



International Journal of Advanced Computer Science and Applications

Volume 7 | Issue 10

October 2016



ISSN 2156-5570 (Online)

ISSN 2158-107X (Print)



www.ijacsa.thesai.org

Editorial Preface

From the Desk of Managing Editor...

It may be difficult to imagine that almost half a century ago we used computers far less sophisticated than current home desktop computers to put a man on the moon. In that 50 year span, the field of computer science has exploded.

Computer science has opened new avenues for thought and experimentation. What began as a way to simplify the calculation process has given birth to technology once only imagined by the human mind. The ability to communicate and share ideas even though collaborators are half a world away and exploration of not just the stars above but the internal workings of the human genome are some of the ways that this field has moved at an exponential pace.

At the International Journal of Advanced Computer Science and Applications it is our mission to provide an outlet for quality research. We want to promote universal access and opportunities for the international scientific community to share and disseminate scientific and technical information.

We believe in spreading knowledge of computer science and its applications to all classes of audiences. That is why we deliver up-to-date, authoritative coverage and offer open access of all our articles. Our archives have served as a place to provoke philosophical, theoretical, and empirical ideas from some of the finest minds in the field.

We utilize the talents and experience of editor and reviewers working at Universities and Institutions from around the world. We would like to express our gratitude to all authors, whose research results have been published in our journal, as well as our referees for their in-depth evaluations. Our high standards are maintained through a double blind review process.

We hope that this edition of IJACSA inspires and entices you to submit your own contributions in upcoming issues. Thank you for sharing wisdom.

Thank you for Sharing Wisdom!

Managing Editor
IJACSA
Volume 7 Issue 10 October 2016
ISSN 2156-5570 (Online)
ISSN 2158-107X (Print)
©2013 The Science and Information (SAI) Organization

Editorial Board

Editor-in-Chief

Dr. Kohei Arai - Saga University

Domains of Research: Technology Trends, Computer Vision, Decision Making, Information Retrieval, Networking, Simulation

Associate Editors

Chao-Tung Yang

Department of Computer Science, Tunghai University, Taiwan

Domain of Research: Software Engineering and Quality, High Performance Computing, Parallel and Distributed Computing, Parallel Computing

Elena SCUTELNICU

"Dunarea de Jos" University of Galati, Romania

Domain of Research: e-Learning, e-Learning Tools, Simulation

Krassen Stefanov

Professor at Sofia University St. Kliment Ohridski, Bulgaria

Domains of Research: e-Learning, Agents and Multi-agent Systems, Artificial Intelligence, Big Data, Cloud Computing, Data Retrieval and Data Mining, Distributed Systems, e-Learning Organisational Issues, e-Learning Tools, Educational Systems Design, Human Computer Interaction, Internet Security, Knowledge Engineering and Mining, Knowledge Representation, Ontology Engineering, Social Computing, Web-based Learning Communities, Wireless/ Mobile Applications

Maria-Angeles Grado-Caffaro

Scientific Consultant, Italy

Domain of Research: Electronics, Sensing and Sensor Networks

Mohd Helmy Abd Wahab

Universiti Tun Hussein Onn Malaysia

Domain of Research: Intelligent Systems, Data Mining, Databases

T. V. Prasad

Lingaya's University, India

Domain of Research: Intelligent Systems, Bioinformatics, Image Processing, Knowledge Representation, Natural Language Processing, Robotics

Reviewer Board Members

- | | |
|---|---|
| <ul style="list-style-type: none">• Aamir Shaikh
Mendeley• Abbas Al-Ghaili
Islamic Azad University Arak Branch• Abbas Karimi
Université Abdelmalek Essaadi Faculté Polydisciplinaire de Larache Route de Rabat, Km 2 - Larache BP. 745 - Larache 92004. Maroc.• Abdelghni Lakehal
Gomal University• Abdur Rashid Khan
Faculty of computers and information, Cairo• ADEMOLA ADESINA
University of the Western Cape• Aderemi A. Atayero
Covenant University• Adi Maaita
ISRA UNIVERSITY• Adnan Ahmad
Department of Mathematics and Informatics, Lucian Blaga University of Sibiu• agana Becejski-Vujaklija
University of Belgrade, Faculty of organizational• Ahmad Saifan
yarmouk university• Ahmed Boutejdar
Ahlia University• Ahmed AL-Jumaily
Menoufia University• Ajantha Herath
Stockton University Galloway• Akbar Hossain
University Of California, San Diego• Albert S
Kongu Engineering College• Alcinia Zita Sampaio
Technical University of Lisbon | <ul style="list-style-type: none">• Alexane Bouënard
Sensopia• ALI ALWAN
International Islamic University Malaysia• Ali Ismail Awad
Luleå University of Technology• Alicia Valdez
Taibah University• Amin Shaqrah
Cisco Systems• Anand Nayyar
KCL Institute of Management and Technology, Jalandhar• Andi Wahju Rahardjo Emanuel
Maranatha Christian University• Anews Samraj
Mahendra Engineering College• Anirban Sarkar
National Institute of Technology, Durgapur• Anthony Isizoh
Nnamdi Azikiwe University, Awka, Nigeria• Antonio Formisano
University of Naples Federico II• Anuj Gupta
IKG Punjab Technical University• Anuranjan misra
Bhagwant Institute of Technology, Ghaziabad, India• Appasami Govindasamy
University Technology Malaysia(UTM)• Arash Habibi Lashkari
ARINDAM SARKAR• Aree Mohammed
Directorate of IT/ University of Sulaimani• ARINDAM SARKAR
University of Kalyani, DST INSPIRE Fellow• Aris Skander
Constantine 1 University• Ashok Matani
Government College of Engg, Amravati• Ashraf Owis
Cairo University• Asoke Nath |
|---|---|

- St. Xaviers College(Autonomous), 30 Park Street,
Kolkata-700 016
- **Athanasios Koutras**
 - **Ayad Ismael**
Department of Information Systems Engineering-
Technical Engineering College-Erbil Polytechnic
University, Erbil-Kurdistan Region- IRAQ
 - **Ayman Shehata**
Department of Mathematics, Faculty of Science,
Assiut University, Assiut 71516, Egypt.
 - **Ayman EL-SAYED**
Computer Science and Eng. Dept., Faculty of
Electronic Engineering, Menofia University
 - **Babatunde Opeoluwa Akinkunmi**
University of Ibadan
 - **Bae Bossoufi**
University of Liege
 - **BALAMURUGAN RAJAMANICKAM**
Anna university
 - **Balasubramanie Palanisamy**
 - **BASANT VERMA**
RAJEEV GANDHI MEMORIAL COLLEGE, HYDERABAD
 - **Basil Hamed**
Islamic University of Gaza
 - **Basil Hamed**
Islamic University of Gaza
 - **Bhanu Prasad Pinnamaneni**
Rajalakshmi Engineering College; Matrix Vision
GmbH
 - **Bharti Waman Gawali**
Department of Computer Science & information T
 - **Bilian Song**
LinkedIn
 - **Binod Kumar**
JSPM's Jayawant Technical Campus,Pune, India
 - **Bogdan Belean**
 - **Bohumil Brtník**
University of Pardubice, Department of Electrical
Engineering
 - **Bouchaib CHERRADI**
CRMEF
 - **Brahim Raouyane**
FSAC
 - **Branko Karan**
 - **Bright Keswani**
Department of Computer Applications, Suresh Gyan
Vihar University, Jaipur (Rajasthan) INDIA
 - **Brij Gupta**

- University of New Brunswick
- **C Venkateswarlu Sonagiri**
JNTU
 - **Chanashekhar Meshram**
Chhattisgarh Swami Vivekananda Technical
University
 - **Chao Wang**
 - **Chao-Tung Yang**
Department of Computer Science, Tunghai
University
 - **Charlie Obimbo**
University of Guelph
 - **Chee Hon Lew**
 - **Chien-Peng Ho**
Information and Communications Research
Laboratories, Industrial Technology Research
Institute of Taiwan
 - **Chun-Kit (Ben) Ngan**
The Pennsylvania State University
 - **Ciprian Dobre**
University Politehnica of Bucharest
 - **Constantin POPESCU**
Department of Mathematics and Computer
Science, University of Oradea
 - **Constantin Filote**
Stefan cel Mare University of Suceava
 - **CORNELIA AURORA Györödi**
University of Oradea
 - **Cosmina Ivan**
 - **Cristina Turcu**
 - **Dana PETCU**
West University of Timisoara
 - **Daniel Albuquerque**
 - **Dariusz Jakóbczak**
Technical University of Koszalin
 - **Deepak Garg**
Thapar University
 - **Devena Prasad**
 - **DHAYA R**
 - **Dheyaa Kadhim**
University of Baghdad
 - **Djilali IDOUGHI**
University A.. Mira of Bejaia
 - **Dong-Han Ham**
Chonnam National University
 - **Dr. Arvind Sharma**

- Aryan College of Technology, Rajasthan Technology University, Kota
- **Duck Hee Lee**
Medical Engineering R&D Center/Asan Institute for Life Sciences/Asan Medical Center
 - **Elena SCUTELNICU**
"Dunarea de Jos" University of Galati
 - **Elena Camossi**
Joint Research Centre
 - **Eui Lee**
Sangmyung University
 - **Evgeny Nikulchev**
Moscow Technological Institute
 - **Ezekiel OKIKE**
UNIVERSITY OF BOTSWANA, GABORONE
 - **Fahim Akhter**
King Saud University
 - **FANGYONG HOU**
School of IT, Deakin University
 - **Faris Al-Salem**
GCET
 - **Fir Khan Ali Hamid Ali**
UTHM
 - **Fokrul Alom Mazarbhuiya**
King Khalid University
 - **Frank Ibikunle**
Botswana Int'l University of Science & Technology (BIUST), Botswana
 - **Fu-Chien Kao**
Da-Yeh University
 - **Gamil Abdel Azim**
Suez Canal University
 - **Ganesh Sahoo**
RMRIMS
 - **Gaurav Kumar**
Manav Bharti University, Solan Himachal Pradesh
 - **George Pecherle**
University of Oradea
 - **George Mastorakis**
Technological Educational Institute of Crete
 - **Georgios Galatas**
The University of Texas at Arlington
 - **Gerard Dumancas**
Oklahoma Baptist University
 - **Ghalem Belalem**
University of Oran 1, Ahmed Ben Bella
 - **gherabi noreddine**

- **Giacomo Veneri**
University of Siena
- **Giri Babu**
Indian Space Research Organisation
- **Govindarajulu Salendra**
- **Grebénisan Gávril**
University of Oradea
- **Gufran Ahmad Ansari**
Qassim University
- **Gunaseelan Devaraj**
Jazan University, Kingdom of Saudi Arabia
- **GYÖRÖDI ROBERT STEFAN**
University of Oradea
- **Hadj Tadjine**
IAV GmbH
- **Haewon Byeon**
Nambu University
- **Haiguang Chen**
ShangHai Normal University
- **Hamid Alinejad-Rokny**
The University of New South Wales
- **Hamid AL-Asadi**
Department of Computer Science, Faculty of Education for Pure Science, Basra University
- **Hamid Mukhtar**
National University of Sciences and Technology
- **Hany Hassan**
EPF
- **Harco Leslie Henic SPITS WARNARS**
Bina Nusantara University
- **Hariharan Shanmugasundaram**
Associate Professor, SRM
- **Harish Garg**
Thapar University Patiala
- **Hazem I. El Shekh Ahmed**
Pure mathematics
- **Hemalatha SenthilMahesh**
- **Hesham Ibrahim**
Faculty of Marine Resources, Al-Mergheb University
- **Himanshu Aggarwal**
Department of Computer Engineering
- **Hongda Mao**
Hossam Faris
- **Huda K. AL-Jobori**
Ahlia University
- **Imed JABRI**

- | | |
|--|---|
| <ul style="list-style-type: none">• iss EL OUADGHIRI
• Iwan Setyawan
Satya Wacana Christian University• Jacek M. Czerniak
Casimir the Great University in Bydgoszcz• Jai Singh W• JAMAIAH HAJI YAHAYA
NORTHERN UNIVERSITY OF MALAYSIA (UUM)• James Coleman
Edge Hill University• Jatinderkumar Saini
Narmada College of Computer Application, Bharuch• Javed Sheikh
University of Lahore, Pakistan• Jayaram A
Siddaganga Institute of Technology• Ji Zhu
University of Illinois at Urbana Champaign• Jia Uddin Jia
Assistant Professor• Jim Wang
The State University of New York at Buffalo, Buffalo, NY• John Sahlin
George Washington University• JOHN MANOHAR
VTU, Belgaum• JOSE PASTRANA
University of Malaga• Jui-Pin Yang
Shih Chien University• Jyoti Chaudhary
high performance computing research lab• K V.L.N.Acharyulu
Bapatla Engineering college• Ka-Chun Wong• Kamatchi R• Kamran Kowsari
The George Washington University• KANNADHASAN SURIYAN• Kashif Nisar
Universiti Utara Malaysia• Kato Mivule• Kayhan Zrar Ghafoor
University Technology Malaysia• Kennedy Okafor
Federal University of Technology, Owerri | <ul style="list-style-type: none">• Khalid Mahmood
IEEE• Khalid Sattar Abdul
Assistant Professor• Khin Wee Lai
Biomedical Engineering Department, University Malaya• Khurram Khurshid
Institute of Space Technology• KIRAN SREE POKKULURI
Professor, Sri Vishnu Engineering College for Women• KITIMAPORN CHOOCHOTE
Prince of Songkla University, Phuket Campus• Krasimir Yordzhev
South-West University, Faculty of Mathematics and Natural Sciences, Blagoevgrad, Bulgaria• Krassen Stefanov
Professor at Sofia University St. Kliment Ohridski• Labib Gergis
Misr Academy for Engineering and Technology• LATHA RAJAGOPAL• Lazar Stošić
College for professional studies educators Aleksinac, Serbia• Leanos Maglaras
De Montfort University• Leon Abdillah
Bina Darma University• Lijian Sun
Chinese Academy of Surveying and• Ljubomir Jerinic
University of Novi Sad, Faculty of Sciences, Department of Mathematics and Computer Science• Lokesh Sharma
Indian Council of Medical Research• Long Chen
Qualcomm Incorporated• M. Reza Mashinchi
Research Fellow• M. Tariq Banday
University of Kashmir• madjid khalilian• majzoob omer• Mallikarjuna Doodipala
Department of Engineering Mathematics, GITAM University, Hyderabad Campus, Telangana, INDIA |
|--|---|

- | | |
|--|--|
| <ul style="list-style-type: none">• Manas deep
Masters in Cyber Law & Information Security• Manju Kaushik• Manoharan P.S.
Associate Professor• Manoj Wadhwa
Echelon Institute of Technology Faridabad• Manpreet Manna
Director, All India Council for Technical Education,
Ministry of HRD, Govt. of India• Manuj Darbari
BBD University• Marcellin Julius Nkenifack
University of Dschang• Maria-Angeles Grado-Caffaro
Scientific Consultant• Marwan Alseid
Applied Science Private University• Mazin Al-Hakeem
LFU (Lebanese French University) - Erbil, IRAQ• Md Islam
sikkim manipal university• Md. Bhuiyan
King Faisal University• Md. Zia Ur Rahman
Narasaraopeta Engg. College, Narasaraopeta• Mehdi Bahrami
University of California, Merced• Messaouda AZZOUZI
Ziane AChour University of Djelfa• Milena Bogdanovic
University of Nis, Teacher Training Faculty in Vranje• Miriampally Venkata Raghavendra
Adama Science & Technology University, Ethiopia• Mirjana Popovic
School of Electrical Engineering, Belgrade University• Miroslav Baca
University of Zagreb, Faculty of organization and
informatics / Center for biometrics• Moeiz Miraoui
University of Gafsa• Mohamed Eldosoky• Mohamed Ali Mahjoub
Preparatory Institute of Engineer of Monastir• Mohamed Kaloup• Mohamed El-Sayed
Faculty of Science, Fayoum University, Egypt | <ul style="list-style-type: none">• Mohamed Najeh LAKHOUA
ESTI, University of Carthage• Mohammad Ali Badamchizadeh
University of Tabriz• Mohammad Jannati• Mohammad Alomari
Applied Science University• Mohammad Haghigat
University of Miami• Mohammad Azzeh
Applied Science university• Mohammed Akour
Yarmouk University• Mohammed Sadgal
Cadi Ayyad University• Mohammed Al-shabi
Associate Professor• Mohammed Hussein• Mohammed Kaiser
Institute of Information Technology• Mohammed Ali Hussain
Sri Sai Madhavi Institute of Science & Technology• Mohd Helmy Abd Wahab
University Tun Hussein Onn Malaysia• Mokhtar Beldjehem
University of Ottawa• Mona Elshinawy
Howard University• Mostafa Ezziyyani
FSTT• Mouhammd sharari alkasassbeh• Mourad Amad
Laboratory LAMOS, Bejaia University• Mueen Uddin
University Malaysia Pahang• MUNTASIR AL-ASFOOR
University of Al-Qadisiyah• Murphy Choy• Murthy Dasika
Geethanjali College of Engineering & Technology• Mustapha OUJAOURA
Faculty of Science and Technology Béni-Mellal• MUTHUKUMAR SUBRAMANYAM
DGCT, ANNA UNIVERSITY• N.Ch. Iyengar
VIT University• Nagy Darwish |
|--|--|

- Department of Computer and Information Sciences,
Institute of Statistical Studies and Researches, Cairo
University
- **Najib Kofahi**
Yarmouk University
 - **Nan Wang**
LinkedIn
 - **Natarajan Subramanyam**
PES Institute of Technology
 - **Natheer Gharaibeh**
College of Computer Science & Engineering at
Yanbu - Taibah University
 - **Nazeeh Ghatasheh**
The University of Jordan
 - **Nazeeruddin Mohammad**
Prince Mohammad Bin Fahd University
 - **NEERAJ SHUKLA**
ITM UNiversity, Gurgaon, (Haryana) India
 - **Neeraj Tiwari**
 - **Nestor Velasco-Bermeo**
UPFIM, Mexican Society of Artificial Intelligence
 - **Nidhi Arora**
M.C.A. Institute, Ganpat University
 - **Nilanjan Dey**
 - **Ning Cai**
Northwest University for Nationalities
 - **Nithyanandam Subramanian**
Professor & Dean
 - **Noura Aknin**
University Abdelamlek Essaadi
 - **Obaida Al-Hazaimeh**
Al- Balqa' Applied University (BAU)
 - **Oliviu Matei**
Technical University of Cluj-Napoca
 - **Om Sangwan**
 - **Omaima Al-Allaf**
Asesstant Professor
 - **Osama Omer**
Aswan University
 - **Ouchtati Salim**
 - **Ousmane THIARE**
Associate Professor University Gaston Berger of
Saint-Louis SENEGAL
 - **Paresh V Virparia**
Sardar Patel University
 - **Peng Xia**
Microsoft

- **Ping Zhang**
IBM
- **Poonam Garg**
Institute of Management Technology, Ghaziabad
- **Prabhat K Mahanti**
UNIVERSITY OF NEW BRUNSWICK
- **PROF DURGA SHARMA (PHD)**
AMUIT, MOEFDRE & External Consultant (IT) &
Technology Transfer Research under ILO & UNDP,
Academic Ambassador for Cloud Offering IBM-USA
- **Purwanto Purwanto**
Faculty of Computer Science, Dian Nuswantoro
University
- **Qifeng Qiao**
University of Virginia
- **Rachid Saadane**
EE departement EHTP
- **Radwan Tahboub**
Palestine Polytechnic University
- **raed Kanaan**
Amman Arab University
- **Raghuraj Singh**
Harcourt Butler Technological Institute
- **Rahul Malik**
- **raja boddu**
LENORA COLLEGE OF ENGINEERNG
- **Raja Ramachandran**
- **Rajesh Kumar**
National University of Singapore
- **Rakesh Dr.**
Madan Mohan Malviya University of Technology
- **Rakesh Balabantaray**
IIIT Bhubaneswar
- **Ramani Kannan**
Universiti Teknologi PETRONAS, Bandar Seri
Iskandar, 31750, Tronoh, Perak, Malaysia
- **Rashad Al-Jawfi**
Ibb university
- **Rashid Sheikh**
Shri Aurobindo Institute of Technology, Indore
- **Ravi Prakash**
University of Mumbai
- **RAVINA CHANGALA**
- **Ravisankar Hari**
CENTRAL TOBACCO RESEARCH INSTITUE
- **Rawya Rizk**
Port Said University

- **Reshmy Krishnan**
Muscat College affiliated to stirling University.U
- **Ricardo Vardasca**
Faculty of Engineering of University of Porto
- **Ritaban Dutta**
ISSL, CSIRO, Tasmania, Australia
- **Rowayda Sadek**
- **Ruchika Malhotra**
Delhi Technological University
- **Rutvij Jhaveri**
Gujarat
- **SAADI Slami**
University of Djelfa
- **Sachin Kumar Agrawal**
University of Limerick
- **Sagarmay Deb**
Central Queensland University, Australia
- **Said Ghoniemy**
Taif University
- **Sandeep Reddivari**
University of North Florida
- **Sanskriti Patel**
Charotar University of Science & Technology,
Changa, Gujarat, India
- **Santosh Kumar**
Graphic Era University, Dehradun (UK)
- **Sasan Adibi**
Research In Motion (RIM)
- **Satyena Singh**
Professor
- **Sebastian Marius Rosu**
Special Telecommunications Service
- **Seema Shah**
Vidyalankar Institute of Technology Mumbai
- **Seifedine Kadry**
American University of the Middle East
- **Selem Charfi**
HD Technology
- **SENGOTTUVELAN P**
Anna University, Chennai
- **Senol Piskin**
Istanbul Technical University, Informatics Institute
- **Sérgio Ferreira**
School of Education and Psychology, Portuguese
Catholic University
- **Seyed Hamidreza Mohades Kasaei**
University of Isfahan
- **Shafiqul Abidin**
HMR Institute of Technology & Management
(Affiliated to G GS IP University), Hamidpur, Delhi -
110036
- **Shahanawaj Ahamad**
The University of Al-Kharj
- **Shaidah Jusoh**
- **Shaiful Bakri Ismail**
- **Shakir Khan**
Al-Imam Muhammad Ibn Saud Islamic University
- **Shawki Al-Dubaee**
Assistant Professor
- **Sherif Hussein**
Mansoura University
- **Shriram Vasudevan**
Amrita University
- **Siddhartha Jonnalagadda**
Mayo Clinic
- **Sim-Hui Tee**
Multimedia University
- **Simon Ewedafe**
The University of the West Indies
- **Siniša Opic**
University of Zagreb, Faculty of Teacher Education
- **Sivakumar Poruram**
SKP ENGINEERING COLLEGE
- **Slim BEN SAOUD**
National Institute of Applied Sciences and
Technology
- **Sofien Mhatli**
- **sofyan Hayajneh**
- **Sohail Jabbar**
Bahria University
- **Sri Devi Ravana**
University of Malaya
- **Sudarson Jena**
GITAM University, Hyderabad
- **Suhail Sami Owais Owais**
- **Suhas J Manangi**
Microsoft
- **SUKUMAR SENTHILKUMAR**
Universiti Sains Malaysia
- **Süleyman Eken**
Kocaeli University
- **Sumazly Sulaiman**
Institute of Space Science (ANGKASA), Universiti
Kebangsaan Malaysia

- | | |
|--|---|
| <ul style="list-style-type: none">• Sumit Goyal
National Dairy Research Institute• Suparerk Janjarasjitt
Ubon Ratchathani University• Suresh Sankaranarayanan
Institut Teknologi Brunei• Susarla Sastry
JNTUK, Kakinada• Suseendran G
Vels University, Chennai• Suxing Liu
Arkansas State University• Syed Ali
SMI University Karachi Pakistan• T C.Manjunath
HKBK College of Engg• T V Narayana rao Rao
SNIST• T. V. Prasad
Lingaya's University• Taiwo Ayodele
Infonetmedia/University of Portsmouth• Talal Bonny
Department of Electrical and Computer Engineering, Sharjah University, UAE• Tamara Zhukabayeva• Tarek Gharib
Ain Shams University• thabet slimani
College of Computer Science and Information Technology• Totok Biyanto
Engineering Physics, ITS Surabaya• Touati Youcef
Computer sce Lab LIASD - University of Paris 8• Tran Sang
IT Faculty - Vinh University - Vietnam• Tsvetanka Georgieva-Trifonova
University of Veliko Tarnovo• Uchechukwu Awada
Dalian University of Technology• Udai Pratap Rao• Urmila Shrawankar
GHRCE, Nagpur, India• Vaka MOHAN
TRR COLLEGE OF ENGINEERING• VENKATESH JAGANATHAN | <ul style="list-style-type: none">• ANNA UNIVERSITY• Vinayak Bairagi
AISSMS Institute of Information Technology, Pune• Vishnu Mishra
SVNIT, Surat• Vitus Lam
The University of Hong Kong• VUDA SREENIVASARAO
PROFESSOR AND DEAN, St.Mary's Integrated Campus, Hyderabad• Wali Mashwani
Kohat University of Science & Technology (KUST)• Wei Wei
Xi'an Univ. of Tech.• Wenbin Chen
360Fly• Xi Zhang
illinois Institute of Technology• Xiaojing Xiang
AT&T Labs• Xiaolong Wang
University of Delaware• Yanping Huang• Yao-Chin Wang• Yasser Albagory
College of Computers and Information Technology, Taif University, Saudi Arabia• Yasser Alginahi• Yi Fei Wang
The University of British Columbia• Yihong Yuan
University of California Santa Barbara• Yilun Shang
Tongji University• Yu Qi
Mesh Capital LLC• Zacchaeus Omogbadegun
Covenant University• Zairi Rizman
Universiti Teknologi MARA• Zarul Zaaba
Universiti Sains Malaysia• Zenzo Ncube
North West University• Zhao Zhang
Deptment of EE, City University of Hong Kong• Zhihan Lv |
|--|---|

Chinese Academy of Science

- **Zhixin Chen**

ILX Lightwave Corporation

- **Ziyue Xu**

National Institutes of Health, Bethesda, MD

- **Zlatko Stapic**

University of Zagreb, Faculty of Organization and
Informatics Varazdin

- **Zuraini Ismail**

Universiti Teknologi Malaysia

CONTENTS

Paper 1: Encryption Algorithms for Color Images: A Brief Review of Recent Trends

Authors: Anuja P Parameshwaran, Wen-Zhan Song

PAGE 1 – 11

Paper 2: Characterizing the 2016 U.S. Presidential Campaign using Twitter Data

Authors: Ignasi Vegas, Tina Tian, Wei Xiong

PAGE 12 – 19

Paper 3: Pentaho and Jaspersoft: A Comparative Study of Business Intelligence Open Source Tools Processing Big Data to Evaluate Performances

Authors: Victor M. Parra, Ali Syed, Azeem Mohammad, Malka N. Halgamuge

PAGE 20 – 29

Paper 4: Diagnosing Coronary Heart Disease using Ensemble Machine Learning

Authors: Kathleen H. Miao, Julia H. Miao, George J. Miao

PAGE 30 – 39

Paper 5: Backstepping Control of Induction Motor Fed by Five-Level NPC Inverter

Authors: Ali BOUCHAIB, Abdellah MANSOURI, Rachid TALEB

PAGE 40 – 44

Paper 6: On Standards for Application Level Interfaces in SDN

Authors: Yousef Ibrahim Daradkeh, Mujahed Aldhaifallah, Dmitry Namiot, Manfred Sneps-Sneppe

PAGE 45 – 51

Paper 7: Impact of Domain Modeling Techniques on the Quality of Domain Model: An Experiment

Authors: Hiqmat Nisa, Salma Imtiaz, Muhammad Uzair Khan, Saima Imtiaz

PAGE 52 – 61

Paper 8: A New Selection Operator - CSM in Genetic Algorithms for Solving the TSP

Authors: Wael Raef Alkhayri, Suhail Sami Owais, Mohammad Shkoukani

PAGE 62 – 66

Paper 9: Automatic Detection of Omega Signals Captured by the Poynting Flux Analyzer (PFX) on Board the Akebono Satellite

Authors: I Made Agus Dwi Suarjaya, Yoshiya Kasahara, Yoshitaka Goto

PAGE 67 – 74

Paper 10: A New Methodology in Study of Effective Parameters in Network-on-Chip Interconnection's (Wire/Wireless) Performance

Authors: Mostafa Haghi, Kerstin Thurow, Norbert Stoll, Saed Moradi

PAGE 75 – 85

Paper 11: Determining the Types of Diseases and Emergency Issues in Pilgrims During Hajj: A Literature Review

Authors: Shah Murtaza Rashid Al Masud, Asmidar Abu Bakar, Salman Yussof

PAGE 86 – 94

Paper 12: Energy Efficient Routing Protocol for Maximizing Lifetime in Wireless Sensor Networks using Fuzzy Logic and Immune System

Authors: Safaa Khudair Leabi, Turki Younis Abdalla

PAGE 95 – 101

Paper 13: A System Framework for Smart Class System to Boost Education and Management

Authors: Ahmad Tasnim Siddiqui, Mehedi Masud

PAGE 102 – 106

Paper 14: A Coreference Resolution Approach using Morphological Features in Arabic

Authors: Majdi Beseiso, Abdulkareem Al-Alwani

PAGE 107 – 113

Paper 15: User Intent Discovery using Analysis of Browsing History

Authors: Wael K. Abdallah, Aziza S. Asem, Mohammed Badr Senousy

PAGE 114 – 120

Paper 16: A Multi-Task Distributed Vision System Embedded on a Hex-Rotorcraft UAV

Authors: Nadir Younes, Boukhdir Khalid, Moutaouakkil Fouad, Hicham Medromi

PAGE 121 – 126

Paper 17: Trending Challenges in Multi Label Classification

Authors: Raed Alazaideh, Farzana Kabir Ahmad

PAGE 127 – 131

Paper 18: AAODV (Aggrandized Ad Hoc on Demand Vector): A Detection and Prevention Technique for Manets

Authors: Abdulaziz Aldaej, Tariq Ahamad

PAGE 132 – 140

Paper 19: Named Entity Recognition System for Postpositional Languages: Urdu as a Case Study

Authors: Muhammad Kamran Malik, Syed Mansoor Sarwar

PAGE 141 – 147

Paper 20: Symbolism in Computer Security Warnings: Signal Icons & Signal Words

Authors: Nur Farhana Samsudin, Zarul Fitri Zaaba, Manmeet Mahinderjit Singh, Azman Samsudin

PAGE 148 – 154

Paper 21: Cross Site Scripting: Detection Approaches in Web Application

Authors: Abdalla Wasef Marashdih, Zarul Fitri Zaaba

PAGE 155 – 160

Paper 22: A Parallel Fuzzy-Genetic Algorithm for Classification and Prediction

Authors: Hassan Abounaser, Ihab Talkhan, Ahmed Fahmy

PAGE 161 – 171

Paper 23: Web Accessibility Challenges

Authors: Hayfa.Y.Abuaddous, Mohd Zalisham Jali, Nurlida Basir

PAGE 172 – 181

Paper 24: Tri-Band Fractal Patch Antenna for GSM and Satellite Communication Systems

Authors: Saad Hassan Kiani, Shahryar Shafique Qureshi, Khalid Mahmood, Mehr-e- Munir, Sajid Nawaz Khan

PAGE 182 – 186

Paper 25: Strength of Crypto-Semantic System of Tabular Data Protection

Authors: Hazem (Moh'd Said) Abdel Majid Hatamleh, Hassan Mohammad, Roba mohmoud ali aloglah, Saleh Ebrahim Alomar

PAGE 187 – 192

Paper 26: New Speech Enhancement based on Discrete Orthonormal Stockwell Transform

Authors: Safa SAOUD, Souha BOUSSELM, Mohamed BEN NASER, Adnane CHERIF

PAGE 193 – 199

Paper 27: SDME Quality Measure based Stopping Criteria for Iterative Deblurring Algorithms

Authors: Mayana Shah, U. D. Dalal

PAGE 200 – 209

Paper 28: Real Time Monitoring of Human Body Vital Signs using Bluetooth and WLAN

Authors: Najeed Ahmed Khan, M. Ajmal Sawand, Marium Hai, Arwa Khuzema, Mehak Tariq

PAGE 210 – 216

Paper 29: Analyzing Distributed Generation Impact on the Reliability of Electric Distribution Network

Authors: Sanaullah Ahmad, Sana Sardar, Babar Noor, Azzam ul Asar

PAGE 217 – 221

Paper 30: An Efficient and Robust High Efficiency Video Coding Framework to Enhance Perceptual Quality of Real-Time Video Frames

Authors: Murthy SVN, Sujatha B K

PAGE 222 – 226

Paper 31: Time-Saving Approach for Optimal Mining of Association Rules

Authors: Mouhir Mohammed, Balouki Youssef, Gadi Taoufiq

PAGE 227 – 233

Paper 32: On the Improved Nonlinear Tracking Differentiator based Nonlinear PID Controller Design

Authors: Ibraheem Kasim Ibraheem, Wameedh Riyadh Abdul-Adheem

PAGE 234 – 241

Paper 33: Automated Imaging System for Pigmented Skin Lesion Diagnosis

Authors: Mariam Ahmed Sheha, Amr Sharwy, Mai S. Mabrouk

PAGE 242 – 254

Paper 34: Improved Association Rules Mining based on Analytic Network Process in Clinical Decision Making

Authors: Shakiba Khademolqorani

PAGE 255 – 260

Paper 35: A Novel Position-based Sentiment Classification Algorithm for Facebook Comments

Authors: Khunishkah Surroop, Khushboo Canoo, Sameerchand Pudaruth

PAGE 261 – 268

Paper 36: Medical Image Fusion Algorithm based on Local Average Energy-Motivated PCNN in NSCT Domain

Authors: Huda Ahmed, Emad N. Hassan, Amr A. Badr

PAGE 269 – 276

Paper 37: Dynamic Inertia Weight Particle Swarm Optimization for Solving Nonogram Puzzles

Authors: Habes Alkhraisat, Hasan Rashaideh

PAGE 277 – 280

Paper 38: Conceptual Modeling in Simulation: A Representation that Assimilates Events

Authors: Sabah Al-Fedaghi

PAGE 281 – 289

Paper 39: Performance Improvement of Threshold based Audio Steganography using Parallel Computation

Authors: Muhammad Shoaib, Zakir Khan, Danish Shehzad, Tamer Dag, Arif Iqbal Umar, Noor Ul Amin

PAGE 290 – 294

Paper 40: A Hybrid Algorithm based on Invasive Weed Optimization and Particle Swarm Optimization for Global Optimization

Authors: Zeynab Hosseini, Ahmad Jafarian

PAGE 295 – 303

Paper 41: A New Internal Model Control Method for MIMO Over-Actuated Systems

Authors: Ahmed Dhahri, Imen Saidi, Dhaou Soudani

PAGE 304 – 309

Paper 42: Inter Prediction Complexity Reduction for HEVC based on Residuals Characteristics

Authors: Kanayah Saurty, Pierre C. Catherine, Krishnaraj M. S. Soyjaudah

PAGE 310 – 318

Paper 43: Recovering and Tracing Links between Software Codes and Test Codes of the Open Source Projects

Authors: Amir Hossein Rasekh, Amir Hossein Arshia, Seyed Mostafa Fakhrahmad, Mohammad Hadi Sadreddini

PAGE 319 – 325

Paper 44: Software Requirements Conflict Identification: Review and Recommendations

Authors: Maysoon Aldekhail, Azzedine Chikh, Djamel Ziani

PAGE 326 – 335

Paper 45: Time Emotional Analysis of Arabic Tweets at Multiple Levels

Authors: Amr M. Sayed, Samir AbdelRahman, Reem Bahgat, Aly Fahmy

PAGE 336 – 342

Paper 46: Towards Multi-Stage Intrusion Detection using IP Flow Records

Authors: Muhammad Fahad Umer, Muhammad Sher, Imran Khan

PAGE 343 – 347

Paper 47: Unsupervised of Morphological Relatedness

Authors: Ahmed Khorsi, Abeer Alsheddi

PAGE 348 – 355

Paper 48: FNN based Adaptive Route Selection Support System

Authors: Saoreen Rahman, M. Shamim Kaiser, Mahtab Uddin Ahmmmed

PAGE 356 – 365

Paper 49: Comparison of Inter-and Intra-Subject Variability of P300 Spelling Dictionary in EEG Compressed Sensing

Authors: Monica Fira, Liviu Goras

PAGE 366 – 371

Paper 50: A Frame Size Adjustment with Sub-Frame Observation for Dynamic Framed Slotted Aloha

Authors: Robithoh Annur, Suvit Nakpeerayuth

PAGE 372 – 376

Paper 51: Evaluating Mobile Phones and Web Sites for Academic Information Needs

Authors: Muhammad Farhan, Nadeem Akhtar, Amnah Firdous, Malik Muhammad Saad Missen, Muhammad Ali Nizamani, Hina Asmat

PAGE 377 – 384

Paper 52: Feasibility Study of Optical Spectroscopy as a Medical Tool for Diagnosis of Skin Lesions

Authors: Asad Saf, Sheikh Ziauddin, Alexander Horsch, Mahzad Ziai, Victor Castaneda, Tobias Lasser, Nassir Navab

PAGE 385 – 395

Encryption Algorithms for Color Images: A Brief Review of Recent Trends

Anuja P Parameshwaran

Department of Computer Science,
Georgia State University (GSU),
Atlanta, Georgia, USA

Wen-Zhan Song

Department of Computer Science,
Georgia State University (GSU),
Atlanta, Georgia, USA

Abstract—The recent years have witnessed rapid developments in the field of image encryption algorithms for secure color image processing. Image encryption algorithms have been classified in different ways in the past. This paper reviews the different image encryption algorithms developed during the period 2007-2015, highlighting their contrasting features. At the same time a broad classification of the said algorithms into: (1) full encryption algorithm and (2) partial encryption algorithm, each further sub-classified with respect to their domain orientations (spatial, frequency and hybrid domains) have been attempted. Efforts have also been made to cover different algorithms useful for color images of various color spaces like Red-Green-Blue (RGB), Hue-Saturation-Intensity (HSI), Cyan-Magenta-Yellow (CMY) etc. Chaotic cryptosystems, various transforms like wavelets, affine transforms etc. and visual cryptography systems are being discussed in detail.

Keywords—RGB; HIS; CMY; Chaotic cryptosystem; wavelets; affine transforms and visual cryptography

I. INTRODUCTION

A. Background/Preliminary:

The field of encryption, which deals with information security, is an active research domain in modern times. Irrespective of the kind of data (multimedia or plain text data) dealt with, security is very crucial, attracting lots of researchers into this important domain. World-over, researchers are worried on security issues during: (1) transmission of data across a secure channel and (2) the storage of data, so that it is not attacked or retrieved by unauthorized parties. Encryption techniques in general help manage these two aspects related to security of any data.

The present review focuses on enlisting and exploring various encryption techniques related to image data. Image is an array or a matrix representation of square picture elements (pixels) that is systematically arranged in rows and columns. For example, a given 2D image I can be represented as MxN matrix where M and N represent the number of rows and columns respectively. Each pixel represented in the image matrix has an intensity value. In case of gray scale images the pixel can take intensity value between the ranges [0,255]. Figure 1 shows an instance of a gray scale image matrix with its intensity value representation.

A given Image data will differ from the corresponding text data in several ways. For instance, an image data is inherently

redundant with the pixels highly correlated (This is generally derived from the fact that an image has smooth texture).

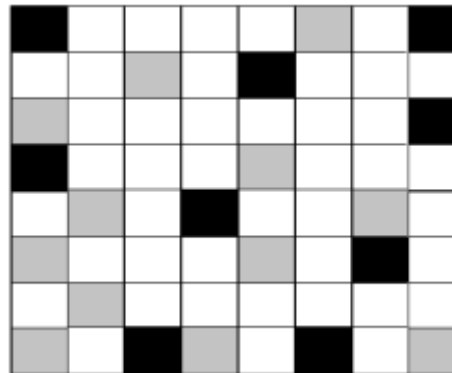


Fig. 1. Each pixel in the gray scale image matrix can take any of the 256 values between [0,255]

Some cryptosystems like the chaotic cryptosystem [1-2] make use of this inherent property of images for encrypting them. Moreover, traditional cryptosystems used for text is not used in case of images for the following two reasons: Firstly, the size of the image data and normal text data varies greatly, with the former being many times bulkier, going up to several Gigabytes in size. Due to the size variation between the two kinds of data at hand, it is obvious that traditional cryptosystems would take a lot more time encrypting image data than normal text data, which is not a very wise choice to go with. A second constraint while dealing with the text data arises out of the requirement that the decrypted data must be same as the original data (in terms of size and content). In contrast, small distortions in the decrypted image data are acceptable as it always depends on human perception which is different for different people. Moreover, lossy compression can be applied to image data before encryption, though this would lead to slight loss of redundant data in the decrypted image [3].

In image encryption, it is important to verify the following three parameters of transmitted digital images: integrity, confidentiality and authenticity [4]. Some of the applications in which image encryption algorithms come really handy are: internet communication, multimedia systems, medical imaging, telemedicine, military communication etc. [3]. Figure 2 shows an illustration of the encryption/decryption process of image data.

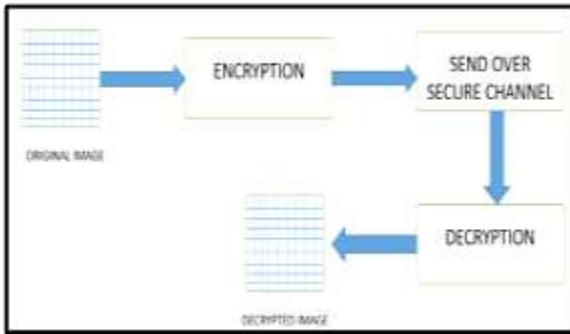


Fig. 2. Encryption and decryption process illustration of a single image matrix

Image compression is another interesting area of research that goes hand in hand with image encryption. Many encryption algorithms like to compress the initial image first before actually encrypting it so as to get rid of any redundant data in the beginning itself [5]. However, some researchers still prefer to encrypt data first and then compress it before transmitting [5] [6] [7] [8]. Compression before encryption works better for data that is highly redundant in nature [5] [6]. In addition to removing redundant data, compression also reduces the bandwidth requirement for transmission of the encrypted image along secure channels. However, it may be added that not all encryption algorithms make use of compression. Most of the algorithms which are frequency domain-oriented and those that involve usage of transforms like DCT, affine etc. have compression either of lossy or lossless form, inherently added to them.

B. Types of Images:

Images can be divided broadly into two categories: (1) Gray-scale images and (2) Color-images. A simple definition of gray scale images would be an image which has only shades of gray and is devoid of any other color. In simpler words gray scale images contain no color information and is mostly referred to as one-color images [29]. The difference between gray-scale images and colored images is that for gray scale images, only less information is required to represent a given pixel of the image. A given pixel of a gray scaled image can take up any of the 256 values ranging from [0-255], which is basically called the intensity of the pixel [9].

Color images can be picturized as a three-band monochrome image data, where each band of the image corresponds to different color [29]. For example: RGB images corresponds to red, green and blue bands if separated into their individual components. Figure-3 shows the famous picture of Lena as a binary image (consists of black and white color only), gray scale image (consists of shades of gray ranging from [0-255] i.e. range from black-shades of gray-white) and RGB colored image (consists of 3 individual components R, G and B) [9].

RGB color images consist of three separate components of 8 bits each. Thus RGB has a color depth of 24 bits in total compared to the 8 bits of gray scaled images. There are various other color space representations of images which are more effective than the RGB representation of images. For instance: YIQ color space (luminance (Y), Chrominance1 (I) and Chrominance2 (Q)), HSI color space (Hue (H), Saturation (S) and Intensity (I)) etc. [9]. Recent experimental results of correlation indicate that YIQ color space algorithm is better than RGB algorithm [9].

and Chrominance2 (Q)), HSI color space (Hue (H), Saturation (S) and Intensity (I)) etc. [9]. Recent experimental results of correlation indicate that YIQ color space algorithm is better than RGB algorithm [9].



Fig. 3. Image of Lena as a binary, gray-scale and RGB color image (courtesy: ref [9])

C. Full Encryption Algorithms vs. Partial Encryption Algorithms:

The image encryption algorithms can be broadly divided into two categories: full encryption algorithms and partial encryption algorithms (selective encryption algorithms). These algorithms will be discussed with respect to their domain orientation, *i.e.*, whether they are spatial domain specific, frequency domain specific or a mix of both (hybrid domain specific) as shown in Figure 4 [4].

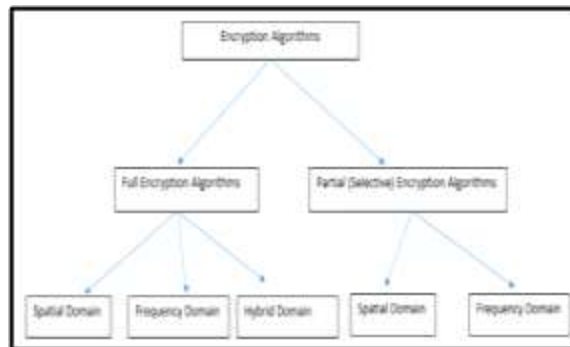


Fig. 4. Broad classification of Image encryption algorithms into full and partial encryption algorithms

Full encryption algorithms, as the name itself suggest, deals with the image as a whole and encrypts the whole image. Partial encryption algorithms encrypts only a part of the image rather than encrypting the whole image. Region of Interest (ROI) is used in selecting the part of image that needs to be encrypted in partial encryption algorithm [20]. Visual cryptography (VC) algorithms also fall into the category of partial encryption algorithms. The application areas of these two classes of encryption algorithms vary greatly. For the first comparison, we look at the computation requirements of both the algorithms. It is seen that in partial encryption algorithms, the computational requirements are greatly reduced as only the lowest portion of data is encrypted. In fact, the full encryption algorithms have greater computational complexity than partial encryption algorithms. For the second comparison, the overall time required by both sections of the algorithms is looked at. Time can be further divided into two categories, (i) the encryption-decryption time (EDT) and (ii) the actual transmission time of the encrypted data over a secure channel.

EDT for full encryption algorithms are bound to be larger as compared to partial encryption algorithms as the latter focuses on encrypting-decrypting only a small region of the image [4]. Figure 5 a) and b) shows the flow and stages of full encryption algorithms and partial encryption algorithms.

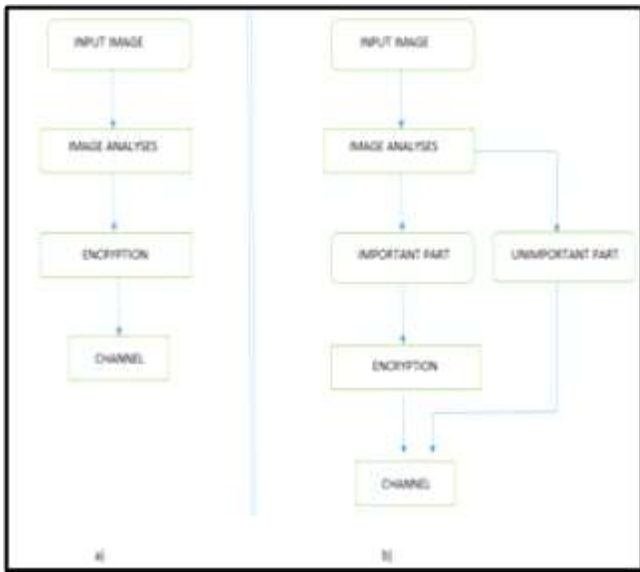


Fig. 5. a) Full encryption algorithm b) partial encryption algorithm

D. Evaluation and Comparison Criteria of Image Encryption Algorithms:

Most of the papers discussed under the category of full encryption based algorithms under spatial domain category [1-4] are evaluated based on the following four parameters:

1) *Security* - Security as an evaluation parameter indicates the confidentiality and robustness of the encryption scheme against various attacks like statistical and differential attacks [9].

2) *Speed*-A factor used to differentiate partial and full encryption algorithms. Less data to encrypt implies usage of less CPU time which further implies faster encryption and decryption. This is the advantage of partial encryption algorithms over full encryption algorithms [9].

3) *Correlation* – Main aim of encryption is to destroy the correlation between adjacent pixels of the encrypted image (which is it will be nearly zero). Image data inherently processes the feature of highly correlated pixels (correlation value close to one), encryption aims to destroy that [1-4] [9].

4) *Key space analysis* – The key space of an encryption space should be large enough so as to avert any brute force or exhaustive attacks from the intruder. Moreover the encryption scheme must also be sensitive to the key [9].

Correlation of adjacent pixels of an encrypted image has to be reduced. But many encryption algorithms on color images existing today are just an extension of the original encryption algorithm on a gray scale image. The correlation analysis does not work out well for such group of algorithms as they apply the encryption schemes on the R, G and B components separately. While doing so, such class of algorithms

conveniently neglect the correlations of the R, G and B components together. Most of the papers discussed here [1] [2-15] are not an extension of the gray scale image encryption scheme, with the exception of [2]. The comparison criteria of most of the papers [1-9] are based on the following:

1) *Number of Pixel Change Rate (NPCR)*–This depicts that the more a particular cryptosystem is sensitive to changing of the original inputted data, the more effective that cryptosystem is to resist a statistical attack from an intruder. The higher the value of NPCR (close to 100%), better is the cryptosystem able to resist statistical attacks.

$$NPCR(R, G, B) = \frac{\sum_{i,j} D(R, G, B)(i, j) \times 100\%}{W \times H}$$

Where, W and H represent the height and width of the image.

2) *Correlation coefficient*–the correlation coefficient between the pixels of the encrypted image should be low i.e. close to zero as it will help resist statistical attacks. The correlation coefficient between each pair of adjacent pixels of an image can be calculated as:

$$D(x) = \frac{1}{N} \sum_{i=1}^N (x_i - E(x))^2$$

Where,

$$\begin{aligned} Cov(x, y) &= \frac{1}{N} \sum_{i=1}^N (x_i - E(x))(y_i - E(y)) \\ E(x) &= \frac{1}{N} \sum_{i=1}^N x_i \\ r\{x, y\} &= \frac{Cov(x, y)}{\sqrt{D(x)} \sqrt{D(y)}} \end{aligned}$$

3) *Unified Average Changing Intensity (UACI)* – UACI values are given so as greater is the possibility that the cryptosystem can avert a differential attack from an intruder.

$$UACI(R, G, B) = \frac{1}{W \times H} \frac{\sum_{i,j} |C(R, G, B)\{i, j\} - C'(R, G, B)\{i, j\}|}{255} \times 100\%$$

Here, W and H represent the width and height of the inputted image and C(R, G, B) and C'(R, G, B) are encrypted images before and after a pixel in the original inputted image has been changed.

4) *Entropy*–This parameter deals with the idea of self-information. It indicates how much of information has been lost in the decrypted image. The ideal value discussed in here for [1-8] is 8. If an encryption scheme has a value closer to 8 means it has lost very little to negligible amount of information. If there are M messages as m is a symbol then entropy H(m) can be defined as:

$$H(m) = \sum_{i=0}^{M-1} p(m_i) \log \frac{1}{P(m_i)}$$

II. FULL ENCRYPTION ALGORITHMS

Full encryption algorithms are discussed in [10-17]. These papers are divided into spatial domain [10-13], frequency domain [14-15] or hybrid domain [16-17] based algorithms. [10], [11] and [13] are encryption algorithms that are based on chaotic cryptosystems. Chaotic cryptosystem is based on the mathematical theory of ‘Chaos’. In theory, chaotic cryptosystems are those dynamic systems that are highly sensitive to system parameters and initial conditions. If the system parameters change by chance then the decrypted image at the receiving end would be totally different from the original inputted image [10]. Chaotic cryptographic systems exploit the inherent feature of bulk data capacity and high data redundancy of an image [30]. The reason chaotic cryptosystems is most useful is because the encryption algorithm destroys any original pattern existing in the reconstructed image, thus making it difficult for an intruder to reconstruct the image based on visual perception of the graphical information. Chaotic cryptosystems are tied to two properties of good ciphers i.e. confusion and diffusion [18]. Diffusion is based on the dependency of the output bits on the input bits whereas confusion is made possible by permuting the data sequence thus guaranteeing the relationship between the key and cipher text to be as complex as possible [18]. The secret key for chaotic cryptosystems described in [10] [11] [13] [16] [17] are the initial conditions and the system parameters defined.

The first step for designing a chaotic cryptosystem is selection of a chaotic map. The dynamics of the chaotic map is determined by control parameters [18]. A particular chaotic cryptosystem will choose the number of chaotic maps it needs. A single chaotic map has only a small key space making it easy for intruders to perform brute force attacks to break the system. Thus to avoid such a situation, multidimensional couple maps can be used together so as to improve the security. A chaotic map is generally used to produce a chaotic sequence after certain number of hops which is very important as this sequence controls the entire encryption process. Though the chaotic cryptosystems seem perfect in theory, in practice they also have a few limitations. First of all, the performance of a chaotic cryptosystem is relatively slow when compared to other cryptosystems (traditional cryptosystems). In addition, the fact that the chaotic cryptosystem is highly sensitive to system parameters and initial conditions of the system sounds great in theory. But in practice, it is difficult to get the correct decrypted image if the processors at the senders and receivers end are different! Because of these limitations, chaotic cryptosystems are very much limited in real world applications [18] [19]. Moreover most of the chaotic cryptosystems are already dysfunctional [31].

Rhouma *et al* [10] have made use of a piecewise linear chaotic map to build their chaotic cryptosystem. The main encryption procedure had three sub procedures which were interleaved with each other. While dealing with color images (in RGB color space) the first step of the encryption algorithm was to convert the image into its three individual vector components by scanning the original image matrix from left to right and top to bottom. The second step involved the division of the phase space of the skew tent map used to build the

cryptosystem into 256 equal width intervals. A mapping function was also defined to help map the respective values. Finally, each of the color pixels belonging to R, G or B were individually encrypted by going through certain number of predetermined rounds. The results of [10] showed that the key space (key space = 1093) was not exhaustive enough (as in the case with most chaotic based cryptosystems) and it was vulnerable to brute force attacks. In order to prove that the encryption algorithm suggested by the authors was a secure one, they proved that the values of NPCR and UACI were high enough to avert any differential attacks. Information loss incurred by [10] was very small, almost negligible, as seen from entropy factor calculations (entropy = 7.9551, as against the ideal value of 8).

Ahmad and Alam *et al* [11] also talked about encryption and decryption of images by using a chaotic cryptosystem. The main difference between [10] and [11] is that in [11], the authors made use of three different chaotic maps namely, 2D cat map, 2D coupled logistics map and 1D logistics map. The original image was initially broken down to 8x8 sized blocks and were then shuffled by using the 2D cat map. The control parameters for the shuffling process were generated randomly as dictated by the 2D coupled logistics map and lastly, the shuffled blocks of the image was encrypted in accordance to the chaotic sequence that was generated by the 1D logistics map. Unlike the work described in [10], [11] surprisingly has a huge key space (about 10112) which was capable of preventing any sort of statistical or differential attack. The information loss as measured by calculating entropy (7.9992, ideal entropy value = 8) was low here too and the coefficient correlation was obtained to be very low as desired (that is, 0.0095, ideally if low correlation that has to be closer to 0). The work in [10] did not really calculate the coefficient correlation value, so was hard to tell whether the correlation of adjacent pixels of the encrypted image was low or high.

Chandell *et al* [12] made use of the color images found in the wang dataset. The security in [12] was increased because of two operations performed one after another: splitting procedure followed by the encryption procedure. Both the procedures have their own respective keys. The encryption algorithm used here is not really new but simple RSA encryption algorithm, which is a public key cryptography method. Initially, the color image from the database was split into many portions by making use of a splitting algorithm. RSA encryption algorithm was then used to encrypt each of the split pieces. On the receiving end, the inverse of RSA was successfully applied to decrypt each of the split pieces and finally all the split pieces were merged together to form the final decrypted image. The keys and number of split pieces were predetermined by the authorized sender in this encryption methodology. This work made use of histograms only to measure the color bins of both the original and the encrypted images. The encryption scheme in [12] did not have an exhaustive analysis of the key space nor did it calculate the coefficient correlation between adjacent pixels of the encrypted image. The only criteria calculated in [12] was the entropy and it consequently proved that the information loss was almost negligible for each of the color images considered from the wang dataset. Since no other analysis was shown by

the authors in [12] against any attacks it is difficult to say how effective this encryption methodology can really be. But on a positive note, the encryption scheme in [12] can be plainly noted for its simplicity.

Just like works in [10] and [11], Wang *et al* [13] was also based on chaotic cryptosystems. This paper made use of a single chaotic map that is the logistics map. The encryption algorithm was very similar to that discussed in [10]. Initially a RGB-color image was broken down to its independent R, G and B components. Then a permutation algorithm was performed on each of the independent component matrices. The permutation algorithm facilitated combined row and combined column scrambling which helped the R, G and B pixels to be mutually permuted. Lastly, a diffusion process was applied to the R, G and B components of the image to give the resultant cipher image. The encryption process discussed when applied in the reverse order gives back the original color image. This algorithm was effective against exhaustive attacks as it had a huge key space which could reach up to 10^{56} . Histogram analysis was also performed which showed that after encryption the R, G and B's components of the cipher image was fairly uniform proving it hard for an intruder to decrypt. Thus the methodology described in [13] was safe against statistical attacks. The correlation coefficient of the cipher image was also very small. NPCR and UACI values calculated by [13] were at a higher range which proved that it was secure against any differential attacks. The authors of [13] also proved that their methodology was safe against cipher text only attacks, known plaintext attacks, chosen plaintext and chosen cipher text attacks.

With Chen *et al* [14] deals with a new domain, *viz.*, frequency domain. This paper made use of two transforms: affine transforms and the gyrator transforms. The affine transform was used twice in the encryption process. The parameters for these transforms served as the secret key in [14]. Initially the RGB image was broken down into its 3 independent components. A function of the affine transform was then used to mix these R, G and B components. Basically, the components were converted to a complex function (real and imaginary parts) with the help of the affine transform. The scrambled pieces of the images was then combined using the gyrator transform. In other words the gyrator function helped to encode and transform the complex function obtained in the first step of using the affine transform. And lastly, the encrypted image came into being by using the final function of the affine transform. The reason the affine transform was performed twice for this encryption scheme was in order to enhance the security of the algorithm. The work in [14] has also demonstrated some numerical simulations to prove that the methodology is valid, secure and robust in nature. Figure 6 shows the encryption scheme as discussed in [14].

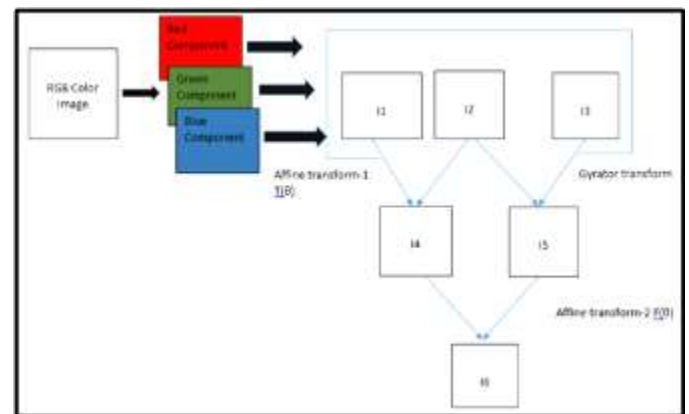


Fig. 6. Encryption algorithm as demonstrated in [14]

Samson *et al* [15] bought in compression before the encryption process. The compression achieved by the use of wavelets in [15] was however lossless in nature. In order to achieve additional compression, [15] made use of lossless predictive coding alongside wavelets. The encryption scheme in [15] flowed as following: firstly, the input color image was compressed using a wavelet of sender's choice, the level of decomposition was also set according to the sender's choice. Then additional compression was achieved using lossless predictive coding. The second step was the encryption process which was achieved using the regular secure advanced hill cipher. This in turn involved a pair of involutory matrices (that is the inverse of a matrix A is equal to the matrix A itself), a mix() function and an XOR operator. The decryption process involved firstly the decryption algorithm followed by the decompression algorithms in order. The wavelet used in [15] was the simple haar wavelet. One of the drawbacks of the methodology in [15] was that there was no analysis of the key space or the nature of attacks possible described in it. The only form of validity [15] has is that the decrypted image obtained was the same as the original inputted image. Figure 7 depicts the flow of stages in [15].

Yu *et al* [16] and Zhou *et al* [17] discussed their methodology in the hybrid domain. Yu *et al* [16] made use of both: the chaotic cryptosystem and the wavelet transform to form its own encryption scheme. This paper made use of the wavelet decomposition and reconstruction processes twice in its encryption scheme. Initially the original color image underwent a 1-level wavelet decomposition. Only the low frequency coefficients were considered of importance at this stage and they were encrypted using a chaotic based encryption algorithm. There were four chaotic maps used for this purpose alone namely: Logistic maps, Chebyshev map, 2D Arnold map and 3D Arnold map.

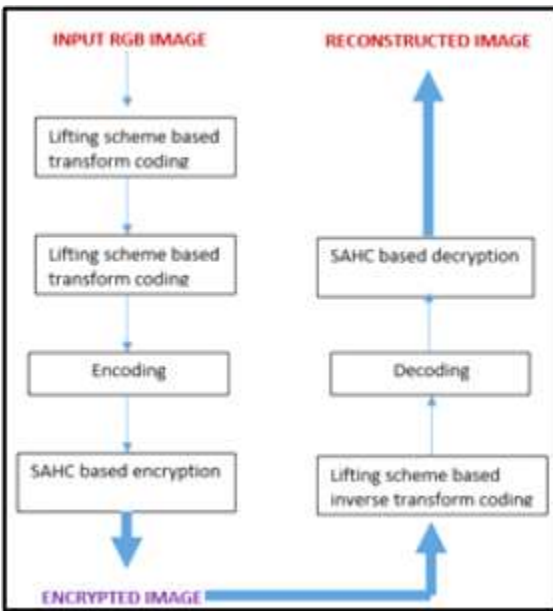


Fig. 7. Flowchart of the encryption scheme followed in [15]

The next step in encryption involved that these encrypted low frequency coefficients act as a key stream and be XORed with the unencrypted high frequency coefficients. This step rendered all the image information held by the high frequency coefficients as hidden. The third step in the encryption process was the wavelet reconstruction which rendered all the encrypted low frequency portions to be equally distributed among the whole image. In order to have effective confidentiality in the encryption scheme of [16], the authors decided to make use of chaotic scrambling for the reconstructed image. Arnold scrambling was used in order to produce a smooth image as the final decrypted image. The wavelet decomposition and reconstruction processes were performed again (level-2 wavelet decomposition). The key space was large enough to resist brute force attacks (2^{128}). The encryption algorithm proved efficient enough against statistical and exhaustive attacks. Overall, methodology discussed in [16] only gave us reasonable performance, but the encryption time taken by the encryption process was determined to be 0.266 seconds (which is still long).

The works from [10], [11], [12], [13], [14], [15] and [16] dealt with image from the RGB color space. Zhou *et al* [17] instead dealt with the image from HSI color space only. The first step in the encryption scheme of [17] was converting the image from any other color space to the HSI color space. New phase plates were generated in this encryption scheme using the fractional fourier transform. The S component obtained a new random phase with the help of random phase encoding which was based on fractional fourier transform. The I component too was transformed into two new phase plates with the help of double random phase encoding which was again based on fractional fourier transform and it made use of the H component and the new random phase component. The final step to the encryption scheme in [17] was chaos scrambling which essentially encrypted the image. The difference between the cipher/encrypted image in [17]

compared to all the other cipher/encrypted images in [10-16] was that it was non-linear in nature and was a combination of gray image and a phase matrix. Numerical simulations had been performed which enabled to illustrate the effectiveness and the level of security obtained by the proposed encryption scheme in [17]. Table-1 summarizes the full encryption algorithms discussed in this section.

TABLE I. SUMMARY OF FULL ENCRYPTION ALGORITHMS. THE WORK DISCUSSED IN [14] & [15] BANKS ITS VALIDITY ON THE FACT THAT THE FINAL DECRYPTED IMAGE SHOULD BE THE SAME AS THE ORIGINAL INPUTTED IMAGE (THIS IS WRT THE VISUAL PERCEPTION ALONE)

Ref No	Category	Domain	Methods used	Number of chaotic maps used	Color space of inputted image	Comparison criteria used wrt security achieved
[10]	Full encryption algorithms	Spatial domain	Purely chaotic cryptosystem	1	RGB color space	-NPCR -UACI -Entropy
[11]	Full encryption algorithms	Spatial domain	Purely chaotic cryptosystem	3	RGB color space	-Larger key space -Entropy -Coefficient correlation
[12]	Full encryption algorithms	Spatial domain	Splitting procedure + RSA encryption algorithm	-	RGB color space	-Entropy
[13]	Full encryption algorithms	Spatial domain	Purely chaotic cryptosystem	1	RGB color space (Made use of color images from wang dataset)	-Huge key space -NPCR -UACI
[14]	Full encryption algorithms	Frequency domain	Affine transforms (used twice) + Gyrator transforms	-	RGB color space	-Security, validity and robustness of methodology illustrated through numerical simulations
[15]	Full encryption algorithms	Frequency domain	Wavelet transforms used for compression prior to encryption	-	RGB color space	-
[16]	Full encryption	Hybrid domain (include	Chaotic cryptosystem +	4	RGB color space	-Huge key space

	algorithms	s both spatial + frequency domains)	wavelet transform [partially chaotic cryptosystems]			
[17]	Full encryption algorithms	Hybrid domain (includes both spatial + frequency domains)	Chaotic cryptosystem + Fractional Fourier Transform [partially chaotic cryptosystems]	1	HSI color space	-Security, validity and robustness of methodology illustrated through numerical simulations

III. PARTIAL ENCRYPTION ALGORITHMS

Partial encryption algorithms are also known as selective encrypted algorithms. The fundamental rule of these algorithms is that there must be independence of the encrypted regions from the unencrypted regions of the image. Since they deal with encrypting only a fraction of the whole image, the computation requirements are greatly lessened by this class of algorithms. Another important point to take into consideration is that this class of algorithms play a very important role in real-time applications. These algorithms play an important role specifically in medical applications. They generally help separate out information into sensitive and insensitive data only based on perception. [20-26] are papers that fall into the category of partial encryption algorithms. [20-26] are further divided into spatial domain [20-24] and frequency domain [25-26] based algorithms.

Along with ROI based algorithms VC algorithms also forms a part of the partial encryption algorithms class. Visual cryptography is a class of encryption algorithms that does not make use of any key. It makes use of a technique where a secret image is hidden inside an image into multiple layers. So each layer of the image essentially holds some secret information. At the receivers end all one has to do is align the layers and the secret information in a proper way and the original image is revealed to the receiver plainly by human perception. The advantage of VC algorithms is that no complex computation is required to be performed in order to get the decrypted image. And since VC algorithms do not use keys, there is no key management needed for these class of algorithms [21].

The methodology of how a VC algorithm work is as following: a secret picture needs to be shared among n participants. So in order to divide this secret image among the n participants, a splitting algorithm is very important. The secret picture is divided into n transparencies/shares based on the splitting algorithm in such a way that if any m shares (as determined by the sender) are placed together then the original image become visible to the authorised receiver. But, if fewer than m shares are placed together than the original image is not revealed to the authorised receiver. The superimposition of the pixels of the various shares is achieved by using a simple logical OR operator. Thus the computational complexity of

the VC class of algorithms is not much [21]. The only disadvantage of the VC class of algorithms is that the quality of reconstructed image could be very poor for certain classes of inputted images.

Wong *et al* [20] proposed a multi-level ROI image encryption universal architecture which dealt with biometric data. It made use of the multi-level encryption in addition with the stream cipher RC4 for encryption purposes. The encryption scheme in [20] made use of multiple ROIs to select the regions of interest for specific users (the authorized users in the receiving end). This implied that a particular user could only see a part of the decrypted image file which it was intended to see and not the other parts of the file which it had no authorized access to. Multiple level ROIs selected for each image and they were encrypted using three levels of authority using RC4 and biometric fingerprinting matching algorithms. If the sender had to send the image to two users at the receiving end, it first requested the authenticated server (AS) for encryption keys for the receivers. The AS generated the keys and send them to the original sender. Using all the keys obtained from AS, the sender then performed multi-level ROI encryption on the main image (the encrypted image is the same but the receivers can only decrypt that part that is sent for it and not the whole image) to form an encrypted image. This encrypted image was then send to the two receivers by the sender. The users at the receiving end send their biometric information to the AS and requested their specific keys from the AS. AS who kept a copy of the keys and the level of authority verifies the same and send the keys to the receivers if the biometric information matched the template already stored in the AS biometric database. Once the receivers received their respective keys from the AS, they can decrypt the image file and read out the portion of the image file meant for them. The encryption scheme implemented by the authors involved implementing two ROIs and also made use of two levels of authority. The work described in [20] made it less susceptible to any kind of thefts as it made use of biometric authentication. The encryption scheme in [20] was thus proved to be one of the most secure encryption schemes discussed in this review paper.

Abdulla and Sozan [21] worked on the subtractive color model CMY (Cyan (C), Magenta (M) and Yellow (Y)). There was no key involved in the encryption scheme of [21] and it was purely based on visual cryptography. The original image was decomposed to its three constituent components based on the CMY color model. Now, if the C primitive matrix was considered then every pixel $P_{i,j}$ in the matrix had $1/4^{\text{th}}$ of its value ($1/4 P_{i,j}$) stored in another matrix which represented a new image. Since the original image was decomposed to its C, M and Y components, which resulted in three cover images existing. The encryption scheme in [21] was very simple and it was based on superimposing (made use of simple OR logical operator) the secret image (size was equal to or smaller than that of the cover image) onto the cover image, thus encrypting the cover image. Three shares were generated such that each share contained a part of the secret image. In this paper, the number of pixels in the decrypted image were the same as the number of pixels in the original image, which was a rule normally followed by text data. The proposed method in

[21] was not a huge success when dark pictures with high contrast were taken into consideration as the decrypted images appeared corrupted with large amounts of noise. This distortion basically happened because the secret image generated was not distinctive. The encryption technique in [21] thus needs to work on how to get a distinct sharp secret image when dark high contrast images are involved. The security of the encryption scheme in [21] depended on the color composition and the color distribution of the secret image. This paper did not mention any detailed analysis of attacks.

Like [21], Patil *et al* [22] was also an encryption technique that was based purely on visual cryptography. The work in [22] also functioned devoid of any key and the encryption process was very simple to execute. The encryption process basically consisted of three main operations namely, sieving (logical XOR operator implemented), division and shuffling. Sieving meant breaking the original RGB image to its individual components. Division meant breaking each of the R, G and B components to numerous number of shares. For example, R could be broken to shares from R_A to R_Z . Shuffling was the last step in the encryption process which dealt with shuffling of the divided shares (from the division step) within itself. These shuffled shares were later combined to generate random shares, for instance in Figure 8 there are two random shares generated. Since majority of the operations in [22] were achieved by using logical operators like OR, XOR and the Mod operator, the computation cost incurred was very less and the implementation in [22] was written purely in java ([10-21] [23-26] implementations were mainly in MATLAB). Since encryption schemes in [21] and [22] do not have keys involved, they do not have to bother about key management or brute force attacks. But the main drawback of the encryption schemes in [21] and [22] was that, generally the quality of the decrypted or recovered image is poor. Figure 8 illustrates the encryption scheme as depicted in [22].

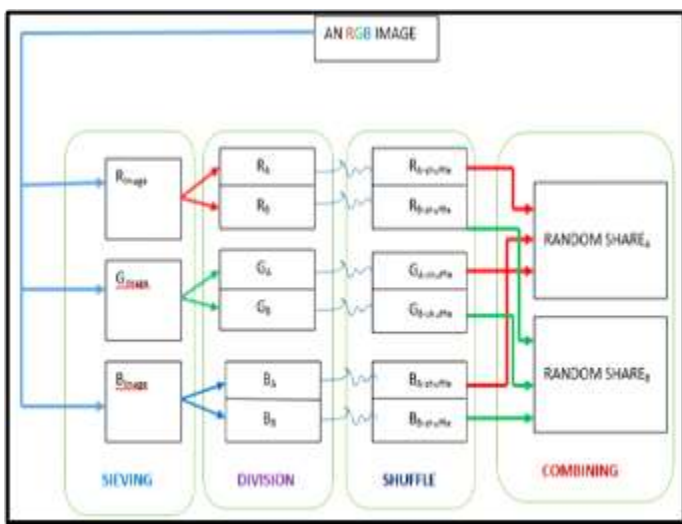


Fig. 8. Encryption scheme as illustrated in [22]

Oh *et al* [23] proposed a selective encryption algorithm

(SEA), which worked on similar lines to the Advanced Encryption standard (AES) algorithm. Like AES, the SEA algorithm also dealt with block cipher. Here the core computation went through several rounds of iteration depending on the key size chosen. In short, the number of iterations required was directly dependent on the key size chosen at the beginning of the algorithm. AES was generally not considered suitable for visual data (included audio, video, image, text etc.) as it could have involved really long computation processes. This work introduced a selector component right at the beginning of the encryption process. The selector component made the selection of ROI from the inputted image and then it performed compression of the ROI based on Huffman coding. The remaining rounds of encryption was very similar to the normal AES algorithm. Figure 9 and Figure 10 depicts the similarity and differences between the SEA algorithm and AES algorithm with the SEA algorithm maintaining the rounds of iteration (computation) same as that as AES.

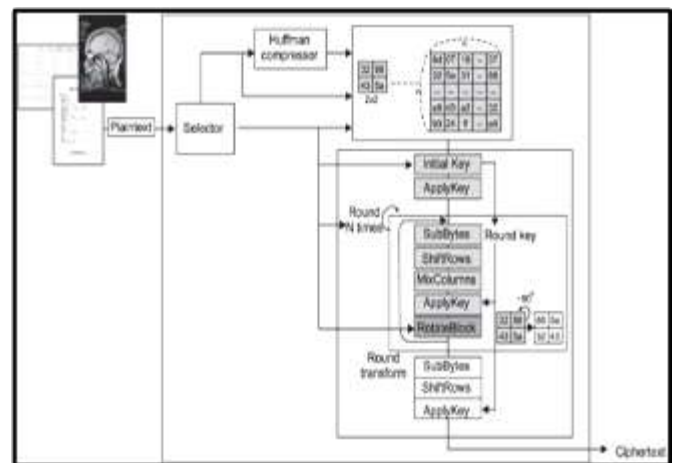


Fig. 9. SEA encryption scheme which is likely to AES (courtesy: ref [23])

SEA algorithm had the same security level that the AES standard algorithm possessed. The only difference between the two seemed to be that the SEA encryption scheme had a compressor component and a selector component to its architecture, something that a normal AES algorithm did not have.

The encryption technique in Parameshachari *et al* [24] was a very simple technique. The key was generated by a random key generator here. The inputted color image was initially broken to sub blocks. The selection of the blocks for encryption happened randomly using the XOR and Mod operators. The randomly selected block along with the random key generator gave the encrypted block. The encrypted block was later combined with all the unencrypted blocks which in turn produced the partially encrypted image for the encryption scheme in [24]. The additional feature [24] had was that it made use of Self-Monitoring Analysis & Reporting Technology copyback system (SMART) to store long term the encrypted images generated. Figure 11 explains the flow of the encryption process at [24].

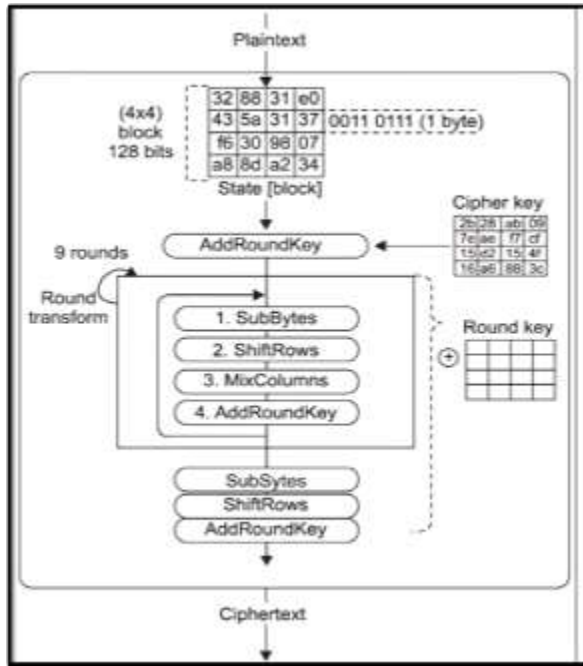


Fig. 10. Encryption scheme of regular AES (courtesy: ref [23])

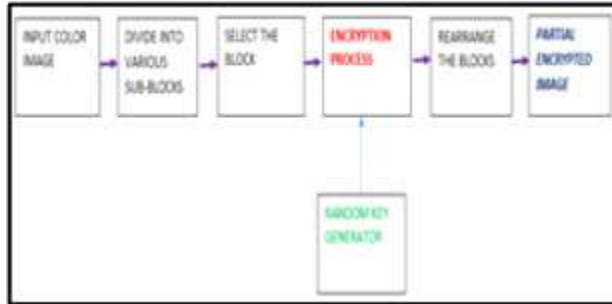


Fig. 11. The flow of the encryption scheme in [24](courtesy: ref [24])

Fan *et al* [25] and Flayh *et al* [26] were partial encryption algorithms which were implemented in the frequency domain. The encoding scheme for [25] was very much similar to the JPEG compression encoding. The only difference between the encoding scheme in [25] and that of the JPEG compression encoding was that, [25] made use of quaternion discrete cosine transforms (QDCT) instead of discrete cosine transforms used in the JPEG encoding scheme. Since the quantization phase was involved in the encryption scheme in [25], the encryption process was rendered to be lossy in nature. Just like the JPEG compression, the encryption scheme in [25] initially divided the original color image into 8x8 sized blocks. The QDCT is performed instead of normal DCT in [25]. The remaining phases remain the same as JPEG compression algorithm. That is, the next subsequent phase was quantization, followed by the zigzag scanning (exploited redundancy and organized coefficients in an array in an order of lower frequency coefficients followed by higher frequency coefficients), sorting of the coefficients and lastly the entropy coding and encryption. Figure 12 and Figure 13 attempt to draw a comparison between the encryption scheme as discussed in [25] and the JPEG compression encoding scheme.

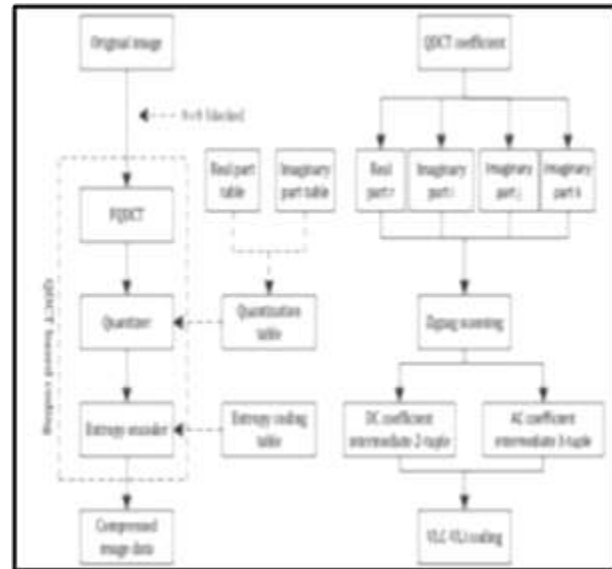


Fig. 12. Encryption scheme in [25] (courtesy: ref [25])

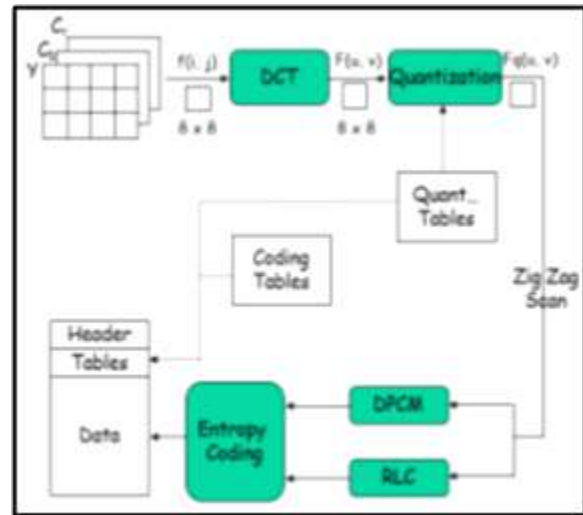


Fig. 13. JPEG compression encoding scheme (courtesy: ref [28])

Flayh *et al* [26] proposed a wavelet based partial encryption algorithm. The first step was to select a key which would be useful in the encryption process. The subsequent step was to select the wavelet filter that one would like to use in the encryption process. The encryption scheme in [26] made use of AES or stream cipher to partially encrypt the inputted color image. The whole idea behind using wavelets was to encrypt only the lower frequency coefficients as opposed to the whole image (consists of lower as well as higher frequencies). The higher frequency coefficients could be discarded or could be coded at a lower bit rate and the lower frequency coefficients could be fully encoded using AES or stream ciphers thus making it a partially encrypted algorithm. If there was a necessity to hide any further details in the cipher/encrypted image then, one could just perform a simple operation like smoothing over the image. The wavelet used for the encryption purpose in [26] was the haar wavelet. The coefficient correlation of the pixels in the cipher image

was nearly equal to zero which was desirable in an encryption scheme. The main problem faced in the encryption scheme in [26] was that, as the amount of encrypted part of the image decreased, the execution time decreased too, which was a good aspect but the coefficient correlation of the pixels in the encrypted image had increased, which was not very desirable in the encryption scheme discussed in [26]. Table-2 summarizes the partial encryption algorithms discussed in this section.

TABLE II. SUMMARY OF PARTIAL ENCRYPTION ALGORITHMS. THE ALGORITHMS MENTIONED IN THE TABLE ARE CAPABLE OF DEALING WITH ANY COLOR SPACE

Ref No	Category	Domain	Class/Method	Type of dataset/Color space	Compression used??
[20]	Partial encryption algorithms	Spatial domain	ROI based algorithms	Biometric data	No
[21]	Partial encryption algorithms	Spatial domain	VC based algorithms	CMY color model	No
[22]	Partial encryption algorithms	Spatial domain	ROI based algorithms	RGB color model	No
[23]	Partial encryption algorithms	Spatial domain	(VC + ROI) based algorithms	Medical/Dicom data	No
[24]	Partial encryption algorithms	Spatial domain	(VC + ROI) based algorithms	Any color space (mostly RGB color models dealt with)	No
[25]	Partial encryption algorithms	Frequency domain	Uses QDCT and very similar to JPEG compression algorithm	Any color space	Yes. Lossy compression by use of QDCT
[26]	Partial encryption algorithms	Frequency domain	Uses Haar wavelets	Any color space	Yes. Mostly lossless compression achieved because of Haar wavelets

IV. FUTURE WORK

The topic of ‘Image Encryption Algorithms for Color Images’ is pretty huge to cover in a single survey paper. This is a topic that has a lot of scope and is still evolving. There is a future and possibility for the partially encryption algorithms to evolve. Chaotic cryptosystem, though very new to explore, having been evolved only during the the last decade, still is not a strong enough system and can easily be broken. Many other transforms in the frequency domain of the various classes of encryption schemes could be explored and their results could be noted. Visual cryptography (VC) has a lot of

scope of improvement in the near future. VC based algorithms generally render poor quality of decrypted image, so a lot of research is going on as to how to handle certain classes of images in a better manner (especially dark high contrasted images). It is difficult to say that any particular cryptosystem or encryption algorithm is the safest as most of the cryptosystems have easily been broken into. This is what makes encryption an ever evolving topic which has a lot of scope to expand in the future.

V. CONCLUSION

Few significant papers on image encryption algorithms for color images were discussed during the period 2007-2015 and the algorithms were classified as full encryption algorithms or partial encryption algorithms. Traditional cryptosystems fail to work for bulky and voluminous data like image data and they fail to produce desirable results for real-time applications. The algorithms in either of the classes were further divided based on whether they were spatial domain, frequency domain or hybrid domain based algorithms. Based on the review one can safely conclude that full encryption based encryption schemes were more suitable for higher security applications while partial encryption based encryption schemes were a lot suitable for real-time applications as they took lesser EDT time and the computational requirements and complexity were smaller.

REFERENCES

- [1] Arroyo, David, Rhouma Rhouma, Gonzalo Alvarez, Veronica Fernandez, and Safya Belghith. "On the skew tent map as base of a new image chaos-based encryption scheme." In Second Workshop on Mathematical Cryptology, pp. 113-117. 2008.
- [2] Yin, Ruming, Jian Yuan, Qiuhua Yang, Xiuming Shan, and Xiqin Wang. "Gemstone: a new stream cipher using coupled map lattice." In Information Security and Cryptology, pp. 198-214. Springer Berlin Heidelberg, 2010.
- [3] Öztürk, İsmet, and İbrahim Soğukpinar. "Analysis and comparison of image encryption algorithms." *International Journal of Information Technology* 1, no. 2 (2004): 108-111.
- [4] Jawad, Lahieb Mohammed, and Ghazali Bin Sulong. "A review of color image encryption techniques." *International Journal of Computer Science Issues* 10, no. 6 (2013): 266-275.
- [5] MULUALEM, GETACHEW MEHABIE. "COMPRESSION AND ENCRYPTION FOR SATELLITE IMAGES: A COMPARISON BETWEEN SQUEEZE CIPHER AND SPATIAL SIMULATIONS." (2015).
- [6] Johnson, Mark, Prakash Ishwar, Vinod Prabhakaran, Daniel Schonberg, and Kannan Ramchandran. "On compressing encrypted data." *Signal Processing, IEEE Transactions on* 52, no. 10 (2004): 2992-3006.
- [7] Klinc, Demijan, Carmit Hazay, Ashish Jagmohan, Hugo Krawczyk, and Tal Rabin. "On compression of data encrypted with block ciphers." *Information Theory, IEEE Transactions on* 58, no. 11 (2012): 6989-7001.
- [8] Zhou, Jiantao, et al. "Designing an efficient image encryption-then-compression system via prediction error clustering and random permutation." *Information Forensics and Security, IEEE Transactions on* 9.1 (2014): 39-50.
- [9] Ali A.Yassin. "Design New Algorithm for Partial Image Encryption Based colors Space." Journal of Babylon University, Pure and Applied Sciences, No.(2), Vol.(20): 2012
- [10] R. Rhouma, D. Arroyo, and S. Belghith, "A new color image cryptosystem based on a piecewise linear chaotic map", in 6th International Multi-Conference on Systems, Signals and Devices, Mar. 2009, pp. 1–6.

- [11] Musheer Ahmad, and M. Alam, "A New Algorithm of Encryption and Decryption of Images Using Chaotic Mapping", International Journal on Computer Science and Engineering, vol. 2, no. 1, 2009, pp. 46–50.
- [12] Chandel, Gajendra Singh, and Pragna Patel. "Image Encryption with RSA and RGB randomized Histograms." *Image* 3, no. 5 (2014).
- [13] Wang, Xingyuan, Lin Teng, and Xue Qin. "A novel colour image encryption algorithm based on chaos." *Signal Processing* 92, no. 4 (2012): 1101-1108.
- [14] H. Chen, X. Du, Z. Liu, and C. Yang, "Color image encryption based on the affine transform and gyrator transform", Optics and Lasers in Engineering, vol. 51, no. 6, Jun. 2013, pp. 768–775.
- [15] Samson, Ch, and V. U. K. Sastry. "An RGB Image Encryption Supported by Wavelet-based Lossless Compression." *International Journal of Advanced Computer Science and Applications* 3, no. 9 (2012).
- [16] Z. Yu, Z. Zhe, Y. Haibing, P. Wenjie, and Z. Yunpeng, "A chaos-based image encryption algorithm using wavelet transform", in 2nd International Conference on Advanced Computer Control, March 2010, Vol. 2, no. 4, pp. 217–222.
- [17] Zhou, Nanrun, Yixian Wang, Lihua Gong, Hong He, and Jianhua Wu. "Novel single-channel color image encryption algorithm based on chaos and fractional Fourier transform." *Optics Communications* 284, no. 12 (2011): 2789-2796.
- [18] Arroyo, David, Rhouma Rhouma, Gonzalo Alvarez, Veronica Fernandez, and Safya Belghith. "On the skew tent map as base of a new image chaos-based encryption scheme." In *Second Workshop on Mathematical Cryptology*, pp. 113-117. 2008.
- [19] Kocarev, Ljupčo. "Chaos-based cryptography: a brief overview." *Circuits and Systems Magazine, IEEE* 1, no. 3 (2001): 6-21.
- [20] A. Wong and W. Bishop, "Backwards Compatible, Multi-Level Region-of-Interest (ROI) Image Encryption Architecture with Biometric Authentication", International Conference on Signal Processing and Multimedia Applications, July 2007, pp. 324 – 329.
- [21] Abdulla, Sozan. "New Visual Cryptography Algorithm For Colored Image." *arXiv preprint arXiv:1004.4445* (2010).
- [22] Patil, Shobha, and V. R. Udupi. "A Secure Approach to Image Encryption of color image without using key." Received from: <http://inpressco.com/category/ijcet> (2013).
- [23] Oh, Ju-Young, Dong-II Yang, and Ki-Hwan Chon. "A selective encryption algorithm based on AES for medical information." *Healthcare informatics research* 16, no. 1 (2010): 22-29.
- [24] Parameshachari, B. D., KM Sunjiv Soyjaudah, and Sumithra Devi KA. "Partial Image Encryption Algorithm Using Pixel Position Manipulation Technique: The SMART Copyback System."
- [25] Fan, Jing, Jinwei Wang, Xingming Sun, and Ting Li. "Partial Encryption of Color Image Using Quaternion Discrete Cosine Transform." *structure* 8, no. 10 (2015).
- [26] Flayh, Nahla A., Rafat Parveen, and Syed I. Ahson. "Wavelet based partial image encryption." In *2009 International Multimedia, Signal Processing and Communication Technologies*. 2009.
- [27] Introduction to image processing - https://www.spacetelescope.org/static/projects/fits_liberator/image_processing.pdf
- [28] Image compression: JPEG, Multimedia Systems (module 4, lesson 1)
- [29] Umbaugh, Scott E. *Digital image processing and analysis: human and computer vision applications with CVIPtools*. CRC press, 2010.
- [30] Debbarma, Nikhil, Lalita Kumari, and Jagdish Lal Raheja. "2D Chaos Based Color Image Encryption Using Pseudorandom Key Generation." *Chaos* 2, no. 4 (2013).
- [31] Pisarchik, Alexander N., and Massimiliano Zanin. "Chaotic map cryptography and security." *International Journal of Computer Research* 19, no. 1 (2012): 49.

Characterizing the 2016 U.S. Presidential Campaign using Twitter Data

Ignasi Vegas, Tina Tian

Department of Computer Science
Manhattan College
New York, USA

Wei Xiong

Department of Information Systems
Iona College
New Rochelle, USA

Abstract—This paper models the 2016 U.S. presidential campaign in the context of Twitter. The study analyzes the presidential candidates' Twitter activity by crawling their real-time tweets. More than 16,000 tweets were observed in this work. We study the interactions between the politicians and their Twitter followers in the retweet and favorite networks. The most frequently mentioned unigrams are presented, which serve the best featuring the political focuses of a candidate. The mention network among the politicians was constructed by parsing the content of their tweets. In this paper, we also study the Twitter profile of the users who follow the presidential candidates. The gender ratio among the Twitter subscribers is examined using the government's census data. We also investigate the geography of Twitter supporters for each candidate.

Keywords—Twitter; social networks; data mining

I. INTRODUCTION

Online social networks, such as Facebook, Twitter and LinkedIn, have gained increasingly popularity over the decade [1]. Vast quantities of real-time, fine grained data are available on social networking sites, including text, images and other multimedia records. The tremendous amount of data on social networks can be extracted using their Application Program Interfaces (APIs), thus be leveraged for analysis. For example, Sakaki et al. monitored real-time activities on Twitter to detect earthquakes [2]. Tian et al. extracted knowledge from Facebook to build an intelligent search system, which improved users' search experience on the web [3] [4]. Archambault and Grudin surveyed the Microsoft employees to study the usefulness of Twitter in organizational communication and information-gathering [5]. Bakhshi et al. studied a pool of images on Instagram and found that photos with faces are more likely to receive likes and comments [6]. Overall, the availability of massive quantities of data on social media has given a boost to the scientific study of the field of social networks [1].

Due to the rapidly growing number of users, online social media has become the ideal platform for politicians to engage and interact with their potential voters. Among all, Twitter, particularly, has become an integral part in the political campaign [7]. Twitter is an online micro blogging service that enables users to share with the public short messages called "tweets". Currently, there are more than 310 million monthly active users on Twitter worldwide [8]. Users may subscribe to other users' tweets, in which case subscribers are called "followers". Users may also rebroadcast other people's tweets

to their own feed, a process known as a "re-tweet". It allows posts to propagate throughout the network and thus raise their visibility [9]. Moreover, individual tweets can be marked as "favorites" by other users. The content of a tweet may contain text, hyperlinks, images and video clips. Messages regarding the same topic can be grouped using hash tags, a form of metadata consisting of words or phrases preceded by a hash symbol ("#"). Similarly, the "@" sign followed by a username is used to refer to a specific user [10].

A. Background on the 2016 U.S. Presidential Election

In this study, we analyze the presidential candidates' Twitter activities by collecting their real-time tweets. We started extracting data from September 26, 2015 and we will keep gathering and monitoring the Twitter data until the Election Day, which will occur on November 8, 2016. At the beginning of the study, there were five active presidential candidates. They are Hilary Clinton and Bernie Sanders from the Democratic Party and Donald Trump, Ted Cruz and John Kasich from the Republican Party. As of the time of writing, only two candidates remain in the presidential campaign: Hilary Clinton as the nominee of the Democratic Party and Donald Trump being the nominee of the Republican Party.

B. Related Work

The exponential growth of Twitter has made it a popular subject for research in multiple disciplines [11]. One stream of research studied the influence and passivity of users. For example, Romero et al. revealed that users with many followers may not necessarily be influential to the community [12]. Another stream of research investigated the commercial and marketing usage of Twitter. For instance, Jansen et al. examined the use of Twitter for sharing consumer opinions to targeting products and brands [13].

With the successful campaign of Barack Obama in the 2008 U.S. Presidential election, the importance of Twitter in politics has become clear [14] [15]. Twitter, being a platform for political deliberation, has attracted attention of many researchers [7]. Tumasjan et al. investigated whether online tweets can reflect offline political sentiment in the context of a German election [7]. Conover et al. examined the re-tweet network and the mention network in pushing the political communication on Twitter during the 2010 U.S. congressional midterm elections [16]. A proof-of-concept model was developed by Livne et al. to predict candidate's victory using data in the same context [17].

The previous studies of Twitter in politics, however, focused on voters instead of the candidates themselves. Livne et al. analyzed the differences between candidates [17], but had an emphasis on each political party as a whole. In this paper, we concentrate our attention on individual candidates.

Our study analyzes the U.S. presidential candidates' Twitter activity by collecting their real-time tweets using Twitter's REST API [18]. The system monitors the interactions between the politicians and their followers by studying the patterns emergent from the re-tweet networks. The paper also investigates and compares the gender ratio and geographical distribution of the candidates' Twitter followers.

The rest of the paper is organized as follows. Section II describes the data set used in the experiment and explains the methods and algorithms adapted in analyzing the data. In Section III, we present the results and visualize them in the form of charts and maps. Section IV concludes the paper and proposes future directions.

II. DATA SET AND METHODOLOGY

The study leverages data crawled from Twitter's REST API between September 26 of 2015 and the time of writing. During the one year of data collection, we observed approximately 16,805 tweets. Tweets were extracted from the candidates' verified Twitter accounts. A verified account is a validation mechanism on Twitter that ensures the identity of the user. One of the candidates, Senator Bernie Sanders, has two verified and highly active Twitter accounts (@BernieSanders and @SenSanders). Therefore, tweets from both accounts are stored. Analysis of Bernie Sanders in this paper is based on the combined data from his two Twitter accounts. Table I shows the total number of tweets and the average number of posts tweeted per day by each candidate. As one can see in the table, the candidates are grouped by their political party. Politicians in the same party are sorted alphabetically by their last name. The same listing order is used for the tables in the rest of this paper.

TABLE I. TOTAL AND DAILY VOLUME OF TWEETS BY CANDIDATES

Party	Candidates	Total number of tweets	Average number of tweets per day
Democratic	Clinton	3075	12
	Sanders	3824	15
Republican	Cruz	2437	10
	Kasich	2309	9
	Trump	5160	21

In this paper, we analyze three aspects of the data – top favorite and re-tweeted posts by candidates, most frequently mentioned terms by candidates, and profile analysis of followers, where we study their gender ratio and geographical distribution. Figure 1 shows the architectural overview of the system. The rest of this section elaborates each module.

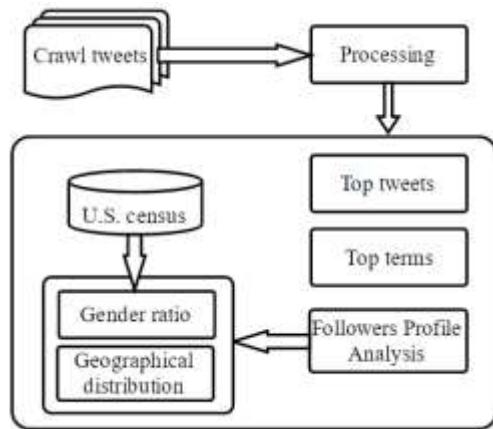


Fig. 1. System architectural overview

A. Top Tweets

As mentioned in Section I, individual tweets can be labeled as "favorites" by other Twitter users. They can also be retweeted, thus to be shared and rebroadcasted. The volume of favorites and the rate of re-tweets of a post indicate its influence on the Twitter network [7]. To evaluate the relationship between the two measures, we extracted the number of favorites and the number of re-tweets of all the tweets posted by the candidates and calculated their correlation. As seen in Table II, the amount of favorites and the level of re-tweets show very high correlation. The overall correlation of all tweets is as high as 0.95. In our data set, the number of favorites of a post is in general larger than the number of re-tweets. Therefore, the former was chosen as the criterion for top tweets. Our system extracts daily tweets published by the candidates and selects the most influential message from the pool with the highest number of favorites, which we refer as top tweets.

TABLE II. CORRELATION BETWEEN THE NUMBER OF FAVORITES AND THE NUMBER OF RE-TWEETS

Candidates	Correlation between favorites and re-tweets
Clinton	0.99
Sanders	0.95
Cruz	0.92
Kasich	0.98
Trump	0.96
Overall	0.95

One factor that needs to be taken into account is the proper interval between the time a tweet is posted and when the volume of favorites is measured, since the latter is a constantly changing variable that accumulates through time. To investigate the scope of this problem, we used a sample of tweets and monitored the evolution of favorites in the next 72 hours after the day those tweets are broadcasted. The level of

favorites was observed every 12 hours. We collected the first record at the end of the day (11:59PM PST), which is denoted as $count_0$ in Table III. The next measure was examined after 12

hours, which is represented as $count_1$ in the table, and so on. In other words, for every tweet in our sample pool, a series of numbers was recorded, ranging from $count_0$ to $count_6$.

TABLE III. OBSERVATION OF THE NUMBER OF FAVORITES

Time	Start of observation	After 12 hours	After 24 hours	After 36 hours	After 48 hours	After 60 hours	After 72 hours
Favorites	$count_0$	$count_1$	$count_2$	$count_3$	$count_4$	$count_5$	$count_6$

To analyze the degree of augmentation of favorites, we calculated E_i , the percentage of increment of the number of favorites compared to the previous record retrieved 12 hours ago:

$$E_i = \frac{count_i - count_{i-1}}{count_{i-1}} \times 100 (\%), \text{ where } i = 1, 2, \dots, 6 \quad (1)$$

Table IV shows the average increment of the volume of favorites from after 12 hours of the day of post to after 72

hours. From the table, one can see that the degree of increment begins with 6.16% after 12 hours and drops significantly after the first 36 hours. After 48 hours from the day of post, the change of favorites reduces to below 1% and becomes relatively stable. Therefore, we adopted 48 hours as the waiting interval. In our experiment, volume of favorites was obtained 48 hours after a tweet is published.

TABLE IV. AVERAGE INCREMENT OF THE NUMBER OF FAVORITES WITH TIME

Time	After 12 hours	After 24 hours	After 36 hours	After 48 hours	After 60 hours	After 72 hours
Percentage of increment (E_i)	6.16%	3.36%	1.48%	0.94%	0.40%	0.25%

B. Top Terms

In this work, we investigate the content of the tweets by extracting unique unigrams from the candidates' accounts. Table V shows the number of unique terms mentioned by candidates in their tweets. Terms are stored in a knowledge base and sorted in the order of their appearances. The top terms play an important role in identifying content produced by each candidate. These keywords serve the best as features to reflect a candidate's political beliefs.

TABLE V. NUMBER OF UNIQUE TERMS IN TWEETS

Candidates	Number of unique terms
Clinton	11456
Sanders	12738
Cruz	6565
Kasich	8135
Trump	12090

Stop words were filtered out from the list of terms. In this study, we considered three types of stop words. They are 1) common functional terms, such as "the", "but", "and", etc., 2) frequently occurred words in a political campaign without individual characteristics, for instance, "America", "people", "president" and so on, and 3) stop words targeting only certain candidates. For example, Bernie Sanders regularly includes his username @BernieSanders in the re-tweets. While it reveals nothing about the content of Sanders' tweets, it can be an important indicator when mentioned by other candidates.

C. Followers Profile Analysis

Previous research suggested that the number of supporters on social media can be successful acting as a sign for electoral success [19]. Some candidate, such as Donald Trump, has more than 9 million followers on Twitter as of the time of writing. In this study, we extract the followers' Twitter profiles and examine them in two facets. We are interested in learning

the gender ratio among the followers for each candidate, as well as their geographical distribution within the U.S..

Twitter does not ask users to share their gender. However, registered users are required to provide their full name when signing up. To determine the gender of a user, our approach utilizes his profile name. We trimmed the name by removing non-English characters and checked it against a list of 4275 female first names and a list of 1219 male given names provided by the U.S. Census Bureau [20]. We were able to identify gender of 55% followers in total. Figure 2 shows the number of followers with gender identified and the number of followers with unknown gender. The gender of a user cannot be determined based on the profile name in the following situations: 1) the name is not in English, 2) it is an unusual name written in English, for example, a foreign name, 3) the name provided in the user profile is a screen name or nickname that does not exist in the lists in [20].

Another aspect we investigated is the geography of the followers. More specifically, we are interested in learning which U.S. state a follower is based in. Twitter allows its users to list their geographical location in the profiles. In most cases, this information is manually entered by the user. Thus, the geographical data for some users may be missing or incorrect [21].

To analyze the location data, first, they were passed to a list of U.S. states, which contains the full name of each state and its abbreviation. If the state of the location cannot be determined, we then queried it in another list, which is constructed with all the cities and towns in the U.S. together with their mapping states [22]. Using this approach, we were able to identify the location of approximately 47% followers. Table VI lists the size of overall followership for each candidate and the number of followers with location identified.

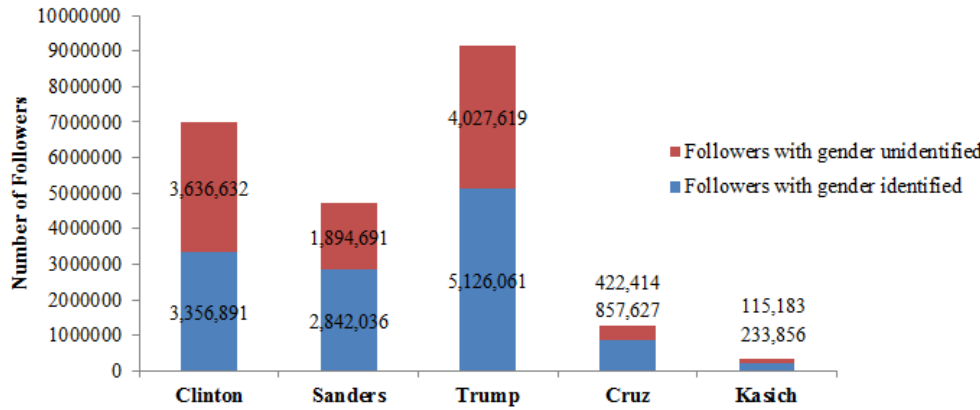


Fig. 2. Number of followers with gender identified

TABLE VI. NUMBER OF FOLLOWERS WITH GEOGRAPHICAL LOCATION IDENTIFIED

Candidates	Total number of followers	Followers with location identified
Clinton	6993523	3007215
Sanders	4736727	2652567
Cruz	1280041	627220
Kasich	349039	209423
Trump	9153680	4119156

The location of a user cannot be analyzed if the data is missing or incorrect. Another scenario is that a city along can be interpreted as different places in the U.S. Two cities from different parts of the country may share the same name. For example, there are Manhattan in New York State, Manhattan in Kansas, Manhattan in the state of Illinois, and so on. If a user specifies his location as Manhattan, we cannot know which Manhattan he is referring to based on this information.

In Section III, we will see that some states have more followers than others for a particular candidate. It is likely that these states are more supportive of the politician. However, there is another possible situation that these states have larger population than others regardless of the public opinions. Therefore, the state population [23] has been considered in the analysis. We used P_i to represent the number of followers per ten thousand among the overall population of a U.S. state:

$$P_i = \frac{\text{follower_count}_i}{\text{population}_i} \times 10000 (0/000), i \in \{\text{U.S. states}\} \quad (2)$$

To further investigate the geography of the followers, we applied Jenks natural breaks classification method [24] to all the P_i values of each candidate. Jenks natural break classification method is a clustering algorithm designed for one dimensional data to arrange values into different groups. In our experiment, we split the P_i data into six classes. The classes with higher P_i values represents the more supportive (positive) U.S. states, while the other groups with lower P_i values indicates the less supportive (negative) states. Results of the method will be demonstrated in Section III.

Our system also examines the percentage of high-impact followers of each candidate. It is anticipated that users with a large number of followers also have strong influence in the real

world. These users may include popular artists, politicians, and so on.

III. RESULTS

This section presents the results of our work using the methodology described in Section II. We divide the section into three subtopics: top tweets, top terms and follower profile analysis.

A. Top Tweets

As previously seen in Section II, our system selects the daily top tweets for each candidate based on the volume of favorites received. Table VII shows the average number of favorites collected per tweet for each candidate. The standard deviation reveals that the amount of variation is large among tweets. In the table, we also list the highest number of favorites a candidate has received during the period of observation.

TABLE VII. AVERAGE NUMBER OF FAVORITES AND HIGHEST NUMBER OF FAVORITES

Candidates	Average favorites	Standard deviation	Highest favorites
Clinton	3881	12751	551388
Sanders	4395	3427	56412
Cruz	901	846	16417
Kasich	409	510	5138
Trump	12911	12830	262457

Figure 3 provides an example of how the system visualizes the change of top tweets. Each data point in the chart represents the number of favorites gained by the top tweet of the day. The line chart is available for demonstration on our website Tweetlitics.net. It provides interaction with the users by displaying the time and content of the top tweet when a user hovers the mouse over a data point. For example, the chart in Figure 3 shows the top tweet of July 20, 2016.

The system monitors the trend of evolution in the number of favorites. A burst in the volume is often caused by emerging events or news. For instance, we can see in Figure 3 that Donald Trump's tweet on July 20 collected 221105 favorites, which is more than twice as many as the favorites of other top tweets in the month. The tweet was posted shortly after the wife of Donald Trump, Melania Trump, delivered her speech at the Republican National Convention.

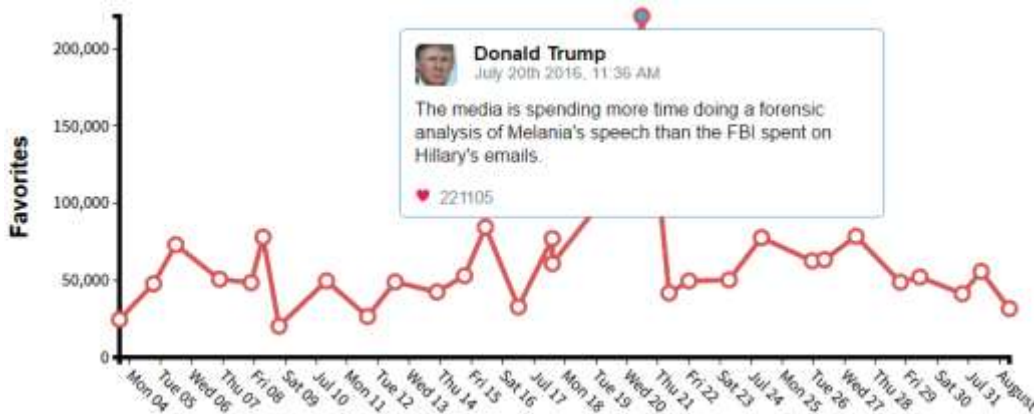


Fig. 3. Example of top tweets by Donald Trump

B. Top Terms

Our system shows the top 20 terms that are regularly tweeted by each candidate. Results are updated periodically. Table VIII gives a glance of some of the top terms in each candidate's profile.

TABLE VIII. TOP TERMS BY CANDIDATE

Clinton	Sanders	Cruz	Kasich	Trump
women	health	#gopdebate	ohio	@foxnews
health	wall	obamacare	#gopdebate	@cnn
trump	wage	#iacaucus	clinton	clinton
gun	jobs	iowa	hilary	cruz
rights	working	tax	work	hilary
families	climate	donald	jobs	crooked
#gopdebate	security	trump	hampshire	ted

We found Donald Trump frequently mentioning other candidates, such as Hilary Clinton and Ted Cruz. His name, on the other hand, is also regularly referred by Hilary Clinton and Ted Cruz. Besides, John Kasich often includes Clinton in his tweets. Figure 4 demonstrates the relationship of mentions among the candidates. An arrow pointing from figure A to figure B represents the mentioning of B in A's tweets.

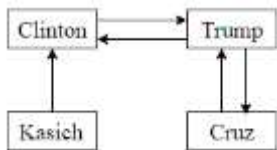


Fig. 4. Relationship of mentions among candidates

Terms relating to health are addressed by a few candidates, including Clinton, Sanders and Cruz. Words about economics (e.g., wage, jobs, work, tax) are frequently mentioned by Sanders, Cruz and Kasich. Compared to the Republican records, the Democratic profile covers a wider range of topics, such as economics, health, security (e.g., gun, security), rights (e.g., women, rights) and climate.

C. Followers Profile Analysis

As mentioned in Section II, we extracted Twitter profile of each candidate's followers and analyzed their gender ratio. Figure 5 shows the number of male and female followers of each candidate. Interestingly, the four male candidates all have

more male followers than female subscribers. Donald Trump, especially, has 66.7% supporters being male. In contrast, Hilary Clinton, who is the only female candidate, has slightly more female followers (50.4%) than male followers (49.6%).

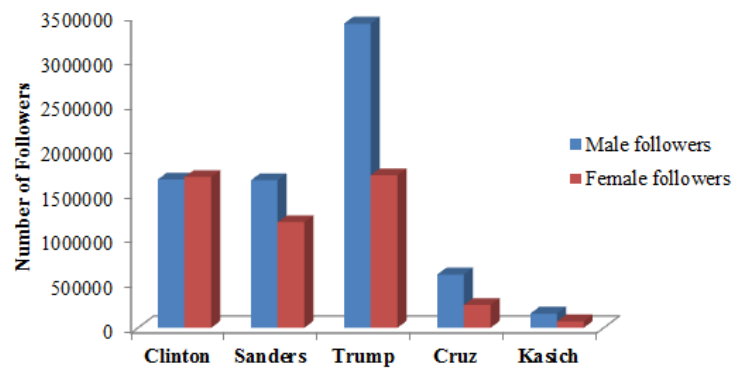


Fig. 5. Gender ratio of followers

Besides gender ratio, we also parsed the geographical data on the followers' records. As previously discussed in Section II, the number of Twitter followers in each state was examined. The size of followership was then compared with the permyriad (one ten-thousandth) of the total population of a state, and the proportion was calculated. Figure 6 shows the results of all U.S. states for Hilary Clinton.

Table IX gives a summary of proportion of followers for each candidate, including the average proportion among the 50 U.S. states and its standard deviation, the highest proportion and the lowest proportion.

TABLE IX. STATISTICS OF PROPORTION OF FOLLOWERS

Candidates	Average proportion	Standard deviation	Highest proportion	Lowest proportion
Clinton	24	28	171	3
Sanders	14	17	105	2
Cruz	7	7	38	1
Kasich	3	3	16	1
Trump	33	37	233	5

This paper also compares the proportion of Twitter followers in each U.S. state among the presidential candidates. As seen in Figure 7, each state is marked with a value, which

specifies the highest proportion of followers of that state. In order to reveal the “winner” of each state, we use different colors to represent the candidates. In Figure 7, states with

Hilary Clinton having the highest proportion of followers are marked with blue, while states that follow Donald Trump the most are illustrated in red.

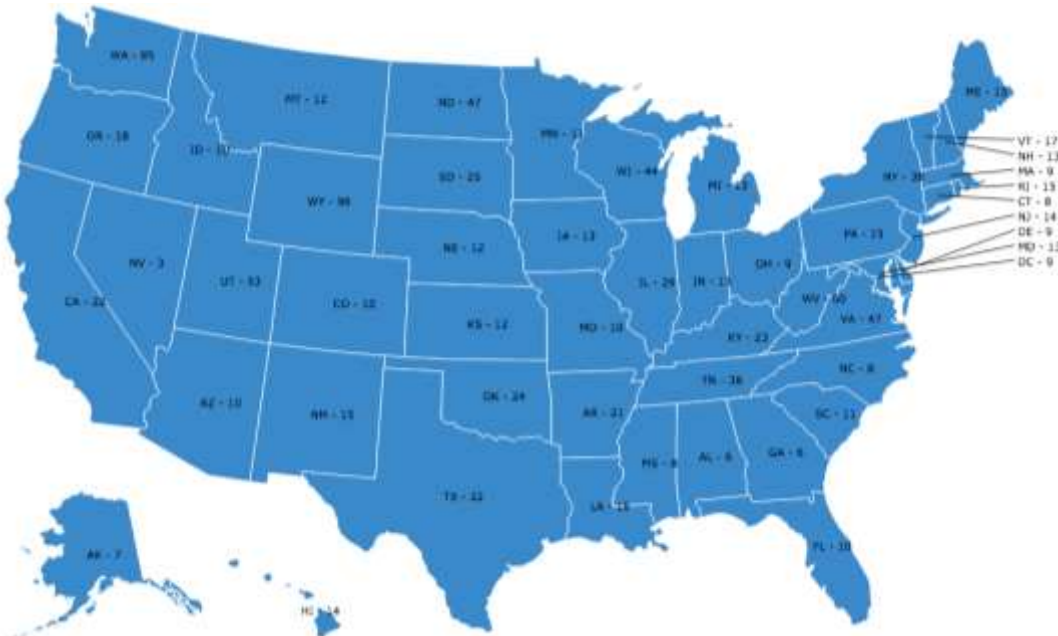


Fig. 6. Proportion of followers of Hilary Clinton

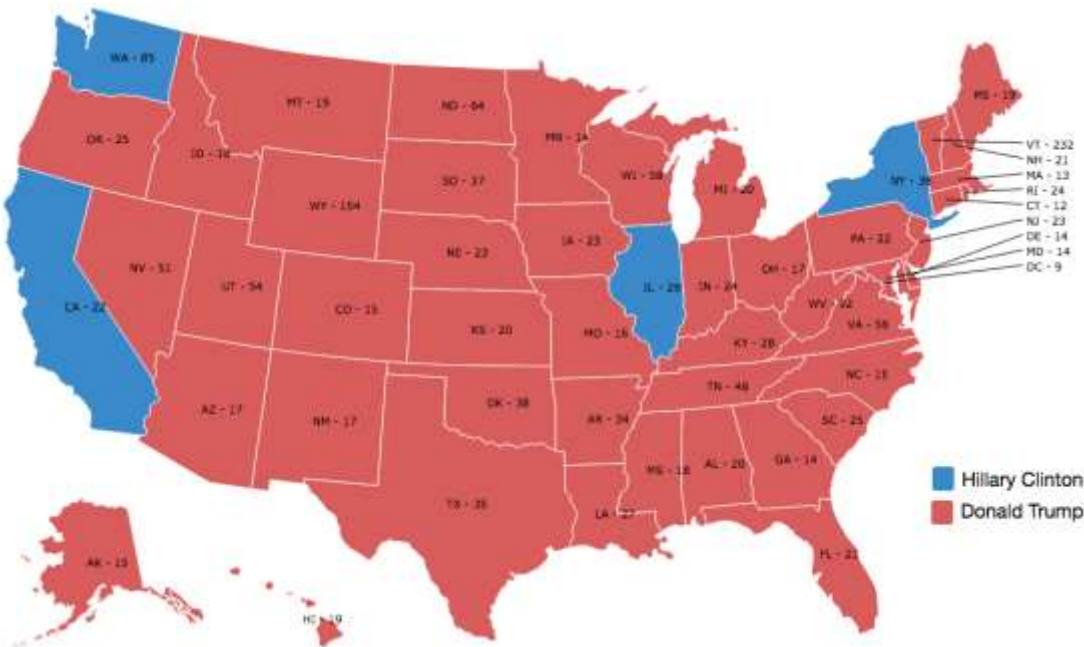


Fig. 7. Highest proportion of followers in each U.S. state

To better understand the geography of supporters for each candidate, we clustered the proportion of followers of each state into different classes by applying Jenks natural breaks optimization [24]. Through experiments, we found that

splitting the states into six groups renders the best classification. Table X summarizes the results in each class, including the range of proportion of followers and the number of states that fall in that range.

TABLE X. RESULTS OF PROPORTION OF FOLLOWERS AFTER APPLYING JENKS NATURAL BREAKS METHOD

	Clinton		Sanders		Cruz		Kasich		Trump	
	Range	States	Range	States	States	States	Range	States	Range	States
Group 1	0 – 3	1	0 – 2	1	1	1	0 – 1	1	0 – 1	1
Group 2	3 – 15	32	2 – 7	15	30	30	1 – 5	27	1 – 2	23
Group 3	15 – 29	8	7 – 13	22	11	11	5 – 9	13	2 – 3	18
Group 4	29 – 47	5	13 – 25	6	5	5	9 – 15	5	3 – 5	4
Group 5	47 – 60	2	25 – 40	4	2	2	15 – 21	3	5 – 8	3
Group 6	60 – 71	3	40 – 105	3	2	2	21 – 38	2	8 – 16	2

Another aspect investigated in this work is the social influence each candidate's followers may have in the Twitter community. To study this matter, we traced the number of fans of every Twitter follower. Table XI lists the number of supporters that have a large social impact. Specifically, we examined the percentage of supporters that have more than 10000 fans, 100000 fans, and 1000000 fans respectively. As

one can see in the table, despite the smaller overall number of followers (recall in Table VI), Ted Cruz and John Kasich have the largest percentage of influential subscribers. Another interesting finding is that between the two nominees of the Republican Party and the Democratic Party, Hilary Clinton has more affecting supporters than Donald Trump does, although the latter is followed the most on Twitter.

TABLE XI. STATISTICS OF FOLLOWERS WITH A SOCIAL IMPACT

Candidates	Followers with over 10000 fans	Percentage	Followers with over 100000 fans	Percentage	Followers with over 1000000 fans	Percentage
Clinton	28396	0.41%	4245	0.06%	462	0.007%
Sanders	23313	0.49%	3028	0.06%	294	0.006%
Cruz	8676	0.68%	1288	0.10%	94	0.007%
Kasich	3370	0.97%	506	0.15%	47	0.013%
Trump	27243	0.30%	3670	0.04%	299	0.003%

We developed a website (Tweetlitics.net) to demonstrate the results of our study and the comparisons between candidates. The website is written in JavaScript. AngularJS was used as the framework for the client-side, while Node.JS was adapted for the server-side. We chose Node.JS mainly for its ability of parallel processing in order to deal with the massive amount of Twitter data. MongoDB was used as the knowledge base for data storage.

IV. CONCLUSIONS AND FUTURE WORK

This paper closely monitors the Twitter activity of the candidates during the 2016 U.S. presidential campaign. We analyzed the interactions between the politicians and their Twitter followers in the retweet/favorite networks. The study collects the real-time tweets published by the candidates and keeps track of the daily top tweets. We found that a burst in the volume of favorites often corresponds to an emerging event. The study also gathers the top terms tweeted by each candidate. These keywords can feature the political focuses of a candidate or a political party. The Democratic Party seems to include a larger range of subjects in their tweets, such as economics, health, rights, security and climate. It is found that some candidates frequently mention others on Twitter. With the extracted top terms, we were able to construct the mention network among the politicians.

This paper also studies the user profiles of the candidates' Twitter supporters. Using the government census data, we examined the ratio of male followers and female subscribers for each candidate. We found that besides Hilary Clinton, the other candidates have the majority of their supporters being male. Moreover, we investigated the geographical distribution of the candidates' Twitter followers. It is found that Donald Trump has the highest number of supporters in most of the

U.S. states. Lastly, we studied the proportion of influential supporters of each candidate. We found that despite the larger volume of Twitter followers, Donald Trump has a smaller number of impacting supporters compared to what Hilary Clinton does.

This study has several limitations. First, we have found in the study that the Twitter followers in the presidential election are a small part of the general voters. Comparing the size of followership with the overall population of a U.S. state, on average, only 0.24% of the population follows Hilary Clinton and 0.33% subscribes Donald Trump on Twitter. Second, the paper only considered unigrams as the top terms extracted from the candidates' tweets. In the future, we plan to include n-grams in the analysis.

Additionally, the results of this paper are based on the tweets broadcasted by the presidential candidates. It would be interesting to study the public opinions by steaming tweets published by the general public. Future work includes conducting a sentiment analysis regarding the election by mining the content on Twitter regarding the candidates and other political events.

REFERENCES

- [1] C. C. Aggarwal, Social Network Data Analytics. Springer, 2011.
- [2] T. Sakaki, M. Okazaki, and Y. Matsuo, "Earthquake shakes Twitter users: real-time event detection by social sensors," Proceedings of the 19th International Conference on World Wide Web, pp. 851–860, 2010.
- [3] S. A. Chun, T. Tian, and J. Geller, "Enhancing the famous people ontology by mining a social network," Proceedings of the 2nd International Workshop on Semantic Search over the Web, article no. 5, 2012.
- [4] S. A. Chun, and T. Tian, "Social Network-based Entity Extraction for People Ontology." Third International Conference on Advances in Information Mining and Management, 2013.

- [5] A. Archambault and J. Grudin, "A longitudinal study of Facebook, LinkedIn, & Twitter use," Proceedings of the SIGCHI Conference on Human Factors in Computing Systems, pp. 2741-2750, 2012.
- [6] S. Bakhshi, D. A. Shamma, and E. Gilbert, "Faces engage us: photos with faces attract more likes and comments on Instagram," Proceedings of the SIGCHI Conference on Human Factors in Computing Systems, pp. 965-974, 2014.
- [7] A. Tumasjan, T. O. Sprenger, P. G. Sandner, and I. M. Welpe, "Predicting elections with Twitter: what 140 characters reveal about political sentiment," Fourth International AAAI Conference on Weblogs and Social Media, pp. 178-185, 2010.
- [8] Twitter, <https://about.twitter.com/company>, retrieved on 09/21/2016.
- [9] D. Boyd, S. Golder and G. Lotan, "Tweet, tweet, retweet: conversational aspects of retweeting on twitter," System Sciences (HICSS), 43rd Hawaii International Conference, pp. 1-10, 2010.
- [10] Twitter, <https://support.twitter.com/articles/166337>, retrieved on 09/21/2016.
- [11] A. Java, X. Song, T. Finin, and B. Tseng, "Why we Twitter: understanding microblogging usage and communities. Proceedings of the 9th WebKDD and 1st SNA-KDD 2007 workshop on Web mining and social network analysis, pp. 56-65, 2007.
- [12] D. M. Romero, W. Galuba, S. Asur, and B. A. Huberman, "Influence and passivity in social media," Proceedings of the 20th International Conference Companion on World Wide Web, pp. 113-114, 2011.
- [13] B. J. Jansen, M. Zhang, K. Sobel, and A. Chowdury, "Twitter power: tweets as electronic word of mouth," Journal of the American Society for Information Science and Technology, vol. 60, pp. 1-20, 2009.
- [14] M. J. Choy, M. L. F. Cheong, N. L. Ma, and P. S. Koo, "A sentiment analysis of Singapore presidential election 2011 using Twitter data with census correction, Research Collection School Of Information Systems, 2012.
- [15] J. Borondo, A. J. Morales, J. C. Losada, and R. M. Benito, "Characterizing and modeling an electoral campaign in the context of Twitter: 2011 Spanish presidential election as a case study," Chaos: An Interdisciplinary Journal of Nonlinear Science, vol. 22, no. 2, 2012.
- [16] M. D. Conover, J. Ratkiewicz, M. Francisco, B. Gonçalves, A. Flammini, and F. Menczer, "Political polarization on Twitter," Proceedings of the Fifth International AAAI Conference on Weblogs and Social Media, 2011.
- [17] A. Livne, M. P. Simmons, E. Adar, and L. A. Adamic, "The party is over here: structure and content in the 2010 election," Proceedings of the Fifth International AAAI Conference on Weblogs and Social Media, 2011.
- [18] Twitter's REST API, <https://dev.twitter.com/rest/public>, retrieved on 09/21/2016.
- [19] C. Williams, and G. Gulati, "What is a social network worth? Facebook and vote share in the 2008 presidential primaries," Annual Meeting of the American Political Science Association, pp. 1-17. 2008.
- [20] US Census data, http://www.census.gov/topics/population/genealogy/data/1990_census/1990_census_namefiles.html, retrieved on 09/21/2016.
- [21] S. Chandra, L. Khan, and F. B. Muhaya, "Estimating twitter user location using social interactions - A content based approach," Proceedings of the 2011 IEEE International Conference on Privacy, Security, Risk and Trust and IEEE International Conference on Social Computing, pp. 838-843, 2011.
- [22] List of cities and towns in the U.S., <https://developers.google.com/adwords/api/docs/appendix/geotargeting>, retrieved on 09/21/2016.
- [23] Population estimates from the U.S. Census Bureau, <http://www.census.gov/popest/data/national/totals/2015/NST-EST2015-popchg2010-2015.html>. retrieved on 09/21/2016.
- [24] G. F. Jenks, "The data model concept in statistical mapping", International Yearbook of Cartography, vol. 7, pp. 186-190, 1967.

Pentaho and Jaspersoft: A Comparative Study of Business Intelligence Open Source Tools Processing Big Data to Evaluate Performances

Victor M. Parra

School of Computing and Mathematics
Charles Sturt University
Melbourne, Australia

Ali Syed

School of Computing and Mathematics
Charles Sturt University
Melbourne, Australia

Azeem Mohammad

School of Computing and Mathematics
Charles Sturt University
Melbourne, Australia

Malka N. Halgamuge

School of Computing and Mathematics
Charles Sturt University
Melbourne, Australia

Abstract—Regardless of the recent growth in the use of “Big Data” and “Business Intelligence” (BI) tools, little research has been undertaken about the implications involved. Analytical tools affect the development and sustainability of a company, as evaluating clientele needs to advance in the competitive market is critical. With the advancement of the population, processing large amounts of data has become too cumbersome for companies. At some stage in a company’s lifecycle, all companies need to create new and better data processing systems that improve their decision-making processes. Companies use BI Results to collect data that is drawn from interpretations grouped from cues in the data set BI information system that helps organisations with activities that give them the advantage in a competitive market. However, many organizations establish such systems, without conducting a preliminary analysis of the needs and wants of a company, or without determining the benefits and targets that they aim to achieve with the implementation. They rarely measure the large costs associated with the implementation blowout of such applications, which results in these impulsive solutions that are unfinished or too complex and unfeasible, in other words unsustainable even if implemented. BI open source tools are specific tools that solve this issue for organizations in need, with data storage and management. This paper compares two of the best positioned BI open source tools in the market: Pentaho and Jaspersoft, processing big data through six different sized databases, especially focussing on their Extract Transform and Load (ETL) and Reporting processes by measuring their performances using Computer Algebra Systems (CAS). The ETL experimental analysis results clearly show that Jaspersoft BI has an increment of CPU time in the process of data over Pentaho BI, which is represented by an average of 42.28% in performance metrics over the six databases. Meanwhile, Pentaho BI had a marked increment of the CPU time in the process of data over Jaspersoft evidenced by the reporting analysis outcomes with an average of 43.12% over six databases that prove the point of this study. This study is a guiding reference for many researchers and those IT professionals who support the conveniences of Big Data processing, and the implementation of BI open source tool based on their needs.

Keywords—Big Data; BI; Business Intelligence; CAS; Computer Algebra System; ETL; Data Mining; OLAP

I. INTRODUCTION

Business Intelligence software converts stored data of a company’s clientele profile and turns it into information that forms the pool of knowledge to create a competitive value and advantage in the market it is in [1]. Additionally, Business Intelligence is used to back up and improve the business with reasonable data and use the analysis of this data, to continuously improve an organisation’s competitiveness. Part of this analysis is to provide timely reports, for management’s to make the decision based on factual information, so their decision-making is based on concrete evidence. Howard Dresner, from Gartner Group [2], was the first to coin the term Business Intelligence (BI), as a term to define a collection of notions and procedures to support the decision-making, by using information found upon facts.

BI system gives enough data to use and evaluate the needs and desires of customers and in addition it allows to: [3]: i) Design reports for departments or global areas in a company, ii) Build a database for customers, iii) Create scenarios for decision-making, iv) Share information between areas or departments of a company, v) Sandbox studies of multidimensional designs, vi) Extract, transform and process data, vii) Give a new approach to decision-making and viii) Improve the quality of customer service.

The benefits of systemizing BI include the amalgamation of information from several sources. [4], creating user profiles for information management, reducing the dependence on the systems department, the reduction in the time of obtaining information, improves the analysis, and also improves the availability to access real-time information according to specific current business criteria.

The recent publication of Gartner Magic Quadrant for Business Intelligence Platforms 2015 [5] has highlighted the changes being taken by the BI sector to rapidly deploy

platforms that can be used by both business users and analysts to extract information from collected data. Traditionally, business intelligence has been understood as a set of methodologies, applications and technologies used to transform data into information and then information into a personal profile of clients that is generated into structured data to serve different areas of business enterprise [6].

Therefore, Big Data will aid to develop better procedures that allow (BI) tools to be used to gather information, such as [7]: i) Process and analyse volumes of information; ii) Increase the universe of data to consider when decision-making: and inherent historical data of the company, to incorporate data from external sources ; iii) Provide an immediate response to the continued provision of real-time data of the devices and the possibilities of interconnections between devices; iv) Working with structures of complex and heterogeneous data: logs, emails, conversations, locations, voice, etc.; v) and lastly, to Isolate from the physical constraints of storage and process by making use of scalable solutions and high availability at a competitive prices.

This paper presents an experimental analysis of the comparison of two of the best positioned open source BI systems in the market: Pentaho and Jaspersoft, processing Big data and focussing on their Extract Transform and Load (ETL) and reporting processes by measuring their performance using Computer Algebra Systems. The aim of this paper is to analyse and evaluate these tools and outline how they improve the quality of data, and inadvertently helps us understand the market conditions to make future predictions base on trends.

Section II describes the capabilities and components of both Pentaho and Jaspersoft BI Open Sources. Section III introduces the computer algebra systems SageMath and Matlab. This is followed by the materials and methods (Section IV) used in the analysis and experimentation, especially the ETL and Reporting measurements and how they were implemented. In Section V, the results of the study for *CPUTime* as a function of the "size" from the input data for the ETL and Reporting processes from both Pentaho and Jaspersoft Business Intelligence Open Sources, applying two different Computer Algebra Systems. Section VI contains the discussion of the experimentation. Section VII, the conclusion of the study.

II. PENTaho AND JASPERSOFT BUSINESS INTELLIGENCE OPEN SOURCES

A. Pentaho

Pentaho, created in 2004 is the current leader of Business Solutions Intelligence Open Source. It offers its own solutions across the spectrum of resources to develop and maintain the operations of BI projects from the ETL with data integration to the dashboards with Dashboard Designer [8]. Pentaho has built its solution Business Intelligence integrating different existing and recognized solvency projects. Data Integration was previously known as Kettle; indeed, it retains its old name as a colloquial name. Mondrian is another component of

Pentaho that retaining its own entity.

Pentaho has the following components:

a) *ETL*: Pentaho Data Integration (previously Kettle) is one of the most widely used ETL solutions and better valued in the market [9]. It has a long history, solidity, and robustness that make it a highly recommended tool. It allows transformations and works in a very simple and intuitive way, as it is shown in Fig. 1. Likewise, the Data Integration projects are very easy to maintain.



Fig. 1. Pentaho Data Integration Interface, the ETL solution allows transformations and works in a very simple and intuitive way

b) *Web Application-BI Server*: The BI Pentaho Server is a 100% Java2EE allows us to manage all BI resources [10]. It has a BI user interface available where reports are stored, OLAP views and dashboards as it is illustrated in Fig. 2. In addition, it offers access to a management support that allows managing and monitoring both application and usage.

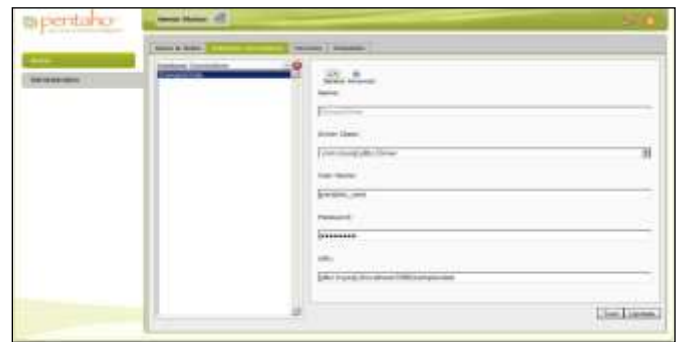


Fig. 2. Pentaho Server User Interface to manage BI resources where all the reports are founded, OLAP views, and dashboards. Also the access to a management supports that allows managing and monitoring both application and usage

c) *Pentaho Reporting*: Pentaho provides a comprehensive reporting solution. Covering all aspects needed in any reporting environment, as shown in Fig. 3. The Pentaho reporting tool is the old form of JFreeReport [11]: i) It provides a tool for reporting (Pentaho Reporting), ii) Provides an execution engine, iii) Provides Metadata tool for conducting reports Ad-hoc, and iv) Provides a user interface that allows ad-hoc reports (WAQR).



Fig. 3. Pentaho Reporting Interface with a comprehensive reporting solution, covering all aspects needed in any reporting environment

d) OLAP Mondrian: Online Analytical Processing is the technology that allows us to organize information in a dimensional structure that will allow us to move information by scrolling through its dimensions [12]. Mondrian is the Pentaho OLAP engine. Although it can be integrated independently on any other platform, and indeed it is the component. Data Integration that is used independently. Mondrian is a Hybrid OLAP engine that combines the flexibility of ROLAP engines with a cache that provides speed.

- **Viewer OLAP:** Pentaho Analyser: OLAP Viewer that comes with the Enterprise version [13]. Modern and easier to use than JPivot as it is illustrated in Fig. 4. AJAX provides an interface that allows great flexibility when creating the OLAP views.

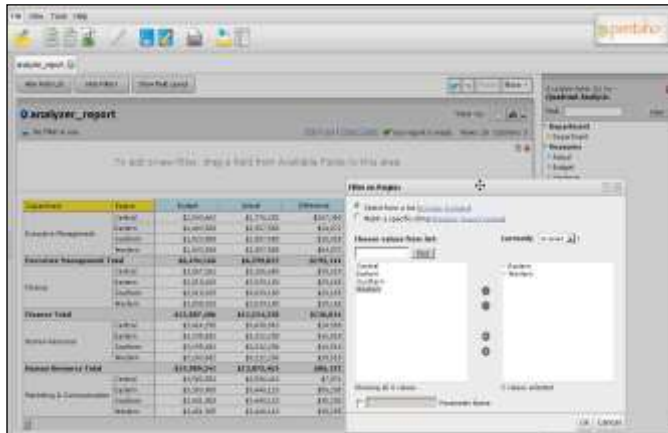


Fig. 4. Pentaho Analyser Interface to create OLAP views that provide a comprehensive reporting solution. Covering all aspects needed in any reporting environment

e) Dashboards: Pentaho provides the possibility of making dashboards [13] through the web interface using the dashboard designer as it is shown in Fig. 5.



Fig. 5. Pentaho Dashboards Interface that provides the possibility of making dashboards through the web interface by using the dashboard designer

B. Jaspersoft

Jaspersoft is the company behind the famous and extended Jaster Reports. Open Source reporting solution preferred by most developers to embed in any Java application that requires a reporting system. Jaspersoft has built its solution B.I. around its reporting engine [14]. This has been done differently from Pentaho. Jasper has integrated its projects that also solves existing and consolidates projects nonetheless, has not absorbed it. This strategy makes it "depend" on Talend solution regarding ETL and Mondrian - Pentaho for the OLAP engine. Jasper has access to the code Mondrian that can adapt and continue its developments with Mondrian.

Jaspersoft has the following components:

a) ETL - JasperETL is actually Talend Studio. Talend, unlike Kettle, it has not been absorbed by Jasper and remains an independent company that offers its products independently [15]. Working with Talend is also quite user-interface intuitive and proprietary although the approach is completely different. Talend is a code generator that is the result of an ETL exercise and it is native Java or Perl code. It can also compile and generate Java procedures or instructions. Talend is more oriented to a type of programmer used with a higher level of technical expertise than it requires by Kettle as it is illustrated in Fig. 6. To sum up, the flexibility is much better with this approach.



Fig. 6. Jaspersoft ETL Interface is actually Talend Studio, it is also quite user-interface intuitive and a code generator

b) Web Application–JasperServer: JasperServer is a 100% Java2EE that allows us to manage all BI resources [16]. The overall look of the web application is a bit minimalist without sacrificing the power as shown in Fig. 7. However, having all resources available on the top button bar makes it a 100% functional application and has all the necessary resources for BI.

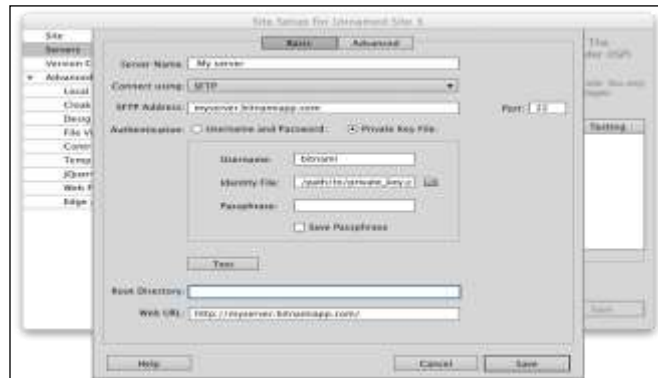


Fig. 7. Jaspersoft Server Interface is a 100% Java2EE to manage business intelligence resources

c) Reports: As described, the report engine is the solution of Jaspersoft as it is illustrated in Fig. 8. The component provides features such as i) Report development environment: Ireport as a system based on environment NetBeans. What makes it challenging to machine resources? In return it offers great flexibility, ii) System of metadata (Domains) the web. These, along with ad-hoc reports, are the strengths of this solution, iii) Web Interface for ad-hoc reports really well resolved, iv) The runtime JasperReports widely was known and used in many projects where a solvent reporting engine is needed, and v) The reports can be exported into PDF, HTML, XML, CSV, RTF, XLS and TXT.

- *Predefined – Ireport:* IReport is a working environment that allows a large number of features [17]. Here something like that Talend is a working environment with larger demands as a result of offering a number of possibilities occurs.

- *Ad hoc:* This is the real strength of Jasper solutions. The editor of ad-hoc reports is the best structured and best featured tool for analysing [17]. It offers: i) Selection of different types of templates and formats, ii) Selection of different data sources, iii) Validation consultation on the fly, iv) Creation of reports by dragging fields to the desired location: i) Tables, ii) Graphics, iii) Crosstable (Pivot), and iv) Edition of all aspects of the reports.



Fig. 8. Jaspersoft Reporting Interface that includes report development environment, a system of metadata (Domains) web, web interface for ad-hoc reports and runtime JasperReports

d) OLAP: The OLAP engine that uses JasperServer is Mondrian and uses a Viewfinder-JasperAnalysis [18], which is no longer JPivot but with a layer of makeup as shown in Fig. 9. Already mentioned in Pentaho paragraph.

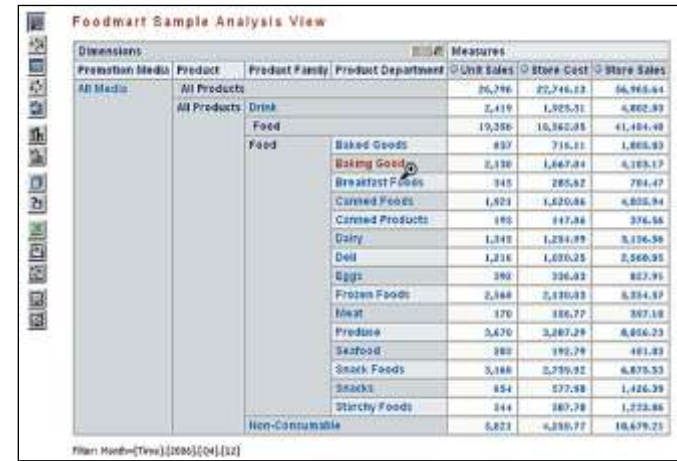


Fig. 9. The OLAP engine that uses JasperServer is Mondrian and uses a Viewfinder-JasperAnalysis which is no longer JPivot but with a layer of makeup

e) Dashboards: Dashboard Designer. Illustrated in Fig.10.

- *Predefined:* They do not make much sense, given the designer panels [19]. In any case, to be a Java platform it can always include proper developments.
- *Ad-hoc:* Dashboard Designer: It is back to a really easy and simple use of the web editor.



Fig. 10. Jaspersoft Dashboards Designers Interface able to select predefined or ad-hoc

III. COMPUTER ALGEBRA SYSTEMS

A. Sagemath

SageMath is a computer algebra system (CAS) that is built on mathematical packages and contrasted as NumPy, Sympy, PARI / GP or Maxima. It accesses the combined power of the same through a common language based on Python. The interaction code combines cells with graphics, texts or formulas enriched with LaTeX rendered. Additionally, SageMath is divided into a core that performs calculations and an interface that displays and interacts with the user. Even, a command line-based text is also available using Python that allows interactive control calculations [20]. The Python programming language supports object-oriented expressions and functional programming. Internally, SageMath is written in Python and a modified version of Pyrex called Cython. It allows parallel processing [21] using both multi-core processors and symmetric multiprocessors. It also provides interfaces to other non-free software as Mathematica, Magma, and Maple (undistributed with SageMath) that allows users to combine software and compare results and performances.

All the packages cover most features such as i) Libraries of elementary and special functions, ii) 2D and 3D graphs of both functions and data, iii) Data manipulation tools and duties, iv) A toolkit for adding user interfaces to calculations and apply, v) Tools for image processing using Python and Pylab, vi) Tools to visualize and analyze graphs, vii) Filters for importing and exporting data, images, video, sound, CAD, and GIS, viii) Sage embedded in documents LaTeX6 [22].

B. Matlab

Matlab is a computer algebra system (CAS) that provides an integrated environment that develops and offers representative characteristics such as the implementation of algorithms, data representation and functions. Also, communication with programs in other languages and other

hardware devices [23], among others are advanced. The Matlab package has two extra tools that extend those functionalities: Simulink is a platform for multi-domain simulation and GUIDE that is a graphic user interface - GUI. Additionally, its potential could be expanded using Matlab toolboxes; and Simulink blocks with block sets.

The language of Matlab is interpreted, and can run in both interactive environments through a script file (*.m files). This language allows vector and matrix operations to function, lambda calculus, and object-oriented programming. An additional tool called Matlab Builder has been launched that contains an "Application Deployment" which allows using Matlab functions, as library files, that provides the ability to be used with environments such as .NET or Java. Matlab Component Runtime (MCR) should be used on the same machine where the main application is set for the Matlab function properly [24]. One of the versatilities of this CAS is that it is quite useful to carry out measurements and it provides an interface to interact with other programming languages. Thus, Matlab can call functions or subroutines written in C or FORTRAN [25]. As the process is accomplished by, creating a wrapper function that allows them to be passed and returned by their data types Matlab.

IV. MATERIALS AND METHODS

Accurately measuring the processing times is not a trivial task, and the results may vary significantly from one computer to another. The number of factors that influence the execution times has used an algorithm, operating system, processor speed, the number of processors and instruction sets that understands the amount of RAM, and cache, and speed of each, math coprocessor, GPU Among each other. Even on the same machine, the same algorithm sometimes takes much longer to give results, due to factors such as using more time than other applications, or if there is enough RAM when running the program.

The objective is to compare only the ETL and Reporting processes, trying to draw independent conclusions from one machine to another. The same algorithm can be called with different input data.

The goal of this study is to measure the run-time as a function of the "size" of the input data. For this, two techniques are used: - Measure run time of programs with different input data sizes and - Count the number of operations performed by the program.

A. ETL Measurement

With Sage was measured the run time and efficiency of ETL processes in both BI tools mentioned previously as it is illustrated in Fig. 11. For the CPU time, Sage uses the concepts of CPU time and Wall time [12], which are the times that the computer is dedicated solely to the program.

The following flow chart shows the ETL process measurement.

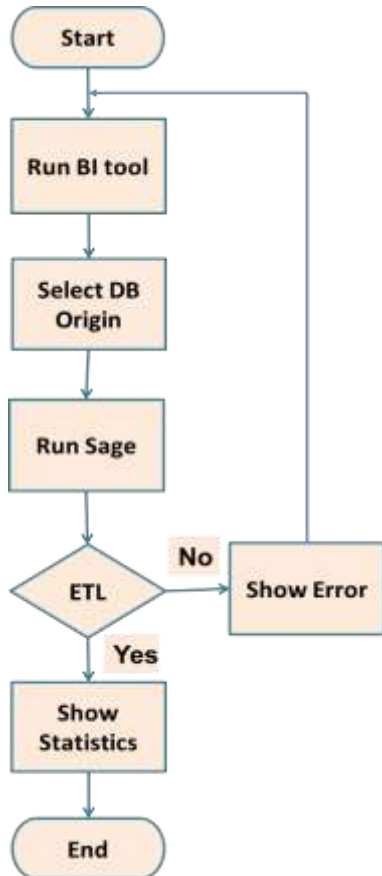


Fig. 11. The ETL process measurement using the Sage computer algebra system for all databases

The CPU time is dedicated to our calculations, and Wall time clock time between the beginning and the end of the calculations. Both measurements are susceptible to unpredictable variations. The easiest way to get the run time of a command is to put the word time to the command as it is shown in Fig. 12.

```

Sage: #To small data size
Sage: Time.is_prime (factorial (500) + 1)
False
Time: 0.09 s CPU, Wall: 0.009 s

Sage: #To higher data size, takes longer (in general)
Sage: time.is_prime (factorial (100) + 1)
False
Time: 0.72 s CPU, Wall: 0.76 s
  
```

Fig. 12. Sage code to measure CPU time of ETL processes in both BI tools for small and higher data sizes

The time command is not flexible enough and needs the *CPUTime* functions and *Walltime*. *CPUTime* is a kind of meter: a meter progresses as the calculations are done, and moves many seconds as the CPU dedicated to Sage. The *Walltime* is a conventional clock (the clock UNIX). For the time spent on the program, also the before and after times of the execution were recorded and calculated and the differences are illustrated in Fig. 13.

```

Sage: #cputime only advances when the cpu runs
Sage: #(a taximeter cpu)
Sage: #runs this function several times to see as time increases
Sage: #if you want. Executes commands in between
Sage: cputime ()
2.0600000000000001

Sage: #walltime inexorable advance (it is an ordinary clock)
Sage: walltime ()
1298369972.163182
  
```

Fig. 13. Sage code using *CPUTime* functions and *Walltime* to measure the ETL process in both tools

The following code saves the list of the CPU times used to run the factorial function with data of different sizes as shown in Fig. 14.

```

Sage: numbers = [2 ^ j for j in range (8,20)]
Sage: time = []
Sage: for number in numbers:
...Tcpu0 = cputime ()
...11 = factorial (number)
...Times.append (cputime () -tcpu0))
  
```

Fig. 14. Sage code to save lists of the CPU times used to run the factorial function with data of different sizes

B. Reporting Measurements

With Matlab the measured run time and efficiency of Reporting processes in both BI tools mentioned previously is shown in the flow chart in Fig. 15.

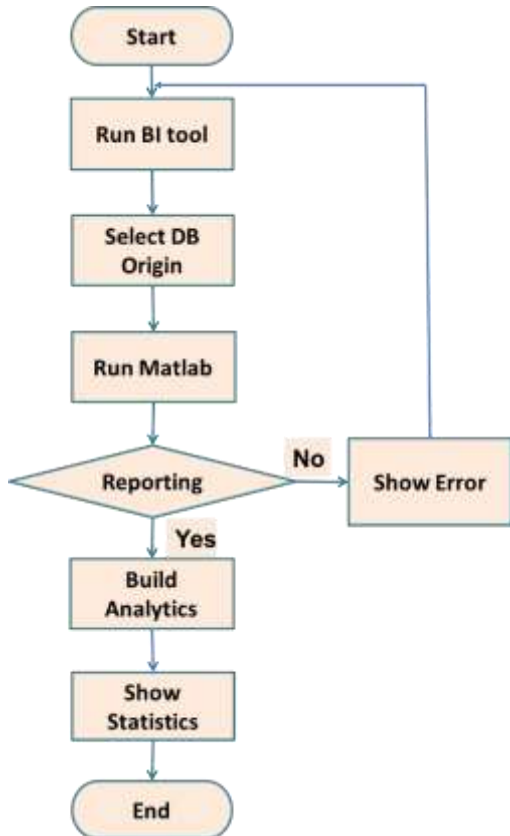


Fig. 15. The Reporting measurement process using the Matlab computer algebra system for all databases

For doing this activity, a C function was used that implemented a High-Resolution Performance Counter for measurement the Reporting processes on both BI tools as it is illustrated in Fig. 16.

```

/* returns "a - b" in seconds */
double performancecounter_diff(LARGE_INTEGER *a, LARGE_INTEGER *b)
{
    LARGE_INTEGER freq;
    QueryPerformanceFrequency(&freq);
    return (double)(a->QuadPart - b->QuadPart) / (double)freq.QuadPart;
}

int main(int argc, char *argv[])
{
    LARGE_INTEGER t_ini, t_fin;
    double secs;

    QueryPerformanceCounter(&t_ini);
    /* ...Reporting... */
    QueryPerformanceCounter(&t_fin);

    secs = performancecounter_diff(&t_fin, &t_ini);
    printf("%.16g milliseconds\n", secs * 1000.0);
    return 0;
}
  
```

Fig. 16. Code to measure the reporting process

In this case, Query Performance Counter acts as a clock () and Query Performance Frequency as CLOCKS_PER_SEC. That is the first function that gives the counter value and the second frequency (in cycles per second, hertz). It is clear that an LARGE_INTEGER is a way to represent a 64-bit integer by a union.

C. Databases Analysis

Six different Excel databases with different sizes have been used to perform the analysis. Those databases were acquired from UCI Machine Learning Repository [26] and their main features are described in Table 1:

TABLE I. DESCRIPTION OF THE SIX EXCEL DATABASES INCLUDING THEIR NUMBER OF ATTRIBUTES, INSTANCES AND SIZES

Database	Number of Attributes	Number of Instances	Size
DB 1	21	65.055	0.009 Mb
DB 2	26	118.439	0.017 Mb
DB 3	35	609.287	0.134 Mb
DB 4	40	999.231	1.321 Mb
DB 5	51	1.458.723	35.278 Mb
DB 6	62	2.686.655	144.195

D. Computer system

In order to perform the experiment and examination, the Business Intelligence Tools, Computer Algebra Systems and Databases are set on and customised in a PC with the following features: i) Operating system: x64-based PC, ii) Operating system version: 10.0.10240 N/D iii) Compilation 10240, iv) Number of processors: 1, v) Processor: Intel (R) Core (TM) i5-3317U vi) Processor speed: 1.7 GHz, vii) Instructions: CISC, viii) RAM: 12 Gb, ix) RAM speed: 1600 MHz, x) Cache: SSD express 24 Gb, xi) Math coprocessor: 80387, xii) GPU: HD 400 on board.

V. RESULTS

In this study, results for *CPUTime* as a function of the "size" was obtained from the data input for the ETL and Reporting processes from both Pentaho and Jaspersoft Business Intelligence Open Sources, applying two different Computer Algebra Systems.

The measurements of the computational times might fluctuate considerably based on many factors such as the used algorithm, operating system, processor speed, number of processors and instruction set that understand the amount of RAM, and cache, of each speed, along with math coprocessor, GPU among others. Even on the same machine, the same algorithm sometimes takes much longer to give the result of others, due to factors that it is more time-consuming than other applications that are running or if it has enough RAM when running the program.

Tables 2 and 3 shows the results of the CPU time (in minutes) of the ETL and Reporting processes and they present the times it took per tool in processing the different sized databases. Additionally, the increment of processing data can be considered as a difference between those BI tools in process. As a result of the first examination (Table 2), it is clear that the computational times for Pentaho ETL process measured by Sage were: 8 min; 12.01 min; 21 min; 32.01 min; 39.06 min and 48.01 min. Conversely, the computational times for Jaspersoft, were 9.54 min; 19.32 min; 31.88 min; 44.73 min; 55 min and 67.69 min, processing 0.009 Mb from DB1; 0.017 Mb from DB2; 0.134 Mb from DB3; 1.321 Mb from DB4; 35.278 Mb from DB5 and 144.195 Mb from DB6, respectively for both tools.

The results of the CPU time of the ETL process is shown in Table 2 and it presents the times that it took per tool in different databases.

TABLE II. RESULTS OF THE CPU TIME OF THE ETL PROCESS WITH THE TIMES TOOK PER TOOL AND THE INCREMENT IN THE PROCESS DATA IN THE DIFFERENT DATABASES

Tool	Process	Time (Minutes)					
		DB1	DB2	DB3	DB4	DB5	DB6
Pentaho	ETL	8	12.01	21	32.01	39.06	48.01
Jaspersoft	ETL	9.54	19.32	31.88	44.73	55	67.69
Increment in the Process of Data							
Jaspersoft	ETL	19.2	60.85	51.79	39.75	40.77	40.99
		2%	%	%	%	%	%

On the other hand, as a result of the second examination (Table 3), we can detect and see that the result of the Pentaho Reporting process measured by Matlab was: 3.75 min; 5.35 min; 8.47 min; 12.03 min; 17.07 min and 22.60 min. Conversely, the reporting process for Jaspersoft were 3 min; 4.02 min; 6.05 min; 8.13 min; 11.16 min and 14.15 min, processing 0.009 Mb from DB1; 0.017 Mb from DB2; 0.134 Mb from DB3; 1.321 Mb from DB4; 35.278 Mb from DB5 and 144.195 Mb from DB6, respectively for both tools. The results of the CPU time of the Reporting process are shown in Table 3 and it presents the time it took per tool in different databases.

TABLE III. RESULTS OF THE CPU TIME OF THE REPORTING PROCESS WITH THE TIMES TOOK PER TOOL AND THE INCREMENT IN THE PROCESS DATA IN THE DIFFERENT DATABASES

Tool	Process	Time (Minutes)					
		DB1	DB2	DB3	DB4	DB5	DB6
Pentaho	Reporting	3.75	5.35	8.47	12.03	17.07	22.60
Jaspersoft	Reporting	3	4.02	6.05	8.13	11.16	14.15
Increment in the Process of Data							
Pentaho	Reporting	25%	32.99%	40%	48%	53%	59.75%
		%	%	%	%	%	%

The Graphical comparison results of the CPU times for the ETL and Reporting processes performed by the BI tools, accessing six different sized databases which is illustrated below. In Fig. 17, we observe that Jaspersoft has significantly increased the results of the CPU time of the ETL process represented by 19.22%, 60.85% 51.79%, 39.75%, 40.77 and 40.99% processing DB1, DB2, DB3, DB4, DB5 and DB6, respectively. This means that in the ETL process, Pentaho had a better performance than Jaspersoft.

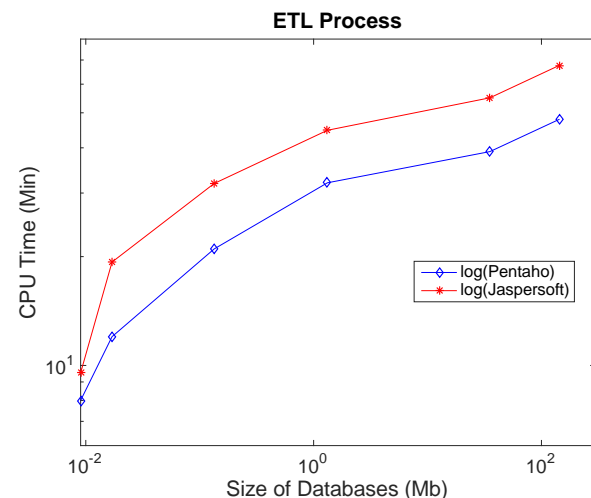


Fig. 17. CPU Time of the ETL process with the times it took per tool in processing data in the different databases

In Fig. 18, it is evident that Pentaho had a considerable rise in the outcomes of the Reporting process denoted by 25%, 32.99%, 40%, 48%, 53% and 59.75% processing DB1, DB2, DB3, DB4, DB5 and DB6, correspondingly. In this case, Jaspersoft had a better performance than Pentaho in the Reporting process.

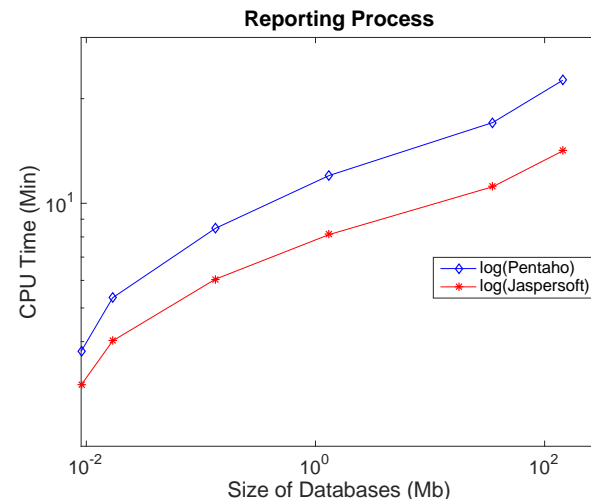


Fig. 18. CPU Time of the Reporting process with the times took per tool in the process data in different databases

The outcomes also showed that both results of CPU time of the ETL and Reporting process are directly related to the

sizes of the databases. What is more, is that the study could identify that Pentaho had a superior performance for ETL process and Jaspersoft an improved performance for Reporting process.

VI. DISCUSSION

The ETL experimental analysis results clearly shows that Jaspersoft BI had an increment of CPU time in the process of data over Pentaho BI, represented in an average of 42.28% of performance metrics over six databases. Pentaho provided its data integration and ETL capabilities as shown in [9], having a better performance. Evidently, for this part of the experimentation, our study has demonstrated that Pentaho had higher performance ETL capabilities with the aim of covering the whole data integration requirements, simultaneously by big data as well. That high performance is provided by its parallel processing engine and these features are shown in [11].

Pentaho BI had a marked increment of the CPU time in the process of data over Jaspersoft evidenced by the Reporting analysis outcomes with an average 43.12% over six databases. Clearly, in this part of the examination, the analysis has confirmed that Jaspersoft has had a higher performance Reporting capability with the objective of generating reports. This particular feature is aligned with other studies, which argue that Jaspersoft extends the range of its BI requirements including reporting based on its operational production, interactive end-user query, data integration and analysis as shown in [11]. On top of this, investigating various security features [27-29] could be an interesting avenue to explore in the future to protect BigData.

VII. CONCLUSION

This study has tested two of the best positioned open source Business Intelligence (BI) systems in the market: Pentaho and Jaspersoft. Both BI systems present notable features on their components. **Pentaho** on one side along with ETL component with great usability, maintainability and flexibility in making the transformations: Web Application with Java j2EE application 100% extensible, adaptable and configurable; the configuration management is integrated in most environments, that communicate with other applications via web services; it integrates all the information resources into a single operating platform; Reports with an intuitive tool that allows clients to create reports easily; OLAP Mondrian with a consolidated engine widely used in environments of JAVA; Dashboard Designer makes dashboards Ad-hoc, dashboards based on SQL queries or Metadata and a great freedom by offering a wide range of components and options. **Jaspersoft** on the other side has JasperETL (Talend) with Java / Perl native, Web Application with a Java j2EE application 100% extensible, adaptable and customizable; the management settings are very well resolved, it allows almost all through the same Web application; It integrates all information resources into a single operating platform; the editor Ad-hoc reports and Box Editor Ad-hoc command are best resolved; Reports are fast; Ad hoc and have a nice interface, with good flexibility and power, simple, intuitive and easy to use.

The experimental analysis has focussed on their ETL and Reporting processes by measuring their performance s using the two Computer Algebra Systems, Sage and Matlab. During the ETL analysis results, clearly showed that it could observe Jaspersoft BI and has an increment of CPU time in the process of data over Pentaho BI, represented in an average of 42.28% of performance metrics over six databases. Meanwhile, Pentaho BI had a marked increment CPU time in the process of data over Jaspersoft evidenced by the Reporting analysis outcomes with an average 43.12% over the databases. This study is a useful reference for many researchers and those who are supporting decisions of Big Data processing and the implementation of BI open source tool based on their process expectations. The future work of the author would involve new studies and implementations of BI with Data warehousing to create a technological tool to support the decision-making at the enterprise level by taking this paper as a base.

REFERENCES

- [1] B. List, R. M. Bruckner, K. Machaczek, J. Schiefer, "A Comparison of Data Warehouse Development Methodologies Case Study of the Process Warehouse," in Database and Expert Systems Applications - DEXA 2002, France, 2002.
- [2] H. Dresner, "Business intelligence: competing Against Time," in Twelfth Annual Office Information System Conference, London, 1993.
- [3] S. Atre, L. T. Moss, "Business Intelligence Roadmap: The Complete Project Lifecycle for Decision-Support Applications, Addison Wesley Professional", 2003.
- [4] J. F. Gonzalez, "Critical Success Factors of a Business Intelligence Project," Novática, no. 211, pp. 20-25, 2011.
- [5] R. L. Sallam, B. Hostmann, K. Schegel, J. Tapadinhas, J. Parenteau, T. W. Oestreich, "Magic Quadrant for Business Intelligence and Analytics Platforms", 23 February 2015. [Online]. Available: www.gartner.com/doc/2989518/magic-quadrant-business-intelligence-analytics. [Accessed 9 Aug 2016].
- [6] Gartner, Inc., "IT Glossary", 2016. [Online]. Available: <http://www.gartner.com/it-glossary/business-intelligence-bi/>. [Accessed 9 Aug 2016].
- [7] R. Kune, P. K. Konugurthi, A. Agarwal, R. R. Chillarige, R. Buyya, "The Anatomy of Big Data Computing", Software: Practice and Experience, pp. 79-105, 2016.
- [8] Pentaho A Hitachi Group Company, "Pentaho | Data Integration, Business Analytics and Bid Data Leaders", Pentaho Corporation, 2005-2016. [Online]. Available: www.pentaho.com. [Accessed 10 Aug 2016].
- [9] D. Tarnaveanu, "Pentaho Business Analytics: a Business Intelligence Open Source Alternative", Database System Journal, vol. III, nº 3/2012, p. 13, 2012.
- [10] T. Kapila, "Pentaho BI & Integration with a Custom Java Web Application", 2014. [Online]. Available: www.neevtech.com/blog/2014/08/13/pentaho-bi-integration-with-a-custom-java-web-application-2/. [Accessed 11 Aug 2016]
- [11] Innovent Solutions, "Pentaho Reports Review ", 2016. [Online]. Available: www.innoventsolutions.com/pentaho-review.html. [Accessed: 12 Aug 2016].
- [12] G. Pozzani, "OLAP Solutions using Pentaho Analysis Services", 2014. [Online]. Available: www.profs.sci.univr.it/~pozzani/attachments/pentaho_lect4.pdf. [Accessed: 12 Aug 2016].
- [13] Sanket, "Fusion Charts Integration in Pentaho BI Dashboards", 2015. [Online]. Available: www.fusioncharts.com/blog/2011/05/free-plugin-integrate-fusioncharts-in-pentaho-bi-dashboards/. [Accessed: 13 Aug 2016].
- [14] TIBCO Jaspersoft, "Jaspersoft Business Intelligence Software", TIBCO Software, 2016. [Online]. Available: www.jaspersoft.com. [Accessed 15 Aug 2016].

- [15] S. Vidhya, S. Sarumathi, N. Shanthi, "Comparative Analysis of Diverse Collection of Big data Analytics Tools", International journal of Computer, Electrical, Automation, Control and Information Engineering, vol. 8, n° 9, p. 7, 2014.
- [16] T. olavsrud, "Jaspersoft Aims to Simplify Embedding Analytics and Visualizations", 2014. [Online]. Available: www.cio.com/article/2375611/business-intelligence/jaspersoft-aims-to-simplify-embedding-analytics-and-visualizations.html. [Accessed: 16 Aug 2016]
- [17] S. Pochampalli, "Jaspersoft BI Suite Tutorials", 2014. [Online]. Available: www.jasper-bi-suite.blogspot.com.au/. [Accessed: 17 Aug 2016].
- [18] J. Vinay, "OLAP Cubes in Jasper Server", 2013. [Online]. Available: www.hadoopheadon.blogspot.com.au/2013/07/setting-up-olap-cubes-in-jasper.html. [Accessed: 19 Aug 2016].
- [19] Informatica Data Quality Unit, "Data Quality: Dashboards and Reporting", 2013. [Online]. Available: www.Markerplace.informatica.com/solution/data_quality_dashBoards_andreporting-961. [Accessed: 21 Aug 2016]
- [20] Sagemath, "Sagemath | Open-Source Mathematical Software System", Sage, 20 March 2016. [Online]. Available: www.sagemath.org. [Accessed 21 Aug 2016].
- [21] AIMS Team, "Sage", 2016. [Online]. Available: www.launchpad.net/~aims/+archive/ubuntu/sagemath. [Accessed: 21 Aug 2016.]
- [22] W. Stein, "The Origins of SageMath", 2016. [Online]. Available: www.wstein.org/talks/2016-06-sage-bp/bp.pdf. [Accessed: 28 2016.]
- [23] MathWorks, "MATLAB - MathWorks - MathWorks Australia", MathWorks, 3 March 2016. [Online]. Available: www.au.mathworks.com. [Accessed 28 Aug 2016].
- [24] M. S. Gockenbach, "A Practical Introduction to Matlab", 1999. [Online]. Available: www.math.mtu.edu/~msgocken/intro/intro.html. [Accessed: 28 Aug 2016]
- [25] K. Black, "Matlab Tutorials", 2016. [Online]. Available: www.cyclismo.org/tutorial/matlab/. [Accessed: 29 Aug 2016].
- [26] M. Lichman, "UCI Machine Learning Repository", 2013. [Online]. Available: www.archive.ics.uci.edu/ml [Accessed 10 Aug 2016].
- [27] D. V. Pham, A. Syed, A. Mohammad and M. N. Halgamuge, "Threat Analysis of Portable Hack Tools from USB Storage Devices and Protection Solutions", International Conference on Information and Emerging Technologies, pp 1-5, Karachi, Pakistan, 14-16 June 2010.
- [28] D. V. Pham, A. Syed and M. N. Halgamuge, "Universal serial bus based software attacks and protection solutions, Digital Investigation 7, 3, pp 172-184, 2011.
- [29] D. V. Pham, M. N. Halgamuge, A. Syed and P. Mendis. "Optimizing windows security features to block malware and hack tools on USB storage devices", Progress in electromagnetics research symposium, 350-355, 2010.

Diagnosing Coronary Heart Disease using Ensemble Machine Learning

Kathleen H. Miao¹, Julia H. Miao¹, and George J. Miao²

¹Cornell University, Ithaca, NY 14850, USA

²Flezi, LLC, San Jose, CA 95134, USA

Abstract—Globally, heart disease is the leading cause of death for both men and women. One in every four people is afflicted with and dies of heart disease. Early and accurate diagnoses of heart disease thus are crucial in improving the chances of long-term survival for patients and saving millions of lives. In this research, an advanced ensemble machine learning technology, utilizing an adaptive Boosting algorithm, is developed for accurate coronary heart disease diagnosis and outcome predictions. The developed ensemble learning classification and prediction models were applied to 4 different data sets for coronary heart disease diagnosis, including patients diagnosed with heart disease from Cleveland Clinic Foundation (CCF), Hungarian Institute of Cardiology (HIC), Long Beach Medical Center (LBMC), and Switzerland University Hospital (SUH). The testing results showed that the developed ensemble learning classification and prediction models achieved model accuracies of 80.14% for CCF, 89.12% for HIC, 77.78% for LBMC, and 96.72% for SUH, exceeding the accuracies of previously published research. Therefore, coronary heart disease diagnoses derived from the developed ensemble learning classification and prediction models are reliable and clinically useful, and can aid patients globally, especially those from developing countries and areas where there are few heart disease diagnostic specialists.

Keywords—accuracy; adaptive Boosting algorithm; AUC; classifier; classification error; coronary heart disease; diagnosis; ensemble learning; F-score; K-S measure; machine learning; precision; prediction; recall; ROC; sensitivity; specificity

I. INTRODUCTION

Globally, heart disease is the leading cause of death for both men and women [1], with more than half of the deaths occurring in men. One in every four people is afflicted with and dies of heart disease, and in the United States, over 610,000 afflicted Americans lose their lives annually [2].

Heart disease encompasses several types of heart conditions. The most common type of heart condition is coronary heart disease [3], which can cause heart attacks that kill more than 370,000 people every year. In the United States, for every 43 seconds, one person suffers a heart attack, and for every minute one person dies of heart disease [2]. As a result, the total annual cost of coronary heart disease, including health care services, medications, and lost productivity, is about \$108.9 billion in the United States.

Coronary heart disease occurs when plaque builds up in a patient's arteries [4]. As plaque continues to accumulate, the patient's coronary arteries detrimentally narrow over time and

reduce blood flow to the heart, thus increasing the risk of heart attack or stroke.

High blood pressure, high cholesterol, and smoking are three key risk factors for heart disease. Several other medical conditions and lifestyle choices, including diabetes, obesity, poor diet, physical inactivity, and excessive alcohol use, can also place people at a higher risk for heart disease.

Currently, there are four main methods that are utilized to diagnose the severity of heart disease in patients. They include chest X-rays, coronary angiograms, electrocardiograms, also known as ECG or EKG, and exercise stress tests [3]. In terms of diagnosing heart disease and saving the lives of patients, time and diagnostic accuracy at early stages are very crucial. Early detection of coronary heart disease aids physicians in determining the most appropriate treatment and enhances the chances of survival for patients. In many developing countries and areas, however, specialists are not widely available to perform these diagnostic tests. Additionally, for many cases, inaccurate diagnoses and erroneously conducted medical procedures could lead to compromises in the patients' health. Thus, early and accurate diagnoses of heart disease have become immensely important in improving the chances of long-term survival for patients.

Diagnosing coronary heart disease is a challenging task, but computer-aided detection (CAD) have been developed to provide automated predictions for heart disease in patients. As one of the modern computer-aided detection methods, machine learning is an emerging technology for analyzing medical data and providing prognosis on early detection outcomes. One research report used CAD approaches to diagnose heart disease patients based on a method of integrating multiple different types of decision trees [5]. In other research reports, methods include support vector machine (SVM) learning [6]-[8], principal component analysis (PCA)-based evolution classifier [9], rotation forest (RF) classifier [10], artificial neural network (ANN) and fuzzy neural network (FNN) [11], and particle swarm optimization [12]. These methods were developed using the medical data of patients to classify and predict heart disease outcomes.

In this research, an alternative and enhanced machine learning approach is proposed for coronary heart disease prediction based on classification and prediction models utilizing an adaptive Boosting algorithm that combines a set of weak classifiers into a strong ensemble learning prediction model. The developed classification and prediction models

contain two components: an ensemble learning-based training model and a prediction model (also called a diagnosis model). The training model is based on the adaptive Boosting algorithm to form ensemble learning consisting of an optimally weighted majority vote on a number of individual classifiers. On the other hand, the diagnosis model is used to distinguish and classify the presence or absence of coronary heart disease for heart disease outcome predictions. The classification and prediction model for diagnosing coronary heart disease was evaluated using the model sensitivity (or recall), specificity, precision, *F*-score, probability of the model misclassification error and the model accuracy, receiver operating characteristic (ROC) curve, area under the ROC (AUC), and Kolmogorov-Smirnov (K-S) measure.

II. MATERIALS AND METHODS

In this section, the coronary heart disease data sets are introduced. The classification and prediction models for the coronary heart disease prediction based on the ensemble learning using the adaptive Boosting algorithm are presented. Lastly, the evaluation methods of the ensemble learning model are discussed in detail.

A. Heart Disease Dataset

The heart disease data sets, which were used in this research, were obtained from the Heart Disease Databases available in the UCI Machine Learning Repository [13]. These databases contain data information on heart disease clinical instances, contributed by the Cleveland Clinic Foundation (CCF), Hungarian Institute of Cardiology (HIC), Long Beach Medical Center (LBMC), and University Hospital in Switzerland (SUH), respectively.

There are 4 different heart disease databases contributed by 4 different medical institutions, including CCF, HIC, LBMC, and SUH. The databases contain 303 clinical instances, 294 clinical instances, 200 clinical instances, and 123 clinical instances in each data set, respectively. This results in a total combination of 920 clinical instances.

Each heart disease database has the same clinical instance format for each patient. Each clinical instance contains a total of 75 attributes and one target attribute. The target attribute refers to the status of the presence of heart disease in the patients. It is represented by an integer valued from "0" to "4," where "0" signifies absence and the values ("1," "2," "3," and "4") signify the presence and severity of heart disease. In this research, the target attribute is reclassified into a binary value of "0" or "1," indicating the diagnoses of absence or presence of coronary heart disease in the patients, respectively.

B. Adaptive Boosting Algorithm and its Classifiers

In this section, the diagnostic method for predicting and classifying the presence or absence of coronary heart disease is designed and developed based on ensemble learning classification and prediction models using an adaptive Boosting algorithm. The developed ensemble learning classification and prediction (or diagnostic) models, associated with their algorithms and methods, are presented in detail.

The adaptive Boosting algorithm, also known as "AdaBoost," is a machine learning meta-algorithm [14]. This

algorithm is adaptive because it runs multiple iterations to generate a strong composite ensemble learning method by using an optimally weighted majority vote of a number of weak classifiers. While the individual weak classifiers are only slightly correlated to the true classifier, the adaptive Boosting algorithm creates a strong ensemble learning classifier, which is well-correlated with the resulting true classifier by iteratively adding the weak classifiers.

Given M training data $\{(\mathbf{x}_1, y_1), \dots, (\mathbf{x}_M, y_M)\}$, \mathbf{x}_i is a vector corresponding to an input sample data, associated with P input attributes, and y_i is a target variable with a class label of either 1 or -1. In this research, the P input attributes are represented by the 75 input attributes in the heart disease data sets that can be utilized to build classification and prediction models.

The adaptive Boosting algorithm can be stated and described in the following [14]-[16]:

$$\text{Initialize weights } D_1[i] = \frac{1}{M} \text{ for } i = 1, \dots, M.$$

For each iteration, $t = 1, \dots, T$:

- Train a weak classifier using distribution D_t .
- Select a weak classifier with low weighted error:

$$\varepsilon_t = Pr_{D_t}[h_t[\mathbf{x}_i] \neq y_i]. \quad (1)$$

- Calculate a new component β_t based on its error:

$$\beta_t = \frac{1}{2} \ln \left(\frac{1-\varepsilon_t}{\varepsilon_t} \right). \quad (2)$$

- Update distribution $D_t[i]$ for $i = 1, \dots, M$:

$$D_{t+1}[i] = \frac{D_t[i] e^{(-\beta_t y_i h_t[\mathbf{x}_i])}}{Z_t}. \quad (3)$$

where Z_t is a normalization constant such that the weights $D_{t+1}[i]$ sum to one.

After all of the boosting iterations, a final ensemble learning classifier, which has a weighted error that is better than chance, is obtained by combining all weak classifiers with an optimal weight,

$$H[\mathbf{x}] = \text{sign}(\sum_{t=1}^T \beta_t h_t[\mathbf{x}]). \quad (4)$$

Eq. (4) is guaranteed to have a lower exponential loss over the training samples. This is equivalent to say that the final classifier $H[\mathbf{x}]$ is computed as a weighted majority vote of the weak classifiers $h_t[\mathbf{x}]$, where each classifier is assigned by weighting β_t .

During the training, the adaptive Boosting iterations also decrease the classification error of the ensemble learning classifier over the training samples. In addition, the classification error must quickly decrease exponentially if the weighted errors of the component classifiers, ε_t , are better than chance, that is, $\varepsilon_t < 0.5$. The ensemble learning-based classification error is bound by

$$\text{err}(H[\mathbf{x}]) \leq \prod_{t=1}^T 2\sqrt{\varepsilon_t(1-\varepsilon_t)}. \quad (5)$$

Furthermore, the weighted error of each new component classifier, ε_t , in Eq. (5) can be expressed:

$$\varepsilon_t = 0.5 - \frac{1}{2} (\sum_{i=1}^M D_t[i] y_i h_t[\mathbf{x}_i]). \quad (6)$$

Eq. (6) shows that the weighted error of each new component classifier tends to increase in association with a function of adaptive Boosting iterations.

During each training round, a new weak classifier is added to the ensemble learning process, and a weighting vector is adjusted to focus on training samples that were misclassified in previous rounds. As a result, the final model $H[\mathbf{x}]$ is a classifier that has a higher accuracy than those of the weak classifiers.

C. The Methods of Adaptive Boosting Model Evaluations

In order to evaluate the performances of the adaptive Boosting algorithm-based ensemble learning classification and prediction models, one of the best methods is to analyze the model's accuracy and misclassification error, sensitivity (also known as recall), specificity, precision, F -score, ROC, AUC, and K - S measure using the training and testing data sets. In this research, these analyses depend on the number of false positive and false negative instances of the heart disease data according to the references [17]-[21]. The diagnostic results, associated with the positive or negative results for distinguishing between presence and absence of coronary heart disease from the ensemble learning classification and prediction model, are shown in Table 1.

TABLE I. A MATRIX OF THE DEVELOPED ENSEMBLE LEARNING CLASSIFICATION AND PREDICTION MODELS' DIAGNOSTIC RESULTS FOR DISTINGUISHING BETWEEN PRESENCE AND ABSENCE OF CORONARY HEART DISEASE

	Actual Heart Disease	Actual No Heart Disease	Total Number
Predicted heart disease patients	True Positive (TP)	False Positive (FP)	TP + FP
Predicted no heart disease patients	False Negative (FN)	True Negative (TN)	FN + TN
Total Number	TP + FN	FP + TN	TP + FP + FN + TN

The sensitivity is defined as the probability of correctly identifying the presence of heart disease in patients given by [18],

$$Sensitivity = \frac{TP}{TP+FN}. \quad (7)$$

The sensitivity is also referred to as the *true positive rate* or *recall* in the field of machine learning.

The *specificity* is defined as the probability of correctly identifying the absence of heart disease in patients given by,

$$Specificity = \frac{TN}{FP+TN}. \quad (8)$$

The specificity is sometimes called the *true negative rate*. The difference of $(1 - specificity)$ is known as the *false positive rate*.

The precision or the positive predictive value is defined as

$$Precision = \frac{TP}{TP+FP}. \quad (9)$$

Thus, the probability of the misclassification error (PME) is obtained by

$$PME = \frac{FN+FP}{TP+FN+FP+TN}, \quad (10)$$

and the model's accuracy is defined by

$$Accuracy = \frac{TP+TN}{TP+FN+FP+TN}, \quad (11)$$

where the model's accuracy = $(1 - PME)$.

Notice that both the recall in Eq. (7) and precision in Eq. (9) are in a mutual relationship based on the understanding and measure of relevance. The recall is a measure of quantity, while the precision is a measure of quality. Thus, based on the harmonic mean of recall and precision, the relationship between the recall and precision definitions is given by a F -score, which is defined as

$$F_score = 2 \left(\frac{Precision \times Recall}{Precision + Recall} \right), \quad (12)$$

where a F -score of 1 would signify the best score in terms of accuracy of the classification and prediction model, and a F -score of 0 would be the worst score.

Thus, the F -score in Eq. (12) is used to measure the model performances and likewise can be used as a single measure of a model's accuracy during the testing. In addition, the F -score can also be interpreted as a weighted average of the recall and precision.

A ROC curve for classification and prediction models is a graph plot, which is obtained by using a set of trade-off points between the sensitivity and the difference of $(1 - specificity)$ for cases classified as presence of heart disease. The corresponding AUC under the ROC curve can be used to evaluate and rank the quality of the performance of classification and prediction models [18]. To estimate the AUC, a trapezoidal approximation formula is given by [18], [22],

$$\int_0^1 f(x)dx \cong \sum_{i=0}^N \left(\frac{y_i+y_{i+1}}{2} \right) (x_{i+1} - x_i), \quad (13)$$

where $f(x)$ denoted the function of the ROC curve analysis, y_i and x_i represented the sensitivity and $(1 - specificity)$ at the i th ($i = 0, 1, 2, \dots, M$) point, respectively. An AUC of 1 represents that the classification and prediction model is a perfect model in terms of diagnostic accuracy in distinguishing the presence of heart disease from absence of heart disease. On the other hand, an AUC of 0.5 indicates that the model is simply based on chance and is unmeaningful. Thus, the higher the AUC is, the better the classification and prediction model performs.

The AUC under the ROC curve is one of the most important parameters to evaluate and rank the quality of the performance of classification and prediction models under a condition of balance samples; that is, the number of presence and the number of absence of heart disease cases are approximately equal in the training and testing data sets. However, if unbalanced samples are represented in the data set, the F -score in Eq. (12) is the most important parameter for quality evaluation of the classification and prediction models. In that case, the AUC would not be an effective method of ranking the quality of the performance of the classification and prediction models.

In this research, the *K-S* measure [20], [21] will also be used to measure performance of the ensemble learning classification and prediction models. More accurately, in our research, the *K-S* measure is used to determine the degree of separation between the distributions of the presence and absence of heart disease in patients. The *K-S* measure can achieve a value of 100% if the scores of the model partition the population into two separate groups, in which one group contains all clinical instances classified with presence of coronary heart disease and the other consists of all clinical instances classified with absence of heart disease. In other words, the *K-S* measure results in 100% if output probabilities (or model scores) of the developed ensemble learning classification and prediction model allow the results of the presence and absence of heart disease in patients to be perfectly separated. In an unusual case, the *K-S* measure would be 0 if the developed ensemble learning classification and prediction model cannot differentiate between presence and absence of coronary heart disease. However, in most cases for classification models, the *K-S* measure will fall in a range between 0% and 100%. Thus, the higher the *K-S* measure value is, the better the developed ensemble learning classification and prediction model is at diagnosing the presence or absence of coronary heart disease in patients.

III. RESULTS

In this paper, an advanced ensemble machine learning technology, utilizing an adaptive Boosting algorithm, is proposed for accurate heart disease diagnosis and outcome predictions. The proposed adaptive Boosting model is an ensemble machine learning meta-algorithm, which combines a set of outputs from other learning algorithms into a weighted sum, thereby converging multiple mathematical models into a strong and enhanced classification and prediction model.

The proposed ensemble learning classification and prediction models were applied to 4 different data sets for coronary heart disease diagnosis. With data collected from four different medical institutions, these 4 data sets contain clinical instances of patients diagnosed with heart disease: 303 instances from the CCF, 294 instances from the HIC, 200 instances from the LBMC, and 123 instances from the SUH. Table 2 shows the details of the clinical instances in terms of the number of cases with the presence or absence of coronary heart disease in each of the 4 data sets, after the removal of clinical instances with missing values.

As can be seen in Table 2, there are large differences in terms of the percentage of the presence of coronary heart disease in patients, with the lowest at 36.18% and the highest at 93.44% in the data sets.

In each data set, each clinical instance consists of 76 raw attributes. Among all of the raw attributes, only 29 of them were used for developing the ensemble learning classification and prediction models due to a large number of missing values. Table 3 lists the detailed 29 raw attributes, which had been used for the model development in this research.

To evaluate the performances of the developed ensemble learning classification and prediction models based on the adaptive Boosting algorithm, the probabilities of the model

misclassification error and the model accuracy were estimated using a nonparametric approach based on a *holdout* method [23]. The holdout method is also known as the *H* method. The pattern data $\{X, \theta\}$ are partitioned into two mutually exclusive data sets $\{X, \theta\}_1$ and $\{X, \theta\}_2$. For the holdout method, the ensemble learning classification and prediction models were trained using the training data $\{X, \theta\}_1$, and then the ensemble learning classification and prediction models were tested using the testing data $\{X, \theta\}_2$.

TABLE II. THE CLINICAL INSTANCES IN TERMS OF THE PRESENCE AND ABSENCE OF HEART DISEASE IN EACH DATA SET

	Cases with Presence of Heart Disease	Cases with Absence of Heart Disease	Total Clinical Instance Cases	Percentage of the Presence of Heart Disease in Data Set
CCF	125	157	282	44.33%
HIC	106	187	293	36.18%
LBMC	113	32	145	77.93%
SUH	114	8	122	93.44%

TABLE III. THE 29 RAW ATTRIBUTE NAMES AND THEIR DESCRIPTIONS

Variable Name	Descriptions	Variable Name	Descriptions
Age	Age in years	Tpeakbps	Peak exercise blood pressure (first of 2 parts)
Sex	Sex (1 = male; 0 = female)	Tpeakbpd	Peak exercise blood pressure (second of 2 parts)
CP	Chest pain type (1 = typical angina; 2 = atypical angina; 3 = non-anginal pain; 4 = asymptomatic)	dummy	Integer, from 94 to 200
Htn	Binary, 0 and 1	tresrbpd	Resting blood pressure
Chol	Serum cholesterol in mg/dl	exang	Exercise induced angina (1 = yes; 0 = no)
Restecg	Resting electrocardiographic results (0 = normal; 1 = having ST-T wave abnormality where T wave inversions and/or ST elevation or depression of > 0.05 mV; 2 = showing probable or definite left ventricular hypertrophy by Estes' criteria)	xhypo	(1 = yes; 0 = no)
Ekgmo	Month of exercise ECG reading	oldpeak	ST depression induced by exercise relative to rest
Ekgday	Day of exercise ECG reading	cmo	Month of cardiac cath
Ekgyr	Year of exercise ECG reading	cday	Day of cardiac cath
Prop	Beta blocker used during exercise ECG (1 = yes; 0 = no)	cyr	Year of cardiac cath
Nitr	Nitrates used during exercise ECG (1 = yes; 0 = no)	Lvx3	Integer, from 0 to 8
Pro	Calcium channel blocker used during	Lvx4	Integer, from 0 to 8

	exercise ECG (1 = yes; 0 = no)		
Thaldur	Duration of exercise test in minutes	lvf	Integer, from 1 to 4
Thalach	Maximum heart rate achieved	num	Diagnosis of heart disease (angiographic disease status) 0 (< 50% diameter narrowing) 1 (> 50% diameter narrowing)
Thalrest	Resting heart rate		

Each data set was separated into equally sized training and testing data sets. The ensemble learning classification and prediction models were trained and tested by using the training and testing data sets, respectively. To train the classification and prediction models, the adaptive Boosting algorithm parameters were set to 100 iterations for the CCF, HIC, LBMC, and SUH.



Fig. 1. The model classification error plot at each iteration, where the red curve represents the training error and the green curve represents the testing error by using the CCF training and testing data sets, respectively

Fig. 1 displays the trained and tested classification error curves at each iteration using the CCF training and testing data sets. Fig. 2 also shows the trained and tested classification error curves at each iteration using the HIC training and testing data sets. For the LBMC, the trained and tested classification error curves at each iteration are shown in Fig. 3, using the LBMC training and testing data sets. Finally, the

trained and tested classification error curves using the SUH training and testing data sets are shown in Fig. 4.

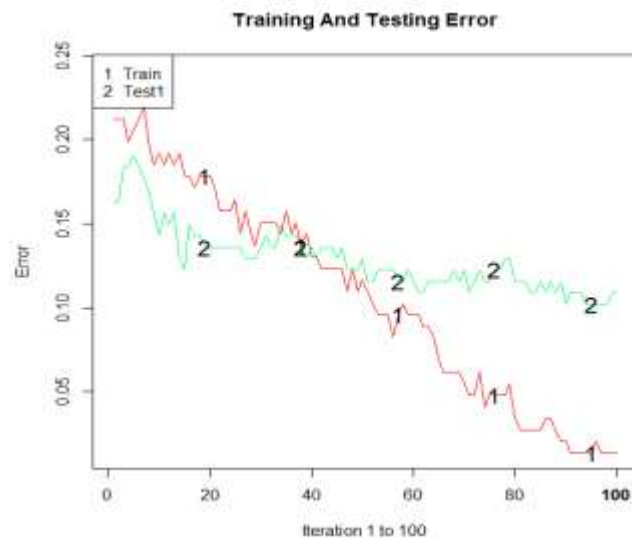


Fig. 2. The model classification error plot at each iteration, where the red curve represents the training error and the green curve represents the testing error by using the HIC training and testing data sets, respectively

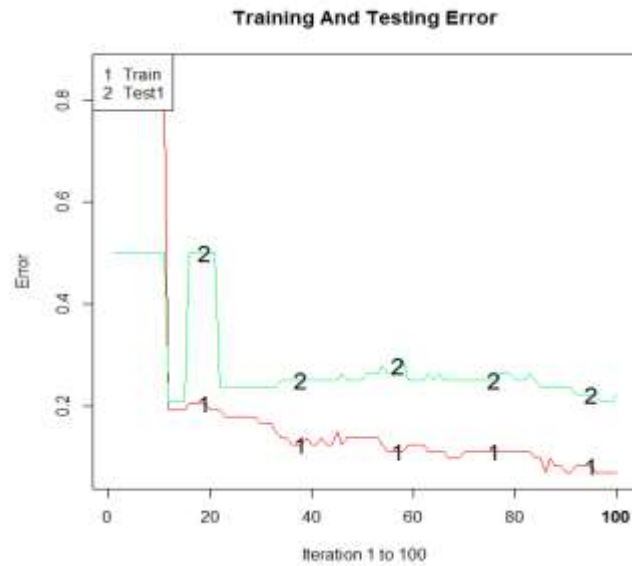


Fig. 3. The model classification error plot at each iteration, where the red curve represents the training error and the green curve represents the testing error by using the LBMC training and testing data sets, respectively

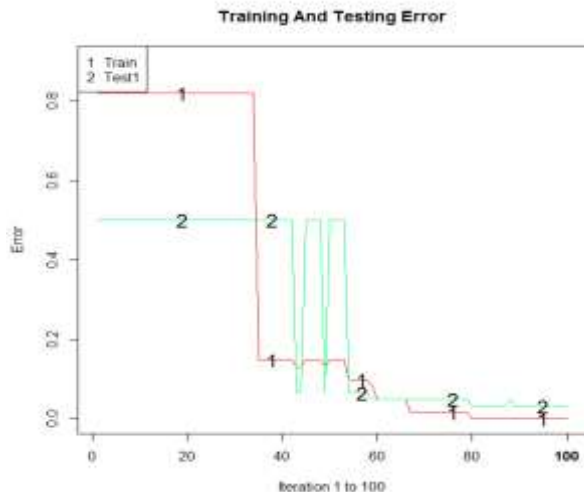


Fig. 4. The model classification error plot at each iteration, where the red curve represents the training error and the green curve represents the testing error by using the SUH training and testing data sets, respectively

TABLE IV. TRAINING RESULTS OF THE MODEL PERFORMANCES FOR THE CCF, HIC, LBMC, AND SUH USING THE TRAINING DATA SETS

	TP	FP	FN	TN	Total	Sensitivity (Recall)	Specificity	Precision	F-Score	Error	Accuracy
CCF	60	1	3	77	141	95.24%	98.72%	98.36%	0.97	2.84%	97.16%
HIC	54	0	2	90	146	96.43%	100%	100%	0.98	1.37%	98.63%
LBMC	57	5	0	11	73	100%	68.75%	91.94%	0.96	6.85%	93.15%
SUH	50	0	0	11	61	100%	100%	100%	1	0%	100%

TABLE V. TESTING RESULTS OF THE MODEL PERFORMANCES FOR THE CCF, HIC, LBMC, AND SUH USING THE TESTING DATA SETS

	TP	FP	FN	TN	Total	Sensitivity (Recall)	Specificity	Precision	F-Score	Error	Accuracy
CCF	44	10	18	69	141	70.97%	87.34%	81.48%	0.76	19.86%	80.14%
HIC	40	6	10	91	147	80.00%	93.81%	86.96%	0.83	10.88%	89.12%
LBMC	54	14	2	2	72	96.43%	12.50%	79.41%	0.87	22.22%	77.78%
SUH	56	2	0	3	61	100%	60.00%	96.55%	0.98	3.28%	96.72%

Table 4 displays the detailed training model performances of the developed ensemble learning classification and prediction models in predicting the presence and absence of coronary heart disease using the training data sets. The training results of the model accuracies of the developed ensemble learning classification and prediction models were the following: 97.16% for CCF, 98.63% for HIC, 93.15% for LBMC, and 100% for SUH. The corresponding *F*-score for the trained ensemble learning classification and prediction models were 0.97 for CCF, 0.98 for HIC, 0.96 for LBMC and 1 for SUH.

Table 5 shows the detailed testing model performances of the developed ensemble learning classification and prediction models in predicting the presence and absence of coronary heart disease using the testing data sets. As shown, the testing results of the model accuracies of the developed ensemble learning classification and prediction models were the following: 80.14% for CCF, 89.12% for HIC, 77.78% for LBMC, and 96.72% for SUH. The corresponding *F*-scores for the tested ensemble learning classification and prediction models were 0.76 for CCF, 0.83 for HIC, 0.87 for LBMC and 0.98 for SUH.

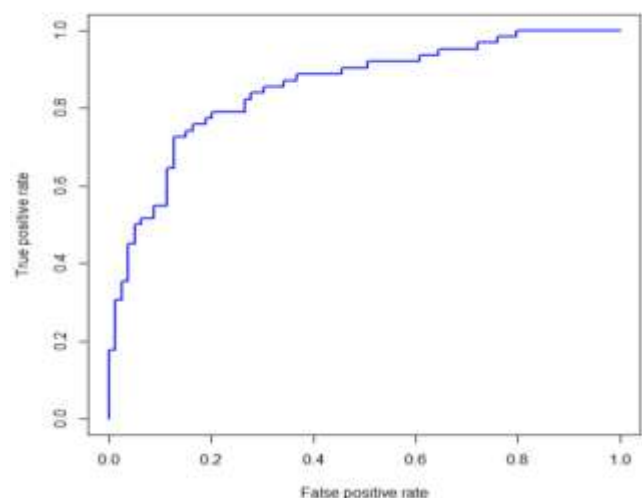


Fig. 5. An estimated AUC under the ROC curve of the developed ensemble learning classification and prediction model for cases classified as presence of heart disease and absence of heart disease in the CCF dataset, where the true positive rate is sensitivity on the y-axis and the false positive rate is the difference ($1 - \text{specificity}$) on the x-axis

The ROC curve results of the developed ensemble learning classification and prediction models were produced by varying a set of trade-off points between the model sensitivity on the y-axis and the difference value ($1 - \text{specificity}$) on the x-axis for CCF, HIC, LBMC, and SUH as shown in Figures 5, 6, 7, and 8, respectively. The corresponding estimated AUCs under the ROC curve for CCF, HIC, LBMC, and SUH were 0.8526, 0.9212, 0.6864, and 0.6357, respectively. The estimated AUCs of the ROC curves based on CCF and HIC implied that the proposed ensemble learning classification and prediction models can provide a consistently high accuracy in diagnosing and classifying presence of heart disease and absence of heart disease for predicting coronary heart disease outcome. Additionally, because the samples are approximately balanced in terms of the presence and absence heart disease cases in both of the CCF and HIC data sets, the AUCs under the ROC curves can be used to evaluate and rank the quality of the performances of the ensemble learning classification and prediction models.

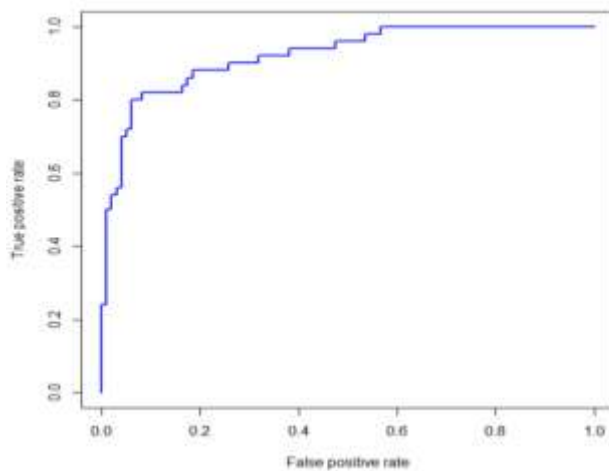


Fig. 6. An estimated AUC under the ROC curve of the developed ensemble learning classification and prediction model for cases classified as presence of heart disease and absence of heart disease in the HIC dataset, where the true positive rate is sensitivity on the y-axis and the false positive rate is the difference ($1 - \text{specificity}$) on the x-axis

The developed ensemble learning classification and prediction models also enabled the production of a set of model probabilities (also called the model scores), which were associated with the presence and absence of coronary heart disease in the cases crossing over the 4 datasets. By sorting the model scores, the $K-S$ charts were generated according to the cumulative counts of instances of the presence and absence of coronary heart disease cases.

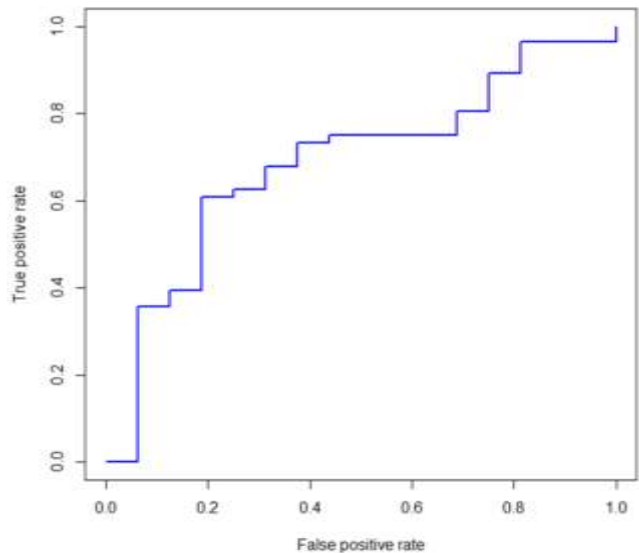


Fig. 7. An estimated AUC under the ROC curve of the developed ensemble learning classification and prediction model for cases classified as presence of heart disease and absence of heart disease in the LBMC dataset, where the true positive rate is sensitivity on the y-axis and the false positive rate is the difference ($1 - \text{specificity}$) on the x-axis

As a result, Fig. 9 shows a $K-S$ chart of the CCF with the highest $K-S$ value of 58.66% at the 4th decile population. Fig. 10 is a $K-S$ chart of the HIC with the highest $K-S$ value of 66.54% located at the 4th decile population. Fig. 11 is the $K-S$ chart of the LBMC with the highest $K-S$ value of 41.96% at the 5th decile population. For the SUH, the $K-S$ chart is shown in Fig. 12 with the highest $K-S$ value of 52.86% located at the 9th decile population. As shown in the charts from Fig. 9 to Fig. 12, the highest $K-S$ values are consistently associated with the tested model accuracies as listed in Table 5. Likewise, the higher the highest $K-S$ test value is, the better and more accurate the developed ensemble learning classification and prediction model is in distinguishing between the presence and absence of coronary heart disease in patients.

Therefore, when applied to patients with chest pain syndromes and intermediate disease prevalence, the diagnostic results of coronary heart disease diagnoses derived from the ensemble learning classification and prediction models are reliable and clinically useful. The results can be used to aid patients, especially those in developing countries and areas where there are few heart disease diagnostic specialists available.

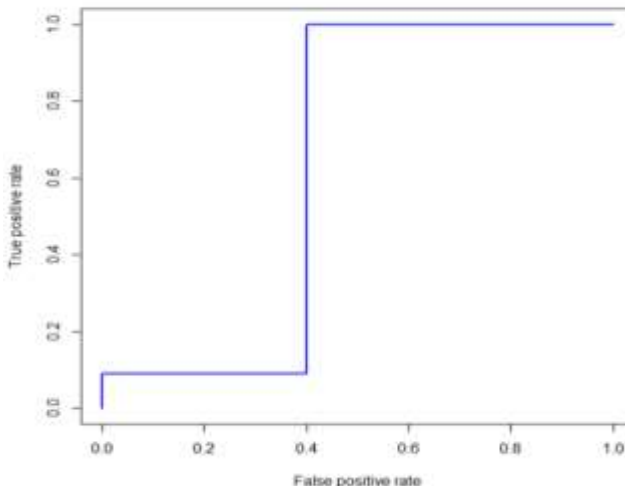


Fig. 8. An estimated AUC under the ROC curve of the developed ensemble learning classification and prediction model for cases classified as presence of heart disease and absence of heart disease in the SUH dataset, where the true positive rate is sensitivity on the y-axis and the false positive rate is the difference ($1 - \text{specificity}$) on the x-axis

IV. DISCUSSION

In this research, the ensemble learning classification and prediction models were designed and developed based on an adaptive Boosting algorithm. The developed classification and prediction models were utilized to diagnose and classify the presence and absence of coronary heart disease in diagnostic outcome predictions. The developed ensemble learning classification and prediction models were applied to 4 different coronary heart disease databases, where data sets were collected from 4 different medical institutions at the CCF, HIC, LBMC, and SUH. The performances of the developed ensemble learning classification and prediction models were tested and measured by using the training and testing data sets. Based on these testing results, the developed ensemble learning classification and prediction models were further evaluated by using the model accuracy and misclassification error, sensitivity (or recall), precision, specificity, *F*-score, ROC curve, AUC, and the *K-S* measure.

As shown in Table 5, the tested model accuracies of the developed ensemble learning classification and prediction models, utilizing the 28 input attributes, were the following: 80.14% for the CCF, 89.12% for the HIC, 77.78% for the LBMC, and 96.72% for the SUH using the testing data sets. Furthermore, the *F*-scores of the developed ensemble learning classification and prediction models were 0.76 for the CCF, 0.83 for the HIC, 0.87 for the LBMC, and 0.98 for the SUH. The corresponding AUCs under the ROC curves were 0.8526 for the CCF, 0.9212 for the HIC, 0.6864 for the LBMC, and 0.6357 for the SUH. In addition, the highest *K-S* values of the developed ensemble learning classification and prediction model were 58.66% for the CCF, 66.54% for the HIC, 41.96% for the LBMC, and 52.86% for the SUH. Thus, based on the testing results, the average diagnostic accuracy of the developed ensemble learning classification and prediction-

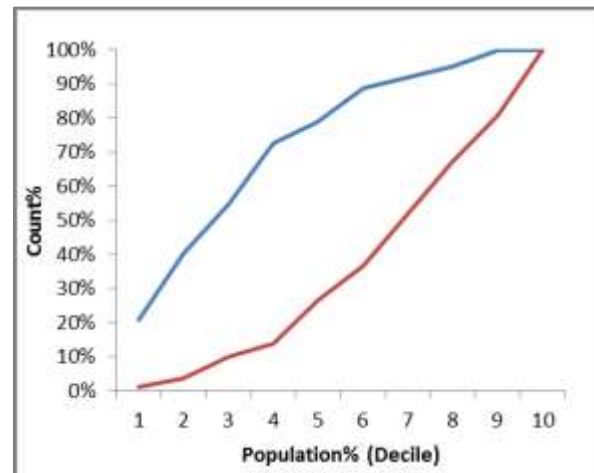


Fig. 9. The *K-S* chart for the CCF was generated by using the model output probabilities. The highest *K-S* value is 58.66%, located at the 4th decile population

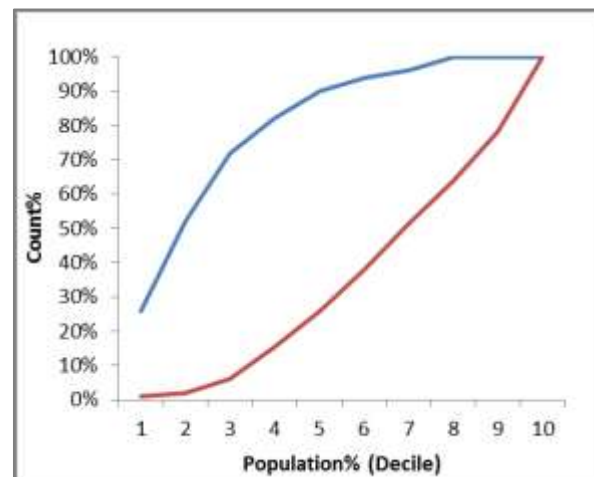


Fig. 10. The *K-S* chart for the HIC was generated by using the model output probabilities. The highest *K-S* value is 66.54%, located at the 4th decile population

-model would be 85.27% accurate in distinguishing between presence and absence of coronary heart disease in a new patient with clinical heart disease data, crossing over the 4 different locations in the CCF, HIC, LBMC, and SUH overall. Additionally, the average developed model sensitivity (or recall) was 86.61%; the average specificity was 83.76%; the average model precision was 85.84%; the average model *F*-score 0.86; and the average highest *K-S* value was 55.01%.

Thus, the developed ensemble learning classification and prediction models were able to achieve a consistently high accuracy in diagnosing the presence and absence of coronary heart disease for heart disease patient outcome predictions.

In comparison to related papers, there were several different methods developed using the same heart disease data sets. However, the methods associated with these developed models only considered 13 input attributes and in most cases were developed to classify and predict heart disease outcomes using only one of the 4 data sets.

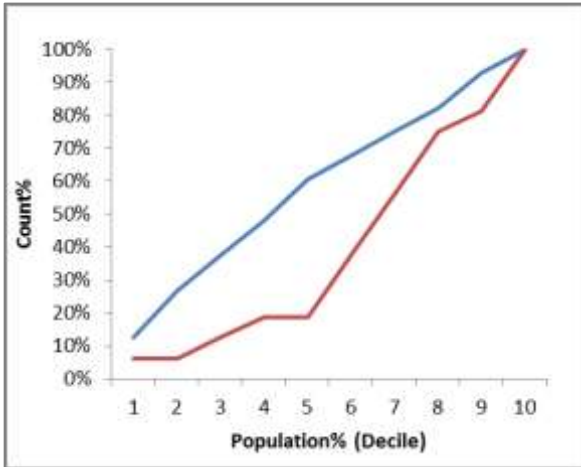


Fig. 11. The *K-S* chart for the LBMC was generated by using the model output probabilities. The highest *K-S* value is 41.96%, located at the 5th decile population

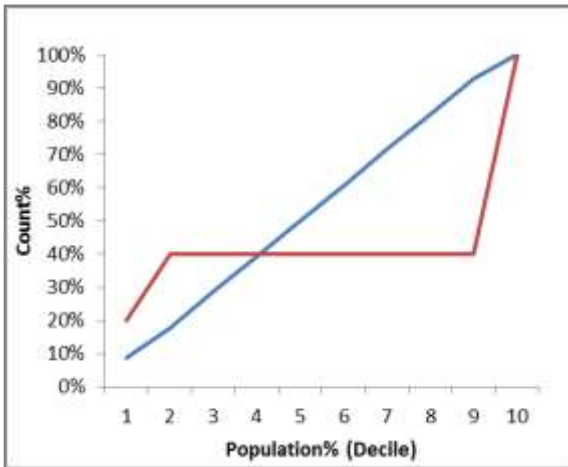


Fig. 12. The *K-S* chart for the SUH was generated by using the model output probabilities. The highest *K-S* value is 52.86%, located at the 9th decile population

In general, these previous methods showed different performances in terms of the model accuracies within a range of approximately 77% to 85%. The previous model accuracies of using a new probability algorithm [24] showed 77% for the HIC, 79% for the LBMC, and 81% for the SUH. The classification accuracy was 77% for the CCF based on the instance-based prediction model [25]. The conceptual clustering model [26] achieved 78.9% accuracy on the CCF data set. A decision tree (J4.8) was 78.9% accuracy and a Bagging algorithm [27] achieved 81.41% accuracy in diagnosing heart disease for the CCF data set. Recently, the data mining approaches [28], including Naïve Bayes, J48 decision tree, and Bagging algorithm, achieved the model accuracies of 82.31%, 84.35%, and 85.03% for the HIC data, respectively.

On the other hand, in this research, the developed ensemble learning classification and prediction models based on the 28 input attributes were not only applied to the CCF data set but also applied to the HIC, LBMC, and SUH data sets. The testing results, as shown in Table 5 and Figures from

5 to 12, also indicate that the model accuracy of the developed ensemble learning classification and prediction models is comparably higher than most of those of the previously published methods. In addition, the developed ensemble learning classification and prediction models had more flexibility due to its use of the adaptive Boosting algorithm, regardless of whether or not there were overlapping data (or clusters) between the presence and absence of heart disease cases. The developed ensemble learning classification and prediction models moreover provided a more reliable and greater percentage of accuracy in distinguishing between the presence and absence of coronary heart disease in the patient outcome predictions.

Therefore, the proposed ensemble learning classification and prediction models achieve significant potential in reducing the number of unnecessary, inaccurate diagnoses and erroneously conducted medical procedures that have compromised patients' health. The proposed ensemble learning classification and prediction models enable early and accurate heart disease diagnose and thus help improve chances of long-term survival for heart disease patients and save millions of lives.

V. CONCLUSION AND FUTURE WORK

In this paper, ensemble learning classification and prediction models have been developed to diagnose and classify the presence and absence of coronary heart disease in patient outcome predictions; additionally, the model accuracies, sensitivities (or recalls), precisions, specificities, *F*-scores, ROC curves, AUCs, and *K-S* measures have been evaluated. The developed classification and prediction models, based on the adaptive Boosting algorithm, were ensemble learning classifiers that had high flexibility in adjusting a weighting vector to generate a strong, single composite ensemble learning classification and prediction model by using an optimally weighted majority vote of a number of weak classifiers.

The developed ensemble learning classification and prediction models were trained and tested using the holdout method based on 4 different data sets from 4 different medical institutions. The testing results showed that the developed ensemble learning classification and prediction models had an average sensitivity (or recall) of 86.61% in diagnosing the presence of heart disease, an average specificity of 83.76% in diagnosing the absence of coronary heart disease, an average model precision of 85.84%, an average model *F*-score of 0.86, and an average model accuracy of 85.27% in diagnosing both the presence and absence of coronary heart disease. In each data set, the accuracies of the testing results of the ensemble machine learning models were the following: 80.14% for CCF, 89.12% for HIC, 77.78% for LBMC, and 96.72% for SUH. Therefore, the developed ensemble learning classification and prediction models using the 28 input attributes can provide highly accurate and consistent diagnoses for coronary heart disease patient outcome predictions, thereby allowing patients to bypass unnecessary, inaccurate diagnoses and erroneously conducted medical procedures.

From Fig. 1 to Fig. 4, the classification errors based on the testing data sets are higher than the classification errors based

on the training data sets at the 100th iterations, where data sets were collected from the 4 different medical institutions. This phenomenon involving the differences of the classification errors between the model training and testing processes is an expected encounter, known as an over-fitting problem in the field of machine learning during model development. Minimizing training error will often result in the over-fitting problem during each iteration in the adaptive Boosting algorithm since the Boosting algorithm is sensitive to noise and/or outlier samples. Thus, in future research, other enhanced methods that prevent and/or reduce the over-fitting problem associated with the adaptive Boosting algorithm during a training process would be investigated, thereby further enhancing the performances of the ensemble learning classification and prediction model and coronary heart disease diagnosis.

ACKNOWLEDGMENT

The authors would like to thank Dr. Andras Janosi from the Hungarian Institute of Cardiology, Budapest; Dr. William Steinbrunn from University Hospital, Zurich, Switzerland; Dr. Matthias Pfisterer from University Hospital, Basel, Switzerland; and Dr. Robert Detrano from V.A. Medical Center, Long Beach and the Cleveland Clinic Foundation, whose heart disease datasets of clinical instances were contributed to and made available from the Heart Disease Databases in the UCI Machine Learning Repository. These datasets contain the clinical instances and information regarding the diagnoses of the presence and absence of heart disease in clinical cases.

REFERENCES

- [1] Centers for Disease Control and Prevention (CDC), Deaths: leading causes for 2008, National Vital Statistics Reports, Vol. 60, No. 6, June 6, 2012.
- [2] Centers for Disease Control and Prevention (CDC), Heart disease in the United States, Available <http://www.cdc.gov/heartdisease/facts.htm>.
- [3] Centers for Disease Control and Prevention (CDC), Know the facts about heart disease, Available http://www.cdc.gov/heartdisease/docs/consumer_heartdisease.pdf
- [4] American Heart Association, What is a heart attack? Available http://www.heart.org/HEARTORG/Conditions/Conditions_UCM_001087_SubHomePage.jsp
- [5] M. Shouman, T. Turner, and R. Stocker, "Using decision tree for diagnosing heart disease patients," Proceedings of the 9th Australasian Data Mining Conference, Ballarat, Australia, pp. 23–29, 2011.
- [6] A. F. Otoom, E. E. Abdallah, Y. Kilani, A. Kefaye, and M. Ashour, "Effective diagnosis and monitoring of heart disease," International Journal of Software Engineering and Its Applications, Vol. 9, No. 1, pp. 143-156, 2015.
- [7] S. Ghumbre, C. Patil, and A. Ghatol, "Heart disease diagnosis using Support Vector Machine," International Conference on Computer Science and Information Technology, Pattaya, pp. 84-88, December 2011.
- [8] S. Bhatia, P. Prakash, and G. N. Pillai, "SVM based decision support system for heart disease classification with integer-coded genetic algorithm to select critical features," Proceedings of the World Congress on Engineering and Computer Science, San Francisco, California, October 22-24, 2008.
- [9] L. Pasi and L. Jouni, "A classification method based on principal component analysis and differential evolution algorithm applied for prediction diagnosis from clinical EMR heart data sets," Computational Intelligence in Optimization, Springer-Verlag, Vol. 7, pp. 263-283, 2010.
- [10] A. Ozciit and A. Gulcen, "Classifier ensemble construction with rotation forest to improve medical diagnosis performance of machine learning algorithms," Journal of Computer Methods and Programs in Biomedicine, Vol. 104, pp. 443-451, 2011.
- [11] H. Kahramanli and N. Allahverdi, "Design of a hybrid system for the diabetes and heart diseases," Journal of Expert Systems with Applications, Vol. 35, pp. 82-89, 2008.
- [12] P. Gayathri and N. Jaishankar, "Comprehensive study of heart disease diagnosis using data mining and soft computing techniques," International Journal of Engineering and Technology, Vol. 5, No. 3, pp. 2947-2957, July 2013.
- [13] UCI Machine Learning Repository, Heart disease data set, available <https://archive.ics.uci.edu/ml/datasets/Heart+Disease>.
- [14] R. E. Schapire and Y. Singer, "Improved boosting algorithms using confidence-rated predictions," Springer, Vol. 37, Issue 3, pp 297-336, December 1999.
- [15] Y. Freund and R. E. Schapire, "Experiments with a new Boosting algorithm," AT&T Research, Murray Hill, New Jersey, pp. 1-15, January 22, 1996, available <http://www.research.att.com/orgs/ssr/people/{yoav,schapire}/>
- [16] R. E. Schapire, "Explaining AdaBoost," in Empirical Inference, B. Scholkopf, Z. Luo and V. Vovk, Eds., Springer Berlin Heidelberg, Chapter 5, pp 37-52, October 2013.
- [17] G. J. Miao, K. H. Miao, and J. H. Miao, "Neural pattern recognition model for breast cancer diagnosis," Multidisciplinary Journals in Science and Technology, Journal of Selected Areas in Bioinformatics, August Edition, pp. 1-8, September 2012.
- [18] K. H. Miao and G. J. Miao, "Mammographic diagnosis for breast cancer biopsy predictions using neural network classification model and receiver operating characteristic (ROC) curve evaluation," Multidisciplinary Journals in Science and Technology, Journal of Selected Areas in Bioinformatics, September Edition, Vol. 3, Issue 9, pp. 1-10, October 2013.
- [19] J. H. Miao, K. H. Miao, and G. J. Miao, "Breast cancer biopsy predictions based on mammographic diagnosis using Support Vector Machine learning," Multidisciplinary Journals in Science and Technology, Journal of Selected Areas in Bioinformatics, Vol. 5, No. 4, pp. 1-9, 2015.
- [20] A. M. Law, "A tutorial on how to select simulation input probability distributions," in IEEE Proceedings of the 2013 Winter Simulation Conference, R. Pasupathy, S. H. Kim, A. Tolk, et al., Eds., pp. 306-320, 2013.
- [21] T. B. Arnold and J. W. Emerson, "Nonparametric goodness-of-fit tests for discrete null distributions," The R Journal, Vol. 3/2, pp. 34-39, December 2011.
- [22] R. L. Finney, F. D. Demana, B. K. Waits, and D. Kennedy, Calculus: A Complete Course, Second Edition, Addison Wesley Longman, Inc., 2000.
- [23] G. J. Miao and M. A. Clements, Digital Signal Processing and Statistical Classification, Artech House, Inc., 2002.
- [24] R. Detrano, A. Janosi, W. Steinbrunn, M. Pfisterer, and J. J. Schmid, et al., "International application of a new probability algorithm for the diagnosis of coronary artery disease," American Journal of Cardiology, Vol. 64, pp. 304-310, 1989.
- [25] D. W. Aha and D. Kibler, "Instance-based prediction of heart-disease presence with the Cleveland database," Technical Report, University of California, Irvine, Department of Information and Computer Science, Number ICS-TR-88-07, 1988.
- [26] J. H. Gennari, P. Langley, and D. Fisher, "Models of incremental concept formation," Artificial Intelligence, Vol. 40, Issues 1-3, pp. 11-6, September 1989.
- [27] M. C. Tu, D. Shin, and D. K. Shin, "Effective diagnosis of heart disease through Bagging approach," IEEE 2nd International Conference on Biomedical Engineering and Informatics, October 17-19, pp. 1-4, 2009.
- [28] V. Chaurasia and S. Pal, "Data mining approach to detect heart disease," International Journal of Advanced Computer Science and Information Technology, Vol. 2, No. 4, pp. 56-66, 2013.

Backstepping Control of Induction Motor Fed by Five-Level NPC Inverter

Ali BOUCHAIB^{1,2}, Abdellah MANSOURI¹, Rachid TALEB²

¹Electrical Engineering Department, ENP d'Oran, BP 1523 El-M'naouer, Oran, Algeria

Laboratoire d'Automatique et d'Analyse des Systèmes

²Electrical Engineering Department, Hassiba Benbouali University, Chlef, Algeria

Laboratoire Génie Electrique et Energies Renouvelables (LGEER)

Abstract—In this paper we will present a contribution to the backstepping control for induction motor (IM) based on the principle of Field Oriented Control (FOC). This law is established step by step while ensuring the stability of the machine in the closed loop, by a suitable choice of the function Lyapunov. In addition it is executed to assure the convergence the error's speed tracking at all initials conditions are possible. Both the speed and the rotor flux are supposed obtained by sensors. The control of the IM by five-level NPC inverter generally uses Pulse-width modulation techniques (PWM). Finally, we represent some of the simulation results by simulations in Matlab/Simulink environment.

Keywords—Backstepping control; Five-level NPC inverter; Field orientated control; Induction motor

I. INTRODUCTION

The control of electric actuators plays a key role in the field of motion control called Mechatronics. Because the simplicity of a control, the DC motor have been the traditional choice for the accurate control with the very high dynamic performance for a large range. The actuators are hard and costly to construct for rapid applications and high power; it is heavy, with an important inertia of the rotor and large dimensions.

Since a long time the AC motor was the choice for industrial applications for high-power and constant speed. These actuators have advantages that the DC motor for simple rotor it has to be no brushes construction contrary to their non-linear dynamics they have been considered unsuitable for high dynamic performance and hard to check.

The new discoveries in electronics powers as well as the apparition of new technologies of microprocessors lows the result of the advance's implementing non-linear checking exploiting ESPACE, DSP and AC machines have been replaced the DC machines in a large application's varieties, there are even plans in the future to replace the traditional choice of hydraulic and pneumatic actuators by the asynchronous motor. About applications include robotics, aviation, and space engines. Because of these factors, AC motors became interesting references problems to try new non-linear control. The challenge of the increasing number of applications and controlling problems has more the incentive

to deal the physical systems class. The importance of electric actuators in industry thousands of paper, and book number with investigations in this field have published through the last thirty years, much time is lost, and it will be a hard undertaking to start all these approaches' details but this is not the objective of the work. The lack of natural decoupling between the inductor and rotor makes the control of the induction motor more difficult, opposite to its structural simplicity, the study of the modeling will be done in the usual context of simplifying hypotheses [1, 2].

Amongst the various techniques of harmonic elimination used there is the technique of multilevel structures. The latter is able to generate numerous voltage levels at the output of the converter. However, the complexity of its structure constitutes an important disadvantage for the number of semiconductors increases with desired levels.[3-5].

The principle of backstepping technique is to establish in a constructive manner the control law of the nonlinear system, considering some state variables as Virtual control and its interim control laws making The application of this backstepping technique on the IM depends on choosing a Lyapunov function [6], ensuring the overall stability of the system. It presents the advantage of being robust to parametric variations of the machine and a good references pursuit. The association of backstepping technique with FOC control gives the induction machine control interesting qualities of robustness. [7, 8].

This work is organized as follows. First, we present the model of IM. After that, we talk about the three-phase five-level NPC inverter. Next give a backstepping application on this IM model, where we will choose both current i_{sd} , i_{sq} as virtual control, we propose to eliminate the conventional PI controller in the FOC of the machine and replace them with control laws by backstepping. Finally, we give some simulation results.

II. PROBLEM FORMULATION

The asynchronous motor can be described by five non-linear differential equations, with two electric coordinates (stator current) and two magnetic coordinates (rotor speed), the stator voltages are the two physical inputs of the system. In a rotating frame d and q -axes, the IM is described by:

$$\begin{bmatrix} \dot{\Omega} \\ \dot{\varphi}_{rd} \\ \dot{\varphi}_{rq} \\ \dot{i}_{sd} \\ \dot{i}_{sq} \end{bmatrix} = \begin{bmatrix} m(\varphi_{rd}i_{sq} - \varphi_{rq}i_{sd}) - c\Omega - \frac{1}{j}T_l \\ -a\varphi_{rd} + (\omega_s - p\Omega)\varphi_{rq} + aM_{sd} \\ -a\varphi_{rq} - (c\omega_s - p\Omega)\varphi_{rd} + aM_{sq} \\ ba\varphi_{rd} + bp\Omega\varphi_{rq} - i_{sd} + \omega_s i_{sq} + m_1 v_{sd} \\ ba\varphi_{rq} - bp\Omega\varphi_{rd} - i_{sq} - \omega_s i_{sd} + m_1 v_{sq} \end{bmatrix} \quad (1)$$

where i_{sd} , i_{sq} , v_{sd} , v_{sq} , φ_{rd} , φ_{rq} , Ω , T_l and ω_s respectively denote the fluxes rotor, the voltage inputs stator, the currents stator, the angular speed, the loading torque and the stator frequency. The s and r subscripts refer to both rotor and stator. The setting are:

$$\left\{ \begin{array}{l} a = R_r/L_r \\ b = M/\sigma L_s L_r \\ c = f_v/J \\ \gamma = (L_r R_s + M^2 R_r)/\sigma L_s L_r^2 \\ \sigma = 1 - (M^2 / L_s L_r) \\ m = pM / JL_r \\ m_1 = 1/\sigma L_s \end{array} \right.$$

we denote by R_s and R_r the resistances, L_s and L_r the self inductances, M the mutual inductance between the stator and rotor windings, P the number of pole-pair, J the inertia of the system (motor and load) and f_v the viscous damping coefficient.

The assumptions are respectively presented:

- 1) The currents stator are capable for measurement also they show the measurable system's outputs;
- 2) The load torque is unchanged, obscure and it is famous with its troubledness;
- 3) The resistance stator known as an overflowing parameter changing with temperature;
- 4) The remained parameters are given by offline identification with limited ambiguity and they are also fixed.

III. MULTILEVEL INVERTER MODELLING

The three-phase five-level NPC inverter, is demonstrated by Figure 1, it has three arms of IGBT or MOSFET with antiparallel diode and three arms of two diodes. Whereas Table 1 shows the five-level output voltage according the states of the switches.

TABLE I. THE SWITCHES STATE FOR THE 5-LEVEL OF OUTPUT VOLTAGE ($K = 1, 2, 3$)

B_{TDk1}	B_{TDk2}	B_{TDk3}	B_{TDk4}	B_{TDk5}	B_{TDk6}	V_{kM}
1	1	1	0	0	0	$2U_c$
1	1	0	0	0	1	U_c
1	0	0	1	0	1	0
0	0	1	1	1	0	$-U_c$
0	0	0	1	1	1	$-2U_c$

PMW strategy is the most discussed method of the

selected switching control methods (in the literature). This strategy is based on comparison between several triangular signals to a sinusoidal reference [9-12]. In the case of five-level converter the strategy consists of comparing four triangular carriers having the same frequency and amplitude to the sinusoidal reference. Thus, the reference waveform is placed in the middle of the carrier bands [13-15].

IV. ROBUST BACKSTEPPING AND FIELD ORIENTED CONTROL

In this section, it is proposed to eliminate conventional PI regulators in vector control of the IM and replace them by backstepping control laws.

The controller design is done in two steps. First step, the control problem is to choose i_{sdref} and i_{sqref} in such a way to force Ω and φ_{rd} to track their desired reference signals Ω_{ref} and φ_{ref} the second step is devoted to the current loops design: find the controls v_{sd} and v_{sq} such that the currents i_{sd} and i_{sq} converge fast to desired references i_{sdref} and i_{sqref} respectively. This design is detailed below.

Step 1: Start with the first equation of (2), we define e_1 , e_2 errors and representing respectively

$$\left\{ \begin{array}{l} e_1 = \Omega_{ref} - \Omega \\ e_2 = \varphi_{ref} - \varphi_d \end{array} \right. \quad (2)$$

The derivative of (2) is computed as

$$\left\{ \begin{array}{l} \dot{e}_1 = \dot{\Omega}_{ref} - m\varphi_d i_{sq} + c\Omega + \frac{T_l}{j} \\ \dot{e}_2 = \dot{\varphi}_{ref} - \dot{\varphi}_d = \dot{\varphi}_{ref} + a\varphi_d - aM_{sd} \end{array} \right. \quad (3)$$

The first Lyapunov v_1 candidates chosen as:

$$v_1 = \frac{1}{2}(e_1^2 + e_2^2) \quad (4)$$

So, the derivative of (4) is computed as:

$$\left\{ \begin{array}{l} \dot{v}_1 = e_1 \left(\dot{\Omega}_{ref} - m\varphi_d i_{sq} + c\Omega + \frac{T_l}{j} \right) \\ \quad + e_2 (\dot{\varphi}_{ref} + a\varphi_d - aM_{sd}) \end{array} \right. \quad (5)$$

The tracking objectives can be satisfied by choosing:

$$\left\{ \begin{array}{l} (i_{sq})_{ref} = \frac{1}{aM} \frac{1}{m} \left[k_1 e_1 + \dot{\Omega}_{ref} + c\Omega + \frac{T_l}{j} \right] \\ (i_{sd})_{ref} = \frac{1}{aM} \left[k_2 e_2 + \varphi_{ref} + a\varphi_d \right] \end{array} \right. \quad (6)$$

where k_1 and k_2 positive design constants that determine the closed loop dynamics.

The derivative of the function Lyapunov becomes:

$$\dot{v}_1 = k_1 e_1^2 - k_2 e_2^2 < 0 \quad (7)$$

so i_{sqref} and i_{sdref} are asymptotically stable.

Step 2: Define other errors signals about currents:

$$\left\{ \begin{array}{l} e_3 = i_{sqref} - i_{sq} \\ e_4 = i_{sdref} - i_{sd} \end{array} \right. \quad (8)$$

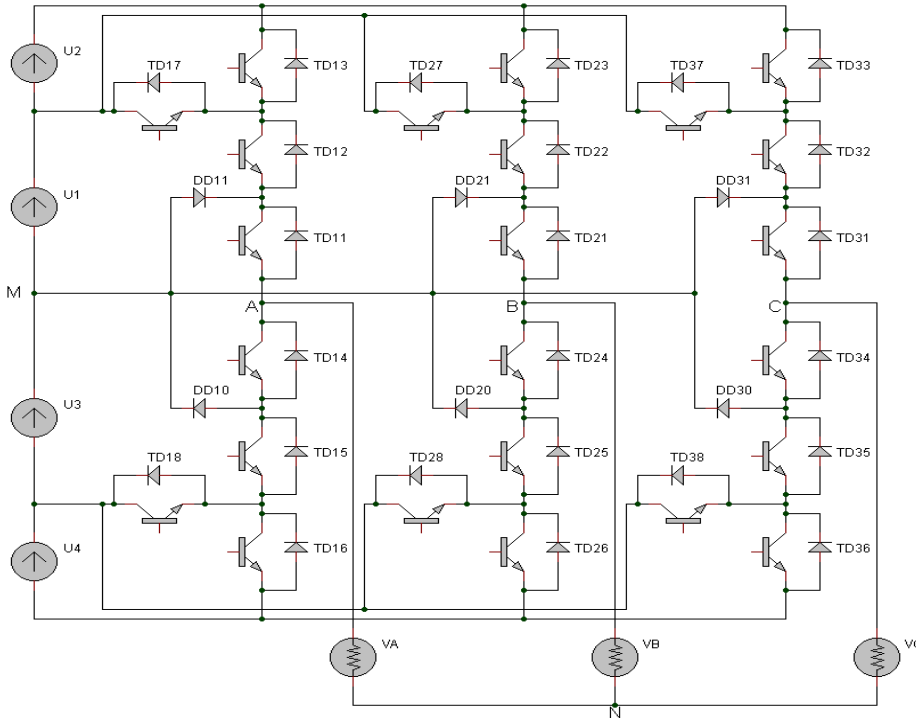


Fig. 1. The three-phase five-level NPC inverter

we find:

$$\begin{cases} e_3 = \frac{1}{m} [k_1 e_1 + \dot{\Omega}_{ref} + c\Omega + \frac{T_l}{j}] - i_{sq} \\ e_4 = \frac{1}{aM} [k_2 e_2 + \dot{\varphi}_{ref} + a\varphi_d] - i_{sd} \end{cases} \quad (9)$$

With this definition, taking into account the system (3) the dynamics e_1 and e_2 are written:

$$\begin{cases} \dot{e}_1 = -k_1 e_1 + m\varphi_d e_3 \\ \dot{e}_2 = k_2 e_2 + aM e_4 \end{cases} \quad (10)$$

From (9), the errors dynamics are given by:

$$\begin{cases} \dot{e}_1 = (\dot{i}_{sq})_{ref} - A - m_1 v_{sq} \\ = \frac{1}{aM} [k\dot{e}_2 + \dot{\varphi}_{ref} + a\dot{\varphi}_d] - i_{sd} \\ \dot{e}_4 = (\dot{i}_{sd})_{ref} - B - m_1 v_{sd} \end{cases} \quad (11)$$

where

$$\begin{cases} A = -\gamma i_{sq} - bP\Omega\varphi_d - Pi_{sd} - aM \frac{i_{sq}i_{sd}}{\varphi_d} \\ B = \gamma i_{sq} - ab\Omega\varphi_d - P\Omega i_{sq} - aM \frac{i_{sq}^2}{\varphi_d} \end{cases} \quad (12)$$

Lyapunov function candidate is chosen following:

$$v_2 = \frac{1}{2} (e_1^2 + e_2^2 + e_3^2 + e_4^2) \quad (13)$$

Its derivative is:

$$\dot{v}_2 = e_1 \dot{e}_1 + e_2 \dot{e}_2 + e_3 \dot{e}_3 + e_4 \dot{e}_4 \quad (14)$$

This equation can be rewritten in the following from

$$\begin{cases} \dot{v}_2 = K_1 e_1^2 - K_2 e_2^2 - K_4 e_4^2 + e_3 (K_3 e_3 + (i_{sd})_{ref}) \\ - A - m_1 v_{sq} + e_4 (K_4 e_4 + (i_{sd})_{ref} - B - m_1 v_{sd}) \end{cases} \quad (15)$$

The choice $k_3 > 0$ and $k_4 > 0$ can be made such that $\dot{v}_2 < 0$. We choose the d -axis and q -axis voltage control input as:

$$\begin{cases} v_{sd} = \frac{1}{m_1} (K_4 e_4) + (i_{sd})_{ref} - B \\ v_{sq} = \frac{1}{m_1} (K_3 e_3) + (i_{sq})_{ref} - A \end{cases} \quad (16)$$

So, (11) can be expressed as:

$$\begin{cases} \dot{e}_3 = -K_3 e_3 - m e_1 \\ \dot{e}_4 = -aM e_2 - K_2 e_4 \end{cases} \quad (17)$$

To show boundedness of all states, we can rearrange the dynamical equations from (10) and (17)

$$\dot{e} = Ae \quad (18)$$

we can prove the boundedness of all the states, where A can be shown to be Hurwitz.

V. SIMULATION RESULTS

In this section we represent a simulation of the model of induction motor fed by a three-phase five-level voltage NPC inverter and controlled by the performing backstepping regulator, using MATLAB/SIMULINK. In order to evaluate the performance of the proposed controller, the testing was led at a high reference change. The dynamic response of IM is shown with Figures 2 to 6, and Table. 2 illustrates the considered simulation parameters for the control system.

Those results, shows; the stator voltage, the rotor speed

and the rotor flux components in which present the performance of the backstepping control in the nominal case. It is observed that the rotor speed converges to the reference one without instabilities effects. As result the decoupling between the flux and the torque is better.

TABLE II. SIMULATION PARAMETERS

	Parameters	Numerical values
Voltage DC bus	V_{DC}	500V
	R_s	4.85
	R_r	3.805
	L_s	0.274
	L_r	0.274
	M	0.258
	P	2
	J	0.031
	f_v	0.001136

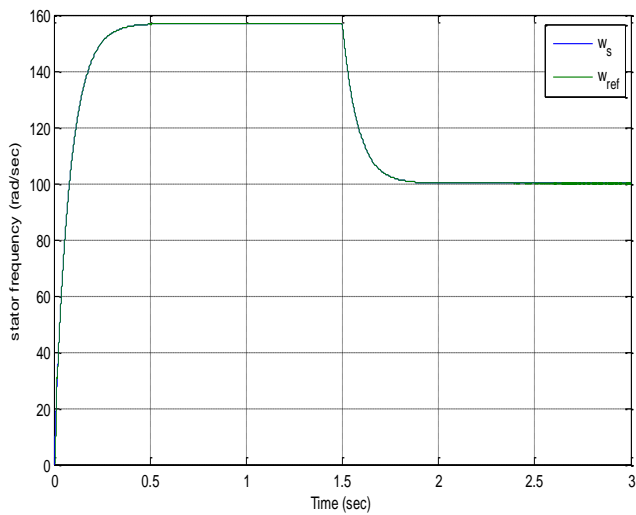


Fig. 2. Speed rotor

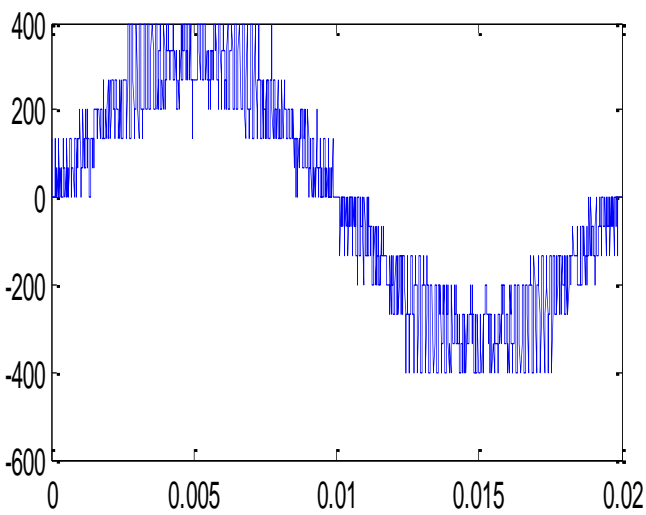


Fig. 3. Stator voltage inputs

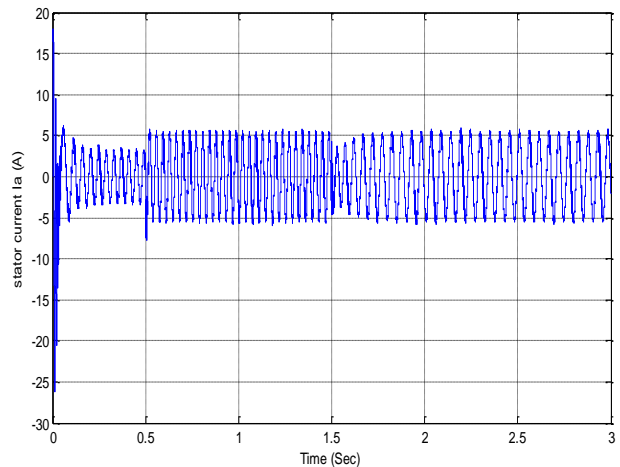


Fig. 4. Stator current

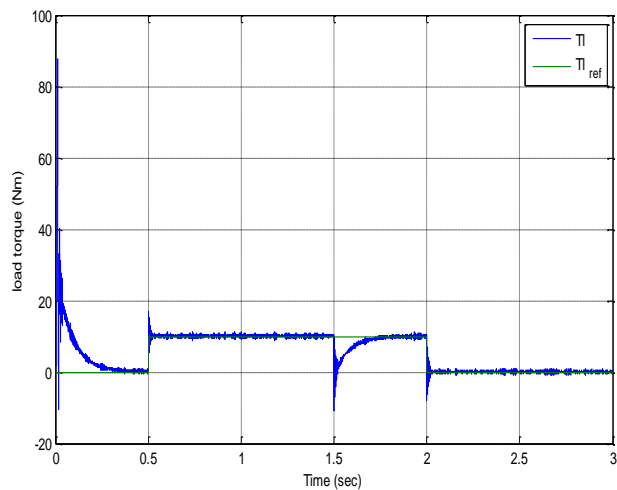


Fig. 5. Load torque

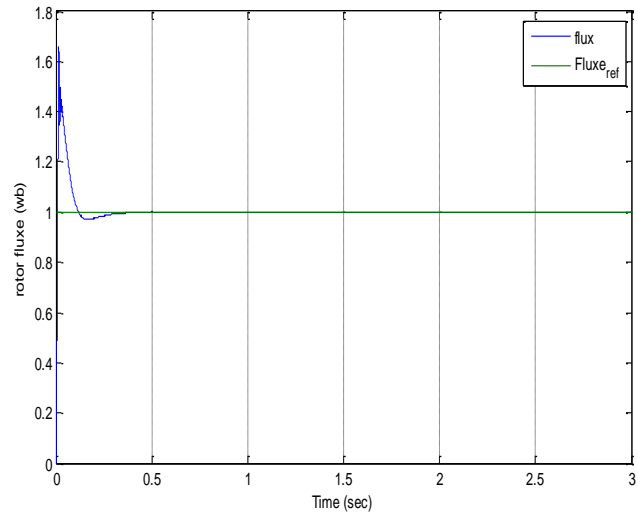


Fig. 6. Rotor flux

VI. CONCLUSIONS

In this paper, a nonlinear feedback controller based on a backstepping method for IM Fed by five-level NPC Inverter has been developed. To achieve global asymptotic stability of the proposed controller, Lyapunov theory is applied. Some simulation results were carried out to illustrate the effectiveness of the proposed control system. It is pointed out that the robustness of the controlled IM drive against speed and load torque variations is guaranteed. Furthermore, the proposed control scheme decreases considerably the torque ripples and assures good speed tracking without overshoot.

REFERENCES

- [1] C. Heising, V. Staudt and A. Steimel, "Speed-sensorless stator-flux-oriented control of induction motor drives in traction", 2010 First Symposium on Sensorless Control for Electrical Drives, Padova, pp. 100-106, 2010.
- [2] S. Chaouch, M.S. Nait Said, "A high performance direct stator flux orientation control (DSFO) for speed sensorless induction motor drive" Second International Conference on Electrical Systems (ICES'06), Oum-Elbouaghi, pp 294-299, 8-10 May 2006.
- [3] H. Chang, R. Wei, Q. Ge, X. Wang and H. Zhu, "Comparison of SVPWM for five level NPC H-bridge inverter and traditional five level NPC inverter based on line-voltage coordinate system", 18th International Conference on Electrical Machines and Systems (ICEMS), pp. 574-577, Pattaya, 2015.
- [4] A. Rufer, N. Koch and N. Cherix, "Control of the Actively Balanced Capacitive Voltage Divider for a Five-Level NPC Inverter - Estimation of the Intermediary Levels Currents", PCIM Europe 2016; International Exhibition and Conference for Power Electronics, Intelligent Motion, Renewable Energy and Energy Management, Nuremberg, pp. 1-7, Germany, 2016.
- [5] H. Dallagi, "Modelling, simulation and analysis of three phase five level NPC inverter for induction motor drive", 16th International Conference on Sciences and Techniques of Automatic Control and Computer Engineering (STA), pp. 562-569, Monastir, 2015.
- [6] I. Benaloui, S. Dridi, L. Chrifi-Alaoui and D. Benoudjite, "Sensorless speed backstepping control of induction motor based on sliding mode observer: Experimental results", 15th International Conference on Sciences and Techniques of Automatic Control and Computer Engineering (STA), pp. 923-928, Hammamet, 2014.
- [7] J. Soltani and R. Yazdanpanah, "Robust Backstepping Control of Induction Motor Drives Using Artificial Neural Networks", Power Electronics and Motion Control Conference (IPEMC'06), pp. 1-5, Shanghai, 2006.
- [8] F. J. Lin, C. K. Chang and P. K. Huang, "FPGA-Based Adaptive Backstepping Sliding-Mode Control for Linear Induction Motor Drive", IEEE Transactions on Power Electronics, vol. 22, no. 4, pp. 1222-1231, July 2007.
- [9] K. Thakre and K. B. Mohanty, "Performance improvement of multilevel inverter through trapezoidal triangular carrier based PWM", International Conference on Energy, Power and Environment: Towards Sustainable Growth (ICEPE), pp. 1-6, Shillong, India, 2015.
- [10] Calais, M., Borle, L. J., & Agelidis, V. G. "Analysis of multicarrier PWM methods for a single-phase five level inverter", In Power Electronics Specialists Conference, 2001. PESC. 2001 IEEE 32nd Annual, vol. 3, pp. 1351-1356, 2001.
- [11] RAHIM, Nasrudin A. and SELVARAJ, Jeyraj. "Multistring five-level inverter with novel PWM control scheme for PV application", IEEE transactions on industrial electronics, vol. 57, no 6, p. 2111-2123, 2010.
- [12] TEKWANI, P. N., KANCHAN, R. S., and GOPAKUMAR, K. "A dual five-level inverter-fed induction motor drive with common-mode voltage elimination and dc-link capacitor voltage balancing using only the switching-state redundancy-Part I", IEEE Transactions on Industrial Electronics, vol. 54, no 5, pp. 2600-2608, 2007.
- [13] J.L. Galvan, "Multilevel Converters: Topologies, Modelling, Space Vector Modulation Techniques and Optimizations", Ph.D. thesis, University of Seville, 2006.
- [14] MCGRATH, Brendan Peter and HOLMES, Donald Grahame, "Multicarrier PWM strategies for multilevel inverters", IEEE transactions on industrial electronics, vol. 49, no 4, p. 858-867, 2002.
- [15] BAI, Zhihong, ZHANG, Zhongchao, and ZHANG, Yao, "A generalized three-phase multilevel current source inverter with carrier phase-shifted SPWM", In IEEE Power Electronics Specialists Conference. IEEE, 2007. p. 2055-2060, 2007.

On Standards for Application Level Interfaces in SDN

Yousef Ibrahim Daradkeh¹

College of Engineering at Wadi Aldawaser
Prince Sattam bin Abdulaziz University
18611, Kingdom of Saudi Arabia

Mujahed ALdhaifallah²

College of Engineering at Wadi Aldawaser
Prince Sattam bin Abdulaziz University
18611, Kingdom of Saudi Arabia

Dmitry Namiot³

Faculty of Computational Mathematics and Cybernetics
Lomonosov Moscow State University
Moscow, Russia

Manfred Sneps-Sneppe⁴

Ventspils International Radioastronomy Centre
Ventspils University College
Ventspils, Latvia

Abstract—In this paper, authors discuss application level interfaces for Software Defined Networks. While the Application Programming Interfaces for the interaction with the hardware are widely described in Software Defined Networks, the software interfaces for applications received far less attention. However, it is obvious that interfaces to software applications are very important. Actually, application level interfaces should be one of the main elements in Software Defined Networks. It is a core feature. In this article, we want to discuss the issues of standardization of software interfaces for applications in Software Defined Networks area. Nowadays, there are several examples of unified Application Program Interfaces in the telecommunications area. Is it possible to reuse this experience for Software Defined Networks or Software Defined Networks standards are radically different? This is the main question discussed in this paper.

Keywords—SDN; REST API; Northbound interface; application

I. INTRODUCTION

Software-Defined Networking (SDN) is a paradigm that separates network's control logic from the underlying hardware (e.g., routers, switches etc.). SDN paradigm promotes the centralization of network control and ability to program the network. It let introduce new abstractions, simplify the network management, and simplify the application programming. Most authors highlight two basic moments for this paradigm:

the abstraction of the network logic from hardware implementation – network logic is a software;

the separation of a control panel and network forwarding

SDN assumes the presence of network controller that coordinates the above-mentioned tasks.

So, SDN concept, by the definition, is based on the various programming interfaces. Actually, SDN controller is a bunch of programming interfaces by itself. In Figure 1, we present the classical model for SDN.

In this paper, we will discuss so-called northbound API.

This open entity enables the network application ecosystem. Actually, this ecosystem is the main promise of SDN. It is what SDN networks are for. The idea is to create an intermediate level independent from equipment vendors. In this case, Network Operators can quickly modify or customize their network control through the application API.

Basically, anyone who wants to develop network applications is the potential user for Northbound API. Of course, the question is to propose a common API on this level. Otherwise, developers will face many different proposals from the vendors. There will be no portability, as well as no way to create 'application store' for network programming.

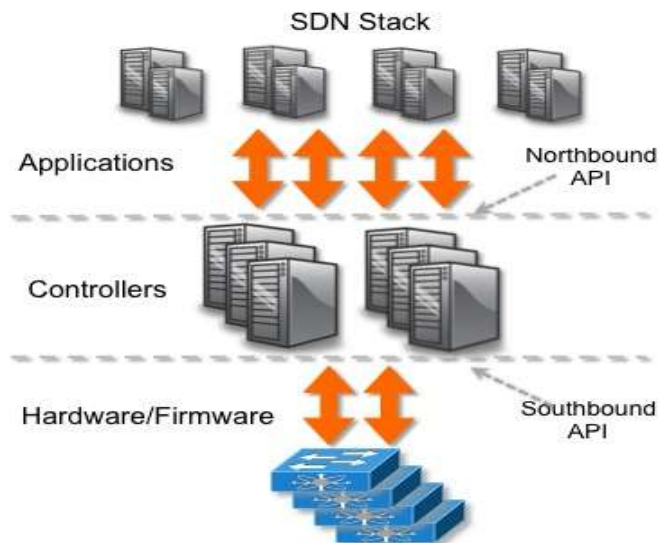


Fig. 1. SDN APIs [1]

Originally, many different sets of northbound APIs are emerging [2]. Currently, more than 20 different SDN controllers are available -- all featuring different northbound APIs. And the Open Networking Foundation (ONF), a consortium dedicated to promoting and commercializing SDN, is studying their variation and why they're all so different [3].

One possible reason is that requirements for a northbound API vary, depending on the needs of the applications and orchestration systems above it. It complicates the collaboration on common API. Actually, one popular opinion is based on ideas to collect market feedback (responses from the developers) first. It makes sense because many programming standards (and Northbound API is about programming only) are based on de-facto approaches, adopted by the majority of developers. For example, as per ONF vision, “the northbound API is a software interface inside a server, and API standards generally emerge from the market, not necessarily from a committee” [4].

The Architecture and Framework Working Group in ONF, originally, set three goals for the Northbound API development:

- 1) to collect use cases for the Northbound API;
- 2) to collect a list of examples of the Northbound API and perform some sort of reverse engineering. The goal is to explore what applications do, describe their data model, and what they require from SDN controller;
- 3) to provide recommendations to industry on required actions.

At this moment, there is no “standard” document that will describe the common requirements to Northbound (application level) API. Typically, a Northbound interface abstracts the low-level instruction sets used by Southbound interfaces to program forwarding devices. Probably, application level interface is the less elaborated area in SDN world [5]. As per this review, most of the existing solutions are either some ad-hoc (proprietary) API or a pure REST API. Authors conclude that it is unlikely that a single Northbound interface emerges as the winner, as the requirements for different network applications are quite different. One possible path of evolution for Northbound APIs are vertically-oriented proposals, before any type of standardization occurs. It is discussed in section 2.

The whole idea of this paper is to discuss the need for application level API for SDN, as well as the possible model for such standard. There are several attempts to create a unified application level program interfaces for telecommunication services. Because this area is very close to SDN, it would be interesting to discuss re-usage of the telecom experience (in the terms of APIs) for SDN. Potentially, it could save a lot of resources (at the first hand, a time for training of developers). It is the main motivation for this paper.

SDN model introduces many new concepts. So, the standardization for SDN is a multi-aspect problem too. In the subsequent sections, the related works in the various aspects of SDN standardization have been discussed.

The rest of our paper is organized as follows. In Section 2, we present the short history of common APIs. In Section 3, we discuss Network Functions Virtualization. In Section 4, we will talk about the Remote Procedure Calls (RPC) and Representational State Transfer (REST) in SDN. In Section 5, we discuss the possible sources for Northbound API requirements. Section 6 presents the discussion. The key question is: what should be included in basic requirements for

application level API and how can we reuse existing unified APIs?

II. ON TELECOM STANDARDS FOR APPLICATION LEVEL API

Probably, the most notable example of application-level API in the area very close to SDN was Parlay. Parlay (Parlay X) is an attempt to present common application level API in telecom world [6]. The main idea behind the Parlay is to combine service delivery mechanisms for network-centric communications (intelligent network) and service delivery approaches in the enterprise world. By enabling access to network capabilities via an API, any solution provider (independent software vendor) can produce new applications that add value to functionality resident in communications networks. The Parlay API hides the basic network complexity (e.g., signaling capability), but is still able to present indirect access to them to enterprise applications and maintain the security level like Network Operators do. This can be achieved by creating an API that resides between the application layer and the service component layer (Figure 2).

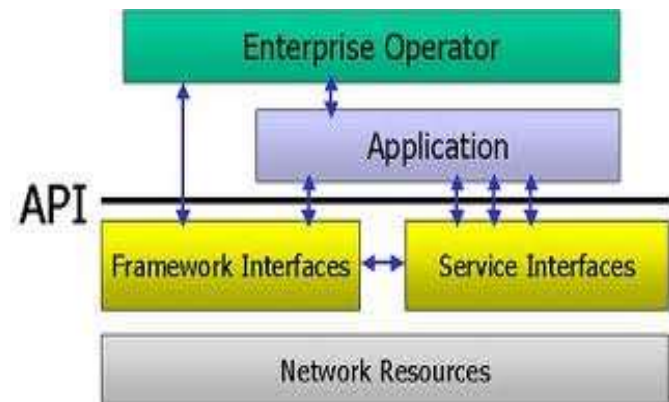


Fig. 2. The Parlay API [7]

The basic principles for API are very transparent:

- 1) The Parlay API is about programming interface, rather than wire-protocols.
- 2) The Parlay API should be network independent.
- 3) End-to-end security.
- 4) Manageability support. It is the ability to manage the operation and provision of the API.
- 5) Simplicity. It should be easy to use for software developers.
- 6) Extensibility. The idea was to expand the API in a series of phases.

At the first hand, it looks very similar to SDN conception. It is the main reason we choose Parlay API for the comparison. It is absolutely the same idea – separate a logic and hardware, convert logical part into pure software services. Actually, even the target areas (developers) are similar. In some sense, a Parlay-related movement in programming was even bigger, because there are more developers of telecom services, rather than programmers for network management systems. So, in our opinion, the lessons from Parlay development (end especially, from Parlay failure) could be used for SDN Northbound APIs.

Let us see the components (parts of API) in Parlay [8]. They are vertical oriented:

- 1) Call Control APIs. It is how to setup and control of connections
- 2) User Interaction APIs. It is how to send SMS, how to recognize tones, etc. So, they are pure telecom services.
- 3) Terminal Capabilities API. It is again pure telecom-related services: how to query to terminal capabilities.
- 4) Connectivity Management API. It is a common API for Quality of Services (QoS).
- 5) User Status APIs. In practice, it is how to get a status of a mobile terminal.
- 6) Data Session Control and Account management. It is about billing and tariffs.

The main conclusion is very transparent. It is an attempt to present a standard for applied services in the telecom world. The key word here is “applied”. The Parlay API was developed with some model for applied services in mind. The Parlay API assumes (proposes) some model for applied services and supports this model with the standard API. Applied services target the end users, at the first hand. Let us see the typical use cases, presented in [7]: services like ‘Buddy List’, ‘Location-based ads’, m-commerce, and ‘Scheduler service using Outlook’, etc. Each of the particular API could be a plain REST, but it is a vertically oriented solution.

In the case of SDN, the original model for application level API has no problem-oriented divisions. It is a conceptual difference. The question here is very obvious. Shall we talk about different types of SDN applications and originally present Northbound API as a collection of problem-oriented APIs? We see that some like this is mentioned in open-source SDN development [9], but have not seen practical results in direction.

III. ON STANDARDS FOR NETWORK FUNCTIONS VIRTUALIZATION

The ONF is working closely with a group of service providers behind Network Functions Virtualization (NFV). The goal is to use Northbound APIs to build top layers for virtual appliances [10].

The NFV was created by a consortium of service providers. It is an attempt to speed up a deployment of new network services. In the basic NFV paper, European Telecommunications Standards Institute described the basic ideas behind NFV [11]. Network Operators’ networks are populated with a large and increasing variety of proprietary hardware appliances. It increases the cost of launching new network services. Moreover, hardware-based appliances rapidly reach an end of life, requiring much of the procure-design-integrate-deploy cycle to be repeated with little or no revenue benefit. NFV aims to address these problems by leveraging standard IT virtualization technology to consolidate many network equipment types onto industry standard high

volume servers, switches, and storage, which could be located in Data-Centers, Network Nodes and in the end user premises.

NFV is highly complementary to SDN, but not dependent on it (or vice-versa). NFV can be implemented without any SDN being required, although the two concepts and solutions can be combined. The approaches relying on the separation of the control and data forwarding planes as proposed by SDN can enhance performance, simplify compatibility with existing deployments, and facilitate operation and maintenance procedures. In the same time, NFV is able to support SDN by providing the infrastructure upon which the SDN software can be run [12].

So, SDN Application API should be able to play a role of application API in NFV. It means that the area of applications is firmly bounded. It is networking. The typical areas for NFV are:

Virtual Switching. In this case, physical ports are connected to virtual ports on virtual servers. VPN gateways could be virtualized too.

Virtualized Network Appliances. For example, firewalls could be virtualized.

Virtualized Network Services. The typical examples of the virtualized services are network monitoring tools, load balancers, SSL accelerators.

Virtualized Applications. The typical example is virtualized data storage.

In our opinion, this classification could be used for the problem-oriented splitting for developers API (see Section 2). NFV by its nature is “close” to the applied application development and Northbound API can borrow ideas from here.

IV. ON REST MODEL AS STANDARDS BASE FOR SDN APIs

According to the fundamental review [5], devoted to SDN, most of the programming interfaces for SDN are based on REST protocol. The conception of programmability is also evolving and is not the pure REST in the case of SDN. Actually, the word ‘Northbound’ for SDN API could be also outdated [13]. Instead of Northbound and Southbound, ONF uses terms data interface and application interface. It could be strange because application interfaces could be data program interfaces too [14]. But this naming (terminology) is not so interesting comparing with the new model based on RESTCONF [15]. There are several new acronyms that we would like to present here: NETCONF, YANG, RESTCONF, TOSCA.

In general, all of them are about describing data for the calls in REST model.

The Network Configuration Protocol (NETCONF) [16] provides mechanisms to install, manipulate and delete the configuration of network devices. It uses an Extensible Markup Language (XML)-based data encoding for the configuration

data as well as the protocol messages.

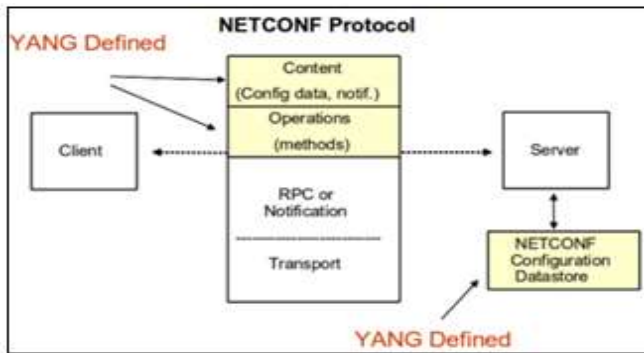


Fig. 3. NETCONF layers [17]

The NETCONF protocol operations are realized as remote procedure calls (RPCs). NETCONF supports devices with multiple configuration datastores. Furthermore, we can also subscribe to notifications or perform other Remote Procedure Calls (RPCs) using NETCONF (Figure 3).

YANG is a data modeling language used to model configuration and state data manipulated by the Network Configuration Protocol (NETCONF), NETCONF remote procedure calls, and NETCONF notifications [18]. As per the specification, YANG is a language used to model data for the NETCONF protocol. A YANG module defines a hierarchy of data that can be used for NETCONF-based operations, including configuration, state data, Remote Procedure Calls, and notifications. This allows a complete description of all data sent between a NETCONF client and server (Figure 4).

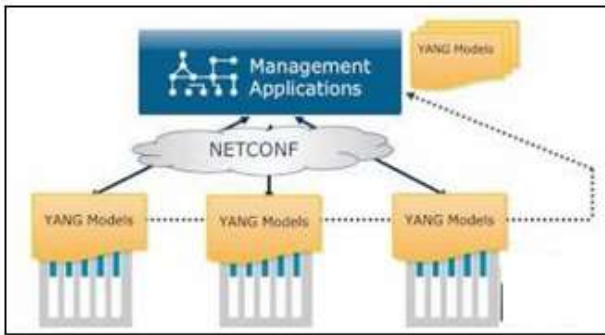


Fig. 4. NETCONF and YANG

YANG models the hierarchical organization of data as a tree in which each node has a name, and either a value or a set of child nodes. YANG provides clear and concise descriptions of the nodes, as well as the interaction between those nodes.

Here is the typical YANG description:

```

list interface {
    key "interface-name";
    leaf interface-name {
        type string;
    }
    leaf speed {

```

type string;

}

leaf duplex {

type string;

}

}

And here is NETCONF XML:

```

<interface>
    <interface-name>TenGigabitEthernet      1/0/1</login-
name>
    <speed>10Gbps</speed>
    <duplex>full</duplex>
    </user>
    <interface>
        <interface-name>TenGigabitEthernet      1/0/2</login-
name>
        <speed>10Gbps</speed>
        <duplex>full</duplex>
        </user>

```

RESTCONF is a model describes a REST-like protocol that provides a programmatic interface over HTTP for accessing data defined in YANG, using the datastores defined in NETCONF [19].

As per RESTCONF specification, the NETCONF protocol defines configuration datastores and a set of Create, Retrieve, Update, Delete (CRUD) operations that can be used to access these datastores. CRUD operation is a standard programming approach for databases. The YANG language defines the syntax and semantics of datastore content, operational data, protocol operations, and notification events. REST-like operations are used to access the hierarchical data within a datastore. So, it is a mapping from NETCONF's CRUD operations to HTTP requests.

What does it mean for SND API? It means a new trend for programmability and APIs for SDN controllers, based on RESTCONF. NETCONF and YANG describe the devices (virtualized devices) and REST (RESTCONF) could be used for access (Figure 5).

OpenDayLight (Open Source SDN controller [20]) proposes a list of Northbound interfaces. Let us see it [21]:

1) Top-Level Inventory: list of all nodes known to the controller.

2) OpenFlow Nodes: extends the top-level inventory node with OF-specific features that allow retrieving and programming of OF-specific states, such as ports, tables, flows, etc.

3) Topology. Base Topology: list of all topologies known to the controller.

4) BGP routing configuration.

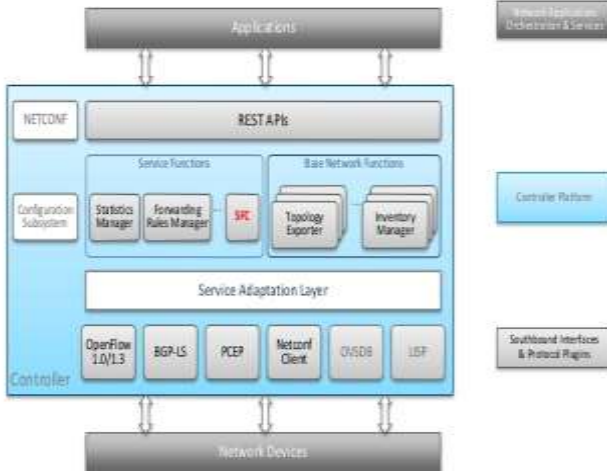


Fig. 5. OpenDayLight model [20]

In other words, it is a very specific networking APIs. In our opinion, the vertical splitting (according to applications area like the above-mentioned list borrowed from telecom world) should be more suitable.

TOSCA is Topology and Orchestration Specification for Cloud Applications [22]. TOSCA should facilitate the creation cloud applications and services. TOSCA provides mechanisms to control workflows, describe relationships and dependencies between resources. TOSCA and YANG can be used together. E.g., in some IaaS (Infrastructure as a Service) configuration the cloud components (compute and storage) could be described by TOSCA. And the connectivity service and networking equipment in the network would be described by YANG.

In other words, all these components bring nothing to Northbound API. All these components are various forms of top-level meta-data and nothing more.

V. ON REQUIREMENTS FOR SDN API

In 2013, the Open Networking Foundation (ONF) established a working group to focus on the Northbound Interfaces (NBI). One of ideas, proposed by this group was the conception of “scopes” for APIs. It is based on the idea that different applications would require the different granularity (levels of abstraction) from API. ONF’s papers use the term “latitude” [23].

One thing that is missed in the above-mentioned NBI paper is resource sharing. As soon as we separate our architecture on levels we need to some arbitrage for resources too. Otherwise, every application will command all the controller’s resources.

The next idea we’ve discovered from NBI paper is an intent-based interface. Technically, such kind of interfaces should be focused on what the application or service needs, rather than the commands to change the status. Intent-based interfaces are more natural for programmers because they do not need to study a new set of commands. Technically, intent-based interfaces have a natural support in the form of web intents. We’ve used them in M2M projects [24], but it looks

like now this direction is closed by Google. So, it looks like the REST will be the prevailing model. But we can make the following important conclusion. Intent-based interface, in general, does not assume the unified model for all devices. So, we should talk, probably, about different NBIs for various SDN controllers.

Technically, building a robust application is not about splitting up their code into smaller services, but instead understanding the connections between these services. So, the connectivity between APIs is more important. And this fact requires a new set of development tools. As an example, we could mention PANE SDN controller [25]. The controller provides an API that allows applications to dynamically add autonomously request network resources. PANE includes a compiler and verification engine to ensure that bandwidth requests do not exceed the limits set by the administrator and to avoid starvation, i.e., other applications shall not be impaired by new resource requests [5].

Top-level classification for NBI could be borrowed from telecom applications. For example, we should follow to [26, 27] and define the following classes:

Model API

Interfaces and objects comprising the domain model. For example the devices, ports, network topology, and related information about the discovered network environment.

Control API

Interfaces to access the modeled entities, control their life-cycles and in general to provide the basis for the product features to interact with each other.

Communications API

Interfaces which define the outbound forms of interactions to control, monitor, and discover the network environment.

Health Service API

Allows an application to report its health to the controller and listen to health events from the controller and other applications.

VI. THE DISCUSSION

Comparing SDN user cases and Parlay. Let us return to the original ONF’s plans and describe the potential use cases for Northbound (Application) SDN API. In general, we present the following uses cases for SDN [28]:

1) Cloud Orchestration

Traditionally, networks and servers were managed separately and independently. SDN is a proper way to integrate management of both network and cloud frameworks. It is, actually, what SDN are for. And for 3-rd party software applications, the API behind SDN is the natural way to get access to the abstracted hardware [29].

2) Load Balancing

Online services, e.g., search engines and web portals, are often replicated on multiple hosts in a data center for efficiency. The load balancer dispatches client requests to a selected service replica based on certain metrics such as server

load. With SDN, the load balancing can be integrated within any element in the network.

3) Monitoring and Measurement

It is a yet another classical task for SDN. We can perform network monitoring operations and measurements without any additional equipment. Also, the monitoring can be integrated with any network element.

4) Routing

The idea is very similar to load balancing. The routing services can be virtualized and implemented via programming modules [30].

5) Network Management and QoS

With SDN, it is very easy to build a centralized solution for traffic analysis, for example. SDN software can analyze traffic patterns as well as a quality of services.

As we see, all the above-mentioned tasks are specific network applications. There is almost nothing common (probably, except management and QoS) with applications for telecom. Parlay (in telecom world) offers (indirectly) some model for the possible services. The key idea for SDN could be shortly described as integration. SDN is about the integration of networking into 3-rd party applications.

This conclusion has a direct implication to the possible solutions for Northbound API. Without Network Functions Virtualization, something conceptually similar to Parlay cannot be expected. Actually, just a list of the various technical APIs with the simple form for 3-rd party integration could be provided here.

REST and meta-data. In this sense, the idea of RESTCONF looks more promising. REST API are easy to use, they are simple and very understandable for the developers. As per [5], most of the existing SDN program interfaces are REST-based. But with REST APIs (in general) programmers will face another issue. In practice, REST is missing meta-data [31]. Let us see one example from Neutron API (OpenStack) [32]. The request is a typical REST:

```
GET /v2.0/networks?limit=2
Accept: application/json
And here is a response (part of it):
{
  "networks": [
    {
      "status": "ACTIVE",
      "subnets": [
        "a318fcb4-9ff0-4485-b78c-9e6738c21b26"
      ],
      "name": "private",
      "admin_state_up": true,
      "tenant_id": "625887121e364204873d362b553ab171",
      "id": "9d83c053-b0a4-4682-ae80-c00df269ce0a",
      "shared": false
    }
  ]
}
```

REST approach proposes the uniform interface. It means that all resources present the same interface to clients. And it is one of the reasons for REST popularity.

SOA and meta-data. Alternatively, the Service Oriented Architecture (SOA) approach (where the REST is from) may

offer personalized interfaces for the different resources [33]. The whole SOA model often compared with REST is based on the idea that different services have different interfaces. It means, immediately, that we need to provide the definition for used interfaces. Indeed, the definition of the services is a key part of SOA. For example, Web Service Definition Language (WSDL) [34] is a part of SOA specification. A WSDL definition of a Web Service defines operations in terms of their underlying input and output messages. Unlike this, REST is based on the self-described messages. WSDL defines the form of the data that accompany the messages in SOA. REST does not provide this information. In other words, SOA has got a rich set of metadata.

On meta-data for REST. The problem with meta-data support is very transparent. Let us see the above-mentioned Neutron API example. How the developers can get information (“get” means programmatically discovery) about the following elements:

- HTTP command (it is GET in this case)
- URI (it is /v2.0/networks)
- Output formats (it is JSON)
- Version (it is 2.0 in this case)
- Optional and mandatory parameters (it is limit=2)?

There are no ways to discover this information programmatically in the modern implementations of REST approach. The key work here is “programmatically”. The typical model for REST-based API deployment includes the “manual” consulting (reading) with the API manual. So, without the metadata, there is no way to automate programming [35]. That is why we can conclude that metadata for Northbound API (application API) is a key problem.

Another classical example is network management. With SNMP [36], an application can programmatically detect new devices and their features. It is a classical example of meta-data deployment.

VII. THE CONCLUSION

As the conclusion of this review, the following suggestions have been made. Unified API for NBI is unlikely. This conclusion is based on the fact that SDN NBI API is not designed to solve applied-level problems. In SDN model, NFV works on an application level. In the same time, we can reuse some developments from telecommunication APIs for SDF. Firstly, in our opinion, the classification for NBI API could be and should be unified. This classification could be directly borrowed from the telecommunications API.

But inside of top-level classes (and this is important in our proposal), the effort should not be focused on developing a common API. The efforts should be concentrated on the search for a unified approach to the description of the APIs. In other words, in our opinion, the developers need unified metadata description, rather than unified API. In practice, this conclusion proposes a fix for meta-data in REST APIs.

The main use cases for NBI applications are the integration and analysis of traffic. These applications should be automated.

It is what NBI APIs are for. But the basis for automating the programming is exactly the meta-data. And the harmonization of metadata is, in our opinion, the main task.

Of course, the lack of meta-data in REST model is not a specific SDN problem. As we stated above, it is a payment for REST model simplicity. But the network programming (network management, for example) really requires automated solutions. And REST programming cannot be automated without some form of meta-data. In this connection, we can conclude that the real problem for application level API in SDN is the way for describing meta-data. In this connection, RESTCONF approach looks promising. It has meta-data for network elements. The question is how to expand this information to REST API. In our opinion, it is what Northbound (or Application level) API standardization should be about.

ACKNOWLEDGMENT

The project was supported by the deanship of scientific research at Prince Sattam bin Abdulaziz University (Kingdom of Saudi Arabia) under the research project # 2014/1/863.

REFERENCES

- [1] The Northbound API- A Big Little Problem <http://networkstatic.net/the-northbound-api-2/> Retrieved: Jul, 2016.
- [2] Sezer, Sakir, et al. "Are we ready for SDN? Implementation challenges for software-defined networks." Communications Magazine, IEEE 51.7 (2013): 36-43.
- [3] Ortiz, Sixto. "Software-defined networking: On the verge of a breakthrough?" IEEE Computer 46.7 (2013): 10-12.
- [4] Do SDN northbound APIs need standards? <http://searchnetworking.techtarget.com/feature/Do-SDN-northbound-APIs-need-standards> Retrieved: Jul, 2016
- [5] Kreutz, Diego, et al. "Software-defined networking: A comprehensive survey." Proceedings of the IEEE 103.1 (2015): 14-76.
- [6] Yates, M. J., and I. Boyd. "The Parlay network API specification." BT Technology Journal 25.3-4 (2007): 205-211.
- [7] Uve Herzog "OSA & Parlay. Enabling an open services market" <http://archive.eurescom.eu/message/messageJun2002/tutorial.asp> Retrieved: Jul, 2016.
- [8] Sneps-Sneppe, Manfred, and Dmitry Namiot. "About M2M standards and their possible extensions." Future Internet Communications (BCFIC), 2012 2nd Baltic Congress on. IEEE, 2012.
- [9] C. E. Rothenberg, R. Chua, J. Bailey, M. Winter, C. Correa, S. Lucena, and M. Salvador, "When open source meets network control planes," IEEE Computer Special Issue on Software-Defined Networking, November 2014
- [10] Schneider, Fabian, et al. "Standardizations of SDN and ITs practical implementation." NEC Technical Journal 8.2 (2014): 16-20.
- [11] NFV White Paper http://portal.etsi.org/nfv/nfv_white_paper.pdf Retrieved: Sep, 2016
- [12] Nunes, Bruno, et al. "A survey of software-defined networking: Past, present, and future of programmable networks." Communications Surveys & Tutorials, IEEE 16.3 (2014): 1617-1634.
- [13] Medved, Jan, et al. "Opendaylight: Towards a model-driven sdn controller architecture." Proceeding of IEEE International Symposium on a World of Wireless, Mobile and Multimedia Networks 2014. 2014.
- [14] Namiot, Dmitry, and Manfred Sneps-Sneppe. "On software standards for smart cities: API or DPI." ITU Kaleidoscope Academic Conference: Living in a converged world-Impossible without standards?, Proceedings of the 2014. IEEE, 2014.
- [15] Bierman, A., Bjorklund, M., Watsen, K., & Fernando, R. (2014). RESTCONF protocol. IETF draft, work in progress.
- [16] Enns, R., Bjorklund, M., Schoenwaelder, J., & Bierman, A. (2011). Network configuration protocol (NETCONF) (No. RFC 6241).
- [17] NETCONF layers <http://itential.com/tech-briefs/> Retrieved: Jul, 2016
- [18] YANG - A Data Modeling Language for the Network Configuration Protocol (NETCONF) <https://tools.ietf.org/html/rfc6020>
- [19] RESTCONF Protocol <http://tools.ietf.org/html/draft-bierman-netconf-restconf-04>
- [20] Baucke, Stephen, et al. "OpenDaylight: An Open Source SDN for your OpenStack Cloud." An Open-Stack Summit, Hong Kong (2013).
- [21] OpenDayLight Northbound API https://wiki.opendaylight.org/view/OpenDaylight_Controller:RESTCONF_Northbound_APIS Retrieved: Jul, 2016
- [22] Mijumbi, Rashid, et al. "Management and orchestration challenges in network functions virtualization." IEEE Communications Magazine 54.1 (2016): 98-105.
- [23] Northbound Interfaces Working Group <https://www.opennetworking.org/images/stories/downloads/working-groups/charter-nbi.pdf> Retrieved: Oct, 2016
- [24] Sneps-Sneppe, Manfred, and Dmitry Namiot. "About M2M standards and their possible extensions." Future Internet Communications (BCFIC), 2012 2nd Baltic Congress on. IEEE, 2012.
- [25] Guha, Arjun, Mark Reitblatt, and Nate Foster. "Machine-verified network controllers." ACM SIGPLAN Notices. Vol. 48. No. 6. ACM, 2013.
- [26] Marie-Paule Odini, Hewlett-Packard, "SDN and NVF for Carriers", ETSI Future Networks Workshop, April 10, 2013
- [27] Chung-Shih Tang, Chin-Ywu Twu, Jen-Hong Ju, Ying-Dian Tsou "Collaboration of IMS and SDN to enable new ICT service creation". Network Operations and Management Symposium (APNOMS), 2014 16th Asia-Pacific 17-19 Sept. 2014 pp.:1-4.
- [28] Jarschel, Michael, et al. "Interfaces, attributes, and use cases: A compass for SDN." IEEE Communications Magazine 52.6 (2014): 210-217.
- [29] M.Banikazemi, D.Olshefski, A.Shaikh, J.Tracey, G.Wang, "Meridian: an SDN platform for cloud network services," IEEE Communications Magazine, vol. 51(2), 2013, pp. 120-127
- [30] C.E. Rothenberg, M.R. Nascimento, et.al. "Revisiting routing control platforms with the eyes and muscles of software-defined networking," Proceedings of the first workshop on Hot topics in software defined networks, Aug. 2012, pp. 13-18.
- [31] Sneps-Sneppe, Manfred, and Dmitry Namiot. "Metadata in SDN API for WSN." 2015 7th International Conference on New Technologies, Mobility and Security (NTMS). IEEE, 2015.
- [32] Denton, James. Learning OpenStack Networking (Neutron). Packt Publishing Ltd, 2014
- [33] Al-Rawahi, N., and Y. Baghdadi. "Approaches to identify and develop Web services as instance of SOA architecture." Proceedings of ICSSSM'05. 2005 International Conference on Services Systems and Services Management, 2005.. Vol. 1. IEEE, 2005.
- [34] Newcomer, Eric, and Greg Lomow. Understanding SOA with Web services. Addison-Wesley, 2005.
- [35] Namiot, Dmitry, and Manfred Sneps-Sneppe. "On IoT Programming." International Journal of Open Information Technologies 2.10 (2014): 25-28.
- [36] Harrington, David, Bert Wijnen, and Randy Presuhn. "An architecture for describing simple network management protocol (SNMP) management frameworks." (2002). <https://tools.ietf.org/html/rfc3411> Retrieved: Aug, 2016.

Impact of Domain Modeling Techniques on the Quality of Domain Model: An Experiment

Hiqmat Nisa

Dept. of Computer Science & Software Engineering
International Islamic University
Islamabad, Pakistan

Salma Imtiaz

Dept. of Computer Science & Software Engineering
International Islamic University
Islamabad, Pakistan

Muhammad Uzair Khan

Dept. of Computer Science National University of Computer
& Emerging Sciences (FAST-NU)
Islamabad, Pakistan

Saima Imtiaz

Dept. of Computer Science & Software Engineering
International Islamic University
Islamabad, Pakistan

Abstract—The unified modeling language (UML) is widely used to analyze and design different software development artifacts in an object oriented development. Domain model is a significant artifact that models the problem domain and visually represents real world objects and relationships among them. It facilitates the comprehension process by identifying the vocabulary and key concepts of the business world. Category list technique identifies concepts and associations with the help of pre defined categories, which are important to business information systems. Whereas noun phrasing technique performs grammatical analysis of use case description to recognize concepts and associations. Both of these techniques are used for the construction of domain model, however, no empirical evidence exists that evaluates the quality of the resultant domain model constructed via these two basic techniques. A controlled experiment was performed to investigate the impact of category list and noun phrasing technique on quality of the domain model. The constructed domain model is evaluated for completeness, correctness and effort required for its design. The obtained results show that category list technique is better than noun phrasing technique for the identification of concepts as it avoids generating unnecessary elements i.e. extra concepts, associations and attributes in the domain model. The noun phrasing technique produces a comprehensive domain model and requires less effort as compared to category list. There is no statistically significant difference between both techniques in case of correctness.

Keywords—Domain Model; UML; Experiment; Noun Phrasing Technique; Category List Technique

I. INTRODUCTION

UML (Unified modeling language) is gaining fame since its inception in 1997; it is being commonly practiced by the industry to model object oriented software systems. UML plays a significant role in reducing the complexity of large software system by modeling different aspects throughout SDLC phases. Object Oriented Analysis (OOA) is carried to understand and model the problem domain in the form of real world objects, which can later be translated into the solution. It describes problem domain from the perspective of objects and emphasizes on identifying and describing the concepts,

attributes and associations in the problem domain [1]. One of the main outcomes of OOA is a domain model which models the problem domain objects along with their associations and attributes.

Domain model is one of the most important UML artifact used to understand the problem domain. It represents vocabulary and key concepts, important to the business world [1] [2] [3] and consists of visual representation of concepts, attributes and association among conceptual classes in the real world domain. It also presents general vocabulary, which helps in clear communication between the team members and helps elevate the level of understanding between the development team and customer side [2] [3]. A solution which is representative of the customer needs requires a domain model that is representative of the domain. A clear and precise domain model can also help in reducing risk [4] and effort and cost of rework required at later stages [5]. Therefore one of the major goals of OOA is to create an accurate and complete domain model.

The domain model can be created using two different techniques suggested by Larman [1]: category list technique and noun phrasing technique. To identify potential candidate classes and associations; category list technique provides a list of categories which are usually important to business information systems. Each category represents entities or concepts related to real-world. Sets of candidate classes produced by all categories are quite independent from each other whereas, noun phrasing technique is linguistic analysis. Noun phrasing technique involves the identification of nouns and noun phrases in the domain description, and considers them as conceptual classes or attributes [1]. These techniques have not been empirically evaluated for their effectiveness in creating a quality domain model. Therefore an experiment was performed to evaluate the effectiveness of techniques in creating a complete and accurate domain model. The experiment was conducted with help of undergraduate students of fourth semester of software engineering, as they are assumed to be familiar with the models and notations of UML. This experiment is focused to answer the below given research questions.

RQ1: What is the effect of noun phrasing and category list technique on the quality of the domain model?

RQ2: What is the amount of effort required to create the domain model using both techniques?

The quality of the domain model is determined on the basis of completeness and correctness of the domain model, whereas the amount of effort is measured in terms time taken to create the model. The rest of the paper is organized as follows: Section 2 presents the Background and Related Work. In Section 3 elaborates on the Design of the Experiment and Section 4 discusses the Analysis and Results. Finally conclusion and future work is given in section 5.

II. BACKGROUND AND RELATED WORK

Domain model is the most important and common model in object oriented analysis. It describes the noteworthy concepts or objects in problem domain. It is a representation of the real-world conceptual classes, attributes of the classes and associations among them Domain model is an improved version of the project dictionary, where the terms used in the project are present along with the graphical visualization of the connections between them. It can be termed as a simplified version of a class diagram, one that does not incorporate responsibility assignment [1]. Most of the conceptual classes modeled in domain model become part of the class diagram, which are important to software development [2] [6].

Domain model can be created using two different techniques namely: noun phrasing technique and category list technique [1]. There are some basic steps involved to create a domain model i.e. identification of conceptual classes along with their attributes and associations and unnecessary candidate classes.

Noun phrasing technique uses grammatical analysis of use case description to identify nouns and noun phrases and consider them as candidate conceptual classes or attributes. For the identification of associations, verb phrases are identified between entities and are considered as relationships between conceptual classes. However, for the identification of potential candidate classes and associations using category list technique Larman [1] provides a list of categories which are usually important to business information system and also provides guideline to eliminate useless concepts which are not appropriate to be implemented

Noun phrasing technique is the simplest approach to create domain model, but result in many imprecision problems e.g. words may be ambiguous or the identification of redundant classes due to synonyms in use case description and noun phrase may also be an attributes rather than a concept [1].Identifying noun and noun phrases is an analyst's job to examine each noun phrase and consider it either as a concept or an attribute. Some guidelines have been proposed by Larman to identify and refine attributes. The research focuses on empirically evaluating both of the techniques to observe their effect on the quality of domain model.

The Literature survey highlights that various empirical studies have been conducted to evaluate the impact of different techniques used to construct different UML models. Most of the target UML models are use case diagram, Class diagram and sequence diagram. The work of T. Yue et.al. [7] for instance, investigated whether restricted use case modeling (RUCM) approach or traditional use case template produced high quality analysis models i.e. Class diagram and sequence model. Subjects designed a class and sequence diagram of a given software systems using RUCM approach and traditional use case template. Results pointed out that RUCM produced better quality model than traditional use case template. Similar experiment was performed S.Tiwari *et al.* [8] [9], where they investigated the impact of use case templates on the quality of class diagram and use case diagram. They concluded [9]that no template is statistically significant better over another in terms of completeness, consistency, understandability, redundancy and fault proneness. However formal use case template produced high quality class diagram as compared to UML use case template and formal use case produced less redundant elements in class diagram [10]. Another study 1 [11], evaluated the effectiveness of two techniques i.e. validation and derivation technique on the quality of class diagram, and concluded that derivation technique produced more complete class diagram as compared to validation technique.

The quality of domain model is also evaluated by some researchers. The impact of system sequence diagram (SSD) and system operation contract (SOC) is observed on the quality of domain model [12]. The subjects designed domain model with SSD and SOC and without SSD and SOC. Two factors were involved to evaluate the quality of domain model, i.e., completeness and time. Author concluded that using SSD and SOC to construct a domain model, improves the quality of domain model in case when subjects have enough practice to take advantage from SSD and SOC. Another study conducted by S. Espana *et al.* [10]evaluated the quality of conceptual model constructed by two alternative techniques i.e. text-based derivation technique and communication based derivation technique. Participants were required to construct conceptual model using two alternative techniques. The quality of derived conceptual model was evaluated according to completeness and number of faults present (model validity) in participants conceptual model. The results highlight that the participants who used communication based derivation techniques produced 9.22% more complete conceptual diagram as compared to those who used text based derivation technique. Briand *et al.* [12] investigated that whether the use of SSD or SOC in domain model construction, improve the quality of domain model or not. Whereas, a main concern is to evaluate domain model construction technique suggested by Larman [1].

Most of the researchers conducted empirically studies, to compare different techniques [10] [7] [11] [13]for the purpose that which technique leads to high quality UML diagram. However most of the target UML models are class, use case diagram and sequence diagram. This research is focused on

the quality of resultant domain model created via noun phrasing and category list technique.

III. EXPERIMENT PLANNING

The research is validated with help of an experiment. This section explains design of the experiment. The experimental guidelines were followed to design the experiment in a controlled environment as suggested by C. Wohlin [14]. All the steps of an experiment to evaluate the quality of domain modeling techniques are reported in this section.

A. Experiment Definition

The purpose of this research is to empirically evaluate the impact of noun phrasing and category list technique on the quality of domain model. Our main concern is the creation of a domain model by the subjects via noun phrase or category list technique. As a result, two treatments are described as independent variable. One describes the creating of domain model using noun phrasing technique, and the other one describe the domain model using category list technique. The aim of this experiment is to evaluate the quality of domain model in terms of correctness, completeness, and effort required to design a complete domain model.

B. Context selection and subject

The selection of the subjects is very important for generalizing the results of experiment. Results generalization can be achieved by satisfactory sample size and random subject selection [14]. This experiment is conducted with 68 fourth year undergraduate computer science students in a famous Science and technology University of Islamabad, Pakistan. The students are familiar with UML notation and domain modeling techniques. They studied UML as part of their software engineering course in initial semesters. All the students have similar experience in modeling UML diagrams. The students were selected as experiment subjects as they fulfill the criteria i.e. participants who have similar education background, adequate knowledge and training of domain modeling.

To avoid biasness simple random sampling [14] is used for subject selection, i.e. subjects are selected from the population at random. Subjects were divided into two groups: group A and group B according to their grades. The categorization of students in two groups according to their grades is done to minimize the impact of students' capability on experiment's results. Before conducting the experiment a brief presentation is given to students about domain modeling techniques and the experiment. However the hypothesis of the experiment is not disclosed.

Two different systems were used as objects in this experiment, Automatic Teller Machine (ATM) and internet book store system (IBS). The ATM use case describes the process of withdraw fund and card verification as discussed in [15]. The IBS system purchases books over internet via credit card and Amazon website as discussed in [16]. We provide the experimental systems of limited complexity due to time constraints, so that subjects are able to finish their task.

C. Dependent and independent variable

There are two independent variables, Technique (category list and noun phrase) and Domain used (ATM and IBS).

Quality of domain model is evaluated by three dependent variables i.e. completeness, correctness and effort. Correctness is calculated in terms of average value of Useless Concepts(UC), Missing Concepts (MC), Extra Relationships (ER), Missing Relationships (MR), Extra Attributes(EA), Missing Attributes (MA) and Missing Generalizations(MG [12]. Completeness is defined as average of correctly identified elements in the domain model i.e. average number of Correct Concepts (CC), Correct Relationships (CR) and correct attributes (CA) and Correct Generalizations (CG) [7]. Table I and table II present the completeness of domain model completeness.

The second dependent variable checks the significant difference between the effort required to design a domain model by subjects who use noun phrase technique and those who use category list technique. The effort is calculated in terms of time, measured in minutes. Only that time was considered which utilized in creation of fully completed or partially completed domain model. The time is computed by subtracting the start time of the experimental task from end time of the experimental task.

D. Hypothesis

Two main research questions are investigated in this experiment. The first question contains a number of hypotheses shown in table III. According to experimental design one independent variable was considered called method, with two treatments: category list technique and noun phrasing technique, and three dependent variables correctness, completeness of domain model and effort required to complete a domain model. Thus two tailed hypothesis i.e. alternate and null hypothesis was formulated. The null hypothesis (H_0) for each dependent variable is: there is no difference between category list technique and noun phrasing technique in terms of completeness and correctness of domain model and required effort. The alternative hypothesis (H_1) is defined as: category list technique produces different quality of domain model, or different effort is required to complete a domain model when compared to noun phrasing technique.

E. Experiment Design

Crossover design is followed in the experiment. Crossover design is a repeated measurement design such that each subject receives different treatments during different time periods. This experiment is conducted in two labs. In first lab, subjects in group A are required to design a domain model for ATM system using noun phrasing technique and group B have to construct a domain model for Internet book store system using category list technique. In second lab, same subjects of group A are required to complete the domain model for Internet book store system using noun phrasing technique and same subjects of group B are required to design a domain model using category list technique for ATM System depicted in table IV. A short

presentation was given to the participants to introduce the domain model and its concepts along with the procedure of the experiment. The hypothesis of the research was not disclosed

to avoid any biases later on. The participants were given 40-45 minutes to finish the domain model.

TABLE I. MEASURES USED TO DERIV DOMAIN MODEL

No#	Measures	Specification
	NRef	Number of correct Concepts in Reference model
	NRRef	Number of correct Relationships in Reference model
	NAref	Number of correct Attributes in Reference model
	NGref	Number of correct Generalizations in Reference model
	NCC	Number of correct Concepts in Subjects model
	NCR	Number of correct Relationships in Subjects model
	NCA	Number of correct Attributes in Subjects model
	NCG	Number of correct Generalizations in Subjects model
	NUC	Number of useless Concepts in Subjects model
	NER	Number of extra Relationships in Subjects model
	NEA	Number of extra Attributes in Subjects model

TABLE II. QUALITY MEASURES FOR DOMAIN MODEL

Dependent		Formula
Completeness	Class Completeness $C_{com} = NCC/Nref$	$Completeness = (C_{com} + R_{com} + A_{com} + G_{com})/4$
	Relationships Completeness $R_{com} = NCR/NRRef$	
	Attributes Completeness $A_{com} = NCA/NAref$	
	Generalizations Completeness $G_{com} = NCG/NGref$	
Correctness	Number of Useless Concepts NUC	$Correctness = (NUC + NMC + NER + NMR + NEA + NMA + NMG)/7$
	Number of Missing Concepts $NMC = Nref - NCC$	
	Number of Extra Relationship NER	
	Number of Missing Relationship $NMR = NRRef - NCR$	
	Number of Extra Attributes NEA	
	Number of Missing Attributes $NMA = NAref - NCA$	
	Number of Missing Generalizations NMG	

TABLE III. HYPOTHESIS FOR DOMAIN MODEL CORRECTNESS, COMPLETENESS AND REQUIRE EFFORT

Dependent variable	Null Hypothesis	Alternative Hypothesis
Correct Concepts (CC)	CC(CLT)=CC(NPT)	CC(CLT) ≠ CC(NPT)
Use Concepts (UC)	UC(CLT)=UC(NPT)	UC(CLT) ≠ UC(NPT)
Missing Concepts (MC)	MC(CLT)=MC(NPT)	MC(CLT) ≠ MC(NPT)
Correct Relationships(CR)	CR(CLT)=CR(NPT)	CR(CLT) ≠ CR(NPT)
Extra Relationships(ER)	ER(CLT)=ER(NPT)	ER(CLT) ≠ ER(NPT)
Missing Relationships(MR)	MR(CLT)=MR(NPT)	MR(CLT) ≠ MR(NPT)
Correct Attributes (CA)	CA(CLT)=CA(NPT)	CA(CLT) ≠ CA(NPT)
Extra Attributes (EA)	EA(CLT)=E(NPT)	EA(CLT) ≠ E(NPT)
Missing Attributes(MA)	MA(CLT)=MA(NPT)	MA(CLT) ≠ MA(NPT)
Correct Generalizations(CG)	CG(CLT)=CG(NPT)	CG(CLT) ≠ CG(NPT)
Missing Generalization(MG)	MG(CLT)=MG(NPT)	MG(CLT) ≠ MG(NPT)
Overall Completeness (Com)	Com (CLT)= Com (NPT)	Com (CLT) ≠ Com (NPT)
Overall Correctness (Corr)	Corr (CLT)= Corr (NPT)	Corr (CLT) ≠ Corr (NPT)
Effort	Time(CLT)=Time(NPT)	Time(CLT) ≠ Time(NPT)

The experiment is performed in supervision of the lab supervisor in both labs. All the required material is provided to the participants. The participants were required to note the time before starting the experiment and after completion of the experiment. Participants were required to construct the domain model using one technique in first half and alternative technique in second half, respective data is collected.

1) Co factors: There are some extraneous factors that affect the experiment results. These are also known as co founding variables that can also affect the results. In case of influence it becomes difficult to infer that the results are due to the independent variable or due to these co-founding variables. These extraneous factors must be minimized to increase the experiment's effectiveness. In this research students' ability and system complexity are considered as co-founding variables. Subjects of the experiment were choose from the same batch i.e. 4th year students to ensure same level of knowledge and skills regarding domain modeling, however we cannot ignore the fact that students belonging to same class may have different analytical and design skills. These skills would also affect the design of domain model from different complexity systems. Therefore we used a block design of experiment to control the impact of these co-founding variables on the output of the experiment.

Subjects were divided into two blocks according to their grades in software engineering course, so that each group consists of students with almost the same ability as far as software engineering knowledge and skills is concerned.

2) Learning and fatigue effect: When subjects deal with the same problem more than once, their response will be better at the second exposure as compared to first one, because human learn from previous experience. As a result any significant changes in the second time can be the effect of practice or learning [14].

In experiment, subjects were required to complete a domain model twice. Different system was used in second half to avoid learning effect.

TABLE IV. EXPERIMENT DESIGN

Lab	Task	Group A	Group B
Lab1	Domain ATM	Category list	Noun phrase
Lab 2	Domain IBS	Noun phrase	Category list

F. Instrumentation

There are three types of instruments associated with experiment: experimental objects, guidelines and measurement [14].

Experimental objects can be a document or source code on which subjects have to work. During experiment planning it is necessary to select appropriate objects i.e. in this experiment; use case description is required for the creation of domain model. In this experiment objects consist of use case description of both software systems (ATM, IBS). Use case description of ATM system [15] and IBS system [16] were selected from literature. A document was provided to students

which contains a brief use case description and students were required to design a domain model using pen and papers.

Regarding experiment guidelines, a brief presentation is given to the students in the beginning of the experiment. In which the students were briefly explained about the list of documents provided, the task to be performed, and the submission strategy. A written instructions document is also given which students return at the end of the experiment. The students were allowed to ask questions before start of the experiment. The students were required to complete the domain model within 45 to 50 minutes. This time selection to construct a domain model is based on the pilot study performed during course work activity.

Measurements contain, documents prepared to collect data and evaluation criteria to compute dependent variables. The use case description documents were prepared and validated. We compared students' domain model with reference model to measure the correctness and completeness of students' domain model. The reference domain model is design by external party, which consists of three researchers having 5 to 10 years of experience in UML and software engineering. The following criteria are followed to evaluate the students' domain model.

- All the concepts were considered correct if different names were used by students for the specific concept in reference model.
- All the relationships belonging to Missing concept in the reference model were considered missing.
- All the relationships of extra concepts were not considered as extra relationships.
- Attribute identified for extra concepts were not considered as extra attributes.
- Attributes were considered as extra identified attributes which are defined in the wrong concept.
- We assume the missing multiplicity to be one.
- In the inheritance, if super class is missing in the students' model, and attributes of super class is correctly defined in the sub class, then those attributes were considered as correctly identified attributes. And missing super class relationships were also considered correct if sub class is correctly associated with the class having direct relationship with super.

G. Analysis Procedure

Data analysis procedure consists of three dependent variables (domain model Correctness, completeness and effort involved to design a domain model), and one independent variable (Method), with two treatments (noun phrase technique and category list technique). The data analysis is performed with help of statistical test. Descriptive statistics presents the initial picture of collected data. Descriptive statistics summarize and presents the quantitative description in an effective way. Some basic descriptive statistics like, mean, standard deviation, minimum and maximum values were presented.

A Mann Whitney U-test was performed for each task related to designing a domain model to compare the means of dependent variables. The dependent variables are not normally distributed therefore we have selected Mann Whitney test which overcame the data normalization assumption.

Three-way ANOVA test is used to analyze combined data collected from lab 1 and lab 2 and extraneous factors which influence the dependent variables. It is used to identify the significance of main effect i.e.: the effect of and interaction between factors [17]. In this experiment two extraneous factors are considered, software systems and students' ability. The purpose of considering these two factors is to analyze the effect of systems' complexity and students' level of understanding on dependent variables and identifying possible interaction between factors.

H. Validity threats

1) Internal validity

Internal validity is concerned with cause-effect relationship among different variables. Internal validity threats can be present when the results of experiment are influenced by extraneous factors like learning and fatigue effect. Learning and fatigue effect is mitigated using cross-over experiment design and two different systems used in different labs.

Although students have same background knowledge but based on their ability subjects were divided into two balance groups according to their grades.

2) Construct validity

Construct validity threats are concerned with the relationship between concepts and construct being studied (correctness and effort). The measurement criteria were briefly explained. We believe that these measurements are reliable. The time factor is directly related to effort being used. Correctness and completeness cover all the domain model elements.

3) External validity

There are two major external validity threats which are related to this experiment, and these threats are usually associated with controlled experiment because of artificial environment used. They are: Are the sample of subjects in this experiment representative of software professionals? Is the material used in experiment representative of real software industry system in terms of complexity and size?

Regarding issue one, 4th year undergraduate student have acceptable knowledge about software engineering and UML modeling. They also practice UML and software engineering concepts during their assignments and projects. Their experience is almost same as junior professionals. Secondly, our purpose is to find the effectiveness of domain modeling techniques which do not need such a high level programming skills and experience. Students do not have exposure about different domain as professionals, but they are familiar about the domain modeling techniques and their usage, which they can apply on any problem domain.

Regarding the second issue, Software systems used in this experiment are small as compared to industrial software systems, because it is not feasible to take large industrial system in limited time [18], but its size and complexity is comparable with other systems used in related experiments [7] [9] [12].

4) Conclusion validity

Conclusions validity threats are related with issues that influence the capability to draw a correct conclusion about experimental hypothesis based on experimental results. Regarding this experiment, appropriate statistical tests were performed to find statistically significant difference. In case where little difference is found but not significant, power analysis was performed to avoid accepting false null hypothesis.

IV. ANALYSIS

Table V and table VI show a Mann-Whitney test results. Overall results show a lack of significant difference between two groups in different dependent variables.

In lab 1, we see a significant difference in the correct concepts ($p\text{-value}=.021$) and correct generalizations ($p\text{-value}=.039$) dependent variables only. From the mean rank of correct concepts show that students produced more correct concepts using category list technique than noun phrase technique.

In lab 2, a significant difference is shown in correct attributes ($p\text{-value}=.000$) and overall completeness ($p\text{-value}=.009$) only. No other dependent variables show significant differences. According to mean rank, subjects produced more correct attributes using noun phrase as compared to category list technique.

Table VI shows the results of overall correctness and effort. As discussed in the dependent variables section that the overall correctness is calculated as average of all the extra dependent variables (concepts, relationships and attributes) and all the missing dependent variables (concepts, relationships and attributes). Lower the overall correctness mean, better will be the quality of domain model.

We can observe from the table VI that those students who used category list technique produced more missing concepts as compare to those who used noun phrase technique in lab 1. However, in lab 2 a significant difference is found in extra attributes ($p\text{-value}=.000$) and missing attributes ($p\text{-value}=.0000$). It can observe from the value of mean rank, that noun phrase technique produced more numbers of correct elements of domain model (concepts, relationships and attributes), However it also produced large number of extra elements in the domain model. No significant difference is found in overall Correctness dependent variable.

We also conduct a power analysis to determine the power of those statistical tests having no significant results. Before accepting null hypothesis we compare minimum effect size required to obtain 80% power with observe effect size. In case of ATM software system, the minimum effect size

required to obtain 80% power for overall completeness is 0.512 but the observed effect size is 0.432. Due to the small effect size the observed power is 70%. So we cannot provide any erroneous conclusion about overall completeness of domain model. On the other hand, the observed power of overall correctness is also very small for IBS system. So we cannot reject the null hypothesis.

According to second research question, a significant difference is observed between effort require in term of time. In lab 1 ($p\text{-value}=.000$) and in lab 2 ($p\text{-value}=.004$) were observed for required effort. So from the mean rank we can say that students spent more time in designing a domain model using category list technique as compare to noun phrase technique.

We apply three-way ANOVA test to analyze the combine data of lab 1 and 2 and possible interaction of co-factors, shown in table VIII. In this experiment, System and Ability factors are considered. We observe a significant main effect for the System factor in overall completeness and overall correctness. This significant main effect is in favor of ATM system. The reason of main effect of system may be that students feel more comfortable and performed better in ATM system. We also observe that noun phrase

technique produced 6% more complete domain model as compared to category list technique. We do not found any significant interactions between System and Method, Ability and Method, System and Ability. Which is further elaborated on interaction plot.

Interaction plots highlight interaction in case of nonparallel lines, whereas parallel lines indicate no interaction at all. It can be seen from figure (a) and (b) that subjects with high and low ability performed similarly in both systems in case of completeness of domain model. However it can also be seen that subjects with high ability were able to make a more complete domain model in ATM system using noun phrasing technique. Regarding correctness it is observed from figure (c) and (d) that high and low ability students performed the same whether they used noun phrasing technique or category list in both software system.

Regarding required effort, we observed a significant time difference to complete the domain model in case of both systems. In both software systems students spent more time to complete a domain model using category list technique as compared to noun phrasing technique. This is also observed from interaction plot (e) and (f).

TABLE V. MANN-WHITNEY U TEST OF OVERALL COMPLETENESS

Dependent variable	Technique	Lab 1			Lab 2		
		Mean	Mean Rank	P-value	Mean	Mean Rank	P-value
Correct Concepts	Noun phrase	5.34	28.4	.021	7.08	32.3	.355
	Category List	5.81	38.5		7.41	36.6	
Correct Relationships	Noun phrase	3.42	34.8	.561	5.79	35.5	.664
	Category List	3.12	32.1		5.23	33.4	
Correct Attributes	Noun phrase	3.45	36.1	.251	3.28	45.8	.000
	Category List	2.66	30.8		1.882	23.1	
Correct Generalization	Noun phrase	2.36	37.5	.039	1.17	36.1	.445
	Category List	1.72	29.4		0.794	32.8	
Overall Completeness	Noun phrase	0.53	36.9	.144	0.29	40.7	.009
	Category List	0.46	30.05		0.23	28.2	

TABLE VII. MANN-WHITNEY U TEST OF OVERALL CORRECTNESS AND EFFORT

Dependent Variable	Technique	Lab 1			Lab 2		
		Mean	Mean Rank	P-value	Mean	Mean Rank	P-value
Useless Concepts	Noun phrase	1.15	36.8	.132	2.50	34.8	.880
	Category List	.88	30.1		2.38	34.1	
Missing Concepts	Noun phrase	2.65	28.4	.021	7.91	36.6	.355
	Category List	2.18	38.5		7.58	32.3	
Extra Relationships	Noun phrase	2.33	36.1	.254	3.02	34.8	.876
	Category List	2.00	30.8		3.05	34.1	
Missing Relationships	Noun phrase	5.57	32.1	.561	13.20	33.4	.664
	Category List	5.87	34.8		13.76	35.5	
Extra Attributes	Noun phrase	4.03	34.9	.404	2.00	45.0	.000
	Category List	3.69	31.0		.352	23.9	
Missing Attributes	Noun phrase	8.54	30.7	.323	12.41	23.1	.000
	Category List	9.33	35.3		15.11	45.8	
Overall Correctness	Noun phrase	4.66	32.97	.822	6.57	30.63	.105
	Category List	3.55	34.03		6.78	38.73	
Effort	Noun phrase	3.60	8.40	.000	23.9	6.36	.004
	Category List	26.8	18.75		41.0	13.8	

TABLE VIII. POWER ANALYSIS

Dependent variables	ATM				IBS			
	Observed Power	Mini. Effect size	Effect size	P_value	Observed Power	Mini. Effect size	Effect size	P_value
Overall Completeness	0.705	0.512	0.432	.144	--	--	--	.009
Overall correctness	0.891	--	0.077	0.822	0.599	0.526	0.376	.105

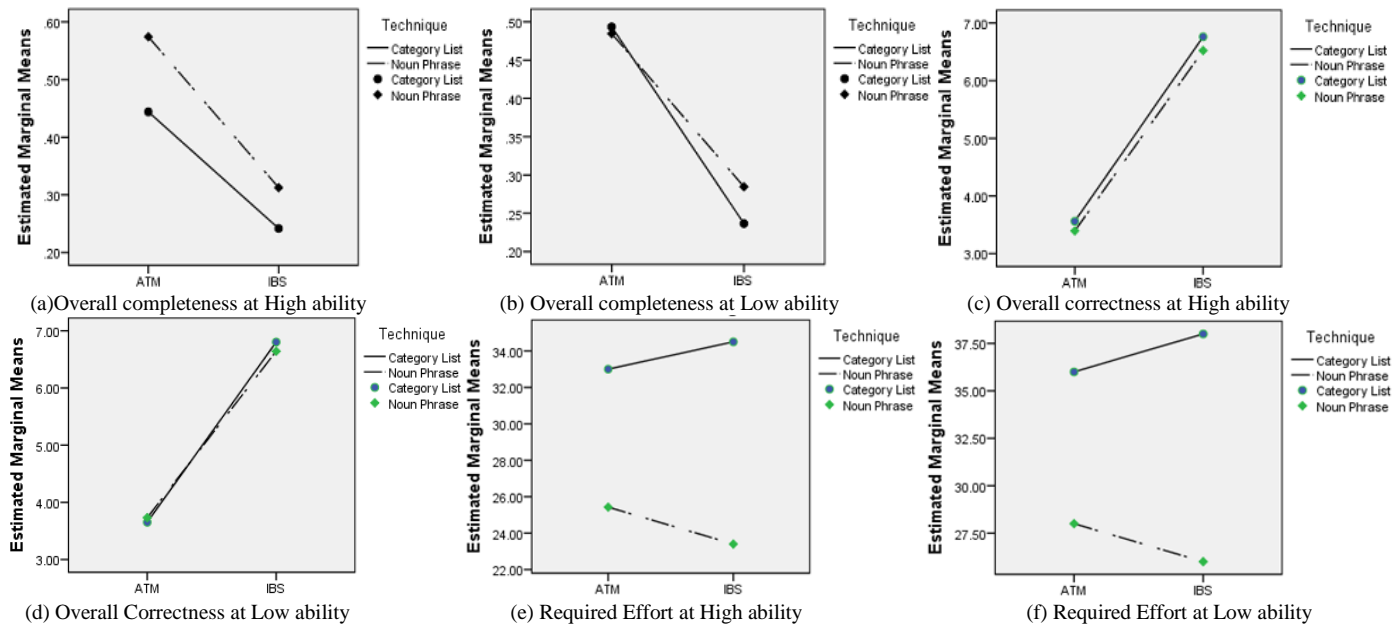


Fig. 1. Analysis results using Interaction Plots

A. Discussion

This experimental study investigates the effectiveness of noun phrase technique and category list technique on the quality of domain model. As already mentioned that the quality of domain model evaluated in terms of completeness, correctness and effort required for constructing the domain model. We summarize the significant results of a main hypothesis.

RQ1: What is the effect of noun phrase and category list technique on quality of the domain model?

This research question consists of number of hypothesis, and each hypothesis represents different domain model elements.

The statistically significant difference is only found between the number of Correct Concepts (CC) and Missing Concepts (MC) identified by noun phrase technique and category list technique when subjects deal with ATM system. In IBS system, statistically significant difference is found between the number of Correct Attribute (CA), Extra Attribute (EA) and Missing Attributes (MA). Those subjects who used noun phrase technique produce a large number of attributes. Some of the attributes are valid. But most of them are useless. This may be the reason that no specific guidelines were provided to extract attributes from requirement specification using noun phrase technique. After identification of noun and noun phrase, subjects skipped to check each and every noun phrase to decide whether it's a concept or attribute. In contrast, using category list subjects identified less valid attributes.

Regarding Overall completeness, a statistically significant difference is found in IBS system only. But both techniques show a lack of domain model completeness. Subjects

produced 29% and 23% complete domain model using noun phrase and category list technique respectively in IBS system. On the other hand, subjects produced almost 53% and 46% complete domain model using noun phrase and category list technique respectively in ATM system. From the combined analysis of both software systems, subjects produced 6% more complete domain model using noun phrase technique as compared to category list.

Regarding overall correctness dependent variables, no statistically significant difference is found in Overall Correctness. On average, subjects produced more extra concepts, relationships and attributes while IBS system using noun phrase technique. So we can say that using noun phrase technique, subjects identified a large number of noun phrases. Some of them were correct and mostly were useless. In addition, satisfactory results were not found while subjects modeled the ATM system. This may be due to the reason that

ATM system is common system and easier as compared to IBS system. A little statistically significant difference is found between the overall correctness in IBS system in favor of category list, but due to the low statistical power we cannot reject the null hypothesis about overall correctness.

RQ2: Which domain modeling technique required more effort to design a domain model?

Regarding required effort statistically significant difference is found between both groups to design domain model. Subjects used more time to design domain model using category list technique.

V. CONCLUSION

There are two basic techniques to model problem domain i.e. noun phrase and category list. In category list technique,

Larman [1] provided a list of candidate conceptual classes, which consists of many categories that are important to the business information system. Noun phrase technique is a grammatical analysis of use case description to recognize conceptual classes.

To evaluate the impact of category list and noun phrase technique on the quality of domain model an experiment was designed and conducted. The purpose of experiment was to investigate that which technique produces high quality domain model in terms of completeness, correctness and effort required to design a domain model.

According to the statistical tests results, category list technique produced more correct concepts in both software system but the difference is statistically significant only in ATM system. So, we can conclude that category list technique is best for identifying concepts which are important to the business world. It also avoids unnecessary concepts in the problem domain. Noun phrase technique is better for identifying attributes for concepts. Both techniques performed same in case of relationships. Overall subjects produce 6% more complete domain model using noun phrase technique however the results are statistically significant in IBS system only. There is no significant difference found between two techniques regarding overall correctness. Minimal significant difference is found in case of IBS system therefore due to low statistical power we cannot reject the null hypothesis. It is also observed that for known system, it does not matter which technique you are using. We suggest that the combined use of both techniques will lead to high quality domain model.

As a future direction the same experiment need to be executed in an industrial environment for more realistic results. In which professional developers are used as subjects and the scenario is also realistic instead of an exemplary one.

REFERENCES

- [1] C. Larman, Applying UML and Patterns, Prentice-Hall, 2004.
- [2] D. Rosenberg, Use Case Driven Object Modeling with UML – A Practical Approach, APRESS, Berkeley, USA, 2007.
- [3] D. R. K. Scott, Applying Use Case Driven Object Modeling with UML: An Annotated e- Commerce Example, Addison Wesley , 2001.
- [4] R. Offen, "Domain Understanding Is the Key to Successful System Development," journal of Requirements Engineering , vol. 7, no. 3, pp. 172-175, September 2002.
- [5] J. Evermann and Y. Wand, "Toward Formalizing Domain Modeling Semantics in Language Syntax," IEEE Transactions on Software Engineering, vol. 7, no. 1, p. 21 – 37, January 2005.
- [6] P. Stevens, Using UML: software engineering with objects and components, Pearson Education, 2006.
- [7] T. Yue, L. C. Briand and L. Yvan, "Facilitating the Transition from Use Case Models to Analysis Models: Approach and Experiments," ACM Transactions on Software Engineering and Methodology (TOSEM), vol. 22, no. 1, p. 5, February 2013.
- [8] S. Tiwari and A. Gupta, "Does increasing formalism in the use case template help?," in Proceedings of the 7th India Software Engineering Conference, 2014.
- [9] S. Tiwari and A. Gupta, "A controlled experiment to assess the effectiveness of eight use case templates.,," in 20th Asia- Pacific Software Engineering Conference (APSEC), 2013.
- [10] S. Espana, M. Ruiz and A. González, "Systematic derivation of conceptual models from requirements models: a controlled experiment.,," in IEEE Sixth International Conference on Research Challenges in Information Science (RCIS), Valencia, 2012.
- [11] B. Anda and D. I. Sjøberg, "Investigating the Role of Use Cases in the Construction of Class Diagrams," journal of Empirical Software Engineering, vol. 10, no. 3, p. 285 – 309, July 2005.
- [12] L. Briand, Y. Labiche and R. Madrazo-R, "An Experimental Evaluation of the Impact of System Sequence Diagrams and System Operation Contracts on the Quality of the Domain Model," in International Symposium on Empirical Software Engineering and Measurement (ESEM), Banff, 2011.
- [13] U. Erra, A. Portnova and G. Scanniello, "Comparing two communication media in use case modeling: results from a controlled experiment.,," in ACM- IEEE International Symposium on Empirical Software Engineering and Measurement, 2010.
- [14] C. Wohlin, P. Runeson, M. Host, M. C. Ohlsson, B. Regnell and A. Wesslen, Experimentation in Software Engineering, Springer Science & Business Media, 2012.
- [15] A. Poul and o. Jeff, Introduction to software testing, 2008.
- [16] Stevens, Perdita and R. J. Pooley, Using UML: software engineering with objects and components., Pearson Education, 2016.
- [17] E. R. Giden, ANOVA Repeated Measures, SAGE Publications.
- [18] G. Scanniello, C. Gravino and G. Tortora, Does the combined use of class and sequence diagrams improve the source code comprehension?: results from a controlled experiment, 12 Proceedings of the Second Edition of the International Workshop on Experiences and Empirical Studies in Software Modeling ACM, 2012.

A New Selection Operator - CSM in Genetic Algorithms for Solving the TSP

Wael Raef Alkhayri

Dept. of Computer Science
Fahed Al duwairi High School
Aljabereyah, Kuwait

Suhail Sami Owais

Dept. of Computer Science
Applied Science Private University
Amman, Jordan

Mohammad Shkoukani

Dept. of Computer Science
Applied Science Private University
Amman, Jordan

Abstract—Genetic Algorithms (GAs) is a type of local search that mimics biological evolution by taking a population of string, which encodes possible solutions and combines them based on fitness values to produce individuals that are fitter than others. One of the most important operators in Genetic Algorithm is the selection operator. A new selection operator has been proposed in this paper, which is called Clustering Selection Method (CSM). The proposed method was implemented and tested on the traveling salesman problem. The proposed CSM was tested and compared with other selection methods, such as random selection, roulette wheel selection and tournament selection methods. The results showed that the CSM has the best results since it reached the optimal path with only 8840 iterations and with minimum distance which was 79.7234 when the system has been applied for solving Traveling Salesman Problem (TSP) of 100 cities.

Keywords—Genetic Algorithm; Traveling Salesman Problem; Genetic Algorithm Operators; Clustering; Selection Operator

I. INTRODUCTION

Genetic Algorithm (GA) is one of the Evolutionary Algorithms (EAs), which is an optimization technique based on natural evolution [2, 4, 6]. GA has evolved into a powerful method for solving hard combinatorial optimization problems that uses a stochastic search technique. It is considered as one of the most important technologies in the search for the perfect choice of a set of solutions available for a particular design. GA proposed by John Holland and it relies on Darwin's principle of eclecticism [1, 6].

Traveling Salesman Problem (TSP) is one of the most intensively studied problems in computational mathematics, and it is a non-deterministic polynomial time problem [2]. TSP requires the most efficient path between the set of cities (i.e., least total distance). There is no general method of such solution known for TSP. TSP focused on an optimize path solution, where the salesman can take through each of the n cities and visits each city exactly only once and finally returning back to the home city [2, 7].

In GA process the selection method is the process of choosing parent(s) from the population for recombination, and mainly the selection step is preceded by the fitness value assignment which is based on the objective value. Where the performance of GA using differing selection methods is usually evaluated in terms of convergence rate and the number of generations to reach the optimal solution of a problem [5].

There are many types of selection methods used in GAs, in this paper the authors will propose a new selection operator.

This research paper proposes a new selection method in GA. The proposed method has been tested and compared with other selection methods which indicate that the new method increases the GA performance by reducing the number of generations.

The paper includes the following sections: introduction is the first part; GA discussed in the second section, TSP has been introduced in the third section. The fourth section explains the research problem statement, then the selection methods were described in the fifth section. The proposed method was discussed in section six, followed by the experimental test in section seven. Finally section eight clarified the conclusions.

II. GENETIC ALGORITHM

Genetic algorithm generally composed of two processes. The first process is the selection to select parents for reproduction to the next generation [4, 6]. The second process is the reproduction by manipulating the selected parents by crossover and mutation operators with respect to the fitness value for the new generation children [3].

Fig. 1 demonstrates the processes of Genetic algorithm [1], where GA consists of the following steps: [6, 7]

- 1) **[Start]** Generate random population of n chromosomes and encoding them.
- 2) **[Fitness]** Evaluate the fitness $f(x)$ of each chromosome x in the population.
- 3) **[New population]** Create a new population by repeating the following steps until the new population is complete:
 - a) **[Selection]** Select parents' chromosomes from a population according to their fitness.
 - b) **[Crossover]** is performed with a probability that crossover the selected parents to produce a new offspring
 - c) **[Mutation]** is performed with a probability that mutates new offspring.
 - d) **[Accepting]** place the new offspring in a new population.
 - e) **[Replace]** use newly generated population for a further run of algorithm

f) [Test] if the termination conditions are satisfied, then stop the algorithm, and return the best solution in current population

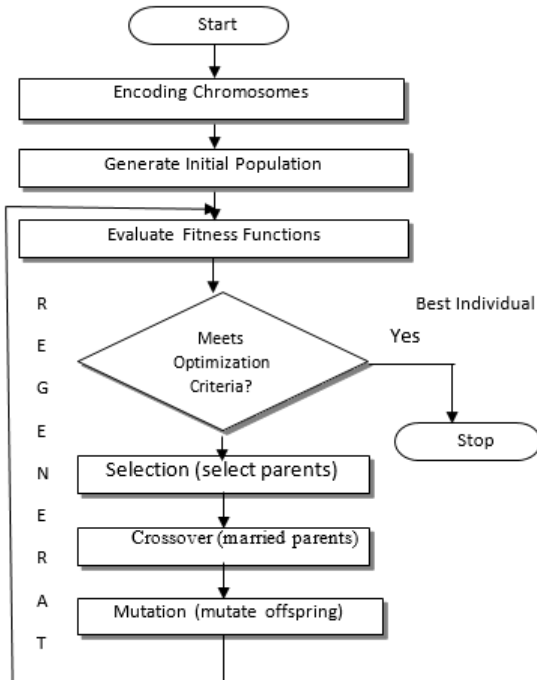


Fig. 1. Genetic Algorithm Processes [1]

III. TRAVELING SALESMAN PROBLEM

The Traveling Salesman Problem consists of a number of cities, where each pair of cities has an equivalent distance. The goal for the salesman is to visit all the cities. So, the total distance travelled will be minimized [7].

TSP is conceptually simple even though it is difficult to get an optimal solution which it is the shortest path between n cities. The major difficulty of this problem is the large number of possible paths; which is estimated by $\frac{(n-1)!}{2}$ for n cities. The problem will be considered when the number of cities increased, the numbers of variations of the valid paths are also increased. Several researchers try to find the optimal path for the TSP using GA [2, 7].

IV. PROBLEM STATEMENT

Parent selection for next generation is the most important operator in GA because the solution of a problem depends on that operator for reproduction; its importance is to choose the successive individuals in the population that will create offspring for the next generation.

There are many selection methods such as roulette, rank, etc. Some of these methods select the parents randomly while others select the parents by sorting them, then choose the highest fitness value parents the thing which is not guaranteed to get the optimal solution with a minimum number of generations. Therefore, the number of generations that evolve depends on whether an acceptable solution is reached as optimal or as the number of iterations is exceeded. Thus, for

the best performance expected is how to get the optimal solution using the minimum number of generations to ensure more efficiency and high speed.

V. SELECTION METHODS

The selection mechanism determines which individuals will be chosen for mating (reproduction) to reproduce new generation [3]. Where the main purpose of selection method is to select parents that can find the better parents in the population to reach the optimal solution.

The most important decision that should be taken into consideration in the selection method in GA is how to decide the most appropriate selection method that should increase the speed of evolution for reaching the optimal path with minimum distance in TSP [8].

There are many selection methods such as Roulette wheel selection; Tournament selection; Elitism Selection; Rank Selection; Stochastic universal sampling; Local selection; Truncation selection and others [8].

VI. PROPOSED CLUSTER SELECTION METHOD

The proposed method Clustering Selection Method (CSM) based on selecting parents from clusters with varying number of individual per each cluster, the cluster will be created by collecting all the closest individuals with respect to their fitness values together in the same cluster for all individuals in the population as shown in Fig. 2. Then parents will be chosen from the cluster that has more elements with respect to the highest or lowest fitness values depending on fitness function.

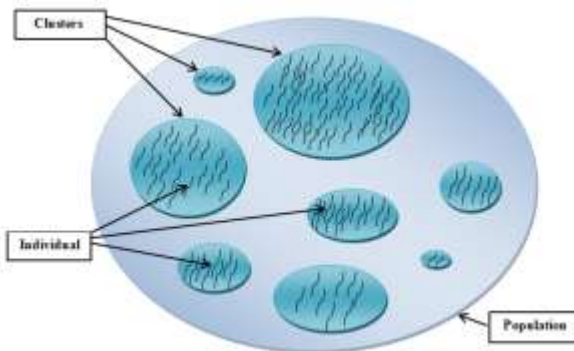


Fig. 2. Clustering individuals in population

The CSM starts by sorting the individuals in the population in ascending or descending order with respect to their fitness values. After that evaluate the ALFA value (α) by using the equation (1), using the standard deviation (STD) because it is the measure of spread out numbers are or how much the individuals in a population (pop) are scattered around the mean. The value of α will be used to determine the clusters, (that means to evaluate the amount of dispersion between individuals in the population). Where, a low standard deviation means that the data are tightly clustered; a high standard deviation means that they are widely scattered, and by using the square root for STD will give more chance to determine the closest individuals to create the clusters.

$$\text{ALFA} = \text{SQRT}(\text{STD}(\text{pop})) \quad (1)$$

After that, to divide the population for clusters with respect to the amount of dispersion between the individuals in the population. The population is divided based on α value that will creates many clusters, where each cluster contains different number of individuals.

Then, for each cluster, evaluate the Cluster_Value (CV) by calculating the STD and the differences (D) using equation (2). By computing the STD for all individuals in a cluster_sub_population (CS_pop) and by computing D between the fitness values for all individuals in the CS_pop. To avoid the division by zero (when the fitness's are equals in a CS_pop or there is no differences) by adding 1 to D.

$$CV = \frac{\sqrt{(STD(CS_pop)) * Count(CS_pop)}}{(D * CS_pop) + 1} \quad (2)$$

Then by comparing the CV values for all clusters, the "highest CV" means that this cluster contains the closest individuals with a high number of individuals which is our goal. Then we will consider this cluster with high CV to select the parents from it for the next generations. For maximization problem consider selecting the highest fitness values from this cluster as parents, and for minimization problem consider selecting the lowest fitness value as parents. As shown in Fig. 3.

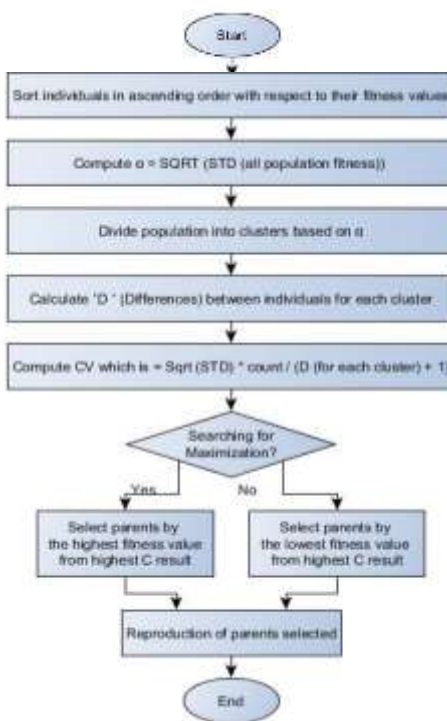


Fig. 3. The Proposed Cluster Selection Method (CSM)

VII. EXPERIMENTAL TEST

The proposed CSM was applied on GA and tested by using MATLAB for solving the TSP on a different number of cities 10, 20, 30, 40, 50, 60, 70, 80, 90 and 100 cities. The system was executed for 10,000 generations for each case or till finding the optimal path, with different selection methods listed in table 1.

TABLE I. SELECTION METHOD AND DESCRIPTION

No.	Method	Description
1	Random selection (Ga)	Random selection
2	Roulette Wheel	Roulette wheel selection
3	Tournament	Tournament selection
4	CSM	Clustering Selection Method using ALFA

TABLE 2. Demonstrates the final results from execution the system implementation with different selection methods and with the proposed CSM, where:

- Dis : the average distances between n cities.
- $O.D$: the order of distances in an ascending order from all paths, if there are any equal values they will have the same order.
- Itr : the average number of iterations to reach an optimal path.
- $O.I$: the order of iteration, if there are any equal values they will have the same order.
- $O.T$: the multiplication of O.I by O.D.

TABLE 3. summarized the final analysis for all cities from 10 – 100 for the TSP. It is obvious that the proposed CSM was the best method based on both values $Sum\ Dis$ and $Sum\ O.T$ because they have the minimum values than the other selection methods. Whereas the $Sum\ Itr$ was the best for the Roulette Wheel selection method.

Other test for the system were done for solving the TSP for 100 cities using three different selection methods in addition to the proposed one.

Fig. 4 shows the system result for the random selection method (Ga), where the optimal path distance was 80.5908 with 9159 iterations.

The distance for the optimal path was 79.9358 and iterations needed was 8864 for the Roulette Wheel selection method as shown in Fig. 5.

Tournament selection method reached the optimal path with 9458 iterations and with distance equals to 82.0521 as presented in Fig. 6.

The proposed method CSM has the best results since it reached the optimal path with only 8840 iterations and with

minimum distance which was 79.7234 as shown in Fig. 7.

TABLE II. SYSTEM RESULTS FOR SELECTION METHODS AND THE PROPOSED ONE

Method	10-Cities					20-Cities					30-Cities					40-Cities					50-Cities					
	Dis	O.D	Itr	O.I	O.T	Dis	O.D	Itr	O.I	O.T	Dis	O.D	Itr	O.I	O.T	Dis	O.D	Itr	O.I	O.T	Dis	O.D	Itr	O.I	O.T	
Ga	22.1	1	80.0	2	10	32.8	1	977.9	3	3	41.1	1	2157.4	9	9	48.1	1	3478.4	8	8	54.2	2	4456.5	3	6	
Roulette Wheel	22.1	1	98.8	4	8	32.8	1	1063.3	6	6	41.1	1	2042.9	4	4	48.1	1	3389.8	1	1	54.1	1	4436.8	2	2	
Tournament	22.1	1	78.5	1	4	32.8	1	1083	8	8	41.1	1	1952.7	1	1	48.2	2	3452.9	6	12	54.2	2	4536.5	7	14	
CSM	22.1	1	82.0	3	3	32.8	1	1081.1	7	7	41.2	2	1999.1	2	4	48.1	1	3470.8	7	7	54.1	1	4511.7	5	5	
60-Cities					70-Cities					80-Cities					90-Cities					100-Cities						
Method	Dis	O.D	Itr	O.I	O.T	Dis	O.D	Itr	O.I	O.T	Dis	O.D	Itr	O.I	O.T	Dis	O.D	Itr	O.I	O.T	Dis	O.D	Itr	O.I	O.T	
Ga	59.8	2	5559.9	8	16	65.1	2	6526.7	4	8	69.9	1	7622	2	2	74.4	4	8534.7	2	8	79.4	2	9160.0	5	10	
Roulette Wheel	59.8	2	5564.7	9	18	65.1	2	6559.7	7	14	70	2	7657.6	4	8	74.3	3	8587.5	5	15	79.5	3	9137.3	3	9	
Tournament	59.7	1	5330.9	1	1	65.1	2	6509.5	2	4	70	2	7648.2	3	6	74.3	3	8596.3	6	18	79.4	2	9136.2	2	4	
CSM	59.7	1	5474.9	6	6	65	1	6517.6	3	3	70	2	7713.5	7	14	74.3	3	8558.7	4	12	79.3	1	9160.0	5	5	

TABLE III. TOTAL ANALYSIS FOR ALL CITIES FROM 10 - 100

Method	Sum Dis	Sum Itr	Sum O.T
Ga	546.9387	48553.474	80
Roulette Wheel	546.9381	48538.407	85
Tournament	546.9383	48324.69	72
CSM	546.638	48569.338	66
Minimum	546.638	48324.69	66

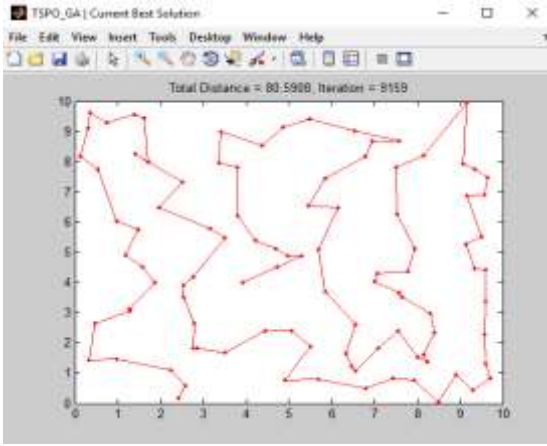


Fig. 4. Random selection method (Ga) results

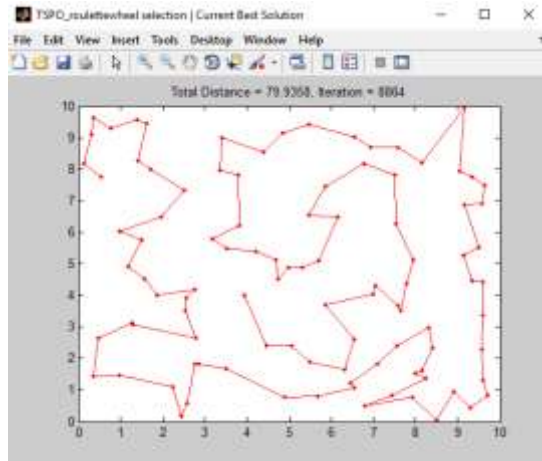


Fig. 5. Roulette Wheel selection method results

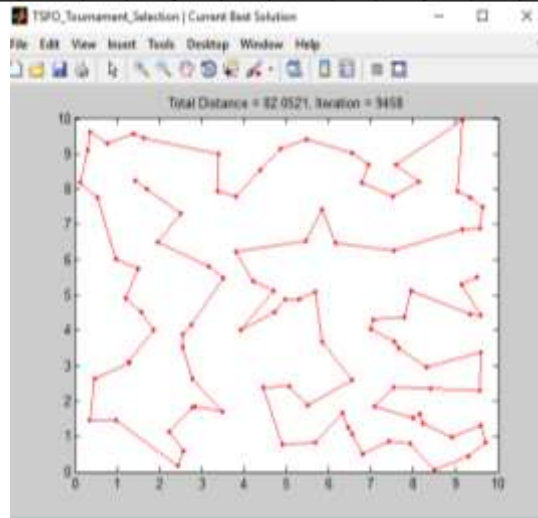


Fig. 6. Tournament selection method results

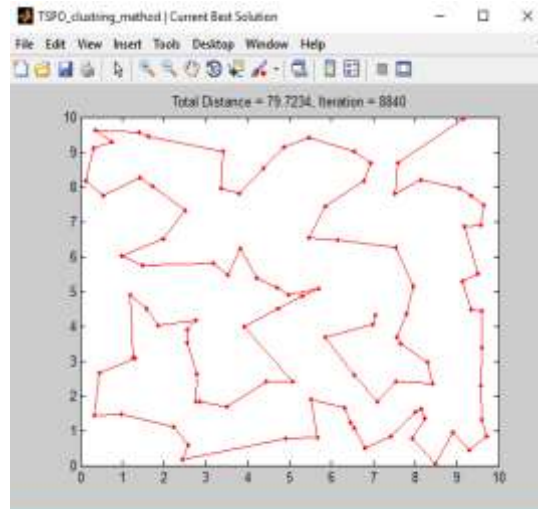


Fig. 7. The proposed CSM selection method results

Table 4 summarizes the results from the figures 4, 5, 6 and 7 which demonstrate the distances and the number of iterations for each method.

TABLE IV. SYSTEM RESULTS FOR 100 CITIES

Method	Distance	Iterations
Ga	80.5908	9159
Roulette Wheel	79.9358	8864
Tournament	82.0521	9458
CSM	79.7234	8840

VIII. CONCLUSION

GA has several operators for solving the optimization problems such as selection, crossover, and mutation operator. Where selection operator considered as one of the most important operators in GA process because it selects parents for recombination and effects on the other operators in the regeneration process.

A new selection method was proposed for selecting parents called Clustering Selection Method (CSM). It divides the population into clusters by collecting all the closest individuals' together with respect to their fitness values in the same cluster, and then selects parents (individuals) from clusters with varying number of individuals per each cluster. Then CSM will choose parents with highest or lowest fitness values based on the chosen cluster depending on Cluster_Value (CV).

TSP has been considered for a different number of cities to test the proposed method, the cities were 10, 20, 30, 40, 50, 70, 80, 90 and 100 cities. The system tested by running it 10,000 generations in each case till finding the best tour path, and the results showed that the proposed method was the best one among the other different types which are Random Selection, Roulette wheel selection, and Tournament selection method.

The result of the proposed CSM was as following: *Sum Dis* is 546.638 and *Sum O.T* is 66; which are the minimum values.

When the system has been tested again for 100 cities also the CSM has showed the best results since it reached the optimal path with minimum distance which was 79.7234 and

with only 8840 iterations.

For the future work authors can modify the proposed method by generating new equations for ALFA in order to get better results.

ACKNOWLEDGMENT

The authors are grateful to the Applied Science Private University, Amman, Jordan, for the financial support granted to this research project.

REFERENCES

- [1] S. Owais, V. Snasel, P. Kromer, and A. Abraham, "Survey: Using Genetic Algorithm Approach in Intrusion Detection Systems Techniques", 7th Computer Information Systems and Industrial Management Applications, IEEE, 2008, pp. 300-307, June 2008.
- [2] F. H. Khan, N. Khan, S. Inayatulla, And S. T. Nizami, "Solving ISP Problem by Using Genetic Algorithm", International Journal of Basic & Applied Sciences IJBAS-IJENS vol. 09, no. 10, 2009, pp. 55-60.
- [3] N. M. Razali, and J. Geraghty, "Genetic Algorithm Performance with Different Selection Strategies in Solving TSP", Proceedings of the World Congress on Engineering, 2011, London, U.K., vol. II, July 2011.
- [4] S. Karakatić, and V. Podgorelec, "A survey of genetic algorithms for solving multi depot vehicle routing problem", Applied Soft Computing, vol. 27, pp. 519–532, 2015.
- [5] A. Sharma, and A. Mehta, "Review Paper of Various Selection Methods in Genetic Algorithm", International Journal of Advanced Research in Computer Science and Software Engineering, vol. 3, no 7, July 2013.
- [6] S. Owais, and J. Atoum, "New Method for Mutation Operator in Genetic Algorithm", Journal of Association for the Advancement of Modelling & Simulation Techniques in Enterprises (A.M.S.E), D Computer Science and Statistics", vol. 14 , no. 2, pp. 17-26, 2009.
- [7] S. Khattar, and Dr.P. Gosawmi, "An Efficient Solution of Travelling Salesman Problem Using Genetic Algorithm", International Journal of Advanced Research in Computer Science and Software Engineering, vol. 4, no. 5, 2014, pp. 656-660.
- [8] C. Chudasama, S. M. Shah, and M. Panchal, "Comparison of Parents Selection Methods of Genetic Algorithm for TSP" , Proceedings published by International Journal of Computer Applications, International Conference on Computer Communication and Networks CSI-COMNET-2011, pp. 85-87, 2011.

Automatic Detection of Omega Signals Captured by the Poynting Flux Analyzer (PFX) on Board the Akebono Satellite

I Made Agus Dwi Suarjaya, Yoshiya Kasahara, and Yoshitaka Goto

Graduate School of Natural Sci. and Tech.
Kanazawa University,
Kakuma-machi, Kanazawa 920-1192, Japan

Abstract—The Akebono satellite was launched in 1989 to observe the Earth's magnetosphere and plasmasphere. Omega was a navigation system with 8 ground stations transmitter and had transmission pattern that repeats every 10 s. From 1989 to 1997, the PFX on board the Akebono satellite received signals at 10.2 kHz from these stations. Huge amounts of PFX data became valuable for studying the propagation characteristics of VLF waves in the ionosphere and plasmasphere. In this study, we introduce a method for automatic detection of Omega signals from the PFX data in a systematic way, it involves identifying a transmission station, calculating the delay time, and estimating the signal intensity. We show the reliability of the automatic detection system where we able to detect the omega signal and confirmed its propagation to the opposite hemisphere along the Earth's magnetic field lines. For more than three years (39 months), we detected 43,734 and 111,049 signals in the magnetic and electric field, respectively, and demonstrated that the proposed method is powerful enough for the statistical analyses.

Keywords—Auto-detection; Satellite; Signal processing; Wave Propagation; Plasmasphere

I. INTRODUCTION

The Akebono (EXOS-D) satellite was launched at 23:30 UT on February 21, 1989 to observe the Earth's magnetosphere and plasmasphere. This satellite has onboard VLF instruments and Poynting flux Analyzer (PFX) is one of the subsystems. The PFX is a waveform receiver that measures two components of electric fields and three components of magnetic fields with a band-width of 50 Hz in a frequency range from 100 Hz to 12.75 kHz [1]. Omega was a navigation system with 8 ground stations transmitter and had transmission pattern repeating every 10 s. Each station transmitted a different pattern of frequency but had a common frequency at 10.2 kHz. The Omega system was terminated in 1997 in favor of the GPS system.

From 1989 to 1997, the PFX on board the Akebono satellite received signals at 10.2 kHz from the eight stations and huge amounts of PFX data became valuable to study the propagation characteristics of VLF waves in the ionosphere and plasmasphere. Once the Omega signals are radiated in the plasmasphere permeating through the ionosphere, they propagate as a whistler mode wave in the plasma. The omega signal data captured by the PFX on board the Akebono has been used to estimate global plasmaspheric electron density. In

particular, a tomographic electron density profile could be determined by calculating the Omega signal propagation path using the ray tracing method. This method could estimate the propagation path within one hour of single satellite observations [2]. The algorithm was further improved with a flexible method and novel stochastic algorithm. This enabled estimates separate from the effects of the ionosphere and plasmasphere [3]. Goto et al. (2003) demonstrated that electron density profile could be drastically changed day by day depending on magnetic activities during a magnetic storm.

Because the transmission pattern of frequency, time, and the location of each station is known, we can easily distinguish the signal source. We can then determine many propagation properties such as attenuation ratio, propagation direction, propagation time (delay time) from the transmission station, and the observation point along the satellite trajectories. Such parameters depend strongly on the plasma parameters along the propagation path. Therefore it is worth to analyze such propagation properties statistically using the long term observation data.

Processing manually all of the data from 1989 to 1997, however, will take a lot of time. Furthermore, more processes and analyses will be needed to see different results such as analysis based on magnetic local time, seasonal propagation analysis, and yearly propagation analysis. Our automatic detection method makes all of the analysis processes simpler and is able to produce most of the required result faster and efficient. This study discusses the automatic detection methods for faster analysis of huge amounts of PFX data to study the propagation characteristics of VLF waves which, in this case, is the Omega signal. An outline of the paper follows. In the second section, we present the technique we are using for automatic detection. It involves identifying a transmission station, calculating the delay time, and estimating the signal intensity. In the third section, we discuss the result of this analysis using an event study and statistical study for the Norway station. In the final section, we present conclusions and summarize our research.

II. DATA ANALYSIS TECHNIQUE

A. Omega Signal

The Omega signal is very low frequency (VLF) signal between 10 and 14 kHz transmitted by the Omega navigation

system that was operational in 1971. Before it shut down in 1997, its purpose was to provide a navigational aid for domestic aviation and oceanic shipping. Omega receiver determines location based on the phase of the signal from two or more of the Omega stations [5]. This Omega signal was transmitted from eight ground stations with each station transmitting a unique pattern, based on which our analyzer software could determine the source of the signal. The location of these Omega stations are Norway (NW), Liberia (LB), Hawaii (HW), North Dakota (ND), La Reunion Island (LR), Argentina (AZ), Australia (AS), and Japan (JP). There are four common frequencies of the Omega signal (10.2, 13.6, 11.33, and 11.05 kHz) with one unique frequency for each station. The transmission pattern at 10.2 kHz from each station is shown in Fig. 1. Each station transmit 10.2 kHz signal at different timing. There is an interval of 0.2 s separating each of the eight transmissions, with variations in the duration for each station.

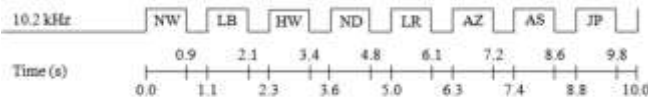


Fig. 1. Transmission Pattern of the 10.2 kHz Omega Signal. There are four common frequencies of the Omega signal (10.2, 13.6, 11.33, and 11.05 kHz) with one unique frequency for each station. There is an interval of 0.2 s separating each of the eight transmissions, with variations in the duration for each station

B. PFX Subsystem of the Akebono Satellite

The PFX subsystem of the Akebono satellite measures 3 components of magnetic fields (B_x , B_y , and B_z) and 2 components of electric field (E_x and E_y). It's comprised five-channel triple-super-heterodyne receivers with an output bandwidth of 50 Hz. It also had a local oscillator that could be stepped or fixed at a specific center frequency with a range from 100 Hz to 12.75 kHz and equipped with Wide Dynamic Range Amplifier (WIDA) hybrid IC to control the gain in the dynamic range for more than 80 dB [1]. WIDA hybrid IC will check automatically averaged signal level every 0.5 seconds and the gain of each channel is changed independently in 25 dB steps from 0 dB up to 75 dB. For our study, we use B_x , B_y , B_z , E_x and E_y in static coordinate system converted from B_1 , B_2 , B_3 , E_x and E_y obtained in the antenna coordinate system fixed to the spinning satellite as defined in Kimura et al. (1990). The static coordinate system is referred to the direction of the geomagnetic field (the geomagnetic field line is in the X-Z plane and Y is perpendicular to the X-Z plane) and the direction of the sun (Z-axis).

Fig. 2 shows the 10 s raw waveform of the PFX data at 18:05:29.503 UT on December 14, 1989. In the figure, we can observe the raised intensity from 18:05:33.500 UT to 18:05:34.900 UT, which in this case is the Omega signal from the Australia station. In the electric field components of E_x and E_y from 18:05:33.800 UT to 18:05:34.300 UT, the PFX receivers both for E_x and E_y were saturated as indicated by the red arrows, because an intense Omega signal was captured. But the gain of these channels was immediately adopted adequately at 18:05:33.800 UT thanks to the WIDA IC. The WIDA IC worked independently for each five components. Therefore, all channels are not necessarily saturated but some components of

the magnetic and/or electric field were occasionally saturated. During the period of saturation, signal intensity is apparently clipped and we cannot estimate absolute intensity. Then we define 'raise time' of Omega signal at the beginning point of the signal, while we use the data 0.5 seconds after the raise time when we evaluate 'absolute intensity' of the signals to exclude the saturated data. The detailed detection algorithm to derive raise time and intensity is described in the next section.

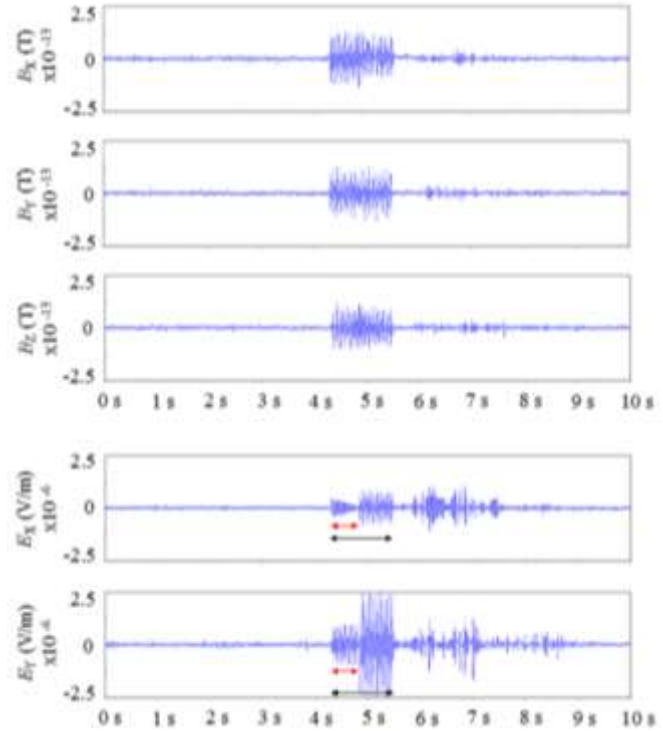


Fig. 2. Raw PFX waveform at 18:05:29.503 UT on December 14, 1989. We can observe the raised intensity from 18:05:33.500 UT to 18:05:34.900 UT, which in this case is the Omega signal from the Australia station. In the electric field components of E_x and E_y from 18:05:33.800 UT to 18:05:34.300 UT, we can observe a 0.5 s saturated intensity signal caused by the WIDA IC

To measure Omega signals, we selected and analyzed the PFX data when its center frequency was fixed at 10.2 kHz. The PFX data was recorded in Common Data Format (CDF) developed by the National Space Science Data Center (NSSDC) at NASA [4]. This ensured standardized read/write interfaces for multiple programming languages and software. The waveforms measured by the PFX were originally two components of the electric field in the spin plane and three components of the magnetic field in the B_1 , B_2 and B_3 directions. These waveforms were orthogonal with respect to each other but different from satellite coordinates. These waveforms were calibrated, converted into static satellite coordinates, and stored in the CDF files. One month of PFX data represented 5–10 GB and one year of data consumed approximately 60–90 GB. In total, the amount of data from 1989 to 1997 is approximately 570 GB.

The PFX data is stored as waveforms sampled at rate of 320 Hz. For FFT analysis, we used FFT size of 32. Therefore, the time resolution was 100 ms and the frequency resolution was 10 Hz. To improve the accuracy of delay time detection,

we applied an overlap-add FFT that moves over three sample points for a higher time resolution (~ 9.4 ms) when the first signal was detected. Although PFX measured only two components of the electric field, we could derive another component (E_Z) if we assumed the measured signal as a single plane wave [5]. This is expressed using (1).

$$E_Z = -\frac{E_X B_X + E_Y B_Y}{B_Z} \quad (1)$$

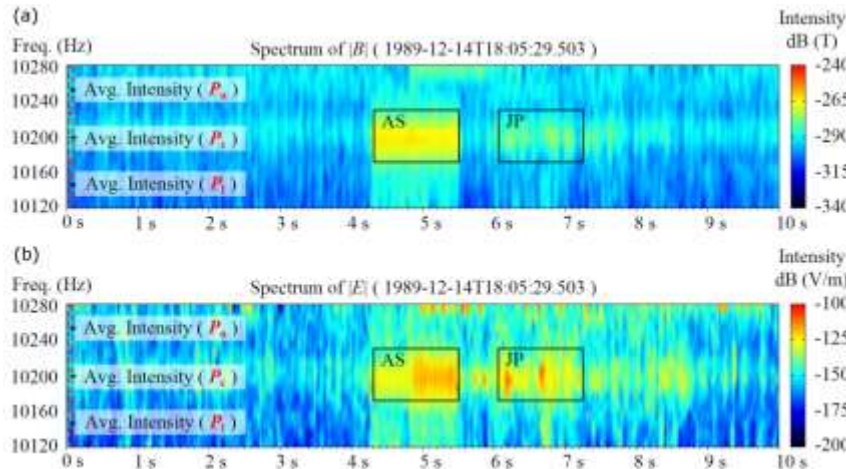


Fig. 3. Spectrum of the Omega signal start at 18:05:29.503 UT on December 14, 1989. We separated it into three frequency area bins (P_c , P_u , and P_l) to compare ambient noise and Omega signal intensity in the magnetic field (a) and in the electric field (b)

III. DETECTION ALGORITHM

A. Detection of the Omega Signal

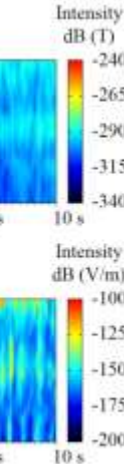
We first estimated the raise time of each signal by comparing the average intensity of specific time frame to the threshold level, expecting a sudden increase in intensity. Second, we determined the transmission station by comparing the raise time with the transmission patterns of the eight Omega stations. At 0000 UT on January 1, 1972, the Omega and UTC scales were identical. However, we subsequently had to conduct a leap seconds calculation to synchronize the omega time and UTC because the Omega had no leap seconds like the UTC [5]. On December 31, 1989, the Omega time led the UTC by 14 s.

The threshold level we use in the detection method, is based on the comparison of ambient noise level and Omega signal intensity. In Fig. 3, we show parameters for the comparison of ambient noise and Omega signal intensity visualized on a spectrogram of 10 s of PFX data in the magnetic field (a) and in the electric field (b) beginning at 18:05:29.503 UT on December 14, 1989 when the Omega signal from Australia and Japan were expected to be received. The spectrogram in Fig. 3 consists of 16 bins in frequency ($\Delta f = 10\text{Hz/bin}$) and 1057 bins in time ($\Delta t = \sim 9.4\text{ms/bin}$). We separated it into three frequency area bins, where P_c denotes the center frequency (consisting of 5 bins in frequency and 1 bin in time), P_u denotes the upper frequency (consisting of 5 bins in frequency and 1 bin in time), and P_l denotes the lower frequency (consisting of 6 bins in frequency and 1 bin in time).

After we calculated the E_Z component, we calculated the absolute intensity of the electric field $|E|$ as shown in (2). In the same way, we also calculated the absolute intensity of the magnetic field $|B|$ using (3). We use dB (V/m) for the electric field measurement unit and dB (T) for the magnetic field measurement unit.

$$|E| = \sqrt{E_x^2 + E_y^2 + E_z^2} \quad (2)$$

$$|B| = \sqrt{B_x^2 + B_y^2 + B_z^2} \quad (3)$$



Based on extracted data from the analyzer, Fig. 4 compares ambient noise and Omega signal intensity in the magnetic field at 18:05:29.503 UT on December 14, 1989. We can see the raised intensity level on P_c compared with P_u and P_l . This raised intensity level occurred within the expected transmission time of the Australia station (from approximately 18:05:33.700 UT to 18:05:34.900 UT) and the Japan station (from approximately 18:05:35.500 UT to 18:05:36.500 UT).

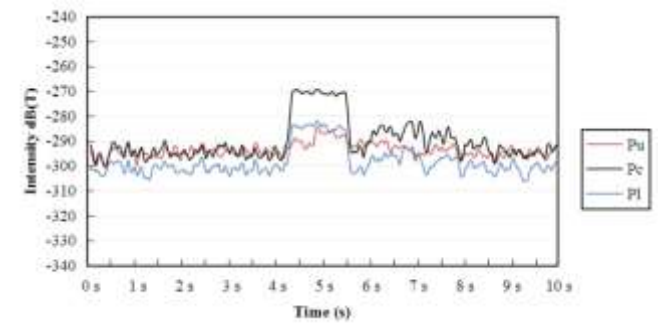


Fig. 4. Comparison of Omega signal intensity and ambient noise level in the magnetic field. Raised intensity level occurred within the expected transmission time of the Australia station (from approximately 18:05:33.700 UT to 18:05:34.900 UT) and the Japan station (from approximately 18:05:35.500 UT to 18:05:36.500 UT)

A comparison of ambient noise and omega signal intensity in the electric field can be seen in Fig. 5, which is based on extracted data from the analyzer at 18:05:29.503 UT on December 14, 1989. In this case, the signal was saturated from

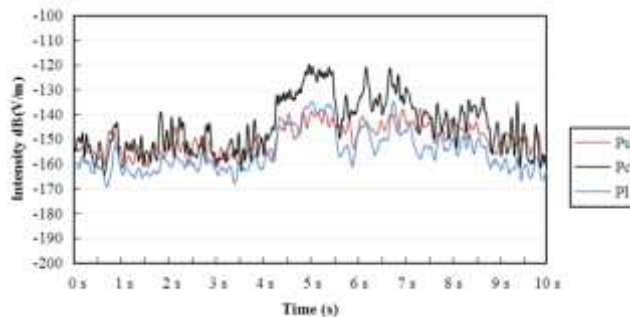


Fig. 5. Comparison of Omega signal intensity and ambient noise level in the electric field. The signal was saturated from approximately 18:05:33.800 UT to 18:05:34.300 UT because the WIDA IC was controlling the gain of receiver

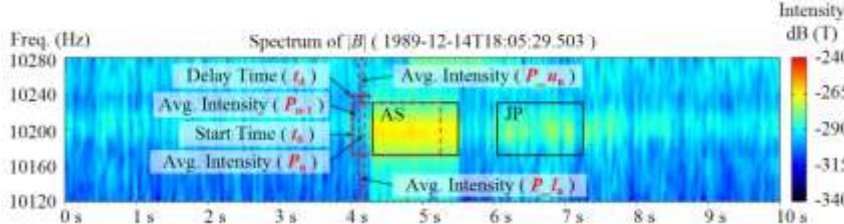


Fig. 6. Parameters used in the delay time detection method. Delay time (t_d) calculated by detecting the raise time of intensity (P_n) and compare it with surrounding frequency (P_{u_n} and P_{l_n}) from start time transmission (t_0) during duration time of each station

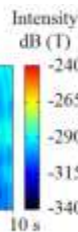
$$t_d = \begin{cases} t_n - t_0 & \text{if } (P_{u_n} + P_{l_n})/2 + T_p < P_n \text{ and } (P_n - P_{n-1}) > T_p \\ 0 & \text{otherwise} \end{cases} \quad (4)$$

where T_p denotes the intensity threshold (8 dB), t_d denotes delay time in seconds, P_n denotes intensity strength of center frequency consists of 5 bins in frequency ($\Delta f = 10\text{Hz/bin}$) and 20 bins in time ($\Delta t = \sim 9.4\text{ms/bin}$), P_{u_n} denotes intensity strength of upper frequency consists of 5 bins in frequency ($\Delta f = 10\text{Hz/bin}$) and 20 bins in time ($\Delta t = \sim 9.4\text{ms/bin}$), P_{l_n} denotes intensity strength of lower frequency consists of 5 bins in frequency ($\Delta f = 10\text{Hz/bin}$) and 20 bins in time ($\Delta t = \sim 9.4\text{ms/bin}$), t_0 denotes start time of the station's transmission, t_n denotes start time of P_n , and n denotes the iteration number for every 1 bin in time ($\Delta t = \sim 9.4\text{ms/bin}$). In Fig. 6, we show the parameters used for the delay time detection visualized on a spectrogram of 10 s of PFX data in the magnetic field start at 18:05:29.503 UT on December 14, 1989, when the Omega signal from Australia and Japan were expected to be received.

approximately 18:05:33.800 UT to 18:05:34.300 UT because the WIDA IC was controlling the gain of receiver. In this case, we need to calculate the intensity of the saturated signal after 0.5 s. We recognized this saturation by calculating and comparing each each signals for any sudden change in the intensity of the constant duration. In this case, the WIDA IC will affect the next 0.5 s sample for increased gain when activated. This type of saturated signal could affect any of the 5 components measured by the PFX subsystem because the WIDA IC works independently for each component.

B. Calculation of Signal Intensity and Delay Time

We calculated the delay time of the signal by detecting the raise time of intensity and compare it with surrounding frequency from start time transmission during each station transmission duration as shown in (4).



In the next step, we determined signal existence by comparing the intensity of the expected duration of the Omega signal with the surrounding intensity (higher and lower frequency points of the center frequency). We determined signal existence and derived the signal intensity (P_{os}) by using (5)

$$P_{os} = \begin{cases} P_s & \text{if } (P_a + P_b)/2 + T_p < P_s \text{ and } (P_w + T_w) < P_s \\ 0 & \text{otherwise} \end{cases} \quad (5)$$

where P_a denotes the intensity strength of the upper frequency bins in decibels, P_b denotes the intensity strength of lower frequency bins in decibels, P_s denotes the intensity strength of center frequency bins in decibels. P_a , P_b , and P_s consists of 5 bins in frequency ($\Delta f = 10\text{Hz/bin}$) and variation (128 bins for Australia and 106 bins for Japan) of bins in time ($\Delta t = \sim 9.4\text{ms/bin}$) depends on the duration of the Omega signal for each station. P_w denotes intensity strength of 16 bins in frequency ($\Delta f = 10\text{Hz/bin}$) and 1057 bins in time ($\Delta t = \sim 9.4\text{ms/bin}$) for every 10 s duration (1 window) in decibels.

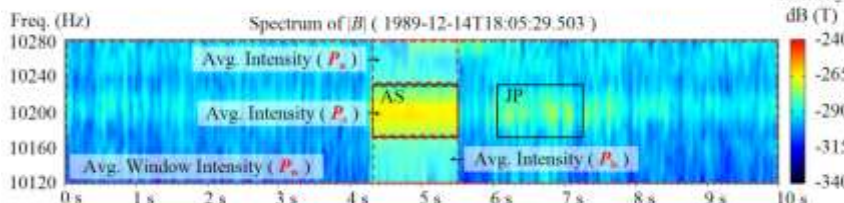


Fig. 7. Parameters used for discrimination and intensity calculations. The signal existence determined by comparing the average intensity of the expected duration of the Omega signal (P_s) with the surrounding frequency (P_a and P_b) and the ambient noise of 10 seconds duration or 1 window (P_w)

In Fig. 7, we show the parameters used for the calculation of the signal visualized on the same spectrogram as shown in Fig. 6. In Fig. 7, for example, P_s has total of 640 bins (5 bins in

frequency and 128 bins in time) because the Omega signal from Australia station has 1.2 s in duration and we used overlap-add FFT. We defined two intensity thresholds T_p and

T_W , where T_P had a fixed value of 8 dB and T_W had a fixed value of 5 dB.

C. PFX Analyzer

We developed software to analyze the Omega signal data measured by the Akebono from 1989 to 1997. The software was written in Java programming language. We can interactively check the waveform measured by the PFX one by one for an event study. It also enables us to detect Omega signals automatically for several months or years and then show the results of electric and magnetic intensity and delay time for specific locations of longitude, latitude, and altitude on

geomagnetic and geographic maps of the Earth. Analyses of local time dependence are also available. An overview of the analyzer software is shown in Fig. 8.

This analyzer connects to the Akebono orbit database and can be used to manually analyze each signal in real time by manipulating the navigation panel. To automatically analyze the CDF files for one month of data, we need 6–9 hours of processing time using an Intel Quad Core with a 3.324 GHz CPU and 4 GB of memory. The computational time depends on the number of available signal data and data size. Depending on the computer specifications, it is possible to run multiple instances of the analyzer to speed up the process.

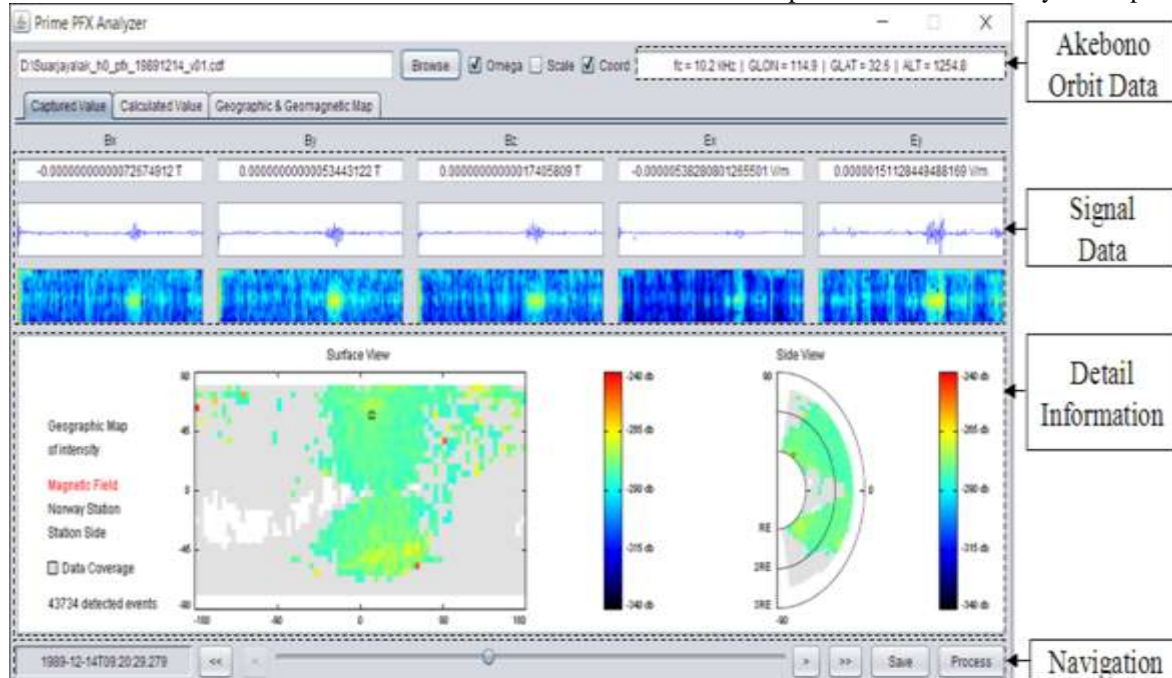


Fig. 8. Overview of the PFX Analyzer, written in Java programming language. It enables us to detect Omega signals automatically for several months or years and then show the results on geomagnetic and geographic maps of the Earth

D. Handling of Error Detection and Evaluation of the System

For accurate results, we also applied error detection handling and a data smoothing process. It is possible for the analyzer to detect a high intensity noise as Omega signal. To handle this type of error detection, we applied a function that ignores a signal that is not detected continuously for a specific duration of time. This is currently set at 40 s. For example, when the signal is only detected for the first 30 s and then disappears in the next 10 s, the analyzer will ignore the signal

and decide there is no signal detected for the entire 40 s. This handling occurs in the background of the analyzer software and the analyzer will still show a rectangle representing the detected signal.

We also applied a time smoothing algorithm to handle sudden peaks of delay time that may reflect false detection. This was accomplished by using the average of every two delay time value of detected signals. We expect to obtain more reliable results using improved detection data.

IV. RESULT OF ANALYSES

A. Event Study

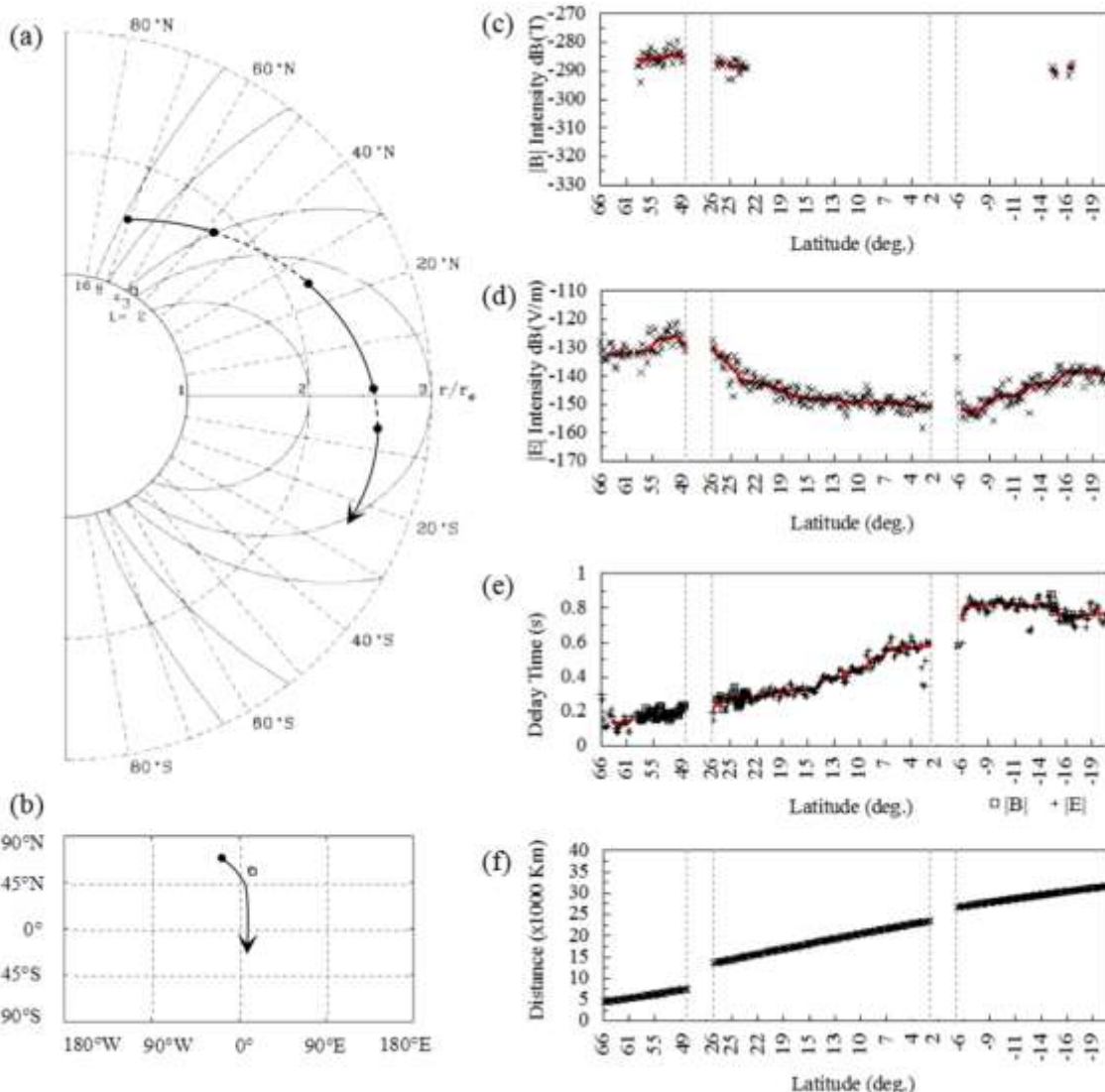


Fig. 9. Trajectory of Akebono, and observed Omega signal of Norway station from 08:29:39.802 UT to 09:55:33.842 UT on October 18, 1989. The PFX data is not available between latitude 49°N to 26°N and 2°N to 6°S and shown as dashed line. Left panels show trajectory line (a) (b) of the satellite. Right panels show (c) absolute intensities of Omega signal in the magnetic fields, (d) absolute intensities of Omega signal in the electric fields, (e) delay times of Omega signal, and (f) the approximate distance of the propagation path to the observation point

Fig. 9 (a) and 9 (b) shows 1.5 hours of trajectory of the Akebono from the northern to southern hemisphere from 08:29:39.802 UT to 09:55:33.842 UT on October 18, 1989. During this period, Omega signals from the Norway station were continuously observed and 344 signals were detected in the electric field and 63 signals were detected in the magnetic field. The location of the Norway station is also shown as a small square in Fig. 9 (a) and (b). The PFX data is not available between latitude 49°N to 26°N and 2°N to 6°S. This unavailable of data is shown as dashed lines in Fig. 9 (a).

Fig. 9 (c) shows absolute intensities of Omega signal in the magnetic fields, Fig. 9 (d) shows absolute intensities of Omega signal in the electric fields, and Fig. 9 (e) shows delay time of the Omega signals. The red curves indicate moving median over 20 points (detected events). The intensity of the magnetic

field and electric field of the Omega signal is showing higher intensity in the northern hemisphere where the Norway station was located. The Norway station was located at latitude 56.42°N, and we can see higher signal intensity around -285 dB (T) for the magnetic field and approximately -125 dB (V/m) for the electrical field. The intensity then becomes lower for the electric field or disappears for the magnetic field near the equator at latitude 0°. The signal for the electric field then increased at approximately -145 dB (V/m) near the southern hemisphere because the signal could propagate along the Earth's magnetic field. The delay time around 0.2 s in the northern hemisphere where the Norway station was located and then increased to more than 0.5 s as the trajectory of the Akebono satellite got closer to the southern hemisphere. This occurred because propagation along the Earth's magnetic field

required more time compared with a direct propagation path. Fig. 9 (f) shows the approximate distance based on a simple magnetic dipole model for the propagation path of the signal

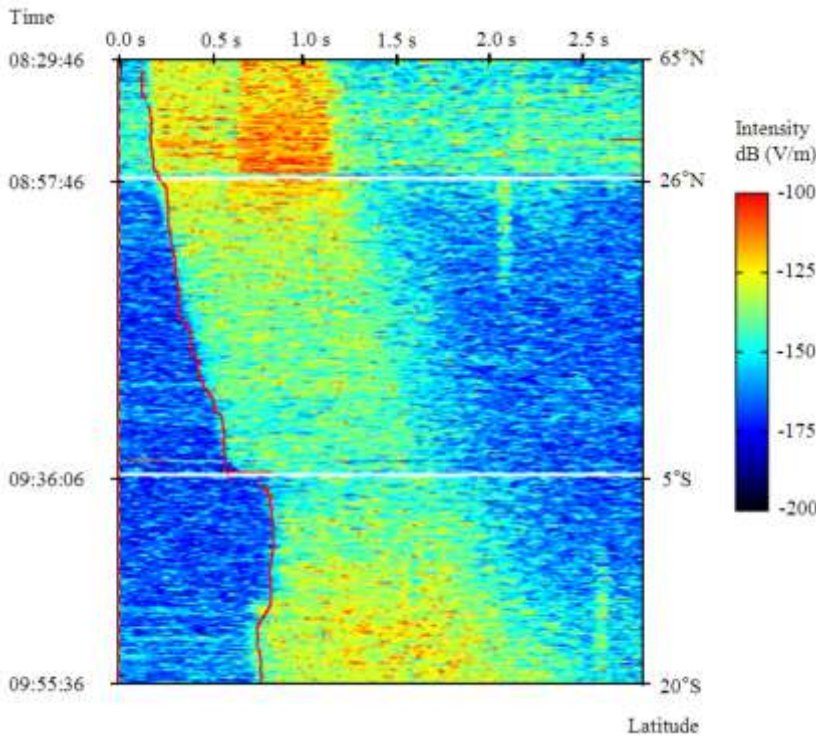


Fig. 10. Sliced Center Frequency in the electric field from 08:29:46 UT to 09:55:36 UT on October 18, 1989. The transmission time of Norway station was 08:29:46 UT and repeated every 10 seconds. Signal from Norway expected to be 0.9 second in duration. Intensification at $t=0.6$ in a period from 08:29:46 UT to 08:57:46 UT was caused by the WIDA IC

For comparison, we calculated the sliced center frequency of each signal in the Electric Field from 08:29:46 UT to 09:55:36 UT on October 18, 1989. We plotted only 1 bin ($\Delta f = 10\text{Hz/bin}$, $\Delta t = \sim 9.4\text{ms/bin}$) of the center frequency spectrum ($\sim 10.2\text{ kHz}$) and arranged it as shown in the Fig. 10. The transmission time of Norway station start at 08:29:46 UT and repeated every 10 seconds. We projected the red curves of trend line in Fig. 9 (e) to Fig. 10. This confirms that the automatic detection of our analyzer produced quite reliable results compared with manual analysis. Deviation occurred at few parts because of false result by multiple high intensity noises and affected moving median of the trend line. Based on the Omega system transmission pattern, we expected signal from Norway should be 0.9 second in duration. Intensification at $t=0.6$ in a period from 08:29:46 UT to 08:57:46 UT was caused by the WIDA IC. Because of its weakness, WIDA IC may cause false intensification of signal as seen at $t=2.05$ in a period from 08:57:46 UT to 09:36:06 UT. The effects of WIDA IC can be seen clearly in Fig. 6. Signal from Liberia station was expected to be delayed and might be received after $t=1.0$. In period from 09:36:06 UT to 09:55:36 UT, overlapped signal between Norway and Liberia is possible.

B. Statistical Study

The results of more than three years data of Norway station (October 1989 to December 1992) is shown in Fig. 11. The longitudinal axis consists of 72 bins of 5° for each bin; the latitudinal axis consist of 36 bins of 5° for each bin; and the

along the Earth's magnetic field. The calculated distance was from the Norway station to the observation point.

altitudinal axis consist of 20 bins of 637.1 Km for each bin. The rectangle on the map shows the location of the transmission station at a longitude of 13.14°E and latitude of 56.42°N . The gray color bin on the map shows the availability of PFX data in the area. However, no Omega signal was detected by the analyzer. The white color bin on the map shows that the PFX data is not available for that location. The meridian plane map shows the average intensity coverage of 10° to the east and 10° to the west from the station. From the figure, We can clearly demonstrate that Omega signal propagated nearly along the geomagnetic field line to the southern hemisphere. The intensity of the signal near the equator shows low intensity at high altitude and no signal at lower altitude. We concluded that this unique propagation is caused primarily by the location of the transmission station, the Earth's magnetic field, and global electron density. Previous study about global electron density had analyzed normal wave direction and delay time of the Omega signal [7][8] and also deduced from whistlers [9][10][11]. For more than three years (39 months), we observed 43,734 detected signals in the magnetic field and 111,049 detected signals in the electric field.

V. CONCLUSIONS

In this study, we developed an advanced detection algorithm to continuously process large amounts of data measured for several years by the PFX subsystem on board the Akebono satellite. The algorithm enables us to distinguish

noise and real omega signals and also detect errors in order to produce more accurate results. When compared with manual analysis, automatic detection can be accomplished with short periods of processing time and does not require human

intervention in the process. We demonstrated that the proposed method is powerful enough for the statistical analyses and further study of the propagation patterns of VLF waves with regard to the Earth's magnetic field and global electron density.

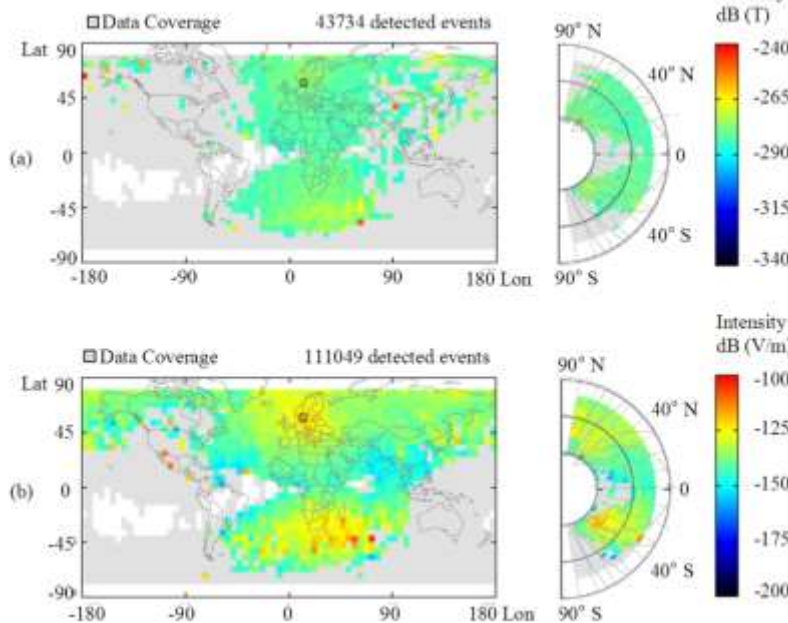


Fig. 11. Omega Signal Propagation of Norway Station from October 1989 to December 1992 in the magnetic field (a) and in the electric field (b). Omega signal is propagated to the southern hemisphere. The intensity of the signal near the equator shows low intensity at high altitude and no signal at lower altitude

ACKNOWLEDGMENT

This research was partially supported by a Grant-in-Aid for Scientific Research from the Japan Society for the Promotion of Science (#24360159 and #16H01172).

REFERENCES

- [1] Kimura, I., K. Hashimoto, I. Nagano, T. Okada, M. Yamamoto, T. Yoshino, H. Matsumoto, M. Ejiri, K. Hayashi, 1990. VLF Observation by the Akebono (EXOS-D) Satellite, *Journal of Geomagnetism and Geoelectricity*, 42, pp. 459-478
- [2] Kimura, I., Y. Kasahara, H. Oya, 2001. Determination of global plasmaspheric electron density profile by tomographic approach using Omega signals and ray tracing, *Journal of Atmospheric and Solar-Terrestrial Physics*, 63, 1157-1170
- [3] Goto, Y., Y. Kasahara, T. Sato, 2003. Determination of plasmaspheric electron density profile by a stochastic approach, *Radio Science*, 38(3), 1060, doi: 10.1029/2002RS002603
- [4] Common Data Format (CDF) Page. <http://cdf.gsfc.nasa.gov/>. Accessed 21 May 2016
- [5] Morris, P. B., R. R. Gupta, R. S. Warren, P. M. Creamer, 1994. Omega Navigation System Course Book, Vol. 1, National Technical Information Service, Springfield, Virginia, 434pp
- [6] Yamamoto, M., Y. Ito, Y. Kishi, A. Sawada, I. Kimura, I. Nagano, E. Kennai, T. Okada, K. Hashimoto, 1991. K vector measurements of VLF signals by the satellite EXOS-D, *Geophysical Research Letters*, 18, pp. 325-328
- [7] Kimura, I., K. Tsunehara, A. Hikuma, Y. Z. Su, Y. Kasahara, H. Oya, 1997. Global electron density distribution in the plasmasphere deduced from Akebono wave data and the IRI model, *Journal of Atmospheric and Solar-Terrestrial Physics*, 59, 1569-1586
- [8] Sawada, A., T. Nobata, Y. Kishi, I. Kimura, 1993. Electron Density Profile in the Magnetosphere Deduced From in Situ Electron Density and Wave Normal Directions of Omega Signals Observed by the Akebono (EXOS D) Satellite, *Journal of Geophysical Research*, 98, A7, 11267-11274
- [9] Tarcsai, G., P. Szemeredy, and L. Hegymegi, 1988. Average electron density profiles in the plasmasphere between $L = 1.4$ and 3.2 deduced from whistlers, *J. Atmos. Terr. Phys.*, 50(7), 07-611, doi:10.1016/0021-9169(88)90058-X
- [10] Collier, A. B., A. R. W. Hughes, J. Lichtenberger, and P. Steinbach, 2006. Seasonal and diurnal variation of lightning activity over southern Africa and correlation with European whistler observations, *Ann. Geophys.*, 24, 529-542
- [11] Lichtenberger, J., C. Ferencz, L. Bodnar, D. Hamar, and P. Steinbach, 2008. Automatic whistler detector and analyzer system: Automatic whistler detector, *J. Geophys. Res.*, 113, A12201, doi:10.1029/2008JA013467

A New Methodology in Study of Effective Parameters in Network-on-Chip Interconnection's (Wire/Wireless) Performance

Mostafa Haghi

Center for life science automation (Celisca)
Rostock University
Rostock, Germany

Norbert Stoll

Institute of Automation
Rostock University
Rostock, Germany

Kerstin Thurow

Center for life science automation
Rostock University
Rostock, Germany

Saed Moradi

Department of Electrical engineering
Isfahan University
Isfahan, Iran

Abstract—Network-on-Chip (NoC) paradigm has been proposed as an alternative bus-based schemes to achieve high performance and scalability in System-on-Chip (SoC) design. Performance analysis and evaluation of on-chip interconnect architectures are widely considered. Time latency and throughput are two very critical parameters which play vital role to improve the system performance. In this work, these two elements are evaluated in both wire and wireless approaches under different conditions for networks contain 64,512 and 1024 number of cores. There are number of parameters those have direct and indirect effects on the delay and throughput, among all, these four are chosen: routing algorithm, buffer size, virtual channel and subnet. Thus this work is clustered into two general parts, in the first section the effect of algorithms and buffer size are calculated and then later on in second part when switching from wire approach to wireless, it's shown that, virtual channel and subnet are able to influence the performance of a network on chip positively under some circumstances. We don't concentrate on approach and techniques here. Our target in this paper is to determine the critical points, trade-off and study the effect of mentioned parameters on entire system. Evaluation is done by means of Booksim and Noxim simulators which are based on system C.

Keywords—network on chip; on-chip interconnection; buffer size; virtual channel; subnet

I. INTRODUCTION

System-On-chip (SoC) has recently emerged as a key technology behind most embedded and smart miniaturized systems to provide high flexibility and better performance. These systems can find an appropriate location in industry and market while in addition to providing high-performance, meet very important system requirements, such as a low power consumption, low time latency and small occupied area. Therefore, the design of these systems should be highly flexible, adaptable, and fulfil stringent time-to-market constraints. A key element in the performance and energy consumption in SoCs is the On-Chip Interconnect (OCI), which allows different SoC components to communicate

efficiently. In some aspect we can claim that the majority of power is consumed by OCI. Network-on-chip has been proposed as an alternative to bus-based schemes to achieve high performance and scalability in SoC design [1], [18]. Different OCI-based architectures using packet-switching have been recently studied and adapted for SoCs. Examples of these architectures and topology are Fat-Tree (FT)[2], 2D mesh[3], Ring[4], Butterfly-Fat Tree (BFT)[5], Torus[6], Spidergon [7], Octagon[8], WK-Recursive[9]. However, as the architecture is improved to enhance the performance of the system, their increasing complexity makes their design extremely challenging. Furthermore, another parameter which is important to be studied is traffic generated between components and traverse the OCI [10]. Therefore, it is very helpful to perform a traffic analysis and predict the process in early stages of the design to determine an appropriate traffic model, such that the designer can select suitable parameters for the on-chip interconnect architecture. Indeed, the selection of the on-chip interconnect architecture, based on traffic patterns as an application, which SoC generates, allows designers to detect and locate network contentions and bottlenecks. Here in this paper as is seen in majority of research works, traffic is assumed to be Random. Generally, the simulation is extremely slow for large systems and provides little insight, on how various parameters affect the actual NoC performance [11].

Two simulators based on system C are applied to evaluate the studied parameters, Noxim and Booksim for wire and wireless sections respectively. However, analytical models, allow fast evaluation of performance metrics in early stages of the design process. This paper extends the work by evaluation of the performance (e.g., latency, throughput) of two on-chip interconnect methodologies under three on-chip routing algorithms architectures for wire-based and wireless using Mesh and Flattened Butter-fly. It is shown how hybrid interconnects can be used to improve the performance and design tradeoffs. The main objective is to illustrate the effectiveness of 4 elements (Buffer Size, Routing Algorithm,

Subnet, Virtual channel) in evaluation of on-chip interconnect architectures. Work is extended by calculation of effect of first two parameters on wire-based section, and next two in wireless part. Furthermore, variation of Packet Injection Rate (PIR), is carefully investigated which always is involved in evaluation of network performance.

The rest of this paper is structured as following: In following section, we summarize the existing research works on performance analysis. Section 2 provides a brief overview of Flattened Butter Fly and methodology in hybrid approach and features. In section 3, work is clustered in 5 subsections, in first and second sections, It will be observed, how buffer size and routing algorithm are able to improve the performance in wire-based approach.

In subsection 3 we compare wire and wireless on delay aspect. In subsection 4 and 5, is proved that virtual channel and subnet can have a direct role in hybrid approach to enhance the different parameters. It's remarkable that, in each subsection a conclusion is provided independently, and finally, in section 5, the conclusion is presented.

II. RELATED RESEARCH WORKS

OCI architecture has some important specifications and features so called: latency, throughput, traffic load, energy consumption, and occupied silicon area requirements. These are adopted in SoCs to characterize the performance. **K. Lahiri and et al.** in [13] have pointed out that the current design tools and methodologies are not suitable for NoC evaluation, and simulation methods, despite their accuracy, are very expensive and time consuming. Therefore, updated techniques and tools are required to extract new communication characteristics, also to estimate the network performance and energy consumption efficiently, and of course area requirements for candidate communication architectures, is always a serious concern. Approaches proposed in the literature can be classified in four main categories: deterministic approaches, probabilistic approaches, physics based approaches, and system theory based approaches. First category is mainly based on graph theory that has been used successfully in many software and computer engineering domains. An example is the work has been carried out by **A. Hansson** in [14], a model using a cycle-static dataflow graph was used for buffer dimensioning in NoC applications. Deterministic approaches assume, the designer has thorough understanding of the communication pattern among cores and switches. Nowadays researchers mostly use probabilistic approaches which are based on queuing theory. For example, an analytical model using queuing theory was introduced in [15] to evaluate the traffic behavior in Spidergon NoC. Simulation results have been reported to verify the model for message latency under different traffic rates and variable message lengths. Most queuing approaches consider incoming and outgoing traffic as probability distributions (e.g., Poisson traffic) and allow designers to perform a statistical analysis on the whole system in order to evaluate certain network metrics, (average buffer occupancy and average buffer delay in an equilibrium state).

In[16], Unlike stochastic approaches that make Markovian assumptions on the network behavior, statistical physics model the interactions among various components while considering the long term memory effects. The main concept in this model is that packets in the network move from one node to another in a manner that is similar to particles moving in a Bose gas and migrating between various energy levels as a consequence of temperature variations. Network Calculus features [17] are derived from system theory which is placed in the fourth category, this strategy has been frequently applied to electronic circuits successfully. Performance bounds (e.g., end-to-end delay) in networks such as the internet is modeled and evaluated. According to shapes of the traffic flows (by analogy, signals in system theory), designers are able to capture some dynamic features of the network [18], [19].

III. SIMULATORS

In this section **BookSim** interconnection network simulator is described which has is widely used in entire work. The simulator is installed on LINUX OS and is open source. To obtain data and simulate a candidate network, there are some parameters to be set. By changing or resetting input parameters, user can simulate the performance of different NOC systems. It's remarkable that the Noxim simulator setting (Fig.1) is the same, but is applied for wire-based only.

Number of virtual channel, depth of buffer size, topology, traffic model, number of IPs, packet injection rate are the parameters to be adjusted before simulator is ran. The parameters like topology, traffic and virtual channel are configured only once, but for the other parameters are changed depending on the delegated task. Here, some important parameters definition are presented:

Virtual channel is the number of the virtual channels per router;

Buffer size means the depth of buffer base on bit;

Traffic model is defined uniform, means each source sends an equal amount of data to destination. The most two important parameters during this work which are frequently varied are PIR and Subnet. PIR unit is either flit/cycle/node or bit/cycle/node. Each flit in this work, contains 6 bits. For example, if the **injection rate** is 0.15, it means that during each cycle, 0.15 bit is injected in every node. Once the parameters were set, simulation is begun. In order to start, type command `\:=booksim [configfile]`" in the `\=src` directory. At the output, following parameters are seen `\average latency`", `\average accepted rate`", which means the average throughput, `\min accepted rate`" and `\average hops`". The unit of *latency* is cycle; the unit of *throughput* is it/cycle/node. Then, by running the simulation for various `\injection rate`", an average latency graph can be obtained. In throughout evaluation, simulator is fed with different number of IPs, subnet and PIR rate which uniquely are able to determine the performance [20]. For large (network containing more than 1024 IPs) networks, during each simulation, under high rate of PIR, simulation takes 20 minutes approximately.

```
Noxim - the NoC Simulator
(c) University of Catania

Reset... done! Now running for 100000 cycles...
Noxim simulation completed.
* 100000 cycles executed
* Total received packets: 696664
* Total received flits: 4179738
* Global average delay (cycles): 4574.38
* Global average throughput (flits/cycle): 0.140845
* Throughput (flits/cycle/IP): 0.048326
* Max delay (cycles): 97249
* Total energy (J): 0.00255775
```

Fig. 1. Noxim Simulator

IV. METHODOLOGY AND APPROACH

A **hybrid** wired/wireless NOC architecture (Fig.2) is used. Hubs are interconnected by both wired and wireless links while the subnets internally are connected via wires only. The hubs those are linked via wireless, have to be equipped with Wireless Base stations (WBs), WBs are responsible to transmit and receive data packets over wireless channels. When a data needs to be sent to a core in a different subnet, it travels from the source to respective hub and reaches to the destination subnet's hub via the **small-world network** consisting of both wired and wireless links, then it is routed to the final destination core. For intra subnet and inter subnet data transferring the **wormhole** routing is adopted [20]. It is remarkable that data packet is broken down to smaller units called flits.

- **Adopted Routing**

In proposed hierarchical NoC [20], two topologies are used. In this work, for inter-subnet we consider mesh topology. For an intra-subnet communication if the destination is more than two hops away, then the flit goes through the central hub to its destination. Thus, within the star-ring subnet, each core is at a distance of at most two hops from any other cores (Fig. 3). To avoid deadlock, the virtual channel management scheme from Red Rover algorithm is adopted, in which the ring is divided into two equal sets of contiguous nodes. Messages originating from each group of nodes use dedicated virtual channels. This scheme breaks cyclic dependencies and prevents deadlock. However, intra-subnet data routing, requires flits to use the upper-level network consisting of wired and wireless links. By using the wireless shortcuts between the hubs with WIs, flits can be transferred in a single hop between them. If the source hub is not equipped with a WI, the flits are routed to the nearest hub with a WI via the wired links and are then transmitted through the wireless channel. Likewise, if for destination hub also a WI is not accessible, then the nearest hub to it with a WI, receives the data and passes it to the destination through wired links. Between a pair of source and destination hubs without WIs, the routing path involving the wireless medium is chosen if it reduces the total path length compared to the wired path. A token flow control (**Kumar**) along with a distributed routing strategy is adopted to alleviate this problem.

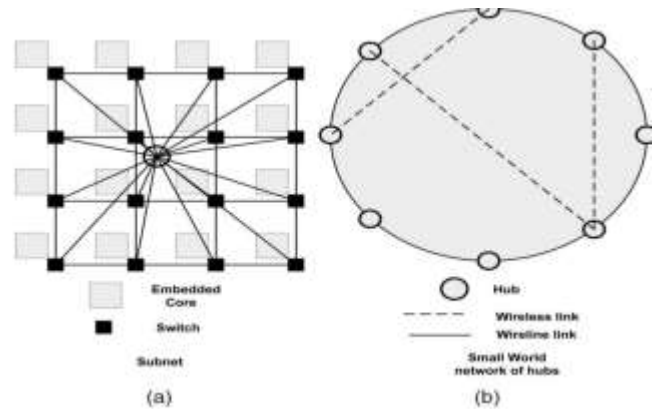


Fig. 2. hybrid structure

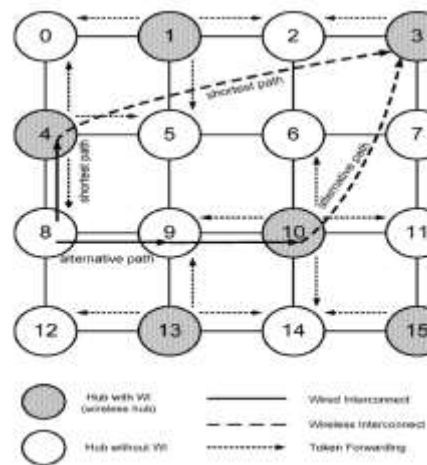


Fig. 3. Adopted Routing in Wireless Communication

- **Flattened butterfly**

Selecting an appropriate topology in the design of an interconnection network is an important task, because it has a direct effect on critical performance metrics such as network's zero-load delay and its capacity, also directly influences the implementation expense, both in terms of on-chip resources and implementation complexity. In this work wire-based and wireless networks are running under mesh and flattened butterfly topology respectively. Here to clarify how Flattened Butterfly topology impresses on network performance we briefly discuss on it.

The flattened butterfly topology is a cost-efficient topology in particular to use with high-radix routers [21]. Flattened butterfly is derived by combining (or *flattening*) routers in each row of a conventional butterfly topology while preserving the inter-router connections. In this design concentration is on the routers, therefore flattened butterfly reduces the wiring complexity of the topology significantly, this is resulted in scaling more efficiently.

Now to make it more understandable, readers are referred to a case study and observe how to map a network with 64-node onto the flattened butterfly topology, we collapse a 3-stage radix-4 butterfly network (4-ary 3-fly) to produce the flattened butterfly shown in Fig. 4(a). The presented flattened butterfly has 2 dimensions and uses radix-10 routers [22]. Each router has a concentration factor of 4. It means, four processor IPs are attached to each router. The remaining 6 router ports are used for inter-router connections: 3 ports are used for the dimension 1 connections, and 3 ports are used for the dimension 2 connections. Routers are placed as shown in Fig. 4(b) to embed the topology in a planar VLSI layout with each router placed in the middle of the 4 processing nodes [22]. Routers connected in dimension 1 are aligned horizontally, while routers connected in dimension 2 are aligned vertically; thus, the routers within a row are fully connected, as are the routers within a column. The wire delay associated with the **Manhattan distance** between a packet's source and its destination provides a lower bound on latency required to traverse an on-chip network. When minimal routing is used, processors in this flattened butterfly network are separated by only 2 hops, which is a significant improvement over the hop count of a 2-D mesh.

V. SIMULATION RESULTS

- Evaluation of effect of Routing Algorithm and PIR on NOC performance**

At the first step to have a transparent idea about range of delay and throughput in NOC, we start with wire-based methodology. Two parameters which NOC performance is extremely influenced by, are routing algorithm and rate (PIR). Therefore fully- adaptive [23], XY [23] and West [23] are picked as samples to feed the simulator. Once the simulator is modelled and adjusted by any of routing algorithm, it shall be kept fixed and another factor (here in this study PIR) is the only variable studied factor to be fed into simulator. The used traffic model is uniform. For each rate of PIR, simulator with all other fixed parameters is executed once. To start simulation, machine is configured under **Fully Adaptive** routing algorithm.

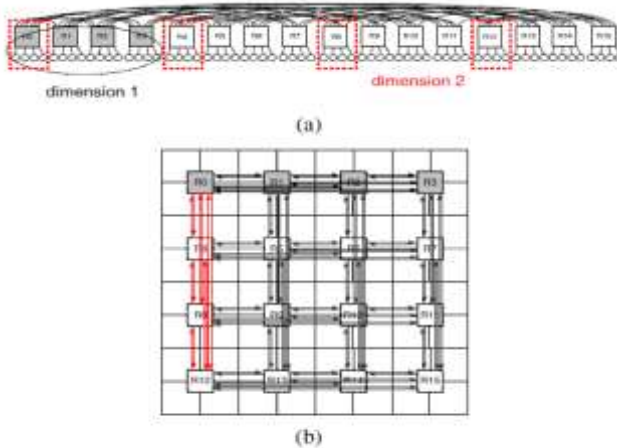


Fig. 4. (a,b)Flattened Butterfly topology with radix-10

As in Fig. 5(a) is seen when PIR is varied between 0.01 and 0.03, in fact rate of data transferring is increased, thus it's expected total received packets become increased and consequently when majority of network's IPs are involved in communication, thus majority of network is active, this causes an IP sends and receives bits with higher potential capacity, the throughput is improved expectedly. On the other, data traffic in directions is increased due to higher rate of bit communication between IPs, which is led to delay, this latency is not desirable but still is controllable.

This policy is same almost for all three routing algorithms with slightly changes. In first case study, when PIR is greater than 0.03 and less than 0.04, an unusual behavior is observed. Throughput is degraded rapidly, on the other side, the slop of figure for delay is getting sharper. For simulation under $PIR > 0.05$, an interesting result is raised up, the simulator fails and no result is obtained for $PIR > 0.05$, this occurs under fully adaptive routing algorithm (see Fig.5(a)). It justifiable that buffer size which is limited to 8bits in this work has no more capacity to reserve the bits. In fully adaptive routing a packet always is transmitted through a not congested route, with increasing the number of received packets, buffer is filled and there is no more space to receive new packets, this causes a block direction. Throughput is zero when no packet is received and the NOC paradigm under fully adaptive routing algorithm is not applicable for $PIR > 0.04$.

In contrast with fully adaptive algorithm, in XY routing algorithm situation is different. In this routing algorithm when the PIR exceeds a certain value, instead of network failure, the saturation state is occurred. For $0.01 < PIR < 0.04$ the same policy with previous routing algorithm is experienced. At $PIR = 0.04$, all Parameters are in MAX level, but the slop of figure for time latency has become sharper. At $PIR = 0.05$, as is shown in Fig.5(a) still all parameters are increasing but two points clearly are observable. First the rate of throughput enhancement

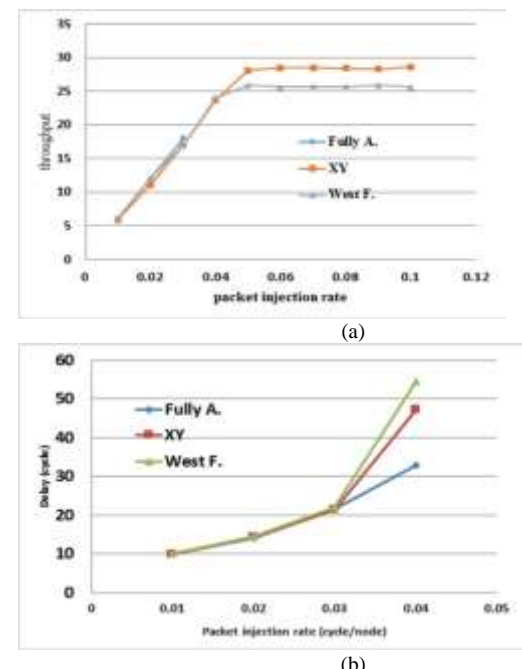


Fig. 5. (a) Throughput under three routing algorithm (b) Delay under Fully A., XY, West F. routing algorithms under xy

has been reduced. Second point is that the number of delay cycles are increased rapidly and is not under control any longer. For instance at $\text{PIR}=0.05$ the latency = 2645, and when $\text{PIR}=0.06$, latency = 107770, this time latency is not acceptable. If packet injection rate is kept increasing, the according to Fig.6(a), for $\text{PIR}>0.05$ the saturation is occurred. In saturation state throughput will be varied between 28.1 and 28.7. Delay in saturation region is very sensitive to PIR, the time latency is rapidly increased, but for $\text{PIR}>0.3$ the rate of delay is decreased and sensitivity degree is reduced, this number of delay cycle kills performance. West first routing algorithm follows the very similar policy to XY algorithm, but obtained information from machine are different. For $0.01<\text{PIR}<0.04$ above under studied parameters are increased, with an almost fixed rate, as is observed in Fig.5(b), at $\text{PIR}=0.05$ time latency is increased with a sharp rate and is out of control. (54.53 at $\text{PIR}=0.04$ to 6240.3 at $\text{PIR}=0.05$). At $\text{PIR}=0.05$ again saturation state is happened.

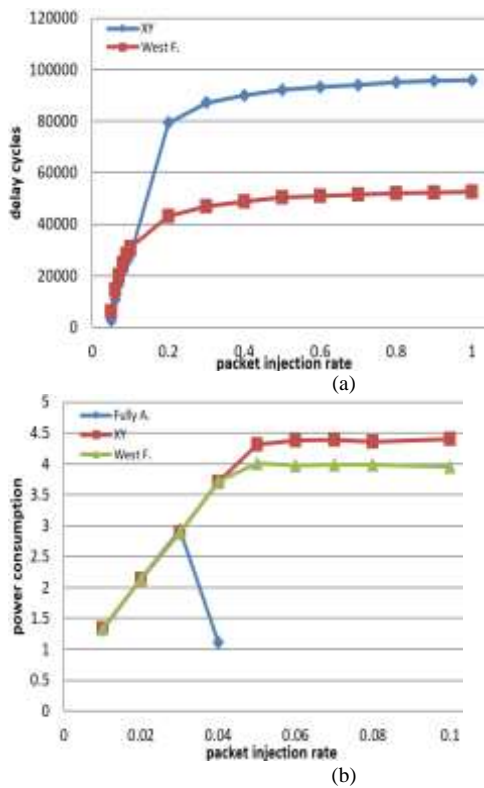


Fig. 6. (a), Full diagram of delay under West F. and XY (b), Power consumption under three routingalgorithms

Number of received packets and average throughput are almost fixed or with a negligible changes. In this case the throughput in saturation area is swing between 25.2 and 25.7.

• Delay

For $0.01<\text{PIR}<0.03$, under three routing algorithms, simulator delivers the same results (Table.1). For $\text{PIR}>0.03$ WEST FIRST routing has higher rate of latency. XY routing algorithm accomplish the better latency than Fully

ADAPTIVE. In Fig. 6(a) It's clearly seen that for $\text{PIR}>0.04$ the rate of latency is decreased and slowly is getting close to saturated surface. One more point is that, the saturation peak for xy routing algorithm is higher than west first routing algorithm, therefore the sensitivity of west first to PIR is lower. These obtained results are due to different definition and design of structures in each routing algorithm.

TABLE I. TIME LATENCY FOR F.A, XY AND W.F UNDER DIFFERENT PIR

PIR	0.01	0.02	0.03	0.04	0.05	0.06	0.07	0.08
F.A	9.9	14.0	21.4	32.9	-	-	-	-
XY	9.8	14.3	21.35	47.1	2645	10777	16693	21739
W.F	10.11	14.44	22.02	54.53	6244.3	14570	20174	24697

• Throughput

According to Fig.5(a) fully adaptive routing algorithm has the best throughput in range of $0.01 \leq \text{PIR} \leq 0.03$. When PIR is greater than 0.03 west stands on higher level, in saturation state the throughput of XY is constant and stays in higher level than west first while swing between 28.1 and 28.6. West first routing algorithm is varying between 25.6 and 25.9(Table.2).

In Fig.6(b), network power consumptions are depicted which are provided to give an idea to reader and are not discussed in this work.

• Buffer size

In this subsection effect of buffer size is studied. Buffer size [24] plays an important role in driving of packets in directions and keep them online when there is a heavy traffic, therefore route congestion depends on capacity of buffer. It means that there is a specific minimum size for buffer size to run the network under an assigned PIR without failure. At the first attempt buffer size is kept fixed, then under variation of PIR, simulator is executed and delay and throughput results are recorded. In second step we apply the worst case of PIR which results under it have been obtained to the machine and this time buffer size is considered as input to be altered. In each round size of buffer is extended and the results are recorded for delay and throughput, therefore by comparing the results in both situations, it could be concluded, by extension of buffer size performance is improved. We take two samples to observe how buffer size influences the network performance.

A) $0.028 \leq \text{PIR} \leq 0.030$, B.S=4

Size of buffer is configured to B.S=4, execution is started with $\text{PIR}=0.028$, different PIR rate are fed into machine. Delay and throughput are obtained 21.56 and 14 respectively, as we see in Fig.7(a) PIR is gradually increased, $\text{PIR}=0.030$ is the maximum rate which still machine can run under it and enhance the delay and throughput, if PIR is kept rising, network will be failed due to full routes capacity. We record the **$\text{PIR}=0.030$ as the worst result for B.S=4**, now we extend the B.S from 4 to 6, obtained results say that throughput is improved dramatically by 30 times (2900%) and delay 22.9%. Buffer size can be extended even more but for B.S>6 saturation state occurs (see Fig.7(b)). To sum up, if B.S is incremented from 6 to 16 gradually, delay is reduced only 3.9% and throughput just -0.5%. It is concluded

TABLE II. THROUGHPUT FOR F.A, XY AND W.F UNDER DIFFERENT PIR

W.F	XY	F.A	PIR
6	6	6	0.01
12	11.9	12	0.02
17	17.7	18	0.03
23	23.7	1.2	0.04
25	28.1	-	0.05
25.6	28.5	-	0.06
25.7	28.5	-	0.07
25.7	28.4	-	0.08
25.6	28.3	-	0.09
25.2	28.6	-	0.1
25.6	28.6	-	0.2
25.5	28.3	-	0.3
25.4	28.5	-	0.4
25.4	28.2	-	0.5

That, the best Buffer Size for $0.028 \leq \text{PIR} \leq 0.030$ is 6. For $\text{B.S} > 6$, PIR is not sensitive to B.S extension (Table.3). This can easily be justified, as the PIR rate and IPs are restricted, therefore the peak of traffic is pre-determinable. It's required to calculate, to match buffer size with maximum traffic to fluent packet travelling. Nevertheless if buffer size would be extended has no mentionable effect on both parameters. Early saturation refers to limited number of IPs in this NOC. Simulator is configured according fully adaptive routing algorithm. b) $0.035 \leq \text{PIR} \leq 0.037$, B.S=8,

The policy is same with previous investigation, two steps, PIR is fed into machine under fixed size of buffer, results are recorded for delay and throughput and then the PIR that the worst results are obtained over it, is considered. Now B.S is extended, then the two states results are compared. It's seen in Fig.8(a) that, time latency is intending toward higher cycles and throughput is reducing gradually while PIR is incremented. In this case also results for $\text{PIR}=0.035, 0.036, 0.037$ are as follow:

Delay=27.9, 30.1, 35.3 and throughput=2, 8, 1. Maximum PIR rate for B.S=8 is 0.037, in next round B.S is extended to 12(by 50%) in Fig.8(b). The obtained results for B.S=12, 16, 20 are provide below:

$$\text{Delay} = 30, 30.64, 28 \quad \text{Throughput} = 22, 22.2, 22.2$$

As the results show in Table 4 and Table 5, we can come up with this fact that, as the PIR rate is ascended, the rate of buffer size has to be extended in a sharper rate to can compensate the much heavier traffic.

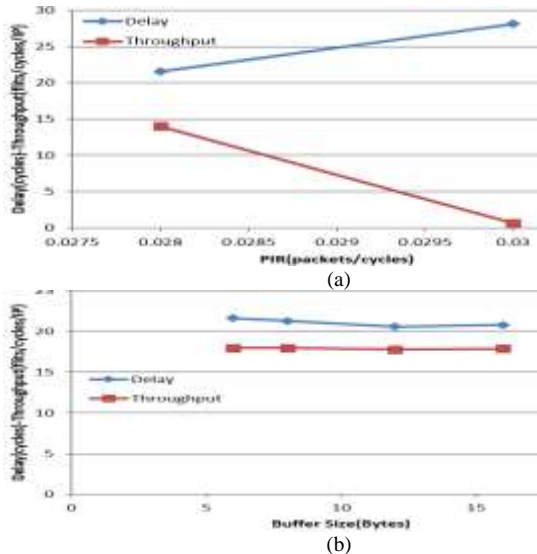


Fig. 7. (a) Delay and throughput under PIR Variant (B.S=4) (b) Delay and throughput under B.S Variant (PIR=0.030)

TABLE III. DELAY AND THROUGHPUT UNDER VARIATION OF B.S AND PIR

B.S	Thr.	Delay	PIR
12	22.7	31.97	0.038
12	23	34.1	0.039
16	24	37	0.040
24	24	37.1	0.041
24	25	39.9	0.042
24	24	42.2	0.043
24	26	52.1	0.045
24	3.2	57.6	0.047
24	1.3	115.7	0.049
72	29	91.5	0.050
72	30	102.5	0.051
72	1	273	0.052
72	1	333	0.054
144	0.7	488.2	0.055
144	0.2	824.2	0.058

TABLE IV. DELAY AND THROUGHPUT UNDER VARIATION OF B.S AND PIR

B.S	Thr.	Delay	PIR
18	23.2	32.64	0.039
24	23.3	32.2	0.039
30	23.3	32.7	0.039
30	8	103.3	0.49
36	19	77.6	0.049
60	29	84	0.049
108	2	310.6	0.054
120	13	250.3	0.054
132	3.6	336	0.054

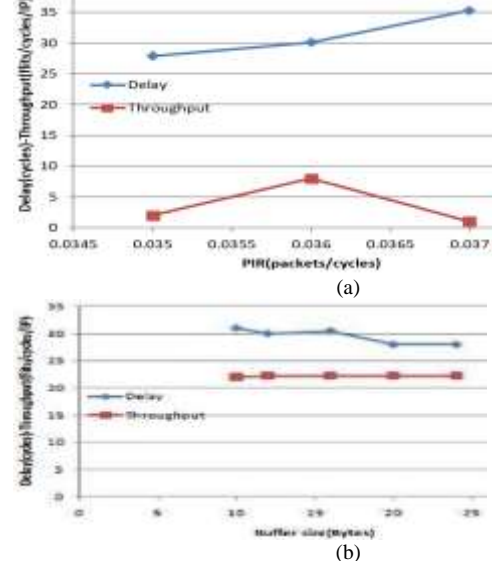


Fig. 8. (a), Delay and Throughput under PIR Variant (B.S=8) (b), Delay and Throughput under B.S Variant (PIR=0.030)

TABLE V. DELAY AND THROUGHPUT UNDER VARIATION OF B.S AND PIR

PIR	0.058	0.058	0.058	0.058	0.058	0.058
Delay	695.7	1110	650	698.9	703.3	940
Thr.	0.1	3	0.8	1.1	2.2	5
B.S	216	288	350	550	570	630

- Comparing Wire vs Wireless in Delay under the Same Conditions

In this section, it's concluded that it's necessary to switch from a wire-based methodology to a hybrid- combination of wire and wireless. The performance of these two approaches are considered under same conditions. Traffic, No. of IP, virtual channel, buffer size and topology are the parameters which are constant for both states. We execute Noxim simulator for wire-based and Booksim for wireless approach under fully adaptive and butterfly algorithm respectively.

Among many solutions that alleviate effect of delay in networks, extending the number of V.C is justifiable. Wormhole routing with virtual channel flow control is a well-known technique from the zone of multiprocessor networks. While area and power consumption are two major overheads, it allows minimization of the size of the router's buffers and providing flexibility and good channel utilization [22].

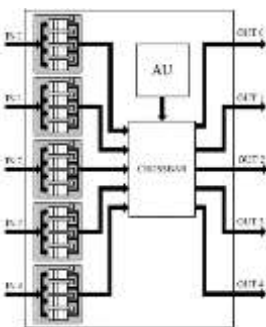


Fig. 9. Structure Virtual channel with 5 I/O

A general structure of a wormhole router with virtual channel flow control is depicted in Fig.9. This router has 5 input/output ports: 4 for connection with the routers those are next to and one to link with the local node. At each input port the virtual channels (VCs), 4 in this example, are de multiplexed and buffering regulation is FIFOs. Status information is saved for every single bit of them. After the bits are out of port through FIFOs they are multiplexed again on a single channel which enters to a crossbar. The operation of the router is controlled by an arbitration unit (AU). It determines on a cycle-by-cycle basis, which virtual channels may advance sooner.

Changing the number of V.C is applicable to both wire and wireless interconnection networks, by using this method, in fact we are dealing with architecture of router. Some modifications have to be completed internally. By doing so, in following section we will observe how the delay is improved:

A) V.C=4, IP=64

At previous subsection delay and throughput in wire-based paradigm and obtained information from the machine were investigated and analyzed. Now we switch to so-called wireless methodology and study same parameters and analyze the obtained results from Booksim simulator under the same conditions. Then these two clusters of information are compared and we come up with a conclusion. In first state,

network contents of 64 IPs which is working under 4 virtual channels. Obtained results in Table.6 show that, delay cycles in wireless network is always in lower level than wire-based. In order to justify the reason of better delay cycle in wireless, we understand that, all intermediate IPs between source and destination nodes are eliminated but two and this reduce the time while transferring data between any two distant IPs.

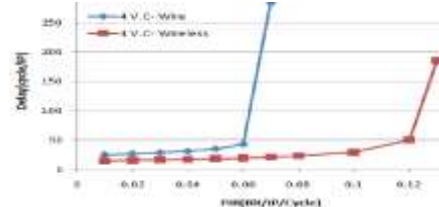


Fig. 10. Delay in wire-wireless networks-64IPS

In table.6 we see that under all PIR rates delay is much more reduced for wireless network. The maximum of improvement before take-off point is belongs to PIR= 0.06(54.4%), and the least one is for PIR= 0.01(43%). Primary level of take-off point is reduced effectively, but as it's still high, is not considered. As it's observed in Fig.10, the PIR range is extended because of delay improvement (reducing the number of delay cycle). It's claimed that under the same conditions, delay is improved at least 43%. When all other states are compared too, we come up with the most enhancement state, which is occurred in high PIR rate, thus it's strongly recommended to use wireless paradigm in higher rate of PIR.

In second investigation PIR safe domain is considered. For wire – based, network just is supported to work up to PIR= 0.06, when PIR is exceeded than 0.06, routes are congested and simulator is dump. Now in wireless based, PIR is extended to 0.13 and network can work in wider range, therefore extension of PIR is led to higher performance. In order to get the best performance in wireless methodology, one of the requirement to run the network under wireless methodology is using it under highest PIR rate. With a quick look at statistics, tables and figures, it's figured out that almost the results for both networks in wireless state under 4 and 8V.C, are same, the only slight change is in PIR rate which in wire-based extended from 0.06 to 0.07, and take off point will occur at PIR=0.08. Network with 64IPs is small enough to meet all condition to run simulator properly with no congestion, that's the reason with extending of the V.C to 8, it has no effect on network delay because there is enough capacity to keep the packets in line, to prevent of traffic.

TABLE VI. COMPARING DELAY IN WIRE-WIRELESS NETWORKS

PIR	0.01	0.02	0.03	0.04	0.05	0.06	0.07
W-Delay	25.4	26.7	28.6	30.9	34.8	42.6	283.4
WL-Delay	14.6 1	15.3 3	16.2 2	17.1 1	18.1 6	19.4 7	21.0 7
Improvement %	43	43	44	45	48	54	93

- Evaluation of Delay and Throughput for: 64 IPs under 4,8,16 V.C,**

Researchers in this work are interested the results and efficiency investigation on incrementing of number of V.C, this proves, this inflation has a positive effect on reducing the delay under some circumstances, and improve the performance. If we take a look carefully into Fig.11(a) we observe, with increasing the number of V.C from 4 to 8 and then 16, under variation of PIR, for all no. of V.Cs, the delay is almost unchanged up to PIR=0.12. If PIR crosses the 0.12, two take-off points (345, 358) are seen for V.C= 4, 8 at PIR=0.13, delay is uncontrollable because congested directions have occurred in network. We can see the advantage of V.C=16, when in same network (64 IPs) for PIR>0.12, delay is still under control and network runs well. In Fig.11(a), delay is out of control and occurs at PIR=0.14, it means that blocked direction happens for a network with 16 V.C in each port too, but where the capacity of router has been expanded from 8 to 16V.Cs, this phenomenon is showed up at higher level of PIR. To conclude we must say if it's supposed to network runs under PIR<0.12, it's better to use 4 virtual channel for each port in router, because it costs less and the delay will be the same as well as two other situations.

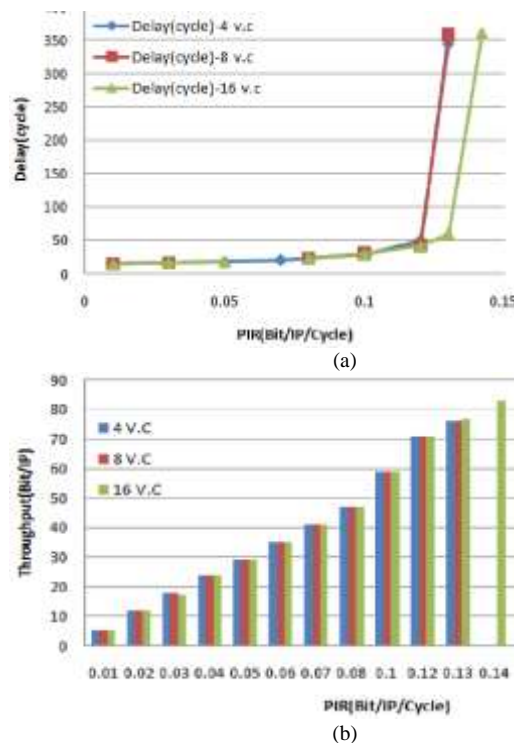


Fig. 11. (a) Delay in network with 64ips (b) Throughput in network with 64 IPs

In Fig.11(b) the effect of virtual channel is studied on throughput. Obtained results for throughput are incredibly similar to each other for various number of V.C (4, 8and16) in each PIR. To study behavior of throughput, networks with different no. of IPs are taken into consideration. It's found out that the number of IPs and V.Cs have to be matched for any network, if V.C is much more bigger than what is required for the network, V.Cs are in idle state and are not useable due to

not having a data transferring between any two source and destination nodes in low rate of PIR, that's the reason throughput descends, but for PIR above 0.13, when network is nearly getting congested, its anticipated that with having more number of V.Cs, it's possible to prevent a traffic or at least reducing it in network , from there all V.C are used and consequently throughput is improved.

- Comparision**

In this part we are going to see how large networks cause congestion in routes and consequently heavy traffic, and end up with an unreliable system if wouldn't be managed by different methods. Three networks with diverse numbers of nodes (64, 512and1024) under same conditions are considered to study behavior of delay parameter. If the number of V.C= 4 are kept fixed for all networks (Fig.12(a)), as we expect, the first network that reaches to take off point is larger one. This was anticipatable, because many nodes are involved in communication and directions are filled with bits carrying data. If designer intends to tackle this issue without any physical alteration or change of design structure, he/she has to keep the PIR less than 0.08, and to be in a safe margin less than 0.07 in cost of performance, or else to hold performance still high and delay acceptable, V.C has to be improved and this requires to an alteration in router design.

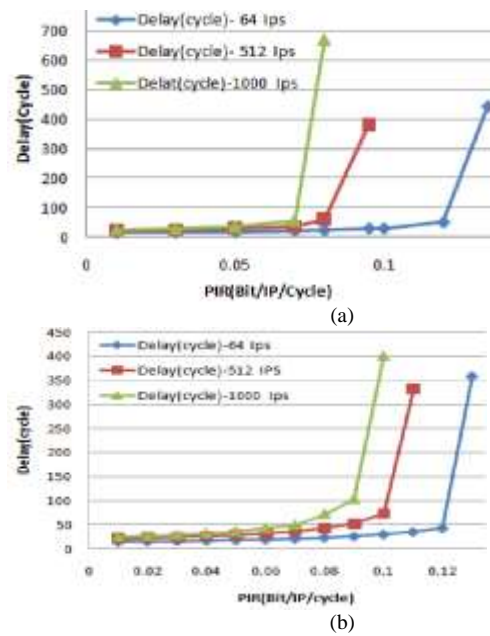


Fig. 12. (a) Delay under 4 V.C (b) Delay under 8V.C

For V.C= 8 (Fig.12(b)) and 16, policy and analyze are similar, the only different is range of PIR, which is extendable by incrementing the number of V.C. In fact we create potential to control delay and even reducing it, to provide this capability, structure of router is changed, but while using this ability, designer has to be aware that, achieving to a desirable delay cycle would be in expense of losing throughput and much more cost. While designing a network, designer needs to know which factor- low delay cycle or higher throughput- is more important to application, then requirements are applied to achieve the best performance.

Basically to get a better efficiency, it's necessary to define for what purpose system is used, because it should be known in trading off between delay and throughput which one should stay in heavy side. Always two policies are observable: first, under equal number of IPs, the network with higher V.C has a lower delay and in high PIR has a better throughput ($4 < 8 < 16$), second, under same number of V.C, a network with lower number of IPs has a lower delay cycle. Throughput is same for different networks under poor rate of PIR, it means that designer has to refuse using much number of V.C under low level of PIR. Using of max. No. of V.C is reasonable if and only if the maximum rate of possible PIR is applied to catch a high throughput.

- **Subnet**

This subsection is divided to 3 parts and in each part delay cycle and throughput of network for various numbers of IPs (64, 512, 1024), under diverse No. of Subnet (1.4.8.16) is evaluated respectively. Critical points, take off spots and domain of PIR are the cases that will be determined accurately. First all network's cores are divided into multiple smaller cluster of neighboring cores and call these smaller networks subnet. Whereas subnets are smaller than entire network, inter-subnet communication will have a shorter average path length than a single NOC spanning the whole system (Fig.13). Size and number of subnets should not be very large because will affect the throughput and performance of the network [26].

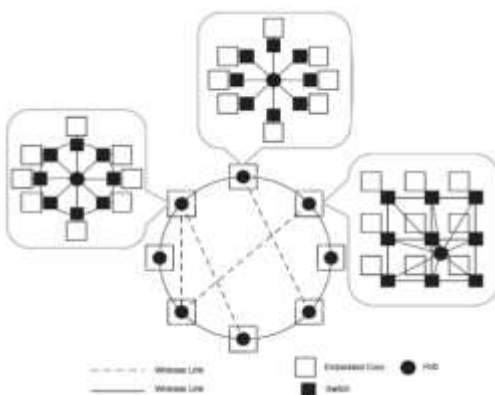


Fig. 13. Clustering of neighboring nodes to subnets

- **Delay and Throughput for 64 IPs**

In this section concentration is on Subnet. In fact with dividing IPs in a network into different clusters, we intend to decrease the physical distance between any two distant IPs. It's quite understandable that the length of communication of any two remote IPs in a coherent network without any subnets, is much more than a network clustering into smaller group of cores as more intermediate cores are there. There is a possibility that any two cores transfer data internally in a same

subnet rather than communication beyond subnets, data transferring is faster because delay cycle is reduced. In this status all switches are linked to a hub, which all other Hubs also from different Subnets communicate in wireless often. This is not discussed in this paper any longer. In first case, a network with 64 IPs is considered.

Simulation is started with Subnet=1, region of PIR is limited to 0.12 due to heavy traffic. Delay cycle is constant for any other of numbers of Subnets (4.8.16). In explain, we say if PIR rate is held low and the network is broken into smaller subnets, as the rate of traffic is fixed, it doesn't affect the performance. Now we discuss on throughput for ($0.01 < \text{PIR} < 0.12$). In spite of delay cycle in Fig.14(b) and Table.8, throughput has the best proficiency for $1 = \text{subnet}$, because running of network in higher level of PIR rate means use of maximum capacity of each node. If we are working with small group of IPs, PIR can be kept in maximum rate with no failure. By developing the number of subnets, network is broken into smaller groups of IPs, this created this potential to run the simulator under higher rate of PIR due to less data communication. When the PIR rate is still low, that is a reason many of IPs are not even involved and throughput would be poor. To reduce the time latency network has to be divided into smaller parts of 4, thus PIR range is extended to 0.5 for 4 Subnets, while PIR is below 0.5 delay cycle is within reasonable range and network works properly. The delay cycle is the same for all number of Subnets like previous case, but throughput is in maximum rate, for 4 Subnets in this range: $0.12 < \text{PIR} < 0.5$ due to using all cores in highest possible efficiency. For each No. of subnet there is an authorized range of PIR. Next step is simulation of network for 8 subnets which PIR is between 0.5 and 0.97. We obtain the results for others subnets too, it's concluded that delay cycle is same for subnet=8and16 but as the network has been divided into very small groups of IPs, Subnets=16 has better delay cycle slightly, but we would prefer to ignore it due to some overheads like cost of design and complicated implementation. The best throughput belongs to Subnets=8 in range of 0.5 and 0.97 for PIR (Fig.14(a) and Table.7). A very important conclusion in this subsection is that, using 16 Subnets for a network with 64 IPs is almost insignificant, because it doesn't create an impressive improvement on performance.

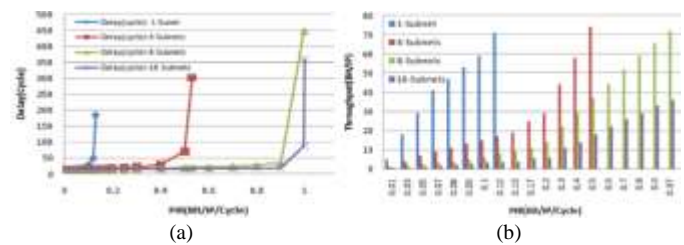


Fig. 14. (a), Delay in a network with 64 IPs (b) Throughput in a network with 64 IPs

TABLE VII. DELAY IN NETWORK WITH 64IPS



- *Delay and Throughput for 512 IPs*

To be continued, numbers of IPs are extended to 512. In contrast with first case two major differences are observable. In delay Fig.15(a), first the domain of PIR has been reduced, in network with 64 IPs, for 1 subnet, PIR can support the network up to 0.1, now in 512 IPs case, PIR is reduced to 0.09, if we extend the Subnets to 4, 8 and then 16, following results are obtained:

TABLE VIII. THROUGHPUT IN NETWORK WITH 64 IPS



TABLE IX. VARIATION OF PIR UNDER DIFFERENT NUMBER OF SUBNETS

PIR-512IPs	0.09	0.3	0.7	0.99
PIR-64IPs	0.12	0.4	0.9	0.97
SUBNET	1	4	8	16

Results are provided in Table 9, for each number of subnets the maximum authorized rate of PIR is shown. The level of PIR under same number of subnets but different number of IPs is decreased.

It was expected, because for equal number of subnets, more cores are located in small networks. To get a higher performance, rate of PIR is enhanced, due to high data transferring traffic, congested directions are raised up and network is dump. As networks become hugger and more complicated, the numbers of Subnets are increased in appropriate ratio. The relation between Subnets and Delay

cycles from one side and the zone of PIR for each numbers of Subnets from the other side, are presented below:

Delay cycle (64 & 512 IPs): 1subnet > 4 Subnets > 8 Subnets >16 Subnets

$0.01 \leq \text{PIR (1.S)} < 0.09 \leq \text{PIR (4.S)} < 0.3 \leq \text{PIR (8.S)} < 0.7 \leq \text{PIR (16.S)} \leq 0.999$

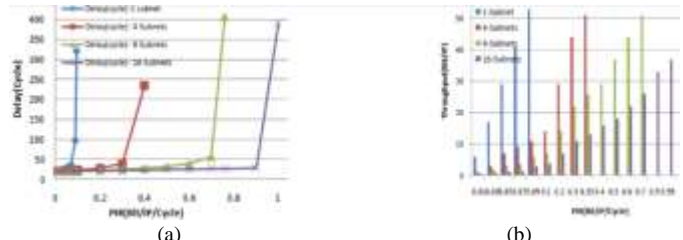


Fig. 15. (a) Delay in a network with 512 IPs (b) Throughput in a network with 512 IPs

For a network with 512 IPs the largest domain of PIR belongs to subnet=8. We discuss on the Fig. 15(a), if we follow the shape of figure for 16 Subnets, it is understood network has less delay cycle in compare with other subnets under same rate of PIR. If quicker data communication in network is the only criteria, designer should go for a highest numbers of Subnets. Now we discuss on Fig. 15(b). Under any circumstance throughput is above 50%, while in case with 64 IPs it was more than 70%. We see that when we have extended the network IPs by factor of 8, (700%), the throughput has reduced just by -20% due to overheads such as power consumption and not using all IPs under maximum rate of PIR. If ignore the range of PIR over than 0.7, in rest of domains we have a competition between Subnets to achieve higher throughput, and always the network with less number of subnets overcomes to others conditions. If level of PIR is increased to greater than 0.7, other players are out of competition one by one, only a network with 16 subnet is supported, if it is supposed to run the network in this range, designer has to use 16 subnets.

- *Delay and Throughput for 1024 IPs*

The same policy is followed, only two differences are pointed out in contrast of networks with 512 and 64 IPs:

a) Largest domain of PIR has been shifted

When size of network is extended almost twice, the safe margin of PIR has moved to range between 0.05 and 0.9 under 16 Subnets. In a network with 512 cores and 8 subnets, every 64 IPs are clustered in a subnet. We compare it with 1024 cores and 8 subnets, every 128 cores are in each subnet. More number of the IPs leads to heavier traffic in data communication and congested direction in lower level of PIR, therefore to prevent unexpected failure in network with 1024 IPs, we need to extend number of subnets, and this is resulted in higher level of PIR.

b) Throughput has degraded by -10%

We have kept the delay cycle under control in expense of cost and losing throughput. In fact when size of network is extended, number of subnets is increased to still control the

delay, but on the other hand for each subnet one Hub is required, thus more number of subnets need more wireless link and more power consumption. It's concluded that sophisticated design reduces throughput. Therefore it's up to user to choose what he needs, whether fast data transferring or high throughput. In this work we have studied the effect of 1,4and8 and 16 subnets on networks with 64,512 and 1024 IPs for PIR variation.

VI. CONCLUSION

Fast data communication and high throughput are always two very important elements which are led to high performance. To achieve high speed, delay should be controlled in data propagation between source and destination IPs. When PIR rate is varied, buffer channel is congested and it causes a traffic in routes, consequently delay is increased and throughput is reduced. To alleviate this issue, one solution is extending of size of buffer. When switching from wire-based network to wireless, in particular in larger network, delay is improved greatly. In a small network with 64 IPs, 512 and 1024 IPs, time latency is improved by 43%, 63.5% and 69% respectively.

Another observation is, when number of subnets are exceeded from an authorized range, throughput is reduced under lower rate of PIR, and therefore user has to choose whether fast data transferring or high throughput is the priority. During this work and simulation we observed that with developing the number of IPs in network, the PIR safe domain is shifted from low rate of PIR and less subnets block towards extended subnets and higher rate of PIR. When V.C is extended for equal number of IPs, the network with more V.C has a lower time latency and only in high rate of PIR has a better Throughput ($4 < 8 < 16$). Refusing apply of extra number of V.C under low level of PIR for poor rate of PIR is another remarkable point, because it delivers same throughput. By extending V.C from 1 to 8, in a small network, delay is enhanced by 18%, and in a large one, its 10%. As an extra ordinary result, if the Subnet would be extended from 1(wire network) to 16 in wireless network, delay is enhanced by 71% in a small network.

Therefore, it's always recommended, wireless interconnection paradigm, has to be applied under high rate of PIR.

REFERENCES

- [1] Senthilkumar et al., International Journal of Advanced Research in Computer Science and Software Engineering 2 (9), September- 2012, pp. 103-108, "A Heterogeneous Network-on-Chip Architecture for Scalability and Service Guarantees"
- [2] P. P. Pande, C. Grecu, M. Jones, A. Ivanov, R. Saleh, Performance evaluation and design tradeoffs for network-on-chip interconnect architectures, IEEE Trans. on Computer 54 (8) (2005) 1025-1040.
- [3] L. Seiler, D. Carmean, E. Sprangle et al., "Larrabee: a many-core x86 architecture for visual computing," IEEE Micro, vol. 29, no. 1, pp. 10-21, 2009.
- [4] L. Bononi, N. Concer, Simulation and analysis of network on chip architectures: Ring, spideron, and 2d mesh, DATE Proc. (2006) 6 pages.
- [5] M. A. Yazdi, M. Modarressi, and H. Sarbazi-Azad, "A load-balanced routing scheme for NoC-based systems-on-chip," in Proceedings of the 1st Workshop on Hardware and Software Implementation and Control of Distributed MEMS, (DMEMS '10), pp. 72-77, Besan, TBD, France, June 2010.
- [6] Y. C. Lan, S. H. Lo, Y. C. Lin, Y. H. Hu, and S. J. Chen, "BiNoC: a bidirectional NoC architecture with dynamic self-reconfigurable channel," in Proceedings of the 3rd ACM/IEEE International Symposium on Networks-on-Chip, (NoCS '09), pp. 266-275, May 2009.
- [7] M. Coppola, R. Locatelli, G. Maruccia, L. Pieralisi, A. Scandurra, Spideron: a novel on-chip communication network, Proc. International Symposium on System-on-Chip (2004) 250-256.
- [8] F. Karim, A. Nguyen, S. Dey, An interconnection architecture for networking systems on chip, IEEE Microprocessors 22 (5) (2002) 36-45.
- [9] S. Suboh, M. Bakhouya, T. El-Ghazawi, Simulation and evaluation of on-chip interconnect architectures: 2d Mesh, Spideron, and WKrecursive networks, NoCS Proc. (2008) 205-206.
- [10] A. Ghasemi , M. Haghi and S. Moradi "An Investigation on the Effects of Subnet Extension in Delay and Throughput in Network-on-Chip" Journal of Circuits, Systems, and Computers Vol. 25, No. 2 (2016) 1650015 (11 pages), Journal of World Scientific Publishing Company DOI: 10.1142/S0218126616500158.
- [11] U. Y. Ogras, R. Marculescu, Analytical router modeling for network-on-chip performance analysis, DATE Proc. (2007) 1-6.
- [12] Pande P.P. et al. Performance Evaluation and Design Trade-Offs for Network-on-Chip Interconnect Architectures. IEEE Computer, vol. 54(8), 2005.
- [13] K. Lahiri, S. Dey, A. Raghunathan, Evaluation of the traffic performance characteristics of system-on-chip communication architectures, VLSI Design Proc. (2001) 29.
- [14] A. Hansson, M. Wiggers, A. Moonen, K. Goossens, M. Bekooij, Applying dataow analysis to dimension buffers for guaranteed performance in networks on chip, NOCS Proc. (2008) 211-212.
- [15] M. Moadeli, A. Shahrabi, W. Vanderbauwheide, M. Ould-Khaoua, An analytical performance model for the spideron NoC, 21st AINA Proc. (2007) 1014-1021.August,2011
- [16] P. Bogdan, R. Marculescu, Quantum-like effects in network-on-chip buffers behavior, Proc. of the 44th Design Automation Conference (2007) 266-267.
- [17] M. Bakhouya, S. Suboh, J. Gaber, T. El-Ghazawi, Analytical modeling and evaluation of on-chip interconnects using network calculus, Proc. of the 3rd ACM/IEEE International Symposium on Networks-on-Chip (2009) 74-79.
- [18] Sheraz Anjum, Ehsan Ullah Munir,Waqas Anwar and Nadeem Javaid, Research Journal of Applied Sciences, Engineering and Technology 5(2): 353-356, 2013, "Object Oriented Model for Evaluation of On-Chip Networks".
- [19] K. change and et al. Performance evaluation and design trade-offs for wireless network-on-chip architectures ACM Journal on Emerging Technologies in Computing Systems (JETC, Volume 8 Issue 3, August 2012 Article No. 23 .
- [20] BookSim 2.0 User's Guide Nan Jiang, George Michelogiannakis, Daniel Becker, Brian Towles and William J. Dally May 7, 2013.
- [21] J. Kim and et al. Flattened Butterfly Topology for On-Chip Networks IEEE Computer Society Washington, DC, USA ©2007 Pages 172-182 ISBN:0-7695-3047-8 doi> 10.1109/MICRO.2007.15
- [22] Kumar, S. ; Lab. of Electron. & Comput. Syst., R. Inst. of Technol., Stockholm, Sweden ; Jantsch, A. ; Soininen, J.-P. ,IEEE Computer Society Ann Published date 24 April 2014ual Symposium on VLSI, "A network on chip architecture and design methodology"
- [23] Ville Rantala, Network on Chip Routing Algorithms University of Turku, Department of Information Technology Joukahaisenkatu 3-5 B, 20520 Turku, Finland No 779, August 2006
- [24] I. Cidon and K. Goossens. Network and transport layers in networks on chip. In G. De Micheli and L. Benini, editors, Networks on Chips: Technology and Tools, The MK Series in SoS, chapter 5, pages 147-202. Morgan Kaufmann, July 2006.
- [25] <http://www.diit.unict.it/users/mpalesi/nocarc09/slides/pande.pdf>

Determining the Types of Diseases and Emergency Issues in Pilgrims During Hajj: A Literature Review

Shah Murtaza Rashid Al Masud

College of Graduate Studies,
Universiti Tenaga Nasional,
Malaysia

Asmidar Abu Bakar

Department of Systems and
Networking,
Universiti Tenaga Nasional,
Malaysia

Salman Yussof

College of Computer Science and
Information Technology,
Universiti Tenaga Nasional,
Malaysia

Abstract—Introduction: Every year 2-3 million pilgrims with different background and most of them are elderly from 184 countries in the world congregate in the holy place ‘Haram’ at Makkah in Saudi Arabia to perform Hajj. During the pilgrimage, they come across a great deal of rough and tough environment, physical hassle and mental stress. Due to the hardship of travel, fluctuation of weather, continuous walking during religious rites at specific time and sites, many pilgrims injury, feel tired, sick, and exhausted. These may also create complications and overburden the physiological functions including heart, chest, abdominal, and kidney of those who suffer from chronic diseases. Besides the problem of diseases, crowds could cause some other significant problems including missing and lost pilgrims, injuries, and even death. **Objective:** To determine the common health problems e.g. diseases and emergency incidents encountered by pilgrims during Hajj was the main objective of this study. **Methods:** An extensive literature review to determine the common health problems and emergency incidents during Hajj was conducted through a systematic literature review. Numerous scholarly databases were used to search for articles published related to health problems and emergency incidents during Hajj from 2008 to 2016. Eligible articles included case reports, experimental and non-experimental studies. Only thirty articles out of two hundred and sixty articles had met the specific inclusion criteria. **Results:** The analysis revealed that respiratory diseases include pneumonia, influenza, and asthma (73.33%) were the main health problems encountered by the pilgrims during Hajj followed by heat stroke or heat attack, sunlight effects (16.67%), cardiovascular disease, heart disease (10%). The analysis also revealed that emergency incidents include traffic accidents, and trauma was 3.33%. Notwithstanding the information given above, according to the analysis, the common health problems during Hajj are mainly divided into two categories: non-communicable diseases (62.5%) and communicable diseases (37.5%). IBM’s statistical package for the social sciences (SPSS) version 22 was used to analysis the result. **Conclusion:** Both communicable and non-communicable health issues are the most common health problems encountered by pilgrims during Hajj. But, due to lack of existing studies associated with this research area, a definite conclusion could not be made. However, our findings demonstrated the necessity of new research to find solutions to pilgrims’ health problems during Hajj.

Keywords—Hajj; pilgrims; health; communicable diseases; non-communicable diseases; emergency

I. INTRODUCTION

The largest yearly religious mass gathering worldwide is the Hajj, one of the obligatory five pillars of Islam. Every year during Hajj event an amount of 2-3 million pilgrims and a total of 10 million pilgrims for Hajj and Umrah from 184 countries congregate in Makkah, Saudi Arabia [1, 2, 3, 4]. The number of Hajj pilgrims has increased rapidly from 58, 584 in 1920 to 20, 00,000 (approx) in 2015 where 13, 84, 931 attended from outside Saudi Arabia. During the last 95 years, the increase rate of foreign pilgrims is 3.5, and the reason is a nonstop expansion of the Grand Mosque at Ka’aba in Makkah [5]. The following Fig. 1 shows the number of pilgrims attending the Hajj during the year 2006-2015. Data were retrieved from the official portal of the royal embassy of Saudi Arabia, Saudi Ministry of Hajj, and central department of statistics and information [5, 6, 7].

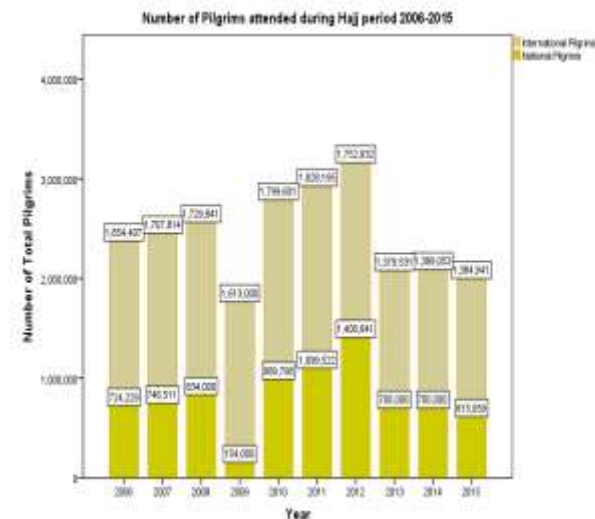


Fig. 1. Statistics of number of pilgrims performed Hajj during the year 2006-2016

Hajj is a dynamic system to appreciate fully the physical dimensions of it which imply movement and travel. Walking Hajj distance: from Kaaba to Mina: 8 km, from Mina to Arafat: 13 km, Arafat to Muzdalifah: 13 km, Muzdalifah to

Mina: 2 km, Mina to Jamarat Akabah: 3.8 km. Makkah to Madina 450 km. On arrival, the pilgrims must don the Ihram and circumambulate the Ka'ba seven times and then perform the Saa'y seven times between the hills Safa and Marwah, a total distance 3.5 km. Crowd densities can increase to seven individuals per m² during Hajj. Overcrowding is one of the major problems since the area is limited and the numbers are increasing annually. The area of pilgrimage rites is a sandy valley embraced by rugged sun-baked mountains. In Makkah, especially during the hot months of May to September the temperature ranges between 38°C and 50°C with a relative humidity of 25% to 50% [8]. This kind of hot environment with high radiant heat favors the development of heat illnesses e.g. heat exhaustion, heat stroke, unintentional physical injuries, and respiratory illnesses, dehydration called as non-communicable diseases or problems [9].

The imminence between pilgrims due to the packed and crowded accommodation, congregation, and prayers creates an ideal atmosphere for spread and transmission of infectious diseases. Influenza, influenza-like illness, meningococcal disease, viral hemorrhagic fevers, yellow fever, cholera, polio, plague, tuberculosis and gastrointestinal infections, foodborne diseases e.g. diarrhea, food poisoning, etc. are examples of communicable diseases [10, 11, 12, 13]. Due to the physical exertion and overcrowding situation, some pre-existing chronic diseases such as asthma, heart disease, chronic chest conditions, diabetes, renal and liver disease may become harmful for pilgrims especially elderly which eventually favors the spread of communicable namely non-chronic diseases or infectious disease [14].

According to the findings, respiratory diseases includes pneumonia, influenza, and asthma 73.33% were the main health problems encountered by the pilgrims during Hajj followed by heat stroke/ attack, sunlight effects 16.67%, diabetic/ diabetes mellitus 13.33%. Cardiovascular disease, heart disease 10%, hypertension 6.67%, dehydration 6.67%, musculoskeletal 6.67%, urinary tract problems 3.33%, meningococcal disease 3.33%, diarrhea and jaundice 3.33%, finally, traffic accidents and trauma 3.33%. According to the studies, the pilgrims encountered 62.5% non-communicable diseases and problems along with 37.5% communicable diseases during Hajj. To determine the common health problems e.g. diseases and emergency incidents encountered by pilgrims during Hajj was the primary objective of this study. Hence, the result from this study could be beneficial in initiating, planning and design the appropriate healthcare system to prevent diseases and emergency situations encountered by Hajj pilgrims.

II. SEARCH STRATEGY AND SELECTION CRITERIA

The Lancet, IEEE Explore, MedLine, EBSCO Host, PubMed, Google Scholar, Science Direct, the Elsevier (Scopus), Academic search complete, Springer Link, ACM digital library, Emerald Insight, Taylors and Francis and Wiley database were used to search for articles published related to health problems and emergency incidents during Hajj from 2008 to 2016. The majority of related articles were published in various prominent journals around the world where most of the studies were carried in Saudi Arabia, Iran,

France, United Kingdom, Malaysia, and Pakistan. Finally, we accessed official Saudi governmental statistics, with a particular emphasis on data from the Saudi Ministry of Health and Saudi Ministry of Hajj and Umrah. The combinations of specific keywords were utilized to retrieve the articles including pilgrims, Hajj, Diseases, healthcare, health problem, medical, medicine, over crowd, emergency incidents, health pattern. Only thirty studies had met the specific inclusion criteria: the subjects were Hajj, pilgrims, health, crowd, emergency; the type of study was experimental or non-experimental study; available full article in English. The research was conducted to find the answers to these questions e.g. What are the major diseases do the pilgrims carry and suffering? What are the reasons behind emergency incidents during Hajj? What are the emergency incidents occur during Hajj? Fig. 2 illustrates the search strategy as depicted. This paper is organized as, Section II: Search strategy and selection criteria; Section III: Data collection and analysis; Section IV: Analyzing the result; Section V: Discussion of the research; and Section VI: Conclusion.

III. DATA COLLECTION AND ANALYSIS

Items and their distributions of all respondents in the studies chosen were well briefed and summarized according to the author, and year. Meanwhile, the subsequent information gathered were objective, study design, the pattern of health problems and emergency situations, analyzing of the result and discussion of research shown in Table I. Table I tabulated all the information from selected articles.

IV. ANALYSING THE RESULT

Universally, elderly pilgrims were vulnerable to get the infection due to decreased rate of immune responses which is actively provoked by other factors such as hard work, lack of sleep and disturbances in the dietary schedule, and mental stress. Main reasons for infectious disease transmission due to airborne agents and pilgrims health hazards; especially injuries, trauma, etc. are extended stays at Hajj sites, and physical exhaustion, extreme heat, and crowded accommodation [15]. The most feared trauma hazard during Hajj is stampede causing huge casualties. Chronicle of Hajj disasters as depicted in Table II, where data retrieved from the official portal of the embassy of Saudi Arabia, Saudi Ministry of Hajj, and central department of statistics and information [5, 6, and 7]. Hajjis face multiple health issues like extreme temperatures, intravascular volume and electrolytes disturbances which also increases the risk of communicable and non-communicable diseases, where Hajj pilgrims encounter a great deal of tough physical and mental stress [16].

Some studies related to the current health and diseases situation during Hajj spotted that, one in three pilgrims experiences such respiratory symptoms [17]. Congestion and close contact stimulate the spread of infection especially upper respiratory tract infections URTIs followed by diseases of the skin, GIT, rheumatology [18, 19], and URTIs as reported among the most common cause of illness among Iranian pilgrims [20]. Other hazards include traffic accidents and fire injuries are reported in the literature [21]. Due to the hazards like accidents, overcrowding situation, and human jam many

pilgrims divert from their groups and get lost, where pilgrims are walking shoulder to shoulder in such massive Hajj gathering.

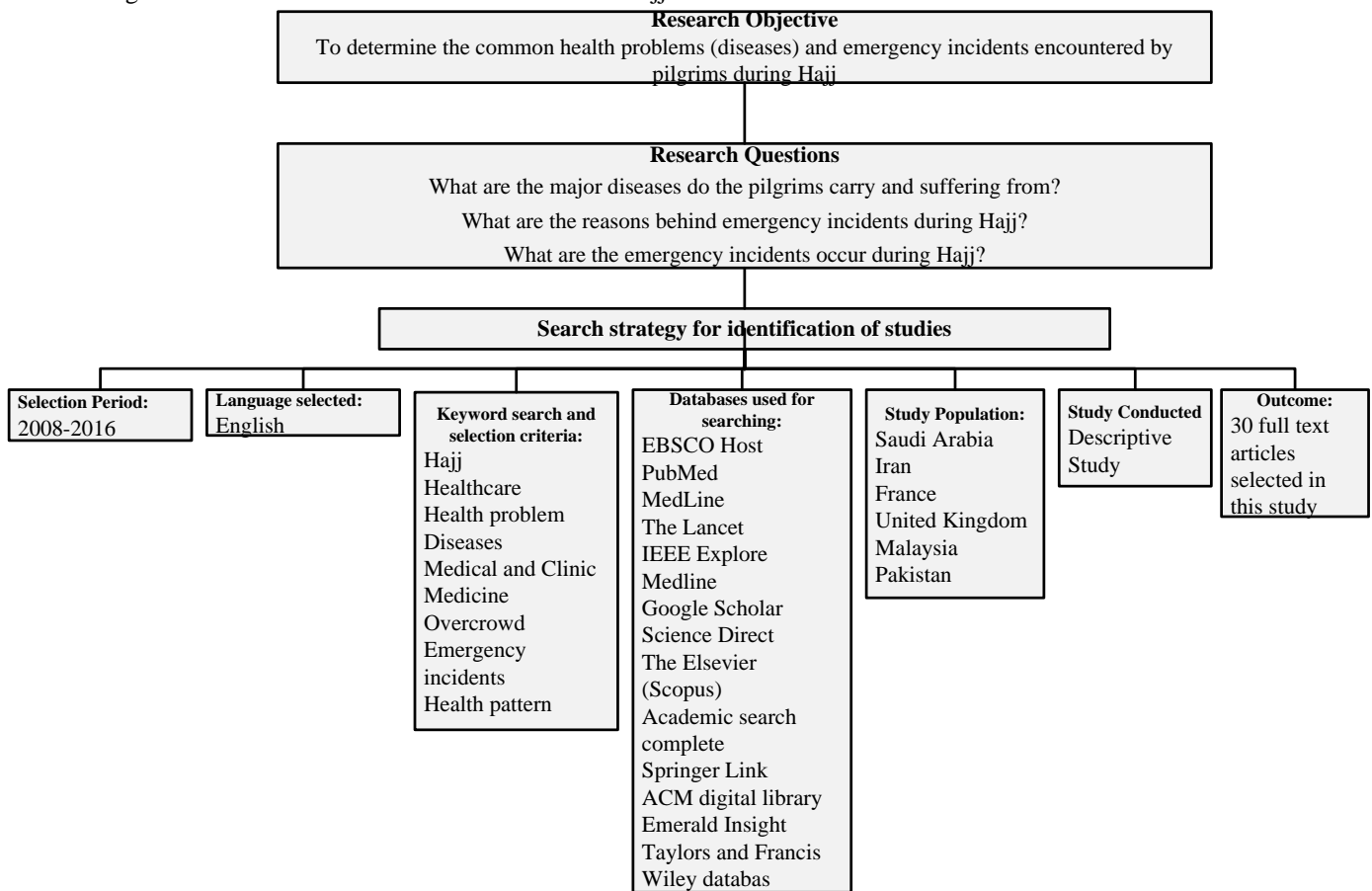


Fig. 2. Flow of the search strategy

TABLE I. EXPERIMENTAL STUDY ON THE BASED ON PILGRIMS' HEALTH PROBLEMS AND EMERGENCY INCIDENTS DURING HAJJ

Research Author, Year [Ref]	Objectives	Method	Result and Discussion
Memish et al. (2016) [22]	Hajj health services emerged as an ad-hoc activity to treat ailing pilgrims which are subject to consultation with global stakeholders for compliance with the International Health Regulations.	Comparative study	Emphasized on non-communicable diseases (NCDs) prevention
Bader et al. (2016) [23]	Clinical pattern of pneumonia during the Hajj period 2004-2013	A retrospective cohort analysis	The mortality rate in the intensive care unit-ICU was 21.45%, while the rate in the ward was 2.4%.
Murtaza et al. (2015)	Pattern of diseases among pilgrims seeking medical	Observational study	Respiratory diseases 52.5%, musculoskeletal

[24]	services		29.6%, skin 5.9%, cardiovascular 2.9%, urinary tract problems 2.3%, diabetic 17.9% and 26.4% hypertensive.
Sindy et al. (2015) [25]	To assess the pattern of patients and illnesses encountered at one health facility at Arafat during Hajj 2013 where acute severe asthma and injuries were the major problems encountered	Cross-sectional study	Bronchial Asthma 34%, Injuries 16%, Diabetes Mellitus 10.4%, Heat effects 6.6%, Hypertension 6.6%, Gastroenteritis 6.63% Dehydration 5.69%
Habsah et al. (2015) [26]	Determining the consequence of influenza vaccination alongside acute respiratory illness amongst Malaysian Hajj pilgrims	Observational cohort study	Respiratory illness was a major problem and caused high hospital admission during Hajj seasons.
Abdulrahman et al. (2015)	Evaluating the diseases pattern among pilgrims during the Hajj	Cross sectional study	Respiratory problems 17.6%, skin diseases 15.7%,

[27]	season 2013		gastrointestinal tract (GIT) diseases 13.2%				accounting for 25-50% of such admission.
Nurul et al. (2014) [28]	Overcrowding, extreme temperatures, and electrolytes imbalance are common among pilgrims. These factors trigger the increased risk for the communicable and non-communicable disease.	Cross-sectional study	The analysis revealed that respiratory diseases 76.2% was the main health problem followed by skin disease 7.4%, meningococcal disease 3.7% and heat stroke 3.7%.	Abdullah et al. (2012) [35]	Establishing a pragmatic system to manage the challenge of cardiovascular morbidities and mortality during Hajj.	Cross-sectional study	Most significant causes of death during 2002 Hajj was cardiovascular diseases (with hypertension) 45.8%, followed by respiratory and cardiac system failure 14.3%, traffic accidents and other traumas 6.4%
Memish et al. (2014) [29]	Infectious disease surveillance during Hajj 2012 and 2013	Descriptive study	Report showed that infectious diseases posed the major threat among pilgrims	Alzahrani et al. (2012) [36]	Seeking medical services for pilgrims suffering from various diseases.	Descriptive study	Respiratory diseases 60.8%, musculoskeletal 17.6%, skin disease 15.0% and gastrointestinal 13.1%.
Habida et al. (2014) [30]	Need for equal attention on infectious and non-communicable diseases during Hajj	Comparative study	The majority about 60% of pilgrims participating in the Hajj are elderly with preexisting chronic conditions. Mental stress, overcrowded conditions, extreme heat and sunlight leading to heat cramps, heat exhaustion, heat stroke, and dehydration which ultimately favors spreading infectious diseases.	Mandourah et al. (2012) [37]	Determining diseases among hospitals providing medical care to Hajj pilgrims.	Prospective cohort study.	Pneumonia was the primary cause of critical illness 27.2%
Osamah et al. (2014) [31]	The attack rate of influenza-like illnesses due to respiratory viruses among the pilgrims from Saudi Arabia, Australia, and Qatar during Hajj 2013	Cross-sectional study	11 % pilgrims had influenza, where rhinovirus was the commonest cause 28%.	Memish et al. (2012) [38]	The occurrence of different respiratory viruses among healthcare worker during Hajj event. Pilgrims' attendance at the Hajj was proportional to the increase of acquiring influenza.	Cross-sectional study	Rhinoviruses and Coronaviruses 22% were detected during the study. Influenza A 0.1-0.2%
Samir et al. (2014) [32]	Specimen of France pilgrims during Hajj 2013 were tested for respiratory viruses and bacteria	Prospective cohort study	Rhinovirus (14.0%), coronavirus E229 (12.4%), and influenza A (H3N2) virus (6.2%)	Moattari et al. (2012) [39]	Seasonal and pandemic influenza attack rate among returning Iranian pilgrims after the 2009 Hajj.	Cross-sectional study	By virus culture, it was recorded that about 9.1% pilgrims had influenza
Samir et al. (2013) [33]	Identifying the pattern of at least 11 respiratory viruses during Hajj 2012 among the pilgrims of France	Prospective cohort study	38.6% pilgrims were affected by different respiratory viruses including rhinovirus, adenovirus, influenza B, and enterovirus	Almaliki et al. (2012) [40]	Estimating the frequency of the cardiovascular diseases during Hajj 2011	Descriptive study	Ischemic heart disease 34%, elevated blood pressure 20% and stroke 17%
Tawfiq et al. (2013) [34]	Causes of respiratory tract infection during Hajj	Cross-sectional study	The most common respiratory tract viruses are influenza and rhinovirus. Pneumonia is a significant cause of an admission	Ziyaeyan et al. (2012) [41]	The occurrence of A (H1N1) among returning Iranian pilgrims.	Cross-sectional study	Influenza A (1.6%)
				Saeed et al. (2012) [42]	The prevalence of three symptoms of interest diarrhea, acute respiratory infection and jaundice among Afghanistan Hajjis during Hajj 2010	Cross-sectional Study	Diarrhea and jaundice remained constant, but Acute respiratory infection 1.4% at pre-transit to 4% at transit area and 37% during Hajj.
				Asghar et al. (2011) [43]	Find the common causes of bacterial pneumonia during the 2005 Hajj season.	Cross-sectional study	Clinically suspected pneumonia 53.9% were confirmed positive.

Mimish et al. (2011) [44]	Electrocardiographic (ECG) changes in exposed to high outdoor temperature 45-degree centigrade, humidity approaching 80% with heat stroke and heat exhaustion.	Case-control study	Sinus tachycardia and ischemic changes.
Mirza et al. (2011) [45]	Predictors of asthma exacerbations during the Hajj.	Cohort study.	46.6% suffered from mild asthma attack, and 31% suffered from moderate asthma attack
Zakuan et al. (2010) [46]	The relationship between pre-morbid conditions and influenza-like illness (ILI) among Malaysian pilgrims during Hajj 2007	Cross-sectional study	Underlying asthma was significantly associated with severe ILI, e.g. a sore throat, longer duration of a cough, runny nose ($p=0.016$) and the Pilgrims who suffered from chronic obstructive pulmonary diseases (COPD), diabetes mellitus and respiratory problem.
Alborzi et al. (2009) [47]	Incidence of the common respiratory viruses among Iranian pilgrims during Hajj 2006	Cross-sectional study	The rates of different types of respiratory virus infections: influenza (9.8%), parainfluenza (7.4%), adenovirus (5.4%) and RSV (1.4%). Where Viral agents (25%) of nasal specimens
Gautret et al. (2009) [48]	The incidence of a febrile cough among French pilgrims during Hajj.	Prospective cohort study	Diabetes mellitus 22.8%, Hypertension 25.3
Gautret et al. (2009) [49]	Investigate prospectively the occurrence of common health hazard in French pilgrims during Hajj 2007	Prospective cohort study	Cough 51%, followed by a headache, heat stress, and fever
Rashid et al. (2008) [50]	Burden of influenza and RSV in asymptomatic British pilgrims during Hajj	Cross-sectional study	Influenza or RSV with 18%
Rashid et al. (2008) [51]	Rates of various influenza virus infections among the UK and Saudi pilgrims during Hajj.	Comparative study	25% the UK and Saudi pilgrims

A total of 30 studies related to communicable diseases or infectious diseases and non-communicable diseases/problems or chronic diseases were used for analyzing the result. Regarding the study design of the selected articles; most of the studies were based on cross-sectional studies 46.67%, prospective cohort study 16.67%, descriptive study 10%, comparative study 6.67%, retrospective cohort analysis 3.33%, comparative study 3.33%, case-control study 3.33%, and Cohort study 3.33% as depicted in Fig. 3. Different types of instruments were used in the quantitative studies.

TABLE II. CHRONICLE OF DISASTER: 1990-2015

1990: 1426 pilgrims killed by stampede/asphyxiation in tunnel leading to holy sites
1994: 270 killed in a stampede
1997: 343 pilgrims died and 1500 injured in a fire
1998: 119 pilgrims died in a stampede
2001: 35 pilgrims died in a stampede
2003: 14 pilgrims died in a stampede
2004: 251 pilgrims died in a stampede
2006: 76 pilgrims died after a hotel housing pilgrims collapsed; a stampede wounded 289, killing 380
2015: 4173 pilgrims died in a stampede

Experimental studies based on pilgrims' health problems and emergency incidents during Hajj

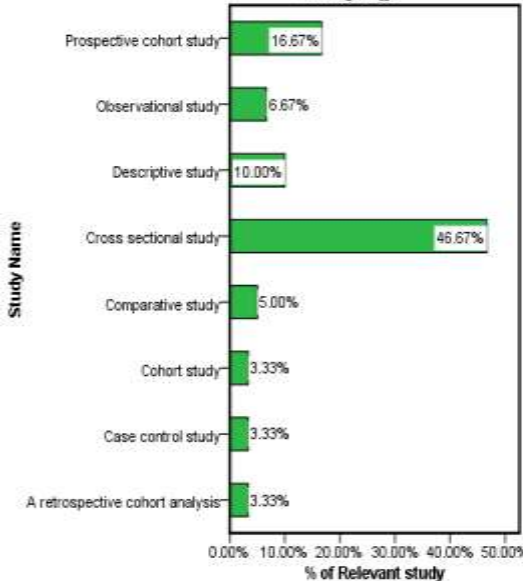


Fig. 3. Percentage of studies based on pilgrims' health problems and emergency incidents during Hajj

Out of 30 selected studies, 22 articles had concluded that respiratory diseases include pneumonia, influenza, and asthma 73.33% were the main health problems encountered by the pilgrims during Hajj as presented in Table III and Fig. 4. The above findings followed by heat stroke/ attack, sunlight effects 16.67%, diabetic/ diabetes mellitus 13.33%, cardiovascular disease, heart disease 10%, hypertension 6.67%, dehydration 6.67%, musculoskeletal 6.67%, urinary tract problems 3.33%, meningococcal disease 3.33%, diarrhea and jaundice 3.33%, finally, traffic accidents and trauma 3.33%.

TABLE III. MAJOR HEALTH PROBLEMS ENCOUNTERED BY PILGRIMS
ACCORDING TO THE STUDIES AND CATEGORIZATION OF DISEASES

Diseases name, major health problems	Number of studies	Percentage of health problems	Category based on Communicable Diseases (CD)/problems-Chronic, Non-Communicable Diseases(NCD)-Infectious
Respiratory disease includes asthma, influenza, pneumonia	[23] [24] [26] [27] [28] [31] [32] [33] [34] [35] [36] [37] [38] [39][41][42] [43][45] [46] [47][50] [51]	22 of 30, 73.33%	Both CD-Infectious (Influenza, Pneumonia), NCD-Chronic (Asthma)
Various communicable diseases	[22]	3.33%	NCD-Chronic
Various infectious disease	[29]	3.33%	CD-Infectious
Cardiovascular disease, heart disease	[24] [35] [40]	10%	NCD-Chronic
Urinary tract problems	[24]	3.33%	CD-Infectious
Skin problem	[24] [27] [28] [36]	13.33%	CD-Infectious
Heat stroke/ attack, Sunlight effects	[25] [28] [30] [44] [49]	16.67%	NCD-Chronic
Diabetic/ diabetes mellitus	[24] [25] [26] [48]	13.32%	NCD-Chronic
Hypertension	[25] [48]	6.67%	NCD-Chronic
Gastroenteritis	[25] [27] [36]	10%	NCD-Chronic
Dehydration	[25] [30]	6.67%	NCD-Chronic
Meningococcal disease	[28]	3.33%	CD-Infectious
Musculoskeletal	[24] [36]	6.67%	NCD-Chronic
Diarrhea and jaundice	[42]	3.33%	CD-Infectious
Traffic accidents and Trauma	[35]	3.33%	NCD-Chronic

Health problems or diseases are categorized into two main classes, namely communicable or infectious diseases and non-communicable or chronic diseases. According to the studies, as shown earlier in Table I and Table III, 62.5% are non-communicable diseases and 37.5% are communicable diseases, as shown in Fig. 5, encountered by the pilgrims during Hajj.

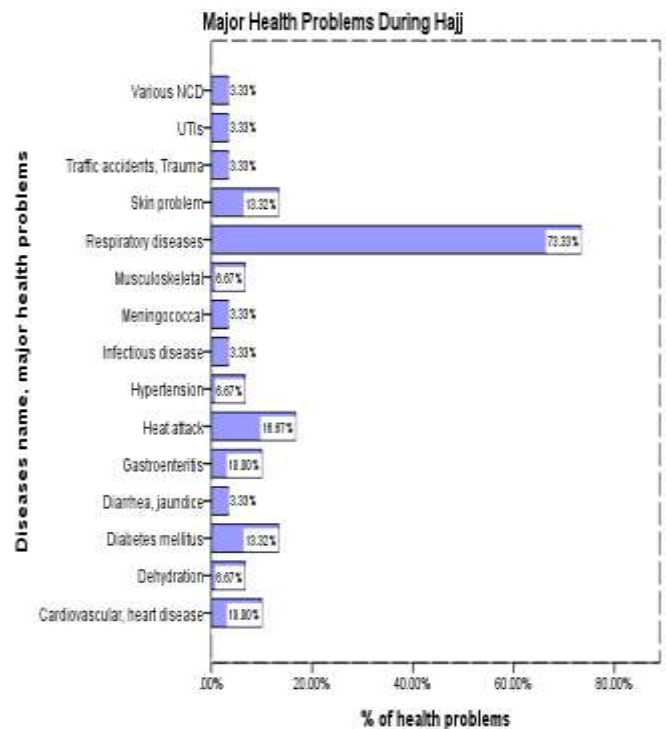


Fig. 4. Percentage of studies according to major health problems

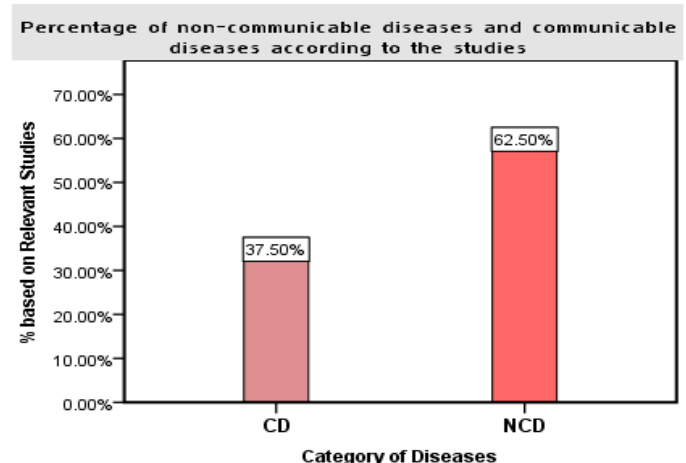


Fig. 5. Percentage of non-communicable diseases and communicable diseases according to the studies

V. DISCUSSION OF THE RESEARCH

This concise review is intended to present a structured analysis of published articles of health problems and emergency situation over the past ten years with regards to Hajj pilgrim. Health problems and their challenges for pilgrims during the pilgrimage, related outcomes, and suggestions for future investigators are highlighted in this study.

Respiratory Tract Infections were considered as the predominant clinical health patterns which encountered by Hajj pilgrims. It continues to be the increasing burden of diseases among Hajj pilgrims, but there is still a lack of studies being conducted to overcome these problems. Researchers had identified respiratory diseases as the most common cause of hospital admission (52.5%) during Hajj, with pneumonia being the leading reason for hospitalization. A prospective study was conducted in two different hospitals during Hajj 2011 [24]. The overall mortality rate in the ward among pilgrims with pneumonia was 2.4% and in the ICU was 21.45% during Hajj period 2004-2013 which is similar to the mortality rates in West [23]. Out of 30 selected studies, 22 of articles had concluded that respiratory diseases includes pneumonia, influenza and asthma 73.33% were the main health problems encountered by the pilgrims during Hajj [23] [24] [26] [27] [28] [31] [32] [33] [34] [35] [36] [37] [38] [39] [41] [42] [43] [45] [46] [47] [50] [51].

Meningococcal Disease: A crowded environment with high humidity and dense air pollution are the main reasons for a meningococcal disease which is defined as an infection as high as 3.33% among all the diseases encountered by pilgrims during Hajj [28].

Skin Infections: Bacterial skin infection is one of the pilgrims' health problems where Makkah is one of the hottest places in the world with the temperature range of 38 to 42°C during Hajj. The studies revealed that 23.6% dermatitis and 11.2% pyoderma patients were reported during Hajj. Among 80 pyoderma cases, 52.5% were primary pyoderma where impetigo was the leading causes for primary pyoderma. Whereas, 47.5% were secondary pyoderma led by *Staphylococcus aureus* responsible as main causative agents and followed by *Streptococcus pyogenes* [24] [27] [28] [36].

Environmental Heat Injury: The main factor of heat stress during Hajj as revealed from the literature are extreme summer temperature, direct and long time heat exposure from the sun, heat from vehicles and internal heat which lead to heat exhaustion or heat stroke among pilgrims [25] [28] [30] [44] [49].

Cardiovascular Diseases: Over the past few years, the study revealed cardiovascular disease with hypertension is one of the important causes of pilgrims' intensive care unit-ICU admission with high mortality rate [24] [40]. During 2002 Hajj, the percentage of cardiovascular diseases was 45.8 [35].

Gastrointestinal infections: Major food-borne outbreaks of gastroenteritis with high mortality rates are common at all religious festivals, including the Hajj [25] [27] [36].

Blood-borne diseases: To shave head during Hajj is compulsory which leads to transmission of blood-borne diseases including hepatitis B, C, and HIV. Illegal unlicensed barbers continue to operate the act whether the Saudi Ministry of health-MoH promotes and encourages all pilgrims to receive hepatitis B vaccination before travel to Hajj [22, 29].

Malaria: Although WHO classifies Saudi Arabia as a low, geographically restricted malaria transmission area and since 2008 has been listed as being in the elimination stage of the program, but the risk during Hajj is still exist. In 2011 Hajj season 19 cases of *P. vivax* malaria was reported where 75% such cases found among the Indian and Ethiopian pilgrims. In 2012, 48 cases of malaria were recorded in Makkah and 78 cases were recorded in Madinah among Pakistan, Nigeria, Guinea, India, Mauritania, Chad, Mali, Afghanistan, Somalia, Ethiopia, Yemen and Ivory Coast pilgrims.

Trauma risks: During Hajj trauma is one of the major causes of morbidity and mortality. In a prospective study of 713 trauma patients, who were injured while performing Hajj, presenting to the emergency room, 248 (35%) were admitted to surgical departments and intensive care. The most common surgical presentations were orthopedic and neurosurgical [35]. For a large part of the Hajj, pilgrims travel either by foot, walking through or near dense traffic, or in vehicles themselves.

Fire-related injury: In 1997, fire devastated the Mina area when makeshift tents were set ablaze by open stoves since banned at the Hajj. There were 343 deaths and more than 1500 estimated casualties. Since then all makeshift tents have been replaced by permanent fiberglass installations. At Hajj time, Teflon-coated awnings are added, and the aluminum frames remain in place the rest of the year. No pilgrim is permitted to set up his own tent. Additionally, pilgrims are not allowed to cook food at Mina. Smoking is forbidden during the Hajj by Islamic teaching, thus reducing the risk of a naked flame. Continuous public education is being undertaken to further reduce fire risk.

Environmental heat injury: Heat exhaustion and heatstroke are a leading cause of morbidity and mortality during the Hajj, particularly in summer. Temperatures in Mecca can rise higher than 45°C. Lack of acclimatization, arduous physical rituals, and exposed spaces with limited or no shade, produces heatstroke in many pilgrims. Adequate fluid intake and seeking shade is essential. Supplicating pilgrims might not notice the dangers of extreme heat exposure until their symptoms are pronounced. Water mist sprayers operate regularly in the desert at Arafat, a time of high risk for heatstroke, when many stand for long hours during the day. Performing rituals at night, using umbrellas, seeking shade, and wearing high-SPF sunblock creams are all advisable and permissible during the Hajj. Children accompanying their parents must be specially protected. The timings of rites are flexible and acceptable at the pilgrim's convenience—it is key that pilgrims are aware of this since, through fear of committing errors, they might not make sensible choices in completing their rituals [25] [28] [30] [44] [49]. Although the Hajj is not due to fall in the summer for

several years, Saudi winters are warmer (35–50°C) than most pilgrims will be used to, and they must seek shade and drink plenty of fluid during their rites.

Occupational hazards of abattoir workers: Abattoir workers at the Hajj are exposed to unique traumatic risks. Over a million cattle are slaughtered each Hajj, up to half a million before noon on the 10th day of the Hajj. In one study, 298 emergency visits for hand injury were treated in Mecca over four Hajj seasons. More than 80% were injuries from animal slaughter; many avoidable injuries were sustained by lay people and not trained abattoir workers. Pilgrims need to be assured that professional slaughtering arrangements are easily available at the Hajj, and far safer.

VI. CONCLUSION

Both communicable and non-communicable health issues are the most common health problems encountered by pilgrims during Hajj. But, due to lack of existing studies associated with this research area, a definite conclusion could not be made. However, our findings demonstrated the necessity of new research to find solutions to pilgrims' health problems during Hajj.

ACKNOWLEDGEMENT

This study obtained no funding. Authors do not have any conflict of interest.

REFERENCES

- [1] Gatrad AR, Sheikh A. Hajj: journey of a lifetime. BMJ 2005; 330: 133–37.
- [2] Kraemer JL. The Hajj: the Muslim pilgrimage to Mecca and the holy places. Hist Religions 2000; 40: 198–203.
- [3] WHO report on Hajj: http://www.who.int/csr/ITH_final.pdf
- [4] Ministry of Health, KSA guideline on Hajj: <https://www.moh.gov.sa/en/Hajj1436/Awareness/Documents/DlelHaj-E.pdf>
- [5] "1,384,941 foreign pilgrims participated in Hajj". Royal Embassy of Saudi Arabia. 22 September 2015. Retrieved 26 Sep 2015.
- [6] Ministry of Hajj, Saudi Arabia. Supreme Hajj Committee. <http://www.hajinformation.com/main/u1.htm> (accessed May-June, 2016).
- [7] Central Department of Statistics and Information. <http://www.cdsi.gov.sa/english/> (accessed May-June, 2016).
- [8] M Khogali, Epidemiology of Heat Illnesses During the Makkah Pilgrimages in Saudi Arabia, International Journal of Epidemiology, Vol. 12, No. 3, 1983,12: 267-273
- [9] Ghaznawi HI, Ibrahim MA. Heat stroke and heat exhaustion in pilgrims performing the Haj (annual pilgrimage) in Saudi Arabia. Ann Saudi Med 1987;7:323-6.
- [10] Z A Memish, S J N McNabb, F Mahoney, F Alrabiah, N Marano, Q A Ahmed, J Mahjour, R A Hajjeh, P Formenty, F H Harmanci, H El Bushra T M Uyeki, M Nunn, N Isla, M Barbeschi, and the Jeddah Hajj Consultancy Group, Establishment of public health security in Saudi Arabia for the 2009 Hajj in response to pandemic influenza A H1N1, Lancet 2009; 374: 1786–91
- [11] Memish ZA, Ahmed QA. Mecca-bound: the challenges ahead. J Travel Med 2002; 9: 202–10.
- [12] Rashid H, Shafi S, Haworth E, et al. Viral respiratory infections at the Hajj: comparison between UK and Saudi pilgrims
- [13] Madani TA, Ghabrah TM, Albarrak AM, et al. Causes of admission to intensive care units in the Hajj season of the Islamic year 1424 (2004). Ann Saudi Med. 27; 2007: 101–105. Available from: URL: <http://www.researchgate.net/publication> /6451514_Causes_of_admission_to_intensive_care_units_in_the_Hajj_p eriod_of_the_Islamic_year_1424_(2004)
- [14] Shuja Shafi, Ziad A Memish , Abdul Rashid Gatrad , Aziz Sheikh, Hajj 2006: communicable disease and other health risks and current official guidance for pilgrims, Eurosurveillance, 15 December 2005
- [15] Ahmed Q, Arabi Y, Memish ZA. Health risks at the Hajj. Lancet 2006;367(9515):1008-15
- [16] Mandourah Y, Al-Radi A, Ocheltree AH, Ocheltree SR, Fowler RA. Clinical and temporal patterns of severe pneumonia causing illness during Hajj. BMC Infect Dis. 12; 2012: 117. Available from: URL: <http://www.biomedcentral.com/1471-2334/12/117>
- [17] Gatrad AR, Shafi S, Memish ZA, Sheikh A. Hajj and the risk of influenza. Br Med J. 33; 2006: 1182–1183. Available from: URL: <http://www.bmjjournals.org/content/333/7580/1182.full.pdf+html>
- [18] El-Sheikh SM, El-Assouli SM, Mohammed KA, Albar M. Bacteria and viruses that causes respiratory tract infections during the pilgrimage (Haj) season in Makkah, Saudi Arabia. Trop Med Int Health. 3(3); 1998: 205–09. Available from: URL: [http://www.researchgate.net/publication/13691513_Bacteria_and_viruse s_that_cause_respiratory_tract_infections_during_the_pilgrimage_\(Haj\)_season_in_Makkah_Saudi_Arabia](http://www.researchgate.net/publication/13691513_Bacteria_and_viruse s_that_cause_respiratory_tract_infections_during_the_pilgrimage_(Haj)_season_in_Makkah_Saudi_Arabia)
- [19] Abdulrahman R. Bakhsh, MBBS, EMDM, Abdulfattah I. Sindy, MBBS, Mostafa J. Baljoon, PhD, Khalid O. Dhafar, FRCS, FACS, Zohair J. Gazzaz, MBChB, PhD, Mukhtiar Baig, MBBS, PhD, Basma A. Deiab, PhD, and Fauzea T. Al Hothali, DN, BSN, Diseases pattern among patients attending Holy Mosque (Haram) Medical Centers during Hajj 1434 (2013), Saudi Med J. 2015 Aug; 36(8): 962–966.
- [20] Meysamie A, Ardakani HZ, Razavi SM, Doroodi T. (2006). Comparison of mortality and morbidity rates among Iranian pilgrims in Hajj 2004 and 2005. Saudi Med J. 27 (7): 1049- 1053. Available from: URL: smj.psmmc.med.sa/index.php/smj/article/viewFile/3733/1507
- [21] British Broadcasting Corporation (BBC) News. 2006. Available from: URL: http://news.bbc.co.uk/2/hi/middle_east/6164337.stm
- [22] Ziad A Memish, Habida Elachola, Mujeeb Rahman, Samba Sow, Nawfal Aljerian, Abdullah Assir, Objection to chronic disease based restrictions during the Hajj, www.thelancet.com Vol 387 April 23, 2016
- [23] Bader Hamza Shiraha, Syed Husham Zafar b, Olayan Ali Alferaidi b, Abdul Momin Muhammad Sabir b, Mass-gathering medicine (Hajj Pilgrimage in Saudi Arabia): The clinical pattern of pneumonia among pilgrims during Hajj, Journal of Infection and Public Health (2016) April
- [24] Murtaza Ali Gowa, Syed Ali Ammar, Ahmed Ali, Syed Muhammad Kashif Kazmi, Rana Farrukh, Ali Abbas Mohsin Ali & Syed Muhammad Mustahsan, Health Issues confronting Muslims on Hajj, International Journal of Endorsing Health Science Research www.aeirc-edu.com Volume 3 Issue 2, July 2015
- [25] Sindy AI, Baljoon MJ, Zubairi NA, Dhafar KO, Gazzaz ZJ, Deiab BA, et al. Pattern of patients and diseases during mass transit: The day of Arafat experience. Pak J Med Sci 2015;31(5):1099-1103. doi: <http://dx.doi.org/10.12669/pjms.315.8017>
- [26] Habsan Hasan, Zakuan Zainy Deris, Siti Amrah Sulaiman, Mohd Suhaimi Abdul Wahab, Nyi Nyi Naing, Zulkefle Ab Rahman, Nor Hayati Othman, Effect of Influenza Vaccination on Acute Respiratory Symptoms in Malaysian Hajj Pilgrims, Journal of Immigrant and Minority Health, August 2015, Volume 17, Issue 4, pp 1114-1119
- [27] Abdulrahman R. Bakhsh, MBBS, EMDM, Abdulfattah I. Sindy, MBBS, Mostafa J. Baljoon, PhD, Khalid O. Dhafar, FRCS, FACS, Zohair J. Gazzaz, MBChB, PhD, Mukhtiar Baig, MBBS, PhD, Basma A. Deiab, PhD, and Fauzea T. Al Hothali, DN, BSN, Diseases pattern among patients attending Holy Mosque (Haram) Medical Centers during Hajj 1434 (2013), Saudi Med J. 2015 Aug; 36(8): 962–966.
- [28] Nurul Diana Dzaraly, Nor Iza A. Rahman, Nordin Bin Simbak, Suhaimi Ab. Wahab, Omar Osman, Salwani Ismail, Mainul Haque, Patterns of Communicable and Non-Communicable Diseases in Pilgrims during Hajj, Research J. Pharm. and Tech. 7(9): Sept. 2014 Page 1052-1059

- [29] Ziad A Memish, Alimuddin Zumla, Rafat F Alhakeem, Abdullah Assiri, Abdulhafeez Turkestani, Khalid D Al Harby, Mohamed Alyemni, Khalid Dhafar, Philippe Gautret, Maurizio Barbeschi, Brian McCloskey, David Heymann, Abdullah A Al Rabeeah, Jaffar A Al-Tawfiq, Hajj: infectious disease surveillance and control, Lancet mass gatherings medicine 1, www.thelancet.com Vol. 383 June 14, 2014
- [30] Habida Elachha, Abdullah M. Assiri, Ziad A. Memish, Sun protection during the Hajj mass-gathering – 2013, Travel medicine and infectious disease, Elsevier, November December, 2014 Volume 12, Issue 6, Part B, Pages 783–784 DOI: <http://dx.doi.org/10.1016/j.tmaid.2014.09.005>
- [31] Osamah Barasheed, Harunor Rashid, Mohammad Alfelali, Viral respiratory infections among Hajj pilgrims in 2013, VIROLOGICA SINICA 2014, 29 (6): 364-371, DOI 10.1007/s12250-014-3507-x
- [32] Samir Benkouiten, Rémi Charrel, Khadija Belhouchat, Tassadit Drali, Antoine Nougairede, Nicolas Salez, Ziad A. Memish, Malak Al Masri, Pierre-Edouard Fournier, Didier Raoult, Philippe Brouqui, Philippe Parola, and Philippe Gautret, Respiratory Viruses and Bacteria among Pilgrims during the 2013 Hajj, Emerging infectious diseases, Volume 20, Number 11—November 2014, DOI: 10.3201/eid2011.140600
- [33] Samir Benkouiten, Rémi Charrel, Khadija Belhouchat, Philippe Gautret et. al. Circulation of Respiratory Viruses Among Pilgrims During the 2012 Hajj Pilgrimage, Clinical Infectious Diseases (2013) 57 (7):992-1000.doi: 10.1093/cid/cit446First published online: July 9, 2013
- [34] Al-Tawfiq JA, Zumla A, Memish ZA. Respiratory tract infections during the annual Hajj: potential risks and mitigation strategies. Current Opinion in Pulmonary Medicine, Infectious diseases, 2013; 19:192–7.
- [35] Abdullah Al Shemeiri, Cardiovascular disease in Hajj pilgrims, Journal of the Saudi Heart Association, Volume 24, Issue 2, April 2012, Pages 123–127
- [36] Alzahrani AG, Choudhry AJ, Al Mazroa MA, Turkistani AHM, Nouman GS, Memish ZA. Pattern of diseases among visitors to Mina health centers during the Hajj season, 1429 H. Journal of Infection and Public Health. 5; 2012: 22-34. Available on <http://Elsevier.com/locate/jiph>
- [37] Mandourah Y, Al-Radi A, Ocheltree AH, Ocheltree SR, Fowler RA. Clinical and temporal patterns of severe pneumonia causing illness during Hajj. BMC Infect Dis. 12; 2012: 117. Available from: URL: <http://www.biomedcentral.com/1471-2334/12/117>
- [38] Memish Z.A, Assiri A.M, Hussain R, Alomar I, Stephens G. Detection of respiratory viruses among pilgrims in Saudi Arabia during the time of a declared Influenza A(H1N1) Pandemic. J Travel Med. 19(1); 2012: 15–2. Available from: URL: [http://www.researchgate.net/publication/51922829_The_prevalance_of_respiratory_viruses_among_healthcare_workers_serving_pilgrims_in_Makkah_during_the_2009_influenza_A_\(H1N1\)_pandemic/file/32bfe50e495caab336.pdf](http://www.researchgate.net/publication/51922829_The_prevalance_of_respiratory_viruses_among_healthcare_workers_serving_pilgrims_in_Makkah_during_the_2009_influenza_A_(H1N1)_pandemic/file/32bfe50e495caab336.pdf)
- [39] Afagh Moattari, Amir Emami, Mohsen Moghadami, Behnam Honarvar, Influenza viral infections among the Iranian Hajj pilgrims returning to Shiraz, Fars province, Iran. Influenza and Other Respiratory Viruses 6(601), 2012, e77–e79
- [40] WH Almalki, The prevalence of cardiovascular diseases_and_role_of_protective_measures_among_hajj_pilgrims 1432)_2011,
- Pakistan Journal of Pharmacology Vol.29, No.2, July 2012, pp.29-34
- [41] Alborzi A, Aelami MH, Ziyaeyan M, Jamalidoust M, Moeini M, Pourabbas B, Abbasian A. Viral etiology of acute respiratory among Iranian Hajj pilgrims. J. Travel Med. 16(4); 2009: 239-242. Available on <http://onlinelibrary.wiley.com/doi/10.1111/j.1708-305.2009.00301.x/pdf>
- [42] Islam Saeed, Jawad Mofleh, Hafiz, Iqbal, Occurrence of acute respiratory infection, diarrhea and jaundice among Afghan pilgrims, 2010, Source: PubMed, December 2012 DOI: 10.1016/j.jegh.2012.11.003
- [43] Asghar AH, Ashshi AM, Azhar EI, Bukhari SZ, Zafar TA, Momenah AM. Profile of bacterial pneumonia during Hajj. Indian J Med Res. 133; 2011: 510–513. Available from: URL: http://www.researchgate.net/publication/51175189_Profile_of_bacterial_pneumonia_during_Hajj
- [44] Mimish, L. Electrocardiograph findings in heat stroke and exhaustion: A study on Makkah pilgrims. J Saudi Heart Assoc. 24; 2012: 35-39. Available from: URL:<http://www.sciencedirect.com/science/article/pii/S1016731511002119>
- [45] Mirza TA, Fillimban A, Maimini O, Khiyat EY, Dhafar KO, Farooq MU, Gazzaz ZJ. Predictors of asthma severity during the pilgrimage to Mecca (Hajj). Pol Arch Med Wewn. 121 (10); 2011: 327-332. Available from: URL:http://allegro.cartel-color.com/sites/default/files/pamw_2011-10_57-Farooq_0.pdf
- [46] Zakuan Zainy Deris, Habsah Hasan, Mohd Suhaimi Ab. Wahab, Siti Amrah Sulaiman, Nyi Nyi Naing and Nor Hayati Othman, The association between pre-morbid conditions and respiratory tract manifestations amongst Malaysian Hajj pilgrims, Tropical Biomedicine 27(2): 294–300 (2010)
- [47] Alborzi A, Aelami MH, Ziyaeyan M, Jamalidoust M, Moeini M, Pourabbas B, Abbasian A. Viral etiology of acute respiratory among Iranian Hajj pilgrims. J. Travel Med. 16(4); 2009: 239-242. Available on <http://onlinelibrary.wiley.com/doi/10.1111/j.1708-305.2009.00301.x/pdf>
- [48] P. Gautret1, W. Yong1,2, G. Soula1,3, J. Gaudart4, J. Delmont1,3, A. Dial, P. Parola1 and P. Brouqui1, Incidence of Hajj-associated febrile cough episodes among French pilgrims: a prospective cohort study on the influence of statin use and risk factors, Journal of Clinical Microbiology and Infect 2009; 15: 335–340
- [49] Gautret P, Soula G, Delmont J, Parola P, Brouqui P. Common health hazards in French pilgrims during the Hajj of 2007. A prospective cohort study. J Travel Med. 16(6): 2009: 377-81. Available from: URL: www.ncbi.nlm.nih.gov/pubmed/19930376
- [50] Rashid H, Shafi, Booy, RS, El Bashir H, Ali K, Zambon, MC, et al. Influenza and respiratory syntical virus infection in British pilgrims. Emerg Health Threats J. 1(2); 2008: 2-5. Available from: URL www.eht-journal.org
- [51] Rashid H, Shafi S, Haworth, E, El Bashir H, Memish ZA, Sudhanya M, et al.. Viral respiratory infections at the Hajj: Comparison between UK and Saudi pilgrims. Clin Microbiol Infect. 14; 2008: 569-74. Available from: URL: <http://onlinelibrary.wiley.com/doi/10.1111/j.1469-0691.2008.01987.x/pdf> on 12/8/14

Energy Efficient Routing Protocol for Maximizing Lifetime in Wireless Sensor Networks using Fuzzy Logic and Immune System

Safaa Khudair Leabi

Mechatronics Engineering Dept
Middle Technical University
Baghdad, Iraq

Turki Younis Abdalla

Computer Engineering Dept
University of Basrah
Basrah, Iraq

Abstract—Energy limitations has become fundamental challenge for designing wireless networks systems. One of the important and interested features is network lifetime. Many works have been developed to maximize wireless sensor network lifetime, in which one of the important work is routing. This paper proposes a new adaptive routing technique for prolonging the lifetime in wireless sensor networks by using Fuzzy-Immune System. The artificial immune system is used to solve the packet LOOP problem and to control route direction. While fuzzy logic system is used to determine the optimal path for sending data packets. The proposed routing technique seeks to determine the optimal route path from source to destination so that energy consumption is balanced. The proposed routing technique is compared with classical method. Simulation results demonstrate that the proposed technique shows significant increase in network lifetime of about 0.93. The proposed technique proved that energy consumption is well managed.

Keywords—routing; fuzzy logic; artificial immune system; network lifetime; wireless sensor networks

I. INTRODUCTION

Recent years advances show serious progress in wireless networking. The progress and growth in wireless communication technology have made WSNs attractive for multiple application areas, such as medical and health, security surveillance, habitat monitoring, military reconnaissance, disaster management, industrial automation, etc. [1-4]. The development of small and ubiquitous WSNs computing devices is ultimately required. WSNs are comprised of considerable number of limited capabilities sensor nodes with one or more high capability base stations. Each sensor node is a small embedded system, low-power, low-cost, multi-functional [3] Each sensor node performs several functions: sensing, data processing, and communication. Sensor nodes perform wireless communications with each other in order for delivering gathered data to base station. The development of ubiquitous, inexpensive, small and low-power computing devices became available through miniaturization technologies [3]. Due to this, using multi-hop communication help to reduce transmission distance as well as increasing network lifetime. Every node consists of four parts: a processor, sensor, transceiver, and battery. Nodes involve bounded power source with abilities of sensing, datum processing along with

communication. The onboard sensors collect datum about the environment through event driven or continuous working mode. The gathered datum may be temperature, pressure, acoustic, pictures, videos, etc. The gathered datum is then transferred across the network in order to form a global monitoring view for objects [5,6].

Since bounded energy source is involved, energy exhaustion is the most important metric for WSNs. In order for maximizing networks lifetime, energy exhaustion must be well managed [7,8]. Balancing energy exhaustion refers to the major problem in characterizing WSNs. Network lifetime might reduce significantly if the energy exhaustion is not balanced, and may lead to network partition quickly. Several techniques can be used for maximizing network lifetime, in which one of the important technique is network layer routing. Generally, in network layer routing algorithm, choosing the best route between nodes and base station represent the main objective of routing algorithms. If same path would be choose for all new communication by taking the benefit of fast transmission at the expense of battery energy exhaustion, sensor nodes of this path will drain its energy quickly and may cause network partition.

In this paper, an adaptive fuzzy-immune routing technique is proposed. The main goal of the proposed routing technique is to make energy consumption balance that prolongs the overall network lifetime.

This paper is organized as follows: section II describe the proposed routing technique. Simulation settings are presented in section III. Simulation results and discussion are presented in section IV. Conclusion is presented in section V.

II. THE PROPOSED ROUTING METHOD

The proposed energy efficient routing protocol is performed by combining artificial immune system and fuzzy logic system. The goal of the proposed routing protocol is balancing energy consumption and extending network lifetime. Artificial immune system is used to solve packet LOOP problem and control route direction. Fuzzy system is used to find the optimum path from sensor nodes to sink.

Sensor nodes are responsible for collecting data from its neighbor's nodes. In this paper, time driven routing schedule is supposed. Each node finds the optimal rout for sending data

packets to the sink in every time cycle. Using this scheduling for routing, the procedure of determining optimum route while sending data packets to the sink for all nodes will be repeated for each round. For the proposed routing protocols: (1) for a specified field random deployment is involved for whole nodes along with knowledge about their positions and their neighbors positions within its range and the position of the sink; (2) initial energy and maximum transmission range are identical for all sensor nodes.

Energy management efficiency is the most important WSNs design challenges; it gives a measure about WSN lifetime which perhaps the most serious metric owing to evaluating WSNs. The definition of net lifetime gives a meaning for time from turning on till first node die within net. The lifetime is the most challenging problem in WSN. Also the packet delivery ratio is used to evaluate the proposed routing technique.

In this paper, an adaptive routing protocol is proposed for managing energy consumption and maximizing the overall lifetime of the network. The proposed routing protocol maximizes the network lifetime by involving the artificial immune system and fuzzy system. Two metrics have been used in our new routing method are the remaining energy (RE) and the shortest hop (SH) to select the optimal next hop node to the current node. Shortest hop (SH) is the distance from sensor node to the sink. Selecting the next hop of highest remaining energy (RE) and shortest hop (SH) to sink is the responsibility of proposed routing algorithm. Hence, energy consumption is balanced and the lifetime of the network is maximized.

The general structure of the proposed routing protocol is illustrated in figure 1. When a sensor node likes to send or forward data packets, firstly find all of its neighbors. Artificial immune negative selection algorithm is then used to control route direction and solve packet LOOP problem. It classifies all neighbor nodes into two categories, good neighbor nodes (GNBR) and bad neighbor nodes (Danger nodes) by using a specified criterion. The good neighbor nodes (GNBR) will contribute in the optimum path finding process. Fuzzy logic system is used to find optimum node from the good neighbor nodes (GNBR) to send or forward the data packets. Fuzzy logic system makes a decision for computing edge cost related to the remaining energy and shortest hop metrics. The favor edge cost is that involves highest remaining energy and shortest hop to sink. Hence, node with highest edge cost value will be selected as next hop node. Depending on this process next hop node is selected and added to OPEN list along with tagging it as current node. If this node is inside sink's range then optimum path is OPEN list. If current node is not inside sink's range, the proposed algorithm is repeated (classifying GNBR nodes, finding their cost function values, and selecting node of highest cost function value) for the current node (the latest node added to OPEN list) to find its next optimum node. The OPEN list is used in the algorithm to store the optimum nodes that finally represent the optimal path. The OPEN list is then stored the optimal path when the algorithm ends and the

optimal path is found. Hence, the operation of the proposed algorithm is repeated for every node like send or forward data packets.

A. Artificial Immune System

The AIS has deduced from biological immune system of humans that defend the body against the threats. Naturally, the immune system is so complicated system and involve several functions. The master function is to defend against attacker cells. This is achieved by using two techniques, which are innate and acquired techniques. The master function takes the responsibility of classifying human cells into two categories which are self and non-self cells [9]. By using special type of defense, the immune system enforces non-self cells for some treatments that led them to disintegration. The immune system has the ability of learning via mutation in order for distinguishing among external antigens, such as bacteria or viruses, and self cells of body.

Immune system framework involves negative selection process. The purpose of this algorithm is providing existence probability of self cells [10]. Processing of this algorithm involves some activities. First is ability of detecting strange antigens along with discarding reaction to self-cells. By using random processing genetical arrangement, receptors are made during T-cells generation. Second, under sensory processing in thymus, receptors' T-cells that affect self-proteins subject for destroying along with allowing ones that not affect self-proteins for leaving thymus. The forward T-cells spread over the body for subjecting to immunity reactions. This processing can protect bodies from strange antigens.

Forrest [11], in 1994, were firstly introduced the algorithm for detecting datum in computer systems when they handle viruses. This processing is carried out by generating two sets. The first set is self-categories that give an indication about normal situation of that system. The second set is detectors that discover S-complement. Hence, datum has to be subjected to detectors set so as for recognizing them as self and non-self.

This section investigates the application of artificial immune in WSNs to solve packet LOOP problem and to control the direction of the routes. Artificial immune system provides the ability for detecting danger neighbor nodes. This is done by classifying nodes as good neighbor nodes (GNBR) and bad neighbor nodes (danger nodes). Route direction control is a crucial feature in the design of any routing algorithm. If this algorithm is not used, the packet may be sent faraway from sink and encounter packet LOOP, which exhaust more energy for the failed packets. Implementing route direction control will improve the routing algorithm, ensure that the packet will not get a path faraway from sink, minimize energy exhaustion, and maximize network lifetime.

Good neighbor nodes (GNBR) will contribute to the optimum path finding, using fuzzy logic system, while the bad neighbor nodes (danger neighbors) will be discarded. The criteria used for classifying the good and bad neighbors nodes depends on the distance to sink metric. The artificial immune negative selection algorithm that is used in the proposed routing

technique is listed below.

AIS-Negative Selection Algorithm

1. Inputs : S has the criteria to classify good neighbor nodes; $S=\{S:s \in P | \text{distance to sink } D(s) < \text{distance to sink } D(n)\}$; where, n is the node want to send packets, s is a neighbor node, P is the set of all neighbors nodes for node n
2. Output : D is the set of good neighbors nodes (GNBR)
3. Repeat for all neighbors nodes in the set P for node n
 - a. Determine the affinity of each member of P with good neighbors criteria S
 - b. If neighbor node satisfies the criteria S, add it to set of good neighbors D
 - c. Else discard the neighbor node and define it as danger node for node n.
4. Stop when all neighbor nodes for node n has been classified

B. The Fuzzy Logic System

Fuzzy logic was first proposed by Zadeh in 1965 [12]. Fuzzy logic is an extension of the classical propositional and predicate logic that rests on the principles of the binary truth functionality. Fuzzy systems implementation was expanded for wide applications like systems identification and control. Fuzzy systems are robust, easy to implement and has the advantage of processing non-linear systems.

For the proposed routing technique, the objective of the fuzzy system is to determine the optimal value of the node edge cost $C(n)$ of node n depending on the remaining energy RE(n) and shortest hop SH(n). The shortest hop (SH) is the distance from sensor node to the sink. Figure 2 depicts the proposed fuzzy system with two inputs remaining energy RE(n) and shortest hop SH(n). The universal of discourse for inputs remaining energy (RE) and shortest hop (SH) and output node cost C, are [0...0.5], [0...120] for area A1; [0...180] for area A2, [0...1], respectively. The design of our fuzzy system uses five membership functions for the two inputs and output as illustrated in figure 3.

For fuzzy system, the inference engine consists of the rule base and processes the fuzzified values. The rule base is a series of IF-THEN rules, which related to fuzzy input variables and fuzzy output variable, and by using linguistic variables, each of which is qualified by fuzzy set. We have used 25 fuzzy rules in our design. Table 1 shows the rules used in the proposed routing technique. Any rule that fire share out in the final fuzzy solution calculation. Using center of area method for defuzzification, the final crisp value is calculated which represent the node edge cost $C(n)$ in per unit. Equation (1) describes the center of area defuzzification method.

$$\text{Node Cost } C(n) = \frac{\sum_{i=1}^n R_i * c_i}{\sum_{i=1}^n R_i} \quad (1)$$

where, R_i is the output of rule base i, and c_i is the center of the output membership function.

This fuzzy design is employed in the proposed routing technique for determining the optimum next hop node with

respect to the current node as well as ensuring energy consumption balance.

TABLE I. FUZZY IF-THEN RULES

RE/SH	Very Low	Low	Medium	High	Very High
Very Low	Low	Very Low	Very Low	Very Low	Very Low
Low	Medium	Medium	Low	Low	Very Low
Medium	High	Medium	Medium	Low	Low
High	Very High	High	High	Medium	Medium
Very High	Very High	Very High	Very High	High	High

III. SIMULATION SETTINGS AND CONFIGURATION

Simulation is carried out in MATLAB. Two topological areas are considered in this paper, which are A1 and A2. A 100 nodes are randomly scattered for every two topological areas. The topological areas A1 and A2 have the dimension of 100mx100m for area A1 and 200mx50m for area A2. One base station “Sink” has been used for each topological area. The position of the sink is (90m,90m) for topological area A1, and is (180m,45m) for topological area A2. Every node operates with maximum transmission range equals to 30m. Every node has initial energy equals to 0.5J. A 200 bit packet length is used for simulation. The value of hop count limit (HCL) is equals to 10 and 15 for areas A1 and A2, respectively. Performance evaluation of suggested routing technique is tested for each of the two topological areas A1 and A2. The proposed routing technique utilized with first order radio model proposed by [13]. This model is shown in the following equations.

$$E_{TX}(pkt_{length}) = E_{elec} * pkt_{length} + E_{amp} * pkt_{length} * d^2 \quad (2)$$

$$E_{RX}(pkt_{length}) = E_{elec} * pkt_{length} \quad (3)$$

where, E_{TX} and E_{RX} are the energy exhaustion for transmitting and receiving respectively. pkt_{length} represents number of bits per packet. d represents distance between two communicating nodes. E_{elec} represents per bit energy exhaustion for broadcasting or receiving for electrical hardware. E_{amp} is the per bit per meter square energy exhaustion. E_{elec} and E_{amp} values that used for simulation are 50nJ/bit and 100pJ/bit/m², respectively.

Routing protocols can be evaluated by using the packet delivery ratio, which is the ratio of successfully packets received packets by sink. The acceptable PDR value is greater than 0.95. The packet delivery ratio (PDR) is calculated by the following equation.

$$PDR = \frac{\text{No. of Successfully delivered Packets to Sink}}{\text{Total No. of Packets Sent}} \quad (4)$$

IV. SIMULATION RESULTS AND DISCUSSION

Simulation is carried out for the two topological areas. Two routing protocols have been considered in the simulation, which are Dijkstra routing, and the proposed routing protocol. Number of alive nodes in each round has used to give the indication about the lifetime of the WSNs. A comparison has been made for the two routing techniques with reference to overall network lifetime beside other metrics. Network lifetime defined as period between network starting work till the first sensor node die or exhaust its energy.

Figure 4 depicts network lifetime for the two topological areas A1 and A2, in terms of number of still alive nodes in

each round till network partition. From this figure, it can be seen that the proposed fuzzy-immune technique is better than the Dijkstra method. It shows an increase in network lifetime of about 0.93 for area A1 and 1.375 for area A2. Also this figure shows the importance of introducing the artificial immune system for solving packet LOOP problem and route direction control, in which the packet delivery ratio will decrease to 0.84 for area A1 and 0.86 for area A2 if the immune system is not used. Result figures show the improvement of the proposed routing technique in comparison with a classical routing method. The proposed technique shows the improvements by investigating energy exhaustion balance, route direction control, and unity PDR along with prolonging overall network lifetime. Depending on the trace of our experiments for searching optimal path, the proposed routing protocol change the optimal path every round depending on the metrics used, the remaining energy (RE) and the shortest hop (SH). This change in the path used to send data packets from any node to sink prove the balance in energy consumption and as a result maximizing network lifetime. Network partition feature has been activated for the simulation. Network partition is work out when any of the 100 deployed sensor nodes has not find a neighbor nodes to send data packet. This is due to the died sensor nodes. Hence, simulation is stopped when network partition is occurred. Table 2 details the overall network throughput (lifetime, partition time, and PDR) for the two methods and for the two topological areas A1 and A2.

Figure 5 illustrates the network average remaining energy in each round for the two topological areas A1 and A2, and also a comparison between the proposed fuzzy-immune method and Dijkstra method. It is obvious from this figure that without using artificial immune system route direction control, the PDR of the network will decrease significantly. This figure shows that the Dijkstra routing method has some nodes exhaust its energy quickly due to the continuous usage of these nodes. This reflects the unbalanced energy consumption in the Dijkstra Routing. This is due to the usage of the same path for sending data packets from sensor node to sink. And this justifies the high average remaining energy in the network. From this figure, the improvement of the proposed fuzzy-immune method can be seen; the average remaining energy has decreased along with the increase in the lifetime due to the use of more nodes that Dijkstra routing has not do. It is obvious that the improvement of the proposed technique is due to artificial immune route direction control and energy consumption balance. In addition, tracing results show that without using the artificial immune route direction control, the packets sent will encounter loops and may not successfully delivered to the sink. The proposed routing technique results in energy exhaustion balance along with extended overall network lifetime, and unity packet delivery ratio.

Figure 6 illustrates average consumed energy for the two topological areas A1 and A2. From this figure, consumed energy for proposed routing is higher than the Dijkstra routing. The key effect of proposed routing protocol is achieving energy consumption balance and avoiding the continuous using of same nodes. This is due to the use of more hop nodes, which lead to maximize total network lifetime as

well as PDR. This reflects the effectiveness of proposed routing protocol for balancing energy exhaustion besides maximizing network lifetime.

Figure 7 illustrates the packet delivery ratio (PDR) for the two topological areas A1 and A2. From this figure the proposed routing shows unity PDR along with higher network lifetime in comparison with Dijkstra routing which shows less network lifetime. This result gives the power point for the proposed routing method which guarantying unity PDR along with higher network lifetime. This figure also shows the importance of artificial immune system for controlling route direction by showing very low PDR as 0.84 for area A1 and 0.86 for area A2 for the proposed routing without using the route direction control. That means not all packets have successfully delivered to the sink and have discarded by hop count limit (HCL) to save network remaining energy.

Figure 8 depicts the maximum number of hops in each round for the two topological areas A1 and A2. This figure shows that proposed routing is better than Dijkstra routing. It changes the path for sending packets continuously depending on the remaining energy and shortest hop metrics by using more hop nodes instead of using the same path as classical routing. Changing transmission path leads to energy consumption balance by using more hops and avoid continuous using for some nodes. Using more hops helps to investigate energy consumption balance, which leads to increase the PDR of the network. This adaptive operation owing to the proposed routing protocol increased network lifetime significantly.

Figure 9 depicts average simulation time (end-to-end delay) in each round for the two topological areas A1 and A2. From this figure, simulation time for proposed routing is a little higher than of Dijkstra routing. So that applying the proposed routing has no effect on computation time for finding the optimal path for sending packets from source to destination. In addition, the figure shows high simulation time for the proposed routing without using the artificial immune system for route direction control. This is because there is high number of packets not delivered to the sink and discarded by hop count limit, which consume more computation time.

TABLE II. NETWORK LIFETIME, PARTITION TIME, AND PDR

Routing Technique	Area	Lifetime	Partition Time	PDR
Dijkstra Routing	A1	1001	2452	1
Fuzzy without AIS	A1	225	More than 10000	0.84
Fuzzy-Immune Routing	A1	1932	2400	1
Dijkstra Routing	A2	602	1498	1
Fuzzy without AIS	A2	1564	More than 10000	0.86
Fuzzy-Immune Routing	A2	1430	1754	1

V. CONCLUSION

WSNs available with limited source power through their life cycle. Since the battery of the sensor node cannot be replaced or recharged, energy preservation occupies first crucial problem in designing WSN infrastructure. This paper presents an adaptive routing technique for maximizing WSNs lifetime using fuzzy logic system and the AIS. The AIS is used for solving packet LOOP problem and to control route direction, so that the packet will not sent far away from the

sink. While fuzzy logic system in the suggested routing algorithm has used for determining optimum routes for sending data packets.

The proposed energy efficient routing protocol ensures that optimum paths from nodes towards base station is determined along with energy balance. Two topological areas have been used for simulation, which are topological areas A1 and A2. Simulations demonstrate that suggested technique has better performance against the Dijkstra routing. Simulation results show an increase in network lifetime of about 0.93 for area A1 and 1.375 for area A2. Simulation results show that without using artificial immune system for route direction control, the packet delivery ratio is decreased to about 0.84 for area A1 and 0.86 for area A2. This proves the importance of introducing artificial immune system for route direction control. Our experiments showed that without the use of the artificial immune route direction control, the goal of the routing protocol would not be satisfied. Simulation results show that the lifetime is maximized and the energy exhaustion is balanced for the proposed routing technique.

The efficiency of suggested method depicts good contribution in field of maximizing network lifetime using adaptive techniques. Simulation results prove the generality of the proposed technique, so that the proposed routing technique could be used for any design framework.

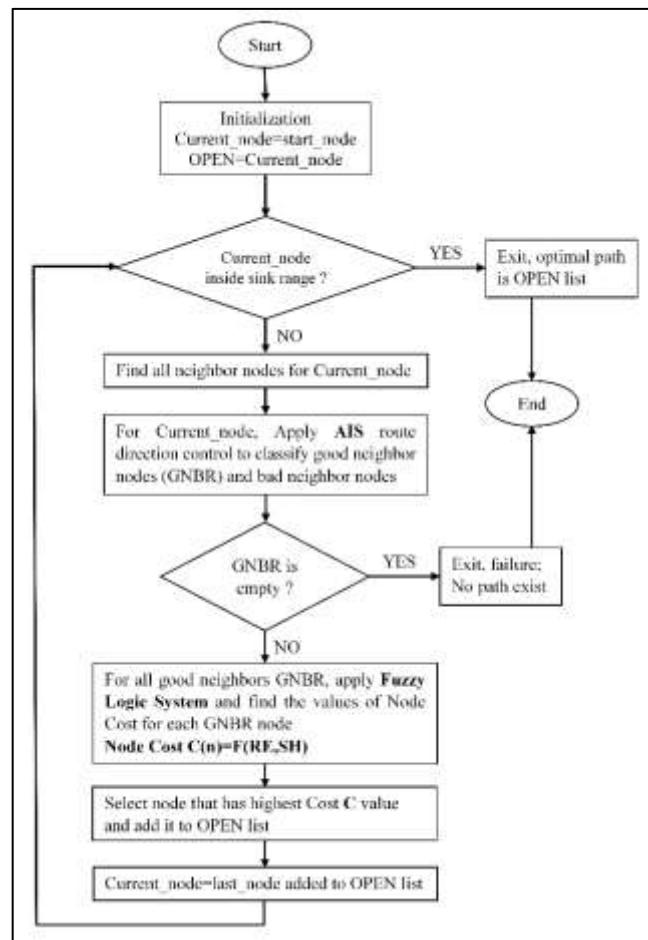


Fig. 1. General structure of the proposed method

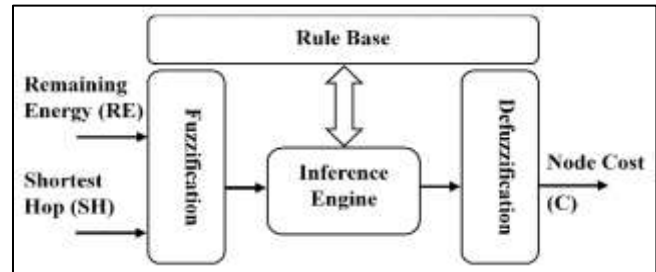


Fig. 2. Designed fuzzy system structure

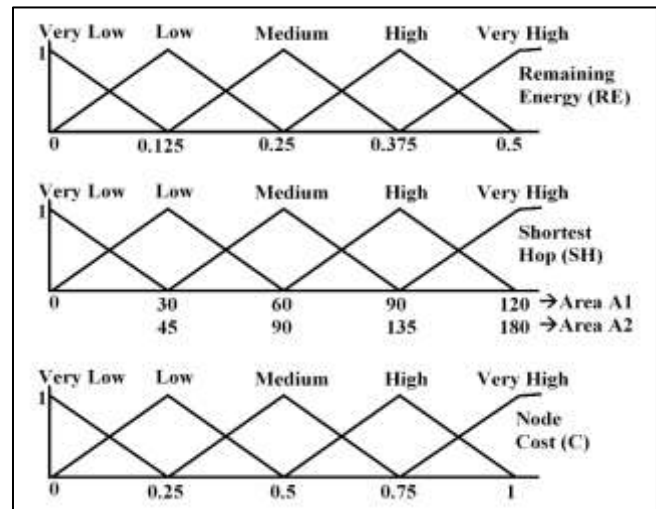


Fig. 3. Designed fuzzy system membership functions

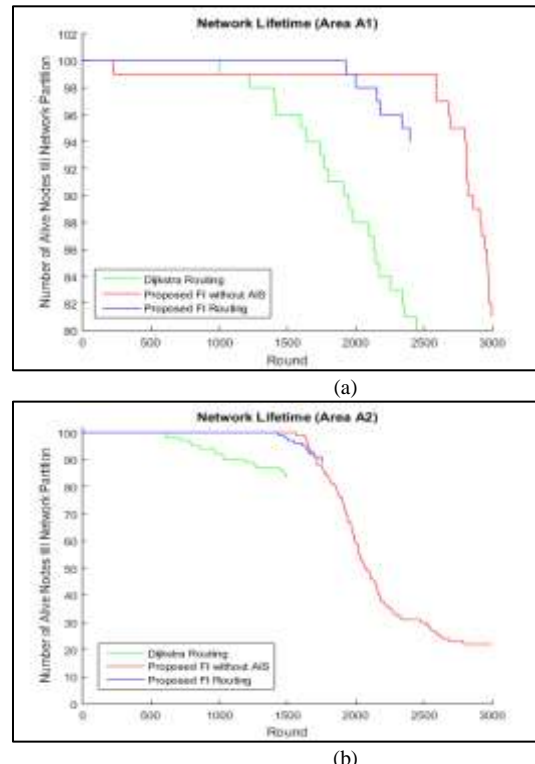
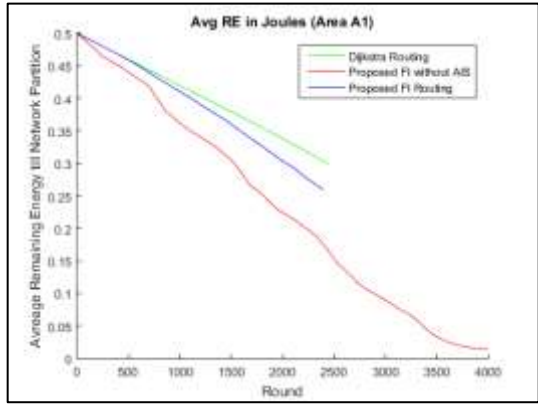
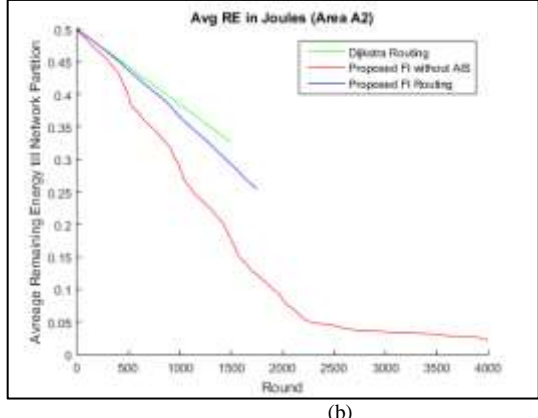


Fig. 4. (a). Number of Alive Nodes for Areas A1 (b). Number of Alive Nodes for Areas A2

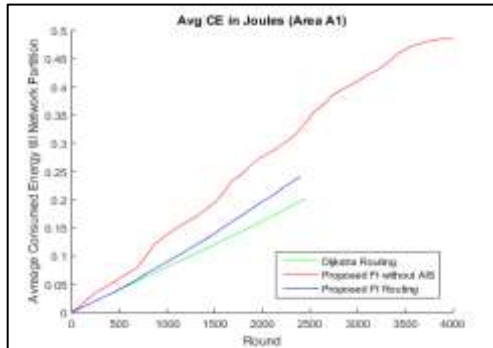


(a)

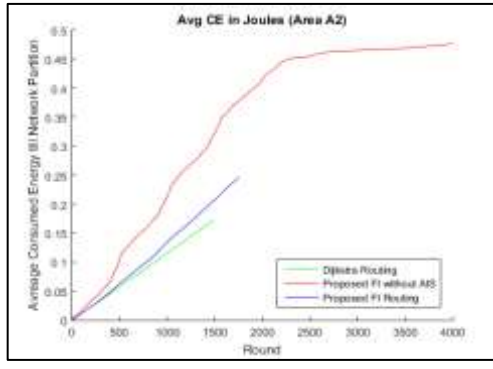


(b)

Fig. 5. (a). Average Remaining Energy for Areas A1 (b). Average Remaining Energy for Areas A2

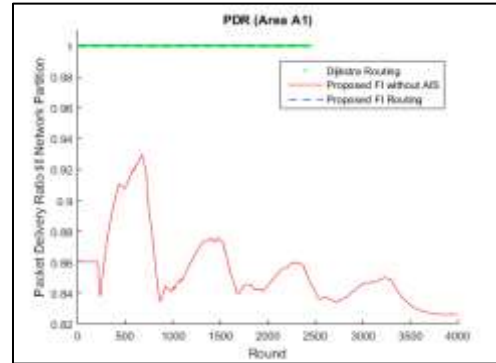


(a)

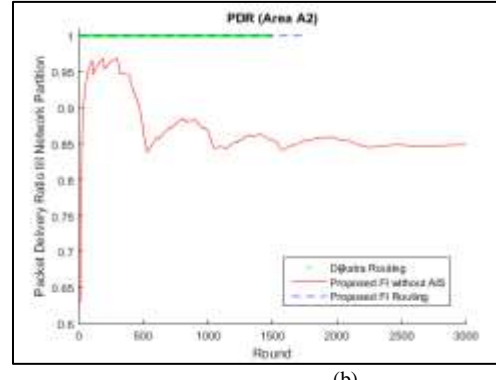


(b)

Fig. 6. (a). Average Consumed Energy for Areas A1 (b). Average Consumed Energy for Areas A2

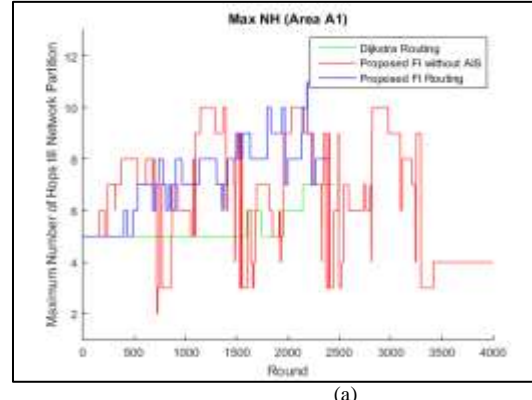


(a)

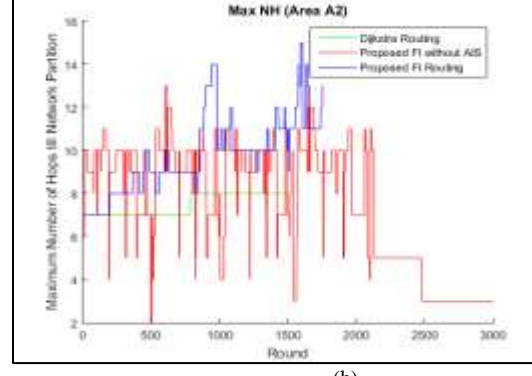


(b)

Fig. 7. (a). Packet Delivery Ratio for Areas A1 (b). Packet Delivery Ratio for Areas A2



(a)



(b)

Fig. 8. (a). Maximum Number of Hops for Areas A1 (b). Maximum Number of Hops for Areas A2

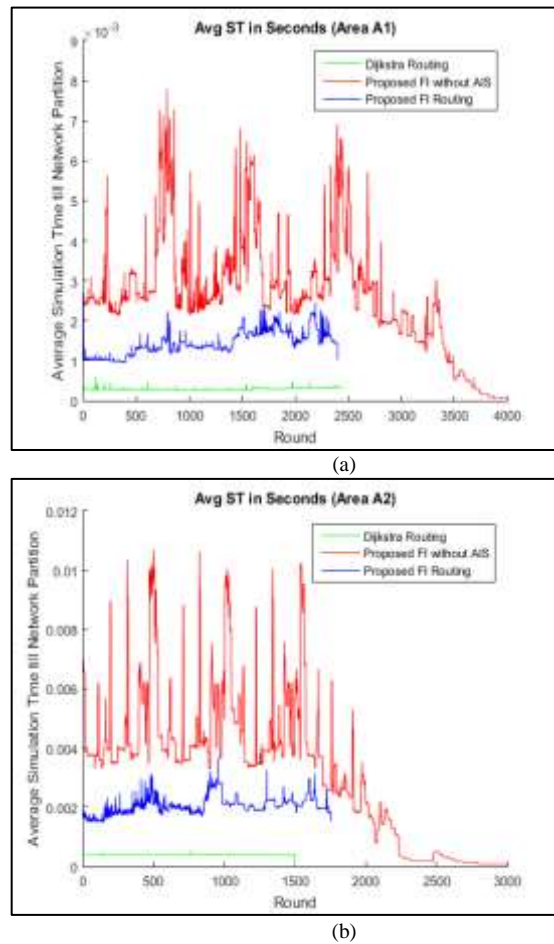


Fig. 9. (a). Average Simulation Time for Areas A1 (b). Average Simulation Time for Areas A2

REFERENCES

- [1] I. F. Akyildiz and M. C. Vuran, "Wireless Sensor Network", John Wiley & Sons Ltd., 2010.
- [2] A. Hac, "Wireless Sensor Network Designs", John Wiley & Sons Ltd, 2003.
- [3] I. Akyildiz, W. Su, Y. Sankarasubramaniam, and E. Cayirci, "A Survey on Sensor Networks," IEEE Communications Mag., Vol. 40, No. 8, Aug. 2002, pp.102-114.
- [4] J. N. Al-Karaki, and A. E. Kamal, "Routing Techniques In Wireless Sensor Networks: A Survey", IEEE Wireless Communication, Vol. 11, 2004, pp.6-28.
- [5] A. Swami, Q. Zhao, Y. Hong and L. Tong, "Wireless Sensor Networks: Signal Processing and Communications Perspectives", John Wiley & Sons Ltd, 2007.
- [6] A. Nayak and I. Stojmenovic, "Wireless Sensor and Actuator Networks: Algorithms and Protocols for Scalable Coordination and Data Communication", John Wiley & Sons, Inc., 2010.
- [7] C. Hua and T. P. Yum, "Optimal Routing And Data Aggregation For Maximizing Lifetime Of Wireless Sensor Networks", IEEE ACM Transection on Network., Vol. 16, No. 4, pp. 892–903, Aug. 2008.
- [8] H. R. Karkvandi, E. Pecht, and O. Yadid, "Effective Lifetime-Aware Routing In Wireless Sensor Networks", IEEE Sensors Journal, Vol. 11, No. 12, pp. 3359–3367, Dec. 2011.
- [9] D. Dasgupta, "Artificial Immune Systems and Their Applications", Springer-Verlag Berlin Heidelberg, 1999.
- [10] D. Dasgupta, "Advances in Artificial Immune System", IEEE Computational Intelligence Magazine, pp.40-49, November 2006.
- [11] S. Forrest, A. S. Perelson, L. Allen, and R. Cherukuri, "Self-Nonself Discrimination in a Computer", Proceedings of the 1994 IEEE Symposium on Research in Security and Privacy, Los Alamitos, CA: IEEE Computer Society Press, 1994.
- [12] L. A. Zadeh, "Fuzzy Sets, Information and Control", Vol. 8, pp.338-353, 1965.
- [13] W. R. Heinzelman, A. Chandrakasan, and H. Balakrishnan, "Energy Efficient Communication Protocol For Wireless Microsensor Networks", Proceedings of the 33rd Annually Hawaii International Conference on Systems Sciences, pp.1–10, 2000.

A System Framework for Smart Class System to Boost Education and Management

Ahmad Tasnim Siddiqui

Department of Computer Science,
Taif University, Taif
Kingdom of Saudi Arabia
Zip – 21974

Mehedi Masud

Department of Computer Science,
Taif University, Taif
Kingdom of Saudi Arabia
Zip – 21974

Abstract—The large number of reasonably priced computers, Internet broadband connectivity and rich education content has created a global phenomenon by which information and communication technology (ICT) has used to remodel education. E-learning can be explained as the use of available information, computational and communication technologies to assist learning practice. In the modern world, education has become more universal, and people are looking for learning with simplicity and interest. Students are looking for more interactive and attractive learning style rather than old traditional style. Using technological learning, we can enhance the education system. We can deliver quality education to students as well as we can ease and uniform the process of education by using the modern technologies and methods. In this paper, we propose a smart class model to manage the entire educational activities and hence to enhance the quality of education.

Keywords—E-Learning; smart class system; quality education; higher education; enhanced education

I. INTRODUCTION

This paper describes the processes of developing and implementing the framework of Smart Class system using e-learning technologies for learning. The main purpose is to raise the competence of quality education of the society for lifelong learning [15]. In this competitive and globalized world, there exists a tremendous focus on having e-learning and e-technology in a variety of working sectors. However, you can find still much scope for improvement on E-learning competency among the scholars, specifically those from rural areas who sadly are still struggling to get the knowledge. Effective work is urgently needed in our educational system in order to secure the futures of students, so that they can remain competitive in the job market. According to the Merriam-Webster dictionary, “Learning is knowledge or skills acquired by instruction, study or experience [1]”. We can also explain the above line as: A continuous process of acquiring knowledge and improving our skills either by practice, experience, study or by being taught by somebody. Using e-learning, we can provide the quality education to remote and rural regions with the help of modern technologies like satellite, internet, and mobiles [2]. Concentration is very much requiring for learning anything. It is a fact; current students are vastly distinct from how they were a long time ago. Reported by Eaton [6], today's students are very much tech-savvy. They're able to access a whole lot of resources and information

just at their fingertips. They are hungry for motivation, inspiration, and guidance.

E-learning involves a very wide range of applications. It includes computational, communication technologies along with other modern devices like interactive TV etc. [2] Smart class system is entirely different from the traditional way of teaching by writing on black boards. It is a modular approach specially designed to help faculties, instructors to compete with new challenges and developing students' capabilities and performance [3]. Smart class can be defined as the improved way of education in which teachers teach and students learn in colleges or universities with advanced and significant use of technology. Smart class means to use the technology right in the way for faculties or instructors in the classrooms or in the laboratories. Students are able to learn and understand difficult concepts and understand the complex problems by watching highly effective audio visuals and animations. By using these we can make learning a fun for the students which will definitely improve their overall performance. Smart class system also enables faculties or instructors to rapidly evaluate the learning by their students in class. The system can automatically mark attendance of students, faculties and instructors by just swapping the smart card and many other activities. Smart class systems are also supposed to be environmental friendly, so that they can provide good environmental practice for the students as well as faculties and instructors.

A. Features of Smart Class System

Smart Class system is a key solution which is intended to support faculties and teaching assistants to overcome with their daily classroom and lab challenges and also improving student's academic interest and performance with easy, practical and significant use of technology. Smart Class helps faculties to make sure that every student in the class is getting knowledge, by providing the wide range of learning patterns in the classroom and in lab sessions. It is also very helpful in managing student's interest and engagement in learning within the classroom. Smart Class makes the problems easy for teacher, abstract curriculum concepts which are difficult to understand and imagine for students or relate by the use of 3-D (three dimensional), interactive multi-media approach.

Smart class have many benefits like: i. Faculty/instructor spends more time in teaching rather than time consuming in

getting started. ii. Can share all the forms, tests, quizzes and assignments to students in just a click. iii. System can collect files automatically after students are finished. iv. Last Class View & Planner, Class Regulation& Monitoring, Assessment of the work, Share Student Screen and Sharing Faculty/Instructor Screen. The term significant use of technology involves a very wide range of technological resources. It includes computers, smart phones, tablets, Internet and web sites, virtual classrooms, projectors, smart boards (interactive white boards, touch screen LCD) and digital association. By providing technological and quality educations along with the quizzes and some other interesting activities, we can provoke the students to learn easily. Smart class also provides a consistent messaging. It minimizes the problems related with different instructors teaching style. Because everyone has their own teaching style and different knowledge base on the same subject. Smart class approach can provide tremendous improved output.

II. LITERATURE REVIEW

E-learning is recognized worldwide in the form of easy learning approach. This is the learning procedure which is delivered through internet, laptops and wireless mobile handheld devices which allows learning anytime and anywhere. Electronic learning takes learning to persons, communities and countries have got previously too remote, socially or geographically, for other categories of educational initiative [7]. E-learning is usually thought as the usage of available information and communication technologies to facilitate learning process. E-learning is a combination of learning as well as the Internet technology [8].

With the advancement in learning technology and change in school education system, it is essential for educators to analyze the classroom situation all the way through the lens of digital interaction. They should propose integrated teaching solutions that put tools such as smart screen, document sharing, on the spot polling and surveys, and remote device management directly by the hands of students and faculties [4].

Electronic learning can be viewed not just being a silver bullet in education, but more as something for learners to gain access to knowledge while there're on the go at anytime and anyplace with full flexibility. Smart class room enabled with interactive white board supports non-linear learning in two different ways: (1) It provides accessing of hypertext and hypermedia online or as external files and (2) It can be accessed by moving back and forth for review slides related to questions/answers of the students and faculties [16]. A lot more educational facilities of the universe are usually on your journey to e-learning and mobile learning so as to take advantage of the ubiquitous quality could possibly offer for educational purposes. An emerging body of literature that explores possibly mobile learning for educational contexts has identified several significant features about mobile learning for example convenience, cost effectiveness, motivation to know,

flexibility, accessibility and also the interaction [9][10][11][12].

Figure 1 explains the U.S. example of growth in tablet, laptops and e-reader expenditure over time. These devices, which make up only 7% of PC spending in the U.S. in 2011, will be increased around 24% of spending by the end of 2016. The increase is mostly due to the advancement in educational technology.

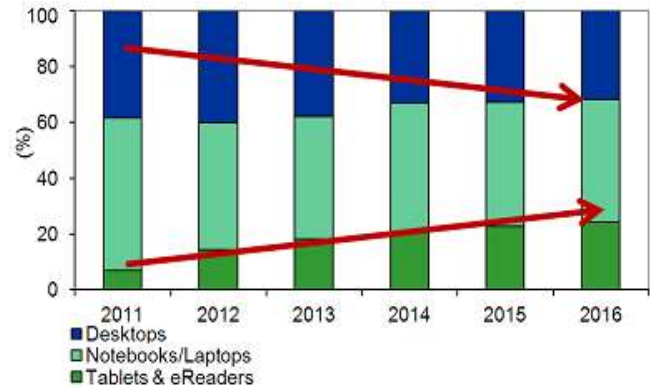


Fig. 1. U.S. Education system spending on Laptops and Tablets as a Percent of Total Spending, 2011-2016 (Source: IDC Global Technology and Research Organization, 2012)

Learner's ability to grasp the knowledge depends on the method of teaching. Figure 2, learning pyramid explains learning retention rates by type of teaching. These days the students have grown up enough with the Internet which provides immediate access to a wealth of information and in multiple formats available such as audio, video, images and text [19].

In the given figure 2, we can see that retention rate is very high in participatory learning as compared to the passive learning which less interactive or non-interactive. Learning through lecture only is very less which is only 5%, while average retention rate is through group discussion which is 50% while learning with practice is 75% and learning with the immediate use of learning that means the applied learning retention rate is 90%. Here the percentage shows the average grasping rate of students.

According to Knight et al., we have to differentiate between the linear and traditional interactivity of teaching and learning where faculty and students interactions as well as interactions of students with their peers takes place and technical interactivity which involves physical interaction with the electronic devices e.g. laptops, tablets, e-pads, e-readers and Smartphone etc [18].

Technical expertise and interactivity can encourage the practice of skills, while pedagogical interactivity provides ability to higher-order thinking and reflections on the learning process [17].

But according to Cisco, these oft-quoted statistics are

unsubstantiated [5]. Below is the Cone of Learning which is developed by Bruce Hyland from material by Edgar Dale.

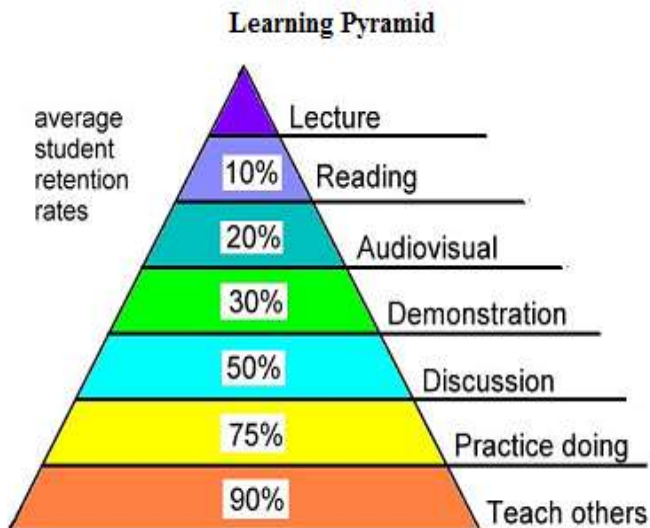


Fig. 2. Learning Retention Rates by Type of Teaching (Source: The World Bank and the National Training Laboratories, Bethel, Maine)

But From the figure 2, one thing is clearly indicated that learning which is interactive and immediately used is more effective than the traditional learning. So, we can make learning more interactive by using advanced technologies.

III. OUR CONTRIBUTION

The main aim of this research is to present a system model for enhancement of education level as well as interest in education. The priority is to provide interactive, uniform academic style and high quality in education. Apart from the traditional black board writing education system we propose a real enhanced education system which is smart class system. It uses more and more advanced technologies to help and support to students as well as faculties and instructors. It uses some inter active learning like forums; quizzes etc. to make the education more interesting, to help students for improving their knowledge level and interest. Students can get proper guidance with the faculties. They can understand and learn every problem easy or complex by audio visual effects, animations and 3-D models. They can get benefits from the special lectures on specific topics by the subject experts. This paper presents a smart class system to enhance the education. Smart classroom covers the whole course of the University/Boards which is flawlessly integrated into the syllabus. The resources include broad learning modules, educational competitions, and interactive e-books, audio, video and soft copies of the study materials in the form of ".pdf" and ".doc(x)" files. In this model we propose smart student tracking system. Every student can be recognized and tracked by the smart card or facial recognition. They can be marked as present when they enter into the class rooms.

The system can also send email and SMS to the parents if students are coming to the classes or bunking schools and colleges. The system also has provision of sending progress reports to the students as well as their guardians.

IV. PROPOSED E-LEARNING SYSTEM ARCHITECTURE

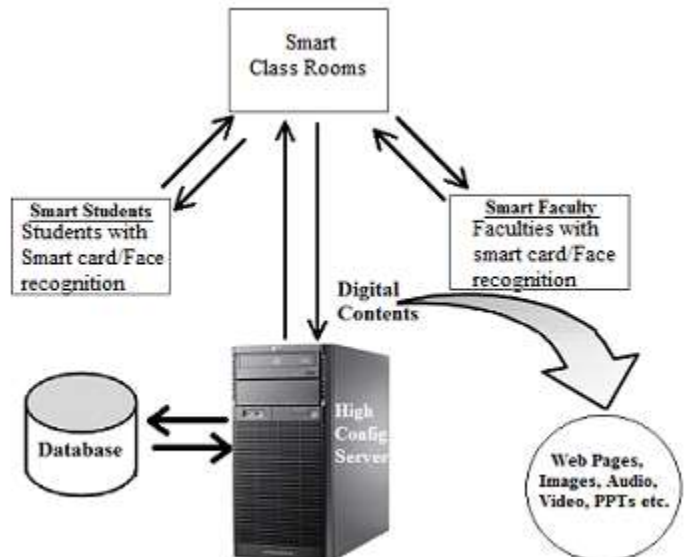


Fig. 3. A Model Framework for Smart Class System

The figure 3 explains our proposed e-learning system; there are four important components in the system. Apart from these four there are two sub components which are used for query processing and sending emails and messages to the students as well as their parents. They are smart class, faculties with smart cards (smart faculties) and students with smart card (smart students). Apart from these main components system includes a database and high configuration server. Each module is integrated. Smart student and smart faculty are directly connected to smart class module.

- **Smart Class:** The first component is Smart Class Room which contains a normal class room equipped with all the modern technologies like computers/laptops, smart phones, interactive TV's, card readers, facial recognitions, high resolution video cameras etc. Whenever any faculty, instructor or student enters into the class he/she has to show the smart card to the card reader or he/she can be recognized by the facial recognition system which marks the attendance of that particular faculty, instructor or student for that particular session. Smart class room is always connected to a high configuration server and a database. Server provides on demand contents to the class room faculties and instructors. The contents are in the form of images, pdf files, 3-D images and models, word document files, audio and video etc. Through the system faculties and instructors can interact to students to explain the topic, to clear the doubts and for other problems. In smart class the faculty or instructor can logged into their session and start the lectures. No need to carry attendance sheets, lecture notes, white board marker and other stuffs which they carry into the normal class rooms. They can browse for the subjects and topics and start the session. They can explain the topics on interactive TV's or monitors. The basic database tables are smart class, students and faculty.

- **Smart Faculty:** The second component is Smart Faculty. It means Faculties with Smart Cards. Smart faculties can log into the respective session and can perform the required tasks like attendance management, lectures, notes, quizzes and other important activities. They can interact to students to explain the topics, to solve their problems in smart class rooms. They can also see the questions posted by the students into their respective subjects. After answering them they can submit and email provider can send email instantly to the students and status of the question is changed from pending to answer.
- **Smart Student:** The third component of this model is Smart Students. Smart students contain a smart card by which they are able to enter into the class, they are also eligible to mark for attendance by showing the smart card inside the smart class rooms. Smart students can always be connected to the smart faculty by using smart class features. They can understand the problems, they can ask questions and they can also post the questions to the concerned smart faculty.
- **Content Centre:** The Content Centre module stores the whole educational materials into the content database which usually are multimedia contents like texts, images, audios, and videos. Materials can be retrieved online through web portal using some secure web services. After this step the contents are delivered to the learners based on their learning style group.
- **Query Processing:** This is a student based application which enables students to have instant feedback and help from the lecturer with regards to the subjects.
- **Alert Messages:** This is the module, in case of instant communications needed, responsible for sending alert messages using SMS and email to the students as well as their parents.
- **Real-time Interaction:** The model represents the ability to support the teaching interaction and human-computer interaction of the Smart class. This involves handy operation and smooth interaction. In smooth interaction, the Smart class should fulfill the interactive needs of the multi-terminal, and a large amount of data. In interactive session, smart class has the feature to record and store the basic data among faculties' students and computer, to support the teachers and students' self-assessment.

These modules worked together and connected to the database [14]. Entire application is hosted at high configuration server, which is able to serve many classrooms, faculties and students at the same time. Through this application every student and staff member can access the digital contents including web pages, images, audio, video, power point presentations etc. after successful login. They can access the content within the smart class rooms.

V. CONCLUSIONS

In this paper we have presented a model framework for Smart Class Room. Smart Class Room is designed to help

faculties, instructors to compete with new challenges and developing students' capabilities and performance. Institutions and organizations financial condition will force them to contemplate adopting a simple and inexpensive solution. This model provides improved way of education in which teachers teach and students learn in colleges or universities with advanced and significant use of technology. They can interact directly without any hesitations. Smart class has many benefits to the students and faculties. It is very clear that innovation in technology is impacting everywhere and bringing new opportunities for schools, universities and educationalists. The system architecture proposed differs in such a way that it provides flexible learning style which is adaptable to students' favorite learning styles. It means to offer a personalized learning environment which suits individual's learning style. Smart class system helps to increase the learning abilities. It can also be used as an alternative learning method to teach the different IQ level students. There must be technological strategy for the classes, schools and entire learning atmosphere. We can help students as well as educators by using advanced technologies to make the future bright.

REFERENCES

- [1] <http://www.merriam-webster.com/dictionary/learning>. Last accessed on 10/05/2016
- [2] Ahmad Tasnim Siddiqui, Dr. Mehedi Masud, An E-learning System for Quality Education, International Journal of Computer Science Issues, Vol. 9, Issue 4, No 1, July 2012
- [3] <http://www.indiastudychannel.com/experts/17114-what-smart-class.aspx>
Last accessed on 10/05/2016
- [4] The Next-Generation Classroom: Smart, Interactive and Connected Learning Environments, IDC Government Insights, White Paper Sponsored by: Samsung
- [5] Multimodal Learning Through Media: What the Research Says, White Paper by Cisco Systems Inc. URL: <http://www.cisco.com/web/strategy/docs/education/Multimodal-Learning-Through-Media.pdf> Last accessed on 30/01/2014
- [6] S. E. Eaton, Global Trends in Language Learning in the 21st Century, Calgary: Onate Press, 2010.
- [7] J. Traxler, "Learning in a Mobile Age", International Journal of Mobile and Blended Learning, vol. 1, pp.1-12, 2009, available at <http://wlv.academia.edu/documents/0009/9949/ijmblproof01.pdf>
- [8] Ahmad Tasnim Siddiqui, Dr. Mehedi Masud, An E-learning System for Quality Education, International Journal of Computer Science Issues, Vol. 9, Issue 4, No 1, July 2012
- [9] D. Laurillard, "Pedagogical forms of mobile learning: Framing research questions", In N. Pachler (Ed.), Mobile learning: Towards a research agenda (Vol. 1, pp. 33-54). London: WLE Centre, Institute of Education, 2007.
- [10] J.-H. Valk, A. T. Rashid, L. Elder, "Using Mobile Phones to Improve Educational Outcomes: An Analysis of Evidence from Asia", The International Review of Research in Open and Distance Learning, vol.11, no.1, pp.117-140, 2010.
- [11] A. Valenta, D. Therriault, M. Dieter, R. Mrtek, "Identifying Student Attitudes and Learning Styles in Distance Education", Journal of asynchronous learning networks, vol. 5, no. 2, pp. 111-127, 2001.
- [12] M. J. W. Lee, A. Chan, "Reducing the Effects of Isolation and Promoting Inclusivity for Distance Learners through Podcasting", Turkish Online Journal of Distance Education, TOJDE, vol. 8, no.1, pp. 85 – 105, 2007.
- [13] Munir Shuib, Amelia Abdullah, Siti Norbaya Azizan, "Designing an Intelligent Mobile Learning Tool for Grammar Learning (i-MoL)", Thenmolli Gunasegaran Universiti Sains Malaysia, Penang, Malaysia
- [14] A. S. Sathishkumar, Dr. P. Karthikeyan, "Emerging Technology of Smart Class Teaching in School Education- A Literature Review", IJSR

- International Journal of Scientific Research, volume 3 issue 8pp. 446 – 449.
- [15] Nataliya Osipova, Olga Gnedkova, Denis Ushakov, "Mobile Learning Technologies for Learning English", ICTERI 2016, Kyiv, Ukraine
- [16] Blau, I. (2011). Being a smart teacher in a "Smart classroom": Assessing teacher professional development for incorporating Interactive WhiteBoards at schools. In Y. Eshet-Alkalai, A. Caspi, & S. Eden (Eds.), Learning in the Technological Era (pp. 63-74). Ra'anana, Israel: Open University of Israel.
- [17] Kennewell, S., Tanner, H., Jones, S., & Beauchamp, G. (2008). Analysing the use of interactive technology to implement interactive teaching. *Journal of Computer Assisted Learning*, 24, 61-73.
- [18] Knight, P., Pennant, J., & Piggott, J. (2004). What does it mean to 'use the interactive whiteboard' in the daily mathematics lesson? *Micromath*, 20, 14-16.
- [19] Whitepaper Sponsored by: SamsungThe Next -Generation Classroom: Smart, Interactive and Connected Learning Environments, October 2012

A Coreference Resolution Approach using Morphological Features in Arabic

Majdi Beseiso

Department of Computer Science
Al-Balqa' Applied University
Alsalt, Jordan

Abdulkareem Al-Alwani

Department of Computer Science & Engineering
Yanbu University College
Yanbu, Saudi Arabia

Abstract—Coreference resolution is considered one of the challenges in natural language processing. It is an important task that includes determining which pronouns are referring to which entities. Most of the earlier approaches for coreference resolution are rule-based or machine learning approaches. However, these types of approaches have many limitations especially with Arabic language. In this paper, a different approach to coreference resolution is presented. The approach uses morphological features and dependency trees instead. It has five stages, which overcomes the limitations of using annotated datasets for learning or a set of rules. The approach was evaluated using our own customized annotated dataset and “AnATAR” dataset. The evaluation shows encouraging results with average F1 score of 89%.

Keywords—Coreference resolution; Anaphora; Alternative Approach; Arabic NLP; morphological features

I. INTRODUCTION

Coreference resolution is an important part of natural language processing. It is the process of identifying natural language expressions and determining which of these different entities refer to the same entity [1, 19, 10, 14, 5]. It is significant for the task of detecting events and entities in a text and cluster them [18]. This process helps in many of the NLP applications such as data extraction, text manipulation, and machine translation [1]. Referents are real word objects or entities, which makes coreference resolution an important hard step towards understanding language [5].

This paper focuses on anaphora, and cataphora coreference resolution in Arabic written sentences. Arabic is morphologically rich language and has a distinctive nature, which makes many of the traditional approaches limited [15]. We present a different approach for coreference resolution using deep morphological and syntactical features as well as dependency trees. The approach makes use of the fact that many Arabic words can be morphologically derived from a set of words or roots, to make relations between different words [5]. Dependency trees provide a different type of relations between words depending on the grammatical rules. In this approach, we use both techniques to determine reference relations. Our model has five stages, text preprocessing, preforms and noun entities (NEs) extraction, morphological analysis, relating NE and preforms, and output validation. The approach includes many linguistic applications such as morphological analysis, POS tagging, tokenization, and

extracting the nouns entities. That is why Different Arabic linguistic tools are used to realize the applications in the different stages. In this paper, we present our own customized and annotated dataset for coreference resolution. It is used for testing along with the “AnATAR” dataset. The evaluation of the system results with average F1 score of 89%.

The paper has seven sections. In section 2, we present some definitions and descriptions related to coreference resolution and after that, in section 3 we review related work. We present the Methodology and the scope of our approach in section 4, which is fully described along with our proposed model in section 5. In section 6, we describe the results of the experiments done and finally in section 7, we conclude and show future work.

II. BASIC CONCEPTS AND CHARACTERISTICS OF ARABIC COREFERENCE RESOLUTION

Anaphora is the process of finding the referent of an anaphor entity that is referring to an entity back in the sentence [14][8]. Cataphora is a similar process where the pro-form precedes the entity, to which it refers [17]. When the anaphor or the cataphor and the entities they are referring to hold the same referent in real world then they are “coreferential” [14][17]. Example 1 is for anaphora coreference and example 2 is for cataphora coreference.

(1) ذهب العلماء إلى المؤتمر وهم كانوا فرحين.

The scientists went to the conference and they were happy.

(2) هو العلم، الذي يغنى الشعوب.

It is science, which enrich people.

Pronominal anaphora is one of the most frequent types of anaphora coreference resolution that deals with pronouns [10]. Pronoun is a type of pro-form that refers to a noun word or a noun expression. In this approach, we deal with certain types of pro-forms, which are all the independent and the attached pronouns (جميع الضمائر المنفصلة والمتعلقة) which falls under the pronominal anaphora.

Typically, coreference resolution is a very hard process even for the English language, as it needs some information about the real world to understand relation between words [18]. There are more challenges that exists when dealing with Arabic language that makes coreference resolution in general and Arabic anaphora in specific a more complicated process.

Arabic language sentences can have complex structure [10].

(3) اعتبرناهم كأصدقائنا

We considered them as our friends.

In example 3, a sentence in Arabic was translated into six words in English, which shows how complex Arabic sentences can be. Arabic language has the feature of free word order, which adds to the complexity of coreference resolution. Free word order means that there are almost no restrictions about words order in a sentence. Sometimes the referent is ambiguous specially that pro-forms could exist in a connected form or separated form [10].

(4) ذهبت سارة إلى مريم وكانت سعيدة

Sara went to Mariam and she was happy.

In example 4, there is a connected pro-form in “كانت” and it has ambiguous coreferenceto either Sara or Mariam. In Arabic language, the consistency between the morphological and syntactical features of the pro-form and the related named entities (NEs)needs to be considered. These morphological includes gender, number (singular, dual, plural), and subject or object reference. Finally, one of the main challenges with Arabic language is that there are not enough annotated corpora for coreference resolution [10].

III. LITERATURE REVIEW

Coreference resolution is an important and complex process, which made it the subject of much research work. Most of the research done on coreference resolution showed common processes done by most of the approaches. Which are identifying the search scope, such as the whole document, a sentence, or a set of sentences, and the preprocessing step where the text is segmented, processed and noun phrases or entities are identified. The last step differs where certain tasks are accomplished to do the resolution [19,10].

A survey about anaphora resolution in general and in the Arabic language in specific was presented in “Arabic Anaphora Resolution Using Holy Qur'an Text as Corpus” [10]. The paper presented two types of anaphora resolution. This first type is rule-based approaches. In which, a knowledge base is built to be used in the process. It is easy to implement and does not require much data, but on the other hand, it needs a large set of human formed rules to cover all the needed features for resolution. The statistical approach or the machine learning approach depends on annotated corpora for both training and testing. This approach can have better results when it comes to accuracy, speed and giving a generalized model, but this depends on the annotated data.

In “A Machine Learning Approach to Coreference Resolution of Noun Phrases”, they took the path of the machine learning approach [19]. In this approach, Annotated corpus is required to be used as training and testingdata. In addition, they have to determine the feature vector. Which is a set of features used to define the relation between two entities. The next step is to generate training examples, then to build the classifier, and the last step is to generate “coreference chains for test documents” [19]. The accuracy was close to the other

approaches. In the types of errors that affect recall, “inadequacy of current surface features” scored 64% of all types. The paper represents a good approach for coreference resolution, but both the features and annotated corpora can restrict the effectiveness of the approach. There has been several trials to overcome these two problems.

In 2012, CoNLL shared task targeted, “modelling of coreference resolution for multiple languages” [18]. The OntoNotes data was the baseline for the modelling, which has different annotation layers, and in the three languages English, Arabic, and Chinese. The paper released by CoNLL 2012 mentioned that the morphology of Arabic language is very complex comparing to English, which has limited morphology and Chinese whichhas very little morphology. The resources available for each language are different and Arabic has the least resources. The shared task presented good data for training and testing coreference resolution in Arabic. CoNLL suggested that a hybrid approach between rules-based approach and machine learning approach to give the highest accuracy.

Chen Chen and Vincent Ng presented a system with a hybrid approach for the CoNLL 2012 in their research [2]. They combined both rule-based approach with statistical approach. They used the lexical information with machine learning to improve the approach. The results showed the effectiveness of the approach. The problem with is hybrid approach is that it showed lower accuracy in Arabic for all the tests that were done. The results on the development set were around 60% for English and Chinese, but for Arabic were around 45%.

In the CoNLL 2012, they stated that Arabic has a complex morphology, and that Arabic has limited resources for comparison. Which lead us to explore Arabic morphological analysis. In the research paper “Arabic Finite-State Morphological Analysis and Generation”, they presented a morphological analysis system, which included displaying the root, pattern, and different affixes, mood, voice, etc. [11]. The paper mentioned that Arabic morphology is very challenging as for example Arabic “orthography displays an idiosyncratic mix of deep morphophonological elements” [11]. They presented a system that can recognise all possible written forms of words and even with varying degrees of diacritical marking [11]. In a different research, morphological stemming was used to improve Arabic Mention Detection and Coreference Resolution [5]. The system make use of “finite state segmentation” and relationships between word stems. The usage of stemming features was very effective in Arabic as it increased the accuracy in the testing data.

The traditional approaches showed to a fair extent inability to accurately solve the challenging problem of Arabic coreference resolution. The need of large set of rules for the rule-based approaches or the annotated data and the set of features for the machine learning approaches made these approaches restricted. Research suggested that machine learning approach or in specific, the hybrid approach for coreference resolution should give the highest accuracy. However, in Arabic, the accuracy was still low comparing to other languages. Where research showed the importance of Arabic morphological analysis and how it can effectively

improve coreference resolution. This showed that in Arabic, it is more effective to depend on the usage of morphological and syntactical features for coreference resolution.

IV. METHODOLOGY AND SCOPE

Arabic is considered as, highly inflected, agglutinative, and morphologically rich language [5, 15]. These features made Arabic language distinctive from many other languages, leading to the limitations of the traditional approaches in coreference resolution. This proposed model makes use of the nature and complexity of the Arabic language to overcome the limitations of other approaches, by including different morphological analysis techniques along with dependency trees.

According to the University of Duisburg-Essen, Morphology is the study of word forms and a morpheme is the smallest unit that has a meaning [16]. Many Arabic words can be morphologically derived or associated with a list of words or roots. This process is done by removing different prefixes and suffixes attached to the word. Not only, Arabic words can be in different forms, but also many pronouns, prepositions, and conjunctions can be attached to words [5]. In Arabic language, the word root is “the original form of the word before any transformation process”, and it has major importance in Arabic language processing [16]. In addition to the different forms of the Arabic word that result from the derivational and inflectional process, most prepositions, conjunctions, pronouns, and possessive forms are attached to words. These orthographic variations and complex morphological structure make Arabic language processing challenging.

كاتب، كتاب، كتب (5)

In example 5, there are two different words that have the same root. They have the same root of three letters, but their meaning are different. Roots can be used to relate the two words. A stem is one morpheme or more that can accept an affix [16].

In this approach “AlkhailMorphoSy” was used, which is a morphological analyzer that provides all possible solutions with their morphosyntactic features for a certain set of words [12]. The tool presents a wide range of features such as, vowelization, proclitics and enclitics, nature of the word, stems, roots, and syntactic form. This tool provides effective analysis, which is done over several steps. The tool is built based on the characteristics of the Arabic language, which makes it suitable for our approach. In addition, Alkhali tool was very effective and more accurate in the evaluation against other analyzers [12].

In addition to the use of a morphological analyser, our approach make use of dependency trees to make relation between different words in a sentence. Stanford dependencies describes the representation of grammatical relations between different words in a sentence [13].

Figure 1 is a graphical representation for the Stanford dependencies for the sentence, “Bell, based in Los Angeles, makes and distributes electronic, computer and building products” [13]. This is a clear directed graph to represent the

relations between the different words as edge labels. Stanford CoreNLP provides such features in Arabic such as, tokenization, segmentation, part of speech, and dependency trees, which is similar to the figure above [3]. In other words, the Stanford CoreNLP tool is used to provide extra information about the whole sentence.

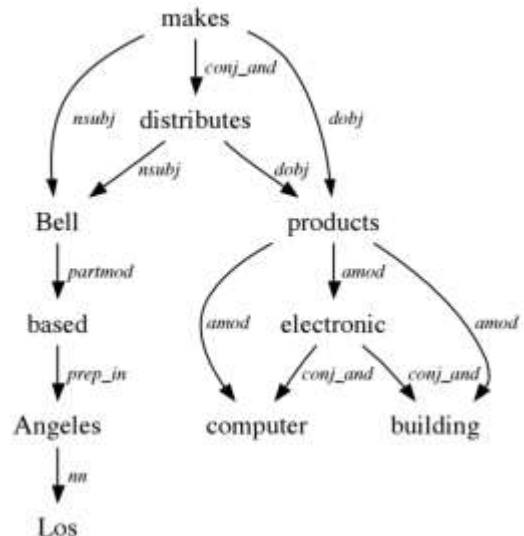


Fig. 1. Standard Stanford dependencies

The approach has a defined scope for the resolution process, which is a sentence with a complete context.

ذهبت سارة إلى مريم فسألتها عن موعد الحفلة(6).

Sara went to Mariam and asked her about the date of the party.

In example 6, it can be Sara or Mariam who asked the question which means that the context not complete and this is out of the scope of this approach.

ذهبت سارة إلى مريم فسألتها عن موعد الحفلة فقالت مريم لم أكن أعلم من (7)
قبل.

Sara went to Mariam and asked her about the date of the party then Mariam said I did not know that before.

In example 7, the context was complete as there is a reference to Mariam in the same sentence. That makes coreference resolution possible and detectable by our approach.

We present an approach that makes use of the nature and “morphology richness” of the Arabic language, which can be considered word-based features. In addition, we include sentence-based features using the Stanford CoreNLP tool. Our approach does not require a wide range of rules neither a large annotated data set, and still provides an effective solution for Arabic coreference resolution.

V. PROPOSED MODEL

The approach consists of five different stages. They are designed in order to make the best use of Arabic words forms, and sentences structure. The stages have different scope, goal,

and complexity in order to reach the maximum accuracy and performance.

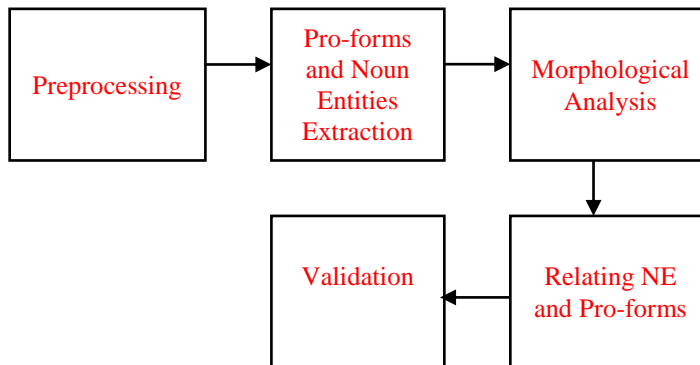


Fig. 2. The four stages of the approach

These five stages are shown in figure 2 as a pipeline of different natural language processing tasks.

A. Preprocessing

In this stage, all sentences will be processed and words to prepare them for the next steps. This stage includes different tasks aiming at making the input text in the correct format for the next stages. The first task is sentence splitting which is done using dots in the sentences. Morphological analysis is the second stage and it is applied to all entities using “AlkhililMorphoSy” with its different features. For the third task, we use Stanford POS Tagger, which includes a module supporting Arabic to perform POS tagging on the input text. The last step is filtering the output of the second step “solutions of Alkhilil” based on the results of the third step or the Stanford POS tagger. “Alkhilil” is a context free analyzer. Which means it does not consider the context of the word it is processing. On the other hand, POS tagger consider the context. When merging the output of the two systems we can have a contextual morphological and syntactical solution. This filtering is applied by comparing the POS-tag, retrieved from Stanford system with Alkhilil solutions and then choosing the solutions, which are compatible with the Stanford tag.

B. Pro-forms and Noun Entities Extraction

The second stage that comes after preprocessing is the extraction of the needed entities, which are pro-forms and noun entities. Both of them have different characteristics that is why each has a different approach for extraction.

In the second stage, we start with extracting pro-forms. The approach uses the output of “Alkhilil” to distinguish between different types of pro-forms, connected and separated pro-form. Connected pro-forms are attached to Arabic words, such as the suffix “هـ” in the word “سألهـ”. Separated pro-forms are not attached to word such as “هـ” “He”. This is can be done with the help of a predefined list of Arabic pro-forms.

The second step in this stage is to find the set of all possible related noun entities (NEs). In the approach, we apply Named-

entity recognition (NER) to extract the noun entities in the following steps. First, we prepare a “gazetteer” which is a list or a corpus of different entities’ names such as names of persons, locations, and organizations. Then we compare the text with the gazetteer and do an initial NE tagging. Last step is to use a set of regular expressions to extract possible NE

C. Morphological Analysis

In the next stage is finding the morphological and syntactical features for pro-forms. We can simply do that using a lookup-table approach since the number of possible pro-forms is limited in Arabic language. Then, we find the morphological features for each possible NE, using the output of the morphological analyzer and the output of POS-tagger. The next step is to filter NE set by removing all inconsistent NEs in terms of morphological and syntactical features. We will call the output of this stage the PCNE (the possible consistent NE).

D. Finding the Related NE and Pro-forms

In this stage, dependency trees are used to relate NEs and pro-forms. First, we find the dependency tree using Stanford Core NLP. If there is a path in the dependency tree between the pro-form and some PCNE, we choose the one with the shortest path in dependency tree graph. Otherwise, we find the nearest NE in term of number of words between the pro-form and each PCNE.

E. Output Validation

The output of the fourth stage can be considered as the final output showing the coreference between different entities. An extra step is performed to reach a more accurate result, which is validation stage. We run different tests on the related entities to validate the relation between them. For example, we check if the pro-form and the noun entity have the same gender, and number. By the end of this stage, we would have completed our model and reached the final output by relating noun entities to pro-forms.

F. Example

In the following example, a text input of an Arabic sentence that goes through the different stages of the approach starting with preprocessing until defining the related pro-forms and noun entities is shown.

(8) محمد هو الطالب الأفضل في الجامعة

Mohamed is the best student in the university.

The tables below show the output of different stages using example 8. Table 1 is the output after applying the first step. After applying the second stage, there is only one pro-form, which is “هو”, or “he” and two NEs are found. Which is shown in Table I. After completing all the stages, in the last step, there is a path in the dependency tree between “هو” and “الطالب” or “he” and “student”. Therefore, the result is, “الطالب” and “هو” are related.

TABLE I. FIRST STAGE OUTPUT

اللائق [1] Suffix	الحالة الإعرابية POS Tags	الجذر Root	الوزن Patt tern	الكلمة [5] Type	نوع [13]	الجذع [6] Ste m	السابق [7] Prefix	الكلمة [8] المشكولة Voweled Word
[9] #	[10] #	[11] #	[12] #	اسم علم [13]	محمد [14]	محمد [15]	[16]	مُهَمَّد
[17] #	[18] #	[19] #	[20] #	صَيْرَ الغائب – للمفرد [21] المُذَكَّر	هو [22]	[23]	[24]	هُوَ
[25] #	مفرد مذكر مرفوع في حالة التعريف	طلب [27]	فَاعِلٌ [28]	اسم فاعل [29]	طالب [30]	ال: [31] التعريف	[32]	الطالب
[33] #	مفرد مذكر مرفوع في حالة التعريف	فضل [35]	أَفْعَلٌ [36]	اسم تقضيل [37]	أَفْضَلٌ [38]	ال: [39] التعريف	[40]	الأَفْضَل
[41] #	[42] #	[43] #	[44] #	حرف جر [45]	فِي [46]	[47] #	[48]	فِي
ة: تاء [49] ة: تاء التأنيث	مفرد مؤنث منصوب في حالة التعريف	جمع [51]	فَاعِلَةٌ [52]	اسم جامد [53]	جامعة [54]	ال: [55] التعريف	[56]	الجامعة

TABLE II. SECOND STAGE OUTPUT

[57] #	مفرد مذكر مرفوع في حالة التعريف [58]	طلب [59]	فَاعِلٌ [60]	اسم فاعل [61]	طالب [62]	ال: التعريف [63]	الطالب [64]
ة: تاء التأنيث [65]	مفرد مؤنث منصوب في حالة التعريف [66]	جمع [67]	فَاعِلَةٌ [68]	اسم جامد [69]	جامعة [70]	ال: التعريف [71]	الجامعة [72]

VI. RESULTS & DISCUSSION

In this approach, we mainly used two annotated corpora for development and testing. For this part, we built our own dataset using different types of emails. In addition, we used “AnATAR” corpus, which consists of 70 different texts of Tunisian books [17].

A. Customized E-Mail Corpus

We built a data set corpus consist of business communication e-mails and e-mails of social Activities. All the emails are in Arabic language. The Arabic Corpus has approximate 900 emails. Which are classified according to different domains. Figure 3 graphically shows the categorization of emails among different domains.

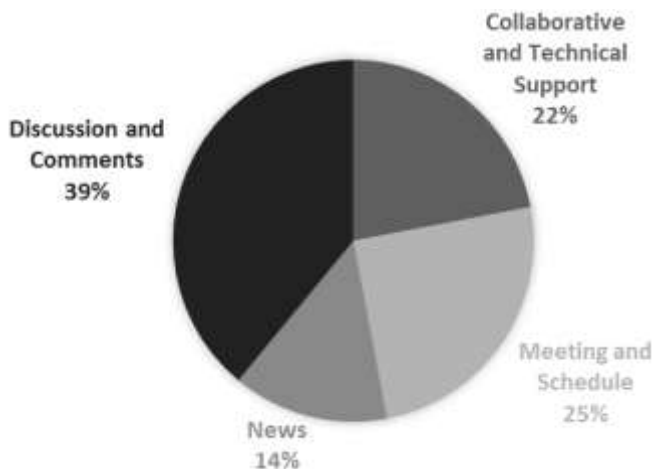


Fig. 3. Email Categorization for Specific Corpus

B. AnATAR” Arabic Corpora

These Corpora were annotated using “AnATAR” tool, consist of “a technical manual, newspaper articles, texts of Tunisian books used for basic education” [17]. Anaphoric relations are annotated in the corpora where some of the pronouns where not included as they were cataphoric.

C. Results

The previous corpora were used in the testing process. Precision, Recall and F Measure are used to evaluate the performance of our method. Assuming that the total number of pronouns in a text has given “R” results and the number of pronouns and referents extracted by the proposed algorithm are “X” of which “N” are correct, then precision is “N” divided by “X” and recall is “N” divided by “R” where F1 measure is calculated according to the following equation, $F1 = (2 * R * P) / (R + P)$. Table 3 shows the results that we got using our approach.

TABLE III. RESULTS

Corpus	R	X	N	Precision	Recall	F1
Customized	1053	1038	951	0.916	0.903	0.909
AnATAR	1148	1190	1018	0.855	0.886	0.87

The results show that the approach effectively and accurately was able to extract pro-forms and NEs while detecting the coreference relations between them. Another observation is that using morphological features along with dependency trees is a successful approach for coreference resolution. This approach was able to achieve high accuracy without the need to define a set of rules or the usage of large amount of annotated data for training. We can also note that the results for our customized set is more accurate than the

“AnATAR” set. The main reason for the difference in the results is due to the difference in annotation scheme. In example (9), the connected pronoun “ت” is not annotated in the “AnATAR” corpus where our approach recognize it as a pronoun and find the coreference relation for it which can affect the accuracy using this set.

(9) فاستيقظت على فراشي.

Then I slept on my bed.

Unfortunately, we could not compare our results to others for multiple reasons. First, annotated corpora and tools for Arabic language coreference resolution are very hard to obtain. Second, the available resources do not have the same scope and same evaluation methods for anaphora [1]. Third, the entities extracted and considered for coreference resolution such as type of pronouns are different from one approach to another. These reasons make comparing the results to other approaches very hard.

Both rule-based and machine learning approaches showed limitations with Arabic language coreference resolution. The first type requires a large set of rules and the second needs annotated data, which add to the limitations of the approaches. The model proposed obtained all the results without the need of both a large set of rules or annotated data, which overcomes a great limitation of traditional approaches. Even a hybrid approach for Arabic coreference resolution, which was suggested by 2012, CoNLL shared task targeted showed many limitations regarding Arabic language coreference resolution [2, 18]. The approach had average results of 60% where in Arabic it dropped to 45%, which means it did not calculate half of the relations right. We cannot compare the numbers directly, but our model does not require the resources that such approach needs and it shows positive results with average F1 score of 89%.

We observed multiple error sources. The complexity of the Arabic language was big challenge for the approach. For example, sometimes some parts of the words were identified wrongly as connected pronouns. Especially that in Arabic most of the connected pronouns are just one letter, which can be easily mistaken as part of any word. Another problem would be the ambiguity of some sentences. The scope of the approach is sentences with complete context, but this cannot easily be identified. An example of ambiguity, the word “كـ” which can be a verb or noun with the same letters, but the diacritics are different.

VII. CONCLUSION AND FUTURE WORK

In this paper, we presented an alternative approach to coreference resolution in Arabic language using morphological features and dependency trees. The approach consists of five stages: text preprocessing, pro-forms and noun entities (NEs) extraction, morphological analysis, relating NE and preforms, and output validation. For testing and evaluation, we designed a customized Arabic annotated corpus using different types of emails for coreference resolution and we used the “AnATAR” dataset. The results indicated the effectiveness of the approach.

In the future, we plan to expand the scope of the approach to include multiple sentences instead of just one sentence,

which means we need to alter the structure of the model to be able to handle the new scope. We plan to explore new ways to improve our results, by for example, combining machine learning in our model. Machine learning can be used for improving the process of morphological analysis by learning new rules for the process. In addition, it can give indication about which morphological features or morphemes have more importance in the process of coreference resolution.

REFERENCES

- [1] A. Soraluze, O. Arregi, X. Arregi, and A. D. de Ilarrazo, "Coreference Resolution for Morphologically Rich Languages," *Procesamiento de Lenguaje Natural*, vol. 55, pp. 23–30, Sep. 2015.
- [2] C. Chen and V. Ng, "Combining the best of two worlds: a hybrid approach to multilingual coreference resolution," *CoNLL '12 Joint Conference on EMNLP and CoNLL - Shared Task*, pp. 56–63, Jul. 2012.
- [3] C. D. Manning, M. Surdeanu, J. Bauer, J. Finkel, S. J. Bethard, and D. McClosky, "The Stanford CoreNLP Natural Language Processing Toolkit," In *Proceedings of the 52nd Annual Meeting of the Association for Computational Linguistics: System Demonstrations*, pp. 55–60, 2014.
- [4] I. A. Al-Sughaiyer and I. A. Al-Kharashi, "Arabic morphological analysis techniques: A comprehensive survey," *Journal of the American Society for Information Science and Technology*, vol. 55, no. 3, pp. 189–213, 2004.
- [5] I. Zitouni, J. Sorensen, X. Luo, and R. Florian, "The impact of morphological stemming on arabic mention detection and coreference resolution," *Association for Computational Linguistics*, pp. 63–70, 2005.
- [6] J. Bajard, L. Didier and P. Kornerup, "An RNS Montgomery Modular Multiplication Algorithm," *IEEE Trans. Computers*, vol. 47, no. 7, pp. 766–776, July 1998.
- [7] J. O. Williams, *Narrow-Band Analyzer*, Ph.D. dissertation, Dept. Elect. Eng., Harvard Univ., Cambridge, MA, 1993.
- [8] J. G. Carbonell and R. D. Brown, "Anaphora resolution," pp. 101–96, Aug. 1988.
- [9] J. Wolf and K. Pattipati, "A File Assignment Problem Model for Extended Local Area Network Environments," *Proc. 10th Int'l conf. Distributed Computing Systems*, pp. 221–230, 1990.
- [10] K. M., A. Farghaly, and A. Aly, "Arabic Anaphora resolution: Corpus of the holy Qur'an annotated with Anaphoric information," *International Journal of Computer Applications*, vol. 124, no. 15, pp. 35–43, Aug. 2015.
- [11] K. R. Beesley, "Arabic finite-state morphological analysis and generation," *COLING '96 Proceedings of the 16th conference on Computational linguistics*, vol. 1, pp. 89–94, May 1996.
- [12] M. Boudchiche, A. Mazroui, A. Lakhouaja, A. Boudlal, and Mohamed Ould Abdallahi Ould Bebah, "AlKhalil Morpho Sys 2: A robust arabic morpho-syntactic analyzer," *Journal of King Saud University - Computer and Information Sciences*, May 2016.
- [13] M.-C. de Marneffe and C. D. Manning, "Stanford typed dependencies manual," Sep. 2008.
- [14] R. Al-sabbagh, "Arabic anaphora resolution using the web as corpus," in *Proceedings of the seventh conference on language engineering*, Cairo, Egypt, 2007.
- [15] R. Roth, O. Rambow, N. Habash, M. Diab, and C. Rudin, "Arabic morphological tagging, diacritization, and lemmatization using lexeme models and feature ranking," *HLT-Short '08 Proceedings of the 46th Annual Meeting of the Association for Computational Linguistics on Human Language Technologies: Short Papers*, pp. 117–120, Jun. 2008.
- [16] "Reviews: Morphology and syntax," in *University of Duisburg-Essen*. [Online]. Available: https://www.uni-due.de/SHE/REV_MorphologySyntax.htm.
- [17] S. Hammami, L. Belguith, B. Hamadou, and Abdelmajid, "Arabic Anaphora resolution: Corpora Annotation with Coreferential links," *International Arab Journal of Information Technology (IAJIT)*, vol. 6, no. 5, pp. 481–490, Dec. 2009.

- [18] Sameer Pradhan, Alessandro Moschitti, Nianwen Xue, Olga Uryupina, and Yuchen Zhang, "CoNLL-2012 Shared Task: Modeling multilingual unrestricted coreference in OntoNotes," Proceedings of EMNLP and CoNLL-2012: Shared Task, pp. 1–40, 2012.
- [19] W. M. Soon, H. T. Ng, and D. C. Y. Lim, "A machine learning approach to Coreference resolution of noun phrases," Computational Linguistics, vol. 27, no. 4, pp. 521–544, Dec. 2001.

User Intent Discovery using Analysis of Browsing History

Wael K. Abdallah

Information Systems Dept
Computers & Information Faculty
Mansoura University
Mansoura, Egypt

Dr. / Aziza S. Asem

Information Systems Dept
Computers & Information Faculty
Mansoura University
Mansoura, Egypt

Prof. /Dr. / Mohammed Badr

Senousy
Computer and Information Systems
Dept
Sadat Academy for Management
Sciences
Cairo, Egypt

Abstract—The search engine can retrieve the information from the web by using keyword queries. The responsibility of search engines is getting the relevant results that met with users' search intents. Nowadays, all search engines provide search log of the user (queries logs, click information besides browsing history). The main objective of this work is to provide features that can help users during their web search by categorizing related browsing URLs together. That will be done by identifying intent groups for each URLs category, then identifying intent-segments for each intent group. Upon clustering the query categories, groups, and intent segments search engines can improve the representation of users' search context behind the current query, this would help search engines to discover the user's intents during the web search. Through the use of the normalized discounted cumulative gain (NDCG), the experimental results show the proposed method can improve the performance of the search engine.

Keywords—component; Information Retrieval; Search Engines; Users' Search Intents; Search Log and Browsing History

I. INTRODUCTION

With the growing of World Wide Web, web search engines have added a big value in web searching. Search engines can find what user search for on the web quickly and easily.

Users issue a query Q and a search engine returns a ranked list of URLs retrieved from the indexed collection of web pages. Developing reliable ranking techniques may be not easy because user search goals are dynamic and depend on their search intents. It is difficult to web search engines to know what the users exactly need. [1]

While searching from the web, users need results based on their interest. For the same keyword two users might require different pieces of information. For a query, a number of documents on different topics are returned by search engines. Hence, it becomes difficult for the user to get the relevant result. Moreover, it is also time consuming. Personalized web search is considered as a promising solution to handle these issues, since different search results can be provided depending upon the information needs of users. It exploits user information and search context to learn in which sense a query refer. [2].

The most important sources help to extract user preferences (i.e. query logs, search engine result page clicks, as well as browsing behavior). Many processes can be done on browsing data, so information extracted from it would become more useful [3].

The proposed method studies the user profiles based on the logs, historical from browsers and clicks. This paper presents a method for the personalization using features based on intentions. It uses resources (browsing history) to categorize URLs in order to extract groups and segments of intents.

There were many studies about the query log that interact with a search is a continuous process to provide a valuable information about the context of the query. So consideration of a given query as a part of large search process could significantly improve the performance of the search engine [3].

But the proposed method studies the browsing history of users to understand how and when information need of a user changes, and it can be very helpful in cold start problem that comes when a new user/query or both just enters the system[4]. As opposed to the previous studies, the proposed method deals not only with search engine result pages but with the whole browsing logs.

The topics categories are used to classify the browsed URLs are based on the most general categories of the Open Directory Project and Alchemy taxonomies like [2]. The second step is grouping each category into intent groups as in [5]. Then for each group, intent segmentation was used like [3]. This categorizing and grouping and intent segmentation information can improve the representation of users' search context behind the current query, this would help search engines to discover the user's intents during the web search and re rank the search results that allow users to find what are they want in the top search results.

Paper organized as the following: the first section discusses the related work. The second section defines the research problem. The third section presents the proposed method. The Fourth section tests the proposed method on data set and evaluates the results. And the last section presents the conclusions and the future work.

II. RELATED WORK

"Personalization is the process of presenting the right information to the right user at the right time." To create the user profile (user context), it needs to collect and analyze user's personal information. User Profile information can be collected from users in two ways: explicitly, i.e. feedbacks; or implicitly, i.e. from user's browsing behavior. The user profile can be presented in the user's preferences and user's interests. Usually, there are three types of a user profile: 1) Content-based profile (i.e. terms), 2) Collaborative profile (i.e. shared similar interest/preference between users' groups) and 3) Rule-based profile: first, users answering the questions about their usage of information. Second, rules are extracted from these answers [4].

Filip and Nicolaas in [6] used complete browsing behavior to build a user interest profile, and then this model was used to re-rank search results.

Ruofan W., Shan J. and Yan Z In [7] proposed a re-ranking method by using semantic similarity to enhance the quality of search results. In the experiment, they used NDCG to evaluate the re-ranking results. The NDCG was used to evaluate our re-ranking results

Fedor et al, in [8] showed how to interact the short-term behavior and long-term behavior (in isolation or combination) to improve the relevance of search results through search personalization

Dixin J., Hang L. and Jian P., in [9] presented a survey that discussed the mining of the search log and the browsing data to improve the search engine components.

Pavel and Yury in [10] tried to solve the problem of the non-existence of the search context by using the short-term browsing.

Anna M., Pavel S. and Yury U., in [3] proposed a technique for automatic segmentation of users' daily browsing activity into intent-related segments. In this paper, the proposed method will use the intent segmentation as a part of intent clustering (besides intent categories and intent groups) of browsing history to understand and discover the user intent during the web search.

Aditi Sharan and R. Kumar In [2] built a framework of an Enhanced User Profile by combining the user's browsing history and the domain knowledge to improve personalized web search. In this paper, the proposed method will use the intent categories (besides intent groups and intent segments) as a part of intent clustering of browsing history to understand and discover the user intent during the web search. Also in the

proposed work, re-ranking the search engine results according to users' discovered intents instead of using the Enhanced User Profile (DMOZ Directory Domain Knowledge) for suggesting relevant pages to the user in this previous work.

Veningston and Shanmugalakshmi In [5] proposed grouping of the search query to allow the search engine to personalize the search results according to user's interests. This paper will use the intent groups for browsed URLs (besides intent categories and intent segments) as a part of our intent clustering of browsing history to understand and discover the user intent during the web search.

III. PROBLEM DEFINITION

First, it is important to provide some definitions: Definition. The browsing log is the recorded daily activity of a user in the browser. The browsing log consists of URLs of visited pages [3].

Definition. Browsing segments (or logical segments) is a subset of the browsing log, consisting of intent-related pages, i.e. pages visited with the same or similar search goal. [3]

Definition. Query logical session is a subset of queries, unified into one search goal (=intent). [3].

The topics categories are used to classify the browsed URLs are based on the most general categories of the Open Directory Project and Alchemy taxonomies. The second step is grouping each category into intent groups. Then for each group, intent segmentation was used as in [3] to obtain a partition of pages visited by a user into intent related goal. Next time when the user issues a query, retrieval process may take place incorporating URL category and its group and its intent segment information in addition to the current query in order to understand and discover the user's intent during the web search. This categorizing and grouping and intent segmentation information can also act to gather a user profile from browsing history which includes users search intents and interests. Thus, web search could be personalized to promote efficient web search.

IV. METHOD

Once all the browsed URLs are classified into predefined intent categories, groups, and segments, then the search result ranking of a user is found out as shown in fig. 1. This is done by creating a database which contains the browsed URLs and its intent classifications (categories, groups, and segments) using intent classification tools such as DMOZ and Alchemy taxonomies and Page Analyzer tools. It also includes the queries and its top results from search engines (and its intent category, intent group, and intent segment). The clustering of

browsed URLs is determined during the clustering phase as training data, and the clustering of top URLs is determined during the clustering phase as testing data. The URLs will be updated in the DB. Then the re-ranking of the top search results of a user.

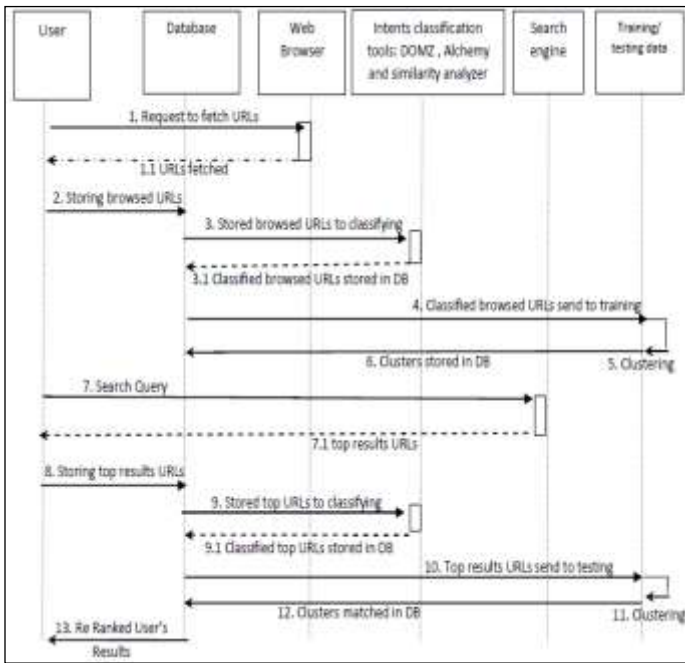


Fig. 1. Process sequence diagram

A. Intent Topic Categorizing, Intent Grouping and Intent Segmentation

a) *The Intent Topic Categories* : The topic categories used to classify the browsed URLs are based on the most general categories of the Open Directory Project and Alchemy taxonomies. The DOMZ₁ Search engine is used to classify the browsed URLs. Also, Alchemy API₂ is used for classifying web pages into particular category after mapping Alchemy API taxonomies to DMOZ Categories.

TABLE I. MAPPING ALCHEMY API TAXONOMIES TO DMOZ CATEGORIES

DMOZ Categories	Alchemy Categories
Art	Arts & Entertainment, Style & Fashion
Education	Education
Home	Family & Parenting, Home & Garden, Pets
Society	Law & Crime, Govt & Politics, Culture, Religion & Spirituality
Business	Business & Industrial, Finance, Real Estate, Careers
Games	Gaming
News	News And Weather
Sciences	Science & Technology
Sports	Sports
References	References
Computers	Technology & Computing
Health	Health & Fitness
Recreation	Automotive & Vehicles, Food & Drink, Travel
Shopping	Shopping
Kids and Teens	Hobbies And Interests

1. <https://www.dmoz.org/>.

2. <http://www.alchemyapi.com/products/demo/alchemylanguage>.

b) *The Intent Groups*: For each previous category, the browsed URLs were classified into intent groups manually with the assistance of DOMZ search engine and Alchemy API. For confirmation, the HTML code of the respective URL's is extracted and crawled to get the content keywords of the page and test theses keywords against the intent groups.

c) *The Intent Segmentation*: Split browsing logs into logical segments manually. During visited pages, search intent segment was assigned to each page. To determine the intent of each page, it is allowed to look through several pages visited after the current one. Then take a collection of pairs (d₁, d₂) of pages visited by one user and manually assign them segments labels S(d₁, d₂, Du) ∈ {0, 1}, choosing 1 if they belong to the same segment and 0 otherwise. With the assistance of similarity-analyzer tool₃ that basically implement the similarity features in 1) HTML code similarity URL Features measuring similarity of URLs and 2)Text similarity textual Features measuring similarity of texts. Similarity-analyzer tool measure the similarity between web pages by giving a similarity score. If the similarity value is above the specified threshold level then only these will be considered belong to one segment.

V. EXPERIMENT AND EVALUATION

A. Experimental Setup

Standard datasets for this research problem are not existent so, the dataset had been designed. In this Experiment, the Lemur toolbar and Google history are used to record the browsing history of the users (researchers in information system filed). Our Experiment is conducted for browsing history for one month for each user. The DOMZ Search engine and Alchemy API are used to cluster the browsed URLs based on the most mapping general categories of the Open Directory Project and API taxonomies. Then, clustering a set of related documents to its group in each category such as art, games, society and so on. Then, the page analyzer is used to determine the intent segment (of related documents) for each group. At last, the browsed URLs had crawled and indexed in each cluster using dtsearch engine₄. Then, keywords have been mined from the crawled web pages. Then calculate the frequency of a specific term in a specific cluster = the number of times that specific term is presented in that specific cluster.

B. Clustering

The input will be a set of URL's from user browsing history as shown in Table 2. The browsed URLs are present in a text file as the training data. The clustering algorithm is applied to it to cluster the input. By the use of Weka₅, the farthest first algorithm [11] is used for clustering the user's intents. A database is created with fields URL, the category field; its group field and its segment field. For each query, the URLs from top five search results is saved in a separate file as test data which is to be tested against predefined clusters of our clustering algorithm in Weka. The last step is the re-ranking of the top search results to improve the web search. The next section will show the clustering results of one user from the dataset as a sample.

C. Clusters

Cluster 0: Computers Web Mining S9, Cluster1: News World News S1, Cluster 2: Sports Football S2, Cluster 3: Education University S4, Cluster 4: Recreation Food S5, Cluster 5: Science Academic Database S7, Cluster 6: Arts Movies S10, Cluster 7: Health Hypertension S11, Cluster 8: Computers Computer Journals S3, Cluster 9: Computers Html Programming Language, S8, Cluster 10: Health Kidney Disease S12, Cluster 11: Computers Software S13, Cluster 12: Arts Music S14, Cluster 13: Recreation Cars S15 and Cluster 14: Recreation Food S6.

D. Clusters Keywords

Now a term cluster matrix can be formed, which specifies by the frequency of the term in that cluster = the number of times the term t is present in the cluster.

TABLE IV. TERMS - CLUSTER MATRIX (TCM)

Term	Cluster0	Cluster	Cluster2	Cluster
t1	C ₁₀	C ₁₁	C ₁₂	C _{1n}
t2	C ₂₀	C ₂₁	C ₂₂	C _{2n}
t3	C ₃₀	C ₃₁	C ₃₂	C _{3n}
.....
t m	C _{m0}	C _{m1}	C _{m2}	C _{mn}

E. Cluster Evaluation

To evaluate the clustering analysis using weka, it can record the recall and precision measures. Precision "is the ratio of the number of documents retrieved that "should" have been retrieved" [12].

$$\text{precision} = \frac{|\{\text{relevant documents}\} \cap \{\text{retrieved documents}\}|}{|\{\text{retrieved documents}\}|} \quad (1)$$

[12].

Recall "is the ratio of the number of relevant documents retrieved to the number of relevant documents" [12].

$$\text{recall} = \frac{|\{\text{relevant documents}\} \cap \{\text{retrieved documents}\}|}{|\{\text{relevant documents}\}|} \quad (2)$$

[12].

TABLE II. CLUSTERING EVALUATION

CLUSTER	TP RATE	FP RATE	PRECISION	RECALL	F-MEASURE	ROC AREA
C0	1	0	1	1	1	1
C1	1	0	1	1	1	1
C2	1	0	1	1	1	0.75
C3	1	0	1	1	1	0.75
C4	1	0	1	1	1	0.667
C5	1	0	1	1	1	0.75
C6	1	0	1	1	1	1
C7	1	0	1	1	1	1
C8	0	0	0	0	0	0.5
C9	0	0	0	0	0	0.5
C10	0	0	0	0	0	0.5
C11	1	0	1	1	1	1
C12	1	0	1	1	1	0.75
C13	1	0	1	1	1	0.75
C14	0	0	0	0	0	?

F. Rand Index

In order to measure the quality of clustering, Rand Index is used. Rand Index is determined as the accuracy of cluster formation. It is a measure of the similarity between two clusters. It is assumed that the two different clusters consist of the same number of data. In order to calculate the Rand Index shown in equation (3), it has to compare pairs as shown in Table 3.

TABLE III. POSSIBLE PAIRS TO COMPUTE RAND INDEX [5]

	Pairs assigned to the same cluster (C1)	Pairs assigned to the different cluster (C2)
Pairs assigned to the same cluster (C1)	A	b
Pairs assigned to the different cluster (C2)	C	d

Count the number of pairs that fall into each of these four options a, b, c & d. C1 & C2 are the two clusters. The four options are expressed in the form of a table. In total there are possible pairs $a+b+c+d = \binom{n}{2}$ of n data points. Once a, b, c & d are identified, the Rand Index is computed as follows;

$$\text{RandIndex} = \frac{(a+b)}{(a+b+c+d)} \quad (3) [5]$$

Where a+b is assumed as the number of agreements between C1 & C2 and c+d as the number of disagreements between C1 & C2.

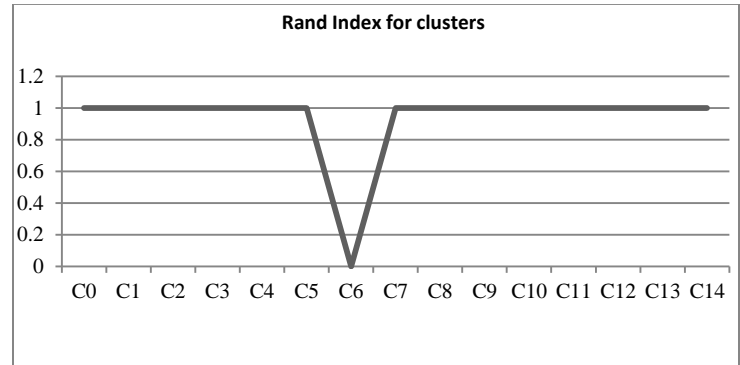


Fig. 2. Rand Index for clusters

Fig. 2 presents Rand Index for the clusters of the proposed method. It was noticed that the Rand Index for all clusters except cluster 6 is one because each cluster contains a few numbers of browsed URLs because clustering depend on many factors; intent categories, intent groups and intent segments. Rand Index of C6=0 because it contains only one URL.

3. <http://tool.motoricerca.info/similarity-analyzer.phpml>.

4. <https://www.dtsearch.com/>

5. <http://www.cs.waikato.ac.nz/ml/weka/>

G. Rand Index Comparison

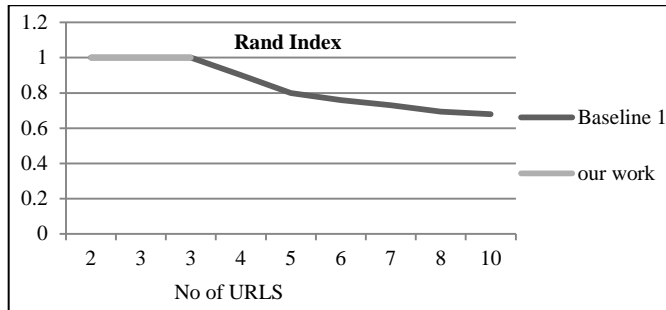


Fig. 3. Rand Index comparison between baseline 1 and the proposed method

Fig. 3 presents the Rand Index comparison between baseline 1 and the proposed method. Work [5] was used as baseline 1. It was noticed that the Rand Index of baseline 1 decrease when the number of browsed URLs increased. But in the proposed method Rand Index is stable because each cluster contains a few numbers of browsed URLs because clustering depends on many factors; intent categories then intent groups and finally intent segments.

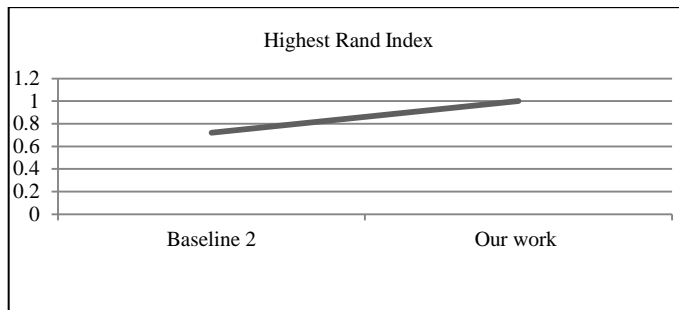


Fig. 4. Highest Rand Index comparison between baseline 2 and the proposed method

Fig. 4 presents the highest Rand Index comparisons between baseline 2 and the proposed method. Work [3] was used as baseline 2. Its highest value is 0.72. But in the proposed method the Rand Index is one because each cluster contains a few numbers of browsed URLs because clustering depends on many factors; intent categories then intent groups and finally intent segments.

VI. RESULTS ANALYSIS

For each query, the top 5 relevant search results provided by Google were collected (many experiments with different accessed times range from August 2015 to February 2016). Then classify them as intent categories, intent groups, and intent segments as discussed before. Consider them as test data for our clustering algorithm to decide whether these top 5 results belong to clusters or not. If the one or more of top results belong to clusters then increase their rank positions to the top else display the original results, but if these top results lately browsed by the user then add them to browsing history data set and re run the clustering algorithms and its followed steps. The analysis of the result is done by discovering the top results for each query belong to each cluster.

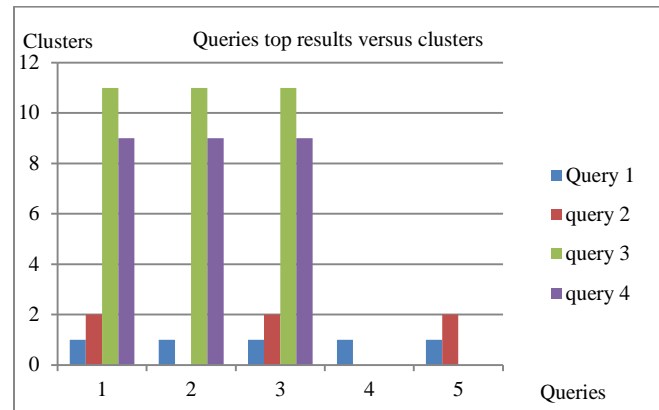


Fig. 5. Queries top 5 results versus clusters

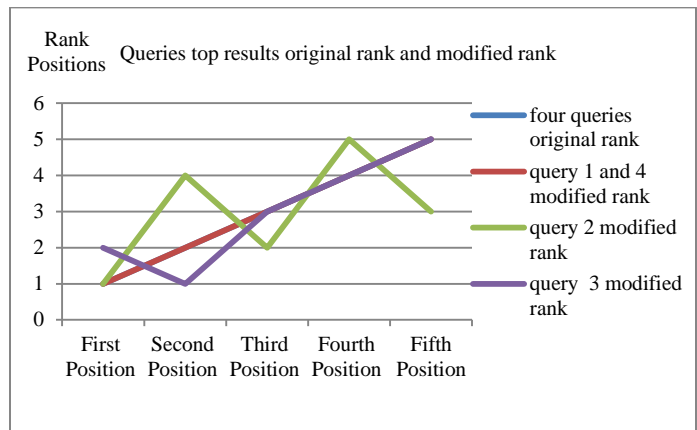


Fig. 6. Queries top results original rank and modified rank

Fig. 5 presents Queries top 5 results versus clusters for the four queries. And Figure 6 presents Queries top results original rank and modified rank for the four queries. For the first query and the fourth query, the search engine should keep the original ranking because the top results match with clusters in their same rank. For the second query and the third query, the search engine should modify the ranking of the top results as showed in the figure 6.

Search Relevance: NDCG Calculation

NDCG is an effective measure mainly used in information retrieval research to evaluate rankings of search documents according to their relevance. It measures how a ranking algorithm is in assigning the proper ranking to relevant documents. For example, if there are three web pages d1, d2, d3 whose relevance scores are (3, 2, 1) respectively (the higher score, the relevant), then the ranking of (d1, d2, d3) will achieve a higher NDCG value than the ranking of (d3, d2, d1). [7]. it can compute NDCG the Normalized Discounted Cumulative Gain of each rank p using the following formula:

$$NDCG_p = \frac{DCG_p}{IDCG} \quad (4) [7]$$

Where IDCG is Ideal Discounted Cumulative Gain calculated when get the search results. it has the best rank. And calculate the order of query of DCG.

And DCG is Discounted Cumulative Gain

$$DCG_p = \sum_{i=1}^p \frac{2^{reli_i}}{\log_2(i+1)} \quad (5) [7]$$

Where p is PageRank serial number and reli is the graded relevance of the result at position i. For simplicity, suppose that on a five-point scale, 0 score given for an irrelevant result, 0 for a partially relevant, 1 for relevant, 1 for relevant again and 2 for perfect according to the percentage of the traffic by Google results positions study⁶.

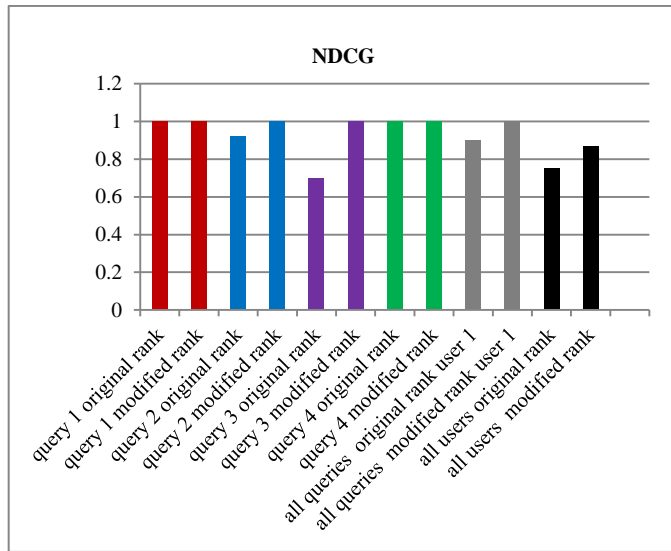


Fig. 7. NDGC for the queries for user 1 and all users

Fig. 7 presents the NDGC for the 4 Queries for original results and after modifying the rank. It was noticed that NDGC increased for queries 2 and 3 after modified the ranked. It stills the same for queries 1 and 4. Then calculate the overall NDGC for all the 4 queries; this improves the search relevance from 0.9 to 1. Then calculate the overall NDGC for all users; this improves the search relevance from 0.75 to 0.87. This proposed method helps the search engine to discover the users' intents during the web search.

VII. CONCLUSIONS

Our work's key objective is to provide features that can help users during their web search by categorizing, grouping, and segmentation of related browsing URLs together. Upon clustering the browsed URLs categories, groups, and intent segments, search engines can improve the representation of user's search context. This would help the search engine to understand better and discover the user's intent during the web search.

From the experiment results, fourteen clusters were proven by high values of recall and precision and f measure metrics. By using the Rand Index metric, it was approved that clusters of the proposed method compared to baselines had high Rand Index values because each cluster contains a few numbers of browsed URLs because clustering depend on many factors; intent categories then intent groups and finally intent segments. Also, term cluster matrix was presented, which specifies the frequency of the term in each cluster.

From the results' analysis, the top search results returned by Google were presented as test data to match them with our clusters from clustering method for four queries. It was found the first five top results of the first query had matched with the clusters 1. And it was found the three top results of the fourth query have matched with the clusters 9, so the search engine should keep the original results ranking for theses queries. It was found the first, the third and the fifth top search results of the second query matched with the clusters 2. And the second, the first, and the third top search results of the third query matched with the clusters 11, so the search engine should modify the ranking of top search results of theses queries as discussed in Fig. 5 and fig.6.

From the results re-ranking and Search Relevance, the proposed method assists in discovering the user intents that enable the search engine to help users to find what they search for by calculating the NDCG metric for the four Queries for original results and after modified rank. It was noticed that NDGC increased for queries 1 and 2 after modified the rank. Then, the overall NDGC was calculated for all the four queries for the first user; this improved the search relevance from 0.9 to 1. And finally, the overall NDGC was calculated for all queries of all users; this improved the search relevance from 0.75 to 0.87. (In the second experiment with different accessed time to top Google results for experiment's queries, the search relevance improved from 0.72 to 0.86).

Future work will include more research to evaluate the proposed method that improved the search engine ranking and its performance complexity. Expanding the experiment with a larger data set is needed. It is interesting to utilize complete knowledge about users' behavior during the web browsing. Also, it is possible to utilize complete browsing history from different resources such as social media links URLs. Also, it can develop more sophisticated similarity method between browsed web pages in segmentation level of user intents.

REFERENCES

- [1] Kiseleva, "Using Contextual Information to Understand Searching and Browsing Behavior", ACM , Information Retrieval , USA, pp. 1059-1059 , 2016 [the 38th International ACM SIGIR Conf. on Research and Development in Information Retrieval USA, 2016].
- [2] Sharan and R. Kumar, "Personalized Web Search Using Browsing History and Domain Knowledge", IEEE, ICICT, Ghaziabad, pp. 493 – 497, 2014. [international Conf. on Issues and Challenges in Intelligent Computing Techniques (ICICT) Ghaziabad , 2014].
- [3] A. Mazur, P. Serdyukov, and Y. Ustinovskiy, "Intent-Based Browse Activity Segmentation", IR, Russia, pp. 242-253, 2013. [the 35th European Conference on IR Research, Russia, 2013].
- [4] D. Gupta, V. Tayal, A. Thakkar3, K.Makvana, "Cold Start Problem in Personalized Web Search", International Journal of Innovative Research in Computer and Communication Engineering, Vol. 4, 2016.
- [5] Veningston .k and dr. R. Shanmugalakshmi, "Personalized Grouping of User Search Histories for Efficient Web Search", Applied Computational Science, 2014.
- [6] Filip Radlinski and Nicolaas Mathijss, "Personalizing Web Search using Long Term Browsing History" , ACM, Web search and data mining, USA, pp. 25-34, 2011. [the fourth ACM international conference on Web search and data mining, USA, 2011].
- [7] R. Wang, S. Jiang, and Y. Zhang, "Re-ranking Search Results Using Semantic Similarity", Fuzzy Systems and Knowledge Discovery, pp. 1047 – 1051, 2011 [the Eighth International Conference on Fuzzy Systems and Knowledge Discovery, 2011].

6. <http://searchenginewatch.com/sew/study/2276184/no-1-position-in-google-gets-33-of-search-traffic-study>

- [8] F. Borisyuk, P. Bailey, P. N. Bennett, R. W. White, S.T. Dumais, W.Chu, and X. Cui, “ Modeling the Impact of Short- and Long-Term Behavior on Search Personalization”, ACM, SIGIR, USA, pp. 185-194, 2012. [the 35th international ACM SIGIR conference on Research and development in information retrieval, USA , 2012].
- [9] D. Jiang, H. Li, and J. Pei, “Mining Search and Browse Logs for Web Search: A Survey”, ACM Transactions on Intelligent Systems and Technology (TIST), Vol. 4, 2013.
- [10] P. Serdyukov and Y. Ustinovskiy, “Personalization of Web-search Using Short-term Browsing Context”, ACM, information & knowledge management , USA, pp. 1979-1988, 2013. [the 22nd ACM international conference on information & knowledge management, USA, 2013].
- [11] J. P. Data, J. Han, and M., Kamber, Data Mining Concepts and Techniques, Elsevier, USA.:2013.
- [12] M.B.Senousy and W. Karam, “A Comparative Study for Internet Search Engines and Web Crawlers”, SAMS, Cairo, Egypt, 2011.

A Multi-Task Distributed Vision System Embedded on a Hex-Rotorcraft UAV

Nadir Younes, Boukhdir Khalid, Moutaouakkil Fouad, Hicham Medromi

Equipe Architectures des Systèmes (EAS), Laboratory of Research in Engineering (LRI)
Université Hassan II of Casablanca, Ecole Nationale Supérieure d'Electricité et de Mécanique (ENSEM)
Casablanca, Morocco

Abstract—In this paper, are presented the general architecture and implementation of a multi-task distributed vision system designed and embedded onboard a Hex-Rotorcraft UAV. The system uses multiple cheap heterogeneous cameras in order to perform various tasks such as: ground target pedestrian detection, tracking, creating panoramic images, video stabilization and streaming multiple data/video feeds over a wireless secure channel. In what follows, are discussed this multi-agent architecture designed to provide our UAV with an embedded intelligent vision system using autonomous agents entrusted with managing the previously listed functionalities. In addition to the cheap set of USB and module cameras, the presented vision system is composed of a Local Data Processing Module connected to each camera and a Central Module used to control the overall system, process the regrouped data and streams it to the ground station. The overall vision system has been tested in real flights and is still under improvements.

Keywords—*multi-agent architecture; image processing; real-time systems; target detection; panoramic images; target following; unmanned aerial vehicles (UAVs); vision systems*

I. INTRODUCTION

In the last few decades, UNMANNED AERIAL VEHICLES (UAV) were employed and adopted in various sectors, ranging from surveillance in both military & industrial, to academic research, agriculture, etc. Specifically, UAV rotorcrafts were mainly used & upgraded by both defense and security communities [1], due to their easy maneuvering and vertical take-off/landing. More specifically, an UAV rotorcraft equipped with a vision system can be used to perform various tasks, ranging from objects investigation, patrolling, to tracking targets, etc...

Since vision is used as our native sensing mean, instead of using basic systems that are only able to acquire/send image & video feeds, researches were mostly focused on implementing embedded systems onboard UAVs able to perform multiple tasks such as: flight control using vision [1] [2], [3], [4], object detection & tracking, etc.

So far, research efforts were mainly geared toward the proposal of solutions answering to specific problems, which makes them optimized to perform the tasks they were conceived for, but they generally lack flexibility and scalability when deployed in other environments, or when they're to be upgraded to add new sensors or features. And so, it is rare to encounter in the literature documentations proposing

implementations, architectures of detailed and exhaustive vision systems designed for UAV rotorcrafts.

In order to bypass the enunciated inconveniences, the present paper introduces the hardware configuration and architecture of our embedded real-time vision system. The developed system is ought to be embedded, cognitive, scalable and based on a flexible multi-agent architecture, able to conduct a panel of image/video processing tasks using a set of low-cost credit-sized cards: Raspberry pi. The implemented software is running on a Raspbian [5] operating system featuring a real-time kernel. In order to develop a detection and tracking of moving targets feature, a variant of the CAMSHIFT algorithm was implemented [6]. This technique is a variant of the histogram based mean shift algorithm [13] altered so that it can adapt to the object's scale and rotation changes. Also, is featured a real-time panorama construction algorithm using simultaneously multiple heterogeneous camera streams. Finally, using the vision feedback, a video stabilization followed by a tracking control setup are presented in order to control a set of pan/tilt servomotors that keeps focusing objects of interest in the center of the video frame.

The rest of the paper is structured as follows. Section 2 briefly justifies the use of a multi-agent architecture as an infrastructure needed to deploy modular embedded vision systems on UAV rotorcrafts. In Section 3, the hardware characteristics are detailed. Section 4 details the architecture of the vision system. Section 5 details the deployment and configuration of the vision system blocs and their functionalities. Section 6 resumes the work and suggests future research lines.

II. MULTI-AGENTS IN VISION SYSTEM

Monitored scenes by UAV vision systems usually are complex and dynamic environments where multiple tasks are to be performed and where the outputs are to be merged in order to display the user requested results. This is why multi-agent systems (SMA) can be seen as an intuitive solution used to devise the vision system into a set of intelligent agents that communicate and cooperate in order to perform the requested tasks.

III. HARDWARE CONFIGURATION

This section describes the hardware configuration of the embedded vision system designed for small UAV. The hardware platform is mostly composed of various video

sensors linked to a couple of credit-card sized computer boards, bounded together using an implemented communication middleware in charge of the tasks distribution, computations and centralization of the outputs sent to the ground station. The hardware configuration that has been used can be justified by the following arguments:

A. Central processing module

First of all, this manipulation aims to implement a low-cost, low power consumption, compact, autonomous and real-time vision system onboard a small UAV rotorcraft. Since the platform ought to run real-time applications, a real-time operating system was chosen to support the implementation [5]. In addition, it is highly recommended to use a hardware platform that supports libraries of programming functions aimed at real-time computer vision such as Aforge, SimpleCv, OpenCv (Open Source Computer Vision), etc. And finally, it is suitable to work with a hardware platform that can use cheap, small and heterogeneous video sensors in addition to regular USB, RS232 or wireless cameras. According to the literature, more than a dozen of small board cards can satisfy parts of these constraints such as Arduino cards, NanoPC-T1, BeagleBone Black or ODROID-XU4, etc... . To meet up all of our expectations, we ended up hesitating between two processing boards: the Raspberry Pi and the BeagleBone Black cards. After comparing all these boards specifications [16], our mind was finally set on using RPI due to their large developing community, diversity of compatible modules that it offers and most of all because it possess a powerful integrated Video-core graphics processor able to decode up to 1080p video streams which is suited in computer vision applications. Is it important to note that this board sole purpose is to run the UAV vision system, and up till now it does not intervene in the flight control process. The separation of the vision system and the flight control system [17] into different computing boards can be justified by the following arguments:

- First, due to the fact that the computation consumption of both these tasks is way too heavy, running them both simultaneously on the same embedded computer board is not possible.

- Also, by distributing the system we can guarantee a better stability of the overall system by protecting the flight system from potential latencies caused by data overload.

B. Visual sensors

Various heterogeneous color video cameras were picked as visual sensors in our system. The default set of cameras that is used in our system is composed of:

- **Camera Module:** This camera plugs into the CSI connector located between the Ethernet and HDMI ports. The cost of the camera module is € 20 in Europe (9 September 2013). [7] It can produce 1080p, 720p and 640x480p video. The dimensions are 25 mm x 20 mm x 9 mm and it weighs less than 30g [7].
- **HERO3+ Black edition camera:** this device offers various functionalities such as the so called “SuperView” which increases the field of view, a panel

video modes (1440p48, 1080p60, 960p100 and 720p120 as well as 4K15 and 2.7K30), can shoot 12MP stills at up to 30 frames per second and also includes a Wi-Fi Remote [8].

- **HD PRO WEBCAM C920:** simple USB webcam, able to save up to 1080p videos.

C. Pan/Tilt servomechanism

In order to maintain a constant visual contact with followed targets, a pan/tilt servomechanism had been used to mount the module cameras, enable them to rotate up to 180 degrees horizontally and 110 degrees vertically.

D. Wireless data link

In order to ensure a permanent wireless communication between the ground operators and the vision system, a 150 Mbps wireless adapter is used in order to perform a Wi-Fi communication -to transmit commands and receive visualization data- between the ground control and the embedded system

IV. PROPOSED ARCHITECTURE

E. Abstract view of proposed architecture

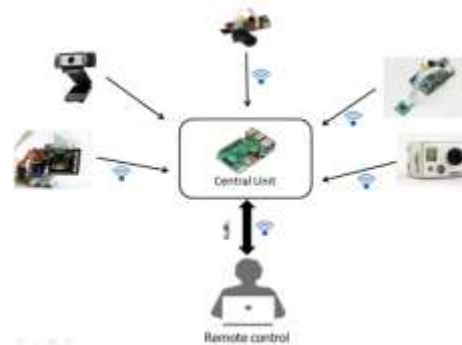


Fig. 1. Abstract view of proposed architecture

As shown in Fig.1, the architecture is mainly composed of a set of raspberry pi board and various types of cameras (USB, module, GoPro ...). Each board can be considered as an independent sub-layer where visual data can be extracted and preprocessed before being sent to the central unit board. In a concern for scalability (possibility to add or suppress boards), and also to keep the system compact as much as possible, communications between these different components have been kept essentially wireless (Wi-Fi).

F. Architecture overview

The system overall architecture (Fig.2) can be structured into three main layers: a reactive layer, deliberative layer, and a user layer. Interactions and communications between these layers are maintained using a communication middleware. Next, characteristics of each level are summarized:

- Basically, the reactive layer is composed of heterogeneous video sensors used to obtain visual information of the UAV in-flight surroundings in addition to agents charged with the unification of the data format on a reactive level.

- The deliberative layer can functionally be split into sub-layers. The first sub-layer (the panoramic editing unit) host agents that register the exploitable collected uniformed data in order to merge them into panoramic images. While in the second sub-layer, are agents entrusted with the construction of a knowledge model

of the environment, so that it can be used in various tasks (such as objects recognition, maintaining the overall system connected to the ground station, pan/tilt object tracking using a set of servomotors).

- The user level allows users to interact and monitor the vision system via a developed web interface.

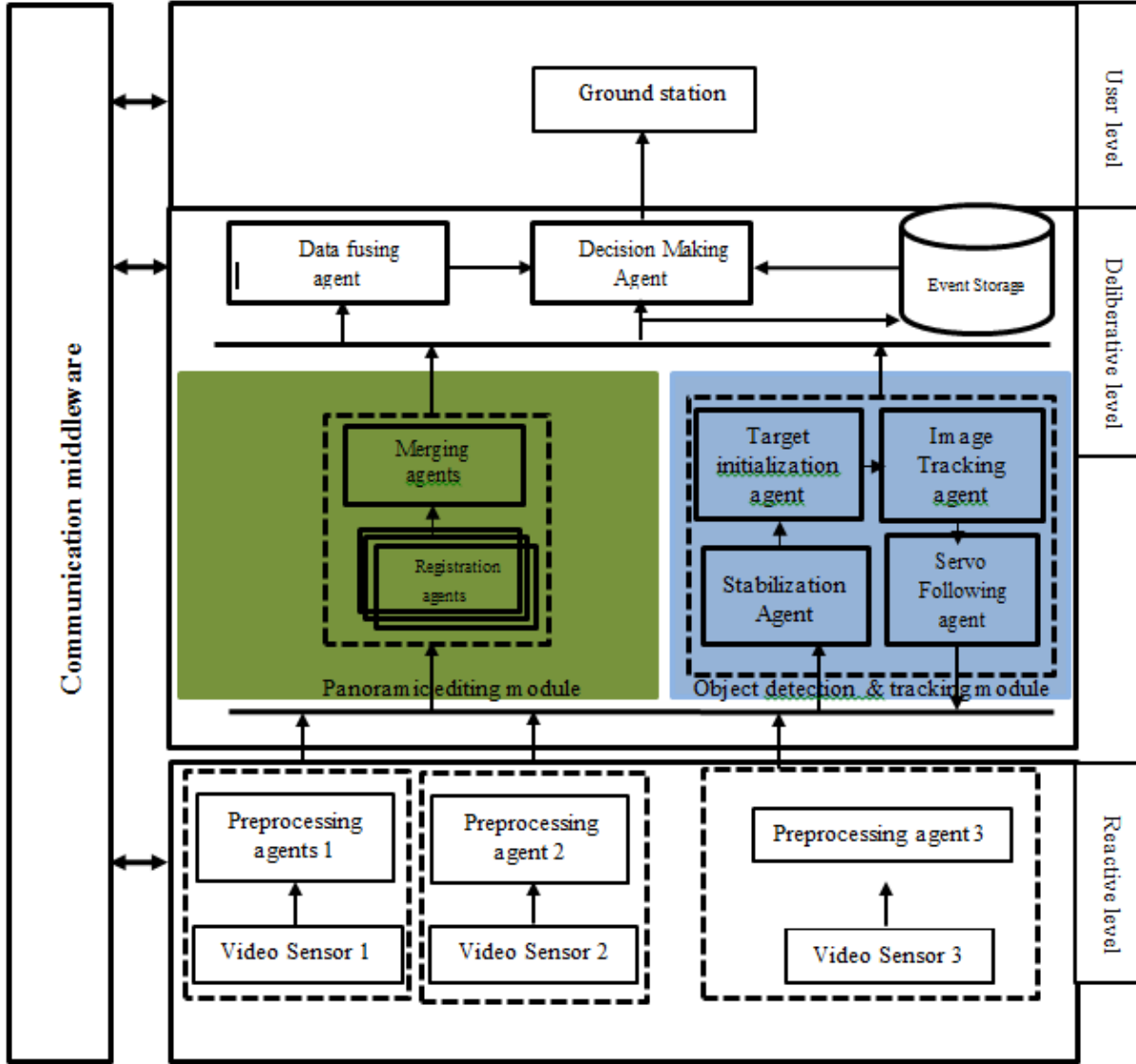


Fig. 2. Architecture of an intelligent and multi-tasked vision system for small UAV

V. DEPLOYMENT AND CONFIGURATION OF THE VISION SYSTEM BLOCS

Each layer in this system incorporates different classes of agents. These agents deal with the problematic of performing simultaneously multiple computer vision tasks using incoming streams of heterogeneous video sensors by treating them locally first on their respective boards, followed by a unification of the retrieved formatted data. In what follows, the data flow between these different layers is detailed.

G. Reactive level: Data Preprocessing

On the reactive level, at the start of the overall process, preprocessing agents are deployed at the end of each video sensor to process the gathered data. And so, these agents are used to unify the gathered streams from the heterogeneous cameras into uniform classes (a VideoClass for video streams and an ImageClass for images) with standard spatial/temporal resolutions. The spatial synchronization mainly consists of a resizing of all the videos based on the one with the smallest resolution while the temporal synchronization is insured by

adjusting the FPS processing rate based on the lowest one. This entire process can be summarized in the following figure (3).

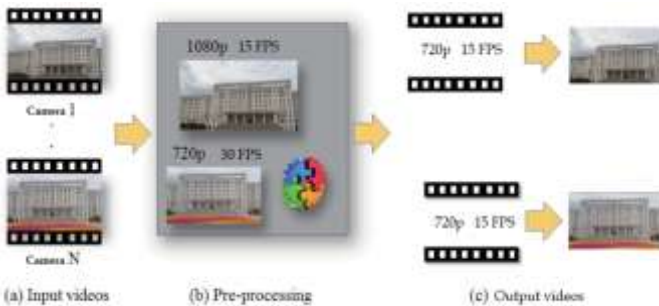


Fig. 3. Pipeline of video preprocessing: (a) input videos that are captured by heterogeneous cameras, (b) auto video synchronization based on lowest FPS/resolution, (c) Output videos generated

H. Deliberative level

On the deliberative level, once the acquired data is uniformed, two scenarios can take place depending on the nature of the requested task.

In the ***panoramic editing module***, are input the collected preprocessed video streams in order to create real-time panoramas. By altering the Panoramic Image Stitching algorithm presented by M. Brown and D. Lowe [9], we were able to extend this technique to real-time videos at the cost of performing it only when the UAV is in stationary flight. The reason behind such a limitation will be addressed later on.

Registration and Merging Agents:

Component heads identify the different components of your system. Assuming that the UAV is performing a stationary flight in order to keep the cameras still, registration agents are used to detect a difference of Gaussian keypoints (DoG) [10] and extract local invariant descriptors SIFT [11] from the previously unified received images. Next, merging agents loop over the previously computed descriptors, compute the distances, find the smallest distance for each pair of descriptors, computes the matches for each pair of descriptors using Lowe's ratio test [9] and estimate their homography matrix by applying RANSAC algorithm [18] on the matched feature vectors. Finally, using the previously created homography matrix, a warping transformation produces a panoramic image that is sent to the user level. The reason behind insisting on having to apply this method only on still cameras resides in the fact that performing these tasks (keypoint detection and matching, SIFT descriptor detection and especially estimating the homography matrix) on successive frames can be computationally heavy. So, applying this algorithm on videos received from moving cameras would make us estimate the homography matrix for each set of frames, making it unmanageable to run it in real-time. However, if by assuming that the cameras are still (as in the case of a stationary flight), the estimation of the homography matrix would only be computed once, resulting in the creation of a video panoramic view using multiple cameras. The overall algorithm can be reviewed in figure 4 while figure 5 gives an inflight example of the image stitching method using frames taken from three video sensors.

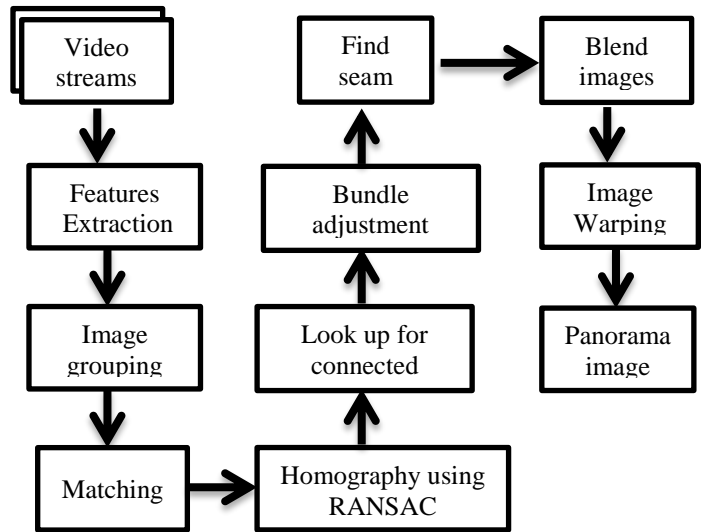


Fig. 4. Real-time panorama stitching algorithm



Fig. 5. Panorama created using three simultaneous frames

On the other hand, the Object detection & tracking module is implemented on the main board (central unit). This board serves to remotely command the overall system, and it is also used to:

- coordinate between all sub-units via a communication middleware,
- stabilize moving videos,
- perform some computer vision tasks using a set of vision algorithms such as HOG + Linear SVM detector [15] for pedestrian detection, CAMSHIFT for scale invariant objects recognition in high altitudes [6], etc.,
- track targets by centering them in the middle of the frame using a couple of pan/tilt servomotors able to perform both vertical and horizontal rotations,
- fuse all the retrieved data before it is sent to the ground station,

- take decisions (send alerts, actuate a command, ...) when a special event (listed in the event knowledge base) is encountered,
- aggregate all the generated outputs destined to the ground station using a **Data Fusing Agent**,
- Interact with the ground station via a wireless secure channel.

Stabilization Agent:

Once video streams have been preprocessed, in order to help performing a robust target tracking, a video **stabilization agent** is first used to reduce the effects of shakiness induced by wind perturbations, forward movements

The hereby **stabilization agent** functioning can be resumed into five steps:

- A look-up for a Euclidean transformation that occurred between the precedent and current frames is conducted using optical flow [20] on all frames. This transformation is only based on three parameters: dx (horizontal), dy (vertical), da (angle). Figure 6 show an example of shakiness in two consecutives frames histograms based on dx and dy.

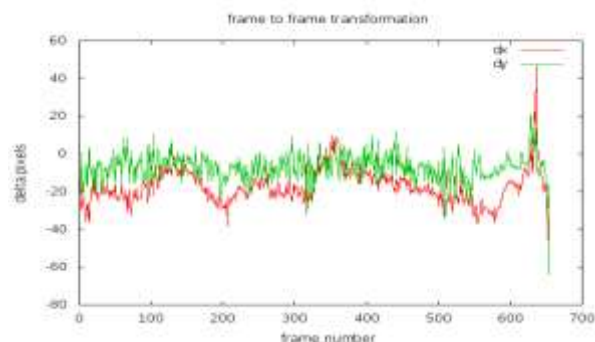


Fig. 6. Example of shakiness on dx and dy from a moving camera

- Stock the consecutives transformations to trace the “trajectories” for x, y, angle, at each frame.
- Smooth out the trajectory using a sliding average window, and defining the window radius as equal to the number of frames used for smoothing. Figure 7 shows an example of smoothing based on dx.

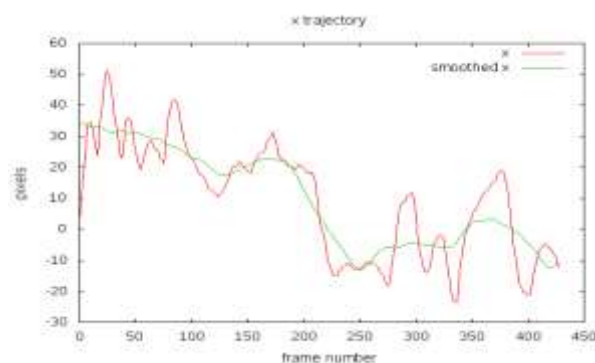


Fig. 7. Example of smoothing based on dx alone

- Create a new transformation defined as:
 $N_{transform} = transformation + (S_{trajectory} - trajectory)$.
- Apply the new transformation to the video (fig 8).

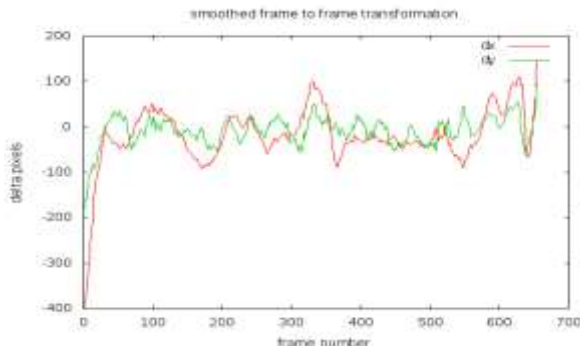


Fig. 8. Final transformation applied to the video

Target initialization agent:

In this section, a particular type of targets was chosen to work on: pedestrian targets. In order to detect this class of targets, an implementation based on HOG + Linear SVM [15] model had been used. Once the stream video is handed, the process begins by initializing the Histogram of Oriented Gradients descriptor.

Then, the Support Vector Machine is set to be pre-trained pedestrian detector. From then, once the pedestrian detector is fully loaded, it is looped on the stream frames.

Image tracking agent:

Figure 9 shows the proposed tracking agent mode of functioning.

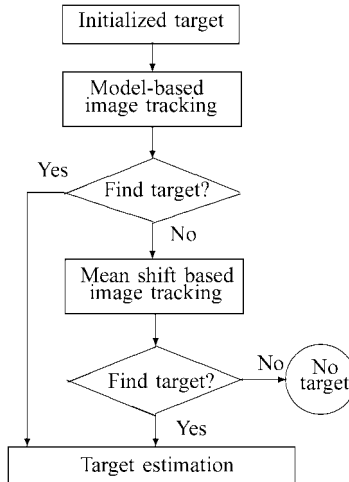


Fig. 9. Tracking image agent

- Once the target is initialized, in the model-based image tracking, a Kalman filtering technique tries to predict the position and velocity of the target in the subsequent frames and then perform data association based on an updated likelihood function [19].

- Once the target gets out of range from the model-based tracker, a changing mechanism check whether the target is still in the image.
- If yes, the mean-shift tracker will be activated. The loss of the target can be attributed to the poor match of features due to noise, distortion, or occlusion in the image. An alternative reason may be the maneuvering motion of the target, and the target is out of the image.
- If the target is still in the image, continuously adaptive mean-shift (CAMSHIFT) algorithm [6] is used to efficiently obtain the optimal location of the target in the search window.

Servo following agent:

In this section is described a target-following system based on a pan/tilt servomechanism. This servomechanism is used to control the orientation of the camera to keep the target in an optimal location in the image plane. The mechanism is operating via i2c and can be fully automated to track a designed target of commanded manually via keyboard.

Data fusing agent:

This agent sole purpose is to aggregate all the data gathered from all the devices and boards, in order to send them to the ground station after to formatting as they were requested.

I. User level:

From this interface, any user can access to the vision system web interface to perform the previously cited functionalities.

VI. CONCLUSION

In this paper, are presented the architecture and functionalities of a remote control wireless vision system embedded onboard a hex-rotorcraft and formed using a distributed multi-agent system architecture. This architecture is validated by an implementation realized onboard a set composed of two raspberry pi, 2 cameras modules, 1 go pro hero + black and one USB camera. The overall functionalities provided by the system can be summarized by the following:

- At the reactive level, all the images and videos gathered from the sensors are preprocessed. This step can be summarized in two big steps: at first, the FPS of all sensors are increased, followed by a unification process that handles all the gathered streams from the heterogeneous cameras in order to uniform them into classes (a VideoClass for video streams and an ImageClass for images) with standard spatial/temporal resolutions.

- On the deliberative level, two units are implemented in order to offer either a live panoramic view using incoming data feeds from heterogeneous cameras, or a pedestrian detection and tracking system using a servomechanism system.

As a further work, the system ought to be improved by:

- Readapting the stitching algorithm so that it can withstand moving cameras,

- Supplying the decision making agent with rules so that respond autonomously to a set of unexpected events,
- implementing a backup wireless communication (radio) adapted to long range data exchange,
- Making the stabilization algorithm more robust and less CPU consuming,
- Extending the target following mechanism so that it can cooperate with UAV following control mechanism.

REFERENCES

- [1] M. J. Adriaans, R. C. Cribbs, B. T. Ingram, and B. P. Gupta, "A160 Hummingbird unmanned air vehicle development program," in Proc. AHS Int. Specialists' Meeting—Unmanned Rotorcraft: Des., Control Test., Chandler, AZ, 2007.
- [2] O. Amidi, T. Kanade, and R. Miller, "Vision-based autonomous helicopter research at Carnegie Mellon Robotics Institute 1991–1997," in Proc. Amer. Helicopter Soc. Int. Conf., Gifu, Japan, 1998, pp. 1–12.
- [3] N. Guenard, T. Hamel, and R. Mahony, "A practical visual servo control for an unmanned aerial vehicle," IEEE Trans. Robot., vol. 24, no. 2, pp. 331–340, Apr. 2008.
- [4] E. N. Johnson, A. J. Calise, Y. Watanabe, J. Ha, and J. C. Neidhoefer, "Real-time vision-based relative aircraft navigation," J. Aerosp. Comput., Inf. Commun., vol. 4, no. 4, pp. 707–738, 2007.
- [5] <http://docs.emlid.com/navio/Downloads/Real-time-Linux-RPi2/>
- [6] G. R. Bradski and S. Clara, "Computer vision face tracking for use in a perceptual user interface," Intel Technology Journal Q2 '98, pp. 1–15, 1998
- [7] "RPI Camera board - Raspberry-Pi - Raspberry Pi Kamera-Board, 5MP | Farnell Deutschland". de.farnell.com. Retrieved 9 June 2013.
- [8] HERO3+ Black Edition, gopro.com
- [9] Brown and D. Lowe. Automatic Panoramic Image Stitching using Invariant Features. International Journal of Computer Vision, 74(1), pages 59-73, 2007.
- [10] Lowe, David G. (1999). "Object recognition from local scale-invariant features" (PDF). Proceedings of the International Conference on Computer Vision pp. 1150–1157. doi:10.1109/ICCV.1999.790410
- [11] U.S. Patent 6,711,293, "Method and apparatus for identifying scale invariant features in an image and use of same for locating an object in an image", David Lowe's patent for the SIFT algorithm, March 23, 2004
- [12] "Deformable Medical Image Registration: Setting the State of the Art with Discrete Methods" Annual Review of Biomedical Engineering, Vol. 12, 2011, pp. 219-244
- [13] Dorin Comaniciu and Visvanathan Ramesh. Mean shift and optimal prediction for efficient object tracking. In Tracking, International Conference on Image Processing, pages 70–73, 2000.
- [14] Unmanned Rotorcraft Systems Par Guowei Cai,Ben M. Chen,Tong Heng Lee
- [15] Histograms of Oriented Gradients for Human Detection, Navneet Dalal and Bill Triggs,
- [16] <http://makezine.com/2014/02/25/how-to-choose-the-right-platform-raspberry-pi-or-beaglebone-black/>
- [17] K.Boukhdir, A. Boualam, S. Tallal, H. Medromi, S. Benhadou "Conception, Design and Implementation of Secured UAV Combining Multi-Agent Systems and Ubiquitous Lightweight IDPS (Intrusion Detection and Prevention System)" IREA Vol 3, No 1 (2015)
- [18] M. A. Fischler, R. C. Bolles. Random Sample Consensus: A Paradigm for Model Fitting with Applications to Image Analysis and Automated Cartography. Comm. of the ACM, Vol 24, pp 381-395, 1981.
- [19] Feng Lin, Kai-Yew, A Robust Real-Time Embedded Vision System on an Unmanned Rotorcraft for Ground Target Following. IEEE TRANSACTIONS ON INDUSTRIAL ELECTRONICS, VOL. 59, NO. 2, FEBRUARY 2012
- [20] Gibson, J.J. (1950). The Perception of the Visual World. Houghton Mifflin.

Trending Challenges in Multi Label Classification

Raed Alzaidah

School of Computing

Universiti Utara Malaysia (UUM)

Sintok-Kedah, Malaysia

Farzana Kabir Ahmad

School of Computing

Universiti Utara Malaysia (UUM)

Sintok-Kedah, Malaysia

Abstract—Multi label classification has become a very important paradigm in the last few years because of the increasing domains that it can be applied to. Many researchers have developed many algorithms to solve the problem of multi label classification. Nevertheless, there are still some stuck problems that need to be investigated in depth. The aim of this paper is to provide researchers with a brief introduction to the problem of multi label classification, and introduce some of the most trending challenges.

Keywords—Challenges; Correlations among labels; Multi Label Classification

I. INTRODUCTION

Classification is an important data mining task that could be defined as the prediction of class label for unseen instances as accurate as possible [1]. Most researchers are interested in single label classification, where the goal is to learn from a set of instances that are associated with a unique class label from a set of disjoint class labels. If the total number of disjoint classes equals two, then the problem is called binary classification, otherwise, the problem is a multi-class classification. On the contrary of the previous problems, Multi-Label Classification (MLC) allows the examples (instances) to be associated with more than one class label at the same time. So, the goal of MLC is to learn from set of instances, where each instance belongs to one or more class labels at the same time [2].

MLC was motivated firstly by text categorization and medical diagnosis [3]. Recently, more researchers pay great attention toward the problem of MLC due to its importance in the real world problems [3]. In many domains where single label classification failed to solve the classification problem, MLC did. For example, single label classification may tag an email message as work or research project but not both, where the fact is, it could be tagged as both work and research project at the same time, which MLC does.

Nowadays, MLC is increasingly required by modern applications such as music categorization into emotions [4], semantic video annotation [5], direct marketing [6], protein function classification [7] and semantic scene classification [8].

MLC is - by its nature- a challengeable problem due to many reasons such as the huge number of labels combinations that grows exponentially, high dimensionality, unbalanced data, and many other reasons [9]. This paper aims to pin point to the most trending challenges in MLC based on extensive

study of many recent researches and articles. These challenges include but not limited to : exploiting correlations among labels from both types conditional and unconditional dependencies, features selection methods that are designed especially to handle multi label datasets, and having new stratification methods that are suitable to the nature of multi label datasets.

This paper is organized as follows. In the next section, we present some of the related work. In section 3, Trending challenges in the field of MLC are introduced. Finally, we conclude and present some of the future works.

II. RELATED WORK

According to [1], there are two approaches that are widely used to handle the problem of MLC: Problem Transformation Methods (PTM) and Algorithm Adaptation Methods (AAM). The former transforms the multi label problem into one or more single label classification problems, which could be solved using any single label classification algorithm [9]. The latter extends a single label algorithm to directly handle a multi label data.

A. Problem Transformation Methods

An algorithmic independent method that handle multi label datasets by transforming it to single label dataset or more as a preprocessing step, and then apply any single label classification algorithm. In fact, there are many transformation methods which could be grouped into two groups:

1) Simple Problem Transformation Methods

The most simple straightforward method is the *ignore* method, which ignores any multi label instances that exist in the dataset [9]. This naïve method is unacceptable, since it causes much of information loss. Other simple methods calculate the frequency of each label and then either select the *most frequent* label, *least frequent* label or *randomly* select any label as transformation criteria [10].

Transformation methods based on label frequency do not reflect any logic in solving the problem of MLC, and may cause different problems like increasing the complexity of the learning process when selecting the least frequent label or imbalance class distribution problem when selecting the most frequent label.

The last transformation method *copies* any multi label instance number of times equals to the number of labels it is associated to, with or without using a weight [11]. This method does not cause any information loss but it neglects the

important correlations among labels and may increase the complexity of the learning process through increasing the number of single label instances in the dataset.

2) Complex Problem Transformation Methods

Roughly speaking, most complex problem transformation methods are based on or inspired by two famous methods: *Binary Relevance (BR)* and *Label Powerset (LP)*[12]. Each algorithm represents different approach in handling the problem of MLC.

BR divides the multi label dataset into q different datasets with each dataset contains all the positive and negative instances for specific label [12]. It then trains q classifiers for all datasets and merge the prediction of all these classifiers to get the final predictions. BR may considered to be simple method with linear complexity with respect to the total number of labels and has the advantage of being executed in parallel, but suffers from many limitations such as : It neglects any correlations among labels, and considers labels to be mutual exclusive, which is totally not correct when handling the problem of MLC. Another limitation for BR is the complexity of the method in the case of huge number of labels [11].

On the contrary of BR, LP considers correlations among labels as it treats every unique combination in the dataset as single class in multi class classification problem. LP exactly transforms MLC problem into multi class problem, and then trains any single label classifier [12]. LP suffers from several drawback as the problem of imbalance class distribution, especially when the number of distinct label sets is high compared to the number of instances in the dataset. Also, LP is capable to predict only those combinations that appeared in the training phase [12].

Although BR and LP are suffering from several limitations, but they inspired many researchers to design many algorithms based on their concepts, or try to do some enhancements to those basic transformation methods through overcoming their limitations. For example *Classifier Chains (CC)* tries to enhance BR through taking label correlations into account by training q classifier that are connected with each other in such a way that the prediction of each classifier is being added to the dataset as new feature, which is used to predict new labels [10]. CC suffers from one drawback that is related to the order of the chain. Different orders give different predictions which may influence the performance and the accuracy of the classifier. This problem has been solved by randomly ordering the classifier chains in new method called *Ensemble of classifier chains (ECC)* [13].

LP by itself has been studied intensively by many researchers, due to its simplicity and its great advantage of taking label correlations into account. The intensive studies of LP result in many algorithms that are based on LP or an enhancement of LP such as The *Random k-labELsets method (RAkEL)* [14] which solved the problem of imbalance class distribution of LP especially when having large number of labels. RAkEL trains an ensemble of LP classifiers, where each classifier is assigned to a small subset of label combinations of size k. RAkEL has the ability to predict combinations that are not exist in the training dataset. The

bottle neck of RAkEL is to determine the optimal value for the combinations size (k); if k is large enough then it will suffer from the same shortcomings of LP, and if it is small enough then it will suffer from information loss especially in correlations among labels , in addition to having low accuracy and high complexity [12].

Pruned set (PS) is another transformation method that solved the problem of imbalance class distribution in LP by pruning instances that have frequency less than specific user defined threshold [13]. This technique reduces the high complexity of LP by considering only the important and frequent combinations of label sets. The price of this solution is to lose important information, and increase the probability of over fitting. An *Ensemble of Pruned Sets (EPS)* [13] enhanced the prediction of PS by considering the prediction of multiple classifiers obtaining by voting while increasing the complexity of the algorithm.

Different approach to solve the problem of MLC is based on Pairwise Methods. The Ranking by Pairwise Comparison (RPC) transformation method divides a dataset with q labels into $q(q-1)/2$ datasets for each pair of labels [15]. Then a binary classifier is trained for each dataset, and a final prediction is built based on counting the votes for each label. RPC was extended by adding a virtual label that has been used as split point between relevant and irrelevant labels. This transformation method is called *Calibrated Label Ranking (CLR)* [16].

B. Algorithm Adaptation Methods

The high efficiency of many algorithms in handling single label classification problems has inspired many researchers to adapt and enhance these algorithms to handle the problem of MLC. ML-C4.5 [17] adapted the popular algorithm C4.5 to handle multi label datasets. Two adaptations has been carried out: the first adaptation allowed the leaves to have multi labels, while the second adaptation was the modifying of the entropy definition in order to have enough information that determine to which classes an exact pattern belonged to.

Multi class Multi label Associative Classification (MMAC) is an algorithm that follows the concepts of Associative Classification (AC) [18]. Firstly, it transforms the multi label dataset into single label dataset using copy as problem transformation method. Then it trains single label associative classifier to predict a single label using if –then rules. Finally it merges the predictions of rules that have the same antecedent to form a rule with more than one label in the consequent of the rule. It is worth mentioning that all the datasets that have been used to evaluate MMAC are single label datasets and have never been tested against multi label datasets.

Rank-SVM is a multi-label ranking algorithm that is based on SVM ranking [19]. This algorithm aims to optimize the ranking loss, but suffer from not taking the important correlations among labels into account, and never been tested against datasets with huge number of labels where it is expected to show very low performance.

Several algorithms are based on the popular K -Nearest Neighbors algorithm (KNN) that is based on the technique of

lazy learning. *ML-KNN* [20] is an example of these algorithms. All of these algorithms share the same first step with KNN (retrieving the k nearest example) and distinguish themselves on the aggregation of the label sets of these examples.

Back Propagation for Multi-Label Learning (BP-MLL) is an adaptation of the traditional feed-forward neural networks. It optimizes an error function that is similar to the ranking loss [21]. *Multilabel Multiclass Perceptron (MMP)* is also another algorithm that uses neural network to handle the problem of MLC [22]. It uses one perceptron for each label as in BR, and the final prediction is calculated using the inner products. MMP is an efficient algorithm especially for large datasets with many labels [9]. Figure 1 depicts a brief taxonomy of MLL methods.

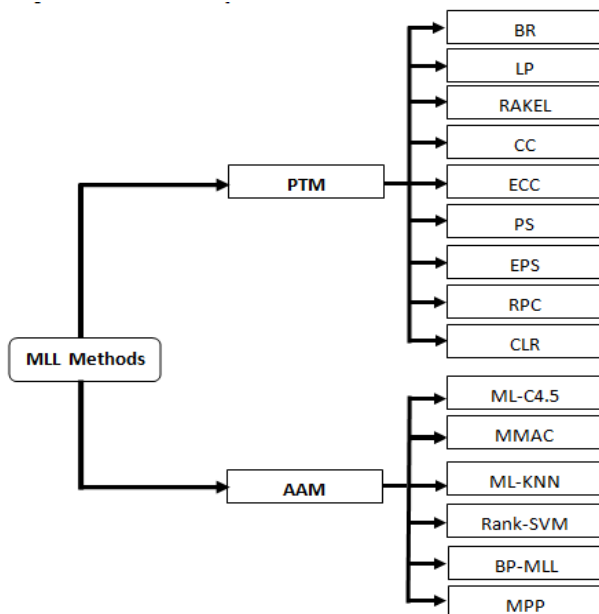


Fig. 1. MLL Methods Taxonomy

In addition to the previous way of categorizing MLC algorithms, there is another interesting way of categorization, which is based on the degree of correlations among labels that has been considered in the algorithms. Based on that, we can distinguish three types of MLC algorithms as shown in Table 1.

TABLE I. CATEGORIZING MLC ALGORITHMS ACCORDING TO THE DEGREE OF CORRELATIONS AMONG LABELS

Type	Characteristics	Examples
First Order	<ul style="list-style-type: none"> The task of MLL considers each label separately. Ignore correlations with other labels. Simple and efficient. Its results are usually suboptimal because of ignoring correlations among labels. 	BR ML-KNN ML-C4.5
Second Order	<ul style="list-style-type: none"> The task of MLL considers the pairwise relationships between labels like classifying labels into relevant and irrelevant labels. Labels correlations are exploited to a limited degree. 	RPC CLR BP-MLL
High Order	<ul style="list-style-type: none"> The task of MLL considers the influence of every label on all other labels and finds a high order correlation among all labels or among random subsets of labels. Demands more computations. 	LP PS, EPS CC, ECC RAKEL

III. TRENDING CHALLENGES IN MLC

A. Exploiting correlations among labels to facilitate multi label learning

Multi label datasets usually have many features that do not exist in single label datasets such as high dimensionality, unbalanced data and the exponential growth of combinations of labels. These features, in addition to the core nature of multi label data; that is based on dependencies among labels, lead to an urgent need to exploit correlations among labels, in order to have additional knowledge that helps in facilitating the learning process [9]. Many algorithms [1] [11] [13] [14] [25] have tried to exploit the correlations among labels to enhance the accuracy of the multi label classifier, but most of these algorithms suffer from high complexity in the learning process [10]. Based on that, the true challenge is to exploit high order labels correlations locally and maintain a linear complexity at the same time [2].

B. Proposing new problem transformation methods based on correlations among labels

Transforming multi label datasets into one single label

dataset or more is a basic step for most multi label algorithms that follow the approach of PTM. The selection of the transformation criteria is usually based on the frequency of a label. Some examples of transformation criteria are: Most Frequent Label (MFL), Least Frequent Label (LFL) or simply by selecting any label randomly [10] [11]. Since multi label datasets is based on a basic assumption which is; labels are not mutually exclusive, and they do have correlations and dependencies among them [9], it would make more sense if the transformation criteria will be based on correlations among labels [1].

C. Proposing new features selection methods that are suitable for the nature of multi label datasets

Features selection is a basic step in many data mining tasks that aims to define the relevant features in the dataset and eliminate irrelevant ones [23]. Labels in single classification are considered to be mutually exclusive, which is not completely true in MLC, and based on that, there is an urgent need to use suitable features selection methods that are designed especially to handle multi label data, and it would be even better if these features selection methods take into account the correlations among labels [23].

D. Hierarchical Multi Label Classification (H-MLC)

In some datasets, labels could be organized in a hierarchical way like "Yeast" dataset where labels are correlated to each other in a hierarchical way. Two types of structures could be used to represent the hierarchical nature of the multi label datasets: a tree or a Directed Acyclic Graph (DAG). In a tree structure a child have one and only one parent, while in DAG a child may have more than one parent at the same time [24]. It would be a nice and promising idea to design an algorithm that manages label correlations using a hierarchical structure with minimum complexity in the learning process. Interesting approaches could be found in [24-25].

E. Proposing new stratification methods that are suitable for the nature of the multi label datasets

Stratification is a techniques that is used in sampling, and take into account the existence of all disjoint groups in the target population, so the chosen sample reflects the whole population in a representative way. In single label classification, stratification is easy since every instance is associated with only one label, and labels are mutually exclusive. Whereas in MLC, the task becomes more and more complicated as instances are usually associated with more than one label, and labels are not mutually exclusive. In [26] two stratification methods were proposed in the context of MLC, but much effort should be done to solve the problem of stratification in the field of MLC.

F. High dimensionality of label space in multi label datasets

High dimensionality is one of the most challengeable issue in MLC, and perhaps the main challenge. In MLC most labels are associated with a few number of training instances in comparison to the total number of instances in the dataset. This situation is similar to the problem of imbalance class distribution in single label classification. And the situation

will be worse when the number of labels in the dataset is very high (more than 100 labels). There is an urgent need to a simple yet fast algorithm that is capable of handling large number of labels that are associated with a few numbers of instances and maintaining a linear complexity at the same time. Example of such an algorithm could be found in [27] where the authors proposed new algorithm HOMER construct a hierarchy of ML classifiers where each classifier considers small subset of labels. This algorithm shows fair performance and good accuracy in only two datasets, and compared only against BR. HOMER needs to be investigated more in depth using larger datasets with a fair evaluation against other algorithms than BR.

IV. CONCLUSION AND FUTURE WORK

In this paper, we have introduced a brief introduction to MLC. Also, we survey some of the most well-known algorithms in the field of MLC. The main contribution of this paper is introducing some of the trending challenges in the domain of MLC. In the near future, we aim to investigate in depth about these trending challenges and propose new methods to exploit correlations among labels. Also, we are now evaluating new transformation methods that are based on the correlations among labels.

ACKNOWLEDGMENTS

The first author would like to thank his family, especially his parent, for their continuous cheer on, patience and empathy. Deep thank to my great friends: Naela Alsalmam and Hazem Nu'man.

REFERENCES

- [1] Raed Alazaidah, Fadi Thabtab and Qasem Al-Radaideh, "A Multi-Label Classification Approach Based on Correlations Among Labels" International Journal of Advanced Computer Science and Applications(IJACSA), 6(2), 2015. <http://dx.doi.org/10.14569/IJACSA.2015.060208>.
- [2] Giorgio Corani , Mauro Scanagatta, Air pollution prediction via multi-label classification, Environmental Modelling & Software, Volume 80, June 2016, Pages 259-264.
- [3] G. Tsoumakas, A. Papadopoulos, W. Qian, S. Vologiannidis, A. D'yakonov, A. Puurula, J. Read, J. Svec, and S. Semenov, "WISE 2014 challenge: Multi-label classification of print media articles to topics," in Web Information Systems Engineering - WISE 2014, Proceedings, Part II, 2014, pp. 541–548.
- [4] Aiyasha Ma, Ishwar Sethi, and Nilesh Patel. 2009. Multimedia content tagging using multilabel decisiontree. In Proceedings of the 2009 11th IEEE International Symposium on Multimedia (ISM'09). 606–611.
- [5] Jingdong Wang, Yinghai Zhao, Xiuqing Wu, and Xian-Sheng Hua. 2010. A transductive multi-label learning approach for video concept detection. Pattern Recognition 44 (2010), 2274–2286.
- [6] Yi Zhang, Samuel Burer, and W. Nick Street. 2006. Ensemble pruning via semi-definite programming. Journal of Machine Learning Research 7 (2006), 1315–1338.
- [7] Kuo-Chen Chou, Zhi-Cheng Wu, and Xuan Xiao. 2011. iLoc-Euk: A multi-label classifier for predicting the subcellular localization of singleplex and multiplex eukaryotic proteins. PLoS ONE 6, 3 (2011), e18258.
- [8] Muhammad A. Tahir, Josef Kittler, Fei Yan, and Krystian Mikolajczyk. 2009. Kernel discriminant analysis using triangular kernel for semantic scene classification. In Proceedings of the 7th International Workshop, (CBMI'09). IEEE, Los Alamitos, CA, 1–6.
- [9] E. Gibaja and S. Ventura. A tutorial on multilabel learning. ACM Computing Surveys, 47(3):Article 52, 2015.

- [10] M.-L. Zhang and Z.-H. Zhou. A review on multi-label learning algorithms. *IEEE Transactions on Knowledge and Data Engineering*, 26(8):1819–1837, 2014.
- [11] Min L. Zhang and Kun Zhang. 2010. Multi-label learning by exploiting label dependency. In Proceedings of the 16th ACM SIGKDD International Conference on Knowledge Discovery and Data Mining (KDD'10). ACM, New York, NY, 999–1008.
- [12] Jesse Read. 2011. Advances in Multi-label Classification. Retrieved from <http://users.ics.aalto.fi/jesse/talks/Charla-Malaga.pdf>.
- [13] Jesse Read. 2008. A pruned problem transformation method for multi-label classification. In Proceedings of the NZ Computer Science Research Student Conference.
- [14] Grigoris Tsoumakas, Ioannis Katakis, and Ioannis Vlahavas. 2010. Random k-labelsets for multi-label classification. *IEEE Transactions on Knowledge and Data Engineering* 23, 7 (2010), 1079–1089.
- [15] Eyke H. ullermeier, Johannes F. urnkranz, Weiwei Cheng, and Klaus Brinker. 2008. Label ranking by learning pairwise preferences. *Artificial Intelligence* 172 (2008), 1897–1916.
- [16] Klaus Brinker, Johannes F. urnkranz, and Eyke H. ullermeier. 2006. A unified model for multilabel classification and ranking. In Proceedings of the 17th European Conference on Artificial Intelligence. IOS Press, Amsterdam, The Netherlands, 489–493.
- [17] Amanda Clare and Ross D. King. 2001. Knowledge discovery in multi-label phenotype data. In Proceedings of the 5th European Conference on Principles of Data Mining and Knowledge Discovery (PKDD'01) (Lecture Notes in Computer Science), Vol. 2168. 42–53.
- [18] Fadi A. Thabtah, Peter Cowling, and Yong hong Peng. 2004. MMAC: A new multi-class, multi-label associative classification approach. In Proceedings of the 4th IEEE International Conference on Data Mining (ICDM'04). 217–224.
- [19] Aiwen Jiang, Chunheng Wang, and Yuanping Zhu. 2008. Calibrated rank-SVM for multi-label image categorization. In Proceedings of the IEEE International Joint Conference on Neural Networks (IJCNN'08). 1450–1455.
- [20] Min-Ling Zhang and Zhi-Hua Zhou. 2005. A k-nearest neighbor based algorithm for multi-label classification. In Proceedings of the IEEE International Conference on Granular Computing (GrC'05). 718–721.
- [21] Min-Ling Zhang and Zhi-Hua Zhou. 2006. Multilabel neural networks with applications to functional genomics and text categorization. *IEEE Transactions on Knowledge and Data Engineering* 18, 10 (2006), 1338–1351.
- [22] Koby Crammer and Yoram Singer. 2003. A family of additive online algorithms for category ranking. *Journal of Machine Learning Research* 3 (March 2003), 1025–1058.
- [23] Suping Xu, Xibei Yang, Hualong Yu, Dong-Jun Yu, Jingyu Yang, Eric C.C. Tsang. Multi-label learning with label-specific feature reduction. *Knowledge-Based Systems*. Volume 104, 15 July 2016, Pages 52–61.
- [24] Celine Vens, Jan Struyf, Leander Schietgat, Sašo Džeroski, and Hendrik Blockeel. 2008. Decision trees for hierarchical multi-label classification. *Machine Learning* 73, 2, 185–214.
- [25] Jaedong Lee, Heera Kim, Noo-ri Kim, Jee-hyong Lee. An Approach for multi-label classification by directed acyclic graph with label correlation maximization. *Information Sciences*. 2016.
- [26] Sechidis, K., Tsoumakas, G., & Vlahavas, I. (2011). On the stratification of multi-label data. *Machine Learning and Knowledge Discovery in Databases*, 145–158.
- [27] Grigoris Tsoumakas, Ioannis Katakis, and Ioannis Vlahavas. 2008. Effective and efficient multilabel classification in domains with large number of labels. In Proceedings of the ECML/PKDD 2008 Workshop on Mining Multidimensional Data (MMD'08).

AAODV (Aggrandized Ad Hoc on Demand Vector): A Detection and Prevention Technique for Manets

Abdulaziz Alidaej

College of Computer Engineering & Sciences
Prince Sattam Bin Abdulaziz University

Tariq Ahamad

College of Computer Engineering & Sciences
Prince Sattam Bin Abdulaziz University

Abstract—Security is a major concern that needs to be addressed in Mobile Adhoc Networks because of its vulnerable feature that includes infrastructureless environment, dynamic topology, and randomized node movement making MANETs prone to various network attacks. Synergetic attacks have raucous effects on MANETs as compared to particular single attack. Various algorithms and protocols have been designed and developed to meet the increasing demand of MANET security but there is still a room for improvement in order to make it more reliable and hassle-free communication. An AggrandizedAODV is presented in this paper to detect and prevent various synergistic and non-synergistic attacks.

Keywords—MANET; AODV; Grayhole; Blackhole

I. INTRODUCTION

MANETs or Mobile Ad hoc Networks are arrangement of non-stationary nodes communicating with each other without any prevailing network infrastructure hence nodes are autonomous i.e. each node acts as source, destination and as router themselves as per need [1]. Nodes or devices enjoy the freedom to move in any direction any time, these nodes inhibit self-configuring or adaptive, self-healing, peer to peer characteristics made possible with introduction of routable network capabilities on the top of Link layer [2]. MANETs flexible mode of operation, least communication infrastructure requirement, adaptability to continually changing scenarios or topologies, operability in low computing capacity, connectivity in scarce bandwidth and communication without any centrally controlled entity provide them special significance in the conditions where making network infrastructure is infeasible or impossible [3].

Because of their special characteristics MANETs have different set of communication protocols especially suited for their needs. Broadly MANET routing protocols can be classified into three categories viz. Reactive Protocols, Proactive Protocols and Hybrid Protocols. Reactive Protocols do not initiate route discovery on themselves unless requested by any node to do so [4]. Their more common name ‘On-Demand’ originate from fact they find route to certain destination node when demanded, Hence don’t consume precious bandwidth of MANETs, These protocol start route discovery with flooding RREQ, destined node or any intermediate node having route information for requested node can send back route information with RREP. Once route becomes active route node keep track of changes, if any intermediate or destination route moves or goes offline

subsequently a RERR is generated to inform neighboring node about link break [5]. Most prominent protocols of this category are Dynamic Source Routing (DSR) and Ad hoc On Demand Vector (AODV) protocols.

Another way around for routing is Proactive Protocols which alike their wired counterparts maintain a routing table and update it regularly for any network changes. Every single node is known to every other node of the network i.e. each node in network has route information about other nodes of the network. In case of any change in network topology all nodes update their routing table to reflect this change [6]. Optimized Link State Routing (OLSR) protocol falls under this category.

As usual, all of these protocols have pros and cons associated with them which vary on routing overheads, throughput and memory overheads etc. none of them is ideal for all situation, although various variation of them have been proposed, researched and tested still wide scope of improvement in detection and defense of MANETs against wide variety of attacks exists. Each protocol has its own issues associated with them.

A compromising solution obtained with combining strengths of these two categories is Hybrid Protocols. MANET is divided into parts or zones, portion of which follows reactive protocols and portion is maintained by proactive protocols [7]. An example of which is Zone Routing Protocol (ZRP) it incorporates proactive protocols for route setup inside zones whereas utilizes reactive protocols for inter zones route setup. A node may have overlapping zones of different routing pattern [8].

Irrespective of routing protocol used security remained a prime concern of MANETs. MANETs are highly prone to a series of attacks exploiting range of features inherent with MANETs, from flexibility to enter and exit from network to scalability attacker had exploited each characteristics of network which distinguish it as MANET [9]. Out of various attack our study is focused upon DoS attacked camouflaged as Black hole attack where a node deliberately drops all packets and keep on sending route message lucrative enough as shortest route in some cases, coordinated black hole attack where more than one compromised node work in tandem to launch Black hole attack and gray hole as special case of black hole attacks where node selectively drops some packets and forward some packets making it more difficult to detect and isolate [10].

II. RELATED WORK

A number of researchers have studied Threat of collaborative attacks on MANETs in recent past, defending mechanism; preventive approaches have been taken on extensively.

In [11] each node incorporated a DRI or Data Routing Table and methods to cross validate it for detecting cooperative black hole nodes in the network. This mechanism was embedded into modified AODV routing protocol. Experimentally it was found this method out performs other proposed solutions.

In [12] author demonstrates some of the frequent attack mechanism and eventually analyses possible collaboration among various attacking entities. Author further tries to evaluate various machine learning techniques viz. DSP (Digital Signal Processing) and ANN (Artificial Neural Networks) in detection and prevention of collaborative attacks in MANETs. Their analysis showed collaborative attack in wireless network is much more devastating and crippling effects than wired one. They also experimentally insinuated effectiveness of the model framed to minimize collaborative attack and immunizing the mobile ad hoc networks.

In [13] the problem of collaborative attack with in from the network was discussed where critical data inside the Information System is at risk from two or more malicious nodes working in some accord. In this proposed approach, authors begins with mutual relation of different illegal information flow diagrams and components of information systems. Later on, he classified and summarized data access patterns on the basis of mutual-access-record's probability value and transaction distance of data items, ultimately proposed an algorithm for early detection of collaborative insider attacks.

In [14] authors have carried out a detailed analysis of MANETs under single and collaborative Black Hole Attacks and based on their analytical finding proposed mechanism to prevent attack by rerouting network traffic to avoid Black Hole nodes. Proposed MANETs utilizes AODV protocol for its robust features, proposed mechanism rely on transmitting only confirmation packets which have been verified by the destination for the presence of black hole in the GAODV routing Protocol.

In [15] the author forwarded a theory that balanced collaborative attackers can eventually bypass security measures imposed by trusted node assistance methods which are readily used in available security setups. Based upon their

theoretical findings, Balanced Collaborative attackers can be seen with highest similarity ratios. Authors forwarded an algorithm to find anomalous behavior of nodes and early detection of balanced collaborative attackers. The only information required for knowledge of reporting channel is bit error probability of secondary users. Simulation results depict efficiency of proposed technique in identification of balanced collaborative attackers. Paper proposes a novel technique for detection and subsequently prevention of collaborative attacks in MANETs focused on detecting and isolating malicious nodes through bridge data items.

III. PROPOSED AAODV (AGGRANDIZED AD HOC ON DEMAND VECTOR)

Two interdependent control packets can be used to enhance and improve the existing AODV.; SRRD_REQ and SRRD REP. their function is same as that of RREQ and RREP but more reliable and with more steps. SRRD_REQ message along with associated SRRD_ID are sent by the source node as destination node's DSN over the MANET on equal continuous intervals and after evaluating the authentic SRRD_ID, SRRD REP packet is sent as response to the SRRD_REQ node by the destination node and generates SRRD REP only to notify that no other node is needed other than destination node and can generate SRRD REP. in addition to this, threshold vale (TV) and Reliability list are added to routing table as new fields. Addition of these two fields doesn't mean that there is going to be any change in the AAODV routing table as compared to AODV routing table but just a couple of more fields.

The reliable list field contains the list of trust worthy and reliable nodes and TV fields contains the DSN average of trustworthy nodes. Following are the two major steps that are used in route discovery.

AAODV Algorithm

The AAODV to detect and defend MANET from attacks is explained in two phases.

Phase I.

Whenever a MANET node wants to communicate with other nodes in the nwtnwork the first thing to do is to check if an updated route is present in the routing table. Forward the data packet in case there is a reliable route otherwise start the route discovery procedure that involves sending SRRD_REQ by the source node to their 1-hop nodes with associated SRRD_ID to create a new route. Following are the steps followed by the immediate node after receiving as SRRD_REQ.

1) Send reply to the requesting node and SRRD_REQ if an updated route is present otherwise forward this request to the first hop nodes.

2) Set up a reverse route discovery for the REP messages.

3) If the node is possess an outdated routing table entry as destination it refreshes it and if RL contains an entry for destination node then erase and update the entry.

4) If there is no entry for the source in the routing table then using RPT create a new entry and in case of various available reliable routes, arrange them in the order of their hop count. After going through all these steps compare the top reliable routes of first node on the basis of DSN having least hop count with TV. In case its value is higher than the route nodes DSNs average then discard this route as it is a malicious node and keep checking until reliable route is found with less DSN value as compared to TV.

5) The source nodes new entry is selected as most reliable route having least hop counts involves hop count, SRRD_REQ sequence number and address of the node which responded first to the broadcasted request packet acts as next hop.

After receiving the SRRD_REQ from the source, the destination node uses reverse path to send SRRD REP. sometimes an intermediate node with a reliable updated route the destination also sends SRRD REP. thus during RRT every node must perform the following tasks after receiving the SRRD REP.

1) If the node contains an outdated route entry for the destination node then it must update the entry otherwise creates a new routing table entry.

2) IP address of the source node must be added to the entry and can be copied from SRRD REP packets originators field. Forward_Data_Packet_Counter and SRRD_ID both are assigned zero and forward it to next node on reverse path.

In normal AODV route discovery procedure is executed when source node receives RREP but in AAODV one more procedure gets invoked from this stage onwards.

Phase I Code.

Input: SRRD_REQ(), reqNode, destNode, relNodeList[],
hopCount, maxHopCount, routeDiscovery(), selRoute(),
sendPckt()

Begin

```

SRRD_REQ()
if (reqNode ∈ relNodeList[]) True then
    selRoute()
    sendPckt()
    stop
else
    routeDiscovery()

```

```

if (SRRD_REQ ← destNode) False
    if (hopCount ≥ maxHopCount) True
        stop
    else
        SRRD_REQ()
    end if
else
    routeForm()
end if
end

```

Phase II

The source floods route requests towards every neighbor node and then sends SRRD packets to all those who responded with RREP (route replies). Following are the steps for that every nodes that received SRRD packets.

1) If routing table contains an entry for reverse path, it sets or initializes SRRD_ID by imitating that from SRRD otherwise a new entry is created by the node.

2) Will send packets to that every node which replied with SRRD REP earlier.

3) Every node must have an entry for the destination that is on the path of SRRD.

The SRRD REP is sent to hop node that responded first with an SRRD packet and ignores the rest after receiving SRRD packet by the destination. Reliability value is set to one (1) in the SRRD REP packet by the destination. During RPT every first hop node receives SRRD REP once only (SRRD_ID=1) for the first time and in SRRD REP assigns 0 to Forward_Data_Packet_Counter and using reverse path forwards it to next node and a unique SRRD REP is received by the source and a reliable route is discovered and no node can generate any SRRD REP at all.

Phase II Code

Input: relRoute(), sortRoute(),
 RevrsTrace(), hopCount, sendPckt(),
 rejectRoute

Begin

```

relRoute()

sortRoute(hopCount)

RevrsTrace(source ← dest)
    if (DSN > TV) True then    ▶ for first
        node at each intermediate node
            rejectRoute ← True
            stop
    else
        routeDiscovery()

```

```

else                                sendPckt()

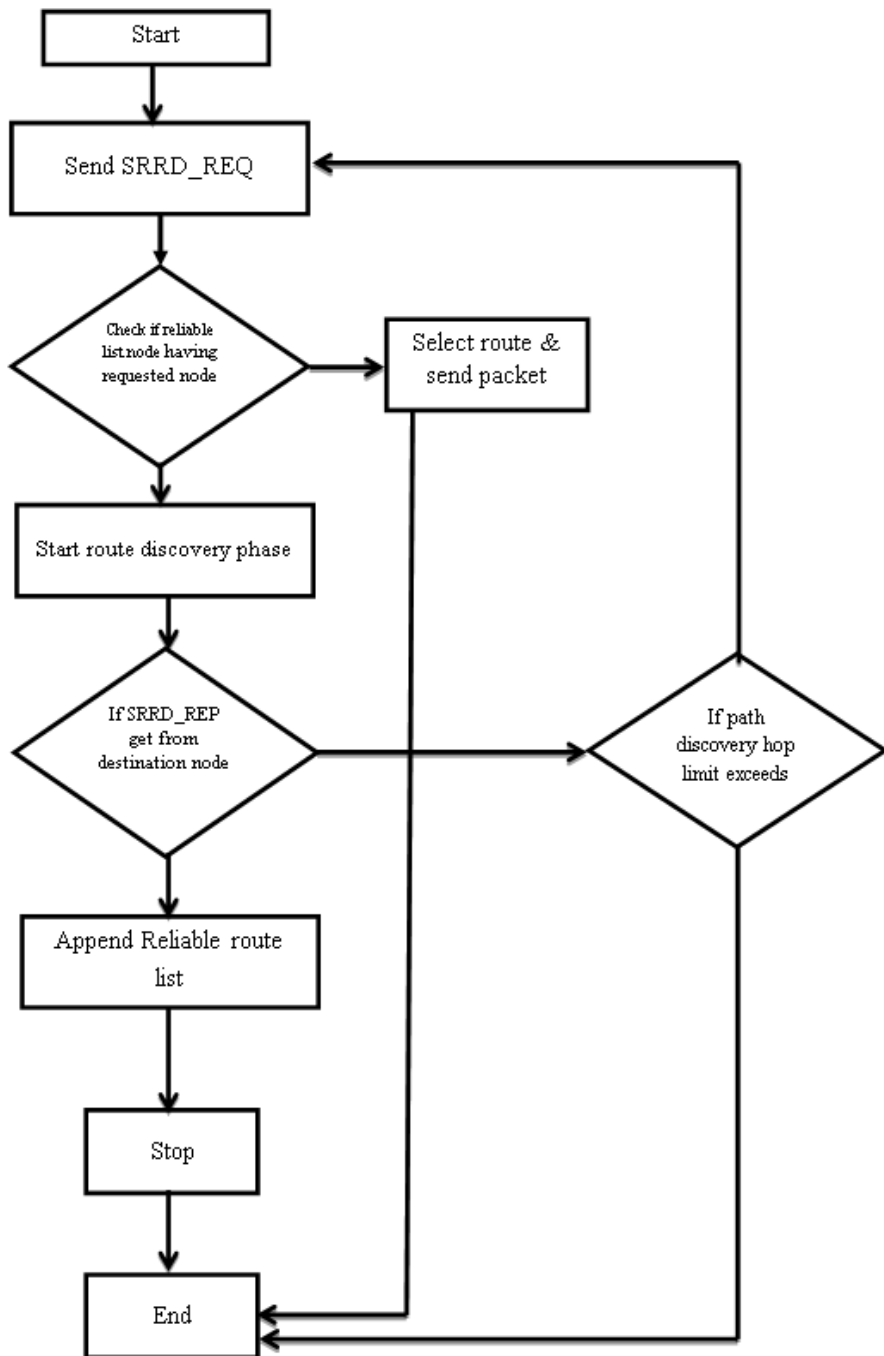
Procedure selRoute(minHop)          end if

Procedure Update(route &relList)    end

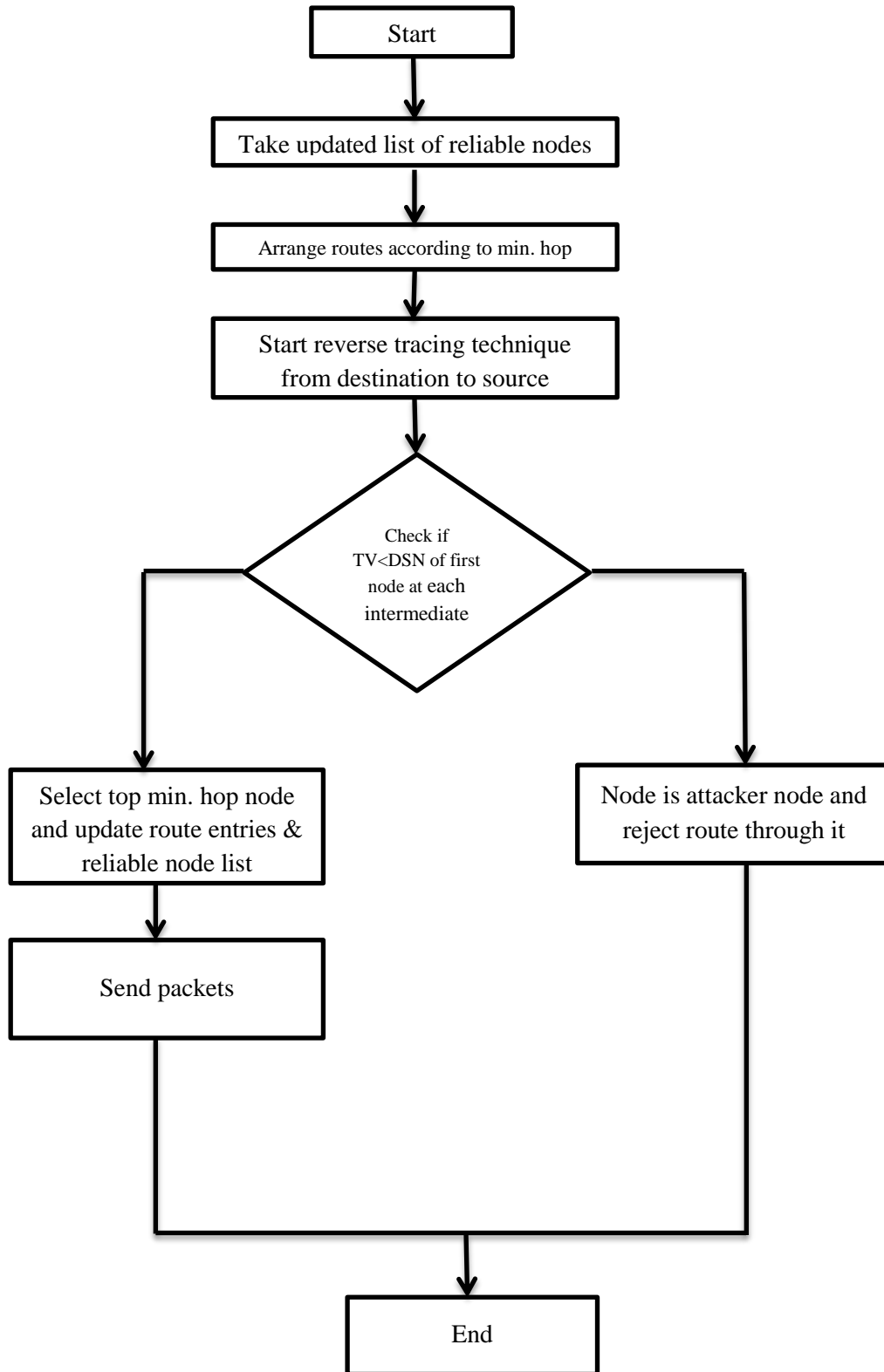

```

Flowchart of AAODV

PHASE 1



Flowchart describing Phase 1 of AAODV



PHASE II

Flowchart describing Phase 2 of AADOV

Simulation and Result

A MANET scenario is designed for the simulation and predefined parameters of the simulator and the necessary attributes of the nodes are configured. We have used NS2 for

simulation in this network model. The complete network model is designed using some values and they will be crucial in providing us with more accurate simulation results as compared to results before this one. Following is the table containing parameters and their values used for simulation.

TABLE I. PARAMETER AND INITIAL VALUES OF THE EXPERIMENT

Parameter	Value
Total Number of Mobile Nodes	25
Total number of Static nodes	4
Total number of Base Station nodes	1
Total number of Black hole nodes	3
Total number of Gray hole nodes	2
Routing Protocol	AODV
Attack Protocols	Black hole AODV, Gray hole AODV
Simulation Time	90 Seconds
Data Rate	10KBPS
Regular Msg Size	512 b
Irregular Msg Size	1024 b

Traffic	CBR
---------	-----

A network with 25 nodes is generated using NS2 allowing some nodes to act as black hole and gray hole like a normal scenario in AODV. Source and destination connection in this MANET is done by UDP and constant packet traffic is generated through the UDP using CBR application. CBR packet size and data rate is set to 512 bytes and 1024 bytes respectively. And this same procedure with same settings, values, connection methodology and traffic generation is used for AAODV.

In figure 1, we observed thoroughly that the normal AODV got affected radically by blackhole and grayhole nodes and gets increased when the number of malicious nodes increases. This acknowledges the fact there is not enough secure technique to detect and prevent blackhole attacks or grayhole attacks using normal AODV. Our proposed AAODV provided better and higher packet delivery ratio as compared to normal AODV in all the conditions (like no attack condition, with black hole only, with blackhole and gray hole together). We also set the number of malicious node in the MANET $\approx 50\%$, AAODV still provided us better results as shown in the figure 1 in detecting and preventing from malicious nodes successfully even after we kept the packet delivery ration more than 75%.

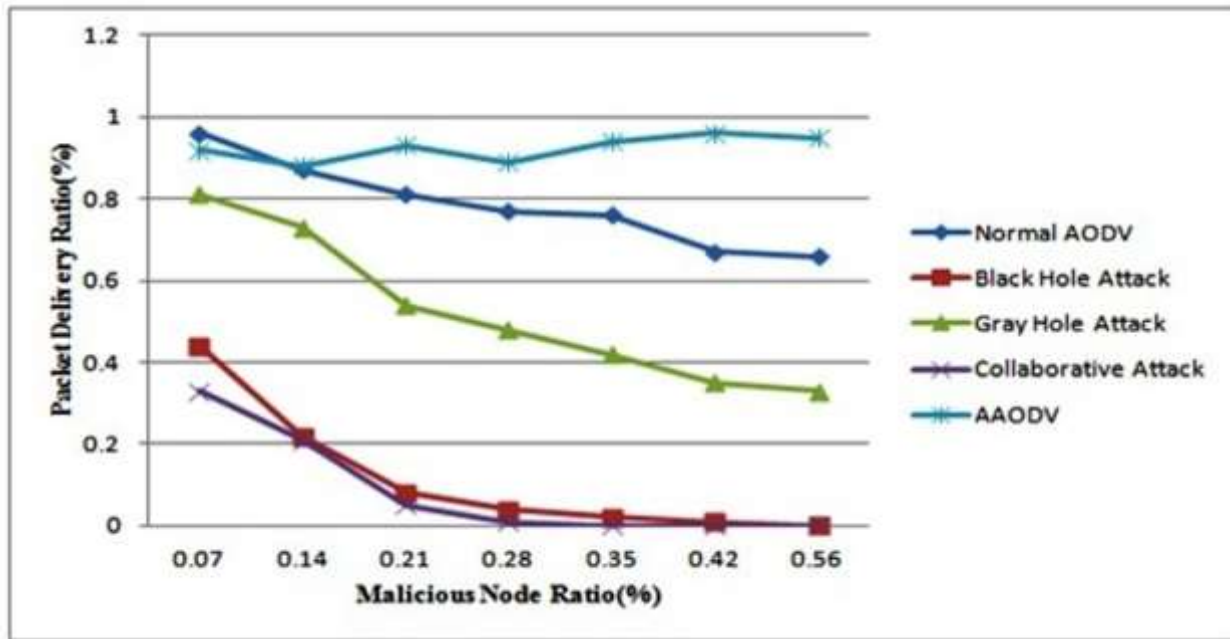


Fig. 1. Packet Delivery Ration of AODV and AAODV in different situations

In figure 2, Keeping malicious node ratio as benchmark, we did a thorough study of AODV's and AAODV's routing overhead and gained result proved that when the number of black hole and Grayhole nodes is increased the proposed AAODV produces better routing overhead AODV. Thus

proving the fact that the existing normal AODV doesn't possess a safe and reliable scheme to detect and defend the Blackhole and gray hole attacks. While the suggested AAODV proves better than the existing one.

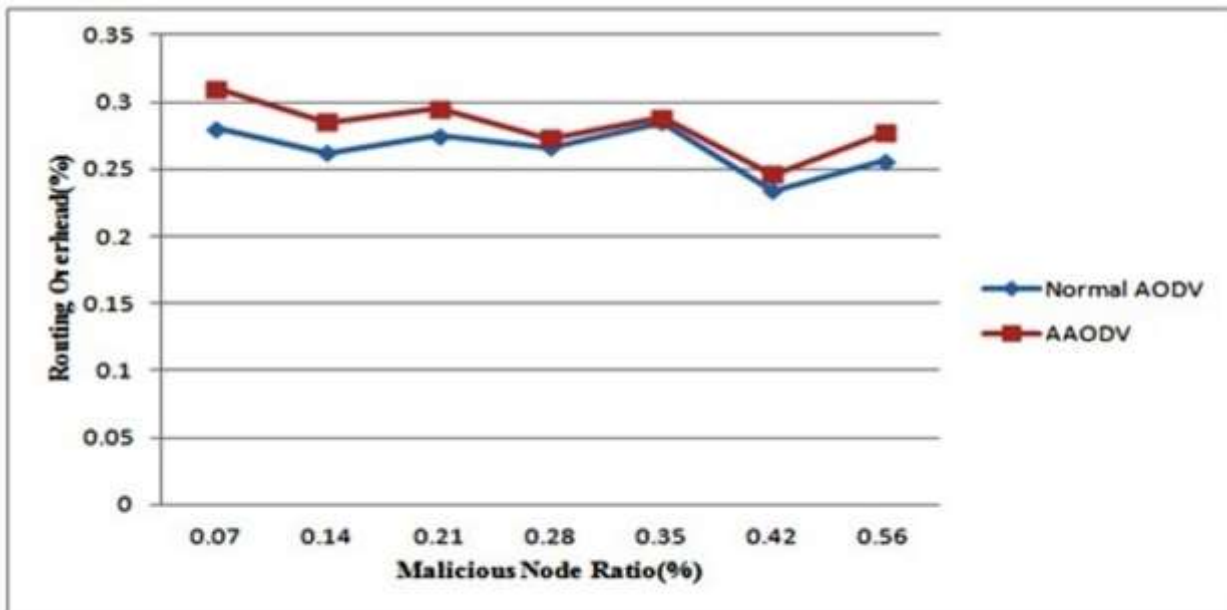


Fig. 2. Routing Overhead of AAODV and AODV

In figure 3, Average end-to-end delay of AAODV and AODV is used to generate the result putting MNR as measurement parameter. Output result graph shows that

proposed AAODV attains better end-to-end delay average than the existing AODV. The result graph also shows that AAODV requires extra time to identify the malicious nodes.

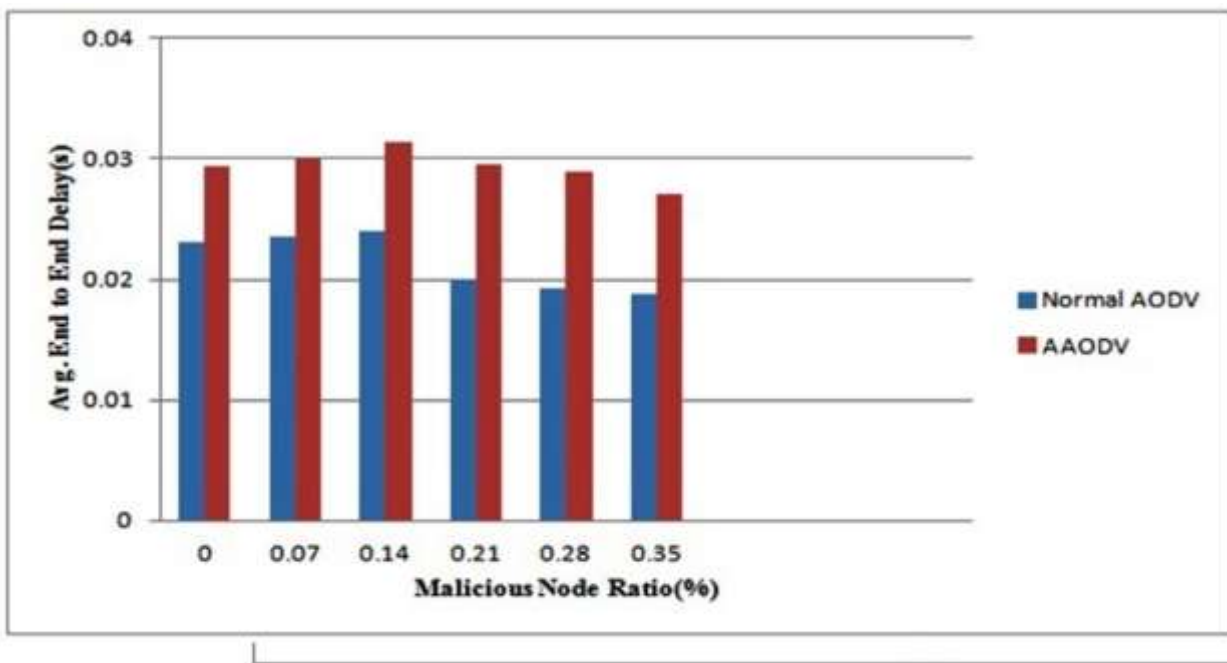


Fig. 3. Average of end-to-end delay in AODV and AAODV

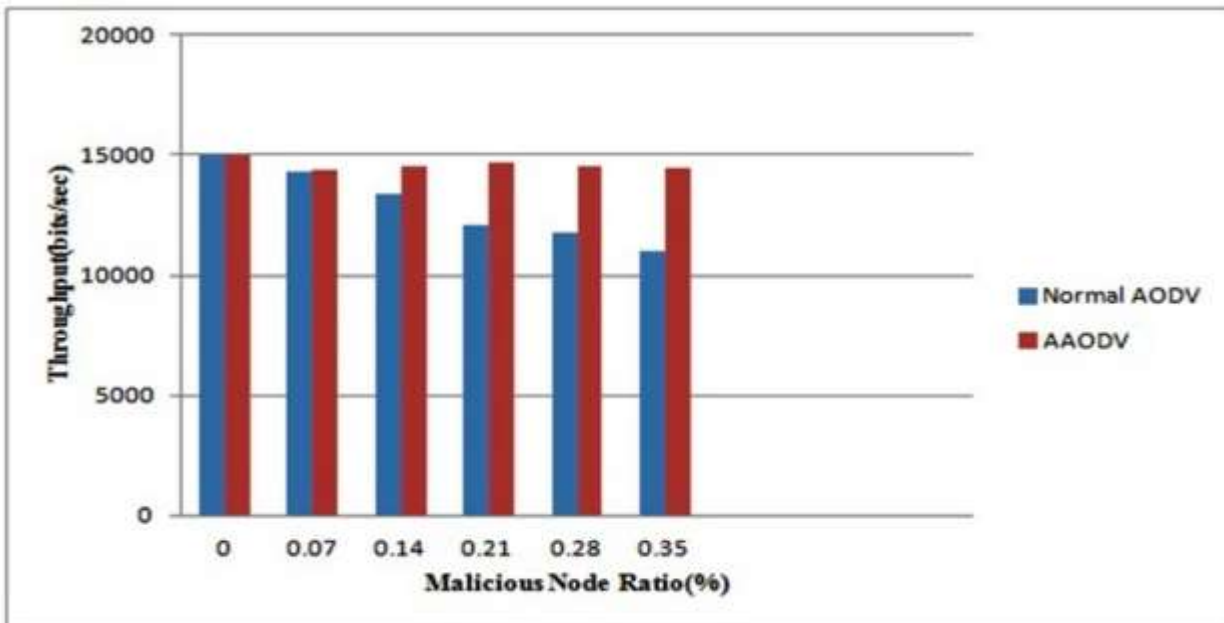


Fig. 4. Throughput of AODV and AAODV

In figure 4, after analyzing the throughput of suggested AAODV and the existing AODV putting MNR as measuring parameter, the result proves that the existing AODV got more Blackhole and Grayhole attacks as compared to AAODV. During a scenario in which the number of Grayhole and Blackhole nodes in the MANET is higher ($\geq 40\%$) the proposed AAODV can still identify the malicious nodes even if the throughput is higher than 14000 b/s.

IV. CONCLUSION

In this research article , we have proposed a AAODV (Aggrandized Ad Hoc On demand Vector) to detect and defend MANETs from malicious nodes during synergistic and single attacks like black hole and gray hole attacks. The proposed AAODV has proven to produce better results as compared to existing AODV protocol as the experimental simulation output graphs of packet deliver ratio, throughput and routing overhead shows improved results. The proposed technique is best appropriate for a MANET up to 50 nodes for detection and prevention from Grayhole attacks and black hole attacks. A minor routing overhead in suggested AAODV that averts the complete efficient application of MANET that is not the case with AODV. This increase in the size of MANET will increase the routing overhead. In future, the simulation can be enhanced to improve this AAODV to overcome this and to tackle with other amalgamation of attacks that can work together to target the MANET.

ACKNOWLEDGEMENT

This research was funded and conducted at Prince Sattam bin Abdulaziz University, Alkharj, Saudi Arabia during the academic year 2016/2017 under research number 2016/01/5693.

REFERENCES

- [1] Ahamad T, Aljumah A. "Detection and Defense Mechanism against DDoS in MANET", Indian Journal of Science and Technology. 2015 Dec Vol 8(33).
- [2] Aljumah A, " Detecting Distributed Denial Of Service (Ddos) Attack Using TTLv Constraint In Mobile Adhoc Networks (MANET) ", Science Internationals, 2015 Dec Vol 27(6),5037-5040.
- [3] Ahamad T, Aljumah A. , "Ad Hoc Network & Black Hole - Threat and Solution". American Journal of Scientific Research , Issue 104 , Nov, 2014.
- [4] Uddin M, Alsaqour R, Abdelhaq M. Intrusion detection system to detect DDoS attack in gnutella hybrid P2P Network. Indian Journal of Science and Technology. 2013 Feb; 6(2):71–83.
- [5] M. Rmayti, Y. Begriche, R. Khatoun, L. Khoukhi and D. Gaiti, "Denial of Service (DoS) attacks detection in MANETs through statistical models," 2014 Global Information Infrastructure and Networking Symposium (GIIS), Montreal, QC, 2014, pp. 1-3. doi: 10.1109/GIIS.2014.6934261
- [6] Tsou PC, Chang JM, Lin YH, Chao HC, Chen JL. Developing a BDSR scheme to avoid black hole attack based on proactive and reactive architecture in MANETs. 13th International Conference on Advanced Communication Technology: Seoul; 2011 Feb 13-16. p. 755–60.
- [7] Baadache A, Belmehdi A. Avoiding black hole and cooperative black hole attacks in Wireless Ad hoc Networks, International Journal of Computer Science and Information Security. 2010; 7(1):10–6.
- [8] Arunmozhi S.A., Venkataramani Y."A Flow Monitoring Scheme to Defend Reduction-of- Quality (RoQ) Attacks in Mobile Ad-hoc Networks", Information Security Journal: A Global Perspective, Vol.19, No.5, 2010, pp.263- 272.
- [9] Hyojin K, Ramachandra B. C., JooSeok S,"Novel Defense Mechanism against Data Flooding Attacks in Wireless Ad Hoc Networks", IEEE Transactions on Consumer Electronics, Vol. 56, No. 2, May 2010, pp. 579-582.
- [10] Mistry N, Jinwala D. C., Zaveri M,"Improving AODV Protocol against Blackhole Attacks", Proceedings of the International Multiconference of Engineers and Computer Scientist, Hong Kong, Vol. II, 2010.
- [11] S. Ramaswamy, H. Fu, M. Sreekantharadhy, J. Dixon, and K. Nygard, "Prevention of Cooperative Blackhole Attack in Wireless Ad-hoc

- Networks”, International Conference on Wireless Networks (ICWN), 2003.p.1-7.
- [12] Tao Gong1 and Bharat Bhargava, “Immunizing mobile ad-hoc networks against collaborative attacks using cooperative immune model”, article published in Wiley Online Library (wileyonlinelibrary.com), Issue: Security and Communication Networks, 2013.p.58-68.
- [13] Khanh Viet, Brajendra Panda, Yi Hu Korea, “Detecting Collaborative Insider Attacks in Information Systems”, IEEE International Conference on Systems, Man, and Cybernetics, Seoul; 2012.p.502-507.
- [14] Sanjay K. Dhurandher, I. Woongang, R. Mathur, P. Khurana, “GAODV: A Modified AODV against single and collaborative Blackhole attacks in MANETs”, IEEE 27th International Conference on AINA Workshops, Barcelona; 2013.p.357-362.
- [15] Mingchen Wang, Bin Liu and Chi Zhang “Detection of Collaborative SSDF Attacks using Abnormality Detection Algorithm in Cognitive Radio Networks”, IEEE International Conference on Communications, Budapest; 2013.p.342 – 346.

Named Entity Recognition System for Postpositional Languages: Urdu as a Case Study

Muhammad Kamran Malik

Punjab University College of Information Technology
University of the Punjab
Lahore, Pakistan

Syed Mansoor Sarwar

Punjab University College of Information Technology
University of the Punjab
Lahore, Pakistan

Abstract—Named Entity Recognition and Classification is the process of identifying named entities and classifying them into one of the classes like person name, organization name, location name, etc. In this paper, we propose a tagging scheme Begin Inside Last -2 (BIL2) for the Subject Object Verb (SOV) languages that contain postposition. We use the Urdu language as a case study. We compare the F-measure values obtained for the tagging schemes IO, BIO2, BILOU and BIL2 using Hidden Markov Model (HMM) and Conditional Random Field (CRF). The BIL2 tagging scheme results are better than the other three tagging schemes using the same parameters including bigram and context window. With HMM, the F-measure values for IO, BIO2, BILOU, and BIL2 are 44.87%, 44.88%, 45.14%, and 45.88%, respectively. With CRF, the F-measure values for IO, BIO2, BILOU, and BIL2 are 35.13%, 35.90%, 37.85%, and 38.39%, respectively. The F-measure values for BIL2 are better than those of previously reported techniques

Keywords—IOB tagging; BIO tagging; BILOU tagging; IOE tagging; BIL2 tagging; NER for Resource-poor languages

I. INTRODUCTION

Named Entity Recognition and Classification (NERC) is a process of identifying categories and classifying them into different groups, for example, person names, location names, organization names, quantities, and date. An NERC system is used in many domains including Information Extraction (IE), Machine Translation (MT), and many other Natural Language Processing (NLP) applications.

There are several ways to automatically identify Named Entities (NEs) in unstructured data. We briefly discuss these approaches.

A. Rule Based approaches

In such approaches, language experts write rules by studying the given text. These rules are used to extract NEs from the text. The drawback of these approaches is that they require in-depth linguistic knowledge.

B. Supervised Learning approaches

A large amount of tagged data is a prerequisite for using this approach. People usually tag data manually and then use this data to train a model. Different supervised machine learning algorithms including Hidden Markov Model (HMM) [2], Decision Trees (DT), Maximum Entropy (ME), Support Vector Machine (SVM), and Conditional Random Fields (CRF) [8] are used to learn patterns or rules from the tagged data.

C. Semi-Supervised Learning approaches

In these approaches, a small degree of supervision is required as compared to the supervised learning approaches that require full supervision. The main technique used in the semi-supervised learning algorithms is called “bootstrapping”. For bootstrapping, a set of manually annotated data, known as seeds, is used for starting the learning process and the system learns rules from this data. These rules are then used to annotate more data. Wrong annotations are corrected manually and corrected data is again used in learning additional rules.

D. Unsupervised Learning approaches

In these approaches, NEs are grouped on the basis of contextual similarity. Different lexical resources such as Wordnet may be used for achieving better results. In such approaches, no supervision is required. Clustering is the primary technique used in the unsupervised learning algorithms to identify NEs of the same types.

In supervised learning, tagged data is required for training and testing. Multiple tagging schemes including IO, BIO, BIO2, IOE, IOE2, and BILOU exist to tag data for NEs. We suggest the use of Begin Inside Last 2 (BIL2) tagging scheme for postpositional languages including Urdu, Japanese, and Hindi. Our hypothesis is that in postpositional languages postposition plays a vital role in the decision making process for identifying NEs. For example, in “Ali (NE) nay (postposition)” and “Muhammad Ali (NE) nay (postposition),” the word “nay” is key to deciding if the preceding word is an NE or not. Only BIL2 tagging scheme tries to capture this behavior, as shown in Table 2. Based on our literature review, we have not seen the use of this technique for postpositional languages. In this paper, we compare the performance of BIL2 with IO, BIO2 and BILOU.

The structure of the paper is as follows. Section 2 describes the related work. Section 3 describes the tagging problem and two machine learning algorithms used to handle the tagging problem. Sections 4 and 5 describe the Urdu language issues and data collection process used for experimentation. Section 6 describes the details and results of experimentation. In Sections 7 and 8, we make conclusion and briefly describe future work.

II. RELATED WORK

For NER chunking and Semantic Role Labeling (SRL) usually two types of tagging schemes are used: Inside/Outside and Start/End. [9] introduces the Inside/Outside representation to solve the Noun Phrase (NP) chunking problem. Three tags

are used to identify chunks: 'I', 'O', and 'B'. 'I' means token is inside of the chunk, 'O' means token is outside of the chunk, and 'B' means token is the beginning of a chunk, immediately following the previous chunk. [11] introduces three new alternate tagging schemes, i.e., IOB2, IOE1, and IOE2, and named IOB1 as the Ramshaw tagging scheme. [13] uses the Start/End tagging scheme that has been used to solve the Japanese NER task, and uses the IOBES (also known as BILOU) tagging scheme.

[10] shows that the choice of NE tags significantly impacts the results of NER. 90.8% F-measure has been reported for an English NER system using the BILOU tagging scheme, which was best result reported at the time on the CoNLL-2003 NER shared task.

[12] also uses two frequently used tagging schemes, BIO and BILOU, for NER of the Estonian language. The results of experiments described in the paper show that BILOU outperformed BIO, and F-measure values of 86.6% and 87% were achieved on BIO and BILOU, respectively.

[4] uses three different variations of the IOB tagging scheme, IOBE, IOBES, and IOB₁₂E, to extract names of chemical compounds and drugs. IOBE uses four tags Begin, Inside, Outside, and End, whereas the IOBES and IOB₁₂E schemes use five tags.

[7] uses the IO, IOB, IOB2, IOE, IOE2 and IOBES tagging schemes to show results on the Conference on Computational Natural Language Learning (CoNLL) dataset. They used Conditional Markov Model (CMM) to calculate F-measure. The paper shows that IOE2 and IOBES yielded better results, with F-measure values of approximately 84% and 85% for IOBES and IOE2, respectively.

[3] discusses different tagging schemes including IOB, IOB2, IOE, and IOBES for Chunking, NER, and SLR purposes.

[6] uses Support Vector Machine (SVM) for the chunking of the English language. The paper describes the use IOB, IOB2, IOE, IOE2, and IOBES tagging schemes to identify chunks. Of all these schemes, IOE2 produced best results.

III. THE TAGGING PROBLEM

NER is considered a sequence-labeling problem where we want to determine a vector $z = \{z_0, z_1, \dots, z_T\}$ of random variables given an observed vector $X = \{x_0, x_1, \dots, x_T\}$. Each variable z_s is the NE of the word at position s, and the input X is divided into feature vectors. Each x_s contains various pieces of information about the word at position s, including its identity, orthographic features such as prefixes and suffixes, membership in the domain-specific lexicons, and information in the semantic databases such as Word-Net.

Let $x_{1:n}$ be the sequence of words in a sentence in the Urdu language, and $z_{1:n}$ be the NE against each word, i.e., Person, Organization, Location, etc. Let X_s be the set of all possible sentences that can be formed from the words in set X . Let S be a sequence of words (i.e., a sentence) from $x_{1:n}$ such that $S \in X_s$ with x_i be the i^{th} word in S and $z_{1:n}$ be the sequence of NEs for these words, with z_i being the i^{th} NE in the sequence.

Now, we define the tagging problem for finding the most probable NE sequence $z_{1:n}$ for the word sequence $x_{1:n}$. More formally,

$$\operatorname{argmax}_{z_{1:n} \in Z} P(z_{1:n} | x_{1:n}) \quad (1)$$

In this expression, we want to find the NE tag sequence that gives maximum probability of NE tags sequence for an Urdu sentence.

A. Hidden Markov Model (HMM)

In HMM, we have two set of states and a triple (π, A, B) . The first element in the triple is a set of observable states, that is, the input sentence or word sequence $X = \{x_{1:n}\}$ such that $X \in X_s$ with x_i being the i^{th} word in X . The second element is the set of hidden states that is represented by NE $z_{1:n}$ for the word sequence $x_{1:n}$ with z_i being the i^{th} NE in the sequence. Each NE represents one of the hidden states in HMM. In the triple (π, A, B) , we define π as the initialization vector containing the initial probabilities of all NEs z_i starting an NE sequence. We define A as a matrix of probabilities (transition or prior probabilities) when the underlying Markov Process transitions from one state (i.e., NE) to another. We define B as a matrix of probabilities (emission or likelihood probabilities) of generating the word sequence $x_{1:n}$ from the underlying NE sequence $z_{1:n}$, i.e., the probability of generating (or emitting) a word x_i once the underlying Markov Process has entered a state x_i . We learn the triple (π, A, B) from our Urdu NE training data.

HMM defines the joint probability distribution over a word sequence paired with an NE sequence as

$$P(x_{1:n}, z_{1:n}) \quad (2)$$

The output of HMM is a tag sequence that maximizes this joint probability distribution, expressed as

$$\operatorname{argmax}_{z_{1:n} \in Z} P(x_{1:n}, z_{1:n}) \quad (3)$$

To model this joint probability we consider our basic NE problem from Equation (1) as

$$\operatorname{argmax}_{z_{1:n} \in Z} P(z_{1:n} | x_{1:n}) \quad (4)$$

Bayes Rule of probability dictates us that we can calculate the probability of $(z_{1:n} | x_{1:n})$ if we know the probability of $(x_{1:n} | z_{1:n})$. It says

$$P(z_{1:n} | x_{1:n}) = \frac{P(z_{1:n})P(x_{1:n} | z_{1:n})}{P(x_{1:n})} \quad (5)$$

By applying Bayes Rule to Equation 3 we get

$$\operatorname{argmax}_{z_{1:n} \in Z} \frac{P(z_{1:n})P(x_{1:n} | z_{1:n})}{P(x_{1:n})} \quad (6)$$

We drop the denominator for being the constant for all NEs and hence Equation 6 becomes

$$\operatorname{argmax}_{z_{1:n} \in Z} P(z_{1:n})P(x_{1:n} | z_{1:n}) \quad (7)$$

This means that for each NE sequence we need to calculate the product of likelihood probability $P(x_{1:n} | z_{1:n})$ and prior probability $P(z_{1:n})$. We make two simplifying assumptions to estimate the probability of the NE sequence. The first

assumption says that the probability of a word is dependent only on its own underlying NE.

$$P(x_{1:n}|z_{1:n}) \approx \prod_{i=1}^n P(x_i|z_i) \quad (8)$$

Since we have used both Bigram and Trigram HMM to formulate our results, therefore, for Bigram HMM we assume that the probability of an NE is dependent only on the previous NE (First Order Markov Assumption). Thus, $P(z_{1:n})$ is expressed as shown below.

$$P(z_{1:n}) \approx \prod_{i=1}^n P(z_i|z_{i-1}) \quad (9)$$

For Trigram HMM we assume that the probability of an NE is dependent only on the previous two NEs (Second Order Markov Assumption). Thus, Equation (9) may be expressed as given below.

$$P(z_{1:n}) \approx \prod_{i=1}^n P(z_i|z_{i-2}, z_{i-1}) \quad (10)$$

With these two assumptions, we can rewrite Equation (2) as

$$P(x_{1:n}, z_{1:n}) \approx \prod_{i=1}^n P(z_i|z_{i-1}) \prod_{i=1}^n P(x_i|z_i) \quad (11)$$

Where $P(z|z_{i-2})$ and $P(z_i|z_{i-2}, z_{i-1})$ are called the Bigram and Trigram parameters, respectively, and $P(x_i|z_i)$ is called the emission parameter of HMM.

B. Conditional Random Field (CRF)

Let $x_{1:n}$ be a sequence of words in an Urdu language sentence with $z_{1:n}$ NEs against each word, i.e., Person, Organization, Location, and Other. A linear chain CRF defines a conditional probability as

$$P(z_{1:n}|x_{1:n}) = \frac{1}{Z} \exp(\sum_{n=1}^N \sum_{i=1}^F \lambda_i f_i(z_{n-1}, z_n, x_{1:n}, n)) \quad (12)$$

The scalar Z is the normalization factor. Z is defined as

$$Z = \sum_{z_{1:n}} \exp(\sum_{n=1}^N \sum_{i=1}^F \lambda_i f_i(z_{n-1}, z_n, x_{1:n}, n)) \quad (13)$$

In the exp() function, all weighted feature functions are summed against each word and for each word values are summed to compute the total score for the sentence. The scalar λ_i is the weight for the features $f_i()$. The λ_i 's are the parameters of CRF model and must be learned.

Feature function: In CRF, the feature function is the key component that consists of the current tag, previous tag, complete input sentence, and current position in the sentence. The output of the feature function is a real value. The general form of a feature function is $f_i(z_{n-1}, z_n, x_{1:n}, n)$.

For example, we can define a feature function that produces binary values: it is one (1) if the current word is Ahmad, and if the current state z_n is PERSON:

$$f_1(z_{n-1}, z_n, x_{1:n}, n) = \begin{cases} 1 & \text{if } z_n = \text{PERSON and } x_n = \text{Ahmad} \\ 0 & \text{otherwise} \end{cases} \quad (14)$$

Depending upon the corresponding weight $\lambda_1 > 0$, f_1 is active only when the word Ahmad is seen and its tag is PERSON, and it increases the probability of the tag sequence $z_{1:N}$. It means that the preferred tag for Ahmad is PERSON. If $\lambda_1 < 0$, then CRF tries to avoid the tag PERSON for Ahmed. Finally, if $\lambda_1 = 0$, it means that this feature has no effect.

Another example of feature is

$$f_2(z_{n-1}, z_n, x_{1:N}, n) = \begin{cases} 1 & \text{if } z_n = \text{PERSON and } x_{n+1} = \text{"nay"} \\ 0 & \text{otherwise} \end{cases} \quad (15)$$

The value of this feature is 1 when the current tag is PERSON and the next word in Urdu sentence is 'nay'. If this pattern is found in the training data then λ_2 will be positive. Furthermore, note that f_1 and f_2 can both be active for a sentence like "Ahmad nay khaa (Ahmad said)". This is an example of overlapping features.

IV. ISSUES WITH THE URDU LANGUAGE

Following are the issue of Urdu language:

- 1) In Urdu, there is no concept of capitalization, which is a major clue of NEs.
- 2) The Urdu language is Agglutinative in nature, i.e., by adding additional features to a word more complex words can be formed.
- 3) Urdu is free word-order language, i.e., a sentence can be written using Subject-Object- Verb or Object-Subject-Verb.
- 4) Very few reliable gazetteers are available for the Urdu language.
- 5) In the Urdu language, words are written sometimes with diacritic and sometimes without diacritic, causing multiple variations of single word.
- 6) Urdu is called a "Lashkari" language, i.e., it contains words of different languages including those of Arabic, Persian, and English.
- 7) Researchers in the field of natural language processing have not spent much time in studying the Urdu language.
- 8) In the Urdu language, there is the issue of word segmentation.
- 9) Urdu has the problem of lack of character level standardization and spelling variation.
- 10) In the Urdu language, depending upon the context, there is a large number of words that can be considered as common nouns as well as proper nouns (i.e., candidate for NE). For example, Shan, Kamran, Fazal, Kiran, Aftab, Manzoor, etc. can be NEs, i.e., Person as well as common nouns. The context may help in identifying proper nouns against common nouns but due to no concept of capitalization,

disambiguation becomes harder than that in the English language.

11) There are multiple ways of representing abbreviations in Urdu.

12) There is a serious lack of labeled data in Urdu required for machine learning.

13) There is a huge variation in the number formats in Urdu, for example, ghiara (11), bara (12), taira (13), ikkees (21), baaees (22), etc.

V. DATA COLLECTION

We took the corpus for our experiments from IJCNLP-08 NERSSEAL shared tasks datasets. For annotation, the first step was to identify whether a word is an NE or not. For example, the word "Fazal" is an NE or not depend on the context. Since Urdu does not have the concept of capitalization, therefore, in the sentence "Us per khuda ka fazal hai (he has the blessing of God)", fazal (blessing) is not an NE, whereas in the sentence "fazal aik laek talabilm hai (fazal is a bright student)", fazal is an NE (PERSON). The next step was to tag maximal entities. For example, "Quaid-e-Azam Library should be tagged as Location. It should not be marked "Quaid-e-Azam" as Person.

We divided the corpus into two sets: training and testing. The following are the details of Urdu that were used in the shared task. The Urdu text was partially taken from the news corpus and partially from other sources. The counts of all NEs used in training and testing are given in the Table 1.

We used 12 tags for tagging the dataset. The details of the tagset are given below:

- NEP (Person): 'Quaid-e-Azam Muhammad Ali Jannah' or simply 'Quaid-e-Azam', or 'Allama Iqbal'
- NED (Designation): 'Prime Minister', 'President' (as in 'President Musharaf'), or 'General' (as in 'General Raheel')
- NEO (Organization): 'State Bank of Pakistan', 'DELL', 'Al Qaida', or 'The Ministry of Defense'
- NEA (Abbreviation): 'PU' (or P.U.), 'CRF', 'AJK', or 'LTV'
- NEB (Brand): 'Pepsi' or 'Windows'
- NETP (Title-Person): 'Mr.', 'Sir', or 'Field Marshall'
- NETO (Title-Object): 'The Seven Year Itch', 'American Beauty', '1984' (as in '1984 by George Orwell'), or 'One Hundred Years of Solitude'
- NEL (Location): 'Lahore', 'Islamabad', or 'Punjab'
- NETI (Time): '19 May', '1965', or '6:00 pm'
- NEN (Number): 'Fifty-five', '3.50', or 'ten lac'
- NEM (Measure): '10 kg', '32 MB', or 'five years'
- NETE (Terms): 'Horticulture', 'Conditional Random Fields', 'Sociolinguistics', or 'The Butterfly Effect'

TABLE I. STATISTICS ABOUT URDU TRAINING AND TESTING DATA

NE	Training Data	Testing Data
NEP	365	145
NED	98	41
NEO	155	40
NEA	39	3
NEB	9	18
NETP	36	15
NETO	4	147
NEL	1118	468
NETI	279	59
NEN	310	47
NEM	140	40
NETE	30	4
NEs	2584	1027
Words	35447	12805
Sentences	1508	498

VI. METHODOLOGY

We assessed the performance of our system using precision, recall, and F1-measure. We used the BIL2 tagging scheme for Subject Object Verb (SOV) ordered languages that usually contain postposition instead of preposition. Table 2 gives details for the IO, BIO2, BILOU and BIL2 tagging for the example "Syed Mansoor Sarwar worked at Punjab University Lahore".

TABLE II. EXAMPLES OF DIFFERENT TAGGING SCHEME

Words	IO	BIO2	BILOU	BIL2
سید (Syed)	I-PER	B-PER	B-PER	B-PER
منصور (Mansoor)	I-PER	I-PER	I-PER	I-PER
سرور (Sarwar)	I-PER	I-PER	L-PER	L-PER
نے (nay)	O	O	O	O
لاہور (Lahore)	I-LOC	B-LOC	U-LOC	L-LOC
کی (key)	O	O	O	O
پنجاب (Punjab)	I-ORG	B-ORG	B-ORG	B-ORG
جامیونیورسٹی (University)	I-ORG	I-ORG	L-ORG	L-ORG
میں (main)	O	O	O	O
کام (kam)	O	O	O	O
کیا (kiya)	O	O	O	O

The IO tagging scheme uses two tags, i.e., I (inside) and O (outside). If an NE, e.g., person name consists of one or more words, I-PER (inside) tag is assigned and O (other) tag is used for the remaining non-NE words. The BIO2 tagging scheme uses three tags to assign particular words. If an NE, e.g., person name is a single word then B-PER (Begin) tag is used. However, if an NE consists of two or more words then the B-PER tag is assigned to first word and the I-PER tag is assigned to all remaining words. The BILOU tagging scheme uses five tags. If an NE consists of a single word then the U-PER tag is used. If an NE consists of two words then the B-PER and L-PER tags are used for first and second words, respectively. If an NE consists of three or more words then the B-PER and L-PER tags are used for the first and last words, respectively, and the I-PER tag is used for all inside words. The BIL2 tagging scheme uses four tags. If an NE consists of a single word then L-PER tag is used. If an NE consists of two words then B-PER and L-PER are used. Finally, if an NE consists of more than

two words then for first word, last word, and all intermediate words are assigned B-PER, L-PER, and I-PER, respectively.

We used the following steps in our approach for Urdu NERC.

- 1) Selection of training and testing data.
- 2) Assignment of IO, BIO2, BILOU, and BIL2 tags to the training and testing data.
- 3) Build models using HMM [1] and CRF [5] for these tagging schemes.
- 4) Calculate F-measures using test data against the respective models.

The BIL2 tagging scheme produced better results than all other schemes for both machine learning algorithms. By using HMM, we used the trigram model with linear interpolation for smoothing. F-Measure for IO, BIO2, BILOU, and BIL2 were 44.87%, 44.88%, 45.14%, and 45.88%, respectively. In case of CRF, we used the base line model without using any features like neighboring words, prefixes, etc. F-Measure of IO, BIO2, BILOU, and BIL2 were 35.13%, 35.90%, 37.85% and 38.39%, respectively. There are chances that by using CRF with other features like previous words and Part Of Speech (POS), previous NE, we may achieve better results. Table 3 and Table 4 show the detailed results for HMM and CRF, respectively.

TABLE III. RESULTS OF FOUR TAGGING SCHEMES USING HMM

	Precision	Recall	F-Measure
IO	52.45	39.21	44.87
BIO2	54.04	38.38	44.88
BILOU	55.08	38.24	45.14
BIL2	55.22	39.24	45.88

TABLE IV. RESULTS OF FOUR TAGGING SCHEMES USING CRF

	Precision	Recall	F-Measure
IO	46.52	28.22	35.13
BIO2	47.34	28.91	35.90
BILOU	55.32	28.77	37.85
BIL2	55.57	29.32	38.39

Overall, the comparison of each tagging scheme with respect to HMM and CRF is shown in Figure 1. We use CRF without using any features like bigram, window size, and context. This is why the values of the performance measures for CRF for all tagging schemes are smaller than those of HMM. As you can see, by using IO tagging, HMM and CRF produced F-measure with least accuracies. Similarly, using BIO2 tagging, HMM and CRF produced F-measure better than IO but smaller than BILOU and BIL2. The same pattern can be observed in BILOU and BIL2 where using BILOU tagging HMM and CRF produced 2nd highest F-measure and using BIL2 both produced highest F-Measure as shown in Figure 1.

Comparison of HMM and CRF on different tagging schemes

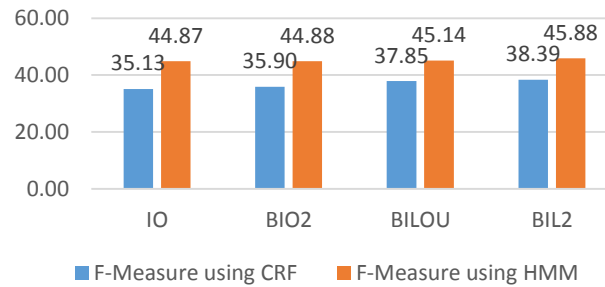


Fig. 1. Overall F-Measure results of CRF and HMM using each tagging scheme

The results of BIL2, IO, BILOU, and IOB2 using HMM on each NE and overall Precision, Recall, and F-Measure are shown in Figure 2, Figure 3, Figure 4, and Figure 5, respectively. With HMM, BIL2 and BILOU could not identify a single instance of NEA, NEB, NETE, NETO, and NETP, as shown in Figure 2 and Figure 4, respectively. NEB, NETE, NETO, and NETP could not be identified using HMM with IO and BIO2 tagging schemes, as shown in Figure 3 and Figure 5, respectively.

Results of BIL2 using HMM

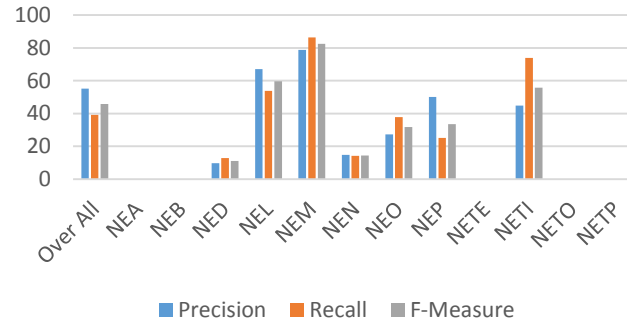


Fig. 2. F-Measure results of BIL2 tagging using HMM of each NE

Results of IO using HMM

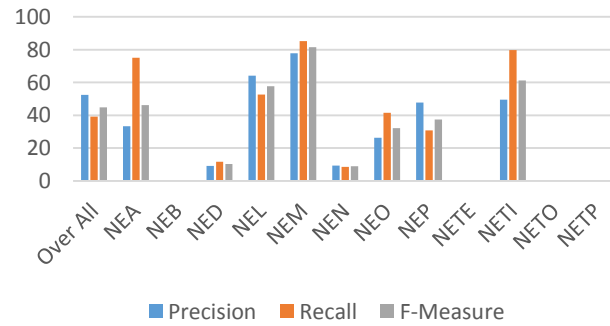


Fig. 3. F-Measure results of IO tagging using HMM of each NE

Results of BILOU using HMM



Fig. 4. F-Measure results of BILOU tagging using HMM of each NE

Results of BIO2 using HMM

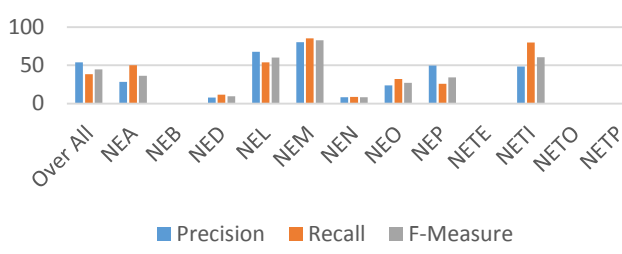


Fig. 5. F-Measure results of BIO2 tagging using HMM of each NE

Results of BIL2, IO, BILOU, and IOB2 using CRF on each NE and overall Precision, Recall, and F-Measure are shown in Figure 6, Figure 7, Figure 8, and Figure 9, respectively. Using CRF with BIL2 tagging did not identify a single instance of NEB, NETE, NETO, and NETP, as shown in Figure 6. NEB, NETE, NETO, and NETP could not be identified using CRF with IO tagging, as shown in Figure 7. The BILOU and BIO2 tagging schemes could not identify a single instance of NEA, NEB, NETE, NETO, and NETP, as shown in Figure 8 and Figure 9, respectively.

Results of BIL2 using CRF

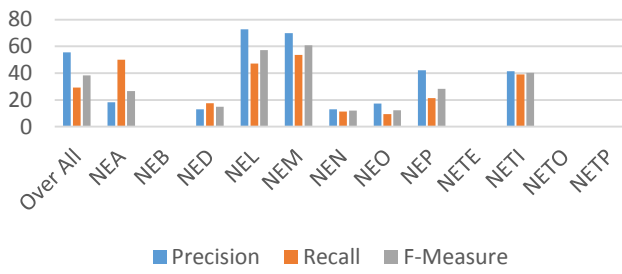


Fig. 6. F-Measure results of BIL2 tagging using CRF of each NE

Results of IO using CRF

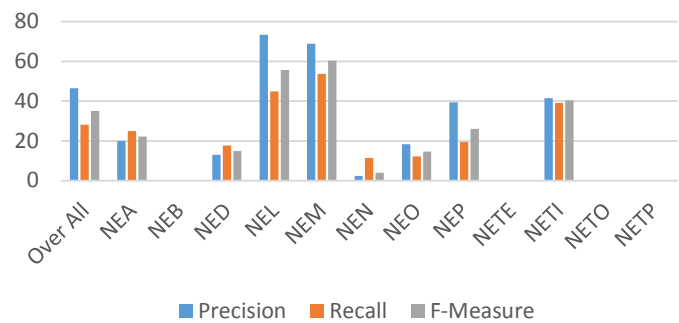


Fig. 7. F-Measure results of IO tagging using CRF of each NE

Results of BILOU using CRF

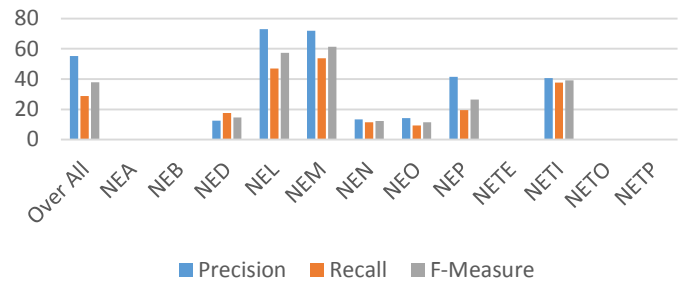


Fig. 8. F-Measure results of BILOU tagging using CRF of each NE

Results of BIO2 using CRF

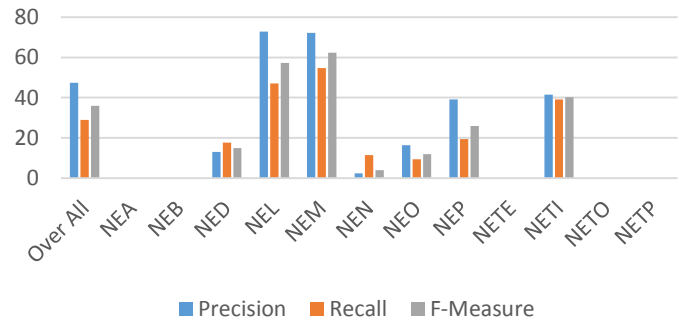


Fig. 9. F-Measure results of BIO2 tagging using CRF of each NE

F-Measure of each NE using HMM on each tagging scheme is shown in Figure 10. The figure shows that using HMM with any tagging scheme could not identify NEB, NETE, NETO, and NETP, and only IO and BIO2 tagging schemes identified NEA.

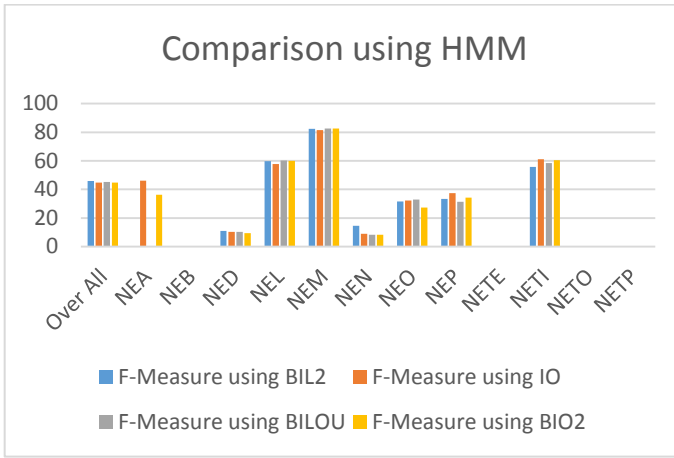


Fig. 10. F-Measure results of all tagging schemes using HMM of each NE

F-Measure of each NE using CRF with each tagging scheme is shown in Figure 11. The figure shows that using CRF with any tagging scheme could not identify NEB, NETE, NETO, and NETP, and only IO and BIL2 tagging schemes identified NEA. In summary, no tagging scheme with MMH or CRF could identify NEB, NETE, NETO, and NETP.

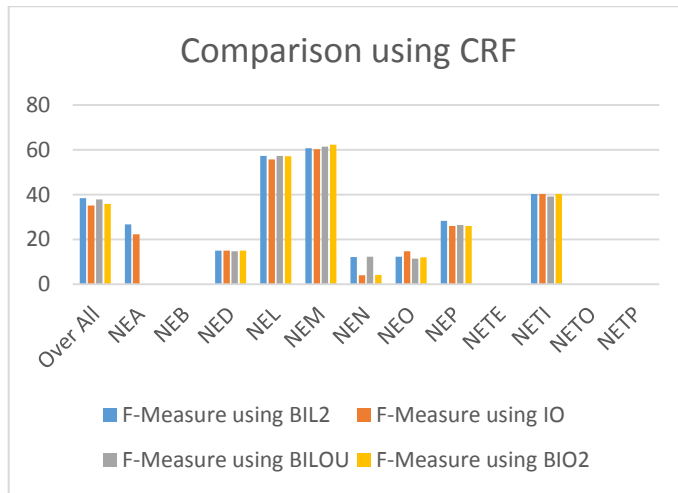


Fig. 11. F-Measure results of all tagging schemes using CRF of each NE

VII. CONCLUSION

The selection of an appropriate tagging scheme and selection of an appropriate ML algorithm may produce good results for the NER problem. In our experiments, we used a new NE tagging scheme for postpositional languages and compared the results with those obtained for the existing tagging schemes using HMM and CRF. The study shows that the NER tagging schemes for the Subject Verb Object (SVO) and SOV languages should be different for building a NER system with good F-measure values, because usually the SVO languages use the concept of preposition and the SOV languages use the concept of postpositional. Finally, our study shows that for Urdu, which is a postpositional language, the BIL2 tagging scheme generates the highest F-measure values using HMM and CRF.

VIII. FUTURE WORK

In future, we can perform experiments on other tagging schemes, including IOE and IOE2, to show a detailed comparison because these tagging schemes also support postposition languages. A NER result with CRF using different features may be conducted to show that the BIL2 tagging scheme still performs better than others or not. Part of speech information can be used to improve the results of NER, and the list of person name, location name, and organization name may be exploited to improve results. We can also observe the improvement in the results of NER by using regular expressions for date, time, numbers, and measures.

REFERENCES

- [1] Brants, T. TnT: a statistical part-of-speech tagger. In *Proceedings of the sixth conference on Applied natural language processing* (pp. 224-231). Association for Computational Linguistics. (2000, April).
- [2] Bikel, D. M., Miller, S., Schwartz, R., & Weischedel, R. Nymble: a high-performance learning name-finder. In *Proceedings of the fifth conference on Applied natural language processing* (pp. 194-201). Association for Computational Linguistics. (1997, March).
- [3] Collobert, R., Weston, J., Bottou, L., Karlen, M., Kavukcuoglu, K., & Kuksa, P. Natural language processing (almost) from scratch. *The Journal of Machine Learning Research*, 12, 2493-2537. (2011).
- [4] Dai, H. J., Lai, P. T., Chang, Y. C., & Tsai, R. T. Enhancing of chemical compound and drug name recognition using representative tag scheme and fine-grained tokenization. *Journal of Cheminformatics*, 7(Suppl 1), S14. (2015).
- [5] Finkel, J. R., Grenager, T., & Manning, C. Incorporating non-local information into information extraction systems by gibbs sampling. In *Proceedings of the 43rd Annual Meeting on Association for Computational Linguistics* (pp. 363-370). Association for Computational Linguistics. (2005, June).
- [6] Kudo, T., & Matsumoto, Y. Chunking with support vector machines. In *Proceedings of the second meeting of the North American Chapter of the Association for Computational Linguistics on Language technologies* (pp. 1-8). Association for Computational Linguistics. (2001, June).
- [7] Krishnan, V., & Ganapathy, V. Named Entity Recognition. 2005. *Dostupno na: http://cs229.stanford.edu/proj2005/KrishnanGanapathy-NamedEntityRecognition.pdf* (13.4. 2012). (2005).
- [8] McCallum, A., & Li, W. Early results for named entity recognition with conditional random fields, feature induction and web-enhanced lexicons. In *Proceedings of the seventh conference on Natural language learning at HLT-NAACL 2003-Volume 4* (pp. 188-191). Association for Computational Linguistics. (2003, May).
- [9] Ramshaw, L. A., & Marcus, M. P. Text chunking using transformation-based learning. *arXiv preprint cmp-lg/9505040*. (1995).
- [10] Ratnovid, L., & Roth, D. Design challenges and misconceptions in named entity recognition. In *Proceedings of the Thirteenth Conference on Computational Natural Language Learning* (pp. 147-155). Association for Computational Linguistics. (2009, June).
- [11] Sang, E. F., & Veenstra, J. Representing text chunks. In *Proceedings of the ninth conference on European chapter of the Association for Computational Linguistics* (pp. 173-179). Association for Computational Linguistics. (1999, June).
- [12] Tkachenko, A., Petmanson, T., & Laur, S. Named Entity Recognition in Estonian. *ACL 2013*, 78. (2013).
- [13] Uchimoto, K., Ma, Q., Murata, M., Ozaku, H., & Isahara, H. Named entity extraction based on a maximum entropy model and transformation rules. In *Proceedings of the 38th Annual Meeting on Association for Computational Linguistics* (pp. 326-335). Association for Computational Linguistics. (2000, October).

Symbolism in Computer Security Warnings: Signal Icons and Signal Words

Nur Farhana Samsudin, Zarul Fitri Zaaba*, Manmeet Mahinderjit Singh, Azman Samsudin

School of Computer Sciences,
Universiti Sains Malaysia, 11800 Minden,
Pulau Pinang, Malaysia

Abstract—Security warning is often encountered by the end users when they use their system. It is a form of communication to notify the users of possible consequences in the future. These threats have always been evolved with the advancement of technologies. The attacks threaten the end users with many harmful effects such as malware attacks. However, security warning keeps being ignored due to various reasons. One of the reasons is lack of attention towards warnings. The end users feels burden and treat security task as a secondary rather than primary task. To divert user's mind to read and comprehend the security warnings, it is important to capture the user's attention. Signal words and signal icons are important in the security warning as it is the elements that could help user to heed the warnings. A survey study has been conducted with 60 participants in regards to the perception towards attractiveness and understanding of the signal words and icons. It can be revealed that end users significantly feel that the icon with the exclamation marks is attractive and easy to understand. However, only one of three hypotheses is proven to be significant.

Keywords—security; signal icons; signal words; usable security; usability; warning

I. INTRODUCTION

Home computer users are more susceptible to security threats such as viruses, worms and phishing attacks with the advancement of Internet and technologies. These threats could lead to possible harm to the computer users and their system in the future such as interruption (i.e. an assets becomes destroyed or unavailable), interception (i.e. an illegitimate party have access to an asset), modification (i.e. the content of an assets is altered) and fabrication (i.e. an illegitimate party inserts a fake objects into the system) [1]. In computer system, the security warning acts as a defense mechanism to resist our system from being harmed. It takes of various forms such as the dialog box, balloon, in-place, banners and notifications [2]. It is usually presented with signal words such as “warning”, “harm” and “danger”. In addition, the signal words are usually being accompanied with signal icons such as a warning icon, an error icon, an information icon and a help icon [2]. These icons have their own meaning and it is utilised based on their respective significance. The signal icon and signal words are some of the important elements in security warnings. Studies revealed that humans process visual data better than text [3]. They claimed that the human brain could process images 60,000 times faster than text. This shows that the visual representations in security warnings could aid the end users in comprehend the security warning faster.

However, security warnings is often being ignored by the users because of various reasons such as they do not understand the messages [4,5], they are unaware of the risk, too much technical words [5,6] and users have an incorrect mental model of risk [6,7]. Users are more focused on their primary task and consider the computer security as secondary tasks [8]. Users also feel like complying with computer security is a burden to them. These problems lead to the lack of usability in computer systems. End users are not able to perform security tasks effectively and the risk communications are not conveyed correctly. In addition, the level of protection offered by the web browsers towards phishing url or malicious site are also very limited [9]. Hence, end-users need to be more alert of the security of their system so that less harm would be experienced.

This paper is organized as follows: Section 2 explores the related work and literature studies; Section 3 describes the methodology implemented in this studies, Section 4 explains the hypotheses used within this study; Section 5 describes the study results and findings, Section 6 presents a brief discussion and finally Section 7 ends with the conclusion highlighting the limitation and current progress of this study.

II. RELATED RESEARCH

Warning is a form of risk communication that is utilized as a message to convey possible consequences of an action [10]. It notifies people about the risk so that possible harm could be avoided. [11] claimed that warning is anything that could interrupts an individual's focus towards possible danger. The warnings in computer context applied the same principle. It is some representations that could prevents the end users from losing several assets such as financial assets and critical data, system access, privacy and valuable time (i.e. user's time) [2].

On the other hand, the end users are still encounter problems with security warnings. [5] have listed six classifications of problems in warnings namely attention towards warnings, understanding of warnings, use of technical wordings, evaluation of risks from warnings, users' motivation towards heeding warnings and users' assessments of the implication of warnings.

This study focuses on the user's attention towards warning with the focus on signal icons and signal words. The attention towards warning is one of the most important aspects in the effort to improve the current implementation of security warnings. People's attention is the fundamental element to

This work is supported by a short term grant from the Universiti Sains Malaysia (USM) [304/PKOMP/6313287]. *Corresponding author

attract the users to read and comprehend the given security warnings. Studies by [12] revealed that there are four categories of reasons for ignoring warnings which are:

- 1) Failures in personal variables: Users do not have the knowledge or experience regarding the security warnings.
- 2) Failures in intention: Users were not motivated to respond to security dialogs.
- 3) Failures communication delivery: The security warnings fail to grab user's attention.
- 4) Failures in communication processing: Users do not understand the message being conveyed.

Studies by [13] revealed that the end users were not attentive towards warning as it is hard to comprehend. The participants of their experimental studies were asked to perform a task of purchasing an item online. It can be revealed that the lock icon in the web browsers are noticed however ignored, and the certificates are rarely used by the users. Users did not look at some indicator such as the certificate icon and even if they look at it (i.e. lock icon), they did not maintain their attention to it. Hence, it can be summarized that it is important to embed a better icon and signal words in order to grasp the user's attention.

[2] Suggests that there are four types of standard icons in Windows namely the error, warning, information and question mark icon. Figure 1 shows the standard icons in Windows. These icons have different usage and meaning as described below:

- 1) Error icon: The problem or error has occurred.
- 2) Warning icon: The condition might cause a possible harm in the future.
- 3) Information icon: Useful information is presented.
- 4) Question mark icon: Indicated a Help entry point.

The questions on icons understanding have also been questioned in previous studies [14]. From the studies it can be found that there are still some misconceptions towards icon understanding in security warning. It is important for warnings to convey the right information to the users in order to aid the users in making the right decision.



Fig. 1. Standard icons in Windows; from left to right; Error icon, Warning icon, Information icon, Question mark icon [2]

The usage of the standard icons takes consideration of the message type, severity of the issues and the context of the situation. It is important to present the appropriate signal icon and words in order to provide a better understanding and correct risk communication.

Studies by [15] revealed how the users of IT perceive the severity of hazard and detailed assessment of the signal icons and signal words. They claimed that by combining signal words and signal icon in a security warnings, the level of

hazard perceive by the end users are higher as shown in Table I. They also conduct an experiment of habituation effects in security warnings. By presenting the combination of signal words and signal icon with three different treatment condition, users became habituated only after a few exposures to the same message. Their study also revealed that the signal word and signal icon combination with higher perceived severity to that of the habituated edit request message have the highest hit rate with 39%.

TABLE I. MEAN VALUES (STANDARD DEVIATION) OF THE PERCEIVED SEVERITY OF SIGNAL WORDS AND SIGNAL ICON [15]

Word	Blank	i	?	!	x
Blank		2.00 (1.43)	2.18 (1.73)	3.74 (1.98)	5.30 (2.29)
Notice	2.23 (1.63)	2.64 (1.76)	2.52 (1.67)	3.89 (1.99)	5.19 (2.35)
Error	3.84 (2.19)	3.85 (1.90)	3.73 (1.92)	4.97 (2.20)	6.24 (2.37)
Warning	4.06 (2.10)	4.09 (2.03)	3.91 (1.96)	5.41 (2.08)	6.65 (2.20)
Urgent	4.09 (2.31)	4.15 (2.14)	3.97 (2.13)	5.34 (2.29)	6.54 (2.37)
Critical	5.11 (2.49)	4.82 (2.42)	4.74 (2.21)	6.01 (2.26)	7.38 (2.22)

On the other hand, a study on end-users' awareness of security indicators have been conducted by [16]. They ask their participants to perform an online transaction in a simulated online banking platform. It can be revealed that none of their participants look at the website address indicator (i.e. lock icon and 'https' wording in address bar). These results are worrisome because the absence of security indicator in address bar might hints insecure connection. This study highlights that most of computer users are not attentive towards details such as the url and signal icons. It is important to draw users attention as soon as they load the page since they are performing task that might cause loss of valuable assets, privacy over confidential information and tricked into fraud [2].

In studies by [17], they revealed that the empirical evidence show that graphical cues such as icons, arrows and boxes attract users attention and the eyes get fixed on the headings first, followed by text blocks and graphics. Their results suggest that the use of visual metaphors aid the users to understand the message better. These finding shows that graphical representations such as icons is important elements in a warning. To access the end users perception of signal words and signal icons in security warning, a survey was conducted to better understand the issues of the current implementation of security warnings.

III. METHODOLOGY

We conduct a survey to discover the user perception and understanding of the security warning dialogs with the focus on signal words and icons.. Participants were recruited through word of mouth and e-mail. The participants were asked to provide a numerical rating on a seven-point Likert scale of



Fig. 2. The study background and computing skills of participants

given scenarios. They could choose the most preferred number where 1 indicate strongly disagree and 7 indicates strongly agree. Studies by [15,17] also conducted the similar survey method to access the end users insights of the current implementation of security warnings however different in scenario used. The Likert-scale is chosen because it is easy to construct, have a high probability of producing a dependable scale and it is easy to be comprehend by the participants [18].

IV. HYPOTHESES

In order to investigate the end users perception towards signal words and icons in security warnings, we proposed three hypotheses to test the significant difference. We would like to explore whether different groups of people have different understanding of security warnings [19]. We have identified two groups from the study which are the technical and non-technical groups. The technical and non-technical groups reflected the user's background. The hypotheses are created based on the questionnaire in the interview sessions. The hypotheses are described in Table II.

TABLE II. SURVEY QUESTIONS AND THE RESPECTIVE HYPOTHESES

Survey Questions	Hypotheses
The use of visual / graphics (e.g. icons, colors, graphics) helps to draw my attention.	There is no difference between technical and non-technical participants in terms of "The use of visual / graphics (e.g. icons, colors, graphics) helps to draw my attention". (H1)
The use of visual / graphics (e.g. icons, colors, graphics) helps me to understand the risk.	There is no difference between technical and non-technical participants in terms of "The use of visual / graphics (e.g. icons, colors, graphics) helps me to understand the risk". (H2)
The words used in the warning is easy to understand.	There is no difference between technical and non-technical participants in terms of "The words used in the warning is easy to understand". (H3)

To test the statistical differences between two groups, we used Chi-square test in order to look for the statistical difference. The purpose of Chi-square test is to evaluate the association between two categorical variables [20]. Studies by [21] revealed that a Chi-square test is utilized as a comparison of more than one group where the differences are related to the actual sample and another hypothetical data. It is considered as a statistical significant findings when $p < 0.05$. In this test, the Likert-scales values were grouped into three classifications with the range of 1 to 3 is equal to No, 4 is equal to Neutral and 5 to 7 is equal to Yes. This classifications have also been conducted by [14,19]. The results of the Chi-square test are explained further in the next section.

V. RESULTS AND FINDINGS

A total of 60 participants were gathered for the survey. The majority of the participants between the age range of 18 – 25 years old and equally distributed between male and female. Since the interview is promoted well in the university, most of the participants are predominantly from the Universiti Sains Malaysia, Penang, Malaysia.

From the overall responses, the gender of our participants is divided almost equally where it comprises of 45% male and 55% female. Majority of the participants are in the range of age of 18-25 years old (95%) and the rest of them were in the range of 26-35 years old. This indicates that they were most likely to grow up in the era of information technology. In addition, the result suggests that the respondents were familiar with the computer and latest technology. Previous studies were also conducted within the university background and majority of the participants were in the range of age between 18-30 years old [8,19]. In addition, most of our participants have high educational background (i.e. postgraduate (8%) and undergraduate (92%)). Figure 3 depicted the study background and computing skills of the study participants.

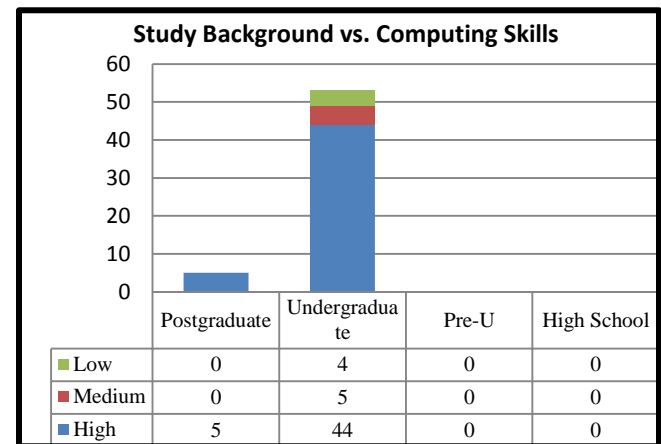


Fig. 3. The study background and computing skills of participants

To classify and determine our study participants skills in computer security, four basic questions were asked in the demographic forms. The questions derived from this section are based on the six tasks from the "Security Center" of Windows Vista [22]. The method of accessing users knowledge by asking a few security questions is also conducted by [23]. The security questions involve knowledge of installing updates, scan for malwares, delete browser's

cookies and setup password. The categorization was high, medium and low. For high level expertise, the participants were able to perform advanced task such as installing updates and patches (i.e. could perform all task). For medium level, the participants were unable to perform one of the tasks given while for the low level, the participants could not performed more than one task.

In the questionnaire, we have included three security warnings example (i.e. in a form of image) to explore the end users understanding and perception of the icons and signal words used in the warnings. Figure 2 shows the security warnings shown to the users. The three security warnings have also been discussed in studies by [4,6,14]. The association of signal words and signal icon used in the three scenarios are depicted in Table III.

TABLE III. SIGNAL WORDS AND SIGNAL ICONS USED IN EACH SCENARIOS

Scenario	Signal words	Signal icons	Background color	Meaning of icons
1	Warning, harm,		Orange	Warning
2	Warning, harm		Yellow	Warning
3	Unavailable		Blue	Help

It can be noted that for scenario 1 and scenario 2, both utilize “warning” and “harm” as a signal words that indicates the possible bad consequences to the system. The icons used are similar which are the exclamation mark icon which means warning. With regards to scenario 3, it can be noted that there is “no signal words” that are available to cues the end users of a possible harm. As for the signal icon, the question mark icon is presented. Generally this icon is a help icon where it will lead users to a guidance page.

A. Scenario 1

Table IV indicates H1 that among those who were from non-technical group, 23 of them found that the icon was more attractive. Despite more non-technical participants found that the icon was attractive, the difference for both version was not statically significant ($p = 0.431$). The icons used in the warning were referring to the exclamation mark icon with the shape of a shield. It can be assumed that most of the participants (43/60) were attracted to the exclamation mark icon. When the user is attracted to the security warning, it can help in providing the users with better understanding of the message in the warning dialogs.

It can be noted that in standard version, 5 participants from the technical groups did not understand the risk while 1 participant from the non-technical version claimed that the icon used did not convey risk. Surprisingly, the number of participants who understand the risk from the technical group was lesser than the non-technical group and the difference was also not statistically significant ($p = 0.181$).

TABLE IV. THERE IS NO DIFFERENCE BETWEEN TECHNICAL AND NON-TECHNICAL PARTICIPANTS IN TERMS OF “THE USE OF VISUAL/GRAFICS (E.G. ICONS, COLORS, GRAPHICS) HELPS TO DRAW MY ATTENTION” (H1) BASED ON SCENARIO 1

Icon Attractiveness	Yes	No	Neutral
Technical	20	1	9
Non-Technical	23	2	5
$\chi^2 = 1.685, p = 0.431, df = 2$			

Even though the results were not statistically significant, majority of our participants agree that the visual in scenario 1 helps them to understand the risk better. With better understanding of the meaning and purposes of the elements in security warning dialogs, the risk communication could better be conveyed.

TABLE V. THERE IS NO DIFFERENCE BETWEEN TECHNICAL AND NON-TECHNICAL PARTICIPANTS IN TERMS OF “THE USE OF VISUAL / GRAPHICS (E.G. ICONS, COLORS, GRAPHICS) HELPS ME TO UNDERSTAND THE RISK” (H2) BASED ON SCENARIO 1

Icon Understanding	Yes	No	Neutral
Technical	23	5	2
Non-Technical	25	1	4
$\chi^2 = 3.417, p = 0.181, df = 2$			

Table VI shows that for the standard version, the result was statistically significant ($p = 0.049$). It can be found that the 26 participants with technical background able to understand the words used easily rather than only 18 participants from the non-technical background. The words used in the standard version were name, from, type, publisher and .exe. It can be noted that there was a difference between the technical and non-technical participants in understanding the words used in the security warning dialogs. These results suggest that the security warnings should minimize the technical jargons in the text blocks.

TABLE VI. THERE IS NO DIFFERENCE BETWEEN TECHNICAL AND NON-TECHNICAL PARTICIPANTS IN TERMS OF “THE WORDS USED IN THE WARNING IS EASY TO UNDERSTAND” (H3) BASED ON SCENARIO 1

Words Understanding	Yes	No	Neutral
Technical	26	1	3
Non-Technical	18	6	6
$\chi^2 = 6.026, p = 0.049, df = 2$			

B. Scenario 2

Table VII indicates H1 that among those who were from non-technical group, 20 of them found that the icon was more attractive. Despite more non-technical participants found that the icon was attractive, the difference for both version was not statically significant ($p = 0.791$). However, we learnt that

majority of the users (65%) were attracted to the icons and colors in scenario 2. The icon used in the warning was referring to the exclamation mark icon.

TABLE VII. THERE IS NO DIFFERENCE BETWEEN TECHNICAL AND NON-TECHNICAL PARTICIPANTS IN TERMS OF “THE USE OF VISUAL/GRAFICS (E.G. ICONS, COLORS, GRAPHICS) HELPS TO DRAW MY ATTENTION” (H1) BASED ON SCENARIO 2

Icon Attractiveness	Yes	No	Neutral
Technical	19	4	7
Non-Technical	20	5	5
$\chi^2 = 0.470, p = 0.791, df = 2$			

It can be noted that in scenario 2, 2 participants from the technical groups did not understand the risk while 4 participants from the non-technical participants claimed that the icon used did not convey risk. The results revealed that the number of participants who comprehended the risk from the technical group and non-technical group were similar with a total of 21 participants from each group. It can be noted that there was no significance difference between both groups as $p = 0.607$. These results indicated that for scenario 2, the use of icon did not help the users in comprehending the risk. This might be resulted from the highly technical message provided in the scenario 2 as it contains words such as “active content”, “ActiveX” and “script”. Studies by [14] revealed that 40% of their participants rated that they were having problems with those technical words. The users might be demotivated because when they read the words and look at the icon, they unable to comprehend the meaning and relate it to the given cues.

TABLE VIII. THERE IS NO DIFFERENCE BETWEEN TECHNICAL AND NON-TECHNICAL PARTICIPANTS IN TERMS OF “THE USE OF VISUAL / GRAPHICS (E.G. ICONS, COLORS, GRAPHICS) HELPS ME TO UNDERSTAND THE RISK” (H2) BASED ON SCENARIO 2

Icon Understanding	Yes	No	Neutral
Technical	21	2	7
Non-Technical	21	4	5
$\chi^2 = 1.000, p = 0.607, df = 2$			

Table IX shows that for the scenario 2, the result was not statistically significant ($p=0.468$). It can be found that 21 participants with technical background can understand the words used easily rather than only 18 participants from the non-technical background. The message given in the security warning is “Allowing active content such as script and ActiveX controls can be useful. But active content might also harm your computer”. It can be noted that there were 11 participants from the non-technical background who could not understand the words in the dialogs.

TABLE IX. THERE IS NO DIFFERENCE BETWEEN TECHNICAL AND NON-TECHNICAL PARTICIPANTS IN TERMS OF “THE WORDS USED IN THE WARNING IS EASY TO UNDERSTAND” (H3) BASED ON SCENARIO 2

Words Understanding	Yes	No	Neutral
Technical	21	5	4
Non-Technical	18	9	3
$\chi^2 = 1.516, p = 0.468, df = 2$			

This result indicated that the non-technical groups were having problems in terms of understanding the technical jargons in computer. Studies by [6] also highlighted the same issues where their participants were having difficulties with the technical words.

C. Scenario 3

Table X indicates H1 that among those who were from non-technical group, 17 of them found that the icon was more attractive. Even though more non-technical participants found that the icon was attractive, the difference was not statically significant ($p = 0.670$). The differences between technical and non-technical users who choose “Yes”, “No” and “Neutral” were not that extensive. The icons used in the standard warning are the question mark icon. It can be noted that scenario 3 receives the lowest “Yes” score between the three scenarios presented to the users. It can be noted that the question mark icon was not an appropriate icon to be used in a critical message such as an email attachment dialogs. It is supposed to be a warning icon rather than question mark icon. When such problems occurs, users’ mental model will shift or learn that “?” icon means warning rather than help (i.e. incorrect mental model). This is not a good signal and it might lead to bad consequences.

TABLE X. THERE IS NO DIFFERENCE BETWEEN TECHNICAL AND NON-TECHNICAL PARTICIPANTS IN TERMS OF “THE ICONS USED ATTRACT MY ATTENTION” (H1) BASED ON SCENARIO 3

Icon Attractiveness	Yes	No	Neutral
Technical	15	9	6
Non-Technical	17	6	7
$\chi^2 = 0.802, p = 0.670, df = 2$			

It can be noted that in scenario 3, 10 participants from the technical groups did not understand the risk while 9 participants from the non-technical version claimed that the icon used did not convey risk. Surprisingly, the number of participants who understood the risk from the non-technical group was larger than the technical group however the difference was also not statistically significant ($p=0.866$). These results also had the least “Yes” choice as compared to

other scenarios. It can be assumed that the question marks icon did not convey the risk communication in a good manner. Users might not realised the importance of responding correctly to the email attachment dialogs since the signal words and icons are not properly utilised.

TABLE XI. THERE IS NO DIFFERENCE BETWEEN TECHNICAL AND NON-TECHNICAL PARTICIPANTS IN TERMS OF “THE USE OF VISUAL / GRAPHICS (E.G. ICONS, COLORS, GRAPHICS) HELPS ME TO UNDERSTAND THE RISK” (H2) BASED ON SCENARIO 3

Icon Understanding	Yes	No	Neutral
Technical	15	10	5
Non-Technical	17	9	4
$\chi^2 = 0.289, p = 0.866, df = 2$			

Table XII shows that the result was not statistically significant ($p=0.936$). It can be found that 22 participants with technical background can understand the words used easily rather than 23 participants from the non-technical background. The words used in the security warnings were trustworthy and .exe. It can be noted that majority of the participants (75%) able to understand the words easily. This might be resulted from the text message that contains the less or minimal technical words. Hence, both groups of users could better comprehend the message in the dialog.

TABLE XII. THERE IS NO DIFFERENCE BETWEEN TECHNICAL AND NON-TECHNICAL PARTICIPANTS IN TERMS OF “THE WORDS USED IN THE WARNING IS EASY TO UNDERSTAND” (H3) BASED ON SCENARIO 3

Words Understanding	Yes	No	Neutral
Technical	22	5	3
Non-Technical	23	4	3
$\chi^2 = 0.133, p = 0.936, df = 2$			

VI. DISCUSSION

One of the main elements that contributed to the attention of users towards warnings is the signal icons and signal words. With the focus of signal words and signal icons, three hypotheses have been constructed to test the usability of the security warning dialogs. It can be revealed that from the three hypotheses for each scenario, only one hypothesis is significant which is H3 for scenario 1 ($p=0.049$). Although most of the scenarios hypotheses are not statistically significant, but it give some indication and basis on how within small sample of participants perceive security cues (i.e. icons an words). The results shows that in terms of icon attractiveness and words understanding, majority of the participants chose scale of (5-7) which reflects their high preference (i.e. Yes) regardless of their study background or major. This result also indicates that the icons and signal words do attracts both groups and there is no significance difference between the two groups in perceiving the signal icon and signal words in general. In addition, it can be noted that in terms of risk understanding of security warnings, more users have better awareness when the exclamation mark icon is presented. Since precaution from possible malwares attacks is important, security warnings

should presents an icon that presents caution in more explicit manner (i.e. rather than using question mark icons which is meant for help). One of the notable findings from the study is within scenario 1. It can be found that the non-technical people have the difficulties in understanding the words (i.e. technical jargons) in the warning. This results shows that it is important to have simpler words that can be understood by users. The similar findings are discovered by [6,14] where they claimed that technical words in warning dialogs should be easy to comprehend. Hence it can be summarised that security warnings should exhibit precise icons with more user-friendly word that could cater for both technical and non-technical users.

VII. CONCLUSION

Security warning is a form of communication that would always be encountered by the end users in order to protect their computer system from being harmed. The hypotheses results revealed that there is no difference between the technical and no-technical participants in perceiving the signal icons and signal words in most of the scenarios. Although the outcome of the Chi-square test did not produce a statistically significant results (i.e. except in one scenario case), the frequency of participants who opt for scale (i.e. point 5-7 – “Yes”) are consistently high. It is believed that given the bigger sample size and different range of end-users’ background might give different impact in regards to the experiments conducted (i.e. testing the hypotheses). Having said that, it can be ascertained that the direction of this research can be expanded further in order to improve the risk communication. On the other hand, it can be noted that the total of participants in this survey is quite low. Given bigger sample size, the results might be different. In addition to that, the effects of habituation in security warnings (i.e. with the usage of signal icons and signal words) potentially can be experimented to find the cause for failure in attention towards warning. In conclusion, this research has shown that the signal words and icons in warnings via symbolism are essential elements in security warnings presentation. Hence the usability of security warning can be further improved for a better risk communication.

ACKNOWLEDGMENT

Token of appreciation to those participate directly or indirectly in this work. This work is supported by a short term grant from the Universiti Sains Malaysia (USM) [304/PKOMP/6313287].

REFERENCES

- [1] B. Jung, I. Han, and S. Lee, “Security threats to Internet: a Korean multi-industry investigation,” *Information & Management*, 38, 8, 2001 pp. 487-498.
- [2] Microsoft, “Warning Messages.” [Online]. Available at: <https://msdn.microsoft.com/en-us/library/dn742473.aspx>, 2015.
- [3] Thermopylae, “Human process visual data better.” [Online]. Available at: <http://www.t-sciences.com/news/humans-process-visual-data-better>, 2014.
- [4] S. M. Furnell, A. Jusoh, D. Katsabas and P. S. Dowland, “Considering the usability of end-user security software”, Proceedings of 21st IFIP International Information Security Conference (IFIP SEC 2006). Karlstad, Sweden, 2006, pp. 307-316.
- [5] Z. F. Zaaba, S. M. Furnell, and P. S. Dowland, “A study on improving security warnings.” In proceedings of the Fifth International Conference

- on Information and Communication Technology for The Muslim World (ICT4M). Kuching, Malaysia, 2014, pp. 1-5.
- [6] C. Bravo-Lillo, L. F. Cranor, J. S. Downs, S. Komanduri and M. Sleeper, "Improving computer security dialogs." *Human-Computer Interaction – INTERACT 2011*, 6949, 2011, pp. 18-35.
- [7] S. Egelman, L. F. Cranor and J. Hong, "You've been warned: an empirical study of the effectiveness of web browser phishing warnings." In proceeding of the twenty-sixth annual SIGCHI conference on Human factors in computing systems. Florence, Italy, 2008, pp. 1065-1074.
- [8] S. Chiasson, M. Modi and R. Biddle, "Auction hero: The design of a game to learn and teach about computer security." In World Conference on E-Learning in Corporate, Government, Healthcare, and Higher Education, 2011, pp. 2201–2206.
- [9] N. Virvilis, A. Mylonas, N. Tsalis, and D. Gritzalis, "Security Busters: Web browser security vs. rogue sites" *Computers & Security*, 52, 2015, pp. 90-105.
- [10] M. S. Wogalter, "Purposes and scope of warnings." *Handbook of Warnings*, USA: Lawrence Erlbaum Associate, ISBN 0-8058-4724-3, 2006, pp. 3-9.
- [11] W. A. Rogers, N. Lamson, and G. K. Rousseau, "Warning research: An integrative perspective." *Human Factors: The Journal of the Human Factors and Ergonomics Society*, 42, 1, 2000, pp. 102-139.
- [12] C. Bravo-Lillo, "Improving computer security dialogs: An exploration of attention and habituation." Phd Thesis. Carnegie Mellon University, 2014.
- [13] T. Whalen and K. M. Inkpen, "Gathering evidence: use of visual security cues in web browsers." *Graphics Interface*, 2005, pp. 137–144.
- [14] Z. F. Zaaba and K. B. Teo, "Examination on usability issues of security warning dialogs". *Journal of Multidisciplinary Engineering Science and Technology*, 2, 6, 2015, pp. 1337-1345.
- [15] T. S. Amer, and J. B. Maris, "Signal words and signal icons in application control and information technology exception messages – hazard matching and habituation effects." *Journal of Information Systems*, 21, 2, 2007, pp. 1-22.
- [16] M. M. Althobaiti and P. Mayhew, "Users' awareness of visible security design flaws" *International Journal of Innovation, Management and Technology*, 7, 3, 2016, pp. 96-100.
- [17] L. Zhang-Kennedy, "Improving mental models of computer security through information graphics." Msc. Thesis, Carleton University, 2013.
- [18] D. Betram, "Likert Scales." Topic Report, The Faculty of Mathematics University of Belgrad, 2009.
- [19] K. Krol, M., Moroz and M. A. Sasse, "Don't work. Can't work? Why it's time to rethink security warnings." In proceedings of the Seventh International Conference on Risks and Security of Internet and Systems (CRISSIS). Cork, Ireland, 2012, pp. 1-8.
- [20] C. Albrecht, "Contingency Tables and the Chi Square Statistic." [Online]. Available at: <https://extension.usu.edu/evaluation/files/uploads/Start%20Your%20EnEngi/Study%20the%20Route/Analyze%20the%20Data/Interpreting%20Chi%20Square.pdf>, n.d.
- [21] E. McCrum-Gardner, "Which is the correct statistical test to use?" *British Journal of Oral and Maxillofacial Surgery*, 46, 1, 2008, pp. 38-41.
- [22] Windows Security, "Using Windows Security Center." [Online]. Available at: <http://windows.microsoft.com/en-ca/windows-vista/using-windows-security-center>, 2010.
- [23] F. Raja, K. Hawkey, S. Hsu, K. L. C. Wang, and K. Beznosov, "A brick wall, a locked door, and a bandit: A physical security metaphor for firewall warnings". Proceedings of the Seventh Symposium on Usable Privacy and Security. Pittsburgh, USA, 2011, pp. 1-20.

Cross Site Scripting: Detection Approaches in Web Application

Abdalla Wasef Marashdih and Zarul Fitri Zaaba

School of Computer Sciences,
Universiti Sains Malaysia, 11800 Minden,
Pulau Pinang, Malaysia

Abstract—Web applications have become one of the standard platforms for service releases and representing information and data over the World Wide Web. Thus, security vulnerabilities headed to various type of attacks in web applications. Amongst those is Cross Site Scripting also known as XSS. XSS can be considered as one of the most popular type of threat in web security application. XSS occurs by injecting the malicious scripts into web application, and it can lead to significant violations at the site or for the user. This paper highlights the issues (i.e. security and vulnerability) in web application specifically in regards to XSS. In addition, the future direction of research within this domain is highlighted.

Keywords—Web Application Security; Security; Software Security; Security Vulnerability; Cross Site Scripting; XSS; Genetic Algorithm; GA

I. INTRODUCTION

Web applications are becoming more important and growing in number as indicated by web browsers being used by almost everyone. Web applications have entered all areas, either for leisure or work, to manage sensitive personal and financial information [1]. These web applications are always available from anywhere with an Internet connection, and they enable us to communicate and collaborate at a speed that was unthinkable just a few decades ago. However, the presence of security vulnerabilities of web application can steal private information (e.g., cookies and session) and perform other malicious operations, and thus limit the use of applications [2].

XSS vulnerability is among the top web application vulnerability according to OWASP top 10 vulnerabilities [4]. The vulnerabilities can lead to significant violations at the site or for the user by injecting malicious scripts to be accepted later by the user. However, if there is no validation on the input of the application, then the malicious code can steal sessions, cookies, or inject and show private data for the user [5,6].

XSS vulnerability is among the top web application vulnerability according to OWASP top 10 vulnerabilities [4]. The vulnerabilities can lead to significant violations at the site or for the user by injecting malicious

The focal point of the study is to investigate the problems, challenges, and approaches to detect XSS vulnerabilities. This paper summarizes the XSS vulnerability on web application. Section II discusses the concept of web application. Section III further explains web application security. Section IV describes

web application vulnerability. Section V and VI narrow the discussion in regards to XSS and the detection approaches. Section VII highlights the related work that has been gathered. Section VIII is a discussion of related work and finally ending with conclusion and future works.

II. WEB APPLICATION

A web application utilizes web and browser technologies to perform tasks over a network using a web browser [7]. The web applications are stored on the web servers, where all their data are stored. Thus, users do not need to spend extra time on hard drives for installation. Some of the popular technologies that help software developers create dynamically generated web pages are PHP, ASP.NET, and Java server pages (JSP) [8].

PHP is easy to use for learning and for building websites, whereas PERL syntax is difficult for beginners to handle. ASP.NET is a product of Microsoft, is only possible in a Windows machine, and is not free. By contrast, PHP is completely free and is an open source. JSP is slower than PHP because JSP libraries are often written for “correctness” and readability but not for performance. Python hosting is hard to find and expensive, while cheap PHP hosting is everywhere. While PHP can mix with HTML in their source code, Python cannot be mixed with HTML (because it needs a template library). Therefore, PHP is the most popular scripting language and is the most commonly used in web applications.

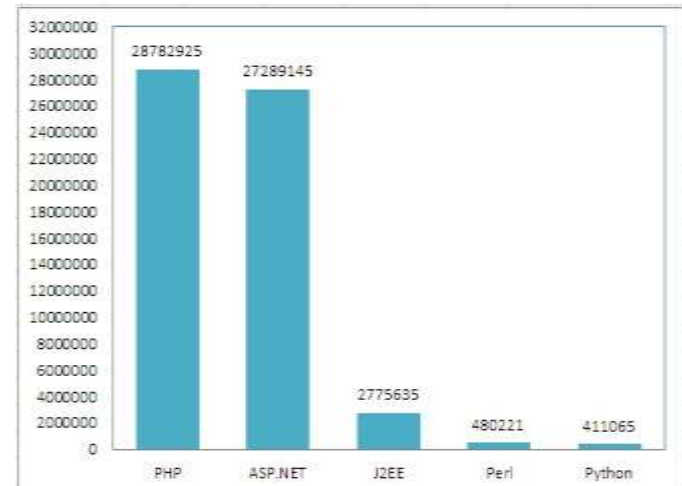


Fig. 1. Usage Statistics of Web Technologies [8]

Fig. 1 shows that PHP is used by more than 28,782,925 websites, thus making it the most used language. PHP is followed by ASP.NET. Statistics show that these two languages dominate all other languages. The number of PHP websites is greater than that of other websites using other web technologies. The user chooses the type of technology to build the website depending on his/her knowledge and the requirements of the facilities offered by the technologies. However, the lack of security of PHP web applications is caused by many programmers', because they do not have enough experience in securing their codes, which makes the applications flawed.

III. WEB APPLICATION SECURITY

Web application security is the practice of safeguarding confidential information stowed online from unlawful access and alteration. It is accomplished by imposing strict policies and practices [12]. In the software domain, security susceptibility is a flaw which could empower an attacker to compromise the veracity, accessibility, or confidentiality of a product. Several web applications set up on the Internet are subjected to security vulnerabilities. According to [13], more than 80% of the websites had experienced at least one grave of vulnerability. Web application security is expected to possess the security properties mentioned below:

- Input Authenticity: The user input should be authenticated before its use by the web application.
- State Integrity: The application state should be maintained unconstrained.
- Logic Exactness: The application logic should be implemented properly, as conceived by the developers.

A web application can be safeguarded through multiple means – for example, administering secure configuration, deploying a secure coding practice, conducting vulnerability evaluation, and employing a web application firewall. However, the total safeguard of the application is not possible. Web applications entail a defence-in-depth tactic to evade and alleviate security vulnerabilities. According to [14], the following is the threat model:

- The application is nonthreatening and hosted on a reliable and hardened infrastructure, i.e. the trusted computing base.
- The attacker hold the potential to regulate or influence the contents or the order of web requests directed towards the web application.

Sometimes, a web application might fail to hold the input validity property. In such a case, the attacker could initiate an XSS attack to thieve the session cookie of the victim, thereby causing an abuse of state integrity property. However, as

mentioned earlier, an exhaustive safeguard of the application is impossible. The emphasis of this paper is on vulnerabilities in input validation, considering that input validity has been noted as the top security vulnerability for web applications (for example, XSS and SQL injection) [16]. In the next section, few of the major vulnerabilities of web applications are outlined.

IV. WEB APPLICATION VULNERABILITY

Application susceptibility is described as a system imperfection or weakness which could be manipulated to compromise the application's security. Attackers are able to abuse the application susceptibility to trigger a cybercrime once they have noted a weakness or vulnerability which can be overpowered [16]. OWASP is a security community which emphasizes on enhancing software security. In 2010, it came up with its annual report that noted the topmost threats and vulnerabilities in web application development; the report was updated in 2013 [4]. Here are the 10 key vulnerabilities identified by OWASP: injection, broken authentication and session management, XSS, insecure direct object references, security misconfiguration, sensitive data exposure, missing function level access control, cross-site request forgery (CSRF), use of components with known vulnerabilities, and invalidated redirects and forwards.

XSS is the most susceptible security threat according to the list [2,4]. The latest report was released in 2013 (Fig. 2), and there has been no new report after that. Veracode, an application security enterprise, has released its state of software security from 2013 until 2015. The report gives information about the number of vulnerabilities for every web technology [17]. A study covering the entire web applications noted that XSS accounts for 25 percent of the vulnerabilities [18].

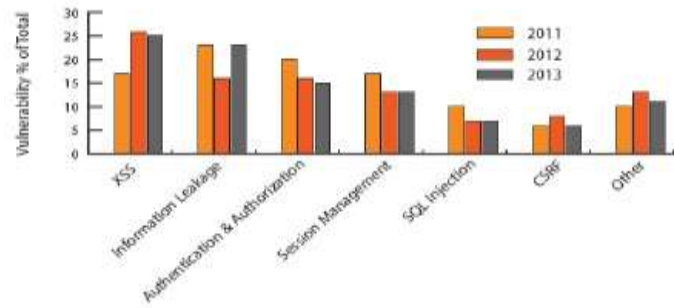


Fig. 2. 2011 vs 2012 vs 2013 Web Application Trends [18]

XSS offers an opening to the invader or hacker to enter the webserver database, mutilate websites, seize the web browser of a user remotely, and compel him/her to take an unfamiliar route [18]. Veracode's state of software security report emphasized on application development and scrutinized over 200,000 individual applications from the period October 2013 to March 2015 [16].

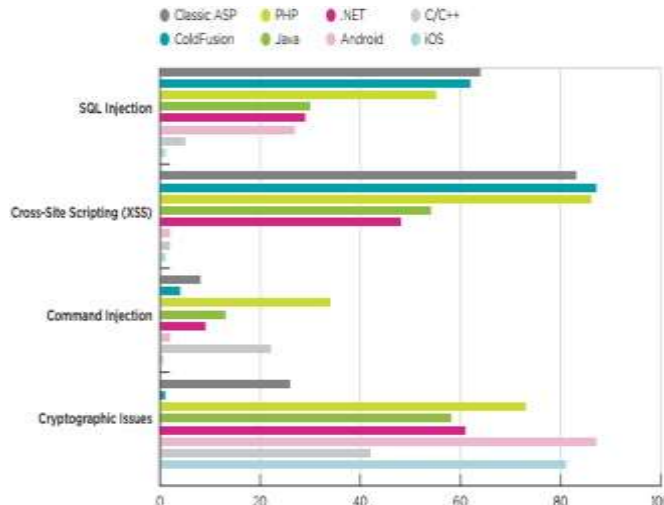


Fig. 3. Comparison of Critical Vulnerability Types [16]

As can be seen in Fig. 3, around 86 percent of PHP and ColdFusion applications comprised at least one XSS susceptibility. SQLi is precarious and easy-to-abuse web application susceptibility. It comprises 62 percent of ColdFusion and 56 percent of PHP applications. ColdFusion is feeble when it comes to supporting OOP, and hence it might jeopardise input validity. Around 58 percent of PHP applications face issues with credentials management, whereas 73 percent of PHP applications involve cryptographic problems. According to [18], XSS vulnerability is the foremost susceptibility among the existing web applications. It is termed as the foremost vulnerability as it offers the basis for other kinds of attacks, including CSRF and session hijacking [19]. Moreover, XSS can inflict damage on website users as well as owners. It easily manipulates and is tough to alleviate. The next section deliberates and elucidates XSS susceptibility.

V. CROSS SITE SCRIPTING (XSS)

XSS is termed as a key threat to web application security. Research is in progress to detect an effectual and convenient mode of analyzing the source code of web applications and eliminating the threat. XSS is triggered by inserting spiteful scripts into the application, causing substantial abuses for the user or at the site. The malicious scripts are inserted at a place where an application admits user input; in case the input is not authenticated, the malicious code can thief cookies or user accounts, or transfer private information [5,6]. These contaminated data might comprise portions of HTML code (for example, JavaScript) which may run into the page being attacked.

According to [19], there are four classes of XSS attacks: (i) stored (persistent); (ii) reflected (non-persistent); (iii) induced-XSS; and (iv) Dom-based XSS. The former two are the most commonplace, while the latter two are lesser known XSS attacks.

A. Stored (persistent) XSS

This susceptibility is triggered when the infused malicious code is forever stored on the victim servers. First, the attacker attempts to detect susceptibility in the web application so that

he/she can inject the malicious script. Next, the attacker robs the confidential information of the users or inflicts other kinds of damages or risks [19].

The threat is more pronounced when this malicious script is forever stored on the server. The malicious script is affected when a user accesses the information by means of the web application, thus allowing the attacker access to it. According to [20], the persistent XSS is more menacing and devastating compared to other types of XSS vulnerabilities. Pure statistical analysis gives a false positive rate that is on the higher side.

B. Reflected (non-persistent) XSS

There is a difference between reflected XSS attacks and stored XSS attacks. Reflected XSS attacks manipulate website elements which reverberate clients' supplied data, including forms. The injected code is not located on the server. The attacker creates a crafted URL that involves a malicious script code, enticing the victim to believe that the URL is reliable [21]. The malicious links are delivered to victims through an email or by embedding the link into a web page which is located on some other server. The injected code is despatched to the web server of the attacker once the user clicks on the link, and the attack is then launched on the target browser.

C. DOM-based XSS

A Dom-based XSS attack is triggered on the client side [19]. DOM allows dynamic scripts, including JavaScript, to reference the document's components – for example, a session cookie or a form field. Such susceptibility could be triggered when an active content (for example, a JavaScript function) is altered by a specially created request, allowing a DOM element to be manipulated by an attacker.

D. Induced XSS

In an induced XSS attack when a web server has an HTTP response splitting susceptibility [7]. The attacker is able to abuse the HTTP header of the server's response in this case. Both Dom-based XSS and induced XSS attacks are uncommon but still mentioned here to ensure the classification is exhaustive.

In contemporary web applications, XSS is a security issue that is exploited the most often [16, 17]. Persistent and non-persistent vulnerability can be observed on either server side or client side codes. However, DOM XSS is only noted in the client side [19]. Much research has concentrated on detecting XSS vulnerability [23, 24, 25, 26, 27]. However, research is still on to determine an effectual and suitable mode of analyzing the source code and identifying the XSS susceptibility in web applications.

VI. DETECTION OF XSS VULNERABILITY

Detecting susceptibility is a process of locating the weaknesses stated in the application's source code. Several web applications utilize the values furnished by users directly in the HTML exhibited in the browser [22]. This input can be fashioned to alter the contents of the web page that the victim can see, thus vesting the control with the attacker. The most standard approaches to spot vulnerabilities are categorized into dynamic analysis, static analysis, and hybrid analysis [15].

A. Static Analysis

Static analysis establishes the fundamental reason behind the security issue. It can detect errors in the initial stages of development and before the program is executed for the first time. The code coverage in static analysis is better compared to dynamic analysis. However, it is not much accurate as it is unable to access runtime information for the evaluated program [15]. Considering the nature of static analysis, approximations are carried out, which might lead to several false positives, i.e. reported vulnerabilities which are not truly vulnerabilities. [11] made a comparison of the different static analysis methods deployed to find out the various kinds of vulnerabilities from the program source code (lexical analysis, data flow analysis, symbolic execution, type inference, and constraint analysis). The data flow analysis approach is deployed to gather dynamic data from the source code. Static taint analysis is a special case of such type of analysis.

B. Dynamic Analysis

Dynamic analysis takes place when a security tool dynamically strikes the running application on the basis of thousands of identified vulnerabilities and attack designs [15]. In spite of utilizing static analysis to locate vulnerabilities in different domains, this method is still ineffective as it has a tendency to come up with false positive and false negative outcomes. Dynamic analysis exposes vulnerabilities by examining the information attained during program implementation.

C. Hybrid Analysis

The hybrid approach combines static and dynamic analysis, wherein the dynamic analysis methods build up on the false alarms of the static analysis methods and offer accurate results. A technique to assist with security auditing and testing offers probabilistic alarms on possibly susceptible code statements.

[10] made a comparison of malware detection approaches on the basis of the dynamic, static, and hybrid analyses. The outcomes of the rates of detection were compared over a considerable number of malware families (Zbot, Security Shield, Smart HDD, Winwebsec, ZeroAccess, Harebot) [10]. The fully static approach is almost effectual in the majority of the circumstances based on API calls. The outcomes of the experiment suggest that a forthright hybrid approach might not be better than a fully dynamic detection or a fully static detection. Conversely, a static/dynamic methodology does not provide a steady improvement.

D. Genetic Algorithm

A genetic algorithm is a search heuristic which simulates the natural selection process. This heuristic (sometimes known as a metaheuristic) is usually used to come up with suitable solutions that can address search and optimization-related issues. Genetic algorithms are founded on the evolutionary notions of natural selection and genetics. Thus, they signify an intelligent manipulation of a random search deployed to address optimization issues [9]. The elementary genetic algorithm steps are converted into a pseudocode (Fig. 4).

```
population = generate_random_population();
for(T in vulnerable paths) {
    while(T not covered AND attempt < max_try) {
        selection = select(population);
        offspring = crossover(selection);
        population = mutate(offspring);
        attempt = attempt + 1;
    }
}
```

Fig. 4. Genetic Algorithm Pseudocode [27]

1) *Initial population:* The most customary kind of encoding or representing chromosomes in genetic algorithms is the binary format. The genetic algorithm population is a suite of likely solutions for a problem.

2) *Fitness function:* This is the assessment of chromosomes as to how effective they are at addressing the issue. The closer the chromosome is to address the issue, the higher is its fitness value.

3) *Selection:* This stage intends to choose the fittest chromosome to reproduce as per certain selection techniques. A chromosome is chosen as per the fitness value to carry on in the next generation.

4) *Crossover and mutation:* This is an offspring produced by perturbing the chosen candidates using genetic operators – for example, mutation rate and crossover rate. The crossover operation combined two chromosomes to reproduce a new solution with better traits. On the other hand and according to specific mutation probability, the mutation operation occurs by altering the chromosome values.

The primary individual population is generated by the high-quality GA of the individuals. A solution is represented by

each individual for the problem [3]. Table (1) presents a review of the approaches, areas of focus, and limitations of detecting XSS vulnerability.

TABLE I. REVIEW APPROACHES AND THEIR FACILITIES IN DETECTION XSS VULNERABILITIES

Article	Approach	Area on focus	Limitation
Shar and Tan [23]	Static Analysis (JAVA)	Detection of SQL Injection and XSS vulnerabilities.	High false positive rate in their detection results.
Toma and Islam [24]	Dynamic Analysis (Javascript)	Detection XSS vulnerability and applied it during the run.	They focused on some types of XSS vulnerability, and their results still not accurate.
Shar, et al. [25]	Hybrid Analysis (PHP)	Detection SQL injection and XSS vulnerabilities.	It is not accurate as full dynamic or static approach.
Avancini and Ceccato [26]	Genetic Algorithm + Static Analysis (PHP)	Detection XSS vulnerability in PHP Web applications.	They detect reflected XSS only.
Hydara et al. [27]	Genetic Algorithm + Static Analysis (JAVA)	Detection XSS vulnerability in JAVA.	The other language is still out side of their area.

As shown in Table 1, [23] use of static analysis still generates false negative and false positive results; and this finding is the main limitation of static analysis while it is executed before the run.

Hybrid analysis combines static and dynamic analyses as a better approach, but the combined approach was focused on to benefit from the two types of analyses (static and dynamic) [25]; nevertheless, it still has some problems in terms of the accuracy of its result, such as the training data.

In PHP, [26] detected one type of reflected XSS vulnerability. On the other hand, [27] proposed an approach based on static analysis with GA on Java web applications. Their approach combines the detection approach from [26] and the removal approach from [25]. [27] approach detects XSS vulnerabilities with significant results as compared with the approach of [25]. However, their approach is only available for Java web application.

VII. RELATED WORK

While there are many approaches used to detect XSS vulnerability in the source code [23,24,25,26,27]. However, research is still on to determine an effectual and suitable mode of analysing the source code and identifying the XSS susceptibility in web applications. [23] proposed an approach to detect XSS vulnerability by using static analysis in Java web application. However, their approach still generates false negative and false positive results; and this finding is the main limitation of static analysis while it is executed before the run. On the other hand, [24] construct the JavaScript's call graph by using dynamic analysis, in a way to secure the client side of web application. Dynamic analysis used to find the limitations

of the graphs art. Then, they evaluated their approach in regards of accuracy, and the results shown that their approach is acceptable.

[25] proposed attributes to check the input validation from SQL injection and XSS vulnerabilities based on hybrid analysis. They adopted static analysis to classify the nodes and dynamic analysis to find the vulnerable nodes. However, the static analysis still imprecise in classification of such nodes. The authors performed the experiments in six PHP web applications, and their results seems to be promised in the future. [26] presented an approach based on taint analysis with GAs as a method to improve taint analysis. They used taint analysis to find the vulnerable paths from the control flow of the program execution. Then, genetic algorithm defines security test cases by re-sorting the paths that enable the execution flow to traverse target paths. They employed the Pixy tool to report the control flow paths from the source code; these paths represent the target paths for genetic search. As their approach is only for detecting the reflected XSS vulnerability in the PHP web application.

[27] used static analysis with genetic algorithm, in a way to minimize the false positives rate in static analysis results. Their results minimize the false positive after embed genetic algorithm with static analysis, and they detect all vulnerabilities in JAVA web applications. Furthermore, the detection of vulnerabilities before run the program for the first time will minimize the threats on applications, rather than dynamic analysis which requires the actual run of the program, and that may leads to security vulnerabilities if they do not detect it quickly.

VIII. DISCUSSION

We discussed the general approaches used to detect XSS vulnerabilities and differentiate their methods in detecting XSS vulnerabilities in Table 1. [26,27] used genetic algorithm with static analysis in a way to decrease the false positive rate in their results. [26] detected one type of reflected XSS vulnerability in PHP web applications using static analysis and GA. However, their approach will be argued because some paths in the source code cannot be executed. To detect XSS vulnerabilities without any false positive results, they need to remove the infeasible paths from the control flow graph. Once they remove the infeasible paths, they will detect the actual XSS vulnerability from the source code without any false positive in their results. [27] detected the three types of XSS vulnerability. While they detected all XSS vulnerabilities in Java source code, their approach still reveals false positive results. Therefore, the removal of the infeasible paths help to minimize the false positive results, because when the GA generator runs only on the feasible paths, it will be more fast and accurate to find the results. Therefore, to complete the approach of using GA with static analysis, the researchers should remove the infeasible paths from the control flow graph, in a way to minimize the false positive rate in their results.

IX. CONCLUSION

Web applications have been deployed to the public with unexpected security holes. The reason for these security holes

is mainly the short time frame of this program's development. Although research on security programs is modern, effective solutions are highly demanded because of the importance of creating programs that are secure and less vulnerable to attacks. Cross-Site Scripting (XSS) vulnerability is one of the most common security problems in web applications. It can lead to the stealing of cookies and user accounts and to the transferring of private data if the input is not validated. While there are many studies have been conducted to address problems related to XSS vulnerability, but their results seems to be not efficient to address the problem as well. Static analysis still contains many false positive and the dynamic analysis still need to improve the accurateness of the results. However, the hybrid approach is not efficient as the fully static or dynamic approaches. On the other hand, genetic algorithm used to detect XSS vulnerability. Genetic algorithm successes to detect all XSS vulnerability in JAVA web application without any false positive results. However, when the researchers implement it in PHP, their results still contain many false positive results, because they did not remove the infeasible paths from the Control Flow Graph.

The future work should involve the removal stage of the infeasible paths from the control flow graph that will lead to minimize the false positive rate in their results and to detect all XSS vulnerability from the source code as well. Since GA has proven to be effective in detection of XSS vulnerabilities, it can used for other web security vulnerabilities, such as (SQL Injection, insecure direct object references and cross-site request forgery).

REFERENCES

- [1] Zhao, J. and Gong, R. "A New Framework of Security Vulnerabilities Detection in PHP Web Application," *Proc. Int. Conf. on Innovative Mobile and Internet Services in Ubiquitous Computing (Munich)*, pp 271-276, 2015.
- [2] Gupta, M. Govil, M. and Singh, G. "Predicting Cross-Site Scripting (XSS) Security Vulnerabilities in Web Applications," *Proc. Int. Joint Conf. on Computer Science and Software Engineering (JCSSE)*, pp 162-167, 2015.
- [3] Gupta, P. and Shinde, S. K. "Genetic algorithm technique used to detect intrusion detection," *Advances in Computing and Information Technology* Springer, vol. 198, pp 122-131, 2011.
- [4] OWASP 2013 Top-10 threats for web application security -2013 [Online] Available: https://www.owasp.org/index.php/Top_10_2013-T10. [Accessed : 23/2/2016]
- [5] Guo, X. Jin, S. and Zhang, Y. "XSS Vulnerability Detection Using Optimized Attack Vector Repertory," *Proc. Int. Conf. on Cyber-Enabled Distributed Computing and Knowledge*, pp 29-36, 2015.
- [6] Dong, G. Zhang, Y. Wang, X. Wang, P. and Liu, L. "Detecting Cross Site Scripting Vulnerabilities Introduced by HTML5," *Proc. Int. Joint Conf. on Computer Science and Software Engineering (JCSSE)*, pp 319-323, 2014.
- [7] Sadana, S. J. and Selam, N. "Analysis of Cross Site Scripting Attack," *Proc. International Journal of Engineering Research and Applications (IJERA)*, vol. 1, no 4, pp 1764-1773, 2011.
- [8] Mishra, A. "Critical Comparison Of PHP And ASP.NET For Web Development - ASP.NET & PHP," *Proc. International Journal of Scientific & Technology Research*, pp 331-333, 2014.
- [9] Duchene, F. Groz, R. Rawat, S. and Richier, J. "XSS Vulnerability Detection Using Model Inference Assisted Evolutionary Fuzzing," *IEEE Fifth Int. Conf. on Software Testing, Verification and Validation*, pp 815-817, 2012.
- [10] Damodaran, A. Troia, F. D. Corrado, V. A. Austin, T. H. and Stamp, M. "A Comparison of Static, Dynamic, and Hybrid Analysis for Malware Detection," *Journal of Computer Virology and Hacking Techniques*, pp 1-12, 2015.
- [11] Bingchang, L. Shi, L. and Cai, Z. "Software Vulnerability Discovery Techniques: A Survey," *Fourth Int. Conf. on Multimedia Information Networking and Security*, pp 152-156, 2012.
- [12] Kumar, R. "Mitigating the authentication vulnerabilities in Web applications through security requirements," *Information and Communication Technologies (WICT)*, vol. 60, pp 651-663, 2011.
- [13] Thankachan, A. Ramakrishnan, R. and Kalaiarasi, M. "Web application security vulnerabilities detection approaches: A systematic mapping study," *Software Engineering, Artificial Intelligence, Networking and Parallel/Distributed Computing (SNPD)*, pp 1-6, 2015.
- [14] Thankachan, A. Ramakrishnan, R. and Kalaiarasi, M. "A Survey and Vital Analysis of Various State of the Art Solutions for Web Application," *Security Information Communication and Embedded Systems*, pp 1-9, 2014.
- [15] Gupta, M. K. Govil, M. C. and Singh, G. "Static Analysis Approaches to Detect SQL Injection and Cross Site Scripting Vulnerabilities in Web Applications: A Survey," *IEEE Int. Conf. on Recent Advances and Innovations in Engineering (ICRAIE-2014)*, pp 1-5, 2014.
- [16] Veracode 2015b Application Security Vulnerability: Code Flaws, Insecure Code [Online] Available: <http://www.veracode.com/security/application-vulnerability>. [Accessed : 13/4/2016]
- [17] Shanmugasundaram, G. "A study on removal techniques of Cross-Site Scripting from web applications," *Proc. Int. Conf. on Computation of Power, Energy, Information and Communication*, pp 0436-0442, 2015.
- [18] Gupta, B. "Cross-Site Scripting (XSS) attacks and defense mechanisms: classification and state-of-the-art," *National Institute of Technology Kurukshetra* (Kurukshetra, India), pp 1-19, 2015.
- [19] Malviya, V. K. Saurav, S. and Gupta, A. "On Security Issues in Web Applications through Cross Site Scripting (XSS)," *Asia-Pacific Software Engineering Conf.*, pp 583-588, 2013.
- [20] Li, Y. Wang, Z. and Guo, T. "Program Slicing Stored XSS Bugs in Web Application," *Fifth IEEE Int. Conf. on Theoretical Aspects of Software Engineering*, pp 191-194, 2011.
- [21] Li, Y. Wang, Z. and Guo, T. "Reflected XSS Vulnerability Analysis," *International Research Journal of Computer Science and Information Systems (IRJCSIS)*, vol. 2, pp 25-33, 2013.
- [22] Fonseca, J. and Vieira, M. "A Practical Experience on the Impact of Plugins in Web Security," *IEEE 33rd Int. Symposium on Reliable Distributed Systems*, pp 21-30, 2014.
- [23] Shar, L. K. and Tan, H. B. K. "Automated removal of cross site scripting vulnerabilities in web applications," *Inf. Softw. Technol.*, vol. 54, pp 467-478, 2012.
- [24] Toma, T. R. and Islam, Md. S. "An Efficient Mechanism of Generating Call Graph for JavaScript using Dynamic Analysis in Web Application," *3rd Int. Conf. on Informatics, Electronics & Vision*, pp 1-6, 2014.
- [25] Shar, L. S. Tan, H. B. K. and Briand, L. C. "Mining SQL injection and cross site scripting vulnerabilities using hybrid program analysis," *Proc. of Int. Conf. on Software Engineering (ICSE '13)* IEEE Press, pp 642-651, 2013.
- [26] Avancini, A. and Ceccato, M. "Towards Security Testing with Taint Analysis and Genetic Algorithms," *ICSE Workshop on Software Engineering for Secure Systems*, vol. 5, pp. 65-71, 2010.
- [27] Hydara, A. I. Sultan, Md. Zulzalil, H. and Admodisastro, N. "An Approach for Cross-Site Scripting Detection and Removal Based on Genetic Algorithms," *Ninth Int. Conf. on Software Engineering Advances*, pp 227-232, 2014.

A Parallel Fuzzy-Genetic Algorithm for Classification and Prediction

Hassan Abounaser

Computer Engineering Department
Arab Academy for Science,
Technology and Maritime Transport
(AASTMT)
Cairo, Egypt

Ihab Talkhan

Computer Engineering Department
Cairo University
Cairo, Egypt

Ahmed Fahmy

Computer Engineering Department
Arab Academy for Science,
Technology and Maritime Transport
(AASTMT)
Cairo, Egypt

Abstract—One of the top challenging problems in data mining domain is the distributed data mining (DDM) and mining multi-agent data. In distributed environment, classical techniques require that the distributed data be first collected in a data warehouse which is usually either ineffective or infeasible. Hence, mining over decentralized data sources can overcome such issues. Rule-based classifiers involve sharp cutoffs for continuous attributes. Fuzzy Logic System (FLS) has features that make it an adequate tool for addressing this shortcoming effectively and efficiently. In this paper, a framework for a Parallel Fuzzy-Genetic Algorithm (PFGA) has been developed for classification and prediction over decentralized data sources. The model parameters are evolved using two nested genetic algorithms (GAs). The outer GA evolves the fuzzy sets whereas the inner GA evolves the fuzzy rules. During optimization, best rules are only distributed among agents to construct the overall optimized model. Several experiments have been conducted over many benchmark datasets. The experiment results show that the developed model has good accuracy and more efficient in performance and comprehensibility of linguistic rules compared to some models implemented in KEEL software tool.

Keywords—Fuzzy Classification; Rule-Base; Fuzzy Logic System (FLS); Genetic Algorithm; Distributed Data Mining (DDM)

I. INTRODUCTION

Data mining, generally, can be described as the process of transforming knowledge from data format into some other human understandable format [1]. This knowledge discovery process has many domains and application areas such as in bioinformatics [2], business analytics [3], text analysis [4], web data analysis [5], health care [1] and many other domains where there is scope for hidden information retrieval.

In literature, data mining systems can be categorized according to data type, data model, task/knowledge type, or exploration technique [1][6]. One form of data mining tasks and Machine Learning (ML) techniques is classification. Classification and prediction are forms of data analysis in order to construct models for describing important data classes or predicting future data trends [7][8]. A classifier model is constructed to predict categorical (discrete, unordered) labels while a predictor model is constructed to predict ordered or continuous valued function. These constructed models give better understanding of the data at large. For example, a marketing manager of a car agency may ask to construct a classifier model to predict to what degree a customer will

accept buying a particular car, given the car profile.

Data mining has some challenges. One of the top challenging problems in data mining domain is the distributed data mining (DDM) and mining multi-agent data [9]. In distributed environment, classical techniques require that the distributed data be first collected in a data warehouse [6]. This Collection of huge volume of data is usually either ineffective or infeasible for many reasons. For example, this may encounter problems belongs to privacy and sensitivity of data in addition to the costs in storage, communication, and computation. Hence, mining over decentralized data sources can overcome the above issues and help to reach all network-related domains. For distributed environment, numerous techniques have been developed for data classification and prediction in order to discover knowledge from distributed data effectively and efficiently [10][11][12]. However, no single data mining technique has been proven appropriate for every domain and dataset [6].

Rules are one way for representing information or bits of knowledge. Rule-based classifiers use a set of IF-THEN rules for classification [13]. However, rule-based classification systems have the shortcoming that they involve sharp cutoffs for continuous attributes. Fuzzy Logic System (FLS) has attractive features that make it an alternative tool to tackle this issue in designing data mining systems performing rule-based classification effectively and efficiently [6].

In this paper, FLS features are explored in next section. In third section, Genetic Algorithms (GAs) are presented as an example of evolutionary computing algorithms (EAs) for evolving fuzzy rule-base. In fourth section, an optimized Parallel Fuzzy-Genetic Algorithm (PFGA) is developed for classification and prediction over decentralized data sources. In fifth section, results of conducted experiments are provided, analyzed and discussed compared with some classification models implemented in KEEL software tool. Finally, a conclusion is presented.

II. FUZZY LOGIC SYSTEMS (FLSS)

One highly successful theory in Computational Intelligence (CI) techniques is fuzzy set theory [14]. The design of FLS was one of the largest application areas derived from fuzzy set theory. FLS have demonstrated their superb ability as system identification tools and has enjoyed wide

popularity in computer science and engineering as an advanced Artificial Intelligence (AI) tool and control technique [15] [16]. The strength of FLS lies in its expressive power and flexibility to handle a complex system even if no precise mathematical model of the underlying processes is available [17]. The key issue resolves around designing the required input and output fuzzy sets that define the semantic of the domain. FLS domains are characterized by linguistic labels rather than by numbers. Hence, FLS is frequently considered as computing with words rather than numbers [17]. This descriptive approach, generally, are suitable for handling the issues related to understandability of patterns, incomplete or noisy data, and can provide approximate solutions faster [18].

As graphically shown in Fig. 1, a general-purpose FLS consists of four generic components. It works by encoding an expert's knowledge into a set of IF-THEN fuzzy rules, which are smoothly interpolated, and the resultant is defuzzified to give the desired behavior in terms of crisp output. Each fuzzy rule is specified as either a trapezoid, triangular, logistic, bell shape, or some other functions, and assigned to some range of input variable. Common sense can provide good estimates for fuzzy sets and membership functions to be associated with each linguistic input and output variables. However, it is the task of the human domain expert to define the function that captures the characteristics of the fuzzy set. Since it tolerates imprecision, FLS is an attractive technique for feature classification because a given feature may have partial membership in different classes. Recent work by data mining researchers has shown that the qualitative nature of FLS makes it a formal tool for constructing classifiers that deal with problems characterized by pervasive presence of uncertainty. For example, Fuzzy-based classifier has been applied successfully in data mining for Hepatitis [19], and data mining for intrusion detection [20]. Fuzzy-based classifier, generally, consists of a set of fuzzy linguistic rules as sentences rather than equations. These fuzzy linguistic rules are easier understood than systems of mathematical equations.

A FLS, generally, is known as knowledge-based system. The Knowledge Base (KB) not only has the rule-base but it also has the fuzzy sets and membership functions of the fuzzy partitions associated to the linguistic input and output variables. Therefore, this specifies a clear distinction between the fuzzy model structure and parameters as defined in classical knowledge discovery techniques [21]. Although the above generic components are common features to all fuzzy-based systems, many design options exist based on this structure[15].

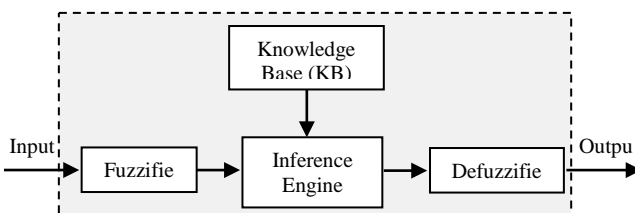


Fig. 1. The structure of a Fuzzy Logic System (FLS) and its components interconnections

Mamdani and Assilian produced the first FLS for control

in 1975 [21]. This type of FLS forms the basis for all types of FLS. It is derived directly from available heuristic control strategies mimicking the control knowledge of a human expert. FLS is statically described by linguistic rules [14]. The output fuzzy sets utilized in Mamdani-type FLS are singletons or combinations of singletons, where the combinations are achieved through application of fuzzy set operators. However, FLS generally has the advantage of allowing two design approaches. The first design approach is applied for real-world applications where the human expert knows the appropriate system response, given particular input variable scenarios. In this case, the FLS parameters can be specified, and they are static (e.g., [22]). This contrasts with Artificial Neural Network (ANN) approaches, where the user is in no position to specify weights values, even if the appropriate system response is known.

The second approach in FLS design is applied for real-world applications where the system response is not known. In this case the FLS parameters can be optimized through learning using some CI techniques such as EAs or ANN strategies, until the overall FLS response matches the desired behavior [23]. Since it is the most natural approach, the use of EAs strategies in designing FLSs is currently a hot topic in classification area and has been largely extended in the last few years to face the tradeoff between interpretability and accuracy as both requirements are clearly in conflict [21]. The developed framework in this paper adopts the second approach in design and utilizes Pittsburgh approach in learning. However, a structure of nested GAs is developed for encoding the whole KB definition such that the performance of the optimized model proposed fits the desired efficiency and accuracy.

III. EVOLUTIONARY ALGORITHMS (EAS)

Optimization is a classical problem in several domain such as in Economy and Biology among others [24]. Analytical techniques were popularly used to solve optimization problems efficiently. However, alternative and competitive methods in CI techniques have appeared such as EAs. EAs have been applied to a wide range of problem areas such as control, function optimization, regression, classification and clustering [14]. One of the most common EAs strategies is the GA. GA generally combines adaptive heuristic search along with mathematical analysis to find approximate or even true solutions for optimization problems. The technique of GAs not only provides alternative methods for solving optimization problems, but it also consistently outperforms other classical methods in most of these problems [25].

The basic concepts in designing GAs follow the principle of survival of the fittest. This principle is inspired by natural selection and natural genetics which is first laid down by Charles Darwin. Although the steps of designing GAs are simple to understand and not difficult in coding, designing a suitable GA for a real-world task is a nontrivial exercise and almost an art [14][25]. However, design a GA has the exploration-exploitation tradeoff due to the interactions between the representation, selection, reproduction, mutation, and replacement operations. The high consumption of computational resources besides this tradeoff has been the

source of active research directions to discover alternative EA strategies [14].

From coding mechanism's perspective, genetic rule-based algorithms in DM can be categorized into three approaches. The first approach is known as "Pittsburgh" approach where each individual encodes a rule set and the best individual in final population represent the rule-based classifier. The second approach is known as "Michigan" approach, where each individual encodes a single rule and the final population represents the rule-based classifier. The third approach is known as Iterative Rule Learning (IRL) approach, where each individual also encodes a single rule but each rule of the rule-based classifier is obtained from each run [8]. The developed framework in this paper utilizes Pittsburgh approach in learning, as mentioned earlier.

IV. PROPOSED PARALLEL FUZZY-GENETIC ALGORITHM (PFGA) FOR CLASSIFICATION AND PREDICTION

A. Fuzzy Logic Classifier & Predictor

The behavior of the FLS is determined by a number of parameters such as the fuzzy sets, the membership functions, and the structure and entries in the Fuzzy Associative Memory (FAM) matrix or fuzzy rules. In addition, some FLSs include parameters that assign a weight for each fuzzy rule to indicate its relative importance in the overall FLS behavior. All of these parameters are possible candidates for optimization using EA strategies, for example. However, it's a daunting task for code developers to design a FLS that optimizes all of these parameters. In this research, the fuzzy sets and the fuzzy rule-base are both the candidates for optimization since they have the most influence in determining the FLS behavior.

A classifier or predictor model is a decision rule that assigns a class to every data point in attribute/feature space. Expert knowledge, in classification and prediction domain, can be effectively used to design a FLS as a set of flexible overlapping fuzzy rules that can be evolved in order to construct an adaptive model that approximate human reasoning in this domain. The fuzzy rules actually represent direct linguistic description of the particular relationships between the given attributes/features and their assigned class. Equation (1) represents the general form of a fuzzy rule:

$$R_i: \text{IF } (x_1 = A_1) \text{ AND } \dots \text{ AND } (x_n = A_n) \text{ THEN } (y = C) \quad (1)$$

Where: R_i is fuzzy rule label number i in rule-base

n is the number of attributes in dataset

x_1, \dots, x_n are input linguistic variables

y is the class linguistic variable

A_1, \dots, A_n are terms in input domains

C is the assigned class term in output domain

For example, one of the evolved fuzzy rules that predict the customer acceptability degree for buying a particular car, given the car profile, specify "*IF (buying=MED) AND (safety=HIGH) THEN (acceptability=ACC)*". In this research, the input attributes/features of a dataset are assumed to be of equal importance and independent of one another. However, the types and the number of membership functions defining

the fuzzy sets utilized for particular attribute is attribute dependent. For continuous attributes, triangular and trapezoid membership functions are selected with symmetry and initial overlap degree criteria of 25% [15] since they are computationally efficient in real-time FLS [6]. Moreover, a range of 3 fuzzy sets is utilized for input variables whereas a range of 5 output rules is utilized as this provides adequate resolution without excessive computational cost. For discrete variables, a singleton membership function is selected in representing discrete domains.

Simplicity of design has been imposed, so the fuzzy rules are assumed to be of equal importance. Hence, all fuzzy rules in the rule-base are used with equal weighting. However, the size of the rule-base is controlled by the size of a dataset. For datasets having more than 1000 tuples, the rule-base is limited to minimum 10 fuzzy rules and maximum 25 fuzzy per agent. Otherwise, the rule-base is limited to minimum 5 fuzzy rules and maximum 15 fuzzy rules per agent. This control approach is necessary in order to avoid ignorance or explosion in case of too small rule-base size or too large rule-base size, respectively, which may results in undesired rules degrading both the accuracy and the interpretability. However, a rule-base size for particular dataset can be computed as a function of its attributes and tuples sizes.

For a low cost in storing fuzzy rules, virtual multidimensional FAM matrix approach is used in this research alternatively to multidimensional FAM matrix of fixed dimension. In this approach, higher-dimensional spaces are separated into two dimensions matrices and only the actually used entries are stored. Hence, no need to allocate the full multidimensional FAM matrix since a fuzzy rule is represented by index information that specifies its location in the virtual matrix. By using this approach, flexible FAM matrix structuring is allowed since rule entries are stored consecutively with variable number of inputs and the storing order becomes insignificant. In addition, huge benefits are also allowed when using this approach such as flexibility, implementation simplicity, ability to handle FAM matrices of arbitrary dimension, and ability to handle multiple lower-dimensional FAM matrices simultaneously. Furthermore, this approach allows for a very compact implementation for the defuzzification process. The firing strength for a FAM entry is computed using the rule of minimum membership degree values as:

$$w_i = \min\{\mu_{A_1}(x_1), \dots, \mu_{A_n}(x_n)\} \quad (2)$$

Where: n is the number of attributes in dataset

x_1, \dots, x_n are input linguistic variables

i is fuzzy rule number in rule-base

μ_{A_i} is the membership function of fuzzy set A_i

w_i is the firing strength of i^{th} fuzzy rule

However, if a membership function for each output fuzzy set is defined as:

$$\mu_{C_i}(y_i) = \text{output membership set} \quad (3)$$

Where: i is fuzzy rule number in rule-base

y_i is the class linguistic variable in i^{th} fuzzy rule

μ_{C_i} is the membership function of fuzzy set C_i

Thereafter, the overall FLS response is computed from the defuzzification process for n output membership fuzzy sets as:

$$output = \frac{\sum_{i=1}^n (w_i \times \mu_{C_i}(y_i))}{\sum_{i=1}^n w_i} \quad (4)$$

Where: n is the number of total current active rules

$(w_i \times \mu_{C_i})$ is the height defuzzification

The height defuzzification method is generally referred to as “clipped center of gravity”. This method is computationally efficient in real-time FLS compared to other methods such as the “center of gravity” or “centroid” defuzzification method, where the output is a combination of centroids for each overlapping fuzzy membership function. Moreover, it is highly recommended since it utilizes better use of the information in the output distribution and generates unique fuzzy centroid [26].

B. Evolved Fuzzy Logic Classifier & Predictor

Normally, a FLS is not adaptive since it has no learning ability in itself. In addition, the design of FLS for certain real-world application is considered as knowledge-intensive and time-consuming. This is due to the rapid increase in the possible combinations of FLS parameters in the KB such as the fuzzy rules, fuzzy rule structure, the number of input and output variable dimensions, fuzzy membership types, number of fuzzy sets per variable, and so on. Hence, FLS is a suitable domain to apply EA or ANN learning strategies to form a hybrid system in order to find an optimum set of fuzzy rules to finally get the desired behavior (e.g., [27]). The real-world application addressed in this research is how to automate the process of designing FLS parameters for a dataset classification and prediction algorithm in distributed environment. Therefore, a framework for a Parallel Fuzzy-Genetic Algorithm (PFGA) has been developed in this paper to evolve the parameters of the FLS that is designed for classification and prediction over multi-agent dataset in decentralized data sources.

The general structure for a FGA agent process is graphically shown briefly in Fig. 2. As shown, the main role for each FGA agent is to construct its local model from the input dataset. In order to construct its local model, the FGA agent uses 70% of the dataset tuples along with their associated class as training data while 30% of the dataset tuples are kept separately independent and used as testing data for validation. The k-fold cross-validation is not used since it has some limitations [28]. The local model parameters of the FGA agent are evolved using two nested GAs. The outer GA evolves the fuzzy sets whereas the inner GA evolves the fuzzy rules. Hence, the chromosome of the outer GA encodes the fuzzy sets whereas the chromosome of the inner GA encodes the fuzzy rules. The global collaborative objective to be solved by the FGA agents is to interact to get the best formation of fuzzy sets and fuzzy rules that best describe and classify the dataset in a more efficient manner than one single FGA agent could. Fig. 3 shows graphically the nested GAs architecture developed for a FGA agent. In this figure, outer GA has population of N_1 chromosomes whereas inner GA has

population of N_2 chromosomes. Given a set of fuzzy rules $R_i=\{R_1, \dots, R_n\}$, a pseudo-code to design the inner GA is given below:

- 1) Initialize population of N_2 chromosomes.
- 2) **for** $i = 1$ to maxGeneration **do**
- a) Evaluate fitness of all chromosomes
- b) Select $N_2/2$ parents for reproduction using roulette wheel selection
- c) Perform crossover operation on the selected pairs at some random point along each chromosome with probability P_c
- d) Perform mutation operation randomly with small probability P_m
- e) Replace the old population P_i with the new population P_{i+1} using elitist strategy
- end for**

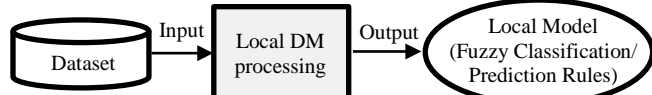


Fig. 2. The brief structure of a FGA agent constructing its local model from the dataset

Since the inner GA evolves fuzzy rules, the inner GA chromosome is designed such that it encodes a rule-base. The encoding scheme here represents each fuzzy rule as an integer array of fixed length equal to size of dataset tuple along with its assigned class. The integer elements in this array represent key values indexing the fuzzy sets utilized in the fuzzy rule, in order. The integer representations of all fuzzy rules are then strung together to form a single and variable-length array of fuzzy rules indices that constitute the inner GA chromosome encoding the rule-base. However, the approach mentioned earlier for controlling the rule-base size has been imposed. Fig. 4 graphically illustrates an example for designing an inner GA chromosome for a dataset having 2 attributes along with its associated class. In this example, the inner GA chromosome is assumed encoding a rule-base having 3 fuzzy rules, with respect to fuzzy sets keys shown in figure. Each inner GA chromosome, or complete FAM matrix, is then evaluated against the fitness function and the normal operations of selection, crossover, mutation, and replacement are applied.

However, in order to evaluate candidate solutions in inner GA, a chromosome from the outer GA must be utilized since it encodes the fuzzy sets definitions required in evaluating the rule-base encoded to obtain the accuracy of classification or prediction. In this case, the fitness function can be simply defined as the testing error:

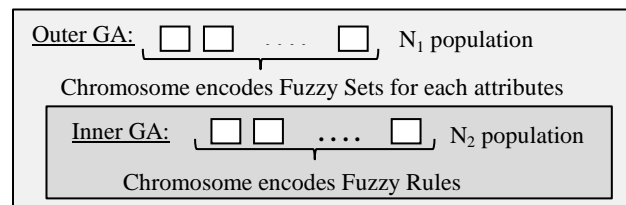


Fig. 3. The structure of nested GAs that evolves local model parameters of FGA agent

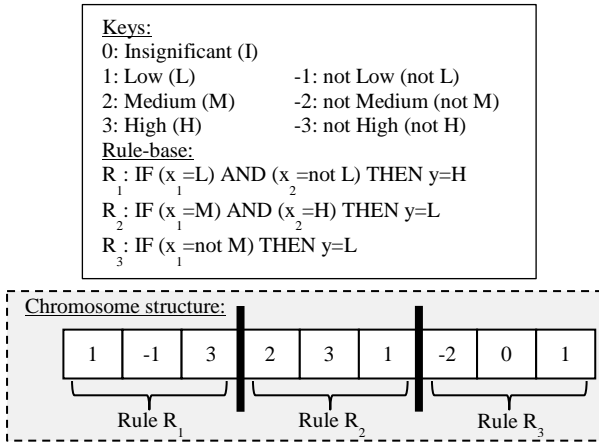


Fig. 4. Example of designing inner GA chromosome encoding rule-base of 3 fuzzy rules

$$f = \frac{1}{e} \quad (5)$$

Where: e is the classification error

However, in case of prediction, the testing error fitness function can be defined as:

$$f = 1 - E \quad (6)$$

Where: E is the root mean squared error (%)

For selecting potential inner GA chromosomes for reproduction, the strategy of roulette wheel technique is utilized due to its implementation simplicity [25]. In this

strategy, the probability of selecting particular individual chromosome is proportional to its fitness. When selecting parents for reproduction, a single-point crossover operation is applied. In this operation, all fuzzy rules beyond that point in either individual chromosome are swapped. The crossover point on either individual is selected randomly and independently between encoded fuzzy rules borders. The resulting individuals are the offsprings. However, once again, the control approach for the size of a rule-base encoded in inner GA chromosome must be preserved for the reasons mentioned earlier. Fig. 5 graphically shows an example of single-point crossover operation between two inner GA parent individuals P₁ and P₂ having chromosome sizes of 3 and 5 fuzzy rules, respectively. In this example, the crossover point for parent P₁ occurred between fuzzy rules R₁ and R₂ whereas the crossover point for parent P₂ occurred between fuzzy rules R'₂ and R'₃. As shown in figure, the reproduction between P₁ and P₂ results in two offsprings O₁ and O₂ having equal size of 4 fuzzy rules.

To preserve and introduce genetic diversity, mutation operation is applied through generations. In this operation, inner GA chromosome is modified per key entry with small probability. To maintain useful genetic diversity and to improve inner GA performance, elitist strategy for replacement is applied. In this strategy, the fittest individuals are selected to replace the old population.

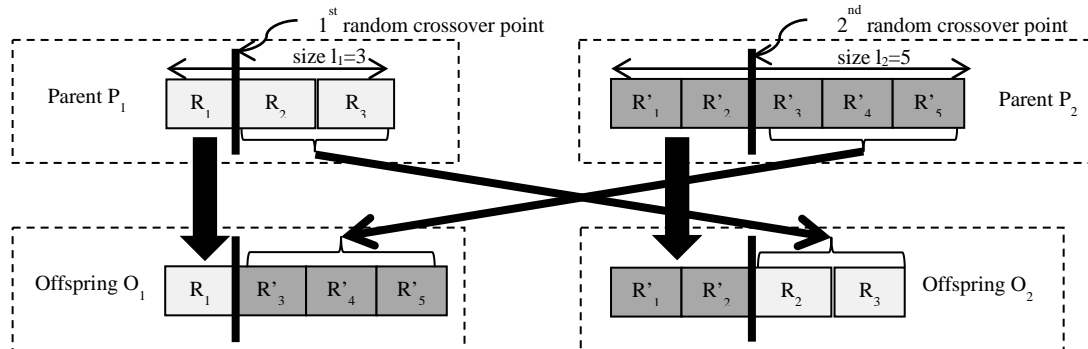


Fig. 5. Example of single-point crossover operation in inner GA where crossover points can be different positions

Given a set of n attributes $x_i = \{x_1, \dots, x_n\}$ along with its associated class attribute y of a particular dataset, a pseudo-code to design the inner GA is very similar to the pseudo-code of inner GA mentioned above. However, the structure of outer GA chromosomes is dissimilar to the structure of inner GA chromosomes since outer GA evolves fuzzy sets whereas inner GA evolves fuzzy rules. Hence, outer GA chromosome is designed such that it encodes the fuzzy sets utilized in dataset attributes along with its associated class attribute. The encoding scheme here represents each attribute as an array of features defining the membership functions selected for the fuzzy sets utilized. Fig. 6 illustrates an example designing a structure encoding 3 fuzzy sets named "LOW" (L), "MEDIUM" (M) and "HIGH" (H) utilized for a continuous input attribute. In this example, triangular membership functions are selected to represent the fuzzy sets utilized,

where fuzzy set L, M, and H are represented by left, regular, and right triangular membership functions, respectively. As shown in figure, the structure of the fuzzy sets utilized is represented as an array of the features defining their membership functions selected. These membership function representations for each attribute are then strung together to form a single and fixed-length array of features that constitute the outer GA chromosome encoding the overall fuzzy sets. Fig. 7 graphically shows the general structure of outer GA chromosome. However, fuzzy sets utilized are attributed dependent, as mentioned earlier.

The difficulty with outer GA is how to evaluate the fitness of candidate solutions. The fitness of each outer GA chromosome cannot be computed in isolation from the inner GA chromosomes since fuzzy sets encoded in outer GA chromosome are contributing in the evaluation of the rule-base

encoded in inner GA chromosomes. A simple solution to this problem is to construct generational fitness regions in inner GA by arranging the fitness of all inner GA chromosomes in equal size regions each generation. The fitness function for an outer GA individual is then can be defined as the average fitness of the majority region. Hence, each outer GA chromosome is evaluated against the fitness function and the operations of selection, crossover, mutation, and replacement are typically applied.

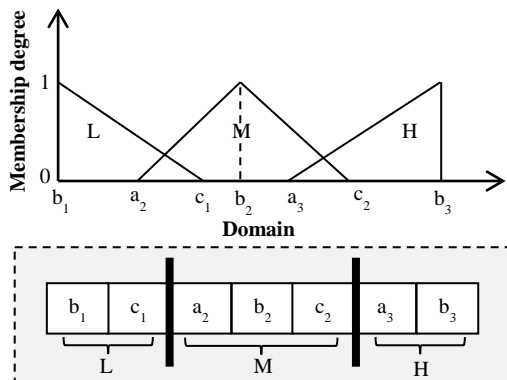


Fig. 6. Example of designing a structure encoding 3 fuzzy sets defined by triangular membership functions utilized for continuous input attribute

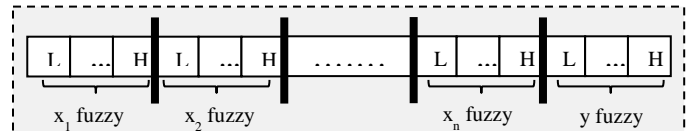


Fig. 7. The general structure of outer GA chromosome encoding fuzzy sets utilized in all dataset attributes along with its class attribute y

Similarly to inner GA, the outer GA utilizes the strategy of roulette wheel technique in selecting potential chromosomes for reproduction. In addition, outer GA applies single-point crossover operation in reproduction. However, in contrast to inner GA, the randomly selected crossover point in outer GA, on either individual, must have identical position between encoded attributes borders to preserve encoded fuzzy sets from being distorted. Fig. 8 graphically shows the single-point crossover operation in outer GA between two parent individuals P_1 and P_2 having fixed chromosome size of n attributes along with its associated class attribute. In this figure, the encoded fuzzy sets $FS_i = \{FS_{i1}, \dots, FS_{in+1}\}$ define the corresponding n input attributes along with the associated class attribute, respectively. As shown in figure, the crossover points for parents P_1 and P_2 have identical position and the reproduction results in two offsprings O_1 and O_2 having permanently identical size to their parents. Moreover, similarly to inner GA, the outer GA applies mutation and replacement operations through generations. Hence, outer GA chromosome is modified per feature entry with small probability and old population is replaced using elitist strategy. However, limits of fuzzy sets in domain must be preserved during mutation operation.

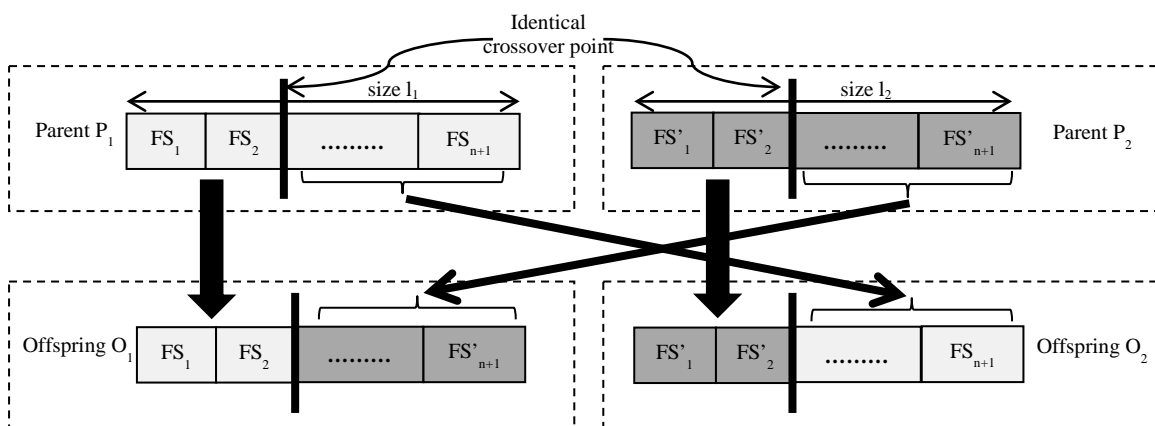


Fig. 8. Single-point crossover operation in outer GA where crossover points must have identical position

Fig. 9 graphically illustrates the detailed structure of a FGA agent showing its components and the interconnections between these components. As shown in figure, the FGA agent consists of two components namely, FLS and nested GAs. In this figure, the FLS uses the nested GAs in learning its KB to get the desired response. As can be seen, the FGA agent uses the structure developed to evolve best parameters in constructing its local model that best describe and classify the local input dataset. However, for a dataset distributed over decentralized sources, a Parallel Fuzzy-Genetic Algorithm (PFGA) framework has been developed. In this framework, all FGA agents are contributing and cooperating in parallel for constructing the final model that best describe and classify the

overall distributed dataset. Fig. 10 graphically shows the structure of PFGA. As can be seen, all FGA agents are first allowed to construct their local models, as mentioned above. During the construction of local models, all FGA agents are allowed to exchange only their best fuzzy rules evolved each particular number of inner GA generations. For simplicity, the distribution strategy for fuzzy rules among FGA agents is applied sequentially and anticlockwise. By using this simple coordination strategy, changes to FGA agents are not only driven through genetic recombination and mutation but also driven through learning from FGA agent peers. In addition, the search process is not only guided by the fitness function but also guided by the interaction among peers.

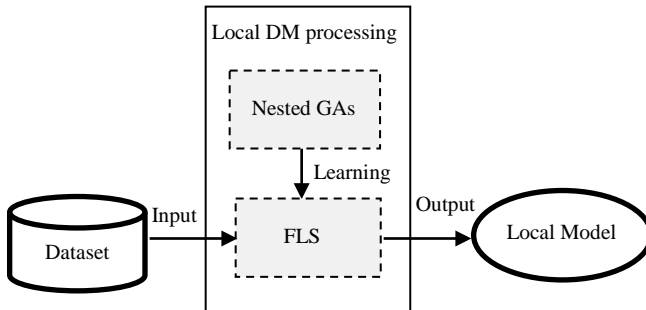


Fig. 9. The detailed structure of a FGA agent constructing its local model from the dataset

As can be also seen, local models of all FGA agents are finally aggregated in order to construct the final model. The adopted aggregation strategy keeps the most common fuzzy rules evolved in local models that give best accuracy and performance whereas eliminates redundant, conflicting and badly-defined fuzzy rules that perturbs the accuracy and performance. To summarize sequence of operations required for these tasks, a pseudo- code for the PFGA is given below:

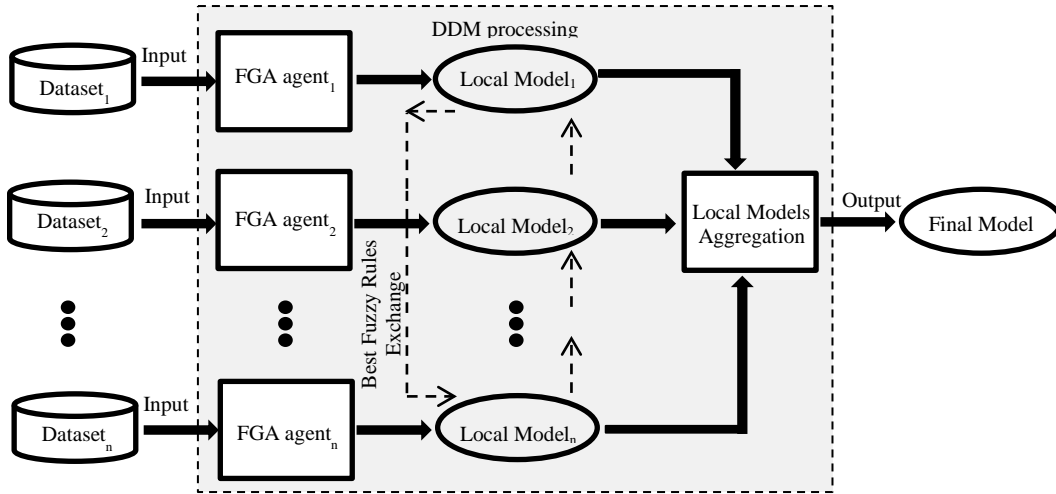


Fig. 10. The structure of PFGA that accepts datasets distributed over decentralized data sources and construct the final model from these cooperative local models of FGA agents

By using the developed framework, storage cost exists in classical knowledge discovery techniques is avoided since distributed datasets are not required to be collected in a data warehouse. In addition, since fuzzy rules are the only thing allowed to be exchanged, many issues such as communication cost, privacy and sensitivity of data are tackled effectively and efficiently. Furthermore, the parallelism and cooperation exist in this framework allows FGA agents to construct the final model in a more efficient manner than one single FGA agent could.

V. EXPERIMENTAL RESULTS AND DISCUSSION

The following results were obtained from a series of experiments conducted using the developed PFGA framework described above, to evolve a model that best describe and classify a distributed datasets. The series of trial runs were performed on i5-3.2 GHz ($\times 4$) system running 32-bit Windows 7 ultimate and having 4.00 GB ram. The

- 1) Initialize nested GAs environments in all FGA agents
- 2) In parallel, build local model per FGA agent:
 - a) Run through outer & inner GAs populations of N_1 & N_2 individuals respectively and assign each pair of inner-outer GAs individuals to a FAM representing candidate solution.
 - b) Input a FAM matrix to classify or predict the training dataset.
 - c) Evaluate current individual of N_2 but evaluate current individual of N_1 each complete generation of N_2 .
 - d) Each particular number of inner GA generations, exchange best fuzzy rules evolved among FGA agents.
 - e) If a prespecified termination condition is satisfied, stop algorithm execution. Otherwise, apply genetic operations to inner & outer GAs individuals, respectively, then return to step (2-a). In experiments conducted, total number of inner GA generations (N_g) is used as a termination condition.
- 3) Aggregate most common and good fuzzy rules evolved in all FGA agents to construct the final model.

performance of the proposed algorithm is measured using two different population sizes, two different numbers of FGA agents and three different policies for best fuzzy rules exchange among these agents. Five different benchmark datasets, listed in Table1, were employed in trial runs which were available from the dataset repository of Knowledge Extraction based on Evolutionary Learning (KEEL) [29]. The trial runs involve using the proposed algorithm against two evolutionary fuzzy rule learning algorithms implemented in KEEL software tool version 3.0 with $P_c=0.5$ and $P_m=0.1$ [30]. In classification, the proposed algorithm is used against the Fuzzy Hybrid Genetics-Based Machine Learning (FH-GBML) algorithm [31]. In prediction, the proposed algorithm is used against the Genetic-Base Fuzzy Rule Base Construction and Membership Function Tuning (GFS-RB-MF) algorithm [32].

In the first set of experiments, a population size $N_1=N_2=20$ is used. In the second set of experiments, a population size $N_1=N_2=40$ is used. For each population size, six experiments

are conducted per dataset then repeated five times to study how the population size (N_1, N_2), number of agents (N_a), and the exchange policy for best fuzzy rules among these agents affect the system behavior.

In each of these six experiments, the system is allowed to run first for $N_g=500$ then for $N_g=1000$. For each of these inner GA generations numbers (N_g), computational experiments are performed to examine various specifications of FGA agents numbers (N_a) along with different exchange policies for best fuzzy rules among these agents in different intervals of N_g . More specifically, the examined numbers of FGA agents $N_a=5, 10$ whereas the examined exchange policies for best fuzzy rules among these agents are: “No Exchange” (Pol_1), “Exchange each 5 generations” (Pol_2), and “Exchange each 10 generations” (Pol_3). The best fitness parameter is recorded for each generation. The average of best fitness parameter is then computed for the total of twelve experiments conducted per dataset, resulting in 500 and 1000 values when using $N_g=500$ and $N_g=1000$, respectively. A time series of this averaged parameter is then plotted using the number of inner GA generations (N_g) for time axis. Specifically, the average fitness is computed for the twelve experiments conducted using the PFGA framework and the average fitness is computed for the experiments conducted using the FH-GBML and GFS-RB-MF algorithms.

TABLE I. LIST OF DATASETS EMPLOYED IN EXPERIMENTS

Name of Dataset	Number of instances	Number of attributes (Real, Integer, Nominal)	Number of classes
Banana	5300	2 (2/0/0)	2
haberman	306	3 (0/3/0)	2
saheart	462	9 (5/3/1)	2
car	1728	6 (0/0/6)	4
plastic	1650	2 (2/0/0)	-

Fig. 11 shows the results when a population size $N_1=N_2=20$ is used in classifying “banana” dataset for $N_g=500$ and $N_a=5$. As can be seen, the best fitness almost reached the same level when using the three exchange policies for best fuzzy rules in PFGA framework. However, it can be also seen that Pol_2 policy outperforms other exchange policies for best fuzzy rules in short run. The reason is that the FGA agents do more exploitation for best fuzzy rules in short interval of times. Moreover, the same figure shows that the convergence time for PFGA framework is slower than the FH-GBML algorithm. This is due to the slow exploration in real attributes. On the other hand, Fig. 12 shows the results when a population size $N_1=N_2=40$ is used in classifying “banana” dataset for $N_g=1000$ and $N_a=5$. As can be seen, the Pol_2 policy performs better in long run and almost reached best fitness value of 0.78. The reason is that using larger population size increases the diversity and, consequently, the exploration for better solutions by FGA agents that exploit best fuzzy rules in short interval of times.

Fig. 13 shows the results when a population size $N_1=N_2=20$ is used in classifying “haberman” dataset for $N_g=500$ and $N_a=10$. As can be seen, the best fitness almost reached a value of 0.74 after 20 generations in PFGA framework when using policies that exchange best fuzzy rules among FGA agents whereas it reached a same value after 80 generations in

a policy that doesn’t exchange best fuzzy rules among FGA agents. This highlights the importance of exchanging best fuzzy rules among FGA agents. As can be seen in Fig. 14, the best fitness using PFGA framework almost reached the same best fitness value of 0.78 using FH-GBML algorithm when classifying “haberman” dataset using $N_1=N_2=40$ for $N_g=1000$ and $N_a=10$. The reason is that the exploration in integer attributes is faster than in exploration in real attributes which results in fast fuzzy rules evolving.

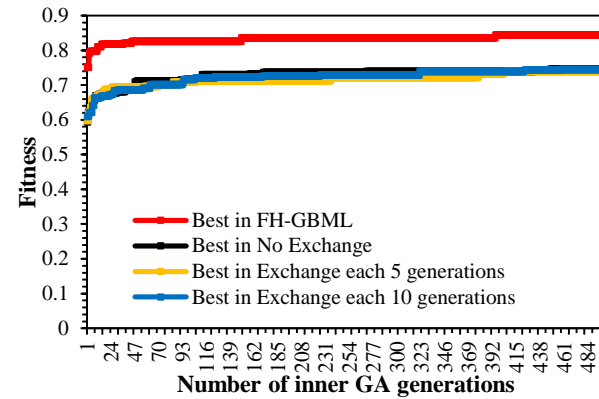


Fig. 11. Example of best fitness data for $N_1=N_2=20$ using “banana” dataset for $N_g=500$ and $N_a=5$

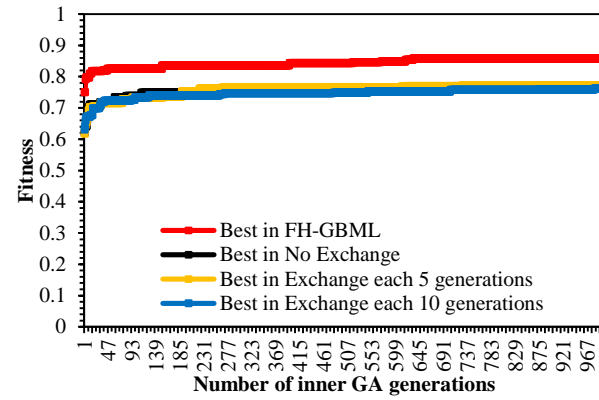


Fig. 12. Example of best fitness data for $N_1=N_2=40$ using “banana” dataset for $N_g=1000$ and $N_a=5$

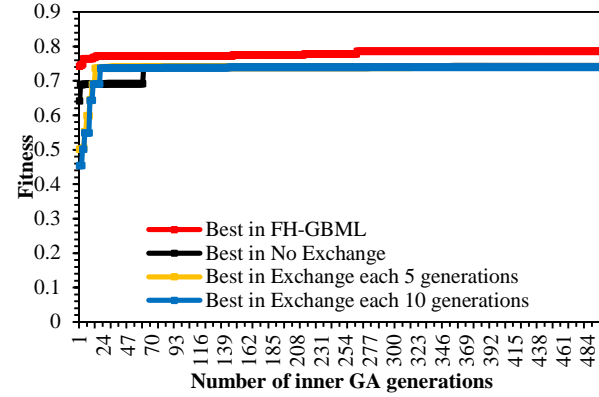


Fig. 13. Example of best fitness data for $N_1=N_2=20$ using “haberman” dataset for $N_g=500$ and $N_a=10$

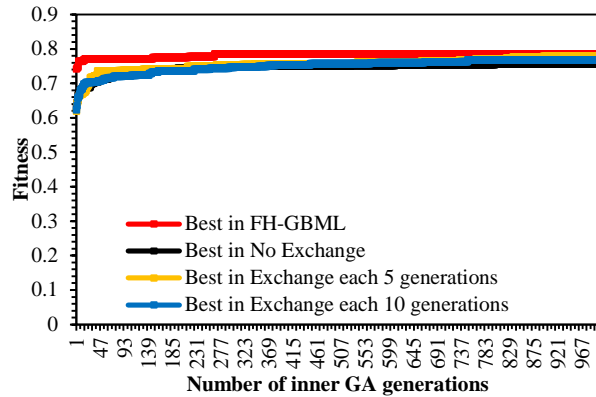


Fig. 14. Example of best fitness data for $N_1=N_2=40$ using “haberman” dataset for $N_g=1000$ and $N_a=10$

Fig. 15 shows the results when a population size $N_1=N_2=40$ is used in classifying “saheart” dataset for $N_g=1000$ and $N_a=10$. As can be seen, the best fitness curve when using Pol_2 policy converges faster than other policies in PFGA framework. However, using the same configuration in Fig. 15, Fig. 16 shows that the FH-GBML algorithm outperforms the PFGA framework. The reason is that the exploration takes longer time when increasing number of attributes in dataset especially when it has real attributes.

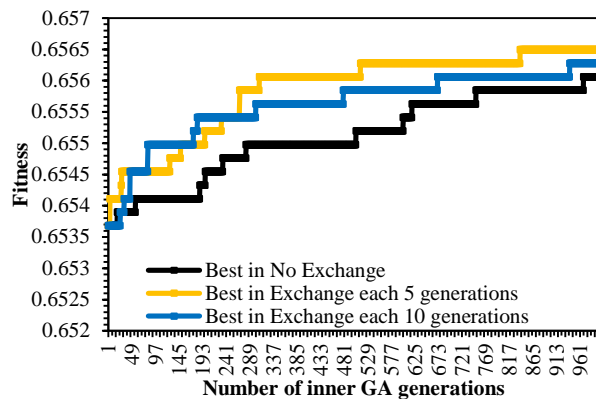


Fig. 15. Example of best fitness data for $N_1=N_2=40$ using “saheart” dataset for $N_g=1000$ and $N_a=10$

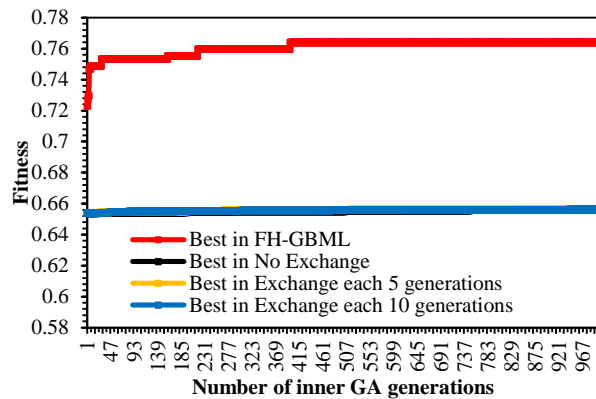


Fig. 16. Example of best fitness data for $N_1=N_2=40$ using “saheart” dataset for $N_g=1000$ and $N_a=10$

Fig. 17 shows the results when a population size

$N_1=N_2=40$ is used in classifying “car” dataset for $N_g=1000$ and $N_a=5$. As can be seen, the best fitness curve when using Pol_2 policy converges slower than Pol_3 policy in PFGA framework whereas it converges faster in Fig. 18. The reason is that using short interval of times for exchanging best fuzzy rules among small number of FGA agents increases the exploitation whereas using larger number of FGA agents increases the exploration. Comparing with results from “saheart” dataset, it can be also seen in Fig. 18 that PFGA framework performs better when number of attributes decreases where it reached almost to fitness value of 0.716 instead of 0.656.

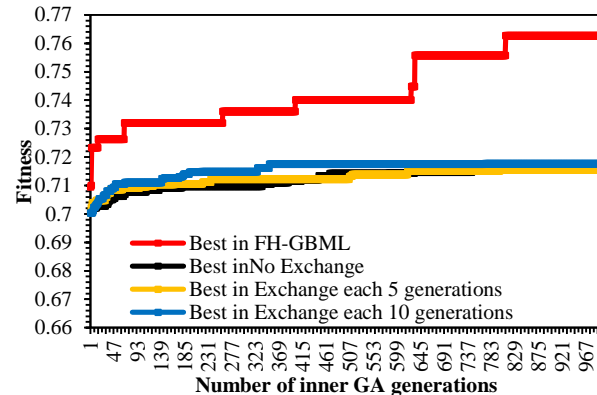


Fig. 17. Example of best fitness data for $N_1=N_2=40$ using “car” dataset for $N_g=1000$ and $N_a=5$

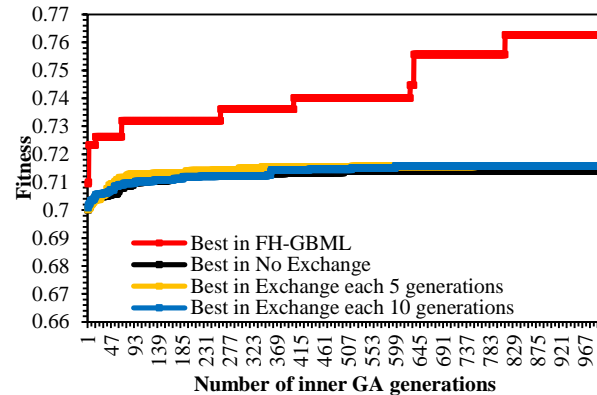


Fig. 18. Example of best fitness data for $N_1=N_2=40$ using “car” dataset for $N_g=1000$ and $N_a=10$

Fig. 19 shows the results when a population size $N_1=N_2=40$ is used in predicting “plastic” dataset for $N_g=1000$ and $N_a=10$. As can be seen, the GFS-RB-MF algorithm outperforms the PFGA framework. The reason is that predicting continuous valued function takes longer time than predicting categorical labels in FLSs. Table 2 shows the summarized average results for the experiments conducted when a population size $N_1=N_2=40$ is used for $N_g=1000$ and $N_a=10$. As shown in the last column, the average computation time were long for some dataset compared with other algorithms (e.g., more than 40 minutes for plastic dataset). However, the first column shows that the average number of fuzzy rules evolved for some dataset has less size along with good accuracy compared with other algorithms (e.g., around 6 fuzzy rules for “haberman” dataset).

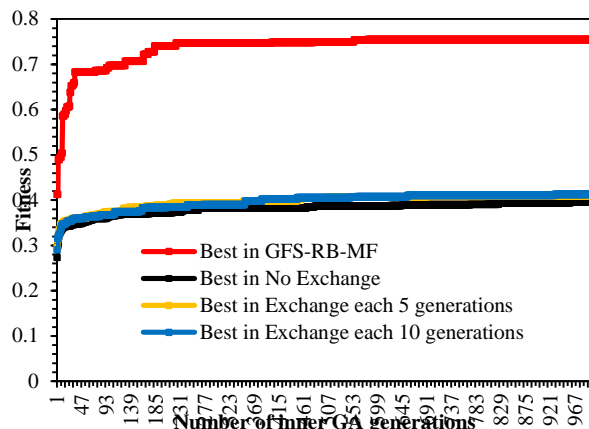


Fig. 19. Example of best fitness data for $N_1=N_2=40$ using “plastic” dataset for $N_g=1000$ and $N_a=10$

VI. CONCLUSION

A new framework for classification and prediction is proposed as a main contribution to the scientific community. The developed Parallel Fuzzy-Genetic Algorithm (PFGA) framework provides flexible mechanism for processing distributed data and offers significant advantage over classical techniques which help to reach all network-related business. Several experiment have been conducted with various specification of population sizes, numbers of FGA agents along with different exchange policies for best fuzzy rules among these agents in different intervals of generations. Small population size does not provide sufficient diversity in individuals for the optimum fuzzy rules to be evolved. Using small interval of times when exchanging best fuzzy rules among FGA agents incorporates more exploitation over exploration whereas using larger number of FGA agents compromises between them. However, using the developed framework with decreasing number of attributes has been shown that it has good accuracy and more efficient in performance and comprehensibility of linguistic rules compared to FH-GBML and GFS-RB-MF models implemented in KEEL software tool.

TABLE II. RESULTS OF PFGA FRAMEWORK VERSUS FH-GBML AND GF-RB-MF ALGORITHMS WHEN $N_1=N_2=40$, $N_g=1000$, AND $N_a=10$

Name of Dataset	Algorithm	Number of fuzzy rules	Accuracy in testing (%)	Time (minutes)
banana	PFGA-Pol ₁	7.2	75.69	83.25
	PFGA-Pol ₂	10.6	77.85	85.5
	PFGA-Pol ₃	10.1	76.86	77.5
	FH-GBML	30	85.83	47
haberman	PFGA-Pol ₁	6.2	74.14	9.5
	PFGA-Pol ₂	5.6	74.18	10.75
	PFGA-Pol ₃	7.1	74.15	10
	FH-GBML	27	77.54	3
saheart	PFGA-Pol ₁	3.8	65.61	18.5
	PFGA-Pol ₂	5	65.65	18
	PFGA-Pol ₃	3.5	65.63	17.5
	FH-GBML	27	76.41	7
car	PFGA-Pol ₁	6.7	71.41	32.5
	PFGA-Pol ₂	7.4	71.59	32.5
	PFGA-Pol ₃	7.3	71.59	32.75
	FH-GBML	29	76.27	8.15
plastic	PFGA-Pol ₁	17.7	39.58	41.75
	PFGA-Pol ₂	19.3	40.93	43.75
	PFGA-Pol ₃	20.4	41.24	42.5
	GFS-RB-MF	9	75.49	1.5

This work can be extended in several directions. For example, part of the dataset can be exchanged along with best fuzzy rules. Furthermore, other exchange policy schemes can be employed in addition to parallelizing data level along with algorithm level per data source such that FLS to evolve to dynamic optimum number of fuzzy rules.

REFERENCES

- [1] M. Sharma, “Data mining: a literature survey”, in International Journal of Emerging Research in Management & Technology, 3(2), 2014.
- [2] X. Hu, “Data mining and its applications in bioinformatics: Techniques and methods”, in 2011 IEEE International Conference on Granular Computing (GrC), Nov. 8-10, IEEE Xplore Press, Kaohsiung, pp. 3-3, 2011.
- [3] G. Shmueli, , N. R. Patel, and P. C. Bruce, Data Mining for Business Analytics: Concepts, Techniques, and Applications in XLMiner, 3rd Ed., John Wiley & Sons. New Jersey, 2016.
- [4] T. Nasukawa, and T. Nagano, “Text analysis and knowledge mining system”, in IBM Systems Journal, 40(4), pp. 967-984, 2001.

- [5] S. Jaideep, R. Cooley, M. Deshpande, and P. Tan, "Web usage mining: discovery and applications of usage patterns from web data", in SIGKDD Explorations Newsletter, 1(2), pp. 12-23, 2000.
- [6] J. Han, J. Pei, and M. Kamber, Data mining: concepts and techniques, 3rd Ed., Elsevier, 2011.
- [7] N. Jain, and V. Srivastava, "Data Mining techniques: a survey paper", in IJRET: International Journal of Research in Engineering and Technology, 2(11), pp. 2319-1163, 2013.
- [8] A. Fernández, S. García, J. Luengo, E. Bernadó-Mansilla, and F. Herrera, "Genetics-based machine learning for rule induction: taxonomy, experimental study and state of the art", in IEEE Transactions on Evolutionary Computation, 14(6), pp. 913-941, 2010.
- [9] Q. Yang, and X. Wu, "10 challenging problems in data mining research", in International Journal of Information Technology & Decision Making, 5(04), pp. 597-604, 2006.
- [10] A. Fariz, J. Abouchabaka, and N. Rafalia, "Using multi-agents systems in distributed data mining: a survey", in Journal of Theoretical & Applied Information Technology, 73(3), 2015.
- [11] S. V. S. G. Devi, "A survey on distributed data mining and its trends", in IMPACT: International Journal of Research in Engineering & Technology, 2(3), pp. 107-120, 2014.
- [12] D. Khan, "CAKE – Classifying, associating and knowledge discovery - an approach for distributed data mining (DDM) using parallel data mining agents (PADMAs)", in WI-IAT '08. IEEE/WIC/ACM International Conference on Web Intelligence and Intelligent Agent Technology, Dec. 9-12, IEEE Xplore Press, Sydney, NSW, pp. 596-601, 2008.
- [13] M. Kantardzic, Data mining: concepts, models, methods, and algorithms, 2nd Ed., John Wiley & Sons. New Jersey, 2011.
- [14] A. P. Engelbrecht, Computational intelligence: an introduction, 2nd Ed., John Wiley & Sons, Chichester. England, 2007.
- [15] D. Driankov, H. Hellendoorn, and M. Reinfrank. An Introduction to Fuzzy Control, 2nd Ed, Springer-Verlag. Berlin, 2013.
- [16] R. G. Hercock, Applied Evolutionary Algorithms in Java, Springer-Verlag Ltd. London, 2013.
- [17] D. Driankov and A. Saffiotti (eds.), Fuzzy Logic Techniques for Autonomous Vehicle Navigation, Physica-Verlag. Berlin, 2013.
- [18] I. Baturone, A. Barriga, S. S. Solano, C. J. Fernandez, and D. R. Lopez, Microelectronic design of fuzzy logic-based systems, CRC Inc. Press, Boca Raton, FL, USA. 2000.
- [19] S. Madhusudhanan, M. Karnan and K. Rajivgandhi, "Fuzzy based ant miner algorithm in datamining for hepatitis", in ICSAP '10. International Conference on Signal Acquisition and Processing, FEB. 9-10, IEEE Xplore Press, Bangalore, pp. 229-232, 2010.
- [20] J. Gomez, and D. Dasgupta, "Evolving fuzzy classifiers for intrusion detection", in Proceedings of the 2002 IEEE Workshop on Information Assurance, JUN. 17, IEEE Computer Press, New York, 6(3), pp. 321-323, 2002.
- [21] O. Cordón, "A historical review of evolutionary learning methods for mamdani-type fuzzy rule-based systems: designing interpretable genetic fuzzy systems", in International Journal of Approximate Reasoning, 52(6), pp. 894-913, 2011.
- [22] P. Singhala, D. Shah, and B. Patel, "Temperature control using fuzzy logic", in International Journal of Instrumentation and Control Systems (IJICS), 4(1), 2014.
- [23] A. Mittal and M. Singh, "Automatic fuzzy rule base generation from numerical data: cuckoo search algorithm", in International Journal of Computer Applications, 133(3), pp. 7-12, 2016.
- [24] D. Corne, et al. (eds.), New ideas in optimization, McGraw-Hill Ltd. Maidenhead, UK, England, 1999.
- [25] D. A. Coley, An Introduction to Genetic Algorithms for Scientists and Engineers, World Scientific Publishing Co. Pte. Ltd, Singapore, 2001.
- [26] S. T. Welstead, Neural Network and Fuzzy Logic Applications in C/C++. 1st Ed., John Wiley & Sons Inc. USA, 1994.
- [27] O. Nasaroui, F. Gonzalez, and D. Dasgupta, "The fuzzy artificial immune system: motivations, basic concepts, and application to clustering and web profiling", in Proceedings of the IEEE International Conference on Fuzzy Systems, May 12-17, IEEE Xplore Press, Honolulu, HI, USA, pp. 711-716, 2002.
- [28] K. H. Esbensen, and P. Geladi, "Principles of proper validation: use and abuse of re-sampling for validation", in Journal of Chemometrics, 24(3-4), pp. 168-187, 2010.
- [29] J. Alcalá-Fdez, et al., "KEEL data-mining software tool: data set repository, integration of algorithms and experimental analysis framework", in Journal of Multiple-Valued Logic and Soft Computing, 17(2-3), pp. 255-287, 2011.
- [30] J. Alcalá-Fdez, et al., "KEEL: A software tool to assess evolutionary algorithms to data mining problems", in Soft Computing 13(3), pp. 307-318, 2009.
- [31] H. Ishibuchi, T. Yamamoto and T. Nakashima, "Hybridization of fuzzy GBML approaches for pattern classification problems", in IEEE Transactions on Systems, Man, and Cybernetics, Part B (Cybernetics), 35(2), pp. 359-365, 2005.
- [32] A. Homaifar, and E. McCormick, "Simultaneous design of membership functions and rule sets for fuzzy controllers using genetic algorithms", in IEEE Transactions on Fuzzy Systems, 3(2), pp. 129-139, 1995.

Web Accessibility Challenges

¹Hayfa.Y.Abuaddous, ²Mohd Zalisham Jali, ³Nurlida Basir

^{1, 2&3}Faculty of Science & Technology, Universiti Sains Islam Malaysia (USIM)
71800, Nilai, Negeri Sembilan, Malaysia

Abstract—Despite the importance of web accessibility in recent years, websites remain partially or completely inaccessible to certain sectors of the population. This is due to several reasons, including web developers' little or no experience in accessibility and the lack of accurate information about the best ways to quickly and easily identify accessibility problems using different Accessibility Evaluation Methods (AEMs). This paper surveys accessibility literature and presents a general overview of the primary challenges of accessibility barriers on websites. In this sense, we critically investigate main challenges forms related to accessibility including standards and guidelines (WCAG 2.0), during website's design and development and during evaluation. Finally, a set of recommendations such as enforcing accessibility legislations are presented to overcome some challenges.

Keywords—component; Website Accessibility; Disabilities; Accessibility challenges; WCAG 2.0; Accessibility automated tools

I. INTRODUCTION

The use of the Internet has been rapidly spreading to most areas of human life. In many industrialized countries, electronic or mobile governmental services are provided in almost all sectors such as immigration, education, commerce, news, workplace interaction, health care, recreation, and entertainment. This would enable citizens and residents to easily and efficiently access different services without usual problems, i.e. long queues, much time and effort. However, it is imperative to provide accessible web services to the majority of people including those with certain disabilities (permanent or temporary) so as to secure equal access and opportunities for everybody.

We can define “web accessibility” as making a website navigable and tractable by various user categories especially those who have disabilities and normally face obstacles when interacting with the web via electronic devices (e.g. blindness). Web accessibility entails overcoming most disabilities that limit Internet access. It means that people with disabilities can use, perceive, understand, navigate, and interact with the web [1]. According to World Wide Web Consortium [2], web accessibility enables people with disabilities, i.e. blind, aged, to utilize the Internet in performing variety of tasks such as online purchasing and browsing. As more accessible websites and software become available, people with disabilities are able to use and contribute to the Web more effectively.

Despite the importance of web accessibility as a research topic, the majority of websites developed remain inaccessible or semi-accessible [3, 4]. This is due to reasons to be discussed in Section II. In addition, web accessibility faces several challenges such as resource allocation, established managerial practices, and time limitation [5]. As a matter of fact, new research findings [6, 7, 8] suggest an imminent need to look beyond the "how to" question of designing websites in order to consider accessibility constraints, accessibility context and the role of professionals who normally are involved in website development, e.g. web designers, web developers, and quality assurance engineers. This will make websites more accessible to different types of Internet users. The following is a list of challenges related to web accessibility in developing countries adopted from [8, 9, 10, 11]:

- Lack of accessibility awareness when designing and implementing websites.
- Limited resources allocated to cover accessibility issues, both tangible and intangible, issues.
- Scarcity of professionals who are familiar with accessibility evaluation tools.
- Dearth of appropriate structured accessibility manuals for web developers and unavailability of web accessibility training courses.

These and some other challenges, like lack of motivation among web developers, contribute to making websites inaccessible for the disabled. Furthermore, lack of efficiency among novices (inexperienced) in the evaluation process may impact web accessibility [12, 13], and web designers and developers may lack the necessary knowledge to implement techniques that support accessibility. All these problems contribute to the existence of several barriers in web accessibility and stimulate interest in this research domain to investigate more the “why” question: “Despite the availability of different resources, why are the majority of online websites still inaccessible?”

This paper critically contrasts various web accessibility challenges raised by current scholars in the last decade. For this purpose, we categorize challenges related to web accessibility using our own taxonomy to stand out from the others, as depicted in Fig.1.

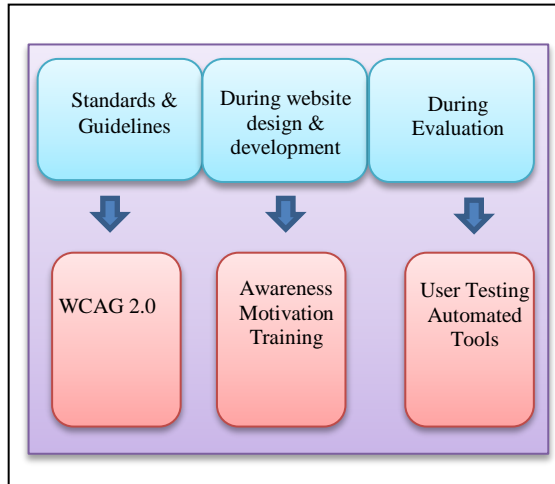


Fig. 1. Web accessibility challenges categories

In fact, many research studies on accessibility have been conducted to evaluate the accessibility conditions of public websites [14,15,16,17]. Nevertheless, few of these studies critically analyzed accessibility challenges [18, 19]. Therefore, this article stresses the vital role of web accessibility not only for disabled Internet users but also for websites developers as well as IT team in charge of building and maintaining websites. We believe that web accessibility is directly related to an organization's profit, legislation, and image within society. It can be seen as a way for an organization to demonstrate its commitment to provide equal opportunities to all users. This can also be seen as a sort of corporate social responsibility. A major benefit of web accessibility for organizations is the potential direct and indirect financial gains from increased access to their websites.

The paper's structure goes as follows: web accessibility challenges section is split into three subsections: the first subsection is devoted to discuss challenges regarding standards and guidelines; second subsection demonstrates various web accessibility challenges during website's design and development and third subsection focuses on common accessibility difficulties faced by website makers (designers, developers) during the process of website evaluation. Recommendations and solutions to handle challenges are discussed in Section III. Section IV summarizes the challenges and Section V concludes this paper.

II. WEB ACCESSIBILITY CHALLENGES

This section is divided into three subsections related to web accessibility challenges:

- Standards and Guidelines.
- During website's design and development.
- During accessibility evaluation.

Website accessibility barriers resulted from the evaluation of a website are discussed based on our own classification of challenges. In particular, we survey the above challenges and evaluate their impact on the accessibility of the website or the users' ability to interact with its content.

A. Challenges related to accessibility standards and guidelines

The increasing number of national laws and policies addressing the accessibility of information and communication technologies (ICT), including the web, resulted in many different approaches in practice. Some of the laws and policies are based on establishing a human right to ICT. Many adhere to the approach in which any ICT purchased by government must be accessible, while others believe that any ICT sold in a given market must be accessible, among other approaches [20]. While many countries such as France and Spain have developed their own accessibility legislations, some developing countries still do not have a specific item of legislation protecting the rights of people with disabilities [21]. These rights are bound in a more general equality act and differ in the level of definition of disabilities and in successfully accessing and using digital content, products and services. Besides the mandatory accessibility legislations enforced by many countries, many voluntary standards and guidelines were founded to support social inclusion of disabled people.

While W3C's Web Content Accessibility Guidelines (WCAG) is the most internationally adopted voluntary web accessibility standard [22], many other guidelines and standards were established as well (e.g. Section 508, BITV, Fujitsu). Furthermore, there is sometimes one version of a guideline or standard at the national level, different versions at the provincial or state level, and yet different versions adopted by commercial, educational, and non-governmental organizations within the same country. This section focuses on WCAG 2.0 since it has been lately the most widely used web standard in the literature [23, 24, 25, 26].

The World Wide Web Consortium [27] is an international consortium that aims to develop web standards. Its mission is pursued through making general guidelines that will lead to web standards. W3C's Web Accessibility Initiative (WAI), which is part of the W3C, focuses on enabling people with disabilities to create and interact with web content. WAI promotes: a) the implementation of web accessibility guidelines in advanced tools, and b) the improvement of accessibility evaluation tools [28]. Together, these may increase the number of disabled people who use the internet.

The WAI has developed: 1) Web Content Accessibility Guidelines (WCAG) which describe how to make Web content and Web sites accessible, 2) Authoring Tool Accessibility Guidelines (ATAG) for the web authoring tools used to create the content, and 3) User Agent Accessibility Guidelines (UAAG) for the tools used to access that content (e.g. browsers and media players). Despite the importance of ATAG and UAAG, we will concentrate on WCAG challenges for two reasons: first, there is enough literature about the WCAG that can allow us to critically analyze it. Second, many automated tools that have been developed to perform website evaluation are using rules/criteria presented within WCAG guidelines. Within WAI, the WCAG documents (WCAG 1.0 and WCAG 2.0) were developed. The WCAG 1.0 was published and became a W3C recommendation in 1999 and was then superseded by WCAG 2.0 in 2008. Although it is possible to conform either to WCAG 1.0 or to WCAG 2.0 (or both), the

W3C recommends the use of WCAG 2.0 for new and updated content.

WCAG 2.0 is organized around four design principles that provide the foundation for web accessibility (perceivable, operable, understandable, and robust) [29]. Under these principles there are 12 guidelines. Each guideline has one or more testable success criteria (SCs). There are 61 SCs at levels A (lowest), AA (medium), and AAA (highest). In WCAG 2.0, a single issue can be covered by more than one SC at different priority levels [29]. Table I demonstrates the WCAG 2.0 conformance levels as classified by [29].

TABLE I. WCAG 2.0 CONFORMANCE LEVELS

Conformance Level	A	AA	AAA
Explanation	All SCs of level A are satisfied. This is the "minimum standard" which a website must meet to be considered accessible for any significant disability groups.	All SCs of Level A and AA are satisfied. This is a "professional practice standard", which a website should meet to be accessible to a broad range of disability groups.	All SCs (at all conformance levels) are satisfied. This is a "gold standard" of maximum accessibility which some websites may choose.

In order to prevent the obsolescence of WCAG against the fast evolution of technology, the WAI removed the technical aspects of accessibility from their guidelines and SC. Technical information regarding how to implement web content with existing web technologies is now provided in separate documents. However, in spite of all of these changes, recent studies [7, 30] have shown that many of the problems raised in WCAG 1.0 still persist in WCAG 2.0 and there have been little improvement in the level of web accessibility.

Although WAI pursues its mission through the creation of guidelines, these do not guarantee accessibility [31]. There is still a lack of empirical evidence to demonstrate that conformance to WCAG 2.0 leads to more accessible websites for disabled users. A study conducted by [7] showed that conformance of a website to WCAG 2.0 Level A does not mean that disabled users will encounter fewer problems.

Many issues have been raised about WCAG 2.0, such as the level of understanding of accessibility issues required when using them [32, 33]. One common challenge that is usually faced by web developers is their inability to interpret or understand guidelines to enable accessibility. WCAG 2.0 documents are not easy to understand and require a certain level of technical knowledge of accessibility. Therefore, when developers or designers are required to implement accessibility, they do not always understand how to achieve the desired requirements. Alonso *et al.* [34] showed that a group of 25 novice evaluators struggled to consistently rate problems according to WCAG 2.0. One cause of this was in the interpretation of the guidelines and the SCs. Besides the manual verification is needed by evaluators and web

developers, guidelines-based accessibility evaluation has several disadvantages [35]. WCAG 2.0 documents are difficult to navigate and locate. All the documents related to this Guideline exceed 450 pages with few hundred navigation links on each single page. Moreover, WCAG 2.0 tends to create supporting documents that can be updated more regularly than the standard itself, which can be a burden to web developers since exploring these updates, necessitates both time and effort. As such, WCAG 2.0 could be unusable by real-world developers. In addition, WCAG 2.0 development itself is inaccessible to anyone who does not understand English.

Loitsch *et al.* [36] pointed out that there exist ambiguities in the language used in WCAG 2.0. For instance, WCAG 2.0 stated that all "the success criteria (SCs) are testable when people who understand WCAG 2.0 test the same content using the same SCs, the same results should be obtained with high inter-rater reliability". However, no explanations were provided about the minimum number of testers needed to fulfill the required "high inter-rater reliability"; also, the level of agreement between evaluators is undefined. Should all the testers obtain the same results or a certain portion of them is enough? Furthermore, [36] mentioned the need for people who understand WCAG 2.0 tests without clarifying the level of expertise needed. This can lead to many different interpretations of what is required. This ambiguity could affect the efficiency and the effectiveness of the evaluation process. Eventually, this may create a gap between evaluators and the evaluation process.

Petrie *et al.* [37] conducted interviews with 14 web accessibility evaluators. They found that they were unclear on the differences between automated and manual testing of accessibility and what can be tested through the automated tools. In addition, [38] had 22 expert and 27 non-expert evaluators to perform accessibility evaluation using WCAG 2.0 and discovered that 50% of testers were unable to come to an 80% level of agreement about whether a problem was present in a webpage. Additionally, when using WCAG 2.0 20% of the problems reported by the evaluators were false positives and 32% of the true accessibility problems had been missed. A false positive occurs if the violation has not taken place and was reported, whereas a false negative occurs if the violation really has taken place and was not reported. For the non-experts, the results were even worse having higher levels of false positives.

The focus of WCAG 2.0 is on the technical artifact, e.g. the webpage - not on users and their goals. This means that the activity of WCAG conformance is oriented towards testing these technical artifacts against SCs - rather than evaluating the user experience with specific impairments trying to complete specific tasks. Although a technical testing's focus can be helpful for programmers treating accessibility evaluation as a bug-fixing activity, this level of technical focus inevitably creates a gap between accessibility and user experience for disabled people [30]. Of a greater concern is WCAG 2.0's emphasis on perfect score on all SCs for a level to get the level conformance logo, which makes it impossible for some websites to achieve any acceptable level of conformance. WAI ignored the fact that in website development process,

developers do not seek perfection; instead, they aim for a continuous, pragmatic improvement over versions [39].

B. Challenges during website's design and development

Many challenges face the staff developing websites before testing and evaluating accessibility, mainly lack of awareness and motivation and the scarcity of professional training courses that may handle accessibility issues. Developing websites requires a team effort that includes developers, designers, content producers and project manager. For the web community, each member of this team has certain responsibilities related to his skills in delivering an accessible website. However, it is the project manager who monitors high-level adherence to business goals, and without his support, there will not be any changes to accessibility unless governments truly start enforcing legislation. Without a managerial impact on accessibility, it is quite normal for a web team to ignore this accessibility issue or pretend they have taken care of it [40]. A project manager should ensure the early engagement of his team in the accessibility process. He should motivate and encourage the web team to get involved in the accessibility issues at early stages. Project managers are responsible for showing the importance of web accessibility to their teams as well as the positive effect of web accessibility on the commercial and community levels. If none of the project members is experienced in accessibility, then a third party can be consulted or out-sourced to perform this task. Lack of accessibility may result in the marginalization of certain user groups, preventing them from accessing the website.

In this section we discuss the main challenges faced in projects related to accessible website during the design and the development of a website. Initially, we highlight the accessibility awareness and motivation among the project's members especially IT developers. Then, we focus on the benefits of web accessibility training for web development staff.

1) Lack of accessibility awareness and motivation

Challenges such as lack of awareness are very common among web developers, besides motivation, knowledge and guidance. The latter challenges are faced by most novice evaluators. Whether facing experienced web developers or novice evaluators, all challenges contribute to the continuing presence of accessibility barriers on websites.

There are moral, legal and economic arguments for implementing accessible websites promoted by advocacy organizations such as disability related charities and academic organizations [41]. Nevertheless, few web designers follow accessibility guidelines [42]. Although the WAI of the W3C have published online guidelines, most IT professionals are unaware of them, and companies that have government contracts are mandated by their government's legislation to make their websites accessible [8]. The low level of accessibility is likely to be the result of several factors. For instance, despite the increase on awareness pertaining to accessibility over the last few years at the level of government and legislation, web designers' knowledge remains quite low [7].

Pye [43] tested the importance of accessibility awareness for IT professionals and its effect on the accessibility level for visually disabled users. The author used a questionnaire and interviewed members of charity organizations that concern themselves with the matters of web accessibility for visually disabled persons. The results of the study revealed that there are certain rules to increase awareness of all individuals involved in web development. Country-specific legislation should be introduced in web accessibility. There is also a key requirement for the continuation of the other current enforcement methods, such as assistive technology, to overcome the accessibility barriers. However, no precise recommendations are given by the author to treat the highlighted awareness problem.

In the USA, [41] showed the lack of awareness in public libraries. These libraries usually do not consider community members with physical disabilities when designing their websites. Therefore, the findings suggested that public library websites are not suited to deliver effective information services for users who need special assistance. Furthermore, this study revealed that public libraries do not consider having an appropriate funding in their reserved budget to support accessibility.

In the research conducted by [3], 20 websites of Finnish higher education's institutes have been examined to evaluate their web accessibility by an application software named TAW [44]. The results showed that 30% of tested websites have full automatic accessibility in priority 'A' level but none of the tested websites has 'AA' compliance. Most of the tested websites have low accessibility issues. The author claims that the lack of accessibility awareness among developers is the main reason.

Until now, the majority of IT professionals, especially those who are involved in developing websites, are not motivated to learn more about accessibility. This is because they do not have a comprehensive knowledge of accessibility and the difference it makes to disabled users and community commercial organizations [24]. So, the challenge is to increase the level of awareness of the IT web team regarding the impact and rewards of web accessibility as well as to motivate them through course training that highlights these rewards and benefits [10]. On the other side, the lack of motivation does not necessarily mean lack of awareness since many IT professionals are aware of web accessibility legislations but not motivated to follow them.

Rosson *et al.* [45] conducted a survey involving 334 web developers. The aim was to understand the needs, problems and the processes that developers follow and the tools they use in websites development. During website implementation, the authors have observed that while developers were quite conscious of the overall quality and usability issues, only 5% of the respondents performed web accessibility testing. They hypothesized that this may be partly due to a lack of knowledge and motivation because of the relatively tedious and time-consuming testing required. Although [45] experiment was conducted 10 years ago, the motivation factor has remained an issue until now. One of the common justifications given by the developers to abandon accessibility

according to [46] is the limited time or resources' incompatibility of technology to accomplish this task. This happens because the accessibility specialist is just a small cog in a big wheel or even there is no specialist at all in the organization.

Trewin *et al.* [5] surveyed IBM rich internet application developers with varying levels of accessibility expertise to explore two concerns: barriers faced by developers when designing accessible web-based products and the value gained from the accessibility test. The findings showed that even for developers with experience in web accessibility, testing has been seen the most time-consuming among other phases with relatively low impact on the website. Nahon *et al.* [4] reported obstacles and incentives for non-professional web makers (e.g. blog writers and/or creators of personal websites) to consider accessibility in their work. The authors presented a theoretical framework that described variables they hypothesized would contribute to designers' intention. They found that intrinsic motivation was the strongest predictor of a positive attitude that affected the intention to make technology accessible.

2) Lack of training

No one can deny that professional training, good education and guidance are crucial to produce skilled IT staff members who can understand the urgent need for accessibility. The lack of skilled staff may eventually negatively impact accessibility. However, accessibility training for web developers is still not available in most IT training centers. Thus, many web developers continue producing websites that are inaccessible.

Many developers claim that accessibility is difficult to accommodate. Part of the problem is a lack of exposure to accessibility during training [13, 25, 47]. Most web designers and developers have little or no experience to ensure that their code meets accessibility requirements. Designers approach accessibility problems differently than other IT professionals, such as Human Computer Interaction (HCI) specialists and developers. Designers and developers typically tend to think that web users are just like them [48].

Recently, developers have indicated a need for more education in accessibility. An exploratory study [49] on the current state of accessibility surveyed more than 400 developers throughout Europe. The study found that 85% of developers wanted more accessibility training with more information on disabilities and the use of assistive devices. Moreover, web testers need training in accessibility evaluation methods like conducting real user testing with blind users and using screening techniques besides assistive technologies. One Brazilian study [50] revealed that while 45% of web-related professionals were aware of screen readers for blind users, they did not know how to make webpages screen reader-compatible.

There are a great number of recommendations for accessible development, but these are often distant from the developers' way of programming. As a consequence, developers do not follow them [32, 50]. Avila *et al.* [6] stated that for web developers to create functionally accessible web resources, more than general guidelines and evaluation tools are required. Thus, it is recommended that more training be given to web development teams in order to raise their awareness and give them a better understanding of end-users.

C. Challenges during evaluation

Web accessibility evaluation methods have been widely studied, and different evaluation methods have been proposed, e.g. [38, 51]. Different AEMs lead to different kinds of results and quality. They require different levels of resources and differ in their applicability [38]. These methods have contrasting pros and cons and various properties [52]. For example, they differ in many ways:

- Method of implementation (analytical or observational).
- Users performing the evaluation.
- Purpose of implementation.
- Methods used in obtaining results.
- Cost/resources spent in evaluation.

This section explores the main challenges in the accessibility evaluation process faced by IT staff when they test websites using an automated method. In the next subsection, we are going to cover challenges related to automated testing and user testing. Screening techniques and other assistive technologies problems are highlighted in subsection (2), since they are related to each another.

1) Automated testing problems

WCAG can be checked manually, though verifying a site's accessibility manually can be time-consuming. Thus, software developers have created a number of tools to simplify this process. Web accessibility testing tools are software programs and web based services that help in determining whether a website meets accessibility guidelines [38]. These tools can help reduce the time and effort required for the evaluation process. Testing normally involves an evaluator to check conformance of a webpage against the accessibility rules encoded in the tool. A-Checker [53], WAVE [54] and TAW [44] are examples of automated evaluation tools. Generally, expert users are required to follow up with the results derived by the tool to determine the rate of accessibility.

Common drawbacks of automatic accessibility tools have been highlighted by many scholars, e.g. [1, 25, 47]. There is not much information about the difficulties that evaluators may face when assessing accessibility using these tools [35]. However, one of the most known deficiencies of automated tools is the difficulty in interpreting results. At first glance, running evaluation using automated tools sounds easy. Unfortunately, they are time consuming when the novice web developers try to analyze their results. Moreover, interpreting these results requires an expert web developer with a technical background in web accessibility. This necessitates constant checking against manuals and documentations. When these tools are used by practitioners who lack experience or knowledge in accessibility, the results can be unpredictable and the quality of findings questionable.

There is high detection rate of defects among many of these evaluation tools, which necessitates a user's manual inspection and, thus, resources are wasted [55]. Automated tools are normally broad in that they apply specific accessibility standards or guidelines and produce a list of automatically

detected problems [47]. Automated testing covers only a small proportion of WCAG 2.0 and is unable to check every aspect of accessibility [56], but they are possibly able to flag items that need to be manually checked. It has been estimated that more than half of the provisions in most accessibility standards ask for human judgment during evaluation process. Some tools like TAW do not evaluate the web content using all guidelines criteria and the rest are usually evaluated by testers who are commonly left to their own interpretation of those guidelines [6].

Trewin *et al.* [5] interviewed 49 IBM web developers and revealed that the majority of the existing evaluation tools are often unclear, cumbersome and incomplete with respect to standards or guidelines that must be met. Moreover, some automated testing tools do not provide support for changed or newly developed accessibility guidelines. While tools can check the adherence to a number of guidelines, some guidelines are not checked properly. For example, it is hard for tools to ascertain whether the “alt” attribute is meaningful or not. This can result in high false positive and inaccurate results. Inaccurate results can decrease the efficiency and increase the cost of accessibility testing. Trewin *et al.* [5] showed a need for new methodologies, particularly mixed ones, that may reduce false positive results. Precisely, to ease end-user interpretability, light-weight visualizations that support novices in performing manual checks and simplification of the automated tools’ results are needed. The research community of accessibility is still unable to standardize ways or methods that are fully automated to generate accessibility rate for a specific website. Developers of interactive systems, especially websites, are frequently not specialists in accessibility and usability techniques. In the absence of an accessibility expert, the evaluation tool might go a long way to find adherence to the standard guideline. But even hiring an accessibility expert may often be beyond the financial capabilities of a typical website development project.

Two experiments were conducted in 2012 and 2013 by [57] using the following tools: Accessibility Check, A-Checker and TAW [44] for 20 public universities in Malaysia in order to diagnose the overall accessibility of these universities’ websites. Unfortunately, none of the websites were fully accessible based on the results obtained by the selected tools. In addition, the results obtained varied and were expressed in different numbers of errors due to the fact that accessibility tools differ in their interpretation of the WCAG, which supports contention [58]. The authors concluded that automated evaluation tools may underestimate or overestimate the number of accessibility errors on a webpage, making the reliability of such tools doubtful.

Choosing website accessibility evaluation tools is not a trivial decision: whether or not to pick the easiest one to use, or the fastest one to learn or the one which produces low false positives. The choice of the tools without previous experience can be a daunting task, especially when working under the pressure of time constraints [59]. Many factors need to be taken into consideration when choosing the suitable evaluation tool. The tool should be clear and user-friendly, provide high quality and reliable results and be capable of testing the browser’s DOM in order to test what users are experiencing.

Additionally, the tool must be suitable to integrate in the development process and flexible enough to be used in any environment by any team in any location. While many tools provide some guidance on verifying results which need to be manually checked, few of them provide easy to follow and user-friendly guidance on performing such manual inspection. There are other factors, including but not limited to the ones mentioned above, to consider when choosing the appropriate evaluation tool [60].

2) Users’ testing problems

Although accessibility tools and guidelines can help in detecting accessibility problems, user testing should be applied whenever it is possible to verify the results [61]. User testing is a process where formal or informal experiments are set up with real users who are asked individually to perform goal-free or oriented navigation on a website, and whose behavior is observed by experienced evaluators. Lab studies with real users are the most effective when conducted early in the lifecycle of a product but can also be conducted towards the end of the iterative design cycle (i.e. when large accessibility problems might be ignored to ship a product or release a site on time). Involving users with disabilities in evaluation has many benefits; however, it cannot alone determine if a website is accessible or not [62].

Several studies of usability evaluation methods [63, 38] have shown that user testing methods may fail in yielding consistent results when performed by different evaluators and that an inspection-based method is not shortcoming free. Other difficulties were observed, like preparing testing materials, developing realistic scenarios of tasks and choosing the right sample size for the test [64]. In addition, this kind of testing has been criticized for being subjective and for depending on the users’ background as well as the Internet skills. Although accessibility and usability are two different properties, there is no reason to assume that the kind of uncertainty that applies to usability evaluation methods should not apply to accessibility as well.

User testing is a part of usability testing, but user testing with disabled users also adds accessibility findings to the normal usability findings. User testing can be conducted in labs or remotely [65]. In lab testing, a live moderator or observer prepares a scenario and uses a think-aloud technique with high facilitator interaction. Data collection and tasks would focus on specific areas of concern for potential accessibility problems, rather than general site usage. On the other hand, in remote user testing, the tester moderates the test via communication means (e.g. phone, webcam, and web-based tool) rather than being on-site with the user. This is often done due to budget constraints in setting up appropriate labs or when the targeted users are scattered across the country.

Recruiting qualified disabled users is not a trifling task since there is a complexity associated with engaging the right users who match the website audience demographics [66]. People with disabilities are diverse and use different interaction techniques and assistive technology. It is important to recruit people with disabilities, characteristics and expertise depending on the target audience. However, accessibility teams often have limited access during testing phase to real disabled users that

meet the end-user profile and who can take time out to do the evaluation. Users regularly have inadequate means to attend to the evaluation. The use of varied assistive devices, like screening techniques, may cause further problems during the evaluation, especially due to the fact that the mastery of a particular device does not mean an automatic skills transfer to another or newer device, besides hardware incompatibility [59]. Thus, recruiting users for testing normally requires that the level of technical savvy of the tester is known and documented [12]. Novice moderators with limited experience can get confused by the type of difficulties being faced by users. It is important to differentiate between challenges in dealing with assistive technology (especially when the assistive tool is a different product than the user is familiar with) and challenges being faced with the website being tested.

User testing with small populations often provides useful information, and normally when combined with more qualitative techniques can help to understand users' behaviors. However, it is not statistically robust due to the small participants' numbers [67]. It is hard to draw conclusions from limited studies, and results cannot be generalized to all people with similar disabilities. User testing with special populations can be beyond the expertise or financial resources of a typical web developer and can incur greater time and monetary costs due to special arrangements for testing [66].

It is important to know the type of the adaptive strategies or the assistive technology being used by users to arrange a lab that simulates their real interaction experience. Assistive technologies are software and hardware that people with disabilities use to improve interaction with products. In the case of web accessibility testing, it is preferable to ask user to bring assistive technology they are familiar with to make them feel relaxed. Unfortunately, it is not always the case that users are being able to bring their assistive technologies. Many assistive technologies being used by real users can be very expensive and demo versions are limited which make the cost of preparing appropriate labs high. Time requirement escalates with the need to prepare labs equipped with appropriate assistive tools. This kind of procedure can be beyond the testing cost of the IT team. In some cases, it might be best to go to the user's place, rather than having the user come to labs. A drawback to this is that limited numbers of the project team get direct interaction with the user.

Generally, remote testing is less expensive than a traditional lab testing [68]. Nevertheless, it embeds many challenges like users being unable to share their screen over the Internet or having unreliable or slow connection speeds. Moreover, there is the restriction of the user's body language that might inhibit some of the cues to their reactions to the website being tested.

III. WEB ACCESSIBILITY CHALLENGES SUMMARY

After we theoretically analyzed the challenges related to web accessibility, we summarize them in a table format along with their various associated forms. Table II depicts forms and examples for "Standards and Guidelines Challenges", "Challenges during Website's Design and Development" and "Challenges during Evaluation", respectively elicited from the previous literature discussed earlier.

TABLE II. WEB ACCESSIBILITY CHALLENGES SUMMARY

Challenge Forms	Examples
Standards and Guidelines Challenges	
Ambiguity	<ul style="list-style-type: none"> The WCAG 2.0 includes some measurements which need to be quantified in order to be interpreted in the same way by all web developers
Only English version is available	<ul style="list-style-type: none"> Inaccessible to developers who do not understand English Language
Incompleteness	<ul style="list-style-type: none"> The application of WCAG 2.0 alone is not sufficient to guarantee website accessibility
Hard to navigate	<ul style="list-style-type: none"> The guidelines normally are presented in descriptive texts, navigation links and tables, which is not an effective display way for the designers and developers.
Not suitable for naïve web developers	<ul style="list-style-type: none"> Following WCAG 2.0 requires qualified web developers with certain level of technical knowledge of accessibility in order to read and interpret the guidelines.
Requires perfection	<ul style="list-style-type: none"> All the SCs on each level have to be met in order to get the conformance logo which could be frustrating to web developers
Inefficiency	<ul style="list-style-type: none"> Following the guidelines could make the accessibility evaluation process slow. Furthermore, even in large companies, resources including time, money and staff are hard to allocate for accessibility.
Challenges during Website's Design and Development	
Lack of Accessibility Awareness	<ul style="list-style-type: none"> Despite awareness about accessibility over the last few years at the levels of government and legislation, web developers are unaware of the legal and industry requirements of effective accessibility and their level of knowledge remains quite low. Despite the availability of WAI guidelines online, most IT professionals are unaware of them and do not use them.
Lack of Accessibility Motivation	<ul style="list-style-type: none"> Lack of knowledge and motivation by developers and designers because of the time consuming accessibility testing process.
Untrained IT Team	<ul style="list-style-type: none"> lack of exposure to accessibility during training courses for Information Systems professionals Most web designers and developers have little experience to ensure that their code attends to accessibility requirements.
Challenges during Evaluation	
Automated Tools Problems	<ul style="list-style-type: none"> Choosing the right accessibility tool can be time consuming. The need for manual inspection along the tools. Some guidelines are not checked properly (e.g. "alt" attribute). Automated tools results are hard to analyze by inexperienced web developers, which can affect the quality of the test process. Can give inaccurate results and results can vary from one tool to another, depending on interpretation of the guidelines.
User Based Testing Problems	<ul style="list-style-type: none"> The cost of setting up labs is quite high. User testing with large samples is often beyond the expertise or financial resources of a typical web developer and is more time consuming than other methods. Finding disabilities that match the website

	<p>audience can be difficult.</p> <ul style="list-style-type: none"> • The need for expert evaluator • Difficulties in preparing testing materials, in developing realistic scenarios of tasks and in choosing the right sample size for the test
--	---

IV. WEB ACCESSIBILITY RECOMMENDATIONS

Now that we have summarized accessibility challenges, we introduce our recommendations and practical solutions to overcome challenges regarding accessibility guidelines and challenges facing developers during website's design and development as illustrated in Fig. 2.

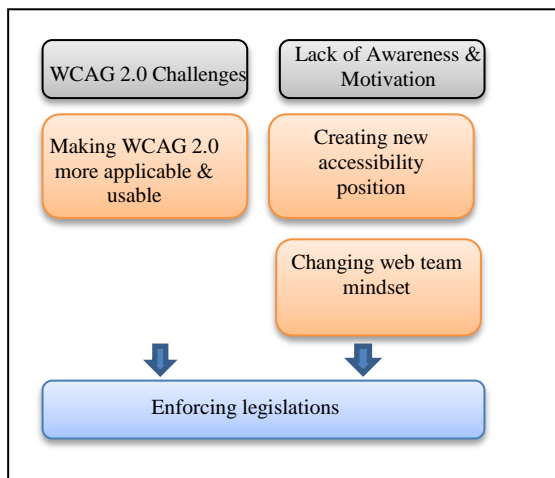


Fig. 2. Suggested solutions to overcome some accessibility challenges

1) Providing applicable and usable guidelines

It is not the case that WCAG 2.0 is not good enough; it will be more useful if the WAI structures the guidelines via job roles that each guideline impacts (i.e. SC will be easier to read if each web team member knows which of them he/she needs to deal with). WAI's assignment of levels to WCAG 2.0 SCs considers the needs of disabled users; however, it will be very helpful if they give an idea of the disability type that would benefit from conforming to each criterion. Moreover, WAI has to be transparent regarding the cost of implementing each guideline. Reasonable measures should include identification of the costs of conforming to accessibility guidelines. Instead of emphasizing the need for perfection, guidelines should be flexible enough to encourage web developers to follow them. This, indeed, will contribute to minimizing the difficulty in both guidelines' structure and presentation.

2) Enforcing accessibility legislation

Widespread recognition of the contribution of ICT, and the web in particular, towards promoting social inclusion and reducing discrimination against people with disabilities is reflected in legislations and policies across the world. Awareness of the nature and implication of legislations and policies regarding web accessibility in different countries is important to guide organizational web accessibility policy. Individual industries and countries need to diligently enhance the enforcement of accessibility legislation. This can be made possible by enacting their own legal standards or legislation rather than following voluntary guidelines.

3) Creating new web accessibility position

One possible viable solution to increase accessibility motivation is to create a new position related to accessibility, e.g. accessibility specialist/expert. This expert can interact with the project team and senior management to make a positive impact on both the community (potential customers) and the organization. In fact, this expert can be a web developer, a quality assurance engineer, or a project manager who takes accessibility training courses and participates in workshops. On the other hand, organizations should start sponsoring workshops for their employees and allocate appropriate funding to support accessibility in their reserved budget.

4) Changing the web team mind-set

To meet end-users' needs, web developers are required to feel as end-users in the accessibility issue. In other words, programmers have to test the website with disabled people or at least use a standardized accessibility testing tool, so that when web developers want to write/change the website's source code, there is a need to change the developers' mind-set to include accessibility. Many web developers do not know the importance of making a website accessible and how this will help disabled people to interact with the web. Moreover, we must change the programmer's perspective regarding the way they code rather than simply asking for a list of changes. Thus, there is a real need to move away from a problem-based approach towards a design principle approach for web accessibility. The whole web team should be inclusive from the beginning when designing an accessible website. Private and public sectors should stress that accessibility is an important indicator of website quality and, without it; the quality of the website will remain low. In addition, emphasizing the importance of accessibility guidelines should start early in web development education. This should take place at the entry level of web development courses. Training and exposing IT professionals and web engineers to accessibility guidelines at an early stage increases their awareness and improves their (programming) attitudes toward this vital issue. Why wait to expose IT students to accessibility until they take senior computing courses when we can make them aware of it earlier? By making accessibility the focus of an introductory level computer science course, we can increase accessibility awareness among IT students.

V. CONCLUSION

Web accessibility is one of the most crucial issues facing the online community. There are various challenges related to websites accessibility that face disabled users and which limit their utilization of the website and may therefore impact their equal rights as well as the organization's revenues. This article has reviewed the negative impact of web accessibility challenges and has critically discussed the primary problems associated with each challenge. Standards and guidelines, during website's design and development (user's awareness, motivation and training) and during-evaluation (automated tools and user testing) have been identified as the three main challenges. Furthermore, we discussed each challenge main problems and their impact on web accessibility. Finally, a list of recommendations was proposed to overcome these challenges. A total collaboration between web team, stakeholders, individual industries and countries is essential to ensure equality and human rights in using the web without

illegal discrimination. We argue that simplifying guidelines and making them more applicable will encourage web developers to follow them. Moreover, we suggest the need for accessibility legislation enforcement by countries rather than following voluntary guidelines. In addition, a project manager has the responsibility to make his web team adhere to accessibility principles. Without a managerial impact on accessibility, it is quite normal for the web team to ignore the accessibility issue or to pretend they have taken care of it. We also need to train and change the web team mind-set regarding how they code to take into consideration the accessibility issue when they program.

REFERENCES

- [1] A. Martínez, J. De Andrés, and J. García, “Determinants of the web accessibility of European banks”, *Information Processing & Management*, Vol. 50 No. 1, pp. 69-86, 2014.
- [2] W3C, “Introduction to web accessibility”, available from: <http://www.w3.org/WAI/intro/accessibility.php> (accessed 2 January 2016)
- [3] B. Hashemian, “Analyzing web accessibility in Finnish higher education”, in *Proceedings of the 13th international ACM SIGACCESS Conference on Computers and accessibility* (Assets '11), ACM Press, New York, NY, Vol. 101, pp. 8-16, 2011.
- [4] K. Nahon, I. Benbasat, and C. Grange, “The missing link: intention to produce online content accessible to people with disabilities by non-professionals”, in *proceeding of 2012 45th Hawaii International Conference on System Sciences* (HICSS), IEEE Computer Society, Washington, DC, pp. 1747-1757, 2012.
- [5] S. Trewin, B. Cragun, C. Swart, J. Brezin, and J. Richards, “Accessibility challenges and tool features: an IBM web developer perspective”, in *Proceedings of 2010 International Cross Disciplinary Conference on Web Accessibility* (W4A '10), ACM Press, New York, NY, pp. 32:1-32:10, 2010
- [6] C. Avila, S. Baldiris, R. Fabregat, and J. Guevara, “Accessibility evaluation improvement using case based reasoning”, *Frontiers in Education Conference* (FIE), Seattle, Washington, pp.1-6, 2012.
- [7] C. Power, A. Freire, H. Petrie, and D. Swallow, “Guidelines are only half of the story: accessibility problems encountered by blind users on the web”, in *Proceedings of the SIGCHI Conference on Human Factors in Computing Systems* (CHI '12), ACM Press, New York, NY, pp.433-442, 2012
- [8] J. Brown, and H. Scott, “The challenges of web accessibility: the technical and social aspects of a truly universal web”, *First Monday*, Vol. 20 No. 9, 2015.
- [9] J. López, A. Pascual, L. Masip, T. Granollers, and X. Cardet, “Influence of web content management systems in web content accessibility”, in *Proceedings of the 13th IFIP TC 13 international conference on Human-computer interaction* (INTERACT11), P. Campos et al. (Eds.), pp. 548–551, 2011.
- [10] M. Baowaly, and M. Bhuiyan, “Accessibility analysis and evaluation of bangladesh government websites”, *Computer Engineering and Intelligent Systems*, Vol. 3 No.4, pp. 46-51, 2012.
- [11] T. Vu, D. Tuan, and V. Phan, “Checking and correcting the source code of web pages for accessibility”, in *proceeding of 2012 IEEE RIVF International Conference on Computing and Communication Technologies, Research, Innovation, and Vision for the Future* (RIVF), IEEE Computer Society, Washington, DC, pp.1-4, 2012.
- [12] G. Brajnik, Y. Yesilada, and S. Harper, “The expertise effect on web accessibility evaluation methods”, *Human-Computer Interaction*, Vol.26 No. 3, pp. 246-283, 2011.
- [13] S.R. Vázquez, “Introducing web accessibility to localization students: implications for a universal web”, in *Proceedings of the 16th international ACM SIGACCESS conference on Computers & accessibility* (Assets '14), ACM Press, New York, NY, pp. 333-334, 2014.
- [14] A. Olalere, and J. Lazar, “Accessibility of U.S. federal government home pages: section 508 compliance and site accessibility statements”, *Government Information Quarterly*, Vol. 28 No. 3, pp.303-309, 2011.
- [15] A.A. Nizar, A. Obeddat, and H.Y. Abu-Addose, “Accessibility as an indicator of Jordanian e-government website quality”, in *Proceedings of 2013 Fourth International Conference on e-Learning Best Practices in Management, Design and Development of eCourses: Standards of Excellence and Creativity*, IEEE Computer Society, Washington, DC, pp. 156-160, 2013.
- [16] S. Lujan-Mora, R. Navarrete, and M. Penafiel, “E-government and web accessibility in South America”, in *Proceedings of 2014 First International Conference on eDemocracy and eGovernment* (ICEDEG), IEEE Computer Society, Washington, DC, pp. 77–82. R. Nicole, “Title of paper with only first word capitalized.” J. Name Stand. Abbrev., in press, 2014.
- [17] Y. Akgül, and K. Vatansever, “Web accessibility evaluation of government websites for people with disabilities in Turkey”, *Journal of Advanced Management Science*, Vol.4 No. 3, pp. 201-210, 2016.
- [18] S. Harper, Y. Yesilada, and S. Abou-Zahra, *Web accessibility evaluation*, Springer, London, pp. 79-106, 2008.
- [19] L. Kubitschke, K. Cullen, C. Dolphin, S. Laurin, A. Cederbom, J. Usero, ...F. Nu., “Study on assessing and promoting e-accessibility”, European Commission, Brussels, available from: <https://ec.europa.eu/digital-single-market/en/news/study-assessing-and-promoting-e-accessibility>, 2013.
- [20] Internet Society, “Internet accessibility: internet use by persons with disabilities: moving forwards”, available from: <http://www.internetsociety.org/>, 2012.
- [21] D. Sloan, and S. Horton, “Global considerations in creating an organizational web accessibility policy”, in *Proceeding of the 11th Web for All Conference* (W4A '14), ACM Press, New York, NY, pp.16, 2014.
- [22] WCAG, available from: <http://www.w3.org/WAI/intro/wcag> , 2016.
- [23] L. Santarosa, D. Conforto, and R. Machado, “Whiteboard: synchronism, accessibility, protagonism and collective authorship for human diversity on web 2.0”, *Computers in Human Behavior*, Vol. 31, pp.591-601, 2014.
- [24] J. Villena, B. Ramos, R.P.M. Fortes, and R. Goulartea, R, “Web videos – concerns about accessibility based on user centered design”, *Elsevier Procedia Computer Science*, Vol. 27, pp. 481-490, 2014.
- [25] S. Gordon, S. and S. Lujan-Mora, “Accessible blended learning for non-native speakers using MOOCs”, *Interactive Collaborative and Blended Learning* (ICBL 2015), IEEE Computer Society, Washington, DC, pp. 19-24, 2015
- [26] J.L. Medina, M. I. Cagnin, and D.M.B. Paiva, “Investigating accessibility on web-based maps”, *ACM SIGAPP Applied Computing Review*, Vol. 15 No. 2, pp. 17-26, 2015.
- [27] W3C, “About W3C”, available from: <http://www.w3.org/Consortium/>, 2016.
- [28] WAI,“WAI guidelines and techniques”, available from: <http://www.w3.org/WAI/guid-tech.html> , 2016.
- [29] WCAG 2.0.,“Web content accessibility guidelines (wcag) overview”, available from: <http://www.w3.org/TR/WCAG20/> , 2016.
- [30] M. Cooper, D. Sloan, B. Kelly, and S. Lewthwaite, “A challenge to web accessibility metrics and guidelines: putting people and processes first”, in *Proceedings of the International Cross-Disciplinary Conference on Web Accessibility* (W4A '12), ACM Press, New York, NY, pp20, 2012.
- [31] G. Miller, S. and Fels, “OpenVL: a task-based abstraction for developer-friendly computer vision”, in *Proceedings of 2013 IEEE Workshop on Applications of Computer Vision* (WACV '13), IEEE Computer Society, Washington, DC, pp. 288-295, 2013.
- [32] T. Bittar, L. Amaral, F. Faria, and R.P.M. Fortes,“Supporting the developer in an accessible edition of web communications: a study of five desktop tools”, in *Proceedings of the Workshop on Information Systems and Design of Communication* (ISDOC '12- EuroSIGDOC), ACM Press, New York, NY, pp.3-9, 2012.
- [33] V. Conway, Website accessibility in Australia and the Australian government's national transition strategy: outcomes and findings, Ph.D. thesis, Western Australia: Edith Cowan University, 2014.

- [34] F. Alonso, L. Fuertes, L. González, and L. Martíez, "On the testability of wcag 2.0 for beginners", in 7th International Cross-Disciplinary Conference on Web Accessibility (W4A'10), ACM Press, New York, NY, pp.1-9,2010.
- [35] E. Tanaka, and H. da Rocha, "Evaluation of Web Accessibility Tools", in Proceedings of the 10th Brazilian Symposium on on Human Factors in Computing Systems and the 5th Latin American Conference on Human-Computer Interaction (IHC+CLIHC '11), Brazilian Computer Society, Porto Alegre, Brazil, pp. 272-279, 2011.
- [36] C. Loitsch, A. Stiegler, C. Strobbe, D. Tzovaras, K. Votis, G. Weber, and G. Zimmermann, "Improving accessibility by matching user needs and preferences", *Assistive Technology: From Research to Practice. In Proceedings of AAATE2013*, IOS Press, Vilamoura, Portugal, Vol. 33, pp. 1357-1365, 2013.
- [37] H. Petrie, C. Power, D. Swallow, C.A. Velasco, B. Gallagher, M. Magenmis, ...K. Down, "The value chain of web accessibility: challenges and opportunities", in *Proceedings of the Workshop on Accessible Design in the Digital World 2011*, CEUR Workshop Proceedings, Lisbon,Portugal,pp.2-12,2011.
- [38] G. Brajnik, Y. Yesilada, and S. Harper, "Testability and validity of wcag 2.0: the expertise effect", in *Twelfth International ACM SIGACCESS Conference on Computers and Accessibility (Assets' 10)*. Orlando, FL: ACM Press, New York, NY, USA. p. 43-50, 2010.
- [39] Hassell Inclusion, "The future of wcag – maximizing its strengths not its weaknesses", available from: <http://www.hassellinclusion.com/2013/01/wcag-future/>, 2013.
- [40] L. Pereira, S. Ferreira, H. Braga, L. Cardoso, D. Salgadob, and R. Nunes, "Using cultural viewpoint metaphors to provide web accessibility for the visually impaired users", *Elsevier Procedia Computer Science*, Vol. 27, pp. 186-196, 2014.
- [41] Y. Yi, and J. Kang, "Do public library websites consider the disabled or senior citizens?", in Proceedings of the 12th ACM/IEEE-CS joint conference on Digital Libraries (JCDL '12), ACM Press, New York, NY,pp.373-374,2012.
- [42] J.T. Nganji, M. Brayshaw, and B. Tompsett, "Describing and assessing image descriptions for visually impaired web users with idat", in *3rd International Conference on Intelligent Human Computer Interaction*. Springer-Verlag, Lecture Notes in Computer Science, August 2011, Reprinted in *Advances in Intelligent Systems and Computing*, Springer Verlag , Vol. 179, pp. 27-37, 2013.
- [43] S.R. Pye, Web Accessibility and its Future: The Requirement of Awareness and Enforcement of Accessibility for those with Visual Disabilities, Graduation Project, Norwich, UK, University of East Anglia, 2011.
- [44] TAW Tool, available from: <http://www.tawdis.net/>, 2016.
- [45] M. Rosson, J. Ballin, J. Rode, and B. Toward, "Designing for the web: revisited: a survey of informal and experienced web developers", *ICWE'05 Proceedings of the 5th international conference on Web Engineering*. Sydney, ACM Press, New York, NY, pp.522-532, 2005.
- [46] S. Gordon, S. and Lujan-Mora, "Web accessibility of moocs for elderly students", *12th International Conference on Information Technology Based Higher Education and Training (ITHET 2013)*, Antalya, Turkey, pp. 1-6, 2013.
- [47] J. Lazar, B. Wentz, A. Almalhem, A. Catinella, C. Antonescu, Y. Aynbinder, ...M. Seidel, "A longitudinal study of state government homepage accessibility in maryland and the role of web page templates for improving accessibility", *Government Information Quarterly*, Vol. 30 No.3, pp. 289-299, 2013
- [48] S. Krug, A common sense approach to web usability, (2nd ed.), New Riders Publishing, Berkeley, California, 2014.
- [49] R. Lopes, K. Isacker, and L. Carricco,"Redefining assumptions: accessibility and its stakeholders", in Proceedings of the 12th international conference on Computers helping people with special needs: Part I (ICCHP'10). Klaus Miesenberger, Joachim Klaus, Wolfgang Zagler, and Arthur Karshmer (Eds.), Springer-Verlag, Berlin, Heidelberg,pp.561-568,2010.
- [50] A.P. Freire, C.M. Russo, and R.P.M. Fortes, "A survey on the accessibility awareness of people involved in web development projects in Brazil", in *Proceedings of 2008 international cross-disciplinary Conference on Web Accessibility (W4A'08)*, ACM Press, New York, NY, pp.87-96, 2008.
- [51] G. Brajnik, and S. Harper, "Model-based engineering of user interfaces to support cognitive load estimation in automotive applications", in Cognitive Load and In-Vehicle Human-Machine Interaction Workshop; adjunct Proceedings of the 5th Int. Conference on Automotive User Interfaces and Interactive Vehicular Applications. Kun, A., Froelich, P. (eds.), Eindhoven, ACM Press, New York, NY, 2013.
- [52] R. Gonçalves, J. Martins, and F. Branco, "A review on the Portuguese enterprises web accessibility levels – a website accessibility high level improvement proposal", *Elsevier Procedia Computer Science*, Vol. 27, pp.176-185, 2014.
- [53] A-Checker Tool, available from: <http://achecker.ca/checker/index.php>, 2016.
- [54] WAVE Tool , available from: <http://wave.webaim.org/>, 2016.
- [55] K. Johari, and A. Kaur, "Measuring web accessibility for persons with disabilities", in Proceedings of 2012 Fourth International Conference on Computational Intelligence and Communication Networks (CICN '12), IEEE Computer Society, Washington, DC, pp.963-967,2012.
- [56] R. Lopes, D. Gomes, D. and L. Carriço, "Web not for all: a large scale study of web accessibility", in *Proceedings of 2010 International Cross Disciplinary Conference on Web Accessibility (W4A '10)*, ACM Press, New York, NY, pp.10:1-10:4, 2010.
- [57] H. Abuaddous, M.Z. Jali, and N. Basir,"Study of the accessibility diagnosis on the public higher institutions websites in Malaysia", in *Proceedings of the 4th International Conference on Computing and Informatics (ICOPI 2013)*, Sarawak, Malaysia, Universiti Utara, pp. 122-127, 2013.
- [58] H. Al-Khalifa, "WCAG 2.0 semi-automatic accessibility evaluation system: design and implementation", *Computer and Information Science*, Canadian Center of Science and Education, Vol. 5 No.6, pp.73-87, 2012.
- [59] M. Greeff, and P. Kotzé, "A lightweight methodology to improve web accessibility", in Proceedings of 2009 Annual Research Conference of the South African Institute of Computer Scientists and Information Technologists (SAICSIT '09), ACM Press, New York, NY, pp.30-39, 2009.
- [60] K. Groves, "A Challenge to Accessibility Testing Tool Vendors", available from: <http://www.karlgroves.com/2012/10/03/a-challenge-to-accessibility-testing-tool-vendors/>, 2013
- [61] M.F. Theofanos, and J.G. Redish, "Bridging the gap: between accessibility and usability", *Interactions*, Vol. 10 No. 6, pp. 36-51, 2003.
- [62] S. Horton, S. and M. Quesenberry, A web for everyone: designing accessible user experience, Rosenfeld Media, 2014.
- [63] J. Nielsen, "Why you only need to test with 5 users", available from: <https://www.nngroup.com/articles/why-you-only-need-to-test-with-5-users/>, 2000.
- [64] S.L Henry, "Just ask: integrating accessibility throughout design", available from: www.uiaccess.com/JustAsk/, 2007.
- [65] K. Madathil, and J. Greenstein, "Synchronous remote usability testing: a new approach facilitated by virtual worlds", in Proceedings of the SIGCHI Conference on Human Factors in Computing Systems (CHI '11), ACM Press, New York, NY, pp.2225-2234, 2011.
- [66] J. Nielsen, "How many test users in a usability study?", available from: <http://www.nngroup.com/articles/how-many-test-users/>, 2012.
- [67] W3C, "Involving users in evaluating web accessibility", available from: <http://www.w3.org/WAI/eval/users.html>, 2010.
- [68] A. Bruun, and J. Stage, "The effect of task assignments and instruction types on remote asynchronous usability testing", in *Proceedings of the SIGCHI Conference on Human Factors in Computing Systems (CHI '12)*, ACM Press, New York, NY, pp. 2117-2126, 2012.

Tri-Band Fractal Patch Antenna for GSM and Satellite Communication Systems

Saad Hassan Kiani, Shahryar Shafique Qureshi, Khalid Mahmood, Mehr-e- Munir, Sajid Nawaz Khan
Electrical Engineering Department, Iqra National University, Peshawar, Pakistan

Abstract—Due to their smaller size and light weighted structures patch antennas are accustomed in modern communication Technology. With additional size in reduction, micro strip antennas are commonly used in handsets, GPS receivers etc. This paper presents a novel design of fractal shape patch antenna using U-slot on patch and defected ground structure. Due to slots on patch and ground, tri-band resonating response is attained with maximum gain and directivity of 4.22dB and 6.51dBi showing high impedance bandwidth and radiation efficiency. The antenna showed good VSWR of 1.63 to 1.02 thus, showing high efficiency. As evident in the simulation results, the proposed antenna has been found useful for W-LAN, GSM, Radio Satellite, Fixed Satellite Services (RSS) & (FSS) and satellite communication systems.

Keywords—miniaturization; directivity; gain; slots; Bandwidth; VSWR

I. INTRODUCTION

The increasing demand of wireless communication and multimedia services has resulted in growing efforts of designing and accomplishment of micro strip patch structures due to their cost efficiency and small size. Applications of such antennas comprise but not restricted to personal communication systems, military applications, jets aircrafts and much more. One of the most necessarily antenna application is in wireless communication. In contrast with classical antennas, patch antennas offer several advantages such as ease in fabrication, low cost light weighted structures. Several techniques have been proposed to reduce the patch antenna size but at the cost of lower gain, lower directivity and reduced bandwidth. Some of the techniques are mentioned below.

With use of split ring resonators, size reduction was only up to 10 to 15% [1-2]. In [3], the dimensions of an antenna are miniaturized to a significant level but gain and the bandwidth is also decreased. By increasing electric permittivity of a substrate, antenna size can be reduced significantly but increase of surface waves in substrate can result in declination of radiation pattern hence worsening antenna bandwidth [4]. Meta materials reduced antenna size when inserted in ground plane structure but the cost surges a bit higher [5-6]. Use of synthetic magnetic conductors resulted with lowered gain at desired resonant frequencies [7]. Hence in simple words patch size reduction has been a very common interesting topic among researchers [8-11].

Therefore, in this paper we have proposed a miniaturized fractal shape patch antenna with u-slots on patch and defected ground structure with good impedance bandwidth, gain and

directivity. The proposed antenna is showing multi frequency response which can be used for various applications systems.

II. ANTENNA DESIGN

The basic patch antenna consists of patch, substrate and ground plane. The basic patch antenna with coaxial probe feed (contacting) is given in fig 1.

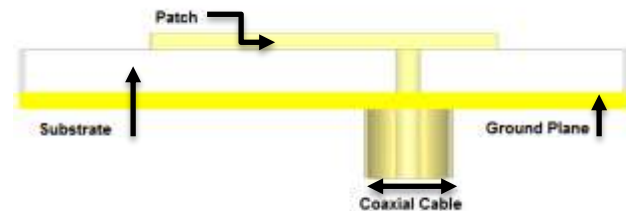


Fig. 1. Normal patch antenna

A. Substrate

The first important task while designing an antenna is selection of a proper substrate with proper dielectric constant.

In proposed antenna design, due its cost effectiveness, moisture withstanding capabilities, FR4 (lossy) is chosen as substrate with dielectric constant of 4.3.

B. Width

In order to derive Patch width, following equation is used. (1).

$$W = \frac{c}{2 f_0 \sqrt{\frac{\epsilon_r + 1}{2}}} \quad (1)$$

Whereas c is the speed of light in free space and f_0 is the resounding frequency and ϵ_r is the relative permittivity.

C. Length

In order to derive Patch length, following equation is used. (2).

$$L = L(\text{eff}) - 2\Delta L \quad (2)$$

Where

$$L(\text{eff}) = \frac{c}{2f_0 \sqrt{\epsilon_{(\text{reff})}}} \quad (3)$$

And

$$\epsilon_{(\text{reff})} = \frac{\epsilon_r + 1}{2} + \frac{\epsilon_r - 1}{4} \left(1 + \frac{12h}{W}\right)^{-1/2} \quad (4)$$

Where h is the height and W as mentioned above is the patch width. Antenna with resonating frequency of 4.5GHz is designed by calculating patch dimensions.

Various dimensions of the proposed antenna technique are provided in table 1.

TABLE I. DIMENSIONS OF PROPOSED ANTENNA

Parameters	Values in MM
Patch Length, PL	16.11
Patch Width, PW	21.43
Ground Length, GL	28.11
Ground Width, GW	33.43
Vertical Fractal Slot Length, VFSL	10.0
Vertical Fractal Slot Width, VFSW	4.0
Horizontal Fractal Slot Length ,HFSL	8.0
Horizontal Fractal Slot Width, HFSW	4.0
U Slot Length, UL	6.0
U Slot Width, UW	1.0
Patch Height, PH	0.0035
Height of Ground, HG	0.08
Height of Substrate, HS	2.0
Horizontal U and H Slot Width, HUW&HHW	1.0
Horizontal U Slot Length, HUL	8.0
Horizontal H Slot Length, HHL	7.0
Vertical U and H Slot Length, VUL&VHL	6.0
Vertical U and H Slot Width, VUW &VHW	1.0

After designing patch antenna for 4.5 GHz, fractal shape is implemented as following.

Patch is slotted by 8mm length and 10mm width horizontally and 10mm length and 4mm width vertically. U shape slot on fractal patch is designed with the following dimensions as shown in Fig 2.

Length of slot is 6mm and width of the slot is 1mm. Now to further reduce size and for efficient frequency response defected ground structure technique is used by adding U and

H slot on a ground plane as shown in fig 2 and figure 3.



Fig. 2. Frontal View of Patch

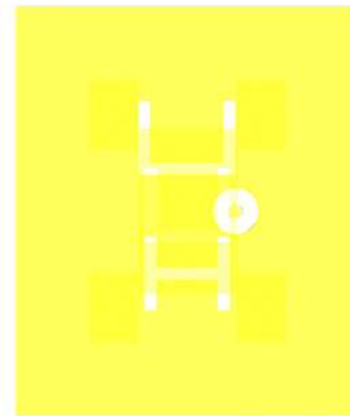


Fig. 3. Frontal View of Ground

The antenna is fed by Co-axial cable a contacting scheme in which inner conductor is mounded to patch through hole from ground through substrate while outer conductor connected with ground plane.

III. RESULTS AND DISCUSSIONS

After simulation, we got the following results in Return loss graph.

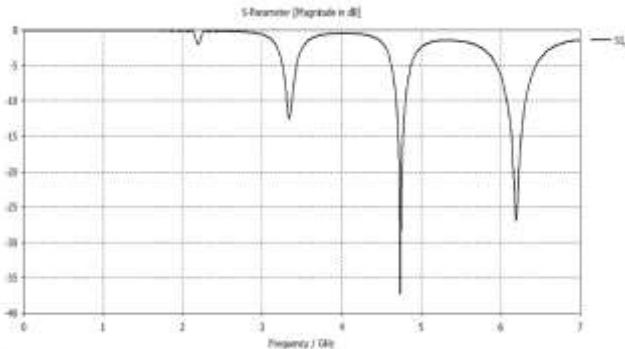


Fig. 4. Return loss graph of antenna

From taking a look at return loss graph shown in Fig 4, we clearly see that we have got a multi frequency response with very good return loss. For frequency 3.349 we have got -12.05dB return loss, 2.92dB of gain 5.64dBi directivity and 60 MHz of bandwidth.

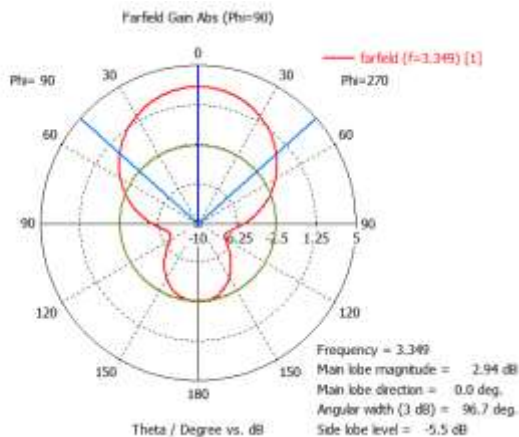


Fig. 5. 1D plot of Gain at 3.349 GHz frequency

In 3.349GHz gain plot, the main front lobe scale is 2.91dB, main front lobe direction is 0 degrees and angular width is 96.8 degrees while back lobe scale is -5.5dB.

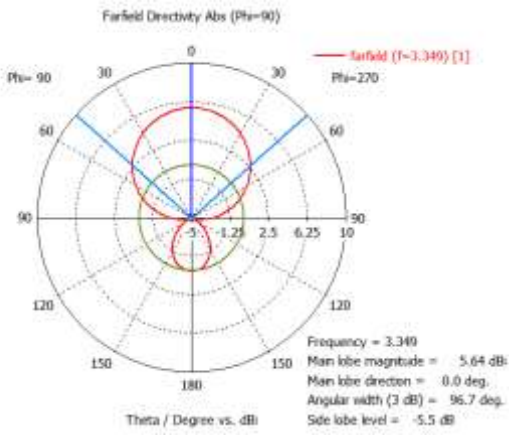


Fig. 6. 1D plot of Directivity at 3.349 GHz frequency

In 3.349GHz directivity plot, the main front lobe scale is 5.64dBi, main lobe direction is 0.0 degrees and angular width is 96.8 degrees while back lobe scale is -5.5dB.

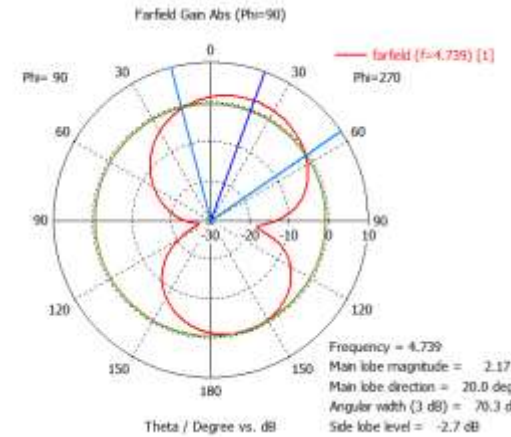


Fig. 7. 1D plot of Gain at 4.739 GHz frequency

In 4.739GHz gain plot, the main front lobe scale is 2.17dB, main lobe direction is 20.0 degrees and angular width is 70.4 degrees while back lobe scale is -2.7dB.

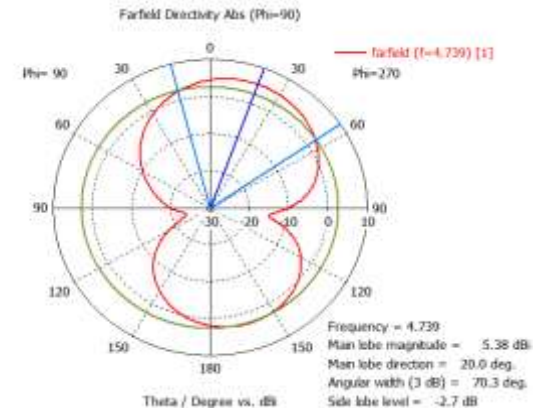


Fig. 8. 1D plot of Directivity at 4.739 GHz frequency

In 4.739GHz directivity plot, the main front lobe scale is 5.38dBi, main front lobe direction is 20.0 degrees and angular width is 70.4 degrees while back lobe scale is -2.7dB.

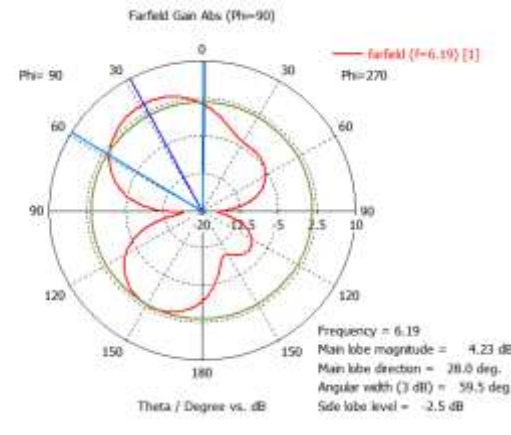


Fig. 9. 1D plot of Gain at 6.19 GHz frequency

In 6.19GHz gain plot, the main front lobe scale is 4.22dB, main front lobe direction is 28.0 degrees and angular width is 59.2 degrees while back lobe scale is -2.5dB.

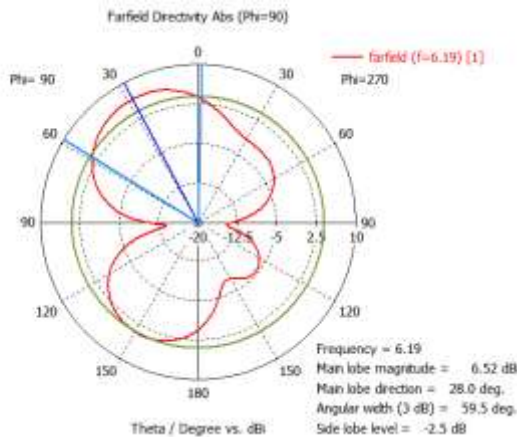


Fig. 10. 1D plot of directivity at 6.19GHz frequency

In 6.19GHz directivity plot, the main front lobe magnitude is 6.51dBi, main front lobe direction is 28.0 degrees and angular width is 59.2 degrees while back lobe scale is -2.5dB.

As goes for VSWR it showed satisfactory results clearly evident from figure 11 as all the resonant frequencies showed response less than 2dB which shows the antenna is efficient as 96 to 98%.

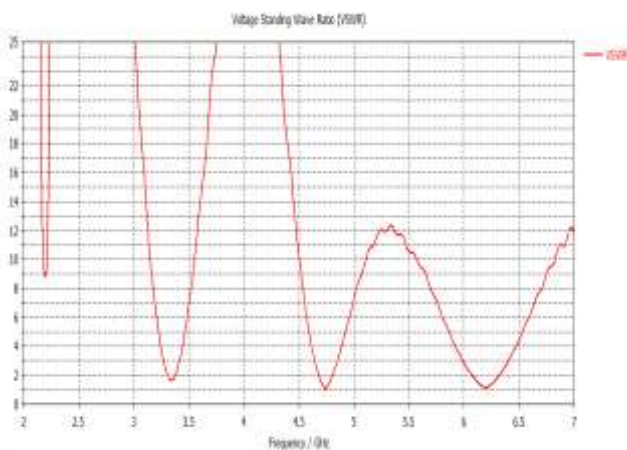


Fig. 11. Voltage Standing Wave Ratio Graph of Antenna

The approximate values of VSWR of the proposed antenna are shown in the following table.

TABLE II. VSWR VALUES OF RESONANT FREQUENCIES

Resonant Frequency	VSWR	Reflection Coefficient	Reflected Power (%)	Reflected Power (dB)	Mismatch Loss (dB)
3.3GHz	1.63	0.24	5.7	-12.41	0.26
4.7GHz	1.02	0.01	0.0	-40.09	0.00
6.1GHz	1.10	0.05	0.2	-26.44	0.01

From results shown in table 2 all the resonant frequencies prove that antenna impedance is matched. For 3.3GHz antenna power delivered is up to 94.3%. For 4.7GHz nearly all the power is delivered from transmitter side. And at last for

6.1GHz power radiated is nearly 99.98%.

The results attained from resonating frequencies both gain and directivity are better than [12-13]. For resonant frequency of 3.3GHz there are no side lob radiations and with the gain exceeding 2dB, makes it suitable for GSM and LTE applications. For 4.7GHz frequency although with slight increase in back radiation, with the higher gain and return loss of resonant frequency it becomes suitable for vehicular and S-band communication applications. At last for 6.1GHz the radiation pattern achieved was very interesting as it was in the form of butterfly. But with the side lobe level of 2.5dB this antenna proves significant response of it making it suitable for Fixed Satellite Services (Earth to Space) applications.

The following table shows all the parameters results of the resonant frequencies of proposed antenna.

TABLE III. PARAMETER RESULTS

Resonant Frequency	Return Loss	Gain	Bandwidth	Directivity
3.3GHz	-12.36dB	2.91dB	60 MHz	5.64dBi
4.7GHz	-37.43dB	2.17dB	110 MHz	5.38dBi
6.1GHz	-26.10dB	4.22dB	300 MHz	6.51dBi

The dimensions of conventional patch antenna with the central resounding frequency of 3.346GHz would require dimensions of $27.94 \times 21.00 = 585 \text{ mm}^2$ while as for proposed design, only by dimensions of $16 \times 21 = 361 \text{ mm}^2$ it is achieved, resulting in shrinking the size up to 61.70%, which is more significant than formerly published methodologies. Also the antenna is showing triple band frequency response with good gain, directivity and good bandwidth for resonant frequencies [12-13].

IV. CONCLUSION

In this paper, a new methodology with tri band resonating frequency is presented. Antenna with size reduction of 61.70% is obtained using defected ground structure and U-Shaped slot on the fractal shape patch. As a result antenna produced responded with a high gain, directivity and good impedance bandwidth for each resonant frequency. The proposed antenna is highly efficient as for all resonating frequencies, the VSWR is seen to be less than 2. The proposed antenna is very useful and can be used for W-LAN, GSM, Radio Satellite, Fixed Satellite Services (RSS) & (FSS) and Satellite communication system applications.

V. FUTURE SCOPE

The proposed tri band antenna can be implemented via MIMO technique and also as in terms of stack configuration. Using stack configuration, further miniaturization can be expected.

ACKNOWLEDGEMENT

The authors would acknowledge the environment and support provided by Iqra National University Peshawar, Pakistan.

REFERENCES

- [1] Kärkkäinen, Mikko, and Pekka Ikonen. "Patch antenna with stacked split-ring resonators as an artificial magneto-dielectric substrate." *Microwave and Optical Technology Letters* 46.6 (2005): 554-556.
- [2] Dong, Yuandan, Hiroshi Toyao, and Tatsuo Itoh. "Design and characterization of miniaturized patch antennas loaded with complementary split-ring resonators." *IEEE Transactions on Antennas and Propagation* 60.2 (2012): 772-785.
- [3] Mosallaei, Hossein, and Kamal Sarabandi. "Antenna miniaturization and bandwidth enhancement using a reactive impedance substrate." *IEEE Transactions on Antennas and Propagation* 52.9 (2004): 2403-2414.
- [4] Yuan, Bo, et al. "An axial-ratio beamwidth enhancement of patch antenna with digonal slot and square ring." *Microwave and Optical Technology Letters* 58.3 (2016): 672-675.
- [5] Singhal, P. K., Bimal Garg, and Nitin Agrawal. "A high gain rectangular microstrip patch antenna using 'different c patterns' metamaterial design in L-band." *Advanced Computational Techniques in Electromagnetics* 2012 (2012): 1-5.
- [6] Dong, Yuandan, and Tatsuo Itoh. "Metamaterial-based antennas." *Proceedings of the IEEE* 100.7 (2012): 2271-2285.
- [7] Rahmadani and A. Munir, "Microstrip patch antenna miniaturization using artificial magnetic conductor," in *Telecommunication Systems, Services, and Applications (TSSA)*, 2011 6th International Conference on, 2011, pp. 219-223.
- [8] Abed, A.T. and Singh, M.S.J., 2016. Slot antenna single layer fed by step impedance strip line for Wi-Fi and Wi-Max applications. *Electronics Letters*.
- [9] Hasan, Mohammed, et al. "A novel miniaturized triple-band antenna." *Electrical & Computer Engineering (ICECE), 2012 7th International Conference on*. IEEE, 2012/
- [10] Yassen, M. T., Hussan, M. R., Hammas, H. A., & Ali, J. K. (2016). A Compact Dual-band Antenna with Fractal Slot Annular Ring and Defected Ground Structure.
- [11] Maiti, Satyabrata, Naikatmana Pani, and Amrit Mukherjee. "Modal analysis and design a planar elliptical shaped UWB antenna with triple band notch characteristics." *Signal Propagation and Computer Technology (ICSPCT), 2014 International Conference on*. IEEE, 2014.
- [12] Farooq U. Multiband microstrip patch antenna using DGS for L-Band, S-Band, C-Band & mobile applications. In *2016 13th International Conference on Modern Problems of Radio Engineering, Telecommunications and Computer Science (TCSET) 2016 Feb 23 (pp. 198-201)*. IEEE.
- [13] Saad Hassan Kiani, Khalid Mahmood, Sharyar Shafeeq, Mehre Munir and Khalil Muhammad Khan, "A Novel Design of Miniaturaized Patch Antenna Using Different Substrates for S-Band and C-Band Applications" *International Journal of Advanced Computer Science and Applications(IJACSA)*, 7(7), 2016.

Strength of Crypto-Semantic System of Tabular Data Protection

Hazem (Moh'd Said) Abdel Majid Hatamleh
Computer Department, Al-Balqa' Applied University,
Faculty of Ajloun, Jordan

Hassan Mohammad
AL-Ahliyya amman university
Department of Engineering, Amman Private University,
Amman, Jordan

Roba mohmoud ali aloglah
Computer Department, Al-Balqa' Applied University,
Faculty of Ajloun, Jordan

Saleh Ebrahim Alomar
AL-Ahliyya amman university
Department of Engineering, Amman Private University,
Amman, Jordan

Abstract—The strength of the crypto-semantic method (CSM) of text data protection based on the use of lexicographical systems in the form of applied linguistic corpora within the formally defined restrictions of selected spheres of applied uses has been analyzed. The levels of cryptographic strength provided by the crypto-semantic method of data protection with due regard of a cryptanalyst's resource capabilities are determined. The conditions under which the CSM provides absolute guarantee of text data protection from confidentiality compromise are determined.

Keyword—cipher key; cryptographic; data protection; crypto-semantic; lexicographical systems

I. INTRODUCTION

In [1], a text data protection method entitled “crypto-semantic method” (CSM) is suggested. The method is based on the use of lexicographical systems in the form of applied linguistic corpora within the formally defined restrictions of selected spheres of applied uses [2,3]. The CSM provides absolute guarantee of text data protection from confidentiality compromise even under the conditions when a sufficiently large number of encrypted information samples (demonstrably larger than the volume of password information) is available to the cryptanalyst. However, in [1] no cryptanalysis as to the CSM's strength has been made. No conditions and restrictions under which the use of the CSM is expedient have been defined. No correspondent formal foundations and proofs have either been provided. The present article aims to eliminate this deficiency.

In this paper, to define the levels of cryptographic strength which the crypto-semantic method of text data protection is capable of providing, with due account of a cryptanalyst's resource capabilities. To define the conditions under which the CSM provides absolute guarantee of text data protection against confidentiality compromise.

II. ANALYSIS OF A CRYPTANALYST'S POSSIBLE ACTIONS

The cryptanalysis of the CSM system of tabular data protection under different conditions of its practical use is presented below.

A. Initial Conditions.

- It is known to the cryptanalyst that the secure text exchange channel functions according to the model presented in figure 1. The flowchart and the performance features of the CSM data protection system implementing this model is dealt with in [1]. The concept of this system is based on the synchronization of pseudo random sequence generators (PRSG) located on the transmitting and receiving sides of the secure exchange channel with the help of a known ciphering key [4-6].
- The text information to be encrypted is presented in a table of an arbitrary type. The form of the table is predefined. No information other than that entered into the table is available.
- The implementers of the CSM protection system, including the application area thesaurus, identical to the implementers of the secure exchange parties are available to the cryptanalyst.

1) Attack model #1

Below, the strength of the CSM protection system under the conditions when at least one pair of corresponding samples of tabular data (i.e. a plain original sample of tabular data and a corresponding sample of encrypted data) are known to the cryptanalyst is analyzed. The aim of the attack is for the cryptanalyst to determine the secret keyword (password) which a priori is unknown. It is appropriate in this case to take as the strength index the criterion K_1 – the maximum possible number of the brute-force search variants of the ciphering key equal to the number of possible ciphering key values:

$$K_1 = a^k$$

where a is the basis of the key information alphabet and k is the ciphering key capacity. The index K_1 under the given conditions characterizes the strength of the CSM protection system on a specified fixed level which can be explicitly ascertained by the cryptanalyst.

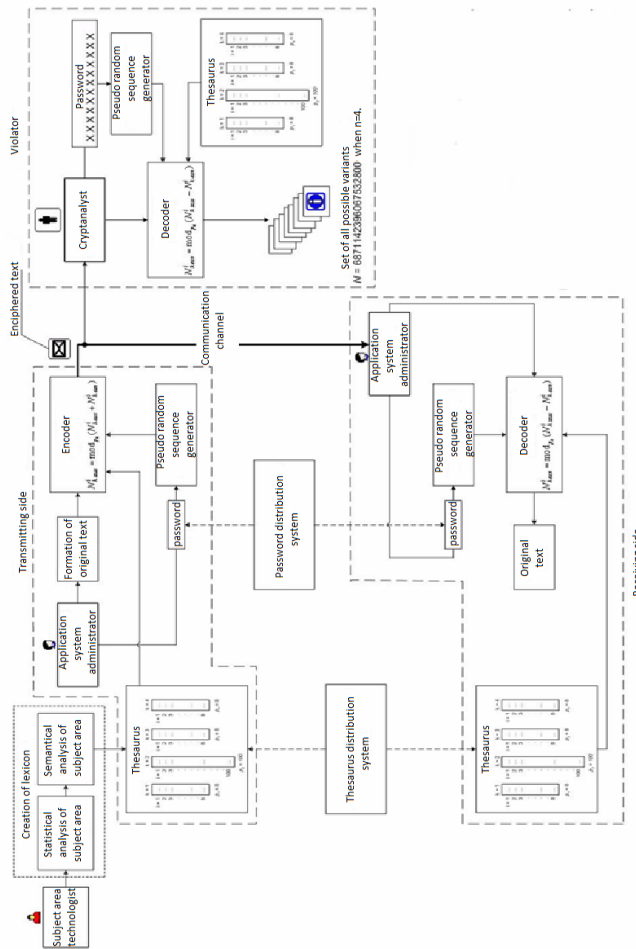


Fig. 1. Functional model of the CSM system of tabular data protection

B. Initial conditions:

- the ciphering key is unknown, but at least one pair of samples – the original data and the corresponding encrypted tabular data – are known to the cryptanalyst.
- the secure exchange parties have not changed the password within the time span when these samples were received.

1) Cryptanalyst's actions

The cryptanalyst repeatedly attempts to decipher the encrypted sample of the tabular data, the original denotation of which is known to them, by brute force attack. In the process of deciphering, the cryptanalyst uses the implementers of the CSM tabular data protection system identical to the implementers of the secure exchange parties. The original denotation of the password is defined as the variant of the keyword with the use of which the corresponding known original sample of tabular data will be obtained as the result of deciphering.

2) Conclusion on the attack model #1:

- the cryptanalyst is able to identify the fact of the successful termination of the attack and, having implemented the attack model #1, to reliably determine the password.

- under these conditions the CSM system is unable to absolutely (according to Shannon [7]) guarantee protection. The CSM system's strength in these circumstances totally depends on the strength of the cryptographic algorithm used.

3) Attack model #2

Below, the strength of the CSM protection system under the conditions when no corresponding pairs of samples of original and encrypted tabular data are available is analysed. Here, the value of the distance of uniqueness does not meet the requirement of absolute protection guarantee (see [7]). The distance of uniqueness (or the point of uniqueness) is defined as such an approximate encrypted data size for which the sum of the real amount of information (entropy) in the corresponding plain data sample plus the keyword entropy equals the number of bits in the encrypted data sample. The distance of uniqueness is the cut-off criterion enabling to evaluate the minimum required volume of encrypted data samples sufficient for their brute-force deciphering. In the case when the analyst deciphers these data they are certain that they have obtained a reliable sample of the original data, as in this case only one reasonable way of their deciphering exists. The distance of uniqueness criterion serves not only as the measure of volume of intercepted encrypted data necessary for their deciphering, but also as the measure of volume of encrypted data samples necessary for the certainty in the uniqueness of the deciphering result obtained to exist. In this case it is considered that the volume of encrypted data available to the cryptanalyst exceeds the distance of uniqueness. Thus, a theoretical possibility of breaking the cipher exists.

4) Initial conditions:

- the absence of any corresponding pairs of original and encrypted information samples, i.e. cryptanalysis can be carried out only on the basis of the intercepted ciphertext;
- the implemented variant of the pseudo random sequence generators in the CSM system (see. [1,6]) provides the randomness of substitutions;
- the cryptanalyst is able to obtain the data on the statistical properties of the application area thesaurus to the extent enabling to construct a function of distribution of a priori probabilities of occurrence of semantic units of the predefined table form on the receiving end of the CSM protection system encoder;
- the cryptanalyst is able to obtain the volumes of ciphertexts exceeding the distance of uniqueness;
- the condition of maintaining the distance of uniqueness is not met; sufficient volume of the intercepted encrypted tabular data samples (obtained within the time span when the ciphering key was not changed) is available to the cryptanalyst in order for them to come to valid statistical conclusions as to the probability of a specific semantic units of the predefined table appearing.

5) Cryptanalyst's actions

a) Preparatory stage.

Preliminary collection of the information on the statistical properties of the secure exchange information:

b) the collection of a batch of tabular data samples from the defined thesaurus within the defined application area with the use of the defined table form;

c) the statistical analysis of the collected batch with the aim of constructing a function of a priori probabilities distribution of occurrence of semantic units on the receiving end of the encoder which are the secure exchange information within the defined table form. This function may be used as a reference for the comparison with a posteriori probabilities distribution in the frequency analysis of the intercepted encrypted tabular data samples.

C. Attack stage.

The cryptanalyst uses the implementers of the CSM tabular data protection system, carries out the enciphering/deciphering of all variants of the semantic units of the defined table form by brute force attack and forms batches of variants corresponding to the intercepted encrypted tabular data samples.

The obtained variant batches are used by the cryptanalyst to construct possible variants of the discrete function of distribution of a posteriori probabilities of occurrence of semantic units on the transmitting end of the decoder.

The constructed variants of the function of distribution of a posteriori probabilities of occurrence of semantic units on the transmitting end of the decoder are compared by the cryptanalyst with the reference function of distribution of a priori probabilities constructed at the preparatory stage in order to make the decision as to the most probable variants of the password.

The cryptanalyst makes the decision as to the most probable variants of the password corresponding to the variants of the function of distribution of a posteriori probabilities most similar to the reference function. The similarity criteria depend on the matter of the applied problem solved by the defined table form.

It is clear that under these circumstances the strength index may not be a fixture as it may occur that the occurrence of specific variants of semantic units of the defined table form at the receiving end of the encoder are not statistically related. Thus, the statistical analysis may turn out to be unsuccessful. Nevertheless, a probability to define the lower threshold of the CSM system strength exists.

In this case it is expedient to present the strength index as

$$K_2 = K_1 \times V \quad (2)$$

where K_1 is the strength index of the implemented cryptalgorith and V is the total number of the brute-force search variants of the tabular data samples in the course of implementing attack model #2. It is clear that $V=V_1V_2$, where V_1 is the number of variants of semantic units of the defined table form sent to the receiving end of the encoder and V_2 is the number of the intercepted encrypted secure exchange information samples used in the course of the analysis.

1) Conclusion on the attack model #2.

a) The results of the frequency analysis of the predefined table form semantic units with the use of intercepted encrypted tabular data samples under certain circumstances may essentially enhance the probability of a correct detection of the password. However, the cryptanalyst is unable to identify the fact of the successful attack completion, and having implemented attack model #2, cannot guarantee the reliability of the password detection.

b) under these conditions the CSM system is unable to absolutely (according to Shannon [7]) guarantee tabular data protection.

c) The strength of the CSM protection system under these conditions even in the worst case, i.e. when attack model #2 has been successfully implemented, is estimated as V times higher than the strength of the cryptographic algorithm used.

Below, a graphic presentation of the dependence of the strength index K on the ciphering key capacity k in relation to the two attack models discussed above is given (see figure 2).

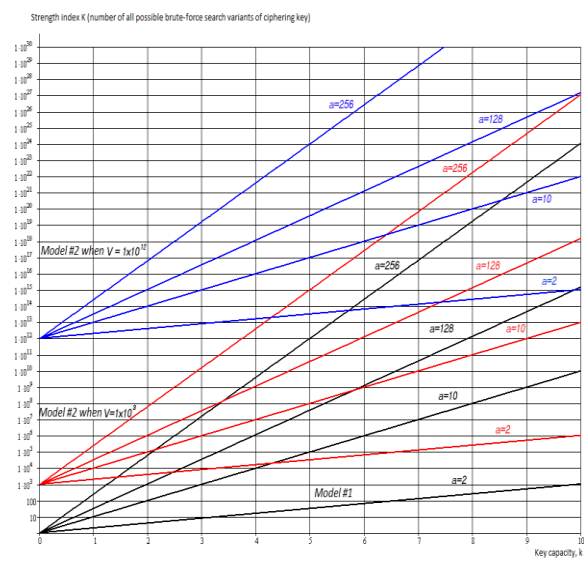


Fig. 2. Graph of strength index against ciphering key capacity

First, a trivial result: with the increase of the ciphering key length the protection system strength is enhanced. Second, in any case the strength of the CSM system against type 1 attacks is significantly lower than the strength of this system against type 2 attacks. Third, with the growth of the batch volume V the CSM protection system's cryptostrength is enhanced.

Below, the dependence of the strength index K on the a parameter, where a is the basis of the key information alphabet, is examined. It is seen in figure 1 that increasing the value of the a parameter will significantly increase the strength index K if $k = \text{const}$. For example, for attack model #1, where the key capacity $k = 8$, the strength index takes on the following values: $K = 256$ where $a = 2$, $K = 1 \cdot 10^8$ where $a = 10$, $K = 1,4064 \cdot 10^{12}$ where $a = 128$ and $K = 1,8447 \cdot 10^{19}$ where $a = 256$.

The CSM system strength against type 1 attacks is significantly lower than this system's strength against type 2 attacks, and, with the growth of the batch volume V necessary for the analysis, the CSM protection system's cryptostrength is enhanced. In its turn, the need to increase V is conditioned by the demands for the increase of the statistical conclusions accuracy as to the character of the function of distribution of the semantic elements of the deciphered tabular data.

Use of the CSM protection system as a perfect secrecy system

As the basic protection effectiveness parameter we chose the so called amount of secrecy according to the terminology used in C. Shannon's works [7]. Also, the notion of the information protection system (IPS) entropy based on the use of key information is used. The IPS entropy is used as a measure of the amount of space of the password information keys. Assume the condition of maintaining the distance of uniqueness in this case is met. Insufficient volume of the intercepted encrypted tabular data samples (obtained within the time span when the ciphering key was not changed) is available to the cryptanalyst in order for them to come to valid statistical conclusions as to the probability of a specific semantic units of the predefined table form appearing.

In most symmetrical key systems, the distance of uniqueness is determined according to the following formula:

$$U = \frac{H(K)}{D} \quad (3)$$

where $H(K)$ is the information protection system (IPS) entropy, K is the number of possible keys in the IPS and D is the redundancy of the language used for message display.

In its turn, the language redundancy D is calculated as

$$D = R - r \quad (4)$$

where R is the maximum entropy of stand-alone metasymbols, and r is the entropy of the language used for displaying the message M, calculated as

$$r = \frac{H(M)}{n} \quad (5)$$

where $H(M)$ is the entropy of the message and n is the message length.

In this case enciphered samples with the total length less than the distance of uniqueness are used for encrypting messages. Thus, it is possible to provide a theoretically perfect protection, as under such circumstances the ambiguity of the cryptanalytical problem solving appears. If by means of the correct thesaurus synthesis one can provide almost equal probability of receiving each solution, under such circumstances the cryptanalyst find themselves in an ambiguous state, in particular they cannot make a valid decision, true on the basis of the deciphered messages.

Thus, in this case we stick to the condition that the volume of the tabular data encrypted by one key does not exceed the distance of uniqueness:

$$U = \frac{\log_2(K)}{D} \quad (6)$$

where U is the distance of uniqueness, K is the maximum possible number of the brute-force search variants of the ciphering key and D is the redundancy of the language used for displaying the semantic units of the predefined table form.

If condition (6) is met, in the case of an exhaustive search of the ciphering key the original sample of the transmitted data will appear on the transmitting end of the decoder not more than once.

Initial condition: the protection system meets the conditions of a perfect secrecy system, i.e. the cryptanalyst is unable to obtain volumes of data encrypted with one key exceeding the distance of uniqueness.

The definition of the strength index under these conditions loses any significance, since it is impossible to identify the moment of the successful attack completion. If the CSM system parameters meet the conditions of a perfect secrecy system, the tabular data protection is absolutely guaranteed. Neither a priori nor a posteriori data on the statistical properties of the secure exchange information can be used. Thus, modelling of any attacks under these circumstances loses its sense.

Also, under these circumstances an absolute protection guarantee is provided by the famous Mauborgne/Vernam scheme [4,5]. Below, the proofs that the CSM system has essential advantages over this scheme are presented.

Below, we plot the uniqueness distance as a function of the message length.

The IPS entropy $H(K)$ is used as the measure of the amount of space of the keys K, namely:

$$H(K) = \log_2 K \quad (7)$$

where K is the number of possible keys in the IPS.

The language redundancy is calculated using formula (4). Consequently

$$R = \log_2 B \quad (8)$$

where B is the number of alphabet symbols calculated using the following formula:

$$B = \prod_{i=1}^s S_i \quad (9)$$

where s is the number of sublexicons in the selected tabular form thesaurus, S_i is the number of words (or phrases) in the ith sublexicon of the thesaurus.

The entropy of the language r, with the help of which the message M is displayed, is calculated using formula (5). The entropy is measured in bits and equals

$$H(M) = \log_2 N \quad (10)$$

where N is the number of possible meanings of the message.

Thus, on the basis of (3), (8) and (5), we have:

$$U = \frac{H(K)}{\log_2(B) - \frac{H(M)}{n}} \quad (11)$$

On account of the perfect secrecy system properties, the number of keys K must equal N – the number of messages having the length of n . Thus, if $H(K)=H(M)=\log_2 N$, the following equation is possible:

$$U = \frac{\log_2 N}{\log_2(B) - \frac{\log_2 N}{n}} \quad (12)$$

It is now necessary to find the dependency of N – the number of possible message meanings – against n – the message length. When calculating N , it is worth keeping in mind that each table row (i.e. each letter in the message) occurs only once (i.e., letters do not repeat). In this case, the maximum possible message length equals the number of letters in the alphabet. Thus, the equation for calculating N – the number of possible message meanings at different n – is as follows:

$$N = \prod_{n=1}^n [B - (n-1)] \quad (13)$$

In order to meet the condition of keeping the distance of uniqueness, it is necessary to correctly calculate the key capacity (length) in correlation with the message length:

$$k = \log_2 N \quad (14)$$

where k is the keyword capacity and N is the number of the possible meanings of a message having the length of n . With due account of (13), the dependency of the ciphering key length against the message length can be expressed in the following way:

$$k = \log_2 \prod_{n=1}^n [B - (n-1)] \quad , \quad (15)$$

where B is the number of the symbols of the alphabet of the language in which the message is presented.

Thus, where $B = \text{const}$ and where $H(K)=H(M)$

(the condition of the perfect secrecy system), the following can be presented (see figure 3):

$$U(n) = \frac{\log_2 \prod_{n=1}^n [B - (n-1)]}{\log_2(B) - \frac{\log_2 \prod_{n=1}^n [B - (n-1)]}{n}} \quad . \quad (16)$$

The dependency of the key entropy $H(K)$ against the message length n can be presented in the following way (see figure 4 for the diagram):

$$H(K) = \log_2 \prod_{n=1}^n [B - (n-1)] \quad (17)$$

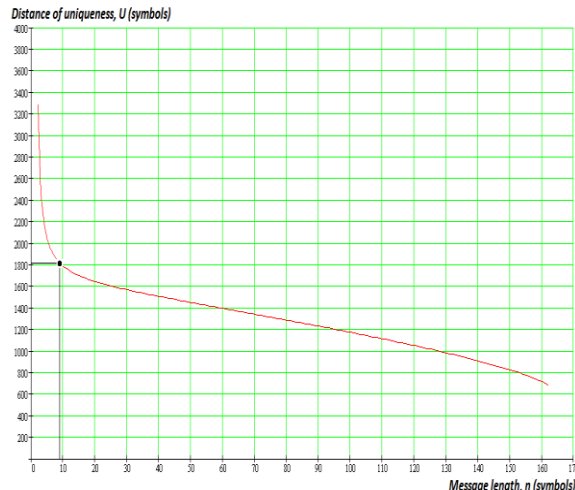


Fig. 3. Graph of the distance of uniqueness U against the message length n

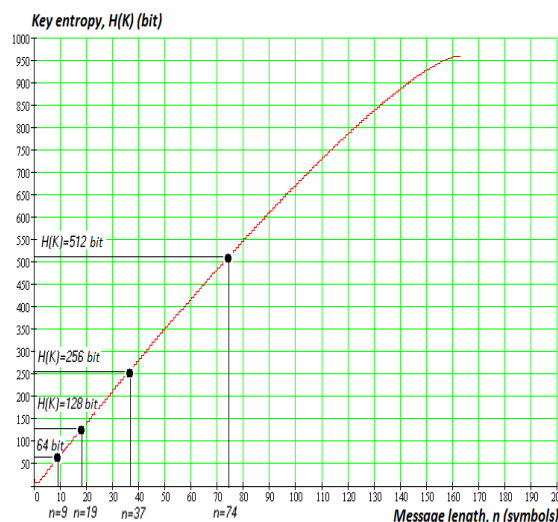


Fig. 4. Graph of the ciphering key entropy $H(K)$ against the message length n

It is advisable to use the graphs in figures 3 and 4 for calculating the maximum possible number of communication sessions without changing the ciphering key while keeping the feature of the perfect secrecy system intact.

It is clear that the CSM protection system in the perfect secrecy system mode, with 64-bit key length with no change in the key, can ensure the absolute protection of 1800 transmitted language elements, while the one-time pad technique provides absolute protection only for 64 language elements. Thus, the

CSM protection system, as opposed to the famous Mauborgne/Vernam scheme, can provide absolute protection under the conditions that the volume of original (plain) text significantly exceeds the volume of key (password) information.

It is worth keeping in mind that the artificial language redundancy dealt with in the given example is negligibly small, which is uncharacteristic of natural languages. Artificial languages are characterized by relatively large value of the distance of uniqueness.

III. MAIN RESULTS AND CONCLUSIONS

The strength of the crypto-semantic method (CSM) of text data protection based on the use of lexicographical systems in the form of applied linguistic corpora has been analysed. The indices of cryptographic strength provided by the crypto-semantic method of text data protection with due regard of a cryptanalyst's resource capabilities are determined and the levels of cryptographic strength are introduced. The conditions under which the CSM provides absolute guarantee of text data protection against confidentiality compromise are determined.

If at least one pair of samples – original ones and corresponding samples of encrypted tabular data – are known to the cryptanalyst, the CSM system's strength in these circumstances totally depends on the strength of the cryptographic algorithm used.

If no corresponding pairs of original and encrypted information sample pairs are available (i.e. cryptanalysis is carried out only on the basis of the intercepted ciphertext), but the cryptanalyst is able to obtain the data on the statistical properties of the application area thesaurus and the volumes of

ciphertexts exceeding the distance of uniqueness, the CSM protection system strength is estimated as V times higher than the strength of the cryptographic algorithm used, where V is the total number of the brute-force search variants of the tabular data samples.

If the CSM system meets the conditions of a perfect secrecy system, i.e. the cryptanalyst is unable to obtain volumes of data encrypted with one key exceeding the distance of uniqueness, protection is absolutely guaranteed. As opposed to the famous Mauborgne/Vernam scheme, the CSM system can provide absolute protection under the conditions that the volume of original (plain) text significantly exceeds the volume of key (password) information.

REFERENCES

- [1] The Art of Deception Kevin D. Mitnick 17 Oct 2003
- [2] McEnery, Tony and Wilson, Andrew. Corpus Linguistics: An Introduction. 2nd Edition, Edinburgh: Edinburgh University Press, 2001.
- [3] Schneier B., Applied Cryptography: Protocols, Algorithms, and Source Code in C, 2nd ed. New York // John Wiley and Sons, 1996.
- [4] Математичні основи криптоаналізу [Текст]: навч. Посібник С.О.Сушко, Г.В. Кузнецов, Л.Я. Фомічова, А.В. Корабльов. – Дніпропетровськ (Україна): Національний гірничий університет, 2010. -465 с.
- [5] Шеннон К.Э. «Теория связи в секретных системах». В кн.: Шеннон К.Э. Работы по теории информации и кибернетике. М.: Иностранный литература. 1963, с. 332-402, -829 с.
- [6] A statistical Test Suite for the Validation of Random Number Generators and Pseudo Random Number Generators for Cryptographic Applications [Text]: NIST Special Publication 800-22 Rev1. – Gaithersburg, Maryland: NIST, 2008. – 153 p.
- [7] Cryptanalysis Helen Fouche Gaines 01 Apr 1989
- [8] Mike Meyers' CompTIA Security+ Certification Passport (Exam SY0-301) T. J. Samuelle 01 Jul 2011

New Speech Enhancement based on Discrete Orthonormal Stockwell Transform

Safa SAOUD

Physics Department
Faculty of Science of Tunis
Tunis, Tunisia

Souha BOUSSELM

Physics Department
Faculty of Science of Tunis
Tunis, Tunisia

Mohamed BEN NASER

Physics Department
Faculty of Science of Tunis
Tunis, Tunisia

Adnane CHERIF

Physics Department
Faculty of Science of Tunis
Tunis, Tunisia

Abstract—S-transform is an effective time-frequency representation which gives simultaneous frequency and time distribution information alike the wavelet transforms (WT). However, the ST redundantly doubles the dimension of the original data set and the Discrete Orthonormal S-Transform (DOST) can decrease the redundancy of S-transform farther. So, this paper aims to propose a new method to remove additive background noise from noisy speech signal using DOST which supplies a multi-resolution analysis (MRA) spatial-frequency representation of image processing and signal analysis. Hence, the performances of the applied speech enhancement technique have been evaluated objectively and subjectively in comparison with respect to many other methods in four background noises at different SNR levels.

Keywords—*MRA; Stockwell Transform; DOST; DWT; speech enhancement*

I. INTRODUCTION

The distortion of signals by noise is a ubiquitous problem. In fact, the background noise deteriorates the intelligibility and quality of the speech signals resulting in a harsh drop in performance of speech applications such as sound recording, telecommunications and teleconferencing. These applications need noise reduction and recover the clean signal from noisy signal. Speech enhancement is the most important technique in speech signal processing domain. It eliminates noise and ameliorates the quality and intelligibility of speech communication.

Over the last decades, noise suppression from speech signals is a very interesting area of researchers during speech processing.

The literature is enriched by many works which treat several methods for speech enhancement has been developed and investigated such as Discrete Fourier transformer (DFT), Discrete Cosine Transformer (DCT), Karhunen-Loeve transformer (KLT), Wiener filtering[2,3], Spectral Subtraction [1], Wavelet Transform (WT) [5-8, 22-26], etc. All the methods have their advantages and inconveniences. Particularly, although the Spectral Subtraction [1]-[12] provides a tradeoff between speech distortion and residual

noise, it suffers from a musical noise artifact that is perceptually annoying. Also, the Wiener estimator has a moderate computation load, but it offers no mechanism to control tradeoff between speech distortion and residual noise. Thus, the one major problem of wiener filter based methods [2]-[3] is the requirement of obtaining clean speech statistics necessary for their implementation. Among the methods using time-frequency analyses, an approach of reducing different types of noise that corrupt the clean speech is the use of Discrete Wavelet Transform (DWT) [5]-[9], which is a superior alternative to the analyses based on Short Time Fourier Transform (STFT).

Even though the wavelet transform (WT) has dominated signal denoising for years, and become a powerful tool of signal analysis and is widely used in many applications which comprise image processing and signal analysis. However, in wavelet transform, only the scale information is supplied, so the applications using the wavelet transform may be limited when the absolutely-referenced frequency and phase information are required [10].

The Stockwell Transform (ST) proposed by R. G. Stockwell in 1996 [11], is a time-frequency analysis method. The ST improves the time-frequency resolution of Short Time Fourier Transform (STFT), and can be regarded as an extension or special case of wavelet transform (WT) in the multi-resolution analysis domain. The use of S-transform can get more precise relationship between the distribution of frequency and time of the signal. Thus, the Stockwell Transforms [11] is a hybrid of the STFT and the WT. It provides a time-frequency representation of a signal with a frequency-dependent resolution and shows a great promise in various applications. However, the ST redundantly doubles the dimension of the original data set. Due to this redundancy; use of the ST is computationally expensive and even infeasible on some large size data sets.

Thus, to improve its computational efficiency, R. G. Stockwell proposed the Discrete Orthonormal S-Transform (DOST) in 2007 [11] which reduce the redundancy of S-transform further and makes S-transform practical in real life

and much more convenient. The DOST is based on a set of orthonormal basis functions that localize the Fourier spectrum of the signal. It samples the time-frequency representation given by the ST with zero information redundancy and retains the advantageous phase properties of the ST. Despite The DOST is fairly young compared to other transform, it has been demonstrated to be useful in some fields Such as in image compression [10][13][14][15], image restoration[12] , and image texture analysis[16] .It has also been successfully applied in signal analysis to channel instantaneous frequency analysis.

Therefore, in order to preserve useful information in a speech signal and eliminate as much noise as possible, we propose in this paper, a new method for speech enhancement using the Discrete Orthonormal Stockwell Transform (DOST). The main objective of the proposed method is to decrease the speech distortion and increase the speech intelligibility of degraded speech signals and reduce the listener's fatigue. This method was compared to the Discrete Wavelet Transform and Spectral Subtraction by means of objective and subjective criteria. The obtained results indicate a good performance of the proposed method and show its high potential for speech enhancement. This paper is organized as follows: Section 2 depicts a brief introduction to the Stockwell transform, the DOST and wavelet theory. Section 3 attempts to explain the methodology for the proposed speech enhancement technique using DOST and DWT. In Section 4, we present the objective and subjective performance measurement parameters used for speech enhancement and we discuss the results. Finally, Section 5 concludes this paper with a discussion and the imagination of our future work.

II. THEORY

A. Stockwell Transform

The Stockwell Transforms proposed in 1996 [11, 17, 18, 19, 20], gives a full time-frequency decomposition of a signal. The Stockwell transforms (ST) of $h(t)$ is defined as the Fourier transform (FT) of the product between a Gaussian window function, and $h(t)$.

$$s(\tau, f) = \int_{-\infty}^{+\infty} h(t) \frac{|f|}{\sqrt{2\pi}} e^{-\frac{(\tau-t)^2 f^2}{2}} e^{-i2\pi f t} dt \quad (1)$$

Where f is the frequency, t and τ are time variables, the Stockwell transform decomposes a signal into frequency (f) and temporal (τ) components. The relation between $S(\tau, f)$ and the Fourier transform of $h(t)$ is expressed as:

$$\int_{-\infty}^{+\infty} s(\tau, f) d\tau = H(f) \quad (2)$$

Where $H(f)$ is the Fourier Transform of $h(t)$.Therefore, we can get the original signal by using this relationship between FT and S-transform:

$$h(t) = \int_{-\infty}^{+\infty} \left\{ \int_{-\infty}^{+\infty} s(\tau, f) d\tau \right\} e^{i2\pi f t} df \quad (3)$$

B. Discrete Orthonormal S-Transform

The DOST is introduced as an orthonormal version of ST. It can be defined as an inner product between a time series $h[k]$ and the basis function $d[k]$. We use v to specify the center of each frequency band, β represents the bandwidth and τ

represents the location in time. Using these parameters, the k th basis vector is expressed as:

$$S_{(v,\beta,\tau)} = \langle d[k]_{[v,\beta,\tau]}, h[k] \rangle = \frac{1}{\sqrt{\beta}} \sum_{k=0}^{N-1} \sum_{f=v-\beta/2}^{v+\beta/2-1} e^{-i2\pi \frac{k}{N} f} e^{i2\pi \frac{\tau}{\beta} f} e^{-i\pi \tau} h[k] \quad (4)$$

For a signal of length N , the discrete ST generates N^2 coefficients, while the DOST can represent the same signal with only N coefficients. For that, the DOST is a non-redundant version of the ST. In order to calculate the DOST much faster we introduce the FFT into DOST:

$$S_{(v,\beta,\tau)} = \langle d[k]_{[v,\beta,\tau]}, h[k] \rangle = \frac{1}{\sqrt{\beta}} \sum_{k=0}^{N-1} \sum_{f=v-\beta/2}^{v+\beta/2-1} \exp \left(-i2\pi \frac{k}{N} f \right) \exp \left(i2\pi \frac{\tau}{\beta} f \right) \exp (-i\pi \tau) H(f) \quad (5)$$

Using FT we can write:

$$S_{(v,\beta,\tau)} = \frac{1}{\sqrt{\beta}} \sum_{f=v-\beta/2}^{v+\beta/2-1} \exp (-i\pi \tau) \exp \left(i2\pi \frac{\tau}{\beta} f \right) H(f) \quad (6)$$

C. Discrete Wavelet Transforms (DWT)

The Discrete Wavelet Transform (DWT) is a powerful tool of signal and image processing that have been successfully used in many scientific fields such as signal processing and image compression. DWT provides sufficient information both for analysis and synthesis and reduce the computation time sufficiently. It analyzed the signal at different frequency bands with different resolutions and decompose the signal into a coarse approximation and detail information. The general form of DWT at L-level expressed in terms of L detail coefficients $d_j(k)$, and the Lth level approximation $a_L(k)$ coefficients can be written as [9]:

$$f(t) = \sum_{j=1}^L \sum_k d_j(k) \Psi_j(t) + \sum_k a_L(k) \phi_L(t) \quad (7)$$

Where, and $\Psi_j(t)$ is the mother wavelet and $\phi_L(t)$ is the scaling function. The approximation and detail at level j are expressed as:

$$a_{j+1}(k) = \sum_m h_0(m-2k) a_j(m) \quad (8)$$

$$d_{j+1}(k) = \sum_m h_1(M-2k) a_j(m) \quad (9)$$

Where $h_0(k)$ and $h_1(k)$ are known as wavelet filters

III. NEW PROPOSED SPEECH ENHANCEMENT METHOD

In this research work, speech enhancement algorithm based on transformation is performed using three most commonly used steps: applying transformation (DOST or DWT), truncate coefficients (thresholding) and applying inverse transformation (IDOST or IDWT) to reconstruct the denoised signal (Figure 2).

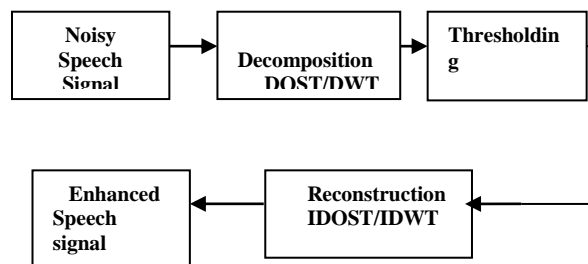


Fig. 1. Block diagram of the suggested method

$$\text{Let: } y(n) = s(n) + w(n) \quad (10)$$

Finally, complete content and organizational editing before formatting. Please take note of the following items when proofreading spelling and grammar

Where $s(n)$ is the clean speech $w(n)$ the noise and $y(n)$ the noisy speech signal. The proposed Discrete Orthonormal S-transform used in speech signal denoising can be represented as follows:

- In this step, the input speech signal is divided into stationary frames and then transformation method (DOST or DWT) is applied of each frame in order to extract coefficients.
- After performing the transformation method of the speech frame, denoising involves truncating the obtained coefficients below a given threshold values. For truncate the small valued coefficients, we calculate the appropriate threshold τ to retain the original signal and restrict the noise and let all the coefficients in DOST domain compare with the threshold. In this case, the threshold value (τ) is manually adjusted and is chosen from coefficients ($0 < \tau < \text{CvalMax}$), where CvalMax is the maximum value of the DOST coefficients or DWT Coefficients. Soft Thresholding was carried out on the DOST or DWT coefficients before reconstructing the signal. In soft Thresholding, the elements whose absolute values are lower than the threshold are first set to zero. Then the nonzero coefficients are shrunked towards 0.

$$X_{soft} = \begin{cases} sign(x)(|X| - |\tau|), & \text{if } |X| > 0 \\ 0, & \text{if } |X| \leq 0 \end{cases}$$

Where X represents the DOST or DWT coefficients and τ is the threshold value.

- After that, we can conduct inverse DOST or inverse DWT to get the denoised speech signal.

IV. RESULTS AND EVALUATION

This section presents the experimental results of the proposed speech enhancement method at various SNR levels from -5 to 15 dB. The speech signal taken from the TIMIT Acoustic-Phonetic Continuous Speech Corpus [21], were used to evaluate the proposed algorithm. For this purpose, clean speech signal sampled at 16 kHz is used and recorded by female voice. To illustrate the performance of the proposed enhancement techniques, Several tests in different various noisy conditions, taken from Noisex-92 database: White Gaussian noise, F16 cockpit noise, Volvo car noise and Pink noise with different values of Signal to Noise Ratio (SNR)from -5dB to 15dB were used.

In order to evaluate the denoising performance of the DOST method and to compare it to DWT denoising and Spectral Subtraction; a number of objective tests used for speech enhancement technique evaluation, are presented in this study. Then, the proposed method is subjectively evaluated in terms of Informal listening tests in order to find the analogy between the objective metrics and subjective sound quality.

A. Objective evaluation

Objective measures [28] are based on mathematical comparison between the original and processed speech signals. The measure of the signal to noise ratio, SNR is one of the most extensively used. As the name suggests, it is computed as the ratio of the signal to noise powers in decibels:

- Signal-to-Noise Ratio

$$SNR = 10 \log_{10} \left[\frac{\sum_n s^2(n)}{\sum_n [s(n) - s^*(n)]^2} \right] \quad (11)$$

where s and s^* are respectively the clean and the enhanced speech signals.

-Peak Signal to Noise Ratio (PSNR)

$$PSNR = 10 \log_{10} \frac{N^2}{\|s - s^*\|^2} \quad (12)$$

Where N is the length of reconstructed signal, S is the maximum absolute square value of signal s and $\|s - s^*\|^2$ is the energy of the difference between the original and reconstructed signal.

-Normalized Root Mean Square Error (NRMSE)

$$NRMSE = \sqrt{\frac{\sum_n (s(n) - xs'(n))^2}{\sum_n (s(n) - \mu s(n))^2}} \quad (13)$$

Here, $s(n)$ is the speech signal, $s'(n)$ is reconstructed speech signal and $\mu s(n)$ is the mean of speech signal

-Perceptual Evaluation of Speech Quality

PESQ (Perceptual Evaluation of Speech Quality) [27] is an objective quality measure that is approved as the ITU-T recommendation P.862. It is a tool of objective measurement conceived to predict the results of a subjective Mean Opinion Score (MOS) test. Particularly, PESQ was developed to model subjective tests commonly to assess the voice quality by human beings

B. Results

Several experiments using the TIMIT database were carried out to evaluate the performance of the proposed method and to compare it to DWT based speech enhancement methods [22], [23], [25] and [26] and Spectral Subtraction [1]. Indeed, in this work, for comparative purposes, the DWT algorithm given in [6], [7], [8] and [9], the used mother wavelet is “db10”, five decomposition levels and Soft thresholding was implemented [24]. In this part of the paper, the obtained results from SNR, PSNR NRMSE and PESQ computation is reported These results are obtained by the application of the proposed speech enhancement technique, the Discrete Wavelet transform and Spectral Subtraction on a number of noisy speech signals which are obtained by corrupting the original signals by different types of noise (White, Pink, Volvo and F16) at different values of SNR (-5dB to 15dB). A comparative study between our proposed speech enhancement system using DOST and the DWT denoising proves that the proposed speech enhancement system using DOST outperforms the DWT and the experimental results are shown in tables and figures bellows;

TABLE I. SNR MEASURES OBTAINED FOR NOISY AND ENHANCED SPEECH SIGNAL

Noise type	Enhancement technique	Improved SNR(dB)				
		-5	0	5	10	15
White	DOST	3,70	6,50	11,63	14,1	17,26
	DWT	-1,21	2,85	7,49	12,43	17,25
	Spectral Subtraction	-0,18	4,08	8,92	13,62	18,23
F16		-5	0	5	10	15
	DOST	-1,65	2,8	6,94	10,98	15,63
	DWT	-1,66	2,4	6,75	10,34	15,08
Pink		-5	0	5	10	15
	DOST	-1,82	1,64	6,68	11,1	15,93
	DWT	-2,95	1,07	5,5	10,19	15,02
Volvo		-5	0	5	10	15
	DOST	-2,9	1,23	5,52	10,25	15,9
	DWT	-2,95	1,07	5,5	10,19	15,02
Volvo	Spectral Subtraction	1,64	6,43	11,28	16,19	21,05

The proposed speech enhancement method is compared with a speech enhancement using DWT and Spectral Subtraction. SNR is calculated under different SNR inputs and the results are shown in Table I and Fig.2.

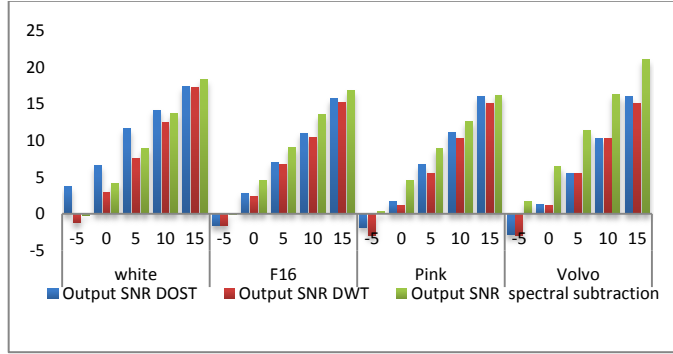


Fig. 2. Comparison of Output SNR for DOST, DWT and Spectral Subtraction

Table 1 and Figure2 below show that the three denoising techniques improve the signal to noise ratio (SNR). The results show also that the DOST based denoising technique is better than the DWT denoising. In fact, the DOST improves the output SNR for SNR input equal to -5dB and 0dB for various noise conditions. It's clear that the Spectral Subtraction denoising is better than the two denoising methods. In case of White Noise, the DOST denoising method is more efficient, however for Volvo noises; the Spectral Subtraction seems to be

more suitable and reliable. From these figures, it can be seen that the DOST method can greatly improve SNR with less distortion of the original speech signal.

TABLE II. PSNR MEASURES FOR ENHANCED SPEECH SIGNAL

Noise Type	Enhancement Technique	PSNR (dB)				
		-5	0	5	10	15
White	DOST	21,0455	23,84	27,97	31,44	34,5625
	DWT	16,1232	20,1927	24,8382	29,7722	33,5986
	Spectral Subtraction	17,1558	21,4244	26,9263	30,9617	34,5760
F16		-5	0	5	10	15
	DOST	16,4876	20,6554	24,0765	29,1221	34,9753
	DWT	15,2148	19,4083	23,1759	28,2993	33,4282
Pink		-5	0	5	10	15
	DOST	17,2635	21,8602	26,4096	30,8378	35,1769
	DWT	15,4752	19,9254	24,4534	29,4447	32,2750
Volvo		-5	0	5	10	15
	DOST	15,5015	18,0198	23,0204	27,4171	32,2530
	DWT	17,6733	21,8828	26,2621	30,9390	35,1534
Volvo		-5	0	5	10	15
	DOST	15,4371	19,4652	24,6547	28,6758	33,2426
	DWT	18,9856	23,7729	28,8233	33,5331	38,3963

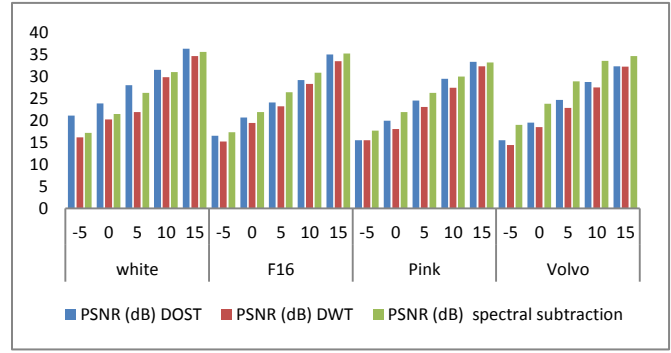


Fig. 3. Evaluating the proposed system based on the PSNR measure

It is observed as the level of Gaussian noise increased from -5dB to 15dB, the output Peak Signal to Noise Ratio (PSNR) values of our speech enhancement system based on DOST outperform the DWT and spectral subtraction. This demonstrates a significant improvement in signal quality and the powerful of the DOST.

However, in case of Volvo noise, the spectral subtraction has the best PSNR.

- Case White Noise

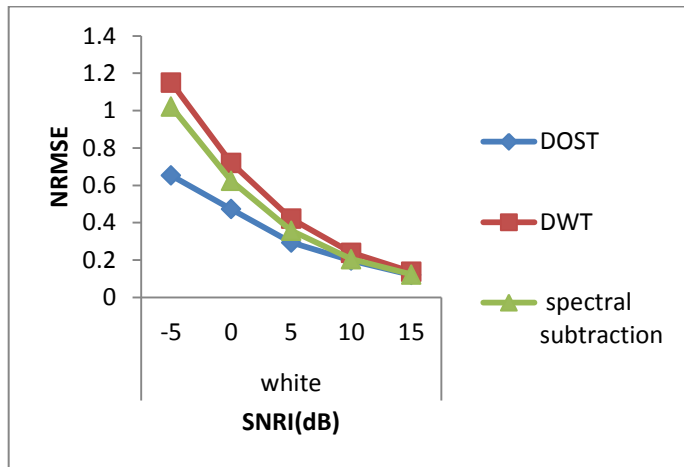


Fig. 4. Comparison of NRMSE for DOST, DWT and Spectral Subtraction for White noise

- Case F16 Noise

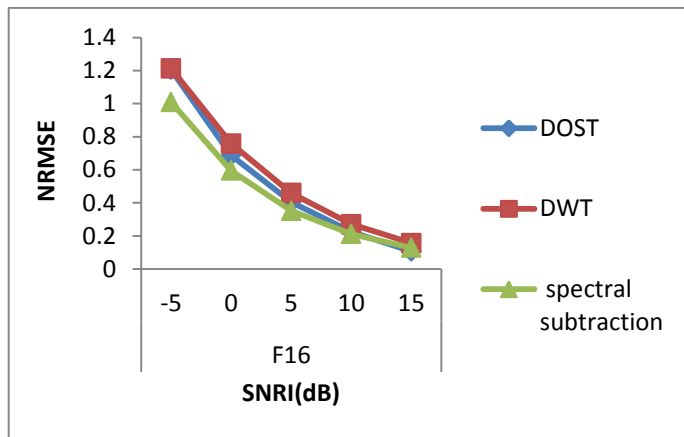


Fig. 5. Comparison of NRMSE for DOST, DWT and spectral subtraction

- Case Pink Noise

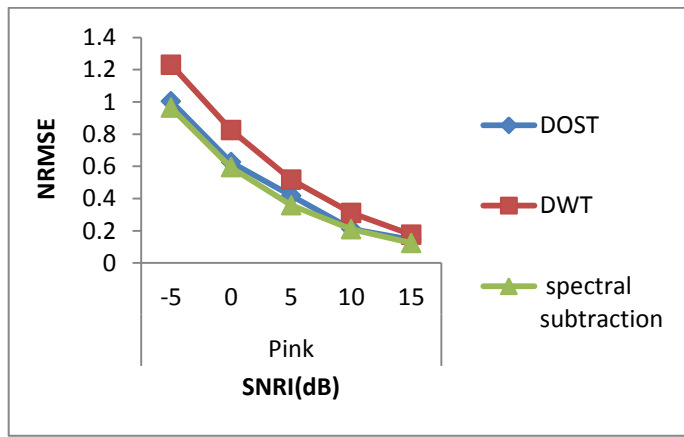


Fig. 6. Comparison of NRMSE for DOST, DWT and Spectral Subtraction for Pink noise

- Case Volvo Noise

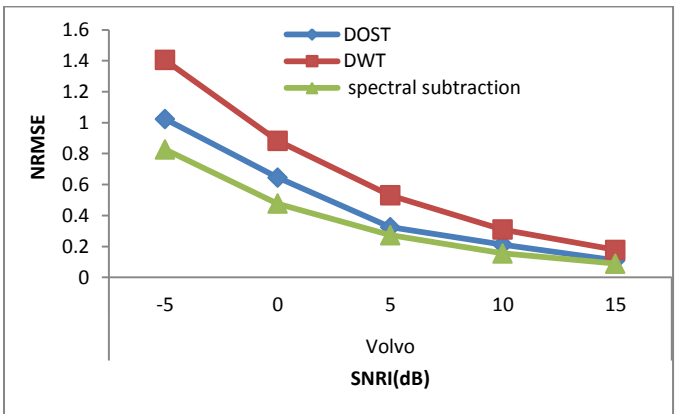


Fig. 7. Comparison of NRMSE for DOST, DWT and Spectral Subtraction for Volvo noise

Figure 4, 5, 6 and 7 below show that NRMSE is less for DOST compared to DWT methods for different types of noise for SNR levels ranging from -5dB, 0dB, 5dB, 10dB and 15dB. In the case of white noise the DOST outperform the DWT and Spectral Subtraction while for Volvo noise the Spectral subtraction has the best performance.

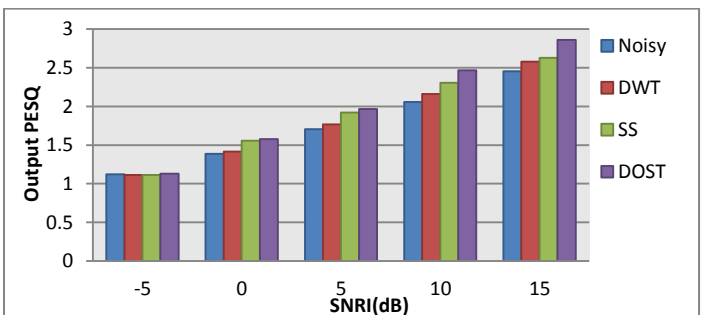


Fig. 8. Performance comparison of PESQ scores for different methods in the presence of White Noise

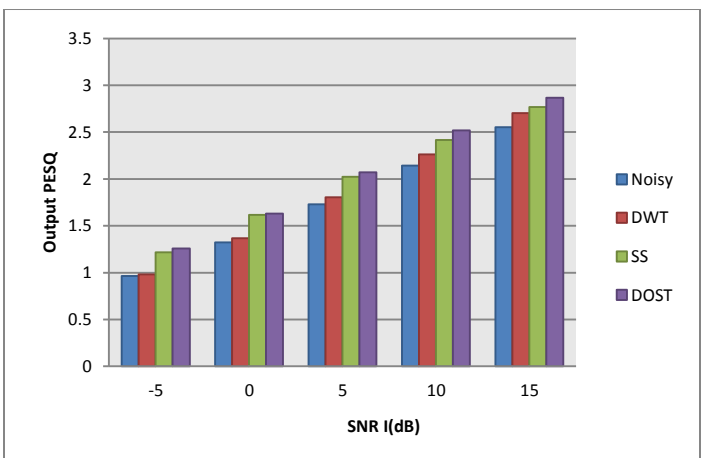


Fig. 9. Performance comparison of PESQ scores for different methods in the presence of Pink Noise

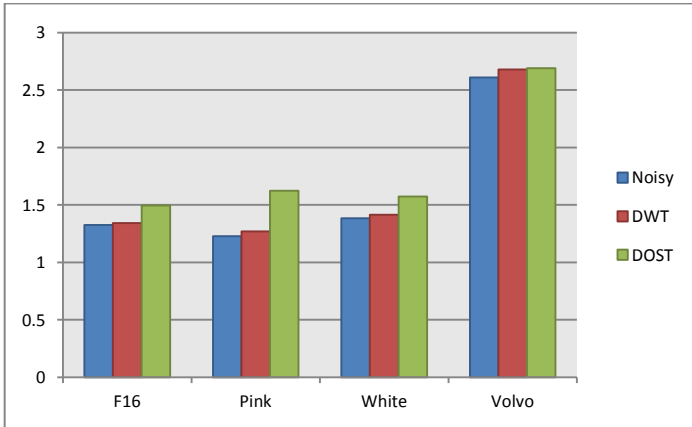


Fig. 10. Performance comparison of PESQ scores for different methods at 5 dB SNR in the presence of various noises

Fig.8 shows the PESQ scores for the noisy signal and the enhanced mentioned signals when the speech is degraded by white noise. As clearly shown in the figure below, PESQ scores of the proposed algorithm are better than PESQ scores given by the algorithm based on the Spectral Subtraction and DWT.

Fig. 9 presents the PESQ scores for the noisy signal and the enhanced mentioned signals when the speech is degraded by Pink noise. Clearly, the PESQ scores of the proposed algorithm outperform the PESQ scores of other methods.

Fig.10 shows the PESQ scores for the noisy signal and the enhanced signals using DWT and DOST over all noise conditions (F16, Pink, White, Volvo) at 5dB SNR. It can be seen from this figure that the proposed method is characterized by the highest PESQ scores showing that the enhanced speech by our method has a better perceived quality. Hence, the high PESQ scores perceived the quality of the enhanced speech.

C. Subjective evaluation

In order to evaluate the enhancement quality of the noisy speech, we have used the Perceptual Evaluation of Speech Quality (PESQ) score which is a mean opinion score, showing high correlations with subjective listening tests. It ranges from 1 to 5. The higher PESQ score shows the higher perceptual quality and the lower speech distortions. Also we have conducted informal listening test where a group of 10 listeners (six women and four men) are permitted and disposed to perceptually evaluate 3 enhanced speech signals from the NOIZEUS database with three background noises (White, F16, and Pink) at three SNR levels (0 ,5 and 10 dB). The listeners have used the MOS (Mean Opinion Score) method to evaluate the difference between the residual noise characteristics of the enhanced speech (1: Bad, 2: Poor, 3: Fair, 4: Good, 5: Excellent). Fig. 7 bellow shows the statistic results of subjective evaluation for 3 speech enhancement methods:

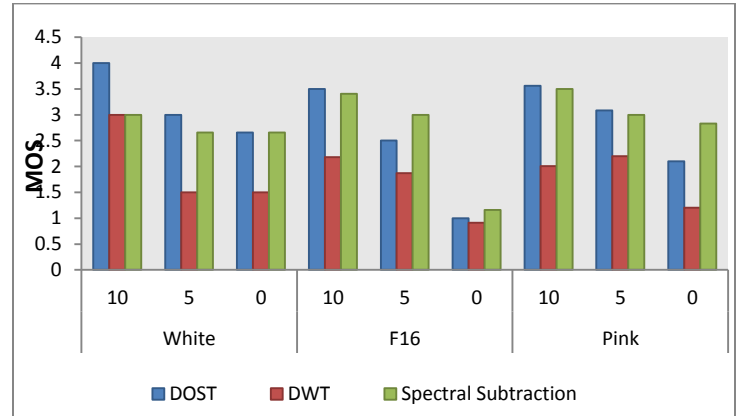


Fig. 11. Subjective evaluation of different speech enhancement methods

The test results show a favorite improvement in the auditory quality of our proposed speech enhancement. In fact, our approach provides a speech signal containing less musical noise while preserving the speech quality.

The listeners found that the subjective sound quality of our proposed method in denoising using DOST has the highest correlation with the objective evaluation in comparison with DWT and spectral subtraction in various noises conditions at different levels of SNR.

V. CONCLUSION

In this paper, a new method for speech enhancement using the Discrete Orthogonal Stockwel Transform has been presented. The evaluation of the proposed technique is performed by comparing it to the speech enhancement technique based on DWT and the technique based on Spectral Subtraction. Both objective and subjective methods used for evaluation of DOST performance in speech denoising. Hence, this evaluation is based on the use of a number of objective criterions which are the SNR, PSNR, NRMSE and PESQ. Also, in this evaluation, a speech signal with a female speaker from the TIMIT database is used and corrupted it by different types of noises which are Pink, White, F16 and Volvo noises at various input SNR levels ranging from -5dB to 15dB. Simulation results show that the proposed method provides better results in terms of higher output SNR, higher output PSNR, higher PESQ score, and lower NRMSE values than the DWT and Spectral subtraction based denoising methods and results in a better enhanced speech. Also, Informal listening tests justify the efficiency of the proposed method that results in a better enhanced speech than that obtained by the other methods.

In the future research works, we will cooperate the proposed speech enhancement method with speech recognition systems in order to increase their recognition rate under noisy environments.

REFERENCES

- [1] G. Ramesh Babu," Modified Kalman Filter-based Approach in Comparison with Traditional Speech Enhancement Algorithms from Adverse Noisy Environments," International Journal on Computer Science and Engineering (IJCSE) Vol. 3 No. 2 Feb 2011.
- [2] I. Almajai and B. Milner, "Visually derived wiener filters for speech enhancement," IEEE Trans. Audio, Speech, and Language Processing, vol. 19, no. 6, pp. 1642-1651, Aug. 2011.
- [3] S. Ben Jebara, "A perceptual approach to reduce musical noise phenomenon with wiener denoising technique," IEEE Int. Conf. Acoustics, Speech and Signal Processing,(ICASSP), vol. 3, may 2006, p. III.
- [4] S. Tabibian, A. Akbari, and B. Nasersharif,"A new wavelet thresholding method for speech enhancement based on symmetric kullback-leiblerdivergence," in Proc. 14th Int.CSI Computer Conference, CSICC), Oct. 2009, pp. 495-500.
- [5] Y. Hu and P. C. Loizou,"Speech enhancement based on wavelet thresholding the multitaper spectrum," IEEE Transactions on Speech and Audio Processing, 12(1):59-67, 2004.
- [6] Slavy G. Mihov, Ratcho M. Ivanov, Angel N. Popov, "Denoising Speech Signals by Wavelet Transform," Annual Journal Of Electronics; 2009; ISSN 1313-1842.
- [7] Mahesh S. Chavan, Manjusha N.Chavan, M.S.Gaikwad," Studies on Implementation of Wavelet for Denoising Speech Signal," International Journal of Computer Applications; Vol. 3: No.2: 2010; 1-7
- [8] Matko Saric, Luki Bilicic, Hrvoje Dujmic," White Noise Reduction of Audio Signal Using Wavelets Transform With Modified Universal Threshold," R. Boskovica B. B Hr 21000 Split, Croatia. 2005
- [9] A. Malayeri, "Noise speech wavelet analyzing an special time ranges," in Int. Conf. Advanced Communication Technology (ICACT), vol. 1, feb.2010, pp. 525-528.
- [10] Y. Wang and J. Orchard, "On the Use of the Stockwell Transform for Image Compression," SPIE Electron. Imaging Algorithms System VII, p. 7245, 2009.
- [11] R. G. Stockwell, "A basis for efficient representation of the S-transform," Digital Signal Processing, vol. 17, no. 1, pp. 371-393, January 2007.
- [12] Y. Wang and J. Orchard, "The Discrete Orthonormal Stockwell Transform for Image Restoration," in 16th IEEE International Conference on Image Processing, 2009, pp. 2761-2764.
- [13] Y. Yan and H. Zhu, "The Generalization of Discrete Stockwell Transforms," EURASIP, pp. 1209-1213, 2011.
- [14] H. Huang, F. Sun, P. Babyn, Z. Zhou, and L. Wang, "Medical-Image Denoising and Compressing Using Discrete Orthonormal S transform," in 2nd International Conference on Electrical, computer Engineering and Electronics (ICECEE 2015), 2015, vol. 291, no.Icecee, pp. 291-296.
- [15] Y. Wang and J. Orchard, "Fast Discrete Orthonormal Stockwell Transform," SIAM. J. Science Computation, 31(5):4000-4012, 2009
- [16] Drabycz, R. G. Stockwell, and J. R. Mitchell, "Image Texture Characterization Using The Discrete Orthonormal S-Transform," J.Digit. Imaging, vol. 22, no. 6, pp. 696-708, Dec. 2009.
- [17] R. G. Stockwell, L. Mansinha, and R. P. Lowe, "Localization of complex spectrum: the S transform," IEEE Transactions on Signal Processing, vol. 144, no. 4, pp. 998-1001, April 1996.
- [18] L. Mansinha, R. G. Stockwell, and R. P. Lowe, "Pattern analysis with two-dimensional spectral localization: Application of two-dimensional S transforms," Physica A, vol. 239, pp. 286-295, 1997.
- [19] L. Mansinha, R. G. Stockwell, R.P. Lowe, M. Eramian, and R. A. Schincariol, "Local S-spectrum analysis of 1-D and 2-D data," Phys. Earth Planet. Inter., vol. 103, pp. 329C336, November 1997.
- [20] M. Eramian, R. A. Schincariol, R. G. Stockwell, R. P. Lowe, and L. Mansinha, "Review of applications of 1D and 2D S-transforms," Proc. SPIE, vol. 3078, pp. 558-568, April 1997.
- [21] J. Garofolo, L. Lamel, W. Fisher, J. Fiscus, D. Pallett, and N. Dahlgren, et al., "TIMIT Acoustic-Phonetic Continuous Speech Corpus: Linguistic Data Consortium, 1993.
- [22] S.Ayat, M.T. Manjuri-Shalmani and R.Dianat, " An Improved Wavelet Based Speech Enhancement by using Speech Signal Features," Computer and Electrical Engineering, 23 May 2006, 411-425.
- [23] P.Sunitha, T.Sekhar,"Speech Signal Enhancement Using Wavelet Threshold Methods,"International Journal of Ethics in Engineering & Management Education Website: www.ijeee.in (ISSN: 2348-4748, Volume 1, Issue 3, March 2014)59
- [24] T. Farah Sanam, C. Shahnaz," An Approach for Noisy Speech Enhancement through soft thresholding function by Employing the Teager Energy Operation on Wavelet Packet," International Journal of Scientific &Technology Research Volume 1, Issue 2, March 2012.
- [25] R.Dhivya, Judith Justin," A novel speech enhancement technique," IRET: International Journal of Research in Engineering and Technology eISSN: 2319-1163 | pISSN: 2321-7308 Volume: 03 Special Issue: 07 | May-2014, Available @ http://www.ijret.org 98
- [26] Kamya Dubey,"A Review on Speech Denoising Using Wavelet Techniques," International Journal of Engineering Trends and Technology (IJETT) – Volume 4 Issue 9- Sep 2013 ISSN: 2231-5381 Http://www.ijettjournal.org Page 3882
- [27] ITU-T P.862, "Perceptual evaluation of speech quality (PESQ), and objective method for end-to-end speech quality assessment of narrow band telephone networks and speech codecs," ITU-T Recommendation p.862, 2000.
- [28] Y. Hu and P. Loizou, "Evaluation of objective quality measures for speech enhancement," IEEE Trans. Audio, Speech, and Language Processing,vol. 16, no. 1, pp. 229.238, Jan. 2008.

SDME Quality Measure based Stopping Criteria for Iterative Deblurring Algorithms

Mayana Shah

Ph.D. student, Electronics & Communication Engineering,
Uka Tarsadia University, Bardoli, India

Dr. U. D. Dalal

Associate Professor in department of Electronics Engineering,
S.V.N.I.T., Surat

Abstract—Deblurring from motion problem with or without noise is ill-posed inverse problem and almost all inverse problem require some sort of parameter selection. Quality of restored image in iterative motion deblurring is dependent on optimal stopping point or regularization parameter selection. At optimal point reconstructed image is best matched to original image and for other points either data mismatch occurs and over smoothing is resulted. The methods used for optimal parameter selection are formulated based on correct estimation of noise variance or with restrictive assumption on noise. Some methods involved heavy computation and produce delay in final output. In this paper we propose the method which calculate visual image quality of reconstructed image with the help of Second derivative like measure of enhancement (SDME) and helps to efficiently decide optimal stopping condition which has been checked for leading image deblurring algorithm. It do not require any estimation of noise variance or no heavy computation are needed. Simulation has been done for various images including standard images for different degradation and noise condition. For test leading deblurring algoritham of Blind and Semi-Blind deblurring of Natural Images using Alternate direction method of minimizer (ADMM) is considered. The obtained results for synthetically blurred images are good even under noisy condition with A ISNR average values 0.2914 dB. The proposed whiteness measures seek powerful solution to iterative deblurring algorithms in deciding automatic stopping criteria.

Keywords—Image deblurring; stopping point; Point Spread Function; Second derivative like measure of enhancement

I. INTRODUCTION

Blind image deblurring is ill-posed inverse problem solved with iterative techniques using regularization methods with reduction of solution space. In regularization methods solutions accuracy and smoothness tradeoff is controlled by regularization parameter selection or by deciding optimal stopping condition. The reconstructed image quality is highly depended on the iteration number and above the optimal iteration point each extra iteration result in amplification of noise and computational cost. If the sharp image is available than one can compute full reference image metrics such as mean-squared error (MSE), peak signal to noise ratio (PSNR) [1], or structural similarity (SSIM) [2] and can decide optimal stopping point when MSE is minimized or PSNR and SSIM is maximized. However, in most practical situations the sharp image is not available and this metrics cannot be used for decision of automatic stopping point determination.

The most commonly used methods for choosing a regularization parameter or for decision of automatic stopping point are as follows.

Visual Inspection: If the prior knowledge of the scene is available one can select the stopping point on the basis of visual inspection of the results. Clearly, as prior information about the scene is not obtainable all the time, the method has very limited application.

L-Curve Method: In any regularization method there are two terms, the data fidelity (residual) and prior information fidelity. The optimal stopping point is determined by plotting the data fidelity term against the prior fidelity term. Graphical behaviour of these two terms forms L-Curve and the optimal stopping point (regularization parameter) is the corner of L-Curve. It requires correct curvature evaluation and can be computationally expensive [3-7].

Discrepancy Principle: If the noise power is known, then the residual norm value can be matched to the noise variance value and on this basis optimal stopping point is selected. If correct noise power is not known it should be estimated and can lead to over smoothing in any inaccurate estimation [8-10]. Its improved versions are based on residual moments [11].

Generalized Cross-Validation (GCV) Method: GCV is an estimator that minimizes the predictive risk. The underlying idea is that the solution that is obtained using all but one observation should predict that left-out observation well if the regularization parameter is a good choice. The total error for a particular choice of the parameter is calculated by summing up the prediction errors over all observations. The optimal parameter value is the one that minimizes the total error. A search technique or an optimization method could be used to determine the optimal value. it does not require knowledge of noise variance and is known to yield regularization parameters for linear algorithms that asymptotically minimize the true MSE [12-14].

SURE: Stein's unbiased risk estimate (SURE) is MSE estimation based method and proved to be good alternative to GCV as almost all algorithm work by minimizing MSE criteria. For blind deconvolution it can't be used as it requires knowledge of noise statistics [15-16].

Statistical Approach: In reconstruction of sharp image using the statistical methods one can estimate regularization

parameter or indirectly optimal stopping point. The methods can be solved using the expectation maximization (EM) technique [17] which alternately restores the image and a new estimate of the parameter is calculated [9].

Whiteness-based method: It measures the whiteness properties such as covariance and power spectral density of the residual image. When residual image is spectrally white, residuals match to the noise having least structure content and it is considered as optimal stopping point [18].

TABLE I. COMPARISON OF DIFFERENT METHODS

Method	Input required	Tuning parameter	Computation	Visual quality consideration
Discrepancy Principle	Noise variance	y	less	No
L-Curve Method	-	n	less	No
whiteness-based method	-	n	heavy	No
General. Cross-Validation	-	n	heavy	No
SURE	Noise statics	n	heavy	No
proposed	-	n	less	yes

All the above summarized methods decide the optimal stopping point without concerning the visual appearance of the reconstructed images. They use the strategy of approximate computation of the metric MSE which is not the idea indicator of the visual quality. So the method is proposed in this paper, which uses SDME measure to decide the optimal stopping point. SDME measure is properly correlated with the noise level and intensity contrast (which indicates the “visibility” [19-21]) of the structured regions of an image. SDME measure is modified such that its value drops if the variance of noise rises or if the blur increases in the image. The contribution of the work lies in the Calculation of SDME measure at every iteration and deciding automatically stopping point. This measure exhibits a clear maximum point and helps to select iteration number. As per indication in Table I the proposed method do not require any input from user and no other parameter tuning is needed. It takes care of visual quality of image with no need of excessive computation. So it seeks powerful solution for determining optimal stopping point in regularized iterative algorithm.

The rest of the paper is organized as follows: Mathematical preliminaries described in section II and the proposed technique is given in section III. Results and discussion are given in section IV. Conclusion is summed up in Section V.

II. MATHEMATICAL PRELIMINARIES

A. Linear and Shift-invariant (LSI) Motion Blur Model

In almost all imaging application observed image is degraded version of original image as it is blurred by some function h which is known as blur or point spread function (PSF). Image deblurring means to solve an inverse problem with the aim of restoring an image which suffered a motion

blur with additive white gaussian noise. The image deblurring methods can be divided into two groups: non-blind deblurring, where the degradation operator of an image is known, and blind deblurring, where the degradation operator is not known. Normally, Degradation process is nonlinear and space varying process but most of the problems can be addressed with a linear and shift-invariant (LSI) model [22]. Output of an LSI system is the convolution of the true image with the impulse response of the system and can be written as,

$$z(x, y) = h(x, y) \bullet g(x, y) + n(x, y) \quad (1)$$

where $g(x, y)$ is the original image that we want to recover from the degraded measurement $z(x, y)$, where (x, y) indicates special coordinates. Here, ‘ \bullet ’ is the convolution operator and n is additive white Gaussian noise involved.

B. Regularized Least Squares Estimation

For any ill posed problem it is difficult to satisfy uniqueness, existence and stability criteria all together. The standard methodology to solve such a problem is to use least squares solution with regularization term. The least squares estimator minimizes the sum of squared differences between the observed image $z(x, y)$ and the predicted image $h(x, y) * g(x, y)$ [22]. Regularization term uses prior information about the true image and helps to obtain a solution with desired properties. The cost function to be minimized in regularized least square estimation can be formulated as:

$$C_s(g, h) = \frac{1}{2} \| z - h \bullet g \|^2 + \beta r[f(g)] \quad (2)$$

Here, h is the PSF kernel to be found, β is the scaling factor and $r[f(g)]$ is the regularization function where $f(g)$ is the edge response. To test the problem we considered deblurring with modification in total variation based solution [23]. Most images have sparse leading edge structure and edges are less sparse for its blurred version as area of the blurred edge is larger. The preferred solution should have sparse edges representation. The scaling parameter is at first a large value and then decreased over iterations. The edge responses of the blurred image are defined by the function $f(g)$ given by [23]:

$$f(g) = \sqrt{\sum_{\phi} q_{\phi}(g)^2}; q_{\phi}(g) = d_{\phi} \bullet g \quad (3)$$

Here d_{ϕ} is directional filter with ϕ values of 0, 45, 90 and 135 to find the edge response. The sparse prior, given the edge intensity for a pixel j represented by $f_j(g)$ is defined by:

$$p[f_j(g)] \propto e^{-k[f_j(g) + \epsilon]^q} \quad (4)$$

k adjusts for the scale of edge intensities and q controls the prior's sparsity and ϵ is a small parameter. Taking the noise into consideration as Gaussian likelihood [23] is given by:

$$p(g, h | z) \propto e^{-\frac{1}{2\sigma^2} \|z - h \bullet g\|^2} \prod_j e^{-k[f_j(g) + \epsilon]^q} \quad (5)$$

The log-likelihood maximization is similar to having the cost function minimized

$$L(g, h | z) = -\frac{1}{2\sigma^2} \|z - h \bullet g\|^2 - k \sum_j [f_j(g) + \epsilon]^q \quad (6)$$

Maximizing this likelihood is equivalent to minimizing the cost function [23]

$$C_s(g, h) = \frac{1}{2} \|z - h \bullet g\|^2 + \lambda \sum_j [f_j(g) + \epsilon]^q \quad (7)$$

Here, $\lambda = k\sigma^2$. The regularization parameter functions over the edge response and regularizer was chosen which favors the sharp edges or the priors are selected that reach sparser edge response.

Algorithm for getting deblurred image:

1. Initialization
2. Initially set PSF (h) to identity matrix keeping dimension of h bigger than that of the actual PSF matrix.
3. Initially set deblurred image (g) equal to blurred image (z).
4. Set λ, q and ϵ to initial values
Loop
5. Find $x = \arg\min(C_s(g, h))$ for given g, z, h, λ, q and ϵ
6. Find $h = \arg\min(C_s(g, h))$ for given g, z, h, λ, q and ϵ . Use the updated x , but keep other parameters constant.
7. Update λ, q, h and ϵ .
8. Repeat from step 4 to step 6 for each iteration and calculate SDME sum at each iteration

Here g is the Deblurred image which has to be found, h is the PSF kernel which has to be found, z is the input normalized blurred image. λ is the scaling parameter which changes over iterations.

C. Second Derivative-like Measure of Enhancement

Second-Derivative-like Measure of Enhancement (SDME) is a visibility operator [19] and a metric for quantitatively assessing image quality [20-21]. This visibility operator can be viewed as a second derivative analogue of the Michelson contrast measure.

Suppose the image I is divided into $a_1 \times a_2$ blocks, and $B_{\max,j,i}, B_{\min,j,i}$ are the maximum and minimum values of the pixels in each block separately, and $B_{cen,j,i}$ is the

intensity of the center pixel in each block, then SDME is defined by the equation:

$$SDME = \sum_{i=1}^{a_1} \sum_{j=1}^{a_2} \left| \frac{B_{\max,j,i} - 2B_{cen,j,i} + B_{\min,j,i}}{B_{\max,j,i} + 2B_{cen,j,i} + B_{\min,j,i}} \right| \quad (8)$$

As per the definition SDME works as local contrast descriptor and it is strongly sensitive to the degradation. Intensity variations are resulted in neighboring pixels of sharp image when blurring takes place. Instead of using direct comparison between the center pixel and its neighborhood pixels, SDME uses order statistics such as B_{\max} and B_{\min} to show sufficient amount of variations. For the digital second derivative spatial differentiation filters the weights are [1 -2 1] and replacement of this spatial weighting is done in the numerator of the SDME contrast with the weighting of order statistics and the central image pixel (1 for B_{\max} , -2 for B_{\min} , and 1 for B_{\min}) [25]. It is observed that the SDME is quite intimately related with the sharpness and contrast of the local region.

To decide the stopping condition we selected only those blocks which are having dominant orientation. The noisy and blurred patches are less structured and do not have dominant orientation so they are removed in calculating global SDME sum over the image. The patches to be selected are decided on the basis of singular value decomposition of gradient vector of the patch. SDME sum is modified in this proposed method and given by;

$$SDME = \sum_{i=1}^{a_1} \sum_{j=1}^{a_2} m(i, j) \left| \frac{B_{\max,j,i} - 2B_{cen,j,i} + B_{\min,j,i}}{B_{\max,j,i} + 2B_{cen,j,i} + B_{\min,j,i}} \right| \quad (9)$$

Where $m(i,j)$ is given by;

$$m(i, j) = \begin{cases} 1 & r(i, j) > T \\ 0 & r(i, j) < T \end{cases} \quad (10)$$

And $r(i,j)$ is given by;

$$r(i, j) = \frac{\text{diff of singular values of gradient}}{\text{sum of singular values of gradient}} \quad (11)$$

The threshold T is empirically selected as 0.3781 for the patch size of 5 and checked over multiple database images. The above expression contains maximization of sum of SDME value with dominantly oriented patches and provides a reasonable solution to the optimal stopping point problem. If $X(t)$ represent reconstructed images over iterations than at the maximum of $SDME(X(t))$ the reconstructed image is best matched to original sharp image, hence further iterations will not enhance the image quality, but may add more noise.

To verify the usefulness of SDME sum in the presence of blur and noise we applied motion blur with different length and theta parameter and recorded resultant SDME values. Its performance is plotted in Fig. 1. Next, we take noise into account. As shown in the graph the visibility operator SDME sum decrease with increase in both blur and random noise. Same experiment is repeated for the image is corrupted by white Gaussian noise and results are noted for increasing

values of noise variance. As per the results obtained the metric has well-behaved characteristics in the presence of both noise and blur and SDME sum values decreases with noise and blur. Thus, SDME has the potential for quality assessment of the blurred image.

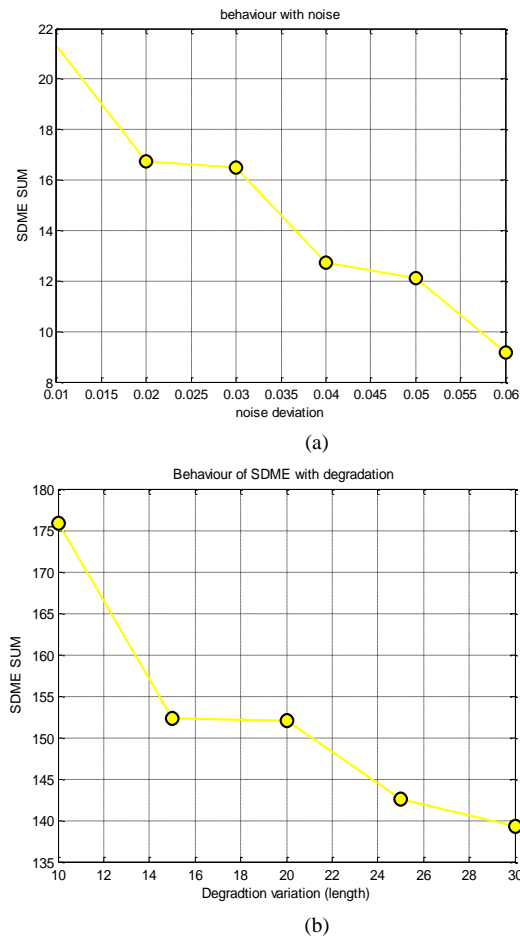


Fig. 1. SDME sum Vs Noise deviation (b) SDME sum Vs degradation

III. PROPOSED METHOD FOR AUTOMATIC STOPPING POINT DETECTION

The proposed stopping criteria are based on measures of the fitness of the estimated data based on SDME .The blurred image was generated by convolution of the original image with a motion blur degradation function with different values of Length and theta and then corrupted by AWGN with different BSNR values dB. We applied the state of art iterative deburring method to restore the blurred version of the image [23]. Reconstructed image generated in all iteration is divided into 5×5 image patches. For each patch we computed horizontal and vertical gradients. Local gradient is used to give us structural information of the patch. In order to extract global information of contrast, the patches with dominant orientation is used .The patch is less structured and will not have dominant orientation when it is more noisy so that patches are neglected in computing global image metric. An accumulation of local contrast SDME information of structured patches of whole image is computed, which can be declared as SDME sum. Iteration are continued till SDME

sum value become 40 and after SDME value reaches 40 at each iteration SDME value is compared with its previous value and when it reaches maximum (before it start decreasing) we stop the iteration. Any impulsive value of SDME that is above than 300 is considered as outliers (empirically setted based on result of database) and SDME sum value is assigned previous value to remove outliers. The flow chart of the algorithm is given in Fig.2.

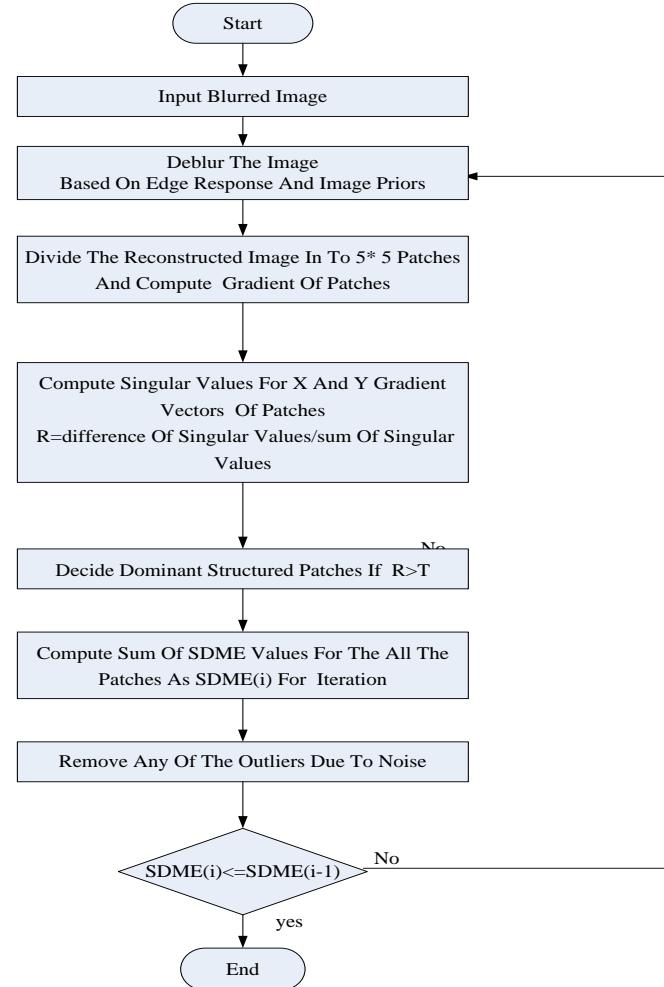


Fig. 2. Block Diagram of the Proposed Technique

Fig. 3 Shows that initially SDME sum value is increasing, reaches to maximum and then decreases because of noise.The results of ISNR graph, sum of SDME graph and MSE curves are plotted for the robot image of size (240×240) are shown in Fig. 3. It can be noted that the quality of the estimated image improves as the iteration increases in the beginning, and corresponding to the change of the estimated images, the SDME sum value become higher, too. Then the distortion caused by noise amplification becomes much stronger, and both the estimated images and the SDME values are affected by random noise. SDME sum graph follows ISNR graph and optimal stopping point is the point with maximal value of SDME sum. Maximum ISNR obtained is for iteration number 22 which is shown in graph of ISNR Vs iteration and iteration number selected on the basis of proposed criteria is 21 as shown.

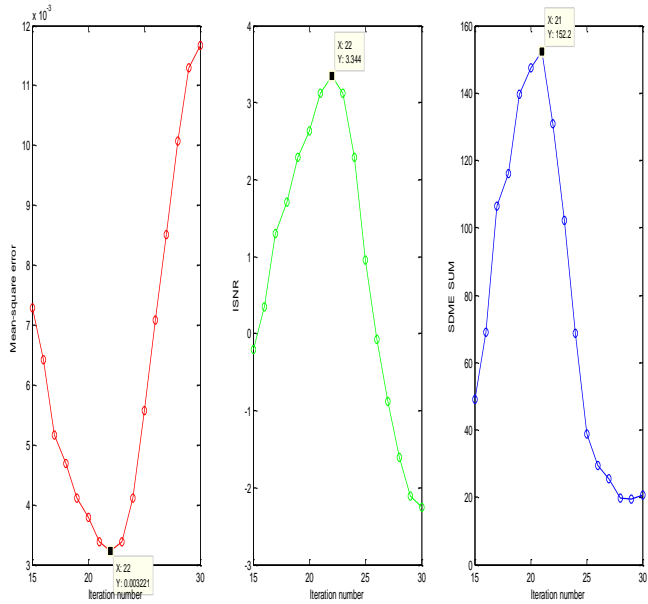


Fig. 3. Performance of Various Measures Vs Iteration

IV. EXPERIMENTAL RESULTS AND DISCUSSION

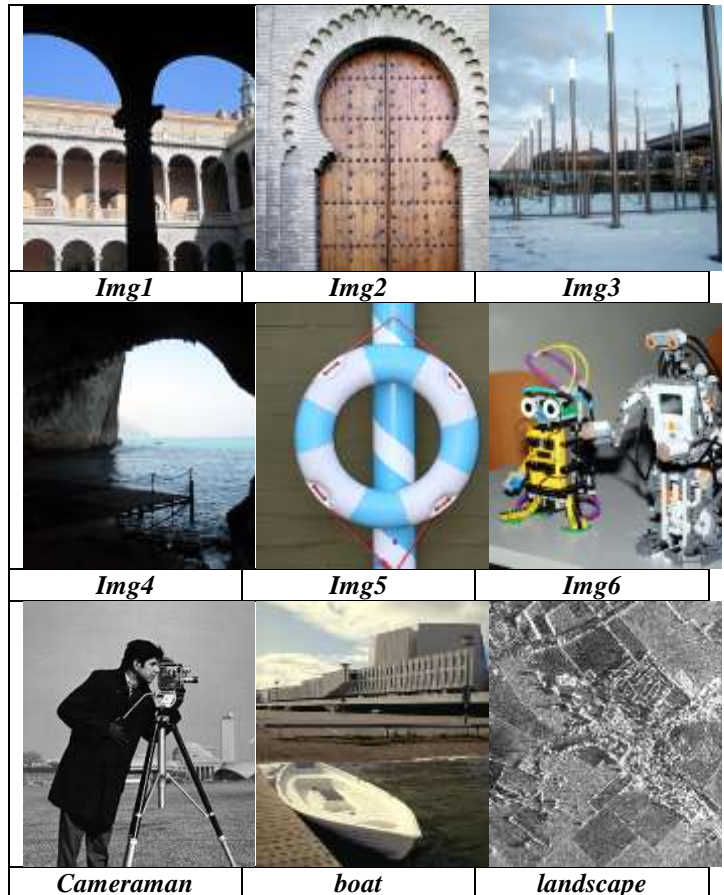
A. Dataset Description, Experimental Set Up and Evaluation Metrics

The dataset consists of various standard images such as Cameraman and other images obtained from public databases. The proposed stopping criteria is tested on a wide dataset of grayscale and color images. Table II gives the sample images. We tested a wide range of white Gaussian noise with noise levels BSNR=25, 30 or 35dB was added to the blurred images. The PSF is a motion blur with different values of length and theta.

For the purpose of comparison of stopping criteria we used state-of-the-art discrepancy principle (DP) method. DP method requires knowledge of the noise variance so its two types DP_{σ} and DP_{MAD} [24] are considered. DP_{σ} uses the true value of the added noise and DP_{MAD} which estimate noise variance by MAD (*Median absolute derivative*) rule. DP_{σ} is considered to be ideal as the true value of the noise variance is unavailable in practice. Numbers of experiments are conducted on numerous test images to validate the use of the proposed algorithm for deciding stopping condition.

The proposed technique is implemented in MATLAB on a system having 8 GB RAM and 2.5 GHz Intel i-7 processor. The evaluation metrics used are: (1) Δ Improve signal-to-noise ratio (Δ ISNR) –the difference of best ISNR and ISNR achieved by manual stopping (low value means good quality reconstruction),(2) Structural Similarity (SSIM) index [2] (lies between 0 and 1,closer to 0 means poor quality and closer to 1 means good quality),(3) Δ MSE is used (low value means good quality reconstruction). Performance of the proposed method is compared with the state-of-the-art methods qualitatively (visual aspects) as well as quantitatively using this metrics.

TABLE II. SAMPLE IMAGES FROM DATABASE



B. Simulation Results

Experiment 1- This experiment is conducted on all images in Table II keeping blurring parameters constant. The image is blurred with PSF parameters, $L = 12$ pixels and $\theta = 230^\circ$ with BSNR of 30 dB. This blurred image is given as an input to algorithms and the stopping point is decided. The Δ ISNR, difference between best ISNR value (with minimum MSE) and ISNR at the iteration where the algorithm stops automatically are recorded. Table III shows iteration stopped with each of automatic criteria and best iteration number with minimum MSE for Length=12, theta=230, BSNR=30 dB and Length=8, theta=120, BSNR=35 dB. As shown in Table VII and Table IV, the reconstructed image quality of proposed method outperforms other algorithms in terms of both visual quality and quantitative evaluation and is close to the best restored image which can be obtained by using minimum mean square error criteria. Table VII shows the simulation results obtained for the proposed technique for three images (robot, cameraman, boat) with degradation parameters length=12, theta=230, noise level=30 dB. All latent images, their blurred versions and final restored image for different automatic stopping criteria are given in Table VII. It is clear that we got better results compared to the state-of-the-art methods.

TABLE III. ITERATION NUMBER SELECTED FOR DIFFERENT METHODS

Images	Length=12, theta=230, BSNR=30 dB				Length=8, theta=120, BSNR=35 dB			
	SDME sum	DP σ Iterati	DP(MAD) Iteration	Best Iteration number	SDME sum	DP σ Iteration	DP(MAD) Iteration	Best Iteration number
	Iteration	on	Iteration		Iteration		Iteration	
Img 1	20	20	26	21	19	21	27	22
Img 2	21	23	28	23	23	24	28	25
Img 3	20	22	28	22	21	26	29	22
Img 4	22	17	26	21	20	20	26	23
Img 5	21	21	27	21	22	24	27	23
Img 6	21	20	28	23	22	21	29	22
Cameraman	21	21	29	22	23	22	30	25
Boats	21	21	27	22	22	22	27	23
landscape	22	23	30	22	21	24	30	23

TABLE IV. EXPERIMENTAL RESULTS (IN DECIBEL FOR TWO DIFFERENT DEGRADATION PARAMETERS). FIRST COLUMN: BEST ISNR OBTAINED DURING THE ITERATIONS. SECOND, THIRD, AND FOURTH COLUMNS: Δ ISNR FOR SDME SUM , DP $_{\text{SIGMA}}$ AND DP $_{(\text{MAD})}$

Images	Length=12, theta=230, BSNR=30 dB				Length=8, theta=120, BSNR=35 dB			
	Best ISNR	SDME sum Δ ISNR	DP σ Δ ISNR	DP(MAD) Δ ISNR	Best ISNR	SDME sum Δ ISNR	DP σ Δ ISNR	DP(MAD) Δ ISNR
Img 1	5.858006	0.2153101	0.2153101	3.800858	4.860949	1.1518	0.1679	3.3567
Img 2	2.537914	0.2485170	0	0.9734740	2.689214	0.1281	0.0284	0.1593
Img 3	3.838959	0.8291039	0	3.668936	2.620799	0.4087	1.6394	3.2842
Img 4	2.964814	0.5373099	1.320347	7.218732	2.591957	0.4002	0.4002	2.8891
Img 5	1.093660	0	0	4.98	-1.466839	0.0860	0.0474	1.1400
Img 6	5.353606	0.3252711	0.8387041	2.287483	2.008620	0	0.0978	0.9491
Cameraman	5.098494	0.2495799	0.2495799	4.680250	6.072667	0.3565	1.4478	4.3235
Boats	3.343654	0.2175529	0.2175529	4.21	3.541060	0.2816	0.2816	2.1739
landscape	1.258956	0	0.0983	0.6815	1.997543	0.1512	0.0502	0.3108
Average		0.2914	0.3266	3.6112		0.3293	0.4623	2.0652

The same experiment is repeated with PSF parameters, $L = 8$ pixels and $\theta = 120^\circ$ with BSNR of 35 dB and results are recorded. Table IV summarizes the results obtained using the global SDME sum stopping criteria and which are on average, only slightly worse (0.29dB, 0.32dB) than the best ISNR

achieved by manual stopping with minimum MSE. Table V and Table VIII shows MSE values and SSIM values. Table VI gives graphical comparison of all the methods in terms of Δ ISNR and Δ MSE. As per the graph SDME sum is best suited to decide the optimal stopping point.

TABLE V. EXPERIMENTAL RESULTS (FOR TWO DIFFERENT DEGRADATION PARAMETERS). FIRST COLUMN: BEST MSE OBTAINED DURING THE ITERATIONS. SECOND, THIRD, AND FOURTH COLUMNS: Δ MSE FOR SDME SUM, DP_{SIGMA} AND DP_(MAD)

Images	Length=12, theta=230, BSNR=30 dB				Length=8, theta=120, BSNR=35 dB			
	Best MSE	SDME sum Δ MSE	DP _σ Δ MSE	DP(MAD) Δ MSE	Best MSE	SDME sum Δ MSE	DP _σ Δ MSE	DP(MAD) Δ MSE
Img 1	0.002884	-0.000147	-0.000147	-0.004036	0.001633	-0.000494	0	-0.001903
Img 2	0.004846	-0.000286	0	-0.001218	0.003374	0	0	-0.000126
Img 3	0.002617	-0.000551	0	-0.003474	0.002131	-0.000210	-0.000978	-0.002409
Img 4	0.002025	-0.000266	-0.000719	-0.008647	0.001393	-0.000135	-0.000135	-0.001317
Img 5	0.002329	0	0	-0.005016	0.002498	0	0	-0.000750
Img 6	0.003608	-0.000281	-0.000769	-0.002502	0.004825	0	-0.000109	-0.001178
Cameraman	0.002351	-0.00014	-0.000139	-0.004557	0.0013	-0.000111	-0.00051	-0.002217
Boats	0.003221	-0.000166	-0.000166	-0.005287	0.002189	-0.000147	-0.000147	-0.001422
landscape	0.017454	0	-0.000399	-0.0030	0.012264	-0.000434	-0.000142	-0.000910
Average		-0.000204	-0.002598	-0.0042		-0.001868	-0.0002375	-0.0014

TABLE VI. (A) Δ ISNR LENGTH=12, THETA=230, BSNR=30 dB (B) Δ ISNR LENGTH=8, THETA=120, BSNR=35 dB (C) Δ MSE LENGTH=12, THETA=230, BSNR=30 dB (D) Δ MSE LENGTH=8, THETA=120, BSNR=35 dB

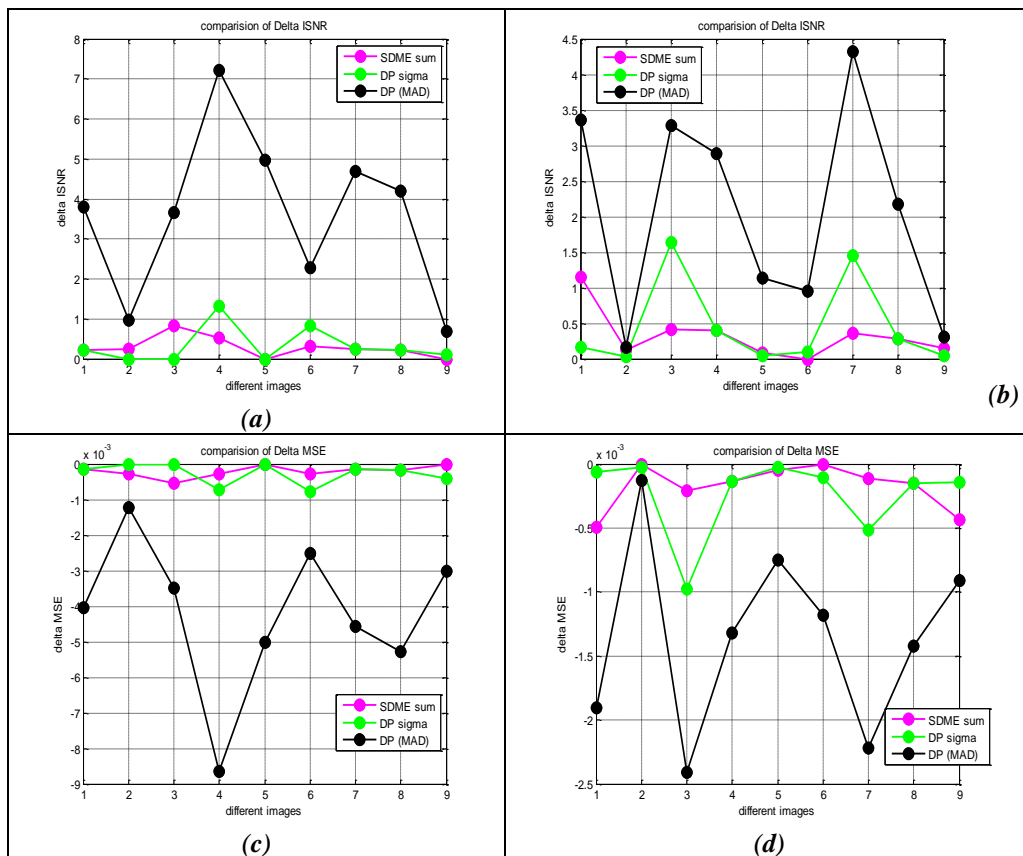


TABLE VII. SIMULATION RESULTS

Input Image			
Blurred Image			
SDME sum			
DPσ			
DP(MAD)			

Fig.4 gives comparison of all the methods for various degradation applied to all the images in the table. As per the chart, one can see that iteration number selected with SDME

sum method is matched to best ISNR iteration in majority cases. DP σ method also seems to be matched with best iteration but the method is based on true value of variance which is unavailable in practice.

TABLE VIII. SSIM VALUES FOR DIFFERENT METHODS

SSIM	Length=12, theta=230, BSNR=30 db			Length=8, theta=120, BSNR=35 db		
	SDME sum	DP σ	DP(MAD)	SDME sum	DP σ	DP(MAD)
Img 1	0.9997400	0.9997960	0.9995880	0.9996170	0.9996170	0.9991770
Img 2	0.9995530	0.9995620	0.9995490	0.9993590	0.9993940	0.9992460
Img 3	0.9997030	0.9996200	0.9994550	0.9995890	0.9996670	0.9992730
Img 4	0.9997880	0.9997880	0.9996620	0.9996580	0.9995810	0.9985820
Img 5	0.9996390	0.9996410	0.9995530	0.9996610	0.9996610	0.9990140
Img 6	0.9992830	0.9992700	0.9991470	0.9994640	0.9993980	0.9992320
Cameraman	0.9998360	0.9997900	0.9995990	0.9996760	0.9996760	0.9991850
Boats	0.9997130	0.9997130	0.9995750	0.9995710	0.9995710	0.9989630
landscape	0.9985110	0.9985660	0.9985010	0.9979270	0.9978840	0.9975340

Comparison of stopping point selection by different methods

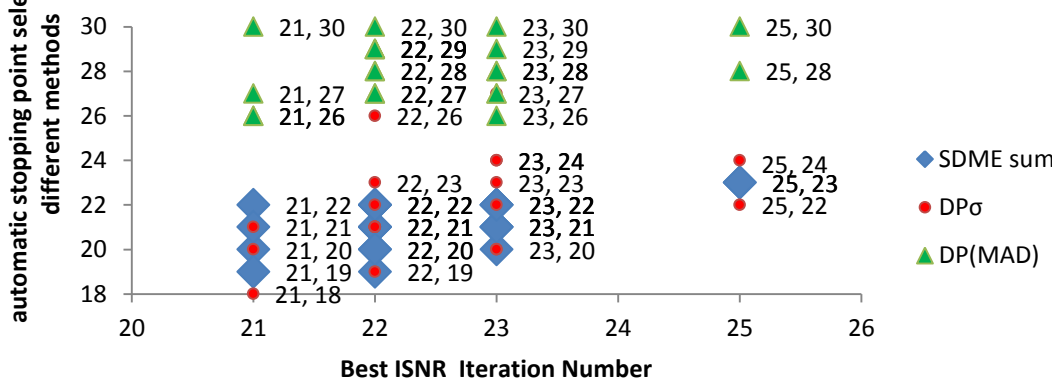


Fig. 4. Comparison of all the methods

Experiment 2 – The proposed technique is evaluated using evaluation metrics employed such as ISNR, MSE, and SSIM for stopping point detection for robot image by varying degradation parameters. Proposed method performs much satisfactorily in this case also.

TABLE IX. ITERATION NUMBER FOR ROBOT IMAGE BY VARYING PARAMETERS

Iteration number	Best Iteration number	SDME sum Iteration number	DP σ Iteration number	DP(MAD) Iteration number
L=8,Theta=120 Noise=35dB	22	22	21	29
L=10,Theta=190 Noise=40dB	23	22	27	29
L=12,Theta=230 Noise=25dB	21	19	18	30
L=5,Theta=45 Noise=30dB	22	20	19	28

Results obtained shows nearer or superior results obtained compare to DP σ method which is based on true value of noise variance which is unavailable for blind image deblurring problems.

TABLE X. SSIM VALUES FOR ROBOT IMAGE BY VARYING PARAMETERS

Degradation parameters	SSIM		
	SDME sum	DP σ	DP(MAD)
L=8,Theta=120 Noise=35dB	0.9995	0.9993	0.9992
L=10,Theta=190 Noise=40dB	0.9989	0.9990	0.9989
L=12,Theta=230 Noise=25dB	0.99934	0.9991	0.9978
L=5,Theta=45 Noise=30dB	0.99958	0.9995	0.9994

TABLE XI. ISNR VALUES FOR ROBOT IMAGE BY VARYING PARAMETERS

ISNR	Best ISNR	SDME sum Δ ISNR	DPσ Δ ISNR	DP(MAD) Δ ISNR
L=8,Theta=120 Noise=35dB	2.0086	0	0.0978	0.9491
L=10,Theta=190 Noise=40dB	1.8336	0.5511	0.2275	0.4789
L=12,Theta=230 Noise=25dB	4.6923	0.5474	1.413	6.26
L=5,Theta=45 Noise=30dB	1.4334	0.4417	0.9449	2.52
Average		0.3850	0.6708	2.54

Inferences from tables 3-12:

- The Tables give the performance evaluation of the proposed technique. Table IV gives the Δ ISNR values Table V gives the MSE values and Table VII gives SSIM values. The values are obtained for nine images. Table 8 shows that visual quality of the reconstructed images for the proposed technique is best compared to other methods.
- The Δ ISNR average values came about 0.2914 dB and 0.32 dB losses with respect to best ISNR. The obtained evaluation metric values confirm the effectiveness of the proposed technique.
- Table IX, X, and XI gives the performance analysis by varying the length, theta and noise level. For robot image the Δ ISNR average values came about 0.3850 dB.

V. CONCLUSION

In this work visibility operator SDME sum is effectively used to decide the optimal stopping point in regularized iterative reconstruction methods which involves intensity contrast of the structured regions of an image. The results are obtained for different images degraded with uniform motion blur. The method calculates the stopping point with less loss of ISNR (0.29dB, 0.32dB) compare to state of art methods and the maximum of SDME sum is located close to the best restored image where MSE is minimum. A large number of experiments are carried out to prove that the SDME measure is highly correlated with noise and contrast of image. The proposed approach is quite general and does not require knowledge about the noise variance. It does not involve any extra parameter tuning and do not allow any visual quality degradation of image. So it seeks powerful solution for determining optimal stopping point in iterative IBD problems.

REFERENCES

- [1] Huynh-Thu, Q., Ghanbari M., "Scope of validity of PSNR in image/video quality assessment", Electronics Letters, Vol. 44, No.13, pp.: 800–801, 2008.
- [2] Z. Wang, A. C. Bovik, H. R. Sheikh and E. P. Simoncelli, "Image quality assessment: From error visibility to structural similarity," IEEE Transactions on Image Processing, vol. 13, no. 4, pp. 600-612, Apr. 2004.
- [3] P. C. Hansen, "Analysis of discrete ill-posed problems by means of the L-curve," SIAM Review, vol. 34, no. 4, pp. 561–580, December 1992.
- [4] N. K. Bose, S. Lertrattanapanich, and J. Koo, "Advances in superresolution using lcurve," in Proceedings of the IEEE International Symposium on Circuits and Systems, vol. 2, pp. 433–436, May 2001.
- [5] C. R. Vogel, "Non-convergence of the L-curve regularization parameter selection method," Inv. Problems, vol. 12, no. 4, pp. 535–547, Aug. 1996.
- [6] P. C. Hansen and D. P. O'Leary, "The use of the L-curve in the regularization of discrete ILL-posed problems," SIAM J. Sci. Comput., vol. 14, no. 6, pp. 1487–1503, 1993.
- [7] T. Regi'nska, "A regularization parameter in discrete ILL-posed problems," SIAM J. Sci. Comput., vol. 17, no. 3, pp. 740–749, 1996.
- [8] A. M. Thompson, J. C. Brown, J. W. Kay, and D. M. Titterington, "A study of methods of choosing the smoothing parameter in image restoration by regularization," IEEE Trans. Patt. Anal. Mach. Intell., vol. 13, no. 4, pp. 326–339, Apr. 1991.
- [9] N. P. Galatsanos and A. K. Katsaggelos, "Methods for choosing the regularization parameter and estimating the noise variance in image restoration and their relation," IEEE Trans. Image Process., vol. 1, no. 3, pp. 322–336, Jul. 1992.
- [10] V. A. Morozov, "On the solution of functional equations by the method of regularization," Soviet Mathematics Doklady, vol. 7, pp. 414–417, 1966.
- [11] L. Dascal, M. Zibulevsky, and R. Kimmel, "Signal denoising by constraining the residual to be statistically noise-similar," Technical Report, Department of Computer Science, Technion, Israel, 2008.
- [12] G. Golub, M. Heath, and G. Wahba, "Generalized cross-validation as a method for choosing a good ridge parameter," Technometrics, vol. 21, no. 2, pp. 215–223, 1979.
- [13] N. Nguyen, G. Golub, and P. Milanfar, "Blind restoration/superresolution with generalized cross validation using Gauss-type quadrature rules," in Proceedings of the Asilomar Conference on Signals, Systems, and Computers, vol. 2, pp. 1257–1261, October 1999.
- [14] N. Nguyen, P. Milanfar, and G. Golub, "Efficient generalized cross-validation with applications to parametric image restoration and resolution enhancement," IEEE Transactions on Image Processing, vol. 10, no. 9, pp. 1299–1308, September 2001.
- [15] Y. C. Eldar, "Generalized SURE for exponential families: applications to regularization," IEEE Trans. Sig. Proc., vol. 57, pp. 471–481, 2009.
- [16] R. Giryes, M. Elad, and Y. C. Eldar, "The projected GSURE for automatic parameter tuning in iterative shrinkage methods," Applied and Computational Harmonic Analysis, vol. 30, pp. 407–422, 2011.
- [17] A. P. Dempster, N. M. Laird, and D. B. Rubin, "Maximum likelihood from incomplete data via the EM algorithm," Journal of the Royal Statistical Society: Series B, vol. 39, no. 1, pp. 1–38, 1977.
- [18] Mariana S. C. Almeida and M'ario A. T. Figueiredo, "Parameter Estimation for Blind and Non-Blind Deblurring Using Residual Whiteness Measure", IEEE transactions on image processing, vol. 19, no. 1, pp. 36-52, 2013.
- [19] S. Delmarco and S. Agaian, "The design of wavelets for image enhancement and target detection," Proceedings of SPIE, vol. 7351, 2009.
- [20] K. Panetta, Y. Zhou, and S. Agaian, "Nonlinear Unsharp Masking for Mammogram Enhancement," IEEE Transactions on Information Technology in Biomedicine, vol. 15, pp. 918-928, 2011.
- [21] M. J. Shah and Upena Dalal, "3D-Image Restoration Technique Using Genetic Algorithm to Solve Blurring Problems of Images" Imaging Science Journal, Volume 62, No. 07, pp.365-374, sept 2014
- [22] Bahadir Kursat Gunturk, and Xin Li, "Image Restoration: Fundamentals and Advances." CRC press, September 11, 2012
- [23] Almeida M.S.C and Almeida L.B., "Blind and Semi-Blind Deblurring of Natural Images", IEEE Transactions on Image Processing, Vol.19, No.1, 2010.
- [24] D. Donoho, "De-noising by soft-thresholding," IEEE Trans. Information Theory, vol. 41, pp. 613–627.
- [25] Human Visual System- Based Multi Scale Tools With Biomedical and Security Application-A dissertation submitted by Shahran Nercessian for the degree of Doctor of Philosophy in Electrical Engineering, Tufts University, May 2012

Real Time Monitoring of Human Body Vital Signs using Bluetooth and WLAN

Najeed Ahmed Khan

Computer Science & IT Department
NED University of Engineering & Technology
Karachi, Pakistan

M. Ajmal Sawand
Department of Computer Science
Institute of Business Administration
Sukkur, Pakistan

Marium Hai

Electronic Engineering Department
NED University of Engineering & Technology
Karachi, Pakistan

Arwa Khuzema, Mehak Tariq

Electronic Engineering Department
NED University of Engineering & Technology
Karachi, Pakistan

Abstract—The technology of telemedicine is emerging and advancing day by day, it is capable of taking the field of healthcare to a whole new level of personalization. A person can keep a close check on his/her health's critical signs and can receive suitable feedback if required, to help maintain the best of health status with the help of Wireless Body Area Network (WBAN) concept. The sensor nodes can wirelessly communicate with any smart phone through an Android application to continuously monitor and have complete access to the medical data of the patient. Moreover it also aims to maintain an efficient electronic medical record of the person. Moreover, the consultant and the caretaker of the patient can have this important information remotely through an internet connection and provide with significant advice which encapsulates the term - *smart first aid technology*.

In the proposed framework miniaturized sensors are worn on the body and non-intrusively monitor a person's physiological state. The body vital signs (e.g.: heart rate, temperature etc.) are recorded through the sensor nodes and transmit to the smart phone via Bluetooth, where the data of vital signs is stored and will further transmitted to remote locations if needed.

Keywords—Telemedicine; smartphone; Vital signs; remote locations; photoplethysmography; e-health; medical telemetry

I. INTRODUCTION

The global cause for death are cardiovascular disease which are increasing day by day, The death statistics are 17.3 million deaths per year and if this is the situation it is expected to increase to reach to 23.6 million by the year 2030 [1]. For improving and avoiding the death risks a contribution to the solution is made. That is an easy access, comfortable and regardless of the hardware sensors should be small, non-invasive method. The work on "WBAN" (wireless body area network) is attempted which supports mobility, data encryption, and authentication. Significant advances in science and technology such as basic developments emerging in the fields of micro/nanotechnology, wireless communication, information technology, and biomedical sciences during the past 10-15 years has brought a clear transformation in the field of medical telemetry [2]. Medical telemetry introduces a new level of personalization, and helps

an individual to have a healthy status of living. For maintaining and arranging high efficient connectivity and processing large data set technology is continuously evolving [3]. This paper is targeted to achieve a practical and affordable health care by allowing an individual (cardiac patients, athletes, sportsmen) to keep a regular check on his cardiac functioning and in any uncertain conditions ; the persons (caretakers , doctors , sports instructors) can provide instant help or advice to be safe from any major health issues.

Selection of sensor nodes is the challenging part due to the accuracy and compatibility issues. For measuring the heart rate (beats per minute) of a person, technique of **photoplethysmography** is used. The technique of photoplethysmography uses Infra-red LEDs (light emitting diodes) and photo detector to measure the blood volume. The sensor should be placed in those areas of body where the blood is having a higher concentration (e.g. finger tips, ear lobes etc.)[4]. Fig.1 shows the principle of measuring heart rate of a person using technique of photoplethysmography.

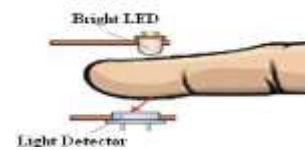


Fig. 1. Principle of photoplethysmography [5]. Contain an infrared Light detector and IR LED, used to record pulse rate

The detection of temperature can be done in two ways either through skin or through mouth. The sensor is used to detect the temperature through skin as it is the more precise way of measuring temperature in medical sciences. If the body temperature is detected to low than a normal threshold value, it is the sign of illness or if the temperature reaches to 104 F, it is the threshold to check body temperature variation.

II. LITERATURE REVIEW

In present days the world is endorsing an increasing pressure on quality and quantity of healthcare due to the increase of aging population, chronic diseases, and health consciousness of people [6]. People put more attention in

prevention and early risk detection. The proposed model is built with the aim of providing early detection of body vital signs based on the concept of Wireless Body Area Network (WBAN). In recent years large amount of work on WBAN has been done in different areas of world but they have certain short comings.

The concept of WBAN was first presented by T. G. Zimmerman in an article from 1996, he gave these body networks the name wireless personal area network (WPAN) from the beginning [7]. Later on PAN (personal area network) was transformed in to WBAN (wireless body area network) by the accumulation of wireless data transmission devices [8] (Bluetooth, ZigBee etc.).

The increasing and continuous demand of sufficient resources placed on the medical society, increasing costs of in-patient care, and a deficit of out-patient surveillance was thoroughly described in a research paper by the scholars of the University of Twente [9].

The author of this paper has defined "extra-BAN communication" (EBAN) as communication between a BAN and other networks. IEEE 802 has established a Task Group called IEEE 802.15.6 in November, 2007 for the standardization of BAN [10]. The purpose of the group was to establish a communication standard optimized for low power, high reliability application for BANs.

In 2009, Young Dong Lee [11] designed a system for cardio vascular patients which measures electrocardiogram (ECG) and acceleration signals. He used smart shirt that can be worn easily and transmit signals using MSBN (mobile body sensor network). The shirt mainly consists of sensors for continuous monitoring the health data and conductive fabrics to get the body signal as electrodes.

There are important limitations observed for wider acceptance of the systems build up till now such as: cumbersome wires between sensors and a processing unit, lack of system integration of individual sensors, interference on a wireless communication channel shared by multiple device and unavailability of proper support for organizing huge data [12]. An interesting solution of Mobi-Health, a BSN (body sensor network) with EBAN (Ethernet body area network) connectivity to a 2.5/3G networks to provide out-patient monitoring of patients vital signs has been reported recently as well [13].

During the last few years there has been a significant increase in the number of various wearable health monitoring devices [14], ranging from simple pulse monitors, activity monitors and portable Holter monitors¹ to sophisticated and expensive implantable sensors. Traditionally, personal medical monitoring systems [10], such as Holter monitors, have been used only to collect data. Systems with multiple sensors for physical rehabilitation often feature unwieldy wires between the sensors and the monitoring system [15]. These wires may limit the patient's activity and level of comfort and thus negatively influence the measured

results. Recent technology advances in integration and miniaturization of physical sensors, embedded microcontrollers and radio interfaces on a single chip; wireless networking; and micro-fabrication have enabled a new generation of wireless sensor networks suitable for many applications [12].

The idea of WBAN consisting of inexpensive, light weight and miniaturized sensors can provide long-term, unobtrusive health monitoring with continuous feedback to the user about the current health status and real-time or near real-time updates of the patient's medical records.

WBAN promises a revolution in medical research through data mining of all gathered information. The large amount of collected physiological data will allow quantitative analysis of various conditions and patterns [16]. Researchers will be able to quantify the contribution of each parameter to a given condition and explore synergy between different parameters, if an adequate number of patients is studied in this manner [12].

In this paper we used the basic WBAN architecture, non-invasive techniques of heart rate and temperature detection. The paper also details the hardware and software platforms used for the monitoring of body vital signs.

III. MATERIAL AND METHODS

A. Objective of the proposed work

The key objective of the proposed model is to provide cardiac patients with such electronic device which can continuously monitor their heart functionality and keep medical log history that is timely updated.

In case of any alarming situations notifications in the form of messages and emails will be generated and sent to relative to take care of the patient. Along with relatives, concerned doctors will also be notified with patient's condition so that instant help can be provided. Another main focus is to provide ambulance service by sending position of the patient to ambulance station using Global Positioning System (GPS) in case of emergency.

- Wireless Body Area Network (WBAN) implemented in the proposed model consists of the following steps: Combination of sensors for detecting physiological parameters.
- The second level encompasses Android based Smart phone device which is the bus station and holds the key position in the proposed model.
- The third level and the final step of the proposed model is a wireless network (caregivers, relatives, doctors) which aims to provide feedback and related first aid services remotely.

Each level is a complex sub-system in itself requiring equal attention for assuring efficiency. Fig. 2 shows the block diagram of the proposed architecture of the model and flow of data transfer.

¹ <http://www.polarusa.com>

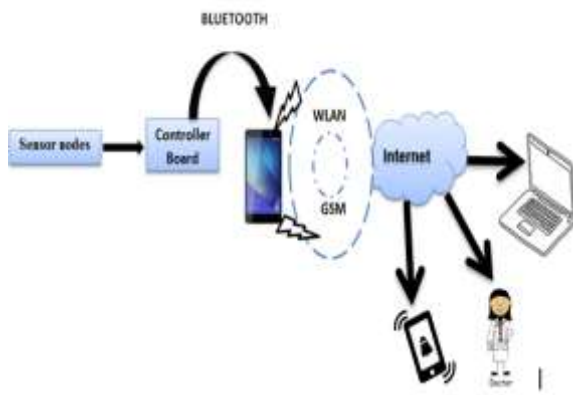


Fig. 2. System architecture of the proposed approach consists of sensors and the micro controller along with the smart phone

The proposed architecture of the model is a composite of hardware part and the software part. The hardware part consists of sensors (Pulse rate sensor SEN-11574 & Temperature sensor LM-35) and a micro controller (Arduino UNO) along with the smart phone (android device), whereas the programming for controller and an android app contribute towards the software aspect of the project. Fig. 3 shows the proposed methodology of the proposed model.

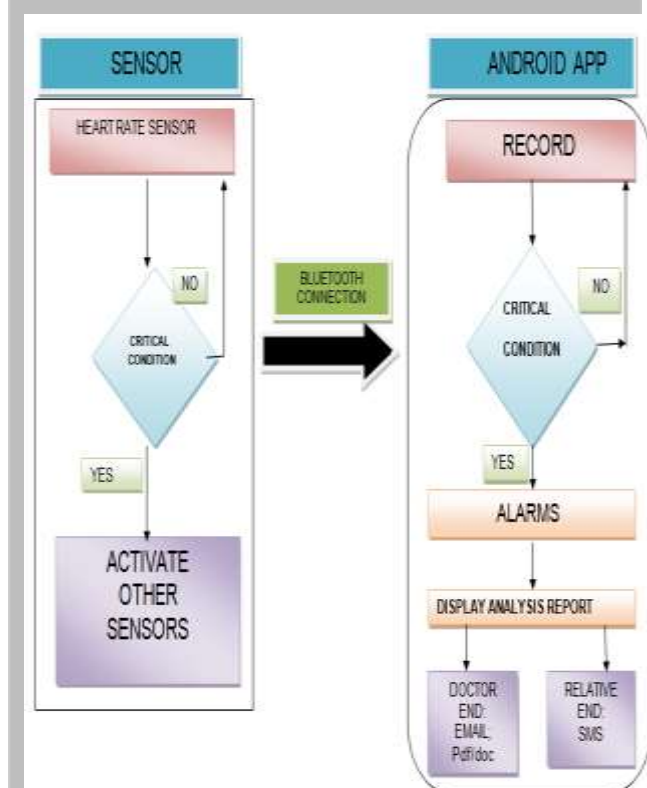


Fig. 3. Work flow of the proposed approach

B. Proposed technique for the detection of pulse rate and temperature

PULSE RATE DETECTION

Photoplethysmography is a technique used nowadays for monitoring patient's pulse rate. The sensor used for this task is pulse sensor (SEN-11574) which is very small in size and can be worn or wrapped around the index finger or on ear lobe. This sensor module consists of light source photo detector and infra-red LEDs (Light emitting diodes). The idea behind the concept is the optical detection of changes in the blood volume. Changes in light intensity are used to check the changes in volume level of blood which is very helpful in cardio vascular systems. Output voltages from this sensor module during the cardiac cycles will be converted into beats per minute through microcontroller board (Arduino UNO) [4].



Fig. 4. Pulse rate sensor SEN-11574

TEMPERATURE DETECTION

Integrated circuit (IC) LM35 is used as a temperature measuring device. The IC is able to provide analog voltages that are proportional to temperature in Celsius ($^{\circ}\text{C}$). The analog voltages are converted into digital values (temperature readings) through a microcontroller platform (Arduino UNO). LM35 is a three pin IC in which first and last pins are for supply and ground respectively whereas the middle one is for output. The following mathematical equation is used to convert output voltage of LM35 (temperature sensor) into temperature in $^{\circ}\text{C}$ (Celsius scale).

$$\text{Temperature } (^{\circ}\text{C}) = \text{Vout} * (100 \text{ } ^{\circ}\text{C/V})$$



Fig. 5. Temperature sensor LM-35

DATA PROCESSING

Arduino UNO is a microcontroller board which is used here to read analog data from all the sensors and convert that data into digital form using mathematical algorithms. The

micro-controller board will also control the series of sensors and sequence of their functioning; in a way that data from heart rate sensor is continuously read by the controller board and when it identifies any abnormal value of heart rate based on predefined threshold values, it will start reading data from other sensors too and transfer that data into the smart phone application through Bluetooth chip which is connected with this board.

DATA TRANSMISSION

Reliable communication is utmost important for health monitoring systems. Bluetooth technology is used for the transmission of data from controller board to bus station (smart phone). HC-05 module is an easy to use Bluetooth SPP (Serial Port Protocol) module, designed for transparent wireless serial connection setup. The module is compatible with micro-controller board (Arduino UNO) and can easily transfer data at the baud rate of 57600 [17]. Fig. 6 shows the connection between micro-controller board and Bluetooth. Smart android device in this project act as a personal server for the patient which collects the data of sensor nodes from Bluetooth and transmits to remote locations via internet or GSM services and also receives the feedback. This application is a significant portion of proposed model.

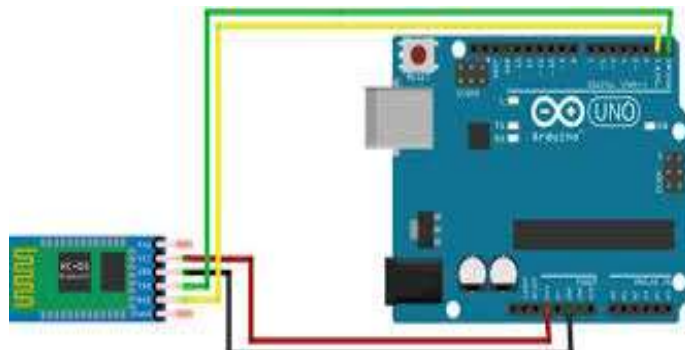


Fig. 6. The circuit diagram shows connectivity between Arduino Board and Bluetooth module

IV. DESIGNING AND DEVELOPMENT OF SOFTWARE APPLICATION

We have chosen **Android studio IDE (version 1.0)** for application developing platform which was launched by Google in December 2014. It is specifically designed for android development based on the *JetBrains* and *IntelliJ IDEA* software and is a successor to *Eclipse Android Development Tools (ADT)* as Google's primary IDE for android application development [18].

The development of the proposed application on android involves the following steps:

- Creating the Project files
- Creating the GUI (.XML) & JAVA files
- Bluetooth connectivity
- Running the application on virtual machine
- Running the application on actual android device [18].

GRAPHICAL USER INTERFACE (GUI) OF APPLICATION

Every screen that we see on an android smart-phone is called an **activity**. A unique name is given to every activity present in an android application called as activity name. Each activity comprises of two files i.e. Layout file (.XML) and the JAVA file (.java). Application in the proposed model comprises of several different activities. Fig. 7 shows the layout of some of the designed activities.



Fig. 7. Screen shots of some activities of Android Application. (a) shows the front end display of application which rests for 5 seconds before the app starts. (b) Shows the sign in activity of application. User must need to provide user Id and password to get access to the application in order to preserve privacy of the patient.(c) shows the registration form for creating account. (d) shows the menu screen of application through which the user can access the available features of application

INTENTS

Intents are basically the messaging objects used for requesting an action from other app contents i.e. calling an activity from other activity. It is communication link between different contents of an application. Fig. 8 shows the methodology followed by intents to call an activity from another one.

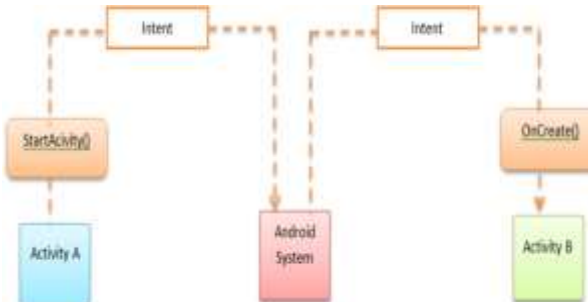


Fig. 8. Intents Methodology – responsible for the messaging objects used for requesting an action from other app contents

V. IMPLEMENTATION AND TESTING

Optical technologies are well suited for non-invasive monitoring of skin blood pulsation. Radiation of the red to near infrared spectral region penetrates several millimeter under the skin surface. Skin blood pumping and transport dynamics can be monitored at different body location (e.g. fingertip, earlobe, and forehead) with relatively simple and convenient PPG contact probes. Reflection PPG method uses the back scattered Optical signals for analysis of skin blood volume pulsation [13]. In the transmission method, an optical signal change according to its absorption at the pulsation as oxygenated blood allows red wavelength more and deoxygenated blood allows infrared wavelength. It employs the principle that oxygenated blood is bright red whereas reduced or deoxygenated blood is dark red so combination of red and near infrared LEDs and photo sensors can be used to monitor the color of blood [13]. The output signal of SEN-11574 is an analog fluctuation in voltage as shown in fig. 9. The depiction of the pulse wave is called as Photoplethysmogram (PPG). It is the function of light intensity. When the heart pumps blood through the body; with every beat there is a pulse that travels along all arteries. A rapid upward rise in signal value occurs as the pulse wave passes under the sensor, then the signal falls back down towards the normal point [19].

1) SYSTOLE: It is the contraction period of the heart in which the heart pumps blood into all parts of the body through arteries.

2) DIASTOLE: It is the relaxation period of the heart in which heart collects blood from all body parts through veins.

The systolic peaks shown in fig. 9 are counted for the period of 60 seconds to compute the number of beats happened in one minute.

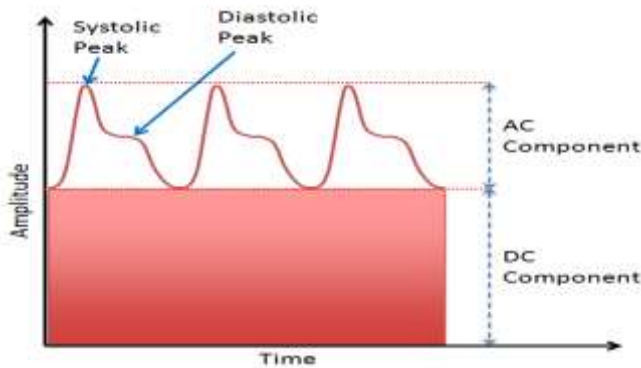


Fig. 9. Model of PPG (photoplethysmography) waveform [21]

The output wave form of SEN-11574 (pulse sensor) is recorded through oscilloscope. Fig. 10 shows the images of PPG (photoplethysmography) waveforms of two patients.

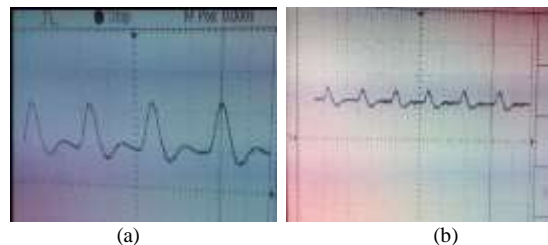


Fig. 10. Photoplethysmography output wave form of SEN-11574 sensor recorded for the patient 1 and patient 2 respectively in figure (a) and (b)

Interfacing of sensors with android application via Bluetooth is carried out by connecting micro-controller board (Arduino UNO). Bluetooth module and smart phone in proper order. 5 volts supply is needed to switch on the micro-controller board. Batteries operating at 5 volts can be used for this purpose. Once the circuit is on, it starts monitoring the data of patient's vital signs and displaying it on the mobile application by transferring it through Bluetooth module. Fig. 10 a and b shows the interfacing of sensor nodes and mobile application.

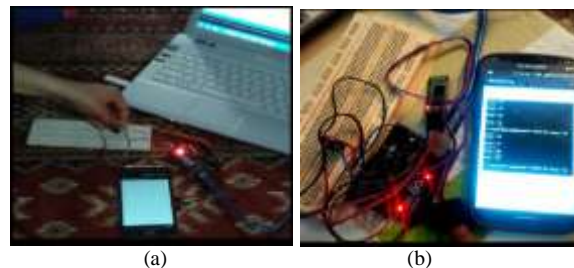


Fig. 11. Interfacing of sensor nodes with android application

Application after displaying the data extracted from sensor nodes; stores it and send it to remote locations via internet and GSM (global system for mobile communication) services. It also generates alert messages to the registered consultants and caretakers in case of any alarming situation. It also aims to send location of a patient to ambulance stations using GPS (global positioning system) services so that ambulance can reach the patient as soon as possible in order to provide first aid services to the patient.

The proposed project is simple and reliable for measuring body vital signs and aims to bring vigorous and rapid change in the field of medical telemetry.

TABLE I. STATISTICS OF RECORDED DATA FOR DIFFERENT PEOPLE THROUGH THE DEVELOPED MODEL USING PULSE SENSOR (SEN-11574) AND BY THE AUTOMATIC MACHINE AVAILABLE FOR BLOOD PRESSURE AND HEART RATE MEASUREMENTS. THE DATA RECORDED THROUGH THE AUTOMATIC MACHINE CONSIDERED AS GROUND TRUTH

PATIENTS	AGE	GENDER	BEATS PER MINUTES	
Name	Years	Male / Female	Proposed model Pulse Sensor(SEN-11574)	Ground Truth (Omron M10-IT Upper Arm BP and heart-rate Monitor)
Person 1	22	Female	92	90
Person 2	22	Female	84	86
Person 3	55	Male	73	72
Person 4	35	Male	67	65
Person 5	16	Female	82	85
Person 6	19	Female	85	82
Person 7	22	Female	82	82
Person 8	20	Male	78	80
Person 9	22	Male	82	82.5
Person 10	40	Female	74	75
Person 11	63	Male	90	92
Person 12	8	Male	82	85

Table 1 shows the recorded data (beats per minute) of 12 different people taken from the developed model and by the automatic machine available for blood pressure and heart rate measurements. The statistics of these numerical values is graphical shows in fig. 12. Graph in fig.12 is drawn to check the fidelity. The graph shows that the readings obtained from the test model (Red color) are in correlation with the readings obtained from an automatic blood pressure and heart rate measuring device (Blue color).

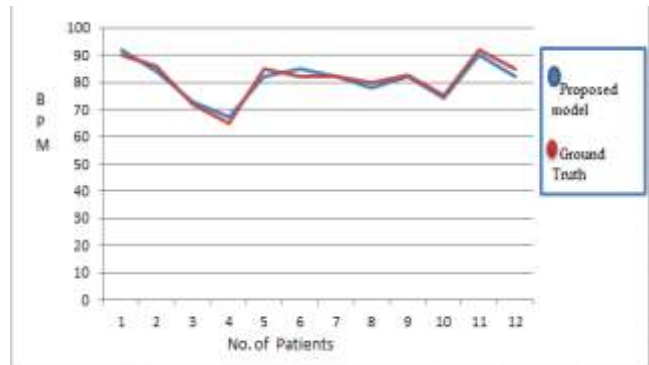


Fig. 12. Graph showing correlation between the readings of test model and Omron M10-IT Upper Arm BP and heart-rate Monitor (ground truth)

VI. CONTRIBUTIONS

The proposed model contributes towards the telemedicine health domain by raising the standards of health care and patient monitoring. It has a great potential in providing the society with cost effective alternative to rehabilitation of health care. It also helps the military personnel, sports persons (athletes, swimmers etc.) in keeping timely record of their health conditions. It aims to reduce sudden death risk and time saving environment to doctors, caretakers and patients as well by getting timely information about the patients and also able to provide timely suggestion to them.

VII. CONCLUSION

Wireless Body Area Network (WBAN) proves to be a milestone in the field of wearable health monitoring providing with the services of cost effective, unobtrusive and continuous monitoring of an individual during his daily activities. As the key objective is to reduce the sudden death risks which are caused by abnormalities in vital signs through ambulatory monitoring, the proposed model has potential to offer a wide range of benefits to patients' medical personnel, and society through continuous monitoring in the ambulatory setting. It aims to provide a great benefit to patients, physicians and society by wirelessly transmitting data of vital signs of patients to remote locations so that they will be provided with first aid and medication at the earliest in case of emergency situations. By recording the daily readings of patient's heart activity and temperature variations, it helps in keeping track of every major and minor details of patient's health. The proposed model of WBAN has a great potential in providing the society with reliable and secured solutions of health care and medical problems.

In future WBAN designs can be improved for providing miniaturization, human friendly devices with more power and

cost effectiveness. To advance this technology more a greater attention is required on portability and affordability of the sensors. To achieve ubiquitous health monitoring challenges of system design, personalization, power sources and application –specific protocols need to be resolved.

REFERENCES

- [1] Subcommittee, A.S.C.a.S.S., Heart disease and stroke statistics., 2014 December.
- [2] Sima Ajami , F.T., Features and application of wearable biosensors in medical care. Journal of Research in Medical Sciences, December 2015: p. 1208–1215.
- [3] Toshiyo Tamura , Y.M., Masaki Sekine , Masaki Yoshida, Wearable Photoplethysmographic Sensors—Past and Present. Electronics 3, 2014 April. Vol. 3(2): p. 282.
- [4] Keith-Hynes, P.M., Benton; Robert, Antoine, A Smartphone-Based System for Real-Time Control of Blood Glucose. Electronics 3, 2014 November. no 4.
- [5] M.K.Chaithanya , K.V.K.K., Avireni Srinivasulu, Blood Pressure Measurement and Data Storing Using Volume Compensation Method. IEEE, 2014 September.
- [6] Abderrahim BOUROUIS, M.F., Abdelhamid UBIQUITOUS MOBILE HEALTH MONITORING SYSTEM FOR ELDERLY (UMHMSE). International Journal of Computer Science & Information Technology 2011 June. Vol 3, No 3.
- [7] Zimmerman, T.G., Personal Area Networks: Near-field intrabody communication. IBM Systems Journal, 1996. Volume 35(Issue 3-4): p. 609 - 617
- [8] Javed Ahmad , F.Z., Review of Body Area Network Technology & Wireless Medical Monitoring International Journal of Information and Communication Technology Research 2012 Feburary. Volume 2 No. 2.
- [9] Aart van Halteren, R.B., Katarzyna Wac, Nicolai Dokovsky, George Koprinkov, Ing Widya, Dimitri Konstantas, Val Jones, Rainer Herzog, Wireless Body Area Networks for Healthcare : the MobiHealth Project. Wearable eHealth Systems for Personalised Health Management, 2004. Vol. 108: p. 181-193.
- [10] Milenković, A., C. Otto, and E. Jovanov, Wireless sensor networks for personal health monitoring: Issues and an implementation. Computer communications, 2006. 29(13): p. 2521-2533.
- [11] Young-Dong Lee , W.-Y.C., Wireless Sensor Network Based Wearable Smart Shirt for Ubiquitous Health and Activity Monitoring. Sensors and Actuators B Chemical 2009 July. 140(2): p. 390-395.
- [12] Konstantas D, H.R. Continuous monitoring of vital constants for mobile users. in 25th International Conference of the IEEE EMBS September 17-21,2003 Cancun, Mexico. .
- [13] Ullah, K.S.K.a.S.U.a.N. An Overview of {IEEE} 802.15.6 Standard. in 3rd International Symposium on Applied Sciences in Biomedical and Communication Technologies. July 2010. IEEE.
- [14] Javier Andreu-Perez, D.R.L., H.M.D. Ip, and Guang-Zhong Yang, From Wearable Sensors to Smart Implants –Towards Pervasive and Personalised Healthcare IEEE, 2014.
- [15] Aleksandar Milenković, C.O., Emil Jovanov, Wireless Sensor Networks for Personal health Monitoring: Issues and an implementation. Computer Communications, 2006. 29: p. 2521-2533.
- [16] Syed Furqan Qadri, S.A.A., Muhammad Amjad, Masood Anwar, Suneel Shehzad, Applications, Challenges, Security Of Wireless Body Area Networks (Wbans) Sci.Int.(Lahore), 2013. 25(4): p. 697-702.
- [17] Currey, M., Arduino with HC-05 (ZS-040) Bluetooth module – AT MODE. Mostly Arduino stuff, 2014 October.
- [18] Lee, W.-M., Beginning Android 4 Application Development. March 2012: Wrox Programmer to Programmer.
- [19] Sukhraj Kaur , D.J.M., Survey on Empirical Channel Models for WBAN International Journal of Future Generation Communication and Networking 2015. Vol. 8 , No. 2.

Analyzing Distributed Generation Impact on the Reliability of Electric Distribution Network

Sanaullah Ahmad¹

Department of Electrical Engineering
IQRA National University
Peshawar, Pakistan

Babar Noor³

Department of Electrical Engineering
IQRA National University
Peshawar, Pakistan

Sana Sardar²

Department of Electrical Engineering
IQRA National University
Peshawar, Pakistan

Azzam ul Asar⁴

Department of Electrical Engineering
CECOS University
Peshawar, Pakistan

Abstract—With proliferation of Distribution Generation (DG) and renewable energy technologies the power system is becoming more complex, with passage of time the development of distributed generation technologies is becoming diverse and broad. Power system reliability is one of most vital area in electric power system which deals with continuous supply of power and customer satisfaction. Distribution network in power system contributed up to 80% of reliability problems. This paper analyzes the impact of Wind Turbine Generator (WTG) as a distribution generation source on reliability of distribution system. Injecting single WTG and close to load point has positive impact on reliability, while injecting multiple WTGs at single place has adverse impact on distribution system reliability. These analyses are performed on bus 2 of Roy Billinton Test System (RBTS).

Keywords—Distribution Generation; Electric Power System Reliability; Wind Turbine Generator; Interruptions; Reliability Assessment

I. INTRODUCTION

Around the world, existing power system is going through different issues like, rising electrical energy demand, growing fuel cost, depletion of fossil fuel and environmental pollution. These issues smoothen way for generation of electrical power at the vicinity of its utilization by means of modular power methods like , micro turbines, fuel cell , photovoltaic cells [1]-[2]. This method of electrical power generation is known as distributed generation.

Reliability is defined as the capability of a system to execute its function in different conditions for given period of time. Customers are directly affected by the interruption in electric power distribution systems, and therefore it is given foremost importance [3].

Usually, each customer in healthy electrical distribution system is energized. In the case of any fault, electric power supply to the customers is interrupted, which is known as outage. Natural causes like lighting, trees and wind, life cycle

of equipment and maintenance are some factors that interrupt standard operating condition [4]–[7]. As the utilization of nonconventional or renewable energy resources increases for generation of electric power, many investigative studies are carried out to establish their viability as DGs. The Interruptions due to different causes as mentioned earlier can be reduced by injection of DG unit and thus improves the power system reliability.

In this paper the impact of DG on reliability is analyzed through increasing number of DG units and varying the distance of DG from feeder. This paper has five sections. Section 1 explains research overview. Section 2 has brief explanation on reliability of distribution system. Section 3 describes the problem formulation and steps for evaluating reliability. Section 4 and 5 explains results and conclusion respectively.

II. RELIABILITY OF DISTRIBUTED SYSTEM

Foul climatic conditions highly influence electric distribution system, winds and lightning are main factors contributing towards outages and failure. Many distribution networks are of radial type. Failure of single section may affect several loads due to radial nature of distribution network. Therefore in such systems reliability is of great concern. IEEE has defined certain indices to assess the reliability of distribution system. Performances are measured by means of these indices [8].

1) *System Average Interruption Frequency Index (SAIFI):*

$$SAIFI = \frac{\sum U_i N_i}{\sum N_i} f / Customer.yr$$

2) *System Average Interruption Duration Index (SAIDI):*

$$SAIDI = \frac{\sum U_i \lambda_i}{\sum N_i} hr / Customer.yr$$

3) Customer Average Interruption Duration Index (CAIDI):

$$CAIDI = \frac{\sum U_i N_i}{\sum N_i \lambda_i} \text{ hr/Customer Interruption}$$

4) Average Service Availability Index (ASAI):

$$ASAI = \frac{\sum N_i \times 8760 - \sum U_i \times N_i}{\sum N_i \times 8760} P.U$$

5) Average Service Unavailability Index (ASUI):

$$ASUI = 1 - ASAI = \frac{\sum N_i \times 8760 - \sum U_i \times N_i}{\sum N_i \times 8760} P.U$$

6) System Expected Energy Not Supplied (EENS):

$$EENS = \sum EENS_i \text{ MWhr/yr}$$

Where,

$$EENS_i = P_i U_i$$

P_i is the load of load Point i .

7) Average Energy Not Supplied (AENS):

$$AENS = \frac{\sum EENS_i}{\sum N_i} \text{ MWhr/Customer.yr}$$

Where,

N_i = Number of Consumers at load point i .

λ_i = Average failure rate at load point i .

U_i = Unavailability.

III. PROBLEM FORMULATION

To analyze the reliability of distribution system with and without DG bus 2 of RBTS is modeled and analyzed. RBTS is developed by university of saskatewan, Canada for reliability research activities [11]. A portion of Bus 2 is modeled in electrical transients analysis program (Etap) for analysis. Etap is fully integrated DC and AC electrical power software tool.[12]. All Passive and active failure rates of each component are taken as per RBTS. Section data, load data, and components reliability data is given in table 1, 2, and 3 subsequently.

Average reliability indices are estimated as:

$$\lambda_t = \sum_i \lambda_i \quad (1)$$

$$U_t = \sum_i \lambda_i r_i \quad (2)$$

$$r_t = \frac{\sum_i \lambda_i r_i}{\sum_i \lambda_i} \quad (3)$$

Where,

r_t = Average outage time

λ_t = Average Failure time

U_t = Average annual outage time

A. Reliability Indices Assessment

Below steps are used to evaluate the reliability indices:

- 1) Failed portion and its location are identified.
- 2) Load points affected due to failed portion and its duration of failure is determined.
- 3) After calculating load indices from equation 1 and 3 system indices are resolved.

TABLE I. FEEDER DATA FOR PORTION OF BUS 2 RBTS

No	Length in KM	Feeder Section
1	0.80	C4, C7, C11, C12, C15, C17, C22, C23, C25.
2	0.75	C1, C3, C6, C8, C9, C14, C16, C19, C24.
3	0.60	C2, C5, C10, C13, C18, C20, C21.

TABLE II. CUSTOMER TYPE, LOAD AND NUMBER DATA

Type of Customer	Load (MVA)	No of Customers
Residential		
Residential 1	0.535	210
Residential 2	0.535	210
Residential 3	0.450	200
Residential 4	0.450	200
Residential 5	0.450	200
Residential 6	0.450	200
Governmental & Institutions (G & I)		
G & I 1	0.566	1
G & I 2	0.566	1
G & I 3	0.566	1
G & I 4	0.566	1
Commercial		
Commercial 1	0.454	10
Commercial 2	0.454	10
Commercial 3	0.454	10
Industrial		
Industrial 1	1.13	1
Industrial 2	1.30	1
Total	8.926	1256

TABLE III. COMPONENTS RELIABILITY DATA

Component	Failure Rate (F/Yr)	Repair Time (Hr)	Switching Time (Hr)
Transformers			
33 KV / 11 KV	0.0150	15.0	1.0
11 KV / 220 V (LT)	0.0150	10.0	1.0
Breakers			
33 KV	0.0020	4.0	1.0
11 KV	0.0060	4.0	1.0
Busbars			
33 KV	0.0010	2.0	1.0
11 KV	0.0010	2.0	1.0
Feeders			
11 KV	0.650	5.0	1.0

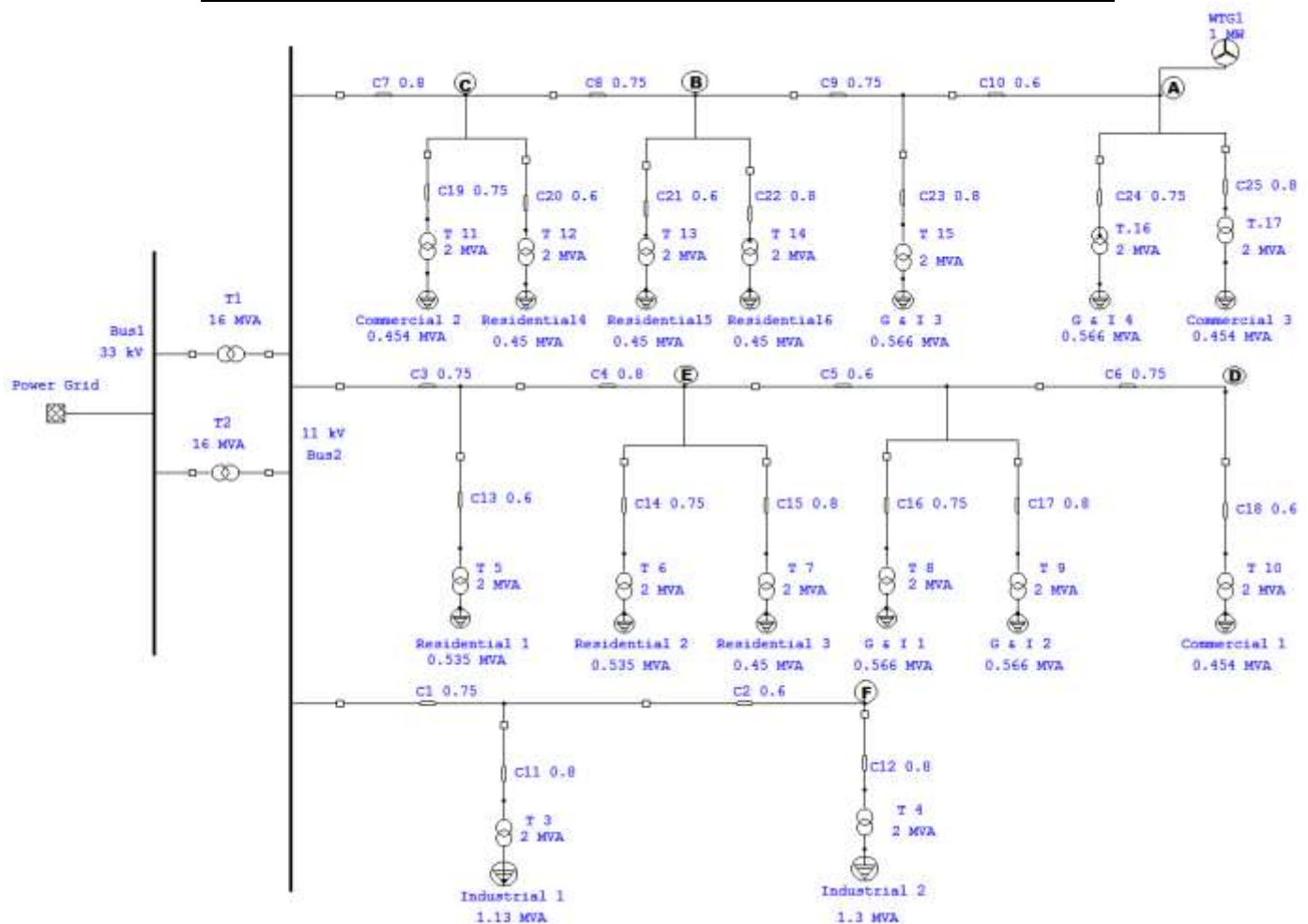


Fig. 1. A portion of Bus 2 of RBTS modeled in Etap

B. DG Reliability Data

WTG is considered as DG source. The WTG is placed at different locations so that the system reliability indices can be recorded. Table 4 lists the reliability data for WTG.

TABLE IV. THE RELIABILITY DATA FOR WTG

Type of Unit	Failure Rate	Repair Time	Switching Time
1 MW (WTG)	0.020 F/Yr	50.0 Hr	1.0 Hr

IV. MODELING AND ANALYSIS

Reliability analysis on bus 2 of RBTS is done using three cases, analysis without DG, analysis with single and multiple DG units, and lastly analyzing reliability by varying DG distance from feeder.

A. Case 1

1) Reliability Analysis without DG

In this case analyses are done without DG and reliability indices are calculated. Table 5 and 6 lists the indices.

TABLE V. RELIABILITY INDICES SAIFI, SAIDI AND CAIDI WITHOUT DG

SAIFI F/ Customer. Yr	SAIDI Hr/ Customer. Yr	CAIDI Hr/ Customer Interruption
3.8680	19.9352	5.154

TABLE VI. INDICES ASAII, ASUI, EENS AND AENS WITHOUT DG

ASAII P.U	ASUI P.U	EENS MWH/Yr	AENS MWH/Customer. Yr
0.9977	0.00228	191.578	0.1525

B. Case 2

1) Reliability VS Penetration of One DG

In this case One DG unit is injected at point A the system indices are calculated. Table 7 and 8 lists the indices.

TABLE VII. RELIABILITY INDICES SAIFI, SAIDI AND CAIDI WITH DG

Point of Injection	SAIFI F/ Customer. Yr	SAIDI Hr/ Customer. Yr	CAIDI Hr/ Customer Interruption
A	1.9957	12.1453	6.086

TABLE VIII. INDICES ASAII, ASUI, EENS AND AENS WITH DG

Point of Injection	ASAII P.U	ASUI P.U	EENS MWH/Yr	AENS MWH/Customer. Yr
A	0.9986	0.00139	120.028	0.0956

The result show positive improvement in reliability indices with injection of one DG unit.

2) Reliability VS Penetration of Multiple DG

With injection of Two DG units at location A the system indices are calculated and results are compared with One DG unit. Table 9 and 10 lists the indices.

TABLE IX. RELIABILITY INDICES SAIFI, SAIDI AND CAIDI

Point of Injection A	SAIFI F/ Customer. Yr	SAIDI Hr/ Customer. Yr	CAIDI Hr/ Customer Interruption
Single DG	1.9957	12.1453	6.086
Multiple DG	1.9959	12.1540	6.090

TABLE X. INDICES ASAII, ASUI, EENS AND AENS

Point of Injection A	ASAII P.U	ASUI P.U	EENS MWH/Yr	AENS MWH/Customer. Yr
Single DG	0.9986	0.00139	120.028	0.0956
Multiple DG	0.9986	0.00139	121.048	0.0964

The results depicted that by injecting multiple DG units at same location in distribution network has adverse effect on the reliability of distribution system.

C. Case 3

1) Reliability VS Distance

In case of one DG penetration at different locations the system indices are calculated and compared with Case1. Table 11 and 12 lists the comparisons.

TABLE XI. RELIABILITY INDICES SAIFI, SAIDI AND CAIDI

	SAIFI F/ Customer. Yr	SAIDI Hr/ Customer. Yr	CAIDI Hr/ Customer Interruption
Without DG	3.8680	19.9352	5.154
A	1.9957	12.1453	6.086
B	2.0119	12.5311	6.228
C	2.2438	14.0404	6.258
D	1.9877	12.1064	6.091
E	2.0036	12.4975	6.238
F	2.5714	15.3795	5.981

TABLE XII. INDICES ASAII, ASUI, EENS AND AENS

	ASAII P.U	ASUI P.U	EENS MWH/Yr	AENS MWH/Customer. Yr
With Out DG	0.9977	0.00228	191.578	0.1525
A	0.9986	0.00139	120.028	0.0956
B	0.9986	0.00143	131.961	0.1051
C	0.9984	0.00160	143.035	0.1139
D	0.9986	0.00138	122.629	0.0976
E	0.9986	0.00143	132.892	0.1058
F	0.9982	0.00176	140.906	0.1122

The results portray that the reliability indices improve when DG is placed near to the load points, the indices shows that optimum location for planting DG in context of reliability is point A.

V. CONCLUSION AND FUTURE WORK

By conducting different reliability tests on Bus 2 of RBTS the results show diverse impact of DG on the reliability of distribution network. The indices clearly shows that reliability of power system improves by injection of DG

into distribution system, injecting DG more close to load points or far from feeder improves the reliability further. However injection of multiple DG units on same location has negative impact on the reliability of distribution network. Furthermore reliability worth assessment can be performed using different renewable or non-renewable energy resources.

REFERENCES

- [1] M. Makandar, C. S. R. Atla and S. Velamuri, "Reliability assessment of distribution system with renewable Distributed Generation," 2016 Biennial International Conference on Power and Energy Systems: Towards Sustainable Energy (PESTSE), Bengaluru, India, 2016, pp. 1-5.
- [2] T. Ackerman, G. Anderson and L. Soder, "Distributed Generation: A Definition", Electric Power Systems Research, vol. 57, December 2001 pp. 195-204.
- [3] C.A Warren, "Distribution Reliability-What is it", Rural Electric Power Conference, April 1995, pp 1-6.
- [4] M.E. Baran and F.F. Wu, "Network Reconfiguration in Distribution Systems for loss reduction and Load Balancing", IEEE Transactions on Power Delivery, Vol. 4, No. 2, April 1989, pp 1401-1407.
- [5] P.P. Barker, De Mello, "Determining the Impact of Distributed Generation on Power Systems.I. Radial Distribution Systems", Power Engineering Society Summer Meeting, Vol. 3, July 2000, pp 1645-1656.
- [6] R.E. Brown and L.A Freeman, "Analyzing the Reliability Impact of Distributed Generation", IEEE Power Engineering Society Summer Meeting, vol. 2, July 2001, pp 1013-1018.
- [7] AC. Neto and M.G. da Silva, "Impact of Distributed Generation on Reliability Evaluation of Radial Distribution Systems under Network Constraints", Proc. Of 9th International Conference on Probabilistic Methods Applied to Power Systems, June 2006, pp 1-6.
- [8] R. K. Matheu, Ashok S. and Kumaravel S., "Analyzing the effect of DG on reliability of distribution systems," Electrical, Computer and Communication Technologies (ICECCT), 2015 IEEE International Conference on, Coimbatore, 2015, pp. 1-4.
- [9] R. Billinton, Reliability Evaluation of Engineering Systems, Plenum Press, New York 1996.
- [10] Y.Sun, M.H.T. Bollen and G.Ault, "Improving Distribution System Reliability by means of Distributed Generation", 19th International Conference on Electricity Distribution, May 2007, pp 1-4.
- [11] R. Billinton and S. Jonnavithula, "A test system for teaching overall power system reliability assessment," in IEEE Transactions on Power Systems, vol. 11, no. 4, pp. 1670-1676, Nov 1996.
- [12] Prakash, Prem, Vivek Anand Verma, and R.C. Jha. "Distribution System Reliability Analysis Using ETAP".srjournal, vol. 02, no. 1, pp. 24-29, Mar 2014.

An Efficient and Robust High Efficiency Video Coding Framework to Enhance Perceptual Quality of Real-Time Video Frames

Murthy SVN

Research Scholar

Department of Computer Science & Engg.
Jain University, Bangalore, India

Dr. Sujatha B K

Professor

Department of Telecommunication & Engg.
MS Ramaiah Institute of Technology, Bangalore, India

Abstract—Different level of compression on real-time video streaming has successfully reduced the storage space complexities and bandwidth constraints in the recent times. This paper aims to design and develop a novel concept towards the enhancement of perceptual quality of a real-time video frames. The proposed model has been experimented considering multi-level compression operation using H.265 where .avi moving frames standards play a crucial role. The study also applies a novel concept of High-efficiency video coding (HEVC) for adaptive live video streaming over a mobile network. The proposed study aims to formulate a multi-level optimization for HEVC to enhance the performance of both encoding and decoding mechanisms at the client as well as server side to ensure higher compression rate. The experimental outcomes also show that the proposed protocol achieves better performance ratio and overall throughput in comparison with conventional H.263, H.264 by enhancing the perceptual quality of .avi format real-time video frames.

Keywords—H.265; HEVC; Video Coding; Compression

I. INTRODUCTION

Video encoding is the way toward diminishing the measure of information required to interpret to an advanced video signal, preceding transmission or capacity. The corresponding operation, decompression or disentangling, recoups an advanced video signal from a compacted representation, before the presentation. Advanced video information tends to take up a lot of capacity or transmission limit thus video encoding and translating, or video coding is a key attribute for any application in which transmission data transfer capacity is compelled and constrained by a limited bandwidth. High-Efficiency Video Coding (HEVC) is right now the freshest video coding standard of the ITU-T Video Coding Experts Group (VCEG) and the ISO/IEC Moving Picture Experts Group (MPEG) [1][2]. The principle objective of the HEVC institutionalization exertion is to empower fundamentally enhanced compression metric execution in respect to existing models – in the scope of half piece rate decrease for equivalent perceptual video quality. HEVC guarantees to diminish the general expense of conveying and putting away video resources while keeping up or expanding the nature of the experience for the viewer. These are the two advantages of HEVC in the spilling space. The principal identifies with encoding existing SD and HD content with HEVC as opposed to H.264, empowering cost reserve funds and the capacity to

stream higher quality video to lower bit rate associations. The second identifies with opening up new markets for ultra-superior quality (UHD) recordings. This research study discusses the retention of higher quality of video file and traffic management when a video is compressed using HEVC over the wireless mobile network. The present pattern in video utilization obviously demonstrates that the officially expansive amount of video material conveyed over communication channels, advanced systems, and bundled media is going to increment in the coming years. As an impact of the developing notoriety, the client's interest for expanded determination and higher quality is driving the endeavors of the technological improvement. Starting here of perspective, the advancement of video obtaining and show advances is much quicker than that of system, the users' demand for increased resolution and higher quality is driving the efforts of the technological development. From this point of view, the evolution of video acquisition and display technologies is much faster than that of network capabilities. Users would like to watch streaming videos on mobile phones on the go. Though H.264 is succeeded in providing a good motion picture in Television, High Definition Television (HDTV), and Full High Definition Television and even to web based applications. But it requires higher bit rate and hence it is failed to deliver high definition videos to mobiles and to tablets.

Therefore, it is an open research problem to conceptualize, design and device a mechanism involves into H.264/AVC encoding processes to achieve higher performance with least computational overhead by low complex implementations. Typically, an H.264/AVC encoding process involves removal of spatial, temporal and statistical redundancy of video signal. The transformation of macro blocks, (a basic coding unit of 16 X 16 block of displayed pixel) by quantization of transform domain (spatial frequency components/ co-efficient) from spatial domain provides a considerable amount of compression. The proposed study aims to design an efficient and novel video compression technique namely HEVC based optimized encoding tool to improve the perceptual quality of real-time encoded video streams on a mobile network. The paper is organized as follows Section II discusses the recent studies towards conventional real-time video compression mechanisms (i.e. using H.263, H.264, H.265) which are followed by problem description in Section III. Section IV discusses proposed system followed by a discussion of algorithm

implementation in Section V. Section VI discusses the result analysis followed by conclusion in Section VII.

II. LITERATURE SURVEY

This section discusses the existing research work being carried out using H.265 video compression standard. Most recently, Chen et al. [3] have introduced a decoder by H.265 using a hardware-based architecture with supportability of the parallel processing. The outcome of the study evaluated on decoding speed shows that presented technique can support decoding of 8K UHD. Dias et al. [4] have presented a study by incorporating H.265 protocol for enhancing the quantization with the aid of rate distortion theory. The presented study has used spatial-based solution to enhance the visual perception of the signal. The study has been testified with mean opinion score and multimedia quality. The similar direction of work by adopting rate-distortion theory has been implemented by Nguyen and Marpe [5]. The authors have used the image as data to be compressed using H.265 protocol. The study outcome found that mean of bit rate saving using JPEG is quite high compared to other compression technique along with H.265. Panayides et al. [6] have presented a study recently that studied comparative analysis of various existing signaling protocols on H.265 taking the case study of medical video dataset. Trzciawski [7] have also presented a study that has focused video coding for legacy protocol e.g. advances video coding.

A very interesting study was put forward by Ye et al. [8] have elaborated about the usage of UHD files and its management over the networks. The author discussed that usage of H.265 can save around 64% of the bit rate as compared to high definition and standard definition video. He et al. [9] have presented a new approximation technique for ensuing processing of UHD files with a major focus on minimizing computational complexity about search-techniques for optimal coefficients of resolutions. The technique was implemented on hardware-based approach over VLSI architecture. Ahn et al. [10] have discussed various optimization techniques using H.265 with the aid of parallel processing. Also, the authors have presented a task scheduling technique along with slicing process in parallelization over multicourse using H.265. Blasi et al. [11] have presented a technique for minimizing the complexity related to motion compensation. Diasi et al. [12] have presented an FPGA-based study for performing compression using H.265 protocol using an integrated scheme of the efficient computational process along with 2D transforms. Mu et al. [13] have presented a cascaded technique for legacy protocols e.g. H.264/AVC and was subjected to H.265 encoding process to extract the encoding coefficients. The focus was laid on enhancing the speed of coding tree unit. Hence, there are various studies that have focused on using video compression algorithm. The techniques are associated with advantages as well as a limitation. However, it has acted as better guidelines for designing a novel protocol of video compression.

III. PROBLEM DESCRIPTION

Existing techniques don't emphasize on developing on-demand video compression techniques which ignore the computational complexity. Existing research work towards

video compression doesn't have the explicit design of wireless communication channel and its associated problems. The entire compression algorithm designed till date seriously lacks multi-level optimization, which will mean that the existing algorithm can offer one round of better solution and cannot go beyond that. Although PSNR is found to be used in literature, its values are less emphasized on 8K or UHD data quality.

IV. RESEARCH METHODOLOGY

The proposed study aims to design and develop an integrated HEVC standard prototype to enhance the perceptual quality of transmitted video frames using H.265 video compression technique. The resulting compressed video frames also support 8K (UHD) resolutions features, and it also maintains the PSNR ratio in between the range of 35-40 dB. The following figure 1 depicts the architecture of the proposed model and the overall flow towards ensuring the better retention of 8 K (UHD) videos after encoding. However, there are conventional techniques used to optimize the 8 K resolution efficiency, but the proposed H.265 prototype | Codec maximizes the perceptual quality and the resolution of an encoded video considering the optimal trade-off. The H.265 protocol runs over a distributed real-time TCP/IP communication scenario where n number of clients is connected to a server using TCP/IP protocol stack based communication terminals. Hence, an analytical methodology has been conceptualized and experimented by streaming standard definition (SD), High Definition (HD) and Ultra High Definition (UHD) in a real time scenario. The proposed study is precisely focused on designing a multi-level HEVC video compression technique to compress 8K videos on real time transmission stage using H.265 without affecting its original quality. The proposed model performs both encoding and decoding in the server and receiver sides respectively, but the compression of the transmitted video happens during the transmission scenario configured by installing and setting up DASH servers for client and receiver units.

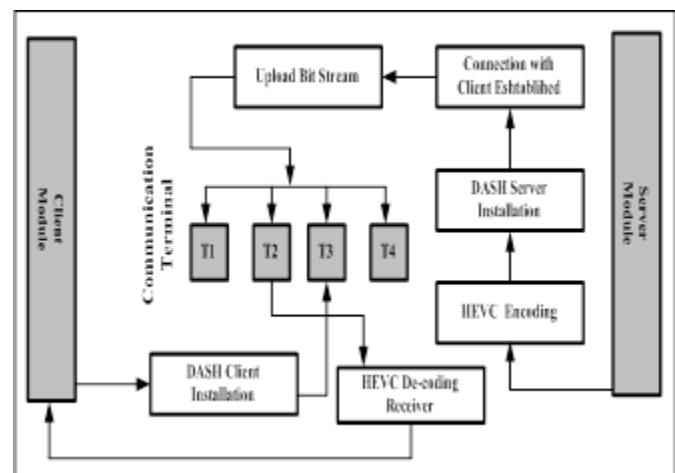


Fig. 1. Proposed Architecture

Apparently, the real-time streaming videos during the buffering time which are usually the time requires to decode the encoded or compressed 8K videos are mostly get affected by the noisy environment of the wireless communication

mediums, and it also degrades the quality of the video even to a minor extent. To address the above-stated issue of 8K (UHD) video frames transmission over a wireless channel DASH server and its functionality initiated in both client and the server side for video quality enhancement. The proposed system initiates a dynamic adaptive streaming over HTTP (DASH) server for transmitting the encoded 8K (UHD) video frames over a wireless channel. It has also been implemented over fast data communication scenario, which enables high quality streaming media contents from conventional HTTP servers using a constraint band-width capacity. The design principles associated with a DASH server configuration and real-time integration is illustrated below.

A. Design Principle of DASH Servers

The principles of DASH servers gained a significant market adoption for the real-time video streaming and compression protocols such as H.265. HTTP-based streaming should be closely inclined on HTTP server based progressive downloading scenario. HTTP based high-resolution video streaming processes are found to give a normative description of media presentation over wireless channels. The proposed HTTP based HEVC protocol incorporates streaming of encoded 8K (UHD) video frames on real-time and on-demand services. It also uses the concept of progressive download for on-demand media delivery from HTTP servers. The proposed system has been designed and experimented considering the following conditions which have been considered referring the conventional design flaws of HTTP/1.1 web server-based progressive downloading.

- The proposed system should effectively utilize the bandwidth even if a client unit terminates the data connection to streaming of the encoded 8K (UHD) videos frames and switch over another content.
- The proposed HEVC protocol is modeled based on the adaptive bit-rate scenario and it also supports the live media services compatible with live video streaming over HTTP-dash addresses.
- It has also been evaluated over a wireless mobile communication medium which ensures reliability and the deployment simplicity of TCP/IP protocol stacks for efficient connection establishment in between client and server units.

The proposed system has also been integrated with The Content Distribution namely CDN Network to reducing the compression and downloading latency of media files. However, initially HTTP streaming has been used in 3GPP adaptive multimedia streaming, hence due to its optimal bandwidth utilization efficiency and adaptive bit-rate switching it is further integrated with 3GPP TS 26.234 for end-to-end packet switch streaming services. The adoption of HTTP based DASH server into the proposed study enhances the effectiveness of live 8K (UHD) video frames streaming and its encoding during a data transmission over a mobile network without affecting its perceptual quality (I.e. PSNR values). The model consider at the HTTP web server unit and client unit communication scenario for uploading and downloading the 8K (UHD) video file. The video is uploaded at the server

side using the efficient HEVC compression technique. After that, the DASH server is initialized to perform further encoding on the digitalized 8K video frames. After successful DASH server initialization and video compression, the server broadcast a request message to the all respective client nodes that are waiting to receive and stream the videos in online buffering. The client establishes a secure TCP/IP integrated connection considering the DASH server's IP address and port number. The successful connection establishment leads to transmitting the 8K video frames over a wireless channel. The H.265 compression also takes place during the transmission to encode the video frames. The client receives the video and performs HEVC decoding and watches the video respectively. The compression of bit-stream over a mobile network doesn't affect the video quality regarding perceptual quality and resolution aspects. Moreover, it enhances the perceptual quality to support the 8 K (UHD) resolutions at the client unit. The next section provides the algorithmic implementation procedures associated with the proposed model.

V. ALGORITHM IMPLEMENTATION

This section introduces the analytical modeling and the algorithmic implementation of the proposed HEVC video compression technique. The algorithm implementation of the proposed prototype has been carried out using Matlab tool. The proposed study develops an optimized HEVC based video compression technique, which connects different level of computations to perform HEVC encoding on the real-time video frame streaming without affecting it's perceptual quality. The proposed HEVC protocol aimed to attain maximum retention of 8K resolution of transmitted UHD video files. The processing of the video frames attains a different level of optimized computation to ensure an effective and optimal performance trade-off of PSNR and network throughput.

Level-1: Modelling of HEVC for processing input 8K video frames.

Input: V_i (input video), f_i (Number of frames), S_l (segment length) where $i \in n$

Output: V_f (video frames)

Start

Step 1. Import $\leftarrow V_i$

Step 2. Initialize f_i, S_l

Step 3. For $i \leftarrow 1: n$

Step 4. Apply HEVC Processing-L1

Step 5. $f \leftarrow$ read pixel information

Step 6. Compute \leftarrow multimedia coefficients

Step 7. **End**

End

The above algorithm shows the level-1 computation of HEVC protocol for the efficient improvement of the perceptual quality of a video frame.

Level-2: Modelling of HEVC protocol using H.265 codec

Input: L (length), W (Width), f_n (frame sequence 1-10)

Output: C_R (compression Ratio), C_{bits} (Number of Compressed bits),

Start:

- Step 1. Initialize $\leftarrow f_1:f_{10}$
- Step 2. for i $\leftarrow 1:n$
- Step 3. N_f $\leftarrow [f(\text{end}) - f(\text{start}) + 1]$
- Step 4. Define $\leftarrow \text{MacroblockSize}(N_f)$
- Step 5. f $\leftarrow \text{read(vid, 1)}$ //read first frame
- Step 6. S_f $\leftarrow \text{Get}(f)$
- Step 7. f $\leftarrow \text{imresize}(f, [128 128])$ //define frame size
- Step 8. I $\leftarrow \eta(.2989*f) + \beta(.5870*f) + \mu(.1140*f)$
- Step 9. Compute $\leftarrow \text{video sequence input}$

End

Level-3: Modelling of HEVC protocol using H.265 encoder

Input: L (length), W (Width), f_n (frame sequence 1-10)

Output: C_R (compression Ratio), C_{bits} (Number of Compressed bits),

Start

- Step 1. Extract $\leftarrow \text{input(Video_seq)}$
- Step 2. Initialize f_{PSNR}, f_{BR}
- Step 3. for i $\leftarrow 1:n$
- Step 4. VideoSeq_rec $\leftarrow n(L, H, f_n)$
- Step 5. Apply $\leftarrow \text{HEVC Encoding Level-2}$
- Step 6. Percentage_t1 $\leftarrow (t1+t2+t3\dots tn)$
- Step 7. B_{size} $\leftarrow B_{\text{size}} * 4$
- Step 8. B_{stream} $\leftarrow [B_{\text{stream}} '0000']$ // appending P-frame
- Step 9. Compute Comratio $\leftarrow [L*H*\text{Size}(\text{VideoSeq_Input}, 3)*8];$

Step 10. Compute $\leftarrow \text{PSNR}$

Step 11. Compute $\leftarrow \text{No_original_Bits} | \text{No_CompressedBits}$

Step 12. End

Step 13. Upload encoded video to the dash server and again perform H.265 standard to enhance the PSNR.

End

The above-connected algorithms show how different level of optimized HEVC encoding has been performed on a real-time video streaming to increase the perceptual quality of high quality (UHD) video frames. The encoding has also been performed on a real-time video streaming followed by appending P-frame in the header. The primary encoding imposed on the input frames and the processed frame is stored in a temporary matrix. The proposed HEVC method ensures the higher reliability on maintaining pixel information along with the superior reduction of media file size to utilize the network bandwidth effectively. The experimental setup and its respective configuration details are provided below.

- *Tool Used:* The proposed mechanism is developed, deployed and executed on both 32 bit as well as on 64 bits machine. The development platform was MATLAB.
- *Specification:* The proposed study has been conducted considering the OFDM wireless channel system OFDM communication and protocol frameworks don't depend on expanded image rates keeping in mind the end goal to accomplish higher information rates. This makes the undertaking of overseeing inter-symbol impedance (ISI) much less complex. OFDM frameworks break the accessible transfer speed into numerous smaller sub-bearers and transmit the information in parallel streams.

VI. RESULT ANALYSIS

The proposed system is integrated with HEVC standard to enhance the perceptual quality of video frames for supporting 8 K (UHD) resolutions. The design and development phase of the proposed model has been carried out using MATLAB 2015 and its two different instances respectively to support the client and server applications. The experimental prototyping also performs a benchmarking by initiating a comparative analysis of the results obtained from the proposed model (H.265) and the conventional H.264 and H.263. The proposed system is found to achieve more precise outcomes (i.e. the enhancement of video quality regarding PSNR) for supporting 8K (UHD) resolution based video frames without affecting the cost effectiveness and the complex hardware unit. Different video files (i.e. no of frames) of few seconds are processed and compressed using HEVC encoding to validate the quality of experimental results.

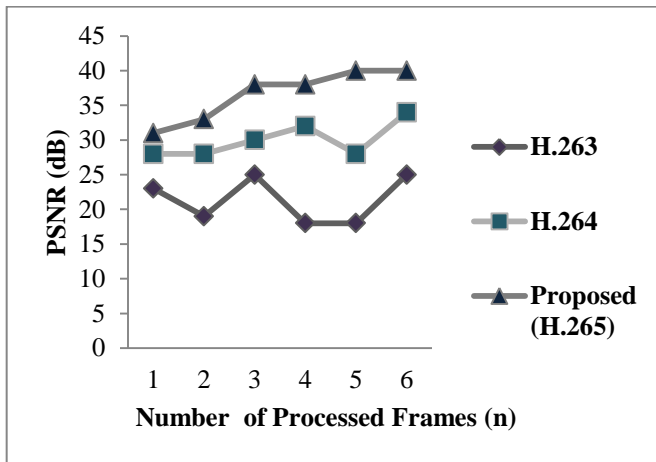


Fig. 2. Perceptual Quality Evaluations

The above-mentioned comparative analysis highlighted in figure 10 depicts that the proposed model not only enhance the perceptual quality of video frames, moreover it also maintains the video compression ratio on standard PSNR (dB) range in between 30-40 (dB). The experimental prototype also suggests that proposed model is capable of maintaining the 8 K (UHD) video resolutions, which requires very less amount of storage space in DASH servers for both client and server units. It also reduces the computational complexities in comparison with the conventional techniques.

VII. CONCLUSION

The proposed study performs a more deep investigation on standard definition (SD), High Definition (HD), and Ultra High Definition (UHD). Usually streaming videos over wireless medium will have possible degradation in the video quality even to minor extent; hence, these issues will be addressed in this phase of the study. The study has accomplished a most superior quality of video that supports 8K features using H.265. The comparative analysis of the proposed H.265 decoder shows that it effectively enhances the PSNR

(perceptual quality of a video signal) by reducing the computational time and space complexities. It also outperforms the conventional H.263 and H.264 standards.

REFERENCES

- [1] I.E. Richardson, "H.264 and MPEG-4 Video Compression: Video Coding for Next-generation Multimedia", John Wiley & Sons, Science, pp.306, 2004
- [2] D. R. Bull, "Communicating Pictures: A Course in Image and Video Coding", Academic Press, Computers, pp. 560, 2014
- [3] Y-H Chen, V. Sze, "A Deeply Pipelined CABAC Decoder for HEVC Supporting Level 6.2 High-Tier Applications", IEEE Transactions On Circuits And Systems For Video Technology, Vol. 25, No. 5, 2015
- [4] S. Dias, M. Siekmann, S. Bosse, H. Schwarz, "Rate-Distortion Optimized Quantization For HEVC Using Spatial Just Noticeable Distortion", IEEE-European Signal Processing Conference, 2015
- [5] T. Nguyen and D. Marpe, "Objective Performance Evaluation of the HEVC Main Still Picture Profile", IEEE Transactions On Circuits And Systems For Video Technology, Vol. 25, No. 5, 2015
- [6] S. Panayides, M. S. Pattichis, C. P. Loizou, "An Effective Ultrasound Video Communication System Using Despeckle Filtering and HEVC", IEEE Journal Of Biomedical And Health Informatics, Vol. 19, No. 2, 2015
- [7] L. Trzcianowski, "Subjective Assessment for Standard Television Sequences and Videotoms H.264/AVC Video Coding Standard", Journal of Telecommunications and Information technology, 2015
- [8] Y. Ye, Y. He, and X. Xiu, "Manipulating Ultra-High Definition Video Traffic", IEEE Computer Society, 2015
- [9] G. He, D. Zhou, Y. Li, Z. Chen, "High-Throughput Power-Efficient VLSI Architecture of Fractional Motion Estimation for Ultra-HD HEVC Video Encoding", IEEE Transactions on Very Large Scale Integration (VLSI) Systems, Vol. 23, No. 12, 2015
- [10] Y-J Ahn, T-J Hwang, D-G Sim, and W-J Han, "Implementation of fast HEVC encoder based on SIMD and data-level parallelism", Springer-EURASIP Journal on Image and Video Processing, Vol.16, 2014
- [11] S. G. Blasi, I. Zupancic, and E. Izquierdo, "Fast motion estimation discarding low-impact fractional blocks", IEEE-Proceedings of 22nd European Signal Processing Conference, pp.201-215, 2014
- [12] T. Diaset, N. Roma and L. Sousa, "Unified transform architecture for AVC, AVS, VC-1 and HEVC high-performance codecs", Springer-EURASIP Journal on Advances in Signal Processing, Vol.108, 2014
- [13] F. Mu, L. Song, Z. Luo, X. Wang, X. Yang, "Speed Up HEVC Encoder by Precoding with H.264", IEEE-Annual Summit and Conference Asia-Pacific Signal and Information Processing Association, pp.1-6, 2014

Time-Saving Approach for Optimal Mining of Association Rules

Mouhir Mohammed

IIMCS Laboratory

Dept. of Mathematics and Computer Sciences

FSTS, University of Hassan 1st

Settat, Morocco

Balouki Youssef

IIMCS Laboratory

Dept. of Mathematics and Computer Sciences

FSTS, University of Hassan 1st

Settat, Morocco

Gadi Taoufiq

IIMCS Laboratory

Dept. of Mathematics and Computer Sciences

FSTS, University of Hassan 1st

Settat, Morocco

Abstract—Data mining is the process of analyzing data so as to get useful information to be exploited by users. Association rules is one of data mining techniques used to detect different correlations and to reveal relationships among data individual items in huge data bases. These rules usually take the following form: if X then Y as independent attributes. An association rule has become a popular technique used in several vital fields of activity such as insurance, medicine, banks, supermarkets... Association rules are generated in huge numbers by algorithms known as Association Rules Mining algorithms. The generation of huge quantities of Association Rules may be time-and-effort consuming this is the reason behind an urgent necessity of an efficient and scaling approach to mine only the relevant and significant association rules. This paper proposes an innovative approach which mines the optimal rules from a large set of Association Rules in a distributive processing way to improve its efficiency and to decrease the running time.

Keywords—MDP_{REF} Algorithm; Association Rules mining; Data partitioning; Optimization (profitability, efficiency and Risks); Bagging

I. INTRODUCTION

Big data is an important research topic and it has attracted considerable attention. The huge numbers of data sets are unused and redundant in the databases of companies, universities, etc. Discovering the unused and redundant information stored in these data bases is grounded on the efficient KDD (Knowledge Discovery in Database) process. This latter does not only retrieve data or let researchers find new information from data [1] but also has the ability to reveal the patterns and relationships among large amounts of data in a single or several data sets. KDD process makes use of several techniques from statistics and artificial intelligence in a variety of activities. The main activities are as follows [2-11]: Association Rules; Clustering; Classification; Regression and Prediction. We are rather interested in the association rules mining, together with classification and clustering which are two of the major data mining applications where pattern mining is extensively used to transform raw data into pattern-based description that is accepted and processed by classification and clustering algorithms. In this context, patterns which occur in data are simply considered as features that characterize data. Patterns describing the data are also called explanatory variables. Whereas Association Rules Mining is one of the most common algorithm-based data

mining techniques which can be defined as the extractor or generator of interesting relationships and correlations among items in large amounts of data. [10] Although Association Rules, Clustering and Classification are the techniques extensively used in this paper, Regression and Prediction are going to be taken into account in our future work to reinforce the reliability and to improve the quality of results. For reasons related to the obviation of a possible confusion or misunderstanding, we provide below the definitions of the activities meant by both concepts:

- **Regression** for a set of items is the analysis of the relationships of dependence between the values of the attributes. A model is automatically produced that can predict attribute values for new items.
- **Prediction** for a specific item and a corresponding model is the ability to predict the value of a specific attribute. For example, in a predictive model for treatment schema, prediction is used to determine the next procedure in the sequence of treatment.

Lately, many algorithms have been suggested in the literature for instance: Close, Close +, Charm, Sky Rules,... to help generate association rules, either by improving the process of "patterns'extraction" or by introducing other criteria and factors in order to determine which rule to keep and which one to discard [3]. However, these algorithms are mainly used to centralize computing systems and relatively evaluate small databases. Yet, the huge numbers of generated association rules and modern databases are growing dramatically in terms of size. Consequently, several parallel and distributed solutions have been proposed to tackle this issue. In addition to that, many distributed frameworks have been used to deal with the existing abundance of data. These distributed frameworks focus on the challenges of distributed system building and on simple programming models for data analysis. To solve these problems, we think that a data partitioning technique considering data characteristics should be applied. In this paper, we propose a scalable and distributive approach for large scale frequent association rules. The proposed approach offers the possibility to apply any of the known association rules mining algorithms in a distributive way. In addition, it allows many possibilities to apply any of the known clustering or classification algorithms as partitioning techniques for the association rules set.

Besides the introduction, the paper is made up of four sections, each of which deals with a particular aspect: section II deals with the necessary definitions, section III describes the proposed approach of large-scale association rules mining. Then, section IV is concerned with the experiments we have carried out to concretize the proposed approach. The last section concludes the paper and reveals our willingness to continue research for better results.

II. BACKGROUND AND PROBLEM DEFINITION

Definition 1 (Association Rules) An Implication expression having the form of $B \rightarrow H$ where: both B and H are sets of items, and are separate itemsets i.e. $B \cap H = \emptyset$. B is called a premise and H is called a conclusion.

Definition 2 (MDP_{REF} rules) MDP_{REF} is an algorithm which is short for the Most Dominant and Preferential rules. It is based on notions of dominance, preference and user profile.

Definition 3 (Loss Rate) Given S_1 and S_2 two set with $S_2 \subseteq S_1$ and $S_1 \neq \emptyset$, we define the loss rate S_2 as compared to S_1 by

$$\text{LossRate}(S_1, S_2) = \frac{|S_1 - S_2|}{|S_1|}$$

Definition 4 (Cost of a partitioning method) Let $R = \{Runtime_j(PM), \dots, Runtime_N(PM)\}$ be a set of runtime values. $Runtime_j(PM)$ represents the runtime of computing MDP_{REF} rules in the partition_j (Part_j) of the database. The operator E denotes the average or expected value of R . Let μ be the mean value of R :

$$\mu = E[R].$$

The cost measure of a partitioning technique is:

$$\text{Cost}(PM) = \sqrt{E[(R - \mu)^2]}.$$

A large cost value indicates that the runtime values are far from the mean value and a small cost value indicates that the runtime values are near the mean value. The smaller the value of the cost is, the more efficient the partitioning is.

III. BIG DATA ANALYSIS

A. Distributed machine learning and data mining techniques

Data mining and machine learning hold a vast scope in using the various aspects of Big Data technologies for scaling existing algorithms and solving some of the related challenges [4]. In the following, we present existing works on distributed machine learning and data mining techniques.

a) NIMBLE

NIMBLE [5] is a portable infrastructure that has been specifically designed to enable the implementation of parallel Machine Learning (ML) and Data Mining (DM) algorithms possible.

The NIMBLE approach allows composing parallel Machine Learning and Data Mining algorithms « ML-DM algorithms » using reusable (serial and parallel), building

blocks that can be efficiently executed using MapReduce and other parallel programming models. The programming abstractions of NIMBLE have been designed so as to parallelize ML-DM computations and allow users to specify several tasks such as parallel data, parallel tasks and even pipelined computations.

The NIMBLE approach has been used to implement some popular data mining algorithms such as k-Means Clustering and Pattern Growth based Frequent Item set Mining, k-Nearest Neighbors, Random Decision Trees, and RBRP-based Outlier Detection algorithm.

As shown in Fig.1, NIMBLE is divided into four distinct layers:

1) The user API layer, which provides the programming interface to the users. Within this layer, users are able to design tasks and Directed Acyclic Graphs (DAGs) of tasks to indicate dependencies between tasks. A task processes one or more datasets in parallel and produces one or more datasets as output.

2) The architecture independent layer, which acts as the middleware between the user specified tasks/DAGs, and the underlying architecture dependent layer. This layer is responsible for the scheduling of tasks, and delivering the results to the users.

3) The architecture dependent layer, which consists of harnesses providing a means allowing NIMBLE to run portably on various and several platforms. Currently, NIMBLE only supports execution on the Hadoop framework.

4) The hardware layer, which consists of the used cluster.

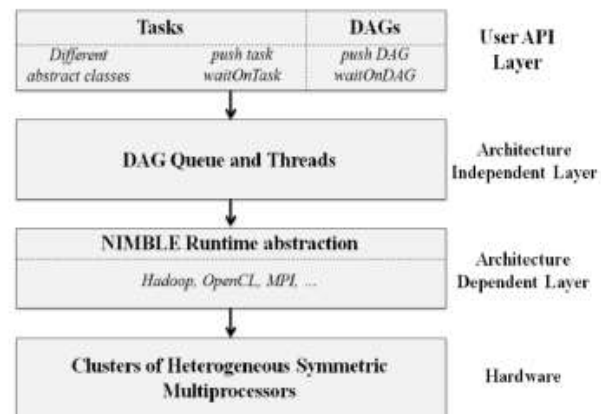


Fig. 1. An overview of software architecture of NIMBLE

b) SystemML

SystemML [6] is a system that enables the development of large scale Machine Learning algorithms. It first expresses a Machine Learning algorithm in a higher-level language called Declarative Machine learning Language (DML). Then, it executes the algorithm in a MapReduce environment.

On the one hand, DML is a system whose main goal is to simplify the usage or development of Machine Learning algorithm, it separates algorithms from data representation and execution plans.

On the other hand, DML language exposes arithmetical and linear algebra primitives on matrices that are natural to express a large class of Machine Learning algorithms.

There are different types of DML such as:

- DML Tasks : (for further clarification please refer to MLbase [18, 21], (fixed task) Columbus [25], DeepDive [20])
- DML Algorithms (fixed algorithm) : (for further clarification please refer to OptiML [23], SciDB [13-22] SystemML [12-16], SimSQL [14])
- Large-Scale ML Libraries (fixed plan) : (for further clarification please refer to MLLib [19], Mahout [24], MADlib [15-17], ORE, Rev R)

As shown in Fig.2, SystemML is classified into four distinct layers:

1) The Language component: It consists of user-defined algorithms written in DML.

2) The High-Level Operator Component (HOP): It analyzes all the operations within a statement block and chooses from multiple high-level execution plans. A plan is represented in a DAG of basic operations (called hops) over matrices and scalars.

3) The Low-Level Operator Component (LOP): It translates the high-level execution plans provided by the HOP component into low-level physical plans on MapReduce.

4) The runtime component: It executes the low-level plans obtained from the LOP component on Hadoop.

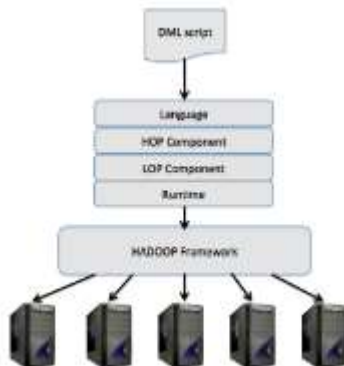


Fig. 2. An overview of software architecture of System ML

a) PARMA

PARMA [7] is a parallel randomized algorithm for mining Frequent Itemsets (FI's) and Association Rules (AR's). PARMA is built on top of MapReduce and the computations are performed twice following the two processing steps of MapReduce. As stressed in Fig.3, the Ellipses represent data, squares represent calculations on that data and arrows show the movement of data through the system.

PARMA creates multiple small random samples of the transactional dataset, at Phase 1 "Map1", and runs a mining

algorithm on the samples independently and in parallel, at Phase 2 "Reduce1". The output results from each sample labeled "id", at Phase 3 "Map 2", are aggregated and filtered, at Phase 4 "Reduce 2", to provide a single collection as output which is a global set of Frequent Itemsets and Association Rules. The final result of PARMA is an approximation of the exact solution since it mines random subsets of the input dataset.

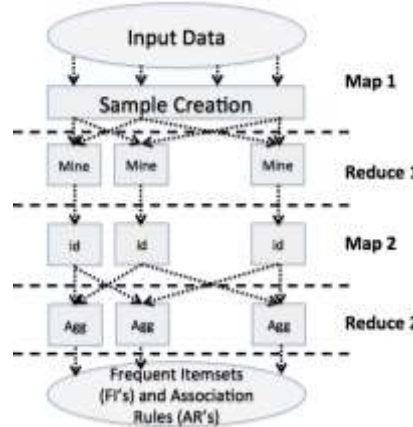


Fig. 3. An overview of the software architecture of PARMA

Table 1 presents the most popular data mining and machine learning techniques. For each technique, it lists the programming model, the implemented techniques and the programming language. We notice that the input and the output of the above presented approaches are user-defined.

TABLE I. OVERVIEW OF DATA MINING AND MACHINE LEARNING TECHNIQUES

Approach	Programming language	Programming model
NIMBLE	Java	MapReduce
System ML	Java and DML	MapReduce
PARMA	Java	MapReduce

IV. OVERVIEW OF THE PROPOSED APPROACH

1) The point of departure is the Association rules set (input) that is first distributed into J partitions (where $1 \leq J \leq k$) which are processed simultaneously by MDP_{REF} algorithm which is in itself distributed among the J partitions (see Fig. 4).

2) $MDP_{REF} - J -$ is an MDP_{REF} algorithm that we execute in the assigned data partition – J^{th} partition – to generate the corresponding, locally most Dominant and Preferential association rules.

3) The Optimizing step uses the sets of locally Most Dominant and Preferential association rules as input and computes profitability, efficiency and risks of each one of the partitions. Then, it outputs the set of the globally optimal Most Dominant and Preferential association rules, i.e., Association Rules that are undominated, most preferable and efficient ones in the whole association rules set (AR-Set).

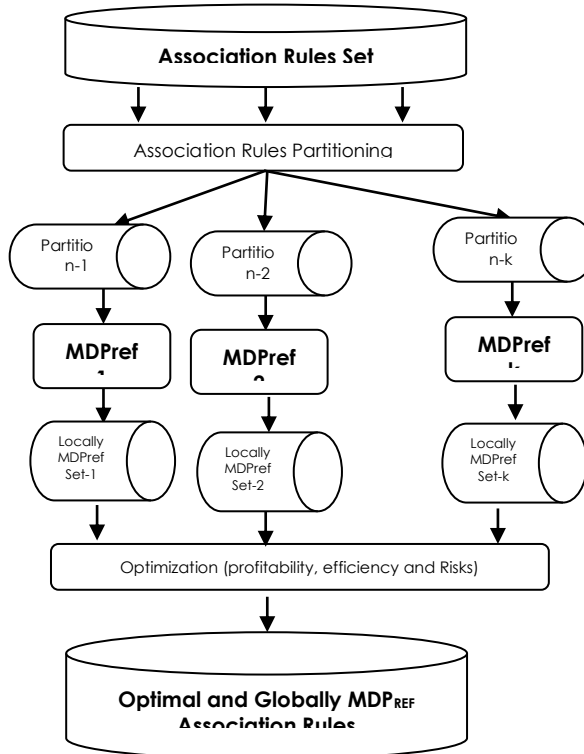


Fig. 4. An overview of the software architecture of our Approach

B. Data partitioning

In the data partitioning step, several techniques intervene to partition the dataset into a number of partitions with respect to particular criteria such as similarity or nearest neighbor criterion. These techniques may involve algorithms using different measures to partition data. It follows that the output (of a technique applied on the input) is a homogenous set, this homogeneity reflects the criterion which this technique uses. Therefore if the output is a group of similar association rules then the criterion used must be that of similarity. If the technique takes into consideration the distance between elements it generates a set of equidistant elements with regard to a determined central point. In our case the input database, a set of Association Rules $AR\text{-Set} = \{AR_1, \dots, AR_n\}$, is partitioned into a user-specified number "k" of partitions. The output is a set of partitions $Part(AR\text{-Set}) = \{Part_1(AR\text{-Set}), \dots, Part_k(AR\text{-Set})\}$.

The proposed framework allows many partitioning techniques for the Association Rules Set, like k-Means, k-Medoids, Décision Tree in addition to other partitioning techniques or meta-algorithms like Bagging and Boosting whose objective is to improve predictions, classification and accuracy.

TABLE II. BAGGING AND BOOSTING FEATURES

	Bagging	Boosting
Partitioning of data into subsets	Random	Giving mis-classified sample higher preference
Goal to achieve	Minimize variance	Increase predictive force
Methods where this is used	Random subspace	Gradient descent

Function to combine single models	(Weighted) average	Weighted majority vote
-----------------------------------	--------------------	------------------------

Let $AR\text{-Set} = \{AR_1, \dots, AR_n\}$ be a set of Association Rules. For $1 \leq j \leq k$, Let $Part_j(AR\text{-Set}) \subseteq AR\text{-Set}$ be a non-empty subset of $AR\text{-Set}$. We define a partitioning of the database over a k partitions by the following:

$Part(AR\text{-Set}) = \{Part_1(AR\text{-Set}), \dots, Part_k(AR\text{-Set})\}$ such that :

- $\bigcup_{i=1}^k \{Part_i(AR\text{-Set})\} = (AR\text{-Set})$
- $\forall_{i \neq j} Part_i(AR\text{-Set}) \cap Part_j(AR\text{-Set}) = \emptyset$

C. Distributive Association Rules mining

The distributive ARM step mines a set of sub-sets of locally Most Dominant and Preferential association rules named MDP_{REF} Association Rules sub-sets. The input of this step is a partition of the $AR\text{-Set}$: $Part(AR\text{-Set}) = \{Part_1(AR\text{-Set}), \dots, Part_k(AR\text{-Set})\}$. The execution of Distributive Association Rules mining step is resumed by running the MDP_{REF} algorithm on each partition $Part_k(AR\text{-Set})$ in parallel.

In the last step, the Optimizing step, we run an algorithm permitting to determine the optimal set formed by the locally MDP_{REF} Association Rules with regard to the minimization of "Risks" and to the maximization of the "profitability - efficiency" of Association Rules.

D. MDP_{REF} Algorithm

MDP_{REF} stands for the **M**ost **D**ominant and **P**referential rules. It is based on dominance, preference and user profile. Besides being threshold-free, MDP_{REF} solves the subjectivity problem and keeps all measures so as no information would be lost. Its main goal is to successfully discover, filter and prune AR into subsets verifying a two-sided criterion. That is to say, each rule in a subset must meet two conditions; it has to be the most dominant as well as the most preferred by the user. To get at the above-mentioned objective, the algorithm takes into account the factor of time during the processing of the following tasks [8]:

- Creates a referential rule (r^T) which dominates all the rules (Having the maximum measurements);
- Computes the degree of similarity of all the rules one by one with the referential rule (r^T);
- Determines the dominant rule r^* (which has a minimal "degree of similarity" with referential rule (r^T));
- Discards all the rules dominated by r^* ;
- If two rules are equivalent, we resort to the user's preferences to determine which one to keep;
- Keep both if the decision maker is indifferent in regard to the equivalent rules, otherwise we keep the one satisfying more preferences;
- Drop all rules where the user's preferences are already covered by those previously handled;

- Keep Rules covering the user's preference other than those already covered by those previously selected [9].

ALGORITHM: "MDPREF" Algorithm

```

1.0 Input : Set of Rules+Set of Measures+Preference Set  $\Omega$  ( $R, M, P_{ref}$ )
2.0 OutPut: The Most Dominant and Preferential Rules  $MDPref$ 
3.0 Begin
4.0  $MDPref \leftarrow \emptyset$ 
5.0  $C \leftarrow R$ 
6.0 while  $C \neq \emptyset$  do
7.0 Create a referential rule  $r^T$  having a max of measure value
8.0  $r^* \leftarrow r \in C$  having a min (DegSim ( $r, r^T$ ))
9.0 For ( $i=1$  to  $k=|C|$ ) do
10.0      $MDPref \leftarrow MDPref U \{r^*\}$ 
11.0      $C \leftarrow C \setminus \{r^*\}$ 
12.0     Foreach  $r_i \in C$  do
13.0         If  $r^* > r_i$ 
14.0             then
15.0                  $C \leftarrow C \setminus \{r_i\}$ 
16.0             else
17.0                 For ( $j=1$  to  $k'$ ) do
18.0                     If  $r_i[m_j] \geq r^*[m_j]$ 
19.0                         then
20.0                              $MDPref \leftarrow MDPref U \{r_i\}$ 
21.0                              $r^* \leftarrow r_i$ 
22.0                     else
23.0                         ( $r_i$  is equivalent of  $r^*$ )
24.0                      $S \leftarrow$  set of equivalent rules
25.0                      $Z \leftarrow \emptyset$ 
26.0             while  $S \neq \emptyset$ 
27.0              $Z_{best}(r_i) = \max \triangleleft S \triangleleft r_i$  the most preferred rule in  $S$ 
28.0              $Z = Z \cup Z_{best}(r_i)$ 
29.0              $P_{ref} \leftarrow \{<t, u> \in P_{ref} / t \triangleleft \neq z_{best} u \text{ the preferences}$ 
30.0                     engendered by  $Z_{best}\}$ 
31.0              $S \leftarrow S \setminus \{Z_{best}(r_i)\}$ 
32.0             end
33.0             end
34.0             end
35.0             end
36.0             end
37.0     end
38.0      $MDPref \leftarrow MDPref U \{Z\}$ 
39.0     end
40.0     Return  $MDPref$ 
41.0 end

```

Concerning the quality of rules, it is assessed by the two measures of dominance and preference which are inherent in the algorithm. The first one is a statistical measure and the second one is subjective – related to users. Rules failing to meet these two measures are not mined.

V. EXPERIMENTS

This section presents an experimental study of the proposed approach on real datasets. First, it describes the datasets that have been used and the details of implementation. Then, it introduces a discussion of the results.

A. Experimental setup

The datasets used in the experimental study are presented in the table III, the proposed approach use six datasets, Diabete, Flare, Iris, Monks, Nursery, and Zoo taken from "UCI Machine Learning Repository". Each dataset deals with a particular

domain such as human health, animals, and agriculture defined by an item count, transaction count and all counts of the association rules.

TABLE III. DESCRIPTIVE OF DATA SETS

DS	Dataset	#Item	# Transaction	#All Rules
DS1	Diabete	75	3196	62132
DS2	Flare	39	1389	57476
DS3	Iris	150	8124	440
DS4	Monks	57	415	181464
DS5	Nursery	32	12960	71302
DS6	Zoo	42	101	25062

Recalling that these experiments have been applied on a machine that has the following characteristics: 1.73 GHz and a memory capacity of 2GB.

The Fig.5 illustrates the effect of the proposed partitioning method on the rate of lost association rules. We can easily see in Fig.5 that the proposed partitioning method allows low values of loss rate especially with low values of tolerance rate.

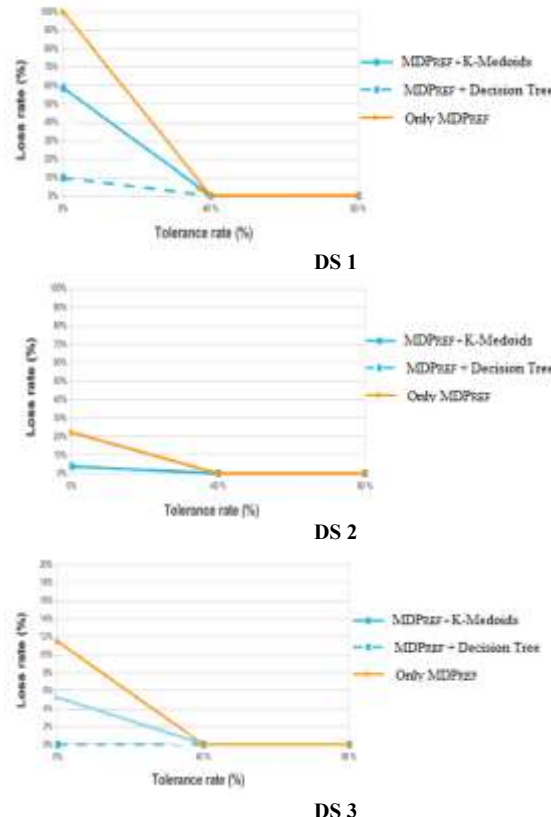


Fig. 5. Effect of partitioning method on the rate of lost Association Rules

In order to study the scalability of the proposed approach and to show the impact of the number of used machines on the large scale Association Rules mining runtime, the Fig.6 present the runtime of the proposed approach for each number of $MDPref(i)$ machines.

As illustrated in Fig.6, the proposed approach scales with the number of machines. In fact, the execution time of the

proposed approach is proportional to the number of machines.

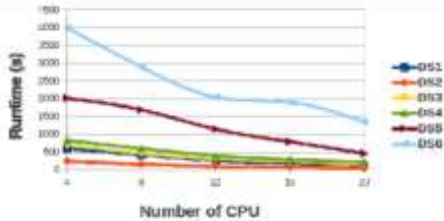


Fig. 6. Effect of the number of workers on the runtime. using K-Medoids as a partitioning method, MDP_{REF} as an association rules extractor

In order to evaluate the influence of some parameters on the performance of the proposed implementation, the block size is varied and computed the runtime of the distributive Association Rules mining process of the proposed approach. In this experiment, six datasets are used and the chunk size is varied from 10MB to 100MB.

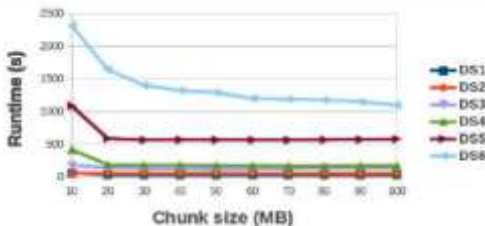


Fig. 7. Effect the varation the chunk size on the runtime. using K-Medoids as a partitioning method, MDP_{REF} as a association rules extractor

The experiment presented in Fig. 7 shows that as long as the data set is large the results are not notably affected no matter how big or small the chunk size values may be. Otherwise, the other values of chunk size do not notably affect the results.

VI. CONCLUSION

In this paper, we addressed the issue of the distributive Association Rules Mining process. We have described the proposed approach for large-scale association rules mining from large-scale association rules sets. The proposed approach relies on clustering / classification methods to build partitions of an association rules set in order to select the locally MDP_{REF} rules for each partition via applying any of the known "clustering / classification" algorithms . Then we apply an optimization algorithm [used in the last step of the distributive ARM process, see section V.B above] to extract a globally optimal MDP_{REF} rules. By running experiments on a variety of datasets, we have shown that the proposed method decreases significantly the runtime. Moreover, it may be functional in the case of large scale databases. This is a significant part of the future work to make sure that the performance and scalability of the proposed approach encompass also big databases.

REFERENCES

- [1] U.M. Fayyad, G. Piatetsky-Shapiro and P. Smyth, 1996. Knowledge Discovery and Data Mining: Towards a Unifying Framework. In KDD 1996, 1996
- [2] M. Goebel and L. Gruenwald "A survey of data mining and knowledge discovery software tools". SIGKDD Explor. Vol.1, Issue 1, pp.20–33, 1999. doi: 10.1145/846170.846172
- [3] M. Mouhir, Y. Balouki, T. Gadi and M. El Far " A new way to select the valuable association rules", in KST 2015: Proceedings of the Knowledge and Smart Technology (KST), 2015 7th International Conference on, 2015 7th KST IEEE, Chonburi, Thailand, pp. 81-86.Junuary 2015. doi: 10.1109/KST.2015.7051464
- [4] O. Y. Al-Jarrah, P. D. Yoo, S. Muhaidat, G. K. Karagiannidis, and K. Taha, "Efficient machine learning for big data: A review. Big Data Research", Vol. 2, No.3,pp.87- 93, 2015.
- [5] A. Ghoting, P. Kambadur, E. Pednault, and R. Kannan. "Nimble: a toolkit for the implementation of parallel data mining and machine learning algorithms on mapreduce". In Proceedings of the 17th ACM SIGKDD international conference on Knowledge discovery and data mining, KDD '11, pp. 334-342, New York, NY, USA, 2011. ACM.
- [6] A. Ghoting, R. Krishnamurthy, E. Pednault, B. Reinwald, V. Sindhwani, S. Tatikonda, Y. Tian, and S. Vaithyanathan, "SystemML: Declarative machine learning on Mapreduce". In Proceedings of the 2011IEEE 27th International Conference on Data Engineering, ICDE '11, pp. 231-242, Washington,DC, USA, 2011. IEEE Computer Society.
- [7] M. Riondato, J. A. DeBrabant, R. Fonseca, and E. Upfal. "Parma: a parallel randomized algorithm for approximate association rules mining in mapreduce" in Proceedings of the 21st ACM international conference on Information and knowledge management, CIKM '12, pp. 85-94, New York, NY, USA, 2012. ACM.
- [8] M. Mouhir, A. Dahbi, Y. Balouki and T. Gadi. "S_{EM}MDP_{REF} : Algorithm to filter and sort rules using a semantically based ontology technique" in ACM-MEDES 2015: Proceedings of the 7th International Conference on Management of computational and collective intElligence in Digital EcoSystems - ACM-MEDES'15, Caraguatatuba, Sao Paulo, Brazil, pp. 29-34, October 2015. doi: 10.1145/2857218.2857223
- [9] M. Mouhir, Y. Balouki and T. Gadi. "Selecting and Filtering Association Rules within a Semantic technique," International Review on Computers and Software (I.RE.CO.S.), Vol. 11, No6, June 2016, pp. 530-538. doi:<http://dx.doi.org/10.15866/irecos.v11i6.9556>
- [10] M. Kamber, and J. Han, Data Mining: Concept and Techniques, 2nd ed., Vol. 6, The Morgan Kaufmann Series in Data Management Systems, Munich, Germany.2006
- [11] S.A. Mahmoodi, K. Mirzaie and S.M. Mahmoudi. "A new algorithm to extract hidden rules of gastric cancer data based on ontology". SpringerPlus, Vol.5, No 312, 2016. doi:[10.1186/s40064-016-1943-9](https://doi.org/10.1186/s40064-016-1943-9).
- [12] M. Boehm D. R. Burdick, A. V. Evfimievski, B. Reinwald, F. R. Reiss, P. Sen and Y. Tian. SystemML's Optimizer: Plan Generation for Large-Scale Machine Learning Programs. IEEE Data Eng. Bull., Vol 37, No 3, 2014.
- [13] P. G. Brown. Overview of SciDB: Large Scale Array Storage, Processing and Analysis. In SIGMOD, 2010
- [14] Z. Cai, Z. Vagena, L. L. Perez, S. Arumugam, P. J. Haas, and C. M. Jermaine. Simulation of Database-Valued Markov Chains Using SimSQL. In SIGMOD, 2013.
- [15] J. Cohen, B. Dolan, M. Dunlap, J. M. Hellerstein, and C. Welton. MAD Skills: New Analysis Practices for Big Data. PVLDB, Vol 2, No 2, 2009.
- [16] A. Ghoting, R. Krishnamurthy, E. Pednault, B. Reinwald, V. Sindhwani, S. Tatikonda and S. Vaithyanathan. SystemML: Declarative Machine Learning on MapReduce. In ICDE, 2011
- [17] J. M. Hellerstein, C. Ré, F. Schoppmann, D. Z. Wang, E. Fratkin, A. Gorajek and A. Kumar. The MADlib Analytics Library or MAD Skills, the SQL. Proceedings of the VLDB, Vol 5, No 12, 2012.
- [18] T. Kraska, A. Talwalkar, J. C. Duchi, R. Griffith, M. J. Franklin, and M. I. Jordan. MLbase: A Distributed Machine-learning System. In CIDR, 2013
- [19] X. Meng, J. Bradley, B. Yuval, E. Sparks, S. Venkataraman, D. Liu and D. Xin. MLLib: Machine Learning in Apache Spark. JMLR, Vol.17, No. 34, pp. 1-7, 2016.
- [20] J. Shin, S. Wu, F. Wang, C. D. Sa, C. Zhang, and C. R é. Incremental Knowledge Base Construction Using DeepDive. PVLDB, Vol 8, No11, 2015.

- [21] E. R. Sparks, A. Talwalkar, D. Haas, M. J. Franklin, M. I. Jordan, and T. Kraska. Automating Model Search for Large Scale Machine Learning. In SOCC, 2015.
- [22] M. Stonebraker, P. Brown, A. Poliakov, and S. Raman. The Architecture of SciDB. In SSDBM, 2011.
- [23] A. K. Sujeeth, H. Lee, K. Brown, T. Rompf, H. Chafi, M. Wu and K. Olukotun. OptiML: An Implicitly Parallel Domain-Specific Language for Machine Learning. In ICML, 2011.
- [24] The Apache Software Foundation. Mahout
- [25] C. Zhang, A. Kumar, and C. Ré. Materialization Optimizations for Feature Selection Workloads. In SIGMOD, 2014.

On the Improved Nonlinear Tracking Differentiator based Nonlinear PID Controller Design

Ibraheem Kasim Ibraheem
Electrical Engineering Department
College of Engineering, Baghdad University
Baghdad, Iraq

Wameedh Riyadh Abdul-Adheem
Electrical Engineering Department
College of Engineering, Baghdad University
Baghdad, Iraq

Abstract—This paper presents a new improved nonlinear tracking differentiator (INTD) with hyperbolic tangent function in the state-space system. The stability and convergence of the INTD are thoroughly investigated and proved. Through the error analysis, the proposed INTD can extract differentiation of any piecewise smooth nonlinear signal to reach a high accuracy. The improved tracking differentiator (INTD) has the required filtering features and can cope with the nonlinearities caused by the noise. Through simulations, the INTD is implemented as a signal's derivative generator for the closed-loop feedback control system with a nonlinear PID controller for the nonlinear Mass-Spring-Damper system and showed that it could achieve the signal tracking and differentiation faster with a minimum mean square error.

Keywords—Nonlinear tracking differentiator; PID; Nonlinear mass-spring-damper; Lyapunov theory; Measurement noise

I. INTRODUCTION

Differentiation of signals in real time is an old and well-known problem. An ideal differentiator would have to differentiate measurement noise with possibly large derivatives along with the signal [1]. In various case studies, the building of a differentiator is inescapable. However, the perfect differentiator could not be synthesized. Without a doubt, together with the principal function, it could differentiate any minor high-frequency noise which is inherent in the signal and may have large derivative values [2].

Designing a differentiator as a single entity is a common design objective for the field of signal processing. The initial procedure is to let some linear dynamical system model to represent the transfer function of the perfect differentiator. Accordingly, the obtained differentiator does not compute the precise derivatives of only noise free signals including the situations when the frequency bandwidth of the signal is limited [2]. Tracking differentiator (TD) design has drawn much consideration in last twenty years because of trailing the high performance of control and navigation system [3].

The traditional high-gain differentiator announced by [4] could follow certain derivatives when the gains lean towards infinity which couldn't feasibly realize. In [2], a sliding mode technique has been used to design differentiator. An upper bound for Lipschitz constant is needed in this kind of differentiator. Nevertheless, the derivative estimation is not soft due to the existence of a discontinuous function. Therefore, a chattering phenomenon occurs in the derivative evaluation. In [5], a universal vigorous precise differentiator

has been developed by integrating a sliding modes differentiation with the high-gain differentiator by means of a switching function. Wang Xinhua [6, 7] has suggested a continuous hybridized nonlinear differentiator in which a smattering phenomenon has been decreased adequately. The differentiators in [8] could regularly approach to the correct solution with finite-time exact convergence and start differentiator error [3]. While linear techniques for tracking differentiators design have been adopted in [9, 10].

In [11], two particular high-gain tracking differentiators were proposed. This differentiator was based on the Taylor expansion, the time lagging phenomenon of the traditional high-gain differentiator is reduced effectively.

Also, a fractional order tracking differentiators have been studied recently. In [12], the tracking differentiator was redesigned with fractional-order to provide a fundament for the design of fractional-order ADRC. An Adaptive controller was developed by Wei [13] using fractional order tracking differentiator. In [14], a discrete analog of a fractional order differentiator over Paley–Wiener space are constructed.

As an improvement, a new meta-heuristic optimization algorithm, called cuckoo search algorithm (CSA) was applied by Kumar [15] to determine the optimal coefficients of the finite impulse response-fractional order differentiator

In practice, to achieve high-performance control, many applications based on tracking differentiators have been proposed, such as, the pitch and depth control problem of autonomous underwater vehicle (AUV) in diving plane [16], detection of harmonic current in single phase active power filters [17], geomagnetic attitude detection systems [18], the position and speed detection system as well as suspension system of maglev train [19], electric vehicles (EVs) [20], etc.

In this work, an improved tracking differentiator is proposed, and its stability is tested based on Lyapunov technique. The peaking phenomenon is presented through time domain analysis, while frequency domain analysis proves that the proposed nonlinear tracking differentiator attenuates signals with a certain frequency band.

The paper is organized as follows: in Section II an improved nonlinear tracking differentiator is proposed, and the main convergence results are presented. Section III explains using the INTD with nonlinear PID controller. The mathematical model of the nonlinear Mass-Spring-Damper is introduced in Section IV. The numerical results are presented

in Section V to verify the effectiveness of the proposed INTD. Finally, the conclusions are provided in section VI.

II. THE IMPROVED NONLINEAR TRACKING DIFFERENTIATOR (INTD)

The enhanced nonlinear tracking differentiator based on the hyperbolic tangent function is proposed as follows:

$$\begin{cases} \dot{z}_1 = z_2 \\ \dot{z}_2 = -R^2 \tanh\left(\frac{\beta z_1 - (1-\alpha)v}{\gamma}\right) - Rz_2 \end{cases} \quad (1)$$

Where z_1 is tracking the input v , and z_2 tracking the derivative of input v . the parameters α, β, γ , and R are appropriate design parameters, where $0 < \alpha < 1, \beta > 0, \gamma > 0$, and $R > 0$.

Lemma 1: (Convergence of the INTD system): the improved tracking differentiator described by (1) with its design parameters is globally asymptotically stable.

Proof: Let us assign $V_l(\mathbf{z}) = R \frac{\gamma}{\beta} \ln \cosh\left(\frac{\beta z_1}{\gamma}\right) + \frac{1}{2} z_2^2$ as a Lyapunov function to system (1). Where $V_l(\mathbf{z}) > 0$ if and only if $\mathbf{z} \neq 0$, and $V_l(\mathbf{z}) = 0$ if and only if $\mathbf{z} = 0$

Now,

$$\dot{V}_l(\mathbf{z}) = -Rz_2^2 \text{ and}$$

$$\dot{V}_l(\mathbf{z}) \leq 0 \text{ for all } z_2$$

This leads to $\dot{V}_l(\mathbf{0}) = 0$ at the origin by Lasalle's theorem[21]. Since $V_l(\mathbf{z}) \rightarrow \infty$ for $\|\mathbf{z}\| \rightarrow \infty$, then the system is globally asymptotically stable (GAS). \square

Lemma 2: (Arrival phase): consider the system (1) if $\frac{\beta z_1 - (1-\alpha)v}{\gamma} \gg 1$; then $\forall t > 0$, the term $\frac{\beta z_1 - (1-\alpha)v}{\gamma}$ will be decreased until it reaches the tracking phase where $\left|\frac{\beta z_1 - (1-\alpha)v}{\gamma}\right| \ll 1$.

Proof: Since $\frac{\beta z_1 - (1-\alpha)v}{\gamma} \gg 1$, Then $\tanh\left(\frac{\beta z_1 - (1-\alpha)v}{\gamma}\right) \rightarrow 1$

So that

$$\begin{cases} \dot{z}_1 = z_2 \\ \dot{z}_2 = -Rz_2 - R^2 \end{cases} \quad (2)$$

The solution of system (2) with the initial condition $\mathbf{z}(0) = [z_1(0) \ z_2(0)]^T$ is given as

$$z_1(t) = -Rt - \left(1 + \frac{z_2(0)}{R}\right) e^{-Rt} + z_1(0) + \frac{z_2(0)}{R} + 1$$

$$z_2(t) = -R + (R + z_2(0))e^{-Rt}$$

If $z_2(0) = 0$, then $z_1(t)$ is a decreasing function for $t > 0$ until it reaches the tracking phase where $\left|\frac{\beta z_1 - (1-\alpha)v}{\gamma}\right| \ll 1$. \square

Corollary 1: for the system given by (1) if $\frac{\beta z_1(t) - (1-\alpha)v(t)}{\gamma} \ll -1$, then $\forall t > 0$, the term

$\frac{\beta z_1(t) - (1-\alpha)v(t)}{\gamma}$ will be increased until the system reaches the tracking phase where $\left|\frac{\beta z_1 - (1-\alpha)v}{\gamma}\right| \ll 1$.

Proof: By the same way of lemma (2), for $\frac{\beta z_1(t) - (1-\alpha)v(t)}{\gamma} \ll 1$, and $z_2(0) = 0$, then $z_1(t)$ increasing for $t > 0$ until it reaches the tracking phase where $\left|\frac{\beta z_1 - (1-\alpha)v}{\gamma}\right| \ll 1$. \square

Lemma 3: (tracking phase): consider system (1) for $\left|\frac{\beta z_1 - (1-\alpha)v}{\gamma}\right| \ll 1$ then both tracking error $e_t(t) = v(t) - \frac{\beta}{1-\alpha} z_1(t)$, and differentiation error $e_d(t) = \dot{v}(t) - \frac{\beta}{1-\alpha} z_2(t)$ tends to zero for finite input signal.

Proof: Since $\frac{\beta z_1 - (1-\alpha)v}{\gamma} \ll 1$, Then $\tanh\left(\frac{\beta z_1 - (1-\alpha)v}{\gamma}\right) \rightarrow \left(\frac{\beta z_1 - (1-\alpha)v}{\gamma}\right)$. So that,

$$\begin{cases} \dot{z}_1 = z_2 \\ \dot{z}_2 = -R^2 \left(\frac{\beta z_1 - (1-\alpha)v}{\gamma}\right) - Rz_2 \end{cases} \quad (3)$$

Taking Laplace transform to (3), then

$$\begin{bmatrix} Z_1(s) \\ Z_2(s) \end{bmatrix} = \begin{bmatrix} \frac{R^2(1-\alpha)}{\gamma} \\ \frac{s^2 + Rs + \frac{R^2\beta}{\gamma}}{\gamma} \\ \frac{R^2(1-\alpha)s}{\gamma} \\ \frac{s^2 + Rs + \frac{R^2\beta}{\gamma}}{\gamma} \end{bmatrix} V(s) \quad (4)$$

The tracking error associated with the tracking phase is

$$e_t(t) = v(t) - \frac{\beta}{1-\alpha} z_1(t)$$

$$E_t(s) = V(s) - \frac{\beta}{1-\alpha} Z_1(s)$$

The transfer function of the tracking error w.r.t input v is given as

$$L_t(s) = \frac{E_t(s)}{V(s)} = \frac{s(s+R)}{s^2 + Rs + \frac{R^2\beta}{\gamma}}$$

So that,

$$l_t(\infty) = \lim_{s \rightarrow 0} s L_t(s) = 0 \quad (5)$$

The differentiation error associated during the tracking phase is described as

$$e_d(t) = \dot{v}(t) - \frac{\beta}{1-\alpha} z_2(t)$$

$$E_d(s) = sV(s) - \frac{\beta}{1-\alpha} Z_2(s)$$

The transfer function of the differentiation error w.r.t the input derivative is

$$L_d(s) = \frac{E_d(s)}{sV(s)} = \frac{s(s+R)}{s^2 + Rs + \frac{R^2\beta}{\gamma}}$$

So that,

$$l_d(\infty) = \lim_{s \rightarrow 0} sL_d(s) = 0 \quad (6)$$

Therefore (5) and (6) complete the proof. \square

Theorem 1: Consider system (1), then for any value of $\left| \frac{\beta z_1 - (1-\alpha)v}{\gamma} \right|$,

$$\lim_{t \rightarrow \infty} \left| \frac{\beta z_1(t) - (1-\alpha)v(t)}{\gamma} \right| = 0$$

and

$$\lim_{t \rightarrow \infty} \left| \frac{\beta z_2(t) - (1-\alpha)\dot{v}(t)}{\gamma} \right| = 0$$

Proof:

By using Lemma (2) and (3). \square

Lemma 4: (Time domain analysis): Consider the system (1) which satisfies (4). If $\beta \gg 1, 0 < \gamma < 1, R \gg 1$, with $0 < \alpha < 1$, then the system (1) has a high undamped natural frequency, a small damping ratio, and peaking phenomenon.

Proof:

$$\frac{Z_2(s)}{sV(s)} = \frac{\frac{R^2(1-\alpha)}{\gamma}}{s^2 + Rs + \frac{R^2\beta}{\gamma}} = \left(\frac{1-\alpha}{\beta} \right) \frac{\omega_n^2}{s^2 + 2\xi\omega_n s + \omega_n^2}$$

Where,

$\omega_n = R \sqrt{\frac{\beta}{\gamma}}$ is the undamped natural frequency (rad/sec)

$\xi = \frac{1}{2} \sqrt{\frac{\gamma}{\beta}}$ is the damping ratio

It's clear that from the values of the parameters β, γ , and R that the damping ratio $\xi \ll 1$ implies that the system has an under damped effect which leads to peaking phenomenon. \square

Lemma 5: (The frequency-domain analysis): Consider a system (1) which satisfies equation (4) with parameters β, γ , and R defined in Lemma 4. The system represents a band-limited differentiator with bandwidth ω_n .

Proof: for

$$\begin{aligned} \frac{Z_2(j\omega)}{V(j\omega)} &= \left(\frac{1-\alpha}{\beta} \right) \frac{\omega_n^2 j\omega}{(j\omega)^2 + 2\xi\omega_n j\omega + \omega_n^2} \\ &= \left(\frac{1-\alpha}{\beta} \right) \frac{j\omega}{\left(\frac{j\omega}{\omega_n} \right)^2 + 2\xi \frac{j\omega}{\omega_n} + 1} \end{aligned}$$

if the magnitude of the transfer function $\frac{Z_2(j\omega)}{V(j\omega)}$ is taken as

$$\begin{aligned} 20 \log \left| \frac{Z_2(j\omega)}{V(j\omega)} \right| &= 20 \log \left(\frac{1-\alpha}{\beta} \right) \\ &\quad + 20 \log \omega \\ &\quad - 20 \log \sqrt{\left(1 - \left(\frac{\omega}{\omega_n} \right)^2 \right)^2 + \left(2\xi \frac{\omega}{\omega_n} \right)^2} \end{aligned}$$

For $\omega \ll \omega_n$ this implies

$$20 \log \left| \frac{Z_2(j\omega)}{V(j\omega)} \right| = 20 \log \left(\frac{1-\alpha}{\beta} \right) + 20 \log \omega$$

Such that $20 \log \left(\frac{1-\alpha}{\beta} \right)$ is the correction gain and $20 \log \omega$ is the differentiator effect.

On the other hand if $\omega \gg \omega_n$, then

$$20 \log \left| \frac{Z_2(j\omega)}{V(j\omega)} \right| = 20 \log \left(\frac{1-\alpha}{\beta} \right) + 20 \log \omega - 40 \log \frac{\omega}{\omega_n}$$

The third term represents the attenuation effect. Therefore, the system has the attenuation effect for $\omega \gg \omega_n$. \square

III. TRACKING DIFFERENTIATOR BASED NONLINEAR PID CONTROLLER

Using nonlinear tracking differentiator, a standard PID controller is transformed into nonlinear PID (NLPID) [22] as shown in Fig. 1. The first tracking differentiator (TD(I)) is used as transient process profile generator, while the second tracking differentiator (TD(II)) is used as state observer to get tracking output z_1 and its differential z_2 . The error, integral, and differential signals are produced by comparing transient process profile to the output of TD(II).

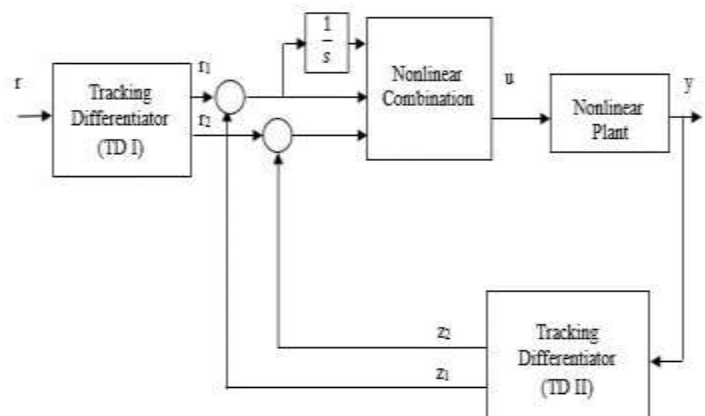


Fig. 1. The traditional structure of NLPID controller

Jing Han has made some investigations on traditional structures and essential properties of nonlinear tracking differentiator. A kind of second-order nonlinear tracking differentiator based on second order bang-bang switch system has been proposed [22]:

$$\dot{x}_1 = x_2$$

$$\dot{x}_1 = -R \operatorname{sign} \left(x_1 - v(t) + \frac{x_2 |x_2|}{2R} \right)$$

where x_1 is the desired trajectory and x_2 is its derivative. Note that, the parameter R is an application dependent and it is set accordingly to speed up or slow down the transient profile. Then, x_2 is denoted as the "tracking differentiator" of $v(t)$.

In order to avoid chattering near the origin, changing the **sign** function to linear saturation function **sat**, then the modified Han TD is represented by:

$$\dot{x}_1 = x_2$$

$$\dot{x}_1 = -R \operatorname{sat}(x_1 - v(t) + \frac{x_2 |x_2|}{2R}, \delta)$$

Where

$$\operatorname{sat}(A, \delta) = \begin{cases} \operatorname{sign}(A), & |A| > \delta \\ \frac{A}{\delta}, & |A| \leq \delta \end{cases}$$

The NLPID takes “nonlinear combination” on the three signals. Han [23] proposed the following nonlinear function:

$$fal(e, \alpha, \delta) = \begin{cases} \frac{e}{\delta^{1-\alpha}} & |e| \leq \delta \\ |e|^\alpha \operatorname{sign}(e) & |e| \geq \delta \end{cases}$$

The control rule takes:

$$u = \beta_1 fal(e, \alpha_1, \delta_1) + \beta_2 fal(\dot{e}, \alpha_2, \delta_2) + \beta_3 fal\left(\int e, \alpha_3, \delta_3\right)$$

Where α_1, α_2 and $\alpha_3 \in [0.5, 1]$

IV. MATHEMATICAL MODELING OF THE NONLINEAR MASS-SPRING-DUMPER (NMSD) PLANT

A simple nonlinear mass-spring-damper mechanical system as shown in Fig. 2. It is assumed that the stiffness coefficient of the spring, the damping coefficient of the damper and the input term have nonlinearity or uncertainty [23]:

$$M\ddot{x} + g(x, \dot{x}) + f(x) = \varphi(\dot{x})u \quad (7)$$

where M is the mass and U is the force, $f(x)$ is the nonlinear or uncertain term with respect to the spring, $g(x, \dot{x})$ is the nonlinear or uncertain term with respect to the damper, and $\varphi(\dot{x})$ is the nonlinear term with respect to the input term.

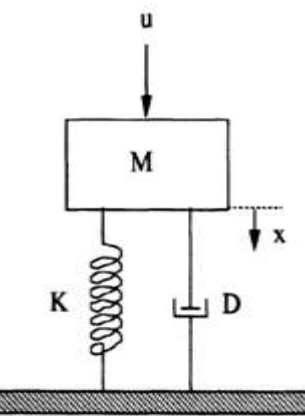


Fig. 2. The nonlinear mass spring damper model

Assume that $g(x, \dot{x}) = D(c_1 x + c_2 \dot{x}^3)$, $f(x) = c_3 x + c_4 x^3$, and $\varphi(\dot{x}) = 1 + c_5 \dot{x}^3$, assume that $x \in [-a, a]$, $\dot{x} \in [-b, b]$, $a, b > 0$. The above parameters are set as follows:

$M = 1.0$, $D = 1.0$, $c_1 = 0.01$, $c_2 = 0.1$, $c_3 = 0.01$, $c_4 = 0.67$, $c_5 = 0$, $a = 1.5$, $b = 1.5$. Then (6) can be written as:

Then, (7) can be rewritten as follows:

$$\ddot{x} = -0.1\dot{x}^3 - 0.02x - 0.67x^3 + u \quad (8)$$

The state space representation of the nonlinear mass-spring-damper model is:

$$\left. \begin{array}{l} \dot{x}_1 = x_2 \\ \dot{x}_2 = -0.1x_2^3 - 0.02x_1 - 0.67x_1^3 + u \\ y = x_1 \end{array} \right\} \quad (9)$$

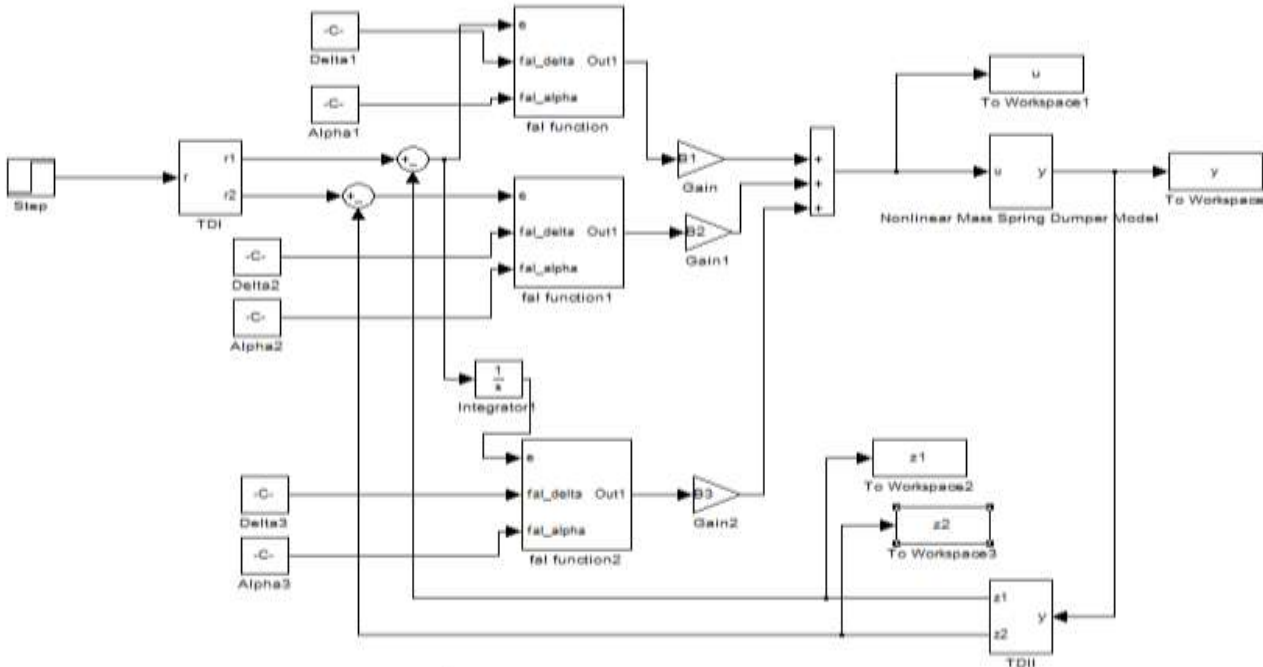


Fig. 3. The Simulink® model for the NPID and the NMSD plant

V. NUMERICAL SIMULATIONS

The NPID controller based on either the modified Han TD or the proposed INTD and the NMSD mathematical models are designed and numerically simulated using Matlab®/Simulink® as shown in Fig. 3. The values of the parameters for these subsystems are listed in Tables I-III.

TABLE I. THE PARAMETERS OF THE CONTROL LAW

Parameter	Value
δ_1	0.1038
α_1	0.7128
β_1	1.9151
δ_2	0.0354
α_2	0.8680
β_2	2.0130
δ_3	1.1916
α_3	0.9888
β_3	0.0800

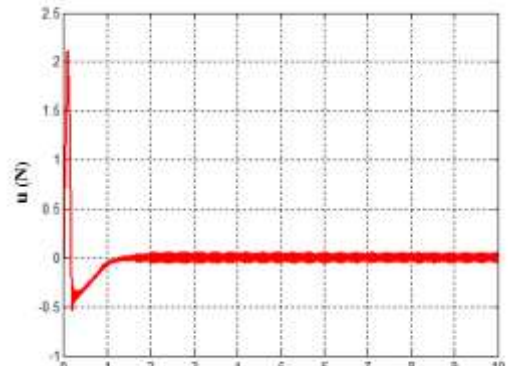
TABLE II. THE PARAMETERS OF THE MODIFIED HAN TD

Parameter	Value
R	11.6000
δ	0.0005

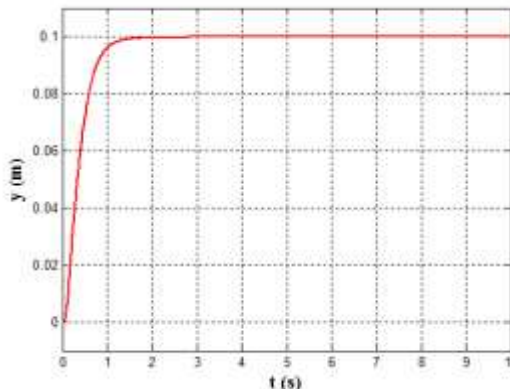
TABLE III. THE PARAMETERS OF THE INTD

Parameter	Value
α	0.9790
β	5.5872
γ	8.3864
R	26.5005

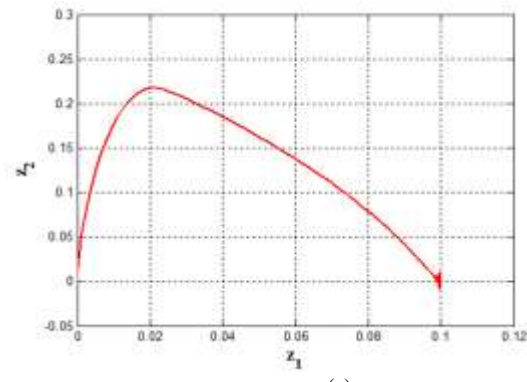
The numerical simulations are done by using Matlab® ODE45 solver for the models with continuous states. This Runge-Kutta ODE45 solver is a fifth-order method that performs a fourth-order estimate of the error. The reference input to the system is constant linear displacement equals to 0.1 m applied at $t = 0$ sec. The NPID controller is tested for two cases. The numerical simulation of the first testing case is done without adding a measurement noise at the output of the NMSD plant, and the results of this case are shown in Fig.4 and Fig. 5. Also, the numerical results are listed in Table IV.



(a)

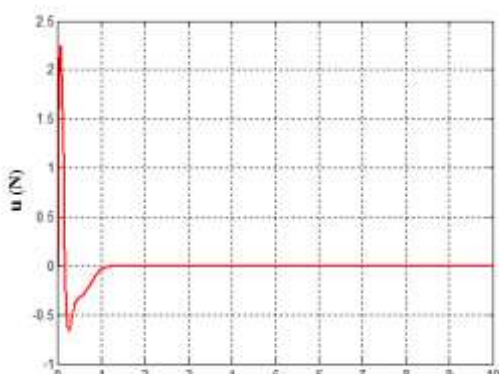


(b)

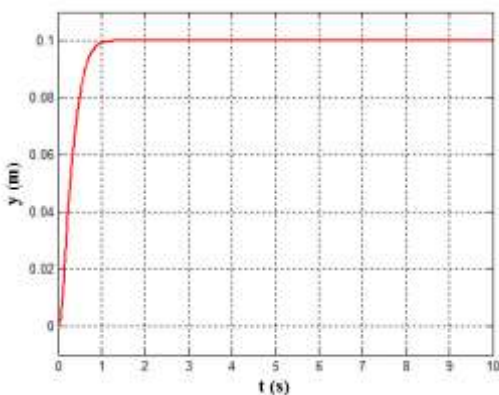


(c)

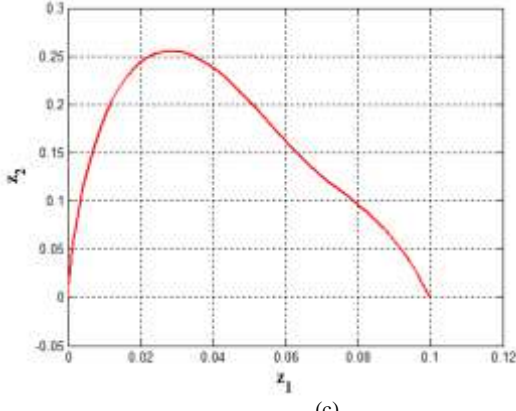
Fig. 4. The simulation results of the NPID based on modified Han TD, (a) The control signal u , (b) The plant output y , and (c) The TD(II) state Trajectory (z_1, z_2)



(a)



(b)



(c)

Fig. 5. The simulation results of the NPID based on proposed INTD, (a) The control signal u (b) The plant output y (c) The TD(II) state Trajectory (z_1, z_2)

TABLE IV. THE NUMERICAL SIMULATION RESULTS OF CASE 1

Performance Index	Modified Han TD	Proposed INTD
IAE	0.062009	0.037965
ITAE	0.017028	0.007961
ITSE	0.000623	0.000325
ISU	0.532537	0.559512
IAU	0.851211	0.540125

Where,

$\text{ITAE} = \int_0^{10} t \times |r - y| dt$ is the integration of the time absolute error for the output signal

$\text{ITSE} = \int_0^{10} t \times (r - y)^2 dt$ is the integration of the time squared error for the output signal

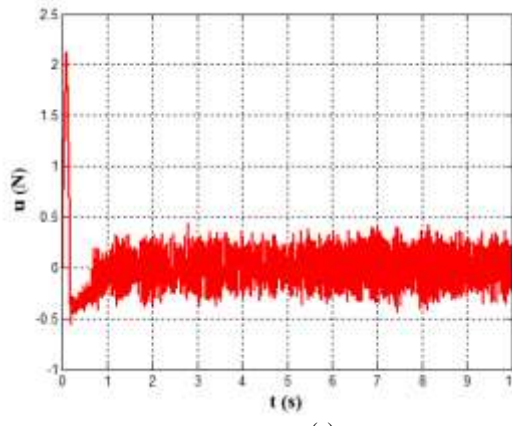
$\text{IAE} = \int_0^{10} |r - y| dt$ is the integration of the absolute error for the output signal

$\text{IAU} = \int_0^{10} |u| dt$ is the integration of absolute of the NPID control signal

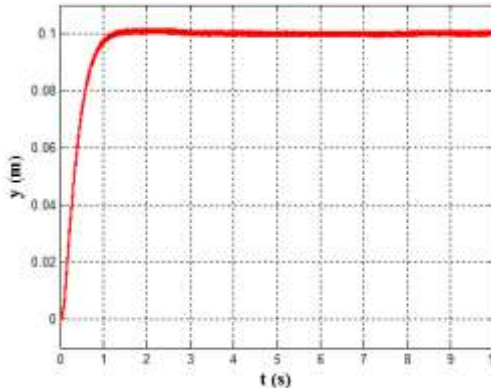
$\text{ISU} = \int_0^{10} u^2 dt$ is the integration of square of the NPID control signal

Figure 4 (a) shows the chattering in the control signal due to the nonlinear signal of the Han TD [12]. By using the proposed INTD, the chattering in the control signal is significantly reduced (figure 5(a)). The IAU performance index reflects this improvement. The peaking phenomenon previously explained in Lemma (4) appears in the ISU performance index and has the benefit of speeding up the time response of plant output.

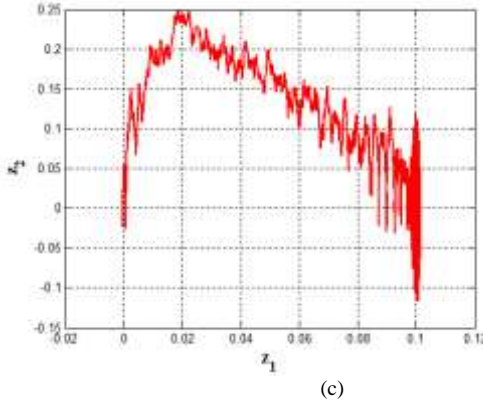
The second testing case demonstrated in this work considers adding a measurement noise at the output of the plant. The measurement noise modeled as uniform in the range [-0.001, 0.001] at sampling time 0.001 s. The result of this case shown in Fig. 6, Fig. 7, and Table V.



(a)

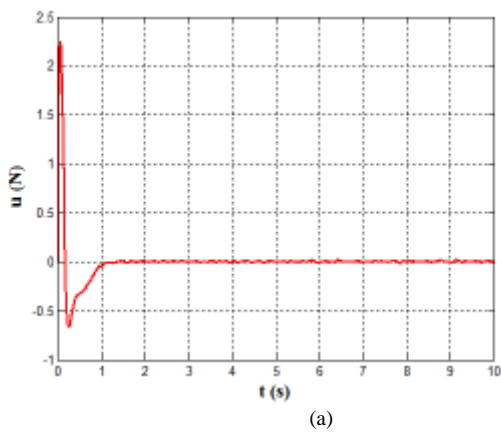


(b)

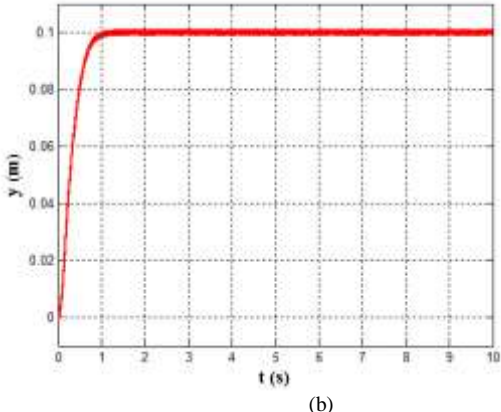


(c)

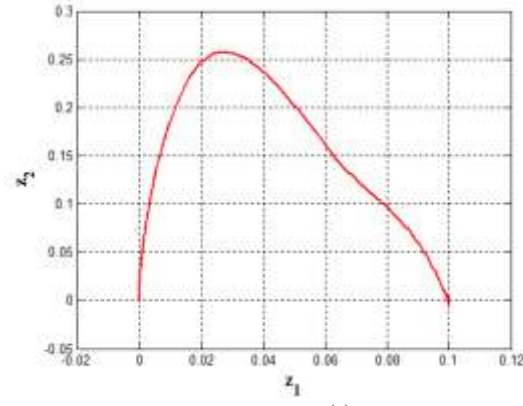
Fig. 6. The simulation results of the NPID based on modified Han TD with measurements noise, (a) The control signal u (b) The plant output y (c) The TD(II) state Trajectory (z_1, z_2)



(a)



(b)



(c)

Fig. 7. The simulation results of the NPID based on proposed INTD with measurement noise, (a)The control signal u (b) The plant output y (c) The TD(II) state Trajectory (z_1, z_2)

TABLE V. THE NUMERICAL SIMULATION RESULTS OF CASE 2

Performance Index	Modified Han TD	INTD
IAE	0.489928	0.384329
ITAE	0.512582	0.327142
ITSE	0.005007	0.003458
ISU	8.449415	5.536271
IAU	26.187044	5.561920

The band-limiting effect is very clear for the INTD as shown in Fig. 7-(a) with very little fluctuations in the steady state. While the control signal u for the case of the TD of [13] is highly affected by the measurement noise (Fig. 6-(a)). Same results are reflected on the output signal y and state-trajectories. Also, the simulations prove that the proposed INTD outperforms the TD offered by [13] with five performance measures as indicated by Table V.

VI. CONCLUSION

In this article, an improved type of nonlinear tracking differentiator is developed to obtain higher derivatives of reference signal to achieve tracking with high robustness against measurement noise. The proposed tracking differentiator is proven to be globally asymptotically stable. It converges to the exact derivatives of the signal independent of the initial differentiation error. The INTD has an under damped effect which lead directly to peaking phenomenon. Knowing

that the INTD is a continuous structure which comprises of rectilinear and non-linear parts, the noise and chattering phenomenon has been reduced adequately, the reason is due of the high fidelity that the INTD has when generating the derivatives of the signal. Also dynamical performance are enhanced apparently. The Simulation experiments show the feasibility of integrating the proposed INTD with the nonlinear combinations of the error profile to design a nonlinear PID controller for MSD system which can be considered as an alternative and efficient control method to solve real control design for such nonlinear systems. The new configuration with the proposed INTD achieves fast arrival and smooth tracking to the input signal. Finally, the performance of the nonlinear MSD system has been enhanced dramatically.

As a future work, the value of R in this work may be varied and based on certain adaptive law, the optimal value for R may be chosen which makes the TD producing better results.

ACKNOWLEDGMENT

The authors appreciate the electrical engineering department laboratories for direct help and support to finish this research.

REFERENCES

- [1] Vasiljevic L. K. and Khalil H. K., "Differentiation with High-Gain Observers the Presence of Measurement Noise," Proceedings of the 45th IEEE Conf. on Decision & Control, CA, USA, pp. 4717-4722, 2006.
- [2] Levant A., "Robust exact differentiation via sliding mode technique," Automatica, 34(3), pp. 379-384, 1998.
- [3] Hongwei W. and Heping W., "A Comparison Study of Advanced Tracking Differentiator Design Techniques," Procedia Engineering 99, pp. 1005 – 1013, 2015.
- [4] Dabroom A. M. and Khalil H.. K., "Discrete-time implementation of high-gain observers for numerical differentiation," INT. J. of CONT., Vol. 72, No. 17, pp.1523- 1537, 1999.
- [5] Nunes E. V. L., Hsu L., and Lizarralde F., " Global Exact Tracking for Uncertain Systems using Output-Feedback Sliding Mode Control," IEEE Transactions on automatic control, Vol. 54, No. 4, 2009.
- [6] X. Wang H. Lin. "Design and analysis of a continuous hybrid differentiator," IET Control Theory Applications, Vol. 5, Iss. 11, pp. 1321–1334, 2011.
- [7] Wangn X., S. Bijan., "The rapid-convergent nonlinear differentiator," Mechanical Systems and Signal Processing 28, pp. 414–431, 2012.
- [8] Angulo M. T., Moreno J. A., Fridman L. "Robust exact uniformly convergent arbitrary order differentiator," Automatica 49, pp. 2489–2495, 2013.
- [9] Guo B. Z., Han J. Q. and Xi B. F., " Linear tracking-differentiator and application to online estimation of the frequency of a sinusoidal signal with random noise perturbation," International Journal of Systems Science, Vol. 33, No. 5, pp. 351-358, 2002.
- [10] Salim Ibrir, "Linear time-derivative trackers," Automatica, 40, 397 – 405, 2004.
- [11] Hongyinping F., Shengjia L., "A tracking differentiator based on Taylor expansion," Applied Mathematics Letters 26 , pp.735- 740, 2013.
- [12] Junxiu W., Zhe G., "Design and analysis on fractional-order tracking differentiator , " 27th Chinese Control and Decision Conference (CCDC), pp. 6128- 6132,2015.
- [13] Yiheng W., Yangsheng H., Lan S. and Yong W., "Tracking Differentiator Based Fractional Order Model Reference Adaptive Control: The $1 < \alpha < 2$ Case," 53rd IEEE Conference on Decision and Control December, Los Angeles, California, USA , pp. 6902-6907, 2014.
- [14] Yan W., "Discretization of fractional order differentiator over Paley-Wiener space," Applied Mathematics and Computation , pp.162–168, 2014.
- [15] Manjeet K., Tarun K. R., "Optimal design of FIR fractional order differentiator using cuckoo search Algorithm," Expert Systems with Applications,Vol. 42, No. 7, pp. 3433–3449,2015.
- [16] Jiang Z., Liu T. Xu H., and Wang F., "Diving Control of Autonomous Underwater Vehicle Based on Cascade Control and Tracking Differentiator,"OCEANS- Shanghai, 2016.
- [17] Guoxian S. , Xiju Z. , Xingong C., "An improved detecting approach of harmonic current in single-phase active power filter based on tracking differentiator," International Conference on Intelligent Control and Information Processing (ICICIP), 2015 .
- [18] HUANG Y., WANG H., "Application of tracking-differentiator in angular measurements on spinning projectiles using magnetic sensors,"International Conference on Intelligent Human-Machine Systems and Cybernetics,2015.
- [19] DOU F., WANG Z., HE H., LONG Z., " On Realization of Signal Processing Based on Tracking-Differentiator for Maglev Train," Proceedings of the 34th Chinese Control Conference July 28-30, 2015.
- [20] Duo Z., Guohai L., Yan J., and Guihua S., "Sliding Mode Control with Linear Tracking Differentiator for Multi-Wheel Independently Driven Electric Vehicles , " International Conference on Electrical Machines and Systems, 2013.
- [21] Khalil H., Nonlinear Control," Pearson, 1st ed., 2015.
- [22] HAN J Q. "Nonlinear PID controller" . Autom., Vol. 20, No. 4, pp. 487–490, 1994. (in Chinese).
- [23] Z. Xiu, W. Wang, "A Novel Nonlinear PID Controller Designed By Takagi-Sugeno Fuzzy Model," Proceedings of the 6th World Congress on Intelligent Control and Automation, Dalian, China, June 21 - 23, 2006.

Automated Imaging System for Pigmented Skin Lesion Diagnosis

Mariam Ahmed Sheha/ Amr Sharwy

Biomedical and system Engineering
Cairo University
Giza, Egypt

Mai S. Mabrouk*

Biomedical Engineering Dept.
MUST University
Giza, Egypt

Abstract—Through the study of pigmented skin lesions risk factors, the appearance of malignant melanoma turns the anomalous occurrence of these lesions to annoying sign. The difficulty of differentiation between malignant melanoma and melanocytic naeve is the error-prone problem that usually faces the physicians in diagnosis. To think through the hard mission of pigmented skin lesions diagnosis different clinical diagnosis algorithms were proposed such as pattern analysis, ABCD rule of dermoscopy, Menzies method, and 7-points checklist. Computerized monitoring of these algorithms improves the diagnosis of melanoma compared to simple naked-eye of physician during examination. Toward the serious step of melanoma early detection, aiming to reduce melanoma mortality rate, several computerized studies and procedures were proposed. Through this research different approaches with a huge number of features were discussed to point out the best approach or methodology could be followed to accurately diagnose the pigmented skin lesion. This paper proposes automated system for diagnosis of melanoma to provide quantitative and objective evaluation of skin lesion as opposed to visual assessment, which is subjective in nature. Two different data sets were utilized to reduce the effect of qualitative interpretation problem upon accurate diagnosis. Set of clinical images that are acquired from a standard camera while the other set is acquired from a special dermoscopic camera and so named dermoscopic images. System contribution appears in new, complete and different approaches presented for the aim of pigmented skin lesion diagnosis. These approaches result from using large conclusive set of features fed to different classifiers. The three main types of different features extracted from the region of interest are geometric, chromatic, and texture features. Three statistical methods were proposed to select the most significant features that will cause a valuable effect in diagnosis; Fisher score method, t-test, and F-test. The selected features of high-ranking score based on the statistical methods are used for the diagnosis of the two lesion groups using Artificial Neural Network (ANN), K-Nearest Neighbor (KNN) and Support Vector Machine (SVM) as three different classifiers proposed. The overall System performance was then measured in regards to Specificity, Sensitivity and Accuracy. According to the different approaches that will be mentioned later the best result was shown by the ANN designed with the feature selected according to fisher score method enables a diagnostic accuracy of 96.25% and 97% for dermoscopic and clinical images respectively.

Keywords—component; Pigmented Skin lesions; Color Space; Bounding box; local range; SVM; local range; KNN; ANN; Experimental models

I. INTRODUCTION AND LITERATURE REVIEW

Patients seeking for dermatologic consultation are steadily increasing worldwide. The most critical type of skin diseases is melanoma, which represents the malignant type of skin cancer. Malignant melanoma usually has slow growth rate the time if the lesion detected in this early stage, it can be easily removed with a relatively low cost and hazard. Thus, the survival rate increased to 95% if detected early. While, progression of the disease in the late stage is associated with poor survival rate of 13% [1].

For that reason, melanoma detection weighted as a challenging problem for dermatologist. Several techniques and procedure were proposed for the purpose of melanoma diagnosis; such as dermoscopy or Epiluminescence (ELM) [2], which was entertained with high expectations inspecting skin lesions. ELM was super promising as it is an in-vivo, noninvasive technique used for structures visualization enhancement under the skin surface by means of oil immersion and magnifying instrument, called a “dermatoscope”[3]. However, dermoscopic images results a magnified view for skin lesions its interpretation and diagnosis accuracy mainly depends on the experience of the viewer. Several diagnosis models with similar reliability have become more widely accepted by physicians [4,5] as, 7-point check, Menzie rule and the most popular scoring system so called ABCD rule.

Determination and extraction of features that mention lesion characteristics are usually the error-prone operation through all automated diagnosis systems. Thus, introducing these automated diagnosis systems, as a non-invasive diagnosis support tool is endless interesting work. A considerable number of resaeches and publications focused on the area of image analysis and pattern classification related to melanoma images identification and classifications. Over the last 20 years, the computer aided diagnosis systems for melanoma diagnosis developed [6] to have diagnosis accuracy around 73% to 98%.

July 2002, P. Rubegni et al. [7] developed an automated diagnosis system for melanoma with a set of 50 objective features regarding the main three categories of features that could accurately describe the malignancy of lesions; geometries, textures and islands of color. Thirteen significant features were selected, that discriminate the 2 groups of

lesions reaching 94% accuracy using an ANN for classification. By 2006, Iris Cheng designed an algorithm using relative color features; the algorithm was tested upon 80 nevus, 160 melanoma and 42 dysplastic nevi, as a database. Result showed [8] the algorithm ability to classify 86% of the malignant melanomas successfully in comparison with approximately 75% success rate of dermatologists.

By the beginning of 2009, José Fernández Alcón, et al proposed efficient automated system [9] for diagnosis of PSL. The system supports conventional clinical images for skin lesions acquired using digital cameras (Consumer level), in addition to a decision support component. The use of decision support component system was significant; it combine the image classification outcome with context knowledge such as skin type, age, gender, and affected body part. Lesions were classified with a sensitivity of 94%, specificity of 68% and accuracy 86%.

Mariam A.Sheha, et al. works toward improving contributions about the essential characteristics of PSL. By March 2010, they proposed [10] a Computer aided diagnosis system (CAD) that mainly concerned by analyzing only dermoscopic images based on gray level Co-occurrence matrix (GLCM) classified by Multilayer perceptron (MLP) to discriminate between melanocytic nevi and malignant melanoma. Moreover it was interesting to study the effect of this system using clinical images and compare results with dermoscopic images that was clearly represented on 2013 [11]. Other different features and classifiers were widely used in all fields of automated analysis and diagnosis that was valuable to introduce and study its effect. On Dec 2014, the effect of morphological features (Geometric and Chromatic) was handled using two different classifiers ANN and SVM [12].

To cope with the development track, this paper presented as a completion for the prior studies. Whereas, its main aim is to design a fully automated computer aided diagnosis system for PSL to increase system flexibility and efficiency. It concerns about different types and a huge number of features to evaluate the efficiency of each upon melanoma diagnosis. Feature extraction is usually based on two different concepts, namely morphological (geometric, chromatic) and texture analysis. Significant features that can accurately describe melanoma were then selected by three different methods of feature selection f-test, t-test and fisher score ranking. Afterwards; the study introduced three classifiers to discriminate between malignant melanoma and benign nevi regarding the selected parameters.

The following sections will mention the system performed for the digital image analysis; system designed using different analytical parameters and classification methods performing different approaches. This paper will be organized as shown; First section presented a brief introduction about the topic and related works. Then, material section will deal with the database and the software tool used in this study. By third section, the work methodology will be discussed in details including main block diagram and different algorithms applied to propose a proper and efficient diagnosis approach for PSL

diagnosis. The results of the constructed approaches were compared to investigate the more suitable approach for melanoma diagnosis through the experimental setup in the fourth section. Finally; Conclusion and expected future work conclusion submitted.

II. MATERIAL

A. Database

Toward productive screening process various non-invasive, in-vivo imaging technique proposed. The imaging modalities used nowadays could also facilities skin lesion structure visualization such as, Positron Emission Tomography (PET), Dermoscopy, Confocal laser scanning microscopy (CLSM), High frequency ultrasound, Optical coherence tomography (OCT) and Magnetic Resonance Imaging (MRI) [13]. The study proposed was applied upon a long time used data as a set of traditional photography, named by clinical images and another set of dermoscopic images [14, 15].

The main aim through this research is to define the effective characteristics for designing a high performance consumer application CAD system with high prediction accuracy. So that, it was recommended to apply the same algorithm on both types of data sets mentioned to caliper the effect of different imaging techniques upon diagnosis.

Database presented through this study consist of 320 images for different pigmented skin lesions. Data were randomly sampled from the skin diseases atlases and doctors' clinics [16,17]. Images were fairly divided to the two basic database types; 160 lesions for each dermoscopic and clinical. To compare between malignant and benign lesion each of the used databases were fairly divided also to 80 lesion of each group. Majority of the dermoscopic images were randomly sampled from [18] as the author of [19] recommended, clinical images used for that purpose are widely available in [20-24].

B. Implementation

For successful diagnosis and high performance automated system a good visualization is essential. Leveraging the rich graphics functionality of MATLAB, system was implemented and tested on the WINDOWS platform with MATLAB version of 2010.

III. METHODOLOGY

The main scope of this paper is to apply different and new features on a computer-based system forming different experimental approaches. For that purpose it is valuable to detect the region of interest so the PSL can be accurately evaluated. Once the lesion boundary had been identified, the program attempts to extract different features to manipulate their importance in that field. The selected features are classified to assess the accuracy degree and evaluate the performance of that approach. The features used with the most accurate approach will be highly recommended as a scientific characteristic to recognize dermoscopic. Fig. 1, outlines the procedure followed by the different approaches used to diagnose clinical and dermoscopic images for PSL.

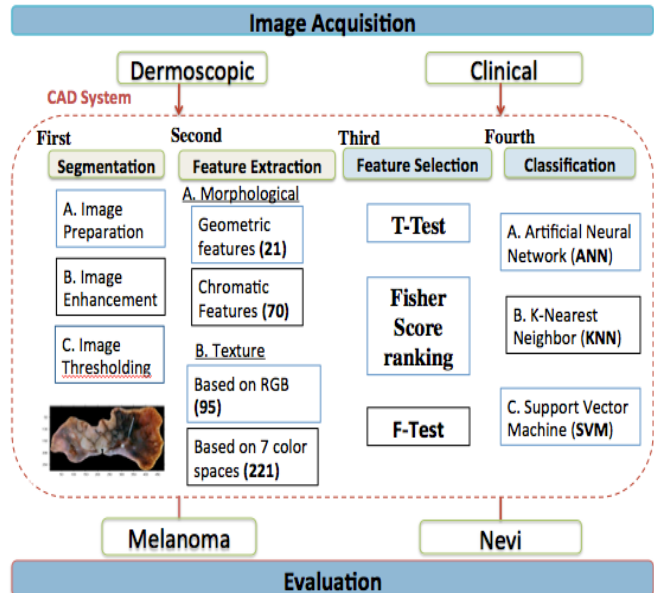


Fig. 1. The Main block diagram

A. Image Segmentation

Skin lesion images, especially clinical and dermoscopic images are often not clear and altered by uneven illumination. Typical skin artifact as hair, skin structures, oil bubbles [25] are usually considered as the main cause for such illumination, which have a direct effect on both segmentation and feature extraction algorithms. Image segmentation is an essential preprocessing step that copes with skin lesions irregularities and artifacts. Sequentially, it is necessary for efficient feature extraction and accurate classification. Thus, image preparation, enhancement and thresholding are considered as the main processing steps for segmentation.

a) Image Preparation: This step deals with scaling all images to one scale (470*640) pixels to avoid the wide size variation in the selected database.

b) Images Enhancement: Segmentation can be distracted by the presence of skin artifacts. Two successive steps are necessary to increase the tumor border visibility and ensure its correct identification. First is image filtration using median filter [26]; considered as a correction tool for reducing noise that corrupt image's clarity. Although this procedure ends in relatively blurring of the image as shown in Fig. 2, it assists the segmentation procedure. Second step is gray level conversion; the RGB colored image is converted into intensity or gray scale image [27], To reduce the effect of different skin color variations and background.

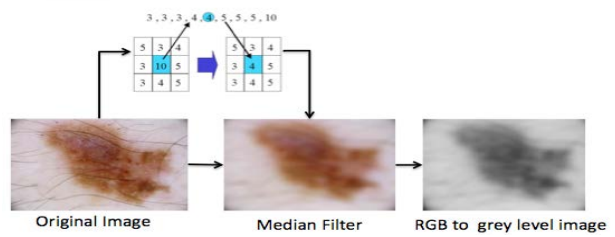


Fig. 2. Image Enhancement process

c) Images Thresholding: The common purpose of segmentation is to group the homogeneous pixels into regions with respect to specific features and semantic content. Segmentation step through this research aims to extract the lesion border from the healthy skin [28]. For accurate segmentation process and correct detection for lesion boundary, image thresholding step should follow contrast adjustment. Through contrast or intensity adjustment, image is adjusted by saturating 1% of the pixels at low and high intensities of the output image. Fig. 3 shows the effect of adjustment process upon the filtered intensity image.

Afterwards; image thresholding process successively occurred. It mainly depends on Otsu's method [29], where it labels each pixel of the entire image as belonging to the lesion or to the background. Thresholding idea can be easily mentioned by separating the pixels whose intensity value is below specific threshold from others that exceeds the same threshold. Then, label each of the two groups according to their definition. Through this research, pixels with low intensity value are considered as the region of interest. Fig. 4 shows the conversion happened as a result of Otsu's threshold.

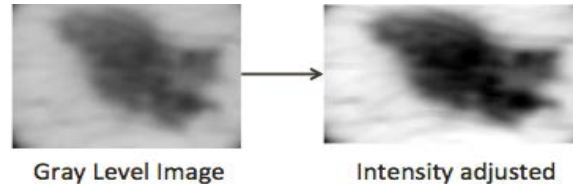


Fig. 3. Image contrast adjustment

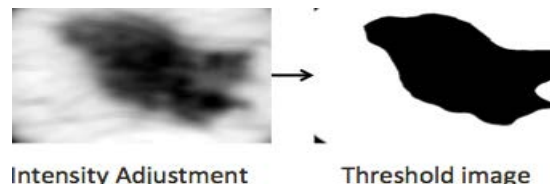


Fig. 4. Threshold process

After the threshold process, it is supposed that segmentation process is almost finished, but important three accomplishment steps still remains, namely for accurate tumor detection. By means of morphological operations [30], an image result from thresholding step was processed. First, any object with size less than 150 pixels were removed. Then, Binary image is inverted to refer for the selected object by white pixels "ones" and black pixels "zero" for background. Finally, any gap that may found at lesion mask was filled to complete tumor holes. After the tumor had been segmented, lesion center (centroid) and bounding box is determined regarding the traced boundary [31]. Fig. 5. Illustrate the full segmentation process.

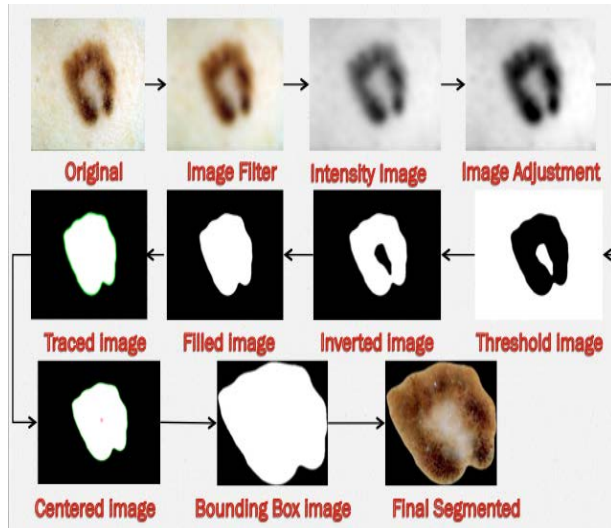


Fig. 5. Schematic representation for image Segmentation steps

B. Feature Extraction

Segmentation operated and reduced pixels number of the pigmented lesion to save time dealing just with the required region. Then sets of different features were extracted to represent the lesion essential characteristics for accurate discrimination between benign and malignant lesions. The most valuable prognostic factor of malignant melanoma is appearance variability. It is irregular in shape and color with differential structure.

On this spot, that research attempt to compromise that heterogeneous phenomena proposing and examining huge different number of features. The features presented study lesion property from three concerned sides geometric for shape, chromatic for color and texture features representing differential structure. Texture features were studied in details in regard to different color spaces and coordinates with respect to GLCM. This section will discuss the different types of features used through this study to correctly define the PSL introduced.

a) Geometric Features: Shape descriptors supply important information to discriminate malignant melanoma from melanocytic nevi. Results shows that geometric features are usually efficient in analyzing region of interest shape in a binary image. This study computed 21 geometric features [9, 32] to describe a set of properties for the segmented binary

image of PSL. Fig. 6 represents a schematic representation of the binary image that shows the geometric representation of each parameter calculated considered as a separate feature as follow. Area (A_p), Perimeter (P_p), Center of gravity (Centroid), Solidity (A_p/A_c), Roundness, Irregularity, Major axis (a_p), Minor axis (b_p), Ratio of axis (a_p/b_p), Eccentricity, Extent (A_p/A_b), Equivalent Diameter, Radius, Bounding Box area (A_b), x-axis of bounding box (b_b), y-axis of bounding box (a_b), Ratio of bounding box axis (b_b/a_b), Estimated borderline, Convex Hull, Convex Hull area (Ac), Orientation.

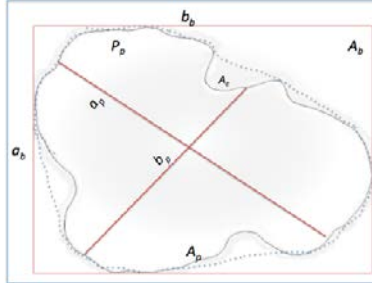


Fig. 6. Binary image lesion representation

b) Chromatic Features: Geometric features were promising in describing the lesion physical structure, but it missed the significance of tumor color, brightness or luminance that could be a guide to distinguish PSL true specification. Different previous studies [33] had proven that color features is useful and robust cue for diagnosing malignant melanoma. Skin lesion could be examined by different color spaces rather than RGB. Various color spaces was introduced through imaging processing field. Color space could be simply defined as different mathematical representation for a set of colors in ways that make certain calculations more convenient, where they provide a method to identify colors that is more intuitive. This section deals briefly with the seven color spaces introduced through this study and the different features vectors extracted from each.

The seven color spaces introduced to study the PSL through them are RGB, HSV, HIS, YIQ, YCbCr, L*u*v* and lab spaces[33-35]. The most common space is the true color space represented by the RGB space, it defines a color as the percentage of red, green and blue hues colors mixed. Also the intuitive notions of hue, saturation, and brightness was represented by HSI and HSV color spaces to simplify processing and identify more details and information about the lesion [34]. In the field of video standards, the most famous color spaces are YIQ and YCbCr. The Y component represents the luminance information, it is the only component used by black-and-white television receivers where I, C_b and Q, C_r represent the chrominance information [33]. However; the five different color spaces mentioned above can help in studying the PSLs but it was interesting to pursue other valuable color spaces, such as L*u*v* and lab spaces [35]. According to the briefly defined color spaces, this study will investigate statistical features depending on each color space. The three different statistical features extracted from each component of the color spaces are specifically the mean, standard deviation, 'coefficient of variation' and the sum of color space component.

1) *Mean (μ)*: It is calculated as the average of the intensity pixels belonging to the lesion.

2) *Standard Deviation (σ)*: This value was taken as the color variation risk. In general, lesions with a higher color standard deviation are considered to be a higher cancer risk. This feature can be represented by the standard deviation value for all the pixels belonging to lesion regions with respect to the 7 different color spaces previously discussed.

3) *Coefficient of variation*: It can be seen as the relative standard deviation that can be represented by division of the lesion standard deviation by its mean value.

4) *Sum of color component*: Another new chromatic feature was proposed that considered the sum of the three channels intensity values of the color space, i.e for the YIQ space the feature represented by the sum of the channel value for luminace (Y), and the 2 chromatic components (I and Q), as $S = Y+I+Q$

Regarding the seven different color spaces mentioned through the above paragraphs and the four parameters explained, 10 features extracted from each space. These results the 70 different chromatic features presented through this study. Fig.7. shows an example for malignant melanoma region represented by the 7 different color spaces to show the different effect of each upon the PSL.

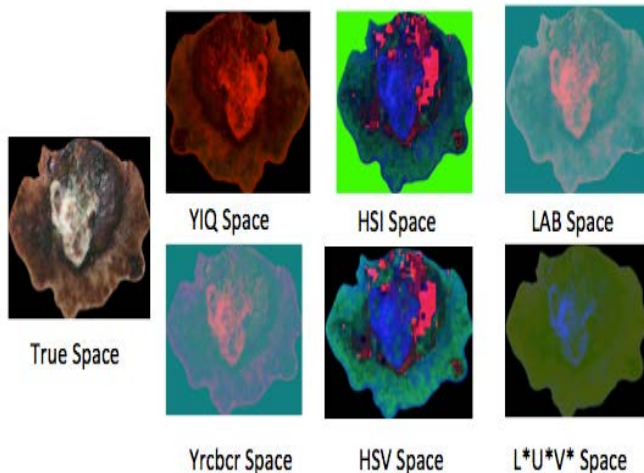


Fig. 7. Malignant melanoma lesion representation regarding the 7 color spaces

c) *Texture Features*: Skin lesion physical shape and color was essentially considered through morphological features. In more advanced melanoma, the skin on the surface may break down and look scraped. Also it may become hard or lumpy; the surface may ooze or bleed. Textures represent tonal variations in the spatial domain and determine the overall visual smoothness or coarseness of image features. Accordingly; texture features extractions stand as the essential accomplishment step to have complete and efficient approach. Texture features are considered to be one of the widely used tools in malignant tissue detection in digital images, where it can describe melanoma's different structures. Texture processing algorithms are usually divided into three major categories: structural, spectral and statistical [36,37].

Statistical texture features have been proven to be powerful in classifying malignant and benign tissues. Texture analysis covers a wide range of techniques based on first- and second order image texture parameters, as the first order statistical features are not at all sufficient to characterize the heterogeneity of the different tumor types.

Since different lightening conditions change the apparent texture of a lesion [38], in addition to these two different groups of texture features it was also interesting to discuss tumor texture with respect to the 7 different color spaces previously proposed to circumvent lightening problem and cope with any variation. Toward the main aim of discrimination between normal and abnormal lesion, this section will deal with all texture features extracted starts with first order statistical features, higher order statistical features (GLCM) and then texture features of 7 color spaces.

1) *First Order Statistical features*: First order statistics can be used as the most basic texture features and are properly named just statistical rather than texture feature. Two groups of statistical features were proposed; one group based on the probability of pixel's intensity values occurring in digital images and independent on spatial distribution of pixels, the other group depends on the histogram statistics. The first order features were extracted depending on spatial distribution of pixels was Mean, Standard deviation, Smoothness, Third Moment and Entropy. Histogram features are extracted depending on the calculated histogram of the lesion image; the six features extracted based on histogram are Mean, Skewness, Entropy, kurtosis, Energy and variance.

2) *Higher order statistical features*: They are second order features that depend on pixel value and their spatial inter-relationships. Higher or second order statistical features are based on statistical parameters such as the Spatial Gray Level Dependence Method (co-occurrence matrices), the Gray Level Difference Method, and the Gray Level Run Length Matrices [39,40]. One of those examples proposed for that study is the gray level co-occurrence matrix, as it is most popular texture analysis used previously for discrimination of melanoma [9,41]. The choice of Haralick features [42,43] based on GCMs was made considering their proven applicability to analyze objects with irregular outlines [44].

Gray level co-occurrence matrix (GLCM) is a tabulation of how often different combinations of pixel brightness values (grey levels) occur in an image. It is constructed by observing pairs of image cells separated distance d from each other and incrementing the matrix position corresponding to the grey level of both cells. Its operation can be simply discussed through the schematic representation example shown on Fig.8. The 21 higher order texture features [42] used in this study are autocorrelation, contrast, correlation, cluster shade, cluster prominence, dissimilarity, energy, entropy, homogeneity, maximum probability, sum of squares (Variance), sum of average, sum of variance, sum of entropy, difference variance, difference entropy, Information measure of correlation 1, Information measure of correlation2, Inverse difference (INV) is homom, Inverse difference normalized (INN), Inverse difference moment normalized (IDM).

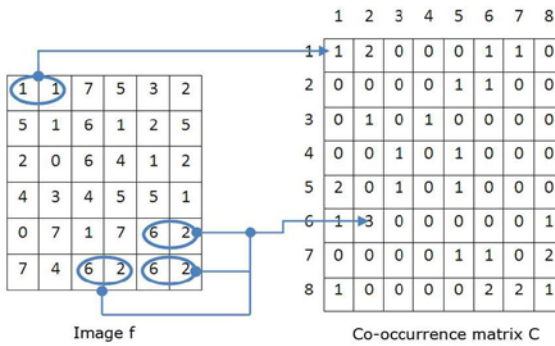


Fig. 8. Example of gray level co-occurrence matrix (GLCM)

The GLCM is determined using gray-tone spatial dependence matrices $D_s^{[K]}(i,j)(K = 1, \dots, 4)$ listening how many times the gray tones i and j are spatial neighbors. So, various co-occurrence matrix realizations depending on distance and angle, and displaying different angular relationships, are introduced through our work. The textural measures were calculated on horizontal, vertical and two diagonal directions on an image as $D_s^{[K]}(i,j)$ is computed for each of the four angles $0^\circ, 45^\circ, 90^\circ$ and 135° , where K denotes the angle of spatial neighborhood. Fig.9 illustrates the geometrical relationships of GLCM measurements made by the four angles under the assumption of angular symmetry. The previously mentioned 21 GLCM features extracted were defined in the four different angles (21 features *4 different angles) to have for total 84 features [45].

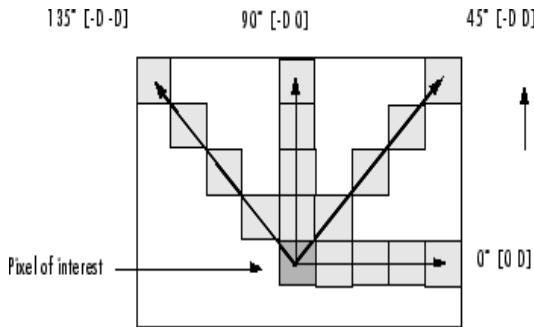


Fig. 9. Geometry directions of adjacency for calculating GLCM features

Texture features of 7 color spaces: Important features about skin texture were extracted by evaluating some statistical parameters about the PSL in regard to the different 7 color spaces mentioned in the chromatic section. In regard to the powerful indication of the tumor specification resulted from measuring its entropy, it was powerful to measure entropy for the PSL based on the 7 color spaces to result 7 different texture features. Furthermore, texture analysis includes several functions that filter an image using standard statistical measures such as range, standard deviation [46]. These statistics can characterize the texture of an image because they provide information about the local variability of the intensity values of pixels in an image. For example, in areas with smooth texture, the range of values in the neighborhood around a pixel will be a small value; in areas of rough texture, the range will be larger. Accordingly, the means and standard deviations of local entropy [46], local standard

deviation and local range [47] of gray scale image are added as separate features for each three color component of the seven spaces ($2 \times 3 \times 7 \times 3$) counting out one hundred and twenty-six feature.

Further information about skin texture can be mentioned by extracting GLCM features out of image transformed to the different color spaces used. Based on the co-occurrence matrix, many different texture descriptors may be computed. To reduce the computational complexity, only four most relevant features were selected out of 21 GLCM features presented above, namely **Energy**, **Homogeneity**, **Correlation** and **Contrast** based on their classification accuracy, computational cost and previously usage in literature [9]. About 88 features were extracted through the present section, where each of the four features was extracted out of each color component of the 7 color spaces ($7 \times 3 \times 4$), In addition to the four features extracted from the gray scale image of the true space on RGB color.

In conclusion, this study presented huge numbers of texture features to fulfill the aim toward having complete definition for the PSL structure and specification. Three hundred-sixteen texture features were extracted considering eleven first order statistical features, eighty-four second order statistical features in addition to texture representation regarding the different seven color spaces, which presented two hundred and twenty one feature. A Simple representation of the distribution for all texture features extracted based on different color spaces is shown in Fig.10.

Texture Features:

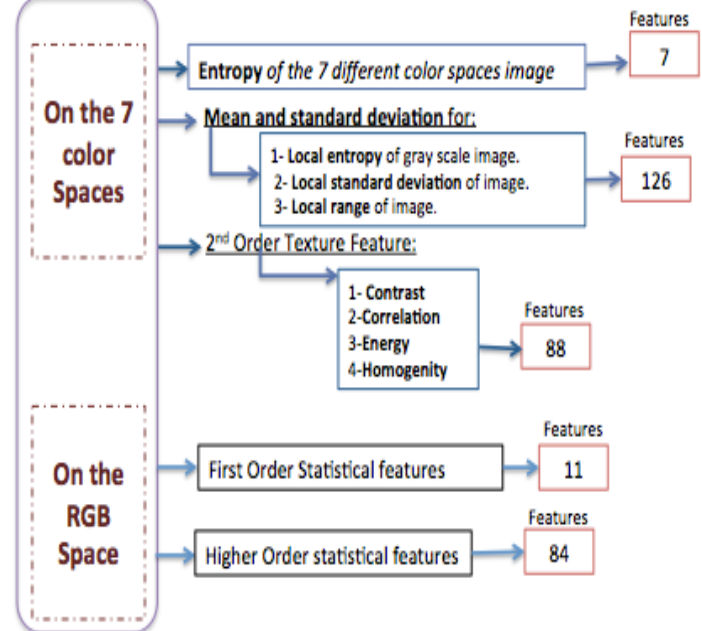


Fig. 10. Texture features diagram

C. Feature Selection

Although, features variety are helpful to screen out tumor properties for accurate diagnosis, but approaches have this huge number of features usually suffer complexity. It is

difficult to experimentally analyze and explicitly recognize patterns in the data of a larger test set, where it will in turn increase processing time, as some of these features are depend on heavy calculations. Features are not equally efficient for classification task due to redundancy or irrelevance. Thus, feature selection techniques used to reduce features quantity significantly, while increasing the detection accuracy. The main idea of feature selection is to choose a subset of input features by eliminating features with little or no predictive information.

All methods begin by having all samples in the feature space of unknown class assignment. The methods described through this study will assign classes by measuring how nearer the samples to a certain limit and similar samples will be grouped by assigning them the same class. Three attribute selection algorithms are used for the dimensionality reduction and identification of the most prominent features to capture efficiently the system. The three statistical methods proposed for the target of feature selection was, the F-test [48,49], the T-test [50] and the Fisher score ranking [51] to compare and increase the detection accuracy.

In statistical significant testing T-test and F-test, the p-value is the significant level of probability. The smaller the p-value, the more significant is the difference between the distributions of the two groups. Features with practically different variance was chosen as significant features where their p-values are suppose to be less than the significant level used for that study which is 0.05. Fig.11 shows simple description for t-value, which used to measure the correlation regarding P-value in the t-test selection method. On the contrary, features selected according to fisher score ranking are those with the highest ranks, where the ranking threshold for this study was 0.5.

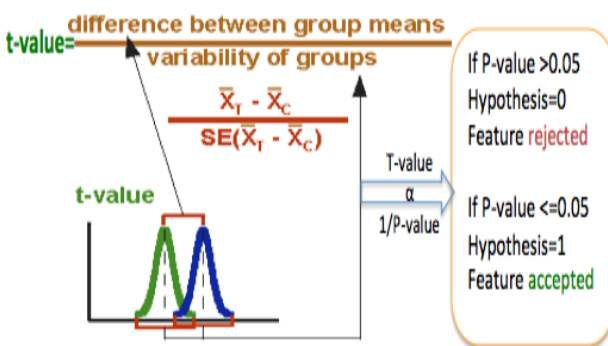


Fig. 11. T-test and P-value relation

D. Classification

The final goal of a skin cancer automatic detection system is to build a decision rule that will discriminate between malignant and benign lesions. Automatic diagnosis system is usually accomplished by means of the classification process, that define as a finding operation for a set of attributes to distinguish between classes of data for the purpose of predicting the class of objects, whose class label is unknown. Generally a classifier generates a decision boundary, which separates the points in feature space into two or more sets of classes. Each type of classifier will arrive at a decision

boundary in a different way according to its working process and the classifier types. Toward accurate diagnosis for PSL different classifying algorithms introduced based on Artificial Neural Network (ANN), the K-Nearest Neighbor classifier (K-NN) and Support Vector Machine (SVM).

This section concerned with discussing the main idea of the three different classification models proposed to differentiate between malignant and benign lesions. As mentioned through material section this study introduces 160 images for each data set whether dermoscopic or clinical image. All images are fairly divided for two classes 50% for learning set and 50% for test set. So, 80 images representing 40 for malignant melanoma cases and 40 of benign nevi cases used as a training set to accomplish the automated detection system of tumors, whereas the other 80 image having the same distribution for testing the automated detection system.

a) *Artificial Neural Network (ANN)*: Artificial neural networks are computational paradigms based on mathematical models that unlike traditional computing have a structure and operation, which resembles the mammal brain. Artificial neural networks or neural networks for short, are also called connectionist systems, parallel distributed systems or adaptive systems, because they are composed by a series of interconnected processing elements that operate in parallel. The main idea of computer-aided diagnosis was to design software having nearly functionality of the human eyes to extract features and the brain to classify them. Thus, ANN was the first choice of classification algorithm among all CAD software programmers [52].

Generally, ANN Classification process usually operated through two successive steps; learning (or training) and testing. The training phase learns the set of examples presented to the network, where the network ‘guesses’ the output for each example. As the training goes on, network internally adjust until it reaches a stable stage at which the provided outputs are satisfactory. Neural networks can learn in two ways: supervised or unsupervised [52].

To decide on a network topology some points must be considered for designing ANN classifier, Number of input nodes represented by the number of selected features feeded into the classifier. Number of output nodes is just one where it suppose to have a clear-cut if that image is whether malignant or benign. Then, Number of hidden nodes and Activation function are selectable according to the designed network and finally the network Training behavior. Accordingly two techniques were proposed for our study, the Automatic and Traditional ANN technique [12].

b) *K-Nearest Neighbor (KNN)*: KNN has recently been recognized as one of the best algorithms for clustering data as it is simple, quick and effective. K indicates the number of neighbors, then each sample, is classified in the same class, as the training data is closest [53]. In other words, there is no explicit training phase or it is very minimal and pretty fast. Each classified sample neighbour in KNN training phase is considered as an item of evidence which supports certain hypotheses regarding the class membership of that pattern.

Finally the test image is classified as belonging to the class, which is most frequent among the K-samples nearest to it.

Support Vector Machine (SVM): Vapnik and Lerner are the first investigators who developed the Support Vector Machine (SVM) algorithm in 1963. The theory has been improved to generalize the ability of learning machines regarding unseen data [54,55]. In the last few years SVM have shown perfect performance in different real-world applications including object recognition and image face detection [56-59]. SVM is based on the idea of minimizing the generalization error when the classifier is applied to test samples, by estimating its magical function that can powerfully classifies data into two classes. Finding the hyper plane that can perfectly discriminate between all data points is the main idea of SVM algorithm. The best hyper-plane for the SVM means the one with the largest margin between the two classes, where margin is the maximal width of the slab parallel to the hyper-plane that has no interior data points. Margin is usually maximized when the norm of the weight vector is minimum. Fig. 12 illustrates SVM methodology of classification.

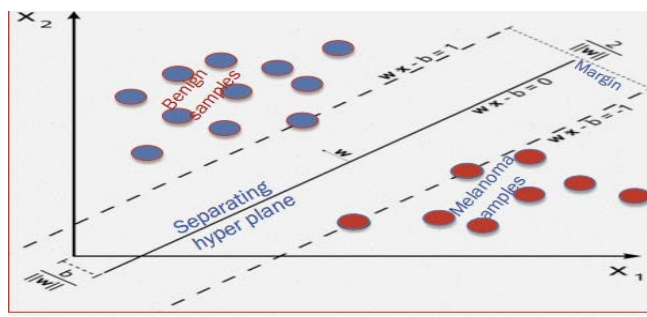


Fig. 12. SVM Classification

In order to obtain satisfactory predictive accuracy, different SVM kernel functions were proposed. Regarding the difference occurred between classifiers due to their training procedure. Three different SVM approaches have been proposed for classification as a result of using three different kernel functions that are linear, quadratic and RBF kernels [60-62].

E. Performance measure

The previously mentioned algorithms and models for detecting melanoma rely on the automatic assessment of the skin to interpret whether a pigmented skin lesion is a melanoma or not. All software developed will have an error rate and occasionally will either fail to identify an abnormality, or well identify an abnormality that is not present. To be able to evaluate the results and assign some kind of performance measure to the diagnosis done by the system. Statistical measures called sensitivity and specificity

calculated to evaluate the diagnostic accuracy, calculated through equation the following three equations 3, 4 and 5. These measures are used to describe the error rate by the terms true and false positive and true and false negative [63,64].

$$\text{Sensitivity} = \frac{\text{TP}}{\text{TP} + \text{FN}} * 100\% \quad (3)$$

$$\text{Specificity} = \frac{\text{TN}}{\text{TN} + \text{FP}} * 100\% \quad (4)$$

$$\text{Accuracy} = \frac{\text{TP} + \text{TN}}{\text{TP} + \text{TN} + \text{FP} + \text{FN}} * 100\% \quad (5)$$

IV. EXPERIMENTAL RESULTS

The previous methodology section illustrated the steps performed for the purpose of PSL diagnosis. As all database images processed and segmented then features were extracted and the most significant was selected. Finally, the promoted features worked as input for the three mentioned classifiers. As result of the huge number of features extracted and the different methods used in both feature selection and classification process, there will be multi different experimental results. This section intent to monitor the classification results according to the testing phase, then, analyzes its performance among different features used. Measuring performance to such huge number of experiments was handled by dividing experiments according to features category. Experimental approaches were divided into single and combined models; Fig. 13 shows the description of the different approaches applied for both single and combined models.

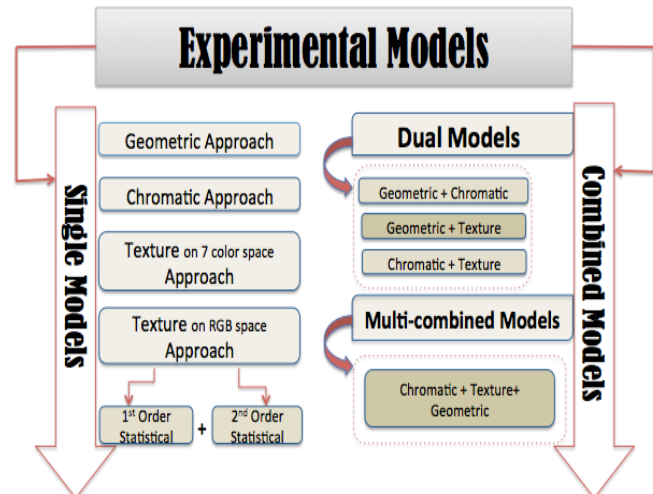


Fig. 13. Single and Combined Model approaches

A. Single Models

These models focus on studying a single type of feature and compare its performance when using three feature

selection methods to choose the most significant features that act as input to different classifiers. According to the different types of features extracted, four single models are proposed. Regarding the 3 sets of chosen features, resulted from f-test, t-test and fisher score raking, fed into the 6 different classification processes applied on both dermoscopic and clinical data set, 36 different experiment is resulted from each single approach. Fig. 14. Shows the general schematic representation for single approach.

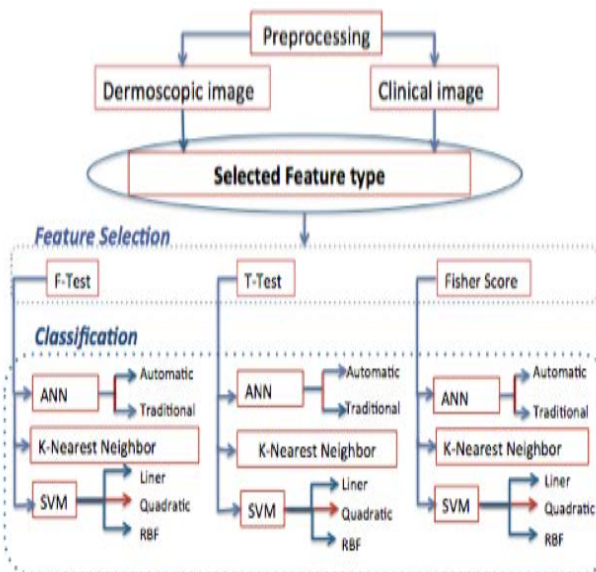


Fig. 14. Single Model Block Diagram

The best accuracy recorded from of all single approach experiments' carried out is discussed as follow:

a) Geometric Approach: The Fisher score method defines the most significant feature for both image types among the geometric features. The most accurate model was presented by introducing the 15 geometric features selected by fisher score ranking to SVM and ANN, which recorded 93.7% regarding both dermoscopic and clinical database.

b) Chromatic Approach: The best two models performed by chromatic features regarding both dermoscopic and clinical images were classified using ANN. Results regarding both datasets were promising where models recorded 92.5% using t-test selected features and 93.75% using fisher selected features for and dermoscopic and clinical database respectively.

c) Texture of 7-color space Approach: Texture features were not very promising for digital images rather than dermoscopic lesions. Clinical data reaches accuracy of 87.5% using t-test features when classified by ANN. On the other

hand, Dermoscopic data reach 90% when fisher-selected features were classified by linear SVM.

d) Texture Analysis using the RGB space Approach:

Through this feature category, the best accuracy recorded for both database types was 87.5 regarding different models. The best dermoscopic model was built up using features selected by f-test model and classified with linear and quadratic SVM. For clinical database, it was observed that the best accuracy recorded was 87.5% according to feature selected by t-test and classified by traditional ANN.

According to the previous results it was observed the first three single approaches (geometric, chromatic and texture based on 7 color spaces) were much more promising than texture features based on RGB space. Thus, first and second order statistical features based only on RGB space were excluded from the group of features used to construct combined models.

Regarding the three selected features category selected it was observed that feature selected upon using the T-test and Fisher score method shows the best results. But since the t-test usually selects a larger set of features compared to the fisher score method reaching very relative results, fisher score method was preferred. Accordingly, the features selected by the fisher score used for the combined model as the most significant. It is valuable to determine the most significant features could be used to determine melanoma, table 1 mentions all the selected features according to the three different categories (Chromatic, Geometric and Texture).

Fifteen and twenty-two features represent geometric and chromatic features respectively for both the dermoscopic and clinical database. Forty- seven and twenty texture features selected to represent dermoscopic and clinical database respectively.

B. Combined Models

After studying each type of features separately through the single models, it was valuable to monitor the effect of combining the most revealing features of each type. Four combined approaches were proposed as a result of amalgamation between the best features extracted out of each feature type. Three approaches were considered by combining two different feature types together (Geometric + Chromatic), (Chromatic + Texture) and (Geometric + Texture), dual models could name those. The fourth approach was proposed by combining the three feature types together (Geometric + Chromatic + Texture).

Therefore, combined models study different types of features together and compare their performance when best features cooperate and feed as input for the different applied classification algorithms. Fig. 15, easily mention the process that the combined model goes through.

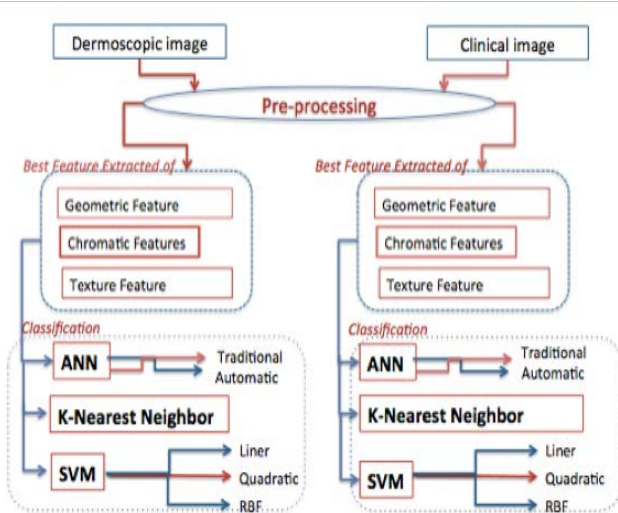


Fig. 15. The Combined Model Block diagram

a) Dual Models: Geometric features record the highest results when combined with texture or chromatic features for the two different types of databases. The best accuracy recorded was 95% for geometric and chromatic features sets of dermoscopic images classified by linear SVM. Where also the combination between geometric and texture feature of clinical images record the same percentage when classified by automated ANN.

1) *Dermoscopic database:* A number of thirty-seven, sixty-two and sixty-nine features were considered the total significant features composed for the three approaches (Geometric + chromatic), (Geometric + Texture) and (Chromatic+ texture), respectively. It was observed that best accuracy recorded was 95% for the combination of geometric and chromatic features classified by linear SVM.

2) *Clinical database:* A number of thirty-seven, thirty-five and forty-four features were considered the total significant features composed of the three approaches (Geometric + chromatic), (Geometric+ Texture) and (Chromatic+ texture), respectively. It was observed that best accuracy recorded was 95% for the combination of geometric and texture features classified by automated ANN.

a) Multiple Models: It was further observed that the amalgamation between the three different features category concluded a well representation for lesions whether of dermoscopic or clinical images.

1) *Dermoscopic database:* Fifteen, twenty-two and forty-seven geometric, chromatic, and texture features respectively were introduced to the six different classification methods to evaluate the model performance. It was remarked that the most accurate model was reached by classifying the three combined features according to the traditional mode of ANN, that record accuracy of 96.25%. Also it was most remarkable that linear SVM yielded very good results that reach 100% for sensitivity and record accuracy 95%.

2) *Clinical database:* Fifteen, twenty-two, and twenty geometric, chromatic and texture features respectively, were

introduced to the six different classification methods to evaluate the model performance. The most accurate model performed to diagnose the PSL was represented in clinical images by classifying the three combined features according to traditional mode of ANN that recorded 97.5%. This was followed by the automatic validation mode of ANN with a recorded accuracy of 95%.

Dermoscopic Combined Models

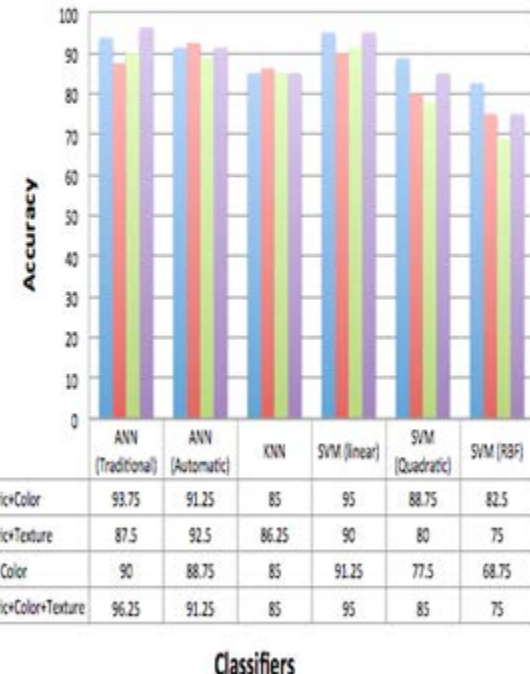


Fig. 16. Dermoscopic combined models results

Clinical Combined Models

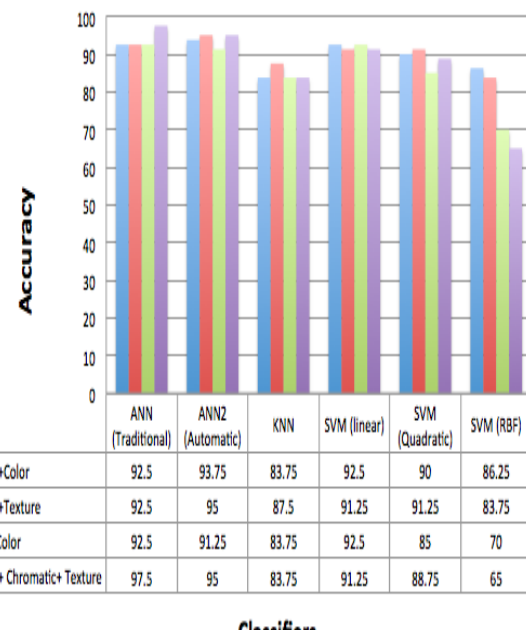


Fig. 17. Clinical combined models results

TABLE I. THE SELECTED FEATURES ACCORDING TO FISHER SCORE METHOD

Selected features				
Geometric	Chromatic		Texture	
Dermoscopic & Clinical Features	Dermoscopic Features	Clinical Features	Dermoscopic Features	Clinical Features
Equivalent Radius	Mean of Red (RGB)	Mean of H (HSI)	Entropy of RGB	Standard deviation of Local entropy for R, G & B of (RGB).
Area	Mean of Y (YIQ)	Mean of I of (YIQ)	Mean of Local entropy for G and B (RGB)	Standard deviation of Local entropy for H & I of (HSI).
Perimeter	Mean of V (HSV)	Mean of S of (HSV)	Mean of Local standard deviation for u* and v* ($L^*u^*v^*$)	Standard deviation of Local entropy for Y of (YIQ).
Solidity	Mean of Y (Ycbcr)	Mean of cr of (Ycbcr)	Mean of Local range for u* ($L^*u^*v^*$)	Standard deviation of Local entropy for H, S & V of (HSV).
Roundness	Mean of L (Lab)	Mean of a (Lab)	Standard deviation of Local entropy for S and V of (HSV)	Standard deviation of Local entropy for Y of (Ycbcr).
Extent	Mean of u* ($L^*u^*v^*$)	Mean of cb (Ycbcr),	Standard deviation of Local standard deviation for R, G & B	Standard deviation of Local entropy for L of (Lab).
Irregularity	Standard deviation of u* ($L^*u^*v^*$)	Mean of b (Lab)	Standard deviation of Local standard deviation for S and I of (HSI)	Standard deviation of Local entropy for L & u* of ($L^*u^*v^*$).
Major Axis	Sum of (R+G+B)	Mean of L ($L^*u^*v^*$)	Standard deviation of Local standard deviation for Y of (YIQ)	Standard deviation of Local Std for u* of ($L^*u^*v^*$).
Minor Axis	Sum of (L+a+b)	Mean of u* of ($L^*u^*v^*$).	Standard deviation of Local standard deviation for V of (HSV)	Standard deviation of Local range of image for u* of ($L^*u^*v^*$).
Equivalent Diameter	Sum of (H+S+I)	Standard deviation of S (HSV).	Standard deviation of Local standard deviation for Y of (Ycbcr)	GLCM Energy of H of (HSI).
Bounding box area	Sum of ($L+u^*+v^*$)	Sum of: (R+G+B)	Standard deviation of Local standard deviation for L of (Lab)	GLCM Energy of H of (HSV).
X-axis of bounding box	Sum of (Y+I+Q)	Sum of (H+S+I)	Standard deviation of Local std for L & u* & v* of ($L^*u^*v^*$)	GLCM Energy of cr of (Ycbcr).
Y-axis of bounding box	Sum of (H+S+V)	Sum of (Y+I+Q)	Standard deviation of Local range for R and G (RGB)	GLCM Energy of (Ycbcr).
Estimated border line	Coefficient variant Of Red	Sum of (H+S+V)	Standard deviation of Local range for I (HSI),	GLCM Energy of b of (Lab).
Convex hull area	Coefficient variant Of I (HSI)	Sum of (L+a+b)	Standard deviation of Local range for Y (YIQ)	GLCM Energy of u* of ($L^*u^*v^*$).
	Coefficient variant Of Y (YIQ)	Sum of ($L+u^*+v^*$).	Standard deviation of Local range for V (HSV)	
	Coefficient variant Of S (HSV)	Coefficient variant Of Red	<input type="checkbox"/> Standard deviation of Local range for L, u*, v*	
	Coefficient variant Of V (HSV)	Coefficient variant Of S (HSV)	Standard deviation of Local range for Y (Ycbcr), ($L^*u^*v^*$),	
	Coefficient variant Of Y (Ycbcr)	<input type="checkbox"/> Coefficient variant Of V (HSV)	GLCM Homogeneity of RGB, R, G	
	Coefficient variant Of L (Lab)	Coefficient variant Of (Y) Ycbcr	GLCM Homogeneity of I (YIQ)	
	Coefficient variant Of L ($L^*u^*v^*$)	<input type="checkbox"/> Coefficient variant Of u* ($L^*u^*v^*$).	<input type="checkbox"/> GLCM Homogeneity of S & V (HSV)	
	Coefficient variant Of u* ($L^*u^*v^*$)	Coefficient variant Of L (HSV)	GLCM Homogeneity of cr (Ycbcr)	
			<input type="checkbox"/> GLCM Homogeneity of L of ($L^*u^*v^*$)	
			Standard deviation of Local range for L (Lab),	
			GLCM Correlation of cb of (Ycbcr),	
			GLCM Homogeneity of H& S&I (HSI)	
			GLCM Contrast of L & u* of ($L^*u^*v^*$).	
			Mean of Local entropy for Y (YIQ)	
			Mean of Local entropy for u* ($L^*u^*v^*$)	

V. CONCLUSIONS & FUTURE WORK

The proposed non-invasive automated system for PSL and melanoma diagnosis tested upon two different types of superficial skin lesions images. The system was tested on 320 melanocytic skin lesions images, fairly divided within both clinical and dermoscopic images. Computer aided diagnosis

systems especially for melanoma begins with image segmentation to extract the infected lesion out of the healthy tissue, this study presented segmentation as first step as well. Then features extraction provides a valuable contribution; it defines the characteristics of the lesion image by illustrating a relevant description for the PSL in a feature space. Features

categories vary between 91 morphological features based on (geometric, chromatic) and 316 representing texture analyses. Features significance level were evaluated and selected regarding three feature selection methods; f-test, t-test and fisher score ranking. Selected features were fed into three different classifiers; ANN, KNN, SVM. Results obtained was very promising concluded that, this study has the ability to define new and efficient features for melanoma diagnosis. Thus, this study presented an efficient software tool which implements different image processing algorithms developed for the automated analysis of clinical and dermoscopic images.

More specifically, the huge number of experiments performed according to the use of different features categories and different classifiers, to PSL images have been resulted in an integrated architecture for CAD. Experimental results show that integration between the most prominent features selected regarding fisher score ranking from the three efficient features categories; geometric, chromatic and texture features had effectively defined the lesion structure rather than single or dual approaches. Where the combined approach records 96.25 and 97.5% as the best accuracy resulted upon classifying dermoscopic and clinical images respectively by ANN.

Comparing results achieved through the last multiple model to the recent studies mentioned in the literature review section, this approach considered as promising completed CAD system that add all different features category to cope with the lesion heterogeneous phenomena and diagnose it with accuracy reaches 97.5 %.

There are many things that need to be improved upon and worthy of further work. According to segmentation step acquired through that study, tumor edges was smoothed and so important features was rejected, so segmentation process could be improved to have better results. Different feature selection methods could be considered to avoid features redundancy or reputation. Also, the most notable is of course to study the dermoscopic differential structure in a larger scale, which requires a more detailed dermoscopic database.

REFERENCES

- [1] U.S. Emerging Melanoma Therapeutics Market, a090-52, Tech. Rep., 2001.
- [2] Ascierto PA, Palmieri G, Celentano E, Parasole R, Caraco C, Daponte A, Chiofalo MG, Melucci MT, Mozzillo N, Satriano RA, Castello G. "Sensitivity and specificity of epiluminescence microscopy: evaluation on a sample of 2731 excised cutaneous pigmented lesions", *BJD*, pp. 142, 893, 2000.
- [3] M. Binder, M. Chwarz, et al., "Epiluminescence microscopy: a useful tool for the diagnosis of pigmented skin lesion for formally trained dermatologists", *Archives of Dermatology*, vol. 131, pp. 286-291, 1995.
- [4] W. Liu, D. Hill, A. Gibbs, M. Tempany, C. Howe, R. Borland, M. Morand, and J. Kelly, "What features do patients notice that help to distinguish between benign pigmented lesions and melanomas? The ABCD(E) rule versus the seven-point checklist," *Melanoma Res.*, vol. 15, no. 6, pp. 549-554, 2005.
- [5] F. Nachbar, W. Stolz, T. Merkle, A. B. Cognetta, T. Vogt, M. Landthaler, P. Bilek, O. Braun-Falco, and G. Plewig, "The ABCD rule of dermatoscopy: High prospective value in the diagnosis of doubtful melanocytic skin lesions," *J. Amer. Acad. Dermatol.*, vol. 30, no. 4, pp. 551-559, Apr. 1994.
- [6] Ho Tak Lau, Adel Al-Jumaily. "Automatically Early Detection of Skin Cancer: Study Based on Neural Network Classification]", *International Conference of SOCPAR*, pp. 375-380, 2009.
- [7] P. Rubegni, G. Cevenini, M. Burroni "Automated diagnosis of pigmented skin lesions", *International Journal of Cancer*, Vol. 101, pp. 576-580, 2002.
- [8] Iris Cheng, Edwardsville, Illinois, "Skin tumor classification using relative color features". *Thesis submitted in partial fulfillment for Master's degree in Electrical Engineering at Southern Illinois University*, Edwardsville, Illinois, 2006.
- [9] José Fernández Alcón, C`alina Ciuhu, Warner ten Kate, Adrienne Heinrich, Natallia Uzunbjakava, Gertrud Krekels, Denny Siem, and Gerard de Haan, "Automatic Imaging System With Decision Support for Inspection of Pigmented Skin Lesions and Melanoma Diagnosis", *IEEE journal of selected topics in signal processing*, VOL. 3, pp.14-25, 2009.
- [10] Mariam A.Sheha, Mai S.Mabrouk, Amr Sharawy,"Automatic Detection of Melanoma Skin Cancer using Texture Analysis", *International Journal of Computer Applications*, VOL 42- pp.20, 2012.
- [11] Mai S. Mabrouk, Mariam A. Sheha, Amr A. Sharawy "Computer Aided Diagnosis of Melanoma Skin Cancer using Clinical Photographic images", *International journal of computer and technology*. Vol.10, No.8, May 2013
- [12] Mariam A. Sheha, Mai S. Mabrouk, Amr A. Sharawy "Pigmented Skin Lesion Diagnosis Using Geometric and Chromatic Features", *Biomedical Engineering Conference (CIBEC)*, Cairo International, IEEE, Dec. 2014.
- [13] K. Korotkov and R. Garcia, "Computerized analysis of pigmented skin lesions: A review", *Artificial Intelligence in Medicine*, vol. 56, no. 2, pp. 69-90, 2012.
- [14] A.Blum, H.Luedtke, U.Ellwanger, R.Schwabe,* G.Rassner And C.Garbe, "Digital image analysis for diagnosis of cutaneous melanoma. Development of a highly effective computer algorithm based on analysis of 837 melanocytic lesions", *BJD*, vol.151, pp.1029-1038, 2004.
- [15] Ratner D, Thomas C, Bickers D. "The uses of digital photography in dermatology". *Journal of the American Academy of Dermatology*, 41(5):749-56, 1999.
- [16] www.dermoscopic.blogspot.com
- [17] www.dermoscopyatlas.com
- [18] http://www.ee.siu.edu/~sumbaug/Borders%20Complete/
- [19] B. Garcia Zapirain, A. Mendez Zorrilla, I. Ruiz Oleagordia, G. Nunez, A. Abtane, "Skin cancer parameterization algorithm based on epiluminescence image processing", *IEEE*,2009.
- [20] www.dermnet.com
- [21] Dermnetnz.org
- [22] DermQuest.com (www.dermQuest.com)
- [23] Dermis.com (dermis.multimedica.de)
- [24] dermatlas.med.jhmi.edu
- [25] Tim Kam Lee, "Measuring border irregularity and shape of cutaneous melanocytic lesions", *thesis submitted in partial fulfillment of the requirements for the degree of doctor of philosophy in the School of Computing Science. Simon Fraser University*, January 2001.
- [26] Bushra Jalil, Dr Franck Marzani, "Multispectral Image Processing Applied to Dermatology" *A Thesis Submitted for the Degree of MSc Erasmus Mundus in Vision and Robotics (VIBOT)*, 2008.
- [27] Tarun Kumar, Karun Verma, "A Theory Based on Conversion of RGB image to Gray Image", *International Journal of Computer Applications* (0975 – 8887) Volume 7 – No.2, September 2010
- [28] G.M. Brake and N. Karssemeijer, 2001. "Segmentation of suspicious densities", *Med. Phys.* 28, pp. 258-266.
- [29] Otsu N, "A threshold selection method for gray-level histograms", *IEEE Trans. Syst., Man, Cyber*, vol. SMC-9, pp.62-66, 1979.
- [30] Soille, P., "Morphological Image Analysis", *Principles and Applications Springer*, pp. 164-165, 1999.
- [31] Di Leo G, Fabbrocini G, Paolillo A, et al. "Towards an Automatic Diagnosis System for Skin Lesions: Estimation of Blue-Whitish Veil and Regression Structures", In: *Proceedings of the IEEE 6th International Multi-Conference on System, Signals and Devices (SSD '09)*, Djerba, Tunisia, March 2009.

- [32] Pietro rubegni*, Gabriele cevenini, Marco burroni, Roberto perotti, Giordana dell'eva, Paolo sbano, Clelia miracco, pietro luizi, piero tosi, paolo barbini and lucio andreassi, "Automated diagnosis of pigmented skin lesions". Publication of the International Union Against Cancer Int. J. Cancer: 101, 576–580 2002 Wiley-Liss, Inc.
- [33] Vladimir V, Vassili .S, Alla A, "A Survey on Pixel-Based Skin Color Detection Techniques", Graphics and Media Laboratory, Moscow state university, Moscow, Russia.
- [34] Chun-Liang Chien and Din-Chung tseng , "Color image enhancement with exact HSI color model" . International journal of Innovative computing , Information and control volume 7, number 12 December 2011.
- [35] S.K. Tasoulis, C.N. Doukas,I. Maglogiannis, V.P. Plagianakos "Classification of Dermatological Images Using Advanced Clustering Techniques", 32nd Annual International Conference of the IEEE EMBS Buenos Aires, Argentina, August 31 - September 4, 2010.
- [36] R. C. Gonzalez, R. E. Woods, "Digital Image Processing", 3rd Edition, Addison-Wesley, Reading, MA, USA, 1992.
- [37] A. Meyer-Baese, "Pattern Recognition in Medical Imaging", Academic Press, Inc., Orlando, FL, USA, 2003.
- [38] Cula O G, Dana K J, Murphy F P, Rao B K. "Skin Texture Modeling", International Journal of Computer Vision IJVC, 2004.
- [39] V. A. Kovalev, F. Kruggel, H.-J. Gertz, D. Y. V. Cramon, "Three-dimensional texture analysis of MRI brain datasets", IEEE Transactions on Medical Imaging, 2001.
- [40] X. Li, "Texture analysis for optical coherence tomography image", Master's thesis, The University of Arizona, 2001.
- [41] Radu Dobrescu, Matei Dobrescu, Stefan Mocanu, Dan Popescu, "Medical images classification for skin cancer diagnosis based on combined texture and fractal analysis", wseas transactions on biology and biomedicine, Issue 3, Volume 7, 2010.
- [42] R. M. Haralick, Dinstein, K. Shanmugam, "Textural features for image classification", IEEE Transactions on Systems, Man, and Cybernetics SMC-3 610–621, 1973.
- [43] R. M Haarlick,"Statistical and structural approaches to texture," Proc. IEEE, vol. 67, pp. 786-804, 1979.
- [44] J. C. Russ, "The Image Processing Handbook", Raleigh, NC: CRC Press, 1995.
- [45] Fritz Albrechtsen, "Statistical Texture Measures Computed from Gray Level Cocurrence Matrices", University of Oslo, November 5, 2008.
- [46] Gonzalez, R.C., R.E. Woods, S.L. Eddins, "Digital Image Processing Using MATLAB", New Jersey, Prentice Hall, Chapter 11,2003.
- [47] <http://www.mathworks.com/help/index.html>
- [48] Markowski, Carol A; Markowski, Edward. "Conditions for the Effectiveness of a Preliminary Test of Variance", The American Statistician 44 (4): 22–326,1990.
- [49] Sawilowsky, S. "Fermat, Schubert, Einstein, and Behrens-Fisher: The Probable Difference Between Two Means When $\sigma_1^2 \neq \sigma_2^2$ ", Journal of Modern Applied Statistical Methods, 1(2), 461–472, 2002.
- [50] McDonald, J.H., Handbook of Biological Statistics Sparky House Publishing, Baltimore, 2008.
- [51] T. Golub, D. Slonim, P. Tamaya, C. Huard, M. Gaasenbeek, J. Mesirov, H. Coller, M. Loh, J. Downing, M. Caligiuri, C. Bloomfield, and E. Lander. "Molecular classification of cancer: Class discovery and class prediction by gene expression monitoring", Science, 286:531-537, 1999.
- [52] Margarita Sordom, "Introduction to Neural Networks in Healthcare", Open Clinical, October 2002.
- [53] R.O. Duda, P.E. Hart, and D.G. Stork, "Pattern Classification", Wiley, 2nd edition, 2001.
- [54] A. J. Smola and B. Schoelkopf, "A tutorial on support vector regression", Neuro COLT2 Technical Report Series NC2-TR-1998-030, ESPRIT working group on Neural and Computational Learning Theory, 1998.
- [55] V. Vapnik, "The Nature of Statistical Learning Theory", Springer, New York, 1995.
- [56] B. Scholkopf, S. Kah-Kay, C. J. Burges, F. Girosi, P. Niyogi, T. Poggio, and V. Vapnik, "Comparing support vector machines with Gaussian kernels to radial basis function classifiers," IEEE trans Signal Processing, vol. 45, pp. 2758-2765, 1997.
- [57] M. Pontil and A. Verri, "Support vector machines for 3-D object recognition," IEEE Trans. pattern analysis, Machine Intel, vol. 20, pp. 637-646, 1998.
- [58] V. Wan and W.M Campbell, "Support vector machines for speaker verification and identification," in Proc. IEEE Workshop Neural Networks for Signal Processing, Sydney, Australia, pp. 775-784, 2000.
- [59] E. Osuna, R. Freund, and F. Girosi, "Training support vector machines: Application to face detection," in Proc. Computer Vision and Pattern Recognition, Puerto Rico, pp. 130-136, 1997.
- [60] B. Schölkopf and A. J. Smola, "Learning with Kernels", MIT Press, 2002.
- [61] T. Hastie, R. Tibshirani, J. Friedman, "The Elements of Statistical Learning", New York, Springer Verlag, 2003.
- [62] N. Cristianini and J. Shawe-Taylor, "An Introduction to Support Vector Machines", Cambridge, U.K, Cambridge Univ. Press, 2000.
- [63] R.M. Nishikawa, M.L. Giger, K. Doi, C.J. Vyborny, and R.A. Schmidt, "Computer aided detection of clustered microcalcifications in digital mammograms," Med. Biol. Eng. Comp. Vol. 33, pp. 174- 178, 1995.
- [64] S. Theodoridis and K. Koutroumbas, "Pattern Recognition", Academic Press, San Diego, 1999.

Improved Association Rules Mining based on Analytic Network Process in Clinical Decision Making

Shakiba Khademolqorani

Department of Industrial Engineering
Sheikh Bahaei University
Isfahan, Iran

Abstract—Association Rules Mining is one of the most important fields in data mining and knowledge discovery in databases. Rules explosion is a problem of concern, as conventional mining algorithms often produce too many rules for decision makers to digest. In order to overcome this problem in clinical decision making, this paper concentrates on using Analytic Network Process method to improve the process of extracting rules. The rules provided by association rules, through group decision making of physicians and health experts, are used to organize and evaluate related features by analytic network process. The proposed method has been applied in the completed blood count based on real database. It generated interesting association rules useable and useful for medical diagnosis.

Keywords—*Clinical Data Mining; Clinical Decision Making; Association Rules Mining; Analytic Network Process*

I. INTRODUCTION

Clinical Data Mining (CDM) involves the conceptualization, extraction, analysis and interpretation of available clinical data for clinical decision making and practitioner reflection. Clinical database can be obtained from various sources which accumulate large quantities of information about patients and their medical conditions. Relationships and patterns within this data could provide new medical knowledge [1, 2].

Popular discourse about CDM focuses on the construction or application of algorithms to acquire medical knowledge. Li et al. have proposed a privacy-preserving method for training a Restricted Boltzmann Machine (RBM) which can be got without revealing their private data to each other when using our privacy-preserving method [3].

Exarchos et al. presented the methodology for the development of the EMBalance diagnostic Decision Support System for balance disorders. Medical data from patients with balance disorders have been analyzed using data mining techniques [4].

Bagherzadeh-Khiabani et al. have shown the application of some variable selection methods, usually used in data mining, for an epidemiological study. Also, they found that the worst and the best models were the full model and models based on the wrappers, respectively [5].

Association rule mining (ARM) is one of the most important methods in DM. In particular, the goal of association rules is to detect relationships or associations between specific values of categorical variables in large data sets, making it possible for analysts and researchers to uncover the hidden patterns. This powerful exploratory technique has a wide range of applications in many areas of business practice, industries, medicine, financial analysis, etc [6, 7].

Babashzadeh et al. proposed a novel approach to modeling medical query contexts based on mining semantic-based AR for improving clinical text retrieval. First, the concepts in the query context were derived from the rules that covered the query and then weighted according to their semantic relatedness to the query concepts. The query context was then exploited to re-rank patients records for improving clinical retrieval performance [8].

Most of the existing studies in temporal data mining consider only lifespan of items to find general temporal association rules. Hong et al. have organized time into granules and considered temporal data mining for different levels of granules. They designed a three-phase mining framework with consideration of the item lifespan definition [9].

Moreover, the purpose of CDM is to help the medical workers, especially physicians, with making decisions according to their own understanding. Then, methods offered to facilitate better decisions should become more descriptive and considerably transparent. Despite the attractive suggestion of fully automatic data analysis, knowledge of the processes behind the data remains indispensable in avoiding many pitfalls of DM.

Based on empirical evidence, ARM faces the rules explosion; consequently, it is complicated to appreciate all discovered knowledge. Based on the literature related to human brain abilities in information processing, when the number of logical phrases and rules is large, it is hard or almost impossible to understand and make a good sense [10, 11].

There are many ideas regarding the application of Multiple Criteria Decision Making (MCDM) in evaluation problems. Wen et al. have presented solutions to incorporate the uncertainty from clinical data into the MCDA model when evaluating the overall benefit-risk profiles among different treatment options [12].

liua have proposed a novel hybrid MCDM model by integrating the 2-tuple DEMATEL technique and fuzzy MULTIMOORA method for selection of health-care waste treatment alternatives. It made use of modified 2-tuple DEMATEL for obtaining the relative weights of criteria and fuzzy MULTIMOORA for assessing the alternatives according to each criterion [13].

Shafii et al. have assessed the service quality of teaching hospitals of Medical Sciences using Fuzzy Analytical Hierarchy Process (FAHP) and Technique for Order Preference by Similarity to Ideal Solution (TOPSIS) [14].

The purpose of this study is to present a solution to this problem in the clinical decision making. It is based on considering the medical experts knowledge to preprocess and evaluate the explored rules by Analytic Network Process (ANP). ANP is one of the main methods of MCDM technique used to make group decision making [15].

Basically, a network model in ANP is constructed based on expert judgments to model an abstract decision problem. A cluster in the ANP network corresponds to a class, and elements in a cluster are equivalent to mainline subclasses in a class. Then, in the ANP context, the resulting network model only includes alternative clusters, contrary to the general network model in the ANP which comprises a goal cluster, criteria clusters, and alternative clusters [16].

Ergu and Peng proposed a framework for SaaS software packages evaluation and selection by combining the virtual team and the BOCR (benefits, opportunities, costs, and risks) of ANP. Their proposed framework has shown great potentials for aiding practitioners and researchers concerned with the cloud services [17].

Nilashi et al. have developed Fuzzy ANP for the Hospital Information System (HIS) to understand the potential factors that importantly driving or inhibiting the decision of HIS adoption from non-adopters' perspective. This study mainly integrated the diffusion of innovation theory, technology-organization-environment framework, institutional theory along with human-organization-technology fit model that can be tailored in understanding of the HIS adoption by Malaysian public hospitals [18].

In this paper, towards CDM, ANP method is applied to improve the process of extracting rules. The clusters provided by ANP through physicians and health experts are used to organize and evaluate related features based on ARM information. To justify our proposed approach, a dataset of Completed Blood Count (CBC) is used. The discovered rules are interesting, useful and influential enough to identify the condition of the cases.

The paper is organized as follows. Section 2 describes ARM and ANP, which are used as the main technologies. Section 3 presents the novel approach used to improve the discovered association rules. Also, in section 4, a case study is carried out to illustrate the proposed method. The paper ends with concluding remarks in section 5.

II. METHODOLOGY

In this section, the methods developed and implemented in our paper are described. First of all, the ANP method is presented. Then, ARM procedure is briefly described.

A. Analytic Network Process (ANP)

The ANP, a generalization of the AHP, is one of the most widely used multiple criteria decision making (MCDM) methods [20]. The ANP incorporates feedback and interdependent relationships among decision elements and alternatives. This method provides a more accurate approach when modeling complex decision problems. The ANP derives relative priority scales of absolute numbers from individual judgments by making paired comparisons of elements on a common property or a control criterion. ANP includes the following steps [16, 19, and 20]:

- Given a decision problem with x_1, x_2, \dots, x_N elements, the first step consists of building a model grouping the elements into c_1, c_2, \dots, c_G clusters.
Let x_i^c the i element of the model, which belongs to cluster c , with $i = 1, \dots, N, c = 1, \dots, G$.
Let x^{c_α} the elements of cluster c_α , $\{x_i^c : c=c_\alpha\}$.
Let n_{c_α} the number of elements of cluster c_α .
- Identify the elements' relationships, ask the DM, and obtain the $(N \times N)$ Elements' Relationships matrix, $R=[r_{i,j}] = [r_{i,j}^{c_\alpha, c_\beta}]$. $r_{i,j}^{c_\alpha, c_\beta} \in \{0,1\}$ where $c_\alpha, c_\beta = 1, \dots, G$ and $i, j = 1, \dots, N$.
 - $r_{i,j}^{c_\alpha, c_\beta} = 0$ indicates that the element $x_i^{c_\alpha}$ has no influence on the element $x_j^{c_\beta}$, and in the graphical model there isn't an edge between $x_i^{c_\alpha}$ and $x_j^{c_\beta}$.
 - $r_{i,j}^{c_\alpha, c_\beta} = 1$ indicates that the element $x_i^{c_\alpha}$ has some influence on the element $x_j^{c_\beta}$, and in the graphical model there is an arc from $x_i^{c_\alpha}$ to $x_j^{c_\beta}$.
- Obtain the $(G \times G)$ Clusters' Relationships matrix, $\hat{R}=[\hat{r}_{c_\alpha, c_\beta}]$. $\hat{r}_{c_\alpha, c_\beta} \in \{0,1\}$ where $c_\alpha, c_\beta = 1, \dots, G$.
 - $\hat{r}_{c_\alpha, c_\beta} = 0$ indicates that any element of cluster c_α has influence on any element of cluster c_β .
 - $\hat{r}_{c_\alpha, c_\beta} = 1$ indicates that some element of cluster c_α has influence on some (at least one) elements of cluster c_β .
- Use usual pair-wise matrices to compare the influence of the elements belonging to each cluster on any element, and derive a priority vector, and obtain the $(N \times N)$ Unweighted Super matrix, $U=[u_{i,j}^{c_\alpha, c_\beta}]$, with $u_{i,j}^{c_\alpha, c_\beta} \in [0,1]$, $c_\alpha, c_\beta = 1, \dots, G$ and $i, j = 1, \dots, N$, where $u_{i,j}^{c_\alpha, c_\beta}$ is the influence of i , which belongs to cluster c_α , on element j , which belong to cluster c_β .
 - $u_{i,j}^{c_\alpha, c_\beta} = 0$ indicates that the element i , which belongs to cluster c_α , has no influence on the element j , which belongs to cluster c_β .

$$u_{ij}^{c_\alpha, c_\beta} = 0 \Leftrightarrow r_{ij}^{c_\alpha, c_\beta} = 0 \quad (1)$$

- $u_{ij}^{c_\alpha, c_\beta} = 1$ indicates that the element i , which belongs to cluster c_α is the unique element of cluster c_α which has influence on element j which belongs to cluster c_β .
- Given a cluster, c_α , and an element j that belongs to cluster c_β , $x_j^{c_\beta}$, the sum of the unweighted values of the elements which belong to c_α , that have influence on x_j is 1. If any element of c_α has influence on x_j then the sum is 0.

Given $c_\alpha ; x_j^{c_\beta}$

$$\sum_{\substack{k=1 \\ k: x_k \in x^{c_\alpha}}}^N (u_{ij}^{c_\alpha, c_\beta}) \in \{0, 1\} \quad (2)$$

Columns sum, $\sum_{i=1}^N (u_{ij})$, indicates how many clusters have influence on the column element. Identify the components and elements of the network and their relationships.

5. Conduct pair-wise comparisons on the clusters, obtaining $\hat{U} = [\hat{u}_{c_\alpha, c_\beta}]$ the $(G \times G)$ Cluster Weights matrix, with $\hat{u}_{c_\alpha, c_\beta} \in [0, 1]$, $c_\alpha, c_\beta = 1, \dots, G$, where $\hat{u}_{c_\alpha, c_\beta}$ is the influence of cluster c_α , on cluster c_β .
 - $\hat{u}_{c_\alpha, c_\beta} = 0$ shows that any element of cluster c_α has influence on any element of cluster c_β .
 - $\sum_{c_\alpha=1}^G (\hat{u}_{c_\alpha, c_\beta}) = 1$
6. Calculate $W = [w_{ij}^{c_\alpha, c_\beta}]$ the $(N \times N)$ Weighted Super matrix, with $w_{ij}^{c_\alpha, c_\beta} \in [0, 1]$, $c_\alpha, c_\beta = 1, \dots, G$ and $i, j = 1, \dots, N$, where $w_{ij}^{c_\alpha, c_\beta} = u_{ij}^{c_\alpha, c_\beta} \cdot \hat{u}_{c_\alpha, c_\beta}$.
 - $w_{ij}^{c_\alpha, c_\beta}$ is the weighted influence of element i , which belongs to cluster c_α , on element j , which belongs to cluster c_β .
7. Calculate $Q = [q_{ij}^{c_\alpha, c_\beta}]$ the $(N \times N)$ Normalized and Weighted Super matrix, with $q_{ij}^{c_\alpha, c_\beta} \in [0, 1]$, $c_\alpha, c_\beta = 1, \dots, G$ and $i, j = 1, \dots, N$, where $q_{ij}^{c_\alpha, c_\beta} = w_{ij}^{c_\alpha, c_\beta} / \sum_i (w_{ij}^{c_\alpha, c_\beta})$.
 - $q_{ij}^{c_\alpha, c_\beta}$ is the normalized weighted influence of element i , which belongs to cluster c_α , on element j , which belongs to cluster c_β .
 - $\sum_i (q_{ij}^{c_\alpha, c_\beta}) = 1$. Q is a left-stochastic matrix.
8. Raise the weighted super matrix to limiting powers until the weights converge and remain stable ($\text{limit super matrix} = \lim_{k \rightarrow \infty} Q^k$). l_i is the final priority of element x_i . If x_i is an alternative, l_i is the rating of the alternative. If x_i is a criterion, l_i is the weight of the criterion.

B. Association Rules (AR)

Mining of association rules was introduced by Agrawal et al. [6]. An association rule is an expression of $X \Rightarrow Y$, where X is a set of items, and Y is a single item. AR is an initial data exploration approach often applied to extremely

large data sets. It provides valuable information in assessing significant correlations. It has been applied to a variety of fields including medicine and medical insurance fraud detection, business applications, market basket analysis, etc.

Let $I = \{i; i = 1, \dots, m\}$ be a set of literals called items. A database D is a set of transactions, where each transaction t is a set of items such that $t \subset I$. An association rule is an implication of the form $X \Rightarrow Y$, where $X \subset I$, $Y \subset I$, and $X \cap Y = \emptyset$. A transaction t is called to contain X , if $X \subset t$.

Let $Dsupp(X)$ be the fraction of transactions that contain X in a database D . The degree of support for a rule $X \Rightarrow Y$ is defined as $Dsupp(X \Rightarrow Y) = Dsupp(XUY)$.

The degree of confidence for $X \Rightarrow Y$ is defined as $Dconf(X \Rightarrow Y) = Dsupp(XUY)/Dsupp(X)$.

The problem of mining association rules is to find all association rules that have their degrees of support and of confidence no less than the pre-specified minimal support α and the minimal confidence β , respectively. Let π denote the set of all discovered rules; then, $\pi = \{r: X \Rightarrow Y | Dsupp(r) \geq \alpha, Dconf(r) \geq \beta, X \subset I, Y \subset I, \text{ and } X \cap Y = \emptyset\}$ [6, 7].

III. THE PROPOSED APPROACH

Although one of the main tasks of DM tools is discovering novel and hidden rules and patterns from database, in practice, data analyzers face the rules explosion. It is not only complicated to appreciate valuable discovered knowledge, but also some of the available rules have no logical and scientific existence, especially in clinical data analysis.

This paper has proposed to apply group decision making, physicians and other medicine experts' knowledge to avoid this trouble. Generally, ANP is a multiple criteria decision making methodology. A network model in ANP is composed of expert judgments to model an abstract decision problem. Then ANP is integrated with ARM to improve the discovered rules for clinical decision makers in medical diagnosis. The proposed approach includes the following steps:

1. Make a list from all attributes of available cleaned database which can biologically influence target variable based on the experts' knowledge. Suppose that $X = \{x_1, x_2, \dots, x_N\}$ as input attributes to exploit ARM.
2. Cluster and group the attributes based on their common biological property. Suppose $C = \{c_1, c_2, \dots, c_G\}$, where $G < (=) N$.
3. Identify the attributes' relationships, inner dependence and outer dependence of attributes of C together, through the group of decision making. Then make \hat{R} , the relationship matrix, and a network model of the problem.
4. Make pair-wised comparison questionnaires to obtain the importance of each cluster, unweighted super matrix, \hat{U} where its elements is the influence of cluster c_α on cluster c_β through group decision making.
5. Calculate the weighted super matrix of W and Q , the importance (weight) of the attribute j of cluster i and each cluster (see steps 6 and 7, section 2.1).

6. Evaluate the significance of each extracted rule based on network model and inner and outer relationship.
- If a rule includes a relationship among the attributes of two independent clusters, then that rule is ignored.
- If a rule includes a relationship among the attributes of a cluster with no inner-dependence, then that rule is ignored.
7. Aggregate the importance level for the rest of rules which could be calculated by the geometric mean of the importance level of each contained attributes in a rule.

$$IL_k = \left(\prod l_i^{w_i} \right)^{\frac{1}{\sum w_i}} \quad (4)$$

where IL_k is the importance level of rule k , l_i is the final priority of attribute i , x_i , and w_i is the weight of cluster i .

8. Prioritize the discovered rules based on their IL.

Hence, in the proposed method, the information obtained from the ANP is then applied to evaluate ARM and recognize the maximum likelihood $X \Rightarrow Y$. The fact, grouping and summarizing all attributes into a network model help data miner to cluster and understand better the structure of database and the interaction of all attributes. Furthermore, ANP presents an overall structure of all features by experts' judgment, thereby avoiding considering all rules where there are not any rational relationships among attributes.

Meanwhile, this approach is not against producing novel and original rules and patterns, one of the essential data mining tasks; the fact, it just improves the process of discovering rules.

Moreover, by implementing ANP, final rules are prioritized based on aggregating the group decision making of medical experts judgments. It is useful to recognize the importance of rules in addition to their support and confidence, as provided by ARM from the database.

IV. APPLICATION OF THE PROPOSED METHOD IN LABORATORY DATA

In this section, we examine our proposed approach by carrying it out on the medical data. These days, access to huge medicine database and the need to extract useful information are much vital. In this paper, we tried to analyze the database of complete blood count to discover novel and practical rules influential to recognize the condition of cases.

The blood count is the most common screening test for virtually every patient and clearly, it plays an important role in Point-of-Care-testing. A routine complete blood count (CBC) is required as part of the evaluation and includes the red blood cell count, hemoglobin, hematocrit, red cell indices (including MCV, MCHC, and MCH), white blood cell count and its differentiation and plate count [21]. Based on the examination of the blood, the physician is directed toward a more focused assessment of the marrow or systemic disorders that secondarily involve the hematopoietic system.

Hemoglobin (Hb), the main component of the red blood cell (RBC), is a conjugated protein that serves as the vehicle for the transportation of oxygen (O_2) and carbon dioxide (CO_2). Also, the most useful parameter is the MCV. The MCV is the average volume of red cells, expressed in Femtoliters or cubic micrometers. The MCH is the content (weight) of Hb of the average red cell. The value is expressed in pictograms. The MCHC is the average concentration of Hb in a given volume of packed red cells, expressed in g/dL [22, 23].

Leukocytes in the blood serve different functions and arise from different hematopoietic lineages, so it is important to separately evaluate each of the major leukocyte types. By using the typical method, it is possible to quantify lymphocytes, Neutrophils and mixed cells (including Monocytes, basophiles and Eosinophil) [24].

Platelets are small cell fragments adapted to adhere to damaged blood vessels to aggregate one with another, and facilitate the production of fibrin [25].

The cleaned database contains: Patient code, patient age, gender, test code, result, test name, normal rang, low and high critical range for the factors of: W.B.C, R.B.C, Hb, Hct, MCV, MCH, MCHC, Platelets, Lymphocytes, Neutrophil, and Mixed (Mono & Eos & Bas). Based on the knowledge of the experts, attributes of patient code, test code, and test name were ignored.

The main objective in this study was to discover significant, reliable and novel rules from CBC register. By implementing ARM, about 240 rules were obtained while it was clear that extracting information from these rules was a complex task.

Then, by implementing the proposed approach, the influenced attributes were organized into some groups. The following groups were revealed in table I, where $X = \{Platelets, Age, Gender, W.B.C, Lymphocytes counts (LC), Neutrophil counts (NC), R.B.C, Hb, Hct, MCV, MCH, MCHC\}$ and $C = \{Platelets, Other Measures, White Blood Measures, Red Blood Measures\}$.

Then, based on the inner and outer interdependences of the grouped attributes, the structure of the network model was in Fig. 1.

TABLE I. GROUPING OF BLOOD FACTORS

Platelets	Platelets					
Other Measures	Age	Gender				
White Blood Measures	W.B.C	Lymphocytes counts	Neutrophil counts			
Red Blood Measures	R.B.C	Hb	Hct	MCV	MCH	MCHC

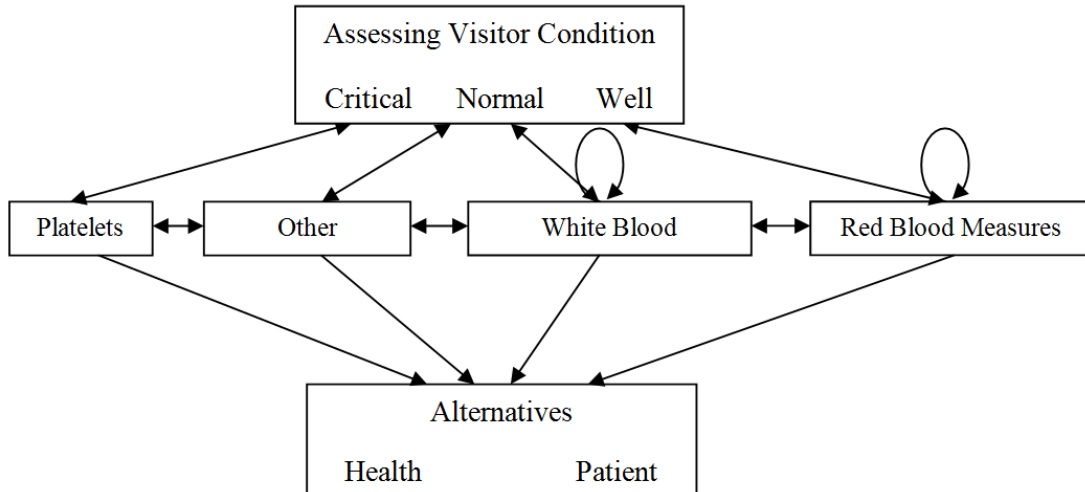


Fig. 1. ANP model used to select the influenced blood factors for assessing the patient

Subsequently, in each assessing level of case condition, we should make a pair-wised comparison of groups and all influenced attributes to determine the importance of each group (c_i) and each attribute (x_j) grouped in c_i on target variable through group decision making. In this application, we have gotten almost 11 pairwised comparison sheets for every expert. For example, if visitor have a critical situation, then the group importance is in table II.

TABLE II. THE PAIRWISED COMPARISON OF THE CLUSTERS IN CRITICAL CONDITION

Critical condition	Platelets	White Blood Measures	Red Blood Measures	Other Measures
Platelets	1	1/5	1/7	1/2
White Blood Measures	5	1	1/2	5
Red Blood Measures	7	2	1	5
Other Measures	2	5	1/5	1

Then, to calculate super matrix of Q , the importance (weight) of each cluster and attribute j of cluster i should be calculated by normalized Eigen vector. The part of super matrix, the weights of the clusters in critical situation, can be seen in table III (w_i).

TABLE III. CLUSTERS WEIGHTS

	Platelets	White Blood Measures	Red Blood Measures	Other Measures
Assessing patient=C	0.042	0.299	0.382	0.277

Therefore, in this case, the Q is a supper matrix with 11 parts and each part has different dimensions depending on its element.

Hence, by using the ANP information, as mentioned in section 3, to make AR, we considered RBC, Hb, Hct and MCV

and disregarded MCH and MCHC; also, association rules between age and sex were ignored. Then, about 23 remaining rules were prioritized where confidences being greater than 60 percent. Moreover, the decision maker's team confirmed that the extracted rules were reasonable, almost interesting and practical. For example:

IF ((404.00 < NC <= 744.50) (HB <= 186.00) (Plate <= 476500.00) (200.50 < LC <= 505.00) (297.00 < RBC) (28.00 < HCT)) THEN (patient = h)

where support=25% and confidence=100%. The useful result from Q calculation is in the calculation of importance level (IL) of each rule by the geometric mean. In this rule, we have IL=18%, where it has the 5th rank among 23 rules.

While this model effectively incorporates qualitative and quantitative measures into the evaluation process, its efficacy depends on the accuracy and the value of judgment provided by the clinical decision making team. The full involvement of the relevant decision makers would help to utilize their experience and expertise in a clinical decision making process.

V. CONCLUSION

Based on the recent studies, this was the first attempt to apply ANP model in the process of ARM in the context of CDM. ANP has the ability to be used as a decision making analysis tool since it incorporates feedback and interdependent relationships among decision criteria and alternatives. In addition, evaluation and selection of novel and reasonable rules can be very useful in both academic research and practice for decision makers. In this paper, organizing all features and summarizing them in a network model helped to group and identify the structure of database through medical experts' knowledge. Furthermore, this approach helped decision makers to avoid considering all rules where there were not any rational relationships between them, thereby strengthening the results. To validate the proposed approach could be effective for clinical decision making, it is exploited the database of complete blood count. The results presented the more influential and practical rules to recognize the condition of cases. Finally, this study is suggested applying more MCDM

methods in DM process, especially for the assessment of results.

REFERENCES

- [1] T.T. J. Chong, V. Bonnelle, and M. Husain, "Quantifying motivation with effort-based decision-making paradigms in health and disease," *Progress in Brain Research*, In Press, Corrected Proof, Available online 7 July 2016, <http://dx.doi.org/10.1016/bs.pbr.2016.05.002>.
- [2] P. Cerrito, "Clinical Data Mining for Physician Decision Making and Investigating Health Outcomes: Methods for Prediction and Analysis," *IGI Global*, 2010.
- [3] Y. Li, Y. Zhang, and Y. Ji, "Privacy-preserving restricted boltzmann machine," *Computational and Mathematical Methods in Medicine*, Vol 2014, <http://dx.doi.org/10.1155/2014/138498>.
- [4] T.P. Exarchos, G. Rigas, A. Bibas, D. Kikidis, C. Nikitas, F.L. Wuyts, et al., "Mining balance disorders' data for the development of diagnostic decision support systems," *Computers in Biology and Medicine*, vol. 77, pp. 240-248, 1 October 2016.
- [5] F. Bagherzadeh-Khiabani, A. Ramezankhani, F. Azizi, F. Hadaegh, E. W. Steyerberg, and D. Khalili, "A tutorial on variable selection for clinical prediction models: feature selection methods in data mining could improve the results," *Journal of Clinical Epidemiology*, vol. 71, pp. 76-85, March 2016.
- [6] R. Agrawal and R. Srikant, "Fast algorithms for mining association rules," *Proceedings of the 20th International Conference on Very Large Databases*, Santiago, Chile, Expanded version available as IBM Research Report RJ9839, 1994.
- [7] J. Han, M. Kamber, and J. Pei, "Data Mining", 3rd Edition, Elsevier Pub, 2012.
- [8] A. Babashzadeh, M. Daoud, and J. Huang, "Using semantic-based association rule mining for improving clinical text retrieval," *Health Information Science*, vol. 7798, pp. 186-197, 2013.
- [9] T. P. Hong, G. C. Lan, J. H. Su, P. S. Wu, and S. L. Wang, "Discovery of temporal association rules with hierarchical granular framework," *Applied Computing and Informatics*, vol. 12, no 2, pp. 134-141, July 2016.
- [10] R. Marois and J. Ivanoff, "Capacity limits of information processing in the brain," *TRENDS in Cognitive Sciences*, vol. 9, no. 6, pp. 296-305, 2005.
- [11] B. Whitworth, "Some implications of comparing brain and computer processing", *Proceedings of the 41st Hawaii Int Conf on Sys Sciences*, IEEE, 2008.
- [12] S. We, L. Zhang and B. Yang, "Two approaches to incorporate clinical data uncertainty into multiple criteria decision analysis for benefit-risk assessment of medicinal products," *Value in Health*, vol. 17, no.5, pp. 619–628, 2014.
- [13] H. Liu, J. You, C. Lu, and Y. Chen, "Evaluating health-care waste treatment technologies using a hybrid multi-criteria decision making model," *Renewable and Sustainable Energy Reviews*, vol. 41, pp. 932–942, 2015.
- [14] M. Shafii, S. Rafiee, F. Abooe, M. A. Bahrami, M. Nouhi, F. Lotfi, and K. Khanjankhani, "Assessment of service quality in teaching hospitals of Yazd university of medical sciences: using multi-criteria decision making techniques," *Osong Public Health and Research Perspectives*, vol. 7, no. 4, pp. 239-247, August 2016.
- [15] V. Belton and T. J. Stewart, "Multiple Criteria Decision Analysis," Kluwer Academics Pub. 2002.
- [16] T. L. Saaty, "Theory and Applications of the Analytic Network Process: Decision Making with Benefits, Opportunities, Costs, and Risks," RWS Publications, Pittsburg, 2005.
- [17] D. Ergu and Y. Peng, "A framework for SaaS software packages evaluation and selection with virtual team and BOCR of analytic network process," *The Journal of Supercomputing*, vol. 67, no. 1, pp. 219-238, 2014.
- [18] M. Nilashi, H. Ahmadi, A. Ahani, R. Ravangard, and O. Ibrahim, "Determining the importance of hospital information system adoption factors using Fuzzy analytic network process (ANP)," *Technological Forecasting and Social Change*, vol. 111, pp. 244-264, October 2016.
- [19] T. L. Saaty, "Decision Making in Complex Environments: The Analytic Hierarchy Process (AHP) for Decision Making and the Analytic Network Process (ANP) for Decision Making with Dependence and Feedback," RWS Publications, Pittsburgh, 2003.
- [20] J. Figueira, S. Greco, and M. Ehrgott, "Multiple criteria decision analysis: state of art survey," Springer, 2005.
- [21] D. Burnett and J. Crocker, "The science of laboratory diagnosis," 2th ed., Hoboken, John Wiley & Sons Ltd, 2005.
- [22] V. F. Fairbanks, "Nonequivalence of automated and manual hematocrit and erythrocyte indices," *American Journal of Clinical Pathology*, vol. 73, no.1, pp. 55-62, 1980.
- [23] T. C. Pearson, and D. L. Guthrie, "Trapped plasma in the microhematocrit," *American Journal of Clinical Pathology*, vol. 78, no. 5, pp. 770-772, 1982.
- [24] W. H. Coulter, "High speed automatic blood cell counter and cell size analyzer," *Proceeding of National Eleceteronic Conferance*, vol. 12, pp. 1034-1040, 1956.
- [25] M. F. Buckley, J. W. James, D. E. Brown, G. S. Whyte, M. G. Dean, C. N. Chesterman, and J. A. Donald, "A novel approach to the assessment of variations in the human platelet count," *Thromb Haemost*, vol. 83, pp. 480–484, 2000.

A Novel Position-based Sentiment Classification Algorithm for Facebook Comments

Khunishkah Surroop

Computer Science & Engineering
Department
Faculty of Engineering
University of Mauritius
Reduit, Mauritius

Khushboo Canoo

Computer Science and Engineering
Department
Faculty of Engineering
University of Mauritius
Reduit, Mauritius

Sameerchand Pudaruth*

Ocean Engineering & ICT
Department
Faculty of Ocean Studies
University of Mauritius
Reduit, Mauritius

Abstract—With the popularization of social networks, people are now more at ease to share their thoughts, ideas, opinions and views about all kinds of topics on public platforms. Millions of users are connected each day on social networks and they often contribute to online crimes by their comments or posts through cyber bullying, identity theft, online blackmailing, etc. Mauritius has also registered a surge in the number of cybercrime cases during the past decade. In this study, a trilingual dataset of 1031 comments was extracted from public pages on Facebook. This dataset was manually categorized into four different sentiment classes: positive, negative, very negative and neutral, using a novel sentiment classification algorithm. Out of these 1031 comments, it was found that 97.8% of the very negative sentiments, 70.7% of the negative sentiments and 77.0% of the positive sentiments were correctly extracted. Despite the added complexity of our dataset, the accuracy of our system is slightly better than similar works in the field. The accuracy of the lexicon-based approach was also much higher than when we used machine learning techniques. The outcome of this research work can be used by the Mauritius Police Force to track down potential cases of cybercrime on social networks. Decisive actions can then be implemented in time.

Keywords—sentiment analysis; Facebook; cybercrime; emoticons

I. INTRODUCTION

The 21st century evokes the magical era of technological advancements amongst which are the evolution of social media sites. People share their thoughts, ideas, opinions, views, knowledge and experiences on platforms such as blogs, social networks, news portals, travel sites and wikis.

“Sentiment analysis, also called opinion mining, is the field of study that analyzes people’s opinions, sentiments, evaluations, appraisals, attitudes, and emotions towards entities such as products, services, organizations, individuals, issues, events, topics, and their attributes.” [1]. Thus, sentiment analysis is a technique that focuses on the detection of favourable and unfavourable opinions about specific subjects. Sentiment analysis usually involves the extraction of sentiments hidden in users’ public texts which they publish on online platforms. In recent years, we have seen people sharing their opinions in diverse fields such as marketing, politics, religion, books, movies, sports, health, etc. This increase in online activities have also led to a consequential rise in the number of scams, cyber bullying, cyberaggression, blackmails,

identity theft, promotion of terrorism and cyber harassment cases. The words and expressions used by users can reveal their intention (sentiment) and therefore necessary measures can be taken to reduce the impact of negative comments. Sentiment Analysis can help to recognize people’s emotions and display the polarity of the comments and help in the making of safer online platforms.

The viral power of online media has proven that threats can be spread within seconds. For example, if anyone is publicly criticizing or judging any other religion, these comments and responses can spread within minutes and after only a very short while can lead to cyber-aggression between Face bookers. As a consequence, these comments could rapidly and easily create social instability in the country. Facebook has become the ideal platform to commit all types of cybercrimes.

Bullying has also taken new dimensions as it has become so easy to create a fake account on Facebook, target a victim, update your status and wait for the awful comments that even people unknown to the victim would be posting about him. This may induce serious damage to the latter’s mental health. For example, a boy who was cyberbullied died as the insults which he received caused a strong emotional stress which he could not digest [2]. On the 5th of September 2015, Mauritians had witnessed a vague of tension that befell over the country due to a racial riot [3]. This particular case was further dramatized by some surfers against racial and religious harmony who opinioned about the matter in a negative way that intimidated people from different ethnicities and this could cause a serious civil conflict in the country.

There are many pending cybercrime cases that the investigators of the Cybercrime Unit (CCU) of Mauritius are scrutinizing [4]. A list of some of the recently reported cases of cybercrime in Mauritius has been provided in Appendix A. Despite the fact that many cases of cybercrime are identified and reported to the Cybercrime Unit, it is a hectic job for investigators to read all the comments, sometimes in thousands and analyze one by one to find potential offenders.

Thus, in this work, we have developed a sentiment analysis tool for the detection of potential threats prevailing on Mauritian Facebook pages. This tool enabled us to process all posts and comments that are extracted from specific pages on Facebook. An analysis of those texts has been done by filtering the useful keywords that could determine the sentiment of the

text and neglect those that are not important. And finally, a classification is done whereby the sentiment of the text is classified as either positive, negative, very negative or neutral.

The language of the texts has also been taken into consideration. They were classified as Creole, English or French. Face bookers also express their emotions by means of animated facial expressions which are known as emoticons. The value of these emoticons has also been assessed. Furthermore, our tool can save the investigators from long hours of hectic work of reading and analyzing thousands of comments which are posted daily on public pages in Facebook. Instead, this tool will highlight only those comments which require immediate attention and where potentially immediate actions may be taken.

The rest of the paper is discussed as follows: Section II focuses on the previous work carried out by researches worldwide. Our proposed approach is described in Section III. Section IV evaluates the tool based on the manual classification. Finally, Section V concludes the study and mentions the future works.

II. RELATED WORKS

Sentiment analysis has been an active field of research since the last decade. However, with the unprecedented growth in the amount of unstructured texts that is being generated online, the field of sentiment analysis is gaining more popularity and is increasingly becoming more important for decision making in large businesses, governmental organizations and many others. However, the increasing usage of social networks has also brought with them new types of social problems and many of them can be categorized as cybercrimes.

Dinakar et al. (2011) emphasized the importance of tracking those harmful comments communicated on the web. They made use of 4500 YouTube comments and classified the data into three areas of bullying based on intelligence, race and culture and sexuality. An overall accuracy of 76% was obtained by using the SMO (Sequential Minimal Optimization) technique [5]. An interesting study by Gerber (2014) analyzed tweets tagged with spatio-temporal information in order to predict crime. Gerber found that the proposed technique was able to improve crime detection for 19 out of the 25 crime types he studied [6].

Bolla (2014) used sentiment analysis techniques to demonstrate that crimes can be detected almost in real-time from social media. He analyzed one hundred thousand tweets from different cities in the United States to determine the crime intensity in each region. It turned out that there was a high correlation with real-life events [7]. Lin (2014) analyzed 180 million tweets after the Boston Marathon bombing events in order to understand how twitter users from 25 major cities expressed fear and/or comfort. He concluded by suggesting that his system could be used to predict perceived threats in the event of natural or man-made disasters [8].

Chen et al. (2012) used comments made on YouTube videos to detect offensive language. They used a combination of lexical and syntactic features to improve the performance of their classifier. They also analysed the writing styles of a

sample of users in order to predict their likeliness to send out offensive content. More recently, Krishna (2014) used comments associated with YouTube videos to demonstrate that it is possible to correlate users' sentiments with real-world events especially for popular events or personalities [9][10].

Qin Li (2015) analyzed the accuracy of the sentiment classifiers provided by four different companies involved in online brand monitoring. He found that most of the commercial classifiers cannot deal with negation, emotions and noisy language [11]. Jurek et al. (2015) smart sentiment classification algorithm considers both the presence of negation words and intensity modifiers. They proposed a new approach to determine the overall polarity of a comment when both positive and negative words are present in that comment. However, their approach did not bring significant improvements and can be used only for short sentences. In a previous work, they had used this tool to estimate the level of public disorder in public events by analysing sentiments in tweets [12][13].

Hosseini mardi et al. (2015) analyzed text comments and images from Instagram to detect incidents of cyberaggression and cyber bullying using machine learning techniques such as support vector machines and logistic regression. They obtained a recall of 79% and a precision of 71% from text comments. For non-text features, the recall was slightly lower at 76% and the precision at 62% [14].

Xu et al. (2012) have detected traces of bullying on the Twitter micro-blogging platform. Their tasks consisted of obtaining traces via the twitter streaming API to find an instance of the word "bully" in tweets and build an eight classes text classifier based on pre-defined emotion classes [15]. Henri et al. (2012) showed that it is possible to predict real-world threats by extracting abnormalities in tweets [16]. Zhang et al. (2011) predicted text sentiments by using machine learning method to build a web-based system called SES. They conducted their experiments on Facebook comments and tweets using four different machine learning models [17].

While previous works have concentrated on finding cyber bullying instances from only one social network, Dadvar et al. (2012) suggest that using information collected from multiple social networks can improve the tracking and prediction of cyber bullying. They have also incorporated gender as a feature which they believe to have increased the defective accuracy. Their main dataset was collected from the MySpace social network [18]. Via a carefully designed Facebook experiment, Anderson et al. (2014) demonstrated that if a third-party provides support to a victim of cyber bullying through a dissenting comment, this encourages other people to provide support and empathy for the victim [19].

While many studies mentioned about how to detect instances of cybercrime, most of them did not explain how this information can be used. Cohen et al. (2014) proposed a safer internet by identifying cyber bullying from Facebook comments and trying to mitigate it by informing the relevant institutions in order to provide assistance to those being bullied. They understood that while technology has made bullying easier and faster, they also proposed that the same technology be used to detect and report such offences [20].

From the analysis of about 7300 tweets related to cyber bullying, Alim (2015) found that a significant minority of users are using tweets for reporting cyber bullying cases and for providing advice to victims, parents or school administrators [21]. Duwairi et al. (2014) has developed a framework to analyze tweets in Arabic dialects and Arabizi. Their proposed framework can handle repetitions, emoticons and negation. The highest accuracy achieved was 76.8% when using the Naïve Bayes classifier. Lexicon expansion through the use of synonym has a drawback of the wording losing its primary meaning after a few recapitulations [22][23].

Troussas et al. (2014) classified Facebook status messages into positive and negative sentiments using three different classifiers. They found that the Naïve Bayes classifier had the highest precision (77%) while the Rocchio classifier had the highest recall (73%) and both classifiers outperformed the Perceptron classifier [24].

In order to detect changes in emotions in Facebook messages, Ortigosa et al. (2013) used a combination of machine learning techniques and hand-crafted lexicons to achieve an overall accuracy of 85% [25]. Agarwal et al. (2011) made use of parts-of-speech (POS) features on tweets which allowed them to use a smaller set of features to achieve similar level of performances as reported in similar works [26]. However, Kouloumpis et al. (2011) concluded that POS features may not be useful at all for classification of tweets [27].

There have been multiple previous works dealing with the number of likes, types of emoticons used or hash tags to predict the emotions or opinions of people based on datasets extracted from Twitter and Facebook. However, these experiments were limited to sentiment classification using the English dictionary only, rather than dealing with sentiments in a multilingual setting dealing with cybercrime. Moreover, there is no research that has been carried out in Mauritius to deal with issues of cybercrimes in the Creole language.

III. METHODOLOGY

Our approach consists of three steps namely data extraction, data processing and data classification. In addition to this, we have catered for colloquial words written differently by different users.

A. Data Extraction

The dataset was extracted using the Facepager tool [29]. Facepager is a tool for fetching data that is publicly available from Facebook and Twitter. All the extracted data are saved in an SQLite database and may also be exported to a csv file. Our dataset consists of comments extracted from different posts including videos, pictures and links. The trilingual dataset consists of 1031 comments each having English, French and Creole words together.

B. Data Processing

The next step is to process and clean the data. The raw data is practically unreadable due to the presence of extra information such as punctuations and other symbols. Tokenization is first applied to break the sentences into distinct words. In the process, emoticons have also been captured. Our

work comprised of finding a link between what people write and what their smileys tend to depict.

1) Emoticons Lexicon

Our tool captured emoticons and displayed them as texts. We assessed the same post in two different desktop computing platforms (Microsoft Windows and Ubuntu) and two different mobile platforms (iOS and Android). It was found that comments from iOS and Android mobile phones generated the same kind of symbols and symbols from the desktop platforms were also similar but were different from each other. However, we noticed that there is a lack of correlation between the sentiments expressed in the text of a comment and the emoticons that are associated with it. Thus, these emoticons are not considered further in this paper.

TABLE I. EMOTICONS FROM DIFFERENT COMPUTING PLATFORMS

Emoticon	Sentiment	Windows/Ubuntu	iOS/Android
	Smile	::)	☺~\$
	Sad	::(☺~'
	Cry	::(☺~¢
	Kiss	::*	☺~
	Confused	::/	☺~
	Laughing	::D	☺~,,

2) Dictionaries

We made use of six dictionaries namely the Creole dictionary containing 3063 Creole words, the English dictionary containing 110 206 English words, the French dictionary containing 336 534 French words, the Positive Words dictionary containing 977 words, the Negative Words dictionary containing 1344 words and the Very Negative Words dictionary containing 200 words. These 200 words are highly offensive and cannot be ignored even if they are preceded by a negation word. Examples of such words are: terrorism, kill, drugs, etc. The last three dictionaries contain words in all the three languages.

3) Language Classification Algorithm

The trilingual dataset consisted of comments having English, French and Creole words extracted from Facebook pages in Mauritius such as L'Express, Le Défi Media and IslandCrisis (Appendix A).

The Language Classification algorithm work as follows. If 30% of the words in a post are in the Creole language or if the number of Creole words is greater or equal to the number of English and French words, the language of the post is classified as Creole. This percentage is calculated by taking the number of Creole words in the post and dividing it by the total number of words in the post. If the number of French words is greater than the number of Creole and English words, the language is classified as French. Finally, if the number of English words is greater than the number of French and Creole words, the

language is classified as English otherwise the language is classified as Other. An example of a post is provided below.

"Its dumb zat an IT specialist wud do such a thing zat 2 frm his own cyber cafe!!Someone dignity is at stake. Eski gouvermen pou dedommage li si li inocen!!ki pu arriv so réputation?"

Creole words: 'Eski', 'gouvermen', 'pou', 'li', 'si', 'li', 'inocen', 'ki', 'pu', 'arriv', 'so'.

English words: 'Its', 'dumb', 'zat', 'an', 'specialist', 'wud', 'do', 'such', 'thing', 'zat', 'frm', 'his', 'own', 'cyber', 'Someone', 'dignity', 'is', 'at', 'stake'.

French words: 'cafe', 'réputation', 'dedommage'.

There are 11 Creole words, 19 English words and 3 French words in this post. The percentage of Creole words in this post is 33.3% and since this is over 305, the post would be classified as being in the Creole language. Words containing only one character are not considered in the calculation.

4) The Mean Algorithm for Sentiment Classification

The Mean Algorithm starts by determining the position of each positive and negative word in a comment. The Mean Positive Score is calculated by taking the sum of all the position of each positive word and dividing it by the total number of positive words. Similarly, for the Mean Negative Score, the sum of all the negative words indexes is calculated and it is divided by the total number of negative words.

If the Mean Positive Score exceeds the Mean Negative Score, the sentiment will be positive. Furthermore, if the Mean Negative Score exceeds or is equal to the Mean Positive Score, the sentiment will be negative otherwise the sentiment is assumed to be neutral. An example is illustrated below:

"Li ene zoli garson. Li ena talen. mai li movai.", which means, "He is a handsome boy. He has talent but he is bad.", in English.

TABLE II. INDEX OF WORDS IN SENTENCE: MEAN ALGORITHM

Index	Creole Word	English Word	Sentiment
1	Li	He	
2	ene	is	
3	zoli	handsome	positive
4	garson	boy	
5	Li	He	
6	ena	has	
7	talen	talent	positive
8	mai	but	
9	li	he	
10	movai	bad	negative

Applying the mean algorithm, the Mean Positive Score is calculated as $(=3+7)/2$ resulting in a score of 5 and the Mean Negative Score is calculated as $(=10)/1$ resulting in a score of 10. The sentiment of this sentence is classified as Negative as the Mean Negative Score exceeds the Mean Positive Score.

5) The Adaptive Algorithm for Sentiment Classification

This algorithm works only in the presence of modifiers such as 'not', 'pa', etc., in a sentence. These modifiers have the effect of reversing the sentiment of the word immediately following them. This algorithm works in the same way as the

Mean Algorithm except that it reverses the polarity of the word if it is preceded by a negation word. For example; "*He is not bad.*" is a positive sentence since 'not' reversed 'bad' into a positive word. An example in Creole is illustrated as shown below:

"Li zourer bouku mai selma li pa mover.", which means "He swears a lot but he is not bad.", in English.

TABLE III. INDEX OF WORDS IN SENTENCE: ADAPTIVE ALGORITHM

Index	Creole Word	English Word	Sentiment
1	Li	He	
2	zourer	swears	negative
3	bouku	a lot	
4	mai	but	
5	selma	but	
6	li	he	
7	pa	not	
8	mover	bad	negative

This sentence contains the 'pa' modifier which means 'not' in English and is followed by a negative word 'mover'. Therefore, the modifier reverses the sentiment into a positive one. Using a naive sentiment classifier, this comment would have been classified as negative because the number of negative words exceeds the number of positive words.

Using the mean algorithm, the result will be negative as the Mean Negative Score which is $5 (=2+8)/2$ exceeds the Mean Positive Score which is 0. Using the adaptive algorithm, the Mean Positive Score will be 8 and the Mean Negative Score will be 2 resulting in having an overall positive sentiment, which is a more appropriate classification for this post.

C. Data Classification

After processing the data, sentiments were assigned to 3 different levels: (i) word-level sentiment in which each word in each comment is assigned a polarity, (ii) comment-level sentiment in which each comment from each post is assigned a polarity, and finally, (iii) post-level sentiment whereby each post on chosen pages is assigned a polarity.

The number of positive, negative and very negative words was also calculated during the process. The number of comments in a post was also noted and the number of words categorized under each language was also done. A further level of classification for the *very negative* category has also been implemented. It has been further classified into 7 categories namely Accident, Crime, Cyber bullying, Drug, Racism, Terrorism and Other.

IV. EVALUATION AND DISCUSSION

Three independent annotators were asked to manually classify the data. Because of different responses from the three annotators, it was necessary for us to assign a final sentiment or language to the comments by using the simple majority rule. In a scenario where one annotator classifies a comment as neutral, another one as positive and the third one as negative, the comment is assumed to be negative.

A. Evaluation of Language Classification Results

An attempt was made to classify each comment into an appropriate language. The highest accuracy was obtained for

the English language, possibly because of the big size of the dictionary. The accuracy of the Creole language was also very high. An overall accuracy of 90.9% was obtained for the whole dataset.

TABLE IV. PERCENTAGE ACCURACY FOR EACH LANGUAGE

Language	Manual Categorization	Automatic Classification	% Accuracy
Creole	696	647	93.0
English	220	216	98.2
French	106	74	69.8
All Three	1031	937	90.9

Some comments that were not properly categorised was due to the use of slangs that were not present in our dictionaries. For example, some people had different ways of writing “good” so all possibilities could not be captured. A lower accuracy was registered for the French language as many of the French words are very similar to the Creole words and are thus classified into the Creole language.

B. Evaluation of Sentiment Classification Results

In this section, the trilingual dataset has been evaluated on their sentiment classification using the adaptive algorithm.

TABLE V. PERCENTAGE ACCURACY FOR SENTIMENT CLASSIFICATION

Sentiment	Manual Categorization	Automatic Classification	% Accuracy
Negative	362	256	77.0
Positive	300	231	70.7
Very Negative	93	91	97.8
Neutral	276	220	79.7
All Four	1031	798	77.4

It was found that 798 comments were properly classified out of the 1031 comments with an overall accuracy of 77.4 % for the sentiment classification.

An accuracy of 97.8% for the *very negative* category will prove to be highly beneficial for this study as the main aim of our work was to identify potential threats on social networks. A lower accuracy was registered for the *negative* sentiment category because of the sarcastic comments that were correctly classified by the human annotators but the algorithm could not recognize them as such.

Sanchez and Kumar (2013) classified Twitter messages using a lexicon of commonly used terms of abuse, which was itself extracted from Twitter. These messages were then classified as either positive or negative. An overall accuracy of 70 % was obtained [28]. Compared to their work, our tool managed to classify comments into four sentiments with a better accuracy of 77.4%. Moreover, we made use of a dataset that consisted of comments written in three different languages. Facebook comments are usually more noisy and lengthy than tweets and people tend to be more informal on Facebook than on Twitter. The adaptive algorithm gave more accurate and precise results than a naive frequency-based sentiment classifier (69.9%) and the mean algorithm (72.4%).

C. Evaluation of Very Negative Sentiments

It was found that 69 comments were probably classified out of the 93 comments. An overall accuracy of 74.2% was obtained.

TABLE VI. ACCURACY OF VERY NEGATIVE SENTIMENTS

Threats	Manual Categorization	Automatic Categorization	% Accuracy
Accident	14	8	57.1
Crime	23	16	69.6
Cyberbullying	5	3	60.0
Drugs	8	7	87.5
Racist	7	6	85.7
Terrorism	27	23	85.2
All Seven	93	69	74.2

The main problem that was encountered was due to the Creole language as it is a language without a universally agreed syntax and grammatical rules. It would not be exaggerated to say that each and every Mauritian has their own unique ways of writing the Creole language. And, therefore, it is very challenging to cater for such a high degree of variability in a language. Furthermore, most Mauritians tend to comment on Facebook in a colloquial manner which sometimes is an amalgam of different languages, all in one sentence only, and this adds another layer of complexity in the classification.

D. Machine Learning Algorithms

To understand the performance and reliability of our proposed algorithm, we also classified the dataset using two well-known machine language algorithms namely the Naïve Bayes and the k-Nearest Neighbour (k-NN) classifiers.

1) Naïve Bayes Classifier

The overall accuracy of the Naïve Bayes classifier for sentiment classification is 45.2%. The highest recall (63.0%) and precision (57.3%) was for the *negative* sentiment. Surprisingly, both the recall and the precision values for the *very negative sentiment* were very low at only 33.3% and 15.4%, respectively. One reason for this is the much lower number of training instances for this category compared to the others. In general, the accuracies for each lower was quite low because the instances from the *neutral* category was uncorrected predicted into the other three categories.

TABLE VII. PERCENTAGE ACCURACY FOR SENTIMENT CLASSIFICATION

Predicted	True Negative	True Positive	True Very Negative	True Neutral	Precision
Negative	228	67	41	62	57.3%
Positive	57	131	13	55	51.2%
Very Negative	48	39	31	83	15.4%
Neutral	29	63	8	76	43.2%
Recall	63.0%	43.7%	33.3%	27.5%	

The overall accuracy of the Naïve Bayes classifier for language classification is 84.6%. The classifier does a much better job at the classification of language than sentiments. The accuracy for the Creole and English are very high (89.1%). The accuracy for the French is probably lower because of the lesser

number of training instances compared to the two others.

TABLE VIII. PERCENTAGE ACCURACY FOR LANGUAGE CLASSIFICATION

Predicted	True Creole	True English	True French	True Other	Precision
Creole	640	31	45	2	89.1%
English	21	172	0	0	89.1%
French	25	9	56	3	60.2%
Other	10	8	5	4	14.8%
Recall	92.0%	78.2%	52.8%	44.4%	

2) K-Nearest Neighbour Classifier

It was found that the overall accuracy for the sentiment classification using the k-Nearest Neighbour (k-NN) was 47.8% which was better than the overall accuracy of the Naïve Bayes classifier. The k-NN classifier also produced much better results for the *very negative* and *neutral* sentiment categories. However, Naïve Bayes outperformed k-NN for the *positive* and *negative* sentiments.

TABLE IX. PERCENTAGE ACCURACY FOR SENTIMENT CLASSIFICATION

Predicted	True Negative	True Positive	True Very Negative	True Neutral	Precision
Negative	165	47	26	66	54.3%
Positive	67	178	16	78	52.5%
Very Negative	26	7	27	9	39.1%
Neutral	104	68	24	123	38.6%
Recall	45.6%	59.3%	29.0%	44.6%	

The overall accuracy for the language categorization was 78.5%. Thus, the k-NN classifier could not match the more accurate results of the Naïve Bayes algorithm. Only the precision for the Creole language and recall for the French language was slightly better.

TABLE X. PERCENTAGE ACCURACY FOR LANGUAGE CLASSIFICATION

Predicted	True Creole	True English	True French	True Other	Precision
Creole	567	34	23	1	90.7%
English	48	166	5	1	75.5%
French	51	8	71	2	53.8%
Other	30	12	7	5	9.3%
Recall	81.5%	75.5%	67.0%	55.6%	

3) Machine Learning v/s The Adaptive Algorithm

In this section, we compare the results obtained from using the adaptive algorithm which we have proposed with two traditional machine learning algorithms. The results are presented in Table XI and Table XII. The precision values have been used for the comparisons.

TABLE XI. PERCENTAGE ACCURACY FOR SENTIMENT CLASSIFICATION

Sentiment	% Accuracy of Novel Algorithm	% Accuracy of Naïve Bayes	% Accuracy of k-NN
Negative	70.7	57.3	54.3
Positive	77.0	51.2	52.5
Very Negative	97.8	15.4	39.1
Neutral	79.7	43.2	38.6
Overall	77.4	45.2	47.8

From Table XI, we observe that the adaptive algorithm outperforms both the Naïve Bayes and the k-NN algorithms in all the four sentiment categories.

TABLE XII. PERCENTAGE ACCURACY FOR LANGUAGE CLASSIFICATION

Sentiment	% Accuracy of Novel Algorithm	% Accuracy of Naïve Bayes	% Accuracy of k-NN
Creole	93.0	89.1	90.7
English	98.2	89.1	75.5
French	69.8	60.2	53.8
Overall	86.8	84.6	78.5

From Table XII, again, we observe that the adaptive algorithm outperforms both the Naïve Bayes and the k-NN algorithms in all the three language categories. Thus, in this paper, we have developed a new polarity assignment technique and we have shown that it performs much better than naïve frequency-based sentiment classifiers and machine learning algorithms. We believe that with more customization of the dictionaries and a larger dataset, it is possible to further improve the overall accuracies of the system.

V. CONCLUSIONS

Due to the rise of cybercrimes, it has become essential for the government to monitor online activities on social networks. Thus, this paper aimed at developing sentiment analyzers to detect potential threats on social networks. After investigating about cybercrime and sentiment analysis related topics, the sentiment analyzer was built using different tools. A novelty aspect of our paper is the sentiment analysis of Creole texts from Facebook, in addition to French and English comments. Another contribution is the analysis of emoticons from different platforms. We have used four different emotion classes compared to most researchers who have used only two. Hierarchical classification of the most serious threats has also been implemented. We also investigated three different algorithms for the classification of comments into an appropriate sentiment class. We also showed that the adaptive algorithm we have proposed produced much better results than machine learning algorithms. This work can be improved by doing the analysis in real-time and communicating the relevant results to the relevant authorities. Using a larger dataset and larger dictionaries will also help to improve the accuracy.

REFERENCES

- [1] Liu, B. *Sentiment Analysis: Opinion Mining, Sentiments and Emotions*. Cambridge University Press, 2012.
- [2] Lexpress.mu. "Cyberbullying: Akash Callikan porte plainte à la cybercrime unit," *Lexpress.mu*, Mar. 16, 2014.
- [3] Hibz, Y. D. "Online Racial Hatred Incitement: Police Elaborated a List of 30 Suspects," *Island Crisis*, Sept. 8, 2015.
- [4] Lexpress.mu. "Cybercrime Unit: dans l'univers des enquêteurs du virtuel," *Lexpress.mu*, Oct. 10, 2015.
- [5] Dinakar, K., Reichart, R. and Lieberman, H., "Modeling the Detection of Textual Cyberbullying," in *The Social Mobile Web (ICWSM) Workshop*, Barcelona, Spain, 2011, pp. 11-17.
- [6] Gerber, M. S., "Predicting Crime Using Twitter and Kernel Density Estimation," *Decision Support Systems*, vol. 61, pp. 115-125, 2014.
- [7] Bolla, R. A., "Crime pattern detection using online social media," M.S. thesis. Missouri University of Science and Technology, USA, 2014.
- [8] Lin, Y. R., "The Ripples of Fear, Comfort and Community Identity During the Boston Bombings," in *iConference*, Pittsburgh, USA, 2014, pp. 708-720.
- [9] Chen, Y., Zhou, Y., Zhu, S., and Xu, H., "Detecting Offensive Language in Social Media to Protect Adolescent Online Safety," in *International Conf. on Social Computing*, Amsterdam, Netherlands, 2012, pp. 71-80.
- [10] Krishna, A., "Polarity trend analysis of public sentiment on YouTube," M.S. Thesis, Iowa State University, Iowa, USA, 2014.

- [11] Li, Q., "Examining the accuracy of sentiment analysis by brand monitoring companies," in *5th IBA Bachelor Thesis Conf.*, Enschede, The Netherlands, 2015, pp. 1-7.
- [12] Jurek, A., Bi, Y., and Mulvenna, M., "Twitter Sentiment Analysis for Security-Related Information Gathering," in *Joint Intelligence & Security Informatics Conf.*, Hague, The Netherlands, 2014, pp. 48-55.
- [13] Jurek, A., Mulvenna, M. and Bi, Y., "Improved lexicon-based sentiment analysis for social media analytics," *Security Informatics*, vol. 4(9), pp. 1-13, 2015.
- [14] Hosseini Mardi, H., Mattson, S. A., Rafiq, R. I., Han, R., Lu, Q. and Mishra, S., "Prediction of Cyberbullying Incidents on the Instagram Social Network," arXiv:1508.06257 [cs.IR].
- [15] Xu, J. M., Zhu, X. and Bellmore, A., "Fast Learning for Sentiment Analysis on Bullying," in *International Workshop on Issues of Sentiment Discovery and Opinion Mining*, Beijing, China, 2012.
- [16] Henri, B., Olga, R., Daniel, W., Corne, V. and Harry, W., "On the early detection of threats in the real world based on open-source information on the internet," in *International Conf. on Information Technologies and Security (ITSEC)*, Hague, The Netherlands, 2012, pp. 1-12.
- [17] Zhang, K., Cheng, Y., Xie, Y., Honbo, D., Agrawal, A., Palsetia, D., Lee, K., Liao, W. nd Choudhary, A., "SES: Sentiment Elicitation System for Social Media Data," in *11th IEEE International Conference on Data Mining Workshops*, Vancouver, USA, 2011, pp. 129-136.
- [18] Dadvar, M. and Jong, F.D., "Cyberbullying Detection: A Step Toward a Safer Internet Yard," in *21st International World Wide Web Conf.*, New York, USA, 2012, pp. 121-125.
- [19] Anderson, J., Bresnahan, M. and Musatits, C., "Combating Weight-Based Cyberbullying on Facebook with the Dissenter Effect," *Cyberpsychology, Behavior, and Social Networking*, vol. 17(5), pp. 281-286, 2014.
- [20] Cohen, R., Lam, D. Y., Agarwal, N., Cormier, M., Jagdev, J., Jin, T., Kukreti, M., Liu, J., Rahim, K., Rawat, R., Sun, W., Wang, D. and Wexler, M., "Using Computer Technology to Address the Problem of Cyberbullying," *Computers & Society*, vol. 44(2), pp. 52-61, 2014.
- [21] Alim, S., "Analysis of Tweets Related to Cyberbullying: Exploring Information Diffusion and Advice Available for Cyberbullying Victims," *International Journal of Cyber Behavior, Psychology and Learning*, vol. 5(4), pp. 31-52, 2015.
- [22] Duwairi, R. M., Marji, R., Sha'ban, N. and Rushaidat, S., "Sentiment Analysis in Arabic Tweets," in *5th IEEE International Conf. on Information and Communication Systems*, Irbid, Jordan, pp. 1-6, 2014.
- [23] Adedoyn-Olowe, M., Gaber, M. M. and Stahl, F., "A Survey of Data Mining Techniques for Social Media Analysis," *Journal of Data Mining & Digital Humanities*, June 2014.
- [24] Troussas, C., Virvou, M., Espinosa, K. J., Liaguno, K. and Caro, J., "Sentiment analysis of Facebook statuses using Naive Bayes classifier for language learning," in *4th IEEE International Conf. on Information, Intelligence, Systems and Applications*, Piraeus Greece, 2013, pp. 1-6.
- [25] Ortigosa, A., Martin, J. M. and Carro, R. M., "Sentiment analysis in Facebook and its application to e-learning," *Computers in Human Behavior*, vol. 31(1), pp. 527-541, 2014.
- [26] Agarwal, A., Xie, B., Vovsha, I., Rambow, O. and Passoneau, R., "Sentiment Analysis of Twitter Data," in *Proceedings of the workshop on Languages in Social Media*, Stroudsburg, PA, USA, 2011, pp. 30-38.
- [27] Kouloumpis, E., Wilson, T. and Moore, J. D., "Twitter Sentiment Analysis: The Good the Bad and the OMG!," in *5th International Conf. on Weblogs and Social Media*, Barcelona, Spain, 2011, pp. 538-541.
- [28] Sanchez, H. and Kumar, S., "Twitter Bullying Detection," University of California, Santa Cruz, California, USA, 2011.
- [29] strohne, "Strohne/Facepager," in github, GitHub, 2016. [Online]. Available: <https://github.com/strohne/Facepager>. Accessed: Oct. 27, 2016.

APPENDIX A: A SAMPLE OF REPORTED CYBERCRIME CASES IN MAURITIUS

Month & Year	Original Title	Title in English	Source
June 2016	Arrêté pour avoir posté des vidéos pornographiques, il est libéré sous caution	Arrested for posting pornographic videos , he was freed on bail.	http://www.lexpress.mu/article/282792/arrete-pour-avoir-poste-videos-pornographiques-il-est-libere-sous-caution
March 2016	Policiers filme: Les commentaires sur facebook font l'objet d'une enquête.	Policemen filmed: Comments on Facebook are subject to an investigation.	http://defimedia.info/policier-filme-les-commentaires-sur-facebook-font-lobjet-dune-enquete-20766/
March 2016	Peut-on tout publier sur Facebook? La Cybercrime Unit démarre une campagne.	Can we all publish on Facebook? The Cybercrime Unit starts a campaign.	http://www.lexpress.mu/article/277175/peut-tout-publier-sur-facebook-cybercrime-unit-demarre-une-campagne
February 2016	Deux internautes arrêtés à la suite d'une plainte de Soodhun.	Two surfers arrested following a complaint made by Soodhun.	http://www.lexpress.mu/article/275235/deux-internautes-arretes-suite-dune-plainte-soodhun
November 2015	Attentats de Paris: L'internaute mauricien présente ses excuses.	Attacks in Paris: the Mauritian surfer apologises.	http://defimedia.info/tag/attentats-a-paris/
October 2015	Cybercrime unit: dans l'univers des enquêteurs du virtuel.	CyberCrime Unit: Investigators in the virtual universe.	http://www.lexpress.mu/article/269976/cybercrime-unit-dans-lunivers-enqueteurs-virtuel
September 2015	Online Racial Hatred Incitement: Police Elaborated a List of 30 suspects.	-	http://news.islandcrisis.net/2015/09/online-racial-hatred-incitement-police-elaborated-a-list-of-30-suspects/
September 2015	Profanation: les auteurs de commentaires violents sur les réseaux sociaux seront arrêtés.	Profanation: The authors of violent comments on social networks will be arrested.	http://www.lexpress.mu/article/268334/profanation-auteurs-commentaires-violents-sur-reseaux-sociaux-seront-arretes
August 2015	Video Posted on Facebook: A Man Threatens to disfigure a teenage girl.	-	http://news.islandcrisis.net/2015/08/video-posted-on-facebook-a-man-threatens-to-disfigure-a-teenage-girl/
June 2015	Profil Facebook piraté: Gurib-Fakim portera plainte à la Cybercrime Unit.	Facebook profile hacked: Gurib-Fakim will submit complaint to the Cybercrime Unit.	http://www.lexpress.mu/article/264556/profil-facebook-pirate-gurib-fakim-portera-plainte-cybercrime-unit

May 2015	Chantage: le sexting prend de l'ampleur.	Blackmail: The sexting is growing.	http://www.lexpress.mu/article/261910/chantage-sexting-prend-lampleur	January 2014	Dérive communale sur Facebook: Suzanne Hervet maintenue en cellule policière.	Communal derivative on Facebook: Suzanne Hervet is maintained in police custody.	http://www.lexpress.mu/article/derive-communale-sur-facebook-suzanne-hervet-maintenue-en-cellule-policiere
May 2014	Facebook: Yatin Varma porte plainte à la Cybercrime Unit.	Facebook: Yatin Varma complains at the Cybercrime Unit.	http://www.lexpress.mu/article/245869/facebook-yatin-varma-porte-plainte-cybercrime-unit	July 2012	Propos sectaires sur Facebook: Krishnee Bunwaree bientôt face à la justice.	Sectarian comments on Facebook: Krishnee Bunwaree soon facing the justice.	http://www.lexpress.mu/article/propos-sectaires-sur-facebook-krishnee-bunwaree-bientot-face-la-justice
March 2014	Cyberbullying: Akash Callikan porte plainte à la Cybercrime Unit.	Cyberbullying: Akash Callikan complains at the Cybercrime Unit.	http://www.lexpress.mu/article/cyberbullying-akash-callikan-porte-plainte-la-cybercrime-unit				
March 2014	Série de dérapages communaux sur Facebook.	Series of communal skids on Facebook.	http://www.lexpress.mu/article/serie-de-derapages-communaux-sur-facebook				
March 2014	Des photos de mineurs en discothèque font polémique sur Facebook.	Minors photos in discothèque controversy on Facebook.	http://www.lexpress.mu/article/des-photos-de-mineurs-en-discotheque-font-polemique-sur-facebook				

Medical Image Fusion Algorithm based on Local Average Energy-Motivated PCNN in NSCT Domain

Huda Ahmed

Department of Computer Science
Cairo University
Giza, Egypt

Emad N. Hassan

Department of Computer Science
Cairo University
Giza, Egypt

Amr A. Badr

Department of Computer Science
Cairo University
Giza, Egypt

Abstract—**Medical Image Fusion (MIF)** can improve the performance of medical diagnosis, treatment planning and image-guided surgery significantly through providing high-quality and rich-information medical images. Traditional MIF techniques suffer from common drawbacks such as: contrast reduction, edge blurring and image degradation. Pulse-coupled Neural Network (PCNN) based MIF techniques outperform the traditional methods in providing high-quality fused images due to its global coupling and pulse synchronization property; however, the selection of significant features that motivate the PCNN is still an open problem and plays a major role in measuring the contribution of each source image into the fused image. In this paper, a medical image fusion algorithm is proposed based on the Non-subsampled Contourlet Transform (NSCT) and the Pulse-Coupled Neural Network (PCNN) to fuse images from different modalities. Local Average Energy is used to motivate the PCNN due to its ability to capture salient features of the image such as edges, contours and textures. The proposed approach produces a high quality fused image with high contrast and improved content in comparison with other image fusion techniques without loss of significant details on both levels: the visual and the quantitative.

Keywords—*Medical image fusion; pulse-coupled neural network; local average energy; non-subsampled contourlet transform*

I. INTRODUCTION

A numerous imaging modalities such as Computed Tomography (CT), Magnetic Resonance Imaging (MRI), Ultrasound, Positron Emission Tomography (PET), and Single Photon Emission Computed Tomography (SPECT) reflect information about the human body from different views. For example, CT can reflect the anatomical structure of bone tissues clearly, while the MRI can reflect the anatomical structure of the soft tissues, organs and blood vessels. The nature of clinical diagnosis and treatment requires a composite

view of two or more modalities, since using a single source of information may not be sufficient to localize lesions and abnormalities during the diagnosis process [1]. Thus, a way is needed to extract and combine information from different modalities to produce clear and rich-information images to provide more reliable and accurate diagnosis. Combining such information manually is time consuming, subject to human error and based on radiologist's experience which may produce misleading results.

The art of combining complementary information automatically from different medical source images for the same organ/tissue being imaged is known as medical image fusion. A major prerequisite should be fulfilled for the fusion process to perform correctly; it is the registration/alignment of the medical source images to be fused. Any fusion scheme should fulfill some generic requirements: First, all the salient features and significant information in the source images should be present in the fused result. Second, no artifacts or unwanted degradations should be introduced by the fusion process. Third, irrelevant features and noise should be discarded and minimized [2].

The core problem of medical image fusion is how to find an efficient way of measuring the contribution of each source image into the resultant fused image which turns the medical image fusion problem into an analysis problem [3]. Medical image fusion can be decomposed into two major steps: measurement of activity level and applying a suitable fusion rule. Activity level refers to the local energy or the amount of information present in an image pixel or coefficient [4]. It can be measured for a single pixel value or by taking into consideration the surrounding neighbors of the pixel. On the other hand, fusion rules should be selected carefully depending on the nature of the source images to be fused. The most common fusion rules are Min, Max and Average.

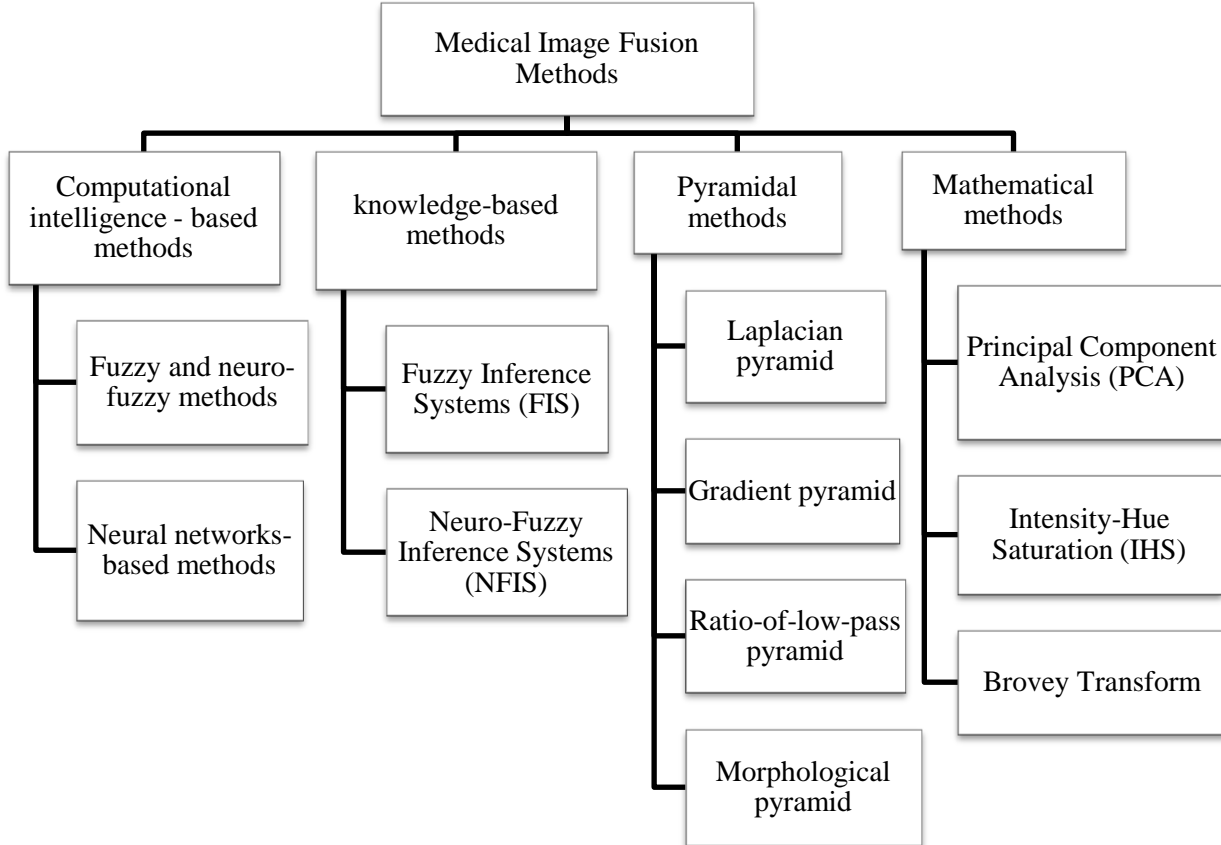


Fig. 1. Medical image fusion methods categorization

PCNN is an artificial neuron model inspired from the visual cortex of the cat. It is characterized by the global coupling and pulse synchronization of neurons, this means that the neurons corresponding to pixels with similar significance tend to fire synchronously. These characteristics of the PCNN make it appropriate for activity level measurement. NSCT is a modified version of the original contourlet transform; it overcomes the Pseudo-Gibbs phenomena because of its shift-invariant characteristic. This characteristic fulfills two major generic requirements of image fusion process: (a) no artifacts or inconsistencies should be introduced in the fused result and (b) the fusion process should be shift invariant.

A variety of medical image methods has evolved across the recent years. Fig. 1 shows the major categories by which medical image methods can be classified. Pixel-level spatial domain techniques such as simple averaging, knowledge based image fusion [5, 6] usually lead to contrast reduction and edge blurring. Pyramidal fusion methods including the laplacian pyramid [7], gradient pyramid [8], ratio-of-low-pass pyramid and the morphological pyramid [9] fail to capture the spatial orientation in the decomposition process; hence cause blocking effects [10]. Mathematical methods including principal component analysis[11, 12], intensity-hue saturation [13, 14] and the Brovey transform [15] offer better results, but suffer from spectral degradation [16].

Several Image Fusion (IF) and Medical Image Fusion (MIF) techniques based on PCNN have been proposed by researchers [15-20]. The majority of the MIF techniques based

on PCNN use the normalized single value of the pixel in the spatial domain or the coefficient in the transform domain as the feeding input to the PCNN which leads to contrast reduction and loss of directional information respectively [19, 21-24]. Moreover, using a single pixel/coefficient value as stimuli for a PCNN neuron is not effective, since the human visual system is more sensitive to the variations in images such as edges, contours and directional features.

Das and Kundu [17] employed a Neuro-fuzzy approach which combines a reduced pulse coupled neural network with fuzzy logic in order to produce fused image with higher contrast, more clarity and more useful subtle detailed information. Kavitha and Chellamuthu [18] enhanced the input before feeding it into the PCNN using the ant colony optimization (ACO) technique. Das and Kundu [16] proposed a modified spatial frequency motivated PCNN to fuse the high frequency sub-bands and max selection fusion rule to fuse the low frequency sub-bands. Xiao-Bo et al. [20] proposed a spatial frequency motivated pulse coupled neural network to fuse low and high frequency sub-bands. It works well for multi-focus IF and visible/infrared IF, but the absence of directional information in SF and using the same fusion rule for both the sub-bands cause contrast reduction and loss of image details [16]. Wang and Ma [19] proposed an image fusion technique based on a modified model of the pulse-coupled neural network; it is called the m-PCNN where m is the number of external input channels. Data fusion happens in the internal activity of the neuron. The process of fusion is completely carried out by the PCNN and the number of

channels can be extended dynamically to fuse more than two images; however, using the normalized gray value of the input image as an input to the PCNN will lead to contrast reduction and edge blurring.

In this paper, a NSCT-based MIF algorithm using local average energy as a feeding input to motivate the PCNN neurons is proposed. Input source images to be fused are assumed to be well-aligned. Rest of the paper is organized as follows: NSCT, simplified model of the PCNN and the proposed MIF scheme are described in the Methodology. Experimental results and discussion are described in Results and discussion section. Finally, conclusions and future work are summarized in Conclusion section.

II. METHODOLOGY

A. Non-Subsampled Contourlet Transform

NSCT is a shift-invariant version of the original contourlet transform proposed by Da Cunha et al. [25] to overcome the contourlet transform limitations. The original contourlet transform lacks shift-invariant characteristic due to down-samplers and up-samplers introduced in both the Laplacian Pyramid (LP) and the Directional Filter Bank (DFB). The absence of shift invariance in the contourlet transform causes pseudo Gibbs phenomena around singularities [20]. In the original contourlet [26], the Laplacian pyramid is firstly applied to capture the point discontinuities and then is followed by a directional filter bank to connect point discontinuities into linear structures [20]. The NSCT is mainly divided into two building blocks: the shift-invariant pyramid filter bank and shift-invariant directional filter bank as shown in Fig.1(a). The

decomposition of an input image into frequency sub-bands using the NSCT is illustrated in Fig.1(b).

The shift-invariant pyramid filter bank is responsible for the sub-bands decomposition. It maintains the multiscale property of the NSCT by using two-channel, non-subsampled filter banks applied iteratively to obtain the multiscale decomposition. The Non-subsampled directional filter bank is used to achieve the multi-direction property of the NSCT. Up-samplers and down-samplers are used to a minimum extent in the Directional Filter Bank by switching them off in every two-channel filter bank in the DFB tree structure and up-sampling the filters accordingly [25].

In our proposed scheme, the decomposition parameters are set to *levels* = [1, 2, 4]. The pyramidal filter is set to ‘*pyrexc*’ and the directional filter is set to ‘*vk*’ in the NCST configuration. The frequency sub-bands obtained after applying the NSCT size are equivalent to the size of the original source images which means that each frequency coefficient corresponds to the pixel of same location in the spatial domain; this characteristic guides the selection of a suitable fusion rule for each sub-band.

B. Simplified Pulse -Coupled Neural Network

PCNN is a 2D single layer, laterally connected network of pulse-coupled neurons, with a 1:1 correspondence between the image pixels and network neurons [27]. No training is required for the PCNN. The three main components of the PCNN are: the receptive field, modulation field and pulse generator as shown in Fig.3.

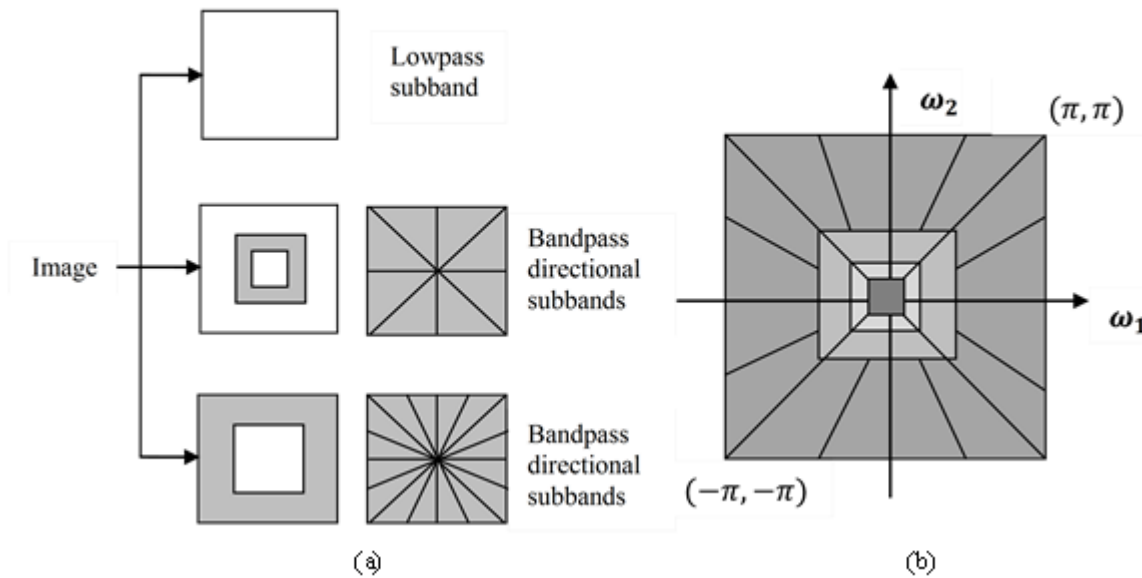


Fig. 2. (a) NSCT structure which consists of bank of filters to split the 2-D frequency plane into frequency and directional subbands. (b) Approximation of the ideal frequency partitioning obtained by NSCT

The output of each neuron is one of two states: firing or non-firing. A firing map is then generated by accumulating each neuron firing times. Firing times of each neuron can be used as an activity level measurement, where the neuron of larger firing times indicates the significance of the

corresponding coefficient. PCNN has several parameters with complex structures and an optimal setting of these parameters is a major limitation to automation and generalization of PCNN [17], that's why a reduced model of the pulse coupled neural

network is used instead. The equations of the reduced PCNN model are described below through Eq.(1) to Eq.(6).

$$F_{i,j}[n] = S_{i,j} \quad (1)$$

$$L_{i,j}[n] = \sum_{k,l} W_{i,j,k,l} Y_{i,j}[n-1] \quad (2)$$

$$U_{i,j}[n] = F_{i,j}[n] (1 + \beta L_{i,j}[n]) \quad (3)$$

$$Y_{i,j}[n] = \begin{cases} 1, & U_{i,j}[n] > T_{i,j}[n-1] \\ 0, & \text{otherwise} \end{cases} \quad (4)$$

$$T_{i,j}[n] = e^{-\alpha T} T_{i,j}[n-1] + V_T Y_{i,j}[n] \quad (5)$$

$$M_{i,j}[n] = M_{i,j}[n-1] + Y_{i,j}[n] \quad (6)$$

The indices i and j refer to the pixel/coefficient location in the image/sub-band, k and l refer to the displacement of the symmetric weights kernel around the image pixel and n refers to the current iteration. $F_{i,j}$ and $L_{i,j}$ are the feeding and linking input respectively. $W_{i,j,k,l}$ is the kernel weights and $S_{i,j}$ is the external stimulus that motivates the neuron. $U_{i,j}[n]$ is the internal activity of the neuron and β is the linking strength parameter. $Y_{i,j}[n]$ is the output of the neuron after applying the

threshold to the internal activity. $T_{i,j}$ is the dynamic threshold, where V_T and αT are normalized constant and time constant respectively.

C. Proposed Approach

Local average energy reflects information about the presence of image variations such as edges, contours and textures, that's why it would be more expressive if the local average energy is used in place of the single pixel/coefficient value as a motivation to the PCNN. Our transform-based approach employs the local average energy to motivate the PCNN in order to measure the contribution of each source image into the fused result. The shift-invariant NSCT is employed to decompose the source images into frequency sub-bands. It is mainly divided into two major steps: high-frequency sub-bands fusion and low frequency sub-bands fusion. The block diagram of our proposed approach is shown in Fig.4.

1) *Low frequency sub-bands fusion:* Max selection fusion rule is applied directly to the absolute value of the LFSs coefficients. The coefficient with higher absolute value is selected as the fused image coefficient.

$$L_F^S(i,j) = \begin{cases} L_A^S(i,j), & |L_A^S(i,j)| \geq |L_B^S(i,j)| \\ L_B^S(i,j), & \text{otherwise} \end{cases} \quad (7)$$

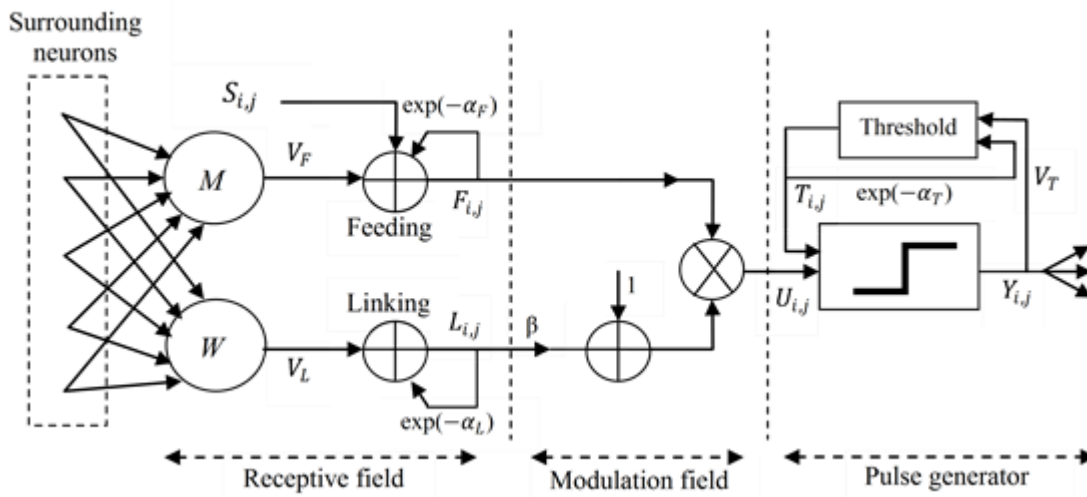


Fig. 3. PCNN's neuron structure

$L_A^S(i,j)$ indicates the low frequency coefficient of image A at location i, j in subband S and the same applies for $L_B^S(i,j)$ and $L_F^S(i,j)$.

2) *High frequency sub-bands fusion:* Since the human visual system is sensitive to image variations such as edges, contours and textures, choosing the absolute value of the coefficient as input to the PCNN may not be the wise choice. Using features rather than raw data or single values, whether

pixel values or frequency coefficients as an input to motivate the PCNN neurons, will be more accurate. Furthermore, it will act as an indicator of the significance of each source image. Local average energy is used as the image features that will motivate the neurons. PCNN is employed as an activity level measurement. For each high frequency sub-band, the local average energy is calculated as follows:

$$LAE_{i,j} = \frac{1}{M \times N} \sum_{m=0}^M \sum_{n=0}^N C(m,n)^2 \quad (8)$$

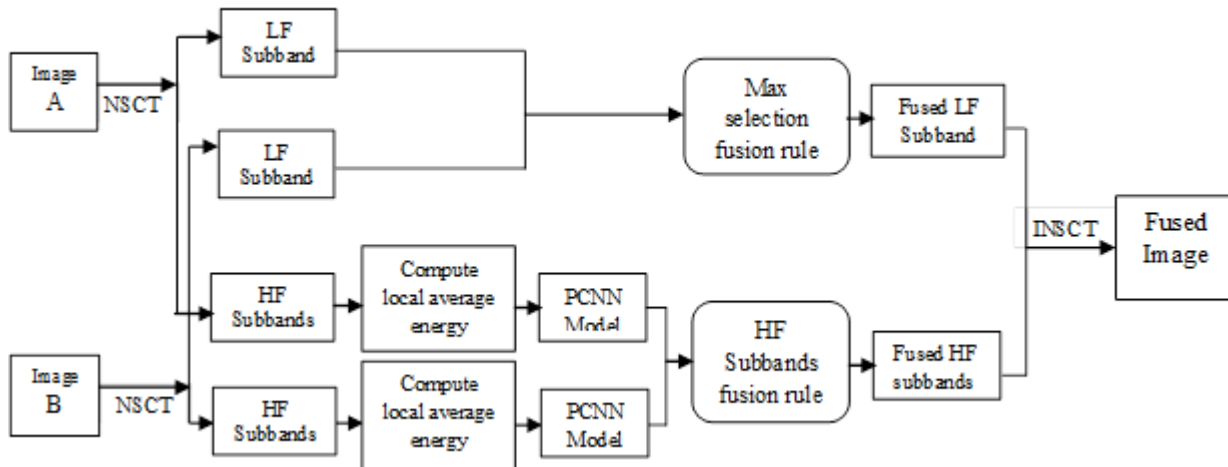


Fig. 4. Block diagram of the proposed MIF Technique

where C is the coefficient value at location m, n in any frequency sub-band. $LAE_{i,j}$ is then used as input to the PCNN. After running the PCNN for several iterations, firing times for each neuron is calculated. The generated firing maps are used to select which coefficient will contribute to the fused result.

3) The proposed MIF algorithm steps:

a) Decompose the pre-registered source images into low/high frequency sub-bands using NSCT, each sub-band size is equivalent to the size of the source images.

b) Apply max selection rule to the Low-Frequency Subbands (LFSs) as described by Eq.(7).

c) Calculate the local average energy for each High-Frequency Sub-band (HFS) as described by Eq.(8) using a slipping window over each HFS coefficients.

d) Motivate the PCNN using the local average energy calculated for every HFS, then calculate the output of each neuron using Eqs.(1) to (5) and generate the firing maps $T_{i,j}[n]$ by Eq.(6).

e) Apply the high frequency fusion rule based on the neurons firing maps. Coefficients that correspond to the neurons with higher firing times are selected to contribute in the resultant fused image as illustrated by Eq. (9).

$$H_F^S(i,j) = \begin{cases} H_A^S(i,j), & M_{i,j}^{S,A}[n] \geq M_{i,j}^{S,B}[n] \\ H_B^S(i,j), & \text{otherwise} \end{cases} \quad (9)$$

f) Apply the inverse NSCT to obtain the fused image.

III. RESULTS AND DISCUSSION

The proposed algorithm was implemented using MATLAB. Source images are of size 256 x 256. The PCNN parameters were configured to $k \times l = 3 \times 3$, $W = [0.707 \ 1 \ 0.707; 1 \ 0 \ 1; 0.707 \ 1 \ 0.707]$, $\beta = 0.2$, and the sliding window of the local average energy = 3 x 3. To evaluate the quality of the output fused images, the following quality metrics are used:

A. Entropy

Entropy is a measure of the information content present in an image. It is described by the equation:

$$E = -\sum_{i=0}^{L-1} p(x_i) \log_2 p(x_i) \quad (10)$$

B. Standard Deviation (STD)

Standard deviation is used to measure the image contrast, where a higher standard deviation value indicates better contrast.

C. Mutual Information (MI)

A measure of how much information is mutual between two images. Given image A and B, the mutual information preserved by the fused image F is computed by the sum of the mutual information between F and A represented by I_{FA} and the mutual information between F and B represented by I_{FB} as illustrated by Eq. (11):

$$MI = I_{FA} + I_{FB} \quad (11)$$

$$I_{MN} = \sum_{x,y} P_{MN}(x,y) \log \frac{P_{MN}(x,y)}{P_M(x)P_N(y)} \quad (12)$$

Larger value of MI indicates that the fused image preserves a significant amount of information from both input images.

D. Edge Association ($Q^{AB/F}$)

An objective performance measure for image fusion was proposed by Xydeas and Petrović [28]. It measures how much of the edge information present in the source images is transferred to the fused image:

$$Q^{AB/F} = \frac{\sum_{n=1}^N \sum_{m=1}^M (Q^{AF}(n,m)w^A(n,m) + Q^{BF}(n,m)w^B(n,m))}{\sum_{n=1}^N \sum_{m=1}^M (w^A(n,m) + w^B(n,m))} \quad (13)$$

E. Universal Image Quality Index (Q_0)

It is a universal objective image quality index proposed by

Wang and Bovik [29]. It is a combination of three elements: loss of correlation, luminance distortion and contrast distortion. Loss of correlation measures how much image A and F are correlated, luminance distortion measures how close the mean luminance is to images A and B and the contrast distortion measures the degree of similarity between the contrast of images A and F. It is calculated for each source image and the fusion result.

$$Q_0(A, F) = \frac{2 \sigma_{af} \cdot 2\bar{a}\bar{f}}{(\sigma_a^2 + \sigma_f^2) \cdot (a^2 + f^2)} \quad (14)$$

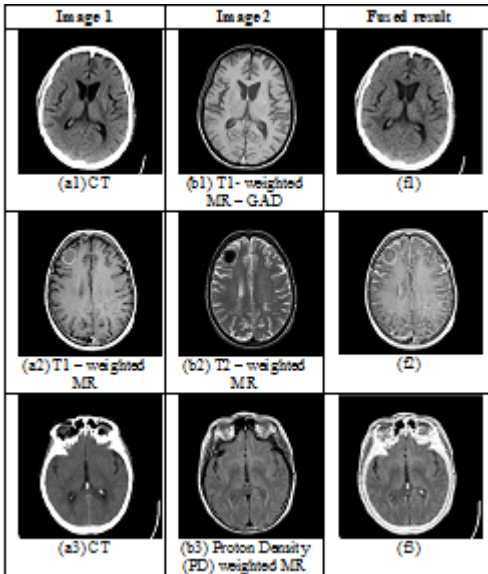


Fig. 5. Three pairs of source medical images (left two images) with the corresponding fusion result of each pair (last column)

Fig. 5 shows three sets of source medical images [30] captured from different modalities used in evaluating the proposed approach. Each set is a pair of two source images, and the corresponding fusion visual result is shown beside each pair. In 'Set1' the CT image in Fig. 5(a1) shows the calcification, while the MR image in Fig. 5(b1) captures several focal lesions. In 'set2' the MR images in Fig. 5(a2) and Fig. 5(b2) reveal a lesion in the frontal lobe. In 'set3' the CT image in Fig. 5(a3) indicates a medical left occipital infarct involving the left side of the splenium of the corpus callosum and the MR image in Fig. 5(b3) reveals only mild narrowing of the left posterior cerebral artery.

For the three sets of medical source images in Fig. 5, a

detailed quantitative evaluation using the previously mentioned quality metrics is presented in Table 1. The best results obtained are formatted in bold in tables 1 and 2.

Table 2 compares the performance of our proposed technique against other existing MIF techniques using the images of *Set3* as the source images to be fused. Fig. 6 shows the visual fusion results produced by the compared MIF methods.

TABLE I. PERFORMANCE EVALUATION OF THE PROPOSED MIF ALGORITHM USING SET1, SET2 AND SET3

Set		Entropy	STD	MI	Entropy	STD
1	a1	3.3019	79.2907	2.9453	4.8045	77.2127
	b1	3.4385	61.7932			
2	a2	3.3046	77.1245	2.2736	4.6308	76.5947
	b2	3.2856	52.6946			
3	a3	2.9001	79.8634	3.187	4.5648	80.9665
	b3	3.6014	61.9829			

The fused images obtained from the three sets combine the information from both corresponding source images as shown in Fig. 4(f1)(f2) and (f3). The fused image of *Set1* combines the bone structure of the CT image (a1) with the soft tissues of the MR image (b2). In *Set2*, the lesion that appears as a black hole in the MR image (b2) is apparent in the fused image. Similarly, the fused image of *Set3* combines both the bone structure of the CT image (a3) and the anatomical structure of the soft tissues of the MR image (b3). In Table 1 the quality of the fusion result is compared respect to the quality of the corresponding pair of source images. Columns 3 and 4 show the entropy and the standard deviation for each pair of the source images respectively. While the rest of the columns show the performance evaluation of the fusion results for each set through different quality metrics. Apparently, the higher entropy values of the fusion results indicate better information content than the source images that participated in the fusion. Similarly, the higher standard deviation value of the fusion result of *Set3* shows better contrast and clarity.

TABLE II. PERFORMANCE COMPARISONS WITH OTHER MIF ALGORITHMS USING SET3

Method	MI	Entropy	STD	$Q^{AB/F}$	Q_0
NSCT+MSF-PCNN [16]	3.0593	4.3645	83.7037	0.5338	0.8796
NSCT+SF-PCNN [20]	2.6651	4.2015	55.6347	0.3163	0.7626
m-PCNN [19]	3.1076	4.1933	55.1152	0.4958	0.8578
DWT+LAE-PCNN	2.6773	4.3800	78.5955	0.4446	0.8757
Proposed Scheme	3.1870	4.5648	80.9665	0.5628	0.8776

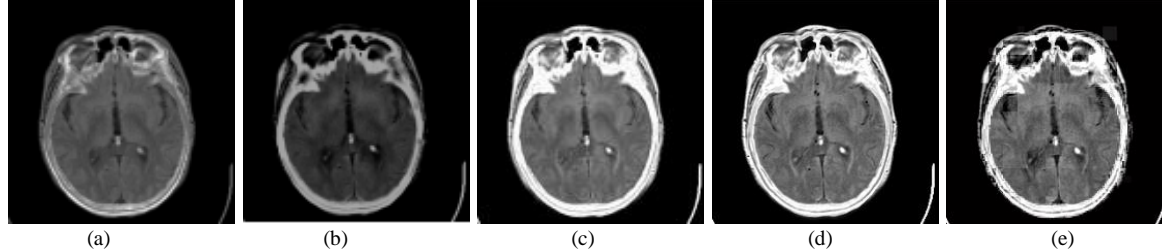


Fig. 6. Resultant fused images on set3 for example: (a) m-PCNN [19], (b) NSCT+SF-PCNN [20], (c) NSCT+MSF-PCNN [16], (d) Proposed Scheme, and (e) DWT+LAE-PCNN

Table 2 shows that the proposed MIF algorithm has the highest entropy, MI and $Q^{AB/F}$. NSCT-MSF-PCNN method [16] has the highest STD and Q_0 values. The higher values of entropy and MI indicate that the fused image produced in this paper preserves more information from the source images and it has higher information content. The visual fused image obtained by NSCT-MSF-PCNN method [16] is very similar to the fused image produced by our proposed approach; however, the quantitative analysis shows that the proposed algorithm provided higher EN, MI and $Q^{AB/F}$ than NSCT-MSF-PCNN method [16]. m-PCNN method [19] in Fig. 5(a) suffers from the contrast reduction problem because of using the normalized value of the coefficient as an input to the PCNN. A close look at Fig. 5(b) shows that NSCT-SF-PCNN method [20] lost large amount of image details. In Fig. 5(e), when NSCT was replaced with the DWT, the fused result revealed unwanted image degradation unlike the proposed method fused result. Careful investigation of the proposed approach in Fig. 5 (d) reveals that it displays very fine details not apparent in the visual result of NSCT-MSF-PCNN [16] in Fig. 5(c).

IV. CONCLUSION

Medical images obtained from different modalities are fused to support a radiologist's task in treatment and diagnosis. Since fusing medical images manually is time consuming and subject to human error, this paper presents an MIF approach based on NSCT and local average energy-motivated PCNN to fuse the medical images. The results show that it overcomes the common drawbacks in the conventional methods such as contrast reduction, edge blurring and unwanted degradations. Using the local average energy as a stimulus to the PCNN is a promising choice, since it doesn't only use the single value of one pixel/coefficient but it also takes into consideration the values of the neighboring pixels. Local average energy extracts features like edges, contours and textures; the human visual system is more sensitive to these features. Selecting the NSCT to transform source images into the frequency domain is a good choice because of its shift-invariant characteristic that overcomes the Pseudo-Gibbs phenomena. Although local average energy showed promising results, we cannot tell that it is the best stimuli for the PCNN to measure the contribution or significance of the source images. Other measurements of activity level instead of the local average energy could be used as a motivation for the PCNN. As a future work, the proposed method in this paper can be extended to fuse multi-focus images, infrared and visible images and remote sensing images. Moreover, the behavior of the algorithm will be tested on noisy modalities images to see how it performs in the presence of noise.

REFERENCES

- [1] A. P. James and B. V. Dasarathy, "Medical image fusion: A survey of the state of the art," *Information Fusion*, vol. 19, pp. 4–19, Sep. 2014.
- [2] V. P. S. Naidu, N. A. Laboratories, Bangalore, and J. R. Raol, "Pixel-level image fusion using Wavelets and principal component analysis," *Defence Science Journal*, vol. 58, no. 3, pp. 338–352, Mar. 2012.
- [3] S. Bedi, J. Agarwal and P. Agarwal, "Image fusion techniques and quality assessment parameters for clinical diagnosis: a review", *International Journal of Advanced Research in Computer and Communication Engineering*, vol. 2, no. 2, pp. 2319-5940, 2013.
- [4] A. Galande and R. Patil, "The art of medical image fusion: A survey," *Advances in Computing, Communications and Informatics (JCACCI)*, 2013 International Conference on, Mysore, 2013, pp. 400-405.
- [5] W. Dou, S. Ruan, Q. Liao, D. Bloyet and J. M. Constans, "Knowledge based fuzzy information fusion applied to classification of abnormal brain tissues from MRI," *Signal Processing and Its Applications, 2003. Proceedings. Seventh International Symposium on*, 2003, pp. 681-684 vol.1.
- [6] J. Teng, S. Wang, J. Zhang and X. Wang, "Fusion algorithm of medical images based on fuzzy logic," *Fuzzy Systems and Knowledge Discovery (FSKD), 2010 Seventh International Conference on*, Yantai, Shandong, 2010, pp. 546-550.
- [7] N. Indhumadhi and G. Padmavathi, "Enhanced Image Fusion Algorithm Using Laplacian Pyramid and Spatial frequency Based Wavelet Algorithm", *International Journal of Soft Computing and Engineering*, vol. 1, no. 5, pp. 298-303, 2011.
- [8] V. S. Petrovic and C. S. Xydeas, "Gradient-based multiresolution image fusion," in *IEEE Transactions on Image Processing*, vol. 13, no. 2, pp. 228-237, Feb. 2004.
- [9] N. Uniyal and S. K. Verma, "Image fusion using morphological pyramid consistency method," *International Journal of Computer Applications*, vol. 95, no. 25, pp. 34–38, Jun. 2014.
- [10] Hui Li, B. S. Manjunath and S. K. Mitra, "Multi-sensor image fusion using the wavelet transform," *Image Processing, 1994. Proceedings. ICIP-94., IEEE International Conference*, Austin, TX, 1994, pp. 51-55 vol.1.
- [11] N. Al-Azzawi, H. A. M. Sakim, A. K. W. Abdullah and H. Ibrahim, "Medical image fusion scheme using complex contourlet transform based on PCA," *2009 Annual International Conference of the IEEE Engineering in Medicine and Biology Society*, Minneapolis, MN, 2009, pp. 5813-5816.
- [12] H. q. Wang and H. Xing, "Multi-Mode Medical Image Fusion Algorithm Based on Principal Component Analysis," *Computer Network and Multimedia Technology, 2009. CNMT 2009. International Symposium on*, Wuhan, 2009, pp. 1-4.
- [13] S. Daneshvar and H. Ghassemian, "MRI and PET image fusion by combining IHS and retina-inspired models," *Information Fusion*, vol. 11, no. 2, pp. 114–123, Apr. 2010.
- [14] C. He, Q. Liu, H. Li, and H. Wang, "Multimodal medical image fusion based on IHS and PCA," *Procedia Engineering*, vol. 7, pp. 280–285, Jan. 2010.
- [15] T.-M. Tu *et al.*, "Adjustable intensity-hue-saturation and Brovey transform fusion technique for IKONOS/QuickBird imagery," *Optical Engineering*, vol. 44, no. 11, pp. 10–116201, Nov. 2005.

- [16] S. Das and I. S. Institute, "NSCT-based multimodal medical image fusion using pulse-coupled neural network and modified spatial frequency," *Medical & Biological Engineering & Computing*, vol. 50, no. 10, pp. 1105–1114, Jul. 2012.
- [17] S. Das and M. K. Kundu, "A Neuro-Fuzzy Approach for Medical Image Fusion," in *IEEE Transactions on Biomedical Engineering*, vol. 60, no. 12, pp. 3347-3353, Dec. 2013.
- [18] K. C.T and C. C, "Medical image fusion based on hybrid intelligence," *Applied Soft Computing*, vol. 20, pp. 83–94, Jul. 2014.
- [19] Z. Wang and Yide, "Medical image fusion using -PCNN," *Information Fusion*, vol. 9, no. 2, pp. 176–185, Apr. 2008.
- [20] X.-B. QU, J.-W. YAN, H.-Z. XIAO, and Z.-Q. ZHU, "Image fusion algorithm based on spatial frequency-motivated pulse coupled neural networks in Nonsubsampled Contourlet transform domain," *Acta Automatica Sinica*, vol. 34, no. 12, pp. 1508–1514, Dec. 2008.
- [21] Z. Baohua, L. Xiaoqi, and J. Weitao, "A multi-focus image fusion algorithm based on an improved dual-channel PCNN in NSCT domain," *Optik - International Journal for Light and Electron Optics*, vol. 124, no. 20, pp. 4104–4109, 2016.
- [22] C. T. Kavitha, C. Chellamuthu, and R. Rajesh, "Medical image fusion using integer wavelet transform and pulse-coupled neural network", *Proceedings of 2011 IEEE International Conference on Computational Intelligence And Computing Research*, 2011, p. 834-838.
- [23] C. T. Kavitha, C. Chellamuthu, and R. Rajesh, "Multimodal medical image fusion using discrete Ripple transform and intersecting cortical model," *Procedia Engineering*, vol. 38, pp. 1409–1414, Jan. 2012.
- [24] C. T. Kavitha, C. Chellamuthu, and R. Rajesh, "Medical image fusion using combined discrete Wavelet and Ripple transforms," *Procedia Engineering*, vol. 38, pp. 813–820, 2012.
- [25] A. L. Da Cunha, J. Zhou and M. N. Do, "The Nonsubsampled Contourlet Transform: Theory, Design, and Applications," in *IEEE Transactions on Image Processing*, vol. 15, no. 10, pp. 3089-3101, Oct. 2006.
- [26] M. N. Do and M. Vetterli, "The contourlet transform: an efficient directional multiresolution image representation," in *IEEE Transactions on Image Processing*, vol. 14, no. 12, pp. 2091-2106, Dec. 2005.
- [27] Z. Wang, Y. Ma, F. Cheng, and L. Yang, "Review of pulse-coupled neural networks," *Image and Vision Computing*, vol. 28, no. 1, pp. 5–13, Jan. 2010.
- [28] C. S. Xydeas and V. Petrovic, "Objective image fusion performance measure," in *Electronics Letters*, vol. 36, no. 4, pp. 308-309, 17 Feb. 2000.
- [29] Zhou Wang and A. C. Bovik, "A universal image quality index," in *IEEE Signal Processing Letters*, vol. 9, no. 3, pp. 81-84, March 2002.
- [30] "The Whole Brain Atlas". *Med.harvard.edu*. N.p., 2016. Web. 31 Aug. 2016.

Dynamic Inertia Weight Particle Swarm Optimization for Solving Nonogram Puzzles

Habes Alkhraisat

Department of computer science
Al-Balqa Applied University
AL salt, Jordan

Hasan Rashaideh

Department of computer science
Al-Balqa Applied University
Al Salt, Jordan

Abstract—Particle swarm optimization (PSO) has shown to be a robust and efficient optimization algorithm therefore PSO has received increased attention in many research fields. This paper demonstrates the feasibility of applying the Dynamic Inertia Weight Particle Swarm Optimization to solve a Non-Polynomial (NP) Complete puzzle. This paper presents a new approach to solve the Nonograms Puzzle using Dynamic Inertia Weight Particle Swarm Optimization (DIW-PSO). We propose the DIW-PSO to optimize a problem of finding a solution for Nonograms Puzzle. The experimental results demonstrate the suitability of DIW-PSO approach for solving Nonograms puzzles. The outcome results show that the proposed DIW-PSO approach is a good promising DIW-PSO for NP-Complete puzzles.

Keywords—Non-Polynomial Complete problem; Nonograms puzzle; Swarm theory; Particle swarms; Optimization; Dynamic Inertia Weigh

I. INTRODUCTION

Most of optimization problems including NP-complete problem, such as Nonograms puzzle, have complex characteristics with heavy constraints. Nonograms are deceptively simple logic puzzles, which is considered as an image reconstruction problem, starting with a blank $N \times M$ grid, Fig. 1.a shows an example for 5×5 Nonograms puzzle.

The solution of the puzzle is an image grid that satisfies certain row and column constraints. The constraints take the form of series of numbers at the head of each line (row or column) indicating the size of blocks of contiguous filled cells found on that line.

The puzzle solvers need to figure out which square will be left blank (white) and which will be colored (black), based on the numbers at the side of the grid. The resulting pattern of colored or left blank squares makes up a hidden picture, which is the solution to the puzzle.

The resulting picture must obey all the following three conditions:

- 1) Each picture cell must be either colored or blanked i.e. black or white.
- 2) The s_1, s_2, \dots, s_k numbers at the side of the row or column: indicated that there are groups of s_1, s_2 , and s_k filled squares, with at least one blank square between consecutive groups.
- 3) Between two consecutive black there must be at least one empty cell.

1	1	3	1	1
1	2		2	1
3				
1	1			
3				

(a) 5×5 Nonograms puzzle

1	1	3	1	1
1	2		2	1
3				
1	1			
3				

(b) 5×5 Nonograms solution

Fig. 1. (a) 5×5 Nonograms puzzle (b) its solution

For example, in the first row the "3" tells that, somewhere in the row, there are three sequential blocks filled in. Those will be the only blocks filled in, and the amount of space before/after them are not defined. The possible solution for the first row are:

Solution 1 

Solution 2 

Solution 3 

The "1 2" in the second columns tells that, somewhere in the column, there is one block filled in, followed by 2 sequential blocks filled in, and also those will be the only blocks filled in, and the amount of space before/after them are not defined. The possible solutions for the second column are:

Solution 1 Solution 2 Solution 3

1
2

1
2

1
2

A puzzle is complete when all rows and columns are filled, and meet their definitions, without any contradictions. Fig. 1 shows an example of a Nonograms and its solution.

Several algorithms have applied to find a solution for the Nonograms problem such as an evolutionary algorithm, a heuristic algorithm, and a reasoning framework [2, 3, 4, and 5].

In this paper, a Dynamic Inertia Weight Particle Swarm Optimization (DIW-PSO) algorithm is proposed for solving Nonograms puzzles. In this work, we demonstrate that DIW-PSO can be specified to NP-Complete puzzle.

II. DYNAMIC INERTIA WEIGHT PARTICLE SWARM OPTIMIZATION

Particle swarm optimization (PSO) is a population based stochastic optimization method, which is an efficient and effective global optimizer in the discrete search domain [6]. PSO has been successfully applied to a wide variety of problems in mechanical engineering, communication, pattern recognition and diverse fields of science.

In PSO, a multiple random candidate solutions, so-called particles, are maintain in the problem search space, where each particle represents a solution to an optimization problem. Each particle is assessed by fitness function to figure out whether a particle is the problem “best” solution or not. A particle then fly through the problem search space with a randomized velocity by combining the current and best potential solution locations.

Let D be the size of the swarm, each particle i is composed of the following D -dimensional vectors: (1) the current position \vec{x}_i , (2) velocity \vec{v}_i , and (3) best value \vec{p}_i .

The PSO algorithm consists of adjusting the velocity and position of each particle toward new current best and global best locations. At each time step, current position \vec{x}_i is updated by velocity and evaluated as a problem solution, in case the particle finds a pattern that is better than any it has found previously, it is recorded in the vector \vec{p}_i . And also the best fitness result value is recorded in $P_{best,i}$, for comparison on the next iterations. The PSO keeps finding better positions and updating both \vec{p}_i and $p_{best,i}$.

Position of individual particles x_i at $k + 1$ iteration is modified according to the following [7]:

$$x_i^{k+1} = x_i^k + v_i^{k+1} \quad (1)$$

The particle position is adjusted using the particle velocity which is calculated using the following equation [8, 9]:

$$v_i^{k+1} = w \times v_i^k + c_1 \times r_1 (P_{best,i}^k - x_i^k) + c_2 \times r_2 (G_{best}^k - x_i^k) \quad (2)$$

where,

- $i = 1, 2, \dots, n$;
- k : iteration index,
- v_i^k , and x_i^k : velocity and position of particle i at iteration k ,
- $P_{best,i}^k$: best position of particle i at iteration k
- G_{best}^k : global best position in the whole swarm until iteration k ,

- c_1 : cognitive parameter coefficient,
- c_2 : social parameter coefficient,
- r_1 and r_2 : predefined random values in rang [0, 1],
- ω : inertia weight factor controlling the dynamics of flying,
- n : number of particles in the group

The inertia weight factor dynamically adjusts the velocity of particle and therefore it controls the exploration and exploitation of the search space. The nonlinearly decreasing inertia weight w is set as follow [10]:

$$\omega = \omega_{min} + \left(\frac{iter_{max} - iter}{Iter_{max}} \right)^n \times (\omega_{max} - \omega_{min}) \quad (3)$$

where,

- ω_{min} , and ω_{max} : lower and upper limit value of inertia weights,
- $Iter_{max}$: maximum number of iteration,
- $Iter$: current iteration,

In each iteration, ω inertia weight will decrease nonlinearly from ω_{max} to ω_{min} and n is the nonlinear modulation index.

Fig. 2 illustrates PSO search mechanism according to “(1)” and “(2)”.

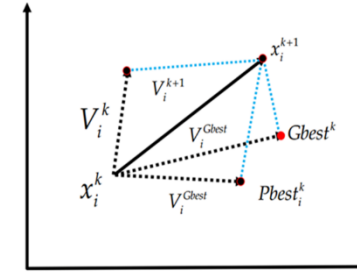


Fig. 2. The search mechanism of the particle swarm optimization

The process of PSO algorithm for solving Nonograms puzzles can be summarized as follows:

- 1) Initialization a population with random positions and velocities of a group of particles in d dimensional problem space while Nonograms puzzles constraints.
- 2) Position updating
- 3) Memory updating P_{best} and G_{best} .
- 4) if stopping criteria is satisfied then stop PSO, else go to Step 2.

III. DIW-PSO FOR SOLVING NONOGRAMS PUZZLES

In this section, the DWI- PSO in solving Nonograms puzzle is described. The fitness function has a major role in the DWI-PSO algorithm, since it is the only standard of judging whether a particle is “best” or not. The fitness function for Nonograms puzzles is calculated as follow:

$$f_k(x_k^i) = \sum_{p=0}^n |r_{i,p} - x_{ip}| + \sum_{p=0}^m |c_{p,i} - x_{p,i}| \quad (4)$$

where

- $\chi_{i,r}$ is the total number of colored pixels at row r of individual i ,

- Q_r is the total number of colored pixels at row r of the puzzle,

- $Y_{i,r}$ is the total number of colored pixels at column r of individual i ,

- P_r is the total number of colored pixels at column r of the puzzle.

The fitness value $f_k^i(x_k^i)$ gives an indication how much the individual $\chi_{i,n}$ far from the optimal solution. Compare current particles fitness value $f(x_k^i)$ with best particles fitness value $f(Pbest_i^k)$. If $f(x_k^i)$ is better than $f(Pbest_i^k)$ then set f_{best}^i value to $f_k^i(x_k^i)$ and the $Pbest_i^k$ location to the location x_k^i . Then compare $f(x_k^i)$ with the population's global best $f(Gbest^k)$. If the $f(x_k^i)$ is better than $f(Gbest^k)$ then reset f_{best}^g to the current particle $f(x_k^i)$, and the $Gbest^k$ location to the location x_k^i . To illustrate the fitness function, consider the figure 2. The fitness function for figure 2 (b), (c) and (d) is calculated as follow:

$$\begin{aligned} f(Pbest_i^k) &= |2 - 2| + |2 - 2| + |1 - 1| + |2 - 1| + |3 - 2| \\ &\quad + |0 - 2| = 4 \\ f(x_k^i) &= |2 - 2| + |2 - 2| + |1 - 1| + |2 - 1| + |2 - 2| \\ &\quad + |1 - 2| = 2 \\ f(Gbest^k) &= |2 - 2| + |2 - 2| + |1 - 1| + |3 - 1| + |2 - 2| \\ &\quad + |2 - 0| = 4 \end{aligned}$$

Since $(x_k^i) < f(Pbest_i^k)$, the current x_k^i is better than $Pbest_i^k$, then set $f_{best}^i = 2$, and $Pbest_i^k = x_k^i$. And also since the $f(x_k^i) < f(Gbest^k)$, which indicates that current x_k^i is better than $Gbest^k$, then set $f_{best}^g = f(x_k^i)$, and $Gbest^k = x_k^i$.

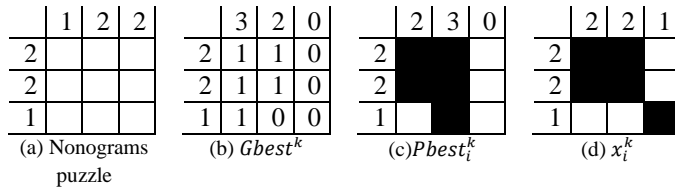


Fig. 3. An example to illustrate the Nonograms fitness function

At each iteration step, velocities of all particles are modified using “(2)”, so the velocity of particle i at iteration k (Fig. 3) according to “(1)” is:

$$\begin{aligned} v_i^{k+1} &= [1 \times 0 + 2 \times 0.2 \times (0) + 2 \times 0.8 \times (4)] \bmod V_{max} \\ &= [6.4] \bmod 3 = 7 \bmod 3 = 1 \end{aligned}$$

where $c_1 = c_2 = 2$, $v_i^k = 0$, $r_1 = 0.2$, $V_{max} = 3$, and $r_2 = 0.8$

After calculating the velocity, and between successive iterations, the modification of the particle position is controlled by the new calculated velocity. The modified position of x_i^k is

done by adding the v_i^{k+1} to the x_i^k , as defined in “(2)”:
$$x_i^{k+1} = x_i^k + 1$$

The result of the above equation means that the current particle x_i^k must be shifted one cell to right. Fig. 4 illustrates the result of shifting x_i^k .



Fig. 4. Particle Position modification

Generally, the procedure for the proposed algorithm consists of the following steps:

Step 1: Initialization

- 1.1. Constant variables c_1, c_2 and k_{max} .
- 1.2. Positions of a group of particles x_i^k .
- 1.3. Velocities of a group of particles v_i^k .

Step 2: Optimization

- 2.1. For each particle, evaluate fitness f_k^i using (4).
- 2.2. Compare the fitness of each individual with each $Pbest_i$.
If $f_k^i \leq f_{best}^i$, then the new position of i^{th} particle is better than $Pbest_i$, then set $f_{best}^i = f_k^i, Pbest_i^k = x_k^i$.
- 2.3. Compare the fitness of each individual with $Gbest^k$.
If $f_k^i \leq f_{best}^g$, the new position of i^{th} particle is better than $Gbest^k$, then set $f_{best}^g = f_k^i, Gbest^k = x_k^i$.
- 2.4. Calculate the inertia weight using (3).
- 2.5. Update all particle velocities according to (2).
- 2.6. Update all particle positions according to (1).
- 2.7. Increment k.
- 2.8. repeat steps 2.1 – 2.4 until a sufficient good fitness or a maximum number of iterations are reached.

Step 3: Terminate

DWI-PSO parameters are as in Table 1. To solve the Nonograms puzzle we set the population size equal to the number of rows times number of columns in the Nonograms puzzle, maximum Number of iterations are considered as 10, 20, 50,100 and 1000, respectively, $c1 = c2 = 2$, and Var_{max} and Var_{min} are equal to the length of the search space [6, 11]. In addition, the inertia weight starts with 1.4 and decreases nonlinearly to 0.4 [12].

TABLE I. PARAMETERS FOR DWI-PSO

Population Size (Swarm Size)	nPop	
Maximum Number of Iterations	$iter_{max}$	10, 20, 50, and 100
Intertia Coefficient	ω	1.0
Intertia Coefficient maximum value	ω_{max}	1.4
Intertia Coefficient minimum value	ω_{min}	0.4
Personal Acceleration Coefficient	c_1	2
Social Acceleration Coefficient	c_2	2
Decision Variables maximum value	Var_{max}	1
Decision Variables minimum value	Var_{min}	0

IV. EXPERIMENTAL RESULTS

To clarify the efficiency of the DIW-PSO algorithm on Nonograms puzzle, several experiments as carried out. The experiment involved three puzzles of each of the following difficulties: “5 × 5”, “10 × 10”, “15 × 15”, “20 × 20”, “25 × 25”, “30 × 30”, “35 × 35”, “40 × 40”, and 45 × 45. All puzzles were selected from <http://www.nonograms.org>.

Table 2 shows the success DIW-PSO in solving Nonograms puzzle. Success rate represents the number of runs out of the maximum number of iterations.

TABLE II. SUCCESS RATE OF VARIOUS METHODS

Problem size	number of runs / maximum number of iterations		
	Puzzle 1	Puzzle 2	Puzzle 3
5 × 5	5/10	6/10	8/10
10 × 10	45/50	40/50	30/50
15 × 15	44/50	32/50	34/50
20 × 20	89/100	70/100	77/100
25 × 25	85/100	87/100	94/100
30 × 30	200/1000	205/1000	194/1000
35 × 35	195/1000	222/1000	275/1000
40 × 40	215/1000	245/1000	320/1000
45 × 45	200/1000	250/1000	310/1000

V. CONCLUSION

In this paper, we presented a new algorithm for solving Nonograms. The process of PSO algorithm in finding optimal values follows the social behavior of bird flocks and fish schools which has no leader. Particle swarm optimization consists of a swarm of particles, where particle represent a potential solution. Particle will move through a multidimensional search space to find the best position in that space. Particle swarm optimization (PSO) is a promising scheme for solving NP-complete problems due to its fast convergence, fewer parameter settings and ability to fit dynamic environmental characteristics.

The Nonograms problem is known to be NP-hard. The challenge is to fill a grid with black and white pixels in such a way that a given description for each row and column,

indicating the lengths of consecutive segments of black pixels, is adhered to.

Firstly, this paper investigates the principles Nonograms puzzle and the general procedure for finding the puzzle solution. Moreover, the principles and optimization steps of Dynamic Inertia Weight Particle Swarm Optimization DWI-PSO and the influence of different parameters on algorithm optimization has been introduced in details.

In this paper, DWI-PSO has been applied for solving Nonograms puzzle. A dynamic inertia weight introduced to increase the convergence speed and accuracy of the PSO while searching for the best solution from Nonograms puzzle. The excremental results demonstrate the effectiveness, efficiency and robustness of the proposed algorithms for solving large size Nonograms puzzles.

In summary, we presented a DWI -PSO algorithm that has been successfully applied to NP-Complete puzzles. For future work, we will consider DWI-PSO for more challenging NP-Complete puzzles such as the Cross Sum, Cryptarithms, and Corral Puzzle.

REFERENCES

- [1] J. Kennedy, R. C. Eberhart and Y. Shi, *Swarm Intelligence*, Morgan Kaufmann Publishers, San Francisco, 2001.
- [2] K.J. Batenburg and W. A. Kosters. A discrete tomography approach to Japanese puzzles. In Proceedings of the 16th Belgium-Netherlands Conference on Artificial Intelligence (BNAIC), pages 243-250, 2004.
- [3] S. Salcedo-Sanz, E.G. Ortiz-Garcia, A.M. Perez-Bellido, J.A. Portilla-Figueras, and X. Yao. Solving Japanese puzzles with heuristics. In Proceedings IEEE Symposium on Computational Intelligence and Games (CIG), pages 224-231, 2007.
- [4] K.J. Batenburg and W.A. Kosters. Solving Nonograms by combining relaxations. *Pattern Recognition*, 42:1672-1683, 2009.
- [5] N. Ueda and T. Nagao. NP-completeness results for Nonogram via parsimonious reductions, preprint, 1996.
- [6] J. Kennedy and R. Eberhart. Particle swarm optimization. *Proceedings, IEEE International Conference on Neural Networks*, 4:1942–1948, 1995.
- [7] A. P. Engel Brecht, *Fundamental of Computational Swarm Intelligent*, First Ed. The atrium, Southern Gate, Chichester, West Sussex PO19 8SQ, England: John Wiley & Sons Ltd, 2005.
- [8] Eberhart R C, Shi Y. (1998). Comparison between genetic algorithms and Particle Swarm Optimization. Porto V W,Saravanan N,Waagen D, et al.*Evolutionary Programming VII.*[S.I.]:Springer,1998:611-616.
- [9] Eberhart R C, Shi Y. (2000). Comparing inertia weights and constriction factors in Particle Swarm Optimization. *Proceedings of the Congress on Evolutionary Computing*, 2000: 84-88.
- [10]A. Chatterjee and P. Siarry, Nonlinear inertia weight variation for dynamic adaptation in particle swarm optimization, *Computers and Operation Researches*, vol.33, no.3, pp.859-871, 2006.
- [11] J. Chen, Z. Qin, Y. Liu and J. Lu, Particle swarm optimization with local search, *Proc. of the IEEE Int. Conf. Neural Networks and Brain*, pp.481-484, 2005.
- [12]Y. Shi and R. C. Eberhart, A modified particle swarm optimizer, *Proc. of the IEEE Conf. Evolutionary Computation*, pp.69-73, 1998.

Conceptual Modeling in Simulation: A Representation that Assimilates Events

Sabah Al-Fedaghi

Computer Engineering Department
Kuwait University
Kuwait

Abstract—Simulation is often based on some type of model of the evolved portion of the world being studied. The underlying model is a static description; the simulation itself is executed by generating events or dynamic aspects into the system. In this context, this paper focuses on *conceptual* modeling in simulation. It is considered the most important aspect in simulation modelling, at the same time it is thought the least understood. The paper proposes a new diagrammatic language as a modeling representation in simulation and as a basis for a theoretical framework for associated notions such as events and flows. Specifically, operational semantics using *events* to define fine-grained activities are assimilated into the representation, resulting in an integration of the static domain description and the dynamic chronology of events (so-called *process* level). The resulting unified specification facilitates understanding of the simulation procedure and enhances understanding of basic notions such as things (entities), events, and flows (activities).

Keywords—events; flow; conceptual modeling; simulation; diagrammatic language

I. INTRODUCTION

Simulation, as employed in this paper, is a technique used to imitate a system or process, as in the case of studying concrete phenomena and their causal relations. It is often based on some type of *model* of the evolved portion of the world under study (the domain – the subject of the simulation study) [1]. Such underlying model is a static description of the domain; the simulation itself is conducted by generating *events* or dynamic aspects into the system. Accordingly, the execution of a model or part of it to reach certain conclusions about the system is known as simulation.

This paper focuses on a *conceptual* model (in contrast to, say, a mathematical or computational model) as an abstract representation of a system intended to replicate some of its properties [2] and to use as a tool for communication between stakeholders. Methods for such representation include texts, diagrams, and logic flow charts [3]. According to Wagner [4], in simulation engineering, a system model consists of both an information model and a process model. “Conceptual modelling, one of the first stages in a simulation study, is about understanding the situation under study and deciding what and how to model” [5]. This phase is considered the most important aspect of simulation modeling [6]; at the same time it is thought to be the least understood [7].

This paper seeks to utilize a new diagrammatic language for conceptual modeling of simulations. Diagrams seem “the

best approach to enhancing *communication* among a wide variety of specification audiences” [8; *italics* added]. According to Zeigler [9], communication is one of the most important and also least appreciated aspects of modeling.

Here the purpose is not to introduce a complete technical solution, which would be outside the limited scope of a conference paper; rather, the aim is to develop an appreciation for the informality of the proposed approach, starting from defining flows and events and ending with a unified description of the system and its environment (simulation). A more ambitious aim is to propose a new approach to conceptual modeling in simulation and to develop a theoretical framework for its associated notions such as events and flows.

A. Focus of study: Diagrammatic representation

Over years of simulation research, many diagrammatic methodologies have been utilized in building models in simulation, e.g., activity cycle diagrams (state diagrams), event graphs, Petri nets, control flow graphs (see [10]), UML, and BPMN. To give an idea of the type of study examined in this paper, we consider a diagrammatic representation introduced in the form of activity cycle diagrams (ACDs) [11].

In the ACD-based approach, a simulation model is viewed as a collection of interacting entities. An active state usually involves the cooperation of different entities. To specify a model using ACDs, an activity cycle composed of queues and activities must be given for each class of entity in the model [10]. ACDs provide a means to recognize and prioritize simultaneous events at the specification level in simulation. “The strongest advantage of these diagrams is that they are simple to work with. However, to fully support the simulation process, these diagrams must be augmented” [10].

An ACD example is the English Pub, where the man entity either drinks or waits to drink. The barmaid either pours a drink or is idle. The glass is either used to drink from, empty, poured into by the barmaid, or full, waiting to be consumed (see Fig. 1) [10].

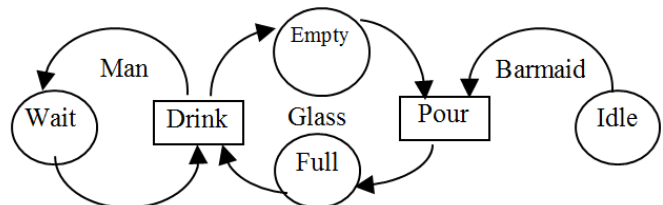


Fig. 1. Activity Cycle Diagram (redrawn, partial from [10])

B. Contribution: Alternative Diagrammatic representation in simulation

This paper presents an alternative to the ACD representation and applies the completed diagram to simulation. Fig. 1 of the English Pub will be recast in the proposed new language of diagramming. The claim is that this methodology provides a more complete specification suitable for a static domain model and its dynamic aspects needed in simulation.

For the sake of a self-contained paper, the next section briefly reviews the diagrammatic language, called the Flowthing Model (FM) that forms the foundation of the theoretical development of the paper, with the *deer dominance* example as a new contribution. With understanding of FM gained from this example, section 3 substantiates the claim that FM offers a more complete specification than the ACD graph of the English Pub discussed in the introduction.

After FM is illustrated with an example and used to support some claims in the introduction, section 4 introduces our research topic of conceptual modeling in simulation by contrasting some notions in the simulation literature against their representation in FM.

Section 5 contains the main contribution of the paper, an exploration of the FM representation in a wider organizational setting. Here we demonstrate that the FM representation embeds operational semantics that simplify the process of modeling a chronology of events.

Section 6 suggests that FM can provide a unifying language for modeling in simulation. Section 7 discusses a specific case study of simulation and applies the FM representation to the case.

II. A DIAGRAMMATIC LANGUAGE

The approach utilized in the paper is called the Flowthing Model (FM), which has been used in a variety of applications (e.g., [12-16]). FM is a uniform method for representing things that “flow”; i.e., things that are *created*, *processed*, *released*, *transferred*, and *received* while retaining their individuality throughout the flow. They may queue in any of the flow stages. They flow within *spheres*, i.e., the relevant environment that encompasses the flow. A sphere may have subspheres.

Things that flow in a flow system are referred to as *flowthings* or, as here, simply as *things*. The life cycle of a thing is defined in terms of six mutually exclusive *stages*: creation, release, transfer, arrival, acceptance, and process (in which its *form may be changed*, but no new thing is generated), as shown in Fig. 2. The flow system shown in the figure is a generalization of the input-process-output model. The reflexive arrow in the figure indicates flow to the *Transfer* stage of another flow system. For simplicity, the stages *Arrive* and *Accept* can be combined and termed *Receive*.

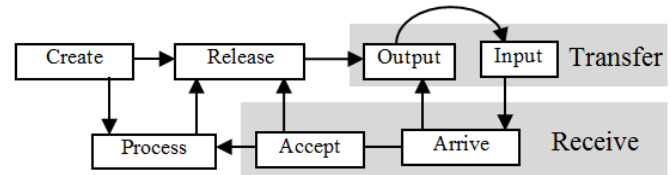


Fig. 2. Flow system

The *stages* in the life cycle of a thing are mutually exclusive (i.e., a flowthing can be in one and only one stage at a time). All other states or conditions of flowthings are not mutually exclusive stages. For example, we can have *stored* created things, *stored* processed things, *stored* received things, etc.; thus *stored* is not an exclusive stage. Things can be released but not transferred (e.g., a channel is down), or arrive but not be accepted (wrong destination), and so on.

The following example illustrates the FM diagrammatic language and its expressive power.

Example: As shown in Fig. 3, Geva [17] provides a text description of behavior of red deer during breeding season, followed by a diagram showing the causal connections described in the text, as produced by a typical student who “has in his repertoire skill for identifying basic meaningful units” [17].

It is frequently necessary to distinguish between dominance—one individual intimidating or threatening another—and leadership—one individual directing the group. Among red deer the dominance shown by males during the breeding season is vastly different from the leadership by the older females who are out ahead of the group and determine its direction without the use of force.

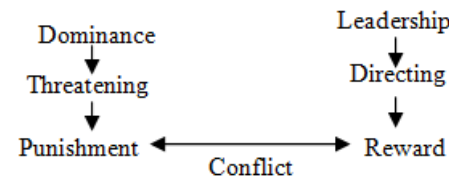


Fig. 3. Diagramming of descriptive text to identify causal relationships (partial, from [17])

Fig. 4 shows the FM representation of *male dominance among deer during breeding season* as interpreted from Fig. 3. The female flows to the male domain (circle 1 in the figure), where she is physically “processed” (2) in different ways. In one scenario she is under threat by the male (3). In case she disobeys (4), she is punished (5). (For simplicity, the flow of the female (1 and 2) is not enclosed in a box.)

The figure can be contrasted with the left side of Fig. 3 where Dominance → Threatening → Punishment.

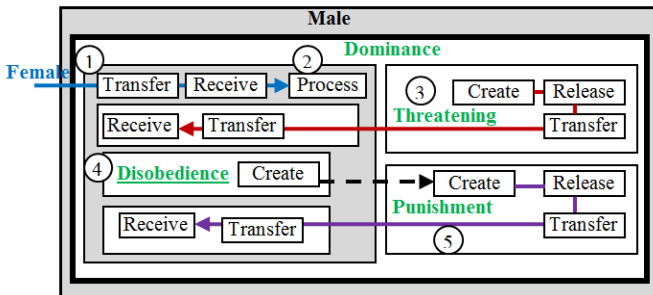


Fig. 4. Deer dominance by males during the breeding season

Similarly, Fig. 5 shows the FM representation of leadership by the older females who are out ahead of the group and determine its direction without the use of force. The process Leadership → Directing → Reward of Fig. 3 is also taken into account. The older female (circle 1) issues a direction (2) that flows (3) to each (4) member of the group (5). Execution of the direction (6) triggers (7) the generation (creation, 8) of a reward that flows to the member.

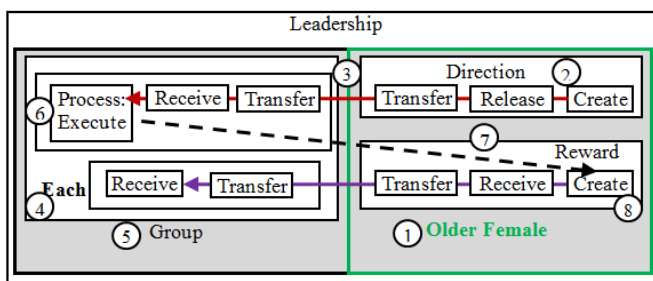


Fig. 5. Deer leadership by the older females who are out ahead of the group and determine its direction

III. THE ENGLISH PUB IN FM

Now, with this understanding of FM, we can substantiate our claim that the specification offered by FM, suitable for static domain modeling along with dynamic aspects needed in simulation, is more complete than the ACD graph of the English Pub discussed previously. Specifically, this section focuses on the static representation, leaving the event-oriented simulation to a later section.

Returning to the example of an English pub discussed in the introduction, from the representational point of view, the diagram of Fig. 1 seems incomplete as a picture of the domain of the pub. The diagram is formed from three separate scenes:

- The state of a Man changes between drinking and waiting
- The state of a Glass changes between empty and full
- The state of a Barmaid alternates between idle and pouring

The resulting conceptual picture is formed by jumping from one state to the next. Thus we find, for example, that the glass is empty during the entire time of pouring, the state specified as (Man: Waiting, Glass: Empty?, Pouring: ON). Modeling of a

domain is selective in its details; nevertheless, in the opinions of the present authors, the model should not “contradict” reality in the domain, e.g., the glass is not empty during the pouring process.

The FM representation provides a “continuous” portrait of the system, as shown in Fig. 6. First, the man orders a drink (circle 1 in the figure) and the order flows to the barmaid (2) to trigger taking an empty glass (3) from storage that flows to the barmaid (4). This triggers release of the liquor (5) to the barmaid, thus creating a filled glass (6) that flows to the man (7) to drink (8).

As we see, inherent characteristics of the FM representation, based on the notion of flow, force the modeler to “connect the dots” and paint a complete chronology of events in the system.

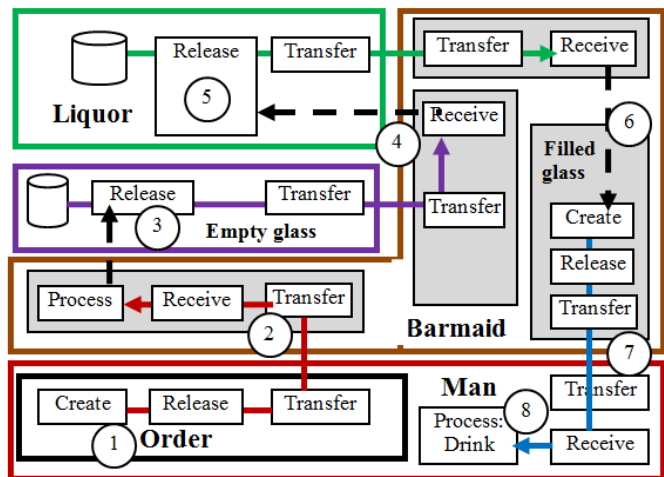


Fig. 6. FM representation

IV. CONTRASTING SOME NOTIONS

This section contrasts some notions used in the simulation literature with their representation in FM. The purpose is to highlight how the FM approach is different from current simulation methods, as an introduction to applying FM in the rest of the paper. Additionally, the discussion in this section shows how FM provides a *unifying* view of many notions in simulation, using the same diagrammatic language introduced in section 2.

In simulation literature, an *object* is typically defined as anything with attributes [18]. Objects and attributes in FM are *things* as defined previously. The two concepts of *time* and *state*, fundamental in the context of simulation, are also things. Similarly, an event is a thing. According to Page [10],

An *event* is a change in an object state, occurring at an instant, and initiates an activity precluded prior to that instant. A process is the succession of states of an object over a span (or the contiguous succession of one or more activities).” [Italics added]

Page [10] illustrates the notions of event, activity, and process in simulation as shown in Fig. 7.

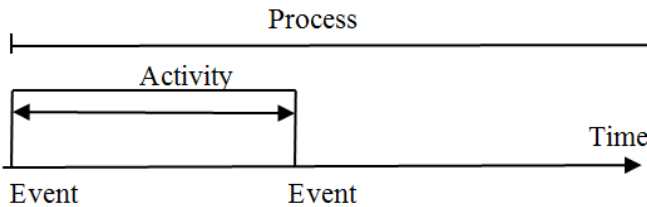


Fig. 7. An illustration of event, activity, and process (redrawn, partial from [10])

An event in FM is a thing since it can be created, processed, released, transferred, and received. It triggers the creation, release, processing, transfer and receipt (“activity” in the above quote) of other things. *Process* in the quote is the *flow* in FM, e.g., a thing is created, released, and transferred. Fig. 8 illustrates the flow, event, and “activities”, i.e., states in a flow system.

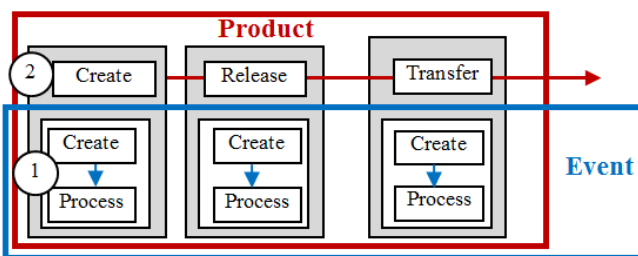


Fig. 8. Illustration of event flow and “activities”

In the figure, the product is modeled from a static description as a thing that is created, released, and transferred; however, such creation, releasing, and transferring occurs only as a result of events. The event is the trigger that activates each stage of flow. Such a distinction between a static description and dynamic activation of a system is a very important aspect in simulation; nevertheless, the two levels of specification (static and dynamic) can be modeled by the same diagrammatic language.

For example, the event at circle 1 activates (causes creation of a product thing: instance). Process (1) in the figure refers to the event (creation) taking its course (e.g., duration). Event scheduling in the diagram could be accomplished through clock “jumps”; e.g., every hour, with each clock tick creating the next period or next new product, etc.

V. APPLYING FM TO EVENTS

This section explores the FM representation in a wider organizational setting. It demonstrates that the FM representation embeds *operational semantics* that simplify simulating the chronology of events in comparison with other diagrammatic representations such as UML sequence diagrams. The resultant operational semantics are conceived along the lines of UM causality model specification in which *events* are used to define fine-grained behaviors. First, let us explore the notion of event in various fields.

According to McKee [19] in the context of English

literature, “STRUCTURE is a *selection of events* ... that is composed into a strategic sequence” [italics added]. Such a definition seems to imply that the structure of a literary piece is the structure of events.

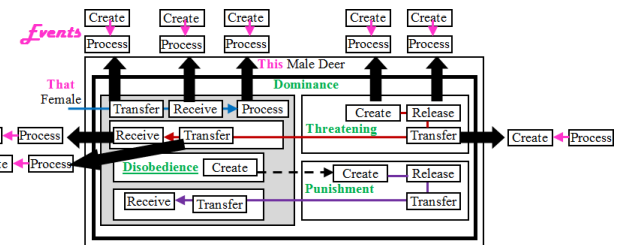


Fig. 9. Example of flows of events

In this paper, structure is the conceptual description of where the flow “takes place.” It is the FM diagram. An *event* is a “happening” or “occurrence” in a point of the diagram (e.g., domain). It may be connected to earlier events (e.g., causal connections). Philosophically, in the context of a definition given by the French philosopher Jean-Luc Marion [20-21],

An event is that which ... changes the given order of things, and then disappears, leaving its mark without return. An event shows itself as much as it gives itself to be seen. An event, properly so-called, poses a problem for thought to think it in ways other than according to the measure of its visible appearance. [22]

Additionally, an event *inaugurates* something new from within a given situation and a break or rupture in the current state of a situation. It is both situated in and supplementary to what the present authors call a structure. (Some of these expression are taken from Butchart [22] describing Badiou’s [23] philosophy, but reinterpreted differently).

This interpretation views the FM diagram as the structure: a static map of things and their flows. Events are *things* of happenings (occurrences), as shown in Fig. 9 for dominance by males described in Fig. 4. This latter figure of dominance by males is a static scenario of the dominance, while Fig. 9 shows actual events (occurrences) as things that can be created, processed, released, transferred, and received.

All things flow in their streams in the basin of flow (the total FM diagram) which forms the *structure* of events, where

- 1) The event in this structure of a specific (that) female transferred to the dominance of a specific (this) male.
- 2) The event in which the female is received.
- 3) The event in which the female is processed, etc.

The scenario is like a scene in a movie being actualized, shot by shot (event by event). Each event “shows itself” and disappears, as in Butchart’s [22] quote: “event, event, event, ... assimilated in a structure.”

As an illustration of assimilation of events in the FM representation, consider the following computer program taken from Podgurski and Clarke [24].

input (X, Y);

1. if X > Y then
2. Max := X;
- else
3. Max := Y;
4. endif;

Fig. 10 shows a partial view of its FM representation (see [25]). The figure also shows different events in this execution.

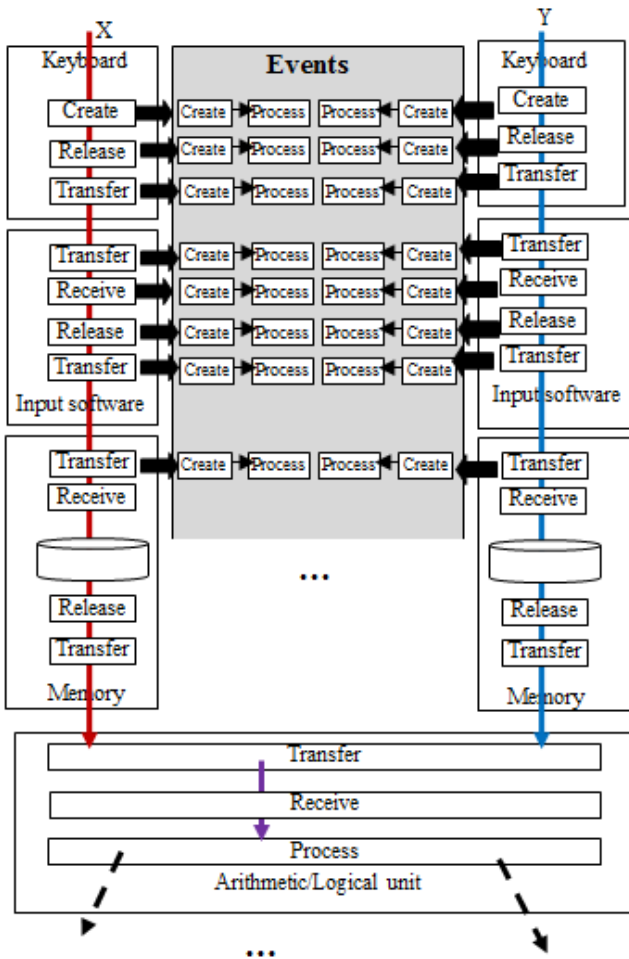


Fig. 10. Events when executing a program

First, the event in which X and Y are created (generated) in the keyboard. The values are release and transfer to the input software (e.g., *cin* in C++). Then the events continue one after another. Note that we have two levels of representation: (a) the structure of the situation, a static FM diagram of the program, and (b) the events, an FM diagram of events at the dynamic level where the event “*inaugurates* something new from within a given situation” [22].

Accordingly, an operational semantics can be defined to describe how to schedule events in the FM representation, therefore specifying the thread of control of execution. Operational semantics can also uncover concurrency of threads of events that offer several options for executions or occurrences, which is required in such systems as distributed systems.

For instance, consider the deer dominance scenario represented in Fig. 4. Two possible sequences of events (behavior – possible execution) are shown in Fig. 11,

1) A female arrives and immediately disobeys; hence, it is punished (1, 2, 3, 4B–10B)

2) A female arrives and immediately faces threats; hence, she immediately submits to the male without disobedience (1, 2, 3, 4A–9A)

Here, the male is assumed to exist prior to the arrival of the female. If we want to express this explicitly, we can add *Create* in the Male sphere to precede these two sequences of events.

Note that the flow and triggering force a partial order on some events; thus, *release* is preceded either by *create*, *process*, or *receive*; a threat is preceded by being communicated by the male (*released* and *transferred*). By the nature of this triggering, punishment is caused by disobedience, hence the sequence 4B, 5B in Fig. 11, etc. Accordingly, alternative sequences of events are modeled at certain points such as circle 3 in Fig. 11 where the A and B threads of events are separated according to circumstances, e.g., actual occurrences or execution.

Similarly, in the execution of the computer program of Fig. 10, the left and right sequences of inputting X and Y can be executed in parallel along the two threads of flow; their arrival at the ALU would then have to be synchronized.

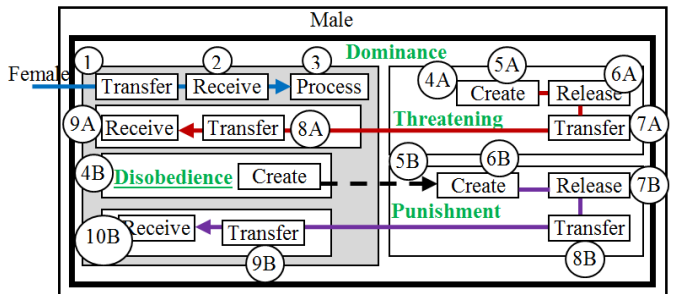


Fig. 11. Two possible sequences of events following the arrival of a female

VI. APPLICATION TO SIMULATION

This section suggests that FM can provide a unifying language that supports modeling in simulation.

According to Wagner [4],

Due to their great expressivity and their wide adoption as modeling standards, UML Class Diagrams and BPMN seem to be the best choices for making information and process models in a model-driven simulation engineering approach. [4]

Wagner [4] illustrates how to develop a simulation of the functions of a *service desk* with the help of UML class diagrams and BPMN diagrams.

In the DES [Discrete Event Simulation] literature, it is often stated that DES is based on the concept of “*entities flowing through the system*”. However, the loose metaphor of a “flow” only applies to entities of certain types: events, messages, and certain material objects may, in some sense, flow, while many entities of other types, such as buildings or

organizations, do not flow in any sense. Also, subsuming these three different kinds of flows under one common term “entity flow” obscures their real meanings. It is therefore highly questionable to associate DES with a “flow of entities”. Rather, one may say that DES is based on a flow of events. [4; italics added]

This view is different from the concept of flow in FM, where the conceptual flow is defined in terms of states of Create, Process, Release, Transfer, and Receive. In FM, buildings can flow conceptually. Suppose that a city zoning board decided to change the zoning for an area containing building 1234, where each zone has different regulations. The building in effect will “flow” to the sphere of a different zone, as shown in Fig. 12. In FM, events, entities, buildings, signals are all things that can flow.

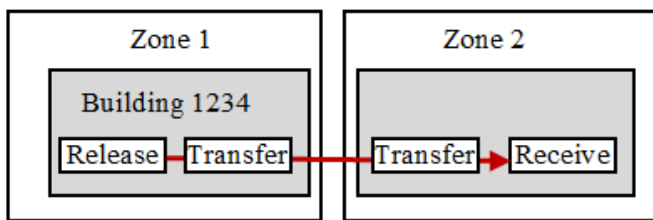


Fig. 12. The flow of a building

According to Wagner [4], ‘‘Unfortunately, this [concept of DES as a flow of events] is often obscured by the standard definitions of DES that are repeatedly presented in simulation textbooks and tutorials.’’ Wagner [4] then describes Pegden’s [26] simulation modeling worldview which provides ‘‘a framework for defining a system in sufficient detail that it can be executed to simulate the behavior of the system.’’

Over the 50 year history of simulation there have been three distinct world views in use: event, process, and objects.

Event worldview: The system is viewed as a series of instantaneous events that change the state of the system over time. This is the basis of the events flow systems in FM.

Process worldview: The system is described as a process flow in which sets of passive entities flow through the system and are subject to a series of process steps (e.g. seize, delay, release) that model the state changes that take place in the system.

Object worldview: The system is modeled by describing the objects that make up the system. The system behavior emerges from the interaction of these objects. [4]

According to Pegden [26], agent based modeling is typically implemented with the object worldview.

So, today’s DES landscape is largely based on the process worldview and object worldview, and the fundamental concept of events is hardly considered anywhere. All three worldviews, and especially the process and object worldviews, which dominate today’s simulation landscape, lack important conceptual elements. The event worldview does not support modeling objects with their (categorical and dispositional) properties. The process worldview does neither support modeling events nor objects. And the object worldview, while it supports modeling objects with their categorical properties, does not support modeling events. None of the three worldviews does support modeling the dispositional properties of objects with a full-fledged explicit concept of transition rules. [4]

Clearly, a Process worldview (the stages of the flow system) and an Object worldview are integrated into the FM diagram, which also includes events as flowthings. The FM description unifies these worldviews through describing them in one language. The FM representation models the system (e.g., deer dominance by males) and models a particular realization of that system using events as things (e.g., arrival of a female with no disobedience), similar to a computer program and testing a path of execution in the program.

Accordingly, we propose that FM can provide a unifying language that supports modeling in simulation.

VII. EXAMPLE: APPLICATION OF FM TO SIMULATION

This section discusses a specific case study of simulation and applies the FM representation to such a case.

Wagner [4] views simulation engineering as a special case of software engineering, hence, applies model-driven development that includes conceptual, design, and implementation models. Wagner [4] uses an example that includes the entity types *Person*, *Customer*, and *ServiceQueue*, as classes in UM. UML stereotypes are utilized to distinguish between object types and event types as two different categories of entity types and use them for categorizing classes.

In the study case, an *event* involves exactly one customer who gets in line at exactly one service queue. The customers wait in a queue; when the queue is empty and the service desk is not busy, they are served. Four entity types can be extracted by analyzing the noun phrases of the description: *ServiceDesk*, *ServiceQueue*, *Service clerk*, and *Customer*. The last two are subclasses of *Person*.

After modeling all relevant object types in the first step, Wagner [4] models the relevant event types in a second step, as shown in Fig. 13. At this point, we reach the focus of our discussion in this paper: Methods of attaching events to the system description.

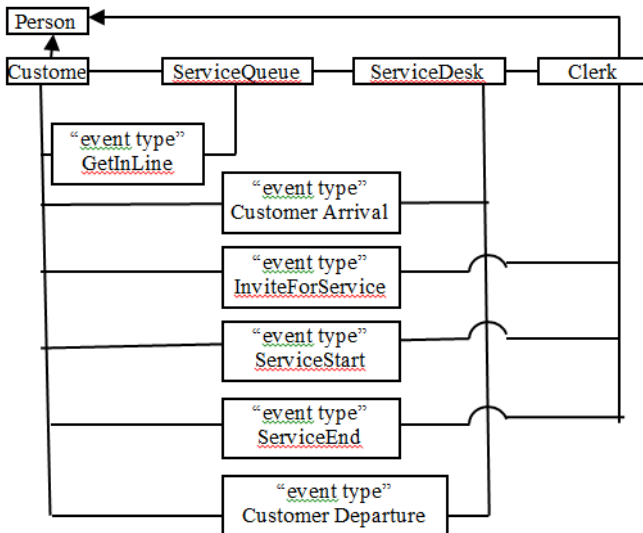


Fig. 13. The complete information model includes event types (redrawn, partial from [4])

Wagner [4] then draws a completely new diagram for the control of the Queue shown partially in Fig. 14, using yet another diagrammatic language, BPMN. Additionally, Wagner [4] models randomness of events using event types. For example, *CustomerArrival* is drawn (not shown here) as an exogenous event type with the class-level attribute *occurrenceTime* having the value (1,8), denoting a random variable with uniform distribution with lower bound 1 and upper bound 8.

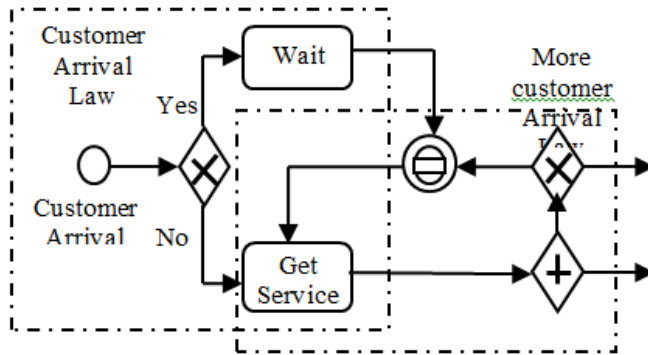


Fig. 14. Queue control (redrawn, partial from [4])

Wagner [4] then introduces a diagram (not shown here) for process design modeling using BPMN.

In the process design model, we turn the causal laws defined in the conceptual process model into corresponding transition rules described as BPMN sub-processes with

- a start/intermediate event for triggering the transition rule;
- tasks expressed as statements that contain typed variables and have a clear computational meaning;
- bindings of variables to entities. [4]

The whole approach exemplified by the case study discussed in this and the previous section seems to lack a unified foundation. First, it is based on “entities flowing through the system,” as mentioned previously. Then it states that “flow” applies only to entities of certain types: events, messages, and certain material objects may, in some sense, flow, while many entities of other types, such as buildings or organizations, do not flow “in any sense” [4]. Finally, it is suggested that one could say that DES is based on a *flow of events*. Accordingly, as shown in the example, heterogeneous types of diagrammatic representations are used, ranging from UML and BPMN either in a mix of hierachal structures with flowing events (Fig. 13) or as refinements of higher-level diagrams (Fig. 14).

The next section introduces the FM representation of the same case study.

VIII. UNIFIED SCHEMATA: ENTITIES, EVENTS, AND FLOWS

To make this example more interesting, we assume two service clerks. Fig. 15 shows the FM representation of this case. Such an addition to the problem will allow us to distinguish between the system (the FM diagram) and its environment: in this case, simulation with events is performed on only one service desk while excluding the other service desk. In the figure, for simplicity, details of the second queue and service clerk are omitted.

Accordingly, in the figure, the customer arrives (circle 1) and proceeds to either Service desk 1 (circle 2) or Service desk 2 (circle 3). At desk 1, the customer is received into its queue (4) then proceeds to Clerk 1 (5) and leaves when finished (6).

We assume that our aim is to simulate the system with only one service desk; thus events are activated only along Service desk 1: circles 1, 2, 4, 5, and 6. Fig. 16 shows the simulated part of the system, with bold boxes (red lines in the online version) indicating activity events (instead of creation and processing of an event).

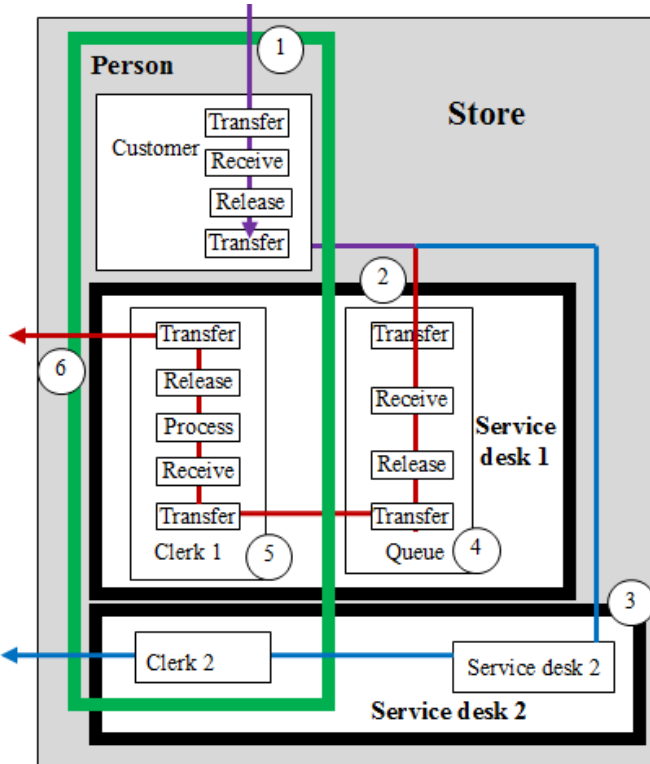


Fig. 15. FM representation

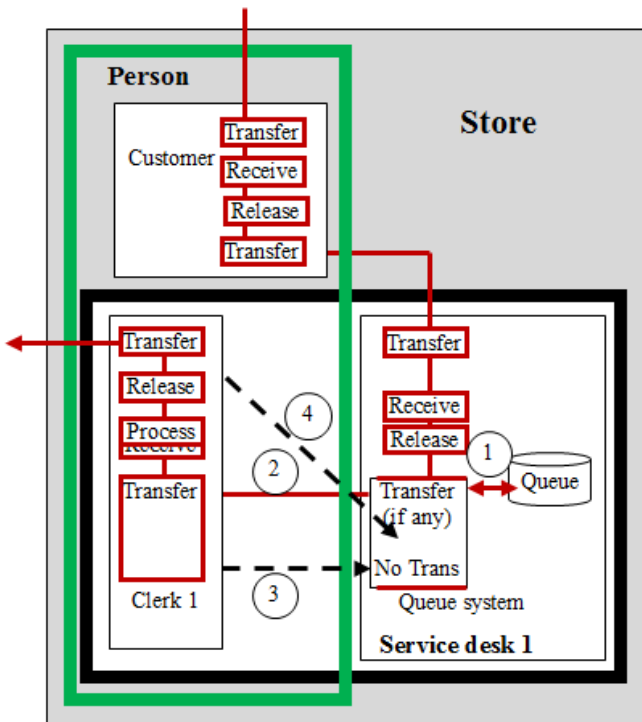


Fig. 16. Activating events of only Service Clerk 1

Active here refers to being in a state of liveliness and reactivity, or in engineering terminology, in the ON state. An *event* is a thing that facilitates such active state by a “switching” or “firing” occurrence (Petri net terminology). A flow (create, process, ...) begins with an event and may end

with the beginning of another event. The event is what causes the flow of things. Note that Create is a type of flow.

Thus, in the figure, a person passes through various active stages. Here we combine the descriptive (static) level and the events level by assuming that each stage is event-active: it performs its function as soon as the thing flows through it. In the queue, the person proceeds to the clerk (2) and this transfer “blocks” any additional flow (3). When the customer leaves the clerk (is released and transferred), the next transfer to the clerk is permitted (4).

Fig. 17 shows the addition of generating random numbers of arrivals, between 1 and 8 (circle 1). The clerk’s processing time (circle 2) can be added in similar fashion.

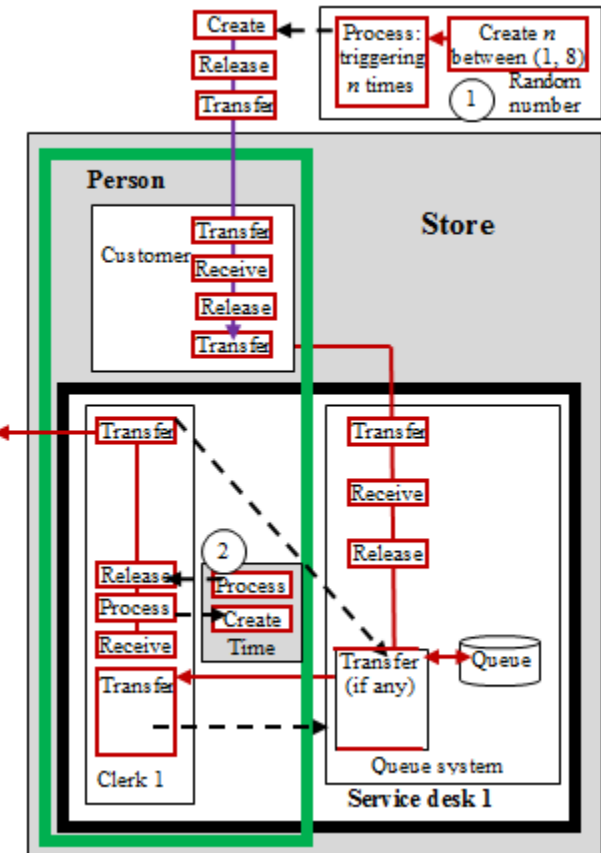


Fig. 17. Activating events of only Service Clerk 1

IX. CONCLUSION

As stated in the introduction, this paper proposes a new diagrammatic language for modeling representations in simulation and as a basis for a theoretical framework incorporating associated notions such as events and flows. Additionally, where events are used to define fine-grained activities, operational semantics are assimilated into the representation, resulting in an integration of the static domain description and the dynamic chronology of events.

We have shown that this unified specification facilitates such goals; nevertheless, the paper is still a theoretical proposal waiting to be realized in an actual simulation project. It is an attempt to point a direction substantiated by examples and re-

casting of work from the published literature. Furthermore, the paper seems to clarify some of the involved issues such as the two-level approach (domain description and events sequences) needed for simulation, and it also seems to enhance understanding of such notions as events and flows.

REFERENCES

- [1] T. Grüne-Yanoff and P. Weirich, "The philosophy and epistemology of simulation: a review," *Simulation & Gaming*, vol. 41, no. 1, pp. 20–50, 2010.
- [2] C. M. Overstreet, (1982). "Model Specification and Analysis for Discrete Event Simulation," PhD Dissertation, Department of Computer Science, Virginia Tech, Blacksburg, VA, December.
- [3] W. Wang and R. Brooks, 2007. Empirical Investigations of Conceptual Modeling and the Modeling Process. In Proceedings of the 2007 Winter Simulation Conference, ed. S.G. Henderson, B. Biller, M.-H. Hsieh, et al., 762-770. Piscataway, NJ: IEEE Computer Society Press.
- [4] G. Wagner, Information and Process Modeling for Simulation, Tutorial, Jan 2015 · Proceedings - Winter Simulation Conference.
- [5] A. A. Tako, K. Kotiadis, and C. Vasilakis, "A participative modeling framework for developing conceptual models in healthcare simulation studies," In Proceedings of Winter Simulation Conference, Baltimore (MD), USA, B. Johansson, S. Jain, J. Montoya-Torres, et al., Eds. 2010, pp. 500–512. <http://www.informs-sim.org/wsc10papers/045.pdf>
- [6] A. M. Law, *Simulation Modeling and Analysis*. Boston: McGraw-Hill, 2007.
- [7] S. Robinson, S. "Conceptual modeling for simulation: issues and research requirements," in Proceedings of the 2006 Winter Simulation Conference, L. F. Perrone, F. P. Wieland, J. Liuet, et al., Eds. Monterey, CA: Institute of Electrical and Electronic Engineers, 2006
- [8] J. W. Brackett, "Formal specification languages: a marketplace failure; a position paper," in Proceedings of the 1988 IEEE International Conference on Computer Languages, Miami, FL, p. 161, October 9-13, 1988.
- [9] B. P. Zeigler, (1976). *Theory of Modelling and Simulation*. New York: John Wiley and Sons, 1976.
- [10] E. H. Page Jr., *Simulation Modeling Methodology: Principles and Etiology of Decision Support*. Ph.D. Dissertation, Virginia Polytechnic Institute and State University, Blacksburg, September 1994.
- [11] R. J. Paul, "Activity cycle diagrams and the three phase approach," in Proceedings of the 1993 Winter Simulation Conference, pp. 123–131, Los Angeles, CA, December 12-15, 1993.
- [12] S. Al-Fedaghi and A. Alrashed, "Threat risk modeling," paper presented at International Conference on Communication Software and Networks (ICCSN 2010), Singapore, February 26–28, 2010.
- [13] S. Al-Fedaghi, "Toward flow-based semantics of activities," *Int. J. Softw. Eng. Appl.*, vol. 7, no. 2, pp. 171-182, 2013.
- [14] S. Al-Fedaghi and B. Al-Babtain, "Modeling the forensics process," *Int. J. Secur. Appl.*, vol. 6, no. 4, 2012.
- [15] S. Al-Fedaghi, "Awareness of context and privacy," *Am. Soc. Inform. Sci. Tech. (ASIS&T) Bull.*, vol. 38, no. 2, 2011.
- [16] S. Al-Fedaghi, "Typification-based ethics for artificial agents," paper presented at Second IEEE International Conference on Digital Ecosystems and Technologies (IEEE-DEST 2008), Phitsanulok , Thailand, February 26–29, 2008.
- [17] E. Geva, Facilitating Reading Comprehension through Flowcharting. University of Illinois, Urbana-Champaign, July 1981. https://www.google.com.kw/url?sa=t&rct=j&q=&esrc=s&source=web&cd=1&cad=rja&uact=8&ved=0ahUKEwjM5ea5jM7OAhUHlxQKHeyiBewQFggMAA&url=https%3A%2F%2Fwww.ideals.illinois.edu%2Fbibtstream%2Fhandle%2F2142%2F18065%2Fcfrstreadtechrepv01981i00211_opt.pdf%3Fsequence%3D1&usg=AFQjCNExx3Z9X8TVvI4G_v4G_lbct3AL0Fg&bvm=bv:129759880.d.d24
- [18] R. E. Nance, "The time and state relationships in simulation modeling," *Comm. ACM*, vol. 24, no. 4, pp.173- 179, 1981.
- [19] R. McKee, *Story: Substance, Structure, Style, and the Principles of Screen Writing*. ReganBooks, 1997. ISBN: 0-06-039168-5.
- [20] J.-L. Marion, *Being Given: Toward a Phenomenology of Givenness*, Jeffrey L. Koskey (trans.). Stanford, CA: Stanford University Press, 2002.
- [21] J.-L. Marion, *Reduction and Givenness: Investigations of Husserl, Heidegger, and Phenomenology*, Thomas A. Carlson (trans.). Evanston, IL: Northeastern University Press, 1998.
- [22] G. C. Butchart, "An excess of signification: or, what is an event?" *Semiotica*, vol. 187, no. 1/4, pp. 291–307, 2011.
- [23] A. Badiou, *Ethics: An Essay on the Understanding of Evil*, Peter Hallward (trans.). London: Verso, 2001.
- [24] A. Podgurski and L. A. Clarke, "The implications of program dependences for software testing, debugging, and maintenance," *ACM SIGSOFT Softw. Eng. Notes*, vol. 14, no. 8, pp. 168-178, December 1989. DOI: 10.1145/75309.75328
- [25] S. Al-Fedaghi, "Conceptual understanding of computer program execution: application to C++," *Int. J. Comp. Sci.*, vol. 10, no. 2, March 2013.
- [26] C. D. Pegden, "Advanced tutorial: overview of simulation world views," in Proceedings of Winter Simulation Conference, Baltimore (MD), USA, B. Johansson, S. Jain, J. Montoya-Torres, et al., Eds., pp. 643–651, 2010.

Performance Improvement of Threshold based Audio Steganography using Parallel Computation

Muhammad Shoaib

Information Technology Department,
Hazara University,
Mansehra, Pakistan

Danish Shehzad

Computer Engineering Department,
Kadir Has University,
Istanbul, Turkey

Arif Iqbal Umar

Information Technology Department,
Hazara University,
Mansehra, Pakistan

Zakir Khan

Information Technology Department,
Hazara University,
Mansehra, Pakistan

Tamer Dag

Computer Engineering Department,
Kadir Has University,
Istanbul, Turkey

Noor Ul Amin

Information Technology Department,
Hazara University,
Mansehra, Pakistan

Abstract—Audio steganography is used to hide secret information inside audio signal for the secure and reliable transfer of information. Various steganography techniques have been proposed and implemented to ensure adequate security level. The existing techniques either focus on the payload or security, but none of them has ensured both security and payload at same time. Data Dependency in existing solution was reluctant for the execution of steganography mechanism serially. The audio data and secret data pre-processing were done and existing techniques were experimentally tested in Matlab that ensured the existence of problem in efficient execution. The efficient least significant bit steganography scheme removed the pipelining hazard and calculated Steganography parallel on distributed memory systems. This scheme ensures security, focuses on payload along with provisioning of efficient solution. The result depicts that it not only ensures adequate security level but also provides better and efficient solution.

Keywords—Steganography; LSB; Steganalysis; Parallel; Pipelining; Processing Efficient; Real time; Security

I. INTRODUCTION

The brisk advancement in internet technology and digital information revolutionized the overall technology and information communication. Easy to use and cheap software have enabled major portion of society to get addicted to these communication systems where they can create, manage and exchange multimedia data. Specifically broadband Internet has facilitated transmission of data at much faster and cheaper rate thus helps people to create and share large amount of audio/ video files [1]. These information sharing requires security of private information on internet as it is shared by billions of users. The provisioning of security over internet is most challenging research area as sending and receiving sensitive data through unsecured internet is very critical. There are three main techniques that are being used for information security and are known as encryption, steganography and watermarking [2].

Steganography hides secret information inside another wrapper that may be text, audio, video and protocol. Steganography originated from steganos meaning covered and graphi means writing. Steganography is that branch of

information security which deals with embedding secret information inside cover on sender side and retrieving it back on receiver. The purpose of steganography may be personal information sharing, private communication or preventing resources from piracy. Stego-message is amalgamation of cover and host message, where message that is hiding information i.e. user's message is called host message [3].

Audio steganography is type of steganography in which secret information is hidden inside audio signal and audio is modified in imperceptible manner. An overall audio steganography system can have following components.

- Message to be sent
- Cover audio signal
- Encoding technique/algorithm
- Stego signal : Audio combined with secret information is known as
- Decoding technique/algorithm

The steganography allows only communicating parties to see inside that what is being transferred and hides this fact from any other party on the same communication channel [4]. Audio steganography can be divided into four key types, where each of these types is beneficial and vary in implementation mechanisms. Though all techniques are significant and have their own beneficial areas.

A. Least Significant Bit Encoding

In order to encode binary information, least significant bit of each audio frame is modified and information is embedded inside it. This technique is simple and has many advantages as high payload in audio but in contrast has low security. File compressions, conversion or other necessary changes can modify and contaminate hidden information [5].

B. Echo Hiding

This mechanism deceives the perception by modifying frames by adding various kinds of sub-perceptible echoes. Three main parameters of the audio frame are varied which

are amplitude of signal, its decay rate and offset as delay. Each parameter is adjusted below human audible threshold so that echo cannot be detected and resolved normally. The offset is different for encoding the binary message, if one offset value represents one the other is representing binary zero. If single information is to be produced from audio signal, single bit information can be encoded only. So, this mechanism audio signal is separated into blocks before encoding, modified and then concatenated to produce the final audio signal [6]. The main drawback of this technique is its low capacity as it is computationally heavy and complex to add echo for each bit.

C. Phase Coding

Phase coding allows replacement of phase components from original audio signal for hiding information inside replaced components. The new amplitude in will not be audible to human. Thus, it results in non-audible encoding of signal to perceived noise ratio (SPNR) resulting in hiding secret message inside audio signal, which cannot be detected by steganalysis based on SPNR [7]. This technique allows controlled phase modifications host in audio to carry secret information.

D. Spread Spectrum

This method allows spreading of secret information in the spectrum inside audio signal using code which is autonomous to that of actual signal. There are two main types of SS for audio steganography: direct sequence spread spectrum (DSSS) and frequency hopping spread spectrum (FHSS). In DSSS, the secret message is spread across the spectrum by constant known as chip rate, and then it is modulated with signal and then interleaved with host signal. In FHSS the frequency of spectrum is modified to allow it to hop briskly between frequencies and allowing fast wrapping of information [6]. The limitation of this method is it introduces distortion to the original audio signal.

The paper is arranged in sections where Section II elaborates the existing work and explains limitations of the existing techniques. In Section III proposed solution is explained with description of encoding and decoding process. Section IV gives the experimental results and comparison that shows the efficiency of the proposed solution. Section V concluded the work.

II. LITERATURE REVIEW

Least significant bit steganography ensures that binary digits are embedded in LSBs in cover file. Various LSB techniques have been developed for ensuring security [9]. GIF based image LSB is explained in [10]. Two bits of cover page pixels help to store one bit message in LSB based on Difference Expansion [11]. Hiding behind corners LSB and edge based LSB are important methods adopted in LSB Steganography [6]. LSB steganography has several important methods that are currently used for hiding data.

A. Parity Coding

In this method parity bits are used for embedding data. Complete signal is broken down into separate small samples.

If bit to be encoded does not match with sample's parity bit then flip LSB of sample [12].

B. XORing Method

XORing method performs XOR operation on LSBs and the message bit and the result of XOR decides whether to modify or to keep LSB unchanged. This approach increases capacity of cover by 8 times and provides comparatively robust encryption [12].

C. Bit Selection

Varying bits are selected inside each sample to hide secret information. The first two MSBs are used for selection of bits from sample to hide secret data and first three LSBs are used for embedding data. If the first two MSBs are 00 then third bit is used for same purpose. This mechanism confuses the intruder and do not allow to obtain secret information [13].

D. Sample Selection

Specified samples from signal are used for data hiding purpose. Here randomness is achieved by the control of 1st three MSBs. If the current sample is i, last column shows next sample containing hidden bit. The space between two consecutive hidden bits in sample is one more than decimal value of 1st three MSBs [14].

E. Lowest Bit Coding

This method embeds the data using least significant bit. Both wave data and secret information to be sent are in binary form, low bit of wave is replaced with bit by bit of message [7]. This method gives capacity benefit of 12.5% and minimizes the transition.

F. Variable Low Bit Coding

This method increases embedding capacity as it introduced advancement in lowest bit coding. Two thresholds are defined like 1 and 2 so that bits information can be embedded between these ranges. If the range of amplitude is less than 1 then data is not embedded. If the range of amplitude is between threshold values, one bit is used for embedding data and if amplitude range is greater than 2 then data is embedded using 2 bits [7].

G. Average Amplitude Method

Average amplitude data of audio in surrounding is used as threshold value. The average is calculated for 10 audio data and after 5 audio data other than own audio data [7]. If level of amplitude is greater than threshold, then 2 bits are used for embedding in any other case bits are not used and number of embedding bits are limited to 2.

III. PROPOSED SOLUTION

In this work a novel method is proposed to reduce the processing time of the steganography, and improve the efficiency of the process. There are two basic steps to improve the efficiency, which are:

1) Divide the cover signal into sub signals according to the number of cores of processor.

2) Mack each sample embedding and extraction process independent from other samples.

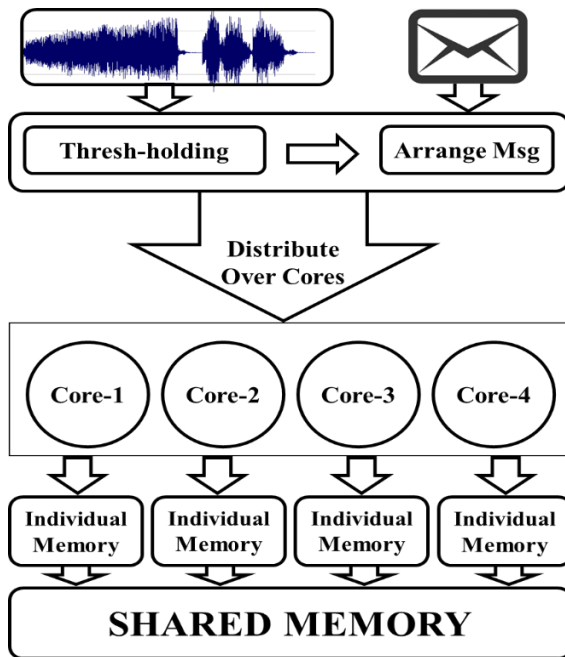


Fig. 1. Distribution of signal over multiple processor cores

In this way the advantage of parallelism and pipelining is achieved as well, which improve the efficiency as compared to all existing techniques. The encoding and decoding process is explained as follows:

A. Encoding Process

The encoding process starts with reading host audio signal then original audio signal is quantized and the samples are converted into discrete form. The formula used for quantization is as follows:

$$\text{Quantized Audio} = \text{Amplitude} \times (2^{\text{No_of_Bits}-1})$$

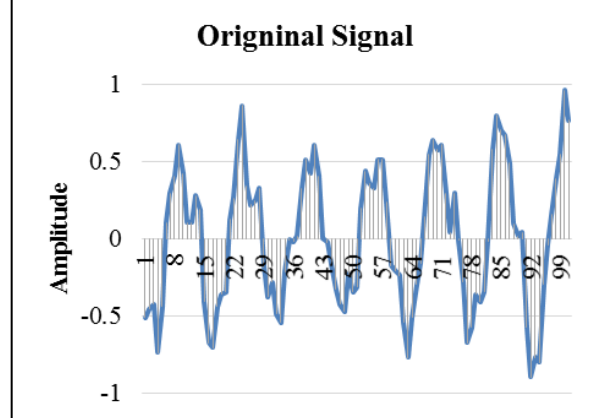


Fig. 2. Original Audio Signal Amplitude

When the numbers of bits in a sample are equal to 16 then quantized value can be calculated as:

$$\text{Quantized Audio} = \text{Amplitude} \times (2^{16-1})$$

$$\text{Quantized Audio} = \text{Amplitude} \times 32768$$

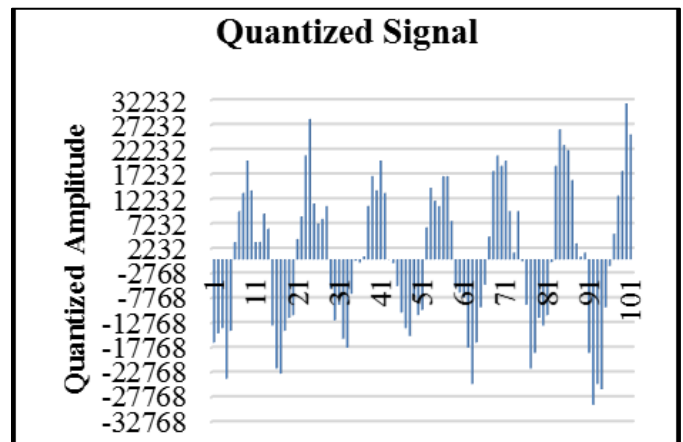


Fig. 3. Quantized Signal Discrete Values

TABLE I. THRESHOLDS FOR 1 TO 8 BITS STEGANOGRAPHY

S. No	Lower Bound	Upper Bound	Stego Bits
1	0	255	8-Bits
2	256	511	7-Bits
3	512	1023	6-Bits
4	1024	2047	5-Bits
5	2048	4095	4-bits
6	4098	8191	3-Bits
7	8192	16383	2-Bits
8	16384	32768	1-Bit

As shown in table 1. Sample capacity is 8 bits but when sample amplitude is greater than 255 then capacity of sample is calculated by following equation as:

$$\text{Capacity of Sample} = 16 - \text{ceil}(\log_2 \text{Sample Amplitude})$$

After the quantization of audio signal and getting discrete values, binary empty array is created for bits to be stored inside the audio signal. After that samples are selected according to Threshold values. If the values lie within threshold limit further process of Steganography is followed. LSB data according to threshold is selected and converted into binary and is appended in binary array string. When the process is complete binary data is written to file for sending it under cover to the destination.

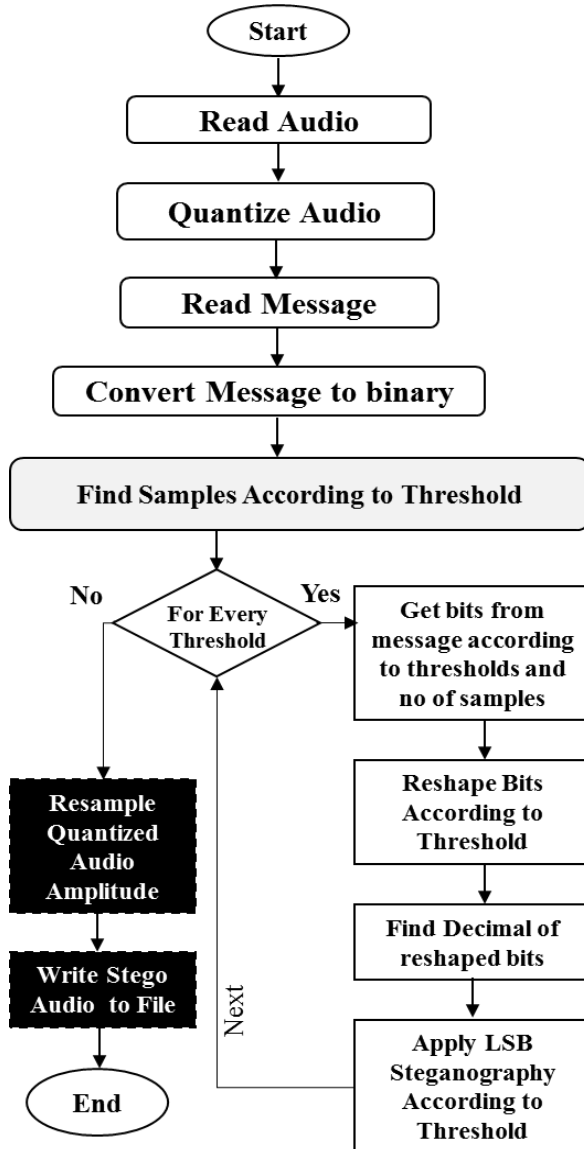


Fig. 4. Encoding Process

B. Decoding Process

On receiver side the received audio signal is quantized again using the same process as shown above. An empty array for storage is created for retrieving hidden data storage. After quantization for each threshold least significant bit is obtained and data is uncovered that was hidden during encoding process. After the parallel unfolding of data as shown in Fig4, through various thresholds, complete data is retrieved at destination.

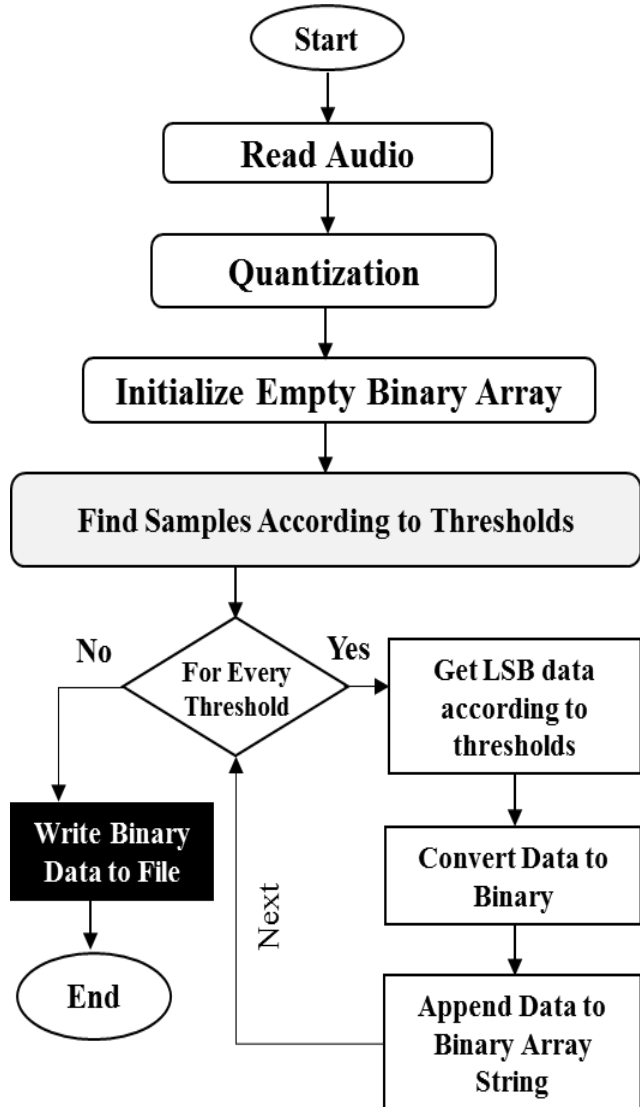


Fig. 5. Decoding Process

IV. EXPERIMENTAL RESULTS

The experiments were conducted in Matlab 2015 on Intel core i5 with 4 cores and using 8 GB RAM for computing the efficiency of the proposed parallel scheme, and the results were compared with existing Hakeem. et al scheme. Results depicts that the proposed scheme is much efficient than existing scheme. The exiting scheme was calculating threshold for each sample, then hiding the data but serially according to threshold was consuming most of the time. This scheme parallelize it by finding threshold, then arranging samples

according to threshold and parallel on multiprocessing systems hiding data through steganography.

TABLE II. PROPOSED SCHEME VS. HAKEEM. ET. AL AUDIO STEGANOGRAPHY EFFICIENCY COMPARISON

Sound	Hakeem	Proposed	Total Efficiency	Efficiency Per Sec
Chirp	110.255	0.889	123.963	77.346
Gong	372.828	0.903	412.977	80.496
Handel	579.918	1.093	530.370	59.426
Laughter	429.817	0.900	477.734	74.356
Splat	85.708	0.871	98.431	80.629
Train	110.889	0.822	134.859	85.772

Table 2 shows that as compared to existing Hakeem. et.al scheme when experiments conducted on different sounds, the proposed scheme is much more times efficient than existing scheme.

V. CONCLUSION

Audio steganography is used to send secret information inside the cover of audio signal for secure transmission. There are various schemes ensuring adequate and efficient security, but due to serial dependency efficiency of existing schemes were causing the computational overhead. The proposed scheme enhanced the existing scheme by eliminating the serial dependency and running the steganography calculations on parallel machines in efficient manner. The result shows that it not only ensures adequate security level but also provides much better and efficient solution.

REFERENCES

- [1] J. Johnston and K. Brandenburg, 1992, "Wideband Coding Perceptual Consideration for Speech and Music". Advances in Speech Signal

- Processing, S. Furoi and M. Sondhi, Eds. New York: Marcel Dekker.
- [2] W. Bender, W. Butera, D. Gruhl, R. Hwang, F. J. Paiz, S. Pogreb, "Techniques for data hiding", IBM Systems Journal, Volume 39 , Issue 3-4, July 2000, pp. 547 – 568.
 - [3] Robert Krenn, "Steganography and steganalysis", An Article, January 2004.
 - [4] F.A.P.Petitcolas, R.J.Anderson, G.Kuhn: "Information Hiding- a Survey", Process of IEEE, vol.87, no.7, pp.1062-1078, July, 1999.
 - [5] P.K.Singh, R.K.Aggrawal, 2010,"Enhancement of LSB based Steganography for Hiding Image in Audio", International Journal on Computer Science and Engineering, Vol. 02, No. 05.
 - [6] F.Djebbar, B.Ayady, H.K.Abed Meraimx, 2011,"A view on latest audio steganography techniques", International Conference on Innovations in Information Technology.
 - [7] P.Dutta1, D.Bhattacharyya, and T.Kim, June 2009" Data Hiding in Audio Signal: A Review", International Journal of Database Theory and Application, Vol. 2.
 - [8] F.Djebbar, B.Ayady, H.K.Abed Meraimx, 2011,"A view on latest audio steganography techniques", International Conference on Innovations in Information Technology.
 - [9] Thomas, P. "Literature survey on modern image steganographic techniques". In International Journal of Engineering Research and Technology. 2013. ESRSA Publications.
 - [10] Bender, W., et al., *Techniques for data hiding*. IBM systems journal, 1996. **35**(3.4): p. 313-336.
 - [11] Tian, J., *Reversible data embedding using a difference expansion*. IEEE Trans. Circuits Syst. Video Techn., 2003. **13**(8): p. 890-896.
 - [12] H.B.Kekre, A.Athawale, S.Rao, U.Athawale, October 2010" Information Hiding in Audio Signals", International Journal of Computer Applications, (0975 – 8887) Volume 7– No.9.
 - [13] H.B.Kekre, Archana Athawale, Swarnalata Rao, Uttara Athawale, October 2010, *Information Hiding in Audio Signals*, International Journal of Computer Applications (0975 – 8887) Volume 7– No.9.
 - [14] M.Asad, J.Gilani, A.Khalid, 2011,"An Enhanced Least Significant Bit Modification Technique for Audio Steganography", IEEE978-1-61284-941-6/11.
 - [15] Hakeem, N. Amin, M. Shah, Z.Khan & A.Qadir, "Threshold Based LSB Audio Steganography", Int'l Conf. on Chemical Engineering & Advanced Computational Technologies, 2014. South Africa.

A Hybrid Algorithm based on Invasive Weed Optimization and Particle Swarm Optimization for Global Optimization

Zeynab Hosseini

Department of Computer Engineering
Urmia Branch, Islamic Azad University
Urmia, Iran

Ahmad Jafarian*

Department of Mathematics
Urmia Branch, Islamic Azad University
Urmia, Iran

Abstract—In this paper, an effective combination of two Metaheuristic algorithms, namely Invasive Weed Optimization and the Particle Swarm Optimization, has been proposed. This hybridization called as HIWOPSO, consists of two main phases of Invasive Weed Optimization (IWO) and Particle Swarm Optimization (PSO). Invasive weed optimization is the nature-inspired algorithm which is inspired by colonial behavior of weeds. Particle Swarm Optimization is a swarm base Algorithm that uses the swarm intelligence to guide the solution to the goal. IWO algorithm is the algorithm which is not benefit from swarm intelligence and PSO converges to the local optimums quickly. In order to benefit from swarm intelligence and avoidance from trapping in local solutions, new hybrid algorithm IWO and PSO has been proposed. To obtain the required results, the experiment on a set of benchmark functions was performed and compared with other algorithms. The findings based on the non-parametric tests and statistical analysis showed that HIWOPSO is a more preferable and effective method in solving the high-dimensional functions.

Keywords—*Invasive weed optimization; Particle Swarm Optimization; Global optimization; Hybrid algorithm*

I. INTRODUCTION

One of the affective methods in finding the best solution in numerical problems is the Optimization technique. In optimization, only a few solutions are considered the best which are called as the goal. Classical optimization techniques have some deficiencies on solving the complex optimization problems. These deficiencies are primarily interdependent on their inherent search systems. These classical optimization methods are strongly under effects of choosing proper objectives, constraints functions and type of variables. They also do not grant a universal result approach that can be used to solve problems where various type of variables, objective and constraint functions, are used [1]. For covering these deficiencies ,a new method with the name of Metaheuristic was designed, which is mainly originated from artificial intelligence research that developed by researchers [2]. A Metaheuristic is an algorithm designed for solving the various types of hard optimization problems without having to fully accommodate to each problem. The Greek word meta indicates that these methods are higher-level heuristics. The primary features of Metaheuristic methods are as follows: they are nature-inspired (meaning that they have originated from

nature physics, behavior and etc); stochastic components are one of the inseparable parts of these methods (involving random variables); they aren't gradient base method and don't use them; at the beginning of program, they have several parameters which needs to adjust properly. Metaheuristic algorithms combine various intelligent procedures and guide basic heuristic methods [3]. These algorithms are inspired from different things such as natural phenomena, natural selections and social behaviors and applied in solving the optimization problems. Examples of the recently metaheuristic algorithms are Vortex search [4], WOA (whale optimization algorithm) [5], MBA (mine blast algorithm) [6], WCA(water cycle algorithm) [7], and SFS (stochastic fractal search) [8].

The PSO [9] is the other Metaheuristic algorithm which has been utilized in the optimization of many problems. This algorithm uses the strategy of birds and folks in migration for finding better solutions. Individuals in the PSO are called as particles and each particle has velocity in the searching space. Particles are distributed randomly in the searching space and positions of the particles are changed based on the velocity which has been calculated. These particles tend to move toward the best positions which causes to seek a better position and find the best. One of the deficiencies that can be specified for PSO is that it often falls to the local minimum quickly, missing better opportunities when facing multimodal functions [10].

IWO is a nature inspired algorithm which is getting much more attention because it shows efficient exploration and dissimilarity properties [11] and took an exceptional place for solving continuous optimization problems. In formal IWO, the seeds are uniformly spread on the search space [11]. After all, if the searching space is too large, its not efficient to use this type of distribution for the searching. Also, initialization of the parameters is so important task in IWO and trapping in local solution is a probable event. Hence ,it was found that the efficiency of an IWO algorithm to achieve success goal in problems relies too much on its initial parameters and these parameters should be wisely selected based on the problem to be solved. To overcome these problems, a novel hybrid IWO and PSO algorithm is proposed and implemented for solving continuous optimization problems. Hybridization of IWO with other algorithms has been investigated in many studies. MICA-IWO [12] is a new type of hybrid method which

combines two well-known Metaheuristic approaches: IWO and imperialist competitive algorithm (ICA) [13]. ICA has outperformed many of the already existing stochastic and direct search global optimization techniques. The hybrid MICA-IWO method has been used for handling optimal reactive power dispatch (ORPD) problem. Other recently hybrid method based on IWO is the hybrid IWO/WDO [14] algorithm. In IWO/WDO, wind driven optimization (WDO) [15] algorithm has been combined with IWO algorithm for nulling pattern synthesis of uniformly spaced linear and non-uniform circular array antenna.

In this paper, we will combine PSO and IWO global optimization algorithms, and propose the novel hybrid algorithm based on these algorithms which are jointly called as HIWOPSO. As PSO has Swarm intelligence, this could provide more variant population for IWO which could help in finding better places by using the previous experiences. To avoidance of trapping in local solutions and searching the large area greatly, the mutation function has been used which applied for checking other places and give chance for them. Proposed method is tested on the benchmark functions and compared with other famous algorithms. The statistical analysis Friedman test [16] is performed on the results and compared with other algorithms results. The Convergence diagram and normality diagrams for the statistical analysis is also presented.

In the real world, many problems have been proposed and optimization problems are one of them [17]. The optimization problems are single or multi-objective. The multi-objective is the problem with more than one objective function ($m > c_1$) and single objective is a problem with one objective function ($m=1$). The main goal in this procedure is to seek the global minimum or maximum. The function may have more than one minimum or maximum which is called as the local, but only one of them is the global maximum or minimum. The point x^* is the global minimum if $f(x^*) \leq f(x)$ for all the x in the searching space S. Optimization problem may consist of one or more mathematical functions which need to be optimized. The general form of the optimization problem is indicated in Eq. (1).

$$\text{Minimize } F(f_1(x); \dots; f_m(x)), \quad x = (x_1, \dots, x_n) \in S. \quad (1)$$

Where n is the decision variables, m is the number of objectives, x is decision vector and S is searching space. If the problem has one objective function ($m=1$), then it should be indicated as Eq. (2).

$$\text{minimize } f(x), \quad x = (x_1, \dots, x_n) \in S. \quad (2)$$

The rest of the paper is organized as follows: Section 2 illustrates the PSO and IWO algorithms, and section 3 discusses the HIWOPSO algorithm, its parameters and boundary control. Section 4 presents 26 benchmark test functions applied for the experiments. Finally, the last section presents the concluding remarks.

II. RELATED WORKS

The PSO is the one of the Metaheuristic algorithms which

is originated from the nature. This algorithm was introduced by Kennedy and Eberhart in 1995 [9]. The PSO is originated from the birds and folks migration behavior, living in small and large numbers of groups. The birds use a method for finding food and migration, which has been used in this algorithm. In this method, only the birds know their distance from food, but they don't know the location of the food thus, following the other neighboring birds is the best way for surviving.

The PSO consist of elements with the name of particles which is a probable solution in the searching space. The main steps in the PSO algorithm are as follow: first, particles are distributed randomly in the searching area and PSO starts the process with these particles. In this searching process, particles only follow the one which is nearer to the goal and has better fitness value. Each particle has a velocity which is represented by V_i and calculated by Eq. (3) in the D-dimensional searching space. Particles are under the effect of personal ($pbest_i^t$) and swarm experiences ($Gbest_i^t$) and the position is updated by Eq. (4).

$$v_i[t+1] = w v_i[t] + c_1 r_1 (x_{i,best}[t] - x_i[t]) + c_2 r_2 (x_{g,best}[t] - x_i[t]) \quad (3)$$

$$x_i[t+1] = x_i[t] + v_i[t+1] \quad (4)$$

In Eq. (3) and (4), X_i represents the i-th particle of the population, c_1 and c_2 are the learning coefficients, r_1 and r_2 are random values between [0, 1], w is the inertia weight, and V_i is the i-th member of particles velocity. $pbest_i^t$ and $Gbest_i^t$ are the personal best and generation best.

PSO algorithm:

- 1: Initialize locations X_i and velocity V_i of n particles.
- 2: Find $Gbest$ from $\min\{f(X_1), \dots, f(X_n)\}$ (at $t = 0$)
- 3: While (criterion)
- 4: for $i = 1, 2, \dots, n$ do
- 5: Generate new velocity V_i^{t+1} using Eq. (3).
- 6: Calculate new locations $X_i^{t+1} = X_i^t + V_i^{t+1}$
- 7: Evaluate objective functions at new locations X_i^{t+1}
- 8: If X_i^{t+1} is better than $Pbest_i^t$ then
- 9: Set X_i^{t+1} to be $Pbest_i^t$
- 10: end if
- 11: end for
- 12: Find the Generation best $Gbest^t$ from particles $Pbest^t$
- 13: iter = iter + 1 (pseudo time or iteration counter)
- 14: end while
- 15: Output the final result $Gbest$

Invasive weed optimization was first introduced by Mehrabian and Locardi [11] and it is one of the population based optimization algorithms which is originated from colonial behavior of weeds. The IWO algorithm is a very simple and yet efficient algorithm in finding optimum solution of the objective function, which is implemented based on the natural and basic features of weeds in a colony such as reproduction, growth and competition to survive. In comparison to other algorithms, IWO is simpler and has adequate ability and convergence rate to the global optimum solution of the objective function. Some of the major features

of this algorithm which specifies it from other methods are reproduction, space distribution and exclusive competition.

In order to simulate behavior of a weed, we have the following algorithm, according to [11].

Step 1: Initial population production: a population of N_0 seeds is randomly distributed in an n dimensional space.

Step 2: Reproduction: each seed grows and turns into a mature plant and then, begins seed production for newer generation. The amount of seeds produced by a plant increases linearly between two possible values of minimum (S_{min}) and maximum (S_{max}) possible amounts of produced seeds. The amount of produced seeds for the i th plant in every repeat is dependent to its goal value (F_i), its best (F_{best}) and worst (F_{worst}) goal values in that repeat and is calculated with the following equation:

$$Numseed(i) = \left[S_{min} + (S_{max} - S_{min}) \frac{f - f_{worst}}{f_{best} - f_{worst}} \right] \quad (5)$$

Step 3: Distribution space the randomness and assimilation of the algorithm are related to this stage. The produced seeds are distributed in the d dimensional search space with normal distribution which has zero mean and different variance of $(N(0; \sigma_t^2))$. In this state, the seeds will be near the breeder plant. Although, the standard deviation decreases from initial amount ($\sigma_{initial}$) to final amount (σ_{final}) in each repeat, in the simulations, non-linear variation of standard deviation causes satisfactory results which are illustrated below:

$$\sigma_t = \left(\frac{T-t}{T} \right)^n \times (\sigma_{initial} - \sigma_{final}) + \sigma_{final} \quad (6)$$

In Eqs. (13)(15), T represents the maximum number of repeats related to (t) and is the non-linear modulation factor. In this status, the positions of seeds (S_j) for the i th plant (w_i) are calculated as follows:

$$S_j = W_i + N(0, \delta_t)^d, 1 \leq j \leq numseed(i) \quad (7)$$

Step 4: Exclusive competition: by several repeats, the number of plants produced by rapid reproduction reaches its maximum value (W_{max}), in this situation, every plant is permitted to produce seeds by in accordance with reproduction method. The seeds are authorized to spread in search space with correspondence to distribution space method, when the seeds find their position; they form a colony alongside their parent plants. Then members with less propriety are deleted in order to number of members reach its maximum allowed value. In this method, the parent plants combine with their children and the plants with most propriety from the group are preserved and allowed for replacement.

This crowd control mechanism will be imposed on next generations until reaching the final period. Step 5: If the criterion satisfied end otherwise, return to Step 2.

III. PROPOSED MODEL

The swarm intelligence is some kind of artificial intelligence which has been established based on group behaviors in decentralized and self-organizing systems. This systems usually included population of the simple agents that

interact locally with each other and their environment. Some samples of this system that can be mentioned are ants groups, birds flock, fishes flock, bacterize bulk and animals herd. In order to use of swarm intelligence, it needs to use the behavior of these systems in the proposed method. So PSO algorithm has been using with IWO algorithm to give the behavior of swarm intelligence to agents of IWO algorithm and use it in guiding the solution of the problems to the goal. As previously mentioned, in IWO algorithm, each father (weed) produce some child (seed) that these Childs distribute around the father with a kind of normal distribution. In proposed hybrid method, this distribution could be based on the some kind of normal distribution or guided through the goal by using the swarm intelligence and previously experience of father. Using the previously experiences is like this, if each weed (w_i) could

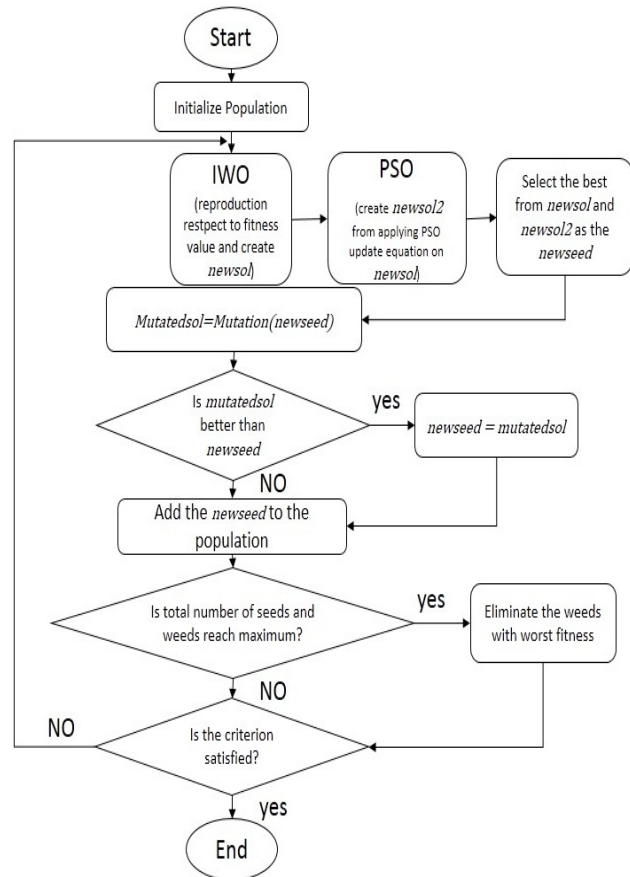


Fig. 1. Flowchart of HIWOPSO algorithm

give good result, it stores the result as the experience in the experience memory and these experiences inherited to this weed Childs and used in guiding the solutions of the problem like the PSO algorithm. Each child in proposed method (HIWOPSO) inherited two things from their father and that is the velocity (V) and experience (w_p). The main process of proposed method is like this: first, the population with size n_{pop0} of weeds (w_i) are distributed randomly around the searching space and their position is initialized randomly. The cost of each weed is computed from the position which calculated previously and at the Start, the value of velocity is zero ($V_i = 0$). first, The experience of each weed is the value

which previously initialized to the position and cost for each weed. After producing population with size of npop0, algorithm enters to the main iteration loop which at start have a section for computing the number of producing child for each weed by Eq. (5) and also the velocity for each weed is computed like the following equation:

$$w_i^{t+1} = w_i^t + c_1 \cdot r_1 \cdot (w_{pi}^t - w_i^t) + c_2 + r_2 \cdot (w_{best}^t - w_i^t) \quad (8)$$

Where w_i is ith weed in population and w_p is personal experience and w_{best} is the global best , other variables are described in PSO algorithm and This equation is same as the PSO velocity update equation. For each of the w_i enters to a loop and one solution is created by the seed distribution formula in IWO (newsol) Eq. (9) and another solution is created by PSO (newsol2) Eq (10).

$$\text{Newsol2} = w_i + N(0, \delta_t)^d \quad (9)$$

$$\text{Newsol} = w_i + V_i \quad (10)$$

New solutions newsol and newsol2 are compared with each other and if newsol2 better than newsol then newsol value will be replaced by the newsol2 value. The newsol is compared with w_i experience and if newsol better than w_p it will set as w_i experience and it also if it is better than global best, the global best will be updated with newsol. After using the PSO and IWO for creating new solutions, its time to reduce the probability of trapping in local solutions.

For decreasing this probable event , using mutation function could be help full after producing new solution. The mutation function applied to the new solution (newsol) and the output (mutatedsol) will be compared with newsol. The mutatedsol is compared with newsol and if the mutation creates better solution then the value of newsol will be replaced by the mutatedsol value and newsol inserted to the population. The mutation function described briefly in next subsection. After inserting the newsol to the population, it must be control the size of population not to exceed from maximum size which was initialized at the start (npop).

The mutation function which has been using in proposed algorithm, uses random selection of dimension and replaces that dimension values with the random values that has been obtained from function domain. For example if the input for the mutation function is the following input=[0.7 0.5 0.6 0.8] with boundary [L U]=[0.4 0.9] and if the mutation function selects random dimensions 2 and 4 then that dimensions values will be changed with random real value from domain [0.4 0.9] and output=[0.7 0.45 0.6 0.65]. Random selection of dimension could be any order of input dimension size for example, if d=30 then random dimension could be f{1 5 18 20} , f1{ 2 3 4 5 6 7 19} and etc... The number of dimension that selected for replacement is determine randomly in each execution of mutation function.

The pseudo code for proposed method described as follows:

```

HIWOPSO algorithm:
1: Input: objective function f, constraints and the dimensions of the problem (d)
2: \Initialization
3: Initial parameters npop0 (initial population size), npop (final population size) S_min, S_max,
σ_max, σ_min, n, ω, c1, c2 , wdamp.
4: Let pop be the set of weeds 1, 2, ..., npop0
5: for i = 1, 2, ..., npop0 do
6: Assign random real number between [varmin , varmax] to the weeds position
7: Calculate fitness (cost) for assigned position
8: Set velocity = 0
9: Set calculated position and cost as best experience (wp) position and cost too.
10: end for
11: \Iterations
12: while (the stopping criterion is not met) do
13: Update standard deviation by Eq. (6)
14: for i = 1, 2, ..., pop-size do (pop-size =population size )
15: Reproduction : calculate numseed(i) for each weeds in population (wi) Eq. (5)
16: Caclulate the velocity for wi Eq. (8)
17: for j = 1, 2, ..., numseed(i) do
18: Create newsol by Eq. (10) and assign wi experience and velocity to newsol
19: Create newsol2 by Eq (9) and assign wi experience and velocity to newsol2
20: if newsol2 better than newsol then newsol= newsol2
19: if newsol fitter than wi then wp_i= newsol and wi= newsol
21: if newsol better than wp then wp= newsol
22: Apply mutation: mutatedsol = mutation(newsol)
23: if mutatedsol better than newsol then newsol= mutatedsol
24: Add the newsol to the new population (newpop)
10: end for j
10: end for i
10: insert the newpop to the population
25: if pop-size > npop then sort the population and select the bests with npop size
26: decrease the inertia weight (ω * wdamp)
27: end while
28: \the final stage
29: output the minimum value found (wp)

```

HIWOPSO algorithm is consists of 2 main parts and these parts are executed in consecutive form in each cycle which are showed at the flow chart Fig. 1. In each part process is performed on weeds of population with size of pop-size and weed position is d dimensional vectors. The main operator for each part effects on time complexity. The sections that alter time complexity are: PSO update equation, IWO position update equation. We can explain complexity analysis of HIWOPSO in worse case and prove the fastest execution of these two algorithms combination like this: As the HIWOPSO algorithms are executed in consecutive form, then the time complexity for IWO is O(nd) and for PSO is also O(nd), therefore the HIWOPSO algorithm is run in O(nd) complexity because of the consecutive form of execution in IWO and PSO algorithms. For analyzing convergence of the Metaheuristic algorithm, Markov chain Monte Carlo method is the one of the preferable methods for this task [18].

Most Metaheuristic algorithms can be sighted in the framework of Markov chain from statically viewpoint. Now if look at the proposed hybrid method closely using the

framework of Markov chain Monte Carlo, each algorithm in HIWOPSO essentially forms a Markov chain and the appropriate better solutions which created in each iteration, replace with previous one. Convergence analyzing based on the Markov chain for algorithm HIWOPSO is performed as follows:

Definition 1. Assume that the best weed is shown by $X^* := \{x^* \in X : f(x^*) = \min(f(x) \mid x \in X)\}$ where X is probable solution and f is fitness function. The number of best weeds in weeds population is shown by $\omega(N) := |N \cap x^*|$.

Definition 2. Algorithm convergence with probability 1 to the best if this condition is true :

$\lim_{g \rightarrow \infty} P\{\omega(N(g)) \geq 1 \mid N(0) = N_0\} = 1$, where g indicates generation number and N_0 is random initial population.

Theorem 1. HIWOPSO algorithm converges to its globally best solution with probability 1.

Proof: Let $P_0(g) = P\{\omega(N(g) = 0)\}$ then the probability due to the Bayesian condition final probability of $P_0(g+1)$ is $P_0(g+1) = P\{\omega(N(g+1) = 0) \rightarrow P\{\omega(N(g+1) = 0) \mid \omega(N(g) \neq 0)\} + P\{\omega(N(g+1) = 0) \mid \omega(N(g) = 0)\}$. Since the best solution replace with previous one in memory, this expression $P\{\omega(N(g+1) = 0) \mid \omega(N(g) \neq 0)\}$ is true

Hence, $P_0(g+1) = P\{\omega(N(g+1) = 0) \mid \omega(N(g) = 0)\} \times P\{\omega(N(g) = 0)\}$.

$P\{\omega(N(g+1) = 1) \mid \omega(N(g) = 0)\} > 0$ is true because of the HIWOPSO algorithm by two main phases IWO and PSO store the best solution.

Make $\Gamma = \min P\{\omega(N(g+1) = 1) \mid \omega(N(g) = 0)\} \min, g = 0, 1, 2, \dots$

Then

$$P\{\omega(N(g+1) = 0) \mid \omega(N(g) = 0)\}$$

$$= 1 - P\{\omega(N(g+1) \neq 0) \mid \omega(N(g) = 0)\}$$

$$= 1 - P\{\omega(N(g+1) \geq 1) \mid \omega(N(g) = 0)\}$$

$$\geq 1 - P\{\omega(N(g+1) = 1) \mid \omega(N(g) = 0)\} \leq 1 - \Gamma < 1$$

Therefore,

$$0 \leq P_0(g+1) = P\{\omega(N(g+1) = 0) \mid \omega(N(g) = 0)\} \leq (1 - \Gamma) \times P_0(g)$$

such that, $0 \leq P_0(g+1) \leq (1 - \Gamma) \times P_0(g)$.

$$\text{Hence, } 0 \leq P_0(g+1) \leq (1 - \Gamma) \times (1 - \Gamma) \times P_0(g-1) \leq \dots \leq (1 - \Gamma)^{g+1} \times P_0(0).$$

Given that $\lim_{g \rightarrow \infty} (1 - \Gamma)^{g+1} = 0$ and $0 \leq P_0(0) \leq 1$.

$$\text{Hence } 0 \leq \lim_{g \rightarrow \infty} P_0(g) \leq \lim_{g \rightarrow \infty} (1 - \Gamma)^g \times P_0(0) = 0$$

$$\lim_{g \rightarrow \infty} P_0(0) = 0$$

Then

$$\lim_{g \rightarrow \infty} P\{\omega(N(g)) \geq 1 \mid N(0) = N_0\}$$

$$1 - \lim_{g \rightarrow \infty} P\{\omega(N(g)) = 0 \mid N(0) = N_0\}$$

$$1 - \lim_{g \rightarrow \infty} P_0(0) = 1.$$

There for, when $g \rightarrow \infty$, $P\{\omega(N(g)) \geq 1 \rightarrow 1$. HIWOPSO algorithm could reach to best solution and assurance convergence with probability 1.

Parameter adjustment is a non-negligible task which is required to be performed properly in order to get a better result in solving various problems. Besides, the parameter adjustment also is necessary for controlling the boundary whenever the algorithm finds a new solution [19]. The (HIWOPSO) needs boundary control for a weed w_i , because its position is required to be in the searching space, which is a boundary between $[L, U]$, (L is the lower bound and U is the upper bound of the searching space). The method that controls the boundary is as follows:

$$p = \text{Max}(X, L); q = \text{Min}(p, U) \quad (11)$$

Where Min and Max are the functions that select the minimum and maximum among the input pairs, X is the input weed position and q is the output which has been controlled in the boundary range $[L, U]$. Since proposed algorithm is combination of two algorithms IWO and PSO then it is consisted of these two algorithms parameters. HIWOPSO parameters with initial settings are mentioned in Table 1.

IV. DISCUSSION AND EVALUATION

In this paper, the proposed algorithm has been evaluated with a set of benchmark functions which are a subgroup of unimodal and multimodal functions. These functions have various dimensions such as 2, 4, 10 and 30. Tables 3 highlights a multimodal test functions and Table 2 shows unimodal test functions.

TABLE I. PARAMETER SETTINGS

Parameter	definition	PSO	IWO	HIWOPSO
T	Maximum number of iterations	5000	5000	2000
N pop	Maximum population size	30	150	150
npop0	Initial population size	-	10	10
Smin	Minimum number of seeds	-	0	0
Smax	Maximum number of seeds	-	5	5
n	Nonlinear modulation index	-	2	2
$\sigma_{initial}$	Standard deviation initial value	-	1	1
σ_{final}	Standard deviation in al value	-	0.001	0.001
c1	cognitive/local weight	2	-	2
c2	social/global weight	2	-	2
ω	Inertia weight	1	-	1
Ω damp	Inertia weight reduction rate	0.9	-	0.9

TABLE II. UNIMODAL TEST FUNCTIONS (D: DIMENSIONS)

Function	D	Range	Min	Formulation
F1(Beale)	2	[4.5,4.5]	0	$f(x) = (1.5 - x_1 + x_1x_2)^2 + (2.25 - x_1 + x_1x_2^2)^2 + (2.625 - x_1 + x_1x_2^3)^2$
F2(Easom)	2	[-100,100]	-1	$f(x) = -\cos(x_1)\cos(x_2)\exp(-(x_1 - \pi)^2 - (x_2 - \pi)^2)$
F3(Matyas)	2	[-10,10]	0	$f(x) = 0.26(x_1^2 + x_2^2) - 0.48x_1x_2$
F4(Colville)	4	[-10,10]	0	$f(x) = 100(x_1^2 - x_2)^2 + (x_1 - 1)^2 + (x_3 - 1)^2 + 90(x_2^2 - x_4)^2 + 10.1(x_2 - 1)^2 + (x_4 - 1)^2 + 19.8(x_2 - 1)(x_4 - 1)$
F5(Zakharov)	10	[-5,10]	0	$f(x) = \sum_{i=1}^D x_i^2 + \left(\sum_{i=1}^D 0.5ix_i\right)^2 + \left(\sum_{i=1}^D 0.5ix_i\right)^4$
F6(Schwefel 2.22)	30	[-10,10]	0	$f(x) = \sum_{i=1}^D x_i + \prod_{i=1}^D x_i $
F7(Schwefel 1.2)	30	[-100,100]	0	$f(x) = \sum_{i=1}^D \left(\sum_{j=1}^i x_j\right)^2$
F8(Dixon-price)	30	[-10,10]	0	$f(x) = (x_1 - 1)^2 + \sum_{i=2}^D i(2x_i^2 - x_{i-1})^2$
F9(Step)	30	[-5,12,5,12]	0	$f(x) = \sum_{i=1}^D (x_i + 0.5)^2$
F10(Sphere)	30	[-100,100]	0	$f(x) = \sum_{i=1}^D x_i^2$
F11(SumSquares)	30	[-10,10]	0	$f(x) = \sum_{i=1}^D ix_i^2$
F12(Quartic)	30	[-1,28,1,28]	0	$f(x) = \sum_{i=1}^D ix_i^4 + Rand$

Multimodal test functions have many local minimums, and therefore, they are hard to be solved simply because of the trapping in local solutions. The (HIWOPSO) has been evaluated by these functions and search the global minimum for them. In Table 4, the results for algorithms GA [20], DE [21], PSO, BA [22] and IWO are compared with HIWOPSO. Conditions for experiment and parameter settings for these algorithms is explained in reference [23]. The experiment has been performed on the computer with following features: CPU 2.1 GHZ, Ram 8 GB and Matlab 2016 running on computer with windows 7. The NFE= 500,000 (number of function evaluation) was set as Stopping criteria and the values minimum than 1E-12, presented as 0 same as other methods. The mean value and Std Dev (standard deviation) have been calculated from 30 independent runs. In Table 4, the HIWOPSO found the minimum results for most of the functions with best standard deviations. The results of Friedman non-parametric test [16] are also presented in this table and HIWOPSO could rank the best with value 2.75. The low p-value indicates that the results are remarkably different with each other and figure 2 depicts the results for this test with a bar diagram. For analyzing the procedure of convergence in (HIWOPSO), figure 3 has been presented. This figure shows the Convergence diagram for functions F8, F9, F18 and F19 in algorithms PSO, IWO and (HIWOPSO).

As it stands, HIWOPSO has reached the desired minimum with

TABLE III. MULTIMODAL TEST FUNCTIONS (D: DIMENSIONS)

Function	D	Range	Min	Formulation
F13(Schaffer)	2	[-100,100]	0	$f(x) = 0.5 + \frac{\sin^2(\sqrt{x_1^2 + x_2^2}) - 0.5}{(1 + 0.001(x_1^2 + x_2^2))^2}$
F14(6 H Camel)	2	[-5,5]	-1.03163	$f(x) = 4x_1^2 - 2.1x_1^4 + \frac{1}{3}x_1^6 + x_1x_2 - 4x_2^2 + 4x_2^4$
F15(Bohachevsky2)	2	[-100,100]	0	$f(x) = x_1^2 + 2x_2^2 - 0.3\cos(3\pi x_1)(4\pi x_2) + 0.3$
F16(Bohachevsky3)	2	[-100,100]	0	$f(x) = x_1^2 + 2x_2^2 - 0.3\cos(3\pi x_1 + 4\pi x_2) + 0.3$
F17(Shubert)	2	[-10,10]	-186.73	$f(x) = \frac{(\sum_{i=1}^5 i \cos(i+1)x_1 + i)}{(\sum_{i=1}^5 i \cos((i+1)x_2 + i))}$
F18(Rosenbrock)	30	[-30,30]	0	$f(x) = \sum_{i=1}^{D-1} 100(x_{i+1} - x_i^2)^2 + (x_i - 1)^2$
F19(Griewank)	30	[-600,600]	0	$f(x) = \frac{1}{4000} \left(\sum_{i=1}^D (x_i - 100)^2 \right) - \left(\prod_{i=1}^D \cos \left(\frac{x_i - 100}{\sqrt{i}} \right) \right) + 1$
F20(Ackley)	30	[-32,32]	0	$f(x) = -20 \exp \left(-0.2 \sqrt{\frac{1}{n} \sum_{i=1}^D x_i^2} \right) - \exp \left(\frac{1}{n} \sum_{i=1}^D \cos(2\pi x_i) \right) + 20 + e$
F21(Bohachevsky1)	2	[-100,100]	0	$f(x) = x_1^2 + 2x_2^2 - 0.3\cos(3\pi x_1) - 0.4\cos(4\pi x_2) + 0.7$
F22(Booth)	2	[-10,10]	0	$f(x) = (x_1 + 2x_2 - 7)^2 + (2x_1 + x_2 - 5)^2$
F23(Michalewicz2)	2	[0,π]	-1.8013	$f(x) = -\sum_{i=1}^D \sin(x_i) (\sin(ix_i^2/\pi))^{20}$
F24(Michalewicz5)	5	[0,π]	-4.6877	$f(x) = -\sum_{i=1}^D \sin(x_i) (\sin(ix_i^2/\pi))^{20}$
F25(Michalewicz10)	10	[0,π]	-9.6602	$f(x) = -\sum_{i=1}^D \sin(x_i) (\sin(ix_i^2/\pi))^{20}$
F26(Rastrigin)	30	[-5,12,5,12]	0	$f(x) = \sum_{i=1}^D (x_i^2 - 10 \cos(2\pi x_i) + 10)$

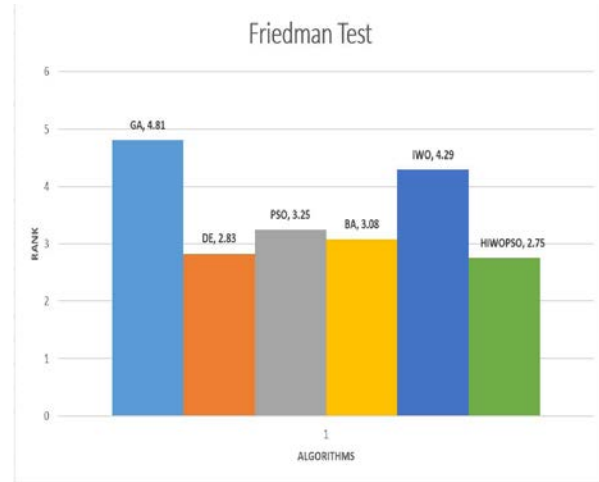


Fig. 2. Bar diagram for non-parametric Friedman test results for Functions F1-F26

minimum CPU Time and faster against the other algorithms IWO and PSO. Also, the test of normality

TABLE IV. HIWOPSO COMPARISON WITH GA, DE, PSO, BA, AND IWO (UNIMODAL FUNCTION SET), BOLD VALUES REPRESENT

Function	Criteria	GA	DE	PSO	BA	I	HIWOPSO
(F1)	Mea	0	0	0	1.88	2.	0
	Std	0	0	0	1.94	4.	0
(F2)	Mea	-1	-1	-1	-	-1	-1
	Std	0	0	0	4.50	0	0
(F3)	Mea	0	0	0	0	0	0
	Std	0	0	0	0	0	0
(F4)	Mea	0.01494	0.04	0	1.11	7.	0
	Std	0.00736	0.08	0	0.46	4.	0
(F5)	Mea	0.01336	0	0	0	1.	0
	Std	0.00453	0	0	0	3.	0
(F6)	Mea	11.0214	0	0	0	2.	1.42E-03
	Std	1.38686	0	0	0	0.	2.242585E-03
(F7)	Mea	7.40E+0	0	0	0	1.	147.401395
	Std	1.14E+0	0	0	0	3	448.571186
(F8)	Mea	1.22E+0	0.66	0.66667	0.66	0.	0.66667
	Std	2.66E+0	E-9	E-8	1.16	0	0
(F9)	Mea	1.17E+0	0	0	5.12	2.	0
	Std	76.56145	0	0	0.39	1.	0
(F10)	Mea	1.11E+0	0	0	0	2.	0
	Std	74.21447	0	0	0	4.	0
(F11)	Mea	1.48E+0	0	0	0	2.	0
	Std	12.40929	0	0	0	4.	0
(F12)	Mea	0.18070	0.00	0.00116	1.72	1.	3.66E-03
	Std	0.02712	0.00	0.00028	1.85	0.	0.001401347
(F13)	Mea	0.00424	0	0	0	7.	0
	Std	0.00476	0	0	0	6.	0
(F14)	Mea	-1.03163	-	-1.03163	-	-	-1.03163
	Std	0	0	0	0	0	0
(F15)	Mea	0.06829	0	0	0	1.	0
	Std	0.07822	0	0	0	7.	0
(F16)	Mea	0	0	0	0	1.	0
	Std	0	0	0	0	2.	0
(F17)	Mea	-186.73	-	-186.73	-	-	-186.73
	Std	0	0	0	0	0	0
(F18)	Mea	1.96E+0	18.2	15.0886	28.8	5	0.03137
	Std	3.85E+0	5.03	24.1701	0.10	3	0.02992
(F19)	Mea	10.63346	0.00	0.01739	0	0.	0
	Std	1.16146	0.00	0.02081	0	0.	0
(F20)	Mea	14.67178	0	0.16462	0	0.	5.62617E-05
	Std	0.17814	0	0.49387	0	0.	0.0001823
(F21)	Mea	0	0	0	0	4.	0
	Std	0	0	0	0	3.	0
(F22)	Mea	0	0	0	0.00	3.	0
	Std	0	0	0	0.00	2.	0
(F23)	Mea	-1.8013	-	-1.57287	-	-	-1.8013
	Std	0	0	0.11986	0	0	0
(F24)	Mea	-4.64483	-	-2.4908	-	-	-4.6877
	Std	0.09785	0.01	0.25695	0	0	0
(F25)	Mea	-9.49683	-	-4.0071	-	-	-9.6602
	Std	0.14112	0.06	0.50263	0	0.	0
(F26)	Mea	52.92259	11.7	43.9771	0	2	0
	Std	4.56486		2.53817	2.	0	

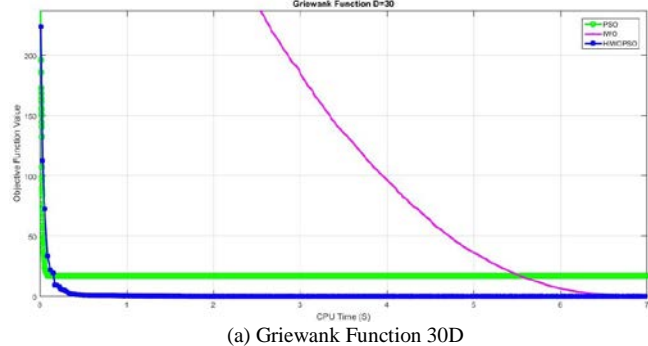
of Kolmogorov-Smirnov and Shapiro-Wilk [16] has been performed for the four functions of F6, F7, F12 and F20 which are hard to be solved, and here, standard deviation is not zero for them. Table 5 presents the results for this test and the p-value, df (degree of freedom), and the statistics for this test are also presented. Accordingly, the p-value which is higher than the significant $\alpha = 0.05$ is considered a normal distribution and the lower than that value is supposed to be an abnormal

distribution. Based on the p-value and the test of normality of Kolmogorov-Smirnov, the function of F7 result is normal and other functions have the abnormal distribution. Figure 4 shows the normal and abnormal distributions, the histogram, QQ-plot and Box-plot for the two functions, F7 and F12. In this figure, F7 is a normal distribution and F12 is considered abnormal. As can be inferred, in normal distributions, the

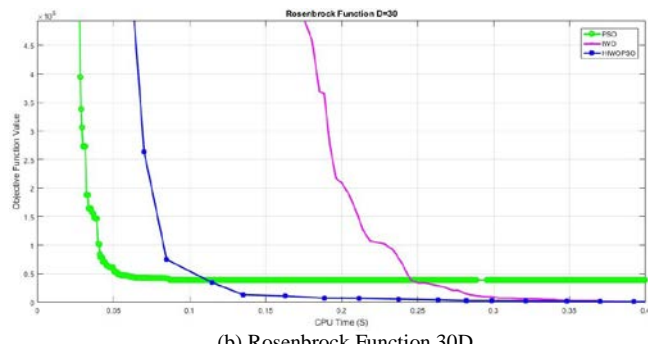
results are in one diagonal line for QQ-plot while in abnormal distributions, this fact does not hold true.

TABLE V. TEST OF NORMALITY KOLMOGOROV-SMIRNOVA AND HAPIRO-WILK FOR FUNCTIONS F7,F25 AND F12

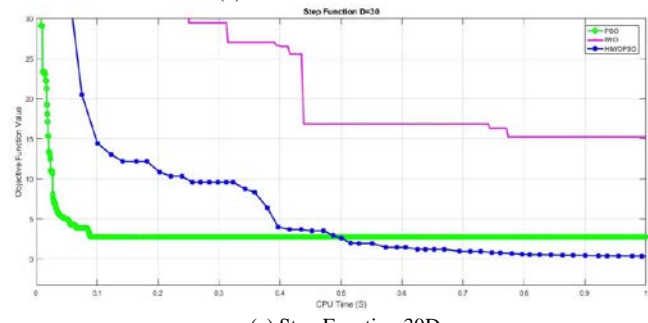
Kolmogorov-Smirnova			Shapiro-Wilk			
Statistic	df	p-value	Statistic	df	p-value	
F6	0.239999	30	0.000	0.858999	30	0.000
F7	0.1259999	30	0.103	0.858999	30	4.0532E-3
F12	0.6268000	30	0.000	0.3579999	30	0.000
F20	0.3219999	30	0.000	0.4839999	30	0.000



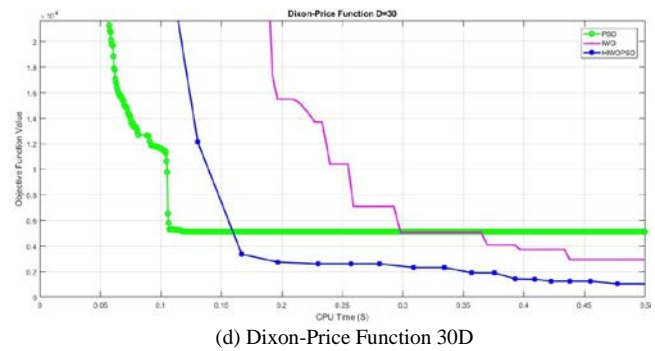
(a) Griewank Function 30D



(b) Rosenbrock Function 30D



(c) Step Function 30D



(d) Dixon-Price Function 30D

Fig. 3. Convergence diagram for functions F8, F9, F18 and F19 in algorithms PSO, IWO and HIWOPSO

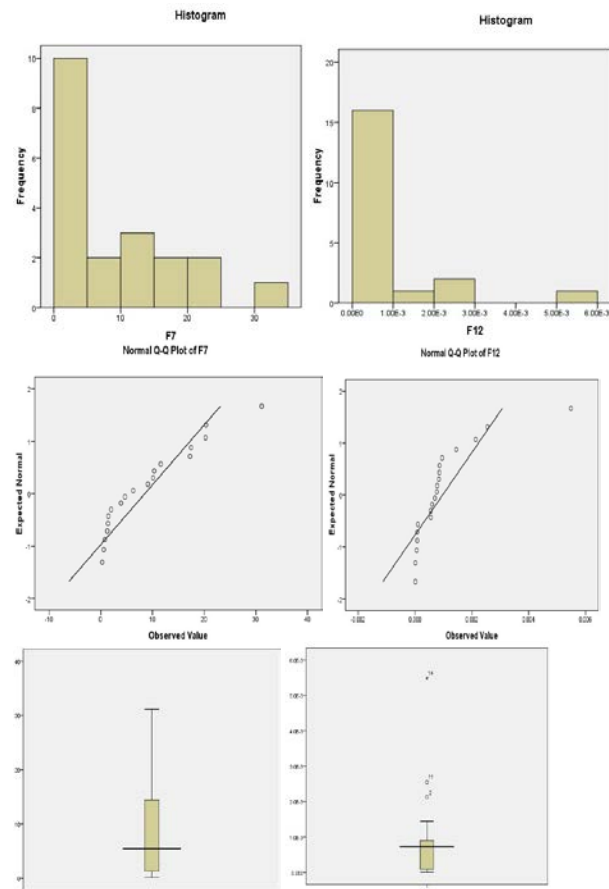


Fig. 4. HIWOPSO algorithm. Left plots are normal for F7 and the Right are abnormal for F12

as studies presented in section 2. Figure (4) and (5) shows these comparisons.

V. CONCLUSION AND FUTURE WORKS

The IWO is, arguably, one of the most efficient nature inspired Metaheuristic algorithms, which has outperformed most of the algorithms in solving the various optimizing numerical problems. Furthermore, one of the practical Metaheuristic algorithms which have been used most widely in the optimization is the PSO. The PSO algorithm is a simple and practical algorithm which is more amenable to combination with others. In the current study, the PSO and IWO algorithms are combined in order to design a new hybrid method for seeking the global solution. The proposed hybrid algorithm begins to search by creating solutions by IWO and PSO algorithms and used the better one as the input to the mutation function. Mutation output is compared with the input and better one selected as the new seed. The experiment based on benchmark functions and non-parametric ranking showed that the proposed hybrid is more dominant and competent than other famous algorithms. Moreover, based on the results of the test of normality and convergence, this proposed hybrid algorithm mostly had abnormal distributions for results and converged to the optimum solutions in minimum CPU Time.

According to the description and assumptions made in this study, the following works are suggested:1.Using compound method for solving engineering problems2.using Compound method for data clustering 3.resolving the distribution of load in power plants according to posed algorithm.

REFERENCES

- [1] C. Grosan, A. Abraham, Intelligent systems a modern approach, Intelligent Systems Reference Library, Springer Berlin Heidelberg, 17 (2011).
- [2] X-S Yang, Introduction to Mathematical Optimization: From Linear Programming to Metaheuristics. Cambridge International Science Publishing , (2008).
- [3] P. Hansen, N. Mladenovic, J. Brimberg, J. Moreno-Prez, Variable neighbor hood Search .In :Handbook of Metaheuristic s.Springer US, (2010) 61 86.
- [4] B. Dogan, T. Omez, A new Metaheuristic for numerical function optimization: Vortex search algorithm, Information Sciences, 293 (2015) 125{145.
- [5] S. Mirjalili, A. Lewis, The Whale Optimization Algorithm, Advances in Engineering Software, 95 (2016) 51-67.
- [6] A. Sadollah , A. Bahreininejad, H. Eskandar, M. Hamdi, Mine blast algorithm for optimization of truss structures with discrete variables, Computers & Structures, 103 (2012) 49-63.
- [7] H. Eskandar, A. Sadollah, A. Bahreininejad, M. Hamdi, Water cycle algorithm a novel Metaheuristic optimization method for solving constrained engineering optimization problems, Computers & Structures, 111 (2012) 151-166.
- [8] H. Salimi, Stochastic fractal search: A powerful Metaheuristic algorithm, Knowledge-Based Systems, 75 (2015) 1-18.
- [9] J. Kennedy, R. Eberhart, Particle swarm optimization. In: Proceedings of the IEEE international conference on neural networks. Perth, Australia, (1995) 1942-1948.
- [10] T. KAY CHEN , Advances in Swarm Intelligence, First International Conference, ICSI 2010, Beijing, China, June 12-15, 2010, Proceedings, Part I, Springer-Verlag Berlin Heidelberg. 6145 (2010).
- [11] Mehrabian AR, Lucas C. A novel numerical optimization algorithm inspired from weed colonization. Ecol Inform 2006;1:35566.
- [12] Mojtaba Ghasemi, Sahand Ghavidel, Mohammad Mehdi Ghanbarian, Amir Habibi, A new hybrid algorithm for optimal reactive power dispatch problem with discrete and continuous control variables, Applied Soft Computing, Volume 22, September 2014, Pages 126-140
- [13] E. Atashpaz-Gargari, C. Lucas, Imperialist competitive algorithm: an algorithm for optimization inspired by imperialistic competition, Proc. IEEE Cong. Evol.Comput. (2007) 46614667.
- [14] Santosh Kumar Mahto, Arvind Choubey, A novel hybrid IWO/WDO algorithm for nulling pattern synthesis of uniformly spaced linear and non-uniform circular array antenna, AEU – International Journal of Electronics and Communications, Volume 70, Issue 6, June 2016, Pages 750-756
- [15] Bayraktar Z, Komurcu M, Bossard JA, Werner DH. The wind driven optimization technique and its application in electromagnetic . IEEE Trans Antennas Propag2013;61:274557.
- [16] S. Garcia, D. Molina, M. Lozano, F. Herrera, A study on the use of non-parametric tests for analyzing the evolutionary algorithms' behavior : a case study on the CEC'2005 Special Session on Real Parameter Optimization. Journal of Heuristics, 15 (2009) 617-644.
- [17] S. Boyd, L. Vandenberghe, Convex Optimization, Cambridge University Press, (2004).
- [18] H. Duan, D. Wang, X. Yu, Markov Chains and Martingale Theory Based Convergence Proof of Ant Colony Algorithm and Its Simulation Platform. in Intelligent Control and Automation, 1 (2006) 3057{3061.
- [19] W. Chu, X. Gao, S. Sorooshian, Handling boundary constraints for particle swarm optimization in high-dimensional search space. Information Sciences, 181 (2011) 4569-4581.
- [20] D. E. Goldberg, Genetic Algorithms in Search, Optimization and Machine Learning, 1st Edition, Addison-Wesley Longman Publishing Co., Inc., Boston, MA, USA, (1989).
- [21] R. Storn, K. Price, Differential evolution a simple and efficient heuristic for global optimization over continuous spaces, Journal of Global Optimization, 11 (1997) 341-359
- [22] D. Pham, A. Ghanbarzadeh, E. Ko, S. Otri, S. Rahim, M. Zaidi, The bees algorithm a novel tool for complex optimization problems, in: D. Pham, E. Eldukhri, A. Soroka (Eds.), Intelligent Production Machines and Systems, Elsevier Science Ltd, Oxford, (2006) 454-459.
- [23] M. Cheng, L. Lien, Hybrid artificial intelligence based pba for benchmark functions and facility layout design optimization, Journal of Computing in Civil Engineering, 26 (2012) 612-624.

A New Internal Model Control Method for MIMO Over-Actuated Systems

Ahmed Dhahri

University of Tunis El Manar,
National Engineering School of
Tunis, Laboratory of research in
Automatic Control, BP 37,
Belvédère, 1002
Tunis, Tunisia

Imen Saidi

University of Tunis El Manar,
National Engineering School of
Tunis, Laboratory of research in
Automatic Control, BP 37,
Belvédère, 1002
Tunis, Tunisia

Dhaou Soudani

University of Tunis El Manar,
Departement of Electrical Engineering, National Engineering School of Tunis,
Laboratory of research in Automatic Control, BP 37, Belvédère, 1002
Tunis, Tunisia

Abstract—A new design method internal model control is proposed for multivariable over-actuated processes that are often encountered in complicated industrial processes.

Due to the matrix that is adopted to describe over-actuated system is not square, many classical multivariable control methods can be hardly applied in such system. In this paper, based on method of virtual outputs, a new internal model control method is proposed.

The proposed method is applied to shell standard control problem (3 inputs and 2 outputs). The simulation results show that the robust controller can keep the set inputs without overshoot, steady state error, input tracking performance and disturbance rejection performance, the results are satisfactory have proved the effectiveness and reliability of the proposed method.

Keywords—internal model control (IMC); over-actuated multivariable system; inverse model; method of virtual outputs; disturbances rejections, stability; state error

I. INTRODUCTION

The multi-input and multi-outputs (MIMO) over-actuated systems exist in industrial and such are a difficult problem in the control [12], [21]. The multivariable over-actuated system is non-square system with the number of inputs is superior to that of outputs [7].

A simple of controlling the MIMO non-square system is transform it into a square system by adding or deleting variables. But adding variables will increase the control cost, while deleting variables reduce the quality of control by reason of missing information and may even make the process unstable between the credible introduction of right half plane [1], [8], [9], [16].

The Internal Model Control (IMC) which due to its simplicity, excellent robustness, and better control performance shows the capacity to solve the control problems

of the multivariable systems. If we combine IMC with multivariable control system, it could be a capable way to solve the control difficulty of multivariable systems [11].

On the basis of the IMC principle, the design of a controller for a square system is generally based on the inverse matrix of system [3], [4], [20]. Nevertheless, considering non-square processes, IMC cannot be applied exactly, as it cannot obtain the traditional sense of inversion [5], [6].

In recent years, many researchers adopted finding the robust controller by internal model control.

Seshagiri [2] designed a PI controller as a Smith delay compensator for non-square system with multiple time delays. This method achieves static decoupling because it is based on the pseudo inverse of the steady-state gain matrix of non-square systems. Only using the steady-state information of the systems will lead to the limitation of control performance.

Chen [17] a modified the IMC el for non-square systems by inserting compensated to remove the terms unrealizable factoring there for obtained from the controller. The objective the controller parameter is to achieve tracking performance and robustness.

Chen [9] proposed a new method using Internal Model Control and smith controller between design a PI controller for multivariable non-square systems with transfer function elements consisting of first order and time delay. The problem of this method is no analysis of load disturbance performance, and the decoupling effect is poor than dynamic decoupling.

Quan [12] proposed a new NERGA based on internal model control method for non-square system. This method calculate the inverse of the matrix, the model controller is designed based on the model of squared subsystem. But when building the subsystem controller, that is to say we eliminate variables the global system will reduce the quality and control performance.

Liu [10] proposed a method a modified two-degrees-of-freedom internal model control method for non-square systems with multiple time delays and right-half-plane zeros. This method, pseudo-inverse is introduced to describe the internal model controller, and an appropriated closed-loop transfer function is designed to eliminate the impracticable factors of the derived controller.

Jin [18] proposed a design method of decoupling IMC for non-square processes with multiple time delays. The method can achieve a realizable decoupling controller of non-square processes by inserting some compensated terms. At the same time, based on the relative normalized gain array, an equivalent transfer function matrix is acquaint to approximate the pseudo-inverse of the process transfer function matrix.

This paper presents a new technique to enquire into the IMC control design for multivariable over-actuated system. In the controller design procedure a simple method designed to uses virtual outputs method [1]. Finally, this method is applied in a system with 3 inputs than two outputs; the simulation results show that the proposed method had good performance of tracking ability and strong performance.

This paper is organized as follows. Section II presents a generality on the internal model control strategy of multivariable system. Section III proposes the design method of the controller for the internal model control for multivariable over-actuated system. In section IV, an example is employed to illustrate the effectiveness of the proposed controller. Some conclusions are drawn in section V.

II. STRUCTURE OF IMC FOR MIMO PROCESSES

The internal model control (IMC) found wide acceptance in process control system, due to be simplicity, excellent robustness, and good control performance, shows the strong vitality to solve the control problems of multivariable non-square and square systems.

The internal model control structure of multivariable process as shown in Fig. 1. Where $G(s)$, $M(s)$, $C(s)$ and $G_v(s)$ represent the transfer functions of the process, the process model, IMC controller and disturbance respectively; y and y_m are the outputs vectors of the process and its model, respectively; r is the input vectors of the process; u represents the control input signal; v is the disturbance.

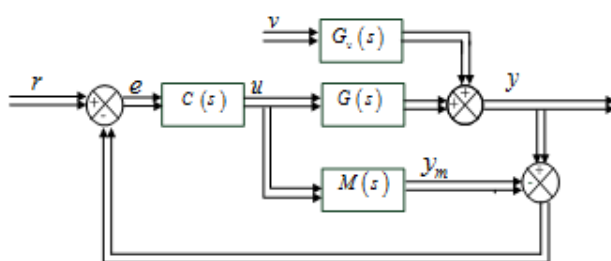


Fig. 1. Structure of Internal model control (IMC)

Where, all elements in $G(s)$, $G_m(s)$ are stable [19].

The equation of input, output and disturbance is given by [19]:

$$y(s) = G(s) \left[I + C(s)(G(s) - M(s)) \right]^{-1} C(s)r(s) \quad (1)$$

$$+ \left[I - G(s) \left[I + C(s)(G(s) - M(s)) \right]^{-1} C(s) \right] G_v(s)v(s)$$

When the model is perfect, the model process is given by:

$$M(s) = G(s) \quad (2)$$

The expression of output transfer function can be obtained to equation (3):

$$y(s) = G(s)C(s)r(s) + \left[I - G(s)C(s) \right] G_v(s)v(s) \quad (3)$$

The MIMO transfer functions for the process $G(s)$ with 'n' inputs and 'm' outputs ($m < n$) is considered as [7]:

$$G(s) = \begin{pmatrix} G_{11}(s) & G_{12}(s) & \cdots & G_{1n}(s) \\ G_{21}(s) & G_{22}(s) & \cdots & G_{2n}(s) \\ \vdots & \vdots & \ddots & \vdots \\ G_{m1}(s) & G_{m2}(s) & \cdots & G_{mn}(s) \end{pmatrix} \quad (4)$$

Transfer function of the controller is :

$$C(s) = \begin{pmatrix} k_{11}(s) & k_{12}(s) & \cdots & k_{1m}(s) \\ k_{21}(s) & k_{22}(s) & \cdots & k_{2m}(s) \\ \vdots & \vdots & \ddots & \vdots \\ k_{n1}(s) & k_{n2}(s) & \cdots & k_{nm}(s) \end{pmatrix} \quad (5)$$

We consider the IMC configuration that is stable for process, the model of the process and the IMC controller.

In IMC, the synthesis of a controller which is equal to the inversion of the model system is paramount to ensure perfect follow instructions. But, the manner of direct inversion is practically impossible for over-actuated systems. To remedy this problem, it is proposed to develop a method of inversion in the case of over-actuated multivariable linear systems.

III. CONTROLEUR DESIGN

A. Structure of the controller to a over-actuated multivariable system

For MIMO non-square system, the input number is unequal to the output number. There are two types of non-square systems: the under-actuated system where the number of inputs is inferior than the number of outputs ($m > n$) and the system over-actuated system the number of inputs is superior to that of outputs ($m < n$) [7].

In this paper we will take an interest in the over-actuated system, and we will follow a methodology to design our controller for this case of system.

Using the method of virtual outputs of adding lines to the transfer matrix of the non-square system, up to have a square transfer matrix that can be reverse [1].

Regarding the virtual outputs that will add to the transfer matrix system, we will copy the outputs of the original system

and the programmation part we will remove them. these virtual outputs will be used to make the square transfer matrix.

The transfer function matrix of the over-actuated system is then a rectangular matrix recess non-singular. If we extend the matrix $G(s)$ to make it square. This amounts to consider $((n-m), n)$ further referred to as the word of virtual outputs.

Our system is represented by the following equation (11),

$$\begin{pmatrix} y_1 \\ y_2 \\ \vdots \\ y_m \end{pmatrix} = \begin{pmatrix} G_{11} & G_{12} & \cdots & G_{1n} \\ G_{21} & G_{22} & \cdots & G_{2n} \\ \vdots & \vdots & \ddots & \vdots \\ G_{m1} & G_{m2} & \cdots & G_{mn} \end{pmatrix} \begin{pmatrix} u_1 \\ u_2 \\ \vdots \\ u_n \end{pmatrix} \quad (11)$$

The transfer matrix that will add to make the over-actuated system square is its size $((n-m), n)$. This matrix has the following form:

$$\begin{pmatrix} y_{m+1} \\ y_{m+2} \\ \vdots \\ y_n \end{pmatrix} = \begin{pmatrix} G_{m+1,1} & G_{m+1,2} & \cdots & G_{m+1,n} \\ G_{m+2,1} & G_{m+2,2} & \cdots & G_{m+2,n} \\ \vdots & \vdots & \ddots & \vdots \\ G_{n1} & G_{n2} & \cdots & G_{nn} \end{pmatrix} \begin{pmatrix} u_1 \\ u_2 \\ \vdots \\ u_n \end{pmatrix} \quad (12)$$

In the system simulation phase, we need to add a function block which eliminates $(m-n)$ output added to visualize the non-square system output.

The simulation block diagram is given in Fig.3.

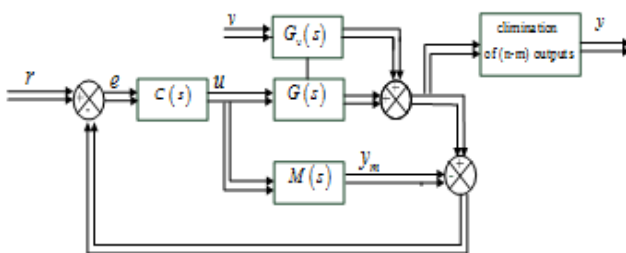


Fig. 2. IMC structure for multivariable over-actuated system

B. Study of the stability of the proposed controller

The IMC controller is present on Fig.2 by using the inversion method proposed [13], [14]. K_1 reversal of the matrix is an invertible square matrix; it must ensure the stability conditions of the controller.

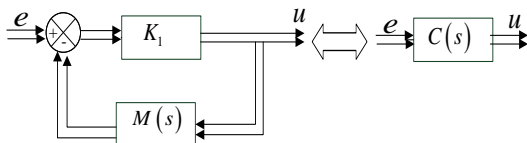


Fig. 3. Structure for model inversion

The expression of internal model controller can be obtained:

$$C(s) = \frac{K_1}{I_m + K_1 M(s)} \quad (6)$$

the K_1 inversion matrix of the form $K_1 = a I_m, a \in \mathbb{R}^+$, I_m is the identify matrix is chosen sufficiently High then $\frac{1}{a}$ is sufficiently low there by approximating given by the equation [15]:

$$\frac{1}{\frac{1}{K_1} + M(s)} = M(s)^{-1} \quad (7)$$

The stability of the structure proposed for the internal model depends of stability of the process control, of the model and of the controller $C(s)$ respectively.

The controller $C(s)$ can be written as follows [15]:

$$C(s) = \frac{t_{com}(I_m + K_1 M(s)) K_1}{\det(I_m + K_1 M(s))} \quad (8)$$

are $N(s)$ and $D(s)$ respectively represent the numerator and denominator of $\det(I_m + K_1 M(s))$.

To ensure the stability of the regulator $C(s)$, it must be ensured that $N(s)$ is a polynomial of Hurwitz. This means that the roots of $N(s)$ must be strictly negative real parts. These roots can be located either using geometric methods such as root locus or algebraic methods such as of Routh criterion.

Given a model $M(s)$ Stable, adequate choice of K_1 inversion matrix then ensures the stability of the regulator $C(s)$.

C. Precision study of the system

To ensure the accuracy of the system, that is to say a zero static error, check that [15]:

$$C(0) = \frac{1}{M(0)} \quad (9)$$

With $C(0)$ is the matrix of the static gains of the controller. It can be expressed as a function of the matrix of the static gains of the system $M(0)$. It is defined by the equation (10):

$$C(0) = \frac{K_1}{(I_m + K_1 M(0))} \quad (10)$$

It can be said the performance of the proposed controller, to ensure a perfect tracking of the reference input independently of external disturbances. This property can only be validated if we choose a sufficiently high.

IV. SIMULATION RESULTS

Consider a 2×3 stable over-actuated multivariable system; the transfer function of the model system is given as:

$$G(s) = \begin{pmatrix} \frac{s+2}{s^2+3s+4} & \frac{1}{s+3} & \frac{1}{s^2+2s+3} \\ \frac{s+1}{3s^2+3s+2} & \frac{3}{s+4} & \frac{1}{s^2+2s+1} \end{pmatrix} \quad (13)$$

Where there are two controlled variables (y_1, y_2) and three manipulated variables (u_1, u_2, u_3).

The model is represented by the following transfer matrix function $M(s)$, it is defined by the equation (14):

$$M(s) = \begin{pmatrix} \frac{s+2}{s^2+3s+4} & \frac{1}{s+3} & \frac{1}{s^2+2s+3} \\ \frac{s+1}{3s^2+3s+2} & \frac{3}{s+4} & \frac{1}{s^2+2s+1} \\ \frac{s+2}{s^2+3s+4} & \frac{1}{s+3} & \frac{1}{s^2+2s+3} \end{pmatrix} \quad (14)$$

In our case, the chosen matrix K_1 is equal to $K_1 = 40 \times I_3$, to ensure the stability of the system $G(s)$ for controlling.

Fig. 4 and Fig. 5 represents the evolution of the internal model controllers $u_1(t)$ and $u_2(t)$. The unit step responses of outputs $y_1(t)$ and $y_2(t)$ are shown in Fig.6 and Fig.7. From the analysis of Fig.6 and Fig. 7, it follows that the system control effect is satisfactory without overshoot, static error and the system has good traceability. The resulting outputs responses of the system are in order affirm the effectiveness of the proposed internal model controller.

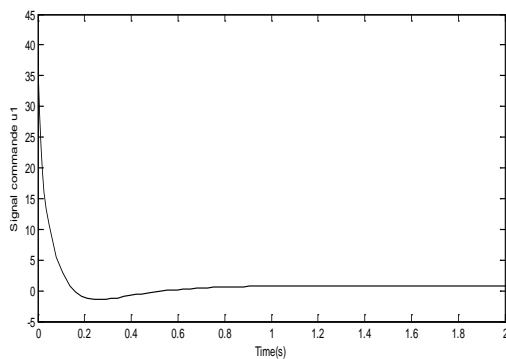


Fig. 4. The control input u

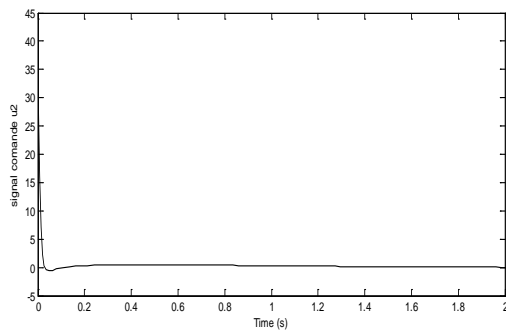


Fig. 5. The control input u₂

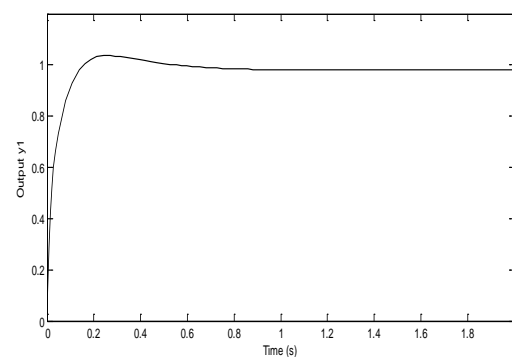


Fig. 6. The step response of output y1

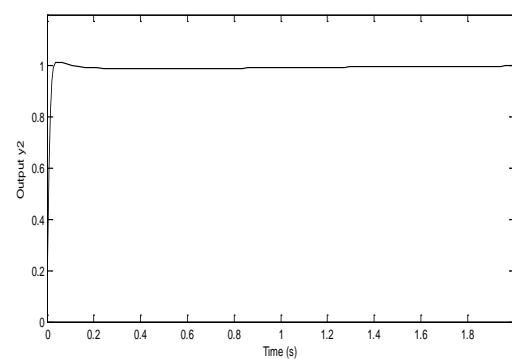


Fig. 7. The step response of output y2

The disturbance signal is expressed by equation (15)

$$G_v(s) = \begin{bmatrix} \frac{e^{-0.5s}}{s} & \frac{e^{-0.5s}}{s} & \frac{e^{-0.5s}}{s} \end{bmatrix}^T \quad (15)$$

In order to assert the disturbance rejection capability of the system, assumed a step disturbance signal with magnitude 1 was added to the input 1, input 2 and input 3 at t=1s.

Fig. 8 and Fig. 9 represents the evolution of the internal model controllers $u_1(t)$ and $u_2(t)$.

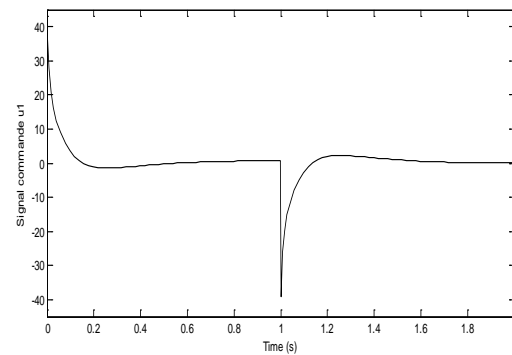


Fig. 8. The control input u₁ with disturbance

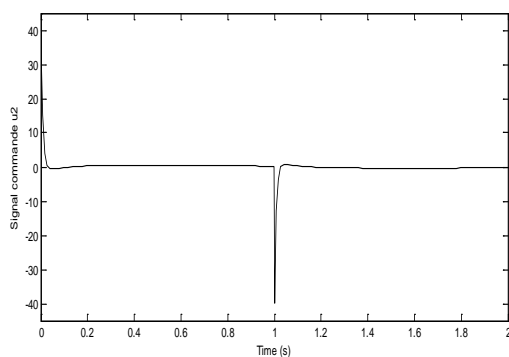


Fig. 9. The control input u_2 with disturbance

The simulation results of model perturbation responses of outputs $y_1(t)$ and $y_2(t)$ are given in Fig.10 and Fig.11. The simulation results show that the proposed method has disturbance rejection performance. It clearly shows that the set-point tracking and disturbance rejection are achieved and it offers robustness.

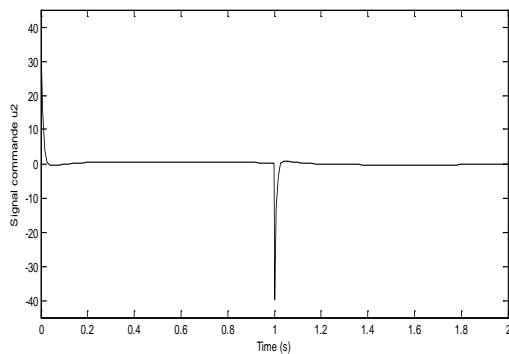


Fig. 10. The step response of output y_1 with disturbance

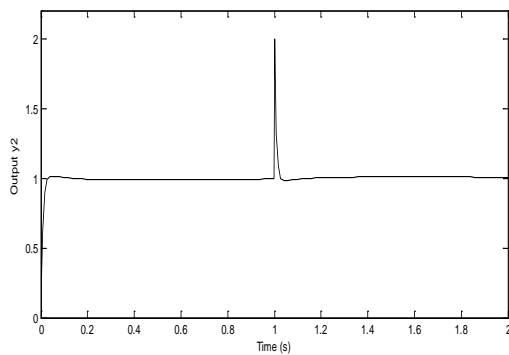


Fig. 11. The step response of output y_2 with disturbance

V. CONCLUSION

For the multivariable system with the number of inputs is superior to that of outputs are habitually met in system industries, we proposed a new method of virtual outputs based on internal model control for over-actuated system has been presented in this paper. This novel method avoids the complex calculation; such as calculate the inverse of this matrix, the controller structure is simple.

The multivariable over-actuated system is not square, so the reverse is not possible with our method of virtual outputs is added, our system becomes square at that moment, and we can build our controller which is based on the reversal of the processes.

The simulation results show that this method proposed has the advantages of small overshoot, the set-point tracking controller and disturbance rejection performance. Meanwhile, better control performance and good robustness than other control methods of over-actuated systems.

Generally, this new method is simple, has robust performance and easy to implement in engineering processes.

REFERENCES

- [1] A. Fossard,"Commande des systèmes multidimensionnels," Dunod, Paris 1972.
- [2] A. Seshagiri Rao, M. Chidambaram, "Smith delay compensator for multivariable non-square systems with multiple time delays," International Journal of Computers and Chemical Engineering, Vol. 30, pp 1243-1255, 2006.
- [3] C. E. Garcia and M. Morari, "Internal model control.1. A unifying review and some results", Industrial Engineering Chemistry Process Design and Development, vol. 21, pp. 403-411, 1982.
- [4] C. E. Garcia and M. Morari, "Internal model control.3.Multivariable control law computation and tuning guidelines," Industrial Engineering Chemistry Process Design and Development, Vol. 24, p.484, 1985.
- [5] C. E. Garcia and M. Morari "Internal model Control.2. Design procedure for multivariable System," Industrial Engineering Chemistry Process Design and Development. Vol.24, p.472, 1985.
- [6] C. G. Economou, M. Morari, and B. O. Palsson, "Internal model control 5. Extension to nonlinear systems," Industrial Engineering Chemistry Process Design and Development, vol. 25, pp. 403-409, 1986.
- [7] D. Shinde, S. Hamde and L. Waghmare, "Predictive PI control for multivariable non-square system with multiple time delays," International Journal for Science and Research in Technology, Vol. 1 No.5, pp. 26-29, 2015.
- [8] D. Shinde, S. Hamde and L. Waghmare, "Predictive PI control for multivariable non-square system with multiple time delays," International Journal for Science and Research in Technology, Vol. 1 No.5, pp. 26-29, 2015.
- [9] H. Trebiber," Multivariable control of non-square system. Industrial & Engineering chemistry," Process Design and development, vol. 23, No.4, pp.854-857, 1984.Journal of Process Control, vol. 21 , pp.538-546, 2011.
- [10] J. C. Lui, N. Chen and X. Yu, "Modified Two-Degrees-of-Freedom Internal Model Control for non-square systems with mutiple time delays," Journal of Harbin Institue of Technology, Vol.21, No.2, pp 122-128, 2014.
- [11] J. Qibing, Q. Ling and Y. Qin, " New internal model control method for multivariable coupling system with time delays," IEEE International Conference on on Automation and Logistics Shenyang, pp. 1307-1312, China, 2009.
- [12] L. Quan and H. Zhang, "Max-Max based internal model control method for multivariable system with time delay," Journal of Applied Mechanics and Materials, Vols. 236-237, pp. 356-359, 2012.
- [13] M. Benrejeb, M. Naceur, D. Soudani, "On an internal mode controller based on the use of a specific inverse model," International Conference on Machine Intelligence ACIDCA 2005, pp. 623-626, Tozeur, 2005.
- [14] N. Touati, D. Soudani, M. Naceur and M. Benrejeb, " On an internal multimodel control for nonlinear multivariable systems - A comparative study," International Journal of Advanced Computer Science and Applications, Vol. 4, No.7, pp. 66-71, 2013.
- [15] N. Touati, "Sur la commande par modèle interne de systèmes continus multivariables", PhD, ENIT, Tunisia, 2015.
- [16] P. Chen, L. Ou, D. Gu and W. Zhang, "Robust Analytical Schema for Linear Non-Square Systems" 48th IEEE Conference on Decision and

- Control and 28th Chinese Control Conference, Shanghai, P.R. China, .pp. 1890-1895. December 16-18 2009.
- [17] P. Y. Chen, L. L. Ou, J. Sun and W.D. Zhang., "Modified internal model control and its application in non-square processes," Control and Decision, vol.23, pp. 581-584, 2008.
- [18] Q. B. Jin and W. B. Huang , "Tuning algorithm of an internal model control decoupler. International Conference on Electrical and Engineering. Wuhan, 2010, pp. 2482-2485.
- [19] S. Dasgupta, S. Sadhu and T.K. Ghoshal, " Internal Model Based V-Norm decoupling control for four tank system" IEEE International Conference on Control, Instrumentation, Energy & Communication (CIEC), Calcutta, pp 31-35.2014
- [20] T. Liu, W. D. Zhang and D. Y. Gu , "Analytical design of decoupling internal model control (IMC) scheme for two-input-two-output (TITO) processes with time delays," Industrial & Engineering Chemistry Research, Vol. 45, pp. 3149-3160, 2006.
- [21] X. Zhang and H. Pang, " Novel Concise Robust Control Design for Non-square Systems with Multiple Time Delays" Journal of Nature and Science, Vol.1, No.2, pp 1-4, 2015.

Inter Prediction Complexity Reduction for HEVC based on Residuals Characteristics

Kanayah Saurty
Faculty of Information and
Communication Technologies
Université des Mascareignes
Pamplemousses, Mauritius

Pierre C. Catherine
School of Innovative
Technologies and Engineering
University of Technology,
La Tour Koenig, Mauritius

Krishnaraj M. S. Soyjaudah
Faculty of Engineering
University of Mauritius
Réduit, Mauritius

Abstract—High Efficiency Video Coding (HEVC) or H.265 is currently the latest standard in video coding. While this new standard promises improved performance over the previous H.264/AVC standard, the complexity has drastically increased due to the various new improved tools added. The splitting of the 64×64 Largest Coding Unit (LCU) into smaller CU sizes forming a quad tree structure involves a significant number of operations and comparisons which imposes a high computational burden on the encoder. In addition, the improved Motion Estimation (ME) techniques used in HEVC inter prediction in order to ensure greater compression also contribute to the high encoding time. In this paper, a set of standard thresholds are identified based on the Mean Square (MS) of the residuals. These thresholds are used to terminate the CU splitting process and to skip some of the inter modes processing. In addition, CUs with large MS values are split at a very early stage. Experimental results show that the proposed method can effectively reduce the encoding time by 62.2% (70.8% for ME) on average, compared to HM 10, yielding a BD-Rate of only 1.14%.

Keywords—HEVC; inter prediction; early termination scheme; complexity reduction; prediction residuals

I. INTRODUCTION

High Efficiency Video Coding (HEVC), produced by the Joint Collaborative Team on Video Coding (JCT-VC) consisting of ISO-IEC/MPEG and ITU-T/VCEG, is currently the latest standard in video image compression [32]. In fact, it makes use of the same hybrid approach, consisting of the intra/inter prediction coupled with 2-D transform coding, which all video compression technology have been using since H.261.

Video coding consists essentially of removing the maximum redundancy possible through intra and inter prediction. While intra prediction, which makes use of data from the same frame, produces a very high quality output, it is also accompanied by a high bitrate. Inter prediction exploits the redundancies among already decoded frames and contributes significantly towards the low bitrate of the compression algorithm.

Unlike its predecessor, H.264/AVC [35], which partitions the frame into 16×16 macroblocks, HEVC makes use of a block of size 64×64 pixels which is also known as the Largest Coding Unit (LCU). This large LCU size is advantageous for smooth regions of a picture although HEVC has to test all the various combinations of CU sizes. In fact, HEVC adopts a highly flexible quad-tree structure as shown in Fig. 1.

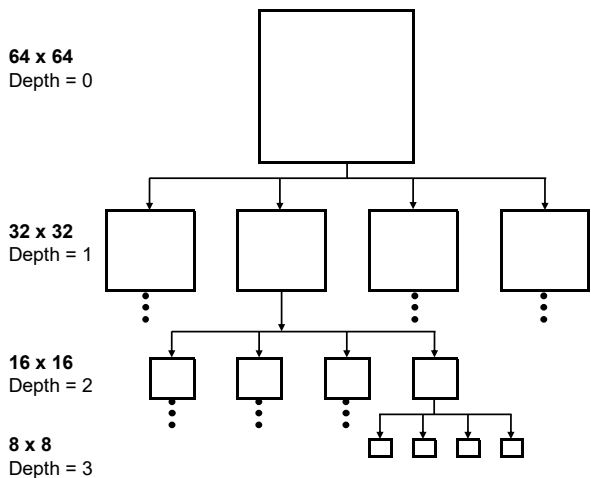


Fig. 1. HEVC quad tree splitting of the LCU

For each CU size, HEVC selects one out of many prediction possibilities resulting in the testing of various Prediction Units (PUs) and Transform Units (TUs) prior to selecting the best one based on the Rate Distortion (RD) cost. In addition, using a bottom up approach in the quad-tree structure, the four aggregated children CUs are compared with their parent to check the possibility of combining them as one CU only. The larger the CU size, the higher will be the compression as the prediction information sent will be less than those required by the four children. This process applies to both the intra and the inter prediction, although the PU partitioning is different for these two modes.

A high proportion of the encoding time is however devoted to inter-prediction during the encoding phase. Inter frame prediction alone consumes from 60% to 96% of the total encoding time [26]. In [13], inter prediction is shown to consume 84% of the encoding time while only 3% is taken by intra prediction for High Definition (HD) sequences.

Consequently, for practical applications such as high-resolution video services and real-time processing, HEVC still requires a significant complexity reduction while maintaining the high coding performance. Several approaches have been proposed to reduce the encoding complexity for both intra-picture and inter-picture prediction. In intra-prediction, com-

plexity reduction is achieved by reducing the number of modes used out of the maximum of 35 and by terminating the CU splitting process as early as possible [5], [6], [9], [22], [27], [28], [31], [40]. While the determination of the CU size at an early stage is also applicable to inter prediction, time reduction is also obtained by optimizing on the Motion Estimation (ME) process.

The complex quad-tree structure of the HEVC standard, which is the basis of the high encoding time, also implies that various optimization techniques could be implemented. Thus, most of the existing works have come up with heuristics to eliminate the processing of some of the possible configurations within the full range available so as to encode the input video with substantial time savings. The results of these techniques to accelerate the encoding process also come along with varied loss in quality and increase in the bit rate.

The high encoding time during inter prediction is largely contributed by the use of various Motion Estimation (ME) and motion compensation techniques to produce accurate prediction. In addition, the use of multiple reference frames in the ME techniques since the H.264/AVC standard, makes the motion estimation process even more complex. The common optimization method to reduce the encoder complexity therefore consists of decreasing the number of ME operations during the inter prediction process.

In this paper, the splitting of CUs in the quad tree is terminated based on the Mean Square (MS) of the residuals. In addition, CUs are also identified as split-CUs during the $2N \times 2N$ PU processing itself. In such cases, the processing for other PU modes are skipped. The different thresholds are identified after analyzing the splitting process of a sample of the sequences. The rest of this paper is thus organized as follows. Section II enumerates the techniques proposed by related works. Section III provides an overview of inter prediction in HEVC. The time consuming elements during inter-prediction are presented in Section IV. Section V describes the proposed approach consisting of the early termination schemes. The experiments conducted and discussions on the results obtained are subsequently presented in Section VI. Finally, Section VII concludes the paper.

II. RELATED WORKS

Several algorithms have been proposed to reduce the HEVC complexity while ensuring negligible loss in quality and bit rate.

For example, significant time savings are obtained by avoiding the unnecessary splitting of some CUs. In [41], the quad-tree CU depth decision process is modeled as a three-level of hierarchical binary decision problem. In addition, a flexible CU depth decision structure is used to allow the performance of each CU depth decision be smoothly transferred between the coding complexity and RD performance along with binary classifiers to control the risk of false prediction. By making use of the mode information of the current CU and a depth range selection mechanism (DRSM), [19] produces an effective splitting decision process. The RD costs of the parent and current levels are used in [11] to terminate the quad-tree-based structure earlier, thus reducing the computational complexity of the encoder. In [38], the CU splitting decision

is constructed on a pyramid motion divergence (PMD) based CU selection along with a k nearest neighboring like method. Splitting and termination decision approaches are also explored in [15], [30]. In [30], a Bayesian decision rule is also used in the splitting decision. The splitting decision in [29] is based on skipping some specific depth levels rarely used in the previous frame and neighboring CUs in addition to using termination methods based on motion homogeneity checking, RD cost checking and SKIP mode checking. An early pruning method based on statistics of the prediction residuals is used in [33] to produce significant time gain. A fast CU decision approach is proposed in [36] based on an exponential model expressing the relationship between the motion compensation R-D cost and the SAD cost for the upper CU and its sub-CUs.

Fast prediction unit decision methods are proposed in [17], [18], [24], [34]. Motion Estimation is performed only on the selected inter prediction mode in [17] based on a priority level. Inter prediction information from previously predicted blocks and neighboring blocks enable the selection of only one inter prediction mode. Spatio-temporal analysis and depth correlations along with a classification of motion activity are explored in [18]. In [34], optimization techniques are proposed based on the rate-distortion-complexity characteristics of the HEVC inter prediction for the different block partitioning structures. In [24], the depth information of a CTU is already determined from information collected in the $2N \times 2N$ PU. It makes use of the high probability of $2N \times 2N$ being the best mode. Thus a fast scheme is proposed to make this decision at an early stage itself. In addition, a merge SKIP extraction method is developed and integrated with the CU depth decision algorithm to effectively decrease the encoding time.

A simple tree-pruning algorithm is proposed in [7] that exploits the observation where the sub-tree computations can be skipped if the coding mode of the current node is sufficient, i.e. a SKIP mode. An early detection of SKIP mode is also proposed in [39] to reduce an encoding complexity of HEVC. The proposed method is similar to the early skip detection scheme implemented the H.264/AVC, but slightly modified to address the different encoding scheme of HEVC. The SKIP mode and the number of transformed coefficients of a CU which are already computed values in HEVC are utilized in [10] and [16] to produce fast mode decision algorithm. A fast rate-distortion estimation algorithm for HEVC is proposed in [10] based on genuine zero blocks (GZBs) and pseudo zero blocks (PZBs) of the transformed coefficients. In [16], the early mode decision is modeled as a binary classification problem of SKIP/non-SKIP or split/unsplit along with the Neyman-Pearson-based rule to balance the rate-distortion (RD) performance loss and the complexity reduction.

In [25], a new global search pattern for finding the global minima and an adaptive early termination condition are proposed to speed up the Motion Estimation (ME) algorithm. By merging $N \times N$ PU partitions in order to compose larger ones, several Motion Estimation (ME) calls during the PU inter-prediction decision are avoided in [26] to reduce the overall encoding process.

Reference [13] proposes a system-level Adaptive Workload Management Scheme (AWMS). The AWMS collect feedbacks at a frame level and dynamically configures different parameters for the video-coding system such as the maximum CU

depth and the search range. A fast CU size decision based on Sobel operator is proposed in [14]. By using textual features of the video images, the algorithm identifies the coding depth of the final CU without having to traverse the coding layers and results in a reduced computational complexity.

III. OVERVIEW OF INTER PREDICTION IN HEVC

Each frame in HEVC is initially partitioned into blocks of 64×64 pixels prior to any prediction and encoding being made. Each of these blocks which is also known as the Largest Coding Block (LCU) is further split recursively into four children until the Smallest Coding Units (SCUs) of size 8×8 are reached. The quadtree structure formed is illustrated in Fig. 1. Intra prediction iterates among the 35 available modes to select the one that results in the cheapest Rate-Distortion (RD) cost. The reference data which are obtained from the already decoded top and left CUs are interpolated to form the prediction for the current CU regarding the angular modes. While intra prediction makes use of reference samples within the same frame, the references of inter prediction comes from the already decoded frames. As such, inter-prediction makes use of a list of reference frames in the case of uni-predictive frame (P-frame) and two lists (list 0 and list 1) for the bi-predictive frame (B-Frame).

Inter prediction exploits the motion data among frames. A block of pixels in a frame generally has a very close match with another block of the same size in a different frame. This match may be at the same location in the reference frame when there is no motion but at a different location when motion is present. HEVC represents this prediction as a set of motion vector which gives the translational movement of the block from the reference frame to the current one. The residuals which is the difference between the original block of pixels and the prediction block is transformed and together with the motion vector constitute the motion data.

During the inter-prediction process, a single motion data may not optimally represents the prediction of the CU in terms of RD cost as objects within this CU may have different motion vectors. CUs are therefore split into PUs to more accurately reflect the different motion vectors within the single block of pixels. In order to determine the best PU configuration, an intensive Motion Estimation (ME) process is undertaken. HEVC has to theoretically search through all the possible blocks in the search window which is commonly known as the full search algorithm so as to reach the best match in terms of minimum distortion and low number of bits to represent the encoded region. There are many fast ME algorithms which optimize this search. Efficient search techniques [20], [25] have been implemented as this process is the most time consuming element in the inter-picture process.

There are 8 possible PU configurations for each CU and they consist of one, two or four PUs. The different PU modes in inter prediction are illustrated in Fig. 2. The PUs are categorized as either symmetric PUs or asymmetric ones. For the symmetric PUs, the CU is either not split or split into 4 PUs or it may be split into two identical PUs (horizontal or vertical). The asymmetric PUs are also known as Asymmetrical Motion Prediction (AMP) and consist of 4 PU configurations: the CU is split into $\frac{1}{4}$ and $\frac{3}{4}$ of the square region. This

is especially useful when only a small part within the region shows a different motion vector. There are four AMP PU modes namely $2N \times nU$, $2N \times nD$, $nL \times 2N$ and $nR \times 2N$. The $N \times N$ PU configuration is only processed for the 8×8 CUs. It is to be noted that the smallest size CUs do not check for the AMP PU modes. They only adopt the $2N \times 2N$, $N \times 2N$, $2N \times N$ and the $N \times N$ PU configurations [4].

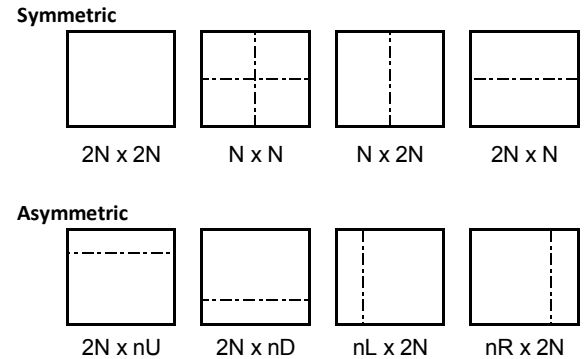


Fig. 2. HEVC inter-picture PU modes

Once the PU modes for each CU size has been identified in the quad tree, a bottom-up approach comparison is performed to determine whether the parent CU is more optimized compared to the combined RD-cost of the four children. In case the parent CU along with the appropriate PU mode is more optimized, it is retained. Otherwise, the 4 children, each with their independent PU configuration, are adopted.

IV. HEVC INTER PREDICTION COMPLEXITY

Although the new features introduced in the HEVC inter prediction contributes to the high performance, it is also the cause for the increase in encoding time compared to AVC. This complexity is distributed among many stages throughout the prediction process. The following sub-sections provide an insight into the time consuming elements during the inter prediction stage.

A. Inter Frames Encoding Time

Inter frame prediction is the most time consuming part in the HEVC encoder. The processing time of inter-predicted frames is in fact higher than their corresponding intra frames within the same sequence. A preliminary experiment is conducted by encoding 10 frames for each sequence and the result is illustrated in Fig. 3. It clearly shows that inter frames processing requires more than *thrice* the processing time of intra frames, indicating the complex nature of the inter prediction process. This higher computing time is associated with the exhaustive Motion Estimation (ME) processing which is performed for each possible PU configuration at the different depth of the quadtree structure.

B. Time spent at different depth of the LCU

The amount of time spent within each CU size or depth is further analyzed by collecting the data from the inter predicted frames for a number of sequences and the result is provided

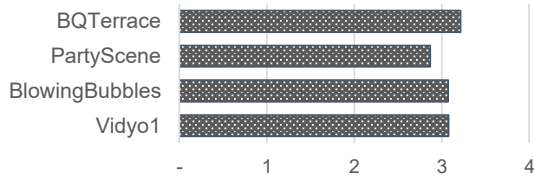


Fig. 3. Inter frames processing time relative to corresponding intra frames

in Fig. 4. It is noticed that the 64×64 CU size shows the smallest percentage of time spent, i.e., 18%. This largest size CU seldom tests all the possible PU configurations and therefore the encoder spends a smaller proportion of time at this depth compared to others. Processing in the other CU depths averagely spend slightly more than 25% of the total inter prediction time spent for the whole LCU. Avoiding the processing of higher depths during inter prediction can therefore bring around 25% time savings for each depth at the level of the CU.

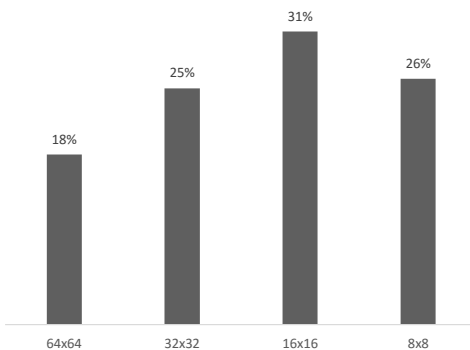


Fig. 4. Time spent within each CU size during inter-prediction

As opposed to intra prediction where the complexity of the texture in the frame normally dictates the granularity of the CU structure, the movement of the objects in the frame relative to the background or to other objects determines the CU structure during inter prediction.

The ME operation precisely maps the region of the CU being processed to those within the searched window in order to determine the closest match in terms of the lowest distortion and bit rate. This intensive ME operation lends itself to a very time consuming process although some of these steps could be avoided by identifying the non-split CUs or specific PU modes at an early stage of the quad-tree traversal.

C. Frequency of PU modes

Data has also been collected from the inter predicted frames for a number of sequences and the frequency of occurrences of the different PU modes is provided in Fig. 5. Among the CUs which are not split, almost 90% of them adopt the $2N \times 2N$ PU mode.

By carefully identifying those terminating CUs that potentially will result in $2N \times 2N$ PU mode, the complexity of

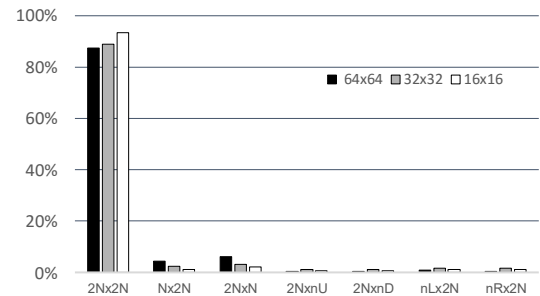


Fig. 5. Occurrences of PU modes for different CU sizes

the inter prediction process may be further reduced. In the following section, a method of reducing these unnecessary computations is proposed by analyzing the residuals formed following the $2N \times 2N$ PU mode operation.

V. PROPOSED APPROACH

Using the *lowdelay B main* profile for HEVC, there are three B-frames for every I-frame in a GOP. As illustrated in Fig. 3, inter-predicted frames encoding consumes more than *thrice* the amount of time compared to intra-predicted frames. The complexity of only the B-frames have therefore been reduced in this approach as they account for the larger portion of the encoding time. Moreover, since regions from the I-frames are the main references in the inter-prediction process and are used for assessing the quality of the predicted CUs, they are encoded using the conventional HEVC process.

The final structure of the LCU is determined after traversing the quadtree formed by HEVC with CUs of size 64×64 down to 8×8 . The proposed approach of complexity reduction targets CUs of size 16×16 and larger only. By terminating CUs of size at least 16×16 , only a reduced number of CUs of size 8×8 will be left. These remaining CUs follow the HEVC conventional processing.

By making an informed decision at the beginning of the CU processing for inter prediction, a number of unnecessary processing can be avoided leading a substantial decrease in the encoding time. For example, by correctly identifying that a CU will be split at the beginning itself can prevent the unnecessary checking of other modes. Next, determining that a CU will not be further divided can avoid the processing at higher depths. Within this very CU, the encoding time may be further reduced by recognizing that this terminating CU may be encoded as a single PU, thus avoiding the verification of other PU modes. These decisions, when applied collectively during the quad tree traversal, can lead to enormous time savings for the encoder.

The CUs under consideration are thus classified as

- 1) Single PU mode ($2N \times 2N$)
- 2) Other PU modes (two PUs), and
- 3) Splitting of the CU into four children

In this paper, CUs are classified into the different categories based on the luma residuals. Once the best $2N \times 2N$ PU motion data is obtained following the merge and the SKIP operations,

the luma residuals which are also of the order of $2N \times 2N$ are further analyzed.

The residuals, which is the difference between the original block of pixels and the prediction block, obtained after performing the $2N \times 2N$ inter prediction processing are analyzed to determine the probable configuration of that CU. The residuals are grouped in blocks of 8×8 and the Mean Square (MS) of the residuals is computed for each one of these blocks as follows

$$MS = \frac{1}{h \times w} \sum_{h,w} [Org(i,j) - Pred(i,j)]^2 \quad (1)$$

where h and w represent the *height* and *width* of the CU and i and j represent the coordinates of each pixel within the block

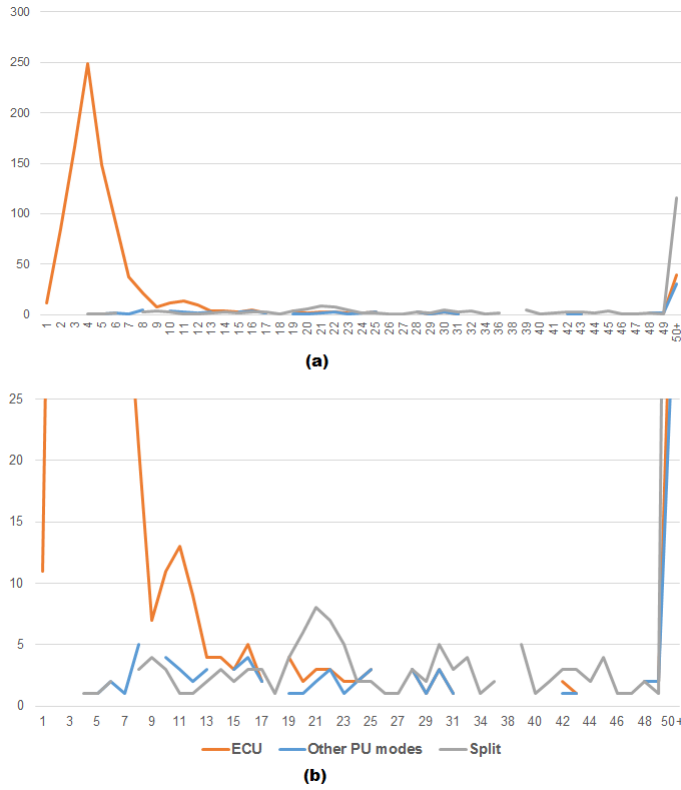


Fig. 6. a) Frequency of occurrence of ECU, Other PU modes and Split CUs as a relationship of MS_{Max} for the *BasketballPass* sequence with QP 22 b) Magnified version for MS_{Max} values for low frequencies of occurrences

The largest MS value, termed as MS_{Max} is used as the coefficient for the threshold values. The first 10 frames of a sample of sequences are studied to find the relationship between the early CU size determination and MS_{Max} . Fig. 6 illustrates the frequency of occurrence of the Early CUs (ECUs), other PU modes and Split CUs as a relationship of MS_{Max} for 16×16 CUs of the *BasketballPass* sequence encoded with a QP value of 22. The ECUs consist of the $2N \times 2N$ CUs (1 PU) as well as those CUs with 2 PUs ($N \times 2N$, $2N \times N$, $2N \times nU$, $2N \times nD$, $nL \times 2N$ and $nR \times 2N$). It is noted that the majority of the non-split CUs (ECUs) are concentrated at the lower MS_{Max} values while the split CUs

are at the other end with relatively larger MS_{Max} values. In Fig. 6, it is observed that the ECUs are found mostly below 25. In addition, CUs adopt the $2N \times 2N$ PU configuration for values of MS_{Max} less than 10.

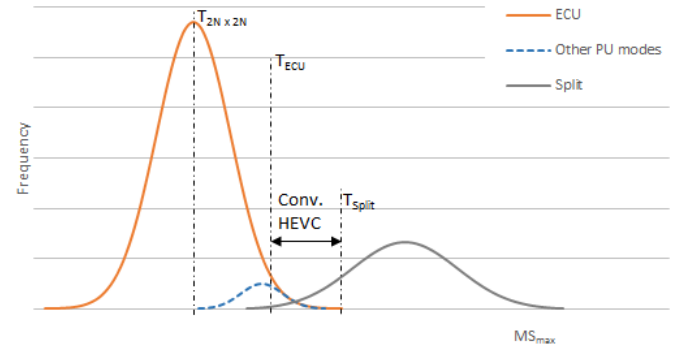


Fig. 7. Using Normal curves to approximate the occurrences of Early CU, Other PU modes and split CUs

The distribution of the three classifications can be approximated to three Normal curves as shown in Fig. 7. The early CU termination threshold is set to the MS_{Max} value for which 90% of the ECUs are captured. A preliminary analysis is performed on the first 10 frames of 4 sequences (one for each class) to determine this value. Table I shows that there is no apparent relationship between the threshold values and the QPs. The thresholds, however, is dependent on the sequences and varies accordingly. In this paper, the average value of 22 is adopted to terminate the CU (for QP = 22) and denoted by T_{ECU} . The threshold value to terminate the CU as $2N \times 2N$ PU is taken as $1/2 T_{ECU}$ and denoted by $T_{2N \times 2N}$. As shown in Fig. 6, most of the CUs with values below $T_{2N \times 2N}$ (11) actually terminates as $2N \times 2N$ PUs. The high MS_{Max} in Fig. 7 values are the split CUs. The split threshold is therefore set above the ECU threshold, i.e. $1.25 \times T_{ECU}$. These CUs will not be allowed to perform the various modes checks but considered directly as split CUs.

TABLE I. 90% THRESHOLD VALUES FOR ECU BASED ON FIRST 10 FRAMES WITH QP=22

Sequence	CU Size		
	16	32	64
Cactus	31	33	29
BasketBallDrill	13	13	14
BlowingBubbles	35	30	-
Vidyo1	18	19	15

It is also observed that the MS of the residuals is proportional to the QP values. A large QP (lower quality) normally results in higher residual values. By observing the MS values obtained with same motion vectors and different QP values, the following relationship is formed

$$MS_{27} = 2.4 \times MS_{22} \quad (2)$$

$$MS_{32} = 5.0 \times MS_{22} \quad (3)$$

$$MS_{37} = 10.0 \times MS_{22} \quad (4)$$

Combining the relationship among the different QP values with the threshold defined above for QP value of 22, the different threshold values are set as shown in Table II.

TABLE II. MEAN SQUARE (MS) THRESHOLD VALUES FOR DIFFERENT QP VALUES

QP	T_{ECU}	$T_{2N \times 2N}$	T_{Split}
22	22	11	28
27	53	26	66
32	110	55	138
37	220	110	275

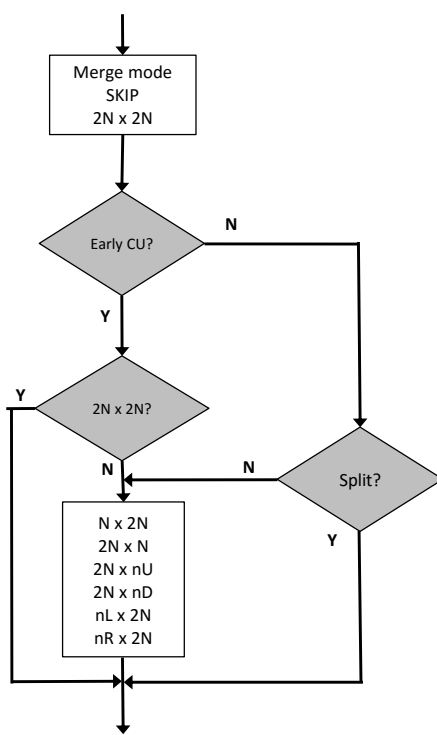


Fig. 8. Illustrating early PU mode decisions based on residuals obtained following the $2N \times 2N$ inter-prediction operation

As illustrated in Fig. 7, the region between the ECU threshold and the split threshold is not considered in our complexity reduction approach. The inter-prediction modes of CUs falling in this area, where the curves intersect, are difficult to predict. The risk of an incorrect decision is quite high and may weight significantly on the quality. For this reason, these CUs have been left to HEVC normal processing.

The overall approach is summarized in Fig. 8 where the highlighted (gray) decision boxes indicate the modifications brought about to the conventional HEVC processing for inter-prediction.

VI. EXPERIMENTS, RESULTS AND DISCUSSION

HEVC Test Model Reference software version 10 (HM10) has been used to implement the proposed early termination

schemes for complexity reduction in inter prediction using the QP values of 22, 27, 32 and 37. Thirteen standard sequences, ranging from class B to class E, as defined in [3] have been used so as to cover a broad range of resolutions. The experiments were performed on 50 frames for each sequence using the *lowdelay B main* encoding configuration with an IBBB Group of Picture (GOP) structure where optimization was carried out on the B frames only.

The performances of the proposed methods, compared to HM10, are reported in terms of the change in average bit rate, peak signal-to-noise ratio (PSNR), Total Encoding Time (TET) and Motion Estimated Time (MET) based on the following formula:

$$\Delta BitRate(\%) = \frac{BitRate(proposed) - BitRate(HM)}{BitRate(HM)} * 100 \quad (5)$$

$$\Delta PSNR(dB) = PSNR(proposed) - PSNR(HM) \quad (6)$$

$$\Delta TET(\%) = \frac{TET(proposed) - TET(HM)}{TET(HM)} * 100 \quad (7)$$

$$\Delta MET(\%) = \frac{MET(proposed) - MET(HM)}{MET(HM)} * 100 \quad (8)$$

TET is the processing time for both the I and the B frames while the MET represents only the encoding time of the B frames for the sequences under consideration. The Bjøntegaard metrics [2] rate distortion performance is used in the computation of BD-Rate and BD-PSNR.

A. Complexity Reduction using Early CU termination

The result of experiments conducted for the early CU termination is presented in Table III. By stopping the splitting process using the early CU termination threshold, T_{ECU} , an average complexity reduction of 41.9% (47.1% for ME) is achieved with a BD-Rate of 0.44%. This reduction is accompanied with a drop of 0.015 dB in terms of PSNR along with a decrease of 0.05 in bitrate. The time savings range from 23.3% for the *PartyScene* sequence to 63.0% for the *Vidyo1* sequence.

Class E sequences show the highest reduction in encoding time as they contain large stationary regions leading to large CUs being formed when encoded. Compared to the *PartyScene* sequence (lowest performance), the *Vidyo1* sequence has more CUs of larger sizes. For example, during the first 10 HEVC encoded frames (7 inter-frames), 54% of the 64×64 CUs are terminated in *Vidyo1* as opposed to only 30% for *PartyScene*. However, these high performance sequences from Class E also display high BD-Rates since the fixed thresholds used are slightly higher for these sequences. CUs containing small regions of motion are incorrectly terminated in the proposed approach leading to a relatively higher drop in quality.

It is also noted that the high complexity reduction of 42.7% achieved for the *BQTerrace* sequence yields a BD-Rate of only 0.09%.

TABLE III. RESULTS OF COMPLEXITY REDUCTION USING EARLY CU ONLY

Class	Sequence	Δ	Δ	Δ	Δ	Bit-	BD-	BD-
		PSNR	TET	MET	Rate	PSNR	[dB]	Rate
		[dB]	[%]	[%]	[%]		[dB]	[%]
B	BQTerrace	-0.004	-42.7	-48.5	-0.06	-0.003	0.09	
	Cactus	-0.010	-42.6	-47.9	-0.08	-0.010	0.44	
	Kimono	-0.010	-42.9	-46.4	0.07	-0.013	0.37	
C	ParkScene	-0.022	-45.1	-50.3	-0.12	-0.030	0.86	
	BasketBallDrill	-0.015	-39.0	-43.7	-0.01	-0.015	0.34	
	BQMall	-0.015	-33.1	-38.0	-0.03	-0.016	0.33	
D	PartyScene	-0.010	-23.3	-26.9	-0.01	-0.011	0.26	
	BasketBallPass	-0.011	-38.5	-44.0	0.09	-0.013	0.36	
	BlowingBubbles	-0.012	-23.8	-26.6	-0.01	-0.013	0.38	
E	BQSquare	-0.015	-29.5	-34.4	-0.10	-0.012	0.18	
	Vidyo1	-0.029	-63.0	-71.0	-0.17	-0.030	0.83	
	Vidyo3	-0.021	-58.0	-64.5	-0.09	-0.015	0.45	
Average	Vidyo4	-0.020	-62.8	-69.9	-0.10	-0.023	0.77	
	Average	-0.015	-41.9	-47.1	-0.05	-0.016	0.44	

B. Complexity Reduction using Early CU and Early PU Termination

Table IV shows the result of applying the early CU and the early PU thresholds simultaneously. An average complexity reduction of 48.1% (54.4% for ME) is achieved with a BD-Rate of 0.55%. The drop of PSNR is only 0.023 dB while a decrease in the bit rate is also observed. In fact, almost half of the number of CUs terminated earlier are identified as $2N \times 2N$ PUs. For these CUs, the other modes processing are avoided leading to the additional time savings. A similar trend as in the early CU threshold is found for the performance of each sequence.

TABLE IV. RESULTS OF COMPLEXITY REDUCTION USING EARLY CU AND EARLY PU

Class	Sequence	Δ	Δ	Δ	Δ	Bit-	BD-	BD-
		PSNR	TET	MET	Rate	PSNR	[dB]	Rate
		[dB]	[%]	[%]	[%]		[dB]	[%]
B	BQTerrace	-0.004	-48.0	-54.4	-0.07	-0.004	0.12	
	Cactus	-0.014	-48.8	-55.0	-0.09	-0.010	0.48	
	Kimono	-0.019	-51.1	-55.2	0.12	-0.022	0.72	
C	ParkScene	-0.034	-51.9	-58.1	-0.15	-0.045	1.24	
	BasketBallDrill	-0.026	-46.6	-52.2	-0.03	-0.023	0.58	
	BQMall	-0.020	-39.9	-45.5	-0.02	-0.022	0.46	
D	PartyScene	-0.015	-27.0	-31.1	-0.04	-0.020	0.32	
	BasketBallPass	-0.023	-46.6	-53.8	0.00	-0.021	0.51	
	BlowingBubbles	-0.016	-26.2	-30.0	-0.07	-0.023	0.46	
E	BQSquare	-0.020	-34.1	-39.4	-0.13	-0.015	0.23	
	Vidyo1	-0.045	-73.2	-82.4	-0.20	-0.041	1.15	
	Vidyo3	-0.031	-67.1	-75.1	-0.09	-0.020	0.70	
Average	Vidyo4	-0.036	-71.9	-80.0	-0.18	-0.034	1.03	
	Average	-0.023	-48.7	-54.8	-0.07	-0.023	0.62	

C. Complexity Reduction using Early CU and Early PU Termination along with Early Splitting

In addition to the early termination of CUs and PU modes, CUs with high MS values at the level of the $2N \times 2N$ mode processing are identified as split CUs. The processing associated with the other modes processing are therefore avoided and the splitting is performed directly. The results of combining all three techniques is provided in Table V. The reduction in TET ranges from 50.1% for the *BlowingBubbles* sequence to 76.0% for the *Vidyo1* sequence. An average overall complexity reduction of 62.2% (70.8% for ME) is thus achieved along with a BD-Rate of only 1.14%. The MET shows an average reduction of 70.8% in encoding time.

TABLE V. RESULTS OF COMPLEXITY REDUCTION USING EARLY CU, EARLY PU AND EARLY SPLITTING

Class	Sequence	Δ	Δ	Δ	Δ	Bit-	BD-	BD-
		PSNR	TET	MET	Rate	PSNR	[dB]	Rate
		[dB]	[%]	[%]	[%]		[dB]	[%]
B	BQTerrace	-0.012	-60.2	-68.9	0.04	-0.017	0.46	
	Cactus	-0.024	-61.5	-69.8	0.16	-0.031	1.13	
	Kimono	-0.030	-64.5	-70.8	0.56	-0.051	1.56	
C	ParkScene	-0.043	-63.6	-71.9	0.00	-0.048	1.47	
	BasketBallDrill	-0.037	-62.3	-70.6	0.37	-0.055	1.28	
	BQMall	-0.040	-58.7	-67.7	0.43	-0.066	1.44	
D	PartyScene	-0.032	-50.1	-58.5	0.18	-0.039	0.84	
	BasketBallPass	-0.033	-62.1	-72.5	0.43	-0.056	1.15	
	BlowingBubbles	-0.038	-50.3	-58.2	0.19	-0.051	1.10	
E	BQSquare	-0.035	-51.5	-60.7	0.06	-0.042	0.64	
	Vidyo1	-0.045	-76.0	-85.8	-0.06	-0.045	1.30	
	Vidyo3	-0.042	-72.7	-81.8	0.21	-0.059	1.23	
Average	Vidyo4	-0.036	-75.1	-83.8	0.02	-0.036	1.28	
	Average	-0.034	-62.2	-70.8	0.20	-0.046	1.14	

The best and worst performances in terms of BD-Rate during the experiments are illustrated in Fig. 9 for the *BQTerrace* sequence and in Fig. 10 for the *Kimono* sequence. The *BQTerrace* sequence shows practically no deviation with the proposed approach from the standard HEVC encoder while the *Kimono* sequence (worst case) indicates only a very slight deviation. This comparison further confirms the high time savings produced by the proposed approach with negligible deterioration in quality.

D. Comparison with related works

A number of works on complexity reduction for HEVC inter prediction have already been published. Comparison with existing works have been limited to those based on the *low-delay main* profile of the HEVC. In addition, since different degree of reductions with varying BD-Rates are achieved, the performance indicator ratio, *BD-Rate/ ΔTET* , proposed in [8] is used for comparison purposes in Table VI. The comparison is grouped into 3 categories with complexity reduction around 40%, 50% and 60%. The proposed approach for each category, outperforms the other works in terms of the ratio *BD-Rate/ ΔTET* , confirming the effectiveness of the proposed approach.

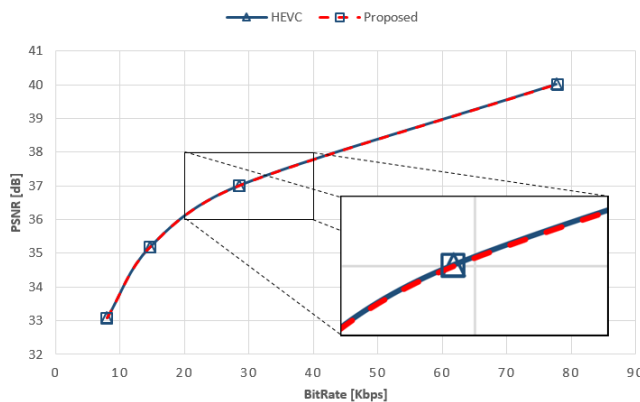


Fig. 9. Performance of *BQTerrace* sequence for complexity reduction using Early CU, Early PU and Early Splitting

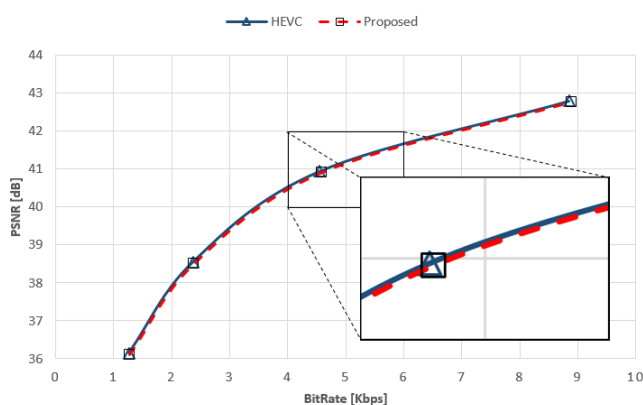


Fig. 10. Performance of *Kimono* sequence for complexity reduction using Early CU, Early PU and Early Splitting

TABLE VI. COMPARISON WITH RELATED WORKS

Category	Related Works	Δ	BD-	BD-Rate/
		TET [%]	Rate [%]	ΔTET [%]
40%	Goswami [12]	-39.53	0.50	1.26
	Shen [29]	-41.00	1.15	2.80
	Ahn [1]	-42.70	1.00	2.34
	Proposed (ECU)	-41.90	0.44	1.05
50%	He [14]	-45.34	1.23	2.71
	Lin [21]	-49.87	0.74	1.48
	Zhang [41]	-51.45	1.98	3.85
	Xiong [36]	-52.00	1.61	3.10
60%	Proposed (ECU+EPU)	-48.70	0.62	1.27
	Liu [23]	-56.71	1.05	1.85
	Xiong [37]	-59.67	2.19	3.67
	Proposed (ECU+EPU+Split)	-62.20	1.14	1.83

For the 40% category, the BD-Rate of 0.44% achieved in the proposed ECU termination approach is well below those of comparable works leading to a $BD\text{-}Rate/\Delta TET$ value of only 1.05. The proposed *ECU + EPU* termination approach in the 50% category results in 48.7% time savings. Compared to other works, the BD-Rate is lower along with a $BD\text{-}Rate/\Delta TET$ ratio of only 1.27. The proposed approach in the high reduction category (60%) also surpasses other works in terms of the $BD\text{-}Rate/\Delta TET$ ratio and with an overall complexity reduction of 62.2%.

VII. CONCLUSION

In this paper, a new approach is proposed to enhance the complexity reduction in the HEVC inter prediction process for the *lowdelay Main* profile. The Mean-Square (MS) of each 8×8 block of the residuals following the $2N \times 2N$ inter prediction processing are computed. The highest MS value is used for comparison with the determined thresholds for early termination of the CU and PU processing along with the early identification of the splitting decision.

When this technique is applied to CUs of size 16×16 , 32×32 and 64×64 , an average overall complexity reduction of 62.2% (70.8% for ME) is achieved at a BD-Rate of only 1.14%.

The proposed approach achieves a higher encoding time reduction compared with the state-of-the-art algorithms while maintaining a good average bitrate performance. In the proposed work, a set of static thresholds are used. The good performances of the proposed work in predicting the termination of CUs and PU processing are observed by the low $BD\text{-}Rate/\Delta TET$ ratios. However, since the proposed approach is based purely on static thresholds, it produces relatively higher BD-Rates when the actual sequence thresholds should have been slightly higher or lower. Therefore, the proposed work can still be enhanced by including in the thresholds some characteristics intrinsic of each sequence.

REFERENCES

- [1] S. Ahn, B. Lee, and M. Kim. A Novel Fast CU Encoding Scheme Based on Spatiotemporal Encoding Parameters for HEVC Inter Coding. *IEEE Transactions on Circuits and Systems for Video Technology*, 25(3):422–435, March 2015.
- [2] G. Bjøntegaard. Calculation of Average PSNR Differences between RDCurves . Doc. VCEG-M33, VCEG, April 2001.
- [3] F. Bossen. Common test conditions and software reference configurations . Doc. JCTVC-B300, JCT-VC, July 2010.
- [4] B. Bross, P. Helle, H. Lakshman, and K. Ugur. Inter-picture prediction in HEVC. In *High Efficiency Video Coding (HEVC)*, pages 113–140. Springer, 2014.
- [5] G. Chen, Z. Liu, T. Ikenaga, and D. Wang. Fast HEVC intra mode decision using matching edge detector and kernel density estimation alike histogram generation. In *Circuits and Systems (ISCAS), 2013 IEEE International Symposium on*, pages 53–56, May 2013.
- [6] G. Chen, Z. Pei, L. Sun, Z. Liu, and T. Ikenaga. Fast intra prediction for HEVC based on pixel gradient statistics and mode refinement. In *Signal and Information Processing (ChinaSIP), 2013 IEEE China Summit International Conference on*, pages 514–517, July 2013.
- [7] K. Choi, S-H Park, and E.S. Jang. Coding tree pruning based CU early termination . Doc. JCTVC-F092, JCT-VC, July 2011.
- [8] G. Correa, P. Assuncao, L. Agostini, and L.A. da Silva Cruz. Four-step algorithm for early termination in HEVC inter-frame prediction based on decision trees. In *Visual Communications and Image Processing Conference, 2014 IEEE*, pages 65–68, Dec 2014.

- [9] T.L. da Silva, L.V. Agostini, and L.A. da Silva Cruz. Speeding up HEVC intra coding based on tree depth inter-levels correlation structure. In *Signal Processing Conference (EUSIPCO), 2013 Proceedings of the 21st European*, pages 1–5, Sept 2013.
- [10] H. Fan, R. Wang, L. Ding, X. Xie, H. Jia, and W. Gao. Hybrid Zero Block Detection for High Efficiency Video Coding. *IEEE Transactions on Multimedia*, 18(3):537–543, March 2016.
- [11] K. Goswami, B-G Kim, D. Jun, S-H Jung, and J.S. Choi. Early Coding Unit-Splitting Termination Algorithm for High Efficiency Video Coding (HEVC). *ETRI Journal*, 36(3):407–417, June 2014.
- [12] K. Goswami, J-H Lee, and B-G Kim. Fast algorithm for the high efficiency video coding (hevc) encoder using texture analysis. *Inf. Sci.*, 364(C):72–90, October 2016.
- [13] M. Grellert, M. Shafique, M.U.K. Khan, L. Agostini, J.C.B. Mattos, and J. Henkel. An adaptive workload management scheme for HEVC encoding. In *2013 IEEE International Conference on Image Processing*, pages 1850–1854, Sept 2013.
- [14] J. He, X. He, X. Li, and L. Qing. Fast Inter-Mode Decision Algorithm for High-Efficiency Video Coding Based on Textural Features. *Journal of Communications*, 9(5):441–447, May 2014.
- [15] W.J. Hsu and H.M. Hang. Fast coding unit decision algorithm for HEVC. In *Signal and Information Processing Association Annual Summit and Conference (APSIPA), 2013 Asia-Pacific*, pages 1–5, Oct 2013.
- [16] Q. Hu, X. Zhang, Z. Shi, and Z. Gao. Neyman-Pearson-Based Early Mode Decision for HEVC Encoding. *IEEE Transactions on Multimedia*, 18(3):379–391, March 2016.
- [17] A. Lee, D. Jun, J. Kim, J.S. Choi, and J. Kim. Efficient Inter Prediction Mode Decision Method for Fast Motion Estimation in High Efficiency Video Coding. *ETRI Journal*, 36(4):528–536, August 2014.
- [18] J.H. Lee, B.G. Kim, D.S. Jun, S.H. Jung, and J.S. Choi. Complexity reduction algorithm for prediction unit decision process in high efficiency video coding. *IET Image Processing*, 10(1):53–60, 2016.
- [19] J.H. Lee, C.S. Park, and B.G. Kim. Fast coding algorithm based on adaptive coding depth range selection for HEVC. In *Consumer Electronics - Berlin (ICCE-Berlin), 2012 IEEE International Conference on*, pages 31–33, Sept 2012.
- [20] X. Li, R. Wang, W. Wang, Z. Wang, and S. Dong. Fast motion estimation methods for HEVC. In *2014 IEEE International Symposium on Broadband Multimedia Systems and Broadcasting*, pages 1–4, June 2014.
- [21] T-L Lin, C-C Chou, Z. Liu, and K-H Tung. HEVC early termination methods for optimal CU decision utilizing encoding residual information. *Journal of Real-Time Image Processing*, pages 1–17, 2016.
- [22] Y. C. Lin and J. C. Lai. Edge Density Early Termination Algorithm for HEVC Coding Tree Block. In *Computer, Consumer and Control (ISCC), 2014 International Symposium on*, pages 39–42, June 2014.
- [23] Z. Liu, T-L Lin, and C-C Chou. Efficient prediction of CU depth and PU mode for fast HEVC encoding using statistical analysis. *Journal of Visual Communication and Image Representation*, 38:474–486, 2016.
- [24] C-S Park, G-S Hong, and B-G Kim. Novel Intermode Prediction Algorithm for High Efficiency Video Coding Encoder. *Advances in Multimedia*, 2014, 2014.
- [25] N. Purnachand, L.N. Alves, and A. Navarro. Fast Motion Estimation Algorithm for HEVC. In *Consumer Electronics - Berlin (ICCE-Berlin), 2012 IEEE International Conference on*, pages 34–37, Sept 2012.
- [26] F. Sampaio, S. Bampi, M. Grellert, L. Agostini, and J. Mattos. Motion Vectors Merging: Low Complexity Prediction Unit Decision Heuristic for the Inter-prediction of HEVC Encoders. In *2012 IEEE International Conference on Multimedia and Expo*, pages 657–662, July 2012.
- [27] K. Saury, P. C. Catherine, and K. M. S. Soyjaudah. Terminating CU splitting in HEVC intra prediction using the Hadamard Absolute Difference (HAD) cost. In *SAI Intelligent Systems Conference (IntelliSys), 2015*, pages 836–841, Nov 2015.
- [28] K. Saury, P. C. Catherine, and K. M. S. Soyjaudah. *Fast Intra Mode Decision for HEVC*, pages 361–383. Springer International Publishing, Cham, 2016.
- [29] L. Shen, Z. Liu, X. Zhang, W. Zhao, and Z. Zhang. An Effective CU Size Decision Method for HEVC Encoders. *IEEE Transactions on Multimedia*, 15(2):465–470, Feb 2013.
- [30] X. Shen, L. Yu, and J. Chen. Fast coding unit size selection for HEVC based on Bayesian decision rule. In *Picture Coding Symposium (PCS), 2012*, pages 453–456, May 2012.
- [31] Y. Shi, O.C. Au, H. Zhang, X. Zhang, L. Jia, W. Dai, and W. Zhu. Local saliency detection based fast mode decision for HEVC intra coding. In *Multimedia Signal Processing (MMSP), 2013 IEEE 15th International Workshop on*, pages 429–433, Sept 2013.
- [32] G.J. Sullivan, J. Ohm, W-J. Han, and T. Wiegand. Overview of the High Efficiency Video Coding (HEVC) Standard. *Circuits and Systems for Video Technology, IEEE Transactions on*, 22(12):1649–1668, Dec 2012.
- [33] H. L. Tan, C. C. Ko, and S. Rahardja. Fast Coding Quad-Tree Decisions Using Prediction Residuals Statistics for High Efficiency Video Coding (HEVC). *IEEE Transactions on Broadcasting*, 62(1):128–133, March 2016.
- [34] J. Vanne, M. Viitanen, and T. D. Hämäläinen. Efficient Mode Decision Schemes for HEVC Inter Prediction. *IEEE Transactions on Circuits and Systems for Video Technology*, 24(9):1579–1593, Sept 2014.
- [35] T. Wiegand, G.J. Sullivan, G. Bjøntegaard, and A. Luthra. Overview of the H.264/AVC video coding standard. *Circuits and Systems for Video Technology, IEEE Transactions on*, 13(7):560–576, July 2003.
- [36] J. Xiong, H. Li, F. Meng, Q. Wu, and K.N. Ngan. Fast HEVC Inter CU Decision Based on Latent SAD Estimation. *IEEE Transactions on Multimedia*, 17(12):2147–2159, Dec 2015.
- [37] J. Xiong, H. Li, F. Meng, S. Zhu, Q. Wu, and B. Zeng. MRF-Based Fast HEVC Inter CU Decision With the Variance of Absolute Differences. *IEEE Transactions on Multimedia*, 16(8):2141–2153, Dec 2014.
- [38] J. Xiong, H. Li, Q. Wu, and F. Meng. A Fast HEVC Inter CU Selection Method Based on Pyramid Motion Divergence. *IEEE Transactions on Multimedia*, 16(2):559–564, Feb 2014.
- [39] J. Yang, J. Kim, K. Won, H. Lee, and B. Jeon. Early SKIP Detection for HEVC . Doc. JCTVC-G543, JCT-VC, November 2011.
- [40] H. Zhang and Z. Ma. Early termination schemes for fast intra mode decision in High Efficiency Video Coding. In *Circuits and Systems (ISCAS), 2013 IEEE International Symposium on*, pages 45–48, May 2013.
- [41] Y. Zhang, S. Kwong, X. Wang, H. Yuan, Z. Pan, and L. Xu. Machine Learning-Based Coding Unit Depth Decisions for Flexible Complexity Allocation in High Efficiency Video Coding. *IEEE Transactions on Image Processing*, 24(7):2225–2238, July 2015.

Recovering and Tracing Links between Software Codes and Test Codes of the Open Source Projects

Amir Hossein Rasekh
Computer Science and Engineering Department
Shiraz University
Shiraz, Iran

Seyed Mostafa Fakhrahmad*
Computer Science and Engineering Department
Shiraz University
Shiraz, Iran

Amir Hossein Arshia
Computer Science and Engineering Department
Shiraz University
Shiraz, Iran

Mohammad Hadi Sadreddini
Computer Science and Engineering Department
Shiraz University
Shiraz, Iran

Abstract—One of the most important controversial issues in the design and implementation of software is the functionality of the designed system. With impressive efforts of different software teams in the field of the system, the primary concern of the developers is its proper and error free functioning of the whole system. Therefore, various tests are defined and designed to help software teams to produce error free software or software with minimum error rate. It is difficult but important to find a proper link between written test class and the class under the test. Discovering these links is useful for programmers to perform the Regression Test more efficiently. In this paper, we are trying to propose a model for the recovery of traceable links between test classes and the classes under the test. The presented model comprises four sections. Firstly, we retrieve the name of similar classes between the test class and source class. Afterward, we extract the complexity, Cyclomatic and design metrics from the source codes and the test classes. Finally, after creating a train set, we implement the data mining algorithms to find the potential relationship between unit tests and the classes under the test. One of the advantages of this method is its language independence; furthermore, the preliminary results show that the proposed method has a good performance.

Keywords—Unit Testing; Source Code; Similarity; Software Engineering; Open Source; Data Mining

I. INTRODUCTION

Designing software without observing software engineering principles is like building a house without a standard and engineered plan. Unfortunately, many producing software companies do not follow the principles of engineering or remove some of the stages, especially the test phase of the software development cycle. This reduces the cost of production of software but multiplies the cost of its support and maintenance. This multiplication of the cost of support and maintenance happens due to most of the problems of the program are resolved in the test phase.

Software test is the software evaluation process to ensure the proper functioning of the various events. In other words, software test is finding the possible errors of software during its use to have software which performs correctly, properly and optimally. The more software could work with different events the better the application performs. A good test refers

to the test that in which there is more probability of finding undetected errors by the evaluation process. A successful test is a test which can find at least one undetected error. The test just shows the existence of error not the non-existence of error. Finding no error in the test doesn't mean that it is not an error-free program. The software testability criteria are as follows:

- Operability: The software can be better assessed when it operates in more environments.
- Observability: having the capacity of observing the results of the evaluation.
- Controllability: having the ability to manage the automated tests, such as the capacity to operate the unit tests with JUnit in Java language automatically.
- Decomposability: assessment could be more purposeful.
- Simplicity: reducing the architectural complexity and application logic.
- Stability: for evaluation needs little changes.
- Understandability: having the capacity of understanding the design and correlations between the components.

Coding and testing are two activities that are entirely integrated with the agile method of software development. These two activities require that the programmer frequently swaps between software source code and test codes.

Unfortunately, the links between software codes and test codes are implicit and hidden; therefore, for developers discovering these links to find connections between test cases and corresponding software codes is very time-consuming.

A. The Beginning Time of the Test

During the Software Development Life Cycle that is called SDLC, test starts and it lasts until the establishment of the software. However, all these tests depend on the model of the development that the company would operate. For example, in

the waterfall model the test is run in the software production phase, but in the incremental model the test is repeated at the end of each increase or change. In every stage of the SDLC, the analysis and approvals required for the test are considered. Reviewing of the design in the design phase to the aim of design improvement in the area of test is also considered. After the completion of the test by a developer, the test is classified as a unit test.

Testing during the SDLC has the following advantages:

- Reducing the production time
- Reducing the costs
- Reducing the reworking
- Reducing the software errors
- Increasing productivity
- Increasing software quality
- On time delivery to the taskmaster
- Improving the customer satisfaction

B. Unit Test

Unit Test is a technique used to test small units of software source code and also ensures they are working properly. In this technique, the integrity of each piece of software source code, which is called "unit", is evaluated using another code written by programmers. In object-oriented languages, this is usually done using a separate class, although it can also be done using only one method. Ideally, each test is independent of the others tests. Unit tests are usually handled by software developers. Method of Unit Test can vary from the evaluation of the result on paper to automatically run multiple tests and analysis of the result by the program itself.

C. The Importance and Benefits of Unit Test

- The compilation of the code does not indicate its correct performance. There need to be methods to test the system. You are not only paid to write code, but you are paid to create executable code.
- In a long time, writing unit tests will result in producing high quality codes. For instance, suppose you've developed a system. Today, an employer asked you to add new functionality to the application. To apply the changes, for example, it is required to modify a portion of the existing code, as well as to add new classes and methods to the program. After the request, you must ensure that the prior parts of the system worked until a few moments ago, now working as before. The volume of written code is high. Manual testing of individual cases may not be possible in terms of time and cost. A unit test is a way to ensure that the delivery of work to taskmaster would happen with no error. In this case, refactoring of the existing code will be done properly, because previous tests can be run immediately; moreover, we can assure that the system performs correctly.
- The procedures of the conducted experiments in the future would become an important reference to understand how different parts of the system perform. How

are they calling, how should they be given value, and so on.

- Using the unit tests, we can consider and assess the possible worst-case scenarios before the outbreak.
- Writing unit tests during operation can make the developer break the parts into smaller units that are capable of independent study. For example, suppose you have developed a method that after three different operations on a string provides a specific output.
- These tests are considered as an ideal part of the process of software development because of their automatic execution.

D. Regression Test

The regression test is a method to test the software. The purpose of regression test is to find new software problems or regressions. The purpose of regression test is to assure that new changes such as changes mentioned will not cause a defect or new error in the software. One of the main reasons for doing regression test is to determine if a change in one part of the system can also affect other parts of the system or not. Among the most common technique of performing regression tests is to apply those tests which were done well and successfully before the application of the new changes in the software. Again, after applying new changes, those tests are applied to the software and are examined whether plan behavior changed after applying new changes; moreover, determine if the deficiencies have already been fixed or are not re-emerged and also determine if the already fixed deficiencies have re-emerged or not.

Unfortunately, at present, connections between application codes and test codes are not very rich, and these links are not easily visible. Even when integrated development environments support building test cases based on the generated classes, finding a proper link between the class code and the test is difficult.

Test cases are a valuable source of documentation for developers which they change them continuously to reflect changes in the generated code of their software and maintain an effective regression analysis. Maintaining links between application codes and test codes are an excellent source for selectively testing the software after applying changes in the generated code.

Discovering these links can also be used in the regression analysis. In large-scale software projects, regression test in the form of retest all approach is a time-consuming duty. In particular, operating some of the cases of the test can take hours or even days of time. So developers cannot test software system quickly or even at an acceptable time. Researches show that only 30% of developers, after applying changes in the generated code of their application, they thoroughly tested it again; however, only 70% test those functions that they have changed them.

II. RELATED WORKS

There are a variety of methods for discovering the links between software codes and test codes. These methods could

then be classified based on the method used. Some of these methods are based on Heuristic Algorithm, some are based on Information Retrieval, some are based on Data Mining and, finally, there are some methods based on Machine Learning.

In recent years, some methods are proposed to retrieve and manage the connections between test classes and software code classes. The researchers proposed the waterfall method to improve the testability of complex classes [1].

In 2007, Bouillon and et al. [2] suggested the Eclipse JUnit to call static graphs. They used a Java icon to identify and communicate the description of generated code of the software.

In 2004, Bruntink and Deursen [3] offered two methods to combine the test case and software generated code. The first method used a name convention and handheld communications for mapping the code functions to the requirements model. In the second method, they proposed the connection between the test case and the code functions with time stamps of the test cases and time-stamp of the code functions.

Ren and et al. [4] proposed a system called Chianati. This system is a software add-on for the Eclipse, which can evaluate the impact of changes in the products with the help of software generated code identification. The system analyzes the changes by the developer between different versions of the system; then it maps them in the test case by analyzing the call graph. Moreover, this system can be implemented after changes; thus, it is not able to identify and maintain the connection between the generated code and test case. This method is also useful to understand the application and test the regression along with effective analysis.

In 2012, Hurdugaci and Zidman [5] wrote a plug-in for visual studio that mapped the changes in the software generated code to the case test code for a change in a piece of code.

In 2009, Rompaey and Demeyer [6] implemented experimentally naming convention, the last call before assertion, Latent Semantic Indexing [8] and co-evolution approach. They discovered the test class naming convention by eliminating the keyword "test" of classes in the software generated. The last call before assertion recognized those classes under the test by the inspection and reviewing of the method in JUnit. It is a Heuristic approach that makes a distinction between the test classes and helper classes. In summary, the last call before the assertion assumes that the test methods immediately call the actual test classes before the confirmation of the orders. The latent naming convention is an Information Retrieval techniques that identified test classes based on context similarity of the JUnit and code classes of the software. Finally, the Co-evolution approach assumes that a JUnit test class is completed again with a relevant test. Their results have shown that the naming convention is more accurate than other methods. Moreover, the latent naming convention has been successful in identifying the relationship between several types of artifacts such as those functions under the test written in the natural language and program codes. They also showed that the use of The latent naming convention to identify relationships between JUnit test class are not satisfied. Naming convention shows a one by one relationship between the test cases and the software generated code.

In 2010, Qusef and et al. [9] proposed the use of data

flow analysis to overcome some restrictions. They considered the test classes as a series of classes that affect the results of the latest announcement of each test. The authors examined decomposability and accessibility based on the dependency of the analysis.

In 2011, Qusef and colleagues [10] proposed using slicing to identify a set of classes that are generated by software and have an effect on commands. It is called SCOTCH. Their results are displayed on three system software called ArgoUML, AgilePlanner, Ant Apache. The advantages of SCOTCH are bright compared to conventional naming techniques and the last call before assertion as well as data flow analysis. In particular, words in class names are important.

In 2014, once again, Qusef and et al. [11], developed their 2011 system based on text filtering strategy from internal and external information communication and called it SCOTCH+. In their work they used name similarity; moreover, they took their results on software systems and with this method they improve their previous result.

III. THE PROPOSED METHOD

In this paper, a method has been introduced based on data mining algorithms to link between the code classes and the test classes. The proposed method includes the following sections.

- 1) Retrieving the name of those classes which have the same name in both test classes and source code classes.
- 2) Extracting features of the source code and test classes:
 - a) Extracting complexity metrics
 - b) Extracting Cyclomatic metrics
 - c) Extracting design metrics
- 3) Creating the train test and the test set
- 4) Operating the data mining algorithms on the obtained file.

Figure 1 and Algorithm 1 demonstrate the full implementation of the proposed method and the pseudo codes presented in this paper. These parts will be explained in the next sections respectively.

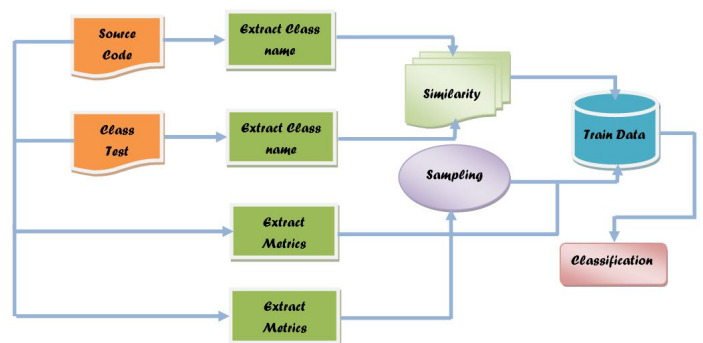


Fig. 1: An overview of the whole system

Algorithm 1 The Pseudocode of the Proposed Method

```

for each (Classname T in TestFolder) do
    for each (Classname C in CodeFolder) do
        if (T equal C) then
            add  $\leftarrow$  T to NamingConventionList
        end if
    end for
end for

for each (Item in TestFolder and CodeFolder) do
    extract (Complexity Metrics)
    extract (Cyclomatic Metrics)
    extract (Design Metrics)
end for

for each (Item in TestFolder) do
    if (Item in NamingConventionList) then
        add  $\leftarrow$  Item and its features to TrainSet
    end if
end for

```

TABLE I: Comparing Similarity Between Two Terms

Term1	Term2	Jaccard Similarity	Proposed Similarity
PropertiesEcho	PropertiesEcho	100%	100%
PropertiesEcho	EchoProperties	100%	85%

A. Recovery of the Name of the Same Classes Between the Test Class and Source Code Class

One of the common approaches among the open source community is the approach of naming the set of test classes. The naming convention of the test class is for selecting the name of the test class. The keyword '*test*' has been located before or after the test name. For example, a class called *TestSample* or *SampleTest* is implementing a test set associated with a class called *Sample*. However, unfortunately, the developers do not follow the class definition of this approach when naming their test series. Accordingly, to make connections between test cases and source codes, initially, we should act in accordance with similarity criteria.

To find such a relationship, initially, the class brand names along with the packages used in this class from the test files should be derived. In particular, the terms used in the class names have much more importance than the name of the other terms in the content of the class. However, it is believed that the terms outlined in the class name offer primary key information, especially when the naming conventions are applied. The names of source code should be scrutinized by using Jaccard similarity criteria with the threshold of 100 and make links between those classes which have quite similar names.

In this method, to find the similarities between the two words, based on the alphabetical order, this task was done which a number of similar letters in the two words divided by the total number of words were counted as it shown in Table III Algorithm 2.

naming conventions create a one-to-one relationship between the test class and the code class based on names, so when there is more than one class tested or when the

Algorithm 2 The Pseudocode of Similarity Measure

```

for each item A in list do
    if (A matches B) then
        return y
    for each char in A or B do
        if (char in both A and B) then
            Di  $\leftarrow$  1
        else
            Di  $\leftarrow$  0
        end if
    end for
    end if
end for

similarity  $\leftarrow$  sum(D)/(|A| + |B|) * 100

return similarity

```

developers are not able to follow the naming based on the smart technology, a shortfall has happened.

B. Feature Extraction of the Source Code and Test Classes

Using the model referred to in phase A, only make links between test cases and source codes for some of the test cases should be found out. If there is no possibility to find such links by class name, the feature extraction model should be used.

In this part, the features such as the technical metrics of the software have been extracted from both sides of the source code and the test classes. These technical metrics are quantitative criteria that can be used for product evaluation. In this paper, complexity metrics, cyclomatic metrics and design metrics have been used.

1) Complexity metrics: In this paper, Halstead complexity measure which was proposed by Howard Halstead in 1977 was used to determine the complexity metrics [12]. These metrics identify those software criteria that reflect implementation or express the algorithm in different languages; also, these metrics are independent of the operation on a specific platform.

Halstead aims to identify the properties of software and relationship between them. For these metrics, a series of initial scale should be applied when the design is complete. These scales are introduced as follows:

n1: number of specified operators that appear in the program
n2: number of specified operands that are displayed in the program
N1: total number of operators
N2: total number of operands
The properties extracted from the Source Code and test file are shown as follows:

- The number of program lines: in this feature, the number of lines of each class of the program was derived.
- The length of the program: the length of the program is the total number of operators and operands.

$$ProgramLength : N = N_1 + N_2 \quad (1)$$

- The number of words of the program: the number of words of the program is the total number of unique operators and operands.

$$n = n_1 + n_2 \quad (2)$$

- Estimation of the length of the program: the following formula can be used for estimation of the length of the program.

$$N = n_1 \log_2 n_1 + n_2 \log_2 n_2 \quad (3)$$

- Volume: volume is the contents of information of the program. Volume size describes the implementation of an algorithm. V calculation is based on the number of operators and operands executable by the control algorithm. Therefore, V sensitivity to LOC criteria is less than code.

$$V = N * \log_2 n \quad (4)$$

- Hard/ Difficulty: the difficulty of the program or error-proneness is assigned by the number of unique operators in the program. The difficulty is also proportional to the quotient between the total number of operands and the number of individual operands. For example, if the same operands are used many times in the program, it is probably more prone to errors.

$$D = n_1 / 2 * N_2 / n_2 \quad (5)$$

- Program effort: program effort (implementation) or understanding of a program is proportional to the volume and level of difficulty of a program.

$$E = D * V \quad (6)$$

- Program level: program level (L) is the inverse of the probability of error in the program. This means that a lower level program is more prone to errors than a higher level program.

$$L = 1 / D \quad (7)$$

- Program Time: time program is proportional to the efforts. The experiments can be used to calibrate this quantity (amount). Halstead has shown that the division of effort (E) by 18 is an approximation for the seconds of time.

$$T = E / 18 \quad (8)$$

2) *Cyclomatic metrics:* In this paper, McCabe criteria were used for Cyclomatic metric. Thomas McCabe proposed this metric in 1976 [13] for the measurement of the complexity of the software. He also considered the number of independent paths covering an entire module or method as the complexity of it. There are different methods to calculate the number of independent paths in the method, and the most formal method is plotting the control graph of the flow of that method. After plotting the control flow graph using the following formula, we can calculate the number of independent paths. This technique is used in the classes of the source code, but the test classes use the properties of the number of calling methods.

$$\text{Cyclomatic Complexity} = EN + 2 \quad (9)$$

$$E : \text{Number of graph edges} \quad (10)$$

$$N : \text{Number of graph nodes} \quad (11)$$

3) *Design metrics:* Software design technique can be useful in evaluating software. In 1974, Steven and colleagues, at the beginning of their work, introduced coupling on the structural development of the content as "measuring the strength of the relationship between a module with another module". The size of the inter-correlation between two objects is called coupling. For example, object "a" and object "b" are coupling if a method of the object "a" is called by a method of "b" or by accessible variables of the object "b". When the defined methods in a class are called by methods or features of the other class, classes are coupled with each other.

Another metric for designing software is Di. Di is a metric for interior design which has the factors related to the internal structure of the module. Di is a basic design metric to evaluate the cohesion of design. The second design software metric is the De. De is an external design metric. De focuses on an external communication of a module with other modules in a software system. So De is a basic metric designed to evaluate coupling of design. The third and the last is the compound design metrics. Dg value is the sum of Di and De.

Coupling factor will display the decimal number that represents the number of communication between the non-inherited classes.

C. Creating the Train Set

For the classification and creating the train set, label one was allocated to the names of those classes which are exactly matched to the source code class which were obtained in phase A; Additionally, those features in phase B from the source codes and test codes were extracted. The sampling method was applied to add the label 0 to the train data.

To perform this process, to determine the distribution of the files, the remaining files were classified.

Then a sample of each source code and test code with their features with zero labels to train data is added. Finally, the train set with features and labels 0 and 1 is available.

D. The Implementation of Data Mining Algorithms on the Obtained Data File

At this phase, the data mining algorithms on the obtained train data from phase C from the source code and test class is run. In this paper, Bayesian learning algorithms, RBF network, logistic regression, SVM, Decision Tree and Part from the data mining algorithms are applied.

1) *Naive Bayes Algorithm:* A very practical approach to learning is the learning Bayesian method, which has been able to provide useful practical solutions [14].

The Bayesian reasoning method is based on the probability to draw inferences.

This method relies on this principle that there is a probability distribution for each quantity. Therefore, an optimal decision may be concluded by observing a new data and having inferences about the probability distribution. This method requires prior knowledge of a large number of probable values. When this information is not available, we are forced to estimate it.

To achieve that, the basic information which was gathered previously and assumptions about the probability distribution was used. Calculation of the optimal Bayesian hypothesis is very costly.

2) RBF Network Algorithm: This algorithm implements a network with radial Gaussian bias function. Here, the K-Means algorithm is used for the bias function; moreover, the logistic regression is used for the nominal properties and linear regression for the numerical regression. Activating the basis functions is normalized before entering into the linear model, by the accumulation of a number. The K-mean applied to each category separately to extract K cluster for each class.

3) Logistic Regression Algorithm: Nowadays, in most of the studies, by using several other factors, a particular purpose should be achieved to get an optimal level. In statistics, such works are done, and the results are analyzed with different regression methods. In regression by independent variables, the responses are estimated. This response variable is the main purpose of the research [15]. Logistic regression is a special case of regression which is used when the variable is a two or more alternative option, i.e. there are two or more different modes for response variable.

4) SVM Algorithm: This algorithm is used in areas that their data are not separated linearly, and the data are mapped into a higher-dimensional space so that they can be separated in this new space linearly.

The basis of SVM classifier is linear classification. In linear dividing of data, that line should be selected which has the most safety margin.

This algorithm does not stick to the local maximum; furthermore, this algorithm almost works well for high-dimensional data.

5) Decision Tree Algorithm: Trees in artificial intelligence are used to show various concepts such as sentence structure, equations, etc. this is one of the most famous inductive algorithms that are successfully used in different applications. The decision tree has application in practical issues that can be raised to provide a single answer like the name of a category or class. The decision tree is suitable for those issues that are determined by the output value of yes or no. The reason for naming it as tree decision is that this tree shows the decision-making process for determining the categories of input data.

6) PART Algorithm: PART is a class to generate a list of decisions. PART algorithm is used to identify the knowledge, templates and also different rules [16].

IV. EVALUATION AND EXPERIMENTAL DATA

The works done in this field are based on some famous data sets. From these sets, three of them has the most similarity; therefore; briefly we will talk about them in follows:

ArgoUML: it is an open source tool for UML modeling. It contains 1430 classes and 124,000 lines of code. For this tool, a total of 163 test classes by JUnit has been written for it. These 163 classes contain 12000 code lines.

Apache Ant: it is a Java library and a command-line tool which has the duty of delivering files of the construction

project. This library contains 851 classes and 108,000 code lines. JUnit writes it a total of 201 test classes for it. These 201 classes include 17000 code lines.

Dependency Finder: it is a set of tool for evaluating and analyzing compiled code in Java language. The kit also contains 498 classes and 29,000 code lines. A total of 193 classes by JUnit is written for it. These 193 classes provide 20,000 code lines.

TABLE II: Characteristics of the Experimented System

Datasets	Source Class (Number)	Test Class (Number)	Links (Number)
Apache Ant	871	75	77
ArgoUML	1424	75	80
Dependency Finder	336	120	96

The results were evaluated by two metrics. Typically, two metric tools called Precision and Recall are used.

The *Recall* is the percent of the correct links found by the proposed algorithm to measure. *Precision* is the accuracy which measures the retrieved candidate list of links.

In this paper, we used the set of test or those samples which are unseen data. The files in phase A cannot be detected. The test file is a subset of data that evaluates the probability of performance of a future model.

Table III shows the number of distinguishable files from phase A on the entire data set separately.

TABLE III: Number of Detected and Undetected Links using Naming Convention Technique

Datasets	Detected	Undetected
Apache Ant	65	12
ArgoUML	62	18
Dependency Finder	67	29

The table IV shows the values obtained from the proposed method of this paper using the Logistic Regression on three data sets; moreover, it shows the results obtained from it using the recall and precision metrics.

TABLE IV: Accuracy of the Proposed System on 3 Open Source Datasets

Code Class To Test Class		
Algorithm	Recall	Precision
Apache ANT	0.94	0.94
ArgoUML	0.88	0.92
Dependency Finder	0.84	0.98

In figure 2, the top line graph shows the results obtained from the Logistic Regression algorithm on all three introduced data set. The first point for each data set indicates Recall, the second point represents Precision and the third point of each data set represents the F-measure.

Figure 3 using the bar graph shows the superiority of the proposed method on the datasets of Apache ANT, ArgoUML and Dependency Finder by SCOTCH+ proposed by Qusef in 2014.

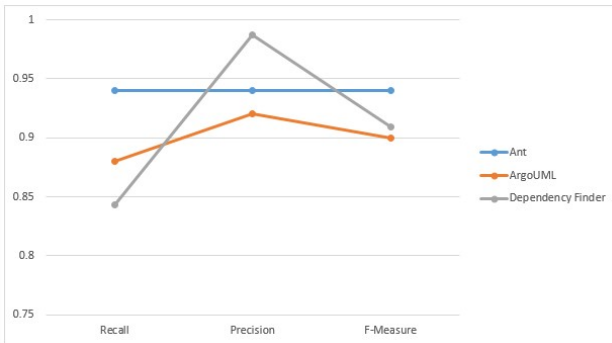


Fig. 2: Accuracy metrics of experimented system

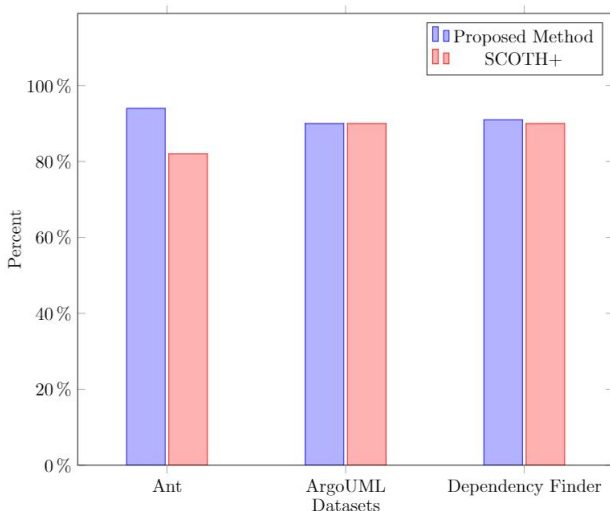


Fig. 3: Comparison proposed method with SCOTCH+ method

V. CONCLUSION AND FUTURE WORK

Recently, several techniques have been provided for identifying the links between test classes and classes under the test. In this paper, we try to not only investigate the available algorithm and guidelines but also propose a method to discover the hidden links and track the correlation between software codes by the test classes. The aim of this paper is to propose a method based on the similarity of the names and packages of a class and also feature extraction from the source code and test classes as well as using data mining techniques to discover hidden relationships between software codes class and test classes. Finally, we compared the proposed method with the available methods. The results show the acceptable performance of the proposed method. Discovering these relationships will help programmers to perform the Regression Test more efficiently.

For future works, it could be possible to use feature selection algorithms to extract features with higher impact on the classes. Afterward, it is recommended to weight the features to reach the new results and compare with the previous results.

REFERENCES

- [1] H. M. Sneed, *Reverse engineering of test cases for selective regression testing*, in Eighth European Conference on Software Maintenance and Reengineering, 2004. CSMR 2004. Proceedings, 2004, pp. 6974.
- [2] P. Bouillon, J. Krinke, N. Meyer, and F. Steimann, *EzUnit: A Framework for Associating Failed Unit Tests with Potential Programming Errors*, in Agile Processes in Software Engineering and Extreme Programming, G. Concas, E. Damiani, M. Scotto, and G. Succi, Eds. Springer Berlin Heidelberg, 2007, pp. 101104.
- [3] M. Bruntink and A. van Deursen, *Predicting class testability using object-oriented metrics*, in Fourth IEEE International Workshop on Source Code Analysis and Manipulation, 2004, 2004, pp. 136145.
- [4] X. Ren, F. Shah, F. Tip, B. G. Ryder, and O. Chesley, *Chianti: A Tool for Change Impact Analysis of Java Programs*, in Proceedings of the 19th Annual ACM SIGPLAN Conference on Object-oriented Programming, Systems, Languages, and Applications, New York, NY, USA, 2004, pp. 432448.
- [5] V. Hurdugaci and A. Zaidman, *Aiding Software Developers to Maintain Developer Tests*, in 2012 16th European Conference on Software Maintenance and Reengineering (CSMR), 2012, pp. 1120.
- [6] B. Van Rompaey and S. Demeyer, *Establishing Traceability Links between Unit Test Cases and Units under Test*, in 13th European Conference on Software Maintenance and Reengineering, 2009. CSMR 09, 2009, pp. 209218.
- [7] S. M. Fakhrahamd, A. R. Rezapour, M. Zolghadri Jahromi, and M. H. Sadreddini, *A novel approach to machine translation: A proposed language-independent system based on deductive schemes*, Iranian Journal of Science and Technology. Transactions of Electrical Engineering, vol. 38, no. E1, p. 59, 2014.
- [8] S. Deerwester, S. T. Dumais, G. W. Furnas, T. K. Landauer, and R. Harshman, *Indexing by latent semantic analysis*, J. Am. Soc. Inf. Sci., vol. 41, no. 6, pp. 391407, Sep. 1990.
- [9] *IEEE Xplore Abstract - Recovering traceability links between unit tests and classes under test: An improved method*. [Online]. Available: <http://ieeexplore.ieee.org/xpl/articleDetails.jsp?arnumber=5609581>. [Accessed: 10-Nov-2015].
- [10] A. Qusef, G. Bavota, R. Oliveto, A. De Lucia, and D. Binkley, *SCOTCH: Test-to-code traceability using slicing and conceptual coupling*, in 2011 27th IEEE International Conference on Software Maintenance (ICSM), 2011, pp. 6372.
- [11] A. Qusef, G. Bavota, R. Oliveto, A. De Lucia, and D. Binkley, *Recovering test-to-code traceability using slicing and textual analysis*, J. Syst. Softw., vol. 88, pp. 147168, 2014.
- [12] M. Halstead, Elements of Software Science, Amsterdam: Elsevier North-Holland, 1977.
- [13] Thomas J. McCabe, *A complexity measure*, IEEE Transactions on software Engineering, vol. 4, pp. 308-320, 1976.
- [14] P. Lucas, *Expert Knowledge and its Role in Learning Bayesian Networks*, Medicine: an Appraisal, Lecture Notes in Artificial Intelligence 2101, pp. 156-166, 2001.
- [15] Xiao, Yuping, M. P. Griffin, D. E. Lake and J. R. Moorman, *Nearest-neighbor and logistic regression analyses of clinical and heart rate characteristics in the early diagnosis of neonatal sepsis*, Medical Decision Making, vol. 30, no. 2, pp. 258-266, 2010.
- [16] Cao, Yongqiang and J. Wu, *Dynamics of projective adaptive resonance theory model: The foundation of PART algorithm*, Neural Networks, IEEE Transactions on , vol. 15, no. 2, pp. 245-260, 2004.
- [17] J. Tahmoresnezhad and S. Hashemi, *A generalized kernel-based random k-samplesets method for transfer learning*, Iranian Journal of Science and Technology. Transactions of Electrical Engineering, vol 39, p. 193-207, 2015.

Software Requirements Conflict Identification: Review and Recommendations

Maysoon Aldekhail
College of Computer and
Information Sciences
King Saud University

Azzeddine Chikh
College of Computer and
Information Sciences
King Saud University

Djamal Ziani
College of Computer and
Information Sciences
King Saud University

Abstract—Successful development of software systems requires a set of complete, consistent and clear requirements. A wide range of different stakeholders with various needs and backgrounds participate in the requirements engineering process. Accordingly, it is difficult to completely satisfy the requirements of each and every stakeholder. It is the requirements engineer's job to trade-off stakeholders' needs with the project resources and constraints. Many studies assert that failure in understanding and managing requirements in general, and requirement conflicts in particular, are one of the main problems of exceeding cost and allocated time which in turn results in project failure.

This paper aims at investigating the different reasons of requirements conflicts and the different types of requirements conflicts. It providing an overview of existing research works on identifying conflicts; and discussing their limitations in order to yield suggestions for improvement.

Objective: To provide an overview of existing research studies on identifying software requirements conflict and identifying limitations and areas for improvement.

Method: A comparative literature was conducted by assessing 20 studies dated from 2001 to 2014.

Keywords—software requirements; requirements engineering; requirements conflicts

I. INTRODUCTION

In requirement engineering, the term conflict involves interference, interdependency or inconsistency between requirements [1].

Different studies state that failure in managing requirement conflicts is one of the main reasons for failure in software projects which is caused by cost and lack of time [2]. It is essential to detect and resolve conflicts in early phases of the project lifecycle to prevent re-iterations of all phases [3]. In recent research studies, a high number of conflicting requirements is stated as in [4], n^2 conflicts are reported in n requirements, whereas [5] reported 40%-60% of requirements were in conflict, In addition, the functional and nonfunctional requirements were both found to be equal in the percentage of conflicts.

Also, most research has shown the risks of working with requirements that are in conflicts with other requirements. These risks are overtime or over budget which can lead to project failure. At the very least, it would result in extra effort expended.

The remainder of the paper is organized as follows: section II gives an overview about requirements conflict, the

different reasons for requirements conflict and the different types of requirements conflict. Section III presents in details the existing techniques for requirements conflict and a comparison between them. Then, section IV, discusses the limitation and research gaps in previous works and gives some recommendations should be taken into consideration when working to find practical techniques for detecting conflict between requirements. Finally, a conclusion of the review is giving.

II. REQUIREMENTS CONFLICT

This section explains the meaning of requirements conflicts, the different reasons that may cause conflict between requirements and the different types of requirements conflicts.

A. Definition of Requirements Conflict

Conflicting requirements is a problem that occurs when a requirement is inconsistent with another requirement [7]. Consistency between requirements requires no two or more requirements contradict each other [8]. In requirements engineering, the term conflict involves interference, interdependency or inconsistency between requirements [1].

Kim et al. [9] gave a good definition of requirements conflict as:

"The interactions and dependencies between requirements that can lead to negative or undesired operation of the system"
An example of a conflict in nonfunctional requirements can be the gap between performance and security; when the client wants certain functionality to be satisfied in minimal time (e.g. calculate something and display it on screen), as well as the use of a secure protocol for data transferee and double password access control.

B. Causes of Requirements Conflict

There are different reasons that cause conflicts between stakeholders' requirements. One good categorization for conflicts reasons is presented in [10]; it classifies the reasons into technical reasons and social reasons. Technical reasons are caused by the following difficulties:

- Massive quantity of requirements can lead to conflicts between them.
- Changes in requirements during system development phases. These changing may occur after the addition of new requirements or the update of old ones [14].

- Complex system domain can lead to misunderstanding of requirements, and therefore, conflicts between them.

Whereas, the social difficulties that lead to requirements conflicts are as follows:

- System has different stakeholders with diverse interests that usually interact with each other and causes conflicts.
- Changes in the system's stakeholders by adding new stakeholders with different needs or by changing stakeholders' requests.

Therefore, there are different sources for inconsistencies between requirements and these may cause problems in the success of the software development. Researchers have been working to find various solutions for this problem.

C. Types of Requirements Conflict

The literature review has shown that there are no predefined classifications for conflicts in requirements. Each work provides a different classification for the conflicts after its found based on the technique used to detect conflicts.

Poort and de With [15] grouped functional requirements based on nonfunctional requirements; this means finding all primary function requirements that share similar nonfunctional requirements and grouping them together. Then two types of conflicts are defined: grouping conflicts which caused by differences in grouping of functions and in-group conflicts that have conflicting requirements within one function group. For example, there are three function groups called workflow, data entry and analysis. For data entry and analysis, security requirements are more restrictive than in the workflow group. Whereas, modifiability for analysis are more stringent than those for data entry and work flow.

Sadana and Liu [16] analyzed functional and nonfunctional requirements and built functionality and quality attributed to hierarchy. Then, two types of conflict in NFR are defined based on comparison of all the lowest level NFRs, if there is still a conflict detected among the NFR. These types are mutually exclusive and partial conflicts. Mutually exclusive conflicts as follows: NFRs A, B are mutually exclusive conflicts if all the lowest level requirements in NFR A have a conflict with the lowest level requirements in NFR B. Partial conflicts as follows: NFRs A, B are in partial conflicts if some of the lowest level requirements in NFR A have a conflict with the lowest level requirements in NFR B.

Heng and Ming [17] defined three types of inconsistent requirements based on multi-coordinated views on requirements. This is common when one stakeholder has an incomplete requirement while others have complete requirements. This creates a situation where requirements overlap when one part of processes in set A is overlapped with another but not fully overlapped, as well as totally disjointed requirements when two views on requirements are totally disjointed.

Butt et al. [2] defined different conflicts based on the classification of the requirements to mandatory, essential and optional. Mandatory requirements are a set of functional and

nonfunctional requirements. Essential requirements are the constraints of the mandatory requirements. Whereas optional requirements are the requirements that if they have conflicts, this would not affect the acceptance of the system. For example, in a hostel management system for a university:

- The system should allow the warden to assign student a seat in his hostel (Mandatory requirement).
- The system should maintain a log of all allotments and vacations in his hostel (Essential requirement).
- The system should allow the warden to shuffle multiple students seats (Optional requirement).

Kim et al. [9] defined two types of requirement conflicts depending on the cause of the conflict and the authoring structure, which is action (verb) + object (object) + resource (resource):

- Source conflict when two requirements use the same resource.

For example, with cellular phones, when a phone call is made from a number that should not answered , the *automatic response function* will try to answer the phone call while the *reception refusal function* will be forced not to answer the call.

- Activity conflict either by opposite verb (verb (different) +object (same)) or by different object (verb (same) +object (different)).

For example, a fire control function is required with an intrusion control function in the home integration system. When those two functions are executed simultaneously, they will try to send messages (fire message and intrusion message) using the same resource (telephone service) at the same time, which will lead to a resource conflict.

Moser et al. [13] [18] defined three types of conflicts that could be detected: conflict between a requirement and a constraint (CRC), conflict between a requirement and a guideline (CRG), and conflict between requirements (CRR). They also gave two classifications for conflicts based on the number of requirements, simple conflicts (between two requirements), and complex conflicts (between three or more).

Urbieta et al. [19] [20] defined three types of conflicts on Web application:

- Structural conflicts: Which means the difference in the data is expected to be presented on a Web page by different stakeholders
- Navigational conflicts: This occurs when two Web application requirements may contradict the way in which links are traversed which in turn produces navigational conflicts; that is, having two targets go to a single source.
- Semantic conflicts: this happens when the same real-world object is described using different terms.

Chentouf [21] defined seven types of conflicts:

- 1) Duplicated requirements: If two requirements are exactly the same or one is included in the other.

- 2) Incompatible requirements: If two requirements are either ambiguous, incompatible or contradictory.
 - a) Two operation frequencies: when the same agent is required to perform the same operation on the same object, but at two different frequencies.
 - b) Start-forbid: when the same event causes the same operation to be performed and forbidden.
 - c) Forbid-stop: when the same operation is stopped under a certain condition event and at the same time, is unconditionally forbidden in another requirement.
 - d) Two condition events: when the same operation is being executed, stopped or forbidden on two different events.
- 3) Assumption alteration: when the output of one requirements' operation is part of the inputs (assumptions) or outputs (results) of the other's operation.
 - a) Input-output: When one of the requirements performs its operation on an object (output) that is an input in other requirements.
 - b) Out-put: This happens if one requirement alters the result (output) or part of another requirement.

Mairiza and Zowghi [21] explained the different categories of conflicts in NFRs as:

- Absolute conflict: represents a pair of NFRs types that are always in conflict.
For example, security and performance, availability and privacy.
- Relative conflict: represents a pair of NFRs that are claimed to be in conflict in some cases but not in all.
For example, usability and security, usability and performance.
- Never conflict: represents a pair of NFRs types that in the software projects are never inconflict. They may contribute either positively through support or cooperation, or may be indifferent to one another.
For example, accuracy and security, usability and maintainability.

In general, we can give general classifications to requirements conflicts based on the types of requirements, functional requirements and nonfunctional requirements. An example for conflicts in nonfunctional requirements is security (privacy metric) with usability (ease of function learning metric) so there is a tradeoff between them. Then the developer must choose a satisfactory solution to find the right balance of attributes that work. Another example is:

- R1: After three continues failed login attempts, the account would be locked by the system.
- R2: Once the account is locked, the system sends an account lock notification email to the account's owner.
- R3: Once an account is locked, the system would also send a SMS message to the account's owner to notify him about the situation owner.

- R4: If a user has already received a notification via email, he will not receive the same notification via SMS.
- There is a conflict between R2, R3 and R4.

Another good classification for requirements conflicts is the one illustrated in [21].

III. REQUIREMENT CONFLICT IDENTIFICATION TECHNIQUES

Owing to the importance of accurate and complete requirements, researchers have tried to identify detection techniques and proposed solutions for requirements conflicts.

This section discusses the different existing detection techniques and their categorization. In the end, a comparison and analysis of the techniques is summarized in a table.

The techniques proposed can have different classifications; the easiest classification is the negotiation or automation techniques. In negotiation techniques, stakeholders and software engineers manually discuss and analyze requirements to detect any conflicts [13]. Some call this approach an informal technique that can be achieved by hiring experts to detect inconsistencies using their experience [22]. This method has some disadvantages because it may take a long time and much effort to negotiate between different stakeholders. Additionally, hiring experts can be very expensive and leave the process to be prone to errors. While in automation approaches, software engineers can use some tools to help with analyzing and managing requirements [13].

In [6], three approaches are proposed to detect requirements conflicts. The ontological approach which uses ontology to extract conflicts between terms and then, between requirements. The methodological approach compares requirement representations to find conflicts and resolve them. The technological approach provides a specific technique or automation to detect potential conflicts.

Methodological approach is almost the same as the negotiation approach since both are manual processes and depend on human efforts. Additionally, technological approach is similar to the automation technique since they both utilize tools to solve problem of requirements conflicts.

Another classification of current detection approaches are formalization-based approaches, model-based approaches and stakeholder priority approaches [23]. The formalization-based approaches use formal specifications for requirements to support seeking conflicts between them. The drawbacks of this approach are the time and effort needed to formalize the requirements and any mistake that could occur during the formalization may lead to incorrect conflict detection. The model-based approach structures the requirements into specific models before conflict identification. If the approach uses a model that is already used in the system then developing it is fine; however, if it uses a different model, this will create additional steps and therefore, extra time and effort. The third approach depends on the stakeholders' discussion and the stakeholders preferences.

A. Existing Techniques

Literature shows that requirements engineering is one of the most active research fields in the recent years. Researchers are continuously working to improve requirements quality and to resolve difficulties that may affect requirements wholeness or accuracy. One of the most common problems is requirements conflicts, and because of the importance of this topic as mentioned in section B, many works have presented different techniques to detect and resolve conflicts between requirements.

This section discusses these techniques, which can be placed in three categories:

- 1) Manual techniques done manually by requirement engineers.
- 2) Automatic techniques applied automatically using software tools.
- 3) General framework, to detect conflicts without using special techniques.

The different techniques are presented in ascending order based on their dates.

1) *Manual*: Most of the proposed methods are performed manually with software engineers and with help of stakeholders. Heisel and Souquierers [3] presented a heuristic algorithm to detect feature interactions in requirements. The algorithm uses the schematic versions for formalized requirements and consists of two parts, precondition interaction analysis to determine any two requirements where both might be applied. Then postcondition interaction analysis to determine the candidate incompatible requirements. As the algorithm is named ‘heuristic’, the candidates need to check with the software engineers and stakeholders to determine if they are actual conflicts or not.

Robinson [6] used a root requirements analysis to detect requirements interactions. The technique is composed of three procedures. First, rewrite the requirements in structure form. Then, produce the root requirements hierarchies. Finally, analyze the root requirements to determine the ordering of the requirements according to their degree of expected conflict. The case study result demonstrated that using root requirement analysis is more accurate and detects more conflicts than without using root analysis.

Poort and de With [15] presented a non-functional decomposition (NFD) model that gives a new classification for requirements. Primary functional requirements and supplementary requirements which is classified as secondary functional requirements, quality attribute requirements and implementation requirements.

The technique defined two types of conflict: grouping conflict caused by differences in grouping of functions and in-group conflicts when conflict happen within one function group. To solve in-group conflicts, requirements will be split into different functions. The new functions will be included in other function groups. This process will repeat until there is no in-group conflict found.

Sadana and Liu [16] have proposed a framework to analyze the conflicts among nonfunctional requirements using the integrated analysis of functional and non-functional requirements.

The conflict detection is performed on the high level NFR based on the relationship between quality attributes, constraints and functionality. The FR and NFR hierarchy are built and integrated to produce high level NFR.

The conflict detection in NFRs is based on relationship among ISO 9126 quality attributes. Two types of conflict in NFR are defined mutually exclusive and partial conflict.

Liu [13] utilized an ontological approach to analyze conflicts in the requirements specification of activity diagrams. The requirements conflict process starts by building an action state ontology and drawing the activity diagram for existing requirements. Then, it detects the requirements conflict based on seven proposed rules: shortcut conflict, initial state conflict, final state conflict, sequence conflict, action state addition conflict, action state deletion conflict and process length conflict.

Heng and Ming [17] proposed a non-mathematical technique called multi-coordinated views that showing different views of multiple stakeholders. The methods used for displaying the different views are color and size. Three types of inconsistent requirements can be found, when one stakeholder has incomplete requirement while other stakeholder has more complete requirement, fully overlapping requirements, and totally disjointed requirements. The conflict resolving is done through agent communication protocol like JADE with ACL.

Mairiza and Zowghi [5] proposed an ontological framework (sureCM) to manage the conflicts between security and usability requirements. The output of the system are lists of conflicts, nature of the conflict based on the impact of the conflicts against different components in software development, and conflict resolution strategy.

Butt et al. [2] proposed a Mandatory, Essential and Optional (MEO-strategy) for requirement conflict resolution. The strategy defined three types of requirements: mandatory requirements, essential requirements and optional requirements.

The output of the framework is a requirement matrix contains the conflicting requirements if any and the suggested solution time. Prevention for mandatory, detection and removal for essential and containment for optional requirements. A case study result shows that the users’ acceptance test for system performance, quality and conformity to user needs was achieved successfully.

Mairiza et al. [11] applied an experimental approach to design a framework that manage the relative conflicts among NFRs. A suitable exterminate is designed to apply the metric and measure of the NFRs with the functionality of the system and how to implement the functionality (operationalization). The result of the experiment is the satisfaction level of NFRs in the system. A two dimensional conflict relationship graph is created to determine if there is a conflict between the two NFRs and the severity of any existing conflicts, means is it a strong or weak conflicts depend on the shape of the graph.

Moreover, Mairiza et al. [24] proposed a novel idea of utilizing TOPIS (Technique for Order of Preference by Similarity to Ideal Solution) to resolve nonfunctional requirements conflicts. TOPIS is a goal-based technique for finding the alternative that is nearest to the ideal solution.

The framework takes a two-dimensional graph that shows the relationship between two NFRs. Then, a decision matrix is constructed based on the graph. The technique calculate the distance to each alternative to the ideal solution and choose the closed one, it is the solution that maximize both NFRs. Alebrahim et al. [25] presented a structural method to detect candidate requirements interaction between functional requirements. The proposed method consists of three phases. The first phase is to remove any conflicts after analyzing problem diagrams. In the second phase, the set of candidates conflict requirements are reduced using the information if requirements have to be accomplished in parallel or not. In last phase, the candidates conflict set are reduced by checking if combination of their precondition is fulfilled. A real life example was studied and the results show that the number of possible interactions was decreased and thus, the time for looking into requirements interactions decrease by 95%. The precision was 33% and a perfect recall with 100%.

2) *Automatic*: The word ‘automatic’ intended using some tools to analyze and detect the requirements conflicts instead of doing that manually.

Egyed and Grunbacher [26] used an automated traceability techniques to eliminate false conflicts and cooperation. The approach automatically analyzing the requirements to identify requirements that conflict based on their attributes, attributes might be indifferent to one another, cooperative or conflicting. Then, the trace analyzer automatically identifies the trace dependencies among the requirements. Based on the knowledge of trace dependencies, the system can determine to what extent the requirements are overlapping. If two requirements overlap, then the two requirement are conflicts. Whereas if there is no overlap between them, they can’t be conflicts.

Kim et al. [9] presented a systematic process to detect and manage requirement conflicts based on requirements partition in natural language. A supporting tool (RECOMA) has been built and two types of conflicts are defined, source conflict and activity conflict. The requirement conflict detection is done through two steps. First, a syntactic method automatically identifies the candidate conflict requirements. Then, the semantic method is used to find the actual requirements conflicts through questions list. By automated a syntactic analysis, the number of requirements to be semantically comparison are reduced. Two cases studies are presented and the results demonstrate that comparison requirements dramatically reduced, and thus the time and effort are decreased.

Kamalrudin et al. [8] explained how to use tractability approach to manage the consistency between textual requirements, abstract interactions and Essential Use Cases (EUCs). An automated tracing tool (Marama AI) is built to help users extract abstract interaction from the textual requirements, mapping the type of interaction and creating the EUC model. It supports traceability and inconsistency checking between the three forms. An experiment results show that 94% of the participants were agree that it is useful and all were say it is user friendly and easy to use.

Moser et al.[13], [18] proposed an automatic semantic based approach for requirements conflict detection. The proposed solution consists of two main phases. First step is to link requirements written in natural language to semantic concepts

to build the project ontology. Then the requirements will automatically and semantically analyzed to identify possible conflicts using sets of assertions that should be true for all existing facts.

They defined three types of conflicts that could be detected: conflict between a requirement and a constraint (CRC), conflict between a requirement and a guideline (CRG) and conflict between requirements (CRR).The evaluation results show that the prototype tool (OntRep) found all conflicts while manual conflict analysis found 30% - 80% of the conflicts. Also, the correctness of the proposed approach is 100% compared to 58.8 of false positive in manual analysis.

While Urbieto et al. [19], [20] proposed a model-driven approach to detect requirement conflicts in Web applications in early stage of software development. The approach starts automatically listing the candidate structural and navigational conflicts by structural analysis using the Navigational Development Techniques (NDT) model. Then semantic analysis on requirements is formalized using Domain Specific Language (DSL) for candidate conflicts to avoid false positives which are conflicts that are actually not in conflict.

Resolving conflicts will be done manually using the proposed conciliation rules or by stakeholders’ negotiations. Compared to manual approach, the evaluation shows that system detects 100% of inconsistencies and the time is reduced by 78% which saves 44% of budget.

Nguyen et al. [27] proposed Knowledge Based Requirements Engineering (KBRE) framework. The domain knowledge and semantics of requirements are centralized using ontology and the requirements goal graph is used to detect requirements inconsistencies and overlaps. The explanation for each detected requirements is provided automatically. The case study shows the performance of the system is satisfactory by calculating the running time to detect inconsistencies and precision of detecting inconsistent requirements.

Chentouf [21] presented a solution to OAM&P (Operation, Administration, Management and Provisioning) requirements conflicts.. The proposed method used an Extended Backus-Naur Form (EBNF) as representation language for requirements. The system automatically validates each requirement statement based on validation rules. Then it compares every pair of requirement to detect conflicts according to the seven conflict inference rules. Seven types of conflicts were defined and a proposed solution for each type was presented. To test the scalability, results show that the proposed solution gives an acceptable computation time less than a minute for more than 10,1000 requirements. Also, it scales very well as the number of requirements increase.

3) *General Framework*: Some works can’t be classified as manual or automatic techniques. Thus, they are only considered as general frameworks to detect the conflicts between requirements.

Shehatam et al. [22] proposed a three-level interaction detection framework (DRI-3). Level-1 uses informal approaches to detect accurate and domain known interaction with the help of experts, Level-2 Identifies requirements interaction using semi-formal, semi-formal means systematic steps without formalized methods. Level-3 applies formal approaches to detect

accurate interaction.

Additionally, the paper presented a set of guidelines describing which techniques from (DRI-3) can be used based on the values of different attributes of project. A case study is carried to evaluate the efficiency of using the model comparing to experts without applying the model. The results show that the number of comparison requirements is decreased by 18%.

Mairiza and Zowghi [28] demonstrated the results of the investigation of research on NFRs conflicts that resulted in a catalogue of conflicts among NFRs. The catalogue is a two-dimensional matrix that represents the interrelationships among twenty types of NFRs.

It shows three categories of relative conflicts between the NFRs, absolute conflicts for NFRs that are always in conflict, relative conflict for pair of NFRs that are sometimes conflicted and not conflict for NFRs that never conflict in the literature of NFRs conflict studies.

B. Comparing between Existing Works

This section analyzes and summarizes the comparison between different techniques to provide a general and quick review on the works done in this area.

To offer better understanding and analysis of existing techniques, they will be classified into different categories as shown in figure 1, categorization is based as follows:

- The first classification is based on the conflict identification method, whether it is done manually by the requirement engineers or automatically using software tools. A class of general frameworks is added to classify some works that detect conflicts without using special techniques.
- The second classification is focused on the type of requirements that the technique will be applied to: functional or nonfunctional requirements.
- The third classification is to determine the scope of the proposed approach to examine if it covers the detection problem, detection and analysis of the conflicts requirements to organize them into different conflict types, and if the proposed approach offers a resolving technique.
- The last classification is based on the representation type for requirements used. If the detection technique uses a specific formalization form, it structures the requirements in a particular model, or it uses an ontology.

Table I summarizes previous works listed by reference number for the research, conflict analysis approach used in identifying conflicts, and category of proposed methods (manually, automatic or just a general framework). It also states the type of requirements the technique is applied to and what is the scope of the technique (i.e. identify, analyze, resolve). It also determines what representation was used to complete or facilitate the technique (formalization, structure model or ontology). The last column indicates whether the proposed technique was supported by evaluation or not. For example, the first row corresponds to a manual technique that

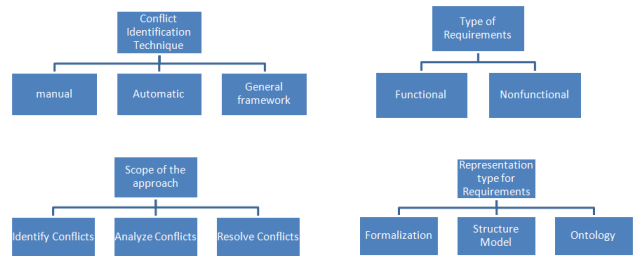


Fig. 1. Categorization of existing techniques for requirements conflicts

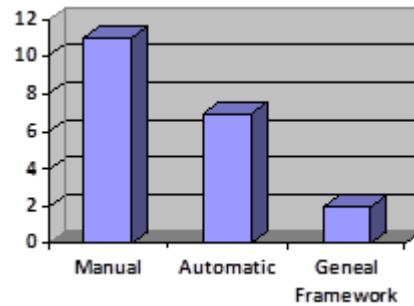


Fig. 2. Analysis results based on identification method

uses a heuristic algorithm to detect functional requirements conflicts and uses schematic versions as formalization form for requirements representation.

The previous works that were studied include 20 papers; these papers are the ones that have a close association with the problem of requirement conflicts. They have proposed different approaches for conflict analysis and detection. For automatic techniques, the conflict analysis approach can be classified into the following four groups: (1) semantic approach for technique that use ontology like [13], [18]; (2) syntax approach when a syntax analysis is done for requirement specification like [9]; (3) graphical analysis when a specific model used like [20], [19], [27]; and (4) tractability approach when tractability technique is used like [26], [8].

The main classification shows that twelve of the works (more than half of them) are manual techniques performed by software engineers whereas only seven are automated tools that help them to find conflicts in requirements, see figure 2.

The analysis of the works as shown in figure 3 demonstrates that eleven of the twenty works work on functional requirements and only six for nonfunctional requirements while there are three works for both of them.

The scope of the proposed solutions was different. As figure 4 shown, almost all research focus on the problem of identifying conflicts, while thirteen of them analyze the conflicts to give different classifications for the conflicts. Only five research studies give guidelines and proposed resolving approaches.

Most techniques used different representation for the requirements to help in analysis and identification of conflicts. Figure 5 indicates that the representation methods used can be divided to three types: either using ontology if the technique using semantic analysis for the requirements like [5], [27],

TABLE I. COMPARISON BETWEEN EXISTING WORKS IN REQUIREMENTS

Reference	Conflict Analysis Approach	Conflict Identification Method	Type of Requirements	Scope of the Approach	Requirement Representation	Evaluation
[3]	Heuristic algorithm	Manual	Functional	Identify	Formalization (schematic versions)	
[6]	Root requirements analysis	Manual	Functional Nonfunctional	Identify Analyze(different degree of conflicts)	Formalization (structure requirement)	✓
[15]	Nonfunctional decomposition model(NFD)	Manual	Nonfunctional	Identify Analyze(grouping conflicts, in-group conflicts) Resolve		
[16]	Integrated analysis of FRs and NFRs	Manual	Nonfunctional	Identify Analyze(mutually exclusive, partial)	Formalization (two canonical form are developed)	
[29]	Model based in UML activity diagram	Manual	Functional	Identify Analyze(7 types of conflicts)	Structure model (Activity Diagram)	
[17]	Non-mathematical technique	Manual	Functional	Identify Analyze (3 types) Resolve	Formalization (semi-formal ontology driven domain-special requirement language)	
[5]	Ontological framework	Manual	Nonfunctional (security and usability)	Identify Analyze (natural of conflict) Resolve	Ontology	
[2]	MEO-strategy	Manual	Functional Nonfunctional	Identify Analyze (mandatory, essential, optional)		✓
[11]	Experimental approach using NFRs metrics and measures as parameters	Manual	Nonfunctional	Identify Analyze (strong, weak)		
[24]	A goal-based technique (TOPIS)	Manual	Nonfunctional	Resolve		
[30]	Graphical method using problem diagram	Manual	Functional	Identify	Structure model (problem diagram)	✓
[26]	Traceability approach	Automatic	Functional Nonfunctional	Identify		
[9]	Requirements partition in natural language	Automatic	Functional	Identify Analyze (source conflicts, activity conflict)	Formalization	✓
[8]	Tractability approach	Automatic	Functional	Identify	Structure model (EUC)	✓
[13],[18]	Semantic based approach	Automatic	Functional	Identify Analyze (CRC,CRG,CRR)	Ontology	✓
[20],[19]	Graphical method using NDT meta model	Automatic	Functional	Identify Analyze	Formalization(DSL) Structure model(NDT requirement meta model)	✓
[27]	Graphical method using requirement goal graph	Automatic	Functional	Identify Analyze	Ontology Formalization(OWL) Structure model(goal graph)	✓
[21]	Validation rules	Automatic	Functional	Identify Analyze (7 types) Resolving for each type	Formalization	✓
[22]	Three-level interaction detection framework	General framework	Functional	Identify		✓
[28]	Investigation of research on NFRs and build a catalogue of NFRs conflicts	General framework	Nonfunctional	Analyze (absolute, relative, no conflict)		

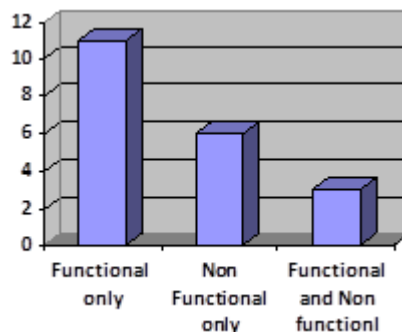


Fig. 3. Analysis results based on type of requirements

[13], [18]; structural model if graphical analysis is used like [20], [19], [8], [29]; or formalization methods which are

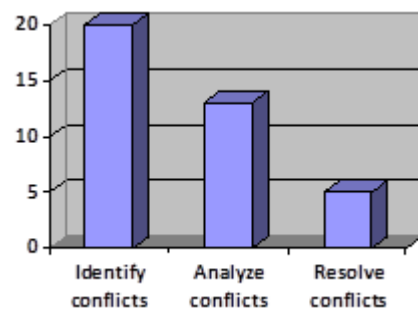


Fig. 4. Analysis results based on scope of the approach

different from schematic version in [3], structure requirements in [6], two canonical forms in [16], semi-formal ontology driven domain-special requirement language in [17], DSL in

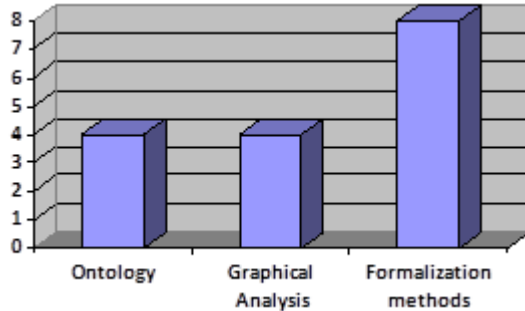


Fig. 5. Analysis results based on requirements representation used

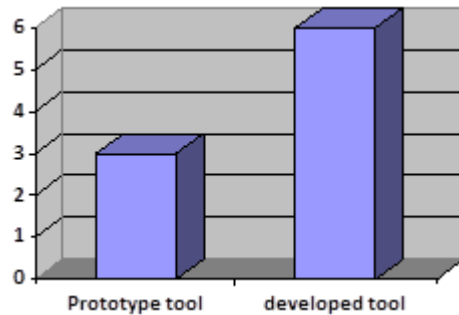


Fig. 6. Analysis results based on type of tool used

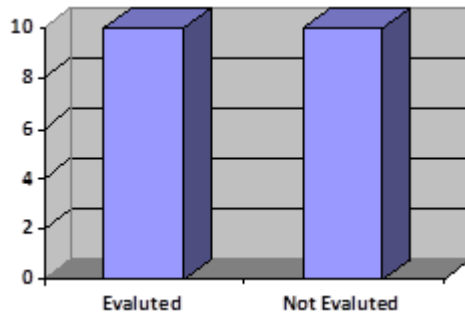


Fig. 7. Analysis results based on if the work is evaluated or not

[20] and [19], OWL in [27], and EBNF in [21]. While some proposed techniques used more than one type of representation like [20], [19] which used ontology and DSL as formalization method, [27] used ontology, OWL as formalization method and goal graph as a structural model.

The tools used in the proposed approaches are either prototype tools like [13], [18], [20], [19], [27]; or developed tools like [26], [9], [8], [21]. [26], [9] developed tracing analysis tools because the conflict analysis approach used is a tractability approach. See figure 6.

Analysis on previous works illustrate that only half of the works were evaluated to test the effectiveness of the proposed method, as shown in figure 7.

According to the importance of evaluation, more analysis was conducted on the evaluated works. Table II summarizes the evaluated works listed by reference number. The second column presents evaluation data that was used to test the

system. The literature illustrates that most works use case studies to test the effectiveness of the proposed method; except for when in two works, one uses a survey and the second uses an experiment. The third column explains the goal of the evaluation. The objectives were differed between the following: assessment of the utility, measuring users' satisfaction, evaluation of the effectiveness, demonstration of the tool feasibility, testing of the usefulness and ease of use, and testing of the completeness and consistence of the proposed method.

The fourth column explains the method used in the evaluation. It is clear that almost all works used the comparison in the number of detected conflicts, the validity of the detected conflicts, and the cost when using the proposed method without using any specific approach. Finally, the evaluation results are presented in the last column.

IV. DISCUSSION

The previous sections have discussed in detail the existing works for detection and managing requirements conflicts. However, the topic is still active for researchers in the field of requirements engineering.

The problem of requirements conflicts can be divided into two main sections: identifying the conflicts in requirements; and resolving them. This paper focused on identifying requirements conflicts. The literature review demonstrated that most techniques that are proposed to decrease risks caused by requirements conflicts are manual techniques while the automated approaches are tools based on human analysis. That may incur costs to the project due to human error and wrong decision making.

There are still many gaps in the previous works in identifying requirements conflicts. Detecting conflicts manually takes a long time and effort which may cause delays in the project. In addition, it is fallible since it is done by human effort. Some conflict techniques have tried to automate the detection process by using or building specific tools. Applying some automation to the process would decrease the human effort and time. However, all the automation approaches are still based on human analysis to detect and resolve conflicts. Also, most techniques are proposed techniques that are not evaluated for their efficiency in detecting and resolving conflicts.

There are some important issues that should be taken into consideration when working to find practical techniques for detecting conflict between requirements. First, define what requirement conflict exactly means and what it includes to find a suitable technique to catch the conflict. Then, determine the type of requirements that the technique will work on and which representation method for requirement specification is the most suitable for use. Also, determine when the technique can be applied and in which phase of software development. As final step, determine how to measure the efficiency of the proposed technique.

V. CONCLUSION

Requirements engineering is a critical part of software development that plays an important role in the software project success. However, there are different issues that may

TABLE II. COMPARISON BETWEEN EVALUATED WORKS

Reference	Evaluation Data	Evaluation Goal	Evaluation Method	Evaluation Results
[6]	Case study: established requirements engineering problem case (Distributed Meeting Scheduler).	Assess the utility.	Compare the number of conflict detection using root analysis and without using it.	Using root analysis technique detects 72 conflicts, while without using it only 9 conflicts is detected.
[2]	Case study: applied MEO-strategy during build (Hostel Management System) as part of university management system.	Measure users' satisfaction.	Conduct a feedback workshop to collect user's feedback.	Users' acceptance test for system performance, quality and conformity to user needs was achieved successfully.
[30]	Case study: proposed approach was used in real life example in domain of (Smart Grids).	Validate the proposed approach.	Compare the number of possible requirements interaction using problem diagram and without using it to measure the effort (time) need to detect the interaction. Measure the precision and the perfect recall using problem domain approach.	The number of possible interactions was decreased and thus, the time for looking into requirements interactions decrease by 95%. The precision was 33% and a perfect recall with 100%.
[9]	Case study: The proposed approach was applied in (Home Integration System (HIS) and (Cellular phone domain).	Demonstrate the tool feasibility.	Compare the total number of comparison to find conflict using the proposed automated tool with the manual approach by developers. Also, compare the time and cost using the two approaches.	The number of comparison using manual approach in His is 378 and in cellular phone case is 666. Comparing to 79 and 100 using the automated proposed approach. While the number of comparison is decreases, the time and cost will decreases.
[8]	Survey: with 8 software engineering post-graduate students.	Test the usefulness and ease of use.	Use Likert scale with five part scale to evaluate the usefulness and ease of use of the proposed approach.	Results show that 94% of the participants were agree that it is useful and all were say it is user friendly and easy to use.
[13],[18]	Case study: real-world industrial case study with 6 project managers and requirement expert.	Evaluate the effectiveness	Compare the number of conflicts detected using the proposed method with the manual approach. Also, compare the percentage of correctness in the two approaches.	The prototype tool (OntRep) found all conflicts while manual conflict analysis found 30% - 80% of the conflicts. Also, the correctness of the proposed approach is 100% compared to 58.8 of false positive in manual analysis.
[20],[19]	Experiment: simulation in real environment of Mosaico.	Measure the efficiency and effectiveness.	Calculate the number of inconsistencies detected and the time and the cost is compared to manual approach.	The evaluation shows that system detects 100% of inconsistencies and the time is reduced by 78% which saves 44% of budget.
[27]	Case study: on traveler social networking system.	Evaluate the effectiveness.	Measure the performance of the system in the number and the precision of detecting inconsistencies.	The performance of the system is satisfactory by calculating the running time to detect inconsistencies and precision of detecting inconsistent requirements.
[21]	Proof-of-concept example , simulation test	Test the completeness and consistence To test the scalability.	Use proof-of-concept Compute the computational time for different number of scalability.	The acceptable computation time less than a minute for more than 10,1000 requirements. Also, it scales very well as the number of requirements increase.
[22]	A case study : smart homes domain	Evaluate the efficiency	Compare the number of comparison done by expert if applying the approach without applying it.	The number of comparison requirements is decreased by 18%.

be caused by giving incorrect requirements and therefore, this results in project failure, which is one of the problems in requirements conflict.

The paper provided a literature review on requirements conflict research and analyzed them to show the limitations and gap in previous works. Also, a more detailed analysis was conducted on the works that were evaluated to illustrate the evaluation methods and data used in the previous works. The literature review demonstrated that most techniques that are proposed to decrease the risks and detect requirements conflicts are manual techniques while the automated approaches are tools based on human analysis. That may incur costs to the project due to human error and wrong decision making. Moreover, most of the proposed approaches were not evaluated to measure their efficiency. At the end, important issues were given as general recommendations when proposing requirements conflicts technique.

REFERENCES

- [1] D. Mairiza, D. Zowghi, and N. Nurmuliani, *Managing conflicts among non-functional requirements*, University of Technology, Sydney, 2009.
- [2] W. H. Butt, S. Amjad, and F. Azam, *Requirement Conflicts Resolution: Using Requirement Filtering and Analysis* in Computational Science and Its Applications - ICCSA 2011, B. Murgante, O. Gervasi, A. Iglesias, D. Taniar, and B. O. Apduhan, Eds. Springer Berlin Heidelberg, 2011, pp. 383-397.
- [3] M. Heisel and J. Souquires, *A Heuristic Algorithm to Detect Feature Interactions in Requirements* in Language Constructs for Describing Features, S. G. Bs. (Hons) and M. R. B. MA, Eds. Springer London, 2001, pp. 143-162.
- [4] M. Ramzan, *Intelligent Requirement Prioritization using Fuzzy Logic*, Ph.D., National University of Computer and Emerging sciences, Pakistan, 2010.
- [5] D. Mairiza and D. Zowghi, *An ontological framework to manage the relative conflicts between security and usability requirements* in 2010 Third International Workshop on Managing Requirements Knowledge (MARK), 2010, pp. 1-6.
- [6] W. N. Robinson, *Surfacing Requirements Interactions* in Perspectives on Software Requirements, J. C. S. do P. Leite and J. H. Doorn, Eds. Springer US, 2004, pp. 69-90.
- [7] B. Schr, *Requirements Engineering Process HERMES 5 and SCRUM*, University of Applied Sciences and Arts, Northwestern Switzerland, 2015.
- [8] M. Kamalrudin, J. Grundy, and J. Hosking, *Managing Consistency between Textual Requirements, Abstract Interactions and Essential Use Cases* in Computer Software and Applications Conference (COMPSAC), 2010 IEEE 34th Annual, 2010, pp. 327-336.
- [9] M. Kim, S. Park, V. Sugumaran, and H. Yang, *Managing requirements conflicts in software product lines: A goal and scenario based approach*, Data Knowl. Eng., vol. 61, no. 3, pp. 417-432, Jun. 2007.
- [10] W. N. Robinson, S. D. Pawłowski, and V. Volkov, *Requirements Interaction Management*, ACM Comput Surv, vol. 35, no. 2, pp. 132-190, Jun. 2003.
- [11] D. Mairiza, D. Zowghi, and V. Gervasi, *Conflict characterization and Analysis of Non Functional Requirements: An experimental approach*, in 2013 IEEE 12th International Conference on Intelligent Software Methodologies, Tools and Techniques (SoMeT), 2013, pp. 83-91.

- [12] Hausmann, Jan Hendrik and Heckel, Reiko and Taentzer, Gabi, *Detection of conflicting functional requirements in a use case-driven approach: a static analysis technique based on graph transformation* in Proceedings of the 24th international conference on software engineering, ACM, 2002, pp. 105-115.
- [13] T. Moser, D. Winkler, M. Heindl, and S. Biffl, *Requirements Management with Semantic Technology: An Empirical Study on Automated Requirements Categorization and Conflict Analysis* in Advanced Information Systems Engineering, H. Mouratidis and C. Rolland, Eds. Springer Berlin Heidelberg, 2011, pp. 3-17.
- [14] M. Shehata, A. Eberlein, and A. Fapojuwo, *IRIS: a semi-formal approach for detecting requirements interactions* in Engineering of Computer-Based Systems, 2004. Proceedings. 11th IEEE International Conference and Workshop on the, 2004, pp. 273-281.
- [15] E. R. Poort and P. H. N. de With, *Resolving requirement conflicts through non-functional decomposition* in Fourth Working IEEE/IFIP Conference on Software Architecture, 2004. WICSA 2004. Proceedings, 2004, pp. 145-154.
- [16] V. Sadana and X. F. Liu, *Analysis of Conflicts among Non-Functional Requirements Using Integrated Analysis of Functional and Non-Functional Requirements* in Computer Software and Applications Conference, 2007. COMPSAC 2007. 31st Annual International, 2007, vol. 1, pp. 215-218.
- [17] T. L. Heng and L. T. Ming, *Using multi-coordinated views with agent communication protocol to detect and resolve inconsistent requirements to improve accuracy* in Information Technology (ITSim), 2010 International Symposium in, 2010, vol. 2, pp. 1041-1044.
- [18] T. Moser, D. Winkler, M. Heindl, and S. Biffl, *Automating the detection of complex semantic conflicts between software requirements* in The 23rd International Conference on Software Engineering and Knowledge Engineering, Miami, 2011.
- [19] M. J. Escalona, M. Urbieta, G. Rossi, J. A. Garcia-Garcia, and E. R. Luna, *Detecting Web requirements conflicts and inconsistencies under a model-based perspective*, J. Syst. Softw., vol. 86, no. 12, pp. 3024-3038, Dec. 2013.
- [20] M. Urbieta, M. J. Escalona, E. R. Luna, and G. Rossi, *Detecting Conflicts and Inconsistencies in Web Application Requirements* in Current Trends in Web Engineering, A. Harth and N. Koch, Eds. Springer Berlin Heidelberg, 2012, pp. 278-288.
- [21] Z. Chentouf, *Managing OAM&P requirement conflicts*, J. King Saud Univ. - Comput. Inf. Sci., vol. 26, no. 3, pp. 296-307, Sep. 2014.
- [22] M. Shehata, L. Jiang, and A. Eberlein, *A requirements interaction detection process guide* in Canadian Conference on Electrical and Computer Engineering, 2004, 2004, vol. 3, pp. 1753-1756 Vol.3.
- [23] A. Sardinha, R. Chitchyan, J. Arajo, A. Moreira, and A. Rashid, *Conflict Identification with EA-Analyzer* in Aspect-Oriented Requirements Engineering, A. Moreira, R. Chitchyan, J. Arajo, and A. Rashid, Eds. Springer Berlin Heidelberg, 2013, pp. 209-224.
- [24] D. Mairiza, D. Zowghi, and V. Gervasi, *Utilizing TOPSIS: A Multi Criteria Decision Analysis Technique for Non-Functional Requirements Conflicts* in Requirements Engineering, D. Zowghi and Z. Jin, Eds. Springer Berlin Heidelberg, 2014, pp. 31-44.
- [25] Alebrahim, Azadeh and Faßbender, Stephan and Heisel, Maritta and Meis, Rene, *Problem-based requirements interaction analysis*.
- [26] A. Egyed and P. Grunbacher, *Identifying requirements conflicts and cooperation: how quality attributes and automated traceability can help*, IEEE Softw., vol. 21, no. 6, pp. 50-58, Nov. 2004.
- [27] T. H. Nguyen, B. Q. Vo, M. Lumpe, and J. Grundy, *KBRE: a framework for knowledge-based requirements engineering*, Softw. Qual. J., vol. 22, no. 1, pp. 87-119, Apr. 2013.
- [28] D. Mairiza and D. Zowghi, *Constructing a Catalogue of Conflicts among Non-functional Requirements* in Evaluation of Novel Approaches to Software Engineering, L. A. Maciaszek and P. Loucopoulos, Eds. Springer Berlin Heidelberg, 2011, pp. 31-44.
- [29] C.-L. Liu, *Ontology-Based Requirements Conflicts Analysis in Activity Diagrams* in Computational Science and Its Applications - ICCSA 2009, O. Gervasi, D. Taniar, B. Murgante, A. Lagan, Y. Mun, and M. L. Gavrilova, Eds. Springer Berlin Heidelberg, 2009, pp. 1-12.
- [30] A. Alebrahim, S. Fabender, M. Heisel, and R. Meis, *Problem-Based Requirements Interaction Analysis* in Requirements Engineering: Foundation for Software Quality, C. Salinesi and I. van de Weerd, Eds. Springer International Publishing, 2014, pp. 200-215.
- [31] *How to Deal with Stakeholders Conflicts in Requirements Gathering?*, [Online]. Available: https://www.researchgate.net/post/How_to_deal_with_stakeholders_conflicts_in_requirements_gathering2. [Accessed: 20-Apr-2016].
- [32] *Scope - How Do You Manage Conflicting Stakeholder Demands? - Project Management Stack Exchange*. [Online]. Available: <http://pm.stackexchange.com/questions/1399/how-do-you-manage-conflicting-stakeholder-demands>. [Accessed: 20-Apr-2016].
- [33] *I Have Two Business Stakeholders Who Have Conflicting Requirements - Projectconnections.com*. [Online]. Available: <http://www.projectconnections.com/knowhow/burning-questions/resolving-conflicting-stakeholder-requirements.html>. [Accessed: 20-Apr-2016].
- [34] *Conflicting Requirements*. [Online]. Available: <http://c2.com/cgi/wiki?ConflictingRequirements>. [Accessed: 20-Apr-2016]

Time Emotional Analysis of Arabic Tweets at Multiple Levels

Amr M. Sayed, Samir AbdelRahman, Reem Bahgat and Aly Fahmy
Computer Science Department
Faculty of Computers and Information
Cairo University
Giza, Egypt

Abstract—Sentiment and emotional analyses have recently become effective tools to discover peoples attitudes towards real-life events. While Many corners of the emotional analysis research have been conducted, time emotional analysis at expression and aspect levels is yet to be intensively explored. This paper aims to analyse people emotions from tweets extracted during the Arab Spring and the recent Egyptian Revolution. Analysis is done on tweet, expression and aspect levels. In this research, we only consider surprise, happiness, sadness, and anger emotions in addition to sarcasm expression. We propose a time emotional analysis framework that consists of four components namely annotating tweets, classifying at tweet/expression levels, clustering on some aspects, and analysing the distributions of people emotions, expressions, and aspects over specific time. Our contribution is two-fold. First, our framework effectively analyzes people emotional trends over time, at different fine-granularity levels (tweets, expressions, and aspects) while being easily adaptable to other languages. Second, we developed a lightweight clustering algorithm that utilizes the short length of tweets. On this problem, the developed clustering algorithm achieved higher results compared to state-of-the-art clustering algorithms. Our approach achieved 70.1% F-measure in classification, compared to 85.4% which is the state of the art results on English. Our approach also achieved 61.45% purity in clustering.

Keywords—Emotional Analysis; Sentiment Analysis; Clustering; Two-Step Classification; Time Analysis

I. INTRODUCTION

Nowadays, social media become interactive environments that present people opinions, emotions, and thoughts regarding specific daily events and aspects. Recently, sentiment and emotional analyses have become very effective mining tools to extract potential and accurate on-time information from tweets [1], [2], [3], [4]. Well-known social media researches were developed to classify, extract, or retrieve information at documents, sentences, expressions, aspects, or words according to some sentiments or emotions [5].

In this research, we are interested in the first three years of Arab Spring - Egyptian Revolution and the related human feelings (emotions) namely: surprise, happiness, sadness, anger, and sarcasm emotion. As well, we identified seven main aspects in that period as explained in the Data Collection and Annotation Section. As our main contribution, we propose a framework to analyze people emotional trends through the aforementioned period at different fine-granularity levels of tweets, expressions, and aspects. The framework comprises four main components namely annotating tweets, classifying

at tweet/expression levels, clustering on some aspects, and analyzing the distributions of people emotions, expressions, and aspects over that time period.

In the classification component, we utilized Conditional Random Fields (CRF) and AdaBoostMH classifiers for classifying emotions at tweets and expression levels in which CRF reported better results. In the clustering component, we evaluated K-Nearest Neighbor (K-NN), Expectation Maximization (EM), and Latent Dirichlet Allocation (LDA) to cluster the tweets with respect to the aspects included in this paper. Moreover, we proposed Tweets Lightweight Clustering (TLC) algorithm that utilizes the tweet short-length nature to achieve better performance. TLC resulted in the highest purity and the lowest Kullback–Leibler Divergence in comparison to the mentioned clustering algorithms. In the time and aspect analysis component, we used Bayesian rules to calculate the probability and cumulative distributions of the emotions, aspects, and expressions over time. As well, we used Pointwise Mutual Information (PMI) to measure the dependency between two emotional expressions.

The rest of this paper is organized as follows. In the second section, some main English and Arabic related works are highlighted. The third section covers our framework details. The specifications and analysis of our experiments are described in the fourth section. We finally pinpoint the paper with main conclusion and future work.

II. RELATED WORK

Despite a lot of research have been conducted in English Language, research in Arabic language is considered immature and developing. Further, less attention has been devoted to the emotional analysis area specially on Arabic language. In the following, we summarize the relevant sentiment and emotional analysis research:

Sentiment Analysis: [6] used n-gram to learn SVM classifier at tweet level to classify Egyptian dialect tweets. [7] used a naive Bayesian classifier on Arabic dialect tweets having the best F-measure for positive class. [8] used logistic regression model to build a sentiment classifier to classify English tweets on expression-level. [9] used deep convolutional neural network to classify the polarity of English sentences. [10] used SVM classifier with semantic and syntactic features learnt by multi-dialectal Arabic tweets. [11] used SVM classifier with Arabic lexicons and n-gram for sentiment classification at tweet level as well as aspect level. [12] classified English

brand-related tweets using Dynamic Architecture for Artificial Neural Networks.

Emotional Analysis: [13] used syntactic and lexical features and a Vector Space Model (VSM) to classify limited types of documents into six classes and got the best F-score on the happiness class. also [14] used Naive Bayes, SVM, Hyperpipes and Voting Feature Intervals to classify Arabic poems into four classes. [15] used syntactic feature to train SMO and SVM classifiers to classify Arabic tweets into six classes and got the best F-score on the Fear class. [3] used hash-tags and logistic regression to classify English tweets into five emotions having the best F-measure on the affection class. [16] used SVM and VSM to classify English documents into seven emotions and got the best F-score on fear class.

III. THE PROPOSED TIME EMOTIONAL ANALYSIS FRAMEWORK

In the following, we present the framework classification and clustering components as three paragraphs discussing the extracted features, techniques, and the related evaluation criteria. The time and aspect analysis component is presented as a set of equations used to study distributions of emotions and expressions overtime per aspect. In the rest of this paper, Arabic text is quoted between double quotes of “ ” and its English translation is presented between rectangular brackets [].

A. Data Collection and Annotation

We used Ekman's set of emotions [17] in classification but with some modifications. We considered anger and disgust as one class and the same for sadness and fear. We have also added the sarcasm class to our set of classes due to the high rate of sarcastic expressions in the collected data. We constructed a lexicon of 563 emotional Arabic words from twitter. We manually classified them into emotional words of happiness (41), surprise (173), sadness (66) and anger (44), sarcasm (16), neutral (103), and multi-emotional (120). Examples of the collected words are: “مبسوط” [glad] happiness, “يقولك” [someone said] sarcasm, “استغرب” [Surprised] surprise, “يرحمه” [Bless his soul] sadness, “فأشل” [Unstuck] anger, “نفسي” [I hope] multi-emotional and “حاليس” [I feel] neutral. We collected Arabic tweets written in Egyptian dialect over the period January 1 2011 through December 31 2013. Each collected tweet should have at least one of seven keywords (aspects) presenting influential figures or events in this period. The keywords are namely: “ثورة ٢٥ يناير” [25 Jan Revolution], “ثورة ٣٠ يونيو” [30 June Revolution], “برنامج البرنامج” [El-Bernameg TV Show], “عبد الفتاح السيسي” [Abdel Fatah El-Sisi], “محمد مرسي” [Mohamed Morsi], “حسني مبارك” [Hosni Mubarak], “الأخوان المسلمين” [Muslim Brotherhood]. Tweets were pulled from twitter search engine. Each tweet contained the user-name, the date, and the associated text. We removed any tweet that contained only URLs and the related replicates (if any). As a result of the previous steps, a corpus of 111,413 tweets was built. Based on the mentioned seven keywords or aspects, we had the related clusters of 6886, 2949, 5736, 11698, 17745, 41075, and 44604 tweets respectively. Of note, we may find a tweet replicated in two or more clusters if it has two or more keywords in common. To build the classification

model, 10,177 tweets were selected randomly from that corpus and all words were normalized. Normalization achieved by removing all non-Arabic characters from the text. These tweets were annotated manually by three specialized linguists and also revised by the authors of the paper. It was made of 608, 1361, 3368, 1056, 1688, 207, 1008 tweets from happiness, sarcasm, surprise, sadness, anger, neutral, and multi-emotional classes respectively. To avoid confusion that might occur during the annotation process among annotators, we used the following criteria: (1) The annotator should not involve his personal feelings towards the matter in concern during the annotation process. (2) To consider a tweet for the annotation, it should contain at least one of the following three items: emotional expression, emotional term (LOL, HHHHH, etc...), and/or emotional symbols (:, :, etc...). (3) Any tweet that contains non-Egyptian dialect was discarded. This annotated corpus was used to develop the classification model which was used to automatically annotate the rest of the 111,413 tweets.

The processes of tweets collection and annotations lasted for around six months. Of note, we aim at releasing the data publicly. As well, since our classifier is effective and it was used to annotate unseen data for clustering component in a systematic manner, it will be very effective and doable to annotate any other amount of Egyptian tweets having similar emotions and aspects. Furthermore, the annotation process could be easily extended to include other emotions and aspects.

B. Classification Component

This component aims at enabling the framework to classify the tweet emotions at levels of expressions and tweets.

Classifiers: In the classification component, we used the two-step classification approach adapted from [18]. At the expression level, we built the one-step and the two-step classifiers using Conditional Random Fields and AdaBoostMH baselines for each step. To classify emotions at tweet level, the following criteria were applied: (1) If a tweet has no clue or it has neutral clues only, then it's considered a neutral tweet. (2) If a tweet contains more than one emotional clue from a specific class, it's considered an emotional tweet that holds emotion from that class. (3) If a tweet contains more than one emotional clue from different classes, then it's considered a multi-emotional tweet.

Classification Features: Following [19], we used four types of features groups with adaptation to Arabic language specially Egyptian dialect. For example we used the Egyptian negation words “مش” [not] and “مكاش” [wasn't]. These features are: (1) word features such as the word itself, part-of-speech, prior polarity, strength and a negation checker, (2) modification features that are related to the context in which the word appears to indicate if a word is preceded by adjective, adverb or intensifier and also to indicate if a word modifies or is modified by a subjective clue, (3) tweet features are counters for strong and weak clues in the context in addition to morphological counters, and (4) structure features that consider the tweet structure and the relations among its words extracted from the Stanford parser [20] dependency parse tree.

Evaluation Criteria: In our experiments, 10-fold cross validation criterion was applied. We used three performance measures for the classification evaluation: (1) precision

that is the percentage of the retrieved emotional clues to the relevant ones, (2) **recall** that is the percentage of relevant emotional clues to retrieved ones, and (3) **F-measure** that is a measure of both precision and recall (equation 1).

$$F - \text{measure} = 2 \cdot \frac{\text{precision} \cdot \text{recall}}{\text{precision} + \text{recall}} \quad (1)$$

C. Clustering Component

This component aims at enabling the framework to partition tens thousands of tweets according to their aspects' similarities. This step is necessary to analyze the aspects' features in the subsequent component.

Clustering Techniques: We evaluated three different clustering algorithms namely **K-Nearest Neighbors (K-NN)** as a baseline, **Expectation Maximization (EM)**, and **Latent Dirichlet Allocation (LDA)**. Our evaluation results showed that: (1) They acquired in general fair results for highly overlapping clusters. (2) The resultant clusters' distributions significantly deviated from the gold standard ones. This clustering performance motivated us to use a sort of bi-gram topic model and we named it **Lightweight Clustering (TLC)** in which each cluster is identified by the most frequent uni/bi-gram and the related subsequent 100 co-occurring uni/bi-grams as bag-of-words. The algorithm could be summarized as follows. In step 1, we generate uni-gram and bi-gram with their frequencies (we excluded all possible stop words). In step 2, we select top frequent (m) uni/bi-grams to present (m) clusters such that: (1) each gram presents one cluster, (2) all clusters have no grams in common (e.g., “عبد الفتاح السيسى” and “السيسى” should not be assigned to different clusters), and (3) they co-occur together in > 70% of the tweets. In step 3, we assign each of the subsequent 100 grams to one of the (m) clusters as related bag-of-words such that the candidate gram co-occur with the cluster gram in > 70% of the tweets. In step 4, we assign each tweet to a cluster where at least one of the tweet's grams appears in the corresponding cluster bag-of-words grams. Of note, a tweet could be assigned to more than one cluster. In all algorithms, we used m = 7 presenting the 7 aspects. In addition, the parameters of our algorithm were selected as the best effective thresholds based on extensive experimentations on this corpus.

Clustering Features: We conducted extensive feature evaluation for each clustering algorithm and the following are the best performing features. In K-NN algorithm, we used only the raw text of a tweet as the bag-of-words feature. For EM algorithm, a feature vector of the binary values was used to present the presence/absence of the most frequent uni-gram, bi-gram, and tri-gram in the tweet. The LDA algorithm uses only one type of features which is a pair of word and its frequency in the given tweet. To overcome this limitation, we combined each two/three words with a delimiter (“.”) to present the related bi/tri-gram level in addition to the uni-gram. We used only the most frequent 20 grams as features for EM and LDA algorithms.

Evaluation Criteria: To evaluate the quality of each clustering algorithm, we used the cluster purity that is the

percentage of the most frequent class in that cluster. **Kullback-Leibler Divergence (D_{KL})** was used to compare how close the algorithm generated word distribution in the clusters is to that of the gold standard; the lower the KL-divergence is, the closer to that of gold standard one is. KL-divergence uses the following equation to quantify the difference between two probability distributions A and T, where T presents the true distribution (gold standard) of the clustering data and A presents the algorithm approximation of T.

$$D_{KL}(T||A) = \sum_{i=1}^n T_i \cdot \log\left(\frac{T_i}{A_i}\right) \quad (2)$$

D. Time and Aspect Analysis

This component is important to show a meaningful analysis on tweets using the classification and clustering components. Analysis on tweets was applied at several levels to generate the most useful and important information. To achieve the component goal, the following equations are used:

- Cumulative probability of emotion (E) given a time interval (T) (with start (s) and end (t)) and a specific cluster (C):

$$P(E|C, T) = \sum_{i=s}^t P(E|C, i) \quad (3)$$

- Probability of emotion (E) given set of tweets (S) of specific time (i):

$$P(E|S_i) = \frac{\# \text{ tweets with emotion E in S}}{\# \text{ tweets in S}} \quad (4)$$

- Probability of emotional expression (Ex) given tweets of a specific cluster (C):

$$P(Ex|C) = \frac{\# \text{ tweets with expression Ex in C}}{\# \text{ tweets in C}} \quad (5)$$

- Pointwise mutual information (PMI) which measures the dependency between two emotional expressions Ex_i and Ex_j :

$$PMI(Ex_i, Ex_j) = \frac{P(Ex_i|Ex_j)}{P(Ex_i)} \quad (6)$$

IV. EXPERIMENT RESULTS AND ANALYSIS

A. Classification Experiments

Our experiments were confirmed [18] conclusion that the two-step classifier results were better than those of the one-step one. Table 1-4 list the results of our two-step classifiers. We can see that multi-emotional class has the lowest scores because multi-emotional tweets are rare and not rich in expressions since the maximum length of a tweet is only 140 letters. Sarcasm class achieved the highest scores due to the significant availability of tweets and the clarity of expressions. The presence of some expressions that can be used the same way in sad and angry contexts led to their weak scores. Neutral class achieved poor results due to the use of emotional expressions and emotion symbols by writers in non-emotional contexts.

TABLE I: Two-Step Step(A) Expression-Level Classifiers Results

Model	CRF Classifier			AdaBoostMH Classifier		
Measure	precision	recall	F-measure	precision	recall	F-measure
Emotional	91.3%	78.3%	84.3%	89.4%	99.0%	94.0%
Neutral	88.1%	46.8%	60.9%	49.5%	07.4%	12.9%
Average	89.70%	62.55%	72.60%	69.45%	53.20%	53.45%

TABLE II: Two-Step Step(B) Expression-Level Classifiers Results

Model	CRF Classifier			AdaBoostMH Classifier		
Measure	precision	recall	F-measure	precision	recall	F-measure
happiness	50.8%	52.1%	51.0%	43.0%	35.9%	38.5%
Sarcasm	63.5%	74.9%	68.1%	58.9%	71.6%	64.1%
Surprise	60.7%	57.4%	58.7%	58.0%	59.2%	58.3%
Sadness	64.4%	66.3%	64.6%	61.4%	59.2%	60.0%
Anger	61.2%	52.5%	56.1%	60.3%	49.6%	54.1%
Multi-emotional	00.2%	05.8%	01.0%	00.0%	00.0%	00.0%
Average	50.13%	51.50%	49.92%	46.93%	45.92%	45.83%

TABLE III: Two-Step Step(A) Tweet-Level CRF Classifier Results

Measure	Precision	Recall	F-measure
Emotional	91.20%	84.20%	87.50%
Neutral	27.30%	42.20%	32.50%
Average	59.25%	63.20%	60.00%

TABLE IV: Two-Step Step(B) Tweet-Level CRF Classifier Results

Measure	Precision	Recall	F-measure
happiness	58.1%	43.6%	49.5%
Sarcasm	70.0%	71.6%	70.1%
Surprise	68.4%	53.8%	60.0%
Sadness	70.1%	63.5%	66.0%
Anger	66.1%	45.4%	53.4%
Multi-emotional	5.7%	31.5%	9.3%
Average	56.40%	51.57%	51.38%

B. Clustering Experiments

Table 5 shows the purities of the clustering algorithms in which the highest values are in bold. Our algorithm, TLC, acquired the best purity on average with only one cluster (30 June Revolution) having the poorest purity. KL-divergence results are 0.043, 0.249, 0.252 and 0.286 for TLC, K-NN, LDA and EM clustering algorithms respectively. TLC showed the nearest distribution of all aspects to the gold standard ones. One may have the following notes. First, LDA acquired the worst purity results since the whole aspects were scattered through the seven clusters and hence there was no clear aspect per each cluster. Second, 30 June Revolution cluster showed the worst cluster purity results because it contained most of other aspects from the other clusters; it is a highly overlapped cluster. Third, although EM obtained higher purity than that of K-NN, it reported the worse KL-divergence since the distribution of all aspects per estimated cluster were not near to those of gold standard one. Finally, TLC resulted in balanced distributions among all main aspects (the most frequent class in the cluster) and that was showed as a good average purity (~61%) and the lowest KL-divergence (0.043).

C. Time and Aspect Analysis

Analysis model was applied on all aspects. In Figures 1-7, we show three different views for each aspect: (a) the cumulative probability of each emotion on a specific time interval, (b) the probability of each emotion given each month tweets, and (c) the most frequent used emotional expressions. We can see many peaks in each emotion line presenting significant events that affect people feelings towards the aspect. As examples, we demonstrate the feelings (emotions) among Egyptians through the revolutions of 25 January and 30 June overtime as follows.

The happiness emotion increased with the beginning of the revolution in January 2011 due to the happiness of the Egyptian people of the successful completion of the revolution. It was also a high curve throughout the year and a half until mid-2012 due to the moving-forward steps of the revolution towards its goals, e.g. the handover of power, the parliamentary elections and the presidency, and the handover of power to the first elected president. The surprise emotion seemed clear in February and March due to the unexpected action of Mubarak when he delivered the power and that the revolution succeeded in its first step. Surprise was also featured in the month of July 2011 because some people attributed the revolution for themselves. The sadness emotion was evident in October 2011 due to the slowdown in achieving the goals of the revolution. The anger emotion appeared clearly in February 2011 because of the violence and the killings of protesters during the revolt against the regime.

A high bending of the happiness emotion began in June 2013 due to the rapid success of the revolution and then began to decline, and increased again in September 2013 because of the happiness of the Egyptians for their ability to maintain the revolution and the beginning of the moving-forward steps towards the revolution goals. The levels of the surprise emotion were not high due to the absence of unexpected events. The grief emotion showed high levels in August 2013 because of the coming together of the people and the emergence of the post-revolution demanding the return of the former regime groups. Anger surfaced at the end of 2013 in sync with the joy due to the conflict situation in Egypt.

TABLE V: 7-Cluster Clustering Results

Cluster	KNN	EM	LDA uni-gram	LDA bi-gram	LDA tri-gram	TLC
25 Jan Revolution	01.59%	14.62%	01.03%	06.96%	04.63%	71.98%
30 Jun Revolution	00.43%	00.08%	02.13%	12.04%	03.75%	06.71%
El-Bernameg TV Show	08.87%	06.03%	18.82%	01.12%	08.32%	68.98%
Abdel Fatah El-Sisi	13.60%	95.70%	18.78%	07.49%	07.62%	66.15%
Hosni Mubarak	11.24%	99.87%	31.66%	20.45%	12.49%	69.62%
Mohamed Morsi	84.33%	84.79%	53.06%	40.68%	31.76%	69.59%
Muslim Brotherhood	36.23%	83.33%	63.41%	35.92%	35.18%	77.10%
Average Purity	22.47%	54.83%	26.98%	17.81%	14.82%	61.45%

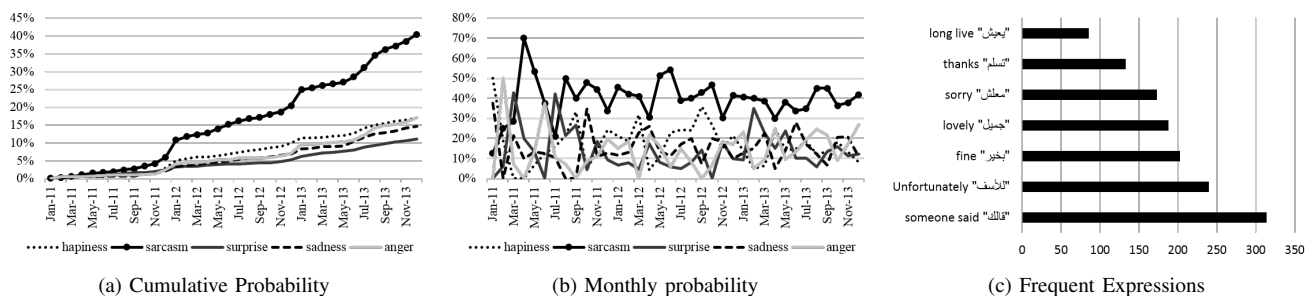


Fig. 1. 25 Jan Revolution

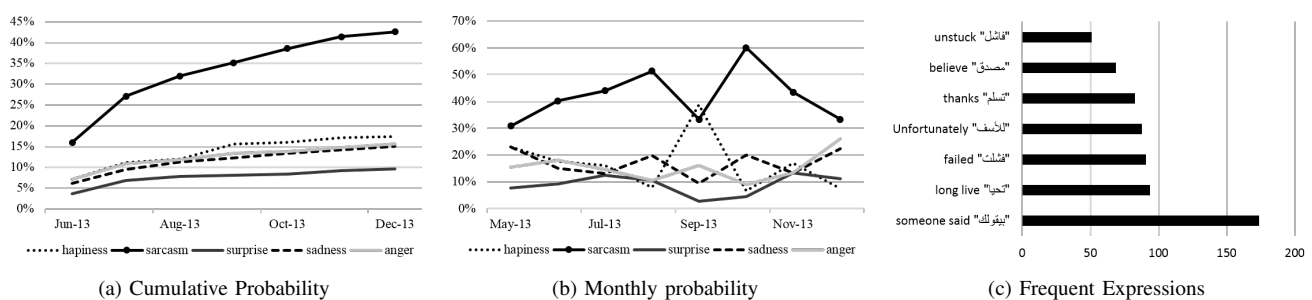


Fig. 2. 30 Jun Revolution

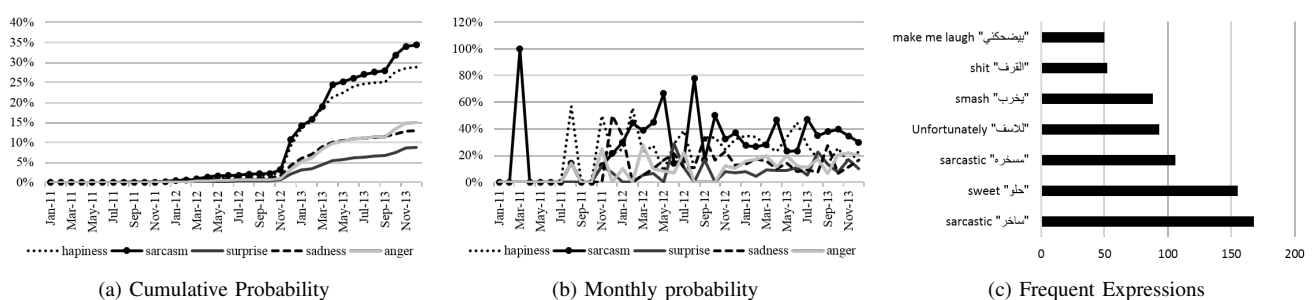


Fig. 3. El-Bernameg TV Show

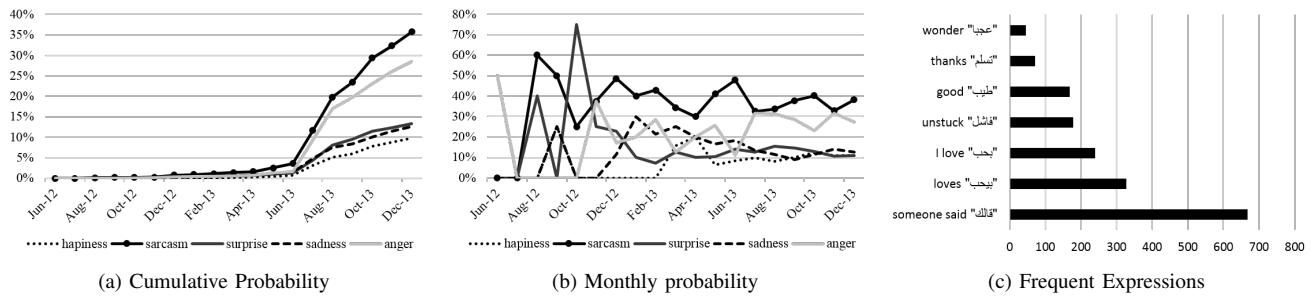


Fig. 4. Abdel Fatah EL-Sisi

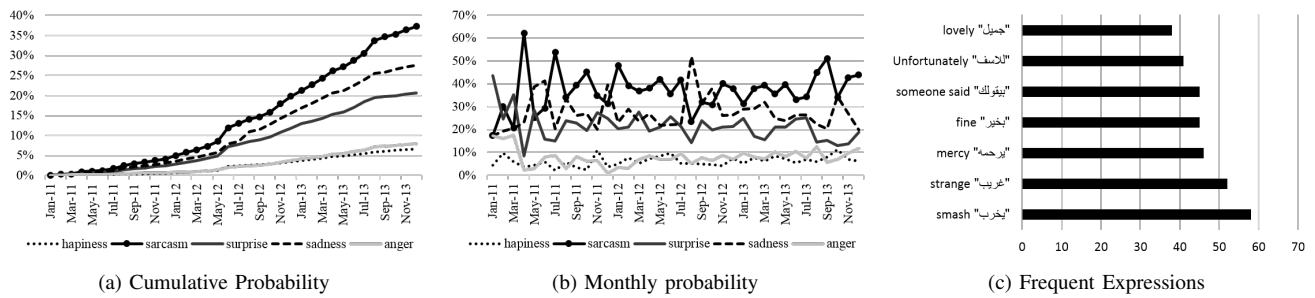


Fig. 5. Hosni Moubarak

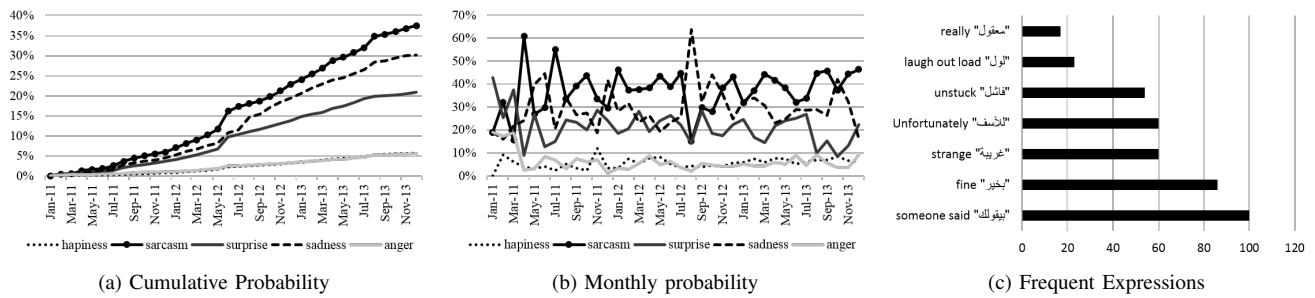


Fig. 6. Mohamed Morsi

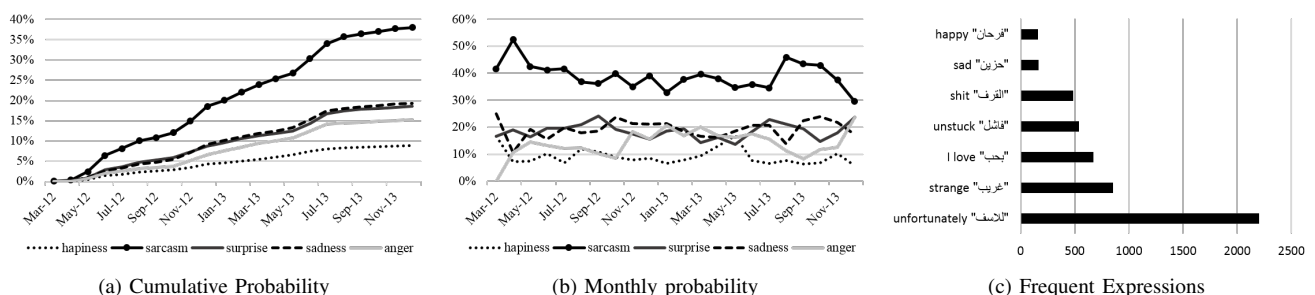


Fig. 7. Muslim Brotherhood

TABLE VI: PMI Measure Examples

Expression(1)	Expression(2)	PMI
“عَمَّة” [His Excellency]	“تحية طيبة” [Greetings]	10.61
“مُقْرَف” [Nasty]	“مُقْرَف” [Disgusting]	10.36
“بِرْحَمَه” [Bless his soul]	“الصَّابَر” [Patience]	8.38
“غُضْبَانَ” [Angry]	“غُبَيْ” [Idiot]	5.65
“اسْتَخْرَبَ” [Surprised]	“خَسَارَةً” [Loss]	2.28
“فَأَشَلَّ” [Unstuck]	“شَكْرًا” [Thanks]	-2.67

PMI measure shows the degree of interdependence between emotional expressions and each others, as a high score means high bonding strength and vice versa as shown in table 6.

V. CONCLUSION AND FUTURE WORK

In this paper, we proposed a framework to effectively analyze people emotional trends over time at different fine granularity levels (tweets, expressions, and aspects). It can be easily adapted to other languages due to the utilization of language independent features. We also developed a lightweight clustering algorithm that benefit from the short length of tweets, for better clustering effectiveness against the state-of-the-art algorithms. Since the algorithm depends on the language grams, it can be utilized in many languages other than Arabic. In the future, the annotated corpus will be freely released to the public as an Arabic natural language community resource. We are planning to expand the set of emotions targeted by the classification model and to apply our work on other domains and languages like English. Moreover, we will investigate how to potentially boost multi-emotional classification performance.

REFERENCES

- [1] E. Kouloumpis, T. Wilson, and J. D. Moore, “Twitter sentiment analysis: The good the bad and the omg!” *Icwsm*, vol. 11, pp. 538–541, 2011.
- [2] S. Mohammad, X. Zhu, and J. Martin, “Semantic role labeling of emotions in tweets,” *Proc. of WASSA*, pp. 32–41, 2014.
- [3] A. Qadir and E. Riloff, “Learning emotion indicators from tweets: Hashtags, hashtag patterns, and phrases.” in *EMNLP*, 2014, pp. 1203–1209.
- [4] H. Saif, Y. He, M. Fernandez, and H. Alani, “Contextual semantics for sentiment analysis of twitter.” *Information Processing & Management*, vol. 52, no. 1, pp. 5–19, 2016.
- [5] B. Liu, *Sentiment analysis: Mining opinions, sentiments, and emotions*. Cambridge University Press, 2015.
- [6] A. Shoukry and A. Rafea, “Preprocessing egyptian dialect tweets for sentiment mining,” in *The Fourth Workshop on Computational Approaches to Arabic Script-based Languages*, 2012, p. 47.
- [7] A. Mourad and K. Darwish, “Subjectivity and sentiment analysis of modern standard arabic and arabic microblogs,” in *Proceedings of the 4th workshop on computational approaches to subjectivity, sentiment and social media analysis*, 2013, pp. 55–64.
- [8] S. Rosenthal and K. McKeown, “Columbia nlp: Sentiment detection of subjective phrases in social media,” in *Second Joint Conference on Lexical and Computational Semantics (* SEM)*, vol. 2. Citeseer, 2013, pp. 478–482.
- [9] C. N. dos Santos and M. Gatti, “Deep convolutional neural networks for sentiment analysis of short texts.” in *COLING*, 2014, pp. 69–78.
- [10] E. Refaei and V. Rieser, “Can we read emotions from a smiley face? emoticon-based distant supervision for subjectivity and sentiment analysis of arabic twitter feeds,” in *5th International Workshop on Emotion, Social Signals, Sentiment and Linked Open Data, LREC*, 2014.
- [11] J. Borge-Holthoefer, W. Magdy, K. Darwish, and I. Weber, “Content and network dynamics behind egyptian political polarization on twitter,” in *Proceedings of the 18th ACM Conference on Computer Supported Cooperative Work & Social Computing*. ACM, 2015, pp. 700–711.
- [12] D. Zimbra, M. Ghiassi, and S. Lee, “Brand-related twitter sentiment analysis using feature engineering and the dynamic architecture for artificial neural networks,” in *2016 49th Hawaii International Conference on System Sciences (HICSS)*. IEEE, 2016, pp. 1930–1938.
- [13] A. F. El Gohary, T. I. Sultan, M. A. Hana, and M. El Dosoky, “A computational approach for analyzing and detecting emotions in arabic text,” *International Journal of Engineering Research and Applications (IJERA)*, vol. 3, pp. 100–107, 2013.
- [14] O. Alsharif, D. Alshamaa, and N. Ghneim, “Emotion classification in arabic poetry using machine learning,” *International Journal of Computer Applications*, vol. 65, no. 16, 2013.
- [15] O. Rabie and C. Sturm, “Feel the heat: Emotion detection in arabic social media content,” in *The International Conference on Data Mining, Internet Computing, and Big Data (BigData2014)*. The Society of Digital Information and Wireless Communication, 2014, pp. 37–49.
- [16] N. Riahi and P. Safari, “Implicit emotion detection from text with information fusion,” *Journal of Advances in Computer Research*, vol. 7, no. 2, pp. 85–99, 2016.
- [17] P. Ekman, “Facial expression and emotion.” *American psychologist*, vol. 48, no. 4, p. 384, 1993.
- [18] T. Wilson, J. Wiebe, and P. Hoffmann, “Recognizing contextual polarity: An exploration of features for phrase-level sentiment analysis,” *Computational linguistics*, vol. 35, no. 3, pp. 399–433, 2009.
- [19] J. Wiebe and E. Riloff, “Creating subjective and objective sentence classifiers from unannotated texts,” in *Computational Linguistics and Intelligent Text Processing*. Springer, 2005, pp. 486–497.
- [20] R. Socher, J. Bauer, C. D. Manning, and A. Y. Ng, “Parsing with compositional vector grammars.” in *ACL (1)*, 2013, pp. 455–465.

Towards Multi-Stage Intrusion Detection using IP Flow Records

Muhammad Fahad Umer, Muhammad Sher and Imran Khan
Department of Computer Science and
Software Engineering
International Islamic University
Islamabad, Pakistan

Abstract—Traditional network-based intrusion detection systems using deep packet inspection are not feasible for modern high-speed networks due to slow processing and inability to read encrypted packet content. As an alternative to packet-based intrusion detection, researchers have focused on flow-based intrusion detection techniques. Flow-based intrusion detection systems analyze IP flow records for attack detection. IP flow records contain summarized traffic information. However, flow data is very large in high-speed networks and cannot be processed in real-time by the intrusion detection system. In this paper, an efficient multi-stage model for intrusion detection using IP flows records is proposed. The first stage in the model classifies the traffic as normal or malicious. The malicious flows are further analyzed by a second stage. The second stage associates an attack type with malicious IP flows. The proposed multi-stage model is efficient because the majority of IP flows are discarded in the first stage and only malicious flows are examined in detail. We also describe the implementation of our model using machine learning techniques.

Keywords—IP flows; Multi-stage intrusion detection; One-class classification; Multi-class classification

I. INTRODUCTION

Network-based Intrusion detection system (NIDS) analyze network traffic to detect malicious activities. Traditional approaches for intrusion detection scan the complete packet content. This method is termed as deep packet inspection (DPI) [18]. However, DPI is difficult to implement when packets are being transferred at gigabit speed. Extensive resources and dedicated hardware infrastructure need to be deployed to perform packet inspection[20]. In most cases, data transmitting through the network is encrypted. DPI techniques cannot scan the encrypted payload. Another drawback of DPI is the compromise of privacy. Even if the data is not encrypted, performing strong packet filtering on the network traffic might not be permitted due to privacy issues [10].

A relatively new approach for intrusion detection analyzes the communication pattern in the network traffic for abnormal behavior[20]. The communication patterns are extracted from the network in the form of IP flow records. The IP flow records contain aggregate packet information and describe the network traffic in a summarized form. An IP flow is defined as a set of IP packets passing through an observation point in the network during a certain time interval. All packets belonging to a particular flow have a set of common properties [6]. The extraction of flow records from the network consists of two processes; flow export and flow collection [20]. The

flow records are exported from the network using flow-enabled devices. Many vendors offer built-in support in the network switches and routers for flow export. The flow collector receives flows from the flow exporter and stores them in a flow database for analysis. A flow exporter can forward flow records to more than one flow collectors. Similarly, a flow collector can receive flow from more than one flow exporters.

The process of transferring flow records between the flow exporter and collector is defined by a flow export and collection protocol. Different vendors have formulated proprietary flow export and collection protocol. However, Cisco's Netflow is a common flow export and collection protocol and is supported by almost all major vendors. Due to the increased requirement of IP flow information for network management, the Internet Engineering Task Force (IETF) has standardized the flow export and collection protocol as IP Flow Information Exchange (IPFIX) protocol [19]. IPFIX is very flexible protocol and defines around 280 attributes for IP flow records.

The IP flow records have a number of applications including billing, congestion control, traffic analysis and intrusion detection. The intrusion detection system using IP flows records for attack detection are called Flow-based IDS. Flow-based IDS have several advantages over DPI-based techniques [12]. The flow records contain aggregate packet data; therefore, fewer resources are required to process the flow data. The flow-based IDS are also not effected by the use of encryption because flow records do not have any payload. Flow-based technique only scans the data up to transport layer, and no confidential information leaves the network [1].

Flow-based Intrusion detection is an on-going research area [20]. This paper proposes a novel multi-stage model for flow-based IDS. The multi-stage model separates malicious flows from normal flows in the first stage. The malicious flows are processed by a second stage which associates an attack type with the malicious flows. We also give implementation details of our model using machine learning techniques. We suggest the use of one and multi-class classification technique for first and second stage intrusion detection processes respectively. Our future work will include a rigorous evaluation of different one-class and multi-class techniques for flow-based intrusion detection. The best performing classification technique will be combined in a multi-stage model for a comprehensive flow-based intrusion detection framework. The multi-stage model will be evaluated on various flow-based intrusion datasets to obtain the performance results.

The organization of the paper is as follows: Section 2 discusses related work in multi-stage intrusion detection systems. The architecture of our proposed model is given in Section 3. Section 4 presents the implementation detail of our model using machine learning algorithms. The conclusion of our work is presented in Section 5.

II. RELATED WORK

The multi-stage detection of network attacks has been applied using two different approaches. The first approach considers a single attack type spanned over multiple stages. Various stages of an attack include vulnerability scan, weakness exploitation, invasion, control, and spread. Every stage of an attack corresponds to a detection stage in the multi-stage IDS. In [9], a technique for detection of a single type of attack using multi-stage traffic analysis was proposed. Similarly, a multi-stage IDS using Hidden Markov Model is presented in [16]. Every attack stage is analyzed by detection agents using predefined attack signals. The signals of all attack stages are estimated by a determination stage using Hidden Markov Model for final intrusion detection decision. The IDS is evaluated on DARPA dataset and achieved a detection rate of 90%.

The other method for multi-stage IDS detects a different type of attack in every stage. In [7], a network intrusion detection technique using Learning Vector Quantization(LVQ) was proposed. The authors used multiple stages to detect different types of attack. The technique was evaluated on DARPA dataset and achieve very low error rate. A multi-stage filter using enhanced AdaBoost for network intrusion detection is presented in [17]. The technique is evaluated on DARPA dataset and achieved good results for some attack types. A malware prevention and detection system using a combination of signature and anomaly-based IDS is presented in [2]. The signature-based IDS uses general characteristics of attack for detection. The anomaly-based IDS is implemented using the RIPPER classifier. The signature and anomaly based IDS are implemented in three stages. The first stage classifies the traffic as normal or malicious. The second stage determines the attack type while the third stage determines the variant of a particular attack type. The technique is evaluated on the NSL-KDD99 dataset and achieved F1-measure of over 0.97 for different stages.

In [22], a multi-stage detection model using time-slot and flow-based detection, is proposed. The time-slot detection stage checks the incoming traffic for obvious traffic characteristic. This stage classifies the traffic into normal, suspicious and malicious categories. The traffic detected as suspicious is converted into IP flows and forwarded to the flow-based detection stage. The technique is evaluated in DARPA dataset and achieved a detection rate of 68.4%.

In [3], the authors proposed a real-time multi-stage intrusion detection system using unsupervised learning to improve the detection rate of unknown attacks. The system uses IP flow records for attack detection. The multi-stage model uses two detection engines. The first engines use sub-space clustering and to detect DoS, DDoS, and other attacks. The second detection engine analyzes the relation between attackers to detect Bot-master. The proposed technique focused on improving the detection rate of unknown attacks by additional flow features.

Our proposed approach differs from the existing work. Unlike most of the techniques, our model uses IP flow records instead of packets for intrusion detection. Our model separates the normal and malicious flow in the first stage and determines the attack type in the second stage. The implementation of our model uses a one-class and multi-class classification at the first and second stage. The use of one-class classification in a multi-stage model is a novel idea. The next section presents the architecture of our proposed model.

III. ARCHITECTURE OF PROPOSED MODEL

Although flow records contain summarized network traffic information, the flow data can be very large in high-speed networks [14]. Flow monitoring and analysis tools employ packet sampling techniques to obtain a subset of flow records [13], [4]. Furthermore, IPFIX defines around 280 flow attributes. Additional flow attributes can also be computed using the base flow attributes by the IDS to detect different types of network attacks. Large input size and high feature space can overload the IDS. Also most of the traffic in the network is normal as compared to malicious traffic. Processing of malicious as well as normal traffic by the IDS will be performance bottleneck.

We propose a multi-stage model for intrusion detection in high-speed networks using IP flow records. Figure II shows the architecture of our proposed approach. The IP flows are collected from the network using a flow-enabled device. These IP flows are passed through an attribute selection step. The multi-stage model uses two stages for attack detection. The first stage selects a minimal set of attributes and determines whether incoming IP flows are normal or malicious. The first stage uses a fast and computationally inexpensive technique for detection. It discards the normal flows and forwards the malicious to the second stage detection process. An initial intrusion alert is also sent to the consolidated intrusion alert module.

The second stage process performs detail intrusion detection on the malicious flows. The size of malicious flows is very small in overall network traffic. Due to small input size, the second stage can commit additional resources for detailed and accurate detection of an attack type. The second stage analyzes the malicious flows and determines the attack type. The second stage can also use additional flow attributes for precise detection of an attack. If the flows do not belong to any attack class, they are marked as unknown in the detail intrusion alert. The unknown flows can belong to an unseen attack, or they can be false postives of the first stage. The second stage sends a detail intrusion alert to the alert module. The alert module raises a consolidated alert combining the alert information received from both detection stages.

Our proposed multi-stage model discards normal flows in the first stage and ensures that only malicious flows are subject to detail intrusion detection. This increase the efficient of our model because no resources are consumed in the processing normal flows. Another benefit of our approach is the reduction of false positives. If the malicious flows detected in the first stage contain false positives, the second stage process does not associate a class type with such flows. The next section gives implementation detail of our model using machine learning techniques.

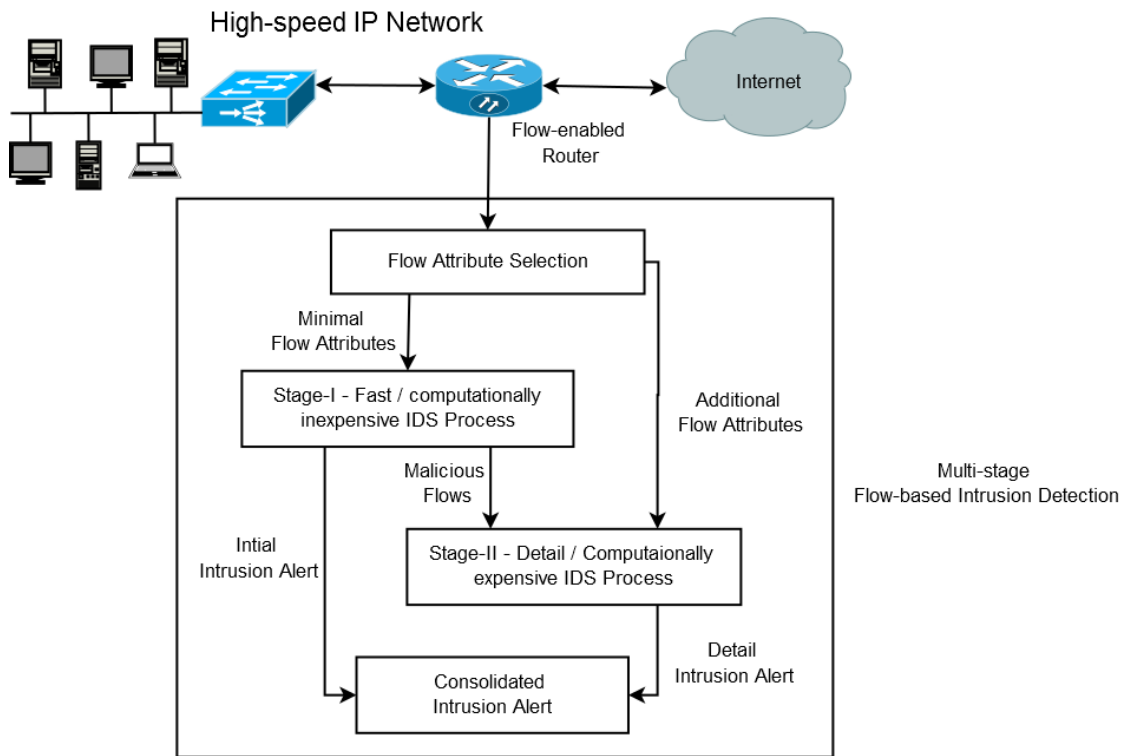


Fig. 1. Architecture of multi-stage intrusion detection model

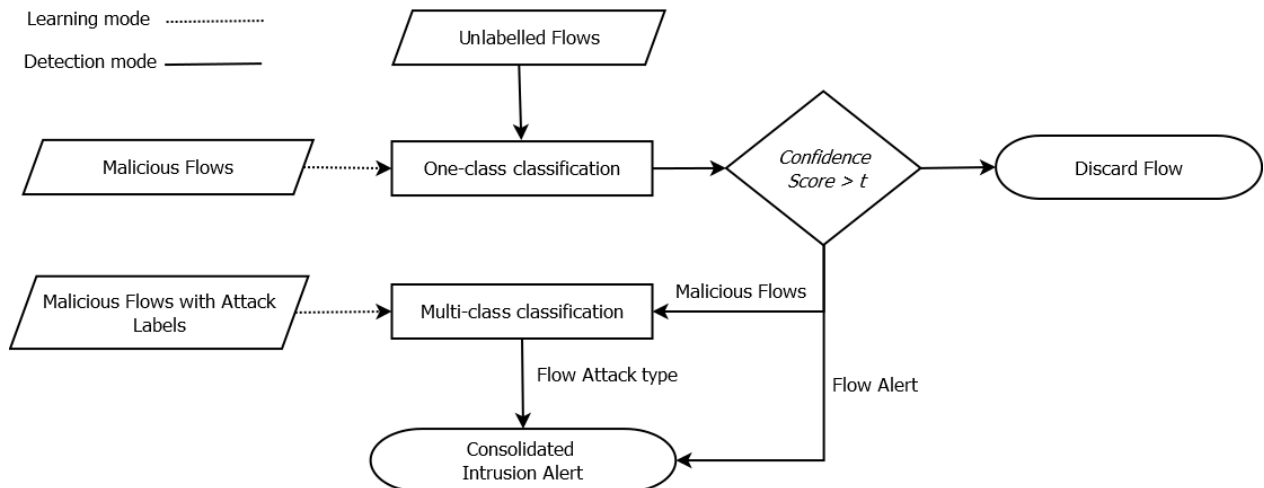


Fig. 2. Architecture of multi-stage intrusion detection model

IV. IMPLEMENTATION

Our work proposes the use of machine learning technique for implementation of the proposed model. Machine learning techniques have been extensively used in intrusion detection systems for adaptability and improvement of detection rate [21], [5].

The implementation of the multi-stage model using machine learning techniques has two modes, learning mode and detection mode. In learning mode, the classification algorithms are trained using a labeled set of IP flows. Our model uses two training sets. The first stage requires a training set consisting of only malicious flow. The second stage uses a training set

of malicious flow with attack labels. In the detection mode, the IDS process unlabeled IP flows and raises consolidated intrusion alerts.

Figure III shows the implementation of our model using machine learning classification algorithms. The first stage detection process only detects malicious IP flows. There is only one target class in the first stage. We have proposed the use of the one-class classification for detection of malicious flows in the first stage. One class classification techniques learn the model for one target class. It only recognizes objects of target class and all other objects are rejected. The training set for one-class classification technique also consists of target class

objects [15].

Mathematically, X is a training set consisting of only malicious IP flows. The one-class classifier learns an output function f_o using the optimized parameter set θ for a given IP flow x_i . The f_o gives a confidence score defining the membership of IP flow x_i with the malicious class.

$$f_o(x_i) = \theta_1 + \theta_2(x_i) \quad (1)$$

The value of f_o is used in a decision function h_o to obtain the classification result. For all unclassified IP flows $z_i \in Z$, if the value of $f_o(z_i)$ is higher than the maliciousness threshold t , the flow is classified as malicious or normal otherwise. The value of maliciousness threshold t is user-defined.

$$h_o(z_i) = \begin{cases} \text{malicious}, & \text{if } f_o(z_i) \geq t \\ \text{normal}, & \text{if } f_o(z_i) < t \end{cases} \quad (2)$$

The malicious flows recognized in the first stage are forwarded to the second stage. The second stage detection process associates an attack type with the malicious IP flows. Since the number of attack types can be more than one, we use multi-class classification technique to classify the IP flows into different attack types [8].

The training set Y contains labeled malicious IP flows for K attack types. The multi-class classifier learns an output function $f_{mk}(y_i)$ for all K attack types using the training set Y where $y_i \in Y$. The function f_{mk} gives a confidence score for all attack types in K .

$$f_{mk}(y_i) = \theta_1 + \theta_2(y_i) \forall k \in K \quad (3)$$

For all unclassified IP flows $z_i \in Z$, The incoming flow is classified into the attack type for which the function $f_{mk}(z_i)$ gives the highest confidence score.

$$h_m(z_i) = \arg \max_{k \in K} f_{mk}(z_i) \quad (4)$$

The classification result of both stages is combined in a consolidated intrusion alert module. The alert module output the maliciousness of flow and the possible attack type in the alert. The information can be used by the security administrator to protect the integrity of the network.

Our future work will explore the application of one-class classification to IP flow records for intrusion detection. We will review available one-class classification methods and evaluate them on flow-based intrusion datasets for detection of malicious flows. Different techniques used for one-class classification include density estimation, reconstruction methods, and boundary methods. The outcome of the step will determine that which one-class classification perform better in intrusion detection using IP flow records.

In the second step, various machine learning technique will be evaluated using flow-based datasets for classification of malicious IP flows in different attack classes. In the third

step, we will combine the best performing one and multi-class classification techniques and develop a multi-stage flow-based intrusion detection model. We will use various flow-based datasets [11] and testbeds to evaluate the performance of proposed intrusion detection system.

V. CONCLUSION

This paper proposes a multi-stage model for intrusion detection using IP Flow records. The first stage classifies the IP flow records into the normal and malicious classes. The second stage detection process performs detail analysis and classifies the flow into different attack types. We also give implementation detail of our model using one and multi-class classification. We conclude that our model is efficient since it discards the majority of the flows in the first stage using a computationally inexpensive algorithm. Only malicious flow are analyzed in detail. The multi-stage detection model also reduces the false positive rate through the application of two different classification techniques.

REFERENCES

- [1] Hashem Alaidaros, Massudi Mahmuddin, and Ali Al Mazari. An overview of flow-based and packet-based intrusion detection performance in high speed networks. In *In Proceedings of the International Arab Conference on Information Technology*, 2011.
- [2] Ammar Alazab, Michael Hobbs, Jemal Abawajy, and Ansum Khraisat. Malware detection and prevention system based on multi-stage rules. *International Journal of Information Security and Privacy (IJISP)*, 7(2):29–43, 2013.
- [3] Payam Vahdani Amoli and Timo Hämäläinen. Real time multi stage unsupervised intelligent engine for nids to enhance detection rate of unknown attacks. In *2013 IEEE Third International Conference on Information Science and Technology (ICIST)*, pages 702–706. IEEE, 2013.
- [4] Karel Bartos and Martin Rehak. Ifs: Intelligent flow sampling for network security—an adaptive approach. *International Journal of Network Management*, 25(5):263–282, 2015.
- [5] Anna L Buczak and Erhan Guven. A survey of data mining and machine learning methods for cyber security intrusion detection. *IEEE Communications Surveys & Tutorials*, 18(2):1153–1176, 2015.
- [6] Benoit Claise, Brian Trammell, and Paul Aitken. Specification of the ip flow information export (ipfix) protocol for the exchange of flow information. Technical report, IETF, 2013.
- [7] Luigi Pietro Cordella, Alessandro Limongiello, and Carlo Sansone. Network intrusion detection by a multi-stage classification system. In *International Workshop on Multiple Classifier Systems*, pages 324–333. Springer, 2004.
- [8] Corinna Cortes, Mehryar Mohri, and Afshin Rostamizadeh. Multi-class classification with maximum margin multiple kernel. In *ICML (3)*, pages 46–54, 2013.
- [9] Jerald Dawkins and John Hale. A systematic approach to multi-stage network attack analysis. In *Information Assurance Workshop, 2004. Proceedings. Second IEEE International*, pages 48–56. IEEE, 2004.
- [10] Christian Fuchs. Implications of deep packet inspection (dpi) internet surveillance for society.(= privacy & security-research paper series 1). Available from http://www.projectpact.eu/documents-1%231_Privacy_and_Security_Research_Paper_Series.pdf, 2012.
- [11] Sebastian Garcia, Martin Grill, Jan Stiborek, and Alejandro Zunino. An empirical comparison of botnet detection methods. *computers & security*, 45:100–123, 2014.
- [12] Mario Golling, Rick Hofstede, and Robert Koch. Towards multi-layered intrusion detection in high-speed networks. In *Cyber Conflict (CyCon 2014), 2014 6th International Conference On*, pages 191–206. IEEE, 2014.

- [13] Rick Hofstede, Pavel Čeleda, Brian Trammell, Idilio Drago, Ramin Sadre, Anna Sperotto, and Aiko Pras. Flow monitoring explained: from packet capture to data analysis with netflow and ipfix. *IEEE Communications Surveys & Tutorials*, 16(4):2037–2064, 2014.
- [14] Jae-Hyun Jun, Dongjoon Lee, Cheol-Woong Ahn, and Sung-Ho Kim. Ddos attack detection using flow entropy and packet sampling on huge networks. *ICN 2014*, page 196, 2014.
- [15] Shehroz S Khan and Michael G Madden. One-class classification: taxonomy of study and review of techniques. *The Knowledge Engineering Review*, 29(03):345–374, 2014.
- [16] Do-hyeon Lee, Doo-young Kim, and Jae-il Jung. Multi-stage intrusion detection system using hidden markov model algorithm. In *Information Science and Security, 2008. ICISS. International Conference on*, pages 72–77. IEEE, 2008.
- [17] P Natesan and P Balasubramanie. Multi stage filter using enhanced adaboost for network intrusion detection. *International Journal of Network Security & Its Applications*, 4(3):121, 2012.
- [18] Thaksen J Parvat and Pravin Chandra. A novel approach to deep packet inspection for intrusion detection. *Procedia Computer Science*, 45:506–513, 2015.
- [19] Anna Sperotto and Aiko Pras. Flow-based intrusion detection. In *Integrated Network Management (IM), 2011 IFIP/IEEE International Symposium on*, pages 958–963. IEEE, 2011.
- [20] Anna Sperotto, Gregor Schaffrath, Ramin Sadre, Cristian Morariu, Aiko Pras, and Burkhard Stiller. An overview of ip flow-based intrusion detection. *Communications Surveys & Tutorials, IEEE*, 12(3):343–356, 2010.
- [21] Chih-Fong Tsai, Yu-Feng Hsu, Chia-Ying Lin, and Wei-Yang Lin. Intrusion detection by machine learning: A review. *Expert Systems with Applications*, 36(10):11994–12000, 2009.
- [22] Yuji Waizumi, Hiroshi Tsunoda, Masashi Tsuji, and Yoshiaki Nemoto. A multi-stage network anomaly detection method for improving efficiency and accuracy. *Journal of Information Security*, 3(01):18, 2011.

Unsupervised Morphological Relatedness

Ahmed Khorsi

Computer Science Department

Al-Imam Mohammad Ibn Saud Islamic University
Riyadh, Kingdom of Saudi Arabia

Abeer Alsheddi

Computer Science Department

Al-Imam Mohammad Ibn Saud Islamic University
Riyadh, Kingdom of Saudi Arabia

Abstract—Assessment of the similarities between texts has been studied for decades from different perspectives and for several purposes. One interesting perspective is the morphology. This article reports the results on a study on the assessment of the morphological relatedness between natural language words. The main idea is to adapt a formal string alignment algorithm namely Needleman-Wunsch's to accommodate the statistical characteristics of the words in order to approximate how similar are the linguistic morphologies of the two words. The approach is unsupervised from end to end and the experiments show an nDCG reaching 87% and an r-precision reaching 81%.

Keywords—Arabic Language; Computational Linguistics; Morphological Relatedness; Semitic Morphology; Unsupervised Learning

I. INTRODUCTION

Expanding a query word to its variants is one of the challenges facing an Information Retrieval (IR) system in order to achieve a decent recall.

Take the Arabic word "كتاب" ([kitaAb]: book)¹. An IR system seeking information related to this word in a collection of documents should pick all the documents in which occur the word itself or any of its variants such as "كاتب" ([kaAtib]: writer), "كتب" ([kutub]: books), "كتيب" ([kutayib]: small book),...etc.

The purpose is to capture the documents in which also occur words with meanings close to the query words. One way to do this is to exploit the fact that two words derived from the same morphological origin are likely to share the same broad meaning.

Experience shows that such technique depends on the type of the language morphology [2], [3]. In languages like English, a word is generally a concatenation of prefixes, stem and suffixes. For instance, the word "unbreakable" is composed of "un", "break" and "able". While the principle of decomposition can be applied to Arabic, words in Semitic languages, such as Arabic, are actually derived by combining two entities; each might be regarded as an origin: *root* and *pattern* [4]. For instance, the word "كاتب" ([kaAtib]: writer) is coined by combining the root "ب ت ك" ([k t b]) and the pattern "كتاب".

This means the normal form an IR system may reduce the Arabic query word to one of three different types, each expressing a different level of similarity.

¹In this paper, Arabic is represented in some or all of three variants according to context: "Arabic word" ([Buckwalter Arabic transliteration] [1]: English translation).

- Stem: The extraction of the stem is simply the elimination of the prefixes and suffixes.
- Root: Specific to the Semitic languages, its extraction is more complicated than the extraction of the stem as it tries to identify the three, four or five core letters among all letters of the words [5]. The words derived from the same root have a common meaning broader than the one shared by words having a common stem.
- Pattern: The extraction of the pattern is the identification of the non-core letters and their positions among the core ones. The authors are not aware of any IR system that makes use of pattern as the normal form of words.

For instance the word "الكاتب" ([alkaAtib]: The writer) might be reduced to its stem "كاتب", to its root "ب ت ك" ([k t b]) or to the pattern "كتاب".

While the trend is to reduce the query words to the normal form then to match them against the stored normal forms, another approach [6] is to redesign the matching itself in such a way that it identifies words morphologically close to the query word by measuring the Morphological Relatedness (MR).

The present work is an attempt to enhance this approach [6] in order to improve the effectiveness of morphology-aware matching. Three major changes are introduced to the computation of the MR:

1. The words are first processed by an unsupervised morpho-segmenter which tries to remove the prefixes and suffixes.
2. The frequency is involved earlier in the computation of the Longest Common Subsequence (LCS). An alignment algorithm is adapted to take into account the frequencies of the letters in the computation of the cost.
3. The comparison is extended to *n*-grams.

Section II reviews the principle of string alignment that will be used to calculate the MR [7]. Section III overview works related to the idea of computing the similarity among natural words. Section IV introduces the proposed approach. Section V details the test and discusses the results.

II. SEQUENCES ALIGNMENT

Sequence Alignment (SA) is the process of identifying the minimal number of edit operations required to transform one string of characters into another [8] [9]. In an edit operation, a character may undergo one of the following changes:

- Indel: The character is simply deleted or a new character is inserted.
- Substitution: The character is substituted by another.

Other operations might be defined on the basis of these. This study will limit this section to the simplest definitions of the underlying concepts. Each edit operation is assigned a cost.

Having two strings (words) at hand, the objective is first to calculate the minimal cost of edit operations required to transform the first string into the second one. Then, to identify what and where are those edit operations. The algorithm which will be focused on in this paper is due to Needleman, Saul and Wunsch, Christian [7]. Algorithm 1 depicts the steps to align two words A and B , where $cost_s$ denotes the cost of a substitution, $cost_{gd}$ and $cost_{gi}$ are a gap penalty pointing out aligned with a null. First, a two-dimensional matrix is built $M[0 \dots n, 0 \dots m]$, where n is the size of A and m is the size of B , and the rows are labeled with letters of A and the columns are labeled with letters of B . The extra row and column at index zero have been added to deal with the empty string. Second, all cells are filled with the similarity values starting from the top row and going to the bottom-right cell from left to right. Each cell in this matrix holds the similarity between two substrings of the two strings whose ends intersect at a given cell; that is, the cell $M[i, j]$ holds the similarity between substrings $A = a_1 \dots a_i$ and $B = b_1 \dots b_j$. Then the last cell $M[n, m]$ holds the similarity between strings A and B .

Algorithm 1: Needleman-Wunsch similarity

Input : Two strings $A = a_1 a_2 \dots a_n$ and $B = b_1 b_2 \dots b_m$

Output: The Needleman-Wunsch similarity between two strings A and B

```

1 M: matrix[0...n, 0...m]
2 M[0, 0] ← 0
3 for  $i \leftarrow 1$  to  $n$  do
4   M[i, 0] ← M[i - 1, 0] + costgd
5 for  $j \leftarrow 1$  to  $m$  do
6   M[0, j] ← M[0, j - 1] + costgi
7 for  $i \leftarrow 1$  to  $n$  do
8   for  $j \leftarrow 1$  to  $m$  do
9     M[i, j] ← max(M[i - 1, j - 1] + costs, M[i - 1, j] + costgd, M[i, j - 1] + costgi)
10 return M[n, m]

```

Example: Table 1 shows an example of applying Algorithm 1 to find the similarity between two words, $A=$ "winter" and $B=$ "write". $cost_s$ was supposed to be equal to 1 when the two letters match, and the other costs are equal to -1. For instance, the value in the cell $M[4, 4]$ indicates that the similarity between "wint" and "writ" is 1.

$$\begin{aligned}
M[4][4] &= \max(M[3, 3] + cost_s, M[3, 4] + cost_{gd}, \\
&\quad M[4, 3] + cost_{gi}) \\
&= \max(0 + 1, 0 - 1, -1 - 1) \\
&= 1
\end{aligned}$$

Table 1: Example of the Needleman-Wunsch similarity

	w	r	i	t	e
0	-1	-2	-3	-4	-5
w	-1	1	0	-1	-2
i	-2	0	0	1	0
n	-3	-1	-1	0	0
t	-4	-2	-2	-1	1
e	-5	-3	-3	-2	0
r	-6	-4	-2	-3	-1

So the value in the last cell $M[6, 5]$ means that the similarity between the words "write" and "winter" is 1.

$$\begin{aligned}
M[6][5] &= \max(M[5, 4] + cost_s, M[5, 5] + cost_{gd}, \\
&\quad M[6, 4] + cost_{gi}) \\
&= \max(0 - 1, 2 - 1, -1 - 1) \\
&= 1
\end{aligned}$$

III.RELATED WORKS

Beside [6], the authors are not aware of any published work on the concept of the MR. This section overviews a number of approaches that make use of the concepts of edit distance in the context of Natural Language Processing (NLP).

Ghafour *et al.* [10] suggest to adapt the Levenshtein's distance [11] in the comparison of compare Arabic words. The cost of the operation captures three levels of similarity: phonetic, character form and keyboard wise similarities. Gomaa & Fahmy [12] proposed a system to automatically grade answers to an essay question. They tested different similarity measures, trying to achieve a maximum correlation value between the proposed system and human experts grades. The Needleman-Wunsch similarity [7] is one of the measures they tested. It achieves 26.5% of the correlation score.

Mustafa & Al-Radaideh [13] who investigated for a n -grams based comparison claim that the bigram based comparison is more effective than the trigram based comparison, and that the use of pure n -grams technique alone does not perform with Arabic words as well as it does with English words. In [14] Mustafa suggests to extend the comparison to non contiguous letters. For instance, the n -grams in the word $W = w_1 w_2 \dots w_n$ might be $\{w_1.w_2, w_1.w_3, \dots, w_{n-2}.w_n, w_{n-1}.w_n\}$. Tested on 160,000 words, the author claims that this approach outperforms the classical one when using a rule-based stemming. The approach meets the balancing point of recall and precision at around 40%.

Reference [15] opted for the rule based approach to match Arabic words. It identifies the common letters between two words, compare their order and checks whether the uncommon letters are valid affixes or not. If these two conditions apply, a match is raised. This approach uses a predefined list of affixes. The authors tested 1,500 distinct words and claim they have achieved a 15% error rate at a 13% missing rate. The error rate measures how many erroneous hits are found among all the relevant variants. While the missing rate measures how many relevant variants are missing among all actual relevant variants in the dataset.

IV.A TWO STEPS MORPHOLOGICAL RELATEDNESS

To the best of the authors' knowledge, the concept of MR was introduced by Ahmed Khorsi [6] where he tried to substitute the classical normalize-then-match approach in the matching process used in the IR systems with a straight comparison that takes into account the core letters intended to carry the core meaning of the word and the non-core ones which are meant to carry the variation in the meaning. Basically, two challenges had to be addressed: 1. How to distinguish the core letters from the non-core ones 2. How to model the matching and mismatching, either within the core letters or the non-core letters.

As the core letters in a word might not be contiguous, the matching made use of the computation of the Longest Common Subsequence (LCS) [16]. As its name suggests, it extracts the longest sequence of letters, either contiguous or not, but in same order shared by the two words. As the LCS does not guarantee that the common letters are all core ones, the formula to calculate the MR tries to exploit the fact that the non-core letters are usually more frequently used than the core ones. The words in a collection of documents found to have the highest MRs with the word at hand were considered the most morphologically related and the most probable to carry a meaning very close to the meaning carried by the word at hand as shown in Algorithm 2. The MR measure is:

Algorithm 2: Top five morphological relatedness

```

input : A word  $w$ 
output: Five words have the highest MRs with  $w$ 
1 foreach word  $w_i$  in a corpus do
  2    $mr_i \leftarrow \text{MR}_{(w,w_i)}$ 
  3    $\text{MR}_{all} \leftarrow \text{MR}_{all} \cup \{mr_i\}$ 
  4    $W_{all} \leftarrow W_{all} \cup \{w_i\}$ 
  5  $\text{MR}_{top} \leftarrow \text{top five values from } \text{MR}_{all}$ 
  6 return  $W_{top}$ 
```

$$MR_{(w_1, w_2)} = \sum_{i=1}^{|LCS_{(w_1, w_2)}|} \log \left(\frac{1}{\text{freq}(LCS_{(w_1, w_2)}[i])} \right) - \sum_{i=1}^{|LCS_{(w_1, w_2)}|} \log \left(\frac{1}{\text{freq}(LCS_{(w_1, w_2)}[i])} \right) \quad (1)$$

Where w_1 and w_2 are two strings whose will be tested, $|w_1|$ is the length of w_1 and $w_1[i]$ is the i^{th} letter in w_1 . $LCS_{(w_1, w_2)}$ is the LCS between w_1 and w_2 , and $LCS_{(w_1, w_2)}$ is LCS's complement (i.e., it contains all letters that are not included in $LCS_{(w_1, w_2)}$). $\text{freq}(a)$ is the frequency (count) of the letter a in a corpus.

Tested on more than 200,000 words, such simple approach could achieve 82% nDCG and 78% R-precision when the five (05) highest MRs are picked.

Based on the analysis of results and the lacks of identification in the original work [6], the present work introduces three major changes to the concept of MR computation:

1. Stemming: To avoid the interference of (pre/suf)fix letters in the computation of the MR, an unsupervised

morphological segmentation is applied beforehand to extract the stems on which the actual computation of the MR is applied.

2. Alignment cost: The LCS extraction in the original approach does not make any distinction between letters. In an attempt to involve the frequency factor early in the process, the cost model of an alignment is adapted to accommodate the frequencies.
3. N-grams: The investigation of this study is extended to the effect of making the comparison unit n -grams of letters rather than single letters.

The first step relies on a morphological segmentation of words, which is also suggested in a separate work. The following paragraphs summarize its main traits.

A. Morphological Segmentation

The objective of this section is to take a quick look at the step introduced before the actual computation of the MR. This step aims at identifying the prefix, stem and suffix of a word, as experience has shown that an unsupervised morphological segmentation is feasible and could reach acceptable performance [17]–[28]. The following paragraphs describe how the unsupervised learning and segmentation of natural words are approached.

Let the word be "*unbreakable*", which is formed by concatenating the prefix "*un*", the stem "*break*" and the suffix "*able*". The vocabulary suggests such segmentation should contain other words with different combinations of prefixes, stems and suffixes (e.g. "*rebreakable*", "*unbreaking*"...etc.), which makes the occurrence of "*un*" have a weak dependence on the occurrence of "*break*", whose occurrence is also relatively independent from the occurrence of the suffix "*able*". On the other hand, it is obvious, but worth mentioning, that each morpheme is not separable, either from its first letter or its last one. The proposed approach is all about exploiting this fact: a morpheme depends on only the letters of which it is formed. To address the challenge of how to assess the dependence among the letters of a word, probabilistic dependence was employed [29].

1) Segmentation Algorithm Algorithm 3 iterates over the word, letter by letter, and, for every position, computes two dependencies: 1. the dependency of the prefix on its last letter; 2. the dependency of the suffix on its first letter, where the prefix starts (inclusive) at the current letter and the suffix ends (inclusive) at it. The difference between the two values then points to which of the two fragments (i.e. the prefix or the suffix) is more attached to the current letter. The algorithm keeps going until it encounters a change of the direction of the highest dependency. If, in the immediately preceding position, the prefix depends on the letter more than the suffix does and, in the current position, the suffix depends on the letter more than the prefix does, a cutting point is marked between the previous and the current letter.

2) Computation of the Dependence By definition, the concept of dependence that used is symmetric [29]. In this context: "*the string depends on the letter*" means "*the letter depends on the string*" and vice versa.

The dependency of a letter a on the prefix α : will be called the forward dependency, and it is denoted $f_{\text{dep}}(\alpha)$

where $u=\alpha a$ is the prefix appended with the letter under consideration a . The dependency of the letter a on the suffix β : will be called the backward dependency, and it is denoted $bdep(v)$ where $v=\alpha\beta$ is the suffix headed by the letter under processing a . The beginning and the end of a word are marked by respectively # and \$. The forward dependency is then:

$$fdep(u) = \frac{P(\alpha \rightarrow a)}{P(a)} \quad (2)$$

and

$$bdep(u) = \frac{P(a \rightarrow \beta)}{P(a)} \quad (3)$$

Where $P(\alpha \rightarrow a)$ is the conditional probability:

$$P(\alpha \rightarrow a) = \frac{\text{Count}(\alpha a)}{\text{Count}(\alpha)} \quad (4)$$

and $P(a \rightarrow \beta)$ is the conditional probability:

$$P(a \rightarrow \beta) = \frac{\text{Count}(a\beta)}{\text{Count}(\beta)} \quad (5)$$

then

$$fdep(u) = \frac{\text{Count}(\alpha a)}{\text{Count}(\alpha)P(a)} \quad (6)$$

and

$$bdep(u) = \frac{\text{Count}(a\beta)}{\text{Count}(\beta)P(a)} \quad (7)$$

Where the probability of a letter a : $P(a)$ is approximated by its normalized frequency in a corpus.

$$P(a) = \frac{\text{Count}(a)}{\sum_{b \in \mathcal{A}} \text{Count}(b)} \quad (8)$$

Where \mathcal{A} is the alphabet. $\text{Count}(\alpha)$ expresses how often an n -gram α occurs in the corpus.

Algorithm 3: Morphological Segmentation

```

input : A word  $w = a_0a_1 \dots a_n$ 
output: Cutting Points
1 foreach  $a_i$  where  $0 < i \leq n$  do
2 if  $fdep(\# \dots a_{i-1}) - bdep(a_{i-1} \dots a_n\$) > 0$  and
    $fdep(\# a_0 \dots a_i) - bdep(a_i \dots a_n\$) < 0$  then
3 add  $i$  to the cutting points
```

Example: Table 2 is a simulation of Algorithm 3 on the word "unbreakable". The second letter "n" depends on the prefix "#u" more than it does on the suffix "breakable\$", where the third letter "b" depends on the suffix "breakable\$" more than it does on the prefix "#un". This change of the dependence direction makes the point "un|breakable" a cutting point. The same logic applies to the seventh letter "k" and the eighth letter "a".

B. Morphological Relatedness

An MR assessment is expected to fulfil two assumptions.

- The longer the shared sequences are, the higher the relatedness should be.
- Words sharing core letters are much more related to each other than are words sharing only non-core letters.

The following shows that an adaptation of a string alignment algorithm might be the answer.

1) Relatedness Algorithm Algorithm 4 is an adaptation of the Algorithm 1, where a word A contains α n -grams and a word B contains β n -grams. Instead of talking about a cost, the term gain will be used which fits well with the aforementioned assumptions.

Algorithm 4: Morphological Relatedness

```

Input : Two words  $A = a_1a_2 \dots a_\alpha$  and
          $B = b_1b_2 \dots b_\beta$ 
Output: The Needleman-Wunsch similarity between
         two words  $A$  and  $B$ 
1  $M$ : matrix[0 …  $\alpha$ , 0 …  $\beta$ ]
2  $M[0, 0] \leftarrow 0$ 
3 for  $i \leftarrow 1$  to  $\alpha$  do
4    $M[i, 0] \leftarrow M[i - 1, 0] + gain_{del}(a_i)$ 
5 for  $j \leftarrow 1$  to  $\beta$  do
6    $M[0, j] \leftarrow M[0, j - 1] + gain_{ins}(b_j)$ 
7 for  $i \leftarrow 1$  to  $\alpha$  do
8 for  $j \leftarrow 1$  to  $\beta$  do
9 if  $a_i = b_j$  then
10    $M[i, j] \leftarrow$ 
         $\max(M[i - 1, j - 1] + gain_{match}(a_i), M[i -$ 
         $1, j] + gain_{del}(a_i), M[i, j - 1] + gain_{ins}(a_i))$ 
11 else
12    $M[i, j] \leftarrow$ 
         $\max(M[i - 1, j - 1] + gain_{subs}(a_i, b_j), M[i -$ 
         $1, j] + gain_{del}(a_i), M[i, j - 1] + gain_{ins}(b_j))$ 
13 return  $M[\alpha, \beta]$ 
```

2) Computation of the Relatedness The following describes how is the gain computed:

1. $gain_{match}(a) = + \frac{1}{freq(a)}$: When two letters match.
2. $gain_{subs}(a, b) = - \frac{1}{freq(a)}$: In case of substitution, the letter a is the one with the lowest frequency.
3. $gain_{del}(a) = - \frac{1}{freq(a)}$: In case of deletion, the letter a is the deleted letter.
4. $gain_{ins}(a) = - \frac{1}{freq(a)}$: In case of insertion, the letter a is the inserted letter.

where $freq(a)$ is the normalized frequency of the letter a :

$$freq(a) = \frac{\text{Count}(a)}{\sum \text{Count}(\cdot)} \quad (9)$$

where \cdot denotes any letter of the alphabet.

Table 2: Example of morphological segmentation

i	u	fdep(u)	v	bdep(v)	Difference	Direction
1	# <u>u</u>	0.46	<u>unbreakable\$</u>	30.97	-30.51	↓
2	# <u>un</u>	6.36	<u>nbreakable\$</u>	5.84	0.52	↑
3	# <u>unb</u>	1.35	<u>breakable\$</u>	46.70	-45.35	↓
4	# <u>unbr</u>	1.94	<u>reakable\$</u>	10.45	-8.51	↓
5	# <u>unbre</u>	3.11	<u>eakable\$</u>	5.01	-1.90	↓
6	# <u>unbrea</u>	6.79	<u>akable\$</u>	1.68	5.11	↑
7	# <u>unbreak</u>	34.71	<u>kable\$</u>	1.50	33.21	↑
8	# <u>unbreaka</u>	5.09	<u>able\$</u>	7.38	-2.29	↓
9	# <u>unbreakab</u>	46.70	<u>ble\$</u>	9.89	36.81	↑
10	# <u>unbreakabl</u>	9.72	<u>le\$</u>	2.76	6.96	↑
11	# <u>unbreakable</u>	10.02	<u>e\$</u>	1.15	8.87	↑

Table 3: Example of the computation of morphological relatedness

	ا	ت	ك	ب	
ا	0	-38.450	-46.760	-62.036	-85.728
ت	-38.450	38.450	30.140	14.864	-8.828
ك	-53.727	23.173	23.174	45.417	21.725
ب	-62.036	14.864	31.483	37.107	21.725
	-85.728	-8.828	7.791	13.415	60.799

Example: The MR between two words $A = \text{"كتاب"} ([ki-taAb])$: book and $B = \text{"كاتب"} ([kaAtib])$: writer is calculated as shown in Table 3, where the frequencies used in this example are shown in Table 4. To fill each cell in the matrix, the maximum value among adjacent cells plus the gain of the underlying operation is picked. The three adjacent cells are those on upper left corner side ($M[i-1, j-1]$), up side ($M[i-1, j]$) and left side ($M[i, j-1]$). The resulting value at the last cell $M[4][4]$ indicates the MR between the two words "كتاب" and "كاتب".

The value in the cell $M[2][2]$ is the relatedness between the two substrings "كت" and "كـ". It corresponds to a substitution of the letter "ا" ([A]: 1st Arabic letter) with "ـ" ([t]: 3rd Arabic letter). The gain $gain_{subs}("ـ", "ا")$ used to evaluate the cell $M[2][2]$ value is the inverse of the frequency of the letter "ـ", which is higher than the inverse of the frequency of the letter "ا". The gain $gain_{del}("ـ")$ uses the frequency of the deleted letter "ـ". The last gain $gain_{ins}("ـ")$ is the inverse of the frequency of the inserted letter "ـ". The value of the cell $M[2][2]$ is calculated as follows:

$$\begin{aligned} M[2][2] &= \max(M[1, 1] + gain_{subs}("ـ", "ا"), M[1, 2] \\ &\quad + gain_{del}("ـ"), M[2, 1] + gain_{ins}("ـ")) \\ &= \max(38.45 - 15.27, 30.14 - 15.27, 23.17 - 8.31) \\ &= 23.17 \end{aligned}$$

As the cell corresponds to a match the gain is a positive used to evaluate the value of $M[2][3]$ is the inverse of the frequency of the matched letter "ـ" ([t]: 3rd Arabic letter) for the three operations: matched, deletion and insertion. Because the cell $M[2][3]$ corresponds to the letter "ـ" at both $M[2]$ and $M[3]$. $M[2][3]$ is calculated as follows:

$$\begin{aligned} M[2][3] &= \max(M[1, 2] + gain_{match}("ـ"), M[1, 3] \\ &\quad + gain_{del}("ـ"), M[2, 2] + gain_{ins}("ـ")) \\ &= \max(30.14 + 15.27, 23.17 - 15.27, 14.86 - 15.27) \\ &= 45.41 \end{aligned}$$

Table 4: A sample of frequencies of Arabic letters

Letter	Count	Frequency	1/Frequency
ـ	3,546,432	-	-
ا	426,784	0.120	8.309
ت	149,688	0.042	23.692
ك	232,146	0.065	15.276
ب	92,234	0.026	38.450

V. TESTS AND RESULTS

This section firsts describes the test settings then discusses the results.

A. Test Dataset

The morphological segmentation is fed with a corpus of plain classical Arabic texts². It contains around 1M distinct (122M in total) words with an average size of 6.22 letters per word. The morphological segmentation step produced 596,356 distinct (1,116,919 in total) stems with an average size of 5.94 letters per stem. The resulting stems were then used to feed the computation morphological relatedness.

B. Performance Metrics

1) Morphological Segmentation Three samples of 100 words each are randomly picked out of the whole segmented corpus. The results of these approaches are evaluated manually by using three metrics: recall, precision and F-measure of the cutting points:

- Recall measures how many correct points are found among all the existing correct points.

$$Recall = \frac{\text{correct points in the result}}{\text{all correct points in the dataset}} \quad (10)$$

- Precision measures how many points are actually correct among all the points the algorithm found.

$$Precision = \frac{\text{correct points in the result}}{\text{all found points in the result}} \quad (11)$$

- F-measure measures the average of the recall and the precision.

$$F\text{-measure} = 2 * \frac{\text{Recall} * \text{Precision}}{\text{Recall} + \text{Precision}} \quad (12)$$

²<https://sourceforge.net/projects/classical-arabic-corpus>

2) *MR Computation Evaluation* The MR computation is ran over the whole set of stems resulting from the previous phase. For every stem, the ten others stems with the highest MRs are picked. Then two metrics are used to assess the performance of the MR computation.

- Normalized Discounted Cumulative Gain (nDCG) measures the number of related stems returned in the results and their order among all existing related stems. The higher is the nDCG, the more related and the better ordered are the results. Related stem means a stem which is derived from the same root. For this purpose, the binary value $rel(s, s_i)$ is defined, which is set to 1 when s and s_i are derived from the same root (relevant to each other) [6] and set to 0 otherwise.

$$nDCG(s) = \frac{DCG(s)}{IDCG} \quad (13)$$

where:

$$DCG(s) = rel(s, s_1) + \sum_{i=2}^k \frac{rel(s, s_i)}{\log_2(i)} \quad (14)$$

$$IDCG(s) = 1 + \sum_{i=2}^k \frac{1}{\log_2(i)} \quad (15)$$

- R-precision measures the number of related stems among all stems that appear at the k^{th} position of the returned stems. The higher is the R-precision, the better the performance is. This study supposes k is equal to 10.

$$R - precision = \frac{\sum_{i=1}^k rel(s, s_i)}{k} \quad (16)$$

C. N-grams vs Letters

The generalization of the approach to make the unit of comparison n -grams rather than letters is investigated. Three cases are tested: unigram (one letter as the original version), bigram (The unit of comparison is two letters) and trigram (three letter).

D. Noise

Typos are known to be a source of errors and a single kind of typo may influence the performance of the whole system. The study seeks to go deeper and investigate the extent of the influence of the misspellings on the performance of the MR computation. The study first runs the computation on a test set without any filtration (normal), then runs it on a test set with simple normalization rules that eliminate the effect of a number of common mistakes (Typos-free):

- "ء" ([']) confused with "ا" ([A]).
- "ى" ([Y]) confused with "ي" ([y]).
- "ه" ([h]) confused with "هـ" ([p]).

Table 5: Morphological segmentation results

	Raw	Nonempty affix	Thresholded
Precision	81.21 ± 2.76	78.73 ± 4.97	89.36 ± 5.18
Recall	48.11 ± 1.32	74.96 ± 2.44	78.69 ± 2.30
F-measure	60.62 ± 1.47	76.80 ± 2.54	83.69 ± 3.49

E. Test Process

1) *Morphological Segmentation* The three metrics are recorded on each of the three sampling settings:

- Raw: Results sample is picked randomly with no restriction.
- Nonempty affix: Samples are picked randomly only among words for which morphological segmentation has carried out at least one cutting point. For a number of words, the segmentation simply did not identify any cutting point. For most of these cases, it was because of the scarcity of the stem or stem+affix remaining combination. The study then tries to assess the impact of such cases on the performance of the segmentation and the accuracy of the identified cutting.
- Thresholded: An additional filter is applied to the nonempty affix sample, where a segmentation is picked only if the affix reappears in more than 1,000 other segmentations.

The results of the raw sample are the lowest on Table 5. The two obvious causes might be the irregularities in Arabic morphology and the typos in the test set. The latter is confirmed by results obtained when the sample is restricted to the words with a relatively high frequency (thresholded) as shown on Fig. 1.

Another reason which affects the performance is the lack of a dataset. The proposed approach works wholly with the unsupervised method and depends only on the count of words in the corpus. However, it is difficult to include all possible derivatives in the corpus. For example, the derivative "الإجحافات" ([Al-o<ij-oHaAfaAt]) the prejudices appears one time in the dataset; that is, there is no other derivative that appears in the dataset without the prefix "الـ", for instance. Indeed, the word "الـجـحـافـات" would be more dependent on the prefix "الـ" and the proposed algorithm does not learn that the prefix "الـ" can be cut off from the word "الـجـحـافـات". This problem will be removed if the word "الـجـحـافـات" is added into the dataset. The approach then finds the segmentation position "الـ"|"ـجـحـافـات".

Running the morphological segmentation over the whole corpus resulted in around 1,805,231 morphemes and 596,358 distinct morphemes with an average size of 5.94 letters per morpheme.

It is worth noting that the objective of the study is to address the classical Arabic (CA) words. To the best of the authors' knowledge, there is no suitable gold standard for CA. The study should build itself a set of words and then proceed to the manual segmentation of three different randomly picked samples for each setting.

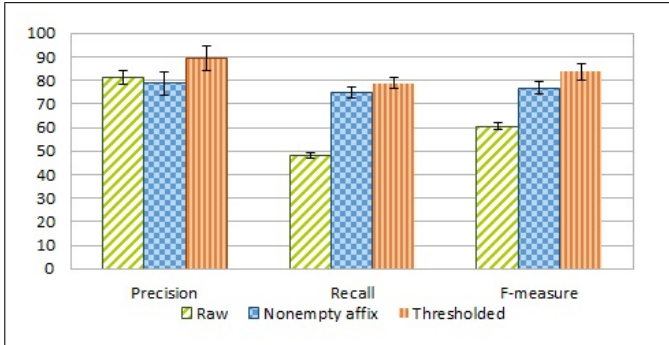


Figure 1: Results of morphological segmentation

Table 6: Morphological relatedness results

		Unigram	Bigram	Trigram
Normal	nDCG	80.38 ± 1.86	84.26 ± 1.11	81.06 ± 1.02
	R-precision	79.33 ± 1.10	81.03 ± 0.75	77.90 ± 0.60
Typos-free	nDCG	86.59 ± 0.94	87.47 ± 0.66	83.01 ± 0.15
	R-precision	83.43 ± 1.11	81.63 ± 1.25	79.03 ± 1.53

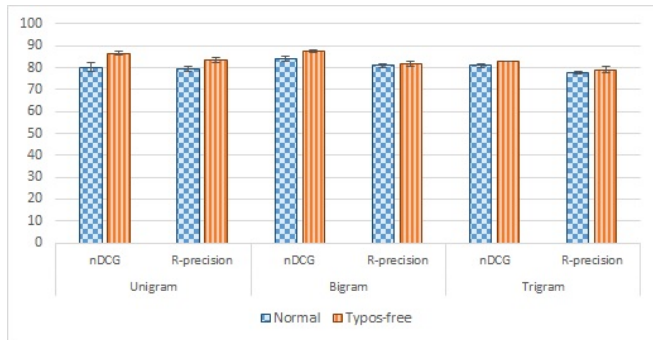


Figure 2: Results of morphological relatedness

2) *Morphological Relatedness* Obviously, checking the whole test set manually is impractical. Thus, the study opts for a sampling approach to approximate the performance. Three samples of 100 words each are randomly picked out of the whole corpus. Along with the nDGC and r-precision computed for every sample, the *average* and the *standard deviation* are recorded. This process is repeated for the different settings explained earlier.

Values in Table 6 and Fig. 2 clearly indicate a high performance of around 80% in all cases. The highest value of nDCG occurs with *bigrams* in the *typos-free* case. This confirms the utility of such simple typos handling. This also suggests that the performance might be enhanced further if a heavier typos filtration is applied.

The combination of letters in bigrams and trigrams shows positive and negative effects. The positive effect is the lowering of the frequencies, which increases the influence of the core (root) letters and widens the differences between the frequencies of the *n*-grams formed of core letters and the frequencies of the *n*-grams formed of non-core letters *n*-grams. A good distinction is then made between the two classes of letters. The negative effect occurs when the combination becomes less common and fails to capture the distinct classes. Instead, it may

mix up letters from both core and non-core letters. The results show that the bigram is a good compromise. The standard deviation is a good indication that the results are reliable.

The changes introduced to the original version [6] were fruitful and the performance increased considerably. It is worth mentioning that the evaluation reported in [6] was on the five top results. The proposed approach is in the top ten and the values are still higher. Of course, one of the factors that boosted the performance is the stemming. However, given that the stemming was also totally unsupervised, this is another proof that an end to end unsupervised method can handle a complex morphology language such as Arabic.

VI. CONCLUSION AND FUTURE WORK

The concept of the Morphological Relatedness seems promising in the area of the unsupervised processing of languages. Even more, it shows a good handling of a complex language, such as classical Arabic. The purpose of the work reported in this article was to enhance the computation of the MR originally suggested in [6] without falling into the trap of human supervision. The study is able to overcome the problem of the long prefixes and suffixes by introducing an unsupervised morpho-segmentation. The study also handles the unclear boundaries between the frequencies by extending the comparison to bigrams.

The study commits itself to keep any processing human independent and as generic as possible. The open issues are diverse, and the exploratory are numerous. A few of them are listed:

- Does the morphological relatedness perform well when generalized to upper levels such as the morphology of partially structured texts?
- Can the computation of the MR be sped up by using an index?
- Can $MR(w_1, w_2)$ be derived from $MR(w_1, w_3)$ and $MR(w_2, w_3)$?

REFERENCES

- [1] N. Habash, A. Soudi, and T. Buckwalter, "On Arabic transliteration," in *Arabic Computational Morphology*, ser. Text, Speech and Language Technology, A. Soudi, A. v. d. Bosch, and G. Neumann, Eds. Springer Netherlands, 2007, no. 38, pp. 15–22.
- [2] I. Al-Sughaiyer and I. Al-Kharashi, "Arabic morphological analysis techniques: A comprehensive survey," *Journal of the American Society for Information Science and Technology*, vol. 55, no. 3, pp. 189–213, Feb. 2004.
- [3] M. Popovic and P. Willett, "The effectiveness of stemming for natural-language access to Slovene textual data," *Journal of the American Society for Information Science*, vol. 43, no. 5, pp. 384–390, Jun. 1992.
- [4] S. Wintner, "Morphological processing of semitic languages," in *Natural Language Processing of Semitic Languages*, I. Zitouni, Ed. Berlin, Germany: Springer Berlin Heidelberg, 2014, pp. 43–66.
- [5] P. Nugues, *An Introduction to Language Processing with Perl and Prolog*. Berlin, Germany: Springer-Verlag Berlin Heidelberg, 2006, pp. 1, 7, 23, 112, 123–129.
- [6] A. Khorsi, "On morphological relatedness," *Natural Language Engineering*, vol. 19, no. 4, pp. 537–555, Oct. 2013.
- [7] S. Needleman and C. Wunsch, "A general method applicable to the search for similarities in the amino acid sequence of two proteins," *Journal of Molecular Biology*, vol. 48, no. 3, pp. 443–453, Mar. 1970.

- [8] C. Manning, P. Raghavan, and H. Schütze, *An Introduction to Information Retrieval*, online ed. Cambridge, England: Cambridge University Press, 2008, pp. 58-60.
- [9] M. Crochemore, C. Hancart, and T. Lecroq, *Algorithms on Strings*, 1st ed. Cambridge University Press, Apr. 2007.
- [10] H. Abdel Ghafour, A. El-Bastawissy, and A. F. Heggazy, "AEDA: Arabic edit distance algorithm towards a new approach for Arabic name matching," in *Proceedings International Conference on Computer Engineering & Systems (ICCES)*, Cairo, Egypt, Dec. 2011, pp. 307–311.
- [11] V. Levenshtein, "Binary codes capable of correcting deletions, insertions, and reversals," *Soviet Physics Doklady*, vol. 10, no. 8, pp. 707 – 710, Feb. 1966.
- [12] W. Gomaa and A. Fahmy, "Short answer grading using string similarity and corpus-based similarity," *International Journal of Advanced Computer Science and Applications (IJACSA)*, vol. 3, no. 11, pp. 115–121, Nov. 2012.
- [13] S. Mustafa and Q. Al-Radaideh, "Using n-grams for Arabic text searching," *Journal of the American Society for Information Science and Technology*, vol. 55, no. 11, pp. 1002–1007, Sep. 2004.
- [14] S. Mustafa, "Character contiguity in n-gram-based word matching: The case for Arabic text searching," *Information Processing & Management*, vol. 41, no. 4, pp. 819–827, Jul. 2005.
- [15] ——, "Word-oriented approximate string matching using occurrence heuristic tables: A heuristic for searching Arabic text," *Journal of the American Society for Information Science and Technology*, vol. 56, no. 14, pp. 1504–1511, Dec. 2005.
- [16] D. Hirschberg, "A linear space algorithm for computing maximal common subsequences," *Communications of the ACM*, vol. 18, no. 6, pp. 341–343, Jun. 1975.
- [17] F. Peng and D. Schuurmans, "A hierarchical EM approach to word segmentation," in *In 6th Natural Language Processing Pacific Rim Symposium (NLPERS2001) Shai Fine, Yoram Singer, and Naftali Tishby*. 1998, 2001, pp. 475–480.
- [18] M. Melucci and N. Orio, "A novel method for stemmer generation based on hidden markov models," in *Proceedings of the twelfth international conference on Information and knowledge management*. ACM, 2003, pp. 131–138.
- [19] K. ur Rehman and I. Hussain, "Unsupervised morphemes segmentation," 2005.
- [20] M. Creutz and K. Lagus, "Unsupervised models for morpheme segmentation and morphology learning," *ACM Transactions on Speech and Language Processing*, vol. 4, no. 1, pp. 1–34, Jan. 2007.
- [21] S. Keshava and E. Pitler, "A segmentation approach to morpheme analysis," in *Working Notes for the CLEF Worksh 2007*, Hungary, 2007, pp. 1–4.
- [22] D. Bernhard, "Simple morpheme labelling in unsupervised morpheme analysis," in *Advances in Multilingual and Multimodal Information Retrieval*. Springer, 2008, pp. 873–880.
- [23] S. Bordag, "Unsupervised and knowledge-free morpheme segmentation and analysis," in *Advances in Multilingual and Multimodal Information Retrieval*. Springer, 2008, pp. 881–891.
- [24] O. Eroglu, H. Kardes, and M. Torun, "Unsupervised segmentation of words into morphemes," 2009.
- [25] H. Poon, C. Cherry, and K. Toutanova, "Unsupervised morphological segmentation with log-linear models," in *Proceedings of Human Language Technologies: The 2009 Annual Conference of the North American Chapter of the Association for Computational Linguistics*. Association for Computational Linguistics, 2009, pp. 209–217.
- [26] H. Hammarström and L. Borin, "Unsupervised learning of morphology," *Computational Linguistics*, vol. 37, no. 2, pp. 309–350, 2011.
- [27] J. Naradowsky and K. Toutanova, "Unsupervised bilingual morpheme segmentation and alignment with context-rich hidden semi-Markov models," in *Proceedings of the 49th Annual Meeting of the Association for Computational Linguistics: Human Language Technologies-Volume 1*. Association for Computational Linguistics, 2011, pp. 895–904.
- [28] B. Can and S. Manandhar, "Methods and algorithms for unsupervised learning of morphology," in *Computational Linguistics and Intelligent Text Processing*. Springer, 2014, pp. 177–205.
- [29] R. Falk and M. Bar-Hillel, "Probabilistic dependence between events," *The Two-Year College Mathematics Journal*, vol. 14, no. 3, pp. 240–247, Jun. 1983.

FNN based Adaptive Route Selection Support System

Saoreen Rahman
Institute of Information Technology
Jahangirnagar University
Dhaka-1342, Bangladesh

M. Shamim Kaiser
Anglia Ruskin IT Research Institute
Anglia Ruskin University
Chelmsford, UK

Mahtab Uddin Ahmmmed
Dept. of Mathematics
Jahangirnagar University
Dhaka-1342, Bangladesh

Abstract—This paper presents Fuzzy Neural Network (FNN) based Adaptive Route Selection Support System (ARSSS) for assisting drivers of vehicles. The aim of the proposed ARSSS system is to select path based on shortest possible time. The proposed system intakes traffic information, such as volume to capacity ratio, traffic flow, vehicle queue length and green cycle length, passenger car unit etc using different types of sensor nodes, remote servers, CCTVs and the road information such as path length, signalized junctions, intersection points between source-destination pair are captured using GPS service. A FNN has been employed to select an optimal path having shortest time. The input parameters of FNN are distance, signal point delay, road type and traffic flow whereas the output parameter is path selection probability which paves the way to identify the best suitable path. The simulation result revels that FNN based ARSSS outperforms more accurate than that of other route selection support system (webster delay model) and artificial neural network (ANN) in estimating path delay.

Keywords—GPS; Fuzzy Neural Network; Path delay; Signal Point Delay; Webster Delay Formula

I. INTRODUCTION

With the increase of metropolitan cities, traffic scenario has become more complex and heavily congested. The road traffic of metropolitan city includes different vehicle types, lane or non-lane base communication, signal points, cross-sections and so on, which introduces long traffic delay. It is a universal truth that people always want to reach their destination in shortest possible time. This human nature introduces the need of an Adaptive Route Selection (ARS) technique, which allows to discover the optimal route between a source-destination pair. An Adaptive Route Selection Support System (ARSSS) assists vehicles to find out the shortest distance path as well as shortest time path for a source-destination pair.

The estimation of traffic delay is one of major requirements for the establishment of ARS technique. There are two major types of traffic delay known as congestion delay and propagation delay. Propagation delay is a unit delay which depends on the path length and its corresponding speed. On the other hand, congestion delay is a random delay depends on various factors such as signalized junction, passenger car unit (PCU), queuing length, cycle length etc. Estimating these types of delay becomes more complicated for metropolitan cities as they include heterogeneous traffic environment [1][2].

Considering heterogeneous traffic environment, researchers have proposed variety of approaches. However, Most of the available delay estimation technique is used for homogenous

traffic environment. But for heterogeneous traffic environment, more feasible, dynamic and real-time approaches should be considered. Keeping in mind of heterogeneous traffic environment, the introduction of artificial intelligence in this research field is more appreciated [3]. Fuzzy Neural Network (FNN) is suitable for uncertain or approximate reasoning which is capable of estimating solutions under certain information. FNN approach also makes a system more adaptive and reliable. As metropolitan cities include heterogeneous traffic environment, FNN is more applicable for traffic delay estimation and optimal route selection between a source-destination pair due to it's nature of adaptivity and flexibility. FNN based ARSSS has the capability of training and learning itself using expert knowledge system and making dynamic result for a source-destination pair.

A well known metropolitan city in Asian subcontinental region is Dhaka, capital of Bangladesh. Unlike other metropolitan cities, Dhaka also includes heterogeneous traffic environment. It needs to maintain non-lane based traffic environment with variety of traffic vehicles. It also supports different types of transportation with low traffic capacity and unstructured road map [4]. Under such circumstances of the city Dhaka, FNN based route selection support system can make its people capable of traveling between a source-destination pair in shortest possible time.

The motivation of the proposed work is to represent a concurrent ARSSS system which is well suited for heterogeneous traffic environment for Dhaka [23]. It intakes route map and traffic information dynamically, delivers optimal possible routes to its user between a source-destination pair. However to identify optimal route with minimum estimated time delay, all kinds of delay needs to be considered for all available routes between a source-destination pair. In a nutshell, it can be said that, the identification of optimal path considers not only distance factor but also time factor which can aid to a more adaptive system of route selection.

In this paper, a FNN based ARSSS is introduced. The proposed system consists of a centralized server, some remote servers which contain DBs, numerous sensors, CCTVs which collect road traffic information and GPS receivers to get latitude longitude information of source-destination points. When a driver submits route selection submits their request to the corresponding server and wait for the result. Here, GPS service is used for determining route information such as coordinates of source-destination points, path length, cross sections, signalized junctions, intersection points etc [5]. Path delay estimation

is a major portion for optimal path identification. To calculate them a classic statistical model is used. To determine a route as an optimal solution FNN is used. It takes various information as input parameters, process them, estimates optimal route and generates the optimal path as output result. In this regard, to train FNN, hybrid learning algorithm is used which makes the performance of FNN more acceptable and realistic.

Based on the above conditions and by considering real time traffic data, the proposed system delivers the best available path which requires least travel time for a specified source-destination pair for its user.

The rest of the paper is organized as follows. Related works have been reviewed in Section II. System model is presented in Section III. System architecture is included in Section IV. Simulation and results are discussed in Section V. Finally our work is concluded in Section VI.

II. RELATED WORKS

In modern road traffic system the most focused problem is efficient and fastest path selection on a busy road. Time that is needed to travel between a source-destination pair, depends on various factors that affects the travel time. Such kinds of affect can be considered as car speed, intersection delay, signalized junction, lane capacity, heterogeneous traffic environment, path distance, queuing length etc. Moreover these factors kill valuable time of passengers [6]. For the above circumstances people have to choose the appropriate path directions from source to destination so that they can reach their destination in time. Efficient route selection system generally considers minimum delay time within source and destination. In a highly populated area one of the most important points of roads and streets are signalized junction. To calculate signalized junction some common measurements are considered like average delay per PCU, cycle length, PCU, green signal ratio, degree of saturation etc. within a path from source to destination [7].

By using deterministic queuing analysis, F. V. Webster, developed a series of traffic theories. His proposal included a statistical regression based model for delay estimation that is experienced by researchers at under saturated signalized intersections. Generally transportation professionals use vehicle delay as a parameter to observe the performance of signalized intersection. Due to random arrival of vehicles (Car, Bus, Mini Bus, Bus, Two-Wheelers) delay estimation is more complex, several populated models have been proposed to handle this complex issue [8] [9].

Among various traffic models, the most well-known model was developed by Miller and Akcelik in Australia [10], which used in HCM model in United States [11] and the model developed by Telyp in Canada [12]. These models are logically superior to Webster's classical model because they can successfully deal with over saturated conditions and homogeneous traffic behaviours.

G.K.H. Pang, K. Takabashi, T. Yokota, proposed an approach named as adaptive route selection for dynamic route guidance system based on fuzzy-neural approaches [37]. In 2005, "Heuristic shortest path algorithms for transportation applications" has been proposed which was a survey review of various heuristic shortest path algorithms for traffic network

[13]. In 2007, Lefebvre and Balmer proposed an approach that computes a time-dependent shortest path for traffic network [14]. In 2010 and 2014, two different shortest path algorithms "Floyd algorithm" and "Dijkstra algorithm" were proposed [15] [16]. They optimized these algorithms to identify shortest path within specific nodes for various traffic networks. Gutsenschwager, Axel Radtke, Volker and Zeller compared different approaches for traffic networks. They also implemented a model for automatic routing of vehicles [17]. In 2013 ANN based Short term traffic flow prediction for a non urban highway was proposed. In these paper author used past traffic data for short term traffic flow prediction [38]. In 2014 a work has been proposed that introduced highway dimensions and efficient shortest path algorithms [18]. For transportation in 2015 a route planning approach has been proposed which considered various techniques for identifying travel time delay within a particular source and destination [19].

However, most of these models are primarily focused on highways and systematic traffic systems that do not generally account with mixed-speed vehicles and multi-lane systems. These models are not suitable enough for a crowded metropolitan city like Dhaka, the capital of Bangladesh, where travellers experience difficulties in multi-lane roads due to chaotic nature of mixed-speed, as well as mixed-type, traffics and not so systematic traffic-controlling mechanisms. To address this problem, Hoque and Imran modified the Webster delay model to make it usable under non-lane based mixed road traffic condition [10]. The model has been calibrated to form a "Modified Webster Delay Formula", which was subsequently validated by comparing the expected delays with observed delays.

In 2009, Chu Cong, Tran Hoai, Tran Thanh and Kazushi proposed an expectation function and Taylor series for Webster formula that estimate delay at pre-timed signalized intersections under heterogeneous traffic conditions [21]. In 2014, Hadiuzzaman, Mizanur, Tanweer and Ahsanul developed heterogeneous traffic model at signalized intersection. Based on field measurement they provide a regression analysis which measures the accuracy of traffic models considering the traffic scenario of Dhaka City [22]. The work of [23] presents a traffic information based adaptive route selection support system by offering a model that helps to calculate the minimum delay for a particular source to destination according to the google map.

Some traffic model designers consider FNN approach as an adaptive solution for route selection. Now-a-days, for the establishment of an ARSSS, FNN have considered one of the most eligible technique for implementing an intelligent route selection support system [1] [26]. In 2011, a bio-inspired integrated with FNN introduced a dynamic route selection system [27]. Following that year, a PSO based dynamic shortest path algorithm using fluid neural network was proposed. That approaches were especially applicable for stochastic traffic network [28]. After few years later, a hybrid optimization algorithm has been proposed which introduced ASO and FNN for better result [29]. A work of ANN based road traffic accidents prediction was introduced in 2014. This work is accomplished based on Jordan [36]. In 2014, R. Yasdi proposed an approach that predicts road traffic using neural network [39]. In 2015, a passenger route selection model

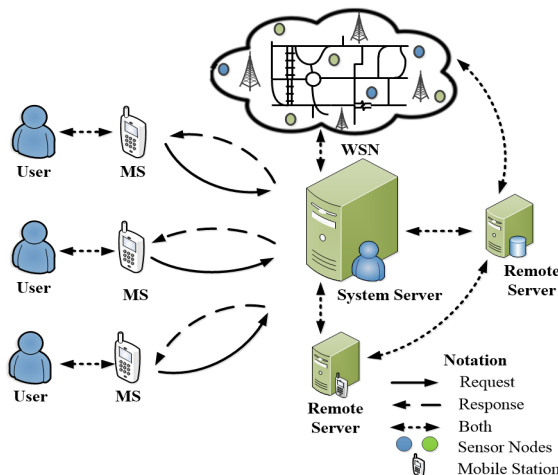


Fig. 1. System Model Scenario.

has been proposed by Fatma Al-Widyan, Nathan Kirchner, Michelle Zeibots [40]. From 2010 to 2016, several FNN based approaches have introduced in work [33][34][35].

In this paper, we use the proposed model scheme of [23] for more realistic modeling of FNN based route selection support system for Dhaka, Bangladesh.

III. SYSTEM MODEL

This section describes the system model, work flow and formulation of the ARSSS.

Figure 1, shows the system model of ARSSS. The entire system can be considered as a real-time client server approach. ARSSS includes users, system server, several remote servers and Wireless Sensor Network (WSN). It uses variety of information which are collected from GPS, CCTVs and others existing real-time remote servers. ARSSS also captures data from sensor nodes which are supported by WSN. The system server takes service request from its client via smart device (mobile phone), generates the result of the service and responses back to its requesting client. In another word, for a source-destination pair, the proposed ARSSS takes predefined features as inputs from its user, processes them using captured information and delivers the best available path as output. The main aim of the proposed system is to define an optimal route among several possible routes between a source-destination pair. Thus, the scenario shown in figure 1, is considered to provide the shortest distance path as well as shortest time path which is optimal path between a source-destination pair.

A. System Work flow

In this paper, a heterogeneous traffic environment is considered which includes mixed-speed, mixed-type vehicles and multi-lane road structure. The work flow of the proposed system is shown in Figure 2.

At the very beginning, the proposed system considers user preference, denoted by Φ , and source-destination pair, denoted by $(s; d)$, as inputs which is defined by users. Φ offers users to declare the presence of priority for a particular route between a source-destination point. Whereas, the other input, $(s; d)$ offers

users to declare the source-destination names or locations. That is, $(s; d)$ takes GPS coordinates (latitudes, longitudes) of user defined source-destination pair. Moreover, each user provides position and movement information to the corresponding server in background mode using GPS. After having basic information (latitudes, longitudes, user-preference) captured from user, it runs query to other information holder nodes (servers, other users, sensor nodes) for capturing other information to generate optimal route between two predefined nodes. A volatile storage is maintained to store concurrent data for the upcoming calculation. After capturing input parameters, a pre-decision phase is considered. Next, based on the decision of previous phase, data per-processing phase is performed. Regarding source destination points it calculates all possible delays for all possible routes using GPS map. After completion of data pre-processing phase, FNN controller identifies an optimal route between a source-destination pair. After that, path identification phase is performed. This phase considers the resulted route of previous phase as the optimal route and declares it as the best one. Finally, the proposed system delivers the identified optimal route to its user and stores the solution for further usage.

B. Initial Decision Method

Initially, the proposed system takes user preference Φ and source-destination points $(s; d)$ these two major parameters as input from the user. To identify an optimal path for a particular location, user must have to define specific source-destination point. Using GPS coordinate service the latitudes and longitudes of user defined source and destination points are determined [30] [31][32]. Therefore, $(s; d)$ input parameter can be functioned as:

$$s = (lat_s, long_s) \quad (1)$$

$$d = (lat_d, long_d) \quad (2)$$

Here, s and d are considered as source-destination locations whereas lat and $long$ are considered as latitude and longitude coordinate values of a source-destination point.

Another major consideration as input parameter is user preference, denoted by Φ which can be declared as

$$\Phi \in [0, 1] \quad (3)$$

Here, $\Phi = 1$ means user declares high level of user preference in choosing route between source-destination pair; $\Phi = 0.5$ means user has confusion in choosing route between source-destination pair and $\Phi = 0.0$ means user has no preference in choosing route between source-destination pair.

If Φ results in high level of user preference then the selected route chosen by the user will be considered as the best path. In this case, no further calculation and decision making is required. For the other two cases the proposed system will calculate total delay time for each possible route and propose a reliable decision by identifying the optimal path between a particular source-destination point. To generate and identify the optimal route several phases have been considered which have been discussed in the upcoming sections.

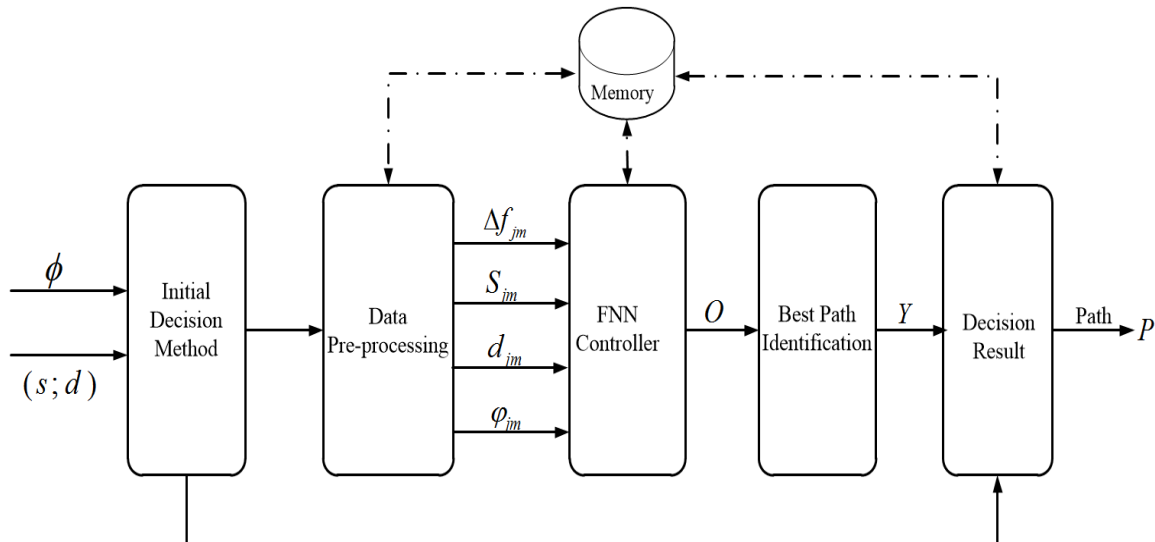


Fig. 2. System Work flow.

C. Data Pre-processing

These phase performs two major activities in optimal path selection process. First one is capturing all necessary information that are required to determine optimal path for a source-destination pair. It collects concurrent usable information from the user in background mode using GPS[30] [31]. It also runs query to other nodes to get required information for further calculation for optimal route selection. All information captured by this phase are memorize and updated in a volatile storage.

And second one is performing delay calculation for all possible routes between a source-destination pair using GPS map. To calculate the total delay time from a particular source-destination pair *straight path delay*, *cross section delay* and *signal point delay* is considered. The *straight path delay* is the time that needed to cover a specific distance. The *cross section delay* is the time that a vehicle takes to cross a crossing-point intersection. The *signal point delay* is the time which is required at a signalized junction [23] [24] [25]. It also considers road type and traffic flow calculation used in FNN controller.

1) *Path Delay*: Path delay includes both *straight path delay* as well as *cross section delay*. It considers path distance along with referred path speed both for straight path and a cross-section point. If j -th route with m branches is chosen to cover the distance d_{jm} with average speed v_{jm} , then the *path delay* can be denoted by D_{jm} and defined as:

$$D_{jm} = \sum_{m=1}^m d_{jm}/v_{jm} \quad (4)$$

Where, $j, m \in \mathbb{R} : \mathbb{R} \leftarrow \text{real_numbers}$.

2) *Signal point Delay*: *Signal point delay* refers the average delay per vehicle at a signalized junction of a particular route with several existing branches. In this paper, *signal point delay* calculation is considered in two steps. First one is the calculation of delay time for a particular signalized intersection

followed by modified Webster Delay Model. Another one is variance calculation for delay time in a particular signalized intersection followed by Taylor Series. The estimated time for signal point delay for j -th route with m branches, can be expressed as:

$$t_{jm} = \xi + \Delta_T \quad (5)$$

t_{jm} calculates congestion delay time at a signalized junction. It includes two basic terms such as ξ = Average delay time. Δ_T = Variance of delay time.

In Equation (17), First term ξ denotes average delay calculation for a signalized junction and second term Δ_T denotes variance of signal point delay for that particular signalized junction.

Average delay time is considered in the first term. This paper uses the modified *Webster delay model* which is discussed in [10]. Therefore, the average delay time at any signalized junction is denoted by ξ . It can be calculated by the following equation.

$$\xi = \frac{c(1 - \lambda)^2}{2(1 - \lambda x)} + \frac{x^2}{2v(1 - x)} + \rho \quad (6)$$

Where,

c = Cycle length of green signal. v = Vehicle flow rate (Passenger Car Unit/hour). λ = Effective green ratio. x = Degree of saturation (volume to capacity ratio).

In Equation (6), the first term represents the average delay to the vehicles assuming uniform arrivals. The second term represents the additional delay due to the random arrivals. The third term is a semi-empirical adjustment term used to maintain accuracy for specific field conditions of vehicle arrivals. The modified Webster delay formula is used to estimate signalized intersections for non-lane based heterogeneous traffic conditions.

The expression for delay, given by Equation (6) was not

derived entirely theoretically. The first and second terms have a theoretical meaning, but the last one is purely empirical. The modification of Websters delay model under non-lane based heterogeneous traffic condition can be measured by adding an empirical adjustment term with first two theoretical terms.

Paper [10] introduced an adjustment term specified for heterogeneous traffic conditions like as dhaka city. In Equation (6) the adjustment term is denoted by ρ . According to the modified Webster delay model, the adjustment term, ρ , can be expressed by,

$$\rho = \alpha_0 + \alpha_1 q + \alpha_2 c + \alpha_3 x + \alpha_4 \lambda + \alpha_5 \eta \quad (7)$$

Where, α_0 = Constant term in the model. α_j = the weighted coefficient for corresponding term.

The equation (7) adjusts the validity of the Webster delay model for Dhaka city with some measurement of field observations. This correction term is taken for best suited local road situation and it dependents on all the previous variables which is unique for non-lane based road traffic and can be measured from field observation data.

Variance of delay time is measured in the second term . The term variance is considered which is followed by *Taylor Series*. For non linear function $Y = f(X)$, the *Taylor Series*(1979) is,

$$Y = f(\mu_x) + (X - \mu_x) \frac{d^2 f}{dX^2} + \frac{1}{2}(X - \mu_x)^2 \frac{d^2 f}{dX^2} \quad (8)$$

Where, μ_x = Mean value. X = Random variable.

The expected value can be derived by the the second order of Taylor Series.

$$E(Y) = \frac{1}{2}Var(X) \frac{d^2 f}{dX^2} \quad (9)$$

Where, $Var(X)$ = the variance of X and estimated by,

$$Var(X) = E(X^2) - \mu_x \quad (10)$$

Here, $E(X^2)$ = the expectation value. μ_x = Mean of x .

The variance of $Y = f(X)$ can be expressed as:

$$\begin{aligned} Var(Y) &= Var(X) \left(\frac{df}{dX} \right)^2 - \frac{1}{4} Var(X)^2 \left(\frac{d^2 f}{dX^2} \right)^2 \\ &\quad + E((X^2) - \mu_x)^3 \frac{df}{dX} \frac{d^2 f}{dX^2} \\ &\quad + \frac{1}{4} E((X^2) - \mu_x)^4 \left(\frac{d^2 f}{dX^2} \right)^2 \end{aligned} \quad (11)$$

The expectation function method is an analytic procedure to overcome shortcomings of estimation procedure. It uses estimate functions which depends on random variable X . In this study, for the modified Webster delay model, the degree of saturation x is considered as random variable.

Considering Taylor Series, Δ_T calculates the variance of delay time for modified Webster Delay model. It indicates how far measured delay time can spread out for particular signalized intersection point. In another word, variance calculates the saturation for estimated value and measured delay time value.

Thereby, Δ_T , can be expressed as,

$$\Delta_T = 1/2p_{xj}q_{xj} \quad (12)$$

Here,

$$p_{xj} = \frac{c(1 - \lambda)^2 \lambda^2}{(1 - \lambda x)^3} \quad (13)$$

and

$$q_{xj} = \mu_x^2(1 + CV^2) - \mu_x \quad (14)$$

Where, CV = Covariance of correlation. μ_x = mean of degree of saturation, x .

Equation (6) is used to calculate delay time for a signalized junction. And Equation (12) is used to calculate the variance of estimated delay time for that particular signalized junction. Thus, Equation (17) calculates signal point delay for a particular signal point intersection.

Therefor, the total delay time for m branches at different signal point can be expressed as:

$$S_{jm} = \sum_{m=1}^m t_{jm} \quad (15)$$

Total Delay Calculation: Total delay for an individual path with m branches for a source-destination pair can be expressed as:

$$\tau_{jm} = D_{jm} + S_{jm} \quad (16)$$

Where, D_{jm} = path delay for branch m of j -th route. S_{jm} = signal point delay for branch m of j -th route.

By using Equation [15] the total delay time of a particular path for a source-destination pair can be measured. It consists of two distinct terms. By using Equation [3], first one calculates all path delay for a particular path. And the last one calculates signal point delay of all signalized junctions for that specific route/path followed by Equation [14].

3) Road Type: Road type parameter considers route category as an express way or high way. As express way requires travel payment, less vehicles prefer to use that route. However, some public transports and private vehicles wish to travel on that route. On the other hand, highway does not require any travel payment which is usually preferable by all types of vehicles. Thus, it can be considered that express way has more traffic flow than that of high way. That is, high way includes more vehicles than that of express way. Therefor, road type parameter for route j -th with branch m denoted as φ_{jm} can be defined as φ_{jm} , which is considered as:

$$\varphi_{jm} = \begin{cases} 1 & jm \in express_way \\ 0 & else \end{cases} \quad (17)$$

4) Traffic Flow: Traffic flow parameter is regarded as traffic load for a particular path with several branches. To identify the optimal path, selection of branches with shortest delay time is equivalently important. Traffic flow defined as Δf_{jm} considers difference between inward vehicle flow, $\zeta_{jm_{in}}$ as well as outward vehicle flow, $\zeta_{jm_{out}}$ of a particular route. Thus, the higher the traffic flow, the high the possibility of traffic load and the lower the traffic flow, the lower the possibility of

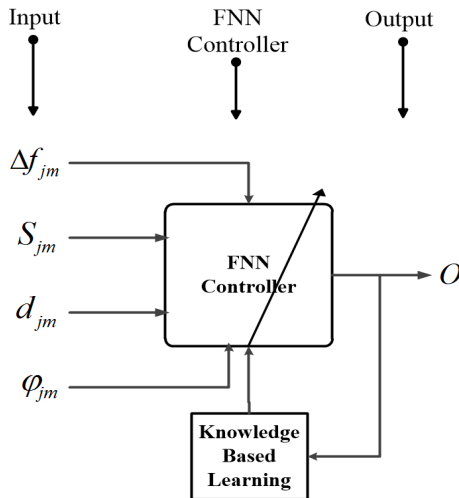


Fig. 3. Block Diagram of FNN_Controller Module.

traffic load. Therefore, the system selects that branch which includes least most traffic flow as well as traffic load. Traffic flow, Δf_{jm} for route j with branch m , can be considered as below:

$$\Delta f_{jm} = \zeta_{jm_{in}} - \zeta_{jm_{out}} \quad (18)$$

D. FNN Controller

In this section we discuss the phase named FNN controller.

1) Block Diagram of FNN Controller Module: These controller uses FNN approach for ARSSS. It includes fuzzy neural network for decision making to identify optimal route. FNN controller takes distance denoted as D_{jm} , signal point delay denoted as, S_{ij} , traffic flow denoted as Δf_{jm} and road type φ_{jm} as input parameters and performs fuzzification-defuzzification calculation and generates the best suitable route between a source-destination pair. Block diagram of FNN controller module is shown in figure 3.

E. General Structure of FNN Controller

Figure 4 shows the general structure of FNN controller for ARSSS. The Fuzzy Neural Network, i.e., FNN model, maps the inputs using input membership function (preceding parameters) into the output using output membership function (consequent parameters). Based on the input features the FNN controller generates the probability of route selection for a source-destination pair. Both the preceding and consequent parameters are adjusted via the learning process. The hybrid of back propagation and least square estimation are used. Based on the chosen error criterion (which is the sum of squared difference between actual and desired outputs), the FNN changes the input and output membership function parameters. Considering our case, FNN is a five-layers fuzzy neural network that simulates the working principle of a fuzzy inference system. The linguistic nodes in layer one and four represent the inputs and output linguistic variables, respectively. There are four input parameters which are X_1 as D_{jm} (distance), X_2 as S_{ij} (signal point delay), X_3 as Δf_{jm} (traffic flow) and X_4 as φ_{jm} (road type). These four input parameters results

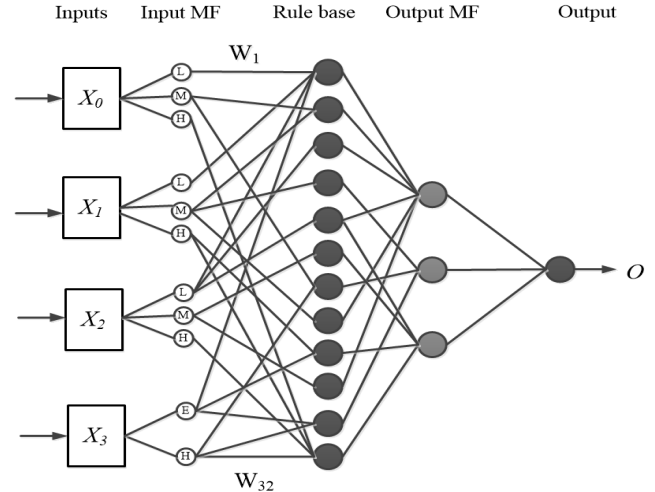


Fig. 4. General Structure of FNN Controller.

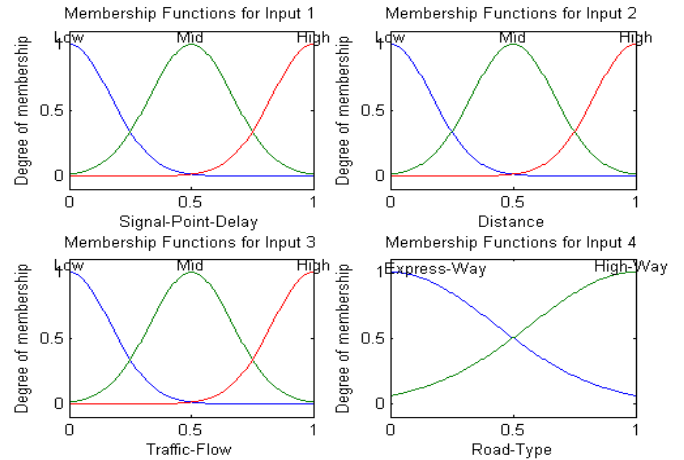


Fig. 5. Membership functions for all input parameters.

in a single output which is path selection probability denoted as O . Nodes in layers two acts as membership functions for input variables and the membership function used in FNN is generalized gaussian membership function. It can be noted that, first three input parameters includes three membership functions whereas the last one includes only two membership functions. Each neuron in the third layer represents one fuzzy rule. FNN used in ARSSS includes 32 fuzzy rules. Here, The third Layer normalizes the strength of all the rules whereas the forth layer used gaussian membership membership function to aggregated results which are forward to the output layer as path selection probability, O .

1) Membership Function for all Inputs: Figure 8 shows four individual plots of membership functions for all input parameters. Figure 8-(a)(b)(c) include fuzzy set [Low, Medium, High] which is applicable for D_{jm} (distance), S_{ij} (signal point delay), Δf_{jm} (traffic flow) these three input parameters. Whereas, Figure 8-(d) includes fuzzy set [Express way, High way] which is only applicable for input variable φ_{jm} (road type) from input layer. All the membership functions were derived from the fuzzy set of input parameters where gaussian

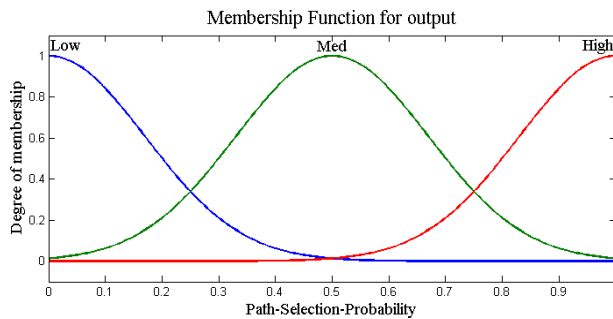


Fig. 6. Output membership function.

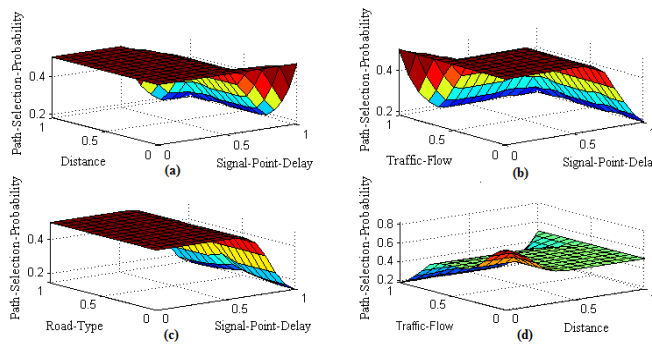


Fig. 7. Surface view of rule base system.

membership function is adopted for transforming the crisp input into linguistic level.

2) Membership Function for Output: Figure 9 shows membership function for output parameter path-selection-probability, O . It includes fuzzy set [Low, Medium, High]. The output membership function is derived by output fuzzy set. When a route holds all features of a best path then the probability of that path selection is high. Otherwise it is low or medium based on the features that it holds. Here, gaussian membership function is considered for output membership function.

3) Surface View: Figure 10 shows four individual plots of surface view of input-output parameters for the proposed system. Here, Both $x - axis$ and $y - axis$ represent input parameters whereas $z - axis$ represents the output parameter. Figure 8-(a) shows the surface view of input parameters signal point delay, distance with output parameter path selection probability, O . Followed by figure 8-(a), 8-(b)(c)(d) show the surface view of input parameters between traffic flow, signal point delay; road type, signal point delay and traffic flow, distance with output parameter path selection probability.

F. Best Path Identification and Decision Result

This phase takes the output of FNN controller. After completing activities of FNN controller, these phase captures the output O (path selection probability) which declares the probability of each available routes between a source-destination pair. It takes that probability result, identifies an optimal route denoted by Y , which includes shortest path delay as well as shortest time delay. At the end of this phase, best suited

path P is defined and send back to its user as a solution of system query. Once a solution is declared for a specific source-destination pair, the resulted optimal path is stored in memory and being updated or modified while it is needed.

IV. SYSTEM ARCHITECTURE

In this section we present the system architecture of our proposed system. First we present an algorithm that supports our system for generating the best possible result. Then we discuss the block diagram of FNN controller which performs decision making of path selection for the proposed adaptive scheme.

A. Algorithm

In this section we propose an algorithm that declares the procedure, step by step, to identify best path between a source-destination point. The algorithm used in our proposed scheme is presented in Algorithm 1

V. SIMULATION AND RESULTS

In this section we discuss the simulation environment used for our proposed adaptive system, and also the results estimated by the scheme. Here, the simulation model is created using MATLAB. For a user-defined source-destination pair, necessary data is fed to model and result is generated to get the most optimum choice of route.

A. Simulation Parameters

The simulation parameters used in ARSSS is given in Table I. For simplicity, we assume that the source-destination pair is fixed, e.g. the source-destination pair in Figure 1 for Panthaphat (23.7515; 90.3861) and Shahbagh (23.7381; 90.3953) in Figure 2 respectively. For a route, our proposed scheme takes all necessary parameters as inputs from the database. The values of different input parameters are varied within a range to analyze the effect of different road and traffic condition. From Table I, d_{jm} and v_{jm} are used for calculating path delay and the remaining parameters are used for signal point delay calculation. Any values that are not shown in the Table I are directly acquired from [10].

B. Simulation Analysis in Route Selection

In this section we discuss the simulation environment for optimal route selection. For the required timing estimation, we consider seven available paths as described in section IV-A using the parameters from Table I. Several parameters are also varied to analyze the impact of different traffic load and road condition.

1) Effects of traffic load: Figure 8 shows the effect of traffic on the seven paths between source-destination pair as described in Section III. It has been found that the delays are different for different paths as the total distances are different. The time delay is proportional to distance if there is no traffic. But the delay changes based on the traffic saturation on the path as greater traffic hinders the movement and slows down average speed and thus increasing the required time. This calculation includes traffic delay for straight paths, cross section points and signal points.

Algorithm 1: Best Path Selection Algorithm

Input:

$(s; d)$ // Source Destination Point

Φ // User Preference

begin

```

1   if ( $\Phi \neq \text{MAX}$ ) then
2       for  $j \leftarrow 1$  to  $(n)$  do
3           for  $m \leftarrow 1$  to  $(m)$  do
4                $S_{jm} \leftarrow \text{signal\_point\_delay}(c, q, x, \lambda, \eta, \alpha_i)$ 
5                $D_{jm} \leftarrow \text{path\_delay}(d_{ij})$ 
6               Return  $S_{jm}, D_{jm}$ 
7           End for
8       End for
9       Input  $S_{jm}, d_{jm}, \Delta f_{jm}, \varphi_{jm}$ .
10      Load  $\text{dataset}_{train} \leftarrow$  data set for training FNN.
11      Load  $\text{dataset}_{test} \leftarrow$  data set for testing FNN.
12      Train FNN on  $\text{dataset}_{train}$  using hybrid learning
13      algorithm.
14       $FNN\_Layer$  // No. of FNN Layers
15      for  $k \leftarrow 1$  to  $(FNN\_Layer)$  do
16          Compute  $O_i$  using equation [16] [17] [18]
17          Return  $Y \leftarrow O_i$ 
18      End for
19      Test FNN on  $\text{dataset}_{test}$  using back propagation
19      algorithm.
20      Select Path  $P \leftarrow Y : Y \in O_i$ 
21      Return Path  $P$ 
22  else
23      Select Path  $P \leftarrow \text{null}$ 
24      Return Path  $P$ 
End if
end

```

Output: Best Path P

TABLE I. PARAMETERS OF STRAIGHT PATH DELAY, CROSS SECTION DELAY AND SIGNAL POINT DELAY

Parameter	Value
d_{jm}	[0.5–2.2] km
d_{jm}	[40, 50, 60] kmh^{-1}
c	540 sec
q	1 (PCU/sec)
x	0.20-0.28
η	0.30
λ	<1
α_0	0.19-0.22
α_i	0.2-0.5
Δf_{jm}	0.5-0.20

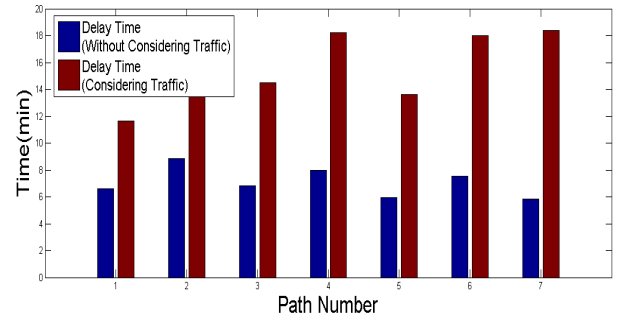


Fig. 8. Effects of S-D paths distance with or without traffic on path delay

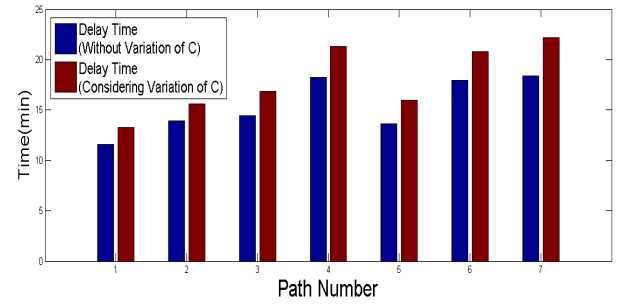


Fig. 9. Effect of cycle length on path delay

TABLE II. TOTAL PATH DELAY

j^{th} Path	D_{jm} (minute)	S_{jm} (minute)	τ_{jm} (minute)
1	6.67	4.94	11.61
2	9.08	4.84	13.93
3	7.00	7.45	14.47
4	8.15	10.06	18.23
5	6.08	7.55	13.64
6	7.74	10.33	17.97
7	5.81	12.58	18.39

2) *Effects of Cycle Length:* Figure 9 shows the effect of cycle length on the seven paths between source-destination pair. The illustration shows that cycle length has direct effect on the path delay. It is additive to total delay.

3) *Effects of Degree of Saturation:* Figure 10 shows the effect of degree of saturation on the seven paths between source-destination pair. It has been found that the degree of saturation has negligible effect on the total path delay, when considering large saturated traffic in the metropolitan area.

4) *Route Selection:* Table II shows the required time for traveling from source to destination via seven paths. Based on the given parameter, our proposed scheme chooses *Path1* to be the best one in terms of minimum time required to travel. It should be noted that both straight path delay and signal point delay play the major role in final path delay whereas cross section delay may be neglected upto a certain magnitude. Based on this result further adjustment can be made in route selection as well as in the overall traffic system.

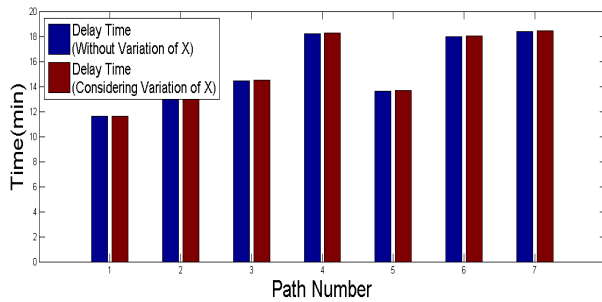


Fig. 10. Effect of degree of saturation on path delay

TABLE III. PERFORMANCE ANALYSIS OF OUTPUT RESULT

Path	Actual Output	Estimated Output	ANN Approach	FNN Approach
1	13.20	11.61	11.58	11.50
2	16.00	13.93	13.80	13.60
3	17.17	14.47	14.31	14.20
4	23.53	18.23	18.10	17.90
5	16.56	13.64	13.80	13.60
6	19.58	17.97	17.80	17.60
7	19.25	18.39	17.50	17.40

TABLE IV. ERRORS IN OUTPUT RESULT ESTIMATION

Path	ANN Approach	FNN Approach
1	0.14	0.01
2	0.16	0.02
3	0.2	0.019
4	0.3	0.018
5	0.2	0.00
6	0.1	0.021
7	0.1	0.057

C. Performance Analysis

In this section we discuss performance analysis of our proposed system in. Table III shows the time delay of actual output without any intelligent system, estimated output by Webster delay model, ANN approach and FNN approach. It has been found that the proposed FNN outperforms the all the other mentioned methods. Table IV shows the error is the delay estimator. It has been found that the accuracy of the FNN approach is higher than that of the ANN approach.

VI. CONCLUSION

This paper presents an ARSSS for a source-destination pair under heterogeneous traffic environment. The Dhaka city is considered to validate the proposed model. ARSSS includes different phases such as initial decision method, data pre-processing, FNN controller and best path identification for a particular source-destination pair. FNN controller takes source-destination pair distance, signal point delay, traffic flow and road type as input parameters and selects best path for a

particular source-destination pair. These input parameters are captured by distributed wireless/wired sensor nodes, remote servers, CCTVs and above all GPS service. This work can be extended by including bio-inspired algorithm instead of FNN for Adaptive road selection support system.

REFERENCES

- [1] Robert L. Bertini and Ahmed El-Geneidy, "Advanced Traffic Management System Data", Proceedings of 92nd Annual Meeting of Transportation Research Board, Washington DC, USA, January 13-17, 2013.
- [2] Chaudhry, M. S. and Ranjitkar, "Capacity and Signal Timing Analysis of Signalized Intersections with Increasing Saturation Flow Rate", Proceedings of 92nd Annual Meeting of Transportation Research Board, Washington DC, USA, January 13-17, 2013.
- [3] Iqbal, M.A., Zahin, A , Islam, Z.S. , Kaiser, M.S. "Neuro-Fuzzy based adaptive traffic flow control system", Communications, Devices and Intelligent Systems (CODIS), International Conference on, Kolkata, India, December 28-29, 2012, pp. 349 - 352, ISBN:978-1-4673-4699-3.
- [4] Robert L. Bertini and Ahmed El-Geneidy. "Traffic Flow Interruptions in Dhaka City: Is Smooth Traffic Flow Possible?", 2013 Journal of PU, Part: B, Presidency University, India, July 13-17, 2013, Vol.2 , No.2, pp.46-54, ISSN: 2224-761.
- [5] Akanbi A. K, Agunbiade O. Y., "Integration of a city GIS data with Google Map API and Google Earth API for a web based 3D Geospatial Application", International Journal of Science and Research (IJSR) , Novembor 23-27, 2013, Vol.2 , No.11 ISSN (Online): 2319-7064.
- [6] Chaudhry,M. S., Ranjitkars ,P., Wilson, D. J. and Hadas, Y., "Investigation of Queue Discharge Behavior at Signalized Intersection based on Analytical and Microsimulation Models", Proceedings of 90th Annual Meeting of Transportation Research Board, Washington DC, USA, January 23-27, 2011.
- [7] Akcelik, R, "Traffic Signals:Capacity and Timing Analysis",Research Report ARR No.123, Australian Road Research Board, Victoria, Australia,Issue (July 2003), pp. 3-4.
- [8] DingXin Cheng, Carroll J. Messer ,Zong Z. Tian, Juanyu Liu, "Modification of Webster Minimum Delay Cycle Length Equation Based on HCM 2000", Transportation Research Board for Presentation and Publication at the 2003 Annual Meeting in Washington, D.C., Texas Transportation Institute, Issue (July 2003), pp. 3-4.
- [9] Webster, F. V., Traffic signal settings, Road Research Technical Paper No. 39, Road Research Laboratory, England, published by HMSO, 1958.
- [10] N. M. Akcelik R, Rouphail, "Over flow queues and delays with random and platooned arrivals at signalized intersections", Journal of Advance Transportation, Vol.3 , pp. 257-251 , Issue (1994).
- [11] TRB (Transportation Research Board),"Highway Capacity Manual", National Research Council, Washington D.C., USA, 2000.
- [12] Teply, S., D. I. Allingham, D. B. Richardson and B. W. Stephenson, Canadian Capacity Guide for Signalized Intersections, Second Edition (S. Teply, ed.), Institute of Transportation Engineering, District 7, Canada, 1995.
- [13] L. Fu, D.Sun, L.R. Rilett, "Heuristic shortest path algorithms for transportation applications: State of the art", Communications, Computers and Operations Research 33 (2006) 3324 - 334, May 3, 2005. pp. 1-3.
- [14] Nicolas Lefebvre, Michael Balmer, "Fast shortest path computation in time-dependent traffic networks", Working Papers Traffic and Spatial Planning, June 2007, pp. 3-4, ISBN:978-1-4673-4699-3.
- [15] Dachuan Wei, "An Optimized Floyd Algorithm for the Shortest Path Problem ", Journal of Networks, Vol. 5, No. 12, December 2010, pp. 1496 - 1497.
- [16] K. Rohila, P. Gouthami, Priya M, "Dijkstras Shortest Path Algorithm for Road Network", International Journal of Innovative Research in Computer and Communication Engineering, Vol. 2, No. 10, Octobor 2014, pp. 349 - 352, ISSN: 2320-9798.
- [17] Kai Gutenschwager, Axel Radtke, Sven Volker, Georg Zeller, "The Shortest Path: Comparison of Different Approaches and Implementations for the Automatic Routing of Vehicles", 2012 Winter Simulation Conference, Octobor 2012, pp. 3312 - 3314, ISSN: 978-1-4673-4780-8.

- [18] Ittai Abraham, Daniel Delling, Amos Fiat, Andrew V. Goldberg, Renato F. Werneck, "Highway Dimension and Provably Efficient Shortest Path Algorithms", Microsoft Research, Microsoft Corporation, One Microsoft Way, Redmond, WA 98052, May 2014, pp. 2- 3.
- [19] Hannah Bast, Daniel Delling, Andrew Goldberg, Matthias Müller-Hannemann, Thomas Pajor, Peter Sanders, Dorothea Wagner, Renato F. Werneck, "Route Planning in Transportation Network", International Journal of Innovative Research in Computer and Communication Engineering, Vol. 2, No. 10, April 20-21, 2015, pp. 2-5.
- [20] Md. Shamsul Hoque, Md. Asif Imran, "Modification of Webster delay formula under non-lane based heterogeneous road traffic condition", Journal of Civil Engineering (IEB)", Issue 7, February 2007, pp. 1-4.
- [21] Chu Cong MINH, Tran Hoai BINH, Tran Thanh MAI and Kazushi SANO, "The Delay Estimation Under Heterogeneous Traffic Conditions", Journal of the Eastern Asia Society for Transportation Studies, Vol. 7, February 2009, pp. 2-9.
- [22] Md. Hadiuzzaman, Md. Mizanur, Tanweer Hasan and Md. A. Karim, "Development of Delay Model for Non-Lane Based Traffic at Signalized Intersection", Journal of Civil Engineering (IJCE), Vol. 3, Issue. 2, March 2014, pp. 69-79.
- [23] Saoreen Rahman, Nilufar Yeasmin, Mahtab U. Ahmed, M. S. Kaiser, "Adaptive Route Selection Support System Based On Road Traffic Information", 2nd International Conference on Electrical Engineering and Information and Communication Technology(ICEEICT), Bangladesh, May 21-23, 2015, pp. 2-4.
- [24] V. K. Arasan , "Modeling Platoon Dispersal Pattern of Heterogeneous Road Traffic.Transportation Research Record", TRB, National Research Council, Washington DC, USA,S.H. (2003).
- [25] R. Underwood, "Speed, volume, and density relationships: Quality and theory of traffic network", Yale bureau of highway traffic, Issue 6-7 (July 2003).
- [26] G. Pang, K. Takahashi, T. Yokota, H. Takenaga, "Adaptive Route Selection for Dynamic Route Guidance System Based on Fuzzy-Neural Approaches ", 1995(IEEE), Japan.
- [27] Sagheer Abbas, M. Saleem Khan, Khalil Ahmed, M.Abdullah and Umer Farooq, "Bio-inspired Neuro-Fuzzy Based Dynamic Route Selection to Avoid Traffic Congestion", International Journal of Scientific and Engineering Research, Vol. 2, Issue. 6, June 2011, pp. 2-4, ISBN:2229-5518.
- [28] Yanfang Deng, Hengqing Tong, "Dynamic Shortest Path Algorithm in Stochastic Traffic Networks Using PSO Based on Fluid Neural Network", Journal of Intelligent Learning Systems and Applications, Vol. 3, February 2011, pp. 11-16.
- [29] Dao Jiang, "A Novel Hybrid Optimization Algorithm based on Improved ACO and FNN", International Journal of Hybrid Information Technology, Vol. 9, April(2016) pp. 173-182, ISBN: 1738-9968.
- [30] A.Renugambal , V.Adilakshmi Kameswari, "Finding Optimal Vehicular Route Based On GPS", International Journal of Computer Science and Information Technologies, Vol. 5(2), June (2016) pp. 1-3, ISBN: 1330-1332.
- [31] Lili Cao , John Krumm, "From GPS Traces to a Routable Road Map", ACM GIS '09, Seattle, WA, USA, November 4-6, 2009 pp. 1-3, ISBN: 978-1-60558-649.
- [32] Jie Liu, Bodhi Priyantha, Ted Hart, Heitor S. Ramos, Antonio A.F. Loureiro, Qiang Wang, "Energy Efficient GPS Sensing with Cloud Offloading", SenSys12, Toronto, ON, Canada., November 6-9, 2012 pp. 1-3, ISBN: 978-1-4503-1169-4.
- [33] ME. Hossain, TN Turna, SJ Soheli, MS Kaiser, "Neuro-fuzzy(NF)-based adaptive flood warning system for Bangladesh ", International Conference on Informatics, Electronics & Vision (ICIEV), 2014, Dhaka, Bangladesh, 23-24, May 2014, pp. 1-3, ISBN:978-1-4799-5179-6.
- [34] MS Kaiser, MH Chaudary, RA Shah, KM Ahmed, "Neuro-fuzzy (NF) based relay selection and resource allocation for cooperative networks", International Conference on Electrical Engineering/Electronics Computer Telecommunication and Information Technology (ECTI-CON), 2010, Chaing Mai, 19-21, May 2010, pp. 224-248, ISBN:978-1-4244-5607-9.
- [35] MS Kaiser, ZI Chowdhury, S Al Mamun, A Hussain, M Mahmud, "A Neuro-Fuzzy Control System Based on Feature Extraction of Surface Electromyogram Signal for Solar-Powered Wheelchair", IEEE Sympo. on Computational Intelligence in Healthcare and e-health (CICARE2015), Cape Town, South Africa, 16 August 2016, pp. 1-9.
- [36] G.K.H. Pang, K. Takahashi, T. Yokota, "Prediction of Road Traffic Accidents in Jordan using Artificial Neural Network (ANN) ", Journal of Traffic and Logistics Engineering, Vol. 2, No. 2, Issue. June 2014, pp. 1-3.
- [37] Khair S. Jadaan, Muaath Al-Fayyad, Hala F. Gammoh, "Adaptive route selection for dynamic route guidance system based on fuzzy-neural approaches", IEEE Transactions on Vehicular Technology, Vol. 48, Issue. 06 August 2002, pp. 1-3, Online ISSN: 1939-9359.
- [38] Kranti Kumar, M. Parida, V.K. Katiyar, "Short term traffic flow prediction for a non urban highway using artificial neural network", 2nd Conference of Transportation Research Group of India (2nd CTRG) ,Kranti Kumar et al. / Procedia - Social and Behavioral Sciences 104(2013)755764, 2013, pp. 757-759.
- [39] R. Yasdi, "Prediction of Road Traffic using a Neural Network Approach", R. Neural Computing & Applications, Springer-Verlag, 03 March 2014, pp. 1-3, ISSN:0941-0643.
- [40] Fatma Al-Widyan, Nathan Kirchner, Michelle Zeibots, "An empirically verified Passenger Route Selection Model based on the principle of least effort for monitoring and predicting passenger walking paths through congested rail station environments", Australasian Transport Research Forum 2015 Proceedings, Sydney, Australia, 30 September - 2 October 2015, pp. 1-4.

Comparison of Inter-and Intra-Subject Variability of P300 Spelling Dictionary in EEG Compressed Sensing

Monica Fira

Institute of Computer Science
Romanian Academy
Iasi, Romania

Liviu Goras

Institute of Computer Science
Romanian Academy
Iasi, Romania

Abstract—In this paper, we propose a new compression method for electroencephalographic signals based on the concept of compressed sensing (CS) for the P300 detection spelling paradigm. The method uses a universal mega-dictionary which has been found not to be patient-specific. To validate the proposed method, electroencephalography recordings from the competition for Spelling, BCI Competition III Challenge 2005 - Dataset II, have been used. To evaluate the reconstructed signal, both quantitative and qualitative measures were used. For qualitative evaluation, we used the classification rate for the observed character based on P300 detection in the case of the spelling paradigm applied on the reconstructed electroencephalography signals, using the winning scripts (Alain Rakotomamonjy and Vincent Guigue). While for quantitative evaluation, distortion measures between the reconstructed and original signals were used.

Keywords—*Biomedical signal processing; Brain-computer interfaces; Compressed sensing; Classification algorithms; Electroencephalography*

I. INTRODUCTION

In the last years, the CS method has attracted considerable attention in areas such as applied mathematics, computer science, and electrical engineering. Basically, the method speculates the fact that, in certain conditions, many signals can be represented using only a few non-zero coefficients in a suitable basis, and nonlinear optimization can be used to recover such signals from very few measurements [1]. The concept of compressed sensing is a classic example of practical use of the new mathematical concepts. The difficulties for using in applications of such concepts are related to the way such results are perceived, in a more or less intuitive manner, in order to facilitate the fusion between theory and applications. The literature of recent years shows a large number of papers in the CS field [2, 3], covering both 1D and 2D medical signals [4, 5, 6]. Among the 1D signals currently used in CS applications, are the electrocardiogram (ECG) and electroencephalogram (EEG) since they are commonly used in the medical world as well. In the case of EEG signals, very often there is a need of records for longer periods of time (i.e., during night) or for a large number of channels. Paralyzed persons (e.g. with lateral amyotrophic sclerosis, cerebral stroke or severe polyneuropathy) or with other motor disabilities need alternative methods for communication and control. Using the EEG signal as a communication vector between human and

machine is one of the new challenges in signal theory. The main element of such a communication system is known as "Brain Computer Interface - BCI". The purpose of BCI is to translate human intentions – represented as suitable signals – in control signals for an output device, e.g. a computer or a neuroprosthesys. A BCI must not depend on normal output traces of peripheral nerves and muscles. In the last two decades, many studies have been carried out to evaluate the possibilities that recorded signals from the scalp (or from the brain) to be used for a new technology that does not imply muscles control.

The BCI that uses the EEG signal is capable of measuring the human brain activity, of detecting and of discriminating certain specific features of the brain. Recent advances in BCI research widened the possibilities of applicability fields. Intelligent devices that are capable to compensate some drawbacks associated with the lack of information from the EEG signals are also useful to persons with milder disabilities.

The definition of BCI largely accepted by the research community given in [7], states that BCI is a system of communication in which the messages or the commands to the outside world by an individual are not passing through the normal brain ways, i.e., those implemented by the peripheral nerves and muscles.

The first mentioning of communication by means of the BCI was made by Vidal in 1973 [8]. Nowadays there are many research teams involved in BCI research. Different approaches and results are achieved, but they are not always precise and imply complicated hardware [8]. Since the development of a BCI combines a great variety of disciplines (e.g. medicine, biology, physics, bioengineering, electronics, computer science, mathematics), the implied aspects are numerous and diverse.

The BCI framework used in this paper is based on P300 Event Related Potentials (ERP), which are natural responses of the brain to some specific external stimuli.

II. COMPRESSED SENSING

Shannon's sampling theory represents, in many cases of signal classes, a too severe limitation. It can be overcome by using the "Compressed sensing" theory (compressive sensing, compressive sampling and sparse sampling) perfected in the

past few years by prestigious researchers such as D. Donoho [10, 11], E. Candès [12], M. Elad, etc. The concept of compressed sensing (CS) is a new and revolutionary method which attracted the attention of many researchers and it is considered to have a high potential, with multiple implications and applications, in all fields of exact sciences. Basically CS is a technique for finding sparse solutions to underdetermined linear systems. In the signal processing domain, CS is the process of acquiring and reconstructing a signal that is supposed to be sparse or compressible.

The advantage of compressed sensing is that the acquisition stage is very fast, with very low complexity, and it is done in real time leading to a compressed EEG signal. The difficult part is the EEG reconstruction where two aspects are crucial: computing complexity (currently there are many mathematical algorithms which can be chosen depending on the needed accuracy, time and available resources) and knowledge of a dictionary for which the initial EEG signal has a satisfactory sparsity.

CS studies the possibility of reconstructing a signal x from a few linear projections, also called measurements, given the a priori information that the signal is sparse or compressible in some known basis Ψ . The vectors on which x is projected onto are arranged as the rows of an $n \times N$ projection matrix Φ , $n < N$, where N is the size of x and n is the number of measurements. Denoting the measurement vector as y , the acquisition process can be described as

$$y = \Phi x = \Phi \Psi \gamma \quad (1)$$

$$\hat{\gamma} = \arg \min_{\gamma} \|\gamma\|_{l_0} \quad \text{subject to} \quad y = \Phi \Psi \gamma \quad (2)$$

$$\hat{x} = \Psi \hat{\gamma} \quad (3)$$

The system of equations (1) is obviously undetermined. Under certain assumptions on Φ and Ψ , however, the original expansion vector γ can be reconstructed as the unique solution to the optimization problem (2); the signal is then reconstructed with (3). Note that (2) amounts to finding the sparsest decomposition of the measurement vector y in the dictionary $\Phi \Psi$. Unfortunately, (2) is combinatorial and unstable when considering noise or approximately sparse signals. Two directions have emerged to circumvent these problems: (i) pursuit and thresholding algorithms seek a sub-optimal solution of (2) and (ii) the Basis Pursuit algorithm [12] relaxes the l_0 minimization to l_1 , solving the convex optimization problem (4) instead of the original.

$$\hat{\gamma} = \arg \min_{\gamma} \|\gamma\|_{l_1} \quad \text{subject to} \quad y = \Phi \Psi \gamma \quad (4)$$

Using the l_0 norm is an NP-hard problem [13] that requires an algorithm of non-polynomial complexity. Such problems are practically impossible to be solved for usual dimensions of data.

III. BRAIN COMPUTER INTERFACE - P300 SPELLER PARADIGM

P300 is an event related potential which occurs at 300 ms after a rare and relevant event.

P300 has two subcomponents (as shown in Fig.1 a): the novelty P3 (also named P3a), and the classic P300 (renamed as P3b). P3a is a wave with positive amplitude and peak latency between 250 and 280 ms; the maximum values of the amplitude are recorded from the frontal/central electrodes. P3b has also positive amplitude with a peak around 300 ms; higher values are recorded usually on the parietal areas of the brain. Depending on the task, the latency of the peak could be between 250 and 500 ms.

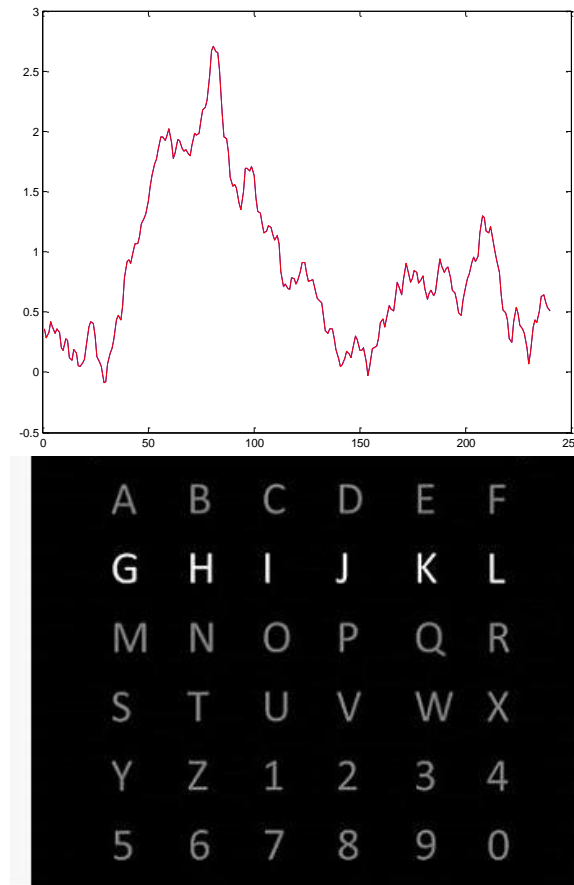


Fig. 1. P300 wave and the classical P300 spelling paradigm described by Farwell-Donchin 1988

Most of the paradigms that use the P300 evoked potentials are derived from the one proposed by Farwell and Donchin in [14].

The P300 speller is based on the so-called oddball paradigm which states that rare expected stimuli produce a positive deflection in the EEG after about 300 ms. It consists of a 6×6 matrix of characters as shown in Figure 1. This matrix is presented on computer screen and the row and columns are flashed in a random order. The user is instructed to select a character by focusing on it. The flashing row or column evokes P300 response in EEG. The non-flashing rows and columns do

not contribute in generating P300. Therefore, the computer can determine the desired row and column after averaging several responses. Finally, the desired character is selected.

For the BCI III competition, the dataset has been recorded from two different subjects in five sessions each. The procedure consists in repeating for 15 times (15 epochs), for each character, followed by a pause of 2.5 seconds. For each given character, there will be $6 \times 2 \times 15 = 180$ intensifications: 2×15 will contain the target character (once when the column is highlighted, second for the line it belongs to, repeated for 15 epochs) and the rest will not contain it. The signals have been bandpass filtered in the range 0.1 - 60Hz and sampled at 240Hz. Each session is composed of runs, and, for each run, a subject is asked to spell a word. For a given acquisition session, all EEG signals of a 64-channel scalp have been continuously collected. The train set contained 85 characters, and the test set of 100 characters for each of the two subjects. A more detailed description of the dataset can be found in the BCI competition paper [15].

The classification problem can be formulated as follows: given the 64-channel signals collected after the intensification of a row or column, we want to predict if such signal includes or not a P300. This first part of the problem is thus a binary classification problem. In accordance with the classification of each post-stimulus signal, the goal is to correctly predict the desired character using the fewest sequences as possible. A second part of the problem deals with a 36-class classification problem as it seeks recognition of a symbol from the 6×6 matrix, as shown in Figure 1 [9].

The competition winners, Alain Rakotomamonjy and Vincent Guigue, proposed a method that copes with such variability through an ensemble of classifiers approach [9]. Each classifier is composed of a linear support vector machine (SVM) trained on a small part of the available data and for which a channel selection procedure has been performed. They achieved a classification rate of 95.5% for 15 sequences and 73.5% for 5 sequences [9]. Thus, in the preprocessing stage, for each channel, all data samples between 0 to 667 ms, posterior to the beginning of an intensification, were extracted. Afterwards, each extracted signal has been filtered with an 8-order band-pass Chebyshev Type I filter with cut-off frequencies 0.1 and 10 Hz and has been decimated according to the high cut-off frequency. At this point, an extracted signal from a single channel is composed of 14 samples. The solution proposed by the winners consists of an ensemble of classifiers, the 85 characters from the training set being divided into 17 groups of 5 characters. The individual classifications are SVM with linear kernel. Each single SVM training involves a model selection procedure for setting its regularization parameter C [9].

IV. METHOD

In general, the biomedical signals do not have a good sparsity in the standard type dictionaries as wavelet, DCT, DST etc. [16]. This is why, for EEG and ECG signals, in most of cases, it is preferred to build signal specific dictionaries, which take into consideration the statistic of the signal, or the repetitive elements from the signal. For example, the ECG signal has a pseudo-cyclicity for the QRS complex, and the P

and T waves which can be exploited. The EEG signal is a much more complex signal that has no visible repeated elements. The EEG signal is mainly composed of alpha, beta, theta, and delta waves which have significance in clinical interpretation but they are visible only in the frequency domain.

A. The dictionary

Taking into account the missing visible, repeated elements from EEG signals and the results obtained previously in [17, 18, 19, 20], it is apparent that, in case of EEG signal, an option to build the dictionary is that of using the EEG signal itself. In the case of the spelling paradigm, the dictionary will be built from the data used in the training set.

We tested the possibility of building an universal mega-dictionary consisting of EEG segments from all 64 channels. Thus, for each channel, three atoms were selected, consisting in EEG segments from the corresponding channel, so that a dictionary made up of $3 \times 64 = 192$ atoms has been obtained. The size of the dictionary is 192×240 , since each atom has the size of 240. For the construction of this dictionary, it was used the training signal from the paradigm of spelling.

The testing of the method was done using EEG test signals which consist in compressed sensed EEG signals. The proposed method is tested also for the inter-subject variability of the dictionary, namely the dictionary with signals from the training set of a subject was tested with signals from the testing set of the other subject. The spelling data base has only two subjects and this led to the following possible combinations to validate the proposed method:

- dictionary from train test of subject A and test by test set for subject A (denoted by **TrainA - TestA**)
- dictionary from train test of subject B and test by test set for subject B (denoted by **TrainB - TestB**)
- dictionary from train test of subject A and test by test set for subject B (denoted by **TrainA - TestB**)
- dictionary from train test of subject B and test by test set for subject A (denoted by **TrainB - TestA**)

B. The acquisition matrix

At the acquisition matrix level, namely the projection matrix, three types of matrices can be used: random matrix, Bernoulli-type matrix (with values of -1, 0, 1 in equal ratios) or an optimized matrix that takes into account the used dictionary for reconstruction. Thus, taking into account the previous results from [17, 19, 20], in this work, we have used the optimized matrix. Shortly, for a given dictionary, if we multiply the projection matrix with the transposed dictionary we will get an optimized projection matrix for that dictionary. This optimization procedure was detailed in [19].

V. EXPERIMENTAL RESULTS AND DISCUSSIONS

For the evaluation of the proposed method, we used the dataset II of the BCI Competition III 2005 -P300 Spelling (the dataset has been recorded from two different subjects; The train set contained 85 characters, and the test set of 100 characters for each of the two subjects).

For compression evaluation, we used the compression rate (CR) defined as the ratio between the numbers of bits needed to represent the original and the compressed signal.

$$CR = \frac{b_{orig}}{b_{comp}} \quad (5)$$

We have also evaluated the distortion between the original and the reconstructed signals by means of the PRDN (the normalized percentage root-mean-square difference (6)) for to validate the compression:

$$PRDN\% = 100 \sqrt{\frac{\sum_{n=1}^N (x(n) - \tilde{x}(n))^2}{\sum_{n=1}^N (x(n) - \bar{x})^2}} \quad (6)$$

where $x(n)$ and $\tilde{x}(n)$ are the samples of the original and the reconstructed signals, respectively, \bar{x} is the mean value of the original signal, and N is the length of the window over which the PRDN is calculated.

For qualitative evaluation of the method based on the classification rate in spelling paradigm, we used scripts from the winners, A. Rakotomamonjy and V. Guigue [9] (the scripts implement classification based on all 64 EEG channels).

In Table 1, we present the classification results in paradigm spelling using original data and the software from [9]. It can be observed that after the reconstruction using a dictionary built with signals for the training stage of subject B, the obtained classification rates in the spelling paradigm are better than in the case of the original signal. This scenario is true for both subject B (92.4% versus 89.37%), and subject A (89.15% versus 87.10%). In the case of using a dictionary built with signals for training from subject A, the obtained results are very close, but a slightly under the performance obtained for the original signals.

TABLE I. CLASSIFICATION PERFORMANCE % AND ERROR (PRDN) IN P300 SPELLING FOR RECONSTRUCTED EEG SIGNAL WITH SOFTWARE FROM [9] FOR A COMPRESSION CR = 10:1

	CR Compression	Max Classification	Average Classification	PRDN
ORIGINAL A	10:1	94 %	87.10 %	-
AA	10:1	90 %	84.29 %	50.17
BA	10:1	95 %	89.15 %	45.09
ORIGINAL B	10:1	93 %	89.37 %	-
BB	10:1	97 %	92.40 %	43.07
AB	10:1	92 %	86.59 %	48.80

In Figure 2, the PRDN errors for the two subjects using the two dictionaries vs. EEG channels are presented. It can be observed a consistency of errors reported to channel, that can be explained as follows: some of channels are reconstructed

with errors, independently of the used dictionary. A possible hypothesis is that those channels have different statistics and a higher variability compared to the other channels.

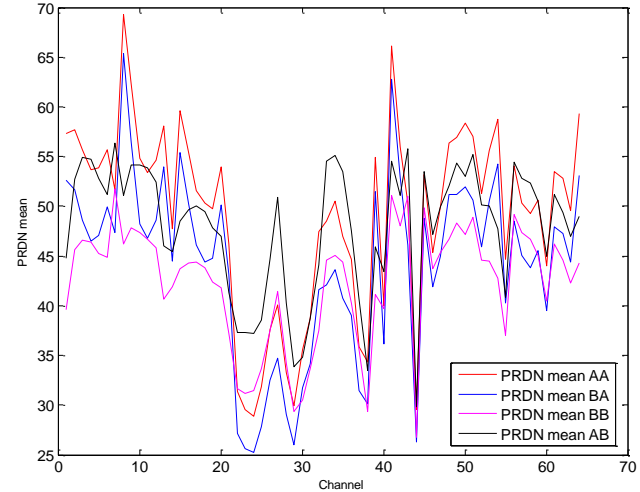


Fig. 2. PRDN_Mean vs. channel for subject A and respectively subject B using dictionaries construct by train test A and train test B

In Figure 3, we present an original EEG segment (red) and its reconstructed variant based on a dictionary built using its own training set (blue) and the alternative with a dictionary built from the signals from the training set of the other subject (black). It can be observed that the shape of the EEG signal is preserved, but there are some variations.

Taking into account the classification results from the spelling paradigm, we may state that those variations of the reconstructed signal do not influence the classification in this paradigm.

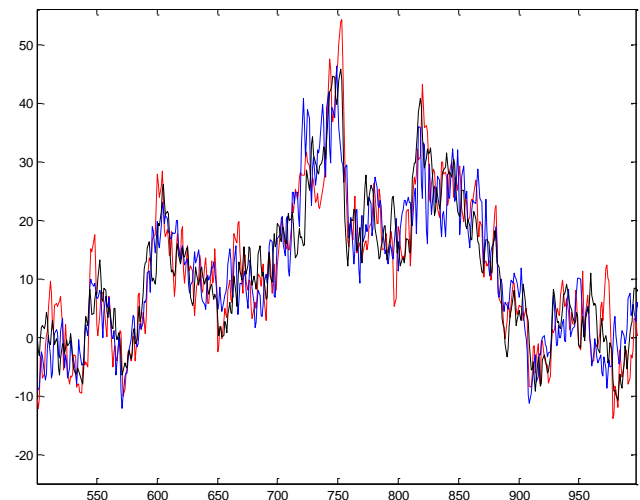
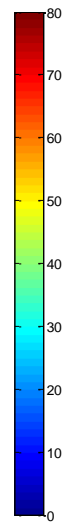
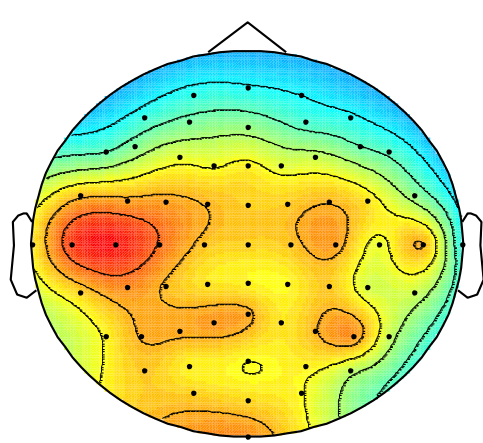
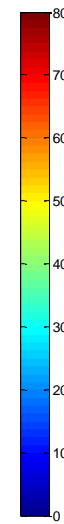
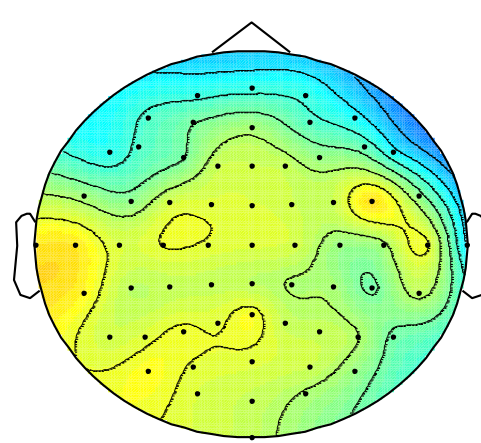


Fig. 3. Example by original signal (subject A with red) and reconstructed signals (TrainA – TestA blue and TrainB-TestA black)

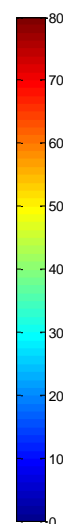
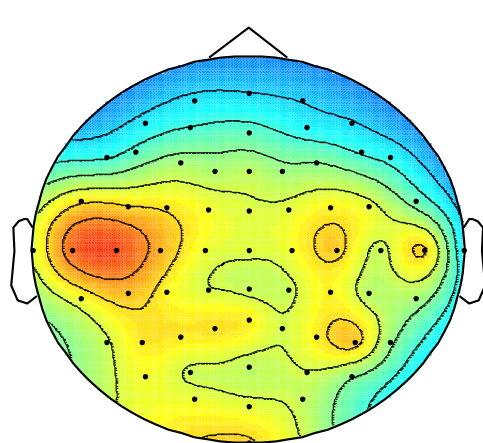
PRDN mean TrainA - TestA Topography



PRDN mean TrainB - TestB Topography



PRDN mean TrainB - TestA Topography



PRDN mean TrainA - TestB Topography

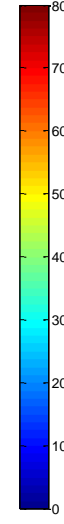
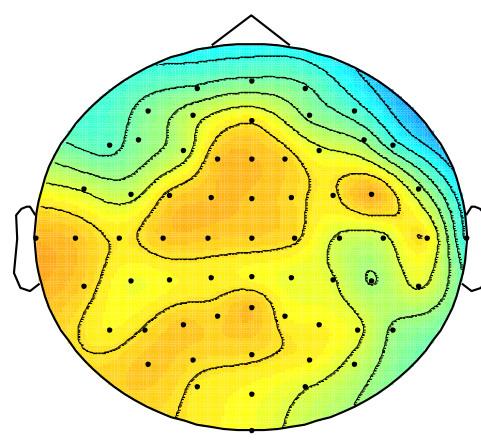


Fig. 4. The topography of PRDN for EEG compressed sensing for subject A and CR = 10:1 (by TrainA – TestA and by TrainB – TestA from up to down)

Figure 4 and 5 show the PRDN topography for subject A and respectively B. This topography shows that frontal/central electrode sites present a PRDN smaller than the other electrodes, a specific area for the P3a wave. Next area, as PRND error is parietal area, specific area for the P3b wave, and the biggest errors are in temporal zone. The temporal area has not too much significance for the P300 generation.

Fig. 5. The topography of PRDN for EEG compressed sensing for subject B and CR = 10:1 (by TrainB – TestB and by TrainA – TestB from up to down)

VI. CONCLUSION

In this paper, it is presented a comparative analysis of results obtained using a mega-dictionary for EEG signals compressed sensing related to the spelling paradigm and using a mega-dictionary built from pieces of the train EEG signals.

For the evaluation of the proposed method, the dataset from the BCI Competition III 2005 - P300 Spelling has been used.

In order to evaluate the results of the EEG signal reconstruction the PRDN was used in parallel with the classification rate of the spelling paradigm assessed using the scripts from the winner of the competition (the version of classification using all 64 channels).

The main result is the verification of the hypothesis that the mega-dictionary is not patient-specific. The testing of this hypothesis involved the construction of a dictionary from the train set of a subject, and using it for the reconstruction of the test signals for other subjects. Even though the used database had only two subjects, the recorded EEG signals were long enough. Thus, both the usages of dictionary for the same subject, and for the other subject were tested. Even though the quantitative measure of the EEG signals reconstruction error expressed by PRDN was around 45, it has been found that the classification rates in the spelling paradigm are very close to the values obtained for the original signal or even above them.

These results can be read in the sense that for the classification rate within the paradigm of spelling it is very important to preserve the shape of the EEG signal while small reconstruction errors do not matter significantly.

The advantage of compressed sensed is that the acquisition stage is very fast, with very low complexity, it is done in real time and, after this stage, it results a compressed EEG signal. The difficult part is the EEG reconstruction and this is due to the following two aspects:

- The complexity of computing, but currently there are different mathematical algorithms and, depending on the needed accuracy, time and available resources, a favourable algorithm can be chosen;
- The knowledge of a dictionary in which the initial EEG signal has a satisfactory sparsity.

The obtained results, in particular the classification rate in the spelling paradigm, demonstrate that the built dictionary ensures the reconstruction of the EEG signal with good results, regardless of the train EEG signal used for the dictionary construction.

ACKNOWLEDGMENT

This work was supported by a grant of the Romanian National Authority for Scientific Research and Innovation, CNCS – UEFISCDI, project number PN-II-RU-TE-2014-4-0832 “Medical signal processing methods based on compressed sensing; applications and their implementation.”

REFERENCES

- [1] M. A. Davenport, M. F. Duarte, Y. C. Eldar, and G. Kutyniok, "Introduction to Compressed Sensing" in Compressed Sensing: Theory and Applications, pp. 1-68, Cambridge University Press, 2012.
- [2] C. Wu, H. Wang, X. Xu, L. Zhao, "Combined Sparsifying Transforms for Compressive Image Fusion", Advances in Electrical and Computer Engineering, Vol. 13, Nr. 4, pp. 79-84, 2013 doi:10.4316/AECE.2013.04014
- [3] D. Giacobello, M. G. Christensen, M. N. Murthi, S. H. Jensen, and M. Moonen, "Retrieving Sparse Patterns Using a Compressed Sensing Framework: Applications to Speech Coding Based on Sparse Linear Prediction", IEEE Signal Processing Letters, vol. 17, no. 1, pp. 103-106, 2010, doi:10.1109/LSP.2009.2034560
- [4] Z. Zhang, T. Jung, S. Makeig, B. Rao, "Compressed sensing of EEG for wireless telemonitoring with low energy consumption and inexpensive hardware", IEEE Transactions on Biomedical Engineering, Vol 60, pp. 221–224, 2013, doi:10.1109/TBME.2012.2217959
- [5] S. Fauvel, K. Rabab, K. Ward, "An Energy Efficient Compressed Sensing Framework for the Compression of Electroencephalogram Signals", Sensors, Vol. 14, pp. 1474-1496, 2014, doi:10.3390/s140101474
- [6] H. Mamaghani, N. Khaled, D. Atienza, and P. Vandergheynst, "Compressed sensing for real-time energy-efficient ECG compression on wireless body sensor nodes," IEEE Transactions on Biomedical Engineering, vol. 58, no. 9, pp. 2456-2466, 2011, doi:10.1109/TBME.2011.2156795
- [7] J. Wolpaw, N. Birbaumer, D. J. Heetderks, D. McFarland et.all, "Brain-Computer Interface Technology: A Review of the First International Meeting", IEEE Trans. on Rehab. Eng., vol. 8, No. 2, June, pp.164-173, 2000, doi:10.1109/TRE.2000.847807
- [8] J. J. Vidal, "Toward direct brain-computer communication", Annu. Rev. of Biophys. Bioeng., pp. 157-180, 1973, doi:10.1146/annurev.bb.02.060173.001105
- [9] A. Rakotomamonjy, V. Guigue, "BCI Competition III: Dataset II- Ensemble of SVMs for BCI P300 Speller", IEEE Transactions on Biomedical Engineering, Vol:55, Issue: 3, pp. 1147 – 1154, 2008, doi:10.1109/TBME.2008.915728
- [10] D. L. Donoho and M. Elad, "Optimally sparse representation in general (nonorthogonal) dictionaries via l1 minimization", Proceedings of the National Academy of Sciences, vol. 100, no. 5, pp. 2197–2202, 2003, doi:10.1073/pnas.0437847100
- [11] D. Donoho, M. Elad, and V. Temlyakov, "Stable recovery of sparse overcomplete representations in the presence of noise", IEEE Transactions on Information Theory, vol. 52, no. 1, pp. 6–18, Jan. 2006, doi:10.1109/TIT.2005.860430
- [12] E. Candes and T. Tao, "Decoding by linear programming", IEEE Transactions on Information Theory, vol. 51, pp. 4203–4215, 2005, doi:10.1109/TIT.2005.858979
- [13] B. K. Natarajan, "Sparse approximate solutions to linear systems" SIAM J. Comput., vol. 24, no. 2, pp. 227–234, Apr. 1995, doi:10.1137/S0097539792240406
- [14] L. A. Farwell, E. Donchin, "Taking off the top of your head: toward a mental prosthesis utilizing event-related brain potentials", Electroencephal and clinical Neurophysiology, 70, 510-523, 1988, doi:10.1016/0013-4694(88)90149-6
- [15] Data Acquired Using BCI2000's P3 Speller Paradigm (<http://www.bci2000.org>)
- [16] M. Fira, L. Goraş, C. Barabasa, N. Cleju, "On ECG Compressed Sensing using Specific Overcomplete Dictionaries", Advances in Electrical and Computer Engineering, Vol. 10, Nr. 4, pp. 23-28, 2010, doi:10.4316/aece.2010.04004
- [17] M. Fira, "Compressed Sensing of Multi-Channel EEG Signals: Quantitative and Qualitative Evaluation with Speller Paradigm", International Journal of Advanced Computer Science and Applications, Vol. 7, No. 6, 2016, doi:10.14569/IJACSA
- [18] M. Fira, V. A. Maiorescu, L. Goras, "The Analysis of the Specific Dictionaries for Compressive Sensing of EEG Signals", Proceedings of the ACHI 2016, Venice, Italy, 2016
- [19] N. Cleju, M. Fira, C. Barabasa, L. Goras, "Robust reconstruction of compressively sensed ECG patterns", Proceedings of The 10-th International Symposium on Signals, Circuits and Systems – ISSCS 2011, 30 June – 1 July 2011, Iasi, pp. 507-510, 2011, doi:10.1109/ISSCS.2011.5978770
- [20] M. Fira, L. Goras, "On Compressed Sensing for EEG Signals - Validation with P300 Speller Paradigm", Proceedings of International Conference on Communications – COMMS 2016, 9 -11 July 2016, Bucharest

A Frame Size Adjustment with Sub-Frame Observation for Dynamic Framed Slotted Aloha

Robithoh Annur

Department of Computer
and Communications Technology
Universiti Tunku Abdul Rahman
Perak, Malaysia

Suvit Nakpeerayuth

and Lunchakorn Wuttitsittikulkij
Department of Electrical Engineering
Chulalongkorn University
Bangkok, Thailand

Abstract—In this paper, a simple frame size adjustment of dynamic framed slotted Aloha for tag identification in RFID networks is proposed. In dynamic framed slotted Aloha, the reader is required to announce the frame size for every frame. To achieve maximum system efficiency, it is essential to set the frame size according to the number unidentified tags appropriately. The proposed approach utilizes the information from a portion of the frame to adjust the size of the next frame. Simulation results show that the smaller number of observed slots results in faster frame adjustment and higher throughput. Compared to the existing anti-collision algorithms, the proposed approach achieves higher throughput and higher identification rate.

Keywords—anti-collision tag identification; RFID; Framed slotted Aloha; frame adjustment

I. INTRODUCTION

Radio Frequency Identification (RFID) is a short range wireless communication technology for identifying a specific object. It is also known as electronic tag. Unlike barcode, it does not require line-of-sight. Moreover, it is able to read, transmit and store the information of the objects. With the development of the RFID technology, it is widely applied in many sectors such as retail trade, services, manufacturing, supply chain management, logistics, information industry, and medical applications. A simple RFID system consists of tags with data memory and antenna, interrogators/ readers, and host with data processing software. A problem so called tag collision may occur when at least two tags respond to the same reader simultaneously. An anti-collision algorithm is performed in such a way to solve this problem and hence increases the tag reading efficiency. To achieve fast tag identification, many tag anti-collision protocols have been proposed. They can be broadly classified into two categories: tree-based and Aloha-based.

Tree based RFID tag anti-collision protocols such as Query tree, M-ary query tree, collision tree [1], consecutive collision bit mapping algorithm (CCMA)[2], Dual Prefix Probe Scheme (DPPS) [3] are developed from the traditional tree algorithm by Capetanakis [4] where the colliding tags are recursively split into subgroups based on the position of the bits in their IDs. However, distribution of tags' ID and collision bit position are the major factors affecting the tag identification speed.

This paper focuses on Aloha based anti-collision algorithm. In the application of RFID systems, framed slotted Aloha receives much attention compared to other types of Aloha

based algorithms. To cope with the problem of tag starvation, many researches have applied adaptive frame size, so called dynamic framed slotted Aloha [5].

In dynamic framed slotted Aloha, the frame size is set dynamically equal to the number of remaining unidentified tags. In fact, the reader usually does not have any information regarding the number of tags. This leads to necessity of an estimation of the number of tags in each frame [6, 7].

In literature, many tag estimate methods have been addressed by observing all slots in the previous frame to find the number of idle (I), successful (S) and collision (C). Schoute's method suggests that the tag number estimate is $\hat{n} = 2.39C$. Vogts method utilizes I , S and C in the tag estimation using mean square error. By assuming that tags in each frame have a multinomial distribution, Chen [8] and Vahedi [9] present a more accurate tag number estimate using a posteriori probability distribution, but at a cost of increased complexity [10]. To achieve a good estimate of number of tags with much reduced complexity, [10] proposed an Improved Linearized Combinatorial Model (ILCM) which uses an efficient interpolation method that is easy to be implemented.

Different from the aforementioned estimate methods that observe the entire slots in the frame, some existing frame size adjustment methods perform frame breaking policy whereby only a portion of the frame is observed. This method allows the reader to end the current frame and start a new frame when an inappropriate frame size is detected. An example of this method is Q algorithm that is adopted in the EPC class 1 Gen 2 of RFID standard [11]. This algorithm is an effective approach to change the frame size of dynamic framed slotted Aloha without requiring the knowledge of the number of unidentified tags, i.e. no explicit estimation of tag numbers is required at the end of each frame. The Q algorithm basically adjusts a parameter called Q with a parameter c in response to the outcome of tag transmission on a slot by slot basis. The Q algorithm is simple, but it is not fully clear how the parameter c should be set [10, 12], despite some efforts by [13, 14]. Chen in [12] (W-T Chen's algorithm) proposed an tag estimation method namely a feasible and easy to implement anti-collision algorithm. When it detects that the frame size is not in the range of optimum value, the frame will end and continue the identification process with new frame. This W-T Chen's algorithm provides a good tag estimation. However, it requires non-empty slot in the first slot of the frame that may not always be true.

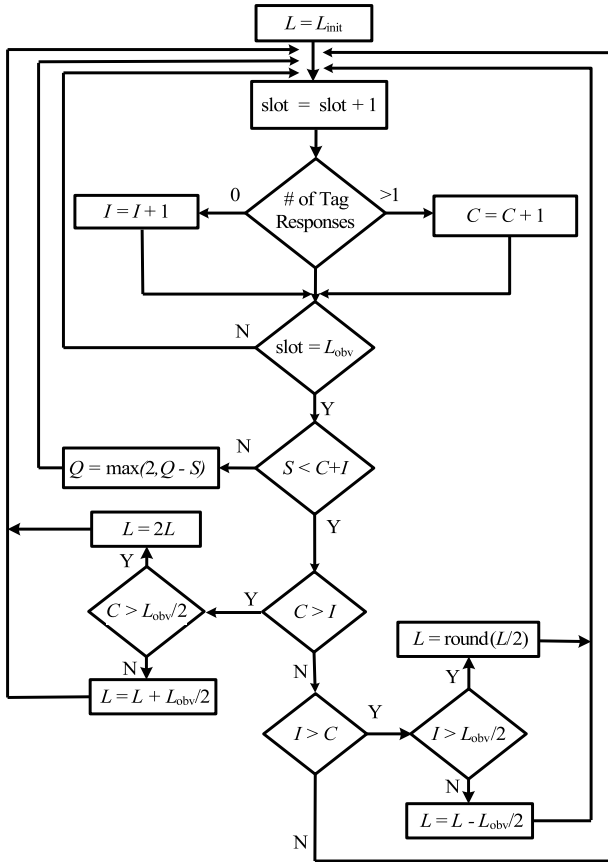


Fig. 1. The flow diagram of the proposed algorithms

In this letter, a simple frame breaking policy for dynamic framed slotted Aloha frame size adjustment is proposed. This aims to reduce the computational complexity and improve the identification speed of the system. The propose algorithm relies on the ratio between the number of collisions and idle slots in a portion of the frame. The proposed method does not apply complex computation but can achieve a considerable performance.

II. SYSTEM MODEL AND FRAME ADJUSTMENT DESCRIPTION

The anti-collision protocol used in this paper is based on the dynamic framed slotted Aloha. To maximize the success probability in each frame, the frame size should be set properly according to the number of collided tags. There will be many collision or idle slots if the frame size is too small or too large compared the number of collided tags.

It is well known that the ideal DFSA achieves a maximum throughput of 36.8% when $L = N$. For this ideal case, the system required the number of collided tags in each frame to set the frame size that can be done by performing tag estimation. Usually, to estimate the number of tags in a frame, it is required to observed all slots in the frame. This approach may not always provide an effective result when the frame size is inappropriate due to error in the estimation. In this case, the reader can break the current frame and initiates a frame with different size.

The proposed frame size adjustment with a breaking policy that is based on the ratio between empty and collision slots in the observed slots in the frame. Fig. 1 depicts the proposed frame size adjustment for framed slotted Aloha. At the beginning of the identification process, the reader will broadcast the initial frame size, denoted as L_{init} and the observed slots denoted as L_{obs} that is the portion of the frame (first several slots in the frame). In every frame, the reader will initiated a new frame after observing L_{obs} . The frame size may be shrunked or enlarged depending on the ratio between empty and collision slots in the observation. If the number of collision slots is greater than the number of idle slots, it is expected that the frame size is too small compared to the number of collided tags. For this case, it is further checked whether the number of collisions is greater than the $L_{obs}/2$. If so, the frame size will increase by $L_{obs}/2$, otherwise it will be doubled. On the other hand, if the number of collision slots is smaller than the number of idle slots, the frame size will reduce by $L_{obs}/2$ if the number of idle slots is greater than $L_{obs}/2$ or will reduce by half for other cases. If the numbers of collision and idle slots are equal, the frame size remains unchanged.

III. SIMULATION RESULTS AND DISCUSSION

This section presents the evaluation of the effectiveness of the proposed frame adjustment approach in terms of two different performance matrices namely throughput or system efficiency and read rate or identification rate.

It will first show the effect of different initial frame size, L_{init} and L_{obs} on the throughput or system efficiency of the proposed algorithm. Computer simulations were conducted with the initial number of tags (N) set up to 1000 tags and run the simulator for each scenario for 10,000 times. To show the effectiveness of the algorithms in resolving collisions, the results are presented in terms of throughput or system efficiency which is normally calculated as the ratio between the number success slots and the total number of slots spent in a collision resolution process that is given by:

$$SE = \frac{S}{S + I + C} \quad (1)$$

Fig. 2 shows the effect of different parameter settings of L_{init} and L_{obs} to the system efficiency. Three different settings of L_{init} are considered, namely 16, 32, and 64. It can be seen that the setting of L_{init} have significant impact to the system efficiency. When the number of tags is far L_{init} , the system efficiency is considerably low, especially when the number of tags is less than the L_{init} . For example, for $L_{init} = 32$ and 64, the system efficiency drop to below 0.3 i.e. 0.22 and 0.125, respectively, when the number of tags is 10. Especially for case when $L_{init} = 16$, the system efficiency is consistently above 0.345 for either small or large number of tags. From these results, $L_{init} = 16$ can be considered as a proposed parameter setting.

To show the influence of the setting of L_{obs} , four different portions of frame to be observed is considered; L , $L/2$, $L/4$, and $L/8$. From Fig.2, it reveals that the setting of L_{obs} gives significant effect to the throughput. For the three different values of L_{init} , each of these four values of L_{obs} presents the same fashion where the smaller number of observed slots, the

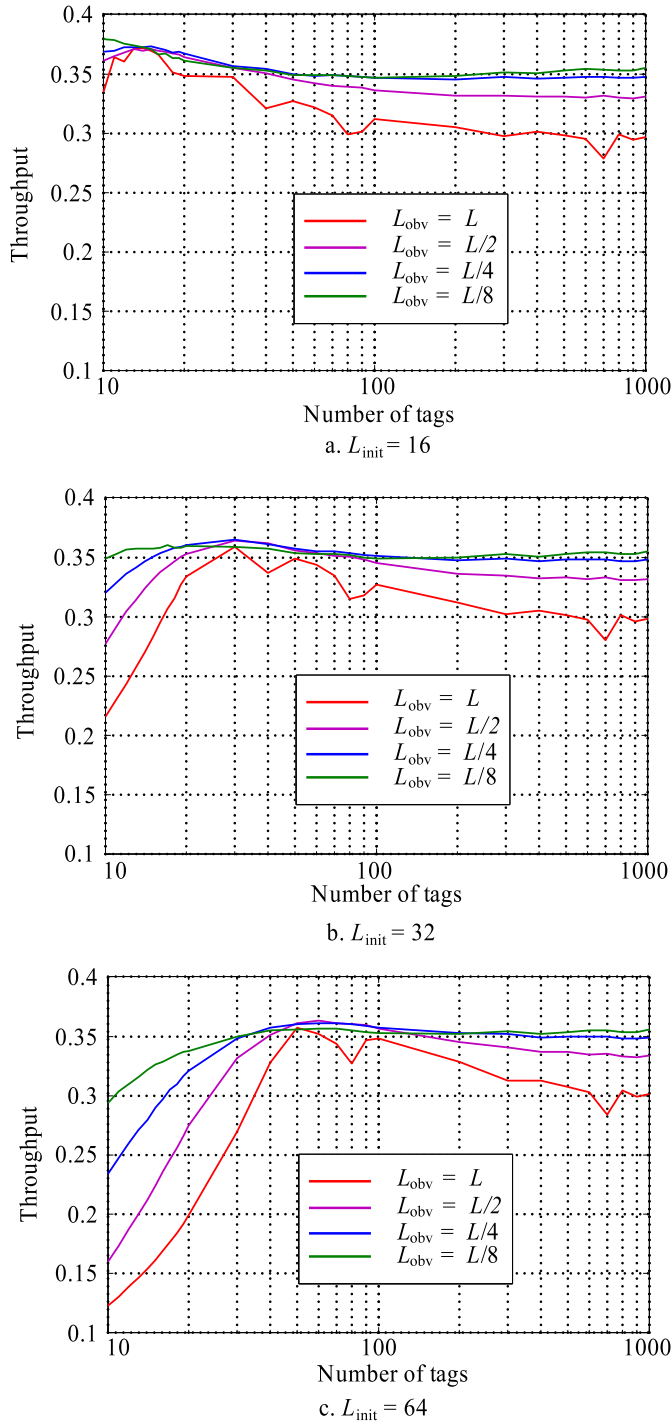


Fig. 2. Normalized throughput of the proposed approach under different initial value of L

better performance is achieved. This is expected because when the observation is for the entire frame, the frame adjustment will be slow to reach the appropriate frame size for the number of remaining unidentified tags. Hence, there is high probability that the slots in the frame will be idle or collision. These reasons will create the drop in the system efficiency of the proposed approach. On the other hand, when small portion of frame is observed, the frame adjustment will be fast to

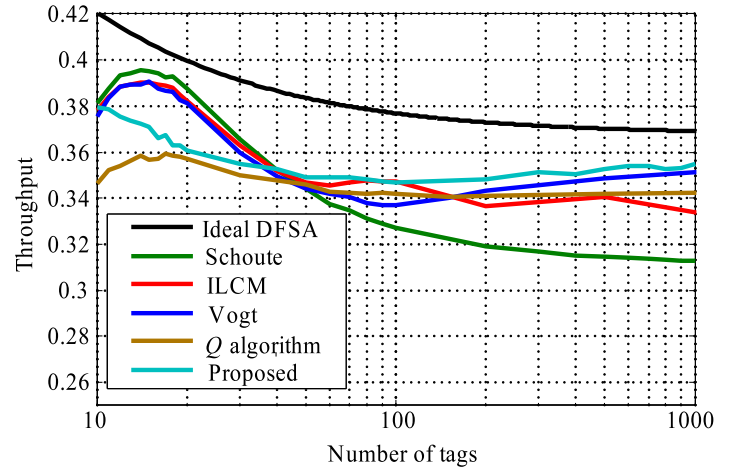


Fig. 3. Normalized throughput comparison between Aloha-based anti-collision algorithms

reach the appropriate frame size. As a result, the probability of success can be maximized. From these results, it suggests that smaller L_{obv} is preferred to achieve a good performance for board range of number of tags.

Fig. 3 compares the throughput of the proposed approach with the existing anti-collision algorithms such as: ideal DFSA, Vogt, Schoutes, ILCM, and Q algorithm. For this comparison, the L_{init} is set to 16 for all algorithms and L_{obv} is $L/8$. It shows that Schoutes, Vogts, ILCM algorithms perform very well for small number of tags, i.e. above 0.36 efficiency for $N < 30$. For larger N , these three existing algorithms exhibit different behaviors. The throughput of Schoutes algorithm drops relatively fast for larger values of N (this is also suggested in [12]), e.g. for $N > 200$ where the efficiency falls below 0.32. The drop also happens to ILCM, but it still maintain the system efficiency of almost 0.34 at large N , i.e. $N > 200$. For Vogts algorithm, the throughput will decrease up to below 0.34 at around $N = 80$ and will rise again up to above 0.34 for $N = 1000$. For the well known Q algorithm, the throughput is less than 0.36 and stable for 0.342 for large vale of N . The proposed algorithms can perform better than all other algorithms in most cases where it can achieve the system performance of almost 35% for the entire range of the number of tags.

Besides the throughput, this section will also compare the identification rate of the proposed approach and the existing anti-collision algorithms. Identification rate is defined as the total number of tags that is successfully identified in a given unit of time. It is referred here as tags/ second. To measure the identification rate, the timing in EPCglobal Class 1 Gen 2 RFID standard is referred. Duration for the empty, success and collisions are defined differently. This is because every slot condition reflects different step of communication between the tags and the reader as illustrated in Fig. 4. It can be seen that the duration of the empty, success and collisions can respectively be given by:

$$T_{idle} = T_{Qrep} + T_1 + T_3 \quad (2)$$

$$T_{success} = T_{Qrep} + T_1 + T_{RN16} + T_2 + T_{ACK} + T_1 + T_{EPC} + T_2 \quad (3)$$

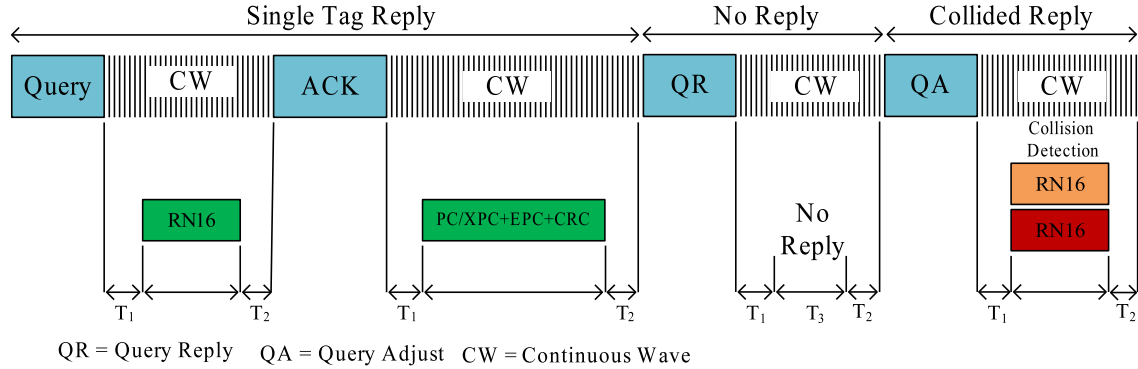


Fig. 4. Timing in EPCglobal Class 1 Gen 2

TABLE I. GEN2 PARAMETER

Parameter	Value
Tari	6.25 μs
TRCal	33.33 μs
T1	33.33 μs
T2	15.63 μs
T3	0.516 μs
TFS	35.94 μs
TQuery	414.06 μs
TQueryRep	104.69 μs
TACK	345.31 μs
TRN16	337.50 μs
TEPC	1.7 ms

$$T_{collision} = T_{Qrep} + T_1 + T_{RN16} + T_2 \quad (4)$$

The identification rate can be then calculated by:

$$rate = \frac{S}{T_{success}S + T_{idle}I + T_{collision}C} \quad (5)$$

The EPCglobal Class 1 Gen 2 RFID standard can operate in several different tag-reader link rates. It uses tag-reader link rates of 640 kbps with the detail parameters given in Table I. It can be seen that the proposed frame adjustment approach offer high identification rate for larger range of the number of tags.

IV. CONCLUSION

Frame size selection is a major challenge in dynamic framed slotted Aloha based RFID anti-collision algorithm since the reader does not have any information regarding the number of tags in the inventory process. This paper has presented a simple frame size adjustment of dynamic framed slotted Aloha that allows early frame adjustment. The algorithm will only observe first few slots of the frame and initiate a new frame. Based on the comparison between the number of idle slots and collisions in the number of observed slots, the new frame size is determined. The results show that this simple approach offers higher throughput and identification rate compared to the other existing algorithms.

ACKNOWLEDGMENT

The authors would like to thank to Ratchadapiseksomphot Endowment Fund from Chulalongkorn University

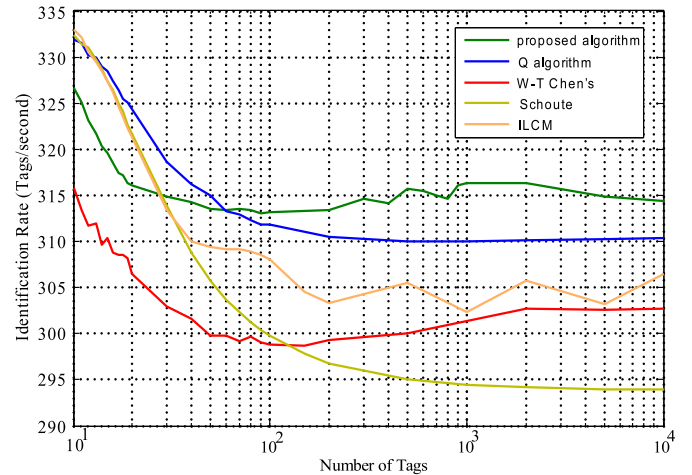


Fig. 5. Identification rate comparison between Aloha-based anti-collision algorithms

and AUN/SEED-Net program, and UTARRF (IPSR/RMC/UTARRF/2015-C2/R02) from Universiti Tunku Abdul Rahman for the financial support.

REFERENCES

- [1] X. Jia, Q. Feng, and L. Yu, "Stability analysis of an efficient anti-collision protocol for rfid tag identification," *IEEE Transactions on Communications*, vol. 60, no. 8, pp. 2285–2294, August 2012.
- [2] H. J.-l. SU Jian, WEN Guang-jun, "An efficient rfid anti-collision algorithm for iso 18000-6b protocol," *Chinese Journal of Electronics*, vol. 42, no. 12, p. 2515, 2014.
- [3] J. Su, Z. Sheng, G. Wen, and V. C. M. Leung, "A time efficient tag identification algorithm using dual prefix probe scheme (DPPS)," *IEEE Signal Processing Letters*, vol. 23, no. 3, pp. 386–389, March 2016.
- [4] J. Capetanakis, "Tree algorithms for packet broadcast channels," *Information Theory, IEEE Transactions on*, vol. 25, no. 5, pp. 505–515, Sep 1979.
- [5] F. Schouste, "Dynamic frame length aloha," *Communications, IEEE Transactions on*, vol. 31, no. 4, pp. 565–568, Apr 1983.
- [6] H. Vogt, "Efficient object identification with passive RFID tags," in *Proceedings of the First International Conference on Pervasive Computing*, ser. Pervasive '02. London, UK: Springer-Verlag, 2002, pp. 98–113.
- [7] C. Floerkemeier, "Bayesian transmission strategy for framed

- Aloha based RFID protocols,” in *RFID, 2007. IEEE International Conference on*, March 2007, pp. 228–235.
- [8] W.-T. Chen, “An accurate tag estimate method for improving the performance of an RFID anticollision algorithm based on dynamic frame length Aloha,” *Automation Science and Engineering, IEEE Transactions on*, vol. 6, no. 1, pp. 9–15, Jan 2009.
- [9] E. Vahedi, V. Wong, I. Blake, and R. Ward, “Probabilistic analysis and correction of Chen’s tag estimate method,” *Automation Science and Engineering, IEEE Transactions on*, vol. 8, no. 3, pp. 659–663, July 2011.
- [10] P. Solic, J. Radic, and N. Rozic, “Energy efficient tag estimation method for Aloha-based RFID systems,” *Sensors Journal, IEEE*, vol. 14, no. 10, pp. 3637–3647, Oct 2014.
- [11] “EPCglobal, EPC radio-frequency identity protocols class-1 generation-2 UHF RFID protocol for communications at 860 MHz-960 MHz,” no. 1.2.0, 2008.
- [12] W.-T. Chen, “A feasible and easy-to-implement anticollision algorithm for the EPCglobal UHF Class-1 Generation-2 RFID protocol,” *Automation Science and Engineering, IEEE Transactions on*, vol. 11, no. 2, pp. 485–491, April 2014.
- [13] D. Lee, K. Kim, and W. Lee, “Q+-algorithm: An enhanced RFID tag collision arbitration algorithm,” in *Proceeding Conference Ubiquitous Intelligence Comput*, 2007, pp. 23–32.
- [14] H. Wu, Y. Zeng, J. Feng, and Y. Gu, “Binary tree slotted aloha for passive RFID tag anticollision,” *Parallel and Distributed Systems, IEEE Transactions on*, vol. 24, no. 1, pp. 19–31, Jan 2013.

Evaluating Mobile Phones and Web Sites for Academic Information Needs

Muhammad Farhan

Dept. of Computer Science and IT
The Islamia Univ. of Bahawalpur,
Pakistan

Nadeem Akhtar

Dept. of Computer Science and IT
The Islamia Univ. of Bahawalpur,
Pakistan

Amnah Firdous

Dept. of Computer Science
COMSATS Institute of Information
Technology

Malik Muhammad Saad Missem

Dept. of Computer Science and IT
The Islamia Univ. of Bahawalpur,
Pakistan

Muhammad Ali Nizamani

Faculty of Engineering, Science and
Tech
Isra University Haiderabad

Hina Asmat

Dept. of Computer Science
Govt. S.E. College, Bahawalpur

Abstract—In the last decade, there has been an exponential growth in use of mobile phones among people. Smart phone invention has digitized life of a common man especially after introduction of 3G/4G technology. People are used to use Internet on the move because of this advancement in technology. This advancement has also motivated usability design researchers to propose more usable designs for both smart phones and web sites. This work focuses on evaluation of web usability of mobile phones as well as usability of university web sites. Evaluation is performed on the most popular mobile phones required by the most common mobile users. Selection of the most popular mobile devices, the most common mobile users and their web usage is done by conducting a very detailed survey in the local market. Survey concludes that students and labors are the most common buyers of mobile phones and we choose three mobile phones from the category of most popular phones that are iPhone (iPhone 4 precisely), Q-Mobile (Q Mobile A35) and Windows phone (Lumia 535). Six participants (three male and three females) are selected for fully detailed and rigorous task-based usability testing with “think aloud” technique. Task scenarios are defined to evaluate the usability of both i.e. smart phones and chosen university web sites. From results of usability testing, we find out that iPhone has better usability design as far as its response time is concerned while Q Mobile ranks second and Microsoft Windows phone takes last position in this ranking. Usability evaluation of university web sites on these mobile phones concludes that web site of Islamia university of Bahawalpur (I.U.B, Bahawalpur) has better mobile usability design and Bahauddin Zakariya university (BZU, Multan) and NFC Institute of Engineering and Technology NFCIET, Multan) second and third respectively and while web site of Institute of Southern Punjab (ISP, Multan) comes last when measured in terms of task completion time. All tests are performed on wireless network when internet download speed is between 3MBPS to 3.2MBPS.

Keywords—Usability Engineering; Smart Phones; Academic information need

I. INTRODUCTION

Since the arrival of mobile phones in the 1980s, they have turned out to be broadly utilized among all ages. In fact, they are turning into the personal computers because users are

increasingly using mobile phones rather than desktops to get to information and services. Due to this significant diffusion of mobile technologies in our lives, the way we used to access information has also changed. For example, we used to visit schools, colleges or universities or their prospectus for getting information of any kind (like course material, degree programs, directory etc). However with the advancement of technology, all such information lies in your hands if you are benefitting from mobile internet. Accessing academic information is not only a need of a causal user but it becomes mandatory for students to get daily information from their university's web site [16]. Students often consult institute's web site for occasional changes in examination schedules, assignments, course material, exam results, news etc. We know that usability of user interfaces are very important for web sites [17] but it becomes more important issue when a web site is being viewed on a mobile and is being frequently visited by many users.

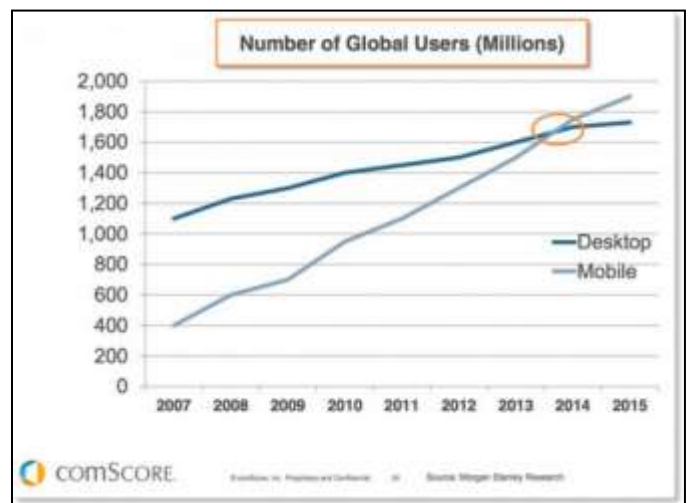


Fig. 1. Mobile Vs Desktop Users¹

¹ <http://www.smartinsights.com/mobile-marketing/mobile-marketing-analytics/mobile-marketing-statistics/>

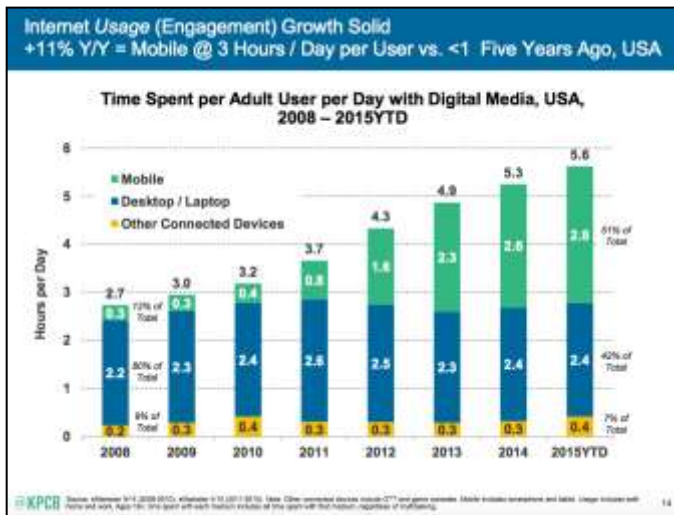


Fig. 2. Internet usage: Mobile Vs Desktop²

Research Objectives

- To find out what kind of smart phones are popular among students,
- To find out what types of tasks student perform while surfing university web sites,
- To evaluate usability of popular smart phones for defined tasks,
- To evaluate usability of different university web sites.

II. RELATED WORK

Our work in this paper basically corresponds to two major issues i.e.

- Usability of mobile web sites
- Usability of mobile phone interactions,

Therefore, in this section of related work we will discuss the work who have worked on both or one of these aspects.

A. Web Site Usability Evaluation

Because our work relates to evaluation of university web sites, we mostly highlight work done on university web sites already.

The work done by Jabar et al. [1] focuses on usability elevation of three Malaysian university Websites. Researchers took support of questionnaires for this purpose. The first portion of their questionnaire directs the demographic of the respondents while the second portion combine twenty four questions that were used to evaluate the usability of educational websites. Overall figure of 351 students were chosen to answer questionnaires for evaluating websites usability depending on Content, organization and readability,

navigation and links, user interface layout and performance and efficiency. The result point out the strengths and flaws for each web site evaluated. Similar kind of work was done by Anwar and Keita [2] on Bangladeshi university web sites with a focus on more technical aspects. Their research evaluates some selective university websites in Bangladesh from the usability aspect. Two online automated appliance namely *web page analyzer* and *html toolbox* were used along with a questionnaire conducted against users of these websites. These appliance were used to evaluate, download time html code flaw, and scope of the html page. The survey questioner was split into two sections. The first part directs the attribute of member and the second part contains thirty survey questions that were used to assess the usability of some university websites in Bangladesh. It is found out that most of the users are not satisfied by usability of these websites while few of them are satisfied with the accessible attributes. However, there are some flaws in some aspects of the design, interface, and performances. Another work [3] in the same category is found on Nigerian universities web site evaluation. This study performs usability evaluation of ten randomly selected Nigerian universities websites. They take support of automated appliances such as *HTML toolbox* and *web page analyzer* for data gathering. The inside characteristic that were taken into review demonstrate entire number of html files, entire size of images, entire number of images, , entire size of external files, as well as Load time, browsers similarity. The finding show that some of universities websites adhered to the laid down threshold values of these characteristic while some are still very much flawed. They found out that no single university adhered to the verge values as provide by the two automated tools used

Another work on university web site evaluation is done by Dr. Ahmet et al. [4] with a slightly different objective of finding impacts of users' demographics on usability. They analyze and evaluate Namik Kemal University (NKU) website and give direction to grow better and more usable web site. The analysis is done by pursuing two various techniques together. First, a few inside participants were individually asked to answer to the online survey questioner. Second, the link to approach the survey questioner was sent to all inside participant through NKU email system. Results acknowledged that some of the demographic part tested, such as gender and web skill, have important impacts on usability approach of separate users. Layla [5] take a very text-book approach for evaluation of three Jordanian web sites. She preferred a heuristic evaluation technique for this purpose and prepared two documents i.e. heuristic guidelines and tasks list. The assessments included testing all pages related to the preferred universities faculties and their corresponding departments. Thirty four (34) specific types of usability problems were determined.

Beside the evaluation of university web sites, there are works that have worked on evaluation of other genre of sites. For example, Walia [6] evaluate the usability features of preferred national libraries websites of Asia with concern to their ordinary attributes of website, URL, window title, time and date, navigation, content, graphic and animation. A usability evaluation checklist was layout on the basis of

² <http://www.smartsights.com/internet-marketing-statistics/insights-from-kpcb-us-and-global-internet-trends-2015-report/attachment/mobile-internet-trends-mary-meeker-2015-1/>

guidelines given by Neilson. Later evaluating the homepage of preferred web sites it was found that the Japan National Library is at position number one among 23 national libraries of Asia and National Library of Maldives at the last position. Similarly another work to be reported is done by Silva [7]. In this work, usability of the library web site of the University of Colombo was measured for its feasibility, profitability and satisfaction through usability testing technique and post-test survey. The study found that general practicality of the library site was 88.69% while efficiency was 1.35 minutes/task. For the most part, the users were extraordinarily satisfied with the library website. A different but related work is on usability evaluation of online news papers [8]. The major focus of this study is to evaluate online newspaper websites. The outcome of this research is that usability component is almost satisfactory for all Jordanian online newspapers whereas the web content element is average.

Another related but different work was done by ShihPeng Hsu [9]. It was different in a way that it tried to show that how a website with improved usability and effectiveness with the no difficulty of learning and memorizing have a strong control over the buying behavior of customer. This study used experimental questionnaire process to assess the usability in different Shopping Mall websites.

B. Mobile Phone Interaction Usability

In this sub-section, we highlight some works related to evaluation of mobile phones usability.

Chi-I Hsu et al. [10] perform mobile usability analysis on basis of two smart mobile phone operating system i.e. iOS and Android. The approach used involved observational experiments and user questionnaire. Total 48 participants are asked to perform five different tasks and rate their satisfaction level on each operating system. The researcher finding is overall iPhone operating system is best as compared to android. Ahmed et al [11] perform a similar type of work by asking questions about usability of Android and iOS. They also proposed an integrated model where both iOS and Android applications can be played in same environment. A similar kind of work is performed by Yong Gu Ji et al [12] where they used heuristic approach. Patrick M. Finley [13] evaluated and compared the usability of different smart phones for table and list based content.

Kimberly [14] found out how smart phone's hardware and operating system impact the usability of library web sites. He performed pre-test and post test surveys on 12 students of age greater than 18 years old.

Comparing our work with the related work, it can be observed that our work is more focused on university's web sites on popular mobile phones in Pakistan. We perform our experiments in a very systematic way by following the findings of our survey. We perform a detailed usability testing by focusing in minor details to give reliable results.

III. SURVEY

This survey is conducted to gather information on

consumer's mobile phone. Our Survey will give you the information you need so that you can create campaigns and improve your services that are geared toward mobile website. Market research concentrating on any survey-based method delivered via a mobile device and website. This includes Apps, SMS, WAP, Location-based Services, Mobile WEB, and both Mobile Terminated and Mobile Originated interactions. Want to ramp up your mobile marketing or improve your cell phone services Send this expert-certified mobile or cell phone survey to get a better understanding of consumer mobile habits. Total round about 100 participant are conduct for survy 50 shopkeapar and 50 customer and the survey questionnaire are given below.

C. Survey Findings

It is found that there are three types of most frequent buyers of mobile phones in the market:

- Daily wage workers
- Students
- Common Men

It is also found out that there are three categories of mobile phones most commonly bought:

- First Category:
 - Popular among workers,
 - Loud sound,
 - Can play video,
 - Long lasting battery,
 - Price range 3K to 5K,
 - Mp 3 Supported.
- Second Category:
 - Popular among students,
 - Loud sound,
 - Can play video,
 - Long lasting battery,
 - 3G/4G supported,
 - Price range 3K to 10K.
- Third Category
 - Popular among common men,
 - Loud sound,
 - Can play video,
 - Long lasting battery,
 - Mp3/Mp4 supported,
 - Price range 3k to15k.

IV. USABILITY TESTING

A. Participant Selection

In our survey, we find out that three types of different customers of frequent mobile buyers exist in the local market. We choose one category among them i.e. students to continue our experiments. We recruit total 6 participants (03 males and 03 females) for usability testing. All of them are studying in educational institutes of South Punjab. Two belong to distt. Rahim Yar Khan, two belong to Bahawalur while remaining two belong to Multan. All of them are IT Graduates having more than 2 years of experience of using Internet on Smart Phones. The students are financially compensated for their time and participation.

B. Mobile Phone Selection

Choosing students as our choice of participants, we choose three mobile sets from different companies belonging to the category students mostly buy (see survey in previous section). The mobile specifications are given below:

TABLE I. SELECTED MOBILE SPECIFICATIONS

1	Microsoft Lumia 535 Release date :2014 December LCD Resolution: 540 x 960 Camera :5 Mega pixel Memory :internal 8 GB RAM 1 GB MP3 Function: Support
2	Q Mobile :A65 Release date: 2013October LCD Resolution: 800 x 400 Camera:3 Mega Pixel Memory: internal 4GB RAM 512 MP3 Function :Support
3	Apple I phone: 4S Release date:2010 June LCD Resolution:540*960 Camer:5 Mega Pixel Memory: internal 16 GB 1GB RAM MP 3 Function: Support

C. Web Site Selection

Following web sites are selected for usability testing.

TABLE II. SELECTED WEB SITES

1	The Islamia Univ. of Bahawalpur Pakistan	http://www.iub.com.pk
2	Institute of Southern Punjab, Multan Pakistan	http://www.isp.edu.pk
3	Bahaduddin Zakaria Univ. Multan Pakistan	http://www.bzu.edu.pk

4	NFC Institute of Engineering and Technology Multan Pakistan	http://nfciet.edu.pk/
---	---	---

D. Evaluation and Results

Few performed usability evaluation in a very detailed way. Each site is evaluated by each participant on each selected mobile phone. In this way, we performed total 72 usability evaluations. For anonymity, we name test participants as A, B, C, D, E and F.

- Usability Goals

TABLE III. WEB USABILITY GOALS

	Goals	Description
1	Goal 1	Accessing University web site
2	Goal 2	Accessing the Basic Information about Program and detail of Syllabus
3	Goal 3	Information About Facility
4	Goal 4	Find fee structure
5	Goal 5	Find Available Job In the University
6	Goal 6	All Information About University Reflected On Home Page
7	Goal 7	Frequently Access Information Available On Single Click
8	Goal 8	News and events Section are clearly visible on home page
9	Goal 9	Applicable Information Available On Website
10	Goal 10	Contents is Visible With looking over or without looking over
11	Goal 11	Easygoing client can Find Information with no assistance
12	Goal 12	un necessary stuff available or not
13	Goal 13	Complete Navigation for client and Search Engine are accessible

- Usability Goals to Usability Task Conversion

It is a general practice to convert the defined usability goals into actions or tasks [15]. Table IV shows defined goals and equivalent tasks defined for our experiments.

TABLE IV. GOAL TO TASK CONVERSION

	Goals	Corresponding Task
1	Goal 1	Open index page of web site of the Institute of Southern Punjab
2	Goal 2	Get the detail of the admission criteria of computer science
3	Goal 3	Find the Syllabus of BS(Cs)&BS(IT) and compare it(Explanation)
4	Goal 4	Check the Profiles of P.H.D professor in computer Science
5	Goal 5	Find Fee Structure of BS (Cs) \$BS (IT)program
6	Goal 6	Check the Different Categories are Provided and Clearly Visible on the homepage(Explanation →About Iub →Administration→Academics→)

		Facilities → Admission → Research → Alumni,)
7	Goal 7	Useful Content is Presented on the Home Page or within one click of the home page.(Explanation to check on one click all link are open and visible Like notification, result etc)
8	Goal 8	Recently Uploaded Features are Displayed in efficient like News, Notification and updates link.
9	Goal 9	Check this Site is Free From Irrelevant, Unnecessary and Distracting Information
10	Goal 10	The Site Requires Minimal Scrolling and Clicking (Explanation open website do you required scrolling to view all the content)
11	Goal 11	A Typical First-Time Visitor can do the most Common tasks without assistance.
12	Goal 12	Unwanted Features (e.g. Flash animations) can be stopped or skipped
13	Goal 13	Check Site map that provides an overview of the site's content.(Explanation you search like keyword for e. g you just click on site map and search keyword like job ,home, contact, etc)

In table V, we describe an example of the evaluation that is performed by each user for each mobile and for each site. Each user is closely observed during each defined task and task completion time is also noted. It is to be notified that we perform open time experiments i.e. there is no limit on time and hence a user can continue till the completion of a task.

TABLE V. EXAMPLE OF AN EVALUATION

Goal No.	Task	Observation	Duration (hh:min.sec)
1	Open index page of web site of the NFC Institute of Engineering and Technology	Successfully open but it take much more time for Loading	00:01:03
2	Get the detail of the admission criteria of computer science	Admission criteria find Successfully	00:00:05
3	Find the Syllabus of BS(Cs)&BS(IT) program	Page are loaded successfully but content are not available	00:00:07
4	Check the Profiles of PhD professor in computer Science	Profile found successfully but content are not showing	00:00:16
5	Find Fee Structure of BS (Cs) \$BS (IT)program	Fee Structure of BS (Cs) \$BS (IT)program Find	00:00:19

		Successfully	
6	check the available job	Available job found successfully	00:00:11
7	Open index page of web site of the NFC Institute of Engineering and Technology	Successfully open but it take much more time for Loading	00:01:03
8	Get the detail of the admission criteria of computer science	Admission criteria find Successfully	00:00:05
9	Find the Syllabus of BS(Cs)&BS(IT) program	Page are loaded successfully but content are not available	00:00:07
10	Check the Profiles of p.h.d professor in computer Science	Profile found successfully but content are not showing	00:00:16
11	Find Fee Structure of BS (Cs) \$BS (IT)program	Fee Structure of BS (Cs) \$BS (IT)program Find Successfully	00:00:19
12	check the available job	Available job found successfully	00:00:11
13	Open index page of web site of the NFC Institute of Engineering and Technology	Successfully open but it take much more time for Loading	00:01:03

Once we have results for all the experiments, Table VI-A and table VI-B describe the results for web site of Bahauddin Zakaria University Multan for all the defined tasks. Due to space limitations, tables of all results cannot be mentioned here. Looking at the results, we can see few interesting patterns like it is obvious that open web site task is taking too much time for all mobile phones. Similar is the case for downloading a file. There are very strong and obvious reasons behind these results which is speed of Internet being used while performing experiments. This is the reason we performed all experiments on the same network. If we look at overall results, it can be concluded that apparently mobile phones interfaces and web site interfaces are providing acceptable usable interfaces; however problems are being caused by Wifi speed apparently. We will have a detailed look at mobile interfaces and web sites usability following in sub-sections.

TABLE VI. A: TASK BASED TIME STATISTICS (IN SECONDS) – PART I

	Login Time	Connect with WIFI	Open Browser	Open Web Site	Open multiple page at a time	Close all tabs time	Download Any file	Save bookmark
Mean	1.44	3.10	3.01	18.29	11.38	4.56	24.18	6.43
Std. Mean of Error	0.09	0.19	0.15	4.02	0.85	0.36	1.10	0.66
Median	1.35	2.67	2.78	3.94	9.31	3.85	22.31	4.29
Mode	1	2	3	3	5	2	22	3
Std. Deviation	0.76	1.68	1.30	34.16	7.23	3.11	9.33	5.59
Variance	0.58	2.85	1.70	1167.39	52.33	9.71	87.19	31.31
Range	3	8	7	148	32	21	45	27
Minimum	1	1	1	1	5	1	2	2
Maximum	4	9	8	149	37	22	47	29
Sum	104	223	217	1317	819	328	1741	463

TABLE VI. B: TASK BASED TIME STATISTICS (IN SECONDS) – PART II

	Delete Temp Files	Web Share Time	Open Home Page	Check Admission Criteria and Course	Check PhD Faculty Profile	Check Fee Structure	Check Available Job	Check All Links
Mean	11.96	73.56	39.97	14.86	21.82	19.40	23.18	44.88
Std. Mean of Error	0.79	2.14	5.16	1.52	2.31	1.44	2.72	7.34
Median	10.80	69.86	12.00	9.92	16.00	18.60	14.00	38.25
Mode	9	60	2	5	10	22	10	33
Std. Deviation	6.72	18.21	43.79	12.94	19.63	12.29	23.10	62.28
Variance	45.19	331.63	1918.33	167.53	385.47	151.20	533.75	3879.06
Range	38	121	116	65	115	90	85	545
Minimum	1	22	2	3	4	3	4	5
Maximum	39	143	118	68	119	93	89	550
Sum	861	5296	2878	1070	1571	1397	1669	3231

E. Mobile Analysis

Based on the results, we find it necessary to discuss few interesting data patterns. In the diagram (figure 3), Y-axes represents the mean time of each specific task mentioned for each mobile on X-axis. It is very obvious from this figure that iPhone beats both other mobiles as far as its response time is concerned. However, it is far behind on one task i.e. opening web site task. We think it could be because of two reasons and one of which is external factor i.e. it does not shows any lacking on iPhone interface. This factor could be speed of Wifi. It is true that all experiments were performed on same Wifi but still speed of Wifi could vary on different times. Another factor could be the relatively smaller size of iPhone that makes typing a difficult task. In short, results shows that iPhone mobile has fast response time and Q mobile is second in ranking and Microsoft mobile is 3rd one in our ranking.

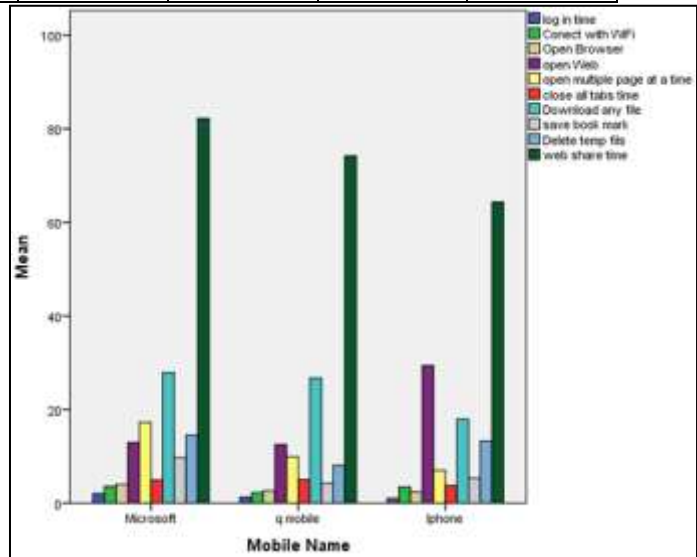


Fig. 3. Web Site Usability Task Based comparison of Mobile Phones

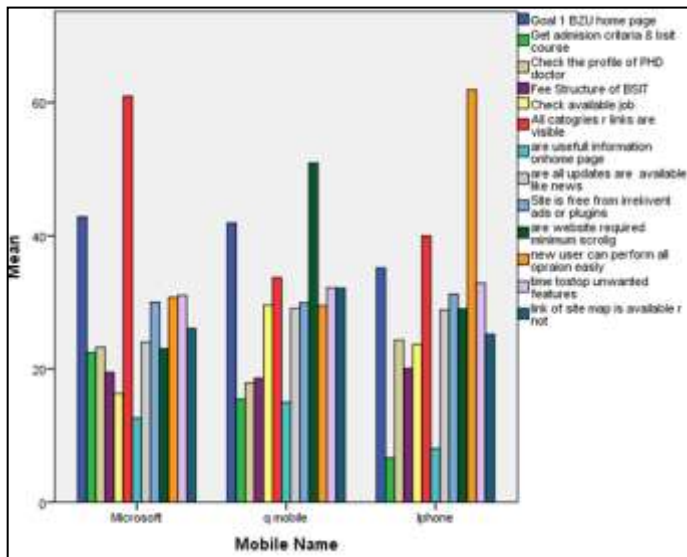


Fig. 4. Mobile Interface Task Based comparison of Mobile Phones

In figure 4 we give thirteen goals to the different users after giving some training that how the different tasks are performed. In this figure, each color represents a different task. A short description of the task is given on right side of the graph. From this histogram, we can easily conclude that over all response time of iPhone mobile performance or response time is also better on average i.e. it is faster due to its simplicity of user interface. On the other hand Q mobile is second fastest mobile in our ranking while Microsoft mobile stands itself on last in our experiments as far as time to complete tasks on these mobile phones is concerned.

F. Gender Based Analysis

In our case study the performance of both males and females are mostly similar because of in our study we take both male and females are educated in IT so that's why the reason of computational capability is same and all goals are related to educational website so there all the information on all websites are same just position of different information is change which is not difficult to trace both of them in our results male are little bit better than female due to experience.

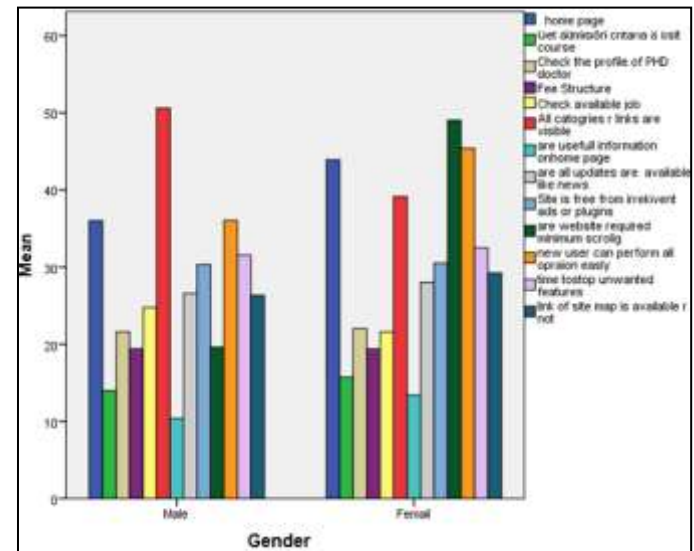


Fig. 5. Gender Based comparison of Task Times

But when we compare the results of male and female participants for evaluation of mobile interfaces (figure 6), it can be concluded that males perform slightly better than females. To find the reasons behind this slight difference, we concluded the pre-test questionnaire filled by each participant and it is found out that males are used to spend more hours on mobiles than females in their free time. Hence, males are more used to perform these operations on mobiles and this is what results are reflecting.

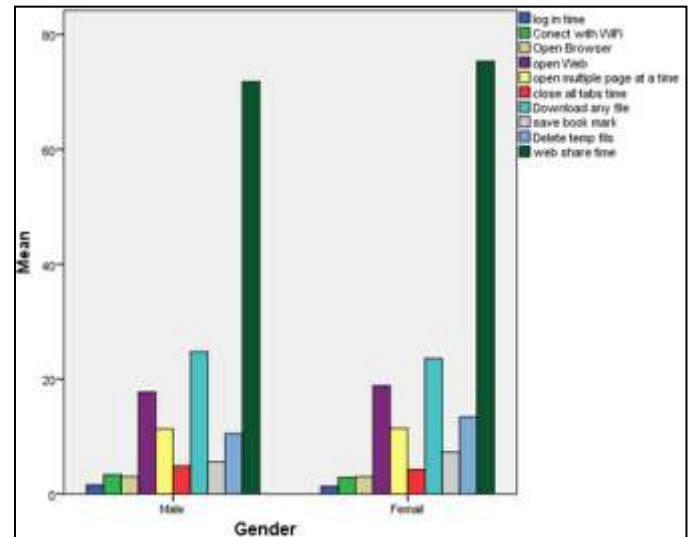


Fig. 6. Gender Based Task Comparisons on Phone Interface

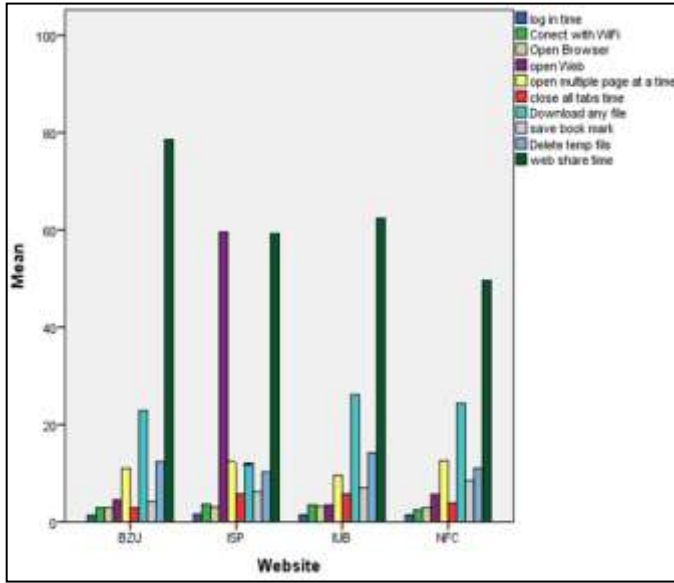


Fig. 7. Comparison of Web Sites Task Based Usability

Figure 7 shows the website analysis to conclude that which web site is better in its usability interface. As shown, Y-axis represents the mean time taken to complete tasks on the web sites mentioned on X-axis of the figure. With respect to completion time, we can conclude from given histogram that NFCEIT has the best user interface among the set of given web sites. Rests of the web sites are almost same with slight differences on different tasks.

V. CONCLUSIONS

This research study focused on very important task of usability engineering where we have evaluated university web sites as far as smart phones for their usability. We know that inaccessibility of information means absence of information which makes a very important thesis for this work. The methodology for this work includes a detailed survey and usability testing. Survey findings reveals the types of most frequent buyer of phones and also the types of the most popular phones among these frequent buyers. Further, we performed a set of 72 usability tests to conclude which smart phones and web sites have better usability interfaces. We also analyzed the results with respect to gender and task performed. We conclude that male perform better than females because they are used to use spend more time on mobile phones. Similarly, it was found out that iPhone has a better usability interface than other smart phones while NFCEIT web site is better from other sites. The conclusions of our experiments are listed below:

- Three most frequent mobile phones buyers are labors, students and rest of the buyers.
- Three types of most commonly bought mobile phones along with their characteristics (see table I).

- iPhone has a better usability interface than other mobile phone used in our experiments.
- NFCEIT web site has a much better interface than rest of the sites.
- The most difficult tasks to perform are downloading files and opening multiple pages at a time on mobile phones.
- Males are better mobile phone users than females.

REFERENCES

- [1] Jabar, M. A., Usman Abbas Usman, and F. Sidi. "Usability Evaluation of Universities' Websites." *International Journal of Information Processing and Management* 5.1 (2014): 10.
- [2] Islam, Anwarul, and Keita Tsuji. "Evaluation of usage of university websites in Bangladesh." *DESIDOC Journal of Library & Information Technology* 31.6 (2011)..
- [3] Kiyea, Celinus, and Aminat Bolatito Yusuf. "Usability Evaluation of some Selected Nigerian Universities' Websites." *International Journal of Computer Applications* 104.3 (2014).
- [4] Mentes, S. Ahmet, and Aykut H. Turan. "Assessing the usability of university websites: an empirical study on Namik Kemal University." *TOJET: The Turkish Online Journal of Educational Technology* 11.3 (2012)..
- [5] Hasan, Layla. "Heuristic Evaluation of Three Jordanian University Websites." *Informatics in Education* 12.2 (2013): 231-251.
- [6] Walia, Paramjeet K., and Monika Gupta. "Usability analysis of Homepage of Websites of National Libraries in Asia." *Library Philosophy & Practice* (2013).
- [7] Silva, M. A. L., and I. D. A. L. Wijayaratne. "Usability evaluation of University of Colombo library website: A case study." *Annals of Library and Information Studies (ALIS)* 62.1 (2015): 40-47.
- [8] Al-Radaideh, Qasem A., et al. "Usability Evaluation of Online News Websites: A User Perspective Approach." *International Journal of Human and Social Sciences* 6.2 (2011).
- [9] Hsu, Shih-Peng, et al. "Usability Evaluation of Mobile Commerce Website on Internet-An empirical study." *WHICEB*. 2014.
- [10] Hsu, Chi-I., Chaochang Chiu, and Wen-Lin Hsu. "USABILITY EVALUATION AND CORRESPONDENCE ANALYSIS OF SMARTPHONE OPERATING SYSTEMS.".
- [11] Ahmad, Naseer, Muhammad Waqas Boota, and Abdul Hye Masoom. "Smart phone application evaluation with usability testing approach." *Journal of Software Engineering and Applications* 7.12 (2014): 1045.
- [12] Ji, Yong Gu, et al. "A usability checklist for the usability evaluation of mobile phone user interface." *International Journal of Human-Computer Interaction* 20.3 (2006): 207-231.
- [13] Finley, Patrick M. "A study comparing table-based and list-based smartphone interface usability." (2013).
- [14] Pendell, Kimberly D., and Michael S. Bowman. "Usability study of a library's mobile website: an example from Portland State University." *Information Technology and Libraries (Online)* 31.2 (2012): 45.
- [15] Kaufman, David R., et al. "Usability in the real world: assessing medical information technologies in patients' homes." *Journal of biomedical informatics* 36.1 (2003): 45-60.
- [16] Zhang, Dongsong, and Boonlit Adipat. "Challenges, methodologies, and issues in the usability testing of mobile applications." *International Journal of Human-Computer Interaction* 18.3 (2005): 293-308.
- [17] Dix, Alan. *Human-computer interaction*. Springer US, 2009.

Feasibility Study of Optical Spectroscopy as a Medical Tool for Diagnosis of Skin Lesions

Asad Safi and Sheikh Ziauddin
COMSATS Institute of Information
Technology Islamabad, Pakistan

Victor Castaneda
Universidad de Chile Independencia 1027
Santiago, Chile

Alexander Horsch
Department of Medical Statistics
and Epidemiology, Technische Universität
München, Germany

Mahzad Ziai
Klinik und Poliklinik für Dermatologie
und Allergologie, Technische Universität
München, Germany

Tobias Lasser and Nassir Navab
Chair for Computer Aided Medical Procedures (CAMP),
Technische Universität München, Germany

Abstract—Skin cancer is one of the most frequently encountered types of cancer in the Western world. According to the Skin Cancer Foundation Statistics, one in every five Americans develops skin cancer during his/her lifetime. Today, the incurability of advanced cutaneous melanoma raises the importance of its early detection. Since the differentiation of early melanoma from other pigmented skin lesions is not a trivial task, even for experienced dermatologists, computer aided diagnosis could become an important tool for reducing the mortality rate of this highly malignant cancer type.

In this paper, a computer aided diagnosis system based on machine learning is proposed in order to support the clinical use of optical spectroscopy for skin lesions quantification and classification. The focus is on a feasibility study of optical spectroscopy as a medical tool for diagnosis. To this end, data acquisition protocols for optical spectroscopy are defined and detailed analysis of feature vectors is performed. Different techniques for supervised and unsupervised learning are explored on clinical data, collected from patients with malignant and benign skin lesions.

Keywords—Melanoma; Classification; Supervised Learning; Computer-Aided Diagnosis; Machine Learning; Optical Spectroscopy

I. INTRODUCTION

Skin cancer is among the most frequent types of cancer and one of the most malignant tumors. The incidence of melanoma in the general population is increasing worldwide [1], especially in countries where the ozone layer is thinning. Its incidence has increased faster than that of almost all other cancers, and the annual rates have increased by 3% to 7% in the fair-skinned population in recent decades [1]. Currently, between 2 and 3 million non-melanoma skin cancers and 132,000 melanoma skin cancers occur globally each year [2].

New technologies to assist the dermatologists in identifying and diagnosing skin lesion have been introduced, such as handheld magnification devices and computer-aided image analysis. Colored image processing methods have been introduced for detecting the melanoma [3] which focused on non-constant visual information of skin lesions. Neural network diagnosis of skin lesion has been applied by classifying extracted features from digitized dermoscopy images of lesions [4] [5].

The extracted features are based on geometry, colors, and texture of the lesions, involving complex image processing techniques. Many other attempts have been made to automate the detection and classification of melanoma from the digital color and surface reflectance images [6][7][8][9][10]. Those attempts involve the initial segmentation of the skin lesion from the surrounding skin followed by the calculation of classification features [11][12][5][13][14][15]. Accurate description and measurement of image features cannot be achieved without accurate image segmentation. Therefore, a wide range of algorithms have been proposed in the past for color image segmentation [16], broadly categorized as pixel-based segmentation, region-based segmentation [17], region-based segmentation and edge detection [18]. However, in the case of optical spectral reflectance images, the research is still limited due to the late introduction of the imaging technology in dermatology.

A. Why Optical Spectroscopy?

One of the substantial features for the diagnosis of malignant melanoma is the skin lesion color [19]. In most of the related research, skin lesion color was investigated to disintegrate malignant melanoma lesions from benign lesions in clinical images [20]. Human skin is a variegated surface, with fine scale geometry, which makes its appearance difficult to model. Furthermore, the conditions under which the skin surface is viewed and illuminated greatly affect its appearance.

As we know that light of different wavelengths access the skin in different depths (as shown in Figure 1). This fact led the researchers to evaluate pigmented lesions under specific wavelengths of light from visible spectrum to near infrared range. Through multi-spectral imaging we can capture light from frequencies beyond the visible light range which allows us to extract additional information that the human eye fails to capture with its receptors for red, green and blue. Furthermore, the spectral information can be employed for the analysis and the information retrieval about the consistency and the concentration of absorbers and reflectors in the skin. Different pigments of the skin absorb different wavelengths of optical spectrum, which helps in determining the reflectance coefficient of the area of the skin.

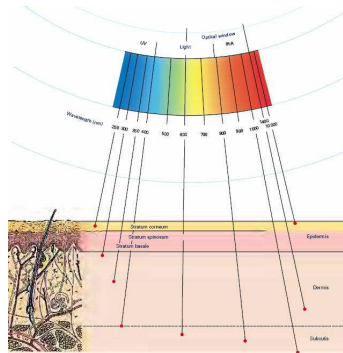


Fig. 1. Different wavelengths penetrate the skin to different depths. Visible light and near infrared penetration in skin is more than other wavelengths (Image source: [21])

One of the most significant features of spectral reflectance is the property that the spectral reflectance curve is based on the material composition of the object's surface, color, biochemical composition and cellular structure. This property can be utilized for recognizing objects and segment regions. Currently there exist only a small number of systems, e.g. spectrophotometric intracutaneous analysis (SIA) scope [22], MelaFind [23] and SpectroShade [24], which use multispectral dermoscopic images as the inputs for subsequent computer analysis. To the best of our knowledge, the systems which have already been developed for the analysis of skin lesion from multispectral images, are based on the images of selected wavelength without keeping record of reflectance spectra. However, as different skin lesions can be investigated more in detail by observing their reflectance, we analyze the feasibility of spectroscopy as a tool to distinguish benign and malign skin lesions.

B. Introduction of Spectroscopy

Spectroscopy is a new imaging technology which is increasingly used to derive significant information about tissue. Due to its multi-spectral nature, this imaging method allows to detect and classify multiple physiological changes like those associated with increased vasculature, cellular structure, oxygen consumption or edema in tumors [25]. The hardware setup for data acquisition is explained in more detail in section III.

Optical spectra in different wavelengths and amplitude is shown in Figure 2 which shows the differences between four colors (red, green, yellow and blue). The experiment is performed on the phantom, where chalks colored with four different inks are used in the experiment. Figure 2 clearly shows that variation in color produces difference in optical spectroscopy.

We design an experiment, to observe the difference between objects based on internal structure. In this experiment we gather six different fruits (Apple, Blueberry, Kiwi, Strawberry, Plum and Orange). Data was collected from each fruit after 12 hours for 7 days consecutively. Due to the change in the internal structure of the fruits the curve was changed, but the main shape of the curve was always constant. Standard deviation of each fruit in wavelength and amplitude is shown in Figure 3.

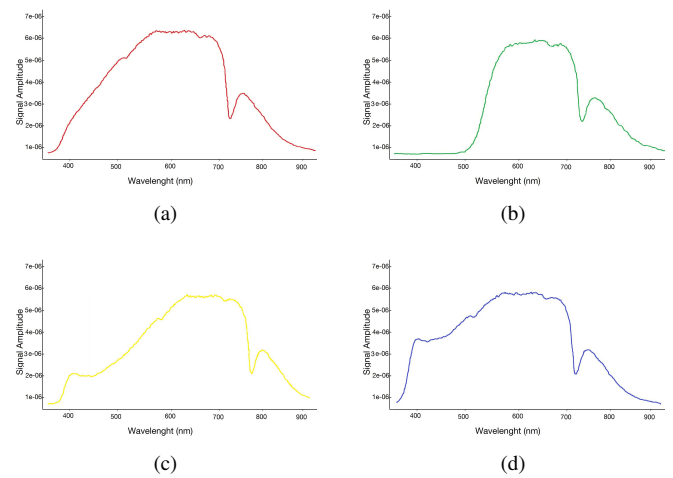


Fig. 2. Optical spectra from chalk with color inks in wavelength and amplitude. (a) Red color, (b) Green color, (c) Yellow color, (d) Blue color

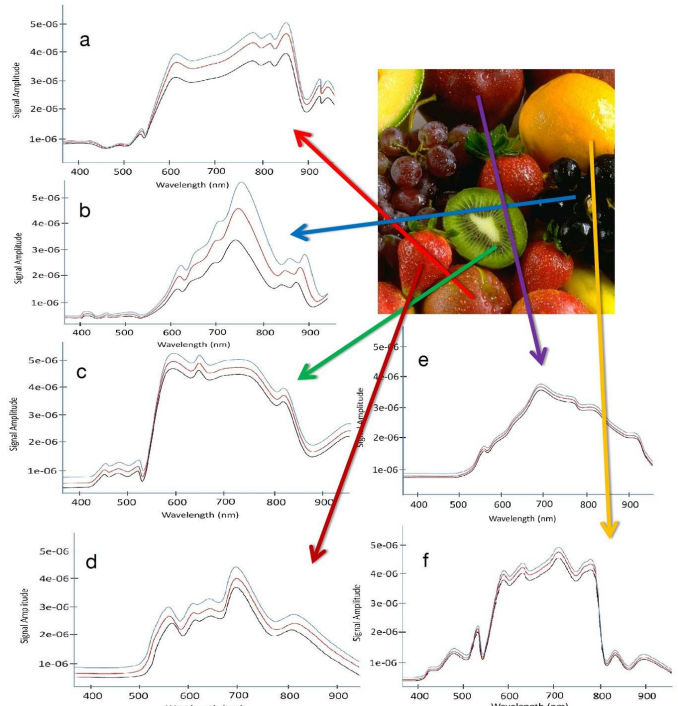


Fig. 3. Spectral standard deviation of each fruit in wavelength and amplitude. Lower curve (Black colored) is the minimum, the upper curve (Blue colored) represents the maximum and the middle curve (Red colored) represents the mean. (a) Apple, (b) Blueberry, (c) Kiwi, (d) Strawberry, (e) Plum, (f) Orange

II. STATE OF THE ART

Skin color measurement through reflectance spectroscopy has received significant attention in the literature [19][26][27][28]. It has been used to provide a numerical index for color, which in turn allows for the study of constriction of a blood vessel and abnormal redness of the skin due to local congestion, such as in inflammation [29]. Dawson et al. [30] worked on the reflectance spectroscopy for the measurement of skin tissue to exemplify the spectral properties. Farrell et al. [31] and Kienle et al. [32] addressed the problem of reflectance measurements to determining in

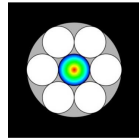


Fig. 4. Schematic representation of the fiber arrangement in the spectroscopy probe: $6 \times 200\mu m$ illumination fibers arrayed around one $600\mu m$ acquisition fiber.

vivo tissue optical properties. Another approach for measuring the optical reflectance over a broad range of wavelengths spectroscopy has been utilized for assessing the skin type and gestation age of newborn infants by Lynn et al. [33].

The first work to evaluate the possibilities of using reflectance spectrophotometry for discriminating between benign and malignant skin lesions was done by Marchesini et al. [34]. Their experiments show that the wavelengths between 400 and 800 nm were highly significant to show the differences between the reflectance spectra of benign and malignant melanomas. Consequently, the authors report a discrimination between 31 primary melanoma and 31 benign lesions with a sensitivity of 90.3% and a specificity of 77.4%, a stepwise discriminate analysis of reflectance spectral features [35].

Moreover, Bono et al. [36] conclude that color is the most important parameter in discriminating melanomas from benign in spectrophotometric imaging of skin lesions using 420–1020 nm. Recently with Raman spectroscopy the molecular structure of skin lesions are explored [37], but due to the side effects of the laser beam on the sensitive skin surface, this technique is not preferred in the dermatology practice.

III. SYSTEM SETUP

A hand-held reflectance spectroscopy probe (StellarNet Inc., Oldsmar, FL, USA) (see Figure 5), consisting of $6 \times 200\mu m$ illumination fibers arrayed around one $600\mu m$ acquisition fiber as shown in Figure 4, was attached to an infrared optical tracking target in order to be able to determine its position and orientation in real-time. The selected tracking system consists of four ARTtrack2 infrared cameras (A.R.T. GmbH, Weilheim, Germany) positioned to be able to track a volume of $2 \times 2 \times 2 m^3$. According to the manufacturer the positional accuracy for such a configuration is 0.4 mm with a maximum error of 1.4 mm (for angle 0.002 rad and 0.007 rad respectively).

A 178–1132 nm, 2048 px, 12 bit CCD spectrometer (StellarNet Inc., Oldsmar, FL, USA) was connected to the acquisition fiber, and a 12 W tungsten lamp was connected to the illumination fibers as a light source. The spectrometer was controlled by a data processing unit to acquire spectra synchronously with the tracking information of the probe. The data-processing unit was also used to run the augmented reality application that combined spectra, positions and orientations. An overview of the entire setup is displayed in Figure 5.

A. Data Acquisition Protocol

In our protocol, the mole selection for the data acquisition is purely based on the doctor's (or physician's) choice based on a visual examination. The labeling of mole is

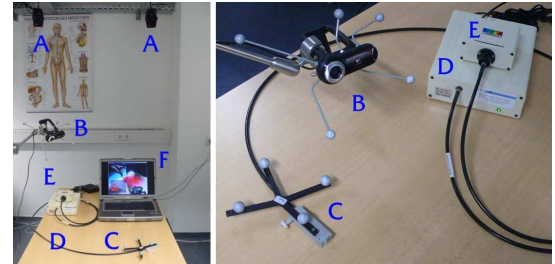


Fig. 5. System setup: (a) tracking cameras, (b) augmented camera, (c) tracked probe, (d) spectrometer, (e) light source, and (f) data-processing unit.

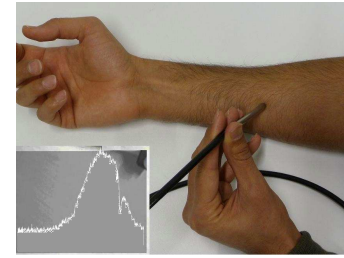


Fig. 6. Covering all the surface of prob tip by contacting skin surface.

performed using two classes: suspicious skin lesion (possibility of malignant melanoma) and normal skin moles based on physician's diagnosis.

The data is stored as a plot of wavelength and amplitude (as shown in Figure 2) by spectrometer without taking into account the mole structure. The time of data acquisition and the number of measurements depend on the number of moles defined on patients, where the time for whole body skin checkup was approximately 20 minutes.

The spatial resolution of sampling region is 1 mm diameter which permits the study of smaller lesions and sampling of several regions within bigger lesions. For mole size bigger than 3 mm and smaller than 6 mm we take 5 measurements (4 from the edges, 1 from the center). If the mole sizes exceeds 6 mm then we take 7 measurements (6 from the edges, 1 from the center). To make sure that the database is consistent and not biased, we only use the measurements which were taken once per mole.

The data acquisition time for one mole is 100 ms. It is important to contact the surface of the mole by the probe tip and keep the probe in a way that no light goes in from outside to ensure that the spectra are only obtained from the lesion itself, as shown in Figure 6. Hair, nails and tattoos are avoided during data acquisition.

B. Data Acquisition

The data collection for this study was performed in collaboration with the dermatology department at Klinikum Rechts der Isar Mnchen; Germany. All lesions in this analysis were selected by dermatology experts. In total, 3072 spectroscopic data vectors were collected from 148 patients, where 2926 measurements were of normal skin moles and 146 measurements from malignant skin lesions. The schematic representation of data acquisition system is shown in Figure 7. Out of 146 malignant skin lesions, 9 cases were histological proven

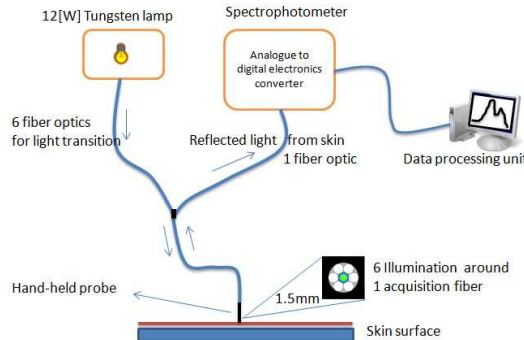


Fig. 7. Schematic diagram of data acquisition system.

melanoma. The remaining 137 are kept under observation. The details of the 9 cases of melanoma are: average Breslow thickness was 1.1 mm , the minimum being 0.1 mm and the maximum 2.8 mm , the average diameter of the lesions was 3 mm , the minimum being 2 mm and the maximum 5 mm . The average age of patients was 40, where the youngest and oldest patients were 2 and 82 years old, respectively. 70% of the examined patients were female. The collected data consists of the following clinical cases:

- Normal skin: spectra were obtained from the inside of the upper arm, groin and inside thigh, a region defined as skin that is not normally exposed to sunlight (i.e. not tanned).
- Normal skin moles: in average 19 spectra per patient were obtained from benign skin moles. Normal skin moles can be visually very similar to malignant moles, as illustrated in Figure 8.
- Malignant skin mole: one spectra was obtained from middle positions on the lesion. Multiple spectra were taken depending on size of the mole as discussed in data acquisition protocol (Section III-A).

Immediately prior to each patient's data collection session, the spectrophotometer probe end was placed in the disinfectant substance to prevent migration of any diseases.

To make sure of reproducibility and accuracy of data acquisition, one concern was that the pressure of the probe on the skin might cause blanching by forcing blood out of local vessels. To test a novel approach to reduce this effect and to assess the magnitude of this problem, a study was performed by Osawa et al. [38]. In their study the probe was held in contact with a flat area of skin and the pressure slowly increased beyond that which would be applied normally for taking skin reflectance measurements. Increasing the pressure caused a decrease in overall reflectance. Osawa et al. suggested three methods for eliminating the effect: (a) a sensor to determine the pressure being applied, (b) an adhesive pad to just hold the probe against the skin, and (c) an electrical contact sensor to feed back information on when the probe makes contact with the skin. In our study the pressure on the skin was reduced by increasing the surface area of contact with a probe holder that was designed to slide in the probe which was also used to keep the tracking points (see Figure 5).

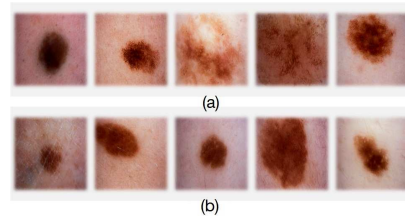


Fig. 8. Skin lesions: (a) Malignant skin lesions, (b) Normal skin lesions.

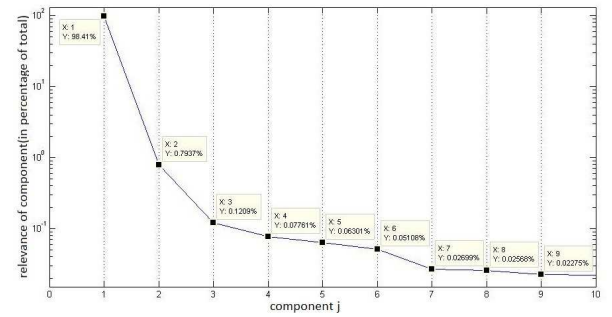


Fig. 9. Representative example of the first part of the sorted PCA eigenvalue spectrum $(e_j^i)_{j=1,\dots,2048}$, the y -axis shows the values of the component as a percentage of the total in log scale.

C. Data Processing

The spectral data is acquired as a $2048D$ vector of the floating points values $x_i \in R^{2048}, i = 1, \dots, n$ where n denotes the number of measurements. Each x_i represents the discretized reflective spectrum from 178 nm to 1132 nm (due to limitation of hardware) of the i th measurement and is stored normalized as

$$\hat{x}_i = \frac{x_i}{\|x_i\|_2} \text{ where } i = 1, \dots, n \quad (1)$$

To reduce the dimensions of the input data, principal components analysis (PCA) is applied. The resulting spectrum of eigenvalues $(e_j^i)_{j=1,\dots,2048}$ is sorted descending by magnitude. Since the highest eigenvalues represent the most relevant components, a cut-off value C_{PCA} is chosen, such that the final input data y_i for the classification algorithm from measurement $x_i (i = 1, \dots, n)$ is

$$y_i = (e_j^i)_{j=1,\dots,C_{PCA}} \quad (2)$$

The cut-off value C_{PCA} is chosen empirically from the data. Figure 9 is showing a representative example of $(e_j^i)_{j=1,\dots,2048}$ from which C_{PCA} was selected as one of $\{2, 3, 4, 5\}$.

IV. CLASSIFICATION

Classification is performed by a support vector machine (SVM) [39]. SVM was selected as the method of choice as it allows to linearly classify data in a high-dimensional feature space that is non-linearly related to the input space via the use of specific kernel functions, such as polynomial functions or

radial basis functions (RBF). This way we can build complex enough models for skin lesion classification while still being able to compute directly in the input space.

The SVM classifier needs to be trained first before using it, thus we partition our already reduced input data $(y_i), i = 1, \dots, n$ into two partitions, $T \subset \{1, \dots, n\}$ the training set and $V \subset \{1, \dots, n\}$ the testing (or validation) set with $T \cup V = \{1, \dots, n\}$ and $T \cap V = \{\}$. The training data set T is labeled manually into two classes with the ground truth, $l(y_i) = \pm 1$. Once the classifier is trained, a simple evaluation of the decision function $d(y_i) = \pm 1$ will yield the classification of any data y_i .

In detail, SVM is trying to separate the data $\phi(y_i)$ mapped by the selected kernel function ϕ by a hyperplane $w^T \phi(y_i) + b = 0$ with w the normal vector and b the translation. The decision function then is $d(y_i) = \text{sgm}(w^T \phi(y_i) + b)$. Maximizing the margin and introducing slack variables $\xi = (\xi_i)$ for non-separable data, we receive the primal optimization problem:

$$\min_{w,b,\xi} = \frac{1}{2} w^T w + C \sum_{i \in T} \xi_i \quad (3)$$

with constraints $l(y_i)(w^T \phi(y_i) + b) \geq 1 - \xi_i, \xi \geq 0$ for $i \in T$. C is a user-determined penalty parameter. Switching to the dual optimization problem allows for easier computation,

$$\min_{\alpha} = \frac{1}{2} \alpha^T Q \alpha - e^T \alpha \quad (4)$$

with constraints $0 \leq \alpha_i \leq C$ for $i \in T$, $\sum_{i \in T} y_i \alpha_i = 0$. The $\alpha = (\alpha_i)$ are the so-called support vectors, $e = [1, \dots, 1]^T$ and Q is the positive semidefinite matrix formed by $Q_{jk} = l(y_j)l(y_k)K(y_j, y_k)$, and $K(y_j, y_k) = \phi(y_j)^T \phi(y_k)$ is the kernel function built from ϕ . Once this optimization problem is solved, we determine the hyperplane parameters w and b , w directly as $w = \sum_{i \in T} \alpha_i l(y_i) \phi(y_i)$ and b via one of the Karush-Kuhn-Tucker conditions as $b = -l(y_i) y_i^T w$, for those i with $0 < \alpha_i < C$. Thus the decision function of the trained SVM classifier ends up as

$$\begin{aligned} d(y_i) &= \text{sgn}(w^T \phi(y_i) + b) \\ &= \text{sgn}\left(\sum_{j \in T} \alpha_j l(y_j) K(y_j, y_i) + b\right) \end{aligned} \quad (5)$$

V. EXPERIMENTS

Data collection of 3072 spectroscopic instances is defined as $(x_i), i = 1, \dots, 3072$ labeled into two classes: normal skin $l(x_i) = 1$ and lesion $l(x_i) = -1$. The 3072 data points were randomly separated into a training data set T and a testing (validation) data set V with $|T| = 2072$ and $|V| = 1000$, however retaining the balance of both sets containing 50% from each of the two classes. A color-coded representation of the normalized skin spectra $\hat{x}_i, i \in T$ of the training data set T is shown in Figure 10.

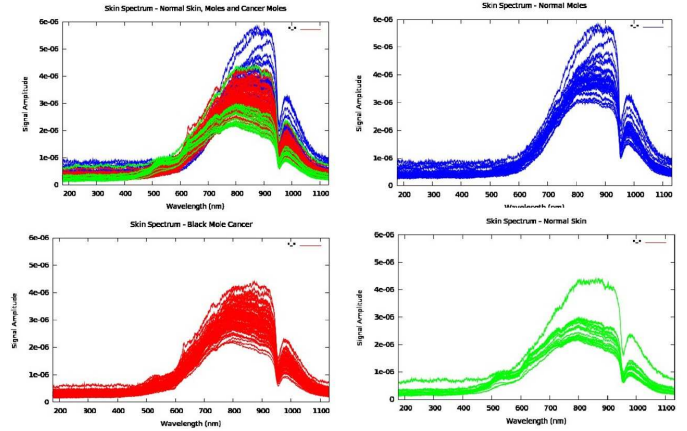


Fig. 10. Plot of all normalized spectra \hat{x}_i from the training data set T , color-coded as blue for normal skin moles, red for malignant mole and green for normal skin. One curve represents one skin lesion data.

TABLE I. RESULTS OF THE CROSS-VALIDATION USING THE TRAINING DATASET T .

Parameters	SVM Training			
	Linear Kernel	Poly Kernel	RBF Kernel	Sigmoid Kernel
$C_{PCA} = 2$	95 ± 9.2	96 ± 8.3	95 ± 7.5	95 ± 9.1
$C_{PCA} = 3$	95 ± 8.3	96 ± 6.7	97 ± 9.5	96 ± 9.5
$C_{PCA} = 4$	95 ± 9.6	97 ± 7.2	97 ± 8.7	96 ± 8.6
$C_{PCA} = 5$	96 ± 9.2	97 ± 9.7	97 ± 8.3	97 ± 7.7

Before classification, PCA was applied to the \hat{x}_i for dimension reduction to yield our classification input y_i . The eigenvalue cut-off C_{PCA} was empirically chosen as one of $C_{PCA} \in 2, 3, 4, 5$.

The SVM classifier (we used LibSVM, [40]) was then trained using the training data set T . As there are multiple parameters to be selected, like for example the penalty parameter C , we performed a cross-validation of 10 folds via parallel grid search. The average accuracy on the prediction of the validation fold is the cross validation accuracy.

A. Discussion

The cross-validation of the training data set T determined, among others, the parameters $C = -5$ and $\gamma = -7$. For the further parameters C_{PCA} and the choice of the kernel (linear, polynomial, radial basis function (RBF) or sigmoid) we performed cross validation of the training data set T , the results are shown in Table I. The best results were received consistently by using the RBF kernel, while for C_{PCA} the value of 5 turned out to be the best choice with an accuracy of 97 ± 8.3 , where 8.3 is standard deviation.

With the training of the classifier completed, we studied the accuracy of the testing (validation) data set V . We compared the manual ground truth labeling $l(y_i)$ for data point y_i with the computed decision function $d(y_i)$ to compute the accuracy as follows

$$\begin{aligned} \text{Accuracy}(\%) &= \frac{\# \text{ of correctly predicted data}}{\# \text{ of total data}} \times 100 \\ &= \frac{|d(y_i)|}{|V|} \times 100 \end{aligned} \quad (6)$$

TABLE II. CLASSIFICATION ACCURACY RESULTS USING THE TESTING DATASET V .

Parameters	SVM Traning			
	Linear Kernel	Poly Kernel	RBF Kernel	Sigmoid Kernel
$C_{PCA} = 2$	86.8%	90.3%	89.9%	88.8%
$C_{PCA} = 3$	89.3%	92.5%	91.8%	90.3%
$C_{PCA} = 4$	91.9%	92.9%	94.9%	94.1%
$C_{PCA} = 5$	92.1%	93.6%	94.9%	94.6%

The results are shown in Table II. We achieve the same accuracy of 94.9% for the kernels RBF with C_{PCA} values of 4 and 5. This corresponds to Figure 9, where it is clear that between C_{PCA} 4 and 5 there is only very little difference. In total we received the best results using the RBF kernel and $C_{PCA} = 5$.

VI. MANIFOLD LEARNING FOR DIMENSIONALITY REDUCTION OF SKIN LESIONS USING OPTICAL SPECTROSCOPY DATA

Most recent applications of machine learning in data mining, computer vision, and in other fields require deriving a classifier or function estimate from a large data set. Modern data sets often consist of a large number of examples, each of which is made up of many features. Though access to an abundance of examples is purely beneficial to an algorithm attempting to generalize from the data, managing a large number of features (some of which may be irrelevant or even misleading) is typically a burden to the algorithm. Overwhelmingly complex feature sets will slow the algorithm down and make finding global optima difficult. To lessen this burden on standard machine learning algorithms (e.g. classifiers, function estimators), a number of techniques have been developed to vastly reduce the quantity of features in a dataset, i.e. to reduce the dimensionality of the data.

Dimensionality reduction has other, related uses in addition to simplifying data so that it can be efficiently processed. The most obvious is visualization; if data lies, for instance, in a 100-dimensional space, one cannot get an intuitive feel for what the data looks like. However, if a meaningful two or three dimensional representations of the data can be found, then it is possible to analyze it more easily. Though this may seem like a trivial point, many statistical and machine learning algorithms have very poor optimality guarantees, so the ability to see the data and the output of an algorithm is of great practical interest. In our case, spectroscopic data is typically acquired as a high dimensional vector (in our case a 2048 element vector); this high-dimensionality, however, creates difficulties for visualization and classification of the data. Manifold learning has a significant role in dimensionality reduction and clustering due to its nature of unsupervised learning [41].

There are many approaches to dimensionality reduction based on a variety of assumptions and used in a variety of contexts. We will focus on an approach initiated recently based on the observation that high-dimensional data is often much simpler than the dimensionality would indicate. In this work, we present results of applying different manifold learning techniques such as Isomap [42], Laplacian Eigenmaps [43] and Diffusion Map [44] to spectroscopy data from 48 patients with normal and malignant lesions to reduce the dimensionality,

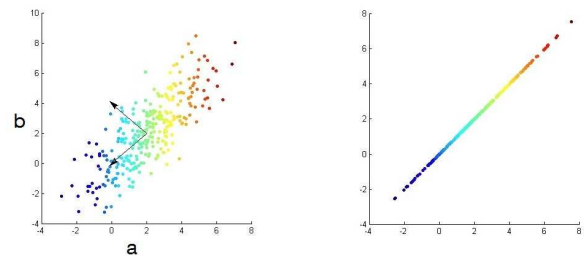


Fig. 11. Working example of PCA. The left image shows a Gaussian distribution together with the two principal components. The coloring is dependent on values of a and b . The right side shows the projection on the eigenvector corresponding to the largest eigenvalue [46].

and compare them to traditional linear technique Principal Component Analysis. Clustering results after dimensionality reduction are shown in Table III for each technique, where some of the method/parameter combinations yield excellent results on the patient data compared to the diagnosis of the treating physicians.

A. Principal Component Analysis

A linear method such as PCA ignores protrusion or concavity of the data [45]. In order to demonstrate the shortcomings of purely linear methods, we will show results using PCA and compare with nonlinear manifold learning. PCA finds a subspace i.e. which finds an optimal subspace that best preserves the variance of the data [46].

The goal of PCA is to find an optimal subspace i.e. the variance of the data is maximized. In general, manifold learning methods do not care about the variance of the data. Non-linear methods in particular, typically famous on preserving neighborhood properties within the data [46]. The input and output of PCA are defined as in equation 7 , given N input points.

Figure 11 shows a Gaussian distribution together with the first (and only) two principal components, calculated by the method described above. The vectors are therefore the eigenvectors of the matrix C .

The coloring is linearly dependent on the values of a and b . The right side shows the projection on the eigenvector corresponding to the largest eigenvalue. As one can see, the variance of the data is preserved.

Figure 12 shows that PCA cannot handle non-linear datasets. The left image shows a spiral distribution (2-d Swiss roll) together with the two principal components. The coloring is dependent on the values of t , where the function is given as $f(t) = (t\cos(t), t\sin(t))$. The right side of Figure 12 shows the overlapping projection on the eigenvector corresponding to the largest eigenvalue. One can observe that blue, red and yellow points are all overlapping in the center of the projected line [46].

This means that most geometric information of the data is lost through this projection. In most cases distances are only meaningful in local neighborhoods, following Non-linear manifold learning methods address this problem.

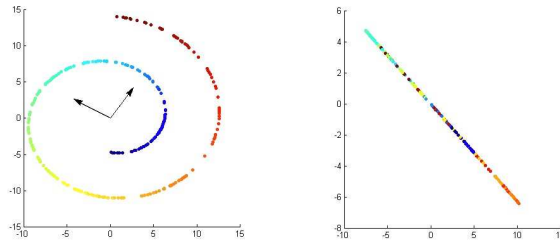


Fig. 12. PCA cannot handle non-linear datasets. The left image shows a spiral distribution (2-d Swiss roll) together with the two principal components. The coloring is dependent on the values of t , where the function is given as $f(t) = (t\cos(t), t\sin(t))$. The right side shows the overlapping projection on the eigenvector corresponding to the largest eigenvalue [46].

B. Non-linear Manifold Learning Methods

Typical non-linear manifold learning methods are graph-based and perform the following three basic steps.

- 1) Build undirected similarity graph $G = (V, E)$, where the vertices V are given by the data points x_i
- 2) Estimate local properties, i.e. the weight matrix W to define the weighted similarity graph $G = (V, E, W)$, where $w_{ij} \geq 0$ represents the weight for the edge between vertex i and j . Weights are obtained by means of a kernel. A weight of 0 means that the vertices are not connected.
- 3) Derive an optimal global embedding Ψ which preserves these local properties.

There are three often used techniques for building the similarity graph G . First, there is the ϵ -neighborhood graph which connects all vertices with distance $\|x_i - x_j\|^2$ smaller than ϵ . The ϵ graph is naturally symmetric [47] [46].

Contrary to this local connection is the fully connected graph which uses a similarity function that incorporates local neighborhood relations such as the Gaussian function: $w_{ij} = \exp(-\|x_i - x_j\|^2 / (2\sigma^2))$. This leads directly to the third step, since it implicitly defines the weights [46].

k -nearest neighbor (kNN) graphs combine both worlds by connecting each vertex only to its k -nearest neighbors.

C. Manifold Learning

In the field of machine learning, a very popular research area is manifold learning, which is related to the algorithmic techniques of dimensionality reduction. Manifold learning can be divided into linear and nonlinear methods. Linear methods, which have long been part of the statistician's toolbox for analyzing multivariate data, include Principal Component Analysis (PCA) and multidimensional scaling (MDS). Recently, researchers focus on techniques for nonlinear manifold learning, which include Isomap, Locally Linear Embedding, Laplacian Eigenmaps, Hessian Eigenmaps, and Diffusion Maps [46]. The algorithmic process of most of these techniques consists of three steps: a nearest-neighbor search, a computation of distances between points, and an eigen-problem for embedding the D -dimensional points in a lower-dimensional space. The manifold learning: Isomap, Laplacian Eigenmaps and Diffusion Maps will be compared and contrasted with the linear

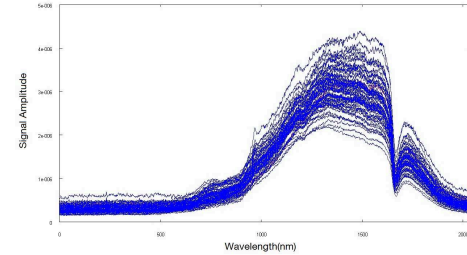


Fig. 13. Normalized spectral graph data sets, malignant skin lesions. Each curve is the vector, representing one skin lesion. Without labeling of the data the overlapping curves are difficult to separate

method PCA for a spectroscopic dataset. The goal is to find a mapping function Ψ from the original D -dimensional data set X to a d -dimensional dataset Y in which distances and information are preserved as much as possible and $d < D$:

$$\Psi : \mathbb{R}^D \rightarrow \mathbb{R}^d \quad (7)$$

In our case, we have $D = 2048$ and thus

$$\Psi : \hat{x}_i \in \mathbb{R}^{2048} \rightarrow y_i \in \mathbb{R}^d \quad (8)$$

where x_i and y_i are vectors and \mathbb{R}^d is a space.

D. System Experiments

We collected 372 spectroscopic data vectors from 48 patients, 326 measurements were of normal skin moles, 46 measurements were malignant skin lesion (as diagnosed by the treating physician). 13 cases out of 46 malignant skin lesions were pathologically verified by the laboratory. All lesions for this experiment were selected by only well-experienced physicians (not by newly joined dermatologists). This was the only additional protocol to the data acquisition protocols as discussed in section III-A. A color-coded representation of the normalized skin spectra data set is shown in Figure 13 and Figure 14. Figure 13 shows malignant skin lesions and Figure 14 shows malignant skin lesions combined with normal skin mole. In Figure 14 one can observe the overlap between two classes of data set.

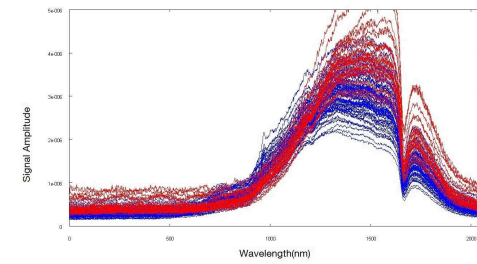


Fig. 14. Normalized spectral graph data sets combined form, blue for malignant skin lesions and red for normal skin mole.

The proposed methods were implemented in Matlab 10.1 using libraries for the dimensionality reduction. Clustering was performed by selecting a separating hyperplane in the processed three-dimensional data.

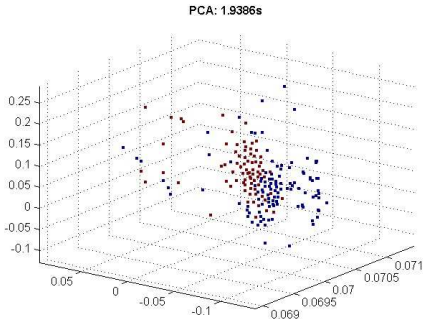


Fig. 15. PCA 3D representation of 2048D dataset. The best possible angle to visualize the data points. Blue for malignant skin lesions and red for normal skin mole. PCA:1.9386s is the runtime of method

TABLE III. CLUSTERING ACCURACY WITH DIFFERENT METHODS AND PARAMETERS. WHERE k IS k -NEAREST NEIGHBORS , A IS FOR ALPHA AND S IS REPRESENTING SIGMA PARAMETER

Parameters	Isomap	Laplacian Eigenmaps	Diffusion Maps
$k = 15, A = 2, S = 20$	88%	0%	10%
$k = 20, A = 2, S = 30$	90%	87%	81%
$k = 30, A = 1, S = 20$	86%	92%	90%
$k = 35, A = 1, S = 20$	94%	96%	92%

Before applying manifold learning we need to elucidate some parameters that play a significant role in producing meaningful data representation. The parameters for the non-linear dimensionality reduction techniques are:

- k : The k -nearest neighbors specify the number of nearest neighbors used to build the graph for the Isomap, Laplacian eigenmaps and Diffusion maps methods. If k is chosen too large or too small, the local geometry may not be interpreted correctly. Here we used the values of $k = 15, 20, 30, 35$.
- Alpha: This parameter controls the normalization.
- Sigma: This specifies the width of the Gaussian kernel. The larger Sigma is, the more weight far-away points will exert on the weighted graph. We used Sigma = 20, 30.

E. Discussion

All four studied methods (PCA, Isomap, Laplacian Eigenmaps and Diffusion maps) were applied independently. PCA is applied on 2048 dimensional data vectors, and the first three most significant components are taken. Each point represents one skin lesion (malignant or benign). The data set is labeled which is represented by two colors red and blue. Red points are malignant and blue are benign. It is clear from the 3D representation of the data shown in Figure 15 that the data is not clearly distinguishable into two clusters. The main reason PCA could not perform well is because PCA maximizes the variance of the data and in our case direction of the variance helps to distinguish between the two classes. The best clustering accuracy PCA achieved is 63%.

The 3D representation of the 2048D data vector after applying Isomap is shown in Figure 16. It is clear from the figure that some area of the data is very nicely clustered.

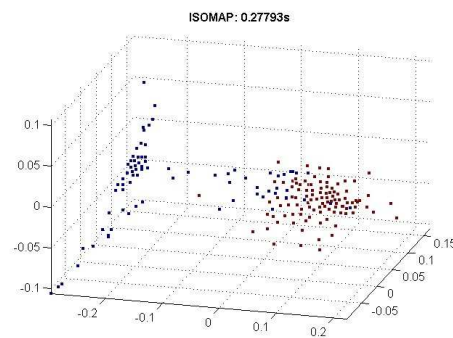


Fig. 16. Applying manifold learning by using Isomap and the output 3D representation as a result. Blue for malignant skin lesions and red for normal skin mole. The points that corresponds to malignant data examples, are well separated from those points corresponds to benign.

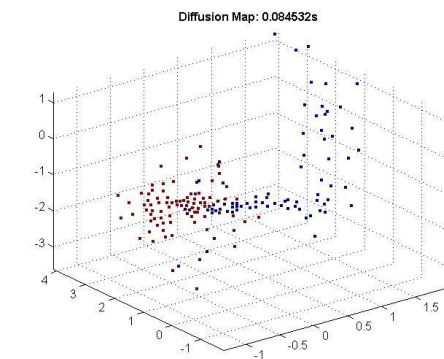


Fig. 17. Diffusion maps 3D data representation. The clusters are clearly visible. Blue for malignant skin lesions and red for normal skin mole.

The Isomap is governed by the geodesic distances between distant points, which causes distortions in local neighborhoods so maybe that is one reason that the data set is not clustered perfectly. Overall Isomap produce better results than PCA.

Figure 17, shows that the Diffusion maps is able to preserve the order of clusters in three dimensions similar as Isomap. Choosing the right parameter(s) is a difficult stage in manifold learning. Experiments are performed with different parameters as in table III. The results were computed as the number of

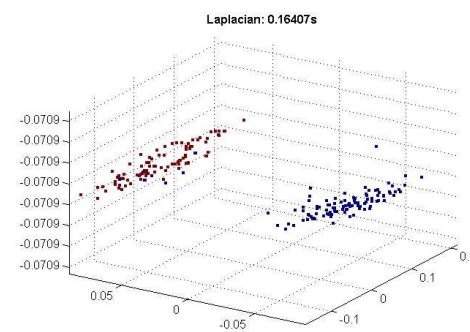


Fig. 18. Laplacian Eigenmaps 3D representation of 2048D dataset. Apart from few points which are in wrong cluster, the two clusters are well separated. Blue for malignant skin lesions and red for normal skin mole.

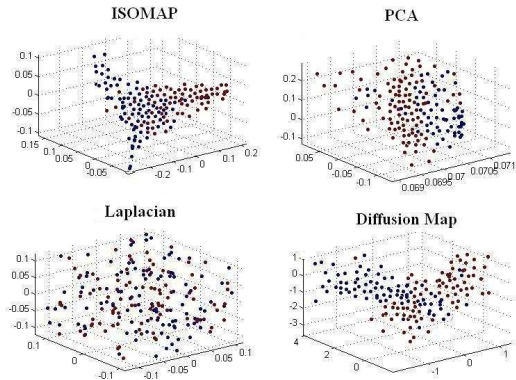


Fig. 19. A reduced 3D representation of spectroscopy 2048D dataset. The worst selection of parameters for all four methods. None of the method produced clear clustering of the dataset. Blue for malignant skin lesions and red for normal skin mole

correctly classified points over the total number of points and as a ground truth we have labeling provided by dermatologist. According to the literature [48], Diffusion maps perform better as compared to other manifold learning techniques but in our case Laplacian eigenmaps produces best results by choosing the right parameters shown in Figure 18. Laplacian eigenmaps preserve local neighborhood of the points which reflect the geometric structure of the manifold.

In Figure 19, all four methods are shown with worst parameters selection. The figure shows that the dataset is not easily distinguishable into two clusters. Variation in parameters for non-linear manifold learning methods are shown in Table III.

Isomap capture local geometry correctly and the dataset is clustered into two parts with an accuracy of 94% as shown in Table III. By increasing the neighborhood size to 20 and Sigma to 30, Laplacian eigenmaps and Diffusion maps perform better. Adding even more neighborhood information, Laplacian eigenmaps clustering accuracy improves to 96%. The parameters shown in the table are the only best combination for our dataset.

Four manifold learning techniques are applied to the problem of dimensionality reduction and clustering of optical spectroscopic data in dermatology. In contrast to the linear method PCA, all studied manifold learning techniques were able to perform satisfactorily in clustering normal skin mole from malignant skin lesions, provided the parameters were chosen correctly. In particular, Laplacian Eigenmaps look very promising for the intended dermatological application.

VII. CONCLUDING REMARKS ON FEASIBILITY OF OPTICAL SPECTROSCOPY FOR SKIN LESIONS CLASSIFICATION

In this part of the paper, optical spectroscopy for skin lesions classification is analyzed. Optical spectroscopy by itself produces data, which, due to its high-dimensionality, cannot be directly utilized for classifying skin lesions. In other words, distinguishing between malignant and benign skin lesions is difficult. First the dimension of the data needs to be reduced in a meaningful way. In this respect, the application of manifold learning techniques to the problem of dimensionality

reduction and clustering of spectroscopic data in dermatology is introduced. One other problem in dermatology is about quantifying the progress of skin lesions. For this purpose, one needs to be able to numerically compare two or more images of e.g. the same lesion taken during different sessions. This involves accurate registration of all those images. Combination of optical spectroscopy with tracking as a solution to this problem is presented. In our approach, this combination is used as a guidance for acquiring spectral measurements at the same positions and orientations as the first acquisition. We defined spectroscopic data acquisition protocol in section III-A for using our system optimally. We also evaluated a patient dataset with an SVM-based classification of skin lesions.

The system opens a new way for utilizing the real potential of optical spectroscopy for noninvasive diagnosis of skin lesions. In taking optical spectroscopy even one step further using the system, it is a promising technique for the discrimination of malignant skin lesions from benign ones. Spectroscopy could form the basis of a clinical method to diagnose skin lesions due to the accuracy and reproducibility of its measurements. Acquisition of spectroscopic data causes little or no patient discomfort, does not alter the basic physiology of the skin, poses no hazard to the patient and does not interfere with any other standard clinical diagnostic practices. The scan could be performed by a non-specialist and therefore might be a useful tool for the prescreening of skin lesions. However, before full integration of spectroscopy into the clinical workflow, some further challenges need to be addressed:

- From our experience, there is need for several spectroscopic probes with different diameter sizes in order **i**) to cover only the area relevant to the lesion during the acquisition, i.e. to avoid getting measurements from the healthy skin region around the lesion and **ii**) to avoid multiple scans of the same lesion.
- In our experiments, we have observed that different samples taken from the same mole led to different spectral readings. A method is required to create a representative measurement from multiple spectroscopic readings for each mole.
- Optical spectroscopy based skin lesion diagnosis systems should be patient specific, since every patient has his/her own individual pattern of lesions which can be monitored throughout his/her body moles. In our study, we have observed that it is important to perform the classification within patient specific data in order to build a reliable system.
- Combining optical spectroscopy with other imaging technologies, e.g. dermoscopy imaging, multispectral imaging and hyperspectral imaging, can improve the diagnosis further, since the optical spectroscopy provides complementary information to these techniques.
- Patient age is an important factor which needs to be taken into account during the acquisition of optical spectroscopy data. As the cellular structures can change according to the age of the patient, differences in spectroscopic readings have been observed between young and elderly people, which can be addressed by creating groups of patients accordingly.

- Accurate data acquisition requires constant contact of the probe with the surface of the lesion which is hindered in some cases by ragged skin lesions. Further studies are required to investigate new techniques for data acquisition without touching the skin surface.
- A more in-depth study on data sets with larger variation is required to demonstrate general utility of optical spectroscopy in the clinical setting. Especially, data accompanied by pathological verification of malignant melanoma would be highly desirable to demonstrate the reliability of the presented methods.

REFERENCES

- [1] R. Marks, Epidemiology of melanoma, clinical excremental dermatology, PMID: 11044179 (PubMed - indexed for MEDLINE) 25 (2000) 395–406.
- [2] W. H. Organization, Ultraviolet radiation and the intersun programme, Website, <http://www.who.int/uv/faq/skincancer/en/> (2007).
- [3] O. Colot, R. Devinoy, A. Sombo, D. de Brucq, A color image processing method for melanoma detection, Medical Image Computing and Computer-Assisted Intervention MICCAI 1496 (1998) 562.
- [4] M. H. Madsen, L. Hansen, J. Larsen, K. Drzewiecki, A probabilistic neural network framework for detection of malignant melanoma, in: artificial neural networks in cancer diagnosis prognosis and patient management, in: 18th IEEE Symposium on Computer-Based Medical Systems, 2001, pp. 141–183.
- [5] P. Rubegni, G. Cevenini, M. Burroni, R. Perotti, G. Dell'eva, P. Sbano, C. Miracco, P. Luzi, P. Tosi, P. Barbini, L. Andreassi, Automated diagnosis of pigmented skin lesions, Publication of the International Union Against Cancer 101 (2002) 576–580.
- [6] J. Sanders, B. Goldstein, D. Leotta, K. Richards, Image processing techniques for quantitative analysis of skin structures, Comput. Methods Programs Biomed. 59 (4) (1999) 167–180.
- [7] A. Bono, S. Tomatis, C. Bartoli, The invisible colors of melanoma. a telespectrophotometric diagnostic approach on pigmented skin lesions, Eur. J. Cancer 34 (10) (1996) 727–729.
- [8] S. Dreiseitl, L. O. Machado, H. Kittler, S. Vinterbo, H. Billhardt, M. Binder, A comparison of machine learning methods for the diagnosis of pigmented skin lesions, Journal of Biomedical Informatics 34 (2001) 28–36.
- [9] A. Blum, H. Luedtke, U. Ellwanger, R. Schwabe, G. Rassner, C. Garbe, Digital image analysis for diagnosis of cutaneous melanoma. development of a highly effective computer algorithm based on analysis of 837 melanocytic lesions, Br. J. Dermatol. 151 (5) (2004) 1029–1038.
- [10] R. J. Stanley, R. H. Moss, W. V. Stoecker, C. Aggarwal, A fuzzy based histogram analysis technique for skin lesion discrimination in dermatology clinical images, Comput. Med. Imag. Graph. 27 (2003) 387–396.
- [11] F. Ercal, A. Chawla, W. V. Stoecker, H. Lee, R. H. Moss, Neural network diagnosis of malignant melanoma from color images, IEEE Trans. Biomed. Eng. 14 (9) (1994) 837–845.
- [12] J. Boldrick, C. Layton, J. Ngyuen, S. Switter, Evaluation of digital dermoscopy in a pigmented lesion clinic: Clinician versus computer assessment of malignancy risk, J. Amer. Acad. Dermatol. 56 (3) (2007) 417–421.
- [13] K. Hoffmann, T. Gambichler, A. Rick, M. Kreutz, M. Anschuetz, T. Grunendick, A. Orlikov, S. Gehlen, R. Perotti, L. Andreassi, J. N. Bishop, J. P. Cesarini, T. Fischer, P. J. Frosch, R. Lindskov, R. Mackie, D. Nashan, A. Sommer, M. Neumann, J. P. Ortonne, P. Bahadoran, P. F. Penas, U. Zoras, P. Altmeyer, Diagnostic and neural analysis of skin cancer (danaos). a multicentre study for collection and computer-aided analysis of data from pigmented skin lesions using digital dermoscopy, Br. J. Dermatol. 149 (10) (2003) 801–809.
- [14] G. Surowka, K. Grzesiak-Kopiec, Different learning paradigms for the classification of melanoid skin lesions using wavelets, in: Proc. 29th Annu. Int. Conf. IEEE EMBS, 2007, pp. 3136–3139.
- [15] Z. Zhang, R. H. Moss, W. V. Stoecker, Neural networks skin tumor diagnostic system, in: in Proc. IEEE Int. Conf. Neural Netw. Signal Process., 2003, pp. 191–192.
- [16] M. Kudo, J. Sklansky, Comparison of algorithms that select features for pattern classifiers, Pattern Recognit. 33 (2000) 25–41.
- [17] S. Umbaugh, Y. Wei, M. Zuke, Feature extraction in image analysis, IEEE Eng. Med. Biol. 16 (4) (1997) 62–73.
- [18] S. E. Umbaugh, R. H. Moss, W. V. Stoecker, Applying artificial intelligence to the identification of variegated coloring in skin tumors, IEEE Eng. Med. Biol. Mag. 10 (4) (1991) 57–62.
- [19] E. A. Edwards, S. Q. Duntley, The pigments and color of living human skin, American Journal of Anatomy 65 (3) (2005) 1–33.
- [20] S. Nischic, C. Forster, Analysis of skin erythema using true color images, IEEE Trans. Med. Imag. 16 (6) (1997) 711–716.
- [21] S. D. Depths, www.missionignition.net/bms/led_heal_clip_image008.jpg
- [22] M. Moncrieff, S. Cotton, E. Claridge, P. Hall, Spectrophotometric intracutaneous analysis: a new technique for imaging pigmented skin lesions, Br J Dermatol. 146 (3) (2002) 448–57.
- [23] P. name: MelaFind(R), Mela sciences, inc., Address: 50 South Buckhout Street, Suite 1, Irvington, NY 10533, <http://www.melasciences.com/> (2004).
- [24] P. name: SpectroShade(R), Mht s.p.a. headquarter, Production and Commercialization Via Milano 12, 37020 Arbizzano di Negar (VR) Italy, www.mht.it (2007).
- [25] A. Kim, U. Kasthuri, B. Wilson, A. White, A. L. Martel, Preliminary clinical results for the in vivo detection of breast cancer using interstitial diffuse optical spectroscopy, MICCAI Workshop on Biophotonics Imaging for Diagnostics and Treatment 75 (2006) 1601–2321.
- [26] H. E. Kuppenheim, R. Raymond Heer, Spectral reflectance of white and negro skin between 440 and 1000 μ m, Journal of Applied Physiology 4 (10) (1952) 800–806.
- [27] R. R. Anderson, J. A. Parrish, The optics of human skin, Journal of Investigative Dermatology 77 (1) (1981) 13–19.
- [28] J. W. Feather, M. Hajizadeh-Saffar, G. Leslie, J. B. Dawson, A portable scanning reflectance spectrophotometer using visible wavelengths for the rapid measurement of skin pigments, Phys. Med. Biol. 34 (1) (1989) 807–20.
- [29] B. L. Diffey, R. J. Oliver, P. Farr, A portable instrument for quantifying erythema induced by ultraviolet radiation, Br. J. Dermatol. 111 (1984) 663–72.
- [30] J. B. Dawson, D. J. Barker, D. J. Ellis, E. Grassam, J. A. Cotterill, G. W. Fisher, J. W. Feather, A theoretical and experimental study of light absorption and scattering by in vivo skin, Phys. Med. Biol. 25 (1980) 695–709.
- [31] T. J. Farrell, M. S. Patterson, B. Wilson, A diffusion theory model of spatially resolved, steady state diffuse reflectance for the non-invasive determination of tissue optical properties in vivo, Med. Phys. 19 (1992) 879–88.
- [32] A. Kienle, L. Lilge, M. S. Patterson, R. Hibst, R. Steiner, B. C. Wilson, Spatially resolved absolute diffuse reflectance measurements for non-invasive determination of the optical scattering and absorption coefficients of biological tissue, Appl. Opt. 35 (1996) 2304–14.
- [33] C. J. Lynn, I. S. Saidi, D. G. Oelberg, S. L. Jacques, Gestational age correlates with skin reflectance in newborn infants of 24 – 42 weeks gestation, Biol. Neonate 75 (1993) 9–64.
- [34] R. Marchesini, M. Brambilla, C. Clemente, M. Maniezzo, A. E. Sichirollo, A. Testori, D. R. Venturoli, N. Cascinelli, In vivo spectrophotometric evaluation of neoplastic and non-neoplastic skin pigmented lesions-i. reflectance measurements, Photochem Photobiol 53 (1991) 77–84.
- [35] R. Marchesini, N. Cascinelli, M. Brambilla, C. C. L. M. E. Pignoli, A. Testori, D. R. Venturoli, In vivo spectrophotometric evaluation of neoplastic and non-neoplastic skin pigmented lesions-2. discriminant analysis between nevus and melanoma, Photochem Photobiol 55 (1992) 515–22.
- [36] A. Bono, S. Tomatis, C. Bartoli, G. Tragni, G. Radaelli, A. Maurichi, R. Marchesini, The abcd system of melanoma detection: a spectrophotometric analysis of the asymmetry, border, color, and dimension, Cancer 85 (1999) 7–72.

- [37] S. Sigurdsson, P. A. Philipsen, L. K. Hansen, J. Larsen, M. Gniadecka, H. C. Wulf, Detection of skin cancer by classification of raman spectra, in: IEEE Trans. Biomed. Eng., 2004, pp. 1784–1793.
- [38] M. Osawa, S. Niwa, A portable diffuse reflectance spectrophotometer for rapid and automatic measurement of tissue, Meas. Sci. Technol. 4 (1993) 668–76.
- [39] N. Cristianini, J. S. Taylor, An Introduction to Support Vector Machines and Other Kernel based Learning Methods, 1st Edition, Cambridge University Press, 2000.
- [40] C.-C. Chang, C.-J. Lin, Libsvm: A library for support vector machines, Open source, <http://www.csie.ntu.edu.tw/~cjlin/libsvm> (2001).
- [41] L. Cayton, Algorithms for manifold learning, TR 2008–0923, University of California, Franklin St., Oakland, (June 15 2005).
- [42] J. B. Tenenbaum, V. de Silva, J. C. Langford, A global geometric framework for nonlinear dimensionality reduction, Science 290 (5500) (2000) 2319–2323.
- [43] M. Belkin, P. Niyogi, Laplacian eigenmaps and spectral techniques for embedding and clustering, in: Advances in neural information processing systems, MIT Press, Cambridge 14 (1) (2002) 585–591.
- [44] R. Coifman, S. Lafon, Diffusion maps: Applied and computational harmonic analysis, Special Issue: Diffusion Maps and Wavelets 21 (1) (2006) 5–30.
- [45] T. Hastie, R. Tibshirani, J. H. Friedman, The elements of statistical learning: Data Mining, Inference and Prediction, Springer, 2001.
- [46] R. Socher, M. Hein, Manifold Learning and Dimensionality Reduction with Diffusion Maps, Tech. report, 2008.
- [47] U. von Luxburg, A tutorial on spectral clustering, Stat Comput, Springer Science and Business Media 17 (5) (2007) 395–416.
- [48] B. Bah, Diffusion maps: Analysis and applications, dissertation 66, Mathematical Modeling and Scientific Computing, Wolfson College, University of Oxford, UK (September 2008).